Electrical Engineering

December 1941

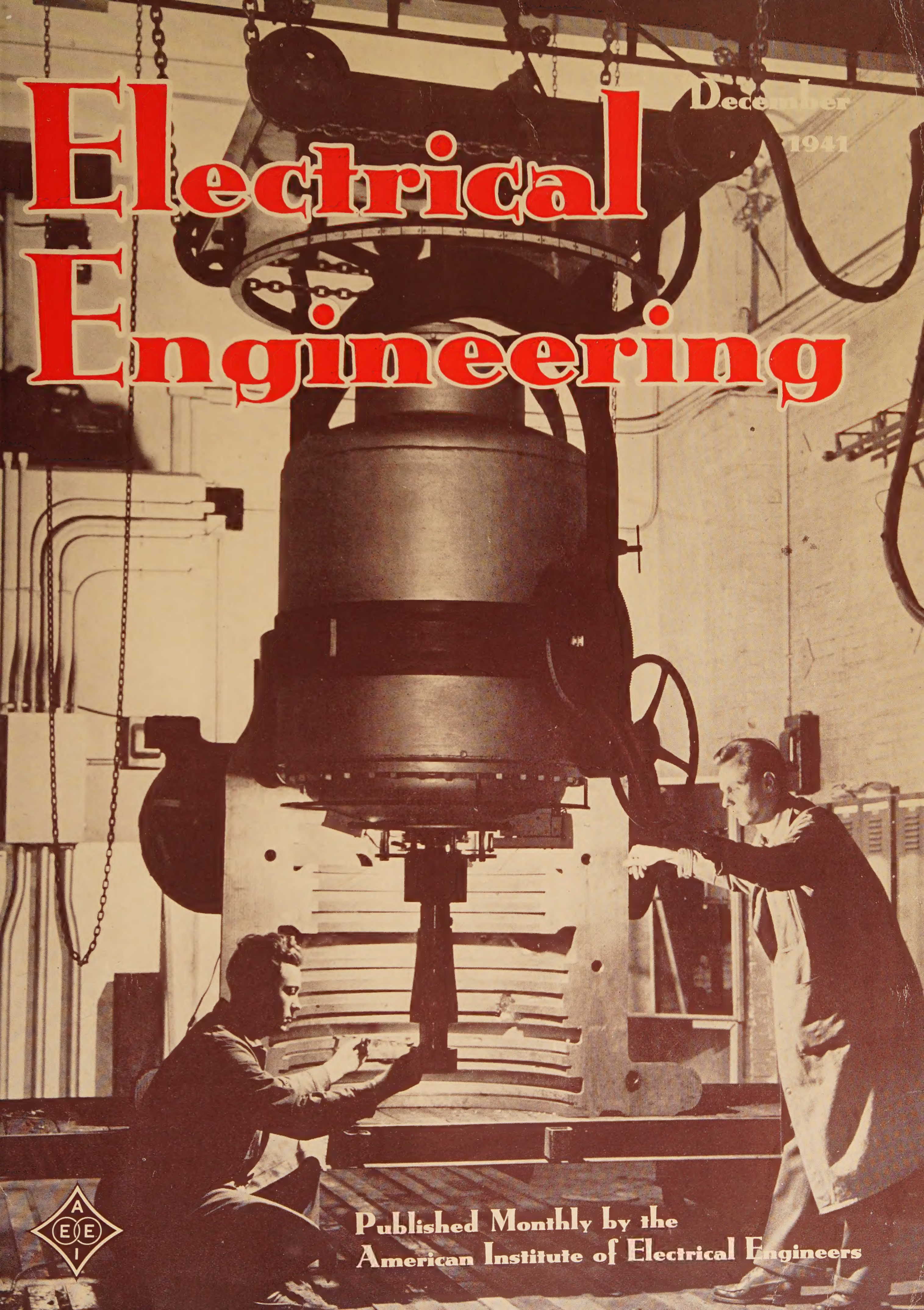

Published Monthly by the
American Institute of Electrical Engineers

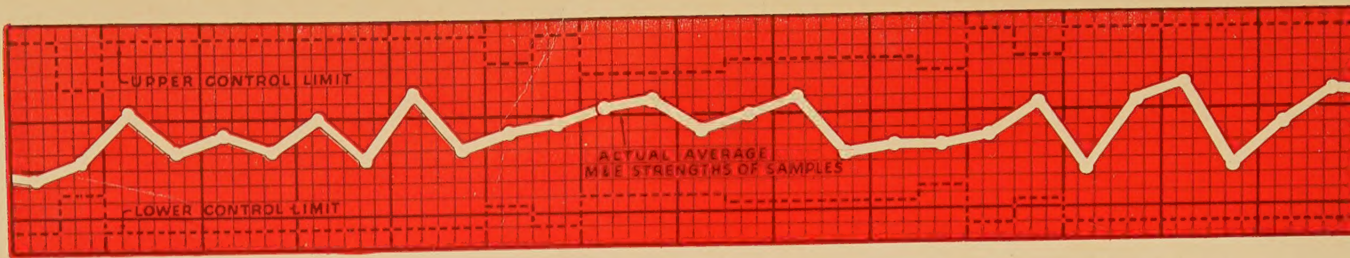

Typical section of an O-B factory control chart, on which the average M & E strengths of the insulators tested each day are plotted. Falling of actual values within the control limits (determined by the number of insulators checked) indicates the desired uniformity is being attained.

Strength Isn't a Straight Line

But the Curves for Average Values and Deviations of O-B Suspensions Are Near the "Straight Line" Ideal

● Uniformity of M & E strength is supremely important for suspension insulators, mainly because the failure of a single unit could drop a line and interrupt service. Uniform insulators allow lines to be designed with a lower factor of safety than would be needed with erratic units. And insulators of uniform strength are superior in other vital properties.

To attain the highest possible degree of uniformity, O-B carefully inspects all raw materials and exercises extremely rigid control in every single manufacturing process. Going even further, O-B uses scientific, large-quantity sampling to secure reliable probability curves which permit accurate, continuous checking of factory control. How this system is applied may be seen in the accompanying typical charts, one for average values and the other for deviations of individual specimens from their average. Control limits are determined by the number of insulators in the samples, and the actual values are the results of *daily* tests. Should any average or deviation value fall outside these control limits, the cause of the observed condition is immediately found and corrective measures taken.

To benefit from this effective factory control system—assuring units with averages safely above rated values and having deviations small enough to guarantee dependable, satisfactory minimum strengths—be sure to specify O-B for your suspension insulators!

BUY THE BEST-BUY O-B!

Ohio Brass

MANSFIELD, OHIO, U. S. A.

Canadian Ohio Brass Co., Ltd., Niagara Falls, Ont.

2208-H

Actual deviations of individual specimens from their average are plotted on this O-B control chart, providing another effective means for checking the uniformity of suspension insulators.

Electrical Engineering

Registered U. S. Patent Office

for December 1941—

The Cover: Million-volt industrial X-ray unit; will radiograph five-inch steel plates and castings in four minutes (see pages 571–3)
Photo courtesy General Electric Company

Transactions Section *(Follows EE page 618; a preprint of pages 1003–50 of the 1941 volume)*

©

VOLUME 60 FOUNDED 1884 NUMBER 12

A Monthly Publication of

American Institute of Electrical Engineers

33 West Thirty-Ninth Street, New York, N. Y.

¶ Statements and opinions given in articles and papers appearing in "Electrical Engineering" are the expressions of contributors, for which the Institute assumes no responsibility.

¶ Correspondence is invited on all controversial matters.

High Lights • •

Generator-Insulation Field Tests. The need for a practical and reliable nondestructive test that will indicate the condition of generator insulation has been the subject of study by a special subject committee of the Edison Electric Institute's electrical equipment committee since 1935; investigation has been directed toward characteristics of insulation for such tests as insulation resistance, power factor, high-voltage alternating current, high-voltage direct current, and ionization as caused by high-voltage application (*Transactions pages 1003–11*).

Metering Development. The series of four articles on the development of the metering art, sponsored by the Institute's committee on instruments and measurements, concludes with a report on developments in calibration, installation, and maintenance of meters (*pages 581–6*). An appendix lists sources of information covering the entire series (*pages 587–9*). The whole report is being issued in pamphlet form (*page 597*).

Automatically Reclosing Breaker. Designed especially for co-ordination on extended distribution systems to eliminate service trips on temporary faults and restrict outages to the immediate neighborhood of a permanent fault, a small automatically reclosing oil circuit breaker has been developed with a pronounced inverse time on tripping; completely self-protecting, it requires minimum maintenance (*Transactions pages 1021–4*).

Relaying Progress. A decade's progress in relaying has been reviewed in a report prepared under the auspices of the AIEE committee on protective devices (*pages 590–2*). This is the second of three reports on developments in the protection of electric power-system circuits and equipment; the first, on circuit interrupters, appeared in November, and the third is scheduled for an early issue.

ECPD Annual Meeting. Rising consciousness of the need for active participation in the affairs of the Engineers' Council for Professional Development by its constituent organizations was indicated at Council's recent ninth annual meeting (*pages 606–08, 610*). The list of curricula accredited by ECPD to date also appears in this issue (*pages 608–09*).

Engineers Defense Board. A central agency prepared to assist the various branches of government with engineering experience has been set up by the formation of the Engineers Defense Board in which six national engineering societies are co-operating (*page 610*). Other news relating to national defense also appears in the section "Of Current Interest".

Wave Analysis. Complex periodic functions, transformed into corresponding voltage waves, may be analyzed with the aid of a cathode-ray oscillograph. The complex wave is represented upon the fluorescent screen of the cathode-ray tube by a vertical displacement, at the same time that a sinusoidal horizontal oscillation exists (*Transactions pages 1032–6*).

Million-Volt X-Ray Unit. Only a few years ago an 800-volt X-ray equipment required a special multistory housing, utilized a tube about a foot in diameter and 14 feet long; today's 1,000-kv unit occupies a 30- by $3^1/_2$-inch envelope, is housed as a self-contained unit in a tank 3 feet in diameter and less than 5 feet high (*pages 571–3*).

Dual Rating. Proposals for the dual rating of electrical apparatus, one governed by strength and the other by endurance limits, are outlined in a report recently issued by the AIEE standards committee. The committee hopes that the report will stimulate discussion that will lead ultimately to an improved system of rating (*pages 569–71*).

Dielectric Strength of Gas. Tests of impulse and 60-cycle breakdown strength have been made of nitrogen and Freon at gauge pressures up to 200 and 70 pounds per square inch, respectively, and dielectric strength values compared with the breakdown of transformer oil under similar conditions (*Transactions pages 1017–20*).

Calculating Motor Performance. A method of predetermining the performance of single-phase induction motors based on the development of charts to determine apparent impedances has been proposed; its practical value has been demonstrated by use in an industrial design department (*Transactions pages 1037–41*).

New Reclosing Relay. A reclosing relay has been designed and built specifically to meet the additional reclosing requirements created by complete automatization of high-voltage oil circuit breakers in transmission networks and on lines containing automatic sectionalizing air-break switches (*Transactions pages 1041–5*).

Transient Overspeeding. The transient swing above synchronous speed observed when a standard squirrel-cage induction motor is started without load has been explained by reference to the frequency modulation of the power supply caused by the rapid variation of the power taken from the line (*Transactions pages 1030–2*).

Inductance of Rectangular Conductors. Formulas have been derived by means of which can be calculated the inductance of single-phase circuits and certain polyphase circuits composed of solid or tubular rectangular conductors; a numerical example illustrates application of the single-phase formulas (*Transactions pages 1046–9*).

Improving Electric Service. Practices used by one power company to improve continuity and quality of service included high-speed circuit reclosure and methods of limiting voltage disturbances, or their effects on motor speeds, to values tolerable in the manufacturing processes of a particular industry (*Transactions pages 1012–16*).

Short Circuits in Armature Coils. An approximate solution for the current in a short-circuited coil or group of coils in the armature of a synchronous machine operating under load is expressed as the sum of a series of harmonics the terms of which are in geometric ratio (*Transactions pages 1024–9*).

Mazda Lamps. The production of incandescent Mazda lamps, from the processing of tungsten ore to the final assembly of parts, is surveyed and illustrated as it is carried on by a large manufacturing company (*pages 574–80*).

Coming Soon: Among special articles and technical papers currently in preparation for early publication are: an article on power-system development on a national scale by T. R. Tate (M'35), Federal Power Commission; an article on Heaviside's operational calculus by J. B. Russell (A'34); an article on protective lighting for American industry by Davis H. Tuck; an article on the cyclotron by W. M. Brobeck; a paper on the acceleration oscillogram method of motor torque measurement by C. R. Atkinson (A'31) and E. G. Downie (A'35); a paper describing field tests on high-capacity station circuit breakers by H. D. Braley (A'18); a paper on the frequency-modulated carrier telegraph system by F. B. Bramhall (M'39) and J. E. Boughtwood; a paper describing the performance of ground-relayed distribution circuits during faults to ground by C. L. Gilkeson (M'34), P. A. Jeanne (M'30), and J. C. Davenport; a paper describing a d-c telemeter or d-c Selsyn for aircraft by R. G. Jewell (A'30) and H. T. Faus (M'34); a paper on the relative values of different types of overcurrent protection for distribution circuits by G. F. Lincks (A'37); a paper on field tests and performance of a high-speed 138-kv air-blast circuit breaker by Philip Sporn (F'30) and H. E. Strang (M'39); a paper on temperature and electric stress in impregnated paper insulation by J. B. Whitehead (F'12) and W. H. MacWilliams (Enrolled Student); a progress report of d-c testing of generators in the field by E. R. Davis (A'41) and M. F. Leftwich (A'30); a paper on a method of calculating performance of current transformers based on admittance vector locus by A. C. Schwager (M'31).

The Dual Rating of Electrical Apparatus

P. L. ALGER
FELLOW AIEE

AIEE Standards Pamphlet No. 1A entitled "General Principles for Rating of Electrical Apparatus for Short Time, Intermittent, or Varying Duty," recently was issued in report form for study and comment. In this article, the chairman of the committee that prepared the report discusses its significance, for the purpose of stimulating discussion of this important topic. Contributions to the Letters columns are invited.

EVERY material or device, from a rubber band to a locomotive, has two independent physical limits, one of strength and one of endurance. The rubber band may support a large weight without rupture, but heat aging or oxygen exposure ultimately will reduce its strength to zero. So also, an induction motor operating at constant voltage has a definite torque limit at which breakdown occurs, but a much lower continuous torque-carrying ability, determined by heating and insulation aging effects.

To select a locomotive for a desired train-speed characteristic on a mountain railroad, or an electric motor for an elevator, or even a type of steel for the buckets of a steam turbine, both the strength and the endurance limits must be recognized and allowed for. When a system is built up of many different apparatus types, therefore, both strength and endurance limits must be properly matched. We cannot attain the perfection of the deacon who designed the "wonderful one-horse shay," but we can very profitably follow the principles he laid down:

"Fur," said the Deacon, "It's mighty plain
That the weakes' place mus' stan' the strain;
'N' the way to fix it, uz I maintain,
Is only jest
To make that place uz strong uz the rest."

For convenience in matching assorted materials or apparatus types, it is very desirable that the name-plate ratings indicate these two limits of strength and endurance separately. That is, a dual output rating is required for any material or apparatus to be used in short-time, intermittent, or varying duty. Examples of such dual ratings in common use are the proportional and fatigue strength limits of metals, the one hour and continuous ratings of railway motors, and the impulse and 60-cycle dielectric strength of insulation.

This problem of suitably describing apparatus for varying-duty service has been under study by an AIEE committee for the past two years. It is of particular importance to the electrical industry because electric motors and controls are now so widely used in association with every variety of mechanical equipment to perform the varied tasks of industry. Electrical engineers have found laymen generally to be singularly impervious to ideas about temperature rise and commutation limits of electric motors; therefore, it is natural that they have sought a more generally acceptable way of defining the output limitations.

The first results of this study have recently appeared in the form of a report, AIEE No. 1A, entitled "General Principles for Rating of Electrical Apparatus for Short-Time, Intermittent, or Varying Duty." This report describes four distinct methods of rating such apparatus that are or have been frequently used, and proposes a new, or modified, "service factor rating" method for general adoption. This method is equally suitable for rating mechanical apparatus and materials, so that its use should facilitate the co-ordination of all the different elements in electromechanical systems of every sort.

The diagrams will assist in understanding the problem and its proposed solution. In Figure 1 is shown the output–time characteristic of an electric motor or other device. The maximum momentary load (P_m) that can be carried (say for one minute) is governed by the strength limit, fixed by breakdown torque, commutation, voltage regulation, or the proportional limit of the mechanical structure; and the endurance limit (P) is fixed by the temperature, chemical stability, and deterioration rates of the materials employed.

For any given type of apparatus, P_m and P may be independently varied over wide limits. For example, increasing the reactance of an electric motor or cable will reduce only its momentary load-carrying ability (for a given voltage), while heat insulating it will reduce only its continuous load-carrying ability (for a given insulation life). The curve equally well applies to a gas engine, a gear, or a steam turbine.

Obviously, the sustained load on the apparatus must be considerably less than P_m, and there must be a reasonable safety margin in addition to provide for unknown conditions of service. It is desirable, therefore, to choose a name-plate rating, P_n, representative of the load that is actually to be carried for repeated or sustained time intervals. Just how P_n is determined will depend on the type of apparatus and the service. It may represent a one-hour rating; or the average of a varying load over any agreed short time interval; or simply an arbitrary fraction of the required P_m value.

However, it is desirable to preserve an approximately fixed ratio of P_n to P_m for any given type of apparatus or system. For example, in the case of an induction motor, the stalled current being closely proportional to the breakdown torque P_m, a fixed ratio of P_n to P_m will make

Essential substance of an address presented at the AIEE South West District meeting, St. Louis, Mo., October 8–10, 1941.

P. L. Alger is staff assistant to the vice-president in charge of engineering, General Electric Company, Schenectady, N. Y.; and chairman of co-ordinating committee 4 of the AIEE standards committee.

the P_n value alone a reliable indicator of all power-supply, fusing, and wiring requirements. A usual ratio of P_n to P_m for induction motors is 0.45 to 0.55, which assures ample torque margin for occasional operating peaks in excess of normal, and which corresponds to a stalled current of about five to six times the full-load value. As another example, in the case of arc-welding generators or transformers, the name-plate rating, P_n, may represent the actually expected welding current at maximum setting. This current is required only intermittently, over periods of a few minutes, as frequent idle periods are necessary for adjusting the work and replacing electrodes. The rms equivalent current over an extended period is rarely in excess of 80 per cent of the actual welding current, and so it is customary to use apparatus with a permissible continuous current materially less than the P_n value.

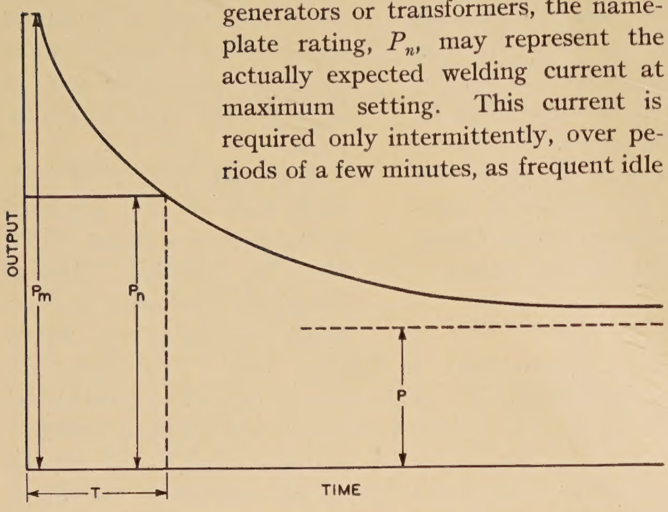

Figure 1. Output-time curve of an electrical device

P_m = Maximum momentary output, fixed by other than thermal limitations
P = Continuous output, or rating for continuous operation under known service conditions
P_n = Name-plate rating, or sustained load that may be carried in intermittent, short-time, or other specified duty. In the case of general purpose apparatus, P_n may be slightly less than P, to provide a margin where service conditions are unknown
T = Time associated with short-time rating
$S = P/P_n$ = Service factor

On this basis, therefore, the name-plate rating of any apparatus for short-time, intermittent, or varying duty ought to define the values of both P_n and P. The remaining question is whether to give both P_n and P directly, or the ratio P_n to P (greater than unity), or the ratio P to P_n (less than unity).

If both P_n and P are given directly, as in the case of the one-hour and continuous horsepower ratings of a locomotive, for example, it becomes necessary always to say which kind of horsepower is intended. It is as confusing as if coal weights were measured in both long and short tons, with the ratio of a long to a short ton varying under different conditions.

Comparison of an electric with a Diesel-electric locomotive, both having the same continuous rating of 4,600 horsepower affords an excellent illustration of this difficulty. The Diesel-electric, having no external source from which to draw power, can deliver 4,600 horsepower continuously, but cannot exceed this output even momentarily. The electric locomotive, being able to draw far more than continuous rated current from the trolley wire, can deliver far more than its continuous rated horsepower for short periods, within the thermal limits of the apparatus, as shown by Figure 2. In the case illustrated, the electric locomotive has a peak capacity of 8,800 horsepower and can deliver 7,000 horsepower for a considerable period, so enabling speed to be maintained on upgrades. It is not fair, therefore, to call them both 4,600-horsepower locomotives, nor is one a 4,600- and the other an 8,800-horsepower unit. They must be compared on a dual-rating basis.

If the continuous rating, P, is taken as the basic value, and the greater-than-unity ratio, P_n/P, is used to indicate the permissible operating load, another sort of confusion arises. Consider the case of a normal open-ventilated motor, with a continuous rating of 100 horsepower, for example. If the ventilation is shut off completely, the motor may become dangerously hot even at no load, and its continuous rating will be reduced to a small fraction of 100 horsepower. Yet, physically, and so far as stalled current, momentary power demand, breakdown torque, and short-time load-carrying ability are concerned, the motor is still a 100 horsepower unit. Conversely, by providing forced ventilation, the permissible continuous rating may be appreciably increased, but the torque limitations and power-demand characteristics will be unchanged. Hence, the continuous rating is greatly affected by ventilation, but is not a good index of physical size, cost, torque ability, or power-supply requirements.

The situation is as if a hoist were designed to lift a ten-ton weight once every ten minutes. Shall this be called a one-ton hoist, because it does the same average amount of work as another hoist lifting a one-ton weight through the same distance once each minute? Certainly the ten-ton lifting capacity requires greater size, stronger foundations, and has a greater cost, than the one-ton lifting capacity. It is, therefore, unreasonable to give them the same name-plate rating.

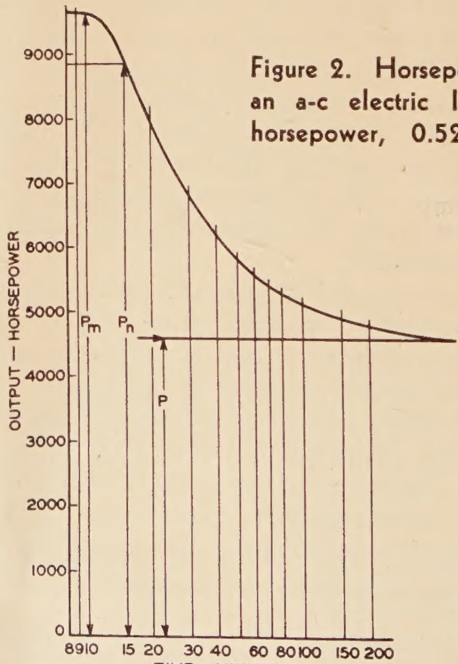

Figure 2. Horsepower-time curve of an a-c electric locomotive (8,800 horsepower, 0.52 service factor)

P_m = 9,600 - horsepower maximum momentary output fixed by mechanical and commutation limitations

P_n = 8,800 - horsepower nominal accelerating rating developed for a fraction of a minute during every acceleration

P = 4,600 - horse power continuous rating

$S = P/P_n$ = 0.52 service factor

There remains the plan of taking the permissible operating load, P_n, as the basic, or name-plate rating, and designating the permissible continuous load by a factor less than unity. As already indicated, with a reasonably uniform ratio of peak output capacity, P_m, to the operating load, P_n, the latter figure gives a fair measure of the physical size, power demand, and basic cost of the apparatus. To give the two hoists of the preceding paragraph ratings of ten tons, 10 per cent time on, and one ton, 100 per cent time on, respectively, is altogether natural and understandable to the layman. This, therefore, is the recommendation made in the AIEE Standards Report No. 1A.

For convenience, and exact expression, the name "service factor" has been given to this ratio, P/P_n, of the permissible continuous load to the normal operating load. The term "service factor" bears a close analogy to the familiar term "load factor," which expresses the ratio of the average to the peak power demand of any system. In each case, a low service factor, or a low load factor, implies a large physical plant and high stand-by charges, compared with a system having a high service factor or load factor and the same annual power consumption. Also, a low service factor, or a low load factor, implies a high ratio of peak-load-carrying ability to continuous capacity.

The recommendations of this AIEE committee report may be summarized in a few brief statements; for all short-time, intermittent, or varying-duty apparatus (referring to Figure 1):

1. The name-plate rating, P_n, should indicate the permissible frequently repeated or sustained load.

2. The momentary peak-load capacity, P_m, should bear an approximately constant relation to P_n, for any given type of apparatus, in associated system elements.

3. The permissible continuous load that may be carried for an indefinitely long period without injury, P, should be indicated by a service factor, S, less than unity, applied to the name-plate rating: $P = SP_n$.

To put these suggestions to practical use, and adopt or modify them for industry standards of rating, is a task for the future that will take considerable time. The report will amply serve its purposes, however, if it excites discussion and ultimate concerted action to improve our American methods of apparatus rating.

In closing this discussion, it should be pointed out that a major reason for bringing this matter to the fore at the present time is the more exact knowledge now available of life temperature effects, or aging, of materials. Chemical knowledge, and many tests, indicate that organic insulating materials deteriorate more rapidly at elevated temperatures, in such a way that the life is halved for each 8- to 12-degree-centigrade increase in temperature. On the basis of this law, and knowing the load–temperature characteristics of the apparatus, it is possible to sketch in the entire load–life curve of Figure 1, if the end points, P_m and P, are given. Hence, it is now possible to fit apparatus for intermittent-duty service much more exactly to the requirements than heretofore.

With the increased variety of industry requirements, it is becoming necessary to secure closer thermal co-ordination of all the elements of an electrical system than ever before. The time–current curves for operating, stalled, and short-circuit conditions must be studied for motors, relays, wiring, and power-supply devices, and made consistent with each other. Better knowledge, coupled with more exacting demands, therefore, give a double indication of the need for more precise methods of apparatus rating, as outlined in the AIEE Standards Report No. 1A.

Million-Volt Industrial X-Ray Unit

THREE DEVELOPMENTS of co-ordinated research stand out as major factors in the General Electric Company's noteworthy achievement of a 1,000-kv portable industrial X-ray equipment: (*a*) dichlordifluormethane ("Freon") instead of air or oil as an electrical insulating medium; (*b*) a compact air-core resonance transformer; (*c*) a multisection X-ray tube small enough to be accommodated within the core space of the transformer. The result of the development and combination of these and other elements is the 1,500-pound self-contained million-volt equipment shown on the front cover and these pages.

An extended investigation of the electrical insulating properties of many gases and chemical vapors disclosed that some of them not only were far superior to air at equivalent pressures, but also provided better insulation than oil and were much lighter in weight. One of these special gases which is readily available and which has good physical and chemical properties is dichlordifluormethane (Freon). It has 2.5 times the insulating strength of air at equivalent pressures.

Freon 12, which has one carbon, two chlorine, and two fluorine atoms per molecule has, at 50 pounds per square inch pressure, a dielectric strength three times as great as the purest transformer oil. In a very high-voltage unit, 100 pounds of this gas will give insulation equivalent to that provided by 12,000 pounds of oil. Gaseous admixtures cannot contaminate Freon the way water or other foreign matter contaminates oil. The breakdown values of Freon are consistent, whereas oil is erratic.

The heat-transfer problem inherent in gas insulation was solved in this X-ray equipment by means of a small built-in cooler which utilizes a 1/15-horsepower fan to circulate the Freon gas over finned water-cooled copper tubing and through the transformer. At low ambient temperatures, such as may occur in industrial plants in winter, the Freon must be kept at summer temperature by electric heaters to keep it from condensing on the tank walls.

In the ordinary high-voltage transformer the charging current serves no directly useful purpose, but is a necessary evil, since it serves to reverse the potential of the high-

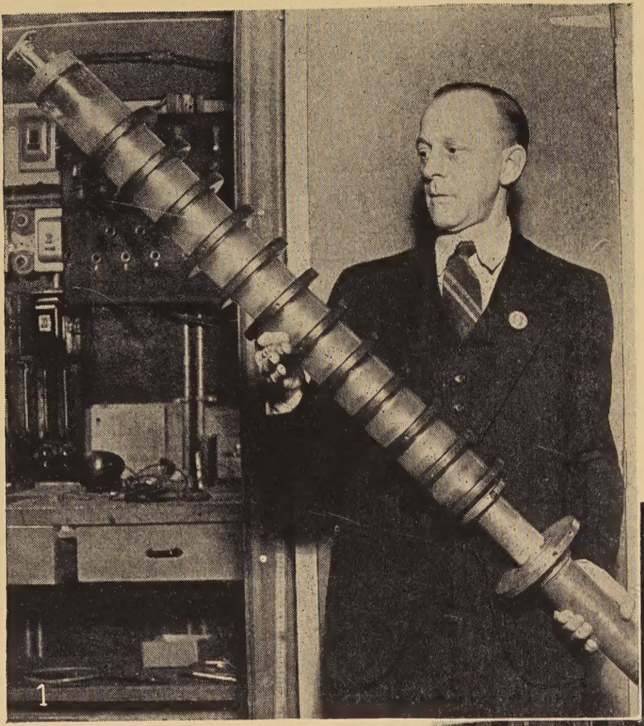

1

A very few years ago an 800-kv X-ray equipment required a special multistory housing (3) and utilized a multisection X-ray tube about a foot in diameter and 14 feet long, as compared with the 30- by $3^1/_2$-inch envelope (1) required for this 1,000-kv tube. Today's million-volt industrial equipment (4) weighs about 1,500 pounds; is housed as a self-contained unit in a tank 3 feet in diameter and less than 5 feet wide; can be swung into any operating position at the touch of a hand. To facilitate a comparison, illustration 3 and its small insert are shown to approximately the same scale in terms of the man shown in (3). In the view of the partially disassembled 1,000-kv unit (2), the resonance transformer may be noted, with its shielding cap and with the tube at its center

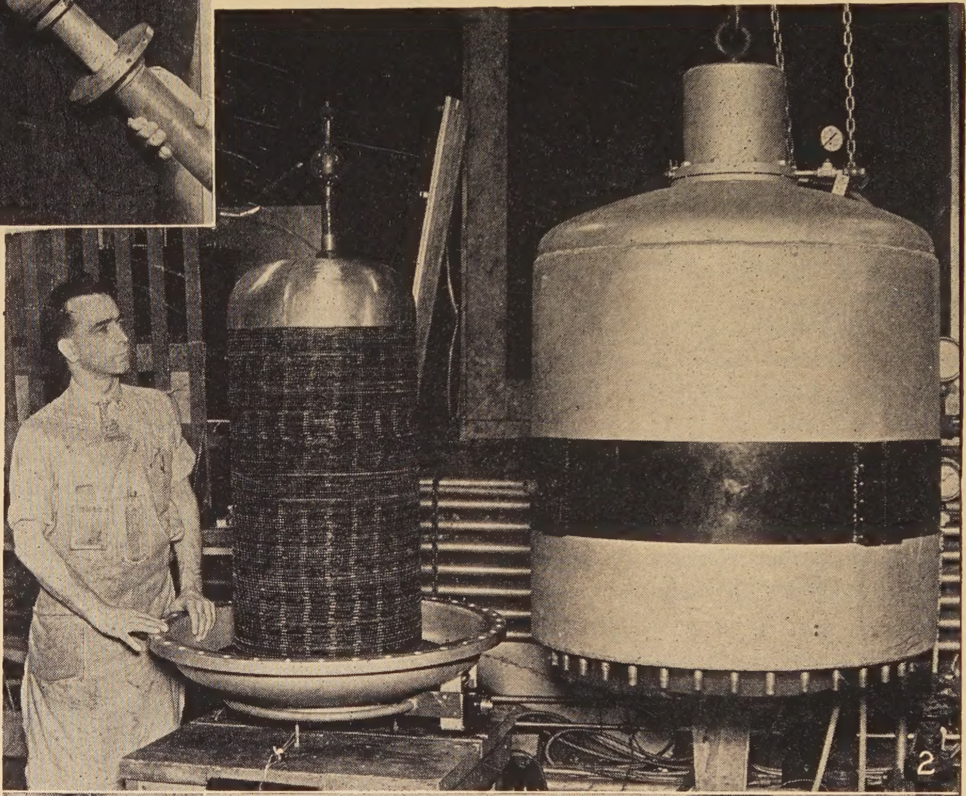

2

Especially under the pressure of defense production, radiography increasingly has become an essential step in the manufacture of vital equipment that must be dependable under severe operating requirements. Time is an essential element in this operation, and the greater the power behind the X rays, the less the time required. Five-inch steel plates and castings that can be radiographed in four minutes with the 1,000-kv equipment require four hours with 200-kv equipment

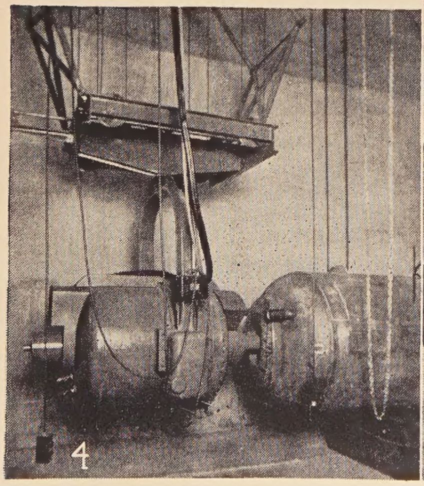

4

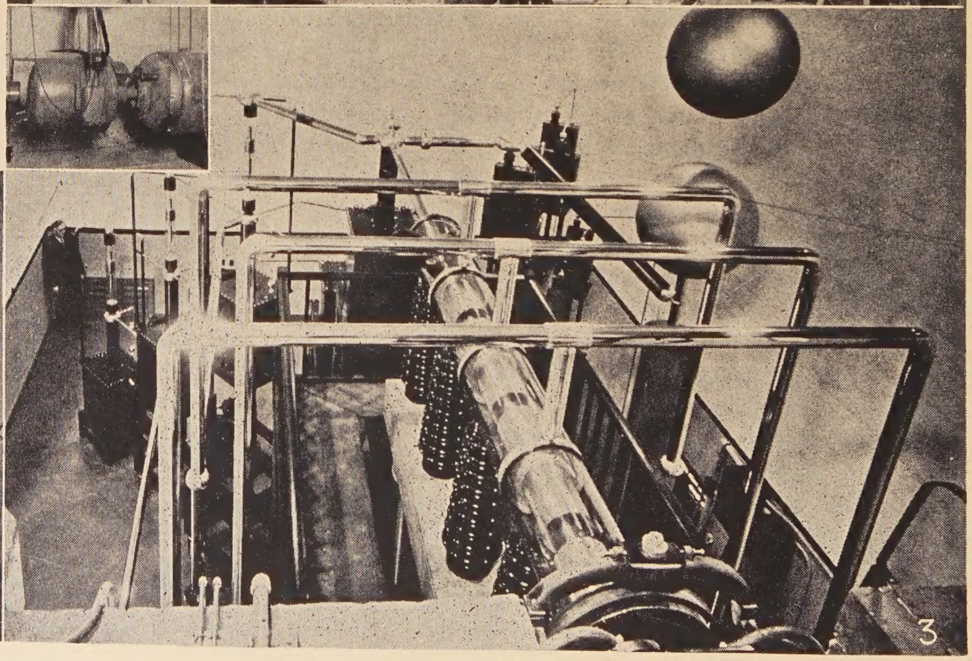

3

voltage terminal of the equipment, which has a considerable capacity to ground. In the resonance transformer this charging current is made to flow through a large inductance coil without iron core and thereby put to good use in producing exactly the high voltage wanted. In other words, the inductance of the coil and the capacity of the high-voltage terminal have been chosen to resonate at the frequency (180 cycles per second) of the power supplied to the transformer.

Some 238 miles of insulated wire are accounted for in the transformer. The high-voltage coil is 30 inches high, with 18-inch outside diameter and 8-inch inside or core diameter, and consists of thin coil elements stacked on top of each other with the primary "pancake" at the bottom. The high-voltage terminal on top of the transformer is a rounded brass spinning, $6^1/_2$ inches high and 18 inches in diameter. A uniform voltage gradient over the 30-inch height of the coil stack makes possible the use of glass rods as mechanical tie-rods to hold the stack together, thereby allowing operation in any position.

The 12-section sealed-off X-ray tube especially designed to go with this resonance transformer has cylindrical accelerating electrodes in each of the intermediate sections between the cathode and the copper-backed tungsten target. These intermediate electrodes are joined to the glass envelope of the X-ray tube with Fernico ring seals. Fernico is a special alloy which has an expansion coefficient comparable with one of the borosilicate glasses, thus permitting heavy metal sections to be fused directly to the glass. This feature allows the tube to be made much smaller than otherwise might be possible (the insulating tube envelope is only 30 inches long, $3^1/_2$ inches in diameter) and also permits the tube to be rigorously exhausted before it is sealed off the pump. The inside glass walls of the tube envelope are sandblasted to reduce the hazards of field emission. The tube is supported entirely by a metal flange joined to the grounded extension chamber. This extension chamber houses the target-end of the X-ray tube and thus permits the target to be placed inside of boiler drums and in other such relatively inaccessible positions.

The tube is mounted in the space at the center of the high-voltage transformer, where it adds nothing to the size of the housing tank required for the equipment. Thus mounted, the tube is located in a uniform electric field and a weak magnetic field, the axes of which parallel the tube axis. Early experiments established that the tube could be shifted sideways in the transformer without effect on the operation or on the size of the focal spot. Small toroidal shields of a conducting Textolite are used around all Fernico seals to reduce the field strength at the Fernico edges, to aid the focusing action of the intermediate electrodes and to provide a contact point for the tap strips which connect the intermediate electrodes to the inside of the transformer coil. The tap connections fix the potential of the electrodes and allow d-c charges to flow from the tube electrodes.

A focus coil is provided outside the tank, around the cooling-water jacket of the extension chamber, to focus the electron beam onto the tungsten target. The focal-spot diameters may be chosen to correspond to the tube current, which can be adjusted from microamperes up to three milliamperes at a million volts. Power for the cathode filament is derived from end-turns on the high-voltage winding and is controlled by means of a variable reactor operated through a glass-rod control shaft by an external filament-control motor.

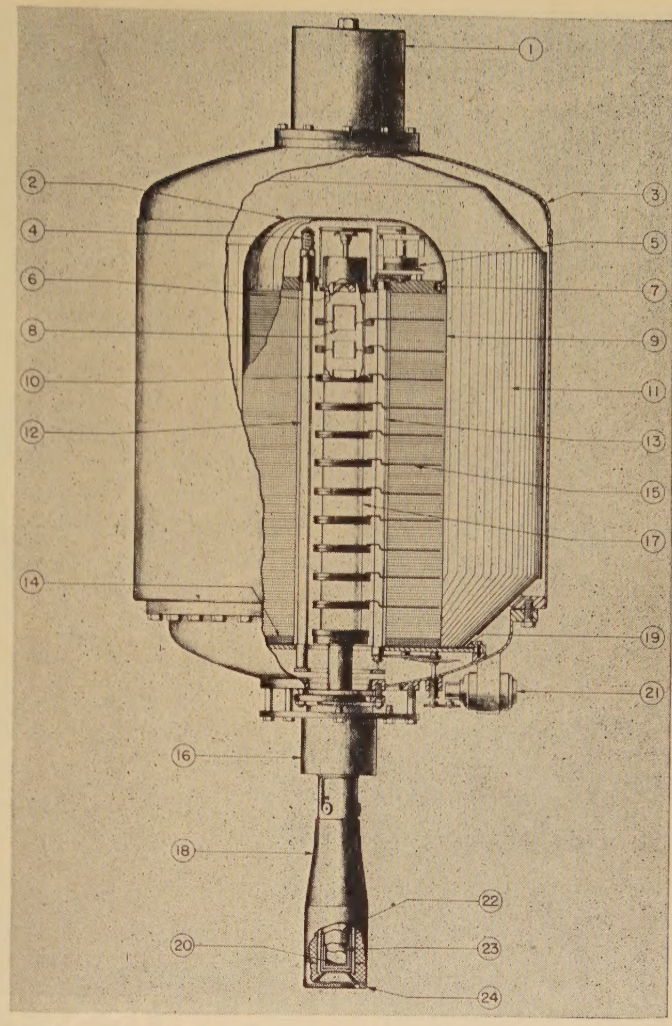

Million-volt portable X-ray unit

1. Cooler
2. Slotted brass shield
3. Steel tank
4. Spring for tie-rod
5. Variable reactor
6. Cathode assembly
7. End-turn filament coil
8. First intermediate electrode
9. Secondary coils
10. Shields around the X-ray tube
11. Laminated shield
12. Glass tie-rod
13. Insulating shaft for filament-control
14. Primary winding
15. Tap lead
16. Focusing coil
17. Glass envelope
18. Lead shield, adjustable
19. Laminated steel bottom
20. Tungsten target
21. Filament-control motor
22. Water jacket
23. Extension chamber
24. Lead diaphragm

Approximately 4 kw of power is required to operate the equipment at 1,000 kv and 3 milliamperes. This is supplied by a small synchronous motor-generator set which serves also to eliminate the effects of fluctuation in line voltage and to maintain accurately the frequency of 180 cycles per second for which the equipment is designed.

JAMES D. HALL

From tungsten ore to assembled lamp, the production of a Mazda lamp at the Westinghouse lamp factory at Bloomfield, N. J., is here surveyed

REMARKABLE AND ROMANTIC as was the transition over the centuries from the caveman's torch to the first incandescent lamp, the advance from that carbon-filament vacuum lamp to the present gas-filled Mazda lamp is even more so. In a relatively short time, the industry has grown from one small workshop, producing a few carbon lamps made entirely by hand, to spacious factories, using raw materials drawn from every corner of the earth and employing thousands of people and amazing automatic machinery to produce annually millions of lamps of many kinds and for many and varied purposes. This rapid advance in the art was accomplished only by the tireless effort of hundreds of scientists, engineers, chemists, and metallurgists, each an expert in his own field and each contributing his bit towards making the Mazda lamp what it is today.

JAMES D. HALL: commercial engineer, Westinghouse Lamp Division, Westinghouse Electric and Manufacturing Company, Bloomfield, N. J.

TUNGSTEN WIRE

Of the many exacting processes used in the various stages of lamp manufacture, none necessitates greater knowledge, accuracy, and care than are required in the making of the tungsten-wire filament, the light-producing element. The high melting point of tungsten (3,392 degrees centigrade) prevents its being melted in crucibles because no crucible material having a higher melting point is available. Its peculiar crystalline characteristics are such that it cannot be drawn in the manner common to the drawing of many other metals, such as iron, copper, nickel; hence there have developed the rather devious and interesting methods used to transform the tungsten

ore into a wire having a tensile strength greater than that of the highest grade of steel.

The tungsten ore, in the form of a coarse brown powder, is first chemically analyzed (figure 1) for detection of 14 different impurities. If an excess of any one of the impurities is found, the lot is rejected. If the chemical requirements are satisfactory, the ore is ground to a talc-like powder in preparation for the chemical processes to follow. Of these highly technical processes it is sufficient to say that from the raw ore to the pure tungsten powder, the tungsten varies in form from a black powder, to a black solution, to a white crystalline powder, then to a yellow sulphur-like mass (tungstic oxide). These processes involve the use of hot and cold water, caustic soda, calcium chloride, hydrochloric acid, ammonia, and caustic potash. Each process is safeguarded by every available type of automatic equipment.

Following these chemical treatments, the yellow tungstic oxide is filtered and then dried in steam-heated kettles and ovens to remove the water (figure 2). The resultant powder is then ground and sifted and is ready for the addition of certain chemicals which produce the desired crystal structure in the finished lamp filament. The nature of this structure varies with different types of lamps, according to the service in which they will be used.

Next the powder in metal containers or "boats" is placed in airtight steel pipes enclosed in gas-heated furnaces. At regular intervals, the "boats" are moved forward through the pipe to meet an increasingly greater temperature as they reach the end of the furnace. During the heating, all water and oxygen are driven off and removed from the pipes by means of a continuous flow of pure hydrogen gas over the powder.

Next, each batch of powder is thoroughly mixed to insure uniformity. After being sieved through a fine silk screen, the powder is placed in a mold and subjected to a hydraulic pressure of some 20 tons per square inch, producing a bar 3/8-inch square by 24 inches long (figure 3). This bar is very brittle, like a cake of compressed talc, and must be handled with great care until it is baked in a hydrogen atmosphere in a gas furnace. This baking, as in a brick kiln, imparts sufficient strength to the bar to allow its handling in the subsequent processes. Following this, the bars are placed in cylindrical airtight metal containers known as "treating bottles." After each bottle is closed, it is filled with pure hydrogen gas and a current of from 1,500 to 2,500 amperes is passed through the bar for varying periods. The passage of the current through the bar fuses the tungsten particles, shrinking the bar, increasing its strength, and causing it to assume a metallic appearance.

From the time the powder is mixed until inspection of the metallic bar is completed, the operations are conducted in a room in which the temperature and the humidity are kept constant by automatic control. Experience has shown that normal fluctuations in weather conditions produce variations in the quality of the tungsten filament.

The next step in the manufacture of the filament wire consists of swaging or hammering the tungsten bar (figure 4) after it has been heated in an electric furnace in an atmosphere of hydrogen. The swaging is continued with the bar changed into a rod which gradually diminishes in diameter and increases in length. When the tungsten has reached the required diameter, it has attained sufficient tensile strength to make it workable in the next process. This increased strength results from elongation and overlapping of the crystals, a transformation that may be compared roughly to that occurring when a mass of hempen fibers, which has little strength, is made into a rope by weaving and intertwining the individual strands.

Further reduction in the diameter of the wire is accomplished by means of a die-drawing process, wherein the wire is lubricated by graphitic carbon and then heated to a carefully regulated temperature and drawn through dies of composition metal. This drawing is continued until the wire is about ten mils in diameter and then as the wire approaches its final size, the ultimate in accuracy as to roundness and diameter is achieved by the use of diamond dies, in the same type of process (figure 5).

The diameter of finished wire is determined by weighing a given length and computing the diameter from the weight and length. For the weighing of filament wire, delicate torsion balances, accurate to 2/1,000,000,000 of a pound, are used. The roundness of the holes in the diamond dies is checked to 1/100,000 inch by means of high-powered optometers. These instruments, like a microscope, enlarge the hole 300 times.

The smallest filament wire now produced is that used for the 3-watt 115-volt lamps. It has a diameter of approximately 3/10 mil or about 1/5 the diameter of a human hair. Specifications require that this diameter be held in commercial production to within plus or minus one per cent, or about 3/1,000,000 inch.

Approved wire is then ready to be wound into spring-like coils. The most commonly used method is that wherein the tungsten wire is wound on a mandrel or core wire of steel. Some filament coils are wound with 2,065 turns per inch, which means that the turns are spaced at intervals of slightly less than 1/2,000 inch. Since none of these turns, which are examined under a microscope, must touch or even vary perceptibly in spacing, machinery of the utmost precision is required.

After completion of the coiling operation, the drums on which the coils with the mandrels are wound are immersed in a solvent to remove any oil or grease. Next follows the annealing operation wherein heat is applied to the coil and its mandrel. This relieves strains and makes the tungsten wire stay set. The wire and its mandrel are then cut into proper lengths, according to the type of lamp for which the coil is to be used.

The next operation consists of dissolving out the mandrel wire (figure 6). Here the coils are immersed alternately in successive steps in acid and hot and cold water. Minus their mandrels, the coils are baked in hydrogen gas. They are then optically inspected (figure 7), the smaller sizes with a special projector by means of which an image of the coil enlarged 60 times is projected on a screen (figure 8).

In the most commonly used types of general lighting service lamps, the filament consists of one continuous

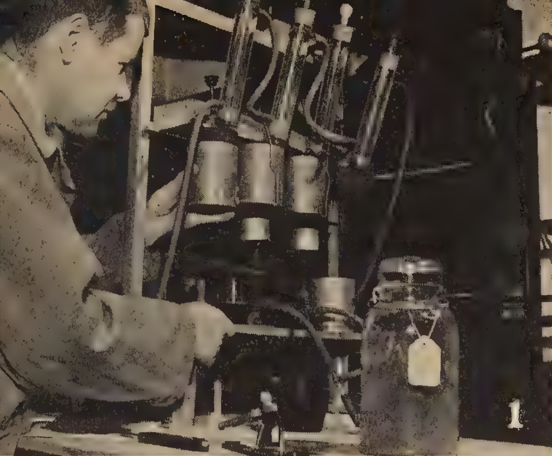

helical coil. For other types of lamps, it is necessary to wind the coils in sections. These sectional coils are then formed into hundreds of different sizes and shapes to meet the requirements of the great variety of lamps in which they are to be used. In order to prevent fracture of the cold tungsten wire, it is formed by bending it over a small electrically heated bar.

"LEAD-IN" WIRES

The wires for conducting the current from the base through the glass bulb to the filament of the lamp are commonly known as "lead-in" wires. Each such wire usually consists of three separate pieces of wire electrically welded into one composite piece. A typical lead-in wire for a gas-filled or Mazda *C* lamp is made of nickel, copper, and "dumet" (dual metal—a copper-coated steel wire with the same coefficient of expansion as the glass in which it is to be imbedded). The nickel is that part of the wire exposed to the inert gas inside the bulb. It is connected to the "dumet" which passes through the glass to the copper wire leading to the base. "Dumet" has replaced the platinum wire used in the early incandescent lamps.

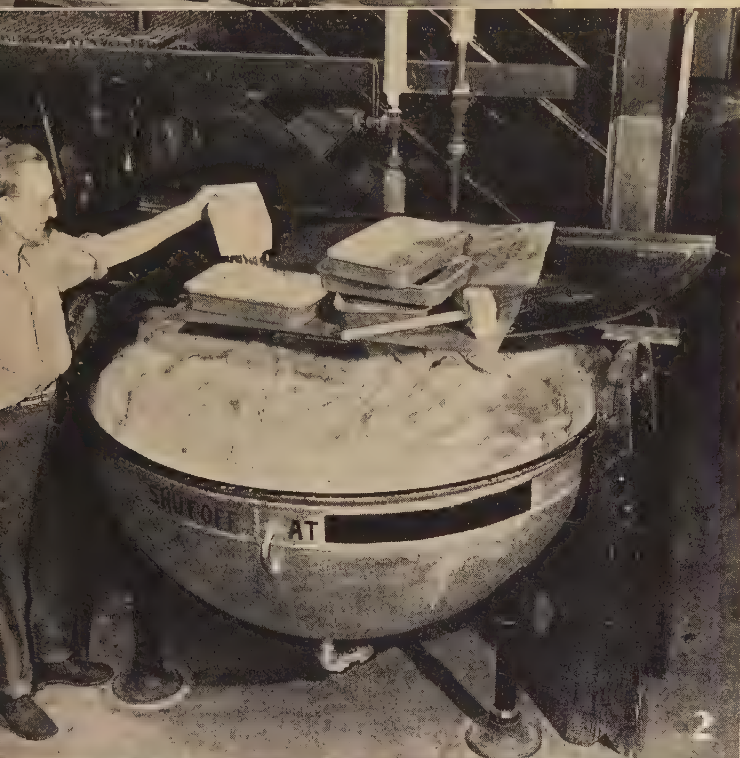

Figure 1. Tungsten ore is analyzed to detect impurities; passes through a variety of chemical treatments to transform it to yellow tungstic oxide

Figure 2. First filtered, tungstic oxide then is dried in steam kettles and ovens

Figure 3. One stage in the treatment of tungsten powder is its formation into bars 24 inches long by 3/8 inch square under a hydraulic pressure of about 20 tons per square inch; the brittle bars are then baked and subjected to high electric currents

Figure 4. Heated in an electric furnace, the tungsten bar is swaged into a rod which gradually diminishes in diameter as it increases in length and tensile strength

FILAMENT SUPPORTS

Inasmuch as the wires supporting a lamp filament reach a high temperature when the lamp is lighted, they necessarily must be made of a material having a high melting point. Molybdenum, having a melting point of 2,625 degrees centigrade, is most commonly used for this purpose, but tungsten or a two-piece support of nickel and molybdenum also may be used. The variety of types of Mazda lamps has required the design of many sizes and types of filament supports.

GLASS

In the making of lamps, some 40 different kinds of glass are used. The characteristics of a glass depend upon the proportion of the ingredients used in its manufacture.

Figure 5. Tungsten wire, reduced to a diameter of about ten mils by being drawn through dies of composition metal, is given its final roundness and diameter by diamond dies

Figure 6. First wound on steel mandrel wires into coils, the coiled tungsten wires, which have been cut into the lengths required for various types of lamps, are immersed successively in acid and hot and cold water to dissolve out the mandrels

Figure 7. Finished tungsten coils are inspected individually

Figure 8. Smaller sizes of tungsten coils are inspected with a projector which produces an image 60 times the size of the coil

Figure 9. "Slip-over" coils are placed over the straight ends of filament coils for high-wattage lamps, to provide greater strength at the point where the lead-in wires are clamped to the filament

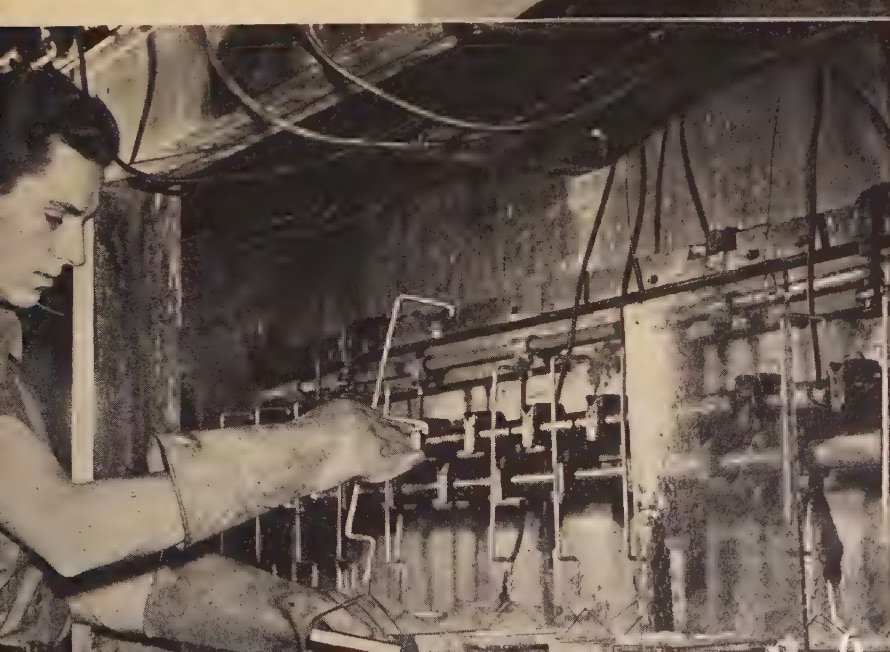

Figure 10. The filament and supporting parts of a lamp are first assembled; then the glass bulb is placed over this "mount" and gas flames applied to seal the two together. Unused portion of the bulb falls off

Among the characteristics which concern the Mazda lamp manufacturer are softening point, uniformity of expansion, electrical resistance, color, ability either to absorb or permit the passage of radiations of certain wave lengths. For example, one type of glass is used where high temperatures are encountered, while another answers the requirements of certain types of ultraviolet lamps, where it is desired to absorb some of the shorter wave lengths and pass the visible light and the longer wave lengths in the ultraviolet range. In other specialized types of lamps, the desire is to absorb as much of the visible light as possible, but at the same time allow the passage of the invisible ultraviolet rays. For this purpose, a dark-colored glass, known as a "black" glass, is used.

Some 300 sizes and shapes of bulbs are received from the glass factory, and a much greater number of sizes and types of cane glass and glass tubing are also used. The proper selection, inspection, and use of glass in the incandescent lamp industry is an art in itself.

BASES

The manufacture of lamp bases requires knowledge of metal forming, stamping, drawing, and glass working. The principal raw materials used in base manufacture are sheet brass and glass. Although there are some 30 different styles and sizes, the larger percentage of general lighting service lamps is confined to types using the medium-screw and the mogul-screw bases.

The problem of base manufacture is one of the oldest in the electric lamp industry. In the earlier days, means had to be provided immediately for connecting the lamp to the lighting circuit. The type of base and socket screw shell which Edison devised has been used for nearly 60 years without any fundamental change. National standards have been adopted for the miniature, candelabra, intermediate, medium, and mogul screw-thread types. Bases are manufactured in accordance with these standards, so as to assure their satisfactory use with the corresponding sockets which likewise have been standardized.

GAS

In addition to the millions of cubic feet of illuminating gas consumed annually in the various heating and glass-working operations, lamp manufacture also involves the use of other gases, some of them rare and little known. Among these gases are hydrogen, oxygen, nitrogen, argon, neon, helium, and krypton. Hydrogen and oxygen gas are manufactured in the lamp factory by electrical decomposition of water. Other gases of standard commercial grades are obtained by fractional distillation of liquid air. These gases are subjected to elaborate purification and drying processes prior to being sealed in the lamp.

The most commonly used Mazda *C* general-lighting-service lamps have bulbs filled with a mixture of argon and nitrogen gases to about 0.65 of atmospheric pressure. In normal operation, because of increased temperature, this pressure is slightly below atmospheric. Other lamps use one of these gases alone, while some of the more specialized types utilize the rarer gases. The proper

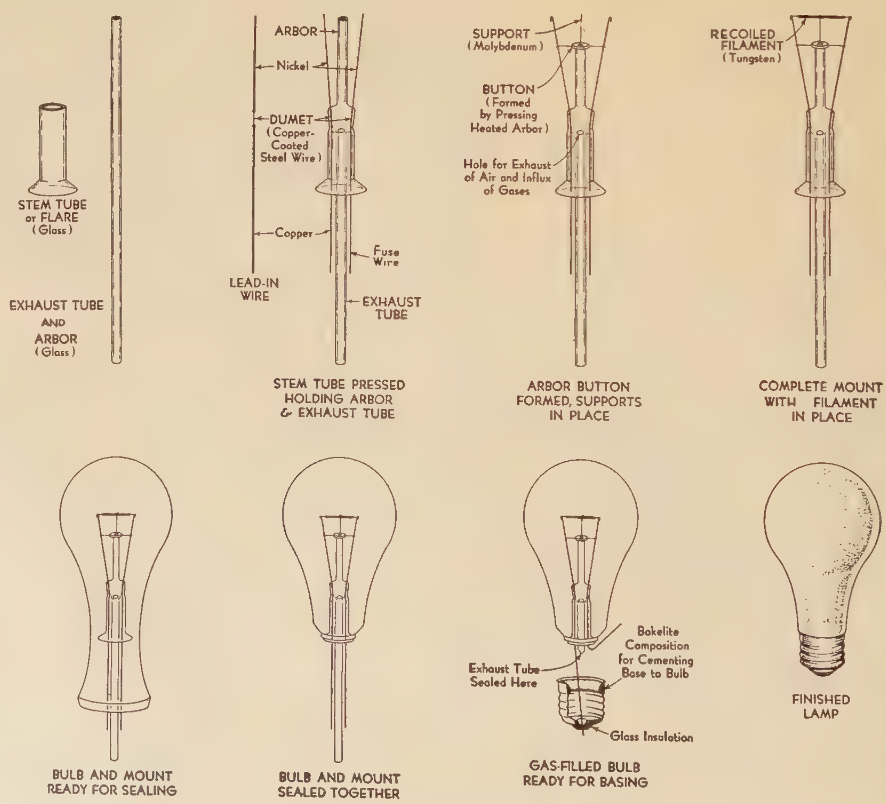

Figure 11. Steps in assembling mount and completed Mazda lamp

performance of a Mazda *C* lamp depends in a large measure upon the purity and freedom from moisture of the gas or gases with which its bulb is filled.

ASSEMBLY

The first step in the assembly of the various parts that make up a finished Mazda lamp is the preparation of the "mount," which consists of the filament and the supporting parts. The flare, the combined arbor and exhaust tubing, and the lead-in wires are grouped in proper relation to each other and gas flames applied to the assembly. The heat softens the two glass parts, causing them to fuse together with the dumet of the lead-in wires embedded in the glass. Then two jaws apply pressure to the softened glass, forming what is known as the "press." While the glass is still soft, a blast of air is blown down the exhaust tubing causing a hole to open through one face of the press. It is through this hole that air is pumped from the bulb and afterwards the filling gas allowed to enter.

The end of the glass arbor then is softened by gas flames and slightly upset, to form the "button". Into the still-soft glass of the button the support wires are inserted. Following this, the ends of the lead-in wires are flattened and bent at the point where they are to be clamped to the filament. The clamping of the filament and the coiling of the support wires, pigtail-like, around the filament coil completes the mount.

In the next operation, the glass bulb is placed over the mount (figure 10) and the gas flames applied to the neck of the bulb at a point opposite to the flare inside the bulb. The softened glass of bulb and flare fuses together and the unused end of the bulb or "cullet" falls off, completing what is known as "sealing in." During this operation, while the glass is still soft, shoulders are formed on the bulb to provide a seat for the base. This makes for accurate over-all length of the lamp and insures precision alignment of the axis of the base with the axis of the bulb, as well as stronger basing.

Next follows one of the most exacting operations in lamp making in which rotary slide valves finished to optical flatness are used in the process wherein the air is removed from the bulbs, and, in the case of the Mazda *C* lamp, replaced by gas. The sealed-in bulbs with the exhaust tubes connected to vacuum line ports are passed through gas flames. The resulting high temperature vaporizes any moisture in the bulbs. The vaporized moisture and most of the air is withdrawn by a vacuum pump.

The bulbs then are flushed out with an inert gas as many times as necessary to assist in removing residual vapor. In the final stage, the bulbs are filled with the required amount of the desired gas and "tipped off" by fusing the exhaust tube.

"GETTERS"

The amount of air left inside the lamp after it is sealed is very small, comparatively speaking, being less than 50 microns, or about 0.00007 of atmospheric pressure. This, however, is still too much for a good lamp. Consequently, "getters" are used to remove the last measurable trace of the remaining air. A getter is a mixture of chemical substances, the action of which is best understood by considering what takes place in a vacuum, or Mazda *B*, lamp. The getter is placed on the filament during the fabrication of the lamp. When the lamp is first lighted, the getter is vaporized and dispersed from the filament. It combines chemically with some of the gases, and, broom-like, sweeps the rest before it, impinging them on the bulb surface and holding them there permanently. This process "cleans up" the residual undesirable gases, water vapor in particular, in the bulb, giving a much better vacuum and producing a good condition for the operation of the filament. In Mazda *C* or gas-filled lamps, the getter's chief function is to clean up the water vapor.

The getter in a Mazda *B* lamp has still an important function to perform after it comes to rest on the bulb. The layer of getter, so formed, is not sufficient to absorb appreciable light. It provides an irregular or increased surface area as a reception place for the black particles of tungsten emitted from the filament while the lamp is operating. So the black particles, instead of falling on a smooth hard surface and making a continuous layer of metal which would absorb light, stagger themselves and bury themselves irregularly in the layer of getter, thus creating an effect similar to venetian blinds, and allowing the light to pass through. This effect of getter action greatly retards the blackening of the bulb, and hence increases the average light output throughout the life of the lamp.

BASING

Following the "tipping off" operation, the sealed-in bulb is ready for application of the base. Contrary to a rather general belief, the base has no part in the airtight sealing of the bulb, but merely supports the bulb and provides a means of connection between bulb and socket.

Preliminary to its cementing to the bulb, the base is filled with a soft cement consisting of some seven ingredients. One of these is a fugitive dye that lends a

Figure 12. Mazda Service inspectors, in addition to lighting sample lamps, check electrical characteristics and light output, dimensions, alignment, and other details

greenish hue to the cement. Upon application of the proper temperature for the required length of time, the green color fades, and the cement assumes a brown color. In the basing operation, the base is placed on the bulb with one of the lead-in wires protruding through the center eyelet and the other wire lying between the bulb and the edge of the base. The cement having hardened from application of heat, the ends of the lead-in wires are cut off and the wires automatically soldered to the base. Both the solder and the soldering flux used must meet definite specifications as to chemical content. During the period in which lamps are on the basing machine, they are lighted five different times. They are again lighted and inspected prior to final packing.

MAZDA SERVICE INSPECTION

The finished lamps are then placed on a conveyor in unsealed cartons and are required to pass in parade, so to speak, before the eyes of Mazda Service inspectors supervised by the Electrical Testing Laboratories of New York. Each package is subject to inspection and sample lamps are selected at random and given a thorough inspection (figure 12). In addition to the lighting of the lamp, this inspection includes a check of electrical characteristics and light output, over-all length, light-center length, base alignment, strength of the bond between base and bulb, and an inspection of details of the base, the bulb, and the mount.

OTHER INSPECTIONS AND TESTS

In addition to the tests and inspections of lamp parts and finished lamps already enumerated, each manufacturing division maintains a photometric and life-test department where representative quantities of lamps from current production are checked for light output and for life. Quick results on these life tests are obtained by burning the lamps at overvoltage—the ratio between the life at this voltage and the life at normal voltage being known. For example, certain types of lamps designed for 1,000 hours average life at normal voltage could be expected to last an average of 5 hours when operated at 50 per cent overvoltage. By means of such forced tests it is possible to keep a daily check on the quality of lamps as they are manufactured without the delay incidental to testing at normal voltage.

Selections of lamps from the various manufacturing divisions are sent to the central life-test department, where, after "seasoning," the lamps first are measured for electrical characteristics and light output by means of photoelectric-cell photometers accurate to less than one fourth of one per cent. The lamps are then placed on test racks, patrolled at least once each half-hour, where they are operated to burn-out, most at normal and a few at forced voltage, on a circuit where the voltage is allowed to vary not more than one tenth of one per cent.

As a lamp burns, there is a certain depreciation in light output caused by bulb blackening, resulting from the normal deposit of sublimated tungsten. A check on the rapidity and amount of this depreciation is determined by photometry of the lamps at various stages during life.

After completion of these tests, the lamps are carefully inspected by representatives of the manufacturing and engineering departments and a record made of the types of failure and their causes. This information is valuable in maintaining and improving the quality of the Mazda lamp.

The life-test department also is provided with equipment for testing lamps under conditions simulating those in actual usage. Racks arranged for producing vibration of varying amplitudes and frequencies assist in the development of lamps best suited for use under vibration conditions such as are encountered in many industrial plants. The susceptibility of a lamp filament to shock is determined by means of the "bump" tester wherein the lamp is attached to a cord and is allowed to swing in an arc and make impact against a board at the lowest point of the arc. The greater the length of the swing necessary to break the filament or the bulb, the greater the strength of the lamp. Other lamps are tested in equipment where shock from battleship gun-fire is simulated.

Shipping strength of lamps and suitability of packing materials are determined on the "package drop tester" by means of which handling and shipping conditions are duplicated. This quick test is later checked by actual freight or express shipment.

Traveling inspectors check and inspect lamps in warehouses, to make sure not only that they are made right, but also that they *stay* right. Inspections also are made and records kept of the performance of thousands of lamps used under actual service conditions. The success of the quality safeguards used in Mazda lamp manufacture is indicated by the fact that inspection of millions of lamps shows serious defects in only about one tenth of one per cent.

Ultraviolet on a Dairy Farm

At Broadacres Farm in Lebanon, N. J., extensive use of ultraviolet radiation is reported to be producing milk of a superior quality—a bacteria count of less than 1,000 per cubic centimeter whereas grade A pasteurized milk allows for 30,000 bacteria per cubic centimeter and grade B 100,000. Two two-hour sunbaths per day—one beginning at five in the morning and the other beginning at six in the evening—are given to all milk cows through the medium of *S*-4 lamps hung on six-foot centers eight feet above the floor down the main aisle of the barn.

General lighting for service maintenance in the barn is provided by fluorescent lamps in simple fixtures appropriately placed.

A liberal installation of germicidal lamps is reported to protect completely every step in the handling, processing, and bottling of the milk. It is said that the milk is never exposed except under direct radiation from germicidal lamps, and that the same type of equipment continually sterilizes the bottles, bottling machines, and cans.

Abstracted from "I Believe in Ultraviolet," *The Magazine of Light*, volume 10, 1941, number 5, pages 26–7.

Progress in the Art of

Metering Electric Energy

IV—Calibration and Installation of Watt-Hour Meters

This article concludes the series on the metering art sponsored by the AIEE committee on instruments and measurements; the complete report is being issued in pamphlet form for immediate distribution, details on page 597

A VITAL ASPECT of the art of metering electric energy is the calibration, installation, and maintenance of the meter that measures this energy. This constitutes an important contact between the utility company and its customers. The diligence with which, since the origin of the art, methods and techniques have been developed and pursued to insure a high degree of accuracy has done much to create on the part of the customer a feeling of confidence in the meter by means of which his charge for the service rendered is computed.

CALIBRATION OF THE WATT-HOUR METER

In most states periodic testing of watt-hour meters is required by law. The period between tests varies, but six-year periods are common practice at present and longer ones are contemplated. If a meter is removed or damaged, or if there is a complaint from a customer, it may receive special tests between the periodic ones.

Tests that can be performed in a laboratory or shop may utilize procedures and equipment not generally applicable to tests made on the customer's premises. It is obvious that test equipment for field use must be primarily portable and self-contained. However, a test, whether in or out of the laboratory, must consist of comparing the performance of the meter to be tested with a certain established standard of performance.

In the very early days calibration of the meter was a major problem, because suitable standards of comparison were not available. At first indicating instruments were used exclusively for calibrating purposes. In order to make a complete calibration, it was necessary to measure voltage, current, watts, and time.

Standardization is important in the manufacture of any electrical equipment but it is obviously of special importance in the manufacture of watt-hour meters. From the beginning, the manufacturers set up standardizing laboratories in which fundamental standards were maintained in close calibration with those of the National Bureau of Standards. Each employed the best techniques then known to make their manufactured product conform to these standards. It must be understood that in the very early days of the art primary, secondary, and working standard instruments, as these are known today, were not available and the problem of standardization was a major one.

Prior to 1900, voltage was measured with a Cardew hot-wire voltmeter (figure 32). Current was measured by means of the Siemens dynamometer (figure 33), or a Kelvin balance (figure 34). Power was measured by the Siemens watt-dynamometer or the Kelvin watt-balance. Figure 35 shows an improved dynamometer-type instrument known as a "precision wattmeter" developed in 1904 by the Westinghouse company. It is a modified Kelvin balance. Time was measured with a stop watch. Frequency in those days was determined by means of a steel wire stretched in the field of an a-c electromagnet. The vibrating length of the wire was varied to secure resonance by use of a rider, and the frequency measured with a stationary scale graduated in "alternations per minute."

By 1897 the Weston Electrical Instrument Corporation had developed a "direct reading" portable wattmeter and its voltmeter. These instruments were push-button-damped at intermediate deflections but were undamped when taking the final reading. Thus with variations in supply voltage, and undamped instruments, the calibration of watt-hour meters in the early days was an exceedingly tedious process.

The uniform calibration of these early indicating standards presented an additional problem. They could not be transported to and from the National Bureau of Standards without their calibration being impaired. Moreover, they all had serious temperature errors. This condition compelled all the manufacturers to establish and maintain their own standardizing laboratories. Such laboratories are equipped to check the indicating standards against primary standards. Standard cells, standard resistances, and other fundamental standards are checked with the National Bureau of Standards at regular intervals. Standards laboratories are maintained as separate units from the main production laboratory.

This report was initiated and sponsored by the AIEE committee on instruments and measurements as part of its regular activities for 1940–41, under the following direction: I. F. Kinnard, West Lynn, Mass., chairman; A. S. Albright, Detroit, Mich., vice-chairman; T. S. Gray, Cambridge, Mass., secretary. Personnel of subcommittee on watt-hour meters: A. S. Albright, chairman; D. T. Canfield, Lafayette, Ind., editor-in-chief; A. L. Brownlee, Chicago, Ill.; A. B. Craig, Boston, Mass.; J. S Cruikshank, Baltimore, Md.; C. L. Dawes, Cambridge, Mass.; A. P. Good; Stanley Green, Lafayette, Ind.; F. C. Holtz, Springfield, Ill.; H. C. Koenig, New York, N. Y.; Paul MacGahan, Newark, N. J.; C. V. Morey, New York, N. Y.; H. C Rankin, Boston, Mass.; A. R. Rutter, Newark, N. J.; F. B. Silsbee, Washington, D. C.; G. R. Sturtevant, Lynn, Mass.; and H. L. Thomson, Hartford, Conn.

Figure 32. The Cardew hot-wire voltmeter, instrument used before 1900

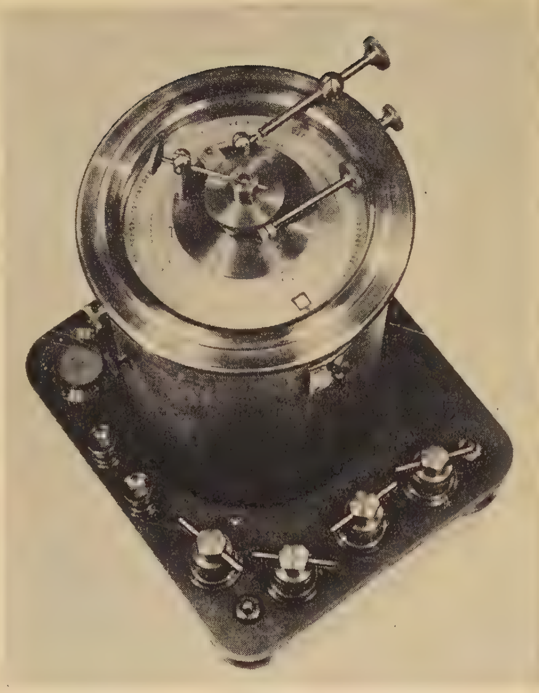

Figure 33. A Siemens dynamometer

Figure 34. A Kelvin watt-balance

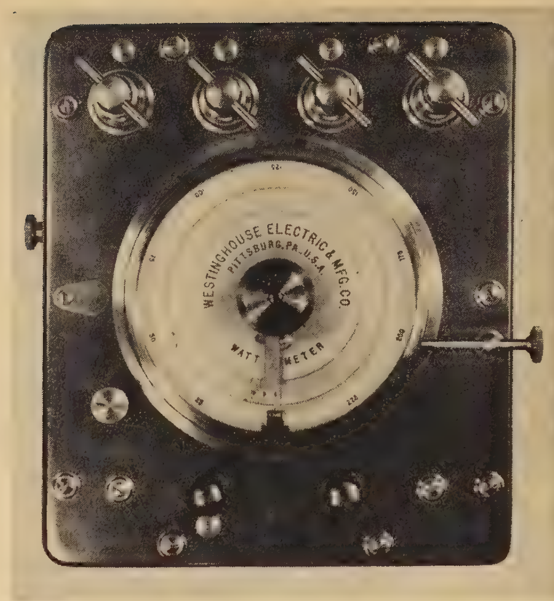

Figure 35. Dynamometer-type precision wattmeter

The early experience of the utilities followed closely that of the manufacturers, and many embarrassing questions arose as to whether the utility or the manufacturer was correct. In some instances standards were shipped back and forth in an attempt to establish comparisons. The difficulties of the early days are suggested by figure 36 which reproduces a photograph (exact date not known) of the "meter shop" of the Commonwealth Edison Company of Chicago, Ill. Considering the type of surroundings and the equipment available it is surprising that the quality of the work done was as good as it was.

The next major improvement in the testing of watt-hour meters was the introduction of the rotating standard by the Westinghouse company in 1899. Early forms of this instrument consisted of a regular watt-hour-meter unit mounted in a box having a suitable case and handle. The disk shaft extended into the lid of the box and was equipped with a sweep hand which revolved over a circular scale divided into 100 equal parts. The total number of whole revolutions was recorded on a separate dial. Thus any number of revolutions of the rotating standard could be determined to 1/100th part of a revolution for any given number of revolutions of the meter being tested.

In 1903 W. J. Mowbray designed and built the first multiple-range rotating standards. These test meters had two voltage ranges and three to five current ranges. The first d-c rotating standards could not be operated by opening and closing the potential circuit but the a-c rotating standards were operated that way from the beginning.

The meter being tested, the rotating standard, and a suitable load all are connected in series. In the simplest case, where the test constants of the meter and standard are identical, a test would be made in the following manner. The standard is run for the exact length of time that it takes the meter to run a specified number of revolutions, say 20. If, for example, the standard runs more than 20 revolutions, the meter being tested is slow and must be adjusted until the revolutions of both meters are the same. Practically all field testing is done this way, and all but the larger companies use this technique in their meter shops and laboratories. This method of testing greatly speeded up the calibration procedure, since any fluctuations in load affected meter and standard alike, and therefore did not alter the result. The accuracy of the standard was maintained by checking it with indicating instrument standards which in turn were checked against primary standards in the standardizing laboratory.

A modified form of the rotating standard was used in the production laboratory by the manufacturers. Test boards or panels were developed to speed up the operation. Gang testing also came into existence. In such arrangements two or more meters were tested at one time, with or without automatic starting and stopping. Master clocks with contacts frequently were used to determine the time interval.

In several instances the improvements already mentioned in the development of the watt-hour meter were first applied to the rotating standard, and only later to the general production of watt-hour meters. In any

event, improvement in the rotating standard at least kept pace with the general advance of the art.

In 1925 development in electronic devices had progressed to the point where the possibility of their use as auxiliaries in the testing process gave promise of both greater speed and greater accuracy. The first recorded device of this character was developed in 1925 by A. R. Rutter of the Westinghouse Electric and Manufacturing Company. This particular arrangement focused a light beam through holes in the meter disk upon a photoelectric cell, which in turn caused marks to be printed on a tape upon which a time scale was placed from contacts on a master clock. Thus the speed of the disk could be determined without actually counting the revolutions.

Some two years later H. P. Sparkes, also of the Westinghouse company, suggested the use of the stroboscopic principle as a method of calibrating watt-hour meters. The principle of the stroboscope may be applied to testing meters in several different ways. Basically, however, the method consists in cutting a number of evenly spaced teeth (for example, 400) on the periphery of the disk, or marking the disk with equally spaced lines, and focusing upon these markings a beam of light that is interrupted at a known rate or turned on or off at a known rate. By such an arrangement it is possible to cause the disk to appear to stand still at the speed at which the meter is correctly calibrated. If the disk appears to drift backward the meter is slightly slow and if it appears to drift forward the meter is slightly fast. Thus the meter may be adjusted visually without the necessity of counting the revolutions.

The larger utilities which have a huge number of meters to handle have found it economical to build and maintain well-equipped establishments for their meter departments. Figures 37 and 38 illustrate what some of the larger utilities are doing. These photographs show the meter laboratories of The Detroit Edison Company, Detroit, Mich. Figure 37 shows the section of the a-c standards laboratory where the rotating standards are checked periodically; figure 38 a section of the main production laboratory with gang testing in operation.

Many of the larger utilities are using the stroboscope in their production laboratories. The fact that meters of more than one manufacture, and therefore of more than one basic test constant, are involved complicates the arrangement somewhat, but the underlying principle is the same as that previously described. Figure 39 shows a stroboscope installation used by the Commonwealth Edison Company, Chicago, Ill.

Some utilities have developed testing boards that are essentially fully automatic. In figure 40 is shown a panel of this kind developed by the Pennsylvania Power and Light Company, Allentown, Pa. The left-hand dial at the bottom sets the test constant for the meter being tested. The right-hand dial at the bottom makes the necessary connection for a two- or three-wire meter of any number of terminals. Immediately above the two bottom dials is a voltage-selector switch and above that is a current-selector switch. The push buttons on the right-hand edge of the panel are the adjusting and starting switches. Relays control the sequence of the operations, the necessary adjustment of the disk to zero, and so on. When the proper test constants, connections, voltage, and load have been selected, the starting button is pressed and the test proceeds under completely automatic operation until it is completed. The resultant registration of the meter is indicated on the appropriate large dial on the upper left-hand side of the panel. If adjustments are necessary, they are made, and the operation is repeated until the desired accuracy is obtained.

One type of test made exclusively by the utilities is that made on the customer's premises. In the very early days this was a difficult and tedious process, but with the development of the rotating standard both difficulty and tediousness were greatly reduced. There still remained, however, the problem of providing a suitable load for the meter. At first the customer's load was used, but since this could not be controlled properly, it was generally unsatisfactory. To avoid the problems involved in using the customer's load, the practice of isolating the meter from this load by by-passing the feeders around the meter during the test became general. Artificial loads then were used in making the test. At first variable resistors of one form or another were used. Later the so-called phantom load came into wide use. This device is an application of the transformer principle to the creation of the desired current at low voltage for testing purposes. It is small, compact, and of light-enough weight to be carried easily by the tester.

The testing of d-c meters was accomplished from the beginning by the use of variable rheostats for meters of

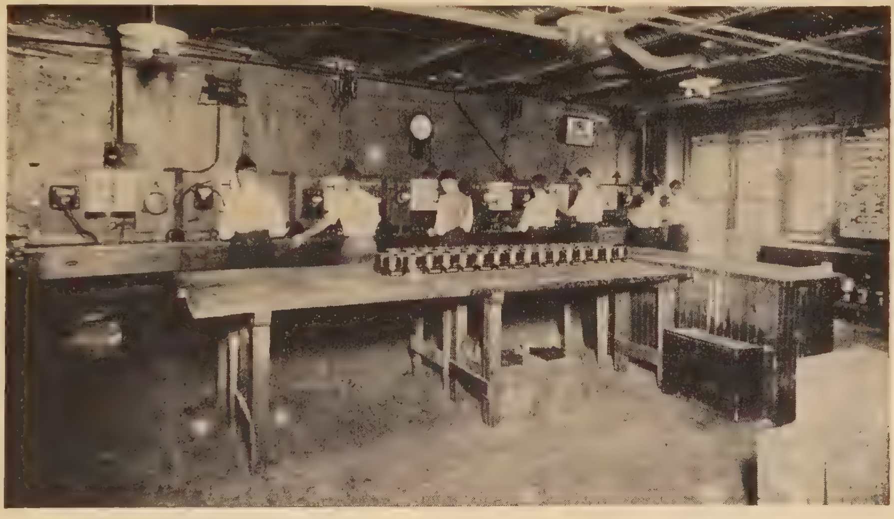

Figure 36. Early meter shop and laboratory of a public utility

Figure 37. Shop testing division of a public utility, modern installation

low rating and by storage batteries when the rating was large. This practice is still in use today and for large-capacity meters requires a considerable number of storage batteries with the necessary transportation to and from the installation.

INSTALLATION OF THE WATT-HOUR METER

Progress has been made in the technique of installing the meter as well as in its manufacture and calibration. In figure 41 is shown an early installation, which in the light of present practice may be described as being everything it should not be. This installation "just grew." There is no indication of a plan and no attempt at protection either of life or of property. In fact, one is forced to conclude either that electric codes were nonexistent or that inspection was reprehensibly lax. Yet to the meterman the picture has a strange fascination. Contrast this picture with figure 42, which shows a modern, completely inclosed indoor installation. In a space little larger than that used for the old installation are 31 meters, each with properly sealed test facilities. In figure 43 is shown a still more modern installation, employing socket-type meters with enclosed test facilities. Here also is illustrated a meter tester at work under conditions that are conducive to high-quality results, obtained with maximum safety for both the tester and the property.

The progress which these pictures illustrate was made possible principally by two factors: a basic change in the National Electrical Code, and the standardization of meter-terminal dimensions and arrangements.

Until about 1931 the Code required that a switch and a main-line fuse be placed between the supply and the meter. Such an arrangement limited the installation largely to indoor arrangements, besides creating a number of complications when more than one meter and service were connected to a single entering circuit. Since access to the line ahead of the meter was at least possible in the old sequence, attempts were made in the early days to seal switches and even fuses, but such practices were generally unsatisfactory. About 1931 the Code was changed to permit the installation of the meter ahead of the switch and fuses. This sequence was a much simpler arrangement, and also removed any possible temptation on the part of an unscrupulous customer to connect loads ahead of the meter.

The standardization of the meter-terminal dimensions and arrangements in 1934 also helped along the progress of standardized meter installations. Meters of any manufacture could be mounted interchangeably, as far as meter trims, test facilities, and conduit arrangements were concerned.

The development and more general use of meter-testing devices has increased greatly the safety of the meter tester,

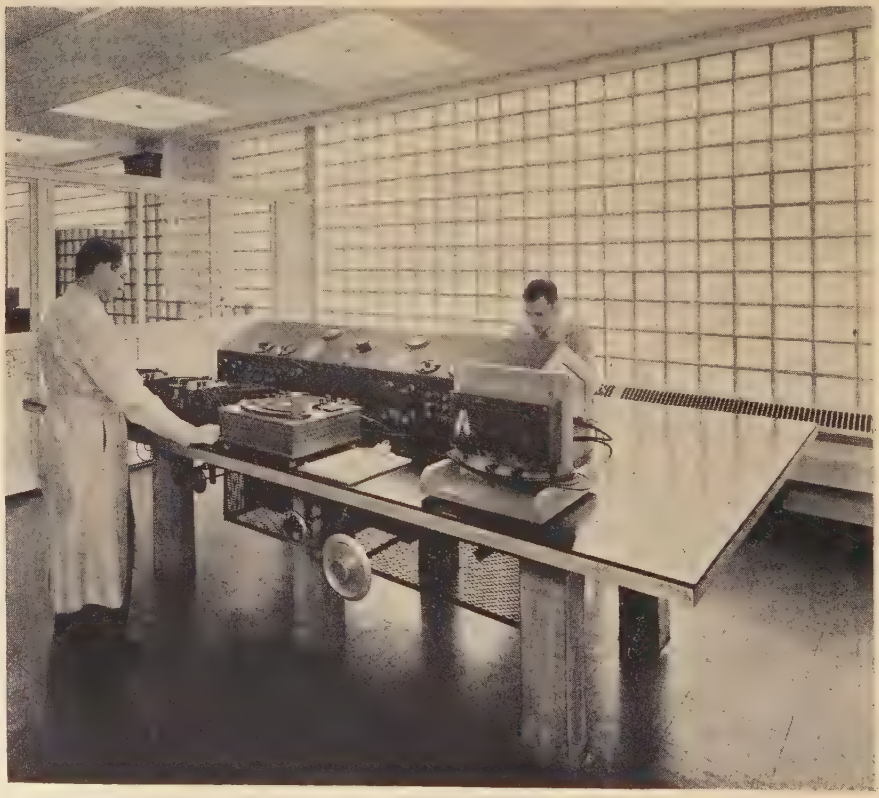

Figure 38. The a-c standards laboratory of a public utility

particularly in respect to power metering at high voltages. Where such devices are economically feasible accidents are reduced materially and much time is saved. Many such devices have been designed, to meet a multiplicity of conditions, but, in general, they consist of switching arrangements which disconnect the meter from the customer's load and at the same time connect that load through to the line and afford access to the meter terminals for test purposes.

Figures 43 and 44 illustrate two such devices. The one in figure 44 is a power-metering installation requiring instrument transformers (not shown) and demand meters. The two meters on the left center of the board are printing-type demand meters. The device just above the tester's head is a demand-totalizing relay. It is used for the purpose of totalizing demand impulses from contactors in each of the four polyphase watt-hour meters shown on the board, adding these impulses, and delivering the result to one of the demand meters. The composite demand of the four circuits being metered is then printed on the tape of the latter. This demand meter is a class II meter, as described in part III of this report.

Figure 41. Early meter installation

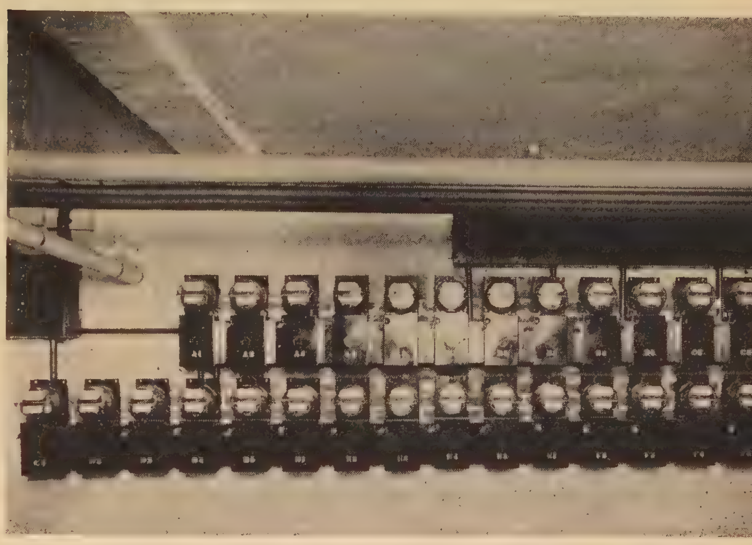

Figure 42. Modern meter installation

Figure 39 (above). Strobometer

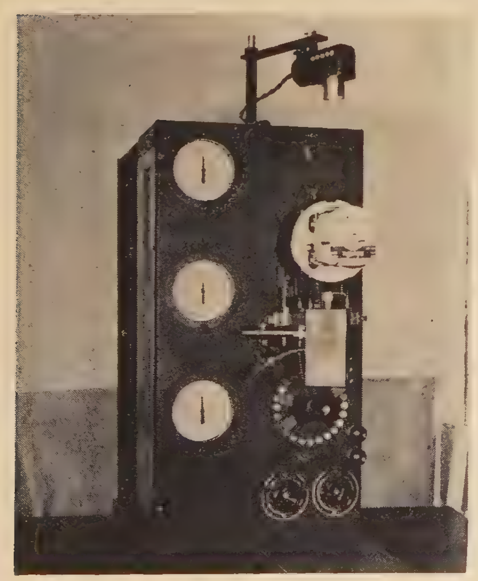

Figure 40. Automatic testing unit

The introduction of a temperature-compensated, weatherproof meter, combined with the revision of the Electrical Code, made outdoor metering physically and economically feasible. One form of such installation before and after a changeover from indoor to outdoor metering is illustrated in parts (*a*) and (*b*) of figure 45. In (*b*) an outdoor meter of the *A*-base type is used in conjunction with a protector case. Figure 45 (*c*) illustrates another method of outdoor metering where a socket-type meter is used without any additional protection being required.

Many different arrangements of meter installations could be illustrated, but the typical examples mentioned

Figure 43 (left). Modern meter installation with built-in test facilities

Figure 44 (below). Modern power-metering switchboard installation

are sufficient to show the progress in this phase of the art. However, occasional installations that have not been modernized are still to be found. Rehabilitation and modernization of meter installations of necessity must lag considerably behind development, for obvious economic reasons.

CONCLUSION

This report has dealt with 60 years of progress in the art of measuring electric energy. Measurement is essential to the progress of any industrial art but the measurement of electric energy was of particular importance to the development of the process of supplying this energy for the improvement of human welfare.

Because this art is more directly affected by economic and sociological trends than are many other industrial arts, its progress has been more difficult to depict. A great diversity of interests was involved in its growth. Such bodies as the national meter committees of the Edison Electric Institute and the Association of Edison Illuminating Companies have had a particularly noticeable influence upon its development.

The nature of this report is such that the operating engineers cannot be given individual recognition, but collectively they are entitled to and should receive a considerable share of the credit for the progress that has been made in the art of metering electric energy.

(a) (b) (c)

Figure 45a. Old-style service drop with indoor metering

Figure 45b. New-style service drop with outdoor metering; meter has protector case

Figure 45c. Outdoor metering with socket meter

Appendix. Guide to Sources of Supplementary Information on Metering

BOOKS

Benjamin Garver Lamme, Electrical Engineer. An Autobiography, **B. G. Lamme.** Published papers, pages 255–63. G. P. Putnam's Sons, New York, 1926, 271 pages.

Commemoration Book Eightieth Birthday of Professor Elihu Thomson, General Electric Company, 1933.

Dictionary of American Biography, volumes 1–20. Charles Scribners' Sons, New York, 1937.

Electric Meter History and Progress, **R. C. Lanphier.** Sangamo Electric Company, Springfield, Ill., 1925, 72 pages.

Electrical Metermen's Handbook, fifth edition. Edison Electric Institute, New York, 1940, 354 pages.

Electric Power Metering; a textbook of practical fundamentals, **A. E. Knowlton.** McGraw-Hill Book Company, New York, 1934, 340 pages.

Electrical Measuring Instruments, two volumes, **C. V. Drysdal** and **A. C. Jolley.** D. Van Nostrand Company, New York.

Electrical Meters, second edition, **C. M. Jansky.** McGraw-Hill Company, New York, 1917, 416 pages.

Electricity Meters, **H. G. Solomon.** L. B. Lippincott, Philadelphia, 1906, 323 pages.

Forty Years of Sangamo, 1896–1936, **R. C. Lanphier.** Privately printed, Chicago, 1936, 107 pages.

George Westinghouse, His Life and Achievements, **Francis E. Leupp.** Little, Brown, and Company, Boston, 1918, 304 pages.

History of the Electric Light, **H. Schroeder.** The Smithsonian Institution, Washington, D. C., 1923, 94 pages.

The Measurement of Alternating-Current Energy, **D. T. Canfield.** McGraw-Hill Book Company, New York, 1940, 210 pages.

Measuring Invisibles. Weston Electrical Instrument Corporation, Newark, 1938, 51 pages.

Science Museum Handbook, South Kensington Museum. His Majesty's Stationery Office, London, 1933–34.

Standard Handbook for Electrical Engineers, seventh edition, edited by **A. E. Knowlton.** McGraw-Hill Book Company, New York, 1941, 2303 pages.

ASSOCIATION REPORTS

Minutes and Serial Reports, Meter Committee, National Electric Light Association.

Reports and Minutes of the Committee on Metering and Service Methods, Association of Edison Illuminating Companies.

PERIODICALS

Aluminum-Nickel-Cobalt Brake Magnets for Watt-Hour Meters, **Stanley Green.** AIEE Transactions, volume 58, 1939, page 791.

Anomalous Behavior of the Moving Systems of Single-Phase A-C Watt-Hour Meters at No Load, **F. C. Holtz.** AIEE Transactions, volume 59 (February section), 1940, page 116.

Character of the Thermal Storage Demand Meter, **P. M. Lincoln.** AIEE Transactions, volume 37, 1918, page 189.

Compensation of Electrical Measuring Instruments, **J. Swinburne.** *Electrical World*, volume 10, September 24, 1887, page 169.

The Development of a Modern Watt-Hour Meter, **I. F. Kinnard** and **H. E. Trekell.** AIEE Transactions, volume 56 (January section), 1937, page 172.

Electricity Meters, Demand Meters, and Instrument Transformers (in French), **W. H. Pratt.** Congrès Internationale d'Electricité, 1932, volume 3, section 2, Gauthier-Villars, Paris, 1932, page 632.

The History of Indicating Meters, **C. R. Riker.** Number 30 in a series of articles on the engineering evolution of electrical apparatus. *Electric Journal*, volume 15, 1818, page 271.

Improved Sheeffer Induction Meter. *Electrical World*, volume 36, September 1, 1900, page 340.

Integrating Wattmeters With Recording Attachments, **H. S. Baker.** *Proceedings*, Annual Convention of the Canadian Electrical Association, 1913, page 32.

The Late O. B. Shallenberger and His Work. *The Electrical Engineer*, volume 25, 1898, page 255.

Magnetic Properties of Hardened Steel (in French), **Madame S. Curie.** Société d'Encouragement pour l'Industrie Nationale, *Bulletin*, volume 97, 1898, page 36.

Measurement of Maximum Demand and the Determination of Load Factor, **P. A. Borden.** AIEE Transactions, volume 39, 1920, page 1847.

Motor Meters, **F. P. Cox.** *Electrical World*, volume 22, September 2, 1893, page 168.

A New Demand Meter, **B. H. Smith.** AIEE Transactions, volume 53 (January section), 1934, page 94.

A New Induction Watt-Hour Meter, **J. Faccioli.** *Electrical World*, volume 47, June 16, 1906, page 1266.

New Types of Shallenberger A-C Meters. *Electrical World*, volume 25, January 5, 1895, page 28.

A New Watt-Hour Meter, **Stanley Green.** AIEE Transactions, volume 54 (October section), 1935, page 1073.

O. B. Shallenberger, an editorial. *Electrical World*, volume 23, June 23, 1894, page 827.

On the Influence of a Plane of Transverse Section on the Magnetic Permeability of Iron, **J. A. Ewing** and **William Low.** *Electrical World*, volume 10, September 24, 1887, page 171.

Polyphase-Meter Applications, **P. MacGahan.** *Electric Journal*, volume 33 1936, page 453.

A Precision Rotating Standard for the Measurement of Kilowatt Hours, **J. H. Goss** and **A. Hansen, Jr.** AIEE Transactions, volume 59 (July section), 1940, page 412.

Rates and Rate Making, **P. M. Lincoln.** AIEE Transactions, volume 34, 1915, page 2279.

Recent Developments in Kilovolt-Ampere Metering, **B. H. Smith** and **A. R. Rutter.** AIEE Transactions, volume 43, 1924, page 297.

Shallenberger's Electric Meter. *The Electrical Engineer*, volume 7, 1888, page 382.

Some New Electric Indicators, **G. B. Prescott, Jr.** *Electrical World*, volume 7, March 27, 1886, page 139.

The Stroboscopic Method of Testing Watt-Hour Meters, **H. P. Sparkes.** AIEE Transactions, volume 46, 1927, page 405.

Temperature Errors in Induction Watt-Hour Meters, **I. F. Kinnard** and **H. T. Faus.** AIEE Transactions, volume 44, 1925, page 275.

Tests on Accuracy of Reactive Metering, **A. E. Knowlton.** *Electrical World*, volume 82, December 29, 1923, page 1309.

Theory of Action of the Induction Watt-Hour Meter and Analysis of Its Temperature Errors, **D. T. Canfield.** AIEE Transactions, volume 46, 1927, page 411.

The Thermal Storage Demand Wattmeter, Its Characteristics and Application, **P. Lincoln.** *Electric Journal*, volume 17, 1920, page 253.

Watt-Hour-Meter Testing With Photoelectric Cells, **S. Aronoff** and **D. A. Young.** *Electric Journal*, volume 26, 1929, page 255.

Weston's New Measuring Instruments. *Electrical World*, volume 12, November 17, 1888, page 263.

Zur Geschichte des Elektrizitätszählers, **W. Stumpner.** *Elektrotechnische Zeitschrift*, volume 47, May 27, 1926, page 601.

MUSEUMS AND COLLECTIONS

Professor Elihu Thomson Collection, General Electric Company, West Lynn, Mass.

Duncan Memorial Museum, Purdue University, West Lafayette, Ind.

Ford Museum, Dearborn, Mich.

Smithsonian Institution, Washington, D. C.

Science Museum, South Kensington, London, England

Meter Patents Listed in the Patent Office Gazette

Some of the more important patents issued to inventors, with brief descriptions of some specifically mentioned in the text or of particular historical interest. Those chosen show important steps in the advancement of the watt-hour meter art, or establish important dates

Name	Patent No.	Date	Description
Gardiner, Sawyer, Fuller and Forbes			
S. Gardiner, Jr.	132,569	October 29, 1872	These devices were all similar to Gardiner's number 1 claim: "1. The combination and arrangement of an electromagnet and its armature with the releasing device of a clock mechanism for indicating upon a dial the time during which an electrical current is in action"
W. E. Sawyer	210,151	November 19, 1878	
J. B. Fuller	210,316	November 26, 1878	
G. Forbes	366,824	July 19, 1887	

Meter Patents Listed in the Patent Office Gazette (Continued)

Name	Patent No.	Date	Description
Edison			
T. A. Edison	240,678	April 26, 1881	"A Weber Meter." Two plates in an electrolyte balanced on a rocking beam. When one plate receives a sufficient deposit of, say, copper it tips the balance in its direction thereby reversing the current through the electrolyte and recording the result on a dial. The process is then repeated in the opposite direction
	242,901	June 14, 1881	A motor meter driving a fan for a load
	248,565	October 18, 1881	Device for decomposition of water, arranged so that the gases released actuate a recording mechanism
	251,545	December 27, 1881	An electrolytic cell in conjunction with an electromagnetic recording mechanism
	251,557	December 27, 1881	Two electrolytic cells, one to operate at a faster rate (across a higher resistance shunt) than the other. Means of heating the electrolyte to keep resistance of shunted circuit constant. One cell was intended to be used for a check meter on the other. This is similar to the meter described in part I of this series of articles (*EE, Sept. '41, p. 421*)
	251,558	December 27, 1881	Antifreezing resistances claimed
	281,352	July 17, 1883	Amalgamated electrodes, zinc, claimed. Reduction of losses in the meter
Weston and Mott			
Edward Weston, Samuel Mott	282,428	July 31, 1883	First recorded patent of the men who later founded the Weston Electrical Instrument Corporation
Thomson			
Elihu Thomson	381,441, 381,442, 381,443	April 17, 1888	Patents for the rocking-beam meter consisting essentially of two glass bulbs connected by a glass tube all mounted on a beam pivoted at the center. Each bulb had a heating element through which the current to be measured passed, first in one bulb, then the other. The heat generated expanded the gas in the bulb, forcing a liquid into the other bulb and thereby rocking the beam in that direction. The process switched the current to the filled bulb and repeated the process. These three patents were followed by some 12 or 15 others covering improvements on this meter. The last of these was issued about 1890
	444,930	January 20, 1891	With this patent Thomson seems to have abandoned the rocking-beam meter and switched to the commutator-type-motor meter. It was filed in 1890. This first patent used electromagnetic retardation
	448,894	March 24, 1891	Permanent magnet retardation used here
	508,661	November 14, 1893	Patent on voltage transformer called a "converter" used in the potential circuit of Thomson's commutator-type-motor meter. Perhaps the first instrument transformer ever used. Also indicates that his meter would operate on alternating current. Followed by many others covering improvements thereon
Aron and Siemens			
H. Aron	374,860	December 13, 1887	Patent covering Aron's pendulum meter, one of the most accurate d-c energy-measuring meters ever designed
E. W. Siemens	415,577	November 19, 1889	Commutator-type motor meter
DeFerranti, Hookham, Halsey, Gutmann, and Lanphier			
S. Z. DeFerranti	338,588	March 23, 1886	The DeFerranti patent discloses the Faraday disk or mercury-motor meter; the Hookham patent is for another mercury motor meter. The five patents listed here represent the backbone of the mercury-motor meter art. All the present meter manufacturers and several others at one time or another obtained patents on a meter of this type. Lanphier of the Sangamo Electric Company seems to have been the only one to persist and eventually to produce an accurate and reliable meter of this type
George Hookham	579,582	March 30, 1897	
E. S. Halsey	626,832	June 13, 1899	
L. Gutmann and R. C. Lanphier	738,902	September 15, 1903	
R. C. Lanphier	843,155	February 5, 1907	
Shallenberger			
O. B. Shallenberger	388,003	August 14, 1888	Patent covering the first induction-type meter in the United States; its number 1 claim reads: "1. The combination of a rotating armature, an inducing circuit polarizing said armature when traversed by alternating electric impulses, a second inducing circuit receiving currents from the first circuit and polarizing said armature in a different direction, and a counting, registering, or indicating device actuated by the movements of the armature"
	388,004	August 14, 1888	Describes some alternative ways of obtaining a shifting field, the use of a shunt coil to overcome friction or to furnish a wattmeter element. Also illustrates the use of reactors and capacitor to produce fluxes out of phase with each other, but apparently not, at that time, in the sense of lagging
	414,595	November 5, 1889	Adds transformer with taps to increase range
	419,367	January 14, 1890	Improvements in construction and movable secondary inducing circuit to adjust speed for a given current
	448,676	March 24, 1891	The inventor seems to have been much worried by what he called "leakage currents," which today would be called exciting currents. The meter was evidently being used on the primary side of distribution transformers and, of course, read even when no lights were turned on the secondary side. To cause the meter to fail to respond on the "leakage currents of the converter" but to respond when any light was used on the secondary of the "converter" the armature of the meter (disk) was flattened on two sides. This patent was followed by several others using electromagnetic and other schemes for the same purpose
	531,866, 531,867	January 1, 1894; January 1, 1895	Patents covering the watt-hour meter—the substitution of coils of wire for the short-circuited secondary or inducing circuit, and the connection of these coils for both potential and current
	548,231	October 22, 1895	Apparently the first patent disclosing the use of a short-circuited coil and series resistance for phasing purposes; represents Shallenberger's most important contribution to the metering art
	591,240	October 5, 1897	Improved means of phasing a meter
Slattery			
M. M. Slattery	404,801	June 4, 1889	Same principle as Shallenberger's meter, but used extra heavy copper grids for the secondary coil
	410,860	September 10, 1889	Overload compensation applied by counterbalanced split vanes which operated by centrifugal force
Duncan			
T. Duncan	500,868	July 4, 1893	Multiphase meter. Refers to an application filed December 21, 1891, serial No. 415,825, giving the principle of the meter
	501,000	July 4, 1893	Describes early air-vane meter mentioned in text
	518,311	April 17, 1894	D-c-motor meters used on alternating current. Shows use of instrument transformers
	523,704	July 13, 1894	Addition of core in secondary to improve torque
	550,823, 551,436	December 3, 1895	Improvements
	560,087	May 12, 1896	Winding of secondary with wire and connecting it in shunt thus making a watt-hour meter. This patent was followed in close order by 25 or 30 patents covering both d-c and a-c meters
	753,193	February 23, 1904	First patent issued to Duncan's Lafayette residence
Gutmann			
Ludwig Gutmann	543,089	July 23, 1895	An air-vane induction-type lamp-hour meter
	614,225	November 15, 1898	Improvement of slanting slots in barrel-like drum used for disk

Name	Patent No.	Date	Description
Conrad, Davis, and Bradshaw			
H. P. Davis and F. Conrad	608,842	August 9, 1898	Show method of measuring energy in a three-phase, four-wire system using three current transformers (secondaries in delta) and a two-element polyphase meter
F. Conrad	716,867	December 30, 1902	
W. Bradshaw	807,435	December 19, 1905	Casing and terminal blocks.
Wood and King			
J. J. Wood	442,501	December 9, 1890	A rocking-beam meter
	469,800	March 1, 1892	A meter which is fundamentally wrong in principle
E. J. King	671,282	April 2, 1901	Describes type *K* meter
	727,640	May 12, 1903	Type *K* meter with forms of potential shunt
J. J. Wood	780,769	January 24, 1905	Correct principles in this meter
Kennelly, Oxley, and Steinmetz			
A. E. Kennelly	479,167	July 19, 1892	A motor meter with drag coil in series with the armature
C. P. Steinmetz	539,452	1895	Two-element d-c meter of commutator type
E. Oxley	588,170	August 1897	Both of these patents covered multi-rate meters
	593,852	November 16, 1897	
C. P. Steinmetz	780,769	August 1, 1905	Shaded pole meter
Pratt, Vaughen, Lunt, Alton, Vogel			
W. H. Pratt	590,648	September 28, 1897	A d-c two-element meter
	645,125	March 13, 1900	Starting coils, consisting of a coil in series with the potential coil to start a meter. First form of light-load or friction compensation. Early coils were not apparently adjustable
F. G. Vaughen	678,075	July 9, 1901	A bent iron-wire clip put on edge of disk to prevent creeping. Apparently first anti-creep device
A. D. Lunt	696,459	April 1, 1902	Copper squares "pasted" on disk to act as anti-creep devices
G. H. Alton	733,611	July 14, 1903	Improvement in jewel mountings
W. H. Pratt	711,932	October 11, 1904	Another form of starting coil
	816,375	March 27, 1906	Two-and-one-half-element meter for use on three-phase four-wire systems. The equivalent of Conrad's three-current transformer scheme
	835,321	November 1906	Covers the first adjustable light-load plate used
F. M. Vogel	941,436	November 30, 1909	Covers a lag plate
W. H. Pratt	984,297	February 14, 1911	Covers grid mounting of the elements in a meter
	1,002,031	May 20, 1913	Improved light-load and lag plate
Lanphier			
R. C. Lanphier	1,010,271	November 28, 1911	Covers the type *H* meter
Harris			
J. Harris	543,865	August 6, 1895	Combination graphic and watt-hour meters
	583,000	August 21, 1900	A summation meter
Stanley			
W. Stanley, Jr.	494,513	March 28, 1893	A two-coil a-c mter
	588,666	August 24, 1897	The magnetic flotation meter
Scheeffer			
G. A. Scheeffer	522,674	July 10, 1894	Early model of Diamond Meter Company meter. Used a cup disk and air-vane damping
	530,351	December 4, 1894	Later model of Diamond Meter Company meter
	591,641	October 12, 1897	Four-magnet meter
	599,302	February 15, 1898	D-c meter
	643,162	February 13, 1900	Round-type Diamond meter
	905,934	December 8, 1908	Inclined-coil type. Columbia Meter Company
	950,074	February 22, 1910	Assigned to General Electric Company
	995,637	June 20, 1911	Columbia Meter Company
	1,082,653	December 30,1913	Roller Smith Company meter
Bláthy, Batault, Tollie, Boddie, Bradshaw, Knight, Kurz			
O. T. Bláthy	423,210	March 17, 1890	Meter with two or more electromagnets one set shunt and the other series, offset from each other with respect to a disk upon which drag magnets also operate
E. Batault	693,537	February 18, 1902	Diverter or saturable member for improving characteristics
O. T. Bláthy	716,372	December 23, 1902	Improved pole tips and magnetic circuits
	853,216	May 14, 1907	Various shunts and special pole pieces for improving load curves
H. Tollie	1,155,384	October 5, 1915	An *L*-shaped bracket placed on both current and voltage magnet to compensate for overloads. A form of saturable member
C. A. Boddie and W. Bradshaw	1,285,911	November 26, 1918	Overload compensation devices
C. A. Boddie	1,290,492	January 7, 1919	Another form of saturable member for overload compensation
J. A. Knight	1,299,736	April 8, 1919	Another form of saturable member for overload compensation
F. Kurz	1,727,509	September 10, 1929	Another form of saturable member for overload compensation
Kinnard and Green			
I. F. Kinnard	1,706,171	March 19, 1929	Temperature compensation with negative temperature coefficient material in shunt with the permanent magnet
Stanley Green	2,110,417	March 8, 1938	Discloses the use of the laminated noninterfering disk for use in single-disk polyphase meters
	2,110,418	March 8, 1938	Discloses the first use of Alnico magnets in watt-hour meters
	2,203,411	June 4, 1940	Patent on new pivot material called Permalloy for use in watt-hour meter pivots
Wright, Merz, Luckee, Steele, Karapetoff, Hall, Mowbray			
A. Wright	702,844	June 17, 1902	Early form of Wright demand meter
	702,847	December 23, 1902	Wright demand meter of the form still used in this country
C. H. Merz	722,030	March 3, 1903	Discloses underlying principle of demand meters
W. W. Luckee and D. J. Steele	933,845	September 14, 1909	Mechanical device embodying all essentials of modern demand meter except clock timing of interval
V. Karapetoff	972,538	October 11, 1910	Demand meter using clock, which may be set for any time interval desired. Several additional features not used on modern indicating block-interval demand attachment
C. F. Hall	1,028,715	June 4, 1912	Five-minute block-interval demand of present type, in which Hall refers to C. H. Merz's work of 1903
W. J. Mowbray	1,024,218	April 23, 1912	Temperature-compensated rotating standard for d-c meters

Ten Years of Progress in Relaying

This is the second of a series of three related articles which together present a review of the progress made in the past decade in the protection of electric power-system circuits and equipment. This article, concerned with protective relaying, has been prepared under the auspices of the AIEE committee on protective devices. The first article of the series, concerned with circuit-interrupting devices, was published last month; the third, dealing with lightning-surge protective devices and the protection of systems against lightning, is now in preparation and is scheduled for publication in a later issue.

JUDGING from the external appearance of relays, one might conclude that protective relaying was an unromantic and prosaic subject. Here are a lot of little devices that spend most of the time sitting still, with not even the little eye-appeal of the moving pointer of an instrument or the passing black spot on the disk of a watt-hour meter. Yet compacted within these small cases is the fruit of the labor of many minds, in such form that, when called upon to function, relays take a set of observations, perform a lightning calculation, and act, all within 1/20 of a second.

Put in more technical terms, the general objectives of protective relaying are: (*a*) the limitation of damage to electric equipment, and (*b*) the maintenance of adequate service with reasonably low investments in generation, transformation, transmission, and distribution equipment. In order to obtain these objectives, the protective-relay system must detect positively the occurrence of a short circuit, determine enough about its location to permit selection of the breakers which must be opened, and control the opening of only those breakers necessary to remove the fault from the system—all in a time short enough to limit equipment damage and reduce system disturbances to a reasonably low value.

In a period of a little more than ten years, a major change has been made in protective-relay methods. From the standpoint of the electrical industry, probably the greatest significance of the change is that modern relaying methods make possible the rendering of improved service with a lower investment in major electric equipment, resulting in savings that many times exceed the total cost of the protective relays.

Previous to 1930, most relay applications for line protection used overcurrent and directional relays with graded time delay to obtain selectivity. As a result the time required to clear many system faults was a matter of seconds. As systems became more complex two limitations of the graded time overcurrent relays became apparent. One was that the prolonged duration of faults sometimes resulted in loss of system stability; the other that, when the maximum load current equaled or exceeded the minimum fault current, overcurrent relays were unable to distinguish between load and short-circuit currents.

During the period since 1930 selectivity has been improved somewhat but the chief improvement has been in speed of operation. The trend has been definitely toward the provision of means whereby at least the more severe faults will be cleared in relay times of the order of one to three cycles. This has brought about the development of new relay systems, such as distance relays and pilot-relays, and also of many new relay elements. These new devices have a much higher torque-inertia ratio than the familiar induction disk formerly used and therefore are inherently much faster in operation.

The relays and relay systems developed during the past ten years and now in common use have two outstanding characteristics. First, if a fault occurs in the area protected by a given relay, the relay operates to energize the breaker trip circuit in a time of the general order of one to three cycles. Second, the relays are capable of distinguishing between load currents and fault currents despite wide variations in system generating capacity. These developments, combined with the parallel development of high-speed circuit breakers, have made it possible so to protect a transmission system that any line fault will be cleared in a total time of ten cycles or even less.

The new relays for line protection may be divided into two classes, the distance relays and the pilot relays. Distance relays may be of either the impedance or reactance type. Pilot relays may operate over physical pilot wires with a-c or d-c excitation, or may use carrier current over the line conductors themselves.

While most of the changes of the past decade have affected line relaying, some marked improvements have been made in relays for apparatus and bus protection, characterized largely by developments making possible faster operation.

The trend in relaying in the immediate future seems to be toward simplification and improved reliability rather than toward any fundamental changes in relays or systems, or in speed of operation. Considerable interest exists in the possibility of using vacuum tubes for relaying. Such use remains a distinct future possibility, and the increasing need for more sensitive devices may result in the development of radically new relay devices for such purposes. Some of the fields where more sensitive operation

might prove helpful are ground protection, bus protection, and pilot-relay systems.

DISTANCE RELAYS

The distance relays used before 1930 were not of the high-speed variety. They were so designed that the time of operation was a direct function of the distance from the relay to the fault. This form of time-distance characteristic produced satisfactory selectivity, but was not suitable for high-speed relaying.

The modern high-speed relay is set to operate on its so-called instantaneous time for any fault within 80 per cent of the protected line section. The so-called instantaneous time step is of the order of one cycle in actual practice. For faults beyond the 80 per cent of the line covered by the instantaneous element, a definite time is introduced into the relay system sufficient to permit a similar relay to clear selectively in the first zone in case the fault is beyond the next station.

The step-distance-time curve can be obtained with relays which have measuring elements operating either to measure impedance or reactance. Both types have been used very widely, although most applications have provided protection only for faults involving more than one phase, that is, either phase-to-phase or three-phase faults. While the theoretical possibilities of applying the step-distance characteristic for single-phase-to-ground faults have long been known, there has been relatively little application in this field because of the variations in distance measurement introduced by ground fault conditions and the cost.

PILOT-WIRE PROTECTION

At the beginning of the last decade, pilot-wire protection of transmission lines was essentially similar to differential protection of generators or transformers, in that the actual secondary output of the current transformers at the two ends of the line was compared physically at a relay having the necessary interconnecting pilot wires. This system not only required a costly multiconductor pilot wire, but imposed a very high burden on the current-transformer system so that accuracy was impaired, and in addition required continuous integrity of the pilot-wire circuit.

Two main developments have characterized this past ten-year period. One is the development of the so-called directional-comparison type of pilot-wire system, whereby the indications of directional relays at the two ends of the transmission line are compared over a physical pilot wire operating as a simple d-c telegraph circuit. In its simplest conception, the contacts of the two directional relays, one at each end of the line, are inserted in series in the pilot-wire circuit and the connections of the relays so made that for any internal fault causing power to flow into the section at both terminals, both relays will close contact and thereby energize the pilot-wire circuit, and in turn cause the tripping of the oil circuit breakers.

The other development has been made possible through the availability of new relay elements requiring materially less energy for operation. It is now possible to supplant the multiconductor pilot wire of the earlier differential systems with a single telephone pair. High-speed differential relays responding to all types of faults are now available for the protection of transmission lines of reasonable length over a conventional telephone pair. Special applications have been made successfully on lines as much as 25 miles long.

Both these systems have been widely used, and have been shown through adequate operating experience to be thoroughly reliable. With either the d-c or the a-c system, tripping times of the order of one to three cycles are now readily available.

CARRIER-CURRENT PROTECTION

The first carrier-current relay system was described before the Institute in 1928. This system proposed to simulate the multiple-conductor pilot systems then in use, and to compare the phase relationships of the currents in the two ends of the line by means of 60-cycle modulation of the carrier system. A number of installations made in 1929, for protection against ground faults only, gave satisfactory results. Attempts in the earlier days of the development to make the system operative on all types of faults were not successful because the power requirements of the relay system at that time were greater than the available output of current transformers.

Subsequently, the comparison of phase relationship of currents was discarded in favor of a comparison of power direction at the two ends of the line similar to the system described for the d-c pilot system. As used today, the carrier impulse is a means of preventing tripping whenever an external fault occurs. In case of an internal fault, directional relays at the two ends of the line, operating in response to power flow into the line, turn off the carrier signal and thereby permit tripping. The relay systems now in use turn on carrier immediately whenever a fault occurs, whether internal or external to the line section, and the carrier subsequently is controlled by the operation of the directional relays to allow or prevent tripping as the fault location dictates.

Improvements in the design of equipment and circuit-control features have permitted a reduction in operating time from between 15 and 30 cycles with the original system to between 1 and 3 cycles with the modern system. Two types of equipment are in use. One consists of simple fault-detecting relays for turning on the carrier signal and directional relays for controlling the signal once started in response to a fault. This system functionally provides the equivalent of differential protection and is operative only in case of internal faults. The other system builds up carrier control about the elements commonly used for distance protection, and embodies in one set of equipment not only the advantages of differential protection for internal faults but also the step-distance characteristic operative as a back-up for external faults when necessary.

INSTANTANEOUS OVERCURRENT RELAYS

While there is nothing essentially new about an instantaneous overcurrent relay, elements of this type have found new application in the last ten years. On many systems it has been found practical to add instantaneous overcur-

rent relays to the graded-time overcurrent relays used for selectivity. These instantaneous relays are given a setting in current value just in excess of the maximum current which could be transmitted to a fault at the remote end of the line that they are protecting. Such relays may be used for phase-to-phase-fault protection or ground-fault protection. It is sometimes necessary to use a directional element in addition to the instantaneous relays to secure proper selectivity on lines forming part of a network. Operating experience has indicated that on some systems where generating conditions are relatively constant, from 80 to 85 per cent of all faults can be cleared by the action of these relays, which have an operating time of about one to three cycles.

BUS PROTECTION

The desirability of always providing automatic protection to remove any type of fault from the system has become much more generally appreciated in the past decade. As a result many bus sections previously left unprotected are being provided with protective relays. The most popular method of protection is the one involving the differential connection of all current transformers in all primary connections to the given bus section. Differential protection of this type may employ either standard-speed induction overcurrent relays or high-speed relays of the multiple-restraint or harmonic-restraint types. Since the application of high-speed relays requires a complete study of current-transformer characteristics, a more thorough investigation and a more complete understanding of the phenomena involved in current-transformer operation, particularly under transient conditions has resulted. Special current transformers capable of maintaining ratio characteristics up to more than 100,000 amperes have been developed for bus-differential purposes.

In certain cases distance relays have been employed to good advantage where feeder reactors are utilized. Fault-bus systems have been employed whereby the fault current to ground resulting from a fault on the protected section is made to flow into the fault bus where its presence can be detected and the desired relay operation performed.

SENSITIVE GROUND PROTECTION

Considerable study has been devoted to the problem of relaying distribution circuits in case of accidental ground. A paper[1] recently presented before the Institute describes a system developed and applied to an ungrounded system. Research has been carried on in the development of a relay system responsive to arc frequencies in connection with high-resistance ground fault. Although many problems remain to be solved, the studies being made in various quarters hold promise that an adequate relay system for the detection of these troublesome faults eventually will be developed.

HIGH-SPEED RECLOSING

High-speed-reclosing relays have been developed for the protection of distribution circuits which, together with instantaneous tripping, permit clearing of temporary faults before the branch fuses blow and the re-energization of the circuit with a total outage time of less than a second.

The reclosing systems also provide that the instantaneous tripping will not be in service on delayed reclosures, so that if the short circuit is of a permanent nature the branch fuses will limit the interruption to a single section. As a result, almost as good service can be provided with relatively inexpensive fuses as would be obtained by the installation of oil circuit breakers and control equipment at each branch sectionalizing point.

The use of pilot wire or carrier current relaying insures simultaneous opening of the breakers at each end of a tie line so that there is no danger of either breaker reclosing before the arc has been de-energized. This scheme of protection and reclosing may make a high-voltage transmission line so reliable as to make unnecessary or to defer the construction of an additional transmission line.

BIBLIOGRAPHY

No references have been cited in this summary of trends in relaying during the past ten years, because a "Bibliography of Relay Literature, 1927–1939" has been prepared by the relay subcommittee of the AIEE committee on protective devices and issued as a special Institute publication.*

1. SENSITIVE GROUND PROTECTION FOR RADIAL DISTRIBUTION FEEDERS, L. F. Hunt and J. H. Vivian. AIEE TRANSACTIONS, volume 59, 1940 (February section), pages 84–90.

* Copies of the "Bibliography of Relay Literature," published July 1941, may be obtained from AIEE headquarters, 33 West 39th Street, New York, N. Y., at a cost of 25 cents per copy to Institute members or 50 cents to nonmembers.

20,000-Kva Synchronous Condenser

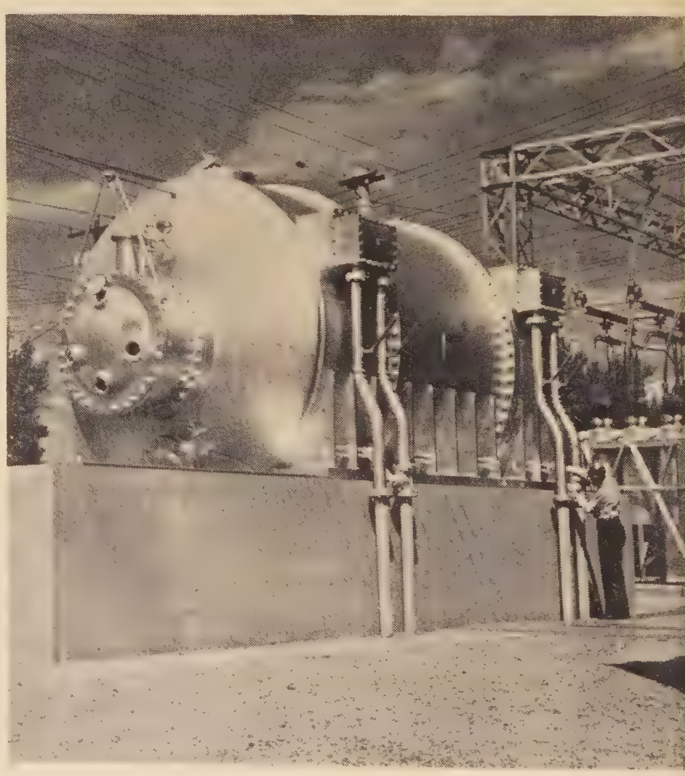

Photo courtesy General Electric

Recently installed at the Denver terminal of the Public Service Company of Colorado, this 13,800-volt synchronous condenser is hydrogen-cooled, and operates at 900 rpm

Institute Activities

Contents of December 1941 Supplement

SUPPLEMENTING the technical papers that have been preprinted from the 1941 volume of AIEE TRANSACTIONS in the monthly TRANSACTIONS sections of ELECTRICAL ENGINEERING for July to December inclusive, a December 1941 "Supplement to ELECTRICAL ENGINEERING—TRANSACTIONS Section" is being issued. This is the second supplement to be issued in 1941, the first being the June 1941 supplement. Both represent the operation of the improved publication procedure adopted at the 1940 AIEE summer convention (*EE, Aug. '40, p. 331–2*).

The December 1941 supplement will contain 32 technical papers and all discussions of these papers and of the papers preprinted in the July–December monthly sections. This supplement, like that of June 1941, will be greatly oversize in order to complete the transition from the previous publication procedure within the current year. Under the present procedure, all papers presented during a calendar year will be contained in the annual volume for that year and preprinted in the monthly sections and semiannual supplements.

Copies of the December 1941 supplement will be mailed when ready to those who entered advance orders. Others may obtain copies at 50 cents each ($1.00 each outside the United States and possessions) from the AIEE order department, 33 West 39th Street, New York, N. Y., as long as the limited supply lasts.

Abstracts of the papers in the current supplement have appeared in the news pages of ELECTRICAL ENGINEERING, where they were published in advance of the meetings and conventions at which the papers were presented, in accordance with the provisions of the current publication policy. Papers appearing in the December 1941 supplement, with references to their abstracts, are:

Basic Sciences

Communication

Electrical Machinery

Electronics

Industrial Power Applications

Instruments and Measurements

Land Transportation

Power Transmission and Distribution

Production and Application of Light

Protective Devices

41-128—Protection of Low-Voltage Circuits by Air Circuit Breakers in Cascade Arrangement; *A. E. Anderson (F'40) and C. H. Black (A'41).* June 1941, page 293.

41-135—New Current Transformer for Bus Differential Protection; *L. F. Kennedy (M'39) and A. T. Sinks (A'36).* June 1941, pages 292–3.

Safety

41-7—Electric Shock; *C. F. Dalziel (M'39), Doctor John B. Lagen, and J. L. Thurston.* January 1941, page 41.

Winter Convention Program to Reflect Concern With Defense

Tentative arrangements for the winter convention, which will be held in New York, N. Y., January 26–30, 1942, with headquarters in the Engineering Societies Building, indicate that a timely program of broad interest is being developed. Preliminary plans provide for a general session, 18 technical sessions, and several conferences, to be held during the mornings and afternoons, while the evenings will be taken up with a smoker, Edison Medal presentation, and a dinner-dance. Special entertainment for women guests will be arranged by the women's entertainment committee, under the chairmanship of Mrs. G. S. Rose.

Among the 18 technical sessions, several will reflect the part being taken by different branches of the profession in national defense. The educational session will have papers dealing with the changes in engineering curricula and advanced training in the graduate field to meet the needs of the emergency. A symposium on electric power distribution systems in the current national defense program will present the steps being taken by several operating companies. Another symposium on asynchronous machines, which will treat the precise speed control of these large motors with variable-speed drive, represents the research and development angle. Other sessions of broad popular interest will deal with the subjects of lightning investigations in the field and distribution switching and relaying.

The general session will be devoted to a topic of timely importance designed to interest as many members as possible.

The members of the 1942 winter convention committee are as follows:

D. A. Quarles, *chairman;* J. W. Barker, T. F. Barton, G. E. Dean, E. E. Dorting, J. F. Fairman, L. C. Miller, D. H. Moore, J. H. Pilkington, C. S. Purnell, and W. W. Truran. *Chairmen of subcommittees:* S. B. Graham, *dinner-dance;* J. E. McCormack, *smoker;* R. F. Brower, *inspection trips;* and Mrs. G. S. Rose, *women's entertainment.*

Board of Directors Meets

The regular meeting of the board of directors of the American Institute of Electrical Engineers was held at Institute headquarters, New York, on October 24, 1941.

A budget for the appropriation year beginning October 1, 1941, was adopted as recommended by the finance committee.

Upon invitation of the Vancouver Section and the District officers concerned, authorization was given to hold the 1942 Pacific Coast convention of the Institute in Vancouver, B. C., September 9–11. A joint conference on student activities of Districts 8 and 9 and the University of British Columbia Branch was authorized to be held in Vancouver during the 1942 Pacific Coast convention.

Approval was given to the dates, April 29 to May 1, 1942, for the North Eastern District meeting previously authorized to be held in Schenectady, N. Y.

Upon recommendation of the executive committee of the North Eastern District and the Sections committee of the Institute, the board authorized the following assignment of territory in that District to Sections in New York State and New England:

State of New York

St. Lawrence County assigned to the Syracuse Section

Franklin and Clinton Counties assigned to the Schenectady Section

State of Vermont

Addison, Chittenden, LaMoille, Franklin, and Grand Island Counties assigned to the Pittsfield Section

Washington, Orange, Caledonia, Essex, and Orleans Counties assigned to the Springfield Section

State of New Hampshire

Grafton County assigned to the Worcester Section, Coos and Carroll Counties assigned to the Boston Section.

Upon recommendation of the standards committee, the board took the following actions:

Approved a revision of the Standard for Railway Motors (AIEE Standard No. 11), developed by a sectional committee under the sole sponsorship of the AIEE and approved by the AIEE committee on land transportation, and its transmittal to the American Standards Association for approval as an American standard.

Approved, for publication as an AIEE standard, a report on "Standards for Wet Tests," developed by a special subcommittee.

Approved the appointment of the following Institute representatives:

C. H. Anderson, Sectional Committee on Definitions of Electrical Terms

R. G. McCurdy, chairman, **H. M. Turner** member of AIEE delegation on Sectional Committee *Z*24, Acoustical Measurements and Terminology (the former succeeding P. L. Alger, who remains a member of the committee, and the latter succeeding Bassett Jones, resigned)

Royce E. Johnson on Section Committees *C*70, *C*71, and *C*72—Domestic Electric Flatirons, Household Electric Ranges, and Electric Water Heaters, respectively.

The following amendments to the Institute bylaws were adopted, in order that they

In Memoriam

THE death, on August 14, 1941, of Bancroft Gherardi removed from the membership of the Institute its 40th president and a leading pioneer in the development of electrical communication, with a career of more than 40 years in that field.

Doctor Gherardi received the degree of bachelor of science from the Polytechnic Institute of Brooklyn in 1891, the degree of mechanical engineer from Cornell University in 1893, and the master's degree in mechanical engineering from that university in 1894. He received the honorary degree of doctor of engineering from the Polytechnic Institute of Brooklyn, 1933, and from the Worcester Polytechnic Institute, 1936.

In 1895, he was employed by the Metropolitan Telephone and Telegraph Company. He was engineer of the traffic department 1900–01, and was transferred to the position of chief engineer of the New York and New Jersey Telephone Company in 1901. In 1906, he returned to New York as assistant chief engineer of the New York Telephone and Telegraph Company and the New Jersey Telephone Company. He was appointed engineer of plant of the American Telephone and Telegraph Company in 1907, became acting chief engineer in 1918, and chief engineer in 1919. From 1920 until his retirement in 1938, he was vice-president and chief engineer.

BANCROFT GHERARDI

He joined the Institute in 1895, and was transferred in 1904 to the grade of Member and in 1912 to the grade of Fellow. He served on many AIEE committees, and represented it on various joint organizations. He was a manager 1905–08, and 1914–17, vice-president 1908–10, and president 1927–28.

RESOLVED: That the board of directors of the American Institute of Electrical Engineers, upon behalf of the membership, hereby expresses sincere appreciation of Doctor Gherardi's numerous contributions, during his membership of 46 years, to the development of Institute activities, and deepest regret at his death, and be it further

RESOLVED: That these resolutions be entered in the minutes and transmitted to the members of Doctor Gherardi's family.

—AIEE Board of Directors, October 24, 1941

might conform with the action of the board of directors on August 8, 1941, abolishing two committees, and with the present rules of the John Fritz Medal Board of Award:

Sec. 65—General Committees. The following committees were deleted: "Committee on Legislation Affecting the Engineering Profession", "Committee on Economic Status of the Engineer".

Secs. 74 and 83 (pertaining to the two former committees mentioned above). Deleted.

Sec. 92—John Fritz Medal. The words "October first" substituted for the words "the third Friday in October" in the second sentence, thus changing that sentence to read: "Each year the President, on October first, shall become a representative of the Institute on the Board of Award of the John Fritz Medal, and the functions of the senior past president of the Institute on this Board shall then cease and determine."

In accordance with section 22 of the by-laws, five members of the board of directors were selected to serve as members of the national nominating committee, as follows:

T. F. Barton, Mark Eldredge, F. Malcolm Farmer, T. G. LeClair, L. R. Mapes; Everett S. Lee and K. L. Hansen *alternates.*

The following additional appointments were made:

H. S. Osborne, an AIEE representative on the Standards Council of the American Standards Association, three-year term beginning January 1, 1942; **H. E. Farrer, R. E. Hellmund,** and **E. B. Paxton** *alternates for 1942.*

John C. Parker, Institute representative on the Hoover Medal Board of Award, for term ending May 1943, succeeding Doctor William McClellan, resigned.

A resolution in memory of Past President Bancroft Gherardi, who died on August 14, 1941, was adopted (page 594).

Other actions taken by the board included the following:

Minutes of the meeting of the board of directors held on August 8, 1941, were approved.

The following actions of the executive committee as of September 16, 1941, were reported and confirmed: 5 applicants transferred to the grade of Fellow; 29 applicants transferred and 19 elected to the grade of Member; 57 applicants elected to the grade of Associate; 24 Students enrolled.

Reports of meetings of the board of examiners held on September 11 and October 23, 1941, were presented, and the recommendations adopted at those meetings were approved. Upon recommendation of the board of examiners, the following actions were taken: 9 applicants were elected to the grade of Member; 42 applicants were elected to the grade of Associate; 585 Students were enrolled.

Monthly expenditures were reported by the finance committee, and approved by the board, as follows: $21,144.46 in August; $24,940.28, September; $31,149.40, October.

Those present were:

President—David C. Prince, Schenectady, N. Y.

Past Presidents—F. Malcolm Farmer, New York, N. Y.; R. W. Sorensen, Pasadena, Calif.

Vice-Presidents—J. W. Barker, New York, N. Y.; J. L. Hamilton, St. Louis, Mo.; K. L. Hansen, Milwaukee, Wis.; N. S. Hibshman, Bethlehem, Pa.; J. Elmer Housley, Alcoa, Tenn.; Everett S. Lee, Schenectady, N. Y.; C. A. Price, Hamilton, Ont.; Walter C. Smith, San Francisco, Calif.

Directors—T. F. Barton, New York, N. Y.; M. S. Coover, Ames, Iowa; Mark Eldredge, Washington, D. C.; Lester R. Gamble, Spokane, Wash.; R. E. Hellmund, East Pittsburgh, Pa.; T. G. LeClair and L. R. Mapes, Chicago, Ill.; Fred R. Maxwell, Jr., Pensacola, Fla.; F. J. Meyer, Oklahoma City, Okla.; W. B. Morton, Philadelphia, Pa.; R. G. Warner, New Haven, Conn.

National Treasurer—W. I. Slichter, Schenectady, N. Y.

National Secretary—H. H. Henline, New York, N. Y.

Institute Finances as Reflected in 1941–42 Budget

At its meeting held on October 24, 1941, the board of directors received from the finance committee a report of the financial operations of the Institute for the appropriation year which ended September 30, 1941, and a recommended budget of income and expenditures for the ensuing year, which was adopted without change. This information is now presented to the membership in the form of a tabulation, with comparable figures for last year and with brief notes regarding those items which deserve special mention.

An increase over last year of 12 per cent in the page content of the TRANSACTIONS section of ELECTRICAL ENGINEERING, a similar increase in the amount of technical material to be published in advance-copy form for use at national and District meetings, one more District meeting than held last year, maximum financial support to Institute Sections under the existing by-laws, increased mileage allowance to delegates because of greater traveling distances to certain meeting places already announced, the restoration of funds for all national prizes, the addition to headquarters' staff of two persons who will serve in a junior clerical capacity, salary increases totaling $1,500 and affecting nine members of the staff—all

Institute Income and Expenses for the Year Ending September 30, 1941, and Budget for Year Ending September 30, 1942

	Actual Income and Expenses, Year Ending 9-30-41	Budget for Year Ending 9-30-42
Income		
Dues	$217,547.35	$224,000.00
Students' fees	13,355.70	13,000.00
Entrance and transfer fees	9,412.73	8,000.00
Advertising	49,788.59	50,000.00
ELEC. ENGG.—non-mem. subscriptions	13,277.52	10,000.00
TRANS. subscriptions	6,875.58	6,500.00
Miscellaneous sales	21,213.46	20,000.00
Interest on securities	6,472.02	5,500.00
Total	$337,942.95	$337,000.00
Expenses		
Publications:		
Text matter (ELEC. ENGG. & TRANS.)	83,094.86	$ 82,410.00*
TRANS. SUPPLEMENT	2,125.01	1,700.00
Preprints	7,369.40	9,000.00
Advertising section—ELEC. ENGG.	22,477.83	23,450.00
Year Book	6,965.73	7,250.00
Miscellaneous expense	1,261.07	1,500.00
Institute meetings	13,485.24	15,150.00
Institute Sections:		
Appropriations	26,576.71	28,500.00
Other expenses	5,856.41	6,050.00
Institute Branches:		00
Meetings expenses	1,046.04	1,200.00
Other expenses	2,320.58	2,700.00
Committees:		
Code of prin. prof. conduct		50.00
Edison Medal	159.86	170.00
Finance	741.68	775.00
Headquarters	183.48	250.00
Lamme Medal	181.30	185.00
Membership	8,756.13	9,240.40
Pension Fund		500.00
Radio broadcasts	504.06	(see text)
Research		150.00
Standards	8,189.74	10,075.00
Technical committees	349.70	500.00
Traveling Expenses:		
Geo. Dist. exec. committees	3,091.94	4,000.00
Section delegates to summer conv.	5,624.96	5,250.00
Counselor delegates to summer conv.	892.94	750.00
Dist. secys. to summer conv.	393.56	750.00
District Student conferences	7,093.63	9,500.00
President's appropriation	960.44	1,000.00
Vice-presidents	697.51	1,000.00
Board of directors	6,808.73	8,000.00
National nominating committee	1,136.22	1,100.00
Past presidents and other AIEE representatives		500.00
Administration:		
Headquarters' salaries	36,273.67	38,585.00
Postage	4,331.46	4,500.00
Stationery & printing	3,824.02	4,000.00
Office equipment	443.93	1,000.00
Trav. expense, bank charges, insurance, misc. supplies and services	4,627.04	4,750.00
Paper prizes	553.05	850.00
Joint activities:		
American Engineering Council	2,075.00	
Amer. Co-ord. Com. Corrosion	25.00	25.00
American Standards Association	1,500.00	1,500.00
ECPD	850.00	1,700.00
Engg. Foundation research projects:		
Impregnated paper insulation	250.00	250.00
Insulating oils and cable saturants	250.00	250.00
Welding	250.00	250.00
Engg. Soc. Personnel Service, Inc.	1,245.45	1,200.00
Engg. Soc. Library	10,072.10	10,260.00
John Fritz Medal	50.00	50.00
N.F.P.A. Dues	60.00	60.00
United Engg. Trustees building assessment	10,984.81	10,985.00
U. S. Natl. Com. I.C.I.	300.00	300.00
Miscellaneous printing, etc.		6,000.00
Authors' reprints	3,902.28	
Reprints of standards	1,780.75	
Miscellaneous	1,082.56	
Other expenses:		
Membership badges	2,209.78	2,400.00
Legal services	250.00	250.00
Pension Fund Reserve	5,000.00	8,000.00
Prepaid ELEC. ENGG. expenses (text paper and env. in storage)	4,181.22	
Depreciation Reserve Fund	69.89	
Unappropriated:		
Reserved for contingencies and additional items		7,180.00
Total	$314,786.77	$337,000.00

*Actual amount available $86,591, including prepaid expenses.

Future AIEE Meetings

Southern District Meeting
New Orleans, La., December 3–5, 1941

Winter Convention
New York, N. Y., January 26–30, 1942

North Eastern District Meeting
Schenectady, N. Y., April 29–May 1, 1942

Summer Convention
Chicago, Ill., June 22–26, 1942

Pacific Coast Convention
Vancouver, B. C., September 9–11, 1942

these are provided for in the budget of expenditures. In addition, the annual appropriation for the proposed pension plan is increased from $5,000 to $8,000 to cover a preliminary estimate of the maximum probable amount of the annual accruing liability to the pension fund. The policy inaugurated last year of allowing for contingencies and probable additional items is continued, the budget including an unappropriated item of $7,180, from which the board subsequently appropriated $500 for radiobroadcasts to be sponsored by several of the engineering societies, and $200 toward the expenses of the Engineers Defense Board.

The increase of income necessary to carry this increased program comes principally through the larger membership of the Institute. The estimated income for the present fiscal year is practically the same as the actual income for the year which has just closed. This is because further increases resulting from continued increase in membership of the Institute during the current year are expected to be largely offset by losses in dues revenue from members now enrolled in military service, from overseas members, and from overseas subscriptions to Institute publications. Losses of this nature, which were not large in the last fiscal year, are expected to be considerably greater this year because of the increasing effect of war conditions.

The July issue of ELECTRICAL ENGINEERING carried in the news section (pages 336–50) the complete report of the Institute board of directors for the fiscal year ending on April 30, 1941, together with financial statements for the corresponding period. In this report will be found a comprehensive statement covering all activities of the organization, making it unnecessary to repeat at this time the details underlying appropriations for the principal activities. Should further information be desired, this can be obtained upon correspondence with Institute headquarters.

Dielectric Strength of Oil for Circuit Breaker Tests Approved

For some time a working group of the AIEE committee on protective devices has been actively studying the subject of the dielectric strength of oil for use when making impulse and low-frequency tests on oil circuit breakers. The results of this study were presented in a report at the 1941 AIEE summer convention, Toronto, Ont. ["Dielectric Strength of Oil for High-Voltage Testing of Oil Circuit Breakers," H. J. Lingal, W. F. Skeats, and H. D. Braley, AIEE TRANSACTIONS, volume 60, 1941 (September section) pages 903–06.] At its meeting of September 25 in Cleveland, Ohio, the committee on protective devices approved the recommendation of the working group (subcommittee on circuit breakers, switches, and fuses) for the use of oil having a dielectric strength of not less than 22 kv (measured under standard test conditions) in making impulse and 60-cycle tests.

The recommendation was made after considering the subcommittee's report, which described impulse tests on oils of different 60-cycle dielectric strength in both sample test gaps and full-size standard circuit breakers. The report showed that the impulse tests of oil circuit breakers were not appreciably changed by the presence of carbon and water in the oil. In some tests the impulse voltages required to break down the oil were higher for oils containing carbon and water than for new clean oil.

New Fault-Current-Calculating Procedure Recommended to Industry

A proposed new procedure for the calculation of short-circuit currents has been embodied in a report prepared under the auspices of the AIEE committee on protective devices, presented at the 1941 summer convention at Toronto, Ont., June 16–20, and published in the AIEE TRANSACTIONS, volume 60, 1941 (September section), pages 877–81. (Discussion of the report, also of interest, will appear in the December 1941 TRANSACTIONS and in the December 1941 Supplement to Electrical Engineering—Transactions Section.) The committee urges the electrical industry to apply the new method and compare it with methods previously in use. Comments or suggestions will be welcomed, and should be sent to J. R. North, chairman, AIEE committee on protective devices, 212 West Michigan Avenue, Jackson, Mich., before May 31, 1942.

The precise determination of short-circuit currents involves a calculation so laborious as to be wholly impractical. Thus, some approximation is required, and a degree of judgment must be applied in any method proposed. The new method is based upon the determination of an initial value of rms symmetrical current with which multiplying factors are used for application purposes. It is proposed that this method be used where applicable, in place of the present method which involves the use of decrement curves. It is believed that the procedure is sufficiently accurate to serve as a reliable basis for the application of interrupting devices and for a preliminary setting for relays.

In the determination of this current, symbols are involved which have the following significance:

E = leg voltage
X_1 = direct axis reactance, either transient or subtransient as specified, in ohms/leg
X_0 = zero-sequence reactance
R_0 = zero-sequence resistance

Table I. Circuit Breakers, Protection Tubes, and Fuses

	Multiplying Factor	Reactance Quantity for Use in X_1: Synchronous Generator	Synchronous Motor	Induction Machine
A. Circuit-Breaker Interrupting Capacity				
1. General case				
Eight-cycle breaker	1.0	Subtransient	Transient	
Five-cycle breaker	1.1			
Three-cycle breaker	1.2			
Two-cycle breaker	1.4			
2. Short circuits fed predominantly by large machines at the point of fault may be increased up to 20 per cent				
3. Air circuit breakers rated 600 volts and less	1.25	Subtransient	Subtransient	Subtransient
B. Mechanical Stresses and Momentary Rating of Circuit Breakers				
1. General case	1.6	Subtransient	Subtransient	Subtransient
2. At 5,000 volts and below, unless current is fed predominantly by directly connected synchronous machines or through reactors	1.4			
C. Protector Tubes				
1. Maximum rating 2. Minimum rating—use minimum system capacity and minimum of E/X_1 or $3E/(2X_1+X_0)$	1.0	Subtransient	Subtransient	Subtransient
D. Fuses				
1. General case	1.6	Subtransient	Subtransient	Subtransient
2. At 15,000 volts or below with interrupting ratings not exceeding 3,000 amperes	1.2			

Table II. Relays

	Multiplying Factor	Reactance Quantity for Use in X_1: Synchronous Generator	Synchronous Motor	Induction Machine
1. High-speed current actuated	1.0	Subtransient	Subtransient	Subtransient
2. Time overcurrent	1.0	Transient	Transient	

The three-phase short-circuit current is $\frac{E}{X_1}$.

The line-to-line short-circuit current is $\frac{\sqrt{3}E}{X_1+X_2}$. Since X_2 is always at least equal to X_1, this quantity never exceeds 86 per cent of the three-phase short-circuit current and consequently may be neglected.

The line-to-ground short-circuit current is $\frac{3E}{X_1+X_2+X_0}$. Since X_2 is usually approximately equal to X_1, this expression is often shortened to $\frac{3E}{2X_1+X_0}$. In practical cases, regardless of the value X_2, this last expression also gives a satisfactory value for the current available from a double line-to-ground fault.

PROCEDURE

The following procedure gives a résumé of the various multiplying factors to be used with currents calculated by the formulas just stated, and Tables I and II show what reactance quantity should be used for representing the machines in the positive-sequence network.

Circuit Breakers, Protector Tubes, and Fuses. Determine "highest value of rms symmetrical current for any type of fault" by $\frac{E}{X_1}$ or $\frac{3E}{2X_1+X_0}$, whichever is greater, except that when R_0 is greater than $5X_1$ no consideration need be given to the latter term.

Basis for Preliminary Relay Settings. Two conditions should be determined for each class:

1. Maximum connected synchronous capacity and "the maximum initial symmetrical current" determined by $\frac{E}{X_1}$ or $\frac{3E}{2X_1+X_0}$, whichever is greater, except that when R_0 is greater than $5X_1$ no consideration need be given to the latter term.

2. Minimum connected synchronous capacity and "the minimum symmetrical current" determined by $\frac{0.866E}{X_1}$ or $\frac{3E}{2X_1+X_0}$, whichever is the smaller. Consideration should be given in particular situations to remote fault locations and fault resistance.

Report on the Metering Art to Be Issued as Pamphlet

The report on "Progress in the Art of Metering Electric Energy" sponsored by the Institute's committee on instruments and measurements, now being published serially in ELECTRICAL ENGINEERING and of which the concluding article appears in this issue, is being reprinted in pamphlet form in response to a demand for such a booklet.

A carefully prepared history of the metering art, the report contains four parts: I. Origins, covering invention and pioneering development before 1900, with particular attention to the men responsible (*EE, Sept. '41, p. 421–7*); II. Growth and Development, outlining progress in the art from 1900 to the present, in improved methods and adaptations to modern production trends (*EE, Oct. '41, p. 469–78*); III. Special Applications, showing how the basic energy-metering unit has been modified for use with three-wire and polyphase circuits and describing the development of demand meters (*EE, Nov. '41, p. 540-6*); and IV. Calibration and Installation of Watt-Hour Meters (*p. 581–6*). An appendix to the series (*p. 587–9*) lists sources of material, not only books and magazine articles, but museums and collections, and includes a tabulation of significant meter patents. Believed to be the first historical survey of this type on the subject of metering, the report not only has great value and significance for all those interested in meters, but also constitutes an important chapter in the yet-unwritten history of the electrical industry.

Copies of the pamphlet "Progress in the Art of Metering Electric Energy" may be obtained from the AIEE order department, 33 West 39th Street, New York, N. Y. Prices are 25 cents per copy to AIEE members; 50 cents per copy to nonmembers; special prices will be quoted on quantity orders.

District • • • •

District 7 Announces 1940 Prizes

The AIEE South West District (7) has announced District prize awards for student papers presented during the academic year ending June 30, 1940. Other District prizes for 1940 papers were announced in ELECTRICAL ENGINEERING, July 1941, page 351, and September 1941, page 428.

District 7

Prize for Branch paper was awarded to Robert P. Watson (Enrolled Student) for his paper "Electronic Visualization of Magnetic Fields," presented at the South West District Branch conference, April 19–20, 1940, Lubbock, Tex. Honorable mention for Branch paper was given to Leroy W. Evans and Raymond E. Glass (Enrolled Student) for their paper "The Study of the Accumulation of High-Potential Static Charges by Wind-Tunnel Method," and to Max H. Mesner for his paper "The Voltage Quadrupler," presented at the same Branch conference.

Prize for graduate student paper was awarded to Luther E. Johnson (A'41) for his paper "A Consideration of Some Possibilities for Electrical Engineering in Ordinary Land Surveying," also presented at the South West District Branch conference, April 19–20, 1940, Lubbock, Tex. Honorable mention for graduate student paper was given to LeRoy C. Tillotson (A'39) for his paper "An Analysis of the Single-Phase Full-Wave Gas Rectifier Loaded with a Choke Input Filter," presented at the same Branch conference.

Section • • • •

Leland Olds Addresses Joint Washington-Maryland Meeting

Reported as one of the most heavily attended AIEE Section meetings to be held in Washington, D. C., was the joint meeting of the Maryland and Washington Sections held November 17 in the auditorium of the Potomac Electric Power Company. Some 300 persons, about 100 of them from the Maryland Section, brought out "S.R.O." signs, according to reports. Some 160 of those attending also attended a dinner in honor of the speaker held in advance of the meeting.

Chairman Leland Olds of the Federal Power Commission, vice-chairman of the National Power Policy Committee, addressed the joint gathering on the subject "Power for National Defense." Mr. Olds discussed in some detail the present power situation, with special reference to the fundamental importance of adequate electric power to the whole national defense program. He discussed the relation of expected power demand to available power supply, and outlined the steps that are being taken to minimize any shortage in any area.

It seems probable that Chairman Olds discussed a good many of the points that will be treated in an article "Power System Development on a National Scale," prepared by Thomas R. Tate, director, National Defense Power Staff, Federal Power Commission, for the forthcoming January issue of ELECTRICAL ENGINEERING.

Sections Committee Urges Action on National Problems

The following letter, sent by the chairman of the AIEE Sections committee to all Institute vice-presidents, District secretaries, and chairmen of Sections, is here presented because it is believed by the Sections committee to be of interest and significance to the membership at large:

To All Vice-Presidents, District Secretaries, and Section Chairmen:

America must not lose its moorings.

Right now America is making a huge effort toward total National Defense.

Its first line of defense is the American home and all that it does or should represent.

Its second line of defense is its vast system of industries and supply of raw materials.

Its third line of defense is national unity.

Those represent preparations for war.

They have been in the process of formulation for years.

Now is the time to prepare for the repercussions of peace.

Emotions must be stabilized by some sound thinking.

Our national spiritual foundation must be reinforced.

Much of the old unrestricted enterprise is gone.

America must face realistically such restrictive regulation as may be needed and exert every influence in the conduct of business to prevent overregulation.

America has the greatest industrial plant in history. It has enormous funds. It has adequate man power and brains. These *must be utilized* to relieve the shock of peace.

Engineers have been held responsible for the recent economic upheaval.

Now the whole world has turned to them pleading for rescue from chaos.

Here is unparalleled opportunity calling for the right kind of leadership supported by teamwork.

America needs it more than at any time in its existence.

Let us as engineers be quick to seize this challenge.

Freedom of religion must be preserved.

Freedom of education must be preserved.

Freedom of speech must be preserved.

Freedom of the press must be preserved.

Freedom of enterprise consistent with social welfare must be preserved.

Freedom to choose and to change representation in government must be preserved.

Plants and employees must be kept busy producing new products and more products for more people at less cost.

The preservation of all of these freedoms is fundamental to the continuance of the American way of life.

The American way of life provides a large measure of individual opportunity, but it requires in return individual responsibility to society as a whole.

Attention has been directed to some of the major problems of the present and future by Charles E. Wilson (ELECTRICAL ENGINEERING, March 1941), by Howard Coonley (ELECTRICAL ENGINEERING, July 1941), by AIEE President D. C. Prince (*General Electric Review*, July 1941), and by many others.

Electrical engineers are among the recognized leaders in our nation.

Your Institute officers urge you to preserve and to strengthen that position of leadership.

There is capable leadership in every Institute Section. Put it to work. Give it your support.

Your Institute officers urge upon each Section:

1. That it will try to develop an increasing sense of professional conscientiousness and a measure of obligation to assume distinctive, constructive leadership in the problems of human relations, community interests, and public relations in the local area.

2. That it will assist in determining the readjustments that must be made, then *work with a will before it is too late*. In many instances members may have the opportunity to work with the local engineering council which, in turn, can co-operate with the local chamber of commerce and other civic bodies.

3. That it will undertake a program of vocational education, especially co-operating with the high schools and the colleges in which this new challenge to the engineering profession will be injected.

4. That it will make this broad effort objective number one by devoting an early meeting at which this next national job may be presented and discussed.

5. That it will appoint one or more of its members to direct this special effort and keep it moving.

6. That it will submit to the chairman of the Sections committee for distribution to all other Sections such materials and ideas as may assist in moving this program forward.

DO NOT WAIT—ACT NOW

M. S. COOVER
Chairman, Sections Committee

Sections Consider Peacetime Planning

Three Institute Sections, Cleveland, Philadelphia, and Niagara Frontier, are giving attention to the development of workable plans for the shift to peacetime production at the end of the present emergency, the Sections committee reports.

The Cleveland Section has set up a "social conditions committee," which held its first meeting October 22, 1941. The desirability of continuing research during the emergency, various aspects of taxation and labor, importance of presenting all sides of economic problems in schools and colleges, consideration of a possible national slogan to identify and stimulate the work of the engineering profession on current problems were among subjects discussed. The committee is considering the feasibility of forming itself into a seminar to meet every two weeks for serious study.

Members Urged To Contact Local Sections

The Institute's Washington Section has sent word to national headquarters urging members normally affiliated with other Sections but now finding themselves more or less temporarily situated in the Washington Section territory, to make their whereabouts known to officers of that Section. It is pointed out that this would enable the Section to circulate meeting notices and would afford opportunity for direct participation in local Section affairs. Members temporarily established in Washington are invited to correspond with F. W. Willcutt, secretary, care Potomac Electric Power Company.

Members temporarily resident in the territory of other Sections likewise may find it profitable to identify themselves with officers of the nearest local Section. A complete listing of Sections will be found in the recent September issue of ELECTRICAL ENGINEERING.

Arizona Section Members Travel

The AIEE Arizona Section, newly organized during 1941, held its first fall meeting at Prescott, Ariz., with 10 members and 14 visitors present. The total mileage traveled by those attending the meeting was reported to be 5,442 miles, with the longest individual round trips 700, 600, and 500 miles. Only two persons present had round trips of less than 64 miles.

The meeting voted formal acceptance to the bylaws previously given tentative approval. The program was concerned with "Use of Electricity in Copper Mining in Arizona."

Abstracts • • •

TECHNICAL PAPERS are previewed in this section as they become available in advance pamphlet form. Copies may be obtained by mail by remitting price indicated to the AIEE order department, 33 West 39th Street, New York, N. Y.; or at five cents less per copy if purchased at AIEE headquarters or at AIEE convention or District-meeting registration desks.

The papers previewed in this issue will be presented at the AIEE Winter Convention, New York, N. Y., January 26–30, 1942.

Air Transportation

42-7—A D-C Telemeter or D-C Selsyn for Aircraft; *R. G. Jewell (A'30) and H. T. Faus (M'34). 15 cents by mail.* A toroidal resistance winding having three taps spaced 120 degrees and a rotatable brush assembly which supplies d-c electric energy at diametrically opposite points constitutes the transmitter. The indicator comprises a permanent-magnet rotor surrounded by a core of low-hysteresis magnetic material carrying three delta-connected coils spaced 120 degrees. The three taps on the transmitter are connected to the three common points of the indicator coils. A diametrical magnetic field is established in the indicator which causes the magnetic axis of the permanent-magnet rotor to come into alignment. The position of the indicator magnetic field is dependent upon the position of the transmitter brushes. The torque, accuracy, size, and weight characteristics make this telemeter particularly suitable for the remote indication of various aircraft functions.

Basic Sciences

42-27—Formulas for the Magnetic Field Strength Near a Cylindrical Coil; *Herbert B. Dwight (F'26). 25 cents by mail.* A group of formulas involving natural logarithms is derived, to give the axial and radial magnetic field intensity at small distances from a solenoid, in the absence of magnetic material. The radial thickness of the solenoid winding is taken care of by additional formulas. Since these and other series formulas are the result of integration from one end of the solenoid to the other, they occur as the difference of two quantities. It is shown in this paper that it is advantageous to give a physical meaning to these two quantities separately, so that, for instance, one may be computed by a long-coil formula and the other by a short-coil formula, if desirable. This greatly increases the range in which the flux density of solenoids under all conditions can be precisely and quickly calculated. In order to express the formulas in the form just described, expressions are derived for the magnetic field strength at points in the end plane of an infinitely long solenoid. By arranging the available series formulas in the manner described, a complete equipment is given for computing the magnetic field of a circular solenoid of any shape and at any point, including points within the cross section of the winding. Several numerical examples are included. A chart is given to assist in choosing the appropriate formulas for a given case.

Electric Welding

42-25—Resistance-Welding Transients; *E. E. Kimberly (M'41). 15 cents by mail.* Many articles published on the subject of resistance welding deal briefly and qualitatively with the importance of switching transients in their effect on the total heat produced in a short-time weld. This paper deals with the same phenomenon quantitatively. Oscillograms of current and power in the weld show that in the first few cycles after random (indiscriminate phase-angle) switching in repetitive welding the heat input to the weld may vary from weld to weld as much as 50 per cent from the optimum. As the number of cycles in the weld period increases, the heat error caused by transient decreases. If the weld period is greater than about one third second, the heat error may be ignored, and although the cost of accurate switching control may be justified because of line-voltage disturbance and because of

exploding or splashing in projection welding, it cannot be justified for accurate heat-control alone. The need for accurate phase-angle switching when the weld time is very short and when the metallurgy of the stock requires accurate temperature limits is clearly shown.

Electrical Machinery

42-1—Progress Report of D-C Testing of Generators in the Field; *E. R. Davis (A'41) and M. F. Leftwich (A'30). 15 cents by mail.* Considerable interest has been shown in field tests of generator insulation, particularly with mobile test apparatus. The development of a portable d-c apparatus with a range of 0–14,000 volts, capable of testing large hydro- and turbogenerators, is set forth in this paper. The initial charging and insulation leakage current at various temperatures is described by several curves. A few interesting tests, which indicate definite possibilities of high voltage d-c testing, are cited to illustrate its feasibility. The method of correlating the test results on individual generators derives from 2,368 periodic field tests made over a period of ten years with high d-c voltage is presented. The detection of latent generator insulation weaknesses without damage to core iron or adjacent coils with a mobile high-voltage d-c test apparatus has proved economical from a service and operating standpoint.

42-3—Equivalent Circuits for the Hunting of Electrical Machinery; *Gabriel Kron (A'30). 15 cents by mail.* A general method is given to establish equivalent circuits for the determination of the hunting characteristics, such as damping and synchronizing torques, of standard types of electrical machines. The method is illustrated by setting up steady-state and hunting equivalent circuits for the salient-pole synchronous machine having amortisseur windings and for the doubly fed single-phase Selsyn with unbalanced windings, special cases of which are the capacitor motor and the doubly fed polyphase motor. A companion paper "The Doubly Fed Machine" (42-4) contains a detailed study of the characteristics of one of the equivalent circuits as measured on the a-c network analyzer.

42-4—The Doubly Fed Machine; *C. Concordia (M'37), S. B. Crary (M'37) and Gabriel Kron (A'30). 15 cents by mail.* This paper presents a general analysis of the doubly fed machine (a synchronous machine with polyphase a-c excitation on both stator and rotor) and shows the characteristic curves of damping and synchronizing torques during hunting, as affected by the machine parameters. Equivalent circuits are presented which may be set up on an a-c network analyzer, so that these damping and synchronizing torques during hunting may be determined simply by direct measurement of watts and vars in the circuit. Equations for the transient short-circuit currents are also included.

Industrial Power Applications

42-19—A Static Voltage Regulator Insensitive to Load Power Factor; *Claude M. Summers (M'39) and T. T. Short. 15 cents by mail.* A new type of static voltage regulator, for those applications where performance is more important than efficiency, is described in this paper. It has the distinction of supplying a constant output voltage which is independent of load power factor. The regulator in its preferred form consists of two reactors and two capacitors. One reactor and one capacitor form a constant-current circuit and the other capacitor and reactor form a constant-voltage circuit, so that the regulator first converts a variable-voltage source to a constant current and then to constant potential. The regulator has many interesting characteristics such as inherent overload protection, and high speed of response, as well as close regulation for simultaneous variation in line voltage, load, and load power factor. Brief descriptions of the design procedure, operating characteristics, and some applications are given.

42-21—The Fundamentals of Industrial Distribution Systems; *D. L. Beeman (A'31) and R. H. Kaufmann (M'41). 25 cents by mail.* The intensive manufacturing activity accompanying the present defense program has stimulated interest in industrial electric-power distribution. The ultimate objective is one of effectively satisfying electric-power requirements with reasonable first cost consistent with a fair standard of safety and service reliability. This paper presents the fundamental aspects of industrial power distribution, with particular reference to low-voltage power supply to distributed electrical machinery and compares various basic system designs, including large concentrated substations and distributed load-center substations with radial and secondary network modifications, as to safety, service reliability, simplicity, etc., relative to estimated installed cost. The comparative analysis comprehends the complete electrical system between high-voltage supply bus and utilization terminal of low-voltage feeders. The ideal size of unit substation as influenced by operating voltage and load density is covered. Principles of system design here disclosed are applicable not only to new plant construction but to expansion or modernization of existing plants as well.

Instruments and Measurements

42-5—The Acceleration-Oscillogram Method of Motor-Torque Measurement; *C. R. Atkinson (A'31) and E. G. Downie (A'35). 15 cents by mail.* The need for an improved method of measuring starting torque of large induction-starting synchronous motors, as compared with the power input and dynamometer methods, has led to the use of the acceleration oscillogram. A low-ripple permanent-magnet-type d-c generator is driven by the motor, and traces a time–speed oscillogram, from which acceleration, and the torque producing it, may be calculated. Comparative torque tests, at full and reduced voltage, made by this and the other methods on the dynamometer-coupled motor, showed the definite advantage of the acceleration tests in combined convenience and accuracy. Interesting facts about synchronous-motor starting torques, not accurately shown by previous tests, have been brought to light. The acceleration or deceleration oscillogram is also applied to the measurement of torques or losses of very small high-speed motors by using other methods of rotation indication involving no loading of the motor.

42-15—Measurement of Maximum Demand; *P. M. Lincoln (F'12). 20 cents by mail.* This paper describes in detail the thermal storage method of measuring the maximum demand of a user of electric service. It makes a comparison between this method and the commonly used block-interval method. It points out that the block-interval method must necessarily be a discontinuous function of time and as such be subject to a possible error of 50 per cent—a possibility that can become a certainty at the option of the service user—while the thermal storage method, being a continuous function of time, can only indicate a single value for maximum demand no matter what may be the character of the load under measurement. Tests on thermal-storage demand meters are given in some detail.

Land Transportation

42-23—Progress in Design of Electrical Equipment for Large Diesel-Electric Locomotives; *Gerald F. Smith (A'13). 15 cents by mail.* During the last eight years, as the result of development of the Diesel engine, Diesel-electric locomotives have come into wide use for heavy switching, passenger, and freight service. There has also been a rapid development in the electrical equipment, going back about 15 years. For present high-speed passenger locomotives, electrical equipment is available with a weight between 20 and 21 pounds per engine horsepower, with continuous rated speed 33 per cent of maximum service speed of above 100 miles per hour and with sufficient maximum tractive effort to slip wheels at 33 per cent adhesion. For freight locomotives with double the number of motors per power plant, the weight per engine horsepower is between 30 and 31 pounds per engine horsepower, and the continuous rated speed 16 per cent of maximum rated speed.

Power Transmission and Distribution

42-2—Relative Value of Different Types of Overcurrent Protection for Distribution Circuits; *G. F. Lincks (A'37). 15 cents by mail.* According to Lord Kelvin, we have only a meager and unsatisfactory knowledge of a subject until it can be measured and expressed numerically. Actual service data on the benefit of branch protection and line sectionalizing with protective devices connected in series are not available. It would be very difficult to obtain such data on all types of protective devices in service at different points on any one distribution circuit. This has been determined by a mathematical study. The actual consumer minutes outage has been expressed as a percentage of the outage time caused by permanent faults alone when no sectionalizing or branch protection is used. The study covered a range of temporary

faults from 25 to 85 per cent of the total number of faults. All types of fuse cutouts and reclosing breaker arrangements at the substation, at sectionalizing points connected in series, and on varying-length branches are included in the study. This knowledge of the relative benefits of distribution overcurrent protective equipments and their applications should be of value in economical system planning.

42-10—Temperature and Electric Stress in Impregnated-Paper Insulation; *J. B. Whitehead (F'12) and W. H. MacWilliams (Enrolled Student). 15 cents by mail.* This paper reports studies of the time rate of change of power factor and loss in thoroughly impregnated paper insulation, due to the separate and to the combined influences of high temperature and high stress. It is found that the rate of deterioration as measured by power factor is very much greater for combined temperature and stress than for either singly, and in fact much greater than that observed when the oil contains a large amount of oxygen. These effects are very pronounced at temperatures and pressures only slightly above those now reached in the operation of power cables. They indicate rapid chemical changes in the insulation and are attributed to a great increase in electrolytic dissociation in the oil. Tests of this character should provide a reliable method for study of the relative chemical stabilities of cable and capacitor saturants.

42-13—Multichannel Carrier-Current Facilities for a Power Line; *P. N. Sandstrom (A'25) and G. E. Foster (A'32). 15 cents by mail.* A carrier-current system providing a relatively large number of channels is in service on a high-voltage power line. The facilities provide:

1. Transmission of signals both ways for the opening of the circuit breakers at the remote end by the operation of relays at the near end.
2. Two-way telephone service between any extension telephone at the remote generating station and any telephone connecting to the main telephone switchboard in the central office building.
3. Two-way telemetering (station generation one way, and system total generation the other way).
4. Transmission from the system operator's office to the station of automatically generated load-control signal used to increase or decrease automatically the station generation.
5. Two channels in each direction for future requirements.

This paper describes the methods employed to obtain these channels over a single power line, including the special precautions taken with the high-speed transferred trip signals to prevent faulty tripping of the line due to external disturbances that might generate carrier-current tripping pulses.

42-14—Shielding of Substations; *C. F. Wagner (F'40), G. D. McCann (A'38), and C. M. Lear. 15 cents by mail.* A previous paper by the authors considered the shielding afforded transmission lines by ground wires and presented a method for suitably simulating the mechanism of natural lightning for laboratory tests with models. This paper continues the investigation as applied to the shielding of substation structures. Recommendations are given for the location of overhead ground wires and vertical masts to provide adequate shielding to the protected object.

42-16—Lightning Investigation at High Altitudes in Colorado; *L. M. Robertson (M'38), W. W. Lewis (F'38), and C. M. Foust (M'31). 25 cents by mail.* An investigation was begun in 1938 on the Shoshone-Denver 100-kv line to determine the probable lightning current at altitudes from 6,000 to 13,500 feet. The results show a decrease of stroke current with altitude, and by extrapolation the entire absence of lightning current at about 18,000 feet is indicated. Observations of temperatures at high altitudes indicate that at 18,000 feet the air temperature never exceeds 32 degrees Fahrenheit. The possible connection between the absence of lightning current and temperatures at or near freezing is discussed. The percentage of positive currents was comparatively high. The investigation was extended to the measurement of corona current at 5,280 and 13,500 feet, and in 1941 measurements were obtained in 51 storms at 13,500 feet. A comparison with similar measurements made at low altitude indicates about the same maximum potential gradient, but a much higher average gradient at the high altitude.

42-17—Field Investigations of Lightning Currents Discharged by Arresters on the American Gas and Electric Company System; *I. W. Gross (M'40), G. D. McCann (A'38), and Edward Beck (M'35). 20 cents by mail.* For the past three years data have been collected on the wave shape of lightning currents discharged by arresters in stations of the Ohio Power Company and the Appalachian Electric Power Company with Fulchronographs, cathode-ray oscillographs, and magnetic surge-front recorders. Fulchronographs and magnetic surge-front recorders have been installed at five three-phase arrester banks. At two of these, cathode-ray oscillographs were also installed. Records have been obtained of 49 single-phase arrester discharges which yielded Fulchronograph records of 88 individual components, cathode-ray oscillographs of 9, and magnetic surge-front records of 18.

42-18—Lightning Investigation on 132-kv System of the American Gas and Electric Company; *I. W. Gross (M'40) and G. D. Lippert (A'38). 25 cents by mail.* This paper presents and discusses field records of natural lightning currents recorded on the 132-kv transmission system of the American Gas and Electric Company during the past nine years, although most of the records have been obtained during the past four years. Magnitude and frequency data on lightning currents in transmission wires, ground wires, tower structures, counterpoises, and ground rods are given. There are also discussed records obtained by the wave-slope indicators on the rate of change of voltages appearing at the entrance to transmission stations, some of which at least are caused by lightning. These data are considered in connection with recorded line currents entering a station and co-ordinated with the rates of voltage rise, calculated line surge impedance, bus voltages, and lightning-arrester performance. Comparison of effectiveness of various lengths and designs of counterpoises and ground rods is given.

42-22—Impulse and 60-Cycle Characteristics of Driven Grounds—II; *P. L. Bellaschi (F'40), R. E. Armington (Enrolled Student), A. E. Snowden (Enrolled Student). 30 cents by mail.* This paper extends the contribution of the first paper experimentally, theoretically, and from the application standpoint. Data are presented on 16 grounds ranging from 8 to 30 feet deep. Eleven are in clay soil, two in gravelly soil, one in sand, and two in a mixture of clay and stones. Sixty-cycle data and impulse data up to 15,500 amperes are given for the single grounds and for parallel combinations. Curves, tables, and typical cathode-ray oscillograms sum up the more pertinent findings. Methods have been developed for determining 60-cycle and impulse characteristics of single and parallel grounds. Curves calculated are in substantial agreement with the experimental results. The discharge-circuit inductance of a ground installation is dealt with and its significance is discussed.

Protective Devices

42-8—Performance of Ground-Relayed Distribution Circuits During Faults to Ground; *C. L. Gilkeson (M'34), P. A. Jeanne (M'30), and J. C. Davenport. 15 cents by mail.* In connection with studies by the Joint Subcommittee on Development and Research of the Edison Electric Institute and Bell Telephone System, of problems of protection where power and telephone circuits are on jointly used poles, extensive oscillographic observations were made of the performance of relaying systems and other equipment for clearing ground faults on power distribution circuits, chiefly on circuits above five kilovolts. Of the data obtained, those relating to feeders equipped with instantaneous ground relays and for immediate reclosure have been selected for presentation in this paper as being of considerable interest outside the specific study for which they were secured. Data are given as to the means by which faults were cleared, speed of initial interruption and of automatic reclosure, per cent of faults clear on first reclosure, fuse and relay co-ordination, fault characteristics, etc. Also limitations on ground relaying imposed by fuse and relay co-ordination, residual load currents and transients following feeder re-energization are discussed.

42-9—Field Tests and Performance of a High-Speed 138-Kv Air-Blast Circuit Breaker; *Philip Sporn (F'30) and H. E. Strang (M'39). 15 cents by mail.* A 138-kv air-blast circuit breaker of novel design has recently been subjected to a series of field tests, up to values of short-circuit duty substantially in excess of its assigned rating of 1,500,000 kva. These tests included both normal interrupting duty and superspeed reclosing service when the breaker was called upon to interrupt, reclose in less than 20 cycles, and again interrupt the fault current. While still somewhat of an innovation in the high-voltage field, the air-blast circuit breaker undoubtedly has certain basic advantages. It is

believed that these tests are an important step forward in developing the possibilities of the air-blast breaker for high-voltage service and that they have brought the entire electric-power industry closer to the possibility of benefit from an application of this interrupting principle.

42-11—Current-Transformer Performance Based on Admittance-Vector Locus; *A. C. Schwager (M'31). 15 cents by mail.* In the past, current-transformer performance has been defined by ratio-error and phase-angle curves in which the abscissa represents primary or secondary current to a linear scale. Numerous curves were necessary for determining the errors for the multiplicity of secondary burdens. This paper shows that a more functional picture of current-transformer operation is obtained by replacing these curves by the admittance-vector locus of the secondary winding. The numerous ratio and phase-angle curves resulting from various secondary burdens and, in case of multiratio transformers, from different numbers of turns, revert to one single curve. Ratio error and phase angle for any burden at any power factor, turn ratio, and secondary current, can be scaled or read directly from a single chart containing the admittance-vector locus.

42-12—Field Tests on High-Capacity Station Circuit Breakers; *H. D. Braley (A'18). 15 cents by mail.* The development of high capacity air-blast breakers in the United States has taken place without the background of operating experience that has attended the use of oil circuit breakers and has, therefore, emphasized the need for testing this equipment at levels comparable with the assigned interrupting ratings. Although field short-circuit tests to verify circuit-breaker performance have been made on operating systems previously, they have been limited in most instances to moderate-duty levels or, in the larger interrupting ratings, to the testing of high-voltage apparatus. Staging severe short-circuit tests at 15 kv introduces operating problems of greater significance since it virtually requires the application of the fault to the generating-station bus. This paper describes such an undertaking and presents:

1. A résumé of the studies which indicated that it would be practicable to stage short-circuit tests ranging up to 2,000 megavolt-amperes directly on a particular generating-station bus.

2. A description of the physical plant equipment assembled for test purposes.

3. Operating experience during a series of 14 short-circuits ranging from 200 to over 1,500 megavolt-amperes at 14.5 kv.

42-20—Loss-of-Field Protection for Generators; *G. C. Crossman (A'30), H. F. Lindemuth (M'41), and R. L. Webb (M'35). 25 cents by mail.* The features of a new protective-relay scheme designed to protect a-c generators for severe reduction in field excitation are described. This scheme operates to remove the underexcited machine from the system upon occurrence of resultant undervoltage before loss of synchronism occurs. Calculation methods required to apply the scheme are covered, together with a sample problem to assist with such applications on any system. A need for loss-of-field protection has been found on the larger machines of a metropolitan operating company. The considerations involved when studying need for such protection are outlined, together with the complete description of machine behavior and records of actual tests to show that those behaviors can be determined with reasonable accuracy.

42-24—High-Speed Single-Pole Reclosing; *J. J. Trainor, J. E. Hobson (M'41), and H. N. Muller, Jr. (A'37). 20 cents by mail.* Recently the Public Service Company of Indiana, Inc., installed the first application of high-speed, single-pole reclosing in the United States. This application is on its single-circuit 132-kv line, extending from Lenore to Newcastle, which line forms part of an interconnection between the Public Service Company of Indiana and the Indiana section of the American Gas and Electric System. Calculations are included which show the comparative transient power limits with gang operation and single-pole operation for speeds of reclosing of 35 and 20 cycles on a 60-cycle basis. Comprehensive tests were conducted to check the single-pole relay and circuit breaker operation for both arcing and solid faults applied at various points on the transmission system. The test results are included in the paper. A general discussion comparing the use of gang operation and single-pole reclosing with other measures for improving transmission-line performance is included.

Personal • • •

D. C. Prince (A'16, F'26) manager, commercial engineering department, General Electric Company, Schenectady, N. Y., and president of the Institute, has been made vice-president in charge of application engineering, apparatus department. **W. R. G. Baker** (A'19, M'41) manager, radio and television department, Bridgeport, Conn., has been appointed vice-president of the radio and television department for the company. **H. A. Winne** (A'16, M'39), staff assistant to the vice-president in charge of engineering, Schenectady, has been appointed vice-president in charge of design engineering, apparatus department. A biographical sketch of Mr. Prince appeared in the March 1941 issue, page 138. Mr. Baker was born November 30, 1892, at Lockport, N. Y., and received the degrees of bachelor of science (1916) and mechanical engineer (1918) and an honorary degree of doctor of science (1935) from Union College. He has been with the General Electric Company since 1917, starting in the research laboratories. In 1924 he was given charge of design of all radio products, and in 1928 complete charge of development, design, and production in the radio field. In 1930 he became vice-president and general manager of the RCA Victor radio plant, Camden, N. J., but returned to General Electric Company in 1935 to become manager of the radio and television department at Bridgeport. Mr. Winne was born October 27, 1888, at Cherry Valley, N. Y., and received the degree of electrical engineer from Syracuse University in 1910. He joined the General Electric Company in 1910, working in the test department. In 1916 he became application engineer in the power and mining and industrial engineering departments, and in 1930 was put in charge of a section of the industrial engineering department. He became manager of sales, mining, and steel-mill section of the industrial department in 1936, and in 1937 was made staff assistant to the vice-president in charge of engineering.

H. L. Crumley (A'26, M'27) formerly general superintendent of operations, Virginia Public Service Company, Charlottesville, has been appointed operating vice-president for the company, with headquarters at Alexandria. **Ivan Buys** (A'24) chief electrical engineer, Illinois Iowa Power Company, Decatur, Ill., has been appointed general superintendent of operations. Mr. Crumley was born in Atlanta, Ga., June 30, 1900, and received the degree of bachelor of science in electrical engineering from the Georgia School of Technology in 1920. He entered the test course of the General Electric Company in 1920, and joined the Georgia Railway and Power Company, Atlanta, in 1921, serving first as tester, and later as assistant foreman of the test department and as protection engineer. He became relay engineer for the Metropolitan Edison Company and New Jersey Power and Light Company, Reading, Pa., in 1926, and was made assistant superintendent of operation in 1927, and chief system operator in 1932. In 1937 he joined the E. M. Gilbert Engineering Corporation as consulting electrical engineer, and went to the Virginia Public Service Company as general superintendent about a year later. Mr. Buys is a native (1896) of Rutherford, N. J., and received the degree of mechanical engineer from Cornell University in 1917. After two years in the United States Army Signal Corps, he joined the Duquesne Light Company, Pittsburgh, Pa., and became successively technical assistant to superintendent of overhead lines, assistant chief of construction, and chief of operation of transmission lines. He became superintendent of transmission for the Kansas Gas and Electric Company, Wichita, Kans., in 1923, and in 1930 transferred to the United Power and Light Corporation of Kansas, Abilene, as chief engineer and later division manager. He joined the Illinois-Iowa Power Company in 1936, as engineering assistant to the vice-president, and was made chief engineer about a year later.

H. P. Charlesworth (M'22, F'28) has retired as assistant chief engineer, American Telephone and Telegraph Company, New York, N. Y. Mr. Charlesworth was born April 7, 1882, at Haverhill, Mass., and graduated in electrical engineering from Massachusetts Institute of Technology. He entered the service of the American Telephone and Telegraph Company at Boston in 1905, and did research and development work in the engineering department. In 1907 he was transferred to New York, to enter the toll traffic department. From 1917 to 1919 he was assigned to problems in connection with the war-time emergency, and later in 1919 was made equipment and transmission engineer for the company. He was appointed plant engineer in 1920, and in

1928 was transferred to the Bell Laboratories as vice-president. He became assistant chief engineer of the American Telephone and Telegraph Company in 1933. Mr. Charlesworth was a manager of the Institute 1923–27, vice-president, 1930–32, and president, 1932–33. He also has been active on many Institute committees. **H. S. Osborne** (A'10, F'21) plant engineer, will carry on Mr. Charlesworth's duties, but will retain his present title of plant engineer. A biographical sketch of Mr. Osborne appeared in the January 1941 issue, page 44.

R. I. Parker (A'14, M'20) district manager, central-station department, General Electric Company, Chicago, Ill., has been appointed assistant district manager of the company's central district. Mr. Parker has been with the company since 1912, having entered the test course at Schenectady, N. Y., and later having been transferred to the lighting engineering department. He was sent to the Chicago district office in 1919, and was made assistant manager of apparatus sales in 1921. He became district manager of the central-station department in 1924. **S. W. Scarfe** (M'40) commercial engineer for the company at Los Angeles, Calif., has been made assistant manager of the Los Angeles central-station department. He joined the company's sales department at San Francisco, Calif., in 1924 transferred to the test department at Schenectady, and returned to San Francisco in 1926. He was made resident sales engineer at Fresno, Calif., in 1927, and at Sacramento, Calif., in 1932, and became assistant to the manager of the company at San Francisco in 1937, and commercial engineer in 1939.

F. C. Weiss (A'14, M'19) manager, engineering and construction department, Alabama Power Company, Birmingham, has been appointed a vice-president of the company. Mr. Weiss was born in Dallas, Tex., March 5, 1892, and received the degree of bachelor of science in electrical engineering from Massachusetts Institute of Technology in 1913. In 1911 he joined the Stone and Webster Corporation, doing construction work in Texas, Iowa, and Missouri, and in 1913 became inspector of transmission-line construction for the Alabama Power Company. He later became assistant to the operating manager, superintendent of line construction, superintendent of electrical construction, and superintendent of construction for the company. After serving as superintendent, construction manager, and vice-president of the Dixie Construction Company, Birmingham, and construction manager of Allied Engineers, Inc., Birmingham, he returned to the Alabama Power Company as manager of the engineering and construction department

E. R. Moore (A'26, M'40) electrical system, Detroit (Mich.) Edison Company, has been appointed budget engineer for the company. **C. F. Ries** (A'19) supervisor of training, has been appointed assistant to superintendent of substations. He will also continue with his former duties. Mr. Moore is a native (1898) of Williamsport, Pa., and received the degree of bachelor of science in electrical engineering from Pennsylvania State College in 1920. He has been with the Detroit Edison Company since 1926, serving first as engineer in charge of design of extensions to d-c substations and system, and later as engineer in charge of the preparation and co-ordination of the electrical system budget and procurement of equipment. A native (1891) of Kenton, Ohio, Mr. Ries received the degree of electrical engineer from Ohio Northern University. He has been with the Detroit Edison Company since 1917, having served successively as tester, electrical engineer, and supervisor of training.

H. H. Barnes, Jr. (A'00, F'13) commercial vice-president, General Electric Company, New York, N. Y., has been appointed AIEE executive committee representative on the newly-formed Engineers' Defense Board, a working organization of engineers and technologists from the several national engineering societies which will deal with technical problems on shortages, substitutions, conservation, raw materials, production and reclamation resulting from the defense effort. The other AIEE representatives are: **Philip Sporn** (A'20, F'30) vice-president in charge of engineering, American Gas and Electric Service Corporation, New York, N. Y.; **C. A. Adams** (A'94, F'13) consulting engineer, Edward G. Budd Manufacturing Company, Philadelphia, Pa.; **C. B. Jolliffe** (M'34) engineer in charge, RCA frequency bureau, Radio Corporation of America, New York, N. Y.; and **R. L. Jones** (A'11, F'31) director of apparatus development, Bell Telephone Laboratories, Inc., New York, N. Y.

W. W. Broadbent (A'16) assistant superintendent, southern division, Narragansett Electric Company, Providence, R. I., has been appointed superintendent of the southern division operating department of the New England Power Association with headquarters at Providence. He received the degree of electrical engineer from Lehigh University in 1910, and after taking the apprentice shop course at the Westinghouse Electric and Manufacturing Company, East Pittsburgh, Pa., became construction inspector for the New York, Ontario, and Western Railroad at Mayfield, Pa. He subsequently served in the same capacity with J. N. Bastress and company, Scranton, Pa.; New England Engineering Company, in Virginia and Ohio; Shore Line Electric Railway Company, Norwich, Conn., and Narragansett Electric Company. He was later made assistant superintendent of production and then assistant superintendent of the southern division, for the company.

L. G. Woodford (M'31) assistance vice-president, American Telephone and Telegraph Company, New York, N. Y., has been appointed chief engineer for the company. Mr. Woodford was born August 10, 1888, at Waterloo, Iowa, and studied engineering at Iowa State College. He joined the Iowa Telephone Company in 1911 as engineering assistant, and became appraisal engineer in 1914. He became appraisal engineer for the Northwestern Group of Bell Telephone Companies in 1916, and was made engineer of costs and practices in 1921. During 1923–24 he engaged in special studies for the American Telephone and Telegraph Company, and in 1924 was made appraisal engineer at New York. He became plant extension engineer in 1933, operating results engineer in 1937, plant operation engineer in 1939, and assistant vice-president in 1940.

E. T. Williamson (A'22) electrical engineer, People's Power Company, Moline, Ill., has been elected vice-president in charge of operations. A native (1897) of Independence, Mo., Mr. Williamson received the degree of bachelor of science in electrical engineering from Kansas State Agricultural College in 1919. He entered the test department of the General Electric Company, Chicago, Ill., in 1919 and was transferred to the a-c engineering department in 1920, and later to the power and mining department. About 1922 he became distribution engineer for the United Light and Railways Company (later United Light and Power Company), Davenport, Iowa, and three years later joined the People's Power Company as engineer. He was made electrical engineer five years ago.

L. E. Johnson (A'41) instructor in electrical engineering, New Mexico State College, State College, N. M., has been awarded the District 7 prize for best graduate student paper presented during the academic year ending June, 1940, for his paper "A Consideration of Some Possibilities for Electrical Engineering in Ordinary Land Surveying." Mr. Johnson was born at Corpus Christi, Tex., July 26, 1910, and received the degrees of bachelor of science in electrical engineering (1935) and master of science in electrical engineering (1940) from Texas Agricultural and Mechanical College. From 1936 to 1939 he was observer for the Texaco Development Corporation, Los Angeles (Calif.) division, and he joined the faculty of Mexico State College in 1940.

R. H. Olson (A'21) New York, N. Y., district sales manager, Electric Machinery Manufacturing Company, Minneapolis, Minn., has been appointed eastern sales manager for the company. Mr. Olson joined the Electric Machinery Company in 1919, as a tester, and was later made erecting engineer. In 1920, he became a partner of the firm Pearson and Olson, service engineers, which was established as the handling service department of the Electric Machinery Company. He returned to the company about 1924 as district sales manager at St. Louis, Mo., and was later also district sales manager at Minneapolis for a short time before being transferred to New York about 1929.

W. L. Cisler (M'35) assistant chief engineer, electrical engineering department, Public Service Electric and Gas Company, Newark, N. J., has been appointed to the staff of the power co-ordinator, Office of Production Management, Washington, D. C. He has been with the Public Service company since 1922 and is currently chairman of the AIEE committee on power generation. Also appointed to the staff of the power co-ordinator are: **F. H. King** (A'31, M'40) superintendent since 1937 of the

electric light department, City of Burlington, Vermont; and **K. W. Miller** (A'23, M'29) secretary, director of research, Utilities Research Commission, Chicago, Ill.

L. C. Tillotson (A'39) graduate assistant, electrical-engineering department, University of Missouri, Columbia, has been given honorable mention in the District 7 award for best graduate student paper presented during the year ending June 1940, for his paper "An Analysis of the Single-Phase Full-Wave Gas Rectifier Loaded with a Choke Input Filter." Mr. Tillotson received the degree of bachelor of science in electrical engineering from the University of Idaho in 1938, and worked for a year as electrician for the Bunker Hill and Sullivan Mining Company, Kellogg, Idaho, before going to the University of Missouri as assistant. He is a member of Sigma Xi.

G. S. Whitlow (A'29, M'39) application engineer, St. Louis (Mo.) office, General Electric Company, has joined the Union Electric Company of Missouri, St. Louis, as electrical engineer. Mr. Whitlow entered the General Electric Company in 1924, as a student in the test courses at Schenectady, N. Y., and Pittsfield, Mass., and in 1925 was made head of automatic switchgear testing at the Schenectady and Philadelphia (Pa.) plants of the company. In 1927 he supervised installation of three automatic substations in Havana, Cuba. He was made application engineer at St. Louis in 1928.

E. G. Thoms (A'28) inductive co-ordination engineer, Indiana Bell Telephone Company, Indianapolis, has been made plant extension engineer. Mr. Thoms joined the company in 1923, serving first in the department of exchange plant engineering. During 1926 he was transmission and distribution engineer for the Indianapolis-Cincinnati Traction Company, Indianapolis. He returned to the Indiana Bell Telephone Company in December 1926, as assistant foreign wire relations engineer, and was made inductive co-ordination engineer about 1930.

C. A. Terry (A'18, F'38) manager of power supply, Central New York Power Corporation, Syracuse, N. Y., has been appointed operating manager. **J. L. Welch** (A'27) general superintendent of distribution, has been appointed general superintendent of the Syracuse-Oswego division, with headquarters at Syracuse. Mr Terry has been with the Central New York Power Corporation as manager of power supply since about 1938. Mr. Welch has been with the company since about 1937, and was made general superintendent of distribution two years ago.

A. F. Brooks (A'24) formerly vice-president and general manager, Southern New England Telephone Company, New Haven, Conn., has been elected president of the company. A native (1890) of Meriden, Conn., Mr. Brooks received the degree of bachelor of philosophy from Yale University in 1911, and soon afterwards joined the Southern New England Telephone Company. He held various positions before being appointed cost and appraisal engineer, and was later made chief engineer. He was appointed vice-president and general manager of the company about 1930.

R. G. Edsall (A'23) electrical engineer-draftsman, Westinghouse Electric and Manufacturing Company, East Pittsburgh, Pa., has been appointed works electrical engineer in the factory service division of the company. Born at Atlantic City, N. J., June 17, 1901, he received the degree of bachelor of science in electrical engineering from Carnegie Institute of Technology in 1935. He has been with the Westinghouse company since 1919 serving successively as electrical apprentice, foreman of the test floor, and draftsman in the works engineering department.

Mildred A. Preen (A'39) junior partner, E. L. and A. G. Preen, contractors, Lebanon, N. J., has been elected representative to the New Jersey State Legislature from Hunterdon County. Miss Preen was born June 13, 1918, at Newark, N. J., and received the degrees of bachelor of science in electrical engineering from Newark College of Engineering in 1938 and master of arts from Columbia University in 1939. She also has completed the first and secondary pilot training courses of the Civil Aeronautics Authority.

R. E. Glass (Enrolled Student) Chicago, Ill., has received honorable mention in the District 7 award for best Branch paper presented during the academic year ending June 1940, for a paper on "The Study of the Accumulation of High-Potential Static Charges by Wind-Tunnel Method," of which he is joint author with L. W. Evans. Born at Hartley, Tex., January 6, 1917, Mr. Glass received the degrees of bachelor of science, Texas Technological College, 1940, and master of science, Illinois Institute of Technology, 1941.

F. L. Arland (A'22, M'30) engineer of special studies, New York (N. Y.) Telephone Company, has retired. Mr. Arland was born January 29, 1880, at Hammondsport, N. Y. He joined the New York Telephone Company in 1911 as division equipment engineer at Albany, and in 1920 became engineering assistant in the engineering department at New York. He later was made assistant engineer and engineer of the department. He was appointed engineer of special studies in the executive department in 1928.

C. A. Butcher (M'22) eastern district service manager, Westinghouse Electric and Manufacturing Company, Newark, N. J., has been made assistant manager of the district manufacturing and repair department with headquarters at East Pittsburgh, Pa. He has been with the Westinghouse company in various cities since 1917, and was made northeastern district engineering manager at New York, N. Y., in 1929, and eastern district service manager in 1936.

W. C. Lenhardt (A'37) electrical engineer, Cornwall ore division, Bethlehem Steel Company, Cornwall, Pa., has been made electrical superintendent for the division. A native (1914) of Syracuse, N. Y., he received the degree of bachelor of science in electrical engineering from Syracuse University in 1936. He joined the Bethlehem company in 1936 as student engineer, and was made electrical engineer about two years later.

C. W. Gustafson (A'25, M'29) chief engineer, Mill Mutual Fire Prevention Bureau, Chicago, Ill., has become sales engineer for I. A. Bennett and Company, Chicago, midwestern agents for the National Electric Products Corporation of Pittsburgh, Pa. He graduated in electrical engineering from Michigan State College in 1922, and immediately joined the Mutual Fire Prevention Bureau as engineer, being made chief engineer in 1926.

H. W. Leitch (A'98, M'13) consultant on special assignments, Consolidated Edison Company of New York, Inc., New York, has retired from active service with the company. He retired from the position of vice-president in charge of electrical operation at the end of 1940, but had remained with the company in a consulting capacity. A biographical sketch of Mr. Leitch appeared in the January 1941 issue, page 43.

F. L. Ball (A'22, M'27) regional executive, New England Power Association has been made president of the Malden (Mass.) Electric Company, and will also continue as an officer of various operating companies of the Association north and northeast of Boston. He has been an executive of the Association since about 1936, having served prior to that as an executive of several New England utility companies.

G. J. Thaler (Enrolled Student) graduate student, Johns Hopkins University, Baltimore, Md., has been awarded the District 2 prize for the best Branch paper presented during the academic year ending June 1940, for his paper "Characteristics of Fluorescent Lamps." Mr. Thaler was born in Baltimore, Md., March 15, 1918, and received the degree of bachelor of engineering from Johns Hopkins University in 1940.

R. P. Watson (Enrolled Student) Dallas Tex., has been awarded the District 7 prize for best Branch paper presented during the academic year ending June 1940, for his paper "Electronic Visualization of Magnetic Fields." Born September 5, 1917, at Dallas, Tex., Mr. Watson received the degree of bachelor of science from Southern Methodist University in 1941.

R. H. Barclay (A'14, F'28) formerly regional director, Federal Power Commission, New York, N. Y., has joined the J. G. White Engineering Corporation, New York, N. Y., as electrical engineer in charge of the division of electrical engineering. A biographical sketch of Mr. Barclay appeared in the September 1941 issue, page 449.

S. A. Moss (A'30) district plant manager, Chesapeake and Potomac Telephone Company, Washington, D. C., has been appointed general plant supervisor. He has been with the Chesapeake and Potomac company since 1924, and was made district plant manager about 1939.

H. L. Bradley (A'15) vice-president and treasurer, Allen-Bradley Company, Milwaukee, Wis., has been elected executive vice-president of the company. He has been with the company for many years, having served as vice-president and treasurer since about 1919.

O. E. Buckley (M'19, F'29) president, Bell Telephone Laboratories, New York, N. Y., has been elected an associate of the Roscoe B. Jackson Memorial Laboratory, Bar Harbor, Me. A biographical sketch of Dr. Buckley appeared in the October 1941 issue, page 506.

T. J. Killian (A'35) technical director, Barkon-Frink-Sterling Corporation, Long Island City, N. Y., has been commissioned lieutenant, senior grade, in the United States Naval Reserve Service. He has joined a special class of physicists at Massachusetts Institute of Technology, Cambridge.

H. L. Logan (A'19, M'28) managing engineer, Controlens division, Holophane Company, Inc., New York, N. Y., has been appointed as a consultant to the Industrial Visual Commission of the Public Health Bureau of the American Optometric Association.

J. G. Strang (A'40) construction engineer, National Broadcasting Company, New York, N. Y., has been put in charge of supervising construction on the new San Francisco (Calif.) Building of the company. He has been with the company since 1927.

I. B. Tilyou (A'38) electrical engineer, Copper Wire Engineering Association of Washington, D. C., Upper Darby, Pa., has joined the consulting engineering staff of the Chase Brass and Copper Company, Inc., Waterbury, Conn.

C. C. Knipmeyer (A'10, M'35) head, electrical engineering department, Rose Polytechnic Institute, Terre Haute, Ind., has been elected president of the National Council of State Boards of Engineering Examiners for 1941–42.

R. W. Beck (M'37) manager, Public Utility District 1, Grays Harbor County, Aberdeen, Wash., has resigned that position; **W. S. Hill** (A'13, M'20) general superintendent of production and construction for the district, has been appointed acting manager.

Robert Paxton (A'26, M'40) assistant to the manager, General Electric Company, Philadelphia, Pa., has been appointed manager of the Philadelphia Works of the company. A biographical sketch of Mr. Paxton appeared in the January 1941 issue, page 44.

C. E. Stephens (M'22) vice-president of the Westinghouse Electric and Manufacturing Company, has been appointed chairman of the electrical committee of the United States Committee for the Care of European Children, New York, N. Y.

R. M. Triest (A'34) manager, educational department, John Wiley and Sons, Inc., New York, N. Y., has been elected head of the editorial department and secretary of the company.

C. I. Maust (A'36) assistant engineer, Public Service Electric and Gas Company, Newark, N. J., has become assistant engineer for Ebasco Services, Inc., New York, N. Y.

C. H. Sharp (A'02, F'12) consulting engineer, White Plains, N. Y., has been awarded an honorary degree of doctor of science by Hamilton College.

Obituary • • •

Frederick F. Elliott (A'19) borough electrical engineer, Woolwich Borough Council, Woolwich, London, England, died May 8, 1941. Mr. Elliott was born February 15, 1892, at Brixton, London, England, and studied electrical engineering at the City and Guilds of London Technical College. During 1912 he was assistant engineer for the Thorpe Meter Syndicate, Ltd., London, and later became charge engineer for the City and South London Railway power station, London. He joined the British Insulated and Helsby Cables, Ltd., Prescot, Lancashire, in 1914, as electrical engineer, and in 1915 became charge engineer for the County of London Electrical Supply Company, Ltd., London. He became station engineer for the Woolwich Borough Council about 1920, and later was made successively electrical engineer in the electricity department, and borough electrical engineer. He was a member of the Institution of Electrical Engineers.

G. S. Lawler (A'11, M'13) chief electrical engineer, Associated Factory Mutual Fire Insurance Companies, Boston, Mass., died October 31, 1941. Born in Boston, Mass., in 1874, Mr. Lawler received the degree of bachelor of science from the Massachusetts Institute of Technology in 1897. From 1897 to 1899 he was electrician for the Halpin Dirigible Torpedo Company. In 1899 he enrolled in the test course of the General Electric Company, and shortly afterward joined the Boston Elevated Railway Company, serving until 1905 in various capacities and finally as superintendent of power distribution. After a brief period with the Brooklyn (N. Y.) Rapid Transit Company, as assistant superintendent of the Williamsburg Power Station, he became electrical inspector for the Associated Factory Mutual Fire Insurance Companies in 1906. He was later made electrical engineer, and became chief electrical engineer about 1918. He had participated in drafting every revision of the national electrical code since 1907.

Willard Ashley Stockbridge (A'11) foreman of power plants, Pennsylvania Railroad Company, Philadelphia, died August 20, 1941. Mr. Stockbridge was born March 31, 1885 at Fort Wayne, Ind., and graduated in electrical engineering from Purdue University in 1910. He joined the Pennsylvania Company, Fort Wayne, in 1910, working first in the photometric division of the company, and later doing tests on power plants and distribution. About 1916 he was employed in the office of the general superintendent of motive power, Pennsylvania Lines West, Pittsburgh, Pa., and five years later became power plant foreman for the Canton (Ohio) Shops of the Pennsylvania Railroad. He was later transferred to the West Philadelphia Shops of the railroad as power plant foreman, and became foreman of power plants at Philadelphia about 1930.

Elmer F. Anderson (A'35) electrical engineer, Portland (Ore.) General Electric Company, died October 4, 1941. Mr. Anderson was born September 3, 1896, at Portland, Ore., and received the degree of bachelor of science in electrical engineering from Oregon State College in 1925. From 1925 to 1927 he was switchboard wireman for the Portland General Electric Company, and in 1927 enrolled in the test course of the General Electric Company at Schenectady, N. Y. He returned to the Portland General Electric Company in 1928, entering the valuation department. He was transferred to the testing department in 1929, and in 1934 was made assistant engineer for the company. He later became electrical engineer.

Warren W. Daugherty (A'37) electrical superintendent, Cornwall ore division, Bethlehem Steel Corporation, Cornwall, Pa., died August 12, 1941. Mr. Daugherty was born in Crisfield, Md., November 11, 1879. From 1905 to 1916 he was general foreman for the Atlantic City and Shore Railroad Company, Philadelphia, Pa., in charge of construction and maintenance work on electric railroad line and car equipment. He joined the Cornwall ore division of the Bethlehem Steel Corporation in 1916, as chief electrician, and became electrical superintendent about 1937.

Membership • •

Recommended for Transfer

The board of examiners, at its meeting on November 27, 1941, recommended the following members for transfer to the grade of membership indicated. Any objection to these transfers should be filed at once with the national secretary.

To Grade of Fellow

Flanders, N. M., dean of faculty and head of department of engineering tests, Bliss Electrical School, Takoma Park, D. C.
Woodford, L. G., chief engineer, American Telephone and Telegraph Company, New York, N. Y.

2 to grade of Fellow

To Grade of Member

Anderson, H. W., professor of electrical engineering, Iowa State College, Ames.
Anthony, B. M., assistant electrical engineer, Tennessee Valley Authority, Tupelo, Miss.
Blake, J. W., assistant superintendent of generation, Oklahoma Gas and Electric Company, Oklahoma City, Okla.
Currie, J. A., director and managing electrical engineer, C. A. Sothers, Ltd., Birmingham, England.
Frisby, E. F., assistant superintendent of production, Virginia Electric and Power Company, Petersburg, Va.
Leonard, M. G. electrical engineer, Westinghouse Electric and Manufacturing Company, Sharon, Pa.
Hamlin, E. W., professor of electrical engineering, University of Texas, Austin, Texas.
Lewis, W. P., electrical cable engineer, American Steel and Wire Company, Worcester, Mass.
Manning, M. L., research engineer, Westinghouse Electric and Manufacturing Company, Sharon, Pa.
Marburger, T. E., engineer, Consolidated Gas Electric Light and Power Company, Baltimore, Md.
Pearson, D. S., professor of electrical engineering, Ohio Northern University, Ada, Ohio.

Peterson, M. M., laboratory engineer, Westinghouse Electric and Manufacturing Company, Sharon, Pa.
Sawvel, J. S., division electrical engineer, Central Ohio Light and Power Company, Findlay, Ohio.
Shelton, S. P., associate laboratory engineer, Bonneville Power Administration, Portland, Ore.
Shuster, J. D., electrical engineer, Bethlehem Steel Company, Quincy, Mass.
Somers, R. M., assistant chief engineer, T. A. Edison, Inc., West Orange, N. J.
Walz, J. O., engineering manager, Westinghouse Electric and Manufacturing Company, Lima, Ohio.
White, W. C., dean of engineering, Northeastern University, Boston, Mass.
Wilson, G., designing engineer, General Electric Company, Oakland, Calif.

19 to grade of Member

Applications for Election

Applications have been received at headquarters from the following candidates for election to membership in the Institute. Names of applicants in the United States and Canada are arranged by geographical Districts. If the applicant has applied for direct admission to a grade higher than Associate, the grade follows immediately after the name. Any member objecting to the election of any of these candidates should so inform the national secretary before December 31, 1941, or February 28, 1942 if the applicant resides outside of the United States or Canada.

United States and Canada

1. North Eastern

Cerwin, F. J., Central New York Power Corporation, Syracuse, N. Y.
Hermann, G. P., General Electric Company, Schenectady, N. Y.
Lindstrom, E., Line Material Company, Oneida, N. Y.
MacMillan, D. G., American Steel and Wire Company, Worcester, Mass.
Ray, J. H., American Steel and Wire Company, Worcester, Mass.
Ray, J. W., American District Telegraph Company, Inc., Boston, Mass.
Shickel, J. B., 208 Syracuse Building, Syracuse, N.Y.
Silver, C. W., General Electric Company, Schenectady, N. Y.
Wahlstrom, E. O., American Steel and Wire Company, Worcester, Mass.
Warchol, M. F., Jackson and Moreland, Boston, Mass.
Wiest, H. G., Jr. (Member), General Electric Company, Lynn, Mass.

2. Middle Eastern

Altar, W., Case School of Applied Science, Cleveland, Ohio.
Ashton, J. O. (Member), Carnegie Illinois Steel Corporation, Pittsburgh, Pa.
Baker, E. P., Westinghouse Electric and Manufacturing Company, Sharon, Pa.
Belinich, J. J., Westinghouse Electric and Manufacturing Company, Sharon, Pa.
Boruh, W. E., General Electric Company, Toledo, Ohio.
Buckley, F.S., United States Navy, Philadelphia, Pa.
Clouse, W. W. (Associate re-election), Consolidated Gas and Electric Company of Baltimore, Baltimore, Md.
Ferlazzo, G., National Bureau of Standards, Washington, D. C.
Fultz, J. M., Jr., Bell Telephone Company of Pennsylvania, Philadelphia, Pa.
Gilfillan, W. C., United States Navy Yard, Philadelphia, Pa.
Gross, K. K., Leeds and Northrup Company, Philadelphia, Pa.
Halpeny, O. M., United States Engineering Department, Cincinnati, Ohio.
Hamner, S. G., Jr., United States Navy, Baltimore, Md.
Harris, F. K., National Bureau of Standards, Washington, D. C.
Hey, J. A., Rural Electrification Administration, Washington, D. C.
Hill, D. A., Alliance Public Service Company and Ohio Public Service Company, Cleveland, Ohio.
Horlacher, P. E., Westinghouse Electric and Manufacturing Company, Sharon, Pa.
Hyde, E. L., Bethlehem-Fairfield Shipyard, Incorporated, Baltimore-Fairfield, Md.
Johnson, C. H., Sun Oil Company, Toledo, Ohio
King, J. A., Westinghouse Electric and Manufacturing Company, Sharon, Pa.
LeBlanc, A. A., Westinghouse Electric and Manufacturing Company, Sharon, Pa.
Mancini, P. A., Rural Electrification Administration, Washington, D. C.
Mason, L. L., Consolidated Gas, Electric, Light and Power Company, Baltimore, Md.
Maxim, G. E. (Member), Picker X-Ray Corporation, Inc., Cleveland, Ohio.
McKeithan, W. L., Westinghouse Electric and Manufacturing Company, Sharon, Pa.
Moody, W. R., National Radio Institute, Washington, D. C.
Ormston, J. J., Jr., Westinghouse Electric and Manufacturing Company, Sharon, Pa.
Phillips, F., Elyria Foundry, Elyria, Ohio.
Phillips, W. E., Leeds and Northrup Company, Philadelphia, Pa.
Ray, B. M., University of Pittsburgh, Pittsburgh, Pa.
Russell, E. H. (Associate re-election), B. F. Goodrich Company, Akron, Ohio
Smith, H. L., Goodyear Tire and Rubber Company, Akron, Ohio.
Voelker, W. D., Leeds and Northrup Company, Philadelphia, Pa.
Wiesner, F. C. (Member), Cramp Shipbuilding Corporation, Philadelphia, Pa.

3. New York City

Dyson, G. W., Consolidated Edison Company of New York, Inc., New York, N. Y.
Humer, R. H., New York Telephone Company, Brooklyn, N. Y.
Meyers, S. T., Bell Telephone Laboratories, Incorporated, New York, N. Y.
Moynihan, V. A., Gibbs and Cox, Incorporated, New York, N. Y.
Smith, W. S., Metropolitan Device Corporation, Brooklyn, N. Y.
Sterner, N. A. (Member), Telefonaktiebolaget L. M. Ericsson, New York, N. Y.
Winans, B., New York State Electric and Gas Corporation, Brewster, N. Y.

4. Southern

Andrews, L. M., United States Navy Yard, Charleston, S. C.
Angelo, E. J., Jr., Tulane University, New Orleans, La.
Brubaker, L. H., United States Navy Yard, Charleston, S. C.
Daniels, P. A., Alabama Power Company, Birmingham, Ala.
Gilbreath, J. H., Tennessee Valley Authority, Chattanooga, Tenn.
Guthrie, R. J., Byrne Organization, Old Army Base, Norfolk, Va.
Long, K. H., United States Navy Yard, Charleston, S. C.
Richardson, O. (Member), Southern States Equipment Corporation, Birmingham, Ala.
Shortley, W. M., Southern Bell Telephone and Telegraph Company, Atlanta, Ga.
Stratton, W. L., Armature Winding Company, Charlotte, N. C.
Sweeting, R. C., United States Navy Yard, Charleston, S. C.
Taylor, E. R., City of Jacksonville, Jacksonville, Fla.

5. Great Lakes

Baird, M. N., General Electric Company, Fort Wayne, Ind.
Belt, D. F., Bendix Products, South Bend, Ind.
Braymer, D. T., Electrical World, Chicago, Ill.
Burian, K., Electrical Engineers Equipment Company, Melrose Park, Ill.
Greene, E. M. (Associate re-election), Albert Kahn, Incorporated, Detroit, Mich.
Heise, E. B. (Member), Northern Indiana Public Service Company, Michigan City, Ind.
Hill, F. E., Fisher Body Corporation, Detroit, Mich.
Juhnke, P. B., Jr., Line Material Company, Milwaukee, Wis.
Killian, S. C. (Associate re-election), Delta-Star Electric Company, Chicago, Ill.
Lawrence, L. E., Allen Bradley Company, Milwaukee, Wis.
Moncher, F. L., Fisher Body Corporation, Detroit, Mich.
Sarafian, K., Fisher Body Corporation, Detroit, Mich.
Siegel, R. C. (Member), Wisconsin Telephone Company, Milwaukee, Wis.
Svec, V., Harnischfeger Corporation, Milwaukee, Wis.
Warnock, E. W., Consumers Power Company, Adrian, Mich.

6. North Central

Becker, S., Hathaway Instrument Company, Denver, Colo.
Dieringer, J. T., Central Nebraska Public Power and Irrigation District, Hastings, Neb.

7. South West

Carothers, B. M., Union Electric Company of Missouri, St. Louis, Mo.
Hansen, E. L., United States Bureau of Reclamation, Elephant Butte, N. Mex.
Maguire, J. C., University of Texas, Austin, Tex.
Milner, M. L., Jr., Ford, Bacon and Davis, Inc., Little Rock, Ark.
Smoll, A. E., General Electric Company, Wichita, Kan.
Tuma, G., University of Oklahoma, Norman, Okla.
Uhr, I. A. (Member), General Electric Company, San Antonio, Tex.
Zeiders, M. L., Southwestern Bell Telephone Company, Oklahoma City, Okla.

8. Pacific

Horton, T. H., Bethlehem Steel Company, San Francisco, Calif.
Larson, P. F., Vega Airplane Company, Burbank, Calif.
O'Hara, P. L., Arizona Edison Company, Incorporated, Gila Bend, Ariz.
Pier, E. H., Douglas Aircraft Company, Incorporated, Santa Monica, Calif.
Ritter, A. L. (Associate re-election), Federal Communications Commission, San Diego, Calif.
Sargeant, G. H., Jr., Employers Liability Assurance Corporation, Limited, San Francisco, Calif.
Thompson, R. J., Trumbull Electric Manufacturing Company, Los Angeles, Calif.

9. North West

Brown, H. R. (Member), Boeing Aircraft Company, Seattle, Wash.
Drewett, G. A. (Member), Northwestern Electric Company, Vancouver, Wash.
Goldberg, M. O., Mountain States Telephone and Telegraph Company, Helena, Mont.
Mayer, R. H., Civil Aeronautics Administration, Anchorage, Alaska.
McGuire, M. H., City Water and Light Department, McMinnville, Ore.
Nystrom, H. R., Washington Water Power Company, Spokane, Wash.

10. Canada

Baxter, S. C., Burrard Dry Dock Company, Ltd., N. Vancouver, B. C.
Briggs, H. L. (Member), Hydro Electric System, Winnipeg, Man.
Faucher, W. (Member), Canadian Light and Power Company, St. Timothee, Beauharnois County, Que.
Lake, F., Burrard Dry Dock Company, Limited, North Vancouver, B. C.
Moss, A. S., Hydro Electric Power Commission, Toronto, Ont.
Rapsey, K. H., Square D Company Canada Limited, Toronto, Ont.
Sanger, J. S. (Member), Hydro Electric System, Winnipeg, Man.
Watson, C. H., Britannia Mining and Smelting Company, Britannia Beach, B. C.

Total, United States and Canada, 110

Elsewhere

Altmann, A. H. (Member), Standard-Waygood Limited, Sydney, N. S. W., Australia.
Anderson, G. A., Canterbury University College, Christchurch, New Zealand.
Brown, D. E. T. (Member), The Surat Electricity Company, Limited, Surat, India.
de la Torre, A. L., Westinghouse Electric International, Mexico, D. F.
Driscoll, W. H. (Member), Anglo-Ecuadorian Oilfields Limited, Casilla 410, Guayaquil, Ecuador.
Escuden, M. M., Westinghouse Electric International, Mexico, D. F.
Graeter, G. E. (Member), care of Contractors, Pacific Naval Air Bases, Midway Islands.
Nava, F. A., Westinghouse Electric International, Mexico, D. F.
Rao, S. K., Tata Oil Mills Company, Ltd., Tatapuram Post, Southern India.
Roldan, D. G., National Economy Bureau, Mexico, D. F.

Total, elsewhere, 10

Addresses Wanted

A list of members whose mail has been returned by the postal authorities is given below, with the addresses as they now appear on the Institute record. Any member knowing of corrections to these addresses will kindly communicate them at once to the office of the secretary at 33 West 39th St., New York, N. Y.

Accioly, Pompeu Barbosa, Caixa Postal 571, Rio de Janeiro, Brazil, S. A.
Anderson, Axel W., Jr., 647 W. Sheridan Road, Chicago, Ill.
Andreasen, Ingwald A., 230—75th St., Brooklyn, N. Y.
Browning, Robert Lee, Jr., c/o Continental Oil Co., Conroe, Texas.
Butler, N. O., Route 1, Moore, Okla.
Butler, Oliver D., 1355 E. 47th Place, Chicago, Ill.
Cohen, LeRoy Daniel, 770 Meridian St., Florence, Ala.
Daily, Charles S., Jr., 1723 Eye St., N. W., Washington, D. C.
Dennis, Roman, Jr., 360 Amherst St., Buffalo, N. Y.
Dively, William L., c/o Ford Hotel, Buffalo, N. Y.
Farmer, Lee Linzey, Balboa Heights, C. Z.
Gould, John P., 2017 S. 59th Court, Cicero, Ill.
Hickey, Frank W., Jr., 750 Taylor St., San Francisco, Calif.
Hurd, Clinton T., Box 178, Seattle, Wash.
Lofstrand, A. L., Box 5043, Quarry Heights, C. Z.
Roberts, C. F., Jr., Houston Lighting & Power Co., Engg. Dept., Box 1700, Houston, Texas.
Romero, Robert F., 3200—13th St., N. W., Washington, D. C.
Schwarz, Donald William, 115 Lincoln Ave., Endicott, N. Y.
Smith, Clement E., 816 Leland Ave., South Bend, Ind.
Swan, Harry C., 586 Shoop Ave., Dayton, Ohio.
Thompson, Haddon, Storden, Minn.
Whitescarver, Robert S., 400 Center St., Wilkinsburg, Pa.
Wood, Frank Preuit, Dallas Power and Light Co., Dallas, Texas.

23 Addresses Wanted

Of Current Interest

Relation of ECPD to Professional Societies Discussed

Speaking at the recent annual dinner of the Engineers' Council for Professional Development, AIEE Representative J. F. Fairman considered his own experience and in that light proffered some pertinent suggestions as to the respective responsibilities of Council, the participating organizations, and the representatives of the latter. The essential substance of Mr. Fairman's address is contained in the following report.

In considering possible inferences to be drawn from the word "relation", and the sequence of mention of the things related I followed the advice I so frequently give my children—go to the dictionary. One of the definitions I found is "the state of being mutually or reciprocally interested, as in social or business matters." This defines for me the "relation" between Council and the participating bodies. To this I would add one other shade of meaning—that implied in kinship, as father to son; or in the relationship of master to servant.

Our charter bears out this idea when it defines ECPD as a conference of engineering bodies organized to do a definite job—to enhance the professional status of the engineer. The text of the charter dealing with our objectives and program further confirms and amplifies this relationship, but in my opinion the argument is clinched by the phraseology of paragraph 4, defining the method of operation, which states "ECPD shall from time to time recommend to the governing boards of the participating bodies procedures considered to be of value or significance in promoting the general objective set forth in paragraph 2 and shall administer such procedures as shall have been approved by those boards." In other words, ECPD is the servant. It is definitely neither a superior body nor an all-powerful co-ordinating agency. It is the servant, to suggest; not the master, to command.

If I may modify the metaphor, ECPD is like unto a beautiful mansion, built by the family of professional societies with a great deal of enthusiasm for the broad outlook on common problems afforded by the site, but visited only occasionally by its masters, because of the pressure of business and other interests located elsewhere. The owners have left the place in charge of a large staff of their own selection. Once a year the servants send their masters a sort of New Year's greeting to reassure them that the house is in order in case they should wish to use it. The greeting is politely acknowledged and that is the end of it. The present major-domo, being a very conscientious man, was distressed not a little by the lack of interest shown by the owners, so he addressed a special message* to them, calling their attention to the fact that the staff desired to be of greater service. This was so extraordinary it commanded more than usual attention, but when the owners found it was not a strike threat, they relaxed again.

The apparent indifference of our masters has lead some of our more enterprising—or shall I say more visionary—associates to dream about how pleasant it would be if we owned the house. Such dreams may cause us to forget our proper place and if indulged in too long may result in unbearable insubordination with the usual consequences. Perhaps if we kept ourselves busier at our job we would not have time for such dreams and we would accomplish more for our masters and for ourselves.

Let me sketch briefly my own experiences, which lead me to this point of view. First, what are we representatives of the professional societies supposed to do?

According to the rules of procedure, "The representatives of each participating body shall be charged with the responsibility of providing its governing board with current information about the plans, program, and proceedings of ECPD, supplementing the reports of the secretary, and of ascertaining the official attitude of its governing board on matters under discussion before ECPD." When I think of this rule and of the actual performance of one of the representatives of one of the participating bodies, I find a reason for the apparent lack of lively interest on the part of that particular body.

In telling my story, I must of necessity make references to persons and events. No criticism is intended or implied.

Experiences of a Representative

When I was first appointed as a representative of AIEE, I knew perfectly well that the appointment must represent a job, since I had not arrived at that time of life when my professional attainments entitled me to be the recipient of honors. So with eager inquisitiveness, I accepted the invitation to attend the next annual meeting of Council after notice of my appointment. I knew little or nothing about ECPD, so I listened carefully. I was much impressed and thoroughly imbued with the idea that here was a chance to be of tangible service to the profession. Then I respectfully waited for an assignment to duty or some instruction either from my master or my companions in service. I waited. A whole year passed. Nothing happened. This bothered me. I began to conceive of myself as the forgotten man, but I also decided that perhaps it was up to me to do something about it. The first annual meeting to which I would be a fully accredited representative was approaching and I thought I ought to try to find out what had been happening during the past year, so that I might take part more intelligently in the business of that meeting. Just at that time there came to me a copy of a draft of the revised pamplet, "Engineering—A Career, A Culture," with an implied invitation to read and comment constructively upon it. Here at last was a job and I went to it with enthusiasm. I received a polite acknowledgment of my letter of comment, so I dared to hope that some of my suggestions might be deemed substantial enough to be incorporated. Imagine my chagrin at the annual meeting when I found that none of them had been. However, I was interested to observe that several other representatives had the temerity to raise questions about some of the same points. Apparently the matter was not closed. I therefore continued my efforts to be constructively helpful.

At this same meeting I was puzzled by the manner in which it was proposed to obtain approval of the participating bodies of the release of this pamphlet for publication. Copies were to be sent to all the members of the governing boards of the participating bodies, but without making any specific recommendation. I arose timidly in the meeting and made the suggestion that it would be helpful to me, were I a member of one of these boards, to be told specifically what ECPD thought about this pamphlet, what they suggested be done with it and why and for how much. The suggestion was ruled out of order as being prejudicial to objective consideration of the pamphlet by the recipients.

A few days after the meeting, I addressed a communication to my two associates representing the same participating body, appealing to their greater length of experience for guidance. I am a rather outspoken individual and I put my request in these words, "I have been trying to ascertain just what a representative of a constituent body is supposed to do, other than attend meetings, look wise, and say 'yes' at appropriate intervals." Now admittedly that is a tough question—I might say it is almost a "Scottian" question. My two experienced associates did their best to be consoling but I remained unenlightened. I followed this up by consultations with assorted past presidents, vice-presidents, and directors, past and present, and got about the same

*ECPD Should Look Ahead, R. E. Doherty, Electrical Engineering, July 1941, pages 318–21.

kind of encouragement. No one had anything specific to suggest, but everyone was willing to have me start something. They would all be right behind me—how far behind was not entirely clear to me.

I didn't do much during the second year, except faithfully attend the few brief meetings of the executive committee to which I had been appointed, and make a scouting expedition on my own to see how the pamphlet was making out in its review by the members of the governing body of AIEE. I started by looking at the replies that came in to headquarters, most of which indicated to me that the pamphlet had not been read. I took my courage in my hands and called on a number of these officers and directors with whom I had a speaking acquaintance. I generally drew the reaction, "Oh, were we supposed to read it?"

During the third year, I stopped running around asking questions and put that same energy, hitherto wasted, to work, in more productive activities. These activities have obtained for me a somewhat questionable recognition by our chairman. I have been given the job of stirring up interest and a feeling of responsibility on the part of the members and officers of the professional societies who may be within sound of my voice and I have assumed for myself the job of stirring up my associates on the Council.

My experiences in that capacity derived of the past three years have served to strengthen my conviction that one gets specific answers to specific questions and general answers, if any, to general questions and that engineers as a group are no different from the rest of humanity in their actions and reactions.

SUGGESTIONS TO SOCIETIES AND REPRESENTATIVES

First, I should like to clean up that part of my assignment dealing with our masters, the officers and members of the participating bodies. My first suggestion to them is that they exercise the greatest care in choosing their servants, bearing in mind that the assignment as representative is not an honor—it is a job.

There is a common fallacy which holds that the busier a man is the more jobs he can take on and the better he will do them. To me this sounds like getting something for nothing. As engineers, believing in the principle of conservation of energy, we should know it just can't be so. Accordingly, a participating body would do well to choose an individual who is reasonably sure that he will have the time to give to the job that the job requires.

ECPD is spending money which the participating bodies supply. The officers and directors of the participating bodies therefore should review periodically what they are getting for the money of their members, to what extent the profession is being advanced as a result of that expenditure, and whether the most effective use is being made of the time and money being expended on their behalf.

Above all things, avoid the common mistake of setting up more committees or new agencies to do the same job. Face the issue squarely and insist that the existing committees and the existing agencies produce or show cause why they cannot. The temptation to start some new group is always a strong one but in the end makes the confusion worse confounded. I submit that a continuing interest and sustained effort are essential factors in the success of any enterprise.

To my fellow representatives my first remark is a corollary of what your sponsors should do in your selection. If, having accepted the job, you find that for any reason you can't see it through with the thoroughness which you know it deserves, or if you just plain don't like it after you have tried it, why not quietly withdraw so that the assignment may be given to someone who has the time or a more active interest or is otherwise better able or better fitted to carry on?

Let's resolve not to ask our principals what they think. Let's tell them what we think and why and what we believe should be done about it. Let them gain respect for us and for their joint enterprise by the way we conduct our business.

After two years of running around trying to find out what other people thought I as a representative should do, or what ECPD should do, I had the very great pleasure of going before the AIEE board of directors with two specific propositions, one of which cost them money, and obtaining their enthusiastic response and prompt action on both proposals. On that same occasion, after obtaining favorable action on the things I specifically requested, I made a general request for ideas, suggestions, and criticism, which was politely received, but to which I have had no reply then or since from the group as a whole, or from any individual member thereof.

NEED FOR A UNITED FRONT

Of course, before we approach our principals with specific proposals, we should be sure that our proposals are sound and reasonable, that they are definitely a part of our general assignment, and that they are important steps in the attainment of our objective. Moreover, in my opinion, it is important that Council, as a whole, present a united front on all such matters. If we cannot agree among ourselves, it is unlikely that the participating bodies we represent will agree.

Even after we have made a sale, our job is not done. Obviously if we are asking for authority for ourselves to do a job and we get that authority, we are obligated to go to work anew. On the other hand, if our recommendation calls for action by some other agency, such as a committee of one of the participating bodies, we should personally see to it that the committee thoroughly understands the job given it to do, and do everything in our power to promote its success. In either case, we cannot relax.

CURRENT PROBLEMS

In the course of preparing these remarks, I reviewed our last annual report. The first thing that hit me was the fact that the only policies listed as adopted by Council are dated October 1933. Does this mean that we found all the answers in October 1933? Obviously, no. To me, it means that we started with enthusiasm, then the going got a little hard, then we began to get cautious, then we began to debate more over the form than the substance. We lost our courage. It was easy to talk but hard to arrive at a conclusion.

What effective action have we taken on the recommendations contained in the reports of our committees? I think I can say the answer as to fundamental recommendations is somewhat embarrassing. To be sure, we did grant the request of the several committees for funds for use during the year, but neither collectively nor individually, so far as I am aware, did we really implement the basic recommendations which we ourselves presumably approved in accepting the committees' reports. Do we seriously expect that anything is going to happen just because a committee makes a report, we accept it for the record, and it is published in our annual report? I don't think we really do if we are honest with ourselves. We probably hope that somebody will do something about it—but somebody else, not me.

Let me suggest just two sample items about which we should be up and doing. Our Committee on Student Selection and Guidance made some suggestions about stimulating the local sections or chapters of our participating bodies to new or renewed efforts in that field. Frankly, it took me nearly a year to give them a hand and then it came about by accident, rather than by design on my part. Similarly, the Committee on Professional Training made certain recommendations as to work that might be handled by local groups in their field of activity. I have done nothing about this and it is on my conscience.

What agency is better organized than ECPD to reconcile the divergent points of view on the so-called model law? To be sure it is not a specific assignment, but it certainly comes within our general scope and we might materially enhance the prestige of the profession if we could get the various societies we represent to stop fighting with each other more or less publicly about model laws and to turn over to us the job of drafting a model law which would take into account not so much diverse points of view as the actual realities of engineering practice. If we cannot do a job like that there is not much excuse for our existence.

There are many problems common to all branches of the profession. Their solution is intimately related to the enhancement of the professional status of the engineer. That is our job. Shall we do it? My answer is—Yes. When shall we begin? My answer is—Now.

Better Understanding of ECPD Objectives Stressed at Ninth Annual Meeting

RECOGNITION of the need for a more general understanding of the major objectives of the Engineers Council for Professional Development among its constituent societies, and constructive suggestions from the official representatives of these sponsoring bodies featured the ninth annual meeting of ECPD, held October 31,

1941, at the Engineering Societies Building, New York, N. Y.

In introducing his report on the work of Council for the past year, its chairman, Doctor Robert E. Doherty, president of Carnegie Institute of Technology, declared that before ECPD could accelerate its progress toward the objectives stated in the charter, it was essential that "not only the officers and boards but also the rank and files of the constituent organizations understand much more fully than they have in the past what these objectives are and the importance of their achievement to the welfare of the country." "An astonishing number of people, including some comparatively close to the work, have felt that the most important activity and the only significant achievement of ECPD have been in connection with the accrediting program," Doctor Doherty said, pointing out that the Charter clearly indicates other purposes and activities relating to selection and guidance, professional training, professional recognition. "From the point of view of further advancement of the profession, and more important still, the welfare of the country, these other purposes and activities are, in the long run, unquestionably of equal importance with accrediting," he said.

Recalling that at the beginning of the year he had strongly urged an educational campaign among the constituent organizations as one of the most important projects the Council could undertake, Doctor Doherty stated his confidence that "as the constructive purposes and results of the Council's work become clear, all constituent bodies will appraise the situation as it exists today, forget misunderstandings of the past, and see their way clear to support the Council's work." He described the projects represented by ECPD's standing committees "and by other objectives having to do with professional development" as affording a basis upon which effective co-operation among the societies can be developed. "But the effectiveness of this co-operation will depend, in my opinion, altogether upon the effectiveness of plans devised by the Council to make use of the machinery wisely set up when it was organized. These plans must, it seems to me, include a more active participation than in the past by the representatives of the constituent bodies; and to accomplish this, there naturally must be a definite and constructive program in which they can find an active interest . . . . The officers and committee chairmen of the Council must work with the delegates to formulate plans and procedures. Fostering co-operative effort has thus become one of our definite plans."

Three steps already taken in the educational campaign, Doctor Doherty said, were his own report to the boards of the societies, "ECPD Should Look Ahead" (*EE, July '41, p. 318–21*); the plan of the committee on information to prepare informative press releases on Council's work, especially publications reaching the engineering profession; and finally a plan to encourage sessions for discussion of ECPD's work at meetings of the societies. Two such meetings have been held and two more are contemplated in this connection he called attention to a suggestion by AIEE Representative J. F. Fairman that the way to achieve understanding and active interest by the societies in ECPD is through their local sections, and that the way to bring this about, in AIEE for example is to have a plan presented and discussed at the conference of officers, delegates, and members, held annually at the summer convention. Of the Council's problems the one most likely to attract Section action, according to Mr. Fairman, is student selection and guidance; a second, suggested by Doctor Doherty, is the work of the committee on professional training among young graduates.

Doctor Doherty's report also touched upon high lights of the work of ECPD's various committees, all of which presented detailed reports at the meeting.

Figures on the progress of the accrediting program were presented by the committee on engineering schools, of which A. A. Potter of Purdue University was chairman. Nearly all the institutions in the United States which grant degrees in engineering have voluntarily submitted curricula for inspection by the Council's committee on engineering schools since the beginning of the accrediting program in 1933, that committee's report shows. In 143 of 166 such institutions, 896 curricula have been inspected, including reinspection, since 1939, of 158 curricula. One or more curricula have been accredited in 129 schools. Accredited curricula number 460; provisionally accredited 105; action was deferred on 6; and accrediting has been refused to 167. Reinspections resulted in change of status for only 26 curricula, in no change for 132. With the inspection program virtually complete, the committee is now engaged chiefly with reinspections of those curricula provisionally accredited.

The short engineering courses provided by the Engineering Defense Training program should not receive credit toward degrees, the committee on engineering schools recommended, pointing out this would interfere with the primary objective of the courses. The defense program has highlighted the lack in the United States of facilities for technical education of a grade between the engineering college and the vocational school, the committee noted, announcing the appointment of a subcommittee to work with the Society for the Promotion of Engineering Education to develop a program for accrediting technical institutes. Attention was called to the increase in engineering schools operated for private profit and granting engineering degrees under existing state laws. A year's study in such schools, in the opinion of the committee, is not equivalent to a year in an accredited curriculum. The committee also recommended that the Engineers' Council for Professional Development continue its policy of limiting the variety of engineering curricula accredited, accrediting specialized curricula only as options under accepted general curricula.

Recognition that the defense program and the probable employment problems following the emergency affect the relationship of younger engineers to their professional societies was indicated in recommendations of the Council's committee on professional training, urging immediate consideration of these problems. This committee also recommended that the national engineering societies hold clinics for professional guidance.

A study of the bases of selection of engineering students to be made jointly by the Society for the Promotion of Engineering Education and the Engineers' Council for Professional Development was recommended by the latter's committee on student selection and guidance, which continues also to encourage engineers to carry on guidance work among high-school students in their communities. A new ECPD guidance booklet, "Engineering as a Career," authorized for immediate publication, is expected to be available soon to take the place of the booklet "Engineering—A Career, A Culture," which is out of print.

During the past year, the Engineers' Council for Professional Development took over the sponsorship of a joint committee on engineering ethics, representing several national engineering societies, and sponsored by the American Engineering Council until the dissolution of that body. Reporting preliminary work in the drafting of a canon of engineering ethics, the committee recommended that a statement on the influence of ethics on the basis of a profession be prepared by the Council's committee on professional recognition. The latter committee reported continued study on the problems related to professional recognition.

Reports of the representatives of ECPD's constituent bodies also reflected the growing interest in closer co-operation. They were concerned chiefly with comments and suggestions on the work of the Council and activities of the societies in support of the work.

J. B. Challies, speaking for the Engineering Institute of Canada, which joined the group of ECPD sponsor societies in 1940, expressed that organization's enthusiasm about ECPD's achievements and discussed the background of organized engineering in Canada and the EIC's activities in initiating a model engineering registration law. While the war economy of necessity limits present activities, the EIC has set up a committee concerned with "servicing the young engineer" and is preparing a Canadian edition of "Engineering as a Career".

Hope for greater understanding and co-operation between the American Institute of Chemical Engineers and ECPD was expressed by S. D. Kirkpatrick, who spoke of the special position of that organization

(*Continued on page 610*)

Notes on List of Accredited Curricula

(See Facing Page)

(*a*). Accrediting applies to both the day and evening curricula.

(*b*). Accrediting applies to the 4-year and 5-year curricula leading to the bachelor of science degree.

(*c*) Accrediting applies to day and to 6-year evening curricula in the Cooper Union Night School of Engineering as submitted to ECPD.

(*d*). Accrediting applies only to curriculum as submitted to ECPD and upon completion of which a certificate is issued by Harvard University certifying that the student has pursued such a curriculum.

(*e*). The accrediting of a curriculum in general engineering implies satisfactory training in engineering sciences and in the basic subjects pertaining to several fields of engineering; it does not imply the accrediting, as separate curricula, of those component portions of the curriculum such as civil, mechanical, or electrical engineering that are usually offered as complete professional curricula leading to degrees in these particular fields.

(*f*). On July 24, 1940, Illinois Institute of Technology was formed by the consolidation of Armour Institute of Technology and Lewis Institute. Curricula now listed under Illinois Institute of Technology were formerly listed under Armour Institute of Technology.

List of Undergraduate Curricula Accredited by ECPD as of October 30, 1941

(Subject to revision. For basis of accrediting see ELECTRICAL ENGINEERING, December 1938, page 515)

Akron, University of: Electrical, mechanical (industrial and aeronautical options)

Alabama Polytechnic Institute: Civil, electrical, mechanical

Alabama, University of: Aeronautical, civil, electrical, industrial, mechanical, mining

Alaska, University of: Civil, mining (including metallurgical and geological—options)

Arizona, University of: Civil, electrical, mechanical, mining

Arkansas, University of: Civil, electrical, mechanical

Brooklyn Polytechnic Institute: Chemical (day and 8-year evening), civil[a], electrical[a], mechanical[a]

Brown University: Civil, electrical, mechanical

Bucknell University: Civil, electrical, mechanical

California Institute of Technology: Aeronautical (5- and 6-year courses), chemical (5-year course), civil, electrical, mechanical

California, University of: Civil, electrical, mechanical, metallurgical (metallurgy), mining, petroleum

Carnegie Institute of Technology: Chemical, civil[a], electrical[a], industrial (management)[e], mechanical[a], metallurgical[a]

Case School of Applied Science: Chemical, civil, electrical, mechanical, metallurgical

Catholic University of America: Aeronautical, architectural, civil, electrical

Cincinnati, University of: Aeronautical, chemical, civil, electrical, mechanical

The Citadel: Civil

Clarkson College of Technology: Chemical, civil, electrical, mechanical

Clemson Agricultural College: Civil, electrical, mechanical

Colorado School of Mines: Geological, metallurgical, mining, petroleum

Colorado State College: Civil, electrical, mechanical

Colorado, University of: Architectural, civil, electrical, mechanical (includes aeronautical option)

Columbia University[b]: Chemical, civil, electrical, industrial, mechanical, metallurgical, mining

Connecticut, University of: Civil, electrical, mechanical

Cooper Union Institute of Technology: Chemical, civil[c], electrical[c], mechanical[c]

Cornell University: Chemical, civil, electrical, industrial (administrative), mechanical

Dartmouth College: Civil

Delaware, University of: Chemical, civil, electrical, mechanical

Denver, University of: Electrical

Detroit, University of: Aeronautical, architectural, chemical, civil, electrical, mechanical

Drexel Institute: Chemical, civil, electrical, mechanical

Duke University: Civil, electrical, mechanical

Florida, University of: Civil, electrical, industrial, mechanical

George Washington University: Civil, electrical, mechanical

Georgia School of Technology: Aeronautical, chemical (including co-operative curriculum), civil, electrical, mechanical

Harvard University[d]: Civil, communication, electrical, industrial (engineering and business administration), mechanical, metallurgical (physical metallurgy), sanitary

Idaho, University of: Civil, electrical, mechanical, metallurgical (metallurgy), mining

Illinois Institute of Technology (Armour College of Engineering)[f]: Chemical, civil, electrical, mechanical

Illinois, University of: Architectural, ceramic (technical option), chemical, civil, railway civil, electrical, railway electrical, general[e], mechanical, railway mechanical, metallurgical, mining

Iowa State College: Agricultural, architectural, ceramic, chemical, civil, electrical, general[e], mechanical

Iowa, State University of: Chemical, civil, electrical, mechanical

Johns Hopkins University: Chemical, civil, electrical, mechanical

Kansas State College: Agricultural, architectural, civil, electrical, mechanical

Kansas, University of: Architectural, civil, electrical, mechanical, mining

Kentucky, University of: Civil, electrical, mechanical, metallurgical, mining

Lafayette College: Civil, electrical, industrial (administrative), mechanical, metallurgical, mining

Lehigh University: Chemical, civil, electrical, industrial, mechanical, metallurgical, mining

Louisiana State University: Chemical, civil, electrical, mechanical, petroleum

Louisville, University of: Chemical, civil, electrical, mechanical

Maine, University of: Civil, electrical, general[e], mechanical

Manhattan College: Civil, electrical

Marquette University: Civil, electrical, mechanical

Maryland, University of: Civil, electrical, mechanical

Massachusetts Institute of Technology: Aeronautical, building engineering and construction, chemical, civil, electrical, electrochemical, general[e], industrial (business and engineering administration), mechanical, metallurgical (metallurgy), naval architecture and marine engineering (including marine transportation), public health, sanitary

Michigan College of Mining and Technology: Civil, electrical, mechanical, metallurgical, mining

Michigan State College: Civil, electrical, mechanical

Michigan, University of: Aeronautical, chemical, civil, electrical, engineering mechanics, mechanical, metallurgical, naval architecture and marine engineering, transportation

Minnesota, University of: Aeronautical, chemical, civil, electrical, mechanical, metallurgical, mining, petroleum

Mississippi State College: Civil, electrical, mechanical

Missouri School of Mines and Metallurgy: Ceramic, civil, electrical, metallurgical, mining (mine) (including petroleum option)

Missouri, University of: Chemical, civil, electrical, mechanical

Montana School of Mines: Geological, metallurgical, mining

Montana State College: Civil, electrical, mechanical

Nebraska, University of: Agricultural, architectural, civil, electrical, mechanical

Nevada, University of: Electrical, mechanical, mining

New Hampshire, University of: Civil, electrical, mechanical

New Mexico School of Mines: Geological (both mining and petroleum options), metallurgical, mining, petroleum

New Mexico State College: Civil, electrical, mechanical

New Mexico, University of: Civil, electrical, mechanical

New York, College of the City of[a]: Civil, electrical, mechanical

New York State College of Ceramics (at Alfred University): Ceramic

New York University: Aeronautical, chemical (day and 7-year evening), civil[a], electrical[a], industrial (administrative), mechanical

Newark College of Engineering: Civil, electrical, mechanical

North Carolina State College: Ceramic, civil, electrical, mechanical

North Dakota Agricultural College: Architectural, mechanical

North Dakota, University of: Chemical, civil, electrical, mechanical, mining

Northeastern University: Civil, electrical, industrial, mechanical

Northwestern University: Civil, electrical, mechanical

Norwich University: Civil, electrical

Ohio State University: Ceramic, chemical, civil, electrical, industrial, mechanical, metallurgical, mining (mine)

Oklahoma Agricultural and Mechanical College: Civil, electrical, industrial, mechanical

Oklahoma, University of: Architectural, chemical, civil, electrical, mechanical, petroleum

Oregon State College: Civil, electrical, mechanical

Pennsylvania State College: Architectural, ceramic (ceramics), chemical, civil, electrical, electrochemical, fuel technology, industrial, mechanical, metallurgical (metallurgy), mining, petroleum and natural gas, sanitary

Pennsylvania, University of: Chemical, civil, electrical, mechanical

Pittsburgh, University of: Chemical, civil, electrical, industrial, mechanical, metallurgical, mining, petroleum

Pratt Institute: Electrical, mechanical

Princeton University: Chemical, civil, electrical, mechanical

Purdue University: Chemical, civil, electrical, mechanical, metallurgical

Rensselaer Polytechnic Institute: Aeronautical, chemical, civil, electrical, industrial, mechanical, metallurgical

Rhode Island State College: Civil, electrical, mechanical

Rice Institute: Chemical, civil, electrical, mechanical

Rochester, University of: Chemical, mechanical

Rose Polytechnic Institute: Civil, electrical, mechanical

Rutgers University: Civil, electrical, mechanical, sanitary

Santa Clara, University of: Civil, electrical, mechanical

South Dakota State College: Civil, electrical, mechanical

South Dakota State School of Mines: Civil, electrical, general[e], metallurgical, mining

Southern California, University of: Petroleum

Southern Methodist University: Civil, electrical, mechanical

Stanford University: Civil, electrical, mechanical, metallurgical, mining, petroleum

Stevens Institute of Technology: General[e]

Swarthmore College: Civil, electrical, mechanical

Syracuse University: Chemical, civil, electrical, industrial (administrative), mechanical

Tennessee, University of: Chemical, civil, electrical, mechanical

Texas, Agricultural and Mechanical College of: Civil, electrical, mechanical, petroleum (4- and 5-year courses)

Texas Technological College: Civil, electrical, mechanical

Texas, University of: Architectural, civil, electrical, mechanical, petroleum (petroleum production)

Tufts College: Civil, electrical, mechanical

Tulane University of Louisiana: Civil, electrical, mechanical

Tulsa, University of: Petroleum (including options in refining and production)

Union College: Civil, electrical

United States Coast Guard Academy: General[e]

Utah State Agricultural College: Civil

Utah, University of: Civil, electrical, mechanical, metallurgical, mining

Vanderbilt University: Civil, electrical, mechanical

Vermont, University of: Civil, electrical, mechanical

Villanova College: Civil, electrical, mechanical

Virginia Military Institute: Civil, electrical

Virginia Polytechnic Institute: Ceramic, chemical, civil, electrical, industrial, mechanical

Virginia, University of: Civil, electrical, mechanical

Washington, State College of: Architectural, civil, electrical, mechanical (basic option), metallurgical, mining

Washington University: Architectural, civil, electrical, industrial (administrative), mechanical

Washington, University of: Aeronautical, ceramic, chemical, civil, electrical, mechanical, metallurgical, mining

Webb Institute of Naval Architecture: Naval architecture and marine engineering

West Virginia University: Civil, electrical, mechanical, mining

Wisconsin, University of: Chemical, civil, electrical, mechanical, metallurgical, mining

Worcester Polytechnic Institute: Civil, electrical, mechanical

Wyoming, University of: civil, electrical, mechanical

Yale University: Chemical, civil, electrical, mechanical, metallurgical (metallurgy)

(*Continued from page 608*)
in regard to accrediting and stated that its procedure had recently been "streamlined" for greater efficiency. In support of the accrediting program, the American Society of Civil Engineers, by recent action of its board of direction, has voted that student chapters at institutions where the civil-engineering curricula have not been accredited by ECPD by January 1, 1944, would have their charters withdrawn at that time, G. W. Burpee reported for ASCE. That society has suggested that ECPD limit accrediting to the five major engineering fields and general engineering.

Declaring that the presentation and discussion of representatives' reports should stimulate activity by the participating bodies and keep the representatives alert to tangible evidences of co-operation with ECPD, J. F. Fairman, AIEE representative, stated that arrangements had been made for the discussion of ECPD objectives and activities at the conference of officers, delegates, and members at the 1942 AIEE summer convention, to which Doctor Doherty had already referred. The AIEE committee on education plans to hold a conference at the 1942 winter convention and a session at the North Eastern District meeting in April 1942 on subjects relating to ECPD activities. The AIEE Sections committee has been studying ECPD proposals with reference to furthering student-guidance programs through local Sections.

Two suggestions for additional activities by ECPD were made by W. R. Chedsey, incoming representative of the American Institute of Mining and Metallurgical Engineers. One was preparation of a booklet offering guidance to engineering graduates, supplementing "Engineering as a Career"; the other was "the encouragement, and possibly some aid in direct development of personnel methods, through the use of scientific and engineering aids—in other words, assisting in the development of so-called human engineering." A booklet providing orientation for the engineering student and the recent graduate was also recommended by N. W. Dougherty, representing the National Council of State Boards of Engineering Examiners, who urged closer co-operation between that body and ECPD.

Joint sessions of ECPD and The American Society of Mechanical Engineers held in June 1941 were sponsored by the ASME committee on education and training for the industries, which also sent copies of ECPD's eighth annual report to section chairmen for study, R. L. Sackett reported for the ASME representative A. R. Stevenson, Jr.

More practicing engineers should be appointed to ECPD, particularly to the accrediting committee, according to R. A. Seaton, representative of the Society for Promotion of Engineering Education who characterized ECPD as "practically the only co-ordinating agency in the engineering profession". ECPD should also urge more participation by practicing engineers in the vocational guidance work of the societies and in the administration of engineering schools, he said. He also urged ECPD to work for greater uniformity among the engineering societies in admission and membership-grade requirements. SPEE has limited its institutional memberships in the United States to schools with accredited curricula, Dean Seaton reported.

Attendance at the annual meeting was much the largest ever recorded, partly because of the concurrent annual meeting of NCSBEE (see page 614). ECPD officers elected for 1941–42 are:

R. E. Doherty, president of Carnegie Institute of Technology, Pittsburgh, Pa., chairman (re-election); H. T. Woolson, executive engineer, Chrysler Corporation, vice-chairman (re-election); H. H. Henline, national secretary, American Institute of Electrical Engineers, New York, N. Y., secretary; A. B. Parsons, secretary, American Institute of Mining and Metallurgical Engineers, New York, N. Y., assistant secretary.

Newly elected committee chairmen are:

D. B. Prentice, president, Rose Polytechnic Institute, Terre Haute, Ind., committee on engineering schools; E. S. Lee, engineer, general engineering laboratory, General Electric Company, Schenectady, N. Y., committee on professional training; G. Ross Henninger, editor, American Institute of Electrical Engineers, New York, N. Y., committee on information. The following committee chairmen were re-elected for the coming year: R. L. Sackett, dean emeritus of engineering, Pennsylvania State College, New York, N. Y., committee on student selection and guidance; C. F. Scott, professor emeritus of electrical engineering, Yale University, New Haven, Conn., committee on professional recognition; D. C. Jackson, professor emeritus of electrical engineering, Massachusetts Institute of Technology, Cambridge, Mass., committee on engineering ethics.

Members of the executive committee are:

G. W. Burpee, consulting engineer, Coverdale and Colpitts, New York, N. Y., ASCE; A. R. Stevenson, Jr., General Electric Company, ASME; J. F. Fairman, Consolidated Edison Company of New York, Inc., AIEE; C. C. Williams, president, Lehigh University, Bethlehem, Pa., SPEE; B. F. Dodge, Yale University, New Haven, Conn., AIChE; C. F. Scott, professor emeritus, Yale University, NCSBEE; J. B. Challies, Shawinigan Water and Power Company, Montreal, Que., EIC; AIME representative to be appointed.

The executive committee will assume also the duties of the committee on ways and means.

Speakers at the 1941 annual dinner, held at the Engineers' Club, New York, October 30, 1941, included N. W. Dougherty, dean of engineering University of Tennessee, Nashville; A. H. White, president, SPEE; and J. F. Fairman, Consolidated Edison Company of New York, Inc. Mr. Fairman's talk appears on pages 606–07.

National Defense

Engineers Defense Board Established by Societies

To provide a central agency that will be prepared to assist the various branches of the government with engineering knowledge and experience on questions connected with military preparedness, six national engineering societies have joined to organize the Engineers Defense Board. Organization plans were completed during September, and since that time the Board and its executive committee have held several meetings. The most recent meeting was that held November 13 at Washington, D. C., jointly with the committee on metals and minerals of the National Academy of Sciences, at which "critical" materials formed the principal subject of discussion. Several committees have been appointed and already are giving attention to such problems as: steel conservation, waste materials, nickel and nickel-steel alloys, substitutes for copper, and aluminum.

Among the functions of the organization, as stipulated in its officially adopted statement of purposes and plan of organization, are:

1. To serve as a channel to inform engineers generally regarding defense problems, especially those involving shortages of materials.
2. To implement and make applicable reports and recommendations of the advisory committees of the National Academy of Sciences.
3. To urge engineers (*a*) to adopt procedures looking toward accomplishment of the objective of defense agencies; (*b*) to promote means of increasing production of raw materials in which shortages exist; (*c*) to conserve the supply of industrial materials; (*d*) to find substitutes; and (*e*) to simplify operations and production.
4. To act as a clearing house between engineers or engineering groups for information regarding substitute materials, waste prevention, and conservation.
5. To appoint, on request of the Army, Navy, or other defense agency, special committees of engineers to deal with specific engineering problems related to defense.
6. To select problems or projects dealing with defense and to study them with due regard to activities of existing agencies.

Initially, the Board consists of five representatives from each of the six participating societies: American Society of Civil Engineers, American Institute of Mining and Metallurgical Engineers, American Society of Mechanical Engineers, AIEE, Society of Automotive Engineers, and American Institute of Chemical Engineers. To these may be added one or more representatives of such other national engineering societies as may be invited to participate, and such additional representatives of the six participating societies as may be requested. The activities of the Board are administered by an executive committee consisting of a chairman, a vice-chairman, and a secretary, elected by the other members of the executive committee, and one representative of each of the six participating societies appointed by the governing bodies of the respective societies.

R. E. McConnell, consultant, Office of Production Management, has been named chairman of the Engineers Defense Board; H. S. Rogers, president, Brooklyn Polytechnic Institute, vice-chairman; and A. B. Parsons, secretary, American Institute of Mining and Metallurgical Engineers, secretary of the Board. Representing the six participating societies, the following have been named members of the Board:

American Society of Civil Engineers. C. S. Proctor, consulting engineer, New York, N. Y.; R. E. Dougherty, vice-president, improvements and developments, New York Central System, New York, N. Y.; C. F. Goodrich, chief engineer, American Bridge Company, Pittsburgh, Pa.; R. R. McMath, chairman of the board, Motors Metal Manufacturing Company, Detroit, Mich.; J. P. H. Perry, vice-president, Turner Construction Company, New York, N. Y.

American Institute of Mining and Metallurgical Engineers. J. F. Thompson, executive vice-president, International Nickel Company, New York, N. Y.; Zay Jeffries, technical director, lamp department, General Electric Company, Cleveland, Ohio; Wilber Judson, vice-president, Texas Gulf Sulphur Company, New York, N. Y.; Frederick Laist, metallurgical manager, Anaconda Copper Mining Company, New York, N. Y.; Wilfred Sykes, president, Inland Steel Company, Chicago, Ill.

American Society of Mechanical Engineers. R. M. Gates, president, Air Preheater Company, New York, N. Y.; H. V. Coes, industrial department, Ford, Bacon and Davis, Inc., New York, N. Y.; K. H. Condit, dean of engineering, Princeton Uni-

versity, Princeton, N. J.; J. W. Parker, vice-president and chief engineer, Detroit Edison Company, Detroit, Mich.; W. R. Webster, chairman of the board, Bridgeport Brass Company, Bridgeport, Conn.

American Institute of Electrical Engineers. H. H. Barnes, Jr., commercial vice-president, General Electric Company, New York, N. Y.; C. A. Adams, consulting engineer, E. G. Budd Manufacturing Company, Philadelphia, Pa.; C. B. Joliffe, engineer in charge, frequency bureau, Radio Corporation of America, New York, N. Y.; R. L. Jones, director of apparatus development, Bell Telephone Laboratories, New York, N. Y.; Philip Sporn, vice-president in charge of engineering, American Gas and Electric Service Corporation, New York, N. Y.

Society of Automotive Engineers. C. L. McCuen vice-president and chief engineer, General Motors Corporation, Detroit, Mich.; F. W. Caldwell, director of research, United Aircraft Corporation, East Hartford, Conn.; C. E. Frudden, Allis-Chalmers Manufacturing Company, Milwaukee, Wis.; Arthur Nutt, vice-president, Wright Aeronautical Corporation, Paterson, N. J.; N. G. Shidle, editor, SAE *Journal*, New York, N. Y.; J. C. Zeder, chief engineer, Chrysler Corporation, Detroit, Mich.

American Institute of Chemical Engineers. F. W. Willard, president, Nassau Smelting and Refining Company, New York, N. Y.; Webster Jones, Carnegie Institute of Technology, Pittsburgh, Pa.; R. L. Murray, vice-president, Hooker Electrochemical Company, Niagara Falls, N. Y.; A. J. Weith, manager of research, Bakelite Corporation, Bloomfield, N. J.; A. E. Wilson, president, Pan American Petroleum and Transport Company, New York, N. Y.

The executive committee, as now constituted, consists of Chairman McConnell, Vice-Chairman Rogers, Secretary Parsons, C. S. Proctor (ASCE), J. F. Thompson (AIME), R. M. Gates (ASME), H. H. Barnes, Jr. (AIEE), C. L. McCuen (SAE), and F. W. Willard (AICE).

Lighting and the Defense Program Discussed by Killian Before IES

The importance of good lighting as a tool in the national-defense program was stressed in an address by Thomas J. Killian (A'35) technical director, The Frink Corporation, Long Island City, N. Y., at a "Residential Lighting Forum" held recently by the Illuminating Engineering Society. Mr. Killian discussed not only the vital role of lighting in industrial defense production, but also the place of residential lighting in the defense program. He also outlined the efforts being made by manufacturers of lighting equipment to conserve critical materials through simplification of design and the use of substitute materials. Essential substance of Mr. Killian's address follows.

Good lighting has proved to be a powerful tool in the defense program. It is now increasingly recognized that high levels of illumination promote speed, accuracy, sustained production effort, and safe operation. Industrial engineers and architects have installed levels of illumination ranging from 25 to 100 foot-candles, which increase the ease and speed of seeing, reduce eye strain and fatigue, and give all employees an equal opportunity to see naturally, whether working near windows or away from them. It is an obvious truism that good artificial illumination makes possible better utilization of floor space and permits arrangements of machines, work tables, and production lines for a most efficient sequence of operations, with little or no dependence upon natural-lighting facilities. This makes 24-hour operation practical with no penalty to the night shift.

Good illumination has made possible the now famous windowless buildings and black-out plants. In England it has been found that in blacked-out factories good lighting is essential for the morale of the workman as well as his health. In the *Transactions* of the British Illuminating Engineering Society for June 1941 appears the following pertinent statement:

"Experience has shown that a few months work in a blacked-out factory may result in marked deterioration in physical and nervous condition, a waste of vital human assets. Faulty lighting produces eye strain, which in turn causes nervous disorder and the lighting engineer has a greatly increased responsibility for industrial health when the eyes are denied lengthy recuperative periods in natural daylight."

It is obvious from the plants now built or being built that the Government recognizes lighting as a powerful tool in its national-defense program. This is proved by the fact that industrial-lighting equipment is given the same priority as machine-tool equipment. In commercial lighting it is also realized that the speed and accuracy of the eye has a greater influence on the speed and accuracy of all kinds of defense work than any other factor. Carefully engineered commercial equipment has been specified and used in drafting rooms, engineering departments, offices, schools, and other important areas.

RESIDENTIAL LIGHTING

When we come to the subject of residential lighting, we find again that the Government recognizes that good lighting is essential to the health and morale of all, and especially the defense workers. The first major step in this recognition is the project-priority-rating plan for privately financed real-estate developments of low-cost housing in defense areas. These ratings will insure materials for the building of up to 200,000 homes throughout the country. The ratings are applicable to materials on the defense-housing critical list of the Office of Production Management, which includes electrical-wiring supplies, devices, and lighting fixtures. As in other types of lighting fixtures the use of aluminum and solid brass or bronze is barred, but copper and brass plating is permissible. Indoor fixtures must be of light-gauge spinnings, stampings, or drawings and nonmetallic elements must be used wherever practical. Outdoor fixtures must be of cast or wrought ferrous metals. There will also be provided additional materials for over 100,000 defense housing units being built by the Government.

An illumination level of 30–35 foot-candles is provided in the plant of the Kelsey-Hayes Wheel Company, Detroit, Mich., by two-lamp fluorescent units using 100-watt white lamps; spacing 10 feet by 13 feet 4 inches; mounting height, 15 feet

So far there have been few restrictions regarding the production of lighting equipment. However, there is a definite shortage of metals, which at present is in the following order: magnesium, aluminum, nickel, copper, zinc, lead, iron, and steel. Manufacturers are doing all they can to substitute and conserve critical metals. Some specific examples of what they are doing are as follows:

1. The use of nickel has been eliminated in the manufacture of lamps and lighting fixtures.
2. As no aluminum has been available since October 1, steel and ferrous metals have, in general, been substituted.
3. Ferrous metals have been substituted for brass in the production of screw-machine parts.
4. Glass and plastics are being substituted for metals wherever possible.
5. The thickness or gauge is being reduced as far as possible without increasing hazards.
6. The tubing or shell for pipe suspensions is being eliminated wherever possible.
7. Designs are being simplified and ornaments with no practical purpose are being eliminated.
8. Ceiling canopies are being simplified.
9. Further simplification has been obtained by a reduction in the number of catalog items.

Because the situation is changing so rapidly, it is difficult to draw specific conclusions. However, manufacturers are urged to avoid "panic" buying, thus paying speculator's prices for materials; not only is this costly, but would invite further Governmental control. To substitute, reclaim, and conserve critical materials is the way to extend and expedite our defense effort. There is a reasonable chance that intelligent study and application of new materials will forestall dangerous reduction in quality of the equipment. The lighting industry is a tool industry, defined as a means for doing work.

If the greatness of a tool is measured by its capacity for doing useful work, we can forecast for lighting a medal of honor in the national-defense program.

All Critical Materials to Be Allocated

Preparation for the allocation of all critical materials throughout American industry was called for November 7, in parallel actions by the Supply Priorities and Allocations Board and the Office of Production Management. SPAB announced that it had authorized its executive director to request OPM to obtain detailed production programs, industry by industry, for 1942. It stipulated that these programs should contain ample information to indicate the month-by-month requirements of critical materials needed for the production of military, industrial, and civilian items, and essential public services. It also directed that these programs should show similar requirements for repair parts and capital expenditures. OPM issued an administrative order setting up the machinery by which the whole program of requirements is to be developed, outlined the manner in which the various industrial branches and other units of OPM are to work together toward this end, and instituted a new system of handling preference ratings in harmony with this program. The program is expected to give greater certainty to American business and industry, and a clear over-all picture of the nation's total requirements for raw materials to defense officials.

In substance the development of an allocation program will proceed roughly as follows: An industrial branch in OPM takes the first step, calling on its several sections to develop requirements programs for each industry that manufactures the products for which the branch is responsible. Each program is built up by the branch or by its section, through consultation with the industry advisory committee involved and also through discussion with either or both of the armed services, depending on the nature of the product and the materials used in its manufacture. When this has been done, the officers of the industrial branch who have the program in charge discuss the entire matter with the industrial branches that have jurisdiction over the materials or the products out of which the article in question is made. Agreement is reached between the branches as to the amount of material that can be allocated, and so on.

Thus, in effect, each program would originate with the group which is responsible for the end product, the raw-materials groups coming into the picture in an advisory and consultative capacity. Since all programs must be decreased or increased as armament production rises, each one will be framed so that it can be modified upward or downward in case of need. When a program has been drawn up, it will be reviewed carefully in order to cut down the use of critical materials to the greatest possible extent through simplification of lines, substitution, and so on. The OPM Bureau of Industrial conservation will work with and through the industrial branches to accomplish this.

CONSERVATION THROUGH SIMPLIFICATION URGED

Manufacturers in every field are being urged by the Bureau of Industrial Conservation to consider how they might reduce the number of varieties or styles of their products. Such a simplification program is needed to save vital materials for national defense as well as for civilian supply. Proposals by each industry for simplification programs will be welcomed by the Bureau, which is also prepared to aid and advise each industry on the subject. In addition, industry advisory committees, already set up within OPM to deal with problems springing from the demands of the defense program, will be used to work out programs of simplification.

It is the task of the Bureau of Industrial Conservation to inaugurate and conduct a "war on waste" combining and expanding to a great degree all previous efforts aimed at conserving the nation's resources. Simplification is being urged by the Bureau as one of the most direct and important methods of conservation of critical materials.

Power Curtailment in Southeast Postponed

Moderate to heavy rains, plus increased power deliveries into the shortage area through power-pooling arrangements have made possible postponement of the power-curtailment program originally scheduled to go into effect November 10 in seven Southeastern states. The 30 per cent curtailment scheduled for Georgia, Tennessee, Alabama, East Mississippi, Southeast North Carolina and Northwest Florida was postponed for a limited time; the 5 per cent curtailment scheduled for the remainder of South Carolina and North Carolina was postponed indefinitely. Immediate and willing cooperation by the public with the "blackout" provisions of the order affecting nonessential lighting services also contributed to the improved situation. The "blackout" provisions, however, will continue in effect in the entire area.

The original program called for:

1. Curtailment of power by large commercial and industrial users in seven states (vital defense industries and a few others providing essential civilian services exempt).

2. Immediate discontinuance of the use of power for such nonessential services as sign lighting, show-window lighting, and floodlighting of athletic fields.

3. Immediate mandatory pooling of power by interconnected systems of 40 publicly and privately owned companies in 13 states.

Rapidly mounting power needs caused by new and expanding defense industries and prolonged drought conditions created the shortage, which has been estimated as high as 72,000,000 kilowatt-hours a week by J. A. Krug, head of the power section, Office of Production Management. Under the general limitation order issued October 30 by Donald Nelson, director of priorities, a consumer could use up to 10,000 kilowatt-hours per month at a rate of not more than 2,500 kilowatt-hours per week without being curtailed. Thus residential and small commercial consumers would not be affected, except that they may not use power for the prohibited services. The curtailment order would apply to every nonexempt consumer who used more than 10,000 kilowatt-hours during the month for which his meter was read between September 15 and October 14, inclusive.

Exemptions from the curtailment order were provided for operations found by the director of priorities to be essential to national defense or to essential civilian services. Seven groups of consumers were listed as exempt from the mandatory curtailment provisions. They include:

1. The following federal, state, county, and municipal services: fire, police, and essential state and highway lighting.

2. The following essential community services: churches, hospitals, newspapers, refrigeration, and food-preservation plants.

3. Transportation services, street cars, railways, waterways, airports, oil and gas lines and pumping stations, and shops used exclusively for transportation services.

4. Communications services, including postoffices, radio, telephone and telegraph, and traffic control.

5. Waterworks, pumping stations, and sewage-disposal plants.

6. Military establishments.

7. Plants exclusively engaged in the production of any of the following munitions or materials: airplanes and airplane engines; naval ships; merchant ships; ordnance items including guns, ammunitions, explosives, and combat vehicles; aluminum; magnesium; copper or brass; zinc; manganese; mercury; ferroalloys; abrasives; graphite electrodes; forgings; machine tools; artificial gas.

New Defense Plant Construction

Among recently reported industrial-plant construction projects related to the national-defense program are the following:

Aluminum Company of America. To supply stock for the manufacture of forgings for airplane motors and fittings, and rod, bar, and wire for national defense industries, this company plans to erect a second blooming mill at its Massena, N. Y., works. The mill and its necessary facilities will be housed in steel and brick buildings to cover an area of more than 450,000 square feet, and its estimated total cost exceeds $15,000,000. A completely new melting department will be established to serve the blooming mill.

Allis-Chalmers Manufacturing Company. A 500- by 800-foot single-floor windowless building to cost more than $9,000,000 is being constructed by this company in suburban Milwaukee, Wis., for the production of airplane superchargers. Scheduled for completion in about six months, the building will be air-conditioned throughout and lighted by fluorescent units. The electrical substation for the plant's power supply will be completely enclosed and protected against the effects of possible bombing.

Fairbanks Morse Company. More than 300,000 square feet of floor space will be provided in a new Diesel-engine plant being built by this company in Beloit, Wis., at a cost of $5,500,000. It will have a frontage of 660 feet and a depth of 460 feet. Production is expected to be under way in about a year.

General Electric Company. Plans for the construction of a new $1,000,000 plant in Pittsfield, Mass., for the manufacture of synthetic phenol, were announced recently by this company. The plant, which is expected to be in operation by September 1942, will comprise four structures.

Mobile Power Plants for Navy. The Bureau of Yards and Docks, Navy Department, has ordered two 10,000-kw mobile steam-electric power plants mounted on

special railway cars from the General Electric Company, Schenectady, N. Y., to supply emergency power wherever its projects may require. One unit will be centrally located on the West Coast and the other on the East Coast. Each of the two units will be housed in two specially built railway cars which can be hauled over the rails at speeds up to 40 miles per hour. The power-generating car will contain a 10,000-kw turbine-generator and accessories, a condenser, and the necessary switchgear. The boiler and its auxiliaries, together with a starting engine-generating set will be housed in the second car. The boilers will be oil-fired and will furnish 140,000 pounds of steam per hour; steam conditions: 550-pounds per square inch, 825 degrees Fahrenheit. The turbines will be of single-cylinder design. The three-phase 60-cycle generators will operate at 3,600 rpm, and the generated voltage will be 13,800 volts.

Westinghouse X-Ray to Move. The administrative departments of the X-ray division of the Westinghouse Electric and Manufacturing Company will be shifted from Long Island City, N. Y., to the radio-division plant at Baltimore, Md., about January 1, 1942, according to a recent announcement by the company. Manufacturing departments, at work on vital X-ray equipment for the armed forces, the medical profession, and industry, will continue in the division's Long Island City factory; manufacturing space will be increased 26 per cent by the move. Scientific and engineering activities for the two divisions will be centralized at Baltimore.

Positions to Be Filled Through Civil Service Examination

Notice of the following positions, which will be filled through civil service examinations, is published here as a service to members of the Institute. Application forms and full information as to requirements for examinations may be obtained from the secretary of the Board of United States Civil Service Examiners at any first- or second-class post office, or from the United States Civil Service Commission, Washington, D. C. Unless otherwise noted, applications will be accepted until further notice.

Radio Mechanic-Technicians (Amended Announcement). A sufficient number of persons did not apply for the radio mechanic-technician positions announced by the Civil Service Commission on September 8, 1941 (*EE, Oct. '41, p. 512*). Accordingly, the examination announcement has been amended:

a. To make it "open continuous", that is, applications will now be accepted until further notice;

b. To add the position of chief radio mechanic-technician at $2,600 a year;

c. To modify the experience requirements and to provide for the substitution of education for part of the experience.

Naval Ordnance Materials Inspectors. In June of this year the U. S. Civil Service Commission announced that it was recruiting inspectors of naval ordnance materials (*see EE, July '41, p. 359–60*). Appointments are being made at the Washington (D. C.) Navy Yard, Naval Torpedo Station in Alexandria, Virginia, and at various contractor plants in the field. The examination announcement covering these positions has just been issued in revised form. The need of the Navy Department for junior inspectors ($1,620 a year) is particularly pressing. The possibility of advancement is good. Requirements have been modified so that the successful completion of an appropriate approved National Defense Training course will meet the full requirements for this grade.

Revised Aeronautical Engineering Inspectors Examination. The examination for inspectors of aeronautical engineering materials (*see EE, Apr. '41, p. 191*) has just been reissued, liberalizing the provision for using National Defense Training Courses. The completion of *any* appropriate engineering defense training course will now be accepted for one year of the prescribed education or experience. There is a particular need for junior inspectors of engineering materials and for these positions applicants need only have completed an appropriate defense training course. Acceptable courses include those in tool engineering, gauging and inspection methods, instrument design, and related courses in materials inspection or engineering fundamentals and basic principles.

Other Societies •

NRC Insulation Conference Held

Taking a modern topic into an historic setting, the National Research Council's 14th annual conference on electrical insulation was held at the Williamsburg Inn., Williamsburg, Va., October 30–November 1, 1941. The registered attendance was 72. Progress reports on the following 23 topics were presented and discussed:

1. The Polarization Parameters of Various Dielectrics Including Rubber and Their Changes With Temperature, R. F. Field, General Radio Company.

2. Susceptance Variation Measurements of Dielectric Constant and Dielectric Loss in Insulating Materials Between 1 and 50 Megacycles, S. I. Reynolds, General Electric Company.

3. An Investigation of the Dielectric Constant and Other Physical Properties of Benzene Solutions of Several Methacrylate Polymers, L. Ackerman, H. C. Ott, and O. M. Arnold, Rensselaer Polytechnic Institute.

4. A-C–D-C Correlation in Dielectrics, J. B. Whitehead and G. S. Eager, Johns Hopkins University.

5. Effect of Aging Semiconducting Rubber-Like Compounds in Insulating Oil, F. L. Downs, C. R. Boytano, and G. M. L. Sommerman, American Steel and Wire Company.

6. Liquid Dielectrics. Power Factor and Related Properties of Solutions of Sulfur and Nitrogen Compounds in Liquid Paraffins, J. D. Piper, The Detroit Edison Company.

7. Anomalous Relation Between Dielectric Strength and Paper Density, W. A. Delmar, C. N. Works, and J. H. Palmer, The Phelps Dodge Copper Products Corporation.

8. Temperature, Oxygen, and Stress in Impregnated Paper Insulation, J. B. Whitehead and W. H. MacWilliams, Johns Hopkins University.

9. The Dielectric Strength and Life of Impregnated Paper Insulation—III, J. B. Whitehead, Johns Hopkins University.

10. Some A-C Properties of Paper Dielectrics Containing Chlorinated Impregnants, D. A. McLean and C. C. Houtz, Bell Telephone Laboratories.

11. Effect of Flow in Molding on the Dielectric Constant and Power Factor of Rubber-Filler Systems, A. H. Scott, National Bureau of Standards.

12. Semiconducting Shielding for Cables, E. J. Merrell, The Phelps Dodge Copper Products Corporation.

13. The Impulse Strength of Solid and Gas-Filled High Voltage Cables, Andrew Gemant, The Detroit Edison Company.

14. Further Tests on Low Pressure Cable, J. A. Scott, General Electric Company.

15. Progress Report on Aging of Cable Insulation Subjected to Elevated Temperatures, Thorstein Larsen, Consolidated Edison Company of New York.

16. A New Test for Evaluating Electrical Insulating Oil, J. C. Balsbaugh and A. G. Assaf, Massachusetts Institute of Technology.

17. A Study of the Electric Hygrometer, R. N. Evans, Consolidated Edison Company of New York.

18. A Manometric Procedure for the Determination of Water in Insulating Oil, R. N. Evans, Consolidated Edison Company of New York.

19. Wax Formation in Stamp Capacitors, W. N. Arnquist and C. E. Trautman, Gulf Research and Development Company.

20. Dielectric Nomenclature, H. H. Race, General Electric Company.

21. The Effect of Corona Deposit on the Flash-over Voltage of Suspension Insulator Units, C. L. Dawes, Harvard University.

22. The Electrical Resistance of the Semiconductor Copper Iodide, R. J. Maurer, Massachusetts Institute of Technology.

23. Resumé of Recent Insulation Researches Undertaken by the Research Department of The Detroit Edison Company, H. S. Walker, The Detroit Edison Company.

Efforts are being made to complete a comprehensive summary of the essential substance of these reports, for publication in an early issue of ELECTRICAL ENGINEERING.

Doctor Ward F. Davidson (A'14, F'26) director of research for the Consolidated Edison Company of New York, Inc., will continue as chairman of the insulation conference for 1941–42. Doctor H. H. Race of the General Electric Company, Schenectady, who has been chairman of the committee on physics relinquished the chairmanship to his vice-chairman, Doctor von Hippel, and a new vice-chairman of that committee is to be appointed. Otherwise the executive committee remains unchanged as follows:

W. F. Davidson, Consolidated Edison Company, New York, N. Y., chairman

Future Meetings of Other Societies

American Association for the Advancement of Science. Winter meeting, December 29–January 3, 1942, Dallas, Tex.

American Institute of Mining and Metallurgical Engineers. Annual meeting, February 9–12, 1942, New York, N. Y.

American Mathematical Society. 48th annual meeting, December 29-31, 1941, Bethlehem, Pa.

American Physical Society. 245th meeting, December 19–20, 1941, Stanford University, Calif.

246th (annual) meeting, December 29–31, 1941, Princeton, N. J.

247th meeting, February 20–21, 1942, Detroit, Mich.

American Society for Testing Materials. Spring meeting, March 2–6, 1942, Cleveland, O.

American Society of Civil Engineers. Annual meeting, January 21–23, 1942, New York, N. Y.

American Society of Heating and Ventilating Engineers. 48th annual meeting and seventh international heating and ventilating exposition, January 26–30, 1942, Philadelphia, Pa.

American Society of Mechanical Engineers. Spring meeting, March 23–25, 1942, Houston, Tex.

Engineering Institute of Canada. 56th annual and general professional meeting, February 5–6, 1942, Montreal, Que.

First Pan-American Congress of Mining Engineering and Geology. January 11–20, 1942, Santiago, Chile.

Institute of Aeronautical Sciences. 10th annual meeting, January 28–30, 1942, New York, N. Y.

Society of Automotive Engineers. Annual meeting, January 12–16, 1942, Detroit, Mich.

S. O. Morgan, Bell Telephone Laboratories, New York, vice-chairman

Thorstein Larsen, Consolidated Edison Company, New York, secretary

Arthur von Hippel, Massachusetts Institute of Technology, Cambridge, chairman, committee on physics

R. N. Evans, Consolidated Edison Company, New York, chairman, committee on chemistry

G. T. Kohman, Bell Telephone Laboratories, New York, vice-chairman, committee on chemistry

C. F. Hill, Westinghouse Electric and Manufacturing Company, East Pittsburgh, Pa., chairman, committee on monographs

H. N. Curtis, Bureau of Standards, Washington, D. C.

W. A. Del Mar, Phelps Dodge Copper Products Corporation, Yonkers, N. Y.

J. B. Whitehead, The Johns Hopkins University, Baltimore, Md.

Perhaps the most actively discussed single topic at the Williamsburg conference was the rapidly increasing necessity for considering substitute materials for electrical insulation. Many traditional practices and materials in the field of electrical insulation are coming to feel increasingly the double impact of increased demand incidental to the national defense activities of the Western Hemisphere and the interruption of supply channels as the result of war conditions in the rest of the world. An informal symposium served as a sharp reminder of the fact that insulating materials important to traditional insulation practices have come from all parts of the world and that some of these distant sources—of shellac and high-grade mica, for example—already have been shut off or diverted so far as the Western Hemisphere is concerned. The effects of the situation will reach into practically every branch of the electrical industry which, in turn, underlies all industry. Research laboratories are busy with the development and application of new materials, new combinations of known materials, and with the improvement and development of domestic supplies. The general consensus seems to be that the end results of the present emergency and the efforts being made to meet it will be a general and material improvement in materials, processes, and practices.

As the Insulation Conference group is holding itself in readiness for close co-operation with other National Research Council defense activities, through the Division of Engineering and Industrial Research, no definite plans have been settled upon at this date with reference to the annual conference for 1942. Electrical Engineering will report on this later.

Better Administration of Laws Stressed by Engineering Examiners

The desirability of more uniform practices in qualifying applicants, for registration, and of improvement in qualifications in certain states, were emphasized at the 22d annual meeting of the National Council of State Boards of Engineering Examiners, held in New York, N. Y., October 27–30, 1941. Registration was larger than for any previous meeting, with 35 of the 44 member boards represented.

The committee on qualifications for registration, noting wide divergence in the practices of the various boards, presented for approval an outline of requirements basic to a determination of competence, a set of general principles to be applied to interviews with applicants, and a set of general requirements basic to all branches of engineering, to be applied in determining whether the four years of qualifying experience usually required meet adequate standards. The latter general statement was supplemented by a detailed statement in regard to civil engineering. The committee's report was approved, and it was instructed to prepare similar detailed statements for the other major engineering fields.

Qualifications for registration are considerably below "model law" standards in about one fourth of the states, notably those with old registration laws, the committee pointed out, urging the Council to work for improvement of such laws.

The secretary of NCSBEE reported that with the passage of registration laws by three states during the current year, only three now lack such laws.

Specifically avoiding any related financial commitment, the Council approved a recommendation from the secretary that NCSBEE undertake the publication of a national directory of registered engineers if satisfactory arrangements can be made.

"Registration by endorsement" rather than reciprocal registration between states was urged by the committee on interstate registration, which pointed out that insistence on reciprocal registration is a form of coercion toward relaxing responsibility and lowering standards, whereas registration by endorsement is permissive rather than mandatory.

Development of a code of engineering ethics by the Engineers' Council for Professional Development was recommended as an objective for the near future, in connection with discussion of the desirability of requiring applicants for registration to endorse a code of professional ethics. Other matters of co-operation with ECPD were discussed.

Officers elected for the coming year are:

C. C. Knipmeyer (A'10, M'35) professor of electrical engineering, Rose Polytechnic Institute, Terre Haute, Ind., *president;* J. H. Dorroh, dean of engineering, University of New Mexico, *vice-president;* G. M. Shepard, St. Paul, Minn., and F. W. Anderson, Lexington, Va., *regional directors.* T. Keith Legaré continues as executive secretary.

National Electrical Safety Code Revision Completed

With the publication of part 2, "Safety Rules for the Installation and Maintenance of Electric Supply and Communication Lines", all six parts of the National Electrical Safety Code are now available in printed form. This represents the completion of a tremendous task by the American Standards Association Sectional Committee on the National Electrical Safety Code under the able leadership of the late Doctor M. G. Lloyd (A'08-F'12), as chairman.

Copies of the various parts of this Code may be ordered from the Superintendent of Documents, United States Government Printing Office, Washington, D. C. The titles, identifying numbers, and prices of each part of this Code are as follows:

1. "Safety Rules for the Installation and Maintenance of Electrical Supply Stations", Handbook H-31, 10 cents
2. "Safety Rules for the Installation and Maintenance of Electric Supply and Communication Lines", Handbook H-32, 65 cents
3. "Safety Rules for the Installation and Maintenance of Electric Utilization Equipment", Handbook H-33, 15 cents
4. "Safety Rules for the Operation of Electric Equipment and Lines", Handbook H-34, 10 cents
5. "Safety Rules for Radio Installations", Handbook H-35, 10 cents
6. "Safety Rules for Electric Fences", Handbook H-36, 05 cents

Machine Tool Builders Adopt New Standards. A new set of electrical standards for machine tools has been adopted by the machine tool industry, in accordance with specifications drawn up by the committee on electrical problems of the National Machine Tool Builders' Association. "Machine Tool Electrical Standards" is planned to relieve customers of the necessity for writing elaborate electrical specifications of their own, and to insure that the machine tools that they buy will be properly wired. There will also be the incidental advantage that assembly of machine tools will be expedited because it will no longer be necessary to make every machine tool a special wiring job to meet special specifications. Copies of the standard may be obtained from the National Machine Tool Builders' Association, Cleveand, Ohio, at $1.00 per copy.

Honors

D. R. Yarnall Receives 1941 Hoover Medal Award

D. R. Yarnall, co-founder and chief engineer, Yarnall-Waring Company, Chestnut Hill, Pa., was awarded the Hoover Medal, joint award of the American Society of Civil Engineers, American Institute of Mining and Metallurgical Engineers, American Society of Mechanical Engineers, and AIEE, at the annual meeting of the American Society of Mechanical Engineers. The medal, presented this year for the fifth time, is awarded "by engineers to a fellow engineer for distinguished public service." Mr. Yarnall received the degree of mechanical engineer from the University of Pennsylvania in 1905, and after a few years as engineer for the Coatesville (Pa.) Boiler Works, and Stokes and Smith Company, he became vice-president and general manager of the Nelson Valve Company, Philadelphia, Pa., in 1912. He was also co-founder in 1912 of the Yarnall-Waring Company, and has been a member of the firm since that date. In 1920 he served as a member of the commission in Europe having charge of feeding German children, and in 1938 was sent to Vienna and to Berlin by the American Friends Service Committee, to aid refugees. He has served as a director of the United Engineering Trustees, and is a former vice-president of the Engineering Foundation, and a past president of the United Engineering Trustees. He is a member of the American Society of Mechanical Engineers and of the American Association for the Advancement of Science. The medal,

established in 1929 by gift of Conrad N. Lauer of Philadelphia, past-president of the American Society of Mechanical Engineers, has been previously awarded to former President Herbert Hoover (HM'29) whose civic and humanitarian achievements it was established to commemorate; to Ambrose Swasey (HM'28) founder of the Engineering Foundation; to John F. Stevens, chief engineer of the Panama Canal; and to Gano Dunn (A'91, F'12) president of the J. G. White Engineering Corporation, New York, N. Y., and past president and Edison Medalist of the AIEE.

American Welding Society Awards Miller Medal

The Miller Memorial Medal, awarded by the American Welding Society for conspicuous contributions to the art and science of welding was presented to David Arnott, chief surveyor and vice-president, American Bureau of Shipping, New York, N. Y., at the annual meeting of the society. The medal was awarded to Mr. Arnott for his work in advancing the application of welding to ship construction. After studying naval architecture at the Royal Technical College, Glasgow, Scotland, Mr. Arnott served an apprenticeship in shipbuilding at the Fairfield Shipbuilding and Engineering Company, Ltd., Glasgow. In 1901 he was made a surveyor for the British Corporation for the Survey and Registry of Shipping, Glasgow, and in 1917 was appointed principal surveyor for the company in Canada. He came to New York in 1918 as deputy chief surveyor of the American Bureau of Shipping, was made chief surveyor in 1925, and chief surveyor and vice-president in 1938.

1941 Chemical Industry Medal Awarded to E. K. Bolton

The Chemical Industry Medal for 1941 has been presented to Dr. Elmer K. Bolton, chemical director of E. I. du Pont de Nemours and Company. The medal, which may be awarded annually for valuable application of chemical research to industry, was presented at a joint meeting of the American Section of the Society of Chemical Industry, the New York Section of the American Chemical Society, and the New York Section of the American Institute of Chemical Engineers.

One of the winners in the industrial class of the sixth annual Modern Plastics competition, held in November 1941, was this ratio adjuster for power transformer, designed and produced by General Electric Company

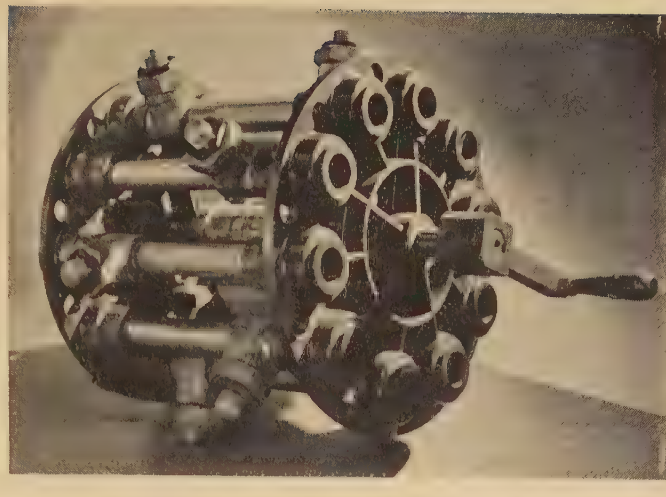

Industry

Iowa University Opens Industrial Film Library. An industrial engineering film library of motion and time study films has been installed at the State University of Iowa. Films in the library, originally used in connection with courses in industrial engineering, will now be available to schools and industrial plants. The motion pictures, contrasting old methods with improved methods, show applications of motion study principles in offices and factories which result in better methods and lower costs. They will be installed by the department of visual instruction of the extension division of the university.

Charles A. Hoxie Dies. Charles A. Hoxie, retired, formerly with the General Electric Company, and inventor of the Hoxie sound-recording machine, died October 13, 1941. Born in Constable, N. Y., he was first engaged in development of an internal telephone system for cities, and was afterward associated with the New England Telephone Company. He joined the Hudson River Telephone Company in 1900 as wire chief. In 1912, he became an engineer for the General Electric Company, and there perfected a machine called a pallophotophone, which would record sound and film for motion pictures simultaneously. This type of recording process now is used by most of the motion-picture companies.

Granite Shaft Over "Time Capsule" Dedicated. A shaft of black granite, marking the spot 50 feet underground where the Westinghouse "time capsule" is buried, has been dedicated by the park department of New York City, at Flushing Meadow Park. Among the records and documents contained in the capsule is a copy of the 50th Anniversary (May 1934) issue of ELECTRICAL ENGINEERING in microfilm. Descriptions of the "time capsule" appeared in the October 1938 issue, page 430, and in the November 1940 issue, page 477.

Letters to the Editor

INSTITUTE members and subscribers are invited to contribute to these columns expressions of opinion dealing with published articles, technical papers, or other subjects of general professional interest. While endeavoring to publish as many letters as possible, Electrical Engineering reserves the right to publish them in whole or in part or to reject them entirely. Statements in letters are expressly understood to be made by the writers; publication here in no wise constitutes endorsement or recognition by the AIEE. All letters submitted for publication should be typewritten, double-spaced, not carbon copies. Any illustrations should be submitted in duplicate, one copy an inked drawing without lettering, the other lettered. Captions should be supplied for all illustrations.

A Matrix Theorem

To the Editor:

From electric circuit theory a theorem in matrix algebra, believed to be new, is suggested and proved. The theorem resembles De Moivre's well-known theorem for complex numbers.

To most electrical engineers the utility of the general circuit constants is quite familiar. Thus if we have a four-terminal network with general circuit constants A_1, B_1, C_1, D_1 terminated in a second network with constants A_2, B_2, C_2, D_2 (figure 1), the constants A, B, C, D of the two networks in cascade considered as a single unit may be obtained by matrix multiplication as follows:

$$\begin{Vmatrix} A & B \\ C & D \end{Vmatrix} = \begin{Vmatrix} A_1 & B_1 \\ C_1 & D_1 \end{Vmatrix} \begin{Vmatrix} A_2 & B_2 \\ C_2 & D_2 \end{Vmatrix} \qquad (1)$$

Applying the above relation repeatedly to n identical networks with constants A_1, B_1, C_1, D_1 in cascade, we get the A, B, C, D of the whole from:

$$\begin{Vmatrix} A & B \\ C & D \end{Vmatrix} = \begin{Vmatrix} A_1 & B_1 \\ C_1 & D_1 \end{Vmatrix}^n \qquad (2)$$

In the special case of a uniform transmission line whose total series impedance and total shunt admittance are respectively Z and Y, the general circuit constants are:

$$\left.\begin{aligned} A_1 &= \cosh\theta \\ B_1 &= (Z/\theta)\sinh\theta \\ C_1 &= (\theta/Z)\sinh\theta \\ D_1 &= \cosh\theta \end{aligned}\right\} \qquad (3)$$

wherein

$$\theta = \sqrt{ZY}$$

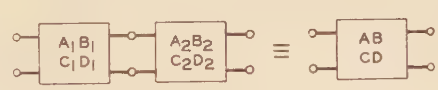

Figure 1

Suppose now n identical lines are connected in series. Then the total series impedance and the total shunt admittance become nZ and nY respectively while the quantity θ becomes also n times as large. The general circuit constants for n such lines in cascade are thus:

$$\left.\begin{aligned} A &= \cosh n\theta \\ B &= (Z/\theta) \sinh n\theta \\ C &= (\theta/Z) \sinh n\theta \\ D &= \cosh n\theta \end{aligned}\right\} \qquad (4)$$

Hence by applying equation 2 we get the following matrix identity:

$$\begin{Vmatrix} \cosh\theta & (Z/\theta)\sinh\theta \\ (\theta/Z)\sinh\theta & \cosh\theta \end{Vmatrix}^n = \begin{Vmatrix} \cosh n\theta & (Z/\theta)\sinh n\theta \\ (\theta/Z \sinh n\theta & \cosh n\theta \end{Vmatrix} \qquad (5)$$

It is obvious from the physical nature of Z and Y that they may assume any value, real or complex, provided the real part is positive. As $\theta=\sqrt{ZY}$, its value is not limited in any way. Similarly let r be written in place of θ/Z to denote any number, real or complex, and multiply element of the left-hand matrix in equation 5 by r. We then get the following relation:

$$\begin{Vmatrix} r\cosh\theta & \sinh\theta \\ r^2\sinh\theta & r\cosh\theta \end{Vmatrix}^n = \begin{Vmatrix} r^n\cosh n\theta & r^{n-1}\sinh n\theta \\ r^{n+1}\sinh n\theta & r^n\cosh n\theta \end{Vmatrix} \qquad (6)$$

or if we take $r=Z/\theta$, the relation assumes the alternate form:

$$\begin{Vmatrix} r\cosh\theta & r^2\sinh\theta \\ \sinh\theta & r\cosh\theta \end{Vmatrix}^n = \begin{Vmatrix} r^n\cosh n\theta & r^{n+1}\sinh n\theta \\ r^{n-1}\sinh n\theta & r^n\cosh n\theta \end{Vmatrix} \qquad (7)$$

It will be noted that these relations have been suggested by physical considerations just like many other interesting relations in pure mathematics. It is not difficult to prove them rigorously. For this purpose we will use mathematical induction. Assume, therefore, that equation 6 is true for $n=k$ and multiply both sides by the matrix:

$$\begin{Vmatrix} r\cosh\theta & \sinh\theta \\ r^2\sinh\theta & r\cosh\theta \end{Vmatrix}$$

We thus obtain:

$$\begin{Vmatrix} r\cosh\theta & \sinh\theta \\ r^2\sinh\theta & r\cosh\theta \end{Vmatrix}^{k+1} = \begin{Vmatrix} r\cosh\theta & \sinh\theta \\ r^2\sinh\theta & r\cosh\theta \end{Vmatrix} \times \begin{Vmatrix} r^k\cosh k\theta & r^{k-1}\sinh k\theta \\ r^{k+1}\sinh k\theta & r^k\cosh k\theta \end{Vmatrix}$$

$$= \begin{Vmatrix} r^{k+1}(\cosh\theta\cosh k\theta+\sinh\theta\sinh k\theta) & r^k(\cosh\theta\sinh k\theta+\sinh\theta\cosh k\theta) \\ r^{k+2}(\cosh k\theta\sinh\theta+\cosh\theta\sinh k\theta) & r^{k+1}(\sinh\theta\sinh k\theta+\cosh\theta\cosh k\theta) \end{Vmatrix}$$

$$= \begin{Vmatrix} r^{k+1}\cosh(k+1)\theta & r^k\sinh(k+1)\theta \\ r^{k+2}\sinh(k+1)\theta & r^{k+1}\cosh(k+1)\theta \end{Vmatrix} \qquad (8)$$

since

$$\cosh(k+1)\theta = \cosh\theta\cosh k\theta+\sinh\theta\sinh k\theta$$

and

$$\sinh(k+1)\theta = \sinh\theta\cosh k\theta+\sinh k\theta\cosh\theta$$

Now equation 8 shows that if equation 6 is true for $n=k$, then it is also true for $n=k+1$. As equation 6 is true for $n=1$, it is therefore true for $n=2$, 3, etc. Hence the relation is true for all positive integral values of n. Similarly we can establish the validity of equation 7. But, as

$$\begin{Vmatrix} \cosh\theta & r^{-1}\sinh\theta \\ r\sinh\theta & \cosh\theta \end{Vmatrix}^{-1} = \begin{Vmatrix} \cosh\theta & -r\sinh\theta \\ -r^{-1}\sinh\theta & \cosh\theta \end{Vmatrix} \qquad (9)$$

and equation 7 is true for any value of θ or r, it is evident that equation 6 holds even when n is a negative integer. By thus permitting n to take any integral value, the two alternate forms equations 6 and 7 become only one.

The close similarity between equations 6 or 7 to De Moivre's well-known theorem for complex numbers,

$$(r\cos\phi+jr\sin\phi)^n = (r^n\cos n\phi+jr^n\sin n\phi)$$

may be noted. This resemblance can be made the more striking, if we let $\theta=j\phi$ and remember $\cosh j\phi=\cos\phi$ and $\sinh j\phi=j\times\sin\phi$, wherein $j=\sqrt{-1}$. Thus using circular instead of hyperbolic functions, our theorem becomes:

$$\begin{Vmatrix} r\cos\phi & j\sin\phi \\ jr^2\sin\phi & r\cos\phi \end{Vmatrix}^n = \begin{Vmatrix} r^n\cos n\phi & jr^{n-1}\sin n\phi \\ jr^{n+1}\sin n\phi & r^n\cos n\phi \end{Vmatrix} \qquad (10)$$

A special case, possessing more symmetry, is to put $r=1$. Then

$$\begin{Vmatrix} \cos\phi & j\sin\phi \\ j\sin\phi & \cos\phi \end{Vmatrix}^n = \begin{Vmatrix} \cos n\phi & j\sin n\phi \\ j\sin n\phi & \cos n\phi \end{Vmatrix} \qquad (11)$$

a corollary of which is evidently

$$\begin{Vmatrix} \cos n\phi & j\sin n\phi \\ j\sin n\phi & \cos n\phi \end{Vmatrix} \begin{Vmatrix} \cos m\phi & j\sin m\phi \\ j\sin m\phi & \cos m\phi \end{Vmatrix} = \begin{Vmatrix} \cos(m+n)\phi & j\sin(m+n)\phi \\ j\sin(m+n)\phi & \cos(m+n)\phi \end{Vmatrix} \qquad (12)$$

A. Pen Tung Sah (A'35, M'36)

(President, National University of Amoy, Changting, China)

Service-Factor Ratings

To the Editor:

I have seen the paper on "The Service Factor Rating of Arc-Welding Generators and Transformers," by R. C. Freeman and A. U. Welch on pages 137–41 of AIEE Transactions, volume 60, 1941 (April section) and I feel that I must send you a note to say how welcome it is. I happen to have been interested in its subject rather intimately for some months past, and I hope that the proposals now made will have their effect in establishing the sound principles they represent. If it were to come to a discussion, I would suggest that a duty-cycle standard of 60 per cent is unnecessarily high, and I should propose something much nearer the 40 per cent of the French rules (much of the evidence of your article, indeed, seems to me to support this); but that is not important at the moment. The main thing is to get the principles of one duty-cycle standard, one service-factor rating, and one set of temperature-rise limits established for all types of hand-welding equipment, including both generators and transformers, no matter what their enclosure or cooling-means may be.

You may be interested to know that thought is proceeding on the same general lines in some quarters over here. An article by J. W. Bayles, MSc. (Eng.), and an associate member of the Institution of Electrical Engineers (a good friend of mine), published in the *BEAMA Journal*, November 1940, treated the subject in outline in very much the same way, and arrived, in principle, at the same conclusions.

Thomas Carter (F'20)

(A. Reyrolle and Company, Ltd., Hebburn-on-Tyne, England)

(*Editor's Note:* See also pages 569–71 of this issue.)

Numerical Solution of Equations

To the Editor:

D. L. Waidelich's article on numerical solutions of equations (*EE, Oct. '41, p. 480–2*) is of some interest, although it is hard to see how Newton's method could be "not very generally known among engineers". Any respectable course in college algebra will include this.

Mr. Waidelich did not mention the "Graeffe method" of solving linear algebraic equations. This method is not as well known as Newton's or the iteration methods, but is much quicker when the degree of the equation is high. Also, a high degree of accuracy is easily obtained.

A very lucid exposition of this method is given by Kurtz and Corcoran in their "Introduction to Electrical Transients".

William M. Breazeale (A'31)

(Radiation Laboratory co-operating with National Defense Research Committee, Massachusetts Institute of Technology, Cambridge)

Copper Shortage

To the Editor:

The October issue of Electrical Engineering carries under the heading "Of Current Interest" an item on copper. I wonder if those in charge in Washington realize that the threatened copper shortage is brought about largely by their action.

If the price of copper is fixed at 12 cents per pound f.o.b. Naugatuck Valley, production is confined to those who can mine, smelt, refine, and lay down copper at this price without loss.

Colorado, Arizona, New Mexico are shot through with low-grade copper ore which would come into the market in quantity under a small increase in price, and elimination of the copper shortage is only a matter of allowing the price to rise to a point where supply equals demand. It is unfortunate that some of the Washington dreamers cannot see the light.

Plenty of copper at 14, 16, or 18 cents per pound would be much better than no copper at 12 cents, which seems to be the impending dilemma.

Frederick G. Strong (A'19, F'13)

(Wethersfield, Conn.)

New Books • • •

"Industrial-Commercial Electrical Reference." Under preparation for more than four years this 1,200-page reference volume by E. S. Lincoln (F'41) consulting engineer, has just been issued by the Electrical Modernization Bureau, representing a group of some 80 manufacturers of electrical equipment. The contents are based upon the wide experience of the author, who has been engaged as industrial consultant for many years, supplemented by selected information furnished by men in the electrical field who have rendered extensive, valuable advisory service to industrials for years. The book is intended to serve primarily electrical men in industrial plants, covering the entire field of industrial electrical operations from service entrance through utilization equipment. Each section devoted to service or utilization equipment is divided into "installation" and "operation" sections. "Installation" covers economic factors, selection of equipment, layout, application, and control; "operation" includes inspection, maintenance, testing, surveys, analysis of performance and operating costs, and correction of faulty operation. Sections are devoted to relations with manufacturers, industrial-plant managements, contractors, consultants, and utilities; industrial and professional associations; distribution systems; protection and control equipment; and various types of utilization equipment. Separate sections also cover such subjects as inspection, maintenance, testing, surveys, performance and cost analysis, power factor, and voltage correction. As an aid to proper installation of equipment, the book includes the complete National Electrical Code, the various sections being reproduced with the material to which they apply. The volume is liberally indexed and arranged so as to assist the industrial electrical man to find with the least possible delay the answers to problems demanding immediate solution. Purchasers of the book will receive a "supplementary service" consisting of new material to be issued periodically which will keep the subject matter continuously up to date. Published by Electrical Modernization Bureau, New York, N. Y.; approximately 1,200 pages, 300 illustrations, 300 tables; 9 by $11^1/_4$ inches, Fabrikoid; price $15, including supplementary service.

"Standard Handbook for Electrical Engineers." Seventh edition, 1941, revised and enlarged. The most recent edition of this electrical encyclopedia has been completely revised, to recognize shifts in order of importance of the branches of the electrical art, and to include new spheres of activity which have appeared in the eight years since the sixth edition was published. To facilitate handling and filing, and to provide a more legible book for reference, the format has been changed to one having larger overall dimensions, less bulk, and a larger type size for easier reading. Presentation of material has been based on the results of interviews with more than 100 electrical engineers, with the result that the handbook aims to answer the demand for an orderly compilation of the "working-tool information of electrical technology" which has been authenticated by research and experience, but is not generally accessible in a compact form. An attempt has also been made to meet a demand for terse condensation of abstract principles, without sacrifice of completeness, so that maximum space might be available for presentation of the accepted data of applied engineering, as given by practical experts. Most of the contributors are new, but have been selected for their authoritative standing, and for their ability to give an up-to-date presentation of the subject in which they are specialists. Changes include: expansion of the section on power-plant electrical equipment to embrace electrical equipment for the whole power system; new treatments of power transmission, electronics and radio, interior wiring, illumination, prime movers, and telephone; recognition of modern developments such as air conditioning, electricity in aviation and in the petroleum industry, lightning technology, high-voltage generators, and cyclotrons; and the expansion of the compilation of codes and standards. The index has been enlarged and elaborately cross-referenced. Edited by A. E. Knowlton (M'17, F'30) associate editor, *Electrical World*. McGraw-Hill Book Company, Inc., New York, 1941, 2303 pages, price $8.00.

"Family Expenditures in the United States," published by the National Resources Planning Board, presents a detailed statistical picture of how American families spend their incomes, based on a survey applying to the year 1935–36. The analysis of family spending and saving at different income levels includes a breakdown of expenditures into more than 90 items, with separate figures for farm, rural nonfarm, and urban families, and with comparative estimates for white and negro families, for five geographic regions, and for three sizes of family. The volume is the third of a series of reports on purchasing power and consumption requirements of the American people, the first two of which were "Consumer Incomes in the United States," and "Consumer Expenditures in the United States." The report shows that of the $41,000,000,000 spent for current consumption needs, less than nine per cent was spent for automobiles, household equipment, and other durable goods, and less than ten per cent for semidurable goods. Food and other perishable goods accounted for 47 per cent. Prepared by Dr. Hildegarde Kneeland and a technical staff. United States Government Printing Office, Washington, D. C., 1941, price 50 cents.

"An Introduction to the Operational Calculus." The purpose of this book is stated as being "to develop some of the methods of the operational calculus for the use of engineering undergraduates whose mathematical equipment is necessarily limited, and for practicing engineers whose mathematical equipment has become rusty through disuse." The material is developed gradually from known mathematical processes to newer ideas and methods, with the first part of the book containing a review of the classical methods of solving linear differential equations with constant coefficients. As opposed to the usual treatment of these subjects, this book makes use of the notation and nomenclature of the operational calculus. The operational calculus as developed in this book is merely a shorthand method of solving certain types of differential equations. By Walter J. Seeley, professor of electrical engineering, Duke University. International Textbook Company, Scranton, Pa., 1941, 167 pages.

"The Engineering Profession." This book describes qualifications and duties of the professional engineer, and his habit of mind. It thus aims to serve as a vocational guide to the young man in his choice of a profession, furnishing him with objective data for forming his own picture of engineering. It should also be of use to the vocational counselor who may be asked to supply information regarding the profession. Points of technology are discussed only by way of illustration. Contents of the books include: fields and functions of engineering; descriptions of the specialized fields of civil, mining, mechanical, electrical, and chemical engineering, and others; the method of engineering and application of this method; vocational guidance in engineering, and the education of the engineer; and requirements for admission to membership in engineering societies. By T. J. Hoover, dean, school of engineering, Stanford University, and J. C. L. Fish, emeritus professor of civil engineering, Stanford University. Stanford University Press, Stanford University, Calif., 1941, 441 pages, price $5.00.

"Electrical Wiring Specifications." This book is a review of design and specification procedure for electrical wiring jobs, presented as a working guide for all concerned with designing wiring installations, laying out wiring systems, and developing specifications for any given job, and containing rules for carrying out these procedures in compliance with the National Electrical Code. It is an authoritative book on a subject of wide importance. Edited by Earl Whitehorne. McGraw-Hill Book Company, Inc., New York and London, 1941, 181 pages, price $2.50.

The following new books are among those recently received at the Engineering Societies Library. Unless otherwise specified, books listed have been presented by the publishers. The Institute assumes no responsibility for statements made in the following summaries, information for which is taken from the prefaces of the books in question.

PRINCIPLES OF MAGNAFLUX INSPECTION. By F. B. Doane. Magnaflux Corporation, Chicago, 1940. 133 pages, illustrated, $9^1/_2$ by 6 inches, cloth, $2.50. A description of magnaflux inspection methods, covering equipment, processes, the inspection medium, detectable defects, demagnetization, and the evaluation of indications. There is a separate chapter on weld inspection, and basic physical principles also are discussed briefly. Bibliography.

THE THEORY OF RATE PROCESSES. By S. Glasstone, K. J. Laidler, and H. Eyring. McGraw-Hill Book Company, New York and London, 1941. 611 pages, diagrams, etc., 9 by 6 inches, cloth, $6.00. This book describes the development and application of a general theory of the kinetics of physical and chemical processes, usually known as the "theory of absolute reaction rates". The fundamental bases are explained, and homogeneous and heterogeneous gas reactions, reactions in solution, viscosity, diffusion, and electrochemical phenomena are considered in terms of the theory.

ATM (Archiv für technisches Messen), Lfg. 119, May 1941. R. Oldenbourg, Munich and Berlin, pages T63–77, F3; illustrated, 12 by $8^1/_2$ inches, paper, 1.50 rm. each. This monthly publication contains classified articles upon various types of apparatus and methods of technical measurement.

There are also descriptions of specific instruments manufactured by German companies.

ELECTRICAL ENGINEERING FUNDAMENTALS. By G. F. Corcoran and E. B. Kurtz. John Wiley and Sons, New York, 1941. 450 pp., diagrams, etc., 9 by 6 inches, cloth, $4.00. The subject matter presented in this textbook is intended as first course material to prepare electrical engineering students for specialized courses. Special emphasis has been given to the arrangement and explanation of basic principles and concepts, although certain chapters deal with more advanced topics.

ENGINEERING DESCRIPTIVE GEOMETRY AND DRAWING. By F. W. Bartlett and T. W. Johnson. John Wiley and Sons, New York; Chapman and Hall, Ltd., London, 1941. 572 pages, illustrated, cloth, $4.50. This comprehensive textbook, developed for use at the United States Naval Academy, consists of three parts: I. Line drawing, which is chiefly concerned with the manner of handling the instruments; II. Engineering descriptive geometry, which deals with the rules of orthographic projection applied to simple geometrical shapes; and III. Engineering drawing, which describes the application of the general principles of drawing to engineering purposes with emphasis on detail drawing.

ENGINEERING ENCYCLOPEDIA. Two volumes. Edited by F. D. Jones. Industrial Press, New York, 1941. 1431 pages, diagrams, etc., $9^1/_2$ by 6 inches, fabrikoid, $8.00. This two-volume reference work supplies practical information such as the various important mechanical laws, rules, and principles; physical properties and compositions of materials used in engineering practice; and the characteristic features and functions of different types of machine tools and other equipment. The 4,500 topics included are alphabetically arranged and cross-indexed, and have been selected for their usefulness in the mechanical industries.

INDEX TO THE LITERATURE ON SPECTROCHEMICAL ANALYSIS, 1920–1939. Second edition. By W. F. Meggers and B. F. Scribner; publication sponsored by Committee E-2 on spectrographic analysis of the American Society for Testing Materials, Philadelphia, 1941. 94 pages, 9 by 6 inches, paper, $1.00. Nearly 1,500 references are contained in this second edition of an index which appeared originally in 1937. This constitutes a 50 per cent increase. The literature from 1920 to 1939 is covered chronologically, with the authors alphabetically arranged within each calendar year. Detailed subject index.

THE SECOND YEARBOOK OF RESEARCH AND STATISTICAL METHODOLOGY BOOKS AND REVIEWS. Edited by O. K. Buros. Gryphon Press, Highland Park, N. J., 1941. 344 pages, 11 by $7^1/_2$ inches, cloth, $5.00. This book consists of carefully selected critical reviews of books dealing with statistical methods and techniques in a variety of fields. Three hundred and fifty-nine books published since 1932 are included, providing a list of the latest publications on the subject and also the means for evaluating them. Indexed by title, subject, and reviewer.

TABLE OF NATURAL LOGARITHMS. Volume 1. Logarithms of the Integers from 1 to 50,000. Prepared by the Federal Works Agency, Work Projects Administration for the City of New York; conducted under the sponsorship of and for sale by the National Bureau of Standards, Washington, 1941. 501 pages, tables, 11 by 8 inches, cloth, $2.00, payment in advance. Continuing the series of mathematical tables being compiled by the Work Projects Administration, this book constitutes volume 1 of a projected four-volume table of natural logarithms. The natural logarithms are given here to 16 decimal places for the integers from 1 to 50,000. Succeeding volumes will carry to 100,000 and cover the range from 0 to 10 at intervals of 0.0001.

PRACTICAL SOLUTION OF TORSIONAL VIBRATION PROBLEMS. Volume 2. By W. K. Wilson. Second edition. John Wiley and Sons, New York, 1941. 694 pages, illustrated, 9 by $5^1/_2$ inches, cloth, $8.50. Owing to the extensive revision and enlargement of the new edition of this work, it was divided into two volumes. The second volume deals with the determination and measurement of stresses owing to torsional vibration, the analysis of torsiograph records, damping devices and rotating-pendulum vibration absorbers, and the dynamic characteristics of electrical-mechanical direct-coupled systems. Practical examples are worked out, and an appendix contains a discussion of harmonic analysis, a bibliography, and a selected list of British patents.

QUARZDRUCKMESSGERÄTE HÖHER EIGENFREQUENZ, Schwingungseigenschaften und Abhilfe gegen die Störung durch Massenkräfte. By W. Gohlke. VDI Forschungshaft 407, March-April, 1941. VDI-Verlag, Berlin. 1–25 pages, illustrated, 12 by 8 inches, paper, 5 rm. The two articles contained in this research publication on piezoelectric measuring devices of high natural frequency deal respectively with their oscillatory properties and with the disturbing effects of inertial forces on readings.

SYMPOSIUM ON COLOR. Its Specification and Use in Evaluating the Appearance of Materials. Jointly sponsored by the American Society for Testing Materials and the Inter-Society Color Council. Washington Spring Meeting, American Society for Testing Materials, Philadelphia, 1941. 79 pages, illustrated, $9^1/_2$ by 6 inches, cloth, $1.25; paper, $1.00. Six technical papers, affording a broad view of the various aspects of color research, are contained in this symposium. The following list of titles indicates the scope: introduction to color; color specifications of transparent materials; hiding power and opacity; color standards for opaque materials; spectrophotometry and color evaluation; photoelectric tristimulus colorimetry.

TABLES OF PROBABILITY FUNCTIONS. Volume 1. Prepared by the Federal Works Agency, Work Projects Administration for the City of New York; conducted under the sponsorship of and for sale by the National Bureau of Standards, Washington, 1941. 302 pages, tables, 11 by 8 inches, cloth, $2.00, payment in advance. The present volume, which is the seventh in the series of mathematical tables now under preparation extends the range of all existing tables of the error function and provides a smaller tabular interval. As in all the volumes of the series, provision has been made to facilitate both direct and inverse interpolation. Entries given to 15 decimal places.

ELEMENTS OF ENGINEERING THERMODYNAMICS. By J. A. Moyer, J. P. Calderwood, A. A. Potter. Sixth edition, rewritten. John Wiley and Sons, New York; Chapman and Hall, London, 1941. 217 pages, diagrams, $9^1/_2$ by 6 inches, cloth, $2.50. In the present edition, as in the previous ones, this book is designed to stress the fundamental principles of engineering thermodynamics as a foundation for the more advanced and practical applications of the theory. It is intended particularly for use in technical colleges having special courses in advanced thermodynamics, steam turbines, internal combustion engines, heating, refrigeration and other applications of thermodynamics.

TRANE AIR-CONDITIONING MANUAL. Revised edition. The Trane Company, La Crosse, Wis., 1941, 376 pages, illustrated, $11^1/_2$ by $8^1/_2$ inches, cloth, $5.00. This publication is primarily concerned with the application of the fundamental facts of engineering to the design of air-conditioning systems. Heat and its transmission, physical comfort, air properties and supply, psychrometry, refrigeration and ventilation processes, the functions of water in air conditioning, and a chapter on ducts and fans, new in this edition, are covered in this comprehensive treatment of the subject. Diagrams, tables, problems and numerical examples.

FUNDAMENTALS OF VACUUM TUBES. By A. V. Eastman. Second edition. McGraw-Hill Book Company, New York and London, 1941. 583 pages, illustrations, $9^1/_2$ by 6 inches, cloth, $4.50. The aim in this work has been to combine in a single text the basic theory underlying the operation of all types of modern vacuum tubes with descriptions of their more common applications in communications and industry. Descriptions and mathematical analyses of the phenomena under consideration are given. Revised and rearranged.

NUCLEAR PHYSICS. (University of Pennsylvania Bicentennial Conference.) By E. Fermi and others. University of Pennsylvania Press, Philadelphia, 1941. 68 pages, diagrams, etc., 9 by 6 inches, paper, $0.75. This pamphlet contains six papers presented at a conference on nuclear physics held in connection with the bicentenary of the University of Pennsylvania.

THROUGH ENGINEERING EYES. Science Selections from Literature. By A. R. Cullimore, re-edited by F. A. Grammer and I. H. Pitman. Pitman Publishing Corporation, New York and Chicago, 1941. 166 pages, illustrated, $7^1/_2$ by $5^1/_2$ inches, linen, $1.00. Presented with the aim of "picturing the development of science and engineering", this volume consists of selections from a variety of books, ancient and modern, written by engineers, scientists, poets, essayists, and philosophers. Each is included because it has "a direct bearing on engineering".

THE THEORY AND APPLICATIONS OF HARMONIC INTEGRALS. By W. V. D. Hodge. University Press, Cambridge, England; Macmillan Company, New York, 1941. 281 pages, tables, 9 by $5^1/_2$ inches, cloth, $4.50. This book is a study of certain integrals defined in a type of space, locally that of classical Riemannian geometry, which is of importance in various branches of mathematics. Topics covered are: Riemannian manifolds; integrals and their periods; harmonic integrals; applications to algebraic varieties; and applications to the theory of continuous groups.

THE TESTING AND INSPECTION OF ENGINEERING MATERIALS. By H. E. Davis, G. E. Troxell, and C. T. Wiskocil. Preliminary edition for Engineering Defense Training Courses. McGraw-Hill Book Company, New York and London, 1941. 372 pages, illustrated, 10 by 7 inches, cloth, $3.50. In view of the increasing importance of quality control in production and its dependence upon tests and inspection, it is the aim of the authors to provide in this book a general treatment of the problems of testing, with specific reference to the mechanical testing of engineering materials, and to establish the principles for the inspection of these materials. Methods of conducting common tests, applicable to most ordinary apparatus, are described in the second section of the book.

TABLE OF NATURAL LOGARITHMS, Volume 2. Logarithms of the Integers from 50,000 to 100,000. Prepared by the Federal Works Agency, Work Projects Administration for the City of New York, conducted under the sponsorship of and for sale by the National Bureau of Standards, Washington, D. C., 1941. 501 pages, tables, 11 by 8 inches, cloth, $2.00, payment in advance. The second volume of this table continues it for the integers from 50,000 to 100,000. Values are given to sixteen decimal places.

THE RUNNING AND MAINTENANCE OF MARINE MACHINERY. Institute of Marine Engineers, London. Second edition. Engineers' Book Shop, New York, 1941. 164 pages, illustrated, 10 by 7 inches, cloth, $2.50. A practical work, prepared for junior members of the Institute of Marine Engineers, intended as a guide for those entering upon a sea-going career. Steam reciprocating engines and turbines, boilers, diesel engines, electrical and refrigerating machinery, pumping arrangements, and steering gears are discussed. A list of books is included.

PRACTICAL SHIP PRODUCTION. By A. W. Carmichael. Second edition. McGraw-Hill Book Company, New York and London, 1941. 283 pages, illustrated, $9^1/_2$ by $6^1/_2$ inches, cloth, $3.00. The present increased interest in shipbuilding is responsible for the revision of this text, which appeared originally in 1919. The book is intended particularly for engineers and technical men who are transferring their activities from other fields to marine engineering and naval architecture. The treatment is practical, rather than theoretical, and concerned with construction, rather than design. The new edition has been partly rewritten, especially the section on electric welding.

MOTION STUDY. By H. C. Sampter. Pitman Publishing Company, New York and Chicago, 1941. 152 pages, ilustrated, $8^1/_2$ by 5 inches, cloth, $1 75. The principles of motion study, as distinct from time study, are clearly presented. Motion symbols are explained, the basic laws and principles for motion economy discussed, and flow process charts to eliminate the study of superfluous operations in a series or complete process.

MODERN MARINE ELECTRICITY. By P. de W. Smith. Cornell Maritime Press, New York, 1941. 279 pages, illustrated, $7^1/_2$ by 5 inches, cloth, $2.50. This handbook is intended to provide the operating marine electrician with a practical guide to the electrical equipment of the modern ship and to its maintenance.

ELECTRONICS. By J. Millman and S. Seely. McGraw-Hill Book Company, New York and London, 1941. 721 pages, illustrated, $9^1/_2$ by 6 inches, cloth, $5.00. This textbook is intended to provide a development of basic electronic principles with applications to many problems in electrical engineering and physics. It co-ordinates the physical theory of electronics and the theory of operation of electronic devices, gives attention to material of present-day commercial importance, and includes both detailed illustrative problems and groups of problems to be worked.

ELECTRICITY APPLIED TO MARINE ENGINEERING. By W. Laws. Institute of Marine Engineers, London; Engineers' Book Shop, New York, 1940. 276 pages, diagrams, etc., $7^1/_2$ by 5 inches, cloth, $2.00. A clear, simple presentation of the fundamental principles of electricity, with special emphasis upon their application in ships. The text is intended for young engineers without much mathematical or technical background, who are preparing for British Board of Trade Certificate examinations, and is based upon articles published in the *Transactions* of the Institute of Marine Engineers.

THE BELL TELEPHONE SYSTEM. By A. W. Page. Harper and Brothers, Publishers, New York and London, 1941. 248 pages, illustrated, 9 by 6 inches, cloth, $2.00. This is a description of the operating policies of the American Telephone and Telegraph Company and its constituent companies, written by the vice-president in charge of public relations. Problems of research, technology, wages, rates and service, relations with the government, and finance are considered, and the methods and achievements of the organization set forth. Much hitherto scattered information is brought together in convenient form.

TEMPERATURE MEASUREMENT AND CONTROL. By R. L. Weber. Blakiston Company, Philadelphia, 1941. 430 pages, illustrated, 9 by 6 inches, cloth, $4.00. This textbook is a revision of a preliminary edition published under the title, "Temperature Measurement". Based upon a course offered to Juniors at Pennsylvania State College, it outlines "an experimental study of the methods of temperature measurement with the theoretical principles necessary for their appreciation, intelligent use and extension".

Any discussion of these papers will appear in the December 1941 "Supplement to Electrical Engineering —Transactions Section"

Large Electric-Arc Furnaces—Performance and Power Supply

B. M. JONES
MEMBER AIEE

C. M. STEARNS
NONMEMBER AIEE

ELECTRIC arc furnaces are desirable loads for power systems, and are becoming more and more used for producing high-grade alloy steels, as well as for other types of steel. The authors believe that the data in this article will be of value and assistance to others in the solution of similar problems.

It is necessary in connecting large electric arc furnaces onto power systems that it be done in such a manner that neither the voltage changes, caused by the violent and rapid load swings of these furnaces, will interfere with other load of the furnace customer nor be permitted to reflect back into the system in such a manner as to interfere with service to adjacent customers. Also precautions must be taken so that such widely fluctuating loads will neither interfere with the operations of any of the equipment on the power system nor interfere with any interconnection with adjacent power companies. Further, precautions must be taken so that voltage regulation caused by large short-time loads will not be too great.

Summary

In March 1940, a 25-ton Heroult 3-phase electric arc furnace using a 10,000-kva furnace transformer was connected to the Duquesne Light Company system, and in August 1940, a second furnace duplicating the first was installed at the same location. These installations were made by the Pittsburgh Crucible Steel Company at their Midland, Pa., plant near Pittsburgh.

It was believed that the load swings on the first furnace with the accompanying voltage changes would exceed the standards which the Duquesne Light Company had established for this type of load, viz.

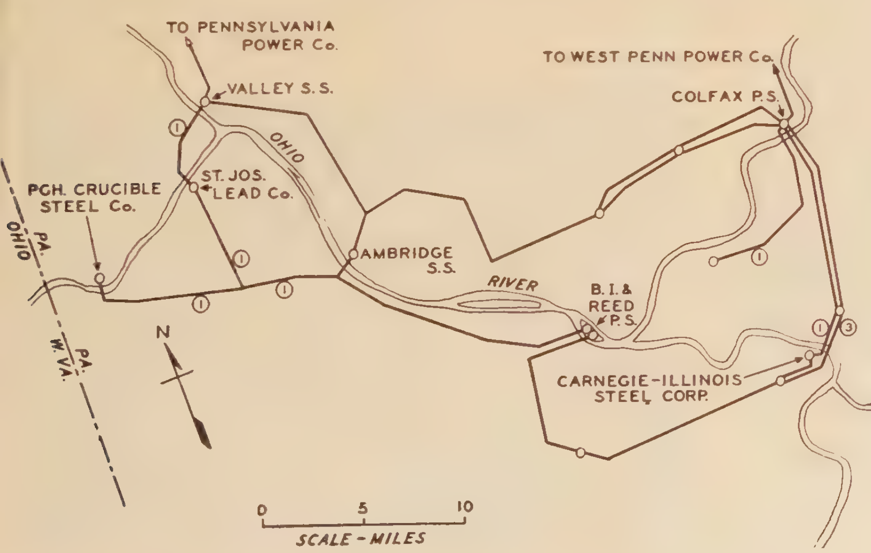

Figure 1. Diagram of power system showing 66-kv lines and power stations

Each line on diagram represents two 50,000-kva lines unless noted. Duquesne Light generating capacity is 504,000 kw with a 60,000-kw unit scheduled for service in July 1941

All lines are double-circuit unless noted by (1) or (3)

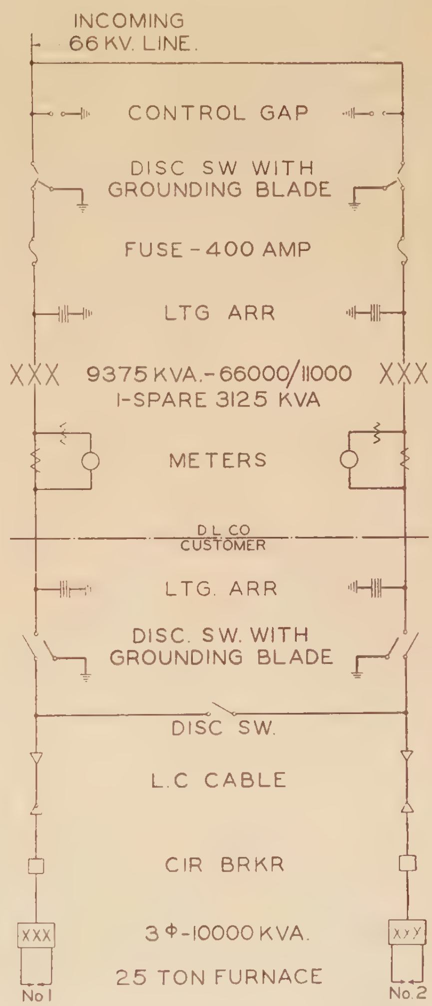

Figure 2. Diagram of power-supply substation and furnace substation

The 400-ampere 66-kv fuses provide protection for high-voltage and low-voltage faults

Paper 41-40, recommended by the AIEE committee on electrochemistry and electrometallurgy, and presented at the AIEE winter convention, Philadelphia, Pa., January 27–31, 1941. Manuscript submitted October 8, 1940; made available for preprinting December 10, 1940.

B. M. JONES is division engineer of system planning and development department, and C. M. STEARNS is subsection engineer of the Duquesne Light Company, Pittsburgh, Pa.

1. For all numbered references, see list at end of paper.

1.5 volts (115-volt base) for the 66-kv system with fluctuations from 3 per hour up to 15 per minute. Precautions were taken in the design of the furnace transformer to include separate reactance to reduce the load swings. Subsequently, it was found that this additional reactance was not eneded and it was removed, thereby improving the operation of the furnace.

The load swings and accompaning voltage changes, after disconnecting the reactance, due to the operation of the first furnace, slightly exceeded the Duquesne Light Company standards. However, no complaints have been received from adjacent customers nor have any difficulties arisen from excessive operation of 4-kv distribution regulators, operation of the power stations, or interconnections.

Second Furnace

Arrangements were made initially to interlock the controls of the two furnaces in such a manner that the furnaces would not melt down simultaneously. Thus the voltage flicker would not exceed that caused by the initial furnace and the regulation would be increased only a small amount.

Following the installation of the second furnace, a test was made with both furnaces melting down simultaneously at the highest secondary voltage. Instead of the load swings of the two furnaces being additive, the swings were diversified to the extent that the net swing of the two furnaces increased only 20 per cent over that of the first furnace. Voltage disturbances increased in the same ratio. In addition, the test showed that the resultant combined swings of the two furnaces were less frequent than for the first furnace alone. Thus the interlocking scheme may not be necessary except as a means of reducing the 15-minute demand.

Method of Approach

This article contains a rather complete treatise of our investigations and presents the industry with these data which the authors hope will be of some use to others in the solution of their furnace problems.

Some data have been published on electric furnace performances and the power system supply (see bibliography), but for the first large installation on any power system the authors strongly recommend getting all data that they can possibly lay their hands on, and making a thorough analysis of them.

Obviously, the correct engineering approach is to determine in advance what the kilovolt-ampere swing and resultant voltage flicker will be, and to provide a suitable system connection with corrective equipment if necessary, to keep the voltage changes within tolerable limits. However, this is not always so easy, for in some cases it is difficult to find out just what the electric performance of the furnace will be.

In addition to the determination of instantaneous load changes, the maximum loads which exist for several seconds at a very poor power factor, and which occur several times during a heat, should be determined. These large loads may result in undesirable voltage regulation on the customer's supply bus or at adjacent customers.

There are many factors involved, and many calculations to be made, not only for normal system conditions but also for the abnormal system condition of reduced capacity, lines out of service, generators off the line, etc. These abnormal conditions may result in voltage disturbances beyond standard voltage limits. However, it will probably not be economical to reduce the voltage changes to standard limitations with lines and equipment out of service because of their infrequent occurrence.

Calculations

Having decided upon the maximum instantaneous furnace load swings, the voltage flicker at the customer's supply bus should be determined from the known or estimated system impedance at that point. The voltage flicker, then, at the nearest customer or substation should also be determined.

The per cent system impedance to the Pittsburgh Crucible Steel Company 66-kv bus in 68-kv terms and on a 10,000-kva base in $R+jX$ terms is:

$(1.1+j4.0)$ per cent

The reactance of each of the 66/11-kv 9,375-kva transformer banks supplying the furnace transformers is 6.0 per cent on a 10,000-kva base. The system impedance is based upon all generating units and all 66-kv lines in service and the West Penn Power tie closed at Colfax.

As the furnace load swings are generally at a very poor power factor, the use of system reactance at the customer's bus will give fairly close results. This system reactance is that ordinarily determined by a short-circuit study. However, the true power does change considerably and if this change and the change in the reactive power are known, then the calculations of the voltage change based upon system impedance rather than reactance will give more accurate results.

The calculations for voltage regulation may be made in substantially the same manner, as described above for voltage flicker.

Application of Corrective Equipment

If the voltage changes calculated as described under the preceding heading

Figure 3. Photograph of power-supply substation—66/11 kv, 18,750 kva—at Pittsburgh Crucible Steel Company, Midland plant

Incoming 66-kv line at left and 11-kv circuits to furnace transformers at right. Lightning arresters mounted at high-voltage transformer bushings

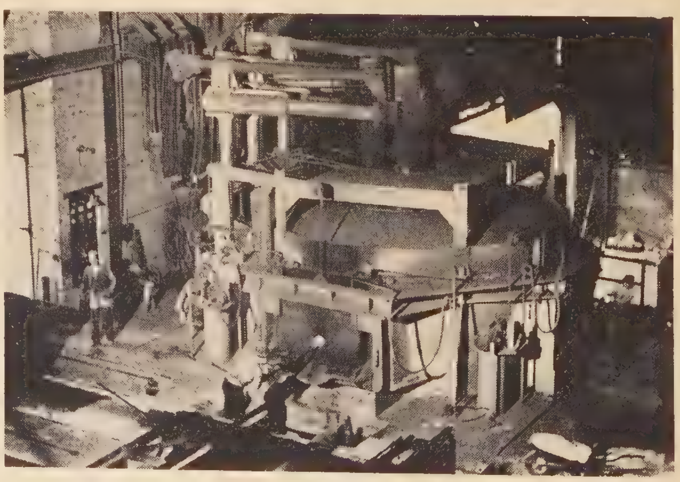

Figure 4. Photograph of charging side of a 25-ton Heroult three-phase electric-arc furnace at Pittsburgh Crucible Steel Company, Midland plant

exceed the allowable values, then corrective equipment should be applied. Discussion here will be limited to correction obtained by synchronous condensers. This as well as other methods of correction have been described by earlier papers, see item 1 in bibliography.

As far as very frequent instantaneous furnace load changes are concerned, the condenser will draw additional leading reactive current to offset some part of the additional reactive furnace load. For a general analysis, it can be considered that the system and the condenser will share the increased furnace reactive load in proportion to the inverse of their respective reactances. Thus the reduction in voltage flicker may be estimated as well as the amount of corrective capacity to obtain the desired reduction.

The condenser can be made to draw more leading reactive current by increasing the system reactance. This may be done by installing a buffer reactor in the furnace supply circuit ahead of the condenser. Actually, this buffer reactor produces increased voltage drop at the terminals of the condenser thus causing it to draw more leading reactive current. The condenser will draw increased leading reactive current in proportion to its subtransient reactance. Thus the speed of condenser field has very little to do with the correction of very rapid furnace reactive changes. Speeding up the field will, however, materially improve regulation for large load changes which last for several seconds.

Duquesne Light Company System and 66-Kv Supply to Furnace

Figure 1 shows the Duquesne Light Company system, including generating stations and the 66-kv transmission ring. The two major sources of interconnections with adjacent utilities are shown, one at Colfax with the West Penn Power Company and the other at Valley substation with the Pennsylvania Power Company. The latter is normally open, but in emergency can be closed and operated in parallel with the other systems, the 40,000-kva regulating transformer between the two systems being able to control both true power flow and reactive flow, the latter providing voltage regulation at this point, see items 6 and 7 in bibliography.

A single 66-kv circuit, ACSR 336,400 circular mils (4/0 equivalent) tapped to the single circuit between Ambridge substation and St. Joseph lead substation, was extended nine miles on wood poles with two ground wires to the Pittsburgh Crucible Steel Company at Midland, Pa. There is an extra degree of insulation and ground protection built into this extension which will make it practically immune from insulation troubles.

Supply Substation

Figure 2 shows the supply substation schematically for the 2 25-ton Heroult furnaces. Figure 3 shows the photograph of the substation with 2 9,375-kva transformer banks and one single-phase spare unit. Normally, each bank supplies one furnace independently and the 11-kv bus tie disconnecting switch is closed only in case one bank is out of service. At this time the furnace must be operated at a reduced secondary voltage to keep the load on the one 9,375-kva bank within its limit.

Figure 5. Photograph showing the pouring of 40 tons of high-grade alloy steel at Pittsburgh Crucible Steel Company, Midland plant

Note the entire furnace tilting to facilitate pouring

Tests on First Furnace

Tests were run during a complete heat on the first 25-ton Heroult furnace shown on figure 4 and figure 5.

Table I. Pittsburgh Crucible Steel Company, Midland, Pa.

Test on 4/10/40

Sec. Voltage	Point No. on Meter Charts	Kw	Reactive Kva	Kva Calculated	Three-Phase Power Factor Calculated*	11-Kv Voltage	Amperes at 11 Kv A	B	C	Kva Calculated**	Single-Phase Power Factor† (Per Cent) Point	Avg.	Max.	Min.
220	1 High	6,550	6,660	9,300	70.5	10,500	655	750	624	12,300	50			
	2 Low	2,280	300	2,300	99.2									
	Inst. change			7,000										
	3 High	7,200	8,700	11,300	64.0	10,000	804	760	792	13,400	50			
	4 Low	2,880	1,680	3,300	87.3									
	Inst. change			8,000								50 Average for 220 volts	98	50
	5 High	7,250	8,640	11,300	64.2	10,350	866	724	892	14,800	54			
	6 Low	2,400	1,200	2,700	89.0	11,000	192	240	240					
	Inst. change			8,600			674	484	652					
	7 High	6,000	9,840	11,500	52.1	10,000	703	792	888	15,000	60			
	8 Low	3,240	1,320	3,500	92.5	10,850								
	Inst. change			8,090										
240	9 High	8,700	11,520	14,430	60.3	9,400	883	1,065	1,100	16,500	50	85	95	50
	10 High	8,650	11,520	14,400	60.0	10,300	1,060	1,026	1,043	18,600	50			
	Low	8,150	4,800	9,400	86.8		556	605	580					
	Inst. change			5,000		9,770	504	421	463					
220	11 High	4,800	11,500	12,460	38.5	9,250	916	960	760	14,100	50	85	97	50

All measurements are "input to furnace transformers" and adjacent to furnace transformer.

*Calculated on basis of three-phase kilowatts and three-phase reactive kilovolt-amperes input.

**Calculated on basis of average amperes per phase and AB voltage.

†Power factor from charts using A amperes and AB and CB voltage.

General: The average power factor for loads during the refining period varies between 85 and 95 per cent. Inst. change—instantaneous change.

Graphic Meter Records

Graphic records were obtained of customer's 11-kv voltage, furnace reactive kilovolt-amperes, kilowatts, amperes in each phase and single-phase power factor, and 66-kv voltages at the nearest attended substations. Sections of these charts during different periods of the heat are shown in figures 6, 8, 10, 12, and 13. These charts were run at approximately six inches per minute speed.

The seven meters at the furnace were driven by a common shaft and a switch was installed to short circuit the current transformers and open the potential leads simultaneously. This switch was operated at 15-minute intervals to aid in synchronizing the charts for analysis purposes.

In order to run the charts at high speed, most of the damping effect is eliminated. This undoubtedly allowed the meters to overswing.

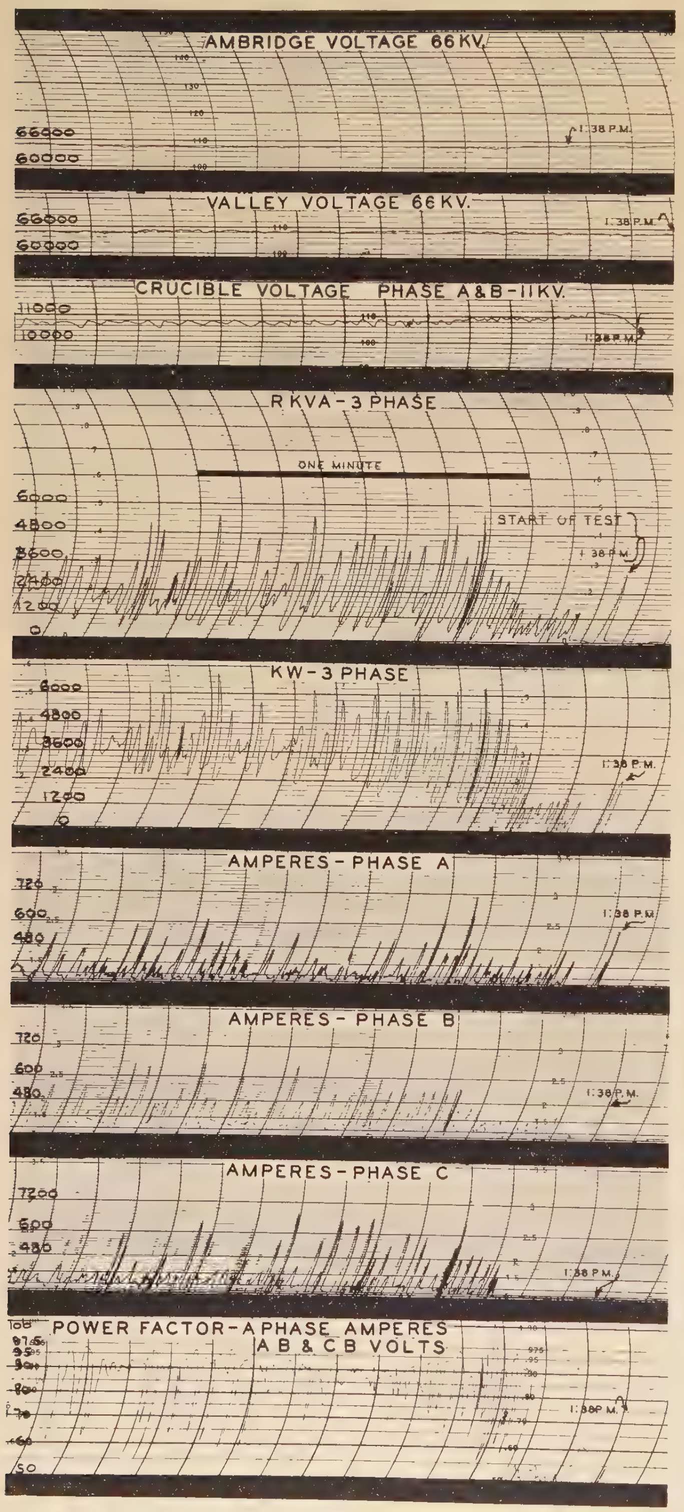

Figure 6. Graphic charts at start of heat at 1:38 p.m.

Furnace swings occur approximately once a second

Figure 7 (below). Oscillograph film at start of heat

A single-phase arc struck and restruck ten times in the space of 15 seconds before all three phases struck. After this initial period, all three phases struck and restruck ten times with currents in all three phases fairly well balanced before the arcs became generally stable. A portion of this performance is shown on this figure

Oscillograph Records

An oscillograph record was taken at several points during the heat. Portions of these records are shown in figures 7, 9, 11, and 14. The record of the single-phase wattmeter is intended to show the rapid changes in furnace consumption and not the true single-phase load, in so far as the single-phase wattmeter is 30 degrees out of phase with three-phase balanced loads.

It is almost impossible to obtain oscillograph records of the maximum loads or changes in loads because of their short duration.

Results

Table I shows various values obtained from the graphic charts of kw, reactive kilovolt-amperes, amperes, volts, and power factor. These values are instantaneous ones taken during maximum furnace load swings or furnace loads. Several of the numbered points are shown on the exhibits.

The maximum instantaneous furnace load swing, lasting a fraction of a second, amounted to 8,600 kva, 3 phase with a calculated power factor of 54.5 per cent (change in load). An analysis of the load swings indicated that the maximum occurred only once and only ten exceeded 7,000 kva during the heat.

The maximum instantaneous load of seconds duration, was found to be 14,400 kva or 144 per cent of the furnace transformer rating.

Based upon maximum load swings (8,600 kva) the voltage flicker at the nearest 66-kv customer (St. Joseph Lead Company) amounts to 2.3 volts, at Valley substation, 2.1 volts, and at Ambridge substation, 1.8 volts. See figure

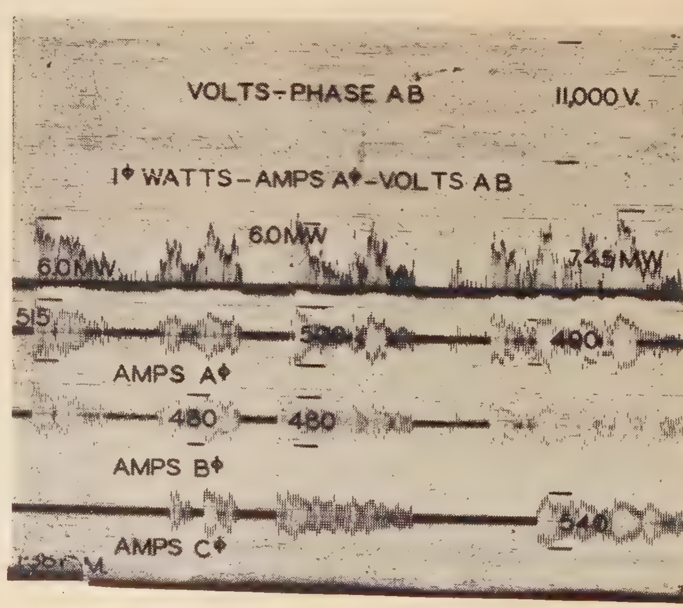

1 for locations. However, due to the fact that the majority of the load swings were considerably less than the maximum, no complaints have been received from adjacent customers and no difficulties have arisen from excessive operation of 4-kv distribution regulators or in the operation of the power station or interconnections.

Thus perhaps corrective equipment should not be installed to correct for the maximum swing but for something less than the maximum, assuming that a few voltage changes in excess of the standard could be allowed.

The location of the furnaces at the end of a long line and with considerable impedance to the supply bus, probably accounts for the fact that the load swings and maximum loads are less than might be expected from a furnace of the size installed.

Due to the fact that no other customers are located near the furnace installation the voltage flicker and regulation at the customer's 66-kv bus are allowed to exceed values that would normally be allowed and the voltage changes at the nearest customer are materially less due to the relatively high impedance between it and the furnace 66-kv bus.

Table II shows the 15-minute kilowatt demand during each 15-minute period of the heat. The maximum demand of 8,400 kw is at approximately 85 per cent power factor or 9,900 kva. Subsequent to this test and prior to the installation of

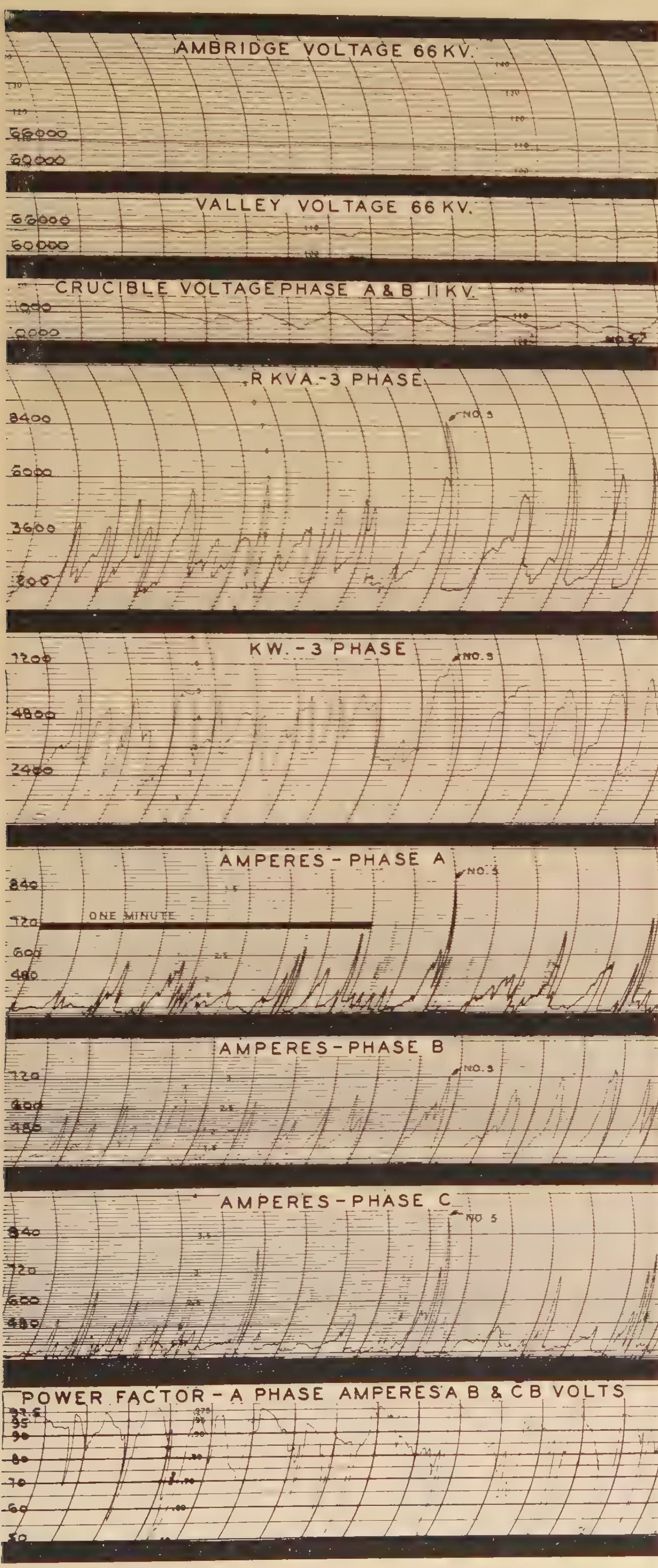

Figure 8. Graphic charts taken 14 minutes after start of heat

The swings have become less frequent, but are greater than shown on figure 6

Table II. Pittsburgh Crucible Steel Company, Midland, Pa.

April 10, 1940

15-Minute Kilowatt Demands

1:30 to 1:45 p.m.	1,800
1:45 to 2:00 p.m.	4,020
2:00 to 2:15 p.m.	3,960
2:15 to 2:30 p.m.	6,720
2:30 to 2:45 p.m.	7,080
2:45 to 3:00 p.m.	8,400
3:00 to 3:15 p.m.	6,480
3:15 to 3:30 p.m.	6,600
3:30 to 3:45 p.m.	3,900
3:45 to 4:00 p.m.	6,960
4:00 to 4:15 p.m.	7,200
4:15 to 4:30 p.m.	3,840
4:30 to 4:45 p.m.	1,680
4:45 to 5:00 p.m.	2,640
5:00 to 5:15 p.m.	1,560
5:15 to 5:30 p.m.	0
5:30 to 5:45 p.m.	1,320
5:45 to 6:00 p.m.	840
6:00 to 6:15 p.m.	1,140
6:15 to 6:30 p.m.	1,200
6:30 to 6:45 p.m.	1,320
6:45 to 7:00 p.m.	360

Next heat started at 7:45 p.m.

Complete heating cycle 6 hours and 15 minutes.

Figure 9 (below). Oscillograph film taken 14 minutes after start of heat

The currents have become more stabilized than in figure 7. The arc did not completely go out during the film

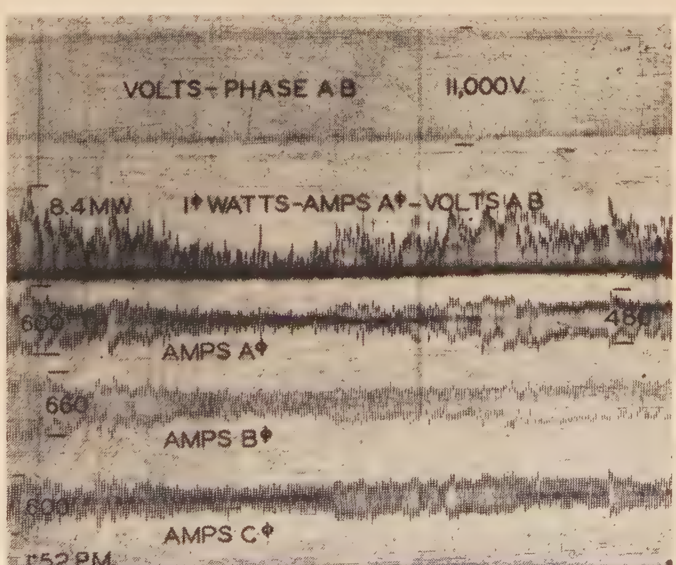

the second furnace the 15-minute demands were somewhat less.

The oscillograms showed maximum amperes of 840 while the graphic charts gave maximum values of 1,100. Probably the true maximum lies between the two, in so far as the graphic meters would probably overswing and the maximum values were probably not recorded on the oscillograph film.

Test on Two Furnaces

Following the installation of the second furnace, test data were obtained of the two furnaces melting simultaneously at the highest secondary voltage. Graphic meter chart records only of voltage, amperes, etc., the same as for the first furnace were obtained. Time has not permitted the preparation of the exhibits for inclusion in this paper but they will be available at a later time for discussion purposes.

During the test, number 2 furnace was melting the initial charge and number 1 furnace was melting the "back charge." Number 2 furnace started the initial melt down 29 minutes prior to number 1 furnace starting the melt down of the "back charge." The test continued from the time number 2 furnace started the melt down of the initial charge until the initial charge was melted, approximately $1^3/_4$ hours. The 11-kv bus tie was closed during the test to facilitate the obtaining of the records.

Results

The maximum combined instantaneous load swing of the two furnaces, lasting a fraction of a second, amounted to 10,580-kva, 3 phase with a calculated power factor of approximately 52.0 per cent (change in load). The next largest swing amounted to 7,500 kva, 3 phase and all other swings were materially less than 7,500 kva.

The maximum instantaneous load of seconds duration was found to be 22,850 kva, and there were several near this value.

Based upon maximum load swings (10,580 kva) the voltage flicker would exceed that of one furnace by about 20 per cent. However, the combined load swings of the two furnaces were much less frequent than for one furnace and actually there seemed to be no flicker

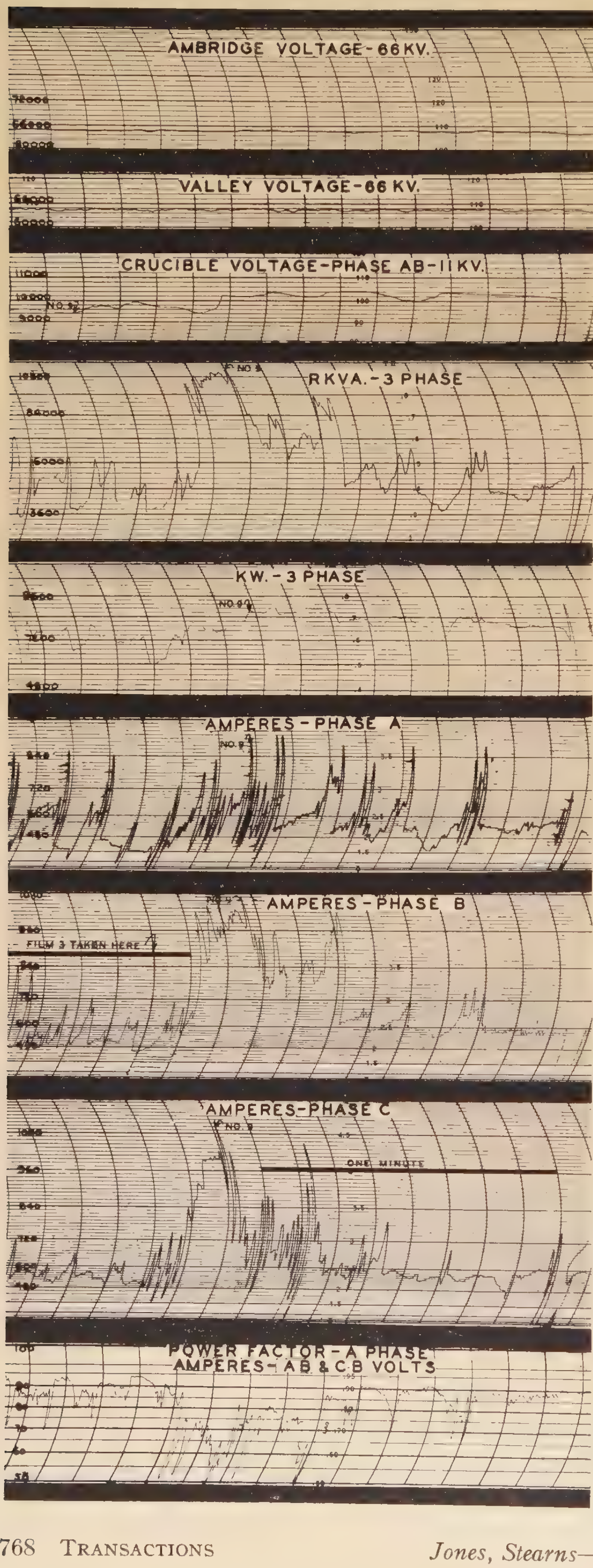

Figure 10. Graphic charts one hour after start of heat

Large furnace swings probably caused by scrap falling against electrodes or falling into molten metal raising its level and short-circuiting the electrodes

Figure 11 (below). Oscillograph film taken during time of figure 10

The exact correlation is not known

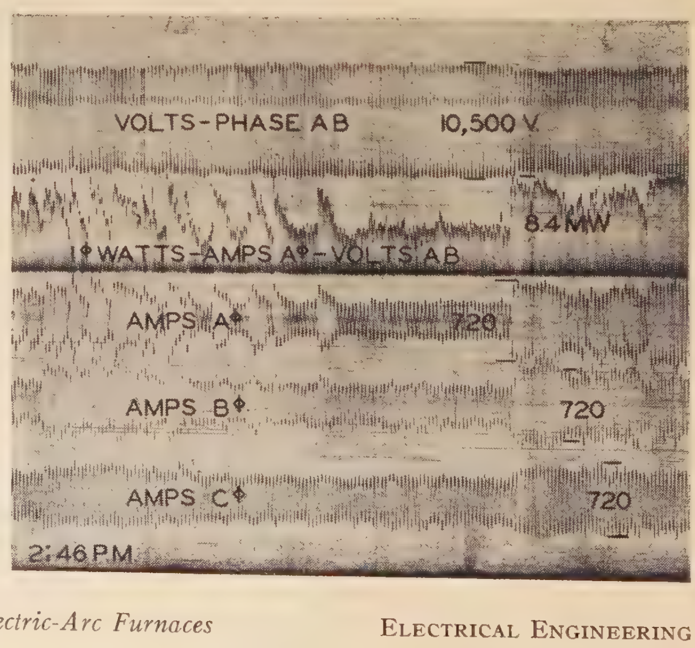

problem. Voltage regulation was of course greater but not intolerable.

The maximum 15-minute kilowatt demand was 15,600 at approximately 75 per cent power factor or 20,800 kva.

The graphic charts show maximum amperes of 1,590 per phase in the 11-kv circuit. Due to the larger ammeter constant, overswinging did not seem to be as pronounced as in the initial furnace test.

References

1. Arc-Furnace Loads on Long Transmission Lines, T. G. LeClair. AIEE Transactions, volume 59, 1940 (April section), pages 234–9.

2. Industrial Electric Heating—Transformers and Reactors for Three-Phase Arc Furnaces, N. R. Stansel. *General Electric Review*, May 1937.

3. Power Company Service to Arc Furnaces, L. W. Clark. AIEE Transactions, volume 54, 1935 (November section), pages 1173–8.

4. Three-Phase Electric Arc Furnace, Samuel Arnold. AIEE Transactions, volume 52, 1933, pages 839–43.

5. Modern Electric Furnace Design and Practice, H. F. Walther. Presented at the 36th Annual Convention Iron and Steel Exposition, Association of Iron and Steel Engineers, Chicago, Ill., September 24, 1940.

6. Application of Large Phase-Shifting Transformer on an Interconnected System Loop, W. J. Lyman and J. R. North. AIEE Transactions, volume 57, 1938 (October section), pages 579–87.

7. Controlling the Power Flow in a 300-Mile Transmission Loop, W. J. Lyman and J. T. Mercereau. *Electrical Journal*, October 1938.

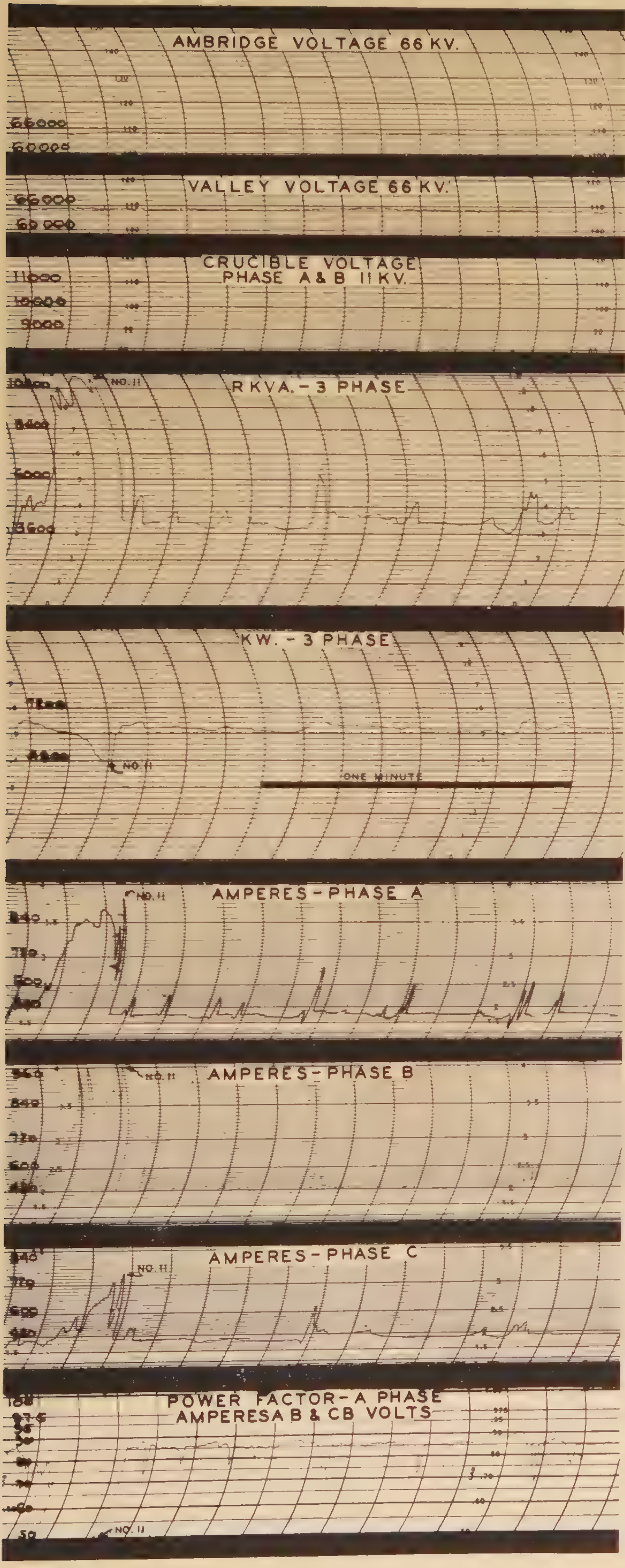

Figure 12. Graphic charts 1 1/2 hours after start of heat

The large load, point 11, was probably caused by scrap falling into molten metal and raising its level

Figure 13. Graphic charts during refining period

A timing device cut off the meters at 4:30 p.m.

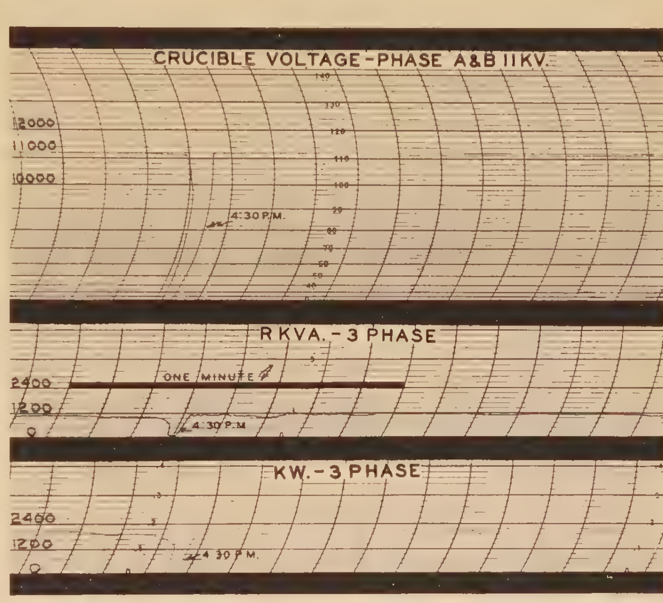

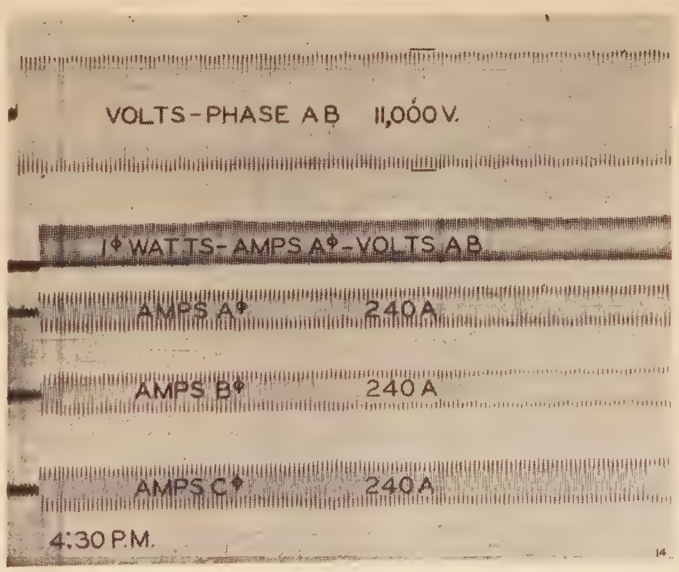

Figure 14. Oscillograph film taken during refining period, corresponding to figure 13

The timing device was operated at the extreme left

The "Electrogear"—A New Electromechanical Vehicle Drive

ERNST WEBER
FELLOW AIEE

Synopsis: Within recent years a new electromechanical transmission known as the "Electrogear" has been developed for use in gas and Diesel engine cars of all types including busses, trucks, rail cars, and track-laying vehicles. The paper describes the principle of its operation which is basically a differential action between direct mechanical power transmission and a generator-motor system, interlinked by means of a permanently engaged planetary differential gear.

At the start, both the electrical and mechanical power flows are in the same direction, giving high torque multiplication. As the vehicle speed increases, the electrical power flow diminishes, goes through zero, and finally reverses its direction, leading to high speed, low torque operation with "overdrive." The torque ratio is thus continuously variable as in the gas-electric drive, and is controlled independent of road conditions by a small auxiliary generator which acts as the "brain" of the system. The design and installation of one specific Bus Electrogear is given in detail in order to illustrate the application to public transportation, though various other models have been built and demonstrated. Extensive test data graphically describe the superior performance of this new vehicle drive which combines the ideal flexibility and low maintenance cost of the gas-electric drive with the economy of the standard gearshift transmission. Actual operation requires only accelerator and brake, both acted on conventionally by means of the conventional pedals, and a selector switch with engine starting, forward and reverse positions. The engine speed varies continuously, and due to the fact that only a comparatively small part of the engine power is circulated through the electrical machines, the weight of the drive is about one-half of that of the gas-electric transmission. Since the Electrogear goes automatically and inherently into "overdrive" at higher car speeds on level road, and can be designed to keep the engine speed in its most economic range during the major part of full throttle acceleration, its fuel economy is at least as good as that of the standard gearshift transmission, and for heavy city schedules becomes even considerably better.

Paper 41-28, recommended by the AIEE committee on land transportation, and presented at the AIEE winter convention, Philadelphia, Pa., January 27–31, 1941. Manuscript submitted October 28, 1940; made available for preprinting December 4, 1940.

Ernst Weber is research professor at the Polytechnic Institute of Brooklyn, Brooklyn, N. Y.

Author's acknowledgments: Save for the enthusiastic and freely given co-operation of all the parties mentioned below, it would not have been possible to carry out successfully the very first design and construction of the Bus Electrogear. It is, therefore, a great pleasure to acknowledge the indebtedness to John Whitson of The Power Transmission Company of New York for providing the background, co-ordination and support, and arranging for the co-operation of all concerned; to Colonel H. W. Alden of The Timken-Detroit Axle Company, who was the first to recognize the possibilities of the Electrogear for use in busses and track-laying vehicles, and who initiated the project for designing and building the first units and assigned the design engineering to R. M. Herron, who also supervised the assembly and participated in the installation of the unit; to C. O. Guernsey of the J. G. Brill Company who furnished the bus and provided generous co-operation; to E. R. Martin of the Delco Products Division of General Motors Corporation, who was in charge of the construction of the electrical machines; to G. M. Stapleton of the Ward Leonard Electric Company for the design of the control equipment; to John H. Gethin of the Pittsburgh Testing Laboratory for faithful assistance in the installation and during the tests; to F. W. Kateley and J. F. Chapman of The J. G. Brill Company for their interest, help, and supervision during the tests in Philadelphia. This paper was prepared at the request of the committee on land transportation of which E. B. Fitzgerald of the American Car and Foundry Company is chairman. The writer is indebted to Mr. Fitzgerald for his many helpful suggestions, and to F. W. Kateley of The J. G. Brill Company and Earl E. Kearns of the General Electric Company for the comparative test data on the gearshift and gas-electric drives.

1. For all numbered references, see list at end of paper.

I. Introduction

EVER since internal combustion engines have been used for the propulsion of vehicles, attempts have been made in great number to overcome the fundamental problem of flexible transmission of torque from the gasoline or Diesel engine to the wheels.[1] Yet no practical solution has been found which merely by mechanical devices produces a continuously variable ratio between engine torque and driving torque and is controlled by the action of the driver of the vehicle.

One of the most unsatisfactory elements of the standard gearshift transmission is the mechanical clutch operated by a separate clutch pedal. Practical ways have been found now to replace this clutch by a hydrodynamic coupling or "fluid flywheel"[2,3] which essentially consists of two rotating vane systems; one connected to the driving shaft, acting as centrifugal pump, and frequently called the impeller; the other connected to the driven shaft, acting as a turbine, and frequently called the runner. Torque transmission is obtained by the fluid circulating through both sets of vanes whereby on account of friction losses a certain amount of slip occurs. Any change in impeller speed causes a corresponding but slightly lagging change in runner speed resulting in a smooth operation of the vehicle without jolts. Since this "fluid flywheel" only acts torque transmitting, it must be used in connection with torque multiplying gears, either manually operated as in Chrysler cars, or in connection with automatic gearshifts as in the "hydra-matic" drive of the Oldsmobile[4] or it can be combined with a semi-automatic transmission as the "Fluid-gear" developed jointly by the A.C.F. Motors Company and the Spicer Manufacturing Company.[5]

A further step is the hydrodynamic transmission or "torque converter";[3,6] this device adds a stationary vane system to the hydrodynamic coupling as a reaction member changing the tangential velocity of the fluid and thus produces torque multiplication. As the vehicle starts, maximum torque multiplication is obtained with a slip of 100 per cent between impeller and runner, and as the vehicle speed increases, slip and torque multiplication decrease. At a predetermined speed of about 17 miles per hour, direct mechanical drive is established automatically, without action of the driver. Obviously, the efficiency and fuel economy in the hydrodynamic range of driving is considerably lower than in the standard gearshift transmission, though the acceleration can be made to be satisfactory.

In spite of this variety of more or less automatic transmissions now available,[7] none of these can truly lay claim to be the

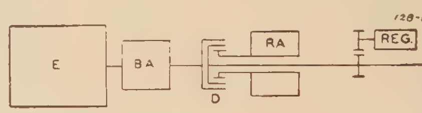

Figure 1. Schematic diagram of Electrogear

BA, RA, REG—Armatures
D—Planetary differential gear
E—Engine
OS—Output shaft

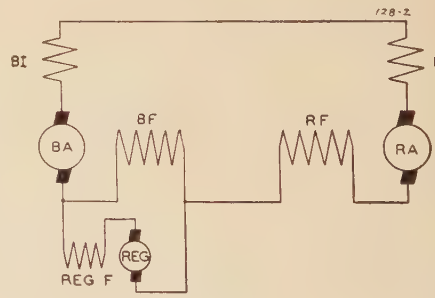

Figure 2. Diagram of Electrogear connections for forward operation

BA, RA, REG—Armatures
BF, RF, REG F—Series field windings
BI, RI—Interpole windings

ultimate solution of the fundamental problem of power transmission in individual vehicles as recently admitted by high authority in the automotive industry.[7a] The only and earliest solution outside the field of strictly mechanical means is the well-known gas-electric transmission in which the engine drives a generator at nearly constant speed and one or two motors are coupled to the driver axle. This gas-electric transmission has recently been considerably improved[8,9] and would appear to be the ideal solution since it gives a continuously variable torque ratio, were it not for the large loss of efficiency and the large size and weight of the electrical machines needed to carry the whole engine power.

The purpose of this paper is to describe the progress in the development of an entirely new principle of power transmission,[10] invented by A. H. Neuland[11] and developed during recent years through the support of The Power Transmission Company of New York City, owners of the patents. Fundamentally, it constitutes an electromechanical drive and is based upon a differential action between directly transmitted mechanical power and d-c electric power furnished by one electrical machine and consumed by another. The driving torque and therewith the torque ratio is controlled by conventional use of the accelerator pedal, and its variation is produced by a small auxiliary generator whose speed is proportional to vehicle speed. Since the transmission embodies electrical machines connected through the elements of a differential gear of the planetary type, the name "Electrogear" has been adopted for it.

The Electrogear has the extreme flexibility of the electric drive and, like this, gives a continuously variable torque ratio. In addition, it has the advantage of high fuel economy, since only a fraction of the mechanical power is transformed into electric power, and since the engine speed though variable can be kept within its most economic range even at the highest vehicle speeds, when overdrive automatically occurs. On account of the partial conversion into electric power, the sizes and weights of the electrical machines are considerably smaller than in the gas-electric drive with the attending advantages of lower currents and smaller commutators.

Designs of the Electrogear have been made and demonstration models built for several 5-passenger cars, for a 36-passenger city bus, and for a 12-ton track-laying vehicle. The Pittsburgh Testing Laboratory made extensive road tests of a five-passenger sedan with the Electrogear

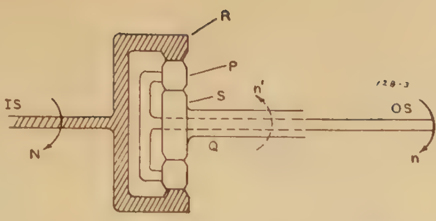

Figure 3. Planetary ring gear differential

R—Ring gear	*Q*—Quill
P—Planets	*IS*—Engine shaft
S—Sun gear	*OS*—Output shaft

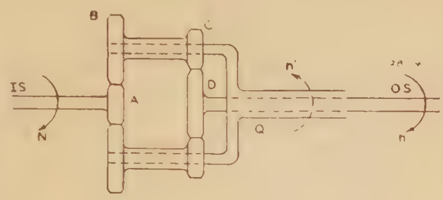

Figure 4. Double-planet differential

A—Input sun gear	*B, C*—Planets
D—Output sun gear	*Q*—Quill
IS—Engine shaft	*OS*—Output shaft

drive, and then duplicated the same tests of the same car with its conventional gearshift drive. The comparative results covered in a report[15] should be of interest to the automotive industry as well as to electrical engineers since they show that a transmission using electrical machines in proper combination with a differential gear can be just as efficient as a purely mechanical transmission.

The detail discussions in this paper however pertain to the bus application because the greatest variety of drives has been developed in this field, so that comparisons can readily be drawn from available commercial test and performance data.

II. Principles of Operation and Design

Figure 1 is a schematic sketch of the Electrogear drive with only the armatures of the electrical machines indicated for simplicity, figure 2 shows the connection diagram for forward operation of the vehicle, and figure 3 gives a more detailed sketch of the differential gear. The armature *BA* of the one electrical machine is directly coupled to the engine shaft *IS* and the ring gear *R* of the differential gear; this machine may, for convenience, be called booster. The armature *RA* of the second electrical machine is coupled to the sun gear *S* of the differential gear and usually is mounted on a hollow shaft or quill *Q*; this machine may, for convenience, be called reducer. Booster and reducer are series-wound d-c machines, both connected in series for forward operation of the vehicle as seen in figure 2. The auxiliary generator has its armature *REG* driven by suitable gears or by belt from the output shaft *OS*, which in turn carries the planet spider with the planets *P* of the differential gear. This auxiliary machine, called regulator for convenience, is connected parallel to the booster field; its function is the distinctive feature of the Electrogear.

1. Operation of the Electrogear

In forward operation, with the vehicle standing still and the engine idling, the ring gear and booster armature *BA* will turn with engine shaft speed, whereas the planet spider and output shaft are at rest. Thus, the sun gear with the reducer armature *RA* has to turn in a direction opposite to engine shaft rotation. Now, the electrical machines are so connected that under these mechanical conditions the reducer will act as self-excited generator and feed current into the booster, which will act as motor permitting just enough current flow to maintain polarities without moving the vehicle.

Depression of the accelerator pedal increases the engine speed and power and therefore the electric power generated by the reducer which drives the booster as motor in the same direction of rotation as the engine. Thus, the ring gear torque is actually the sum of engine and booster torques. Since both ring gear torque and reactive torque of reducer act in the same direction upon the planet spider, a considerable driving torque multiplication takes place comparable to "first gear" in mechanical transmissions; the planet spider starts revolving and the vehicle starts moving. As the vehicle, and with it the planet spider, speeds up, the reducer slows down so that without any further action the vehicle could reach only a comparatively low speed determined by the electromechanical balance of torques.

However, part of the main current is shunted through the regulator which has its field so connected as to generate a voltage in opposition to the voltage drop across the booster field. Since the regulator speed increases with vehicle speed, the regulator voltage also increases and eventually reverses the current in the booster field. The electrical design must, of course, correlate this period with the period in which the reducer has slowed down enough to be unable to drive the booster as motor, so that the regulator, furnishing from now on the field excitation of the booster in reversed direction, forces it to act as generator. With the main cur-

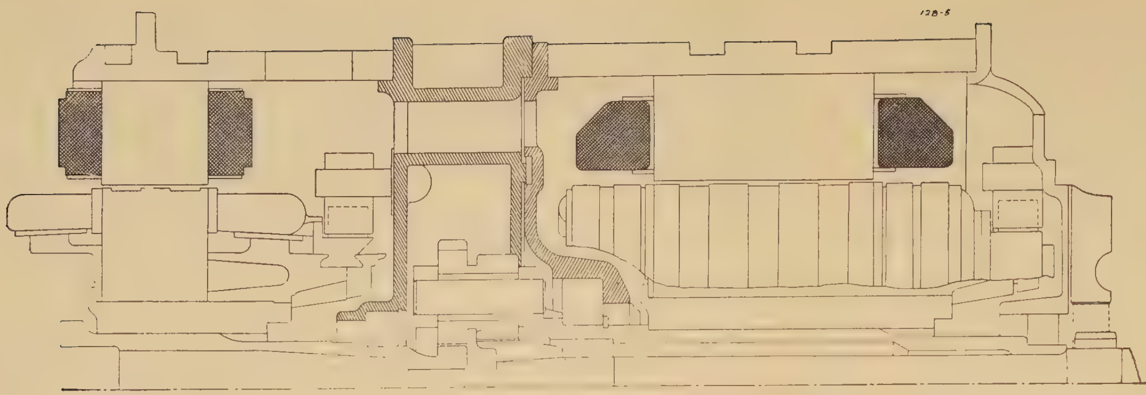

Figure 5. Simplified drawing of Electrogear layout for a city bus

rent continuing to flow in its original direction, the reducer must now reverse its direction of rotation to run as motor. It is quite obvious, at this point, that the regulator is the automatic governor of the booster and determines the over-all action of the electrical power flow which is differentially superimposed upon the mechanical power transfer. Since, in operation, the transitions from motor-to-generator state and vice versa are accomplished smoothly and without any interruption, the resulting variation in driving torque is also continuous and responsive to the degree of depression of the accelerator pedal which, in fact, is an inherent feature of this transmission.

As soon as the reducer reverses its direction of rotation, all three elements of the differential gear, namely ring gear, planet spider, and sun gear are rotating in the same direction. Obviously, at some particular vehicle speed the differential gear will rotate as a solid unit in which case the torque ratio between input and output must be unity, corresponding to "high gear" in the usual mechanical transmission. Advantageously, one can choose to have this occur well below top speed of the engine, preferably close to the most economic speed of the engine with respect to fuel consumption. Further increase of vehicle speed automatically brings about the condition of "overdrive," since the regulator output also increases and forces the booster to generate an increasing voltage at almost constant speed, which in turn speeds up the reducer as motor; thus the ratio of engine to vehicle speed decreases to a value below unity, which is determined primarily by the amount of conversion into electric power at top speed of the vehicle.

Reverse operation of the vehicle is obtained as in any electric drive by reversing the fields of both booster and reducer with the regulator disconnected from the booster field. The booster now acts as self-excited generator driven by the engine and the reducer runs as motor, speeding up in its idling direction of rotation which is opposite to engine shaft rotation. This forces the planet spider also to rotate in the direction opposite to that of the engine shaft which gives backward motion of the vehicle. The maximum reverse speed is of course limited by the electromechanical torque balance under these conditions but is sufficient for all practical purposes, since the maximum tractive effort in reverse operation is as high as 60 to 65 per cent of that in forward operation.

2. Special Features of the Design

The design of this electromechanical transmission requires a careful study of the interrelation of all component elements in order to obtain proper functioning and the economy in weight and cost which is all important for any vehicle drive. The choice of the rear axle ratio (for rear axle drive) and that of the ratio in the planetary differential are interdependent and are determined by the desired rate of initial acceleration and by the top speed of the vehicle. As mentioned above, the fuel economy can be influenced decisively by proper choice of the vehicle speed in full throttle acceleration at which "overdrive" sets in; in this respect particular attention has to be paid to the auxiliary generator or regulator. For best results, individual designs are desirable for different performance requirements, though within any particular class of vehicle a standard design can be used for the average requirements and adjustments made by the use of slightly different rear axle ratios as is customary with the standard mechanical transmissions.

The planetary differential gear of the ring gear type is most commonly used in vehicle drives. Referring to figure 3 and denoting with r the ratio of the number of ring gear teeth to the number of sun gear teeth one finds for the ratio G of the torques on output and input shafts the value

$$T_{OS}=\frac{r+1}{r}T_{IS}=GT_{IS} \qquad (1)$$

Obviously, the largest value of G is obtained for the smallest value of r; for mechanical reasons, therefore, $G \leq 1.8$ which restricts this type of planetary differential to use in vehicles with low torque multiplication, as for example in passenger cars.

In order to obtain larger torque multiplication, a differential gear of the type shown in figure 4 and known as "reverted train" has to be used; on account of the two sets of planets it is often called double-planet gear. For reasons of con-

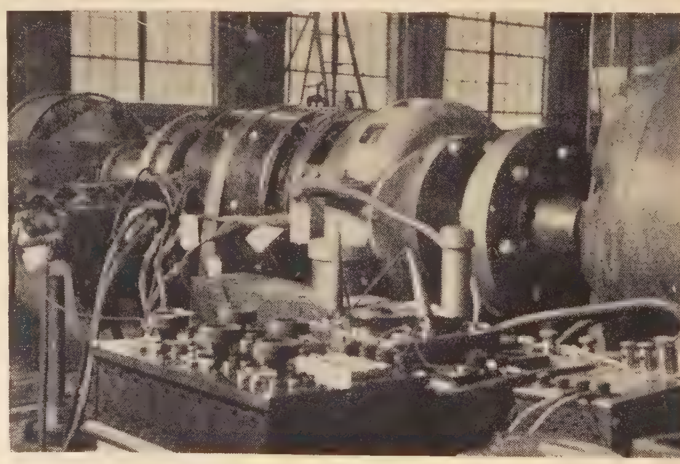

Figure 6. Photographic view of Electrogear on the dynamometer stand

struction the ratio of teeth in B to A is usually the same as that in D to C, and denoting it as q, one has for the torque ratio G of output to input shafts

$$T_{OS}=q^2T_{IS}=GT_{IS} \tag{2}$$

This type of planet gear can, therefore, be used for any large torque multiplication within practical values, and has the further advantage that the quill Q carrying the reducer can be located either to the left or to the right of the planet gear. It has been applied in the bus drive and the drive for the track-laying vehicle.

The main electrical machines have to be designed with utmost economy in the use of materials. In a bus drive with a definite schedule the power requirements can easily be evaluated; the effective mean value of the losses with proper consideration of cooling conditions at the various vehicle speeds will lead to the customary one-hour rating as a basis for the design. In the case of vehicles for general service suitable assumptions must be made with respect to most frequent driving conditions and maximum possible overloads. In the designs built for the bus and track-laying vehicles glass insulation was used throughout to take full advantage of the maximum temperatures permitted by AIEE Standards for traction machines. Of course, only experience can tell what effective cooling the machines may have on account of their particular location on the moving vehicle. The test data below will illustrate these points more fully.

The most important element in the Electrogear transmission is the regulator since it determines and controls the operation of the booster as motor or as generator. Being connected in parallel to the booster field, it carries a large part of the main current in addition to the current which it produces by self-excitation. Furthermore, its magnetic characteristic must be such that at the highest vehicle speeds it will not, or only slightly, saturate in order to provide adequate excitation for the booster. Since it is a very low voltage machine, care has to be taken to obtain good commutation under all driving conditions. All these are requirements that can easily be satisfied by an adequate design, but they are quite different from those met with in the design of general purpose machines.

3. Example of Installation

As an illustration the Electrogear designed for an A.C.F. bus weighing 14,220 pounds empty and 19,420 pounds with seated load will be described. The basic data for the bus were furnished by the engineers of The J. G. Brill Company at

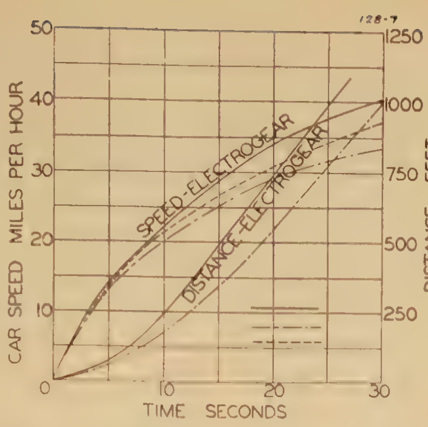

Figure 7. Full throttle acceleration of city bus

Electrogear
Gas-electric
Gearshift

Philadelphia. The bus was to be equipped with a Hall-Scott 135 engine mounted under the floor and delivering 116 brake horsepower at 2,000 rpm of which approximately 9 horsepower were used in accessories so that only 107 horsepower were available for the transmission. As a city bus the requirements were assumed to be 10 stops per mile, 11 seconds for each full stop, a scheduled speed of 11 miles per hour and acceleration up to 25 miles per hour between stops. The one-hour ratings of the electrical machines were—

Booster as motor
..........22.5 horsepower at 1,900 rpm
Reducer as generator
....................20 kw at 1,200 rpm

with maximum speeds of the booster about 2,600 rpm, of the reducer about 2,200 rpm; each had four main and four commutating poles, was series wound and designed for optimum voltage from the point of view of economy. Both main machines as well as the regulator were built and individually tested by the Delco Products Division of General Motors Corporation at Dayton, Ohio.

The mechanical layout was primarily determined by the available space between engine shaft flange and universal joint of the propeller shaft in the standard bus chassis. This put a limitation upon the axial extension of the armature end connections, but by placing the planet gear between booster and reducer and shortening the propeller shaft a solution was found satisfactory from all angles. The planet gear is of the double-planet type and uses the smallest feasible sun gear on the input side in order to utilize the space between the two main machines most economically. The complete layout, in simplified lines shown in figure 5, was made by The Timken-Detroit Axle Company, who also designed and built all mechanical parts and assembled the complete unit for installation. As seen, the assembly is extremely compact and utilizes the space within the bell housing, it provides excellent paths for the cooling air which is supplied through air cleaners, and it gives easy access to all brushes for examination and service. A photographic view of the assembly given in figure 6 shows the mounting on the dynamometer stand during preliminary tests. The mechanical construction also involves the brake drum as an integral part of the output shaft flange. Oil seals are incorporated in suitable form and number to insure proper local lubrication without permitting oil to enter into the electrical machines.

The actual weights (in pounds) of the various parts were as follows:

Booster (complete with shaft)	393
Reducer (complete with quill)	534
Regulator (complete with drive)	82
Planet gears	18
Electric control (complete without cover and brake resistor)	56
Air cleaners and miscellaneous parts	29
Total weight	1,112

Inasmuch as this was a sample unit and time was of essence, the material and dimension specifications of the design were not followed closely, so that the above actual weights of the booster and reducer exceeded the computed weights by about 150 pounds. Therefore the given weights do not in any sense constitute the most economic construction.

The electrical control[12] consists principally of a selector switch which connects the electrical machines for the three distinct operations: engine starting, forward, and reverse; and several relays which reduce the effort of the driver to a minimum, namely conventional operation of accelerator and brake pedals, and at the same time provide appropriate interlocks. The control equipment was designed with the co-operation of, and furnished by, the Ward Leonard Electric Company of Mount Vernon, New York.

The "starting" relay is operative only in the "engine starting" position of the selector switch and by interlock only when the accelerator pedal is depressed so as to avoid an accidental short circuit of the battery over the main circuit. Depression of the start button connects the conventional starting motor to the battery to start the engine and also sends current through the booster armature and the booster and reducer main fields in series, establishing the proper polarities for operation in either forward or reverse

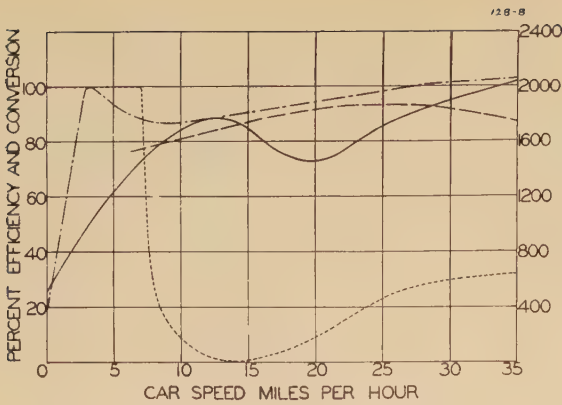

Figure 8. Characteristic performance of city bus Electrogear in full throttle acceleration

— · — · — Gas-electric engine speed
———— Electrogear engine speed
– – – – – – – Electrogear conversion ratio (per cent of engine power)
— — — — Electrogear efficiency (driver to engine)

direction. This is entirely sufficient for all subsequent operations of the vehicle and no further teasing of the generator is required at any time.

With the selector switch in forward position, depression of the accelerator pedal operates the "accelerator" relay, which permits the reducer to build up self-excitation as generator and to accelerate the vehicle as previously described.

In order to provide the very desirable benefits of electrodynamic braking, the brake relay connects a brake resistor parallel to the two main armatures as soon as the brake pedal is slightly depressed, whereas full depression applies additionally the air brakes. Again, an interlock prevents simultaneous accelerating and braking by de-energizing the accelerator relay when the brake pedal is depressed.

As a protective feature a temperature-operated contact system is inserted close to the reducer main field. Should the temperature of the field coils exceed a critical value, these contacts open and prevent further operation of the accelerator relay and thus of the Electrogear until the electrical machines have cooled down sufficiently to avoid damage. Though this protector never had occasion to act even during the most severe test runs, there might be conditions of getting into deep ruts or similar difficulties when this feature would prove desirable.

III. Comparative Test Data on Bus Transmission

As mentioned above, the bus transmission was chosen as a representative illustration, because in commercial transportation fuel economy, low maintenance cost, durability, acceleration, gradability, ease of operation, and comfort of the driver are of particular importance. Consequently many attempts have been made to develop a bus transmission which would satisfactorily meet all these requirements. Thus, there are at present in actual use, in addition to the standard gearshift transmission, the torque converter[6] developed by the Spicer Manufacturing Company in collaboration with General Motors Corporation, the "Fluidgear" developed jointly by A.C.F. Motors Company and Spicer Manufacturing Company,[5] and the gas or Diesel-electric drives developed by the General Electric Company[8] and the Westinghouse Electric Manufacturing Company.[9] Both the torque converter and the Fluidgear have somewhat lower performance[13] than the standard gearshift transmission, the first with respect to fuel consumption, the second with respect to acceleration, so that comparison of the Electrogear performance will be made with the standard mechanical and the gas-electric drives.

In comparing Electrogear with gearshift performance it should be borne in mind that the test data available on the gearshift transmission are obtained with a skilled driver and constitute optimum results which are seldom attained in actual commercial service, whereas Electrogear as well as gas-electric test performance is reproducible uniformly with any driver, no skill being involved in the operation of these drives, as they require only conventional use of conventional accelerator and brake pedals.

For a fair comparison of these drives it is also necessary to take into consideration the differences in bus weight on account of the drive. It was agreed by the engineers consulted in the preparation of this paper that all test data should be compared on the basis of the following bus weights; with standard gearshift transmission 18,000 pounds; with Electrogear 18,500 pounds; with gas-electric drive 19,200 pounds.

1. Performance Tests With the Electrogear

During the summer of 1939 extensive tests were run with an A.C.F. bus equipped with the Electrogear transmission and a standard $6^1/_6$ ratio rear axle. In all tests the total weight of the bus was about 18,500 pounds. After preliminary tests had demonstrated the satisfactory over-all performance of the transmission and necessary adjustments had been made, final tests were run with calibrated measuring equipment. All the tests were carried on under the supervision of The J. G. Brill Company's (or A.C.F. Motors Company's) engineers and a representative of the Pittsburgh Testing Laboratory.

The acceleration runs were made on a concrete highway west of Philadelphia, and the average taken for several runs in each direction in order to even out possible differences in slight slopes. Speeds were measured by means of a "fifth wheel," mounted on the side of the bus and driving a Hasler-Tel integrating accelerometer, giving mean speed values for each second. The result is shown in figure 7 where speed and distance are plotted against time. According to the records the Electrogear accelerated to 40 miles per hour in 29.2 seconds, and to a distance of 1,000 feet in 26 seconds, which must be considered excellent for any bus of this size. As mentioned before, the Electrogear performance being inherently automatic it can always be reproduced by drivers without skill or familiarity with the principles of operation.

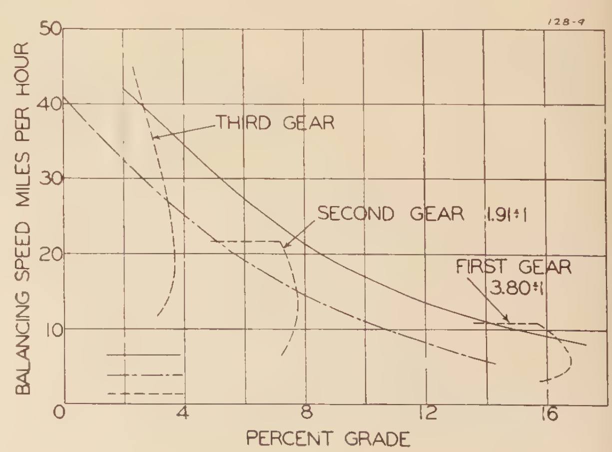

Figure 9. Gradability curves of city bus in terms of balancing speed against per cent grade

———— Electrogear
— · — · — Gas-electric
– – – – – – – Gearshift

From readings of the currents and voltages during acceleration, the circulating electric power can be computed and compared with engine power. The conversion ratio plotted in figure 8 against car speed graphically shows the percentage of engine power which the Electrogear converts into electric power, and checks very well the theoretical values used in the design. It is quite obvious that during the major part of the acceleration period only a very small fraction of engine power is circulated electrically, so that the losses of the double conversion are very small. This is also expressed in the high values of efficiency, defined here as the ratio of power at the wheels to engine power and shown in figure 8. Finally, in the same figure, the engine speed during full throttle acceleration is also given; the moderate values up to 20 miles per hour vehicle speed, in spite of the high rate of acceleration, are indicative of low fuel consumption for heavy schedules.

In normal driving (at constant speed on level road) the above advantages are, of course, much more marked. Thus, in the present installation the "overdrive" becomes noticeable at about 35 miles per hour, i.e., the engine speed is held below the values which the direct drive of a mechanical transmission would require. Equally, the conversion ratio becomes lower than in acceleration, which improves the over-all efficiency particularly at the higher car speeds.

Gradability tests were made on a special test hill near Philadelphia, which is about 700 feet long and has for the major part a grade of 15 per cent, tapering to about 12 per cent toward the top. From a standstill at the foot of the hill the bus was traveling at a speed of 10 miles per

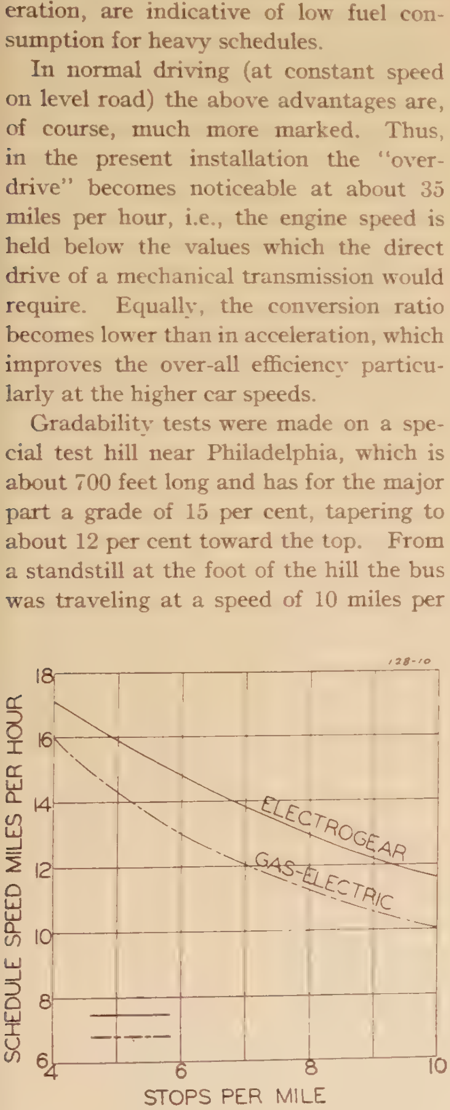

Figure 10. Schedule speed. Stops 11 seconds. Acceleration to about 25 miles per hour

———— Electrogear
— · — · — Gas-electric

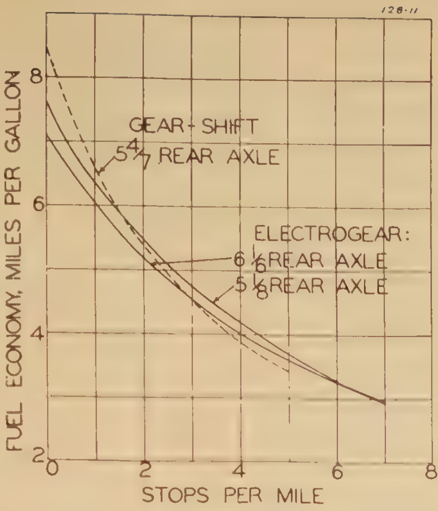

Figure 11. Fuel economy for various stops per mile and different rear axle ratios

———— Electrogear (18,500 pounds)
- - - - - - - Gearshift (19,980 pounds)

hour in less than 15 seconds, and was at the top of the hill at 14.5 miles per hour still accelerating. During this climb the engine speed was very low, with a maximum of 1,650 rpm at the top of the hill. Again, according to the records available to date, this performance was the best obtained on that hill with any bus transmission. On the basis of these and other tests, a gradability curve was computed giving the maximum speed of the bus attainable on various grades; the curve is shown in figure 9.

In order to check continuous performance and temperatures under severe strain the bus was operated for 3 miles with 13 stops per mile, and after a 5-minute interval for $7^1/_2$ miles with 10 stops per mile and 11 seconds per stop, and acceleration up to 25 miles per hour between stops. At the 114th stop the cooling water of the engine boiled over and the brakes were smoking hot. Yet the temperature of the Electrogear machines measured with thermocouples inserted in the field coils was 25 degrees centigrade for the reducer and 43 degrees centigrade for the booster lower than the permissible maximum temperature. The schedule speed during this breakdown test run, as checked repeatedly, was 11.6 miles per hour, taking 5 minutes 11 seconds for every 10 stops. On the basis of this as well as other tests, the schedule speed for various stops per mile was computed and is shown in figure 10. Gasoline consumption was also measured during the runs, giving 2.67 miles per gallon on this severe schedule.

For comparison with other drives, independent fuel consumption tests were carried on at length, for various stops per mile and acceleration up to 30 miles per hour. Figure 11 shows the results for two different rear axle ratios. It is most interesting to observe that the larger ratio $6^1/_6$ which was chosen in the design actually leads to higher fuel economy at heavier schedules than the $5^1/_8$ ratio, which in turn shows up slightly better up to 6 stops per mile. This justifies the selection of the $6^1/_6$ axle for the originally specified schedule of 10 stops per mile, and illustrates the flexibility of the Electrogear showing that it is easily possible to choose the most economical combination for every operating condition. An Electrogear design made for a schedule of 5 stops per mile shows a fuel economy of 8.5 miles per gallon at 30 miles per hour, and of about 4 miles per gallon at 5 stops per mile, which is considerably better than with the design for 10 stops per mile.

2. Comparison With Mechanical Gearshift Transmission

Through the courtesy of The J. G. Brill Company's engineers comparative test data were made available on the standard gearshift transmission in a bus of about the same seated weight and with the same size engine as used for the Electrogear. The ratios in the gearshift transmission were 3.80 for low gear, 1.91 for intermediate, and $5^4/_7$ for the rear axle. The acceleration curves were referred by adjustment of the acceleration rates to the comparative test weight of 18,000 pounds stipulated for the bus with the gearshift drive. The result is plotted in figure 7, demonstrating the superiority of the available continuous driving torque in the Electrogear as compared with the twice interrupted power flow in the gearshift transmission, which in spite of the almost equal initial acceleration rate causes a loss in momentum serious enough to affect the performance. This can be seen very much better in figure 12 in which the available instantaneous acceleration rates are plotted against car speed, and the vertical dotted lines represent the necessary interruptions in acceleration during the shifting of gears. Though the effect is pronounced in acceleration from a standstill, it is much more impressive when accelerating from a given car speed. Thus at 20 miles per hour the mechanical gearshift can produce only 0.76 mile per hour per second acceleration without shifting to second gear, whereas the Electrogear can deliver 1.52 miles per hour per second by mere normal use of the accelerator pedal.

The comparative gradability is plotted in figure 9 in terms of balancing speed, and demonstrates a further advantage of

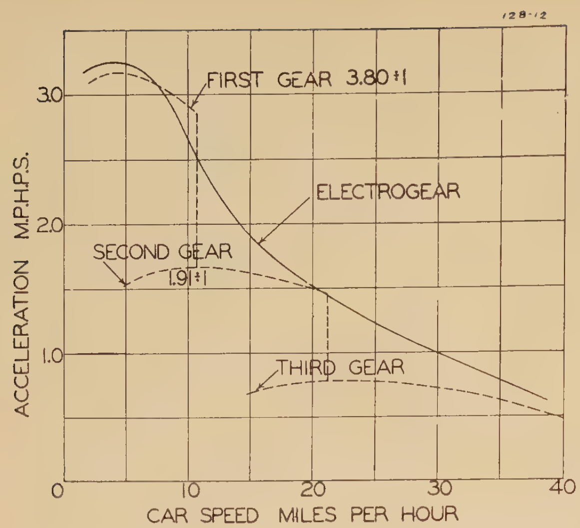

Figure 12. Available instantaneous rate of acceleration of a city bus with a gearshift transmission (- - - -) as compared with the Electrogear

the Electrogear in hilly terrain where the loss of momentum during back shifting of gears is particularly annoying and traffic delaying. Thus, while the standard gearshift bus climbs a grade of only 3.5 per cent at 25 miles per hour, the same bus with an Electrogear will climb a 6.6 per cent grade at 25 miles per hour, which is important with respect to schedule speed on routes with grades. Obviously, this free availability and automatic adjustment of driving torque under all circumstances also indicates a considerable saving in fuel consumption for vehicles traveling in hilly country.

Though no curves are available to show the schedule speed of the gearshift bus directly, reference can be made to an available actual service comparison with the gas-electric drive,[14] which shows that at about the same acceleration rate the gearshift bus schedule is about six to eight per cent slower than that of the gas-electric bus. Since the Electrogear, as shown in figure 7, has better acceleration than the gearshift transmission, the difference in schedule speed in favor of the Electrogear bus would be even greater. At that, it should be kept in mind, in comparing the acceleration curves, that in the case of the gearshift transmission they are obtained with the best driver continuously using extreme care in shifting at the proper moment; such ideal conditions, however, cannot be continuously reproduced in actual service, so that actual schedule speed with gearshift transmissions (manual or automatic) must be lower than theoretically expected, whereas, as pointed out, the Electrogear performance is not dependent on driving skill for uniform efficiency.

In order to compare fuel consumption for various stops per mile and acceleration up to 30 miles per hour, figure 11 shows in dotted line latest data obtained by The J. G. Brill Company on a bus weighing 19,980 pounds and using the same type engine as the Electrogear bus. Since fuel consumption is not proportional to bus weight, reference cannot easily be made to the comparative weight of 18,000 pounds; however, it is quite apparent that the repeated shifting of gears decreases relatively the fuel economy at the heavier schedules, bringing it into the range and below that of the Electrogear beyond about five stops per mile. The influence of shifting gears can best be seen in figure 14 in which the specific fuel consumption for full throttle acceleration is plotted against bus speed, based upon a typical fuel consumption curve of the Hall-Scott 135 engine shown in figure 13 and the engine speed variation shown in figure 8 for the Electrogear, and computed from the gear ratios for the gearshift bus. Over the entire range from 5 to 26 miles per hour (the speed most frequently used in city service) the Electrogear designed for heavy city service keeps the engine in the range of lowest possible fuel consumption. Flexibility of the Electrogear design makes equal or better fuel economy available in busses with lighter city service or for intercity use. In general, then, the Electrogear proves to be at least as efficient as the gearshift drive, and for any particular operating requirements can be made more economical. This clearly shows that the low efficiency of electric drives disappears when the electrical machines are used in proper combination with mechanical elements.

3. Comparison With the Gas-Electric Drive

Through the courtesy of the General Electric Company the performance data of a gas-electric transmission using the same Hall-Scott 135 engine as the Electrogear and the standard gearshift transmission were made available, so that a direct comparison is possible. On account of the greater weight of the gas-electric drive the test weight of the bus in this case was 19,200 pounds. The shunt-wound generator is of the type *GT* 1501 and has a net engine power of 107 horsepower at 2,000 rpm; the series-wound motor is of the type *GE* 1205; the rear axle ratio is $6^1/_8$, comparing with $6^1/_6$ for the Electrogear.

The speed-time curve of figure 7 indicates that the gas-electric acceleration is considerably less than that of the Electrogear, especially at car speeds beyond about eight miles per hour. This is easily accounted for by the fact that for city bus installation the Electrogear is designed to have very little engine power circulating through its electrical machines between 8 and 24 miles per hour car speed, as seen from figure 8, so that there is hardly any conversion loss in that range of car speed. On the other hand in the gas-electric drive the electrical machines continuously carry all the available power so that a considerable conversion loss is sustained. The same explanation holds, of course, for the divergence of the distance-time curves, also shown in figure 7.

For the same reason, the gradability of the Electrogear is considerably higher than that of the gas-electric drive using the same engine, as seen in figure 9, where the balancing speeds are plotted against per cent grades. However, these curves also illustrate particularly well the singular advantage of a continuously variable torque ratio; namely, to permit considerably higher speeds on grades on which the mechanical drive must shift gears and thus lose momentum. Thus at 15 miles per hour car speed the bus with mechanical transmission can climb only a 3.5 per

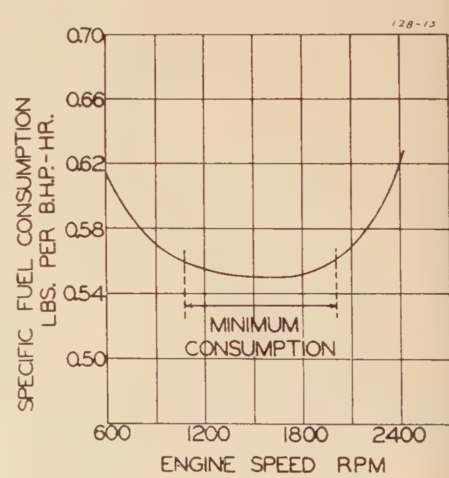

Figure 13. Specific fuel consumption of Hall-Scott 135 engine for full throttle setting

cent grade, the gas-electric bus about a 7.7 per cent grade, and the Electrogear bus even an 11 per cent grade as demonstrated in tests.

Figure 10 shows that the schedule speed of the gas-electric drive is about 1.6 miles per hour lower than that of the Electrogear, assuming 11-second stops in each case. Obviously this difference is due to the considerable difference in acceleration rates already pointed out in connection with figure 7.

Comparison of the fuel consumption per engine horsepower-hour is plotted in figure 14 on the basis of the full throttle specific fuel consumption of the engine given in figure 13 and of the engine speed curves for the various drives. For the gearshift the engine speeds are computed according to the gear ratios with the assumption that shifting is done when the engine speed reaches 2,000 rpm. For the gas-electric drive the engine speed variation was supplied with the performance data as plotted in figure 8 for comparison with the actual engine speed in Electrogear performance. Figure 14 shows the fuel consumption per engine horsepower-hour in full throttle acceleration to be as follows: highest with the gearshift drive (due to the fact that the engine goes through its entire speed range for each gear ratio); up to 12 miles per hour the same with the Electrogear as with the gas-electric drive; lowest with the Electrogear above 12 miles per hour; since the Electrogear uses much less engine power under all conditions it is evident that its total fuel consumption in full throttle acceleration must be the lowest.

Though no curves are available which would permit a direct comparison of the total fuel economy in commercial service of the gas-electric drive with that of the Electrogear, one can judge from comparisons of the gas-electric drive with the equivalent gearshift transmissions obtained in actual operation[14] that the average fuel consumption of the gas-electric drive is about 20 per cent higher if the acceleration is about the same in both cases. The gas-electric total fuel consumption should be even higher in comparison with the Electrogear since it has been established by tests that in a schedule of five stops per mile or more the Electrogear city bus is even more economical than the gearshift bus.

IV. Summary

The five principal requirements of an ideal power transmission from the gasoline (or Diesel) engine to the driver axle of a vehicle can be formulated as: first, a continuously variable torque ratio; second, effective loading of the engine under all driving conditions; third, uniformly economic operation at all vehicle speeds; fourth, driving ease; fifth, durability and low maintenance.

The Electrogear has demonstrated that it satisfies all of the above requirements to a higher degree than any known mechanical, hydraulic, or electrical transmission. There is no loss of momentum as in shifting gears, and the engine is never disconnected. Effective engine loading and "overdrive" are inherent features, fully automatic without any facilitating device. The all-around performance of the Electrogear as demonstrated by the Philadelphia tests is superior to that of other known transmissions, and it is significant that the best performance is always automatically produced without calling for skill or judgment. The driver has only the conventional accelerator and brake pedals to use in a conventional way, he has nothing to think about and no controls to manipulate. The durability and low maintenance cost of electrical machines are sufficiently well established by the gas-electric drives still in operation with 400,000 miles or more to their credit. Auxiliary electrodynamic braking (to reduce brake maintenance cost), particularly valuable in busses with heavy city schedules, can easily be made available with the Electrogear.

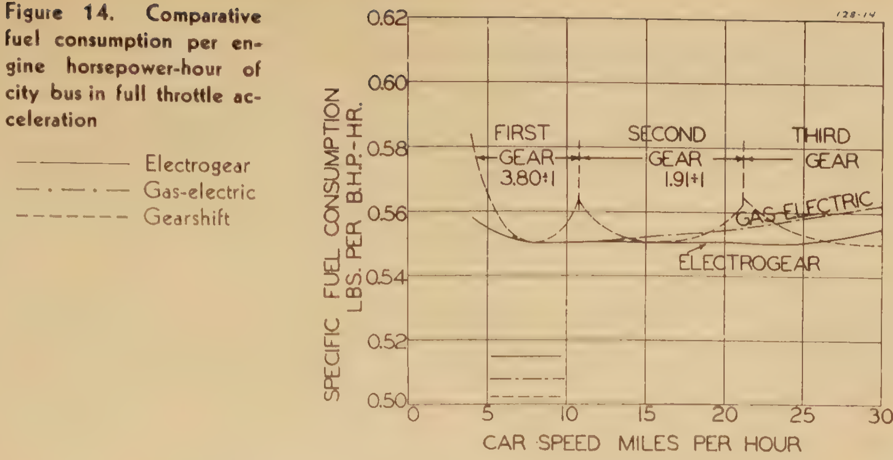

Figure 14. Comparative fuel consumption per engine horsepower-hour of city bus in full throttle acceleration

The design of the Electrogear is simple and flexible, permitting adaptation to any type vehicle. In large vehicles using conventional gas-electric or automatic multishift drives the Electrogear saves space, weight, fuel, and possibly initial cost. Its comparatively low weight opens a wide field of application in medium and light-weight vehicles in which automatically variable infinite ratio transmissions are desirable. To be simple, such transmissions must be electrical.[7a] It is not possible to simulate even by complicated mechanical devices all the desired transmission characteristics which are normally inherent in electric drives. Attempts by mechanical engineers to do so have resulted in increasing the weight and cost of mechanical transmissions to an extent approaching the Electrogear in large production.

Bibliography

1. Automatic Transmissions, **P. M. Heldt.** *Transactions S.A.E.*, volume 32, 1937, page 206.

2. Fluid Flywheels, **P. M. Heldt.** *Automotive Industries*, volume 80, 1939, page 109.

3. Hydrodynamic Power Transmission for Motor Cars, **W. Spannhake.** *Journal S.A.E.*, volume 45, Transactions section, October 1939, page 433. Also *Transactions S.A.E.*, volume 34, 1939, page 433.

4. Trends in Design of 1940 Cars, **Th. A. Bissell.** *Journal S.A.E.*, volume 45, Transactions section, November 1939, page 461. Also *Transactions S.A.E.*, volume 34, 1939, page 461.

5. Fluidgear, **C. O. Guernsey.** *Bus Transportation*, volume 18, 1939, page 466.

6. New Hydraulic Drive of Yellow Coach Corporation, **G. A. Green.** *Bus Transportation*, volume 18, 1938, page 448A. Also *Automotive Industries*, volume 79, 1938, page 438.

7. Power Transmission for Busses, **G. A. Green** *Journal S.A.E.*, volume 46, Transactions section, 1940, page 1.

7a. As in 7, page 16.

8. Electrical Drive Provides Automatic Transmission for Busses, **J. C. Aydelott.** *General Electric Review*, volume 40, 1937, page 531.

9. Electric Bus Drives Come Back, **C. A. Atwell.** *Electric Journal*, volume 35, 1938, page 181.

10. New Type of Electro-Mechanical Transmission, **P. M. Heldt.** *Automotive Industries*, volume 76, 1937, page 236. Also in *Transactions S.A.E.*, volume 32, 1937, page 206.

11. **A. H. Neuland:** U. S. Patents No. 2,000,786 of May 7, 1935, No. 2,045,197 of June 23, 1936, and numerous other patents owned by The Power Transmission Company.

12. **E. Weber:** U. S. Patent No. 2,179,364 of November 7, 1939.

13. Hydraulic Drives, **E. S. Pardoe.** *Bus Transportation*, volume 18, 1939, page 462.

14. Operating Experiences With Gas-Electric-Drive Motor Busses, **R. H. Stier.** AIEE Transactions, volume 57, 1938 (June section), page 318. Also in *General Electric Review*, volume 41, 1938, page 229.

15. Report on tests of the Electrogear transmission, Pittsburgh Testing Laboratory. March 1937.

Factors Influencing the Mechanical Strength of Cellulose Insulation

F. M. CLARK
ASSOCIATE AIEE

CELLULOSE insulation, like mineral oil with which it is usually associated in high-voltage electrical apparatus, is subject to deterioration in an increasing degree as the temperature of exposure is raised. This deterioration is a manifestation of the chemical instability of the cellulose. For a proper understanding of this change, it must be recognized that the fundamental chemical reactions involved are of two types. There are those changes which result from the oxidation of the cellulose and those which arise from the decomposition of its molecule. These changes are invariably intermingled in the normal commercial use of cellulose dielectric materials. To prevent dangerous deterioration and to secure the maximum service life of cellulose insulation, the effect produced by each type of reaction, the probability of its occurrence, and the means for its control must be carefully evaluated.

In a previous article[1] the author has described the mechanical and electrical changes in cellulose promoted by thermal decomposition in contrast to oxidation effects. It has been shown that cellulose will change mechanically and electrically with accompanying increase in color and acidity when heated at temperatures even as low as approximately 130 degrees centigrade under conditions which exclude the possibility of oxidation. These changes have been attributed to a molecular decomposition of the cellulose which culminates in the active evolution of gases, water, and other volatile products at temperatures above 130 degrees centigrade.

One of the objects of the present paper is to evaluate from the standpoint of mechanical strength those deteriorating changes in cellulose insulation which are caused by oxidation in contrast to those which result from the purely thermal decomposition of the cellulose molecule. Linen capacitor paper and Manila paper are used to illustrate the test results. These papers are selected because of their industrial importance. Other cellulose insulations, as for example kraft paper, have been found to be of similar behavior. The tensile strength of the insulation has been accepted as a gauge of its mechanical properties.

The Dormant Period

Cellulose insulation when heated actively exhibits evidence of molecular de-

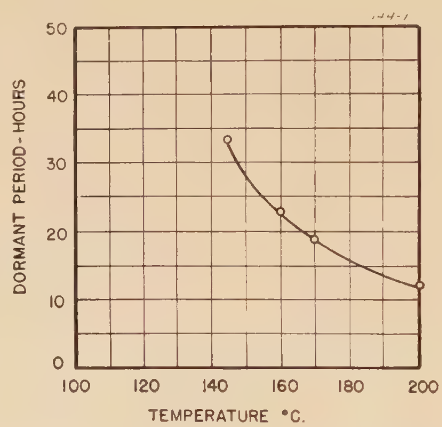

Figure 1. The "dormant" period is the duration of heat treatment which can be applied to cellulose insulation in the absence of oxidation without evolution of gases indicating molecular decomposition

The insulation used is vacuum-dried, oil-impregnated, and oil-immersed linen paper

composition only after a "dormant" period, the length of which depends on the conditions of the heat treatment. Foremost among the conditions of importance are the temperature applied, the accumulated thermal history of the cellulose, and the presence or absence of an impregnating liquid such as mineral oil. In general, for unimpregnated insulation, gas evolution and other evidence of serious decomposition are observed after about 12 hours of heating at temperatures higher than 130 degrees centigrade. With oil-treated cellulose insulation, the effect of temperature has been more carefully delineated. Figure 1 illustrates for oil-immersed linen paper the length of the "dormant" period within which no gas is evolved at temperatures from 145 degrees centigrade to 200 degrees centigrade.

It is obvious that the single effect of oxidation in promoting cellulose deterioration becomes of major importance only when the effects of molecular decomposition are avoided. It is within this range that the use of an inert gaseous atmosphere such as nitrogen can be expected to have its greatest stabilizing effect. When exposed to more severe conditions of temperature and time so that the "dormant" period is exceeded, molecular decomposition may become the dominant deteriorating factor. Adverse results are produced both directly as a result of pyrochemical change and indirectly because of the corrosive character of the decomposition products formed. It is during this period that the beneficial effects of a nonoxidizing atmosphere such as nitrogen gas are of decreasing, and frequently of negligible, importance.

Conditions Which Affect Aging

When cellulose insulation is exposed to temperatures of normal dielectric use, the rate of deterioration in tensile strength is dependent on the conditions of the heat treatment. Important factors are the temperature applied, the length of the exposure, and the presence or absence of an oxidizing atmosphere. The close intermingling of these factors and the great importance of the first two in producing radical changes in the tensile strength of the cellulose insulation have served to confuse their proper evaluation

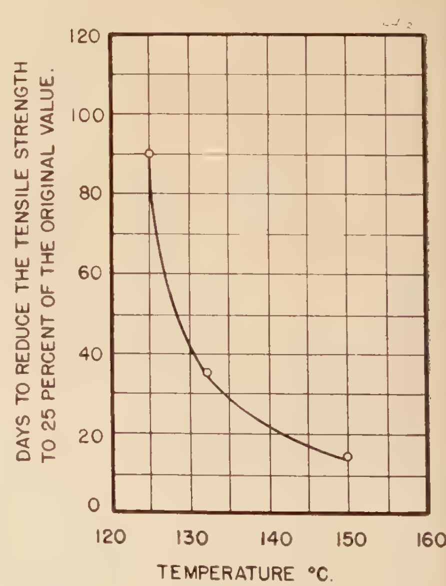

Figure 2. Dry Manila paper will deteriorate mechanically when heated in sealed tubes in contact with nitrogen gas

Paper 41-44, recommended by the AIEE standards committee, and presented at the AIEE winter convention, Philadelphia, Pa., January 27–31, 1941. Manuscript submitted October 25, 1940; made available for preprinting December 11, 1940.

F. M. CLARK is technical assistant for the General Electric Company, Pittsfield, Mass.

1. For all numbered references, see list at end of paper.

to the extent that oxidation is frequently looked upon as the fundamental cause of all of the deterioration observed. This is not true, for cellulose insulation will deteriorate even in the complete absence of any oxidizing gas or other source of oxygen. This is illustrated in the data of figure 2. In this series of tests, Manila paper, vacuum dried but not oil impregnated, has been heated in sealed bombs at temperatures from 125 degrees centigrade to 150 degrees centigrade under 250 pounds of dry nitrogen gas. The results are expressed in terms of that period of time necessary to reduce the tensile strength to 25 per cent of the original value. The rapid loss in tensile strength with the increasing temperature of the exposure in nitrogen gives warning against too great an emphasis of the oxidation factor as the fundamental cause of cellulose deterioration.

The Stable Period

Available data indicate that, even under the most severe deteriorating conditions, there is an initial period during which the cellulose insulation suffers no loss in tensile strength. During this interval it may even exhibit slight increases. This period has been termed the "stable period." It corresponds to but is not of as great a duration as the "dormant" period discussed in a previous paragraph. After passing through the "stable period" chemical reactions are initiated which affect the mechanical strength of the insulation and which at temperatures above 130 degrees centigrade culminate in the evolution of gases, water, and other volatile products.

The duration of the "stable period" decreases sharply with increased temperature above 100 degrees centigrade. The period of stability is clearly evident in the tests of figures 10 and 11 which describe the behavior of vacuum-dried, oil-treated, and oil-immersed 0.003-inch Manila paper. The "stable period" for each of the relations of figures 10 and 11 is reproduced for purpose of clarity in figures 3 and 4.

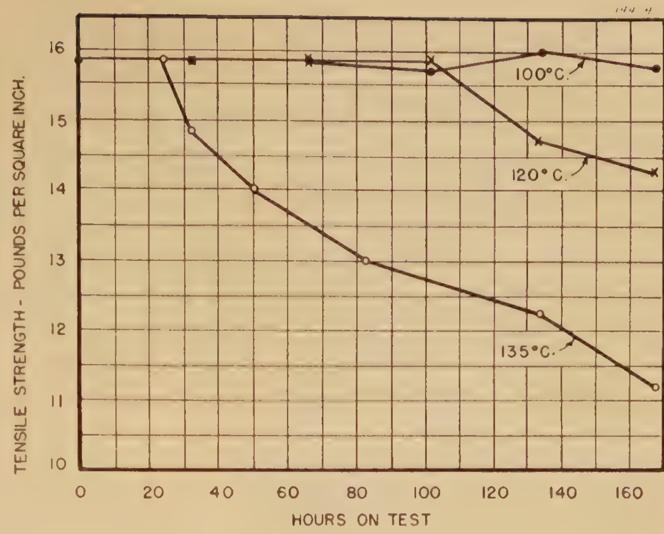

Figure 4. Showing the "stable period" of vacuum-dried, mineral-transformer-oil-treated, and oil-immersed 0.003-inch Manila paper when heated in contact with nitrogen gas

The length of the "stable period" is affected by the presence of an oxidizing atmosphere. This is demonstrated in the following data taken from figures 3 and 4.

Test Temperature (Degrees Centigrade)	Length of "Stable Period" in Hours: For Run in Oxygen Gas	For Run in Nitrogen Gas	Per Cent Decrease in Duration of Stable Period Due to Oxidation
100	101	168	40
120	33	101	68
135	16	24	33

The effect of oxidation on the duration of the "stable period" of oil-treated and oil-immersed Manila paper decreases as the temperature is lowered. As illustrated in figure 5, at temperatures as low as 85 degrees centigrade, the accelerating effect of oxidation can be expected to disappear. Tests at temperatures in the range of 85 degrees centigrade are of long duration and subject to wide variation, but in general, have served to substantiate this expectation.

When the cellulose is exposed to higher temperatures, the effect of oxidation on the length of the "stable period" does not increase indefinitely. This results because of the increasing importance of the second major factor, molecular decomposition which also greatly affects the rate of cellulose deterioration. The advantageous effect of the presence of nitrogen gas in prolonging the "stable period" of oil-treated cellulose reaches its maximum value at approximately 120 degrees centigrade. With higher temperatures of aging, the pyrochemical decomposition of

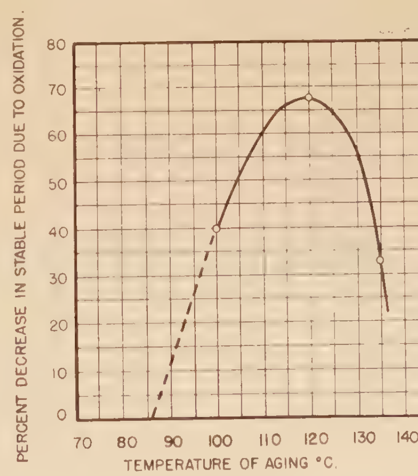

Figure 5. The effect of oxidation on the duration of the "stable period" for vacuum-dried oil-impregnated, and oil-immersed 0.003-inch Manila paper reaches its maximum at approximately 120 degrees centigrade

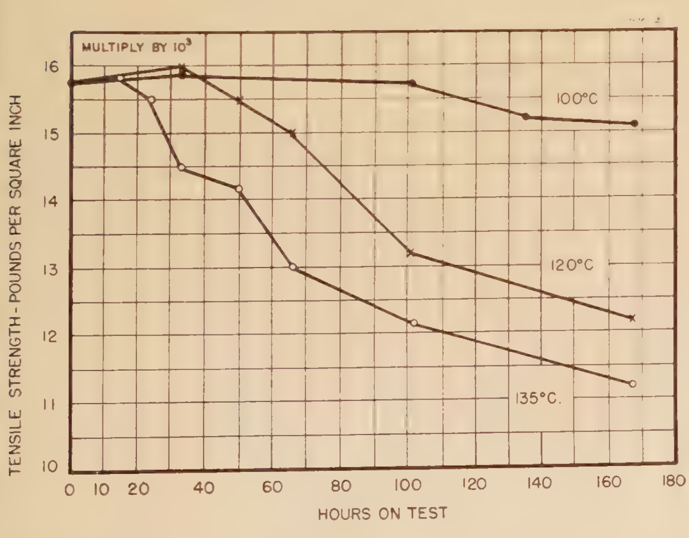

Figure 3. Showing the "stable period" of vacuum-dried, mineral-transformer-oil-treated, and oil-immersed 0.003-inch Manila paper when heated in contact with oxygen gas

the oil-treated cellulose assumes increasing importance. As a result, the duration of the "stable period" rapidly decreases even though all oxidizing gases are eliminated by the use of nitrogen. This is also illustrated in figure 5.

The existence of a "stable period" is of importance in the application of cellulose insulation in oil-filled electrical apparatus. The prolongation of this period is the most important result obtained by the elimination of an oxidizing atmosphere in contact with the oil-immersed insulation. The beneficial results obtained by the use of nitrogen gas, however, are largely limited to temperatures between 100 degrees centigrade and 120 degrees centigrade. For lower temperatures, the oxidation effect is of negligible importance. For higher temperatures, the pyrochemical decomposition reaction

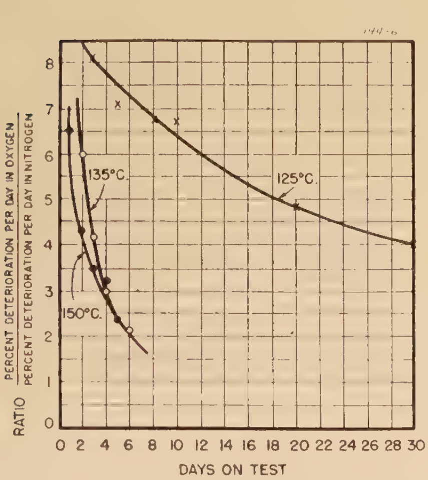

Figure 6. In the heat treatment of vacuum-dried but unimpregnated 0.003-inch Manila paper in sealed bombs under 250 pounds gas pressure, the deterioration in tensile strength is accelerated by the presence of oxygen

of the cellulose rapidly increases in importance and ultimately masks the advantages normally associated with the use of nitrogen gas.

The Oxidation Factor in the Aging of Unimpregnated Insulation

In studying the importance of the oxidation reaction in the deterioration of cellulose insulations, it is necessary to differentiate between its effect on those insulations which have been oil-treated and are tested under mineral oil and those insulations which are tested without oil impregnation and in direct contact with an oxidizing atmosphere. In order to illustrate more clearly the effects of oxidation in terms of tensile strength, it has

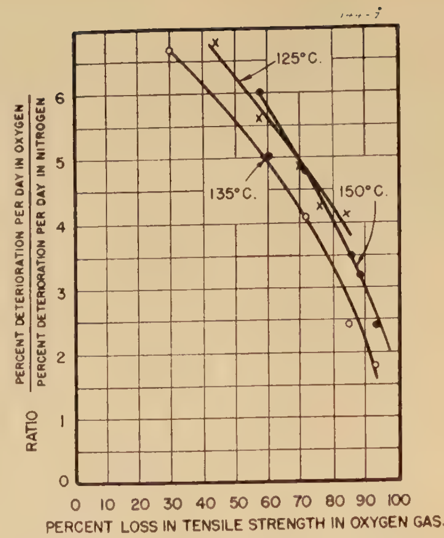

Figure 7. When vacuum-dried but unimpregnated 0.003-inch Manila paper is heated in sealed bombs under 250 pounds of gas pressure, the loss in tensile strength is accelerated by the presence of oxygen gas to approximately the same extent as the temperature is changed within the range from 125 degrees centigrade to 150 degrees centigrade

been found desirable to exaggerate the oxidation reaction by the use of oxygen gas in place of air. The effect on unimpregnated insulation is easily demonstrated. Figure 6 illustrates the importance of oxidation as a factor in the mechanical deterioration of dried but unimpregnated 0.003-inch Manila cable paper, aged at 125 degrees, 135 degrees, and 150 degrees centigrade in sealed bombs under 250 pounds of gas pressure. The results are expressed in terms of the accelerated rate of deterioration produced by the presence of oxygen gas as compared to similar aging in the presence of nitrogen. As the deterioration of the cellulose progresses, irrespective of the temperature of test, the accelerating effect of oxygen gas rapidly diminishes. During the initial state of the temperature exposure, however, the increased rate of aging due to the oxidation of the unimpregnated insulation reaches a high value.

The marked effect of the oxidation reaction during the initial stages of the high-temperature exposure of dried but unimpregnated cellulose results from the longer duration of the "stable period" when the insulation is in contact with a nonoxidizing atmosphere. When once the "stable period" in nitrogen gas has been passed, however, and the paper begins to deteriorate because of pyrochemical decomposition, the increased rate of deterioration in oxygen gas as compared to that observed in nitrogen rapidly decreases. The decrease is substantially independent of the temperature. This is illustrated in the data of figure 7 which correlate the accelerating effect of oxidation caused by the presence of oxygen gas with the degree of deterioration observed. It is important to note that with dried but unimpregnated Manila paper, even though the effect of oxidation decreases as the deterioration progresses, there is nevertheless a pronounced acceleration of deterioration throughout the whole mechanical life of the insulation.

The Oxidation Factor in the Aging of Oil-Impregnated Insulation

In order to evaluate the importance of oxidation in the deterioration of oil-treated and oil-immersed cellulose insulation, it has been found desirable, as in the study of the unimpregnated insulation, to exaggerate those factors which accelerate oxidation. For this purpose, pure

Figure 8. When vacuum-dried, oil-treated, and oil-immersed 0.003-inch Manila paper is aged in glass tubes sealed at atmospheric pressure, the presence of oxygen gas accelerates the loss in mechanical strength as compared to that which is obtained when air is used

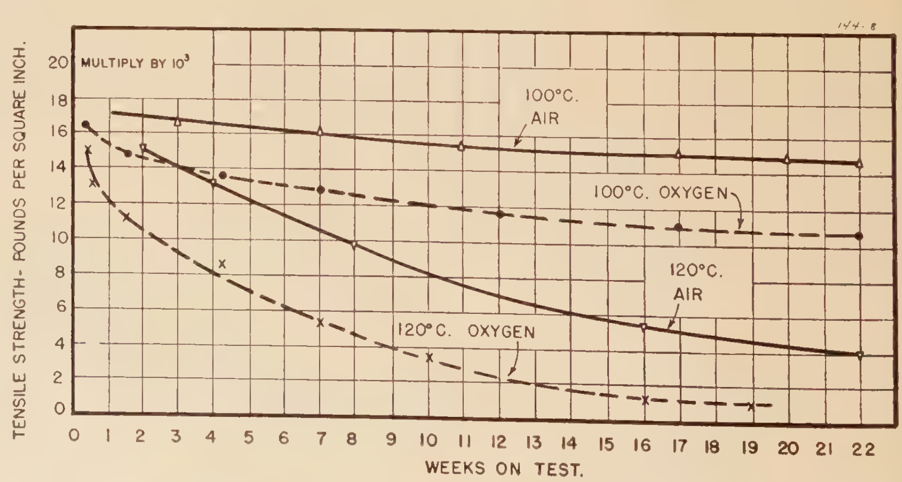

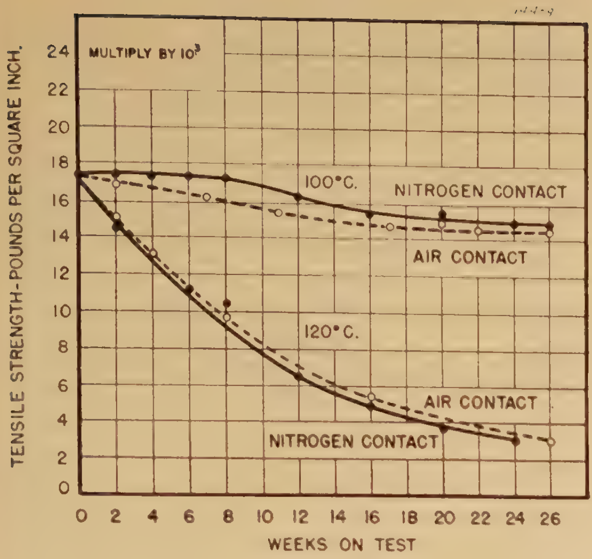

Figure 9. The loss of the tensile strength for vacuum-dried, oil-treated, and oil-immersed 0.003-inch Manila paper when aged in contact with nitrogen gas in glass tubes sealed at atmospheric pressure closely duplicates the deterioration observed when air is substituted for the nitrogen

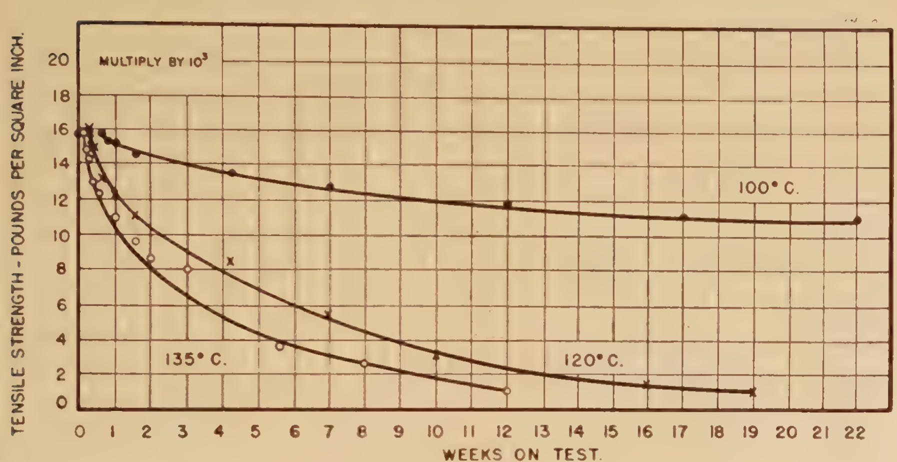

Figure 10. The loss in mechanical strength of vacuum-dried, oil-impregnated, and oil-immersed 0.003-inch Manila paper when heated in sealed tubes in contact with oxygen gas

oxygen has been used in place of air. The oxygen gas has been applied both at atmospheric pressure and at 250 pounds per square inch in sealed bombs. Temperatures of test as high as 200 degrees centigrade have been investigated.

The results of accelerated tests in which the possibility of oxidation has been greatly exaggerated must be considered merely as the ultimate limit of oxidation. It must not be concluded from such tests that an equal degree of deterioration will be obtained for the same oil-treated and oil-immersed insulation in contact with the air which is normally present in commercial usage. A typical comparison of the aging of 0.003-inch Manila paper in air and in oxygen is illustrated in figure 8 for tests at 100 degrees and 120 degrees centigrade. The deterioration observed in the insulation aged in contact with air in figure 8 is substantially the same as that observed when the insulation is aged in contact with nitrogen under similar test conditions (figure 9).

Despite the difference in the rate of aging in oxygen and in air, the use of oxygen serves the practical laboratory purpose of bringing out the effects of oxidation under the most favorable, lower temperature conditions at which the effect of nonoxidizing chemical changes are reduced or eliminated. Figures 10 and 11 give detailed illustrations of the aging of 0.003-inch vacuum oil-treated and oil-immersed Manila cable paper sealed in glass tubes at atmospheric pressure, the surface of the oil being in contact with oxygen and with nitrogen gas.

One of the outstanding characteristics which distinguishes the aging of cellulose insulations in contact with oxygen gas from similar aging in contact with nitrogen is the shorter duration of the "stable period" when oxidation occurs. It is obvious from the data presented that any evaluation of the possible acceleration of aging due to oxidation will depend upon that stage of the heat treatment selected for the comparison. If an interval during the "stable period" is selected as the time of comparison, it will be concluded that oxidation is of serious import. If on the other hand, the point of comparison is taken after considerable mechanical deterioration has occurred, entirely different conclusions will be drawn. This is illustrated in figure 12, based on the data of figures 10 and 11. The acceleration of mechanical deterioration due to the presence of oxygen as compared to nitrogen gas is shown as a function of the duration of the aging exposure at 100 degrees centigrade, 120 degrees centigrade, and 135 degrees centigrade. At the lower temperature pronounced oxidation effects are observed during the initial stages of the test. At the end of about four days of aging, the deterioration in oxygen gas at 120 degrees centigrade is approximately $4^1/_2$ times faster than in nitrogen. This results from the longer duration of the "stable period" in the absence of oxi-

Figure 11. The loss in mechanical strength of vacuum-dried, oil-impregnated, and oil-immersed 0.003-inch Manila paper when heated in sealed tubes in contact with nitrogen gas

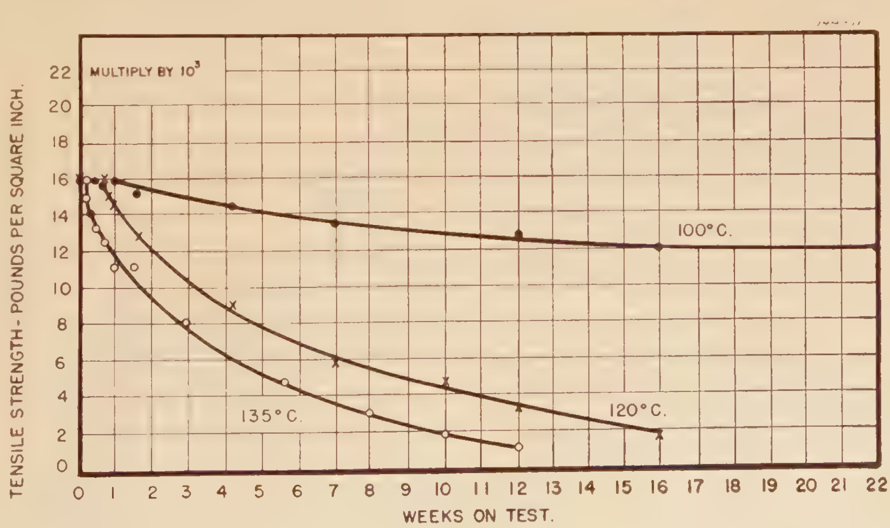

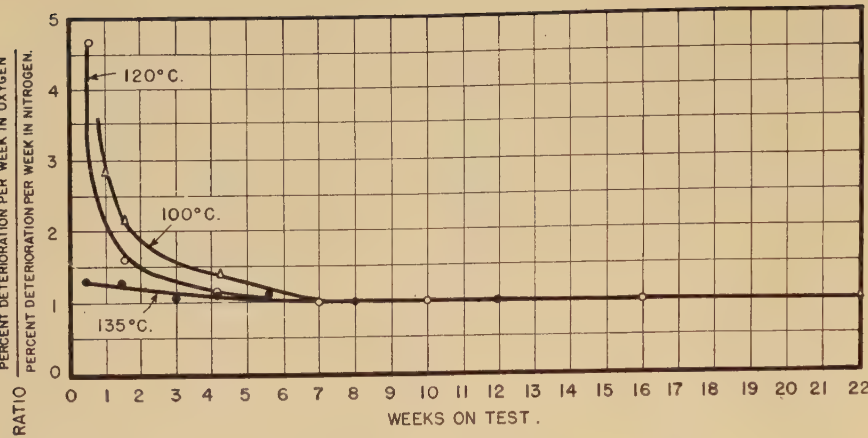

Figure 12. When vacuum-dried, oil-treated, and oil-immersed 0.003-inch Manila paper is heated in glass tubes sealed at atmospheric pressure, the oxidation factor assumes decreasing importance as the aging run progresses

dation effects. At the end of this "stable period" however, rapid changes in the oxidation ratio occur. Deterioration of the insulation in contact with nitrogen gas causes the oxidation ratio to fall rapidly. Within the limits of the available data, it is concluded that the rate of deterioration of the cellulose is progressively less affected by oxidation as the aging continues. When the deterioration has progressed to the extent that approximately 50 per cent of the original strength has been lost, the effects of the oxidation reaction are masked by the increasing importance of pyrochemical deterioration.

A further illustration showing the change from a condition of oxidation type of deterioration to a condition where the pyrochemical type predominates is illustrated in figure 13. In this study the dried, oil-impregnated, and oil-immersed 0.003-inch Manila paper insulation is heat treated at 200 degrees centigrade in contact with oxygen gas and with nitrogen gas. Under this type of deterioration both factors of oxidation and pyrochemical change are greatly exaggerated. As illustrated in the analysis of figure 13 the "stable period" in nitrogen gas under these conditions of heat treatment is approximately one-half hour in duration. Following the "stable period" in nitrogen, the deterioration increases rapidly to a maximum, after which the rate of deterioration in nitrogen and in oxygen appears of approximately equal value. During subsequent heat treatment, the only distinguishable feature between the deterioration resulting from the aging in nitrogen gas as compared to oxygen gas is attributable to the longer duration of the "stable

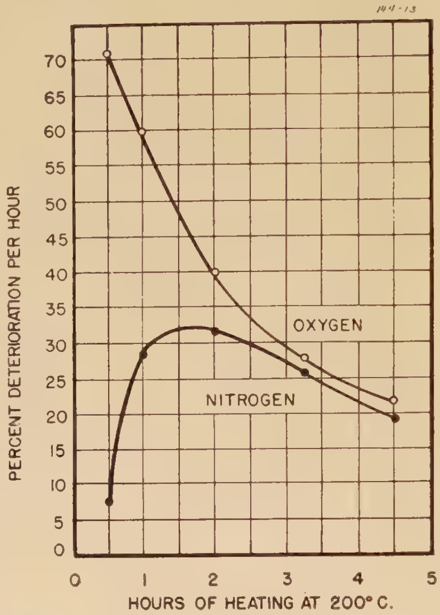

Figure 13. When vacuum-dried, oil-treated, and oil-immersed 0.003-inch Manila paper is aged at 200 degrees centigrade in glass tubes sealed at atmospheric pressure, the effects of oxidation, clearly evident in the initial stages of the heat treatment with oxygen are later masked by the presence of pyrochemical deterioration which occurs even in the presence of nitrogen gas

period" in nitrogen gas during which period the oxidation ratio as illustrated in figure 14 reaches its maximum value.

The Contrasting Behavior of Unimpregnated and Oil-Treated Insulation

Cellulose insulation whether tested before or after mineral oil impregnation and immersion shows the same peculiarities in its chemical behavior. High-temperature exposure in the presence of an oxidizing gas causes an initial deterioration which is traceable to the effect of oxidation on the duration of the "stable period." Examined during this interval, a marked deterioration attributable to the presence of oxygen gas as compared to the corresponding change in nitrogen gas is clearly evident. With continued heating, however, pyrochemical decomposition changes are initiated which become of increasing importance as the insulation is subjected to exhaustive treatment. It is the interrelation of these two types of chemical change and their modification as a result of oil impregnation and immersion which compels special consideration.

When dried but unimpregnated cellulose insulation is aged in an oxidizing atmosphere, the fibers are in intimate contact with what may be considered an unlimited supply of oxygen. Aged after oil impregnation and oil immersion, the amount of immediately available oxygen is limited to that supplied from oil solution. The result is that at temperatures where the oxidation reaction would normally be predominant, as for example at 120 degrees centigrade, unimpregnated paper shows a more rapid loss in tensile strength than similar paper oil impregnated and oil immersed. This is illustrated in figure 15 for tests on Manila paper.

A similar relation holds true when the cellulose deterioration is caused by the application of temperature in the range

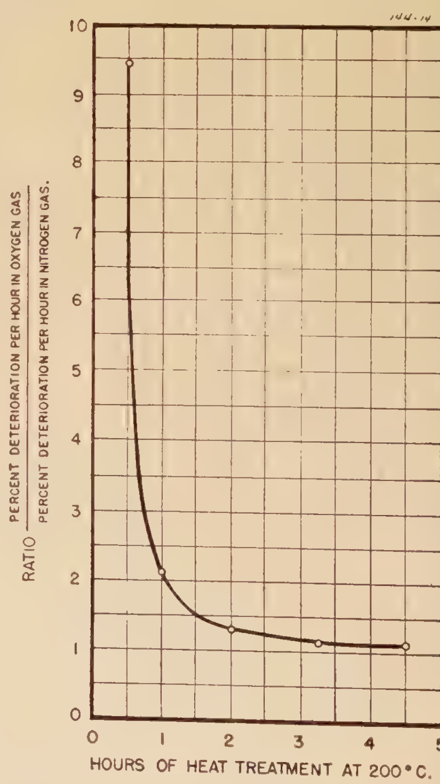

Figure 14. Showing the marked decrease in the oxidation factor after the end of the "stable period" for the aging of vacuum-dried, oil-treated, and oil-immersed 0.003-inch Manila paper in sealed glass tubes at 200 degrees centigrade

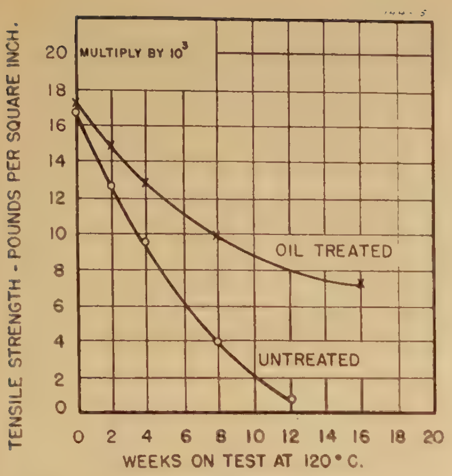

Figure 15. The mechanical aging of vacuum-dried 0.003-inch Manila paper is decreased as the result of impregnation and immersion in mineral transformer oil

The heat treatment in this illustration is carried out in glass tubes sealed at atmospheric pressure, the gas present being dried air

where pyrochemical decomposition is rapid and severe even in the presence of nitrogen. This is not unexpected in view of the fact that, as already described in a previous paragraph, the "dormant" period is increased as a result of oil impregnation and immersion. The longer duration of the dormant period for oil-treated and oil-immersed insulation in the absence of oxidation is undoubtedly related to the slower rate of acid formation in paper when exposed to high temperatures after oil treatment.[1] The result is that at a temperature of 135 degrees centigrade, dried but unimpregnated Manila paper deteriorates in tensile strength at a more rapid rate than does similar paper after oil impregnation and oil immersion. This is illustrated in figure 16.

In comparing the stability of cellulose insulation before and after oil impregnation the conditions of the comparison must be carefully stated. Dried but unimpregnated cellulose may be expected to deteriorate more rapidly than the same material after oil impregnation when the conditions of the temperature treatment are such that severe oxidation or pyrochemical reactions are possible. Heated under conditions such that oxidation and pyrochemical changes are of minor importance, the mechanical deterioration of the cellulose insulation is substantially unaffected by the presence of the impregnating mineral oil in which the material may be immersed.

Summary

1. Cellulose insulation will deteriorate in mechanical strength at a rate which increases with the increasing temperature of exposure. Deterioration will occur in the absence of an oxidizing atmosphere.

2. The rate of cellulose deterioration at a fixed temperature varies as the heat treatment is continued.

3. The mechanical deterioration of cellulose insulation at elevated temperature is the result of oxidation and pyrochemical decomposition.

4. When heated, cellulose passes through a "stable period" during which the mechanical properties are maintained. The presence of oxygen is chiefly effective in reducing the duration of this "stable period."

5. The single effect of oxidation is restricted to the initial periods of treatment at temperatures lower than approximately 120 degrees centigrade. At higher temperatures, pyrochemical decomposition occurs. Even in the most favored temperature range, the effect of cellulose oxidation merges into the effects produced by pyrochemical decomposition as the deterioration progresses.

6. Heated under conditions which favor oxidation or pyrochemical change, the unimpregnated cellulose insulation deteriorates more rapidly than the same insulation after oil treatment and immersion.

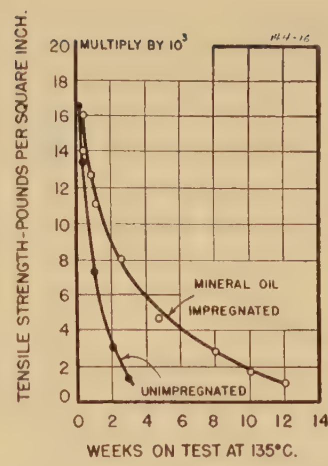

Figure 16. When heated at 135 degrees centigrade in sealed glass containers in contact with nitrogen gas, the rate of loss in tensile strength of dried 0.003-inch Manila paper is substantially decreased as a result of impregnation and immersion in mineral transformer oil

7. The effect of oxidation is accelerated when pure oxygen gas is in contact with the insulation. No substantial difference in the rate of mechanical deterioration is observed when the oil-treated and oil-immersed insulation is aged in contact with nitrogen gas as compared to aging in contact with air.

Bibliography

1. Pyrochemical Behavior of Cellulose Insulation, **F. M. Clark.** AIEE Transactions, volume 54, 1935, pages 1088–94.

2. Correlation of the Chemical and Electrical Changes Observed During the Oxidation of Mineral Insulating Oil, **F. M. Clark.** ASTM Preprint number 99, 1940.

3. Loading Transformers by Temperature, **V. M. Montsinger.** AIEE Transactions, volume 49, 1940, pages 776–90.

4. Temperature Aging Characteristics of Class A Insulation, **J. J. Smith** and **J. A. Scott.** AIEE Transactions, volume 58, 1939 (September section), pages 435–42.

5. Temperature Limits Set by Oil and Cellulose Insulation, **C. F. Hill.** AIEE Transactions, volume 58, 1939 (September section), pages 484–7.

Rotor-Bar Currents in Squirrel-Cage Induction Motors

J. S. GAULT
MEMBER AIEE

Introduction

THE rotor of a squirrel-cage induction motor is an extremely simple and rugged piece of mechanism; and due largely to this simplicity, it resists accurate analysis of its behavior by ordinary testing technique. Its design has been perfected by cut and try methods, making assumptions with respect to rotor current to simplify the theory; but the actual current in the bars has remained a mystery. The purposes of this paper are: first, to present oscillograms of rotor-bar currents; second, to extend the theory of induction motors to include the computation of rotor-bar currents; and third, to show the effect of the rotor current harmonics upon the efficiency of the motor.

Rotor-Bar Currents

The current in the rotor bars of a squirrel-cage induction motor is a composite wave of complicated form in which, however, three main components are prominent. In addition to the slip-frequency component which increases directly with load, there is a component due to nonuniform reluctance, the tooth-frequency component. The magnitude of this component depends primarily upon flux density but also increases with load; its frequency depends upon the number of stator teeth and the speed. The tooth-frequency component is very pronounced in a machine with open slots and is considerably reduced by using closed slots or nearly closed slots. The third main component of rotor frequency is caused by the nonsinusoidal distribution of stator current, and will be designated the band-frequency component.

A polyphase stator winding excited by current of sinusoidal wave shape gives a stator magnetomotive force with nonsinusoidal distribution. This would produce a rotating field with nonsinusoidal shape, although the flux density at every point along the air gap would vary sinusoidally in time to give a sinusoidal generated voltage in the stator. In a wound-rotor motor, space harmonics in the stator flux wave produce corresponding harmonics in the rotor generated voltage; but in a squirrel-cage motor, irregularities in the flux wave are practically eliminated by currents induced in the short-circuited rotor conductors. The rotor current distribution is such that the total current distribution, rotor plus stator, is sinusoidal. This hypothesis is given in Professor Bailey's book,[1] and is substantiated by analysis of the rotor current oscillograms included in this paper.

Computation of Band-Frequency Component

The method of computing the band-frequency component of rotor current will be shown by a specific example, using a three-phase winding with two-thirds pitch, 12 slots per pole. The curves of stator current distribution over two poles, and the corresponding rotor current distribution curves, are shown in figure 1, at time intervals of 15 electrical degrees. In the stator winding distribution diagram at the top of the figure, the arrows indicate the positive direction of current in each coil side, not the current distribution at a particular time. The cyclic maximum value of stator current per coil side (turns per coil times maximum stator current per conductor) is denoted by I_s. At the time ($\theta=0$ degrees) the instantaneous values of currents, indicated in the vector diagram at the left, are:

Phase $A=0$
Phase $B=-0.866I_s$
Phase $C=0.866I_s$

Using these values with the winding distribution diagram, the curve of stator current distribution, S, is obtained for time ($\theta=0$). The rotor current distribution curve, R, is drawn so that the total current curve, T, is the sinusoidal equiva-

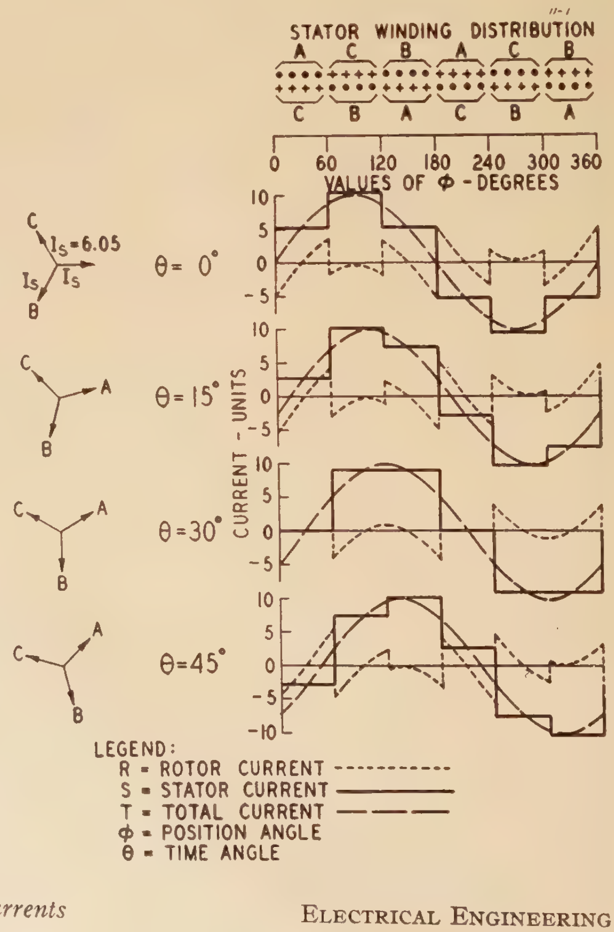

Figure 1. No-load current distribution curves of three-phase winding with 2/3 pitch

Paper 41-1, recommended by the AIEE committee on electrical machinery, and presented at the AIEE winter convention, Philadelphia, Pa., January 27–31, 1941. Manuscript submitted April 6, 1940; made available for preprinting October 23, 1940.

J. S. Gault is assistant professor of electrical engineering, University of Michigan, Ann Arbor, Mich.

Acknowledgments: For materials and aid in this investigation, a grant was obtained from the department of engineering research at the University of Michigan. Professor Lewis N. Holland, electrical engineering department, designed the amplifier and power supply, and supervised its construction and testing. Acknowledgement is also made to Professor Benjamin F. Bailey, chairman of the department of electrical engineering, for inspiration and guidance during the investigation and for valuable help in preparation of this paper.

1. For all numbered references, see list at end of paper.

lent of the stator current curve, that is the fundamental component of the curve S. The amplitude, T_m, may be obtained by use of the formula for the co-

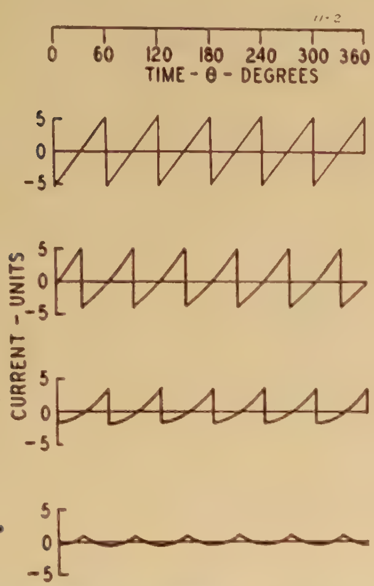

Figure 2. Rotor-bar current at zero slip for three-phase winding with 2/3 pitch

efficient of the fundamental term of the Fourier series:

$$T_m = \frac{2}{\pi} \int_0^{\pi} S \sin \phi d\phi \tag{1}$$

For the time ($\theta = 0$) the values of stator current shown give:

$$T_m = \frac{2}{\pi}\left[\int_0^{\pi/3} 0.866 I_s \sin \phi d\phi + \int_{\pi/3}^{2\pi/3} 1.732 I_s \sin \phi d\phi + \int_{2\pi/3}^{\pi} 0.866 I_s \sin \phi d\phi\right]$$

$$= \frac{3\sqrt{3}}{\pi} I_s \tag{2}$$

and at any other time, the same value will be found for T_m. In figure 1, a value of I_s is chosen arbitrarily to make T_m = ten units, so:

$$I_s = \frac{10\pi}{3\sqrt{3}} = 6.05 \text{ units} \tag{3}$$

and all the curves are drawn to this scale.

The rotor current distribution curves may be used to obtain the time curve of current in a particular bar by following a point on the rotor as it turns with the field. Due to discontinuities in the distribution curves, the time curves of rotor current cannot be obtained by Fourier analysis; however by using the values on the curves in figure 1, the curves of figure 2 may be obtained. The curve ($\phi_0 = 0$)

Figure 3. Full-load current distribution curves of three-phase winding with 2/3 pitch

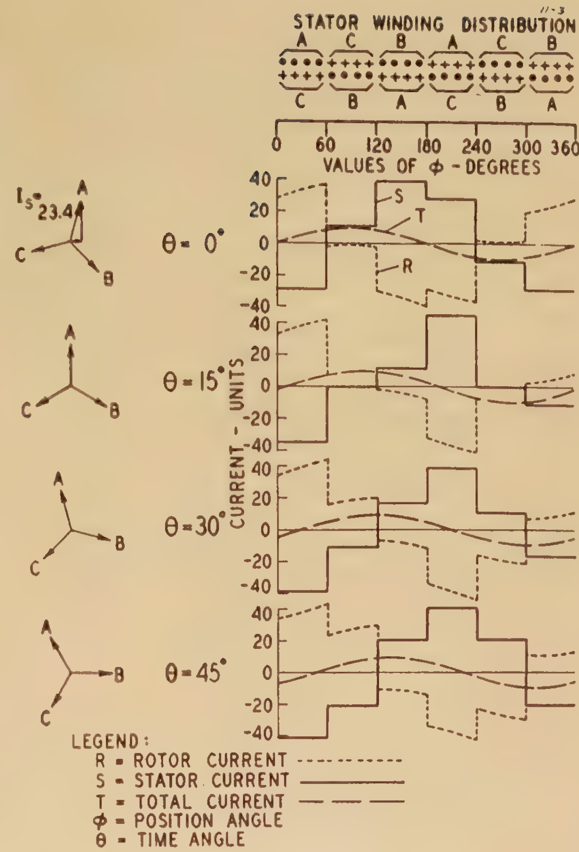

shows current in the rotor bar which is in position ($\phi = 0$) at time ($\theta = 0$), so the value 5.24 units is taken at the point ($\phi = 0$) on the curve for time ($\theta = 0$) in figure 1. At time ($\theta = 15$ degrees) the rotor has moved 15 degrees to the right, so the value of rotor current is taken from the ($\theta = 15$ degrees) curve at point ($\phi = 15$ degrees). The values of rotor current in this bar at $\theta = 30$ degrees and 45 degrees are read similarly from the corresponding curves at the 30-degree and 45-degree points respectively. At ($\theta = 60$ degrees) the distribution curves are like the ($\theta = 0$) curves and the rotor current wave repeats, so the rotor-bar current in this case is a 360-cycle wave of nearly triangular wave shape. The curve ($\phi_0 = 30$ degrees) in figure 2 is obtained similarly; the first point is taken from the ($\theta = 0$) curve at ($\phi = 30$ degrees), etc. For different bar positions, the magnitude of this band-frequency component changes as well as the wave shape with a maximum value for the position ($\phi_0 = 0$):

$$R_b = 6.05 \sin 60° = 5.24 \text{ units} \tag{4}$$

and only 0.67 unit for the bar in the ($\phi_0 = 90$ degrees) position.

The curves of figure 2 represent rotor-bar currents in a machine running at synchronous speed. At no load with a small amount of slip, these curves show some of the phases through which the rotor current passes slowly as the bar changes its position with reference to the revolving field.

Effect of Load Upon Rotor Current

When the motor is loaded, the stator current is increased by the addition of a

Figure 4. Rotor-bar current at full-load with 5 per cent slip, for three-phase winding with 2/3 pitch

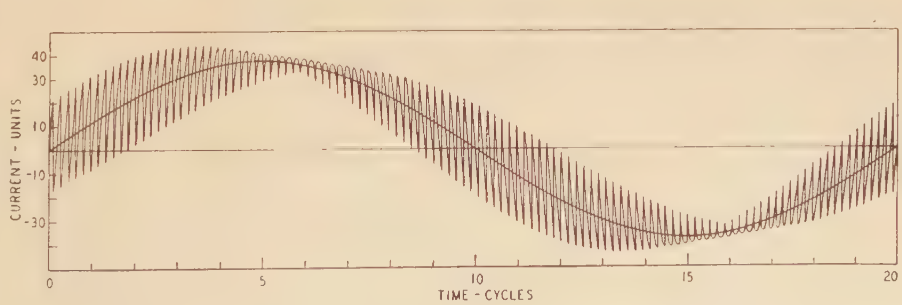

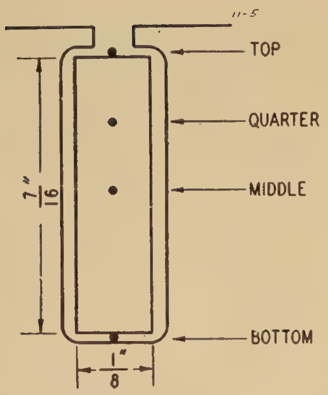

Figure 5. Positions of search conductors in rotor bar

power component in quadrature with the magnetizing component. Since the total current distribution remains practically unchanged, the rotor current distribution curve shows a corresponding increase. Figure 3 shows full-load distribution curves, similar to the no-load curves of figure 1. The value of magnetizing current is taken as 6.05 units, the same as the no-load value given in equation 3. For the power component a value of 22.6 units is assumed, so the value of I_s used in drawing the curves of figure 3 is:

$$I_s = 6.05 + j22.6 = 23.4 \text{ units (at 75 degrees)} \quad (5)$$

The total current, T_m, equals ten units as before.

The curve of rotor-bar current in figure 4 is obtained from these distribution curves by following a point on the rotor, using a slip of five per cent which corresponds to full load. The rotor current now shows a slip-frequency component with amplitude, R_s, proportional to the power component of stator current:

$$R_s = 22.6 \times \frac{3\sqrt{3}}{\pi} = 37.35 \text{ units} \quad (6)$$

The band-frequency component increases with the stator current, so the maximum amplitude:

$$R_b = \frac{23.4}{6.05} \times 5.24 = 20.3 \text{ units} \quad (7)$$

The frequency of this component also changes. At synchronous speed each 60-degree band of the stator winding produces one cycle of the band-frequency wave. As the speed decreases, the band-frequency drops; and for each cycle of slip frequency, the band-frequency component passes through all its phases corresponding to a complete cycle. The band frequency for a value of slip, s, is:

$$f_b = (1-s)6f + sf = (6-5s)f \quad (8)$$

and at five per cent slip, this frequency is 345 cycles. This band-frequency component is superposed on the sinusoidal (slip-frequency) component; and it passes progressively through the various phases shown in figure 2. In these computed curves the tooth-ripple frequency is omitted, and this should be kept in mind when comparing them with the oscillograms shown later.

Method of Measuring Rotor-Bar Current

In February 1937, an article by Narbutovskih[2] showed a method of obtaining rotor-bar current curves by placing search conductors in the rotor bar. The search conductor is an insulated wire running through the rotor bar under observation, and connected to it at the back end. The front end of the test conductor and the front end of the rotor bar are connected through sliding contacts to the first stage of an amplifier, so no current is drawn from this test circuit. The voltage between the leads is equal to the instantaneous value of iR drop in the bar material adjacent to the test conductor and therefore is proportional to the current density.

The article is most interesting because these oscillograms constitute the first published record of actual rotor-bar currents which has come to the writer's attention. The tests were run on an early type of machine with nearly square rotor bars, and an open slot stator which produced a large tooth ripple in the rotor current. From a study of the oscillograms, it is not apparent that the amplifier used had a frequency range low enough to show slip frequency. The band-frequency component is discernible but is nearly covered up by the large tooth-frequency component.

Preliminary tests showed that this method would permit the study of harmonics in the rotor-bar current, which would be even more interesting in a machine of modern design. An amplifier was constructed with a power stage suitable for direct connection to a magnetic oscillograph; with maximum voltage amplification about 50,000. Used in combination with a power supply of special design, it has a flat-frequency response from 1 to 2,000 cycles.

Current Distribution in a Single Bar

As pointed out by Narbutovskih,[2] the current density throughout a rotor bar is far from uniform, particularly for high-frequency components, due to rotor leakage flux. A search conductor in the rotor bar does not, therefore, measure the current in the bar, but rather the current density adjacent to the test conductor. In a narrow rectangular bar the current density across the bar will be nearly uniform, except for very high-frequency components, but will vary with the depth in the bar. For the tests reported in this paper, four search conductors were used, placed as shown in figure 5. Specifications on the machine tested were:

Rating: 220 volt, 3 phase, 60 cycle, 5 horsepower, 1,800 rpm

Stator: 48 coils, 22 turns No. 15, throw 1–9, connected parallel-wye

Rotor: 45 copper bars, $^1/_8$ by $^7/_{16}$ inch, length 2.38 inches copper end rings, $^1/_4$ by $^{29}/_{32}$ inch, mean radius 2.89 inches

The dimensions of rotor slots and teeth, air gap, and stator slot openings are shown in figure 6, all dimensions in inches.

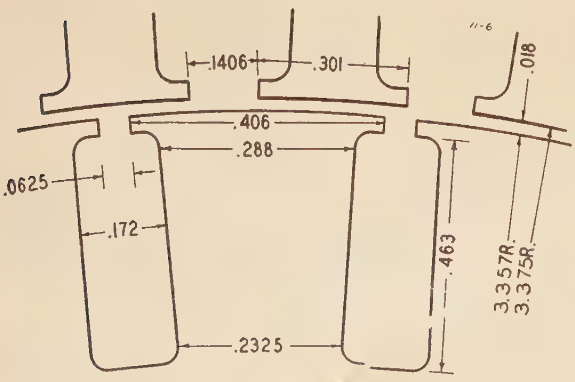

Figure 6 (left). Rotor slot and tooth dimensions

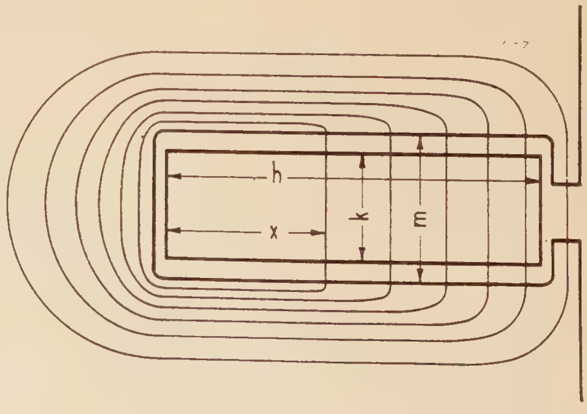

Figure 7. Rotor-bar leakage flux pattern

Figure 7 shows a bar of thickness, k, and depth, h, in a slot of width, m, with all dimensions in inches. Certain simplifying assumptions are made concerning the leakage flux pattern which are quite valid for a narrow rectangular bar nearly filling the slot. Due to the higher reactance of the lower part of the bar, the current density is highest at the top of the bar and diminishes to a minimum at the bottom. Also the current in lower layers is lagging in phase. Both of these effects are most noticeable at high frequency, are relatively small at 60 cycles, and are practically negligible at slip frequency. The current distribution for a particular frequency is given by the formulas:

$$U_x = A\sqrt{2\cosh(2ax)+2\cos(2ax)} \tag{9}$$

$$\tan\psi_x = \tanh(ax)+\tan(ax) \tag{10}$$

where U_x is the cyclic maximum current

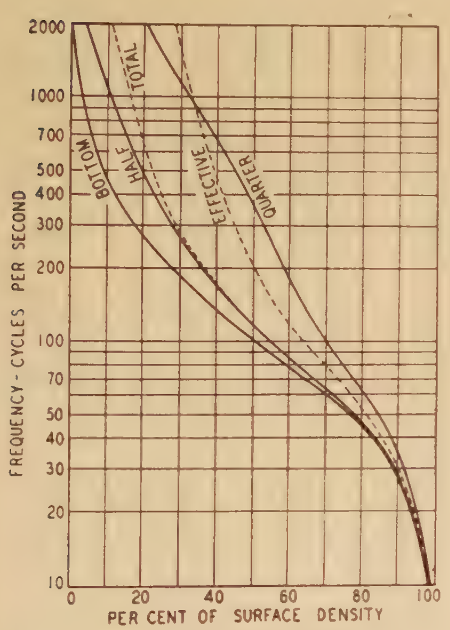

Figure 8. Current density at different levels in per cent of surface density

density at a distance, x, from the bottom of the bar.

$$A = \frac{U_h}{\sqrt{2\cosh(2ah)+2\cos(2ah)}} \tag{11}$$

where U_h = current density at the top of the bar.

$$a = \sqrt{\frac{1.003kf}{\rho m 10^7}} \tag{12}$$

ρ = resistivity in ohms per inch cube

f = frequency in cycles per second

ψ_x = phase angle of current at point x with respect to that at the bottom of the bar

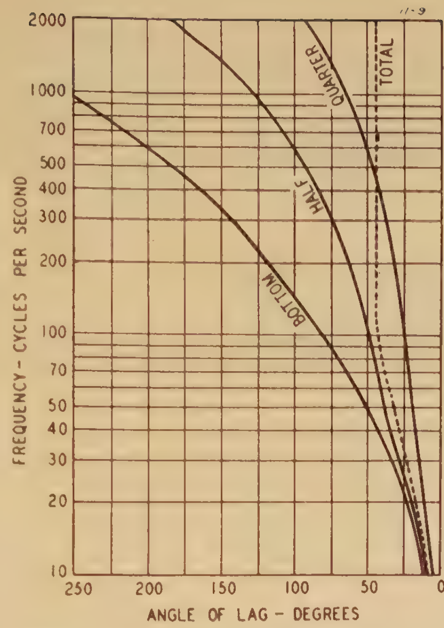

Figure 9. Angle of lag at different levels referred to current at top of bar

In accordance with these formulas, the curves of figure 8 are computed to show the current density at the quarter, middle, and bottom of the bar used, in per cent of the value at the top, for the range of frequencies encountered. Figure 9 shows the angle of lag of the current at the same levels with respect to that at the top of the bar. For the 360-cycle band-frequency component discussed previously, for example, the distribution and phase, taken from these curves, are shown in table I. The current density falls off rapidly with the depth, also the phase shift is large, therefore the average density is only 26 per cent of the density at the surface. The formula for computing this average is:

$$U_{av} = \frac{A}{ah}\sqrt{\cosh(2ah)-\cos(2ah)} \tag{13}$$

and the phase angle with respect to the current at the bottom of the bar is ψ_{av}, where:

$$\tan\psi_{av} = \frac{\tan(ah)-\tanh(ah)}{\tan(ah)+\tanh(ah)} \tag{14}$$

It should be noted that the formula is developed in terms of "amperes per bar", that is, the density in amperes per square inch multiplied by the bar area; so the average current density is numerically equal to the total bar current. The formula for effective or rms density, in the same units, is:

$$U_{eff} = A\sqrt{\frac{\sinh(2ah)+\sin(2ah)}{ah}} \tag{15}$$

These formulas are developed on the basis of sinusoidal wave shape. The band-frequency wave is very nearly triangular so the current density drops a little faster than for a sine wave of the same frequency, due to the higher frequency components of the wave. The wave shape also improves, and becomes nearly sinusoidal near the bottom of the bar. Nevertheless, the curves of figure 8 give a reasonably correct picture of current distribution, especially if a small correction is made for wave shape, and they agree closely with the results obtained by measurements on oscillograms.

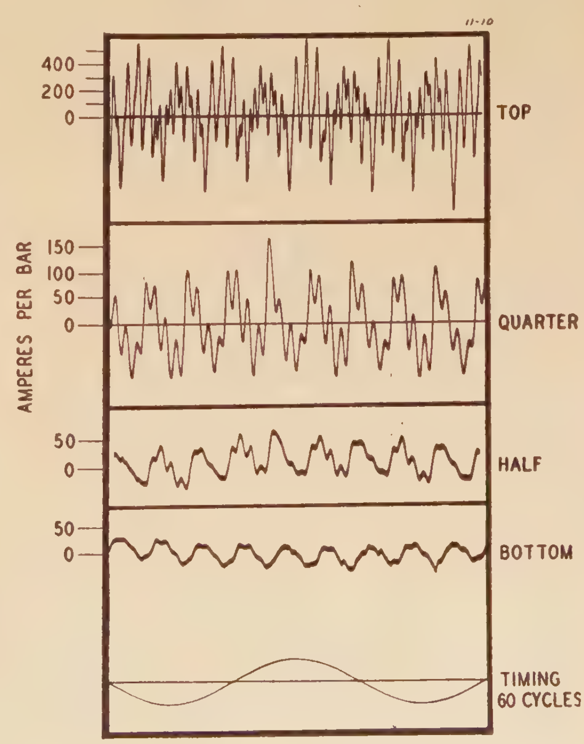

Figure 10. Rotor-bar currents of three-phase four-pole motor at synchronous speed, 1,800 rpm, 220 volts, 3.31 amperes

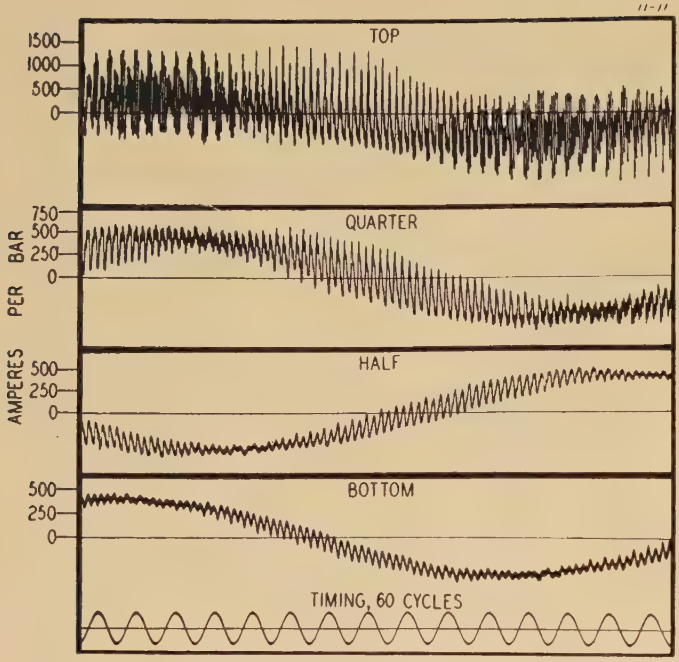

Figure 11. Rotor-bar currents of three-phase four-pole motor at full load with 5 per cent slip 1,710 rpm, 220 volts, 13.15 amperes

Rotor Current Oscillograms

Figure 10 shows rotor current oscillograms for the three-phase motor running at synchronous speed, 1,800 rpm, together with a 60-cycle timing wave. The curves at the different levels in the bar were not actually taken simultaneously, since only one amplifier was used. By means of a stroboscope, the curves were all taken at the same point in the band-frequency cycle; then the waves were lined up on the sheet by means of their separate timing waves, of which only one is shown. By noting the current scales, it is seen how the band-frequency wave diminishes and changes its shape as the depth in the bar increases; also there is a gradual shift to the right, indicating a greater angle of lag. These effects are hidden by the prominent 1,440-cycle tooth ripple, particularly at the upper levels. In some oscillograms shown later, for a different setup, the band-frequency waves show more clearly. In table II, these oscillograph curves are analyzed into the tooth-frequency and band-frequency components. Also in the table is given a column of computed values of the band-frequency component. The agreement is very good considering that the wave shape introduces a little error. All the figures in the table are maximum cyclic values in terms of amperes per bar.

On this test, at synchronous speed, with 220 volts, the current was 3.31 amperes. From equation 4, the maximum band-frequency amplitude, R_b, is 5.24 units. To convert this to amperes per bar, the value of stator maximum amperes per coil side is determined and this is multiplied by the ratio of stator to rotor slots. By equation 3, this is equal to 6.05 units. So:

$$6.05 \text{ units} = \frac{3.31\sqrt{2}}{2} \times 22 \times \frac{48}{45} \text{ amperes}$$

or

$$1 \text{ unit} = 9.09 \text{ amperes per bar} \qquad (16)$$

and

$$R_b = 5.24 \times 9.09 = 47.5 \text{ amperes per bar} \qquad (17)$$

This value appears in table II for "total" current (or average current density). The computed values of current density at the different levels and the "effective" value are figured from this value of total current using the percentages in table I. The tooth-frequency component is more prominent in the top layer, but falls off rapidly. Its effective value is rather hard to determine, but will undoubtedly be lower than that of the band-frequency component in this case.

In figure 11, are shown oscillograms taken under load with readings as follows:

Input—220 volts, 13.15 amperes, 4,570 watts
Output—5.03 horsepower, 1,710 rpm

No attempt has been made to line up this series of oscillograms with the single 60-cycle timing wave shown, and this is included merely to give the time scale which is the same for all curves. A little over one-half cycle of the three-cycle slip-frequency wave is shown at all four levels. As before, the tooth-frequency wave masks the band-frequency wave at the top of the bar. But at the quarter level, and especially at the middle of the bar, the tooth ripple is small and the band-frequency wave is quite prominent; also the similarity between these curves and the computed wave of figure 4 is very marked. The cyclic maximum values of the various components, scaled from these oscillograms, are given in table III.

To check the computation of band-frequency components, from equations 16 and 17 a stator current of 3.31 amperes gives $R_b = 47.5$ amperes per bar. Since this component varies directly with stator current, the value for the "total" under load is:

$$R_b = 47.5 \times \frac{13.15}{3.31} = 189 \text{ amperes} \qquad (18)$$

The maximum values at various levels are computed from this using the percentages of figure 8 for a frequency of 345 cycles. The computed magnitude and distribution of band-frequency current agree very well with the values measured on the oscillograms. Also the effective value of this component is of the same order of magnitude as the slip-frequency component.

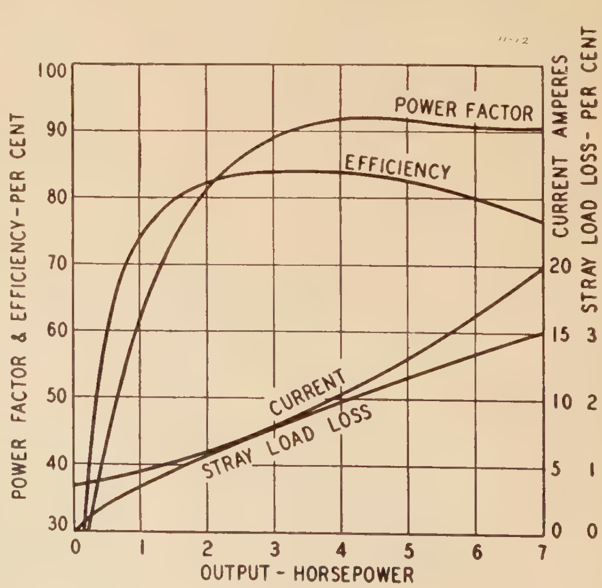

Figure 12. Load-test curves of squirrel-cage motor rated 5 horsepower, 1,800 rpm, three-phase 220 volts. Temperature 55 degrees centigrade

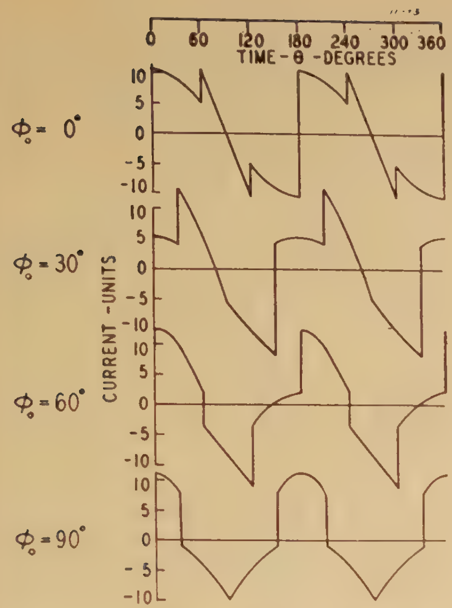

Figure 13. Rotor-bar current at zero slip for single-phase winding with 2/3 pitch

The slip frequency is only three cycles, so the value of this component at various levels should be the same as the total. This fact is clearly shown in the oscillograms, although the magnitude does not check so well. The slip-frequency component of rotor current is in space phase with the total magnetomotive-force wave, and is computed from the power component of stator current. The maximum value of this is approximately:

$$\sqrt{2}\times\sqrt{13.15^2-3.31^2}=12.72\sqrt{2}$$
$$=18 \text{ amperes} \quad (19)$$

Figure 15. Rotor-bar currents of single-phase four-pole motor with 3.6 per cent slip

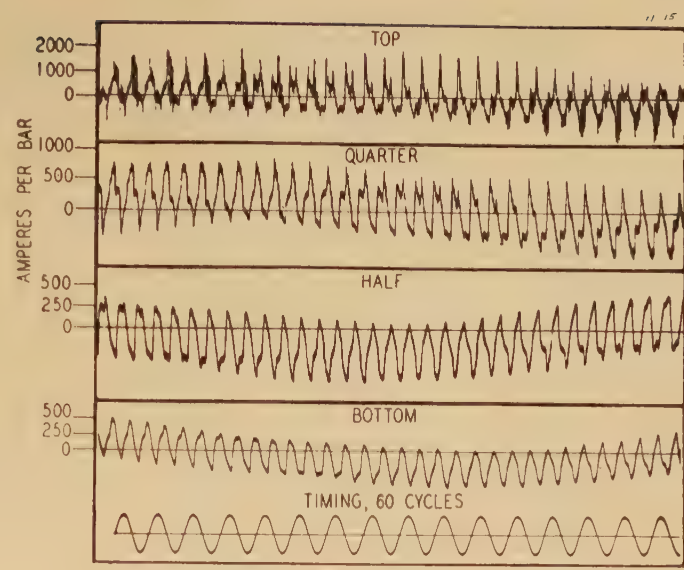

The corresponding rotor-bar current, by equations 1 and 2, is:

$$R_s=\frac{3\sqrt{3}}{\pi}\times\frac{18\times22}{2}\times\frac{48}{45}=350 \text{ amperes} \quad (20)$$

As a further check upon the magnitude of the slip-frequency component, the slip-frequency loss was computed, also the total resistance per bar. The stator resistance between terminals was 1.139 ohms at 55 degrees centigrade, so the stator copper loss was 295 watts. The fixed loss was 220 watts. Therefore:

Rotor input = 4,570 − 295 − 220 = 4,055 watts

$$\text{Slip-frequency loss}=\frac{90\times4{,}055}{1{,}800}=203 \text{ watts} \quad (21)$$

The total rotor resistance per bar at 55 degrees centigrade is:

$$r=69\times10^{-6} \text{ ohms} \quad (22)$$

The amplitude of the slip-frequency component of current, then, computed from the value of loss shown in equation 21 is:

$$R_s=2\times\frac{203\times10^6}{45\times69}=359 \text{ amperes} \quad (23)$$

and this result checks very closely with the value shown in equation 20, but is 13 per cent less than the value scaled from the oscillograms, as shown in table III. This may indicate an error of approximately 15 per cent in the computed scale of the oscillograms, in spite of the care taken to obtain an accurate calibration.

Effect Upon Motor Efficiency, Stray Loss

The total loss determined by the conventional method of losses is:

295 + 220 + 203 = 718 watts (24)

But the total loss determined by a careful dynamometer test is:

4,570 − 3,750 = 820 watts (25)

The stray loss at this load therefore is:

820 − 718 = 102 watts (26)

which is over two per cent. Performance curves for this motor are shown in figure 12, including a curve of stray loss in per cent of input. The shape of this curve is in substantial agreement with other published material.

Several writers on the subject of stray-load loss in induction motors agree that the loss is largely due to high-frequency flux pulsations in the stator teeth, plus a relatively small tooth-frequency eddy-

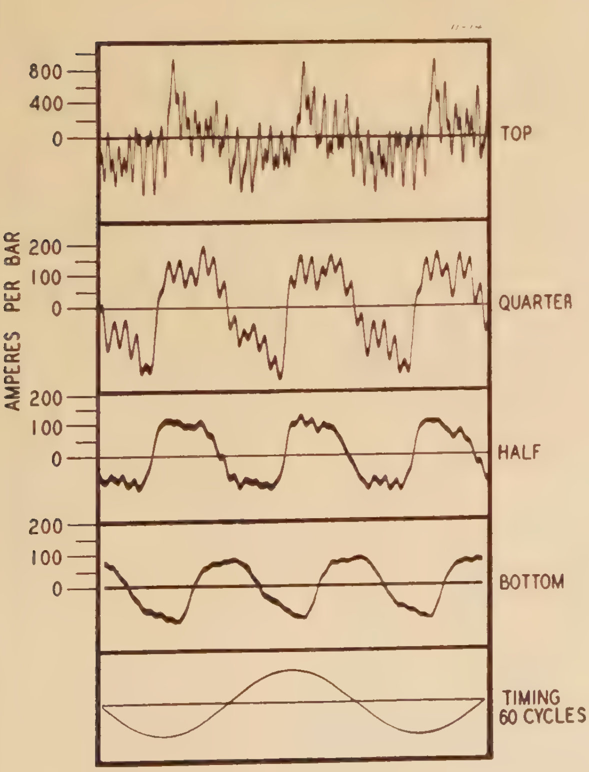

Figure 14. Rotor-bar currents of single-phase four-pole motor at synchronous speed, 1,800 rpm, 220 volts, 5.13 amperes

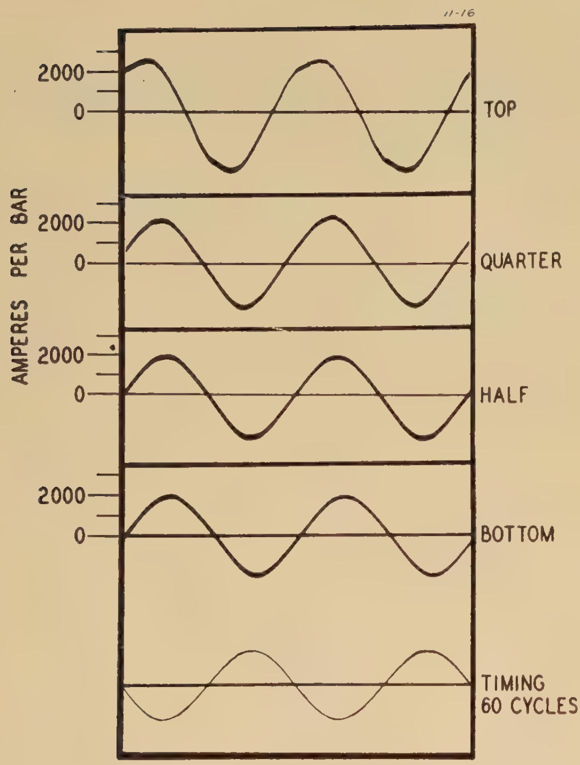

Figure 16. Rotor-bar currents of single-phase four-pole motor with rotor locked, 220 volts, 47.6 amperes

current loss in the rotor bars. In the tests reported herewith, the tooth-frequency eddy-current loss was found to increase with load. The lower frequency band-frequency eddy-current loss was found to be of even greater importance. At full load, this component (see figures 4 and 11) has a frequency of 345 cycles, and its amplitude rises and falls with a beat frequency of $2fs=6$ per second. The rms value of this component per bar is computed to be:

$$I_b=\frac{U_{\text{eff}}}{2.38}=\frac{304}{2.38}=128 \text{ amperes} \qquad (27)$$

Table I. Current Distribution and Phase for 360-Cycle Component

Level	Current Density (Per Cent)	Angle of Lag (Degrees)
Top	100	0
Quarter	50.1	39.1
Middle	24.2	79.3
Bottom	13.4	155.0
Average (total)	26.0	45.3
Effective	42.6	

Table II. Rotor-Bar Current Distribution in Figure 10

Level	Tooth-Frequency 1,440 Cycles	Band-Frequency = 360	
		Measured	Computed
Top	350	187	183
Quarter	33	55	91
Middle	10	30.5	44
Bottom	3	20	24.5
Total			47.5
Effective			78

Due to the distribution of this component in the end rings, the loss there is very small, and the resistance per bar may be taken as 34×10^{-6} ohms instead of the value given in equation 22. The rotor loss produced by this component therefore is:

$$W_b=45\times(128)^2\times34\times10^{-6}=25 \text{ watts} \qquad (28)$$

This is about a quarter of the stray load loss.

In table III is shown a value of 225 amperes for the peak rms value of the tooth-frequency component. This was computed from the curve of measured current density values shown. The loss produced by this component is about 15 watts, so the total high-frequency rotor current loss is 40 watts, which is nearly one per cent of input.

Single-Phase Operation

The same motor was operated single phase by opening one line after it was up to speed. At synchronous speed the computed band-frequency wave shapes are shown in figure 13; the underlying frequency of course is 120 cycles. A set of rotor current oscillograms taken at synchronous speed is shown in figure 14. As before the full-load pictures of figure 15 show the band-frequency wave superposed on the power current, but for single-phase operation the band-frequency current (118 cycles) is a little larger than the slip-frequency current (2.2 cycles).

A locked test was also run on this motor connected single phase, and oscillograms are shown in figure 16. At standstill, all frequency components reduce to 60 cycles, giving a sine wave of current in the rotor bars. The shift in phase is shown by the drift to the right at the lower levels. Values of current density and phase angle with respect to the current at the top are shown in table IV; measured values taken from the film are compared with computed values. The check on phase angle is quite close. There is a satisfactory qualitative check on amplitude also, but the measured values seem to be too high, as noted previously in table III.

Consequent-Pole Winding

By reconnecting the coils of this motor, a three-phase consequent-pole winding

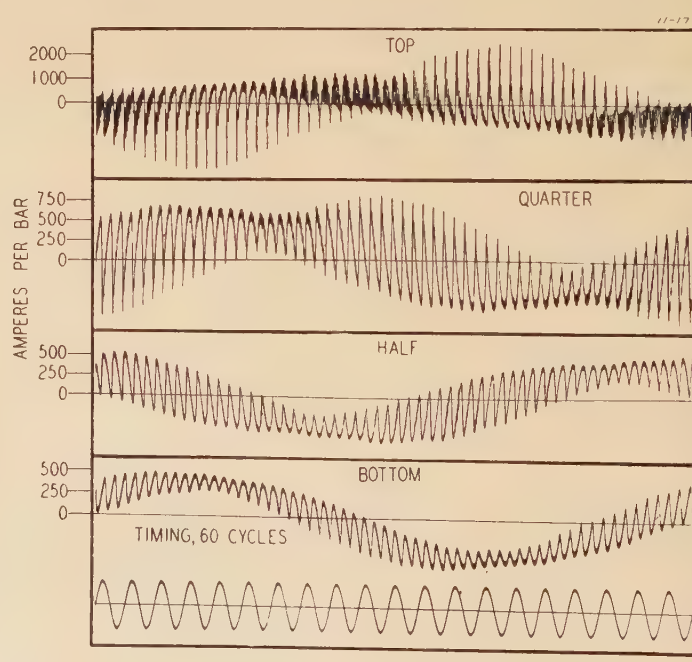

Figure 17. Rotor-bar currents of three-phase four-pole motor, consequent-pole connection 1,710 rpm, 190 volts, 14.4 amperes

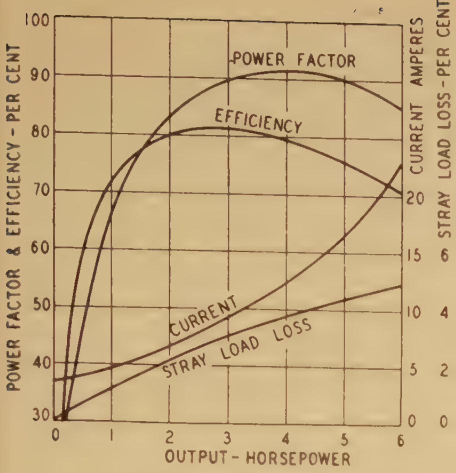

Figure 18. Load-test curves of three-phase four-pole motor, consequent-pole connection, 190 volts. Temperature 55 degrees centigrade

was produced with eight coils per phase group for four-pole speed, that is using a phase band width of 120 degrees instead of 60 degrees and only two polar groups per phase. Upon analysis this gave a band-frequency wave similar to that shown in figure 2, but of half its frequency (180 cycles at synchronous speed) and approximately twice its amplitude. This is noted in the load oscillograms of figure 17. The load-test curves of figure 18 show decreased efficiency, particularly at heavier loads, and a considerable increase in stray-load loss, due almost entirely to the larger band-frequency current in the rotor bars. The test was run on 190 volts to get the same flux density in the motor.

Eight-Pole Operation

The stator winding was reconnected for three-phase eight-pole operation. Using the same coils as before, the coil pitch is four-thirds, which produces a band-frequency wave like that in figure 2; so the load oscillograms shown in figure 19 are quite similar to those in figure 11 except that the tooth ripple is almost entirely gone.

Conclusions

High-frequency components in the rotor-bar current may contribute a considerable portion of the stray-load loss in a squirrel-cage motor. By proper slot design, the tooth-frequency component may be controlled. The band-frequency component, however, depends upon the winding, and may be decreased by coordinating pitch and number of phases. If a pitch of five-sixths instead of two-thirds had been used with the three-phase four-pole winding, the band-frequency wave would be as shown in figure 20 instead of that shown in figure 2. An analysis of this wave shows a band-frequency current loss of about one-third as much.

Table III. Rotor-Bar Current Distribution in Figure 11

Level	Tooth-Frequency 1,368 Cycles	Band-Frequency = 345		Slip-Frequency = 3	
		Measured	Computed	Measured	Computed
Top	930	873	707	417	350
Quarter	61	295	357	418	350
Middle	25	137	177	405	350
Bottom	19	86	102	415	350
Total			189	414	350
Effective	225	306	304	414	350

Table IV. Rotor-Bar Current Distribution and Phase in Figure 16

Level	Amperes Per Bar		Phase Angle—Degrees	
	Measured	Computed	Measured	Computed
Top	2,628	2,168	0	0
Quarter	2,153	1,756	28.1	20.4
Middle	1,943	1,578	39.7	40.7
Bottom	1,870	1,530	57.3	57.9
Total		1,578		35
Effective		1,675		

References

1. The Induction Motor (a book), **Benj. F. Bailey.** McGraw-Hill Book Co., pages 102–4, 195–8.

2. Tooth-Frequency Eddy-Current Loss, **Paul Narbutovskih.** AIEE Transactions, volume 56, 1937 (February section), page 253.

3. Measurement of Stray Load Loss in Polyphase Induction Motors, **C. J. Koch.** AIEE Transactions, volume 51, 1932, page 756.

4. Zusätzliche Verluste in Kleinen Drehstrommotoren, **Rogowski and Vieweg.** *Archiv für Elektrotechnik,* volume 14, 1925, page 574.

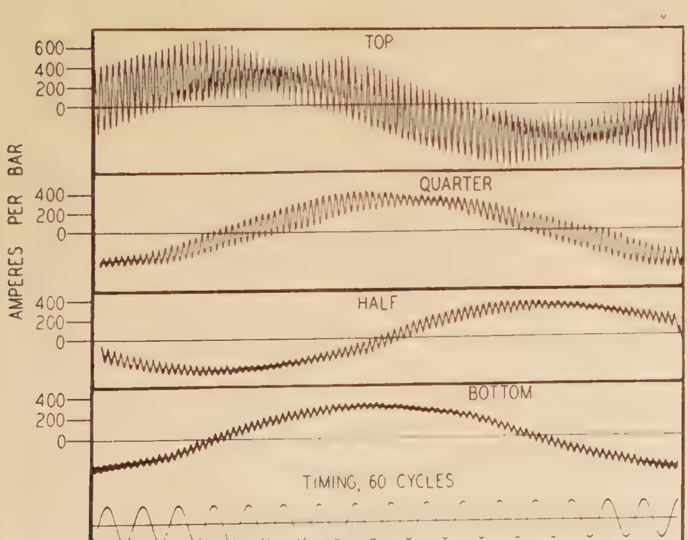

Figure 19. Rotor-bar currents of three-phase eight-pole motor under load with 5.55 per cent slip, 850 rpm, 224 volts, 6.1 amperes

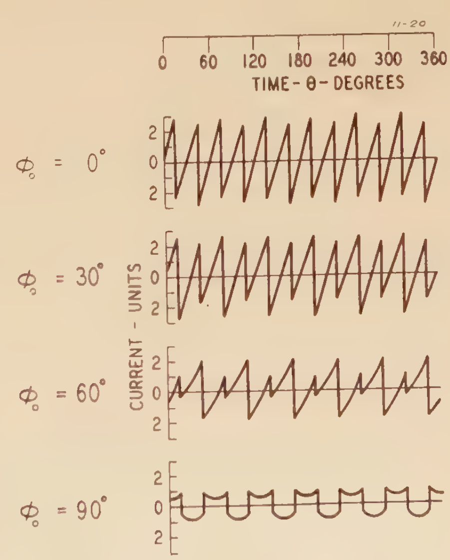

Figure 20. Rotor-bar current at zero slip for three-phase winding with 5/6 pitch

Classification and Co-ordination of Short-Time and Intermittent Ratings and Applications

R. E. HELLMUND
FELLOW AIEE

Synopsis: The paper makes a comparison of permissible temperature rises for short-time and intermittent ratings and permissible rises for continuous ratings. It suggests methods for the application of short-time ratings to various typical classes of intermittent load conditions and presents for each of these classes ways and means for properly co-ordinating the ratings of the major devices (motors and generators) and the ratings of the auxiliary devices and conductors.

Introduction

THE present commercial standards for electrical apparatus and conductors usually provide continuous ratings and short-time ratings for periods of 5, 15, 30, 60, and 120 minutes. The methods used for selecting ratings for various classes of intermittent or varying loads from these available ratings are rather indefinite and at times result in applications which, although generally satisfactory, are often not the most economical. It is shown in this paper that by following essentially the present practices of rating and application but also properly co-ordinating them and supplementing them with additional data, a selection of the most suitable short-time ratings can be made. A very simple procedure applying to the proper co-ordination of the main apparatus and the auxiliary devices and conductors is outlined at the end of the paper. To facilitate this co-ordination, standard temperature-rise values which seem suitable for short-time ratings of the main and auxiliary apparatus and conductors are derived and tabulated.

Short-Time Ratings and Loads

In many standards the short-time ratings are based on temperature rises higher than those on which the continuous ratings are based. Although the differences between the values for short-time and continuous ratings generally were selected arbitrarily, the basic principle of having a difference between them is sound. With short-time loads the maximum temperatures obtained can last for only a relatively small part of the total time. Since the deterioration of insulation depends not only upon temperature but also upon the length of time the higher temperatures prevail, satisfactory life can be obtained if relatively high temperatures prevail for only a small part of the time. Tests have indicated that the life of insulation is halved for each eight- to ten-degree-centigrade increase in temperature, particularly for insulation exposed to oxygen in the air. It is proposed to use this rule here and to calculate for some typical short-time ratings the permissible maximum temperature rises which result in insulation life about equal to that obtained with temperatures specified as standard for continuous operation. (Methods suggested by V. M. Montsinger for transformers[1,2] and also outlined by P. L. Alger and T. C. Johnson[6] will be used for this purpose. These methods and the eight- to ten-degree-centigrade value may not apply to applications where oxygen is excluded, as in oil-insulated transformers with inert air protection or hydrogen-cooled machines.)

Figure 1 shows a number of typical time-temperature curves for short-time ratings of a small induction motor. These curves have been calculated under the assumption that each eight-degree-centigrade increase in temperature halves the life of the insulation. On this basis, each of the curves shown will give insulation life equal to that obtained with a uniform rise of 60 degrees centigrade (by resistance) over the same period of time. Since the cooling curves approach the zero temperature line asymptotically (reaching zero after an infinite time), it was necessary to limit arbitrarily the time for each curve, and the point at which the temperature rise drops to ten degrees centigrade was taken. This provides a margin of safety and results in conservative curves. (All calculations and discussions in this paper deal with temperature rise by resistance; the thermometer method is not very satisfactory for the study proposed.)

It is seen from figure 1 that the permissible temperature rises range from 80 to 93 degrees centigrade, or an excess of 33 to 55 per cent over the 60-degree temperature rise permissible for continuous operation.[10] The use of these higher permissible temperature rises is of importance economically because, according to curve 1, a five-minute rating with a 60-degree limit can be raised to an 11-minute rating for the higher temperature. Similarly, curve 2 shows an increase from a 15-minute to a 46-minute rating; curves 3 and 4 show increases from 30 to 80 minutes and from 38 to 116 minutes respectively. Curve 4 has been chosen as a limiting case with a rate of temperature rise of about one-half degree a minute at 60 degrees centigrade; for major devices such as generators, motors, etc., it is customary to apply continuous ratings rather than short-time ratings if the rate of temperature rise is lower.

The curves of figure 1 are typical of most apparatus, the principal difference being that with larger devices the time values increase. This, however, does not affect the values of the maximum permissible temperatures, which are influenced essentially by the shapes of the curves and which vary to some extent with different types and sizes. Allowing for such variation within usual limits, it seems safe to select for standardization purposes temperature rises 25 to 40 per cent higher for short-time ratings of major devices than for continuous ratings. Table I, column 2, suggests standard values of temperature rise for short-time ratings of major devices corresponding to the values for continuous ratings in the first column. The values are conservative and higher values might be justified. (After testing class *B* insulated d-c motors for short-time ratings now based on 75 degrees temperature rise by thermometer, F. A. Compton recommends a temperature rise of 105 to 120 degrees centigrade by resistance;[8] the table gives 100 or 110 degrees centigrade.)

The considerations thus far can be applied to any type of apparatus or conductors within the limits stated. (Naturally modifications in some of the values mentioned must be made when values

---

Paper **41-13,** recommended by the AIEE committee on standards, and presented at the AIEE winter convention, Philadelphia, Pa., January 27–31, 1941. Manuscript submitted November 8, 1940; made available for preprinting November 27, 1940.

R. E. Hellmund is chief engineer of the Westinghouse Electric and Manufacturing Company, East Pittsburgh, Pa.

The author wishes to acknowledge his indebtedness to C. S. Hague, Jr., for his assistance in the calculation of the curves.

1. For all numbered references, see list at end of paper.

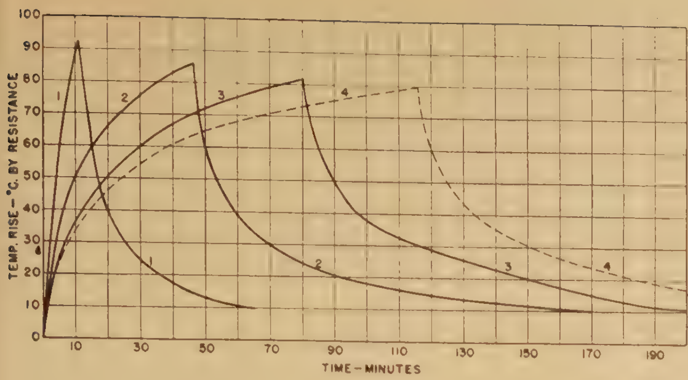

Figure 1. Permissible temperature rises for various short-time loads

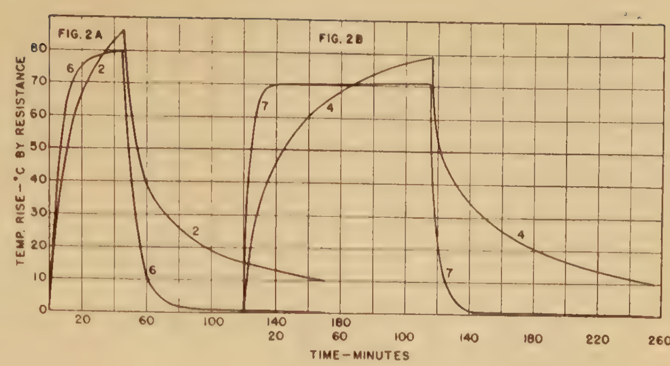

Figure 2. Comparison of permissible temperature rises for short-time loads of apparatus with different time constants

other than 60 degrees permissible temperature rise for continuous load apply.) However, if the main devices are connected in series with various auxiliary devices or conductors having much smaller time constants than the main device, the conclusions derived so far must be modified for the auxiliary devices or conductors. This is demonstrated in figure 2*a*, curve 2 of which corresponds to curve 2 of figure 1 and is considered representative of main devices such as generators, motors, etc. Any smaller device or conductor connected in series with the main device and having a smaller time constant will show more rapid initial temperature rise, and if loaded as long as the main device, will run at temperatures near the maximum for longer periods than the main device. This in turn means that to get equally satisfactory insulation life the maximum temperature-rise values must be kept lower. Curve 6, figure 2*a*, applies to an auxiliary device with a small time constant giving the same insulation life (with the same class of insulation) assumed for the main device. It is seen that 80 degrees centigrade is the maximum permissible value for the auxiliary device instead of 86 degrees centigrade indicated for the main device. Curve 4 in figure 2*b* corresponds to curve 4 in figure 1 and is another typical curve for the main device. Curve 7 has been calculated for an auxiliary device with a smaller time constant to give the same insulation life. Again a smaller maximum temperature rise (71 degrees centigrade) must be chosen for the auxiliary device than the 80 degrees for the main device. Here the auxiliary device reaches constant temperature during the load period.

Table I. Suggested Relation of Temperature Rises (by Resistance) for Short-Time Ratings to Rises for Continuous Ratings

Continuous Ratings (Deg C)	Short-Time Ratings (Deg C): Main Apparatus	Short-Time Ratings (Deg C): Small Auxiliary Apparatus or Conductors*
20	25	25
25	30 or 35	30
30	40	35
40	50 or 55	45 or 50
50	60 or 70	55 or 60
60 (class *A* insulation)[10]	80	70
80 (class *B* insulation)[10]	100 or 110	90 or 100
100	125	110 or 125

The values in this table are chosen from the preferred values suggested in AIEE Standard number 1.[10] In general they should give satisfactory life of insulation if the rated load is continually reapplied after the apparatus temperature has dropped to about ambient temperature. Practical cases of application of this kind are rare. As a rule, considerable time elapses between the applications of loads, and whenever this is the case the application of apparatus can be made so as to reach even higher temperature-rise values than those suggested for standard rating purposes in the table. Although the value of 80 degrees centigrade suggested in the table to correspond to 60 degrees rise for continuous load does not take full advantage of the permissible rises indicated in figure 1, the increases in time over the 60-degree values are still appreciable, ranging from 65 to 250 per cent.

*These values also may be used if the short-time operation of small auxiliary apparatus or conductors results in the same temperature rise obtained with continuous operation at the same load.

In view of the conditions just described, it seems advisable to use lower maximum values of temperature rise for the rating of small auxiliary devices and conductors intended for short-time service. This practice need not be altered by the fact that, as in figure 2*b*, the short-time ratings of the auxiliary devices or conductors give the same temperatures as obtained with continuous operation at the same load. The values in column 3 of table I are suggested for the standardization of small auxiliary devices and conductors used in conjunction with main devices in short-time service. In general, where two values are given, the lower value of one column should be used with the lower value of the other column.

Intermittent and Varying Loads

Typical intermittent and varying load cycles are illustrated in figure 3. During the time (T_r) the apparatus is heavily loaded and carries a current (I), while for the remaining period (T_i) it may carry no load, as in the case of a welding generator[9] (figure 3*a*). Figure 3*b* represents such apparatus as a-c induction motors, which are loaded during the period (T_r) and not loaded during (T_i), but which have to carry a magnetizing current (i_i) during the off periods. There is little change in principle if the motor, instead of carrying a magnetizing current, carries a light load (i_i) as indicated in figure 3*c*. This might occur with an industrial mill which is driven light during (T_i) and loaded during (T_r). In all the applications cited, the rms current (i) is, of course, less than the current (I) during the heavy-load period. (In this discussion, service conditions as illustrated in figures 3 and 10 are of the type which as a rule can be handled by devices having

Figure 3. Typical intermittent and varying (periodic) load cycles

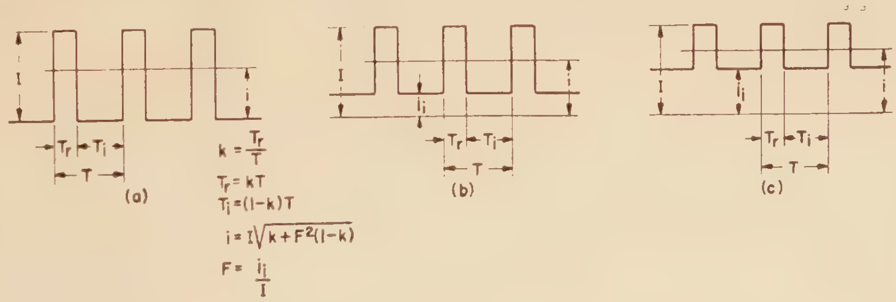

"short-time" ratings. Although many of the considerations in the paper are applicable to other cases, no attempt has been made to include a complete study of varying loads which are generally handled by devices having continuous ratings or a combination of continuous ratings and certain overload ratings.)

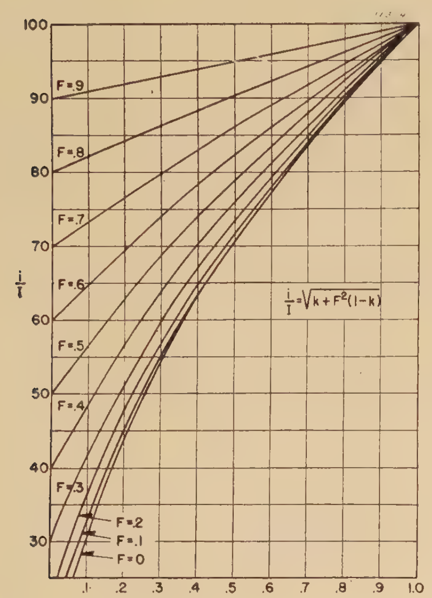

Figure 4. Ratio of rms current to load current for intermittent and varying load cycles

Very often the current (I) during the load period is a significant value in machine design for considerations other than heating. A commutator machine, such as a welding generator[9] for instance, must be able to commutate the current (I) satisfactorily during long periods of machine operation. In an induction motor the value (I) is equivalent to a torque required for driving the load and it is necessary that the pull-out and starting torques of the motor have certain definite relations to the running torque if satisfactory operation and a sufficient margin of safety are to be obtained. Again, the value (I) may be of significance in the regulation of the machine or apparatus. In these examples, current (i) is of importance only in the heating of the machine, while current (I) has considerable bearing on various other characteristics, including the mechanical design. It should therefore appear in the rating structure and it is suggested that the nominal rating of the apparatus be selected to correspond to the current (I) and that the heating current (i_h) which it can carry within safe limits of temperature rise continuously, be indicated by a suitable service factor

$$S_1=\frac{i_h}{I} \tag{1}$$

This has been previously suggested by others (Alger,[4,6] Johnson,[5,6] and Hildebrand[7]) and seems to be a simple method for supplying fairly complete information about heating as well as other characteristics of practical importance. It has also been suggested that no reference whatsoever be made to temperature conditions in connection with the nominal rating corresponding to current (I).[6] However, since practically all nominal ratings of electrical apparatus are now tied in with temperature considerations in some way or other, it seems desirable to retain the temperature rating as the primary basis for all nominal ratings. This can very readily be done because current (I), although it cannot be carried continuously with many devices, can always be carried for at least limited periods and be tied in with one of the standard short-time (5-, 15-, 30-, 60-, or 120-minute) ratings. In this way the length of time the machine can carry the current (I), starting with the machine cold, is indicated. This additional information makes it possible to select for all applications the proper wiring and devices connected in series with the main apparatus, which is very essential for an economical and successful combination of all parts of the circuit. (If the conditions are such that any of the factors, such as commutation, torque, regulation, etc., call for a main device which can carry the current (I) continuously, it can be given a continuous rating (I) and the methods described here will then be of no practical importance with reference to the main apparatus. However, they may be of assistance in the most economical selection of auxiliary apparatus and conductors.)

The rms current (i), dependent upon the load cycles shown in figure 3, is

$$i=I\sqrt{k+F^2(1-k)} \tag{2}$$

in which (k) is the ratio of the load period (T_r) to the total period of the cycle (T), and (F) is the ratio of the rms current during the low-load periods to the rms current during the heavy-load periods. In figure 3a, with $F=0$, we have

$$i=I\sqrt{k} \tag{3}$$

Figure 4 has been calculated from formula 2 and gives the rms current for any value of k and F.

With the regularly repeating (periodic) load cycles shown in figure 3, it is evident that the drop in temperature during each light- or no-load period must at least equal the rise in temperature during each heavy-load period in order to obtain a stable cyclic temperature condition in which permissible temperature values are not exceeded. (See figure 5.) It follows directly that with a heavy-load period (T_r), a time (T_i) must be allowed for the light- or no-load period, resulting in a total time (T) for each cycle. With the time-temperature curves A and B fixed by the loads and apparatus characteristics, the maximum ratio of $T_r/T=k$ is definitely limited. It is dependent upon the ratio (R) of the average rate of drop (B_1) to the average rate of rise (A_1) and follows from

$$k=\frac{R}{1+R} \tag{4}$$

These relations are basic to all regularly repeating (periodic) intermittent or varying loads. A more complete outline of this method of analysis by time-temperature curves is given in a previous paper.[3] In that paper it was generally assumed that the peak temperature rises reached with short-time ratings and during intermittent loads should be the same as the permissible temperature rises for continuous loads. This, however, does not take advantage of the fact that the latter temperature may be safely exceeded for limited periods. An attempt will therefore be made in the following to take advantage of this possibility for

Figure 5. Temperature variation with intermittent and varying (periodic) load cycles of long duration

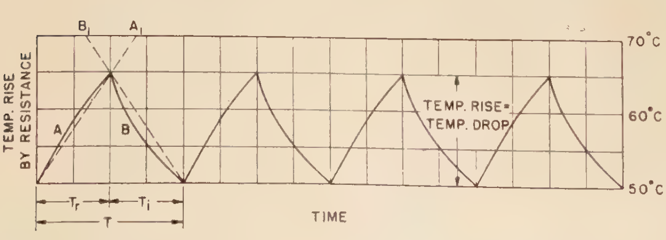

Figure 6. Permissible temperature rises for typical periodic loads

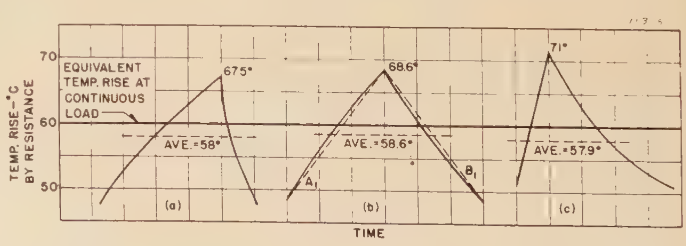

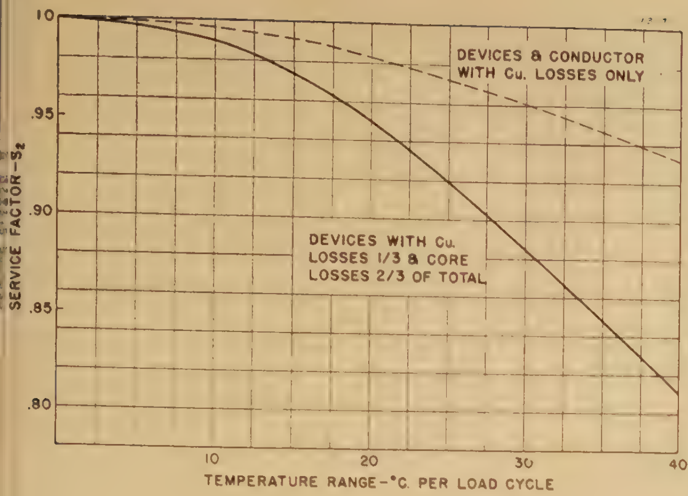

Figure 7. Service factor S_2 takes into account the amplitude of the cyclic temperature variation

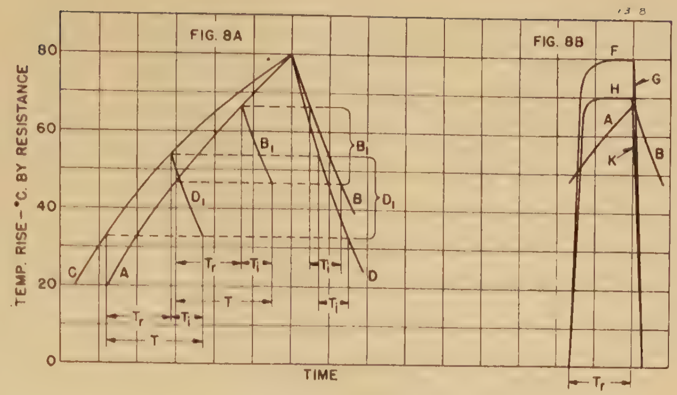

Figure 8. Comparative analysis of temperature conditions for apparatus of different time constants during periodic load cycles

intermittent load applications as in figure 5.

Class 1A Intermittent Service

For this class of service it is assumed that the ventilation conditions are not appreciably changed between the heavy-load and the light- or no-load periods. This applies to most stationary devices or conductors unless they are equipped with adjustable forced ventilation; it also applies in general to constant-speed machinery while running. It is further assumed that the load periods are rather short and the variation in temperature rise will be so small that it can be neglected.

Since with these assumptions the temperature of the machine is about constant, the value (i) should be such as to give a safe temperature rise for continuous operation. For this type of service it is therefore necessary merely to select apparatus having a short-time nominal rating (I) with a service factor at least equal to

$$S_1 = \frac{i}{I} = \frac{i_h}{I} \tag{5}$$

The method outlined under class 1A should be satisfactory if its use is confined to applications where the heavy-load period is limited to ten per cent of the time (T_s) on which the nominal rating is based; that is, in the case of a 30-minute rating, for instance, the load period (T_r) does not exceed three minutes. Then the total temperature variation during the cycle will as a rule be less than ten per cent of the temperature rise for continuous operation and the excess temperature will be less than five per cent.

The wiring and auxiliary devices connected in series with the main machine or apparatus usually have smaller time constants. Therefore, their temperature variations in percentage of the average temperature rise during the time periods just indicated may be larger. This makes it advisable to select them for a continuous rating five to ten per cent larger than the rms value of the load.

Class 2A Intermittent Service

For class 2A applications, it is assumed that the cooling conditions are essentially the same during the entire load cycle but that the time for each cycle is increased to the point where the variations in temperature can no longer be neglected. Figure 6 shows three typical time-temperature curves, each for a single cycle with a total temperature change of 20 degrees centigrade. These curves also have been calculated to give a life of insulation equivalent to that obtained with continuous operation at 60 degrees centigrade rise. Figure 6b has a curvature in the rising curve about equal to that of the dropping curve. This means that the results are the same as they would be with the triangular time-temperature curve A_1B_1. The maximum permissible temperature rise is 68.6 degrees centigrade. With curves 6a having more curvature in the rising curve and thus giving longer periods for the higher temperatures, the maximum must be kept lower, that is to about 67 degrees centigrade. The opposite condition shown in 6c led to a higher maximum of 72 degrees centigrade. The average of the temperature rises for these cycles varies within the narrow range of 57.9 to 58.6, that is, 1.4 to 2.1 degrees centigrade, or 2.3 to 3.5 per cent below the temperature-rise value for continuous load. Thus, in order to obtain satisfactory operation the losses must be lowered 2.3 to 3.5 per cent. In devices having only copper losses, this means a reduction of only 1.1 to 1.7 per cent in rms current. In machines designed for intermittent service the core losses are often relatively high, and therefore the copper losses may be as low as one-third of the combined losses. The same reduction in total losses may therefore require a reduction of about 7 to 10.5 per cent in the copper losses, which means 3.5 to 5.5 per cent reduction in the rms current. This is too liberal because the influence of the core losses upon the copper temperature is usually much less than that of the copper losses. It would thus seem that an allowance of five per cent, or a service factor $S_2 = 0.95$, to cover the difference between case 1A and 2A would be quite safe for a variation of 20 degrees centigrade. The curve for S_2 in figure 7 has been based on this line of reasoning and covers the range of temperature variations usually found in practice.

Determination of the exact temperature variation would require a complete time-temperature curve analysis. It can be safely assumed, however, that it usually does not exceed the value $r(T_r) \div (T_s)$ in which T_r = the time of heavy load per cycle, T_s = the time used as a basis for the short-time rating, and r = the temperature rise upon which this rating is based. It is thus possible to calculate safe maximum limits for the temperature variation and then find the value S_2 for this cycle from figure 7. The service factor for class 2A applications is then

$$S = S_1 S_2 \tag{6}$$

The application of smaller auxiliary devices and conductors with main devices in intermittent service of this class cannot be made safely by the method outlined under class 1A. Depending upon their time constants, the temperature

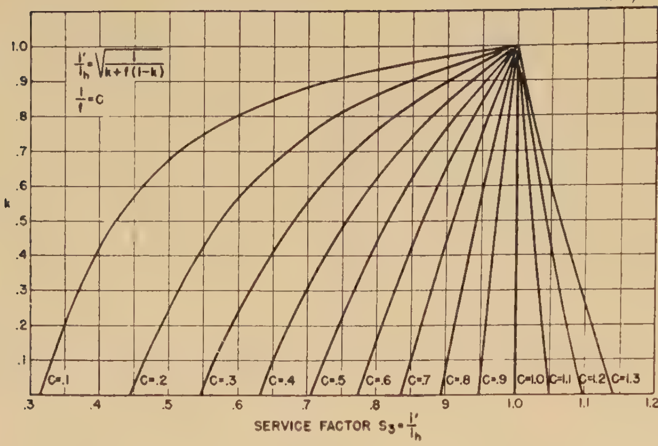

Figure 9. Service factor S_3 takes into account variations in ventilation during the load cycle

rises of the auxiliary devices and conductors may vary over wide ranges and it is hardly feasible to set any safe practical limits for the variation.

Two distinctly different typical conditions are shown in figure 8. In figure 8*a* we have heating curve A and cooling curve B for a main device. An auxiliary device with smaller time constant and designed for the same short-time temperature rise will have a flatter curve (C) for the upper part of the heating curve, and a steeper curve (D) for the cooling curve. With a load time (T_r) and idle time (T_i), stable repeating conditions are obtained with a maximum temperature rise of 68 degrees centigrade for the main device and 54 degrees centigrade for the auxiliary device, as found by the methods described in a previous paper.[3] It follows that with conditions shown in figure 8*a*, the auxiliary device will have lower temperature rises than the main device if based on the same temperature rise for the same short-time rating.[9] Entirely different results are obtained if the time constant of the auxiliary device or conductor is so small that maximum temperature is reached during the time (T_r), as shown by curve F, figure 8*b*. It is at once evident that with curves F and G of the auxiliary device or conductor, insulation life will be shorter than with curves A and B of the main device. This undesirable condition can be largely eliminated by lowering the rating temperature of the auxiliary device or conductor as suggested under short-time ratings in column 3, table I and illustrated by curves H and K in figure 8*b*. It can therefore be concluded that for intermittent service of this 2*A* class, the auxiliary devices and conductors having the same short-time ratings as the main device can be selected if ratings are based on

(*a*). The same temperature rises (column 2, table I) as the main device, if the auxiliary device does not reach its maximum temperature during the load period (T_r);

(*b*). A somewhat lower temperature rise (column 3, table I) if the auxiliary device reaches its maximum temperature during the load period (T_r).

In general, conditions under (*a*) will apply to all except very small auxiliary devices, while conditions under (*b*) may be found to apply frequently to conductors. If suitable temperature rises, as indicated here, are used in the standardization of devices and conductors for intermittent service, their application becomes exceedingly simple and consists merely in combining apparatus and conductors having the same short-time rating with reference to current and time.

Class 1B Intermittent Service

In some classes of application, ventilation conditions are considerably different during the periods of heavy and light load or no load. This is true in any case where artificial cooling is automatically stopped, except during the heavy-load period. A more common application is represented by motors carrying a current (I) while loaded and running and which stand still during idle periods. In these applications the rate of cooling is usually reduced because of the reduced ventilation, although with motors standing still this is at least partially compensated by the absence of those losses (essentially core losses) occurring with the motor running light. In some applications, especially enclosed motors, the elimination of losses may more than counteract the reduced cooling.

If the ratio of the cooling rate for class 1*A* to that for class 1*B* during no-load periods is assumed to be (f), it follows that the necessary drop in temperature for each cycle can be obtained for class 1*B* if the no-load time is increased from T_i to $T_i^1=fT_i$. Consequently, we can analyze class 1*B* applications the same as class 1*A* merely by substituting the time (T_i^1) for (T_i). By replacing in formulas 2 and 3 the value k by $k^1=\frac{T_r}{T_r+T_i^1}$, we find a reduced current (i^1) which the motor is able to carry continuously regardless of the reduced ventilation, assuming that the total time per cycle is too short to give appreciable temperature variations. The ratio of this current (i^1) to the current (i_h) which the motor can carry while running continuously may be represented by another service factor (S_3). It can be calculated for $F=0$ from the following formula

$$S_3=\frac{i^1}{i_h}=\sqrt{\frac{T_r+T_i}{T_r+fT_i}}=\sqrt{\frac{1}{k+f(1-k)}} \quad (7)$$

Figure 9 gives this service factor for various values of k and f. With the aid of these curves the current (i_h) can be found directly from the smaller actual rms current (i^1). The total service factor for class 1*B* applications is, therefore, $S=S_1S_3$. Suitable values for (f) can be determined by the test method described in a previous paper,[3] taking cooling curves with the motors running and at rest. The method here outlined for class 1*B* motors should be satisfactory if the running time per cycle does not exceed ten per cent of the rating time (T_s).

The application of conductors and auxiliary devices follows the same general principle as suggested for class 1*A*, using the actual rms current as a basis. This, of course, is under the assumption that the cooling conditions of the conductors and auxiliary devices are the same for both the load and the idle period, which is generally true.

Class 2B Intermittent Service

For class 2*B* applications it is assumed that the ventilation is different for the high-load and the low-load or no-load periods, but that the time for each load cycle is so long that temperature variations become of practical importance. Thus, class 2*B* applications have the same relation to class 1*B* as class 2*A* have to class 1*A*. It is therefore necessary to introduce, in addition to the service factor (S_3), the service factor (S_2), which leads to the service factor

$$S=S_1S_2S_3 \quad (8)$$

If auxiliary devices and conductors are combined in this service with the main devices by the methods suggested for class 2*A* applications, they will as a rule have an unnecessarily large margin of safety. The reason for this is that the

cooling conditions of the auxiliary devices and conductors usually remain unchanged, while those of the main device are reduced during the ideal periods. However, it is not safe to suggest any other practice which is generally applicable. In specific applications, with known conditions and additional analysis, further economies may be accomplished, but as a rule the gains possible will be of minor importance in the total cost.

General Discussion of Service Factors

S_1 indicates the ratio of the current giving a safe temperature rise with continuous operation to the current corresponding to the nominal (short-time) rating. It is governed by the design of the apparatus and the temperature rises used as a basis for short-time and continuous ratings; it must be determined by test. Minimum values for (S_1) should be known and be standardized for certain types, classes, and ranges of ratings, the same as is done with torque ratios. This is exemplified in table II.

Table II

5-minute ratings	$S_1=0.50$
15-minute ratings	$S_1=0.60$
30-minute ratings	$S_1=0.70$
60-minute ratings	$S_1=0.80$
120-minute ratings	$S_1=0.87$

S_2 makes allowance for temperature variation during long load cycles. It is governed partly by the type of application and partly by the design of the apparatus. However, since it does not vary widely, it can be shown with sufficient accuracy for most practical purposes by curves as shown in figure 7. As pointed out there, higher values than those indicated for S_2 in the full-line curve apply to cases where the copper losses essentially govern the temperature rise of the windings (dotted curve in figure 7).

S_3 makes allowance for differences in ventilation which may exist between the heavy-load and the light- or no-load periods. It is influenced by both the type of application and characteristics of the apparatus. The influence of the former is covered in formula 7 by the factor (k) determined from the service condition. The factor (f), depends upon the apparatus characteristics. It is not recommended here that (f) be made a part of the rating structure but that for various types of motors, values for (f) be established which are safe but which do not result in uneconomic applications.

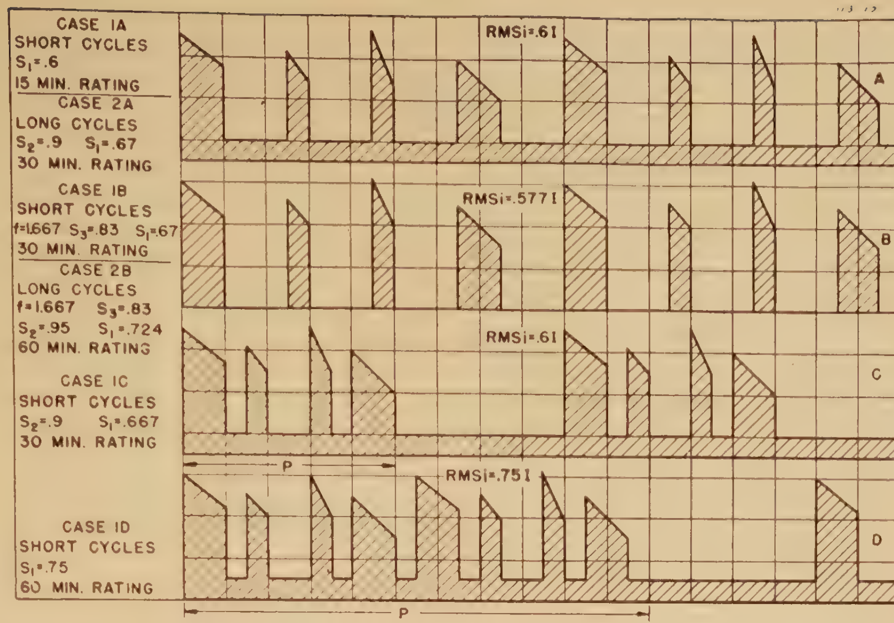

Figure 10. Some typical load cycles analyzed by the methods suggested

Selection of Short-Time Ratings for Intermittent or Varying Loads

(a). Main Apparatus

The variety of conditions met in practice makes it impossible to outline a method of application suitable under all circumstances. However, the data presented here are suitable for the majority of applications and should prove helpful in giving results quickly. Both periodic load cycles as shown in figure 3 and load cycles with irregular intermittent loads as in figure 10 can be calculated as follows.

Divide the entire time into high- and low-load or no-load periods; then calculate the rms current for all the high-load periods. The resultant value is the current (I) of our previous analysis and it is used for the selection of the current value of the nominal short-time rating (or horsepower or kilowatt ratings corresponding to this current value).

The current value (i_l) previously used is found by calculating the rms current for all the low-load periods and it permits the calculation of $F=i_l/I$. The value (k) is obtained by dividing the time of all high-load periods by the total time. The resultant actual rms current (i) can now be found from formula 2 or figure 4. From here on we have to distinguish between different classes of applications.

Class 1A: If with a load as shown in figure 3 or 10*A* the ventilation is essentially constant and the load periods short, find i/I. Then select from such tables as table II the nominal short-time rating for the current I which has a value S_1 at least equal to i/I.

Class 2A: If, again, with the load as shown in figure 3 or 10*A* the ventilation is essentially constant but the periods for some of the heavier loads are long, find S_2 from figure 7; determine i/S_2I, and select a rating having a value (S_1) which is at least equal to i/S_2I.

Class 1B: If the ventilation changes between heavy- and light- or no-load periods and the load periods are short (figure 3*a* or 10*B*), find S_3 from formula 7 or figure 9, determine i/S_3I, and select a rating at least equal to i/S_3I.

Class 2B: If the ventilation changes between heavy- and light- or no-load periods and some of the periods for the heavier loads are long, find both S_2 and S_3, determine i/S_2S_3I, and select a rating with S_1 at least equal to i/S_2S_3I.

If the load cycles are distributed rather unevenly in time as in figure 10*C*, it is evident that there will be some fluctuation in the temperature rise even though the individual load cycles are very short. If the periods (P) over which the load cycles are distributed are shorter than the rating time of the device, the use of a service factor of the general order of S_2 will give reasonably correct results. If, on the other hand, the period (P) is rather long as shown in figure 10*D*, it is safer to calculate results under the assumption that the load conditions prevailing during (P) are continuous. The loads in figures 10*A* to 10*D* have all been assumed to have the same value (I) and thus the same nominal current rating. It will be interesting to note the rms values of i/I and S_1 in figure 10 and the time values to be

Atmospheric Variations and Apparatus Flashover

P. H. McAULEY
ASSOCIATE AIEE

I. Introduction

IN practically all electrical apparatus use is made of the insulating properties of air. The electrical breakdown strength of air, for the electrode arrangements found in apparatus, depends upon air temperature, pressure and moisture content. This condition has long been appreciated and recognized in various standards for testing and for determining insulation ratings. However, the range and significance of the extreme conditions encountered, is not always appreciated. It is proposed, therefore, to consider the variations found in actual service and determine how well current standards and application practices cover these variations. In addition, the desirability of uniform application practices and reference ranges for different apparatus is suggested.

Paper 41-35, recommended by the AIEE committee on standards, and presented at the AIEE winter convention, Philadelphia, Pa., January 27–31, 1941. Manuscript submitted September 5, 1940; made available for preprinting December 9, 1940.

P. H. McAuley is laboratory engineer for the Westinghouse Electric and Manufacturing Company, East Pittsburgh, Pa.

1. For all numbered references, see list at end of paper.

II. Current Practice

Wherever test margins are important, test values obtained under various actual weather conditions are corrected to the American standard conditions, which are:

Temperature	77 degrees Fahrenheit
Barometric pressure	29.92 inches of mercury
Humidity	0.6085 inches of mercury

According to most apparatus standards, equipment which meets the specified voltage tests, corrected to these conditions, may be used at any of the temperature and humidity conditions encountered in nature and at any barometric pressure encountered at altitudes up to 3,300 feet. The corrections for different air conditions are in many cases quite large and the actual flashover voltage of a piece of equipment in service may differ by as much as 25 per cent from the value for standard test conditions. The internal insulation of apparatus is not affected by the changing dielectric strength of the ambient air and in some cases the internal insulation may not be applied effectively and economically because of this situation. On the other hand, the internal insulation may be overstressed when conditions of unusually high external flashover prevail. Thus the variations in air conditions also are of some concern to the designer in that equipment insulation must be suitable for the most unfavorable conditions encountered in use.

III. Temperature, Pressure, Humidity

(a). Temperature

Flashover (and sparkover) voltages through air vary inversely with the absolute temperature. Figure 1 shows the variation in per cent for temperature ranges encountered in the U.S.A.

(b). Barometric Pressure

Flashover voltages vary directly with the barometric pressure. In a given location the pressure ordinarily does not vary through more than a five per cent range. However, barometric pressure and the dielectric strength of air do vary with altitude. Figure 2 indicates the relation.

(c). Humidity

Flashover voltages for nonhomogeneous dielectric fields vary with the absolute humidity of the air. The change in these voltages depends upon wave form, polarity, and the kind of apparatus tested. Correction curves, of which figure 3 is typical, must be obtained experimentally.

(d). Relative Air Density

The effect of temperature and of pressure have been combined into a single

---

chosen for the ratings; the latter range from 15 to 60 minutes for the various service conditions.

(b). Auxiliary Devices and Conductors

For all classes of applications discussed under "main devices," safe temperature rises are obtained for the auxiliary devices and conductors if they are rated for the same current value (I) and the same time as the main apparatus, assuming that the method of establishing short-time ratings outlined under class $2A$ is followed. For applications $1A$ and $1B$ with short-load periods which are definitely limited by the type of application, further economies can be safely effected by selecting auxiliary devices and conductors having continuous ratings corresponding to the actual rms values, as discussed under $1A$ and $1B$.

Obviously, all the methods outlined here may have to be modified in extreme or unusual cases which depart from the assumptions and limitations indicated in the paper.

Conclusions

The selection of the most suitable and economical short-time ratings of main devices, auxiliary devices, and conductors, all properly co-ordinated, has been reduced to an extremely simple procedure for many of the intermittent and varying loads found in practice. Uncertainties and uneconomical combinations previously encountered can be eliminated by the co-ordinated practices suggested for rating and application.

References

1. Effect of Load Factor on Operation of Power Transformers by Temperature, **V. M. Montsinger.** AIEE Transactions, volume 59, 1940 (November section), pages 632–6.

2. Temperature Limits for Short-Time Overloads for Oil-Insulated Neutral Grounding Reactors and Transformers, **V. M. Montsinger.** AIEE Transactions, volume 57, 1938 (January section), pages 39–44.

3. A Study of Short-Time Ratings and Their Application to Intermittent Duty Cycles, **R. E. Hellmund** and **P. H. McAuley.** AIEE Transactions, volume 59, 1940, pages 1050–5.

4. Discussion of reference 3, **P. L. Alger.** AIEE Transactions, volume 59, 1940, pages 1221–2.

5. Discussion of reference 3, **T. C. Johnson.** AIEE Transactions, volume 59, 1940, pages 1222-3.

6. Rating of General-Purpose Induction Motors, **P. L. Alger** and **T. C. Johnson.** AIEE Transactions, volume 58, 1939 (September section), pages 445–56.

7. Duty Cycles and Motor Rating, **L. E. Hildebrand.** AIEE Transactions, volume 58, 1939 (September section), pages 478–83.

8. The Application of Class B Insulation to Auxiliary Type D-C Motors in Severe-Duty Service, **F. A. Compton, Jr.** AIEE Transactions, volume 59, 1940, pages 828–34.

9. Report on Standards Conference at 1940 AIEE Summer Convention, Electrical Engineering, volume 59, August 1940, pages 337–8.

10. AIEE Standard No. 1, General Principles Upon Which Temperature Limits Are Based in the Rating of Electrical Machinery and Apparatus, June 1, 1940.

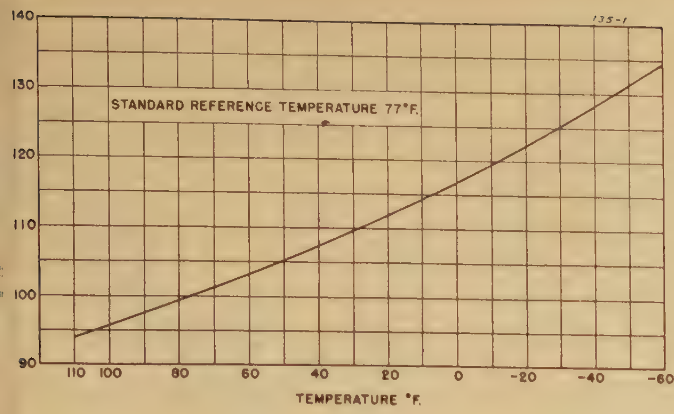

Figure 1. Flashover voltages vary through a range of over 30 per cent due to temperature changes of ambient air

actor, known as relative air density, vhich is unity for the standard conditions of temperature and pressure. For other conditions the relative air density is

$$\frac{17.95\times\text{bar. press. (inches)}}{460+\text{temp. degrees Fahrenheit}}$$

Flashover voltages actually vary at a ate less than the relative air density, out for practical purposes, the slightly oessimistic assumption that they follow he relative air density directly is satisfactory.[1]

(e). Magnitude of Changes

It is seen that temperature alone may oroduce a change in flashover voltage of 30 per cent. An elevation of 3,300 feet educes flashover voltage 11 per cent, neglecting daily variations. Annual variations in humidity cause a change in lashover through a 20 per cent range. These effects, therefore are important and heir combined results are of interest.

V. Service Conditions

(a). Temperature

Temperatures in the continental U. S. vary from 120 degrees Fahrenheit to −50 degrees Fahrenheit. In terms of the variation from 100 per cent flashover at 77 degrees Fahrenheit, these correspond o −8 per cent and +31 per cent change. Maximum and minimum temperatures or some typical cities, where high voltage apparatus may be used, are given in able I.

(b). Barometric Pressure

An altitude map of the U.S.A. is shown n figure 4. Maximum and minimum ltitudes by states are given in table II. t follows that a considerable part of the vestern states is above the 3,300-foot evel to which standard apparatus is applicable. From table I also, the elevaions of the cities listed range up to 7,000 eet. Consequently, a good deal of equipnent is installed at altitudes above the tandard range of 3,300 feet.

(c). Humidity

In general, the absolute humidity is lowest at low temperatures, where the air becomes saturated at very low moisture contents. For locations near large bodies of water high temperatures and high humidities tend to coincide and these two factors tend to cancel in their effect on flashover. However, table I indicates

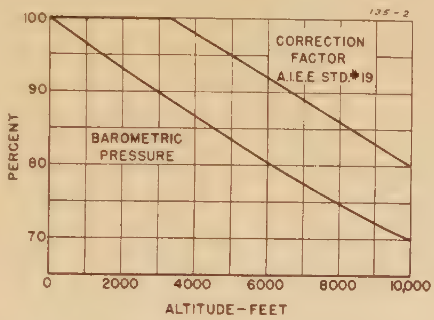

Figure 2. Flashover voltages vary directly with the barometric pressure which is 70 per cent of mean sea level pressure at 10,000 feet altitude

that, for the high inland locations, absolute humidities are quite low, even at times of maximum temperature, at Denver, for example.

(d). Combined Effects

The change in flashover voltages for these extreme conditions in certain cities has been calculated and is shown in table III. The range of the variations likely to be encountered in extreme cases is around 27 per cent. Attention is called, however, to Great Falls, Montana, which is just below the 3,300-foot altitude limit. At this location, standard apparatus would at times suffer a reduction in flashover strength of practically 25 per cent. It should be pointed out that variations in barometric pressure and in humidity from the values assumed or recorded might influence the figures given another two or three per cent in either direction.

V. Rain, Fog, Dirt, Salt Spray

In addition to encountering a reduction in the dielectric strength of air, electrical insulating surfaces, such as porcelain bushings and insulators, frequently are subjected to rain, fog, and foreign deposits. A heavy rain will reduce the flashover voltage of a new clean insulator 30 per cent. Fog or rain on a dirty insulator may reduce the effectiveness of the insulator to the point where operation at rated voltage is impaired. In such cases special types of insulation may be applied or periodic cleaning may be found necessary. Wanger[2] and others have presented quantitative data on this subject, which is outside the scope of this paper.

VI. Apparatus

For a practical illustration of apparatus application, bushings will be considered. The basic insulation levels, based on an impulse voltage-withstand test, for different voltage classes have been suggested for standardization.[3] These levels are shown in figure 5, with the reduced corresponding values for altitudes of 5,000 and 10,000 feet. For the higher voltage classes, the next higher voltage class applies quite well for steps in elevation of the order of 3,000 to 5,000 feet. From 15 to 69 kv the insulation steps do not lend themselves as readily to this practice. Naturally, in any practical application compromises must be made between maintenance of insulation levels and subjecting internal insulation of apparatus to excessive voltages. To avoid an excessive number of designs, it probably is

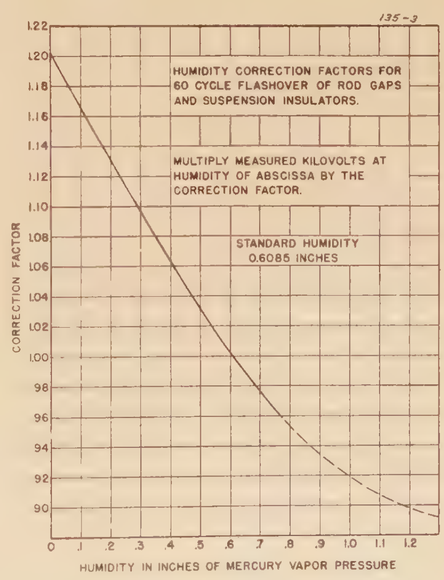

Figure 3. Flashover voltages vary with absolute humidity. The annual range is over 20 per cent for locations at moderate altitudes

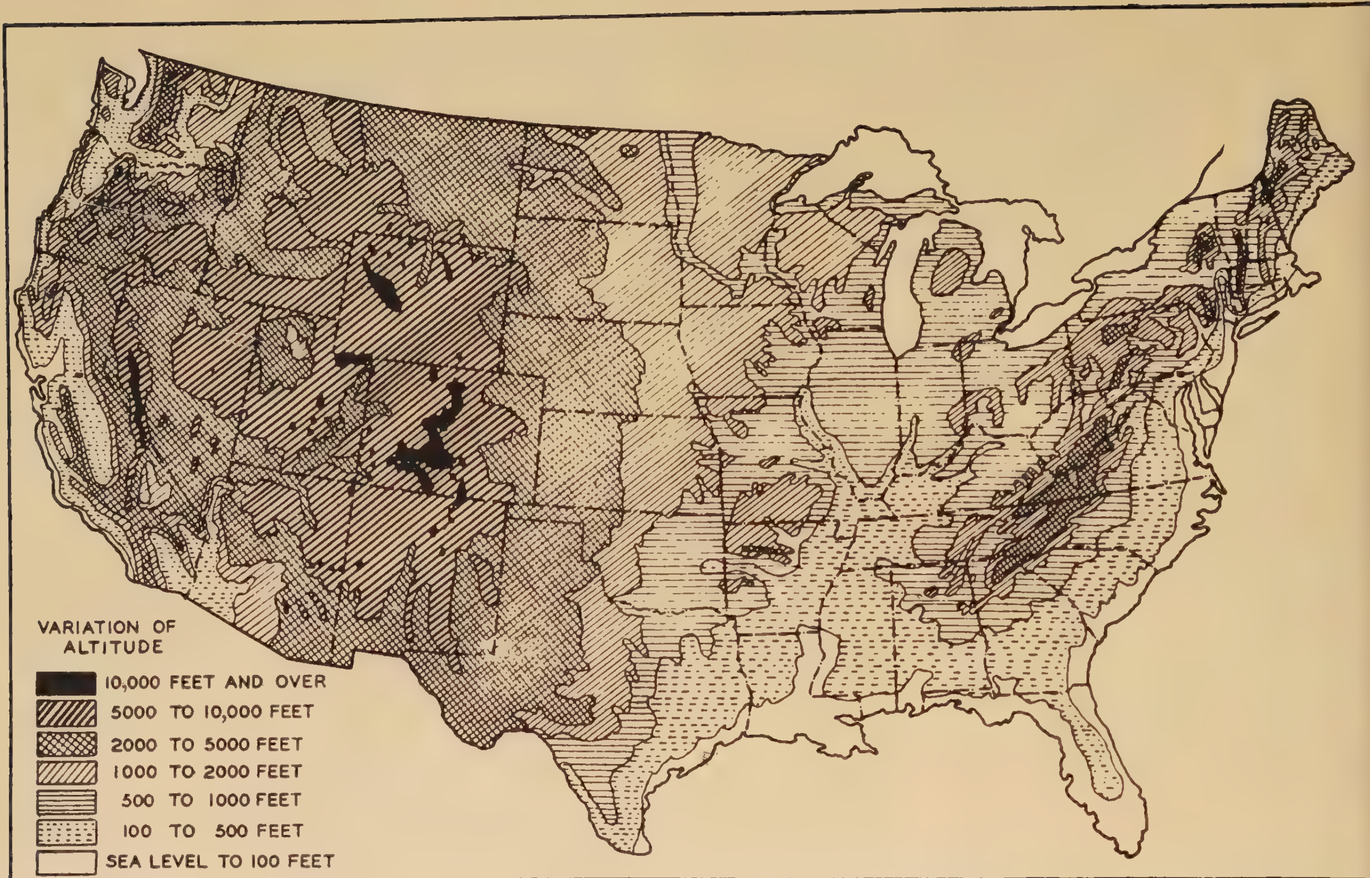

Figure 4. The mean elevation of the United States, including Alaska, is 2,500 feet. About 8.3 per cent of the earth's land lies above 6,000 feet and about 2.5 per cent is above 12,000 feet elevation

most economical to use the next largest bushing with a gap to reduce its flashover at the altitude in question to the basic insulation level of the apparatus. The variations due to temperature and humidity cannot be controlled. Hence, excessive approximations in apparatus application for a given altitude are to be avoided.

Figure 6 shows the effect of altitude on the flashover of 34.5- and 115-kv bushings. The relative flashovers of the next higher voltage steps in 3,300-foot ranges also are indicated. For the 115-kv case, the maximum spread from the basic level using the next higher class of standard bushings is seven per cent. This is likely to be further decreased in practice on account of the lower humidities encountered at higher altitudes. In general, the relative flashover levels lead to a fortunate situation. This is not the case for the 34.5-kv class. The spread between the 46- and 69-kv classes is too great for application in the simple manner found above. For this reason, it has been the practice to use "high-altitude" bushings of appropriate flashover in this range.

VII. Testing Margins

Since apparatus is now tested on a withstand voltage basis, all equipment has a small margin over the basic levels to avoid troubles in acceptance tests. These margins, of course, raise the actual flashover range in terms of voltage. However, although the mean flashover is thereby raised, the width of the band due to atmospheric variations remains the same. The net result is that the internal insulation may be worked a little harder in actual service.

VIII. Upper Air Investigations

A subject of increasing interest is the weather conditions at high altitudes above the ground. Figure 7 gives some early data[7] on this point. Temperature pressure and humidity decrease with altitude, of course. However, the very rapid decrease in absolute humidity and the low moisture content at an altitude of 20,000 feet even with a high value at sea level are very striking.

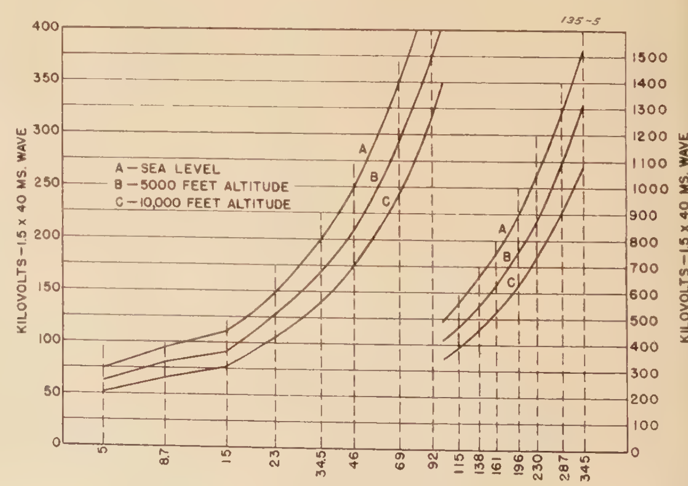

Figure 5. The impulse-withstand voltage ratings of bushings are affected as shown at the 5,000- and 10,000-foot levels

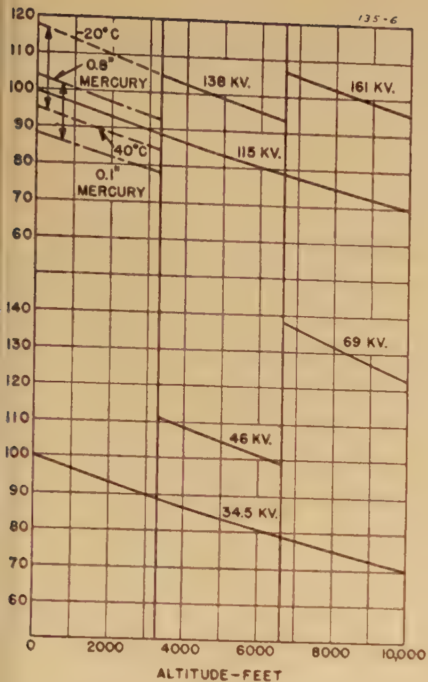

igure 6. The relation of adjacent voltage asses of apparatus permits applying the next igher classes for different altitude ranges in the igher voltage cases and not in the lower operating voltage classes

‹. Apparatus Standards

As already stated, apparatus standards ermit apparatus of standard voltage ratg for elevations up to 3,300 feet. AIEE andard No. 19 for oil circuit breakers ates, "for application at altitudes eater than 3,300 feet, it is recommended at the standard voltage rating of the

Figure 7. Upper air investigations give the variations in weather conditions with altitude. Conditions change of course, with geographical location and with the seasons and time of day

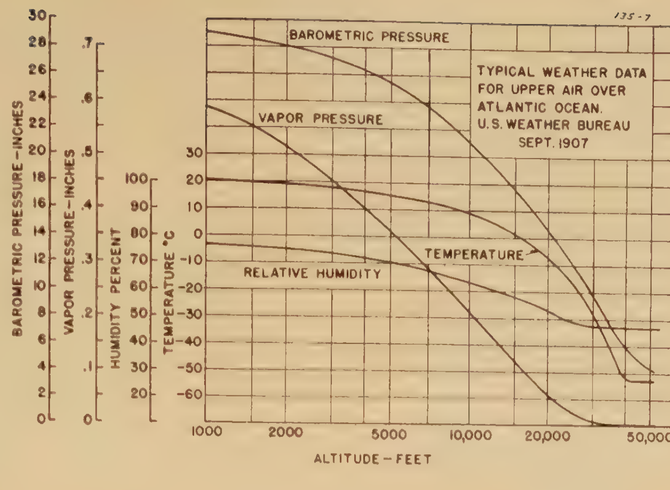

apparatus should be multiplied by the following factors to obtain the modified voltage rating."

Altitude in Feet	Correction Factor
3,300	1.00
4,000	0.98
5,000	0.95
10,000	0.80

These recommended corrections are shown in figure 2 and their actual relation to the decreasing barometric pressure can be seen. There are a few exceptions to the 3,300-foot standard range, based on thermal rather than flashover limitations. Railway motors, AIEE Standard No. 11, may be used through a range up to 4,000 feet. NEMA Industrial Control Standard gives a range of 6,000 feet and a derating factor for the 6,000–15,000-foot range. These are practical figures based on much experience which help to simplify application problems. However, the adoption of a multitude of ranges as a result of selecting the optimum for each type of apparatus is not to be recommended.

X. Conclusions

1. Temperature changes of the ambient air in the U.S.A. change the flashover voltage of apparatus through a range of 39 per cent.

2. An elevation of 10,000 feet reduces flashover voltages 30 per cent from those at sea level.

3. Variations in absolute humidity result in changes in flashover voltage of nearly 20 per cent.

4. In any one location the combined ef-

Table I. Unusual Air Conditions for Certain Cities of the U.S.A.

Place	Elevation, Feet	Highest–Lowest Temperatures Ever Recorded, Degrees Fahrenheit		Highest Wet Bulb at Noon During July and August for a Six-Year Period			Highest Dry Bulb at Noon During July and August for a Six-Year Period			Mean Relative Humidity at Noon in July
				Dry	Wet	Vapor Pressure*	Dry	Wet	Vapor Pressure*	
›uquerque, N. M.	4,930	104	−10							
ıarillo, Tex.	3,676			88	74	0.689	100	70	0.402	
smarck, N. D.	1,690			90	76	0.747	111	70	0.278	46
ise, Idaho	2,705	121	−28	93	72	0.55	104	65	0.184	26
tte, Mont.	5,485	100	−52							
eyenne, Wyo.	6,088	100	−38							40
nver, Col.	5,292	105	−29	92	65	0.319	98	61	0.126	35
Paso, Tex.	3,778	106	− 5	96	70	0.447	99	67	0.307	33
ıgstaff, Ariz.	6,935	99	−25							
and Forks, N. D.	830	108	−43							
eat Falls, Mont.	3,200	107	−49							
‹ksonville, Fla.	100	104	10	98	82	0.921	98	82	0.921	63
nsas City, Mo.	730	111	−22	98	80	0.829	108	74	0.463	51
not, N. D.	1,557	109	−49							
oenix, Ariz.	1,075	118	16							30
eblo, Col.	4,665	104	−27							33
no, Nev.	4,500	106	−19	94	66	0.330	99	65	0.240	18
t Lake City, Utah	4,360	105	−20	97	69	0.399	99	63	0.176	29
ux Falls, S. D.	1,425	110	−42							
ıte Fe, N. M.	7,013									
ma, Ariz.	141	120	22							27

mperatures from "Air Conditioning Engineer's Atlas," The Industrial Press, New York.

apor pressures correspond to temperatures shown for 30-inch barometric pressure.

Table II. Highest and Lowest Altitudes in the United States

(From the United States Geological Survey)

State or Territory	Highest Altitude, Feet	Lowest Altitude, Feet
Alabama	2,407	Sea level
Alaska	20,500	Sea level
Arizona	12,611	100
Arkansas	2,800	55
California	14,501	276 (below sea)
Colorado	14,402	3,350
Connecticut	2,355	Sea level
Delaware	440	Sea level
District of Columbia	420	Sea level
Florida	301	Sea level
Georgia	4,768	Sea level
Idaho	12,078	720
Illinois	1,241	279
Indiana	1,210	316
Iowa	1,800	477
Kansas	4,135	700
Kentucky	4,100	257
Louisiana	400	Sea level
Maine	5,273	Sea level
Maryland	3,340	Sea level
Massachusetts	3,505	Sea level
Michigan	2,023	573
Minnesota	1,920	602
Mississippi	600	Sea level
Missouri	1,750	210
Montana	12,850	1,800
Nebraska	5,350	825
Nevada	13,058	470
New Hampshire	6,293	Sea level
New Jersey	1,809	Sea level
New Mexico	13,306	2,876
New York	5,344	Sea level
North Carolina	6,711	Sea level
North Dakota	3,500	790
Ohio	1,550	425
Oklahoma	4,750	300
Oregon	11,225	Sea level
Pennsylvania	3,136	Sea level
Rhode Island	805	Sea level
South Carolina	3,548	Sea level
South Dakota	7,242	962
Tennessee	6,636	182
Texas	9,020	Sea level
Utah	13,498	2,000
Vermont	4,364	95
Virginia	5,719	Sea level
Washington	14,408	Sea level
West Virginia	4,860	240
Wisconsin	1,940	582
Wyoming	13,785	3,100

fects of these variables is not likely to exceed a 25 per cent range.

5. Standard apparatus applied at different locations in the range of elevations up to 3,300 feet will vary in flashover over a possible range of 35 per cent.

6. For many applications standard apparatus of the next higher voltage class fits the mean flashover range of the location.

7. For other cases it is necessary to use special apparatus or to gap equipment of excessively high rating to meet the average flashover requirements for the conditions encountered at a given location.

8. The desire to maintain flashover values and to avoid overstressing internal insulation prescribes permitting wide departures from basic insulation levels due to conditions of application.

9. This survey would seem to show greater variations in flashover voltages due to changing weather conditions in service than is generally realized. Although the situation is not to be regarded as alarming, it is well to keep it in mind. A full appreciation of the facts in a particular case should lead to a more effective application of apparatus to meet the conditions. On the other hand, certain applications which may have proved unsatisfactory might be explained by these simple natural phenomena. In addition, standardizing groups often find it necessary to consider information of this nature in formulating and revising standards.

References

1. Effect of Altitude on the Sparkover Voltages of Bushings, Leads, and Insulators, F. W. Peek, Jr. AIEE Transactions, volume 33, 1914, page 923.

2. La Tension de Contournement, Sous Ondes de Choc de Differentes Durees, des Isolateurs Salis et Sous Pluie, W. Wanger. CIGRE, Paris, 1939.

3. Proposed Standards for Outdoor Bushings, AIEE Transactions, volume 59, 1940 (October section), pages 590–1.

4. Temperature Survey of the United States, J. J. Smith and H. W. Tenney. AIEE Transactions, volume 59, 1940, pages 769–75.

5. Recommendations for High-Voltage Testing, AIEE Transactions, volume 59, 1940 (October section), pages 598–602.

6. Reference Values for Temperature, Pressure, and Humidity, P. L. Bellaschi and P. H. McAuley. AIEE Transactions, volume 59, 1940 (December section), pages 669–75.

7. The Elements of Hydrology, a book, Adolph F. Meyer. John Wiley and Sons, Inc.

Appendix

Altitude Corrections

The effect of altitude on apparatus rating is given in at least four different forms in the AIEE and ASA standards. Altitude affects voltage rating (flashover through air), cooling (air density) and losses (windage). More uniformity of terminology and method of specification appears possible and desirable.

In Standard No. 19 correction factors for voltage rating are given in the form of a table as given in section IX of this paper. The table values correspond exactly to one per cent reduction for each 330 feet above 3,300-feet altitude. In the same standard the correction for temperature rise is given as 0.4 per cent reduction for each 330 feet above 3,300 feet at which the actual installation is to take place.

In ASA Standard *C*-50 for rotating electrical machinery, the probable decrease in

Table III. Effect of Extreme Air Conditions on Flashover Corrections

Location	Boston, Mass.	Bismarck, N. Dak.	Great Falls, Mont.	Denver, Colo.	Cheyenne, Wyo.
Elevation—feet	Sea level	1,690	3,200	5,292	6,088
Barometer—inches	29.92	28.2	26.6	24.6	24.0
Highest temperature recorded	104		107	105	100
Corresponding relative air density	0.952	0.886	0.843	0.782	0.769
Highest dry bulb*	96	111		98	
Corresponding wet bulb	75	70		61	
Corresponding absolute humidity	0.64	0.278	0.2**	0.2	0.2**
Humidity correction	0.993	1.081	1.101	1.101	1.101
Flashover reduced to	0.958	0.819	0.765	0.710	0.698
Altitude rating standards number 19	100	100	100	94	91.6
Lowest temp. recorded	−18	−45**	−49	−29	−38
Corresponding relative air density	1.216	1.22	1.162	1.025	1.021
Humidity correction	1.12**	1.12**	1.12**	1.12**	1.12**
Flashover reduced to	1.085	1.089	1.038	0.915	0.912
Range in per cent	12.7	27.0	27.3	20.5	21.4

*At noon during July and August in a six-year period.

**Estimated.

Volt-Time Areas of Impulse Spark-Over

J. H. HAGENGUTH
ASSOCIATE AIEE

ynopsis: On the basis of classification of npulse wave shape, the paper shows that npulse spark-over characteristics of elecodes with nonuniform fields cannot be presented by single volt-time curves but ust be represented by volt-time areas of onsiderable extent. This classification exains the large difference obtained by arious laboratories when investigating parkover between one and five microconds. The effect of impulse generator ischarge circuits in producing these differences is explained. The necessity of inılation co-ordination on the basis of voltme areas is pointed out.

ntroduction

EVER since it was definitely established that lightning strokes conribute the greatest amount of insulator ashovers on transmission lines as well as amage to important equipment such as ransformers and circuit breakers, the roblem of insulation co-ordination on ne basis of impulse sparkover has beome of great concern to the operating ngineer, not only as a means of eliminatıg damage, but also of preventing flashvers causing system outages. Many apers[1] have been written on the large roblem of co-ordination.

Co-ordination has been defined in arious ways. One of the more recent efinitions[2] is as follows:

Insulation co-ordination may be defined as ıe process of setting standards of insulation rength and assigning them to all the items equipment in the various insulation classes in such a manner as to produce, from an economic and operating standpoint, both a maximum of protection, and, if failure results, a minimum damage to the system."

From this definition it is apparent that the impulse strength of all types of apparatus comprising a transmission system has to be known, within fairly accurate limits, before co-ordination can be applied effectively. Consequent studies of the impulse flashover characteristics of suspension insulators, apparatus insulators, bushings as well as transformer insulation revealed that the impulse flashover in air, oil, or breakdown of solid insulation is not a constant value, but varies with time. Therefore, impulse strength of a given electrode arrangement and dielectric can be represented by a volt-time curve which correlates the spark-over voltage with the time at which the insulator will spark over.

Present Concept of Impulse Spark-Over Characteristics

In figure 1 a series of such volt-time curves are shown for different types of electrodes. The curves are plotted as overvoltage-time curves to show the relative increase of spark-over voltage as affected by the electrode arrangement. Overvoltage is the actual spark-over voltage expressed in per cent of the critical* spark-over voltage of the apparatus.

It is evident from a study of these curves that co-ordination on the basis of the critical spark-over voltage of different types of apparatus only cannot be effective, but that co-ordination must be based on the volt-time impulse characteristics of the apparatus. While the various laboratories in the United States of America conducting high-voltage research did agree within fairly close limits on the critical spark-over voltages of rod gaps and insulators,[3] considerable differences in results were obtained for volt-time spark-over curves.[4,5] For instance, the differences in measured spark-over voltages for rod gaps were found to be as great as 20 to 40 per cent at times to sparkover of two microseconds and less. These large differences were at first attributed to measuring methods such as the type of divider—resistance divider, shielded and unshielded, and capacitance divider—as well as insufficient precaution in the oscillograph technique. However, it was soon discovered that the shape of the applied impulse wave before sparkover occurs has a distinct bearing on the spark-over voltage of different types of apparatus.[6] The effect of wave shape,

Paper 41-75, recommended by the AIEE committee on instruments and measurements, and presented at the AIEE winter convention, Philadelphia, Pa., January 27–31, 1941. Manuscript submitted November 27, 1940; made available for preprinting December 26, 1940.

J. H. Hagenguth is an electrical engineer for General Electric Company, Pittsfield, Mass.

The author wishes to acknowledge the assistance of A. F. Rohlfs in the preparation of the paper and of G. G. Poulsen and J. W. Albright in obtaining the test data.

1. For all numbered references, see list at end of paper.

*The critical spark-over voltage of a test specimen under an impulse of any given wave shape and polarity is the crest value of that impulse when its amplitude is adjusted to cause flashover on 50 per cent of the applications.

---

nbient temperature at higher altitudes is ecognized and applications at normal rating pproved if the operating conditions are ithin the limits given in the following table.

Altitude In Feet	Altitude In Meters	Maximum Temperature of the Cooling Air in Degrees Centigrade
0– 3,300	0–1,000	40
3,300– 6,600	1,000–2,000	35
6,600– 9,900	2,000–3,000	30
9,900–13,200	3,000–4,000	25

ı this case the percentage change varies ith the different values of temperature se since corrections are given in degrees temperature.

In standard *C*-50 also, a correction of one per cent per 330 feet above 3,300 feet is specified for temperature-rise tests at low altitude on apparatus destined for use at altitudes above 3,300 feet.

ASA standard *C*-57 for transformers, regulators, and reactors gives corrections for temperature rise in per cent per 330 feet above 3,300 feet. Rates from 0.4 to 1 per cent are given depending on whether cooling is largely by radiation or conduction.

AIEE Standard No. 4 for voltage measurement gives a correction for spark-over voltages in air which includes both temperature and pressure (altitude) factors. Measured voltage values are divided by the relative air density to correct to standard conditions.

$$\text{relative air density} = \frac{0.392B}{273+T}$$

where

T = temperature degrees centigrade
B = pressure in millimeters of mercury

ASA standard *C*-50 gives a correction formula for windage losses for different temperature and pressure (altitude) conditions. The losses measured at a given temperature and pressure are multiplied by the factor $690\ \frac{(1+0.004T)}{B}$, in which T = temperature degrees centigrade and B = pressure in millimeters of mercury. Both this and the relative air density formula are unity at 25-degrees-centigrade and 760-millimeter pressure and one is the reciprocal of the other for practical purposes.

The International Electrotechnical Commission proposed specification for a-c circuit breakers (May 1938) states that the limits of temperature rise shall be reduced one per cent for each 300 meters (990 feet) above sea level at which the breaker is intended to work in service. The correction is not applied below 1,000 meters. In this case both the rate and the starting point of the correction are different from American Standards.

however, could not be classified, and, therefore, useful engineering data could not be supplied. Owing to the differences obtained by various laboratories, the volt-time curves were assigned plus and minus corrections of arbitrary value to account for what was thought to be erratic spark-over characteristic of certain types of apparatus.

New Concept of Impulse Spark-Over Characteristics

It will be left to the physicist to translate the following data into electrons, ions, and terms of photo-ionization. This paper will attempt to present the data in terms which the engineer interested in co-ordination and, therefore, in impulse spark-over characteristics of different kinds of apparatus, can use to apply to his problems.

The effect of wave shape is well illustrated by figure 2 which shows a series of volt-time curves and spark-over points for a 20-inch rod gap at negative polarity. Each of these curves was obtained with a constant impulse generator discharge circuit. For the lower curve the impulse wave had a front of 0.5 microseconds, for the middle curve a front of 2.4 microseconds and for the upper curve, 9.6 microseconds at the critical spark-over potential. It can be seen that the spark-over voltages associated with a given time to sparkover vary greatly with the shape of the wave front. For instance, at two microseconds the spark-over voltages for the two extreme wave fronts used are 495 kv and 625 kv respectively with a difference of 25 per cent. If, at the same time to sparkover, widely differing voltage values are obtained, gap spark-over has to be classified as either very erratic or the difference must be due to some physical characteristics of the spark-over phenomenon. If spark-over voltages at two microseconds of 495 kv and 625 kv of a 20-inch rod gap had been obtained in isolated tests and not in the course of obtaining volt-time curves, the spark-over characteristic of the gap would indeed appear erratic.

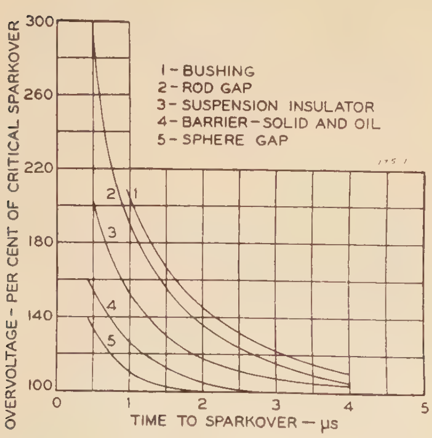

Figure 1. Comparison of overvoltage characteristics of different types of gaps

Negative polarity

Figure 2. Effect of wave front on spark-over volt-time curves for a 20-inch rod gap

Negative polarity. Vapor pressure 0.26 inch mercury; air density 0.983

Impulse circuit adjusted for: 1—9.6-microsecond wave front, 2—2.4-microsecond wave front, 3—0.5-microsecond wave front

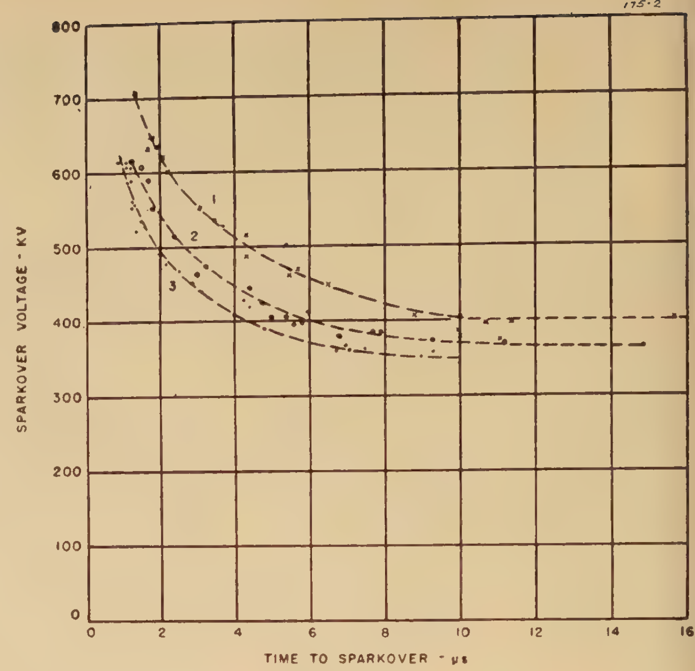

However, since the results shown in figure 2 were obtained with impulse waves of different shapes, it is logical to attribute the difference to wave shape. Since the front of the wave definitely appears to have considerable influence on the variations in spark-over voltage, but, on the other hand, the front of the wave does not stay constant when sparkover occurs between two and ten microseconds, it was decided that the effective front might be used to derive a practical answer for classification of impulse wave shape. The effective front is specified by the slope of the line through the $0.3E$ and $0.9E$ points on the front, where E is the crest of the measured wave. The effective front in microseconds T_1 is the time between the $0.3E$ and $0.9E$ points multiplied by 1.66. For the tests with the slow front, this definition of effective front did not permit sufficient differentiation. Since slow fronts in all cases were of the exponential form, the initial rate of rise was used as the effective front. The time to sparkover T_2 in microseconds is the time from virtual zero time to a point on the wave where voltage is rapidly decreasing toward zero. Virtual zero time is defined as the intersection of the line through the $0.3E$ and $0.9E$ points with the zero line.

The same test points as shown in figure 2 were then replotted as function of kilovolt spark-over and the ratio of T_1/T_2 = (effective front)/(time to sparkover) with time to sparkover T_2 as parameter. Such a plot shows a scattering of points, indicating the trend of lower spark-over voltage for small ratios of T_1/T_2 and higher spark-over voltages for large ratios of T_1/T_2 for equal times to sparkover. In figure 3 the test points were plotted to show the range over which data have been obtained, but the time to

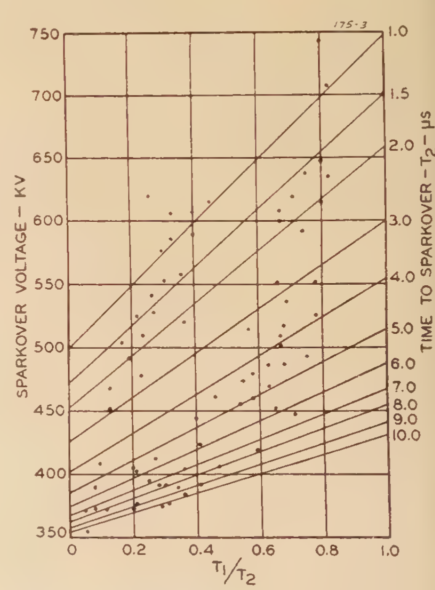

Figure 3. Effect of wave shape on spark-ove voltage of 20-inch rod gap

Negative polarity. Vapor pressure 0.26 inc mercury; air density 0.983

T_1 = effective wave front; T_2 = time to spark-over

Test points indicate range investigated

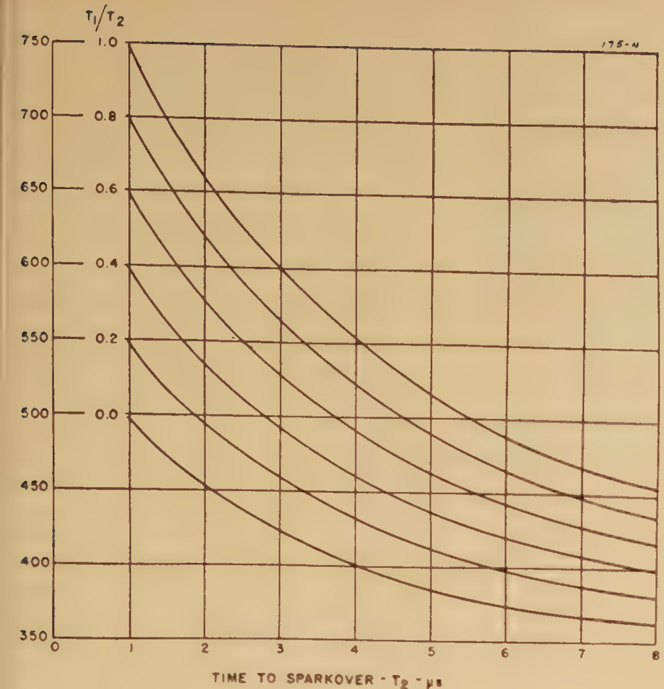

gure 4. Spark-over volt-time area of 20-inch rod gap

oundaries are $T_1/T_2=0$ and $T_1/T_2=1$. egative polarity. Vapor pressure 0.26 inch mercury; air density 0.983

$=$effective wave front; $T_2=$time to spark-over

arkover associated with each test point as omitted for reasons of reproduction. he network of straight lines, indicating ark-over voltage trends for a given time sparkover, has been placed such that most nearly represents the correct in-rpretation of the test results.

The lower limit $T_1/T_2=0$ and the upper nit $T_1/T_2=1$ have not been reached iring these tests. The lower limit, of urse, represents a wave with abrupt sing front and practically rectangular il, while the upper limit represents a ont rising in a straight line from the ro point to the spark-over point. Both these limits are difficult to obtain in actical impulse testing. However, the ror in extending the straight lines to th of these limits beyond the available st points should not result in appreci-le errors.

To reduce the results to the customary rm of the volt-time curves, the straight ies of figure 3 have been used to draw e curves of figure 4, where spark-over ltage in kilovolts is plotted as function time to sparkover with the ratio T_1/T_2 parameter.

This figure shows clearly that spark-er of a rod gap for instance cannot be presented by a single "volt-time curve" t rather by a "volt-time area." This lt-time area, in contrast to previous attempts of using correcting factors in connection with volt-time curves, is well defined by recognition of the influence of impulse wave shape on spark-over voltage. It will be shown that the use of the wave shape definition adopted gives results within a few per cent of expected spark-over voltages. Therefore, the use of volt-time areas will eliminate to a large extent the uncertainty heretofore associated with short-time sparkover of insulators, bushings, rod gaps, and other apparatus. It is important to note that this spark-over area, of course, is subject to the variations in spark-over voltage due to humidity and air density. The correct method of correcting for humidity throughout this spark-over area is not known. If the method at present used for volt-time curves is adopted[7] it means that at short times to sparkover the spark-over values will remain practically the same while at the longer times the spark-over voltages will be raised, so that the individual volt-time curves for different $T_1/T_2=$constant will have a reduced slope at the longer times to sparkover, and the total spark-over area will be reduced when based on standard conditions of humidity. The air density correction probably will be the same regardless of wave shape.

It has been shown that the impulse spark-over voltage (e) of an electrode arrangement producing a nonuniform field, such as the rod gap, is a function not only of the time at which sparkover occurs, but also of wave shape represented by the ratio of T_1/T_2. Therefore $e=f(T_2, T_1/T_2)$. The physical condition for this dependence of spark-over voltage on wave shape is primarily the fact that corona currents of considerable amplitude have to flow through the dielectric to obtain sufficient ionization before sparkover can be completed.[8] The amplitude of these corona currents in turn depends on the voltage applied to the gap and the length of time voltage has been applied to the electrodes. Obviously wave shape cannot accurately be described by a ratio of T_1/T_2, especially for waves with unusual shapes, but in the range below six microseconds the results obtained indicate a sufficient consistency to justify the use of this approximation until more exact methods are available.

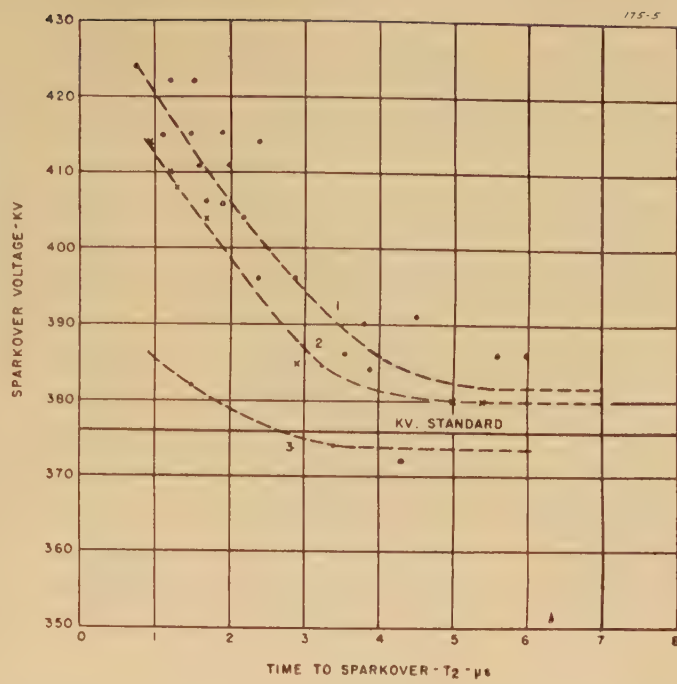

Figure 5. Spark-over volt-time curves of 50-centimeter spheres spaced 15.5 centimeters

Negative polarity. Air density 1

Impulse circuit adjusted for: 1—9.6-microsecond wave front, 2—2.4-microsecond wave front, 3—0.5-microsecond wave front

Volt-Time Areas of Different Types of Electrodes

The Quasi-Uniform Field

From the foregoing discussion it should be expected that spark-over voltage of electrode arrangements producing a uniform field should be represented by straight lines parallel to the zero axis (each spacing between electrodes represented by one line) and without the tendency of spark-over areas because heavy corona currents are not required to initiate sparkover. The closest approximation to the uniform field available for testing at higher voltages is the sphere gap at spacings small with respect to the diame-

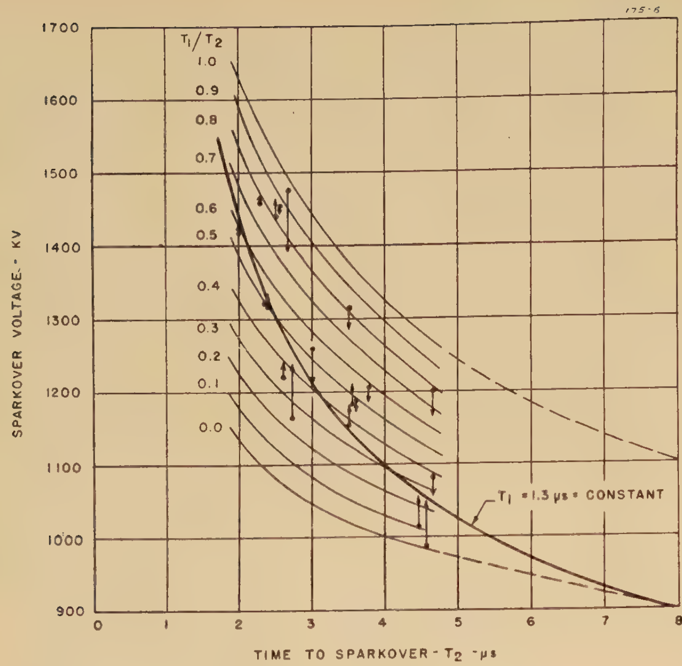

Figure 6. Spark-over volt-time area of 50-inch rod gap

Boundaries are $T_1/T_2 = 0$ and $T_1/T_2 = 1$. Negative polarity. Standard conditions of humidity and air density

T_1 = effective wave front; T_2 = time to spark-over

Points indicate measured values. Arrows point to correct location of test point based on T_1/T_2

T_1 = 1.3-microsecond curve from tests with 1.5x40 wave

ter of the sphere. The same types of waves used for the rod gap were applied to a 50-centimeter sphere gap spaced 15.5 centimeters. This spacing was chosen because it required a spark-over voltage approximately equal to the critical spark-over of the 20-inch rod gap.

The results of these tests are shown in figure 5. This figure shows in a greatly enlarged scale the test points and the probable volt-time curves for the three test conditions as outlined for the 20-inch rod gap. Only two test points were obtained for the short front-long tail wave. The differences between the two slow front waves are insignificant. At one microsecond the difference between minimum and maximum measured voltages is only nine per cent. Since the probable measuring error is of the order of three per cent, it can be said that the volt-time area of a sphere gap, representing a nearly uniform field is extremely small as compared to that of a rod gap at times to sparkover of one microsecond and greater. The data do not permit drawing of T_1/T_2 = constant curves as shown for the 20-inch rod gap in figure 4.

The Nonuniform Field

In addition to the 20-inch rod gap at negative polarity, volt-time areas have been obtained for the 50-inch rod gap at negative polarity, figure 6, and the 20-inch rod gap at positive polarity, figure 7. In the latter two figures the test points have been superimposed on the plot of the T_1/T_2 = constant curves as follows: The spark-over potentials in kilovolts as function of time to sparkover are represented by the solid points. From these test points an arrow is drawn to the expected location of the point according to the ratio T_1/T_2 of the wave. It is apparent that the test points check the expected values very closely. In figure 6 is also shown a conventional volt-time curve for the 50-inch rod gap taken with a 1.5x40 wave. It is evident that such a curve cannot represent the spark-over characteristics of the rod gap. Data of figure 6 and figure 7 have been corrected to standard conditions of humidity and air density according to accepted methods.[7]

Further tests have been made on a string of three suspension insulators (figure 8), a stack of two apparatus insulators (figure 9), and a bushing (figure 10). Only the T_1/T_2 = constant curves for these different insulating elements have been plotted to indicate the slope of the curves and the extent of the volt-time areas for comparison with the other electrode arrangements investigated.

A comparison of the volt-time characteristics of the electrode arrangements of approximately equal critical spark-over voltages shows that the slope of the T_1/T_2 = constant curves is steepest for the bushing, rod gap, line and apparatus insulators in the order named, while the extent of the spark-over areas is greatest for the rod gap, line insulators, bushing and pedestal insulators in the order named. This sequence corresponds well to the trend indicated by the single volt-time curves of figure 1. The electrode arrangement with the least overvoltage—the sphere gap—has the smallest volt-time area, while the higher overvoltages at a given time to sparkover of the single volt-time curve are indicative of larger volt-time areas.

The effect of wave shape on breakdown characteristics of barriers (representing major insulation of oil-filled transformers)—represented by overvoltage-time curve 4, figure 1—has not been investigated. Judging from this volt-time characteristic, the volt-time breakdown area of such a barrier should be intermediate between the spark-over areas of the sphere

Figure 7. Spark-over volt-time area of 20-inch rod gap

Boundaries are $T_1/T_2 = 0$ and $T_1/T_2 = 1$. Positive polarity. Standard conditions of humidity and air density

T_1 = effective wave front; T_2 = time to spark-over

Points indicate measured values. Arrows point to correct location of test point based on T_1/T_2

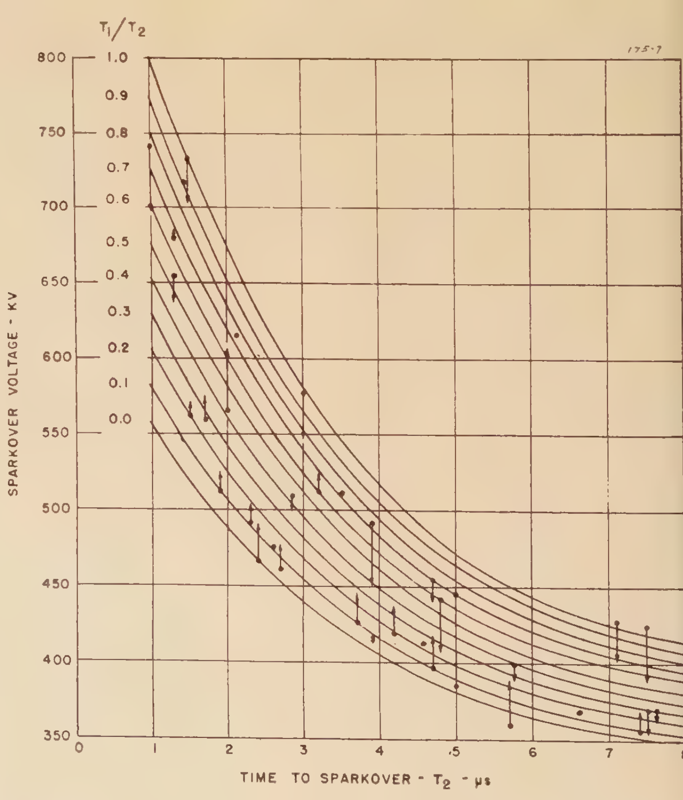

ap and the line insulators, depending reatly on the type of electrodes and the eld between them. Further tests are eeded to obtain data comparable to those epresented in the paper for air dielectrics.

It has been customary[9,10] to represent od gap spark-over voltages as function f rod gap spacing with the time to spark-ver as parameter; similarly, insulator parkover is represented as function of umber of insulators or string arc-over istance. Such curves were based on ingle volt-time curves taken at various pacings using a standard 1.5x40 wave. On the basis of spark-over volt-time areas, uch curves should be drawn for each T_1/T_2=constant curve, or, since the miting conditions are of greatest impor-ance, for the two conditions $T_1/T_2=0$ nd $T_1/T_2=1$.

The results of the tests presented here ermit the plot of such curves for the rod ap between 20-inch and 50-inch spacing t negative polarity (figure 11). To con-erve space, curves for the two extremes ave been plotted on the same figure and, o avoid overlapping of the extreme anges, the curves shown range only be-ween two microseconds and four micro-econds to sparkover. In addition, typi-al curves as obtained with the 1.5x40 vave are included.

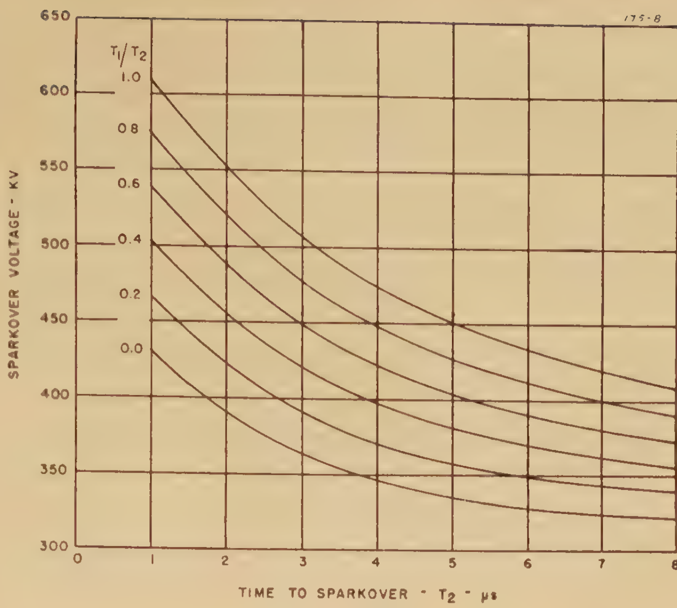

Figure 8. Spark-over volt-time area of a three-unit string of suspension insulators

Boundaries are $T_1/T_2=0$ and $T_1/T_2=1$. Negative polarity. Vapor pressure 0.26 inch mercury; air density 0.983

T_1 = effective wave front; T_2 = time to spark-over

Effect of Impulse Generator Circuits on Spark-Over Voltage

It is interesting to note that the solid wo-microsecond curve as obtained from ests with a 1.5x40 wave (figure 11) is a urve rather than a straight line. This neans, of course, that the wave shape at wo microseconds to sparkover of the 20-nch rod gap was different from the wave hape during tests on the 50-inch rod gap, lthough the wave shape at the longer imes to sparkover was practically the ame in both tests as indicated by the traight lines for three microseconds and our microseconds.

This difference in wave shape at the hort times to sparkover is due to the ef-ect of the corona currents required for onization of the gap to complete spark-ver and the resulting voltage drop in ne series impedance—inductance and re-istance—of the impulse generator dis-harge circuit. The resulting change of ne wave shapes is shown in figure 12. n this figure the wave shape at two mi-roseconds to sparkover is compared with ne wave shape at critical sparkover for vo types of impulse generator discharge rcuits. In figure 12*a* the wave shape is ontrolled by a series resistance and a nall load capacitance which principally consists of the inherent capacitance of the impulse generator plus a small additional load capacitance, a total of approximately 300 micromicrofarads. In order to obtain a 1.5-microsecond front with such a small capacitance, it is necessary to use a series resistance of 1,700 ohms. The corona currents through the gap have an amplitude of the order of hundreds of amperes and, therefore, the voltage drop through the resistor is several hundred thousands of volts. This voltage drop subtracts from the wave as it would have appeared, if the corona currents had not flown through the gap. The effective wave front is, therefore, changed from a 1.2-microsecond front at critical sparkover to 0.6 microsecond at 2 microseconds to sparkover. Therefore, the ratio of T_1/T_2 for this wave at two microseconds is $0.6/2=0.3$ which results in a spark-over voltage of 534 kv from figure 4 when corrected for air conditions. This checks the value of 535 kv obtained from figure 11.

In the other circuit, figure 12*b*, the load capacitance is concentrated close to the rod gap and has a value of 800 micromicrofarads. The series resistance is 800 ohms giving a front of 1.8 microseconds and an effective front of 1.3 microseconds. For equal amounts of corona currents, as for the circuit 12*a*, the voltage drop across the resistor due to the corona is considerably reduced because it can be supplied by the capacitor direct without any appreciable voltage drop. Consequently, the effective front is not changed and at two microseconds to sparkover the ratio $T_1/T_2=1.3/2=0.65$. From figure 4 a spark-over voltage of 587 kv results, which, when corrected to standard conditions of humidity and air density, gives 610 kv as compared to 534 kv obtained with impulse generator circuit of figure 12*a*. This spark-over voltage of 610 kv was actually obtained during tests on the 20-inch rod gap with circuit of figure 12*b* in the process of obtaining a volt-time curve before and independent of this present investigation. Data of figure 4 have been obtained recently. It is, therefore, significant to the value of this proposed classification of impulse wave shapes in terms of T_1/T_2 that test data on the same type of gap taken several years ago should check so well when analyzed on the basis of that ratio.

The solid curves shown in figure 11 were obtained with an impulse generator connected as in figure 12*a* for the 20-inch and 30-inch gap, while the tests for the 50-inch gap were made with circuit of figure 12*b*. If the value of 610 kv for the 20-inch rod gap is plotted on figure 11, a straight line for the two-microsecond test curve results.

These examples show that

1. Differences in spark-over voltages obtained on electrode arrangements with non-uniform field are directly due to differences in impulse generator discharge circuits.

2. Spark-over voltages, when classified according to wave shape as expressed by the ratio of effective front to time to sparkover, are consistent on the basis of spark-over volt-time areas, although they appear erratic on the basis of volt-time curves.

3. The effective wave front produced by some types of impulse generator discharge circuits during investigations of impulse volt-time curves of apparatus with non-uniform field varies considerably throughout the range of times to sparkover from critical to one to two microseconds. Such generators produce volt-time curves where neither T_1=constant nor T_1/T_2=constant. The change in effective front depends on the type of apparatus tested, whether large or

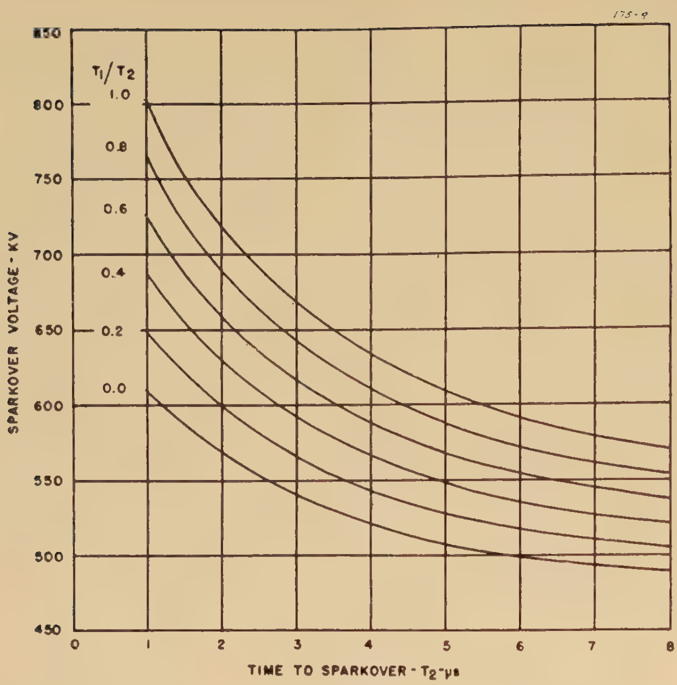

Figure 9. Spark-over volt-time area of a two-unit stack of apparatus insulators

Boundaries are $T_1/T_2=0$ and $T_1/T_2=1$. Negative polarity. Vapor pressure 0.26 inch mercury; air density 0.983

T_1 = effective wave front; T_2 = time to spark-over

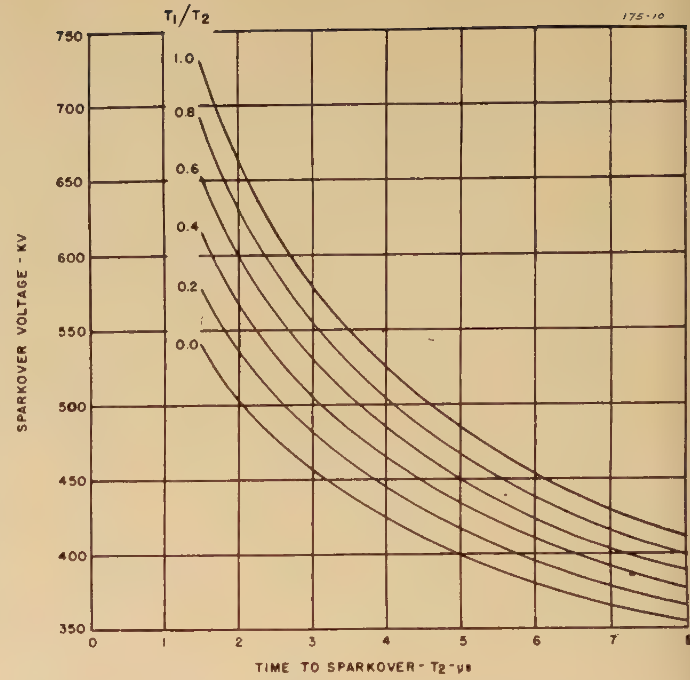

Figure 10. Spark-over volt-time area of a bushing

Boundaries are $T_1/T_2=0$ and $T_1/T_2=1$. Negative polarity. Vapor pressure 0.26 inch mercury; air density 0.983

T_1 = effective wave front; T_2 = time to spark-over

small corona currents are required to complete sparkover.

4. The effective wave front produced by the other type of generator is constant throughout the same range of time to sparkover. Therefore, the volt-time curve produced has a constant T_1. Wave shape at any given time to sparkover is practically independent of the type of apparatus tested. It is, therefore, clear that for purposes of comparison of volt-time curves of apparatus with great differences in electric field distribution, tests made with an impulse generator discharge circuit of the type shown in figure 12*b* are directly comparable. Similar tests made with a generator of the type shown in figure 12*a*, however, are not directly comparable and have to be interpreted with considerable care. Until volt-time areas of all types of insulation structures are available, the effective fronts obtained during tests on volt-time curves should be recorded throughout the range investigated, since they have such a profound effect on the values of spark-over voltages obtained.

Effect of Volt-Time Areas on Co-ordination

The data are obtained on too few types of apparatus to enable complete understanding of all the requirements for effective co-ordination. However, sufficient data are presented to make general recommendations. For this purpose the term co-ordination is used in a restricted sense, such that "co-ordination between two apparatus is obtained if the impulse strength of one of them is below the other, so that sparkover always occurs on the apparatus with lower strength." On the basis of volt-time curves this means that the volt-time curve of apparatus *A* is lower than that of apparatus *B* throughout the expected spark-over time range.

As shown by the examples of the sphere gap and the insulators, quasi-uniform fields between electrodes are associated with small impulse spark-over areas, while the nonuniform field is associated with large impulse spark-over areas. The problems of co-ordinating voltage levels for the large variety of electrode fields encountered in electrical apparatus, therefore, consists in co-ordinating according to spark-over areas rather than according to single volt-time curves. This, of course, complicates the co-ordinating problem to a certain extent.

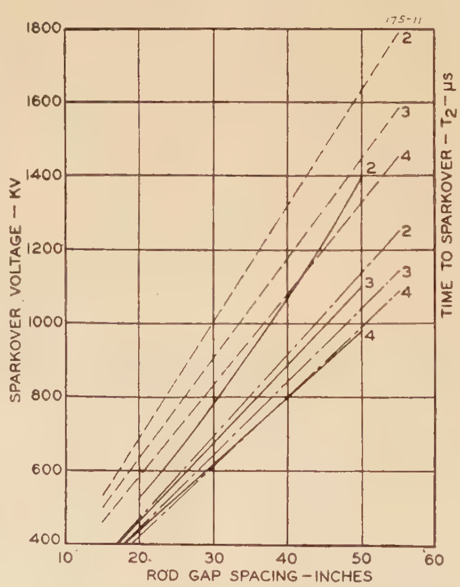

Figure 11. Impulse spark-over characteristics of rod gaps

Negative polarity. Standard conditions of humidity and air density

Solid lines—tests with 1.5x40 wave
Dashed lines—$T_1/T_2=1$ curves
Dot-dash lines—$T_1/T_2=0$ curves

T_1 = effective wave front; T_2 = time to spark-over

However, the problem can be reduced to three fundamental conditions (figure 13):

(*a*). Apparatus with the lower impulse strength (*A*) has a narrow band spark-over area; apparatus with the higher impulse strength (*B*) has a wide band spark-over area (for instance, a sphere gap (*A*) and insulator string (*B*)).

In this case co-ordination can be made effective if the $T_1/T_2=0$ spark-over curve of (*A*) is below the $T_1/T_2=0$ spark-over curve of (*B*) because regardless of wave shape, the impulse strength of (*A*) will be exceeded before that of (*B*) is reached.

(*b*). Apparatus with the lower impulse strength (*A*) has a wide band spark-over area; apparatus with the higher impulse strength (*B*) has a narrow band spark-over area. In this case, co-ordination can be made effective if the $T_1/T_2=1$ spark-over curve of (*A*) is below the $T_1/T_2=1$ spark-over curve of (*B*).

(c). Regardless of the band of the spark-over areas of both apparatus co-ordination is effected if the $T_1/T_2=1$ spark-over curve of (A) is below $T_1/T_2=0$ spark-over curve of (B).

Condition (c), of course, is the most satisfactory method of assuring that apparatus with the lower impulse strength will reduce the impulse voltage before the impulse strength of (B) is reached. However, under conditions where the margin between apparatus (A) and (B) can be kept to a minimum, matching of the spark-over areas as indicated in figure 13, (a) and (b) should give considerable improvement as compared to a consideration of single volt-time curves only. It is obvious that apparatus with nonuniform field and consequent wide band spark-over areas are not suited to limit impulse spark-over voltages in stations where costly equipment may be damaged if the limiting level of the apparatus is set too high. If, on the other hand, the limiting level is set sufficiently low, following condition of figure 13c, the spark-over characteristics will be such that switching surges and other low and medium system disturbances will result in a large number of system outages.

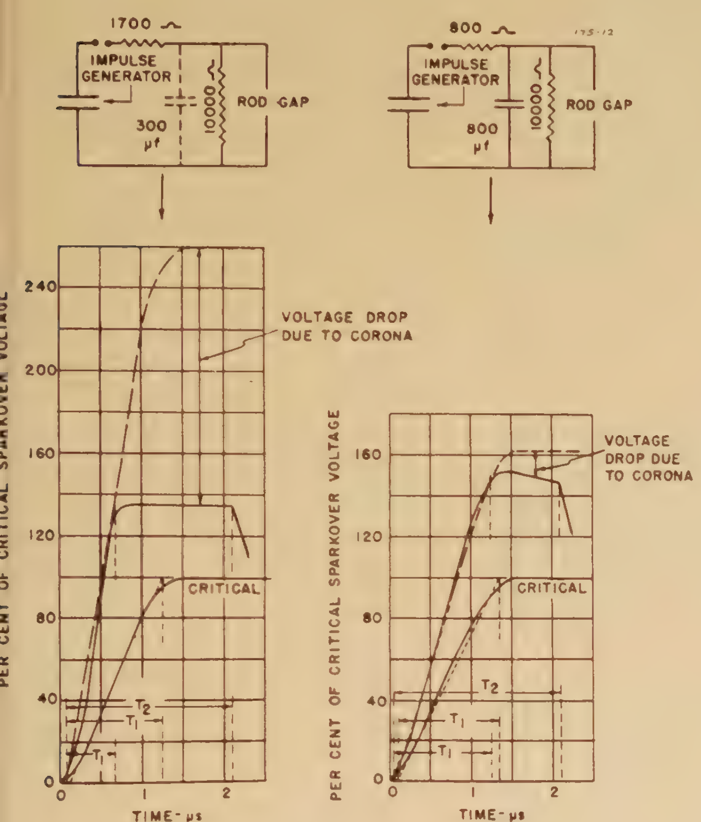

Figure 12. Effect of impulse generator discharge circuits on effective wave front—T_1

Wave Shape Variations on Transmission Lines

The question naturally arises whether apparatus in service will be subjected to waves of such a great variety of shapes as to warrant the investigation of impulse sparkover of areas as has been done in this paper for a few types. The available data are limited, due to the very costly nature of investigations of wave shapes of natural lightning on transmission lines, but approximate limits can be given.

Lewis and Foust[11] give a summary of a study of natural lightning on transmission lines in the United States of America which shows that wave fronts may vary between 1 microsecond and 80 microseconds wave tails between 4 and 160 microseconds. Berger[13] in Switzerland recorded wave fronts up to 80 microseconds causing flashover of insulation at a terminal station. From these limited measurements of traveling waves on actual transmission systems, the possibility of great variations in wave fronts and wave shapes is indicated. Therefore, the large variations in spark-over voltages, as shown to exist for electrode arrangements with nonuniform field, are a distinct possibility and should be taken into account in the co-ordination problem.

Conclusions

1. Impulse spark-over voltages of electrode arrangements with nonuniform field—such as insulators, bushings, rod gaps—cannot be represented with sufficient accuracy by volt-time curves, but must be represented by volt-time areas.

2. The extent of these areas may be considerable. The spark-over voltage of a string of three suspension insulators for instance, ranges between 430 kv and 620 kv with sparkover taking place at one microsecond, a difference of 45 per cent, or at six microseconds to sparkover the spark-over voltage ranges between 330 kv and 430 kv, a difference of 30 per cent.

3. The great differences in voltages at any given time to sparkover are not due to erratic nature of sparkover, but due to differences in the shape of the applied impulse wave before sparkover occurs.

4. The experimental data show that differences in wave shape can be classified by the ratio of the effective front of the wave to the time to sparkover—T_1/T_2. $T_1/T_2=0$ represents a wave with very steep front and practically rectangular tail while $T_1/T_2=1$ represents a wave with a front rising in a straight line from zero time to the time of

Figure 13. Co-ordination on basis of spark-over volt-time areas

A—Apparatus with lower spark-over strength
B—Apparatus with higher spark-over strength
a—A has narrow band spark-over area, B has wide band spark-over area
b—A has wide band spark-over area, B has narrow band spark-over area
c—Band width of spark-over area irrelevant

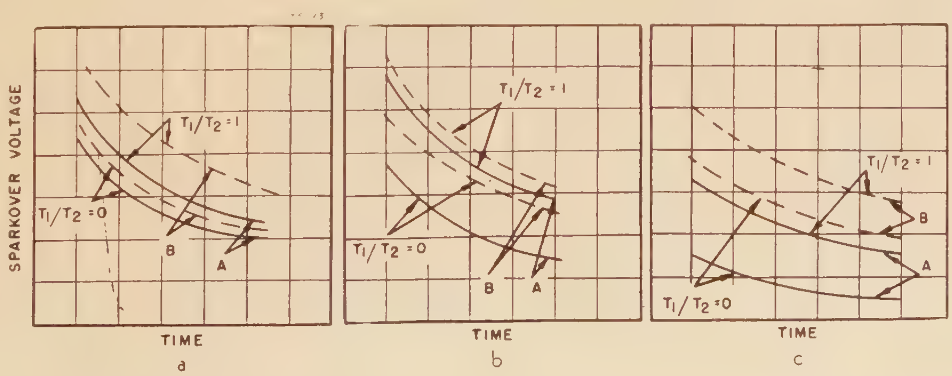

sparkover. Wave shapes where the ratio T_1/T_2 is small are associated with the lower spark-over voltages while straight line voltage rise produces the highest spark-over voltage at any given time to sparkover.

This means that the customary volt-time curves give only a very incomplete spark-over characteristic for any given electrode arrangement. The deviations from such curves are summarized in the following table (data from figure 6) for the 50-inch rod gap.

		Time to Spark-Over—Microseconds				
		2	3	4	5	6
Total spread of spark-over voltage in per cent of lower boundary		44	38	33	28	25
Per cent difference from typical volt-time curve with $T_1 = 1.3$ microseconds	+	13	19	21	21	22
	−	28	16	11	6	2

The maximum and minimum differences between the boundaries of the spark-over areas and volt-time curves depend on the impulse generator connection used for obtaining the curves.

5. The dependence of spark-over voltages on wave shape explains the great difference of spark-over voltage for a given electrode arrangement reported from different laboratories. The differences, in the range of one microsecond and more, are principally due to the difference in types of impulse generators used for the investigations. Although two impulse generators may produce the same wave shape at critical sparkover, at shorter times to sparkover (four microseconds and less) the wave shapes become radically different. One type produces a wave with a short effective front. Therefore, T_1/T_2 is small and the resulting spark-over voltage is low; the other produces a wave with a practically constant effective front. Therefore, T_1/T_2 is large and the resulting spark-over voltage is high.

Thus, this classification of wave shape is a satisfactory means for explaining the large voltage differences observed by various laboratories at times to sparkover of one microsecond or more.

6. The same phenomena which cause the upturn of spark-over volt-time curves are responsible for spark-over volt-time areas. Impulse sparkover in the nonuniform field requires corona currents of considerable amplitude to complete sparkover. The amplitude and the length of time of current flow determine the time to sparkover and the crest voltage of the wave causing sparkover. Therefore, for equal times to sparkover, a wave shape for which corona starting voltage is attained in a short time will require a lower spark-over voltage than a wave shape where corona starting voltage is attained later. Likewise, for equal sparkover voltages, early start of corona current will produce a shorter time to sparkover than a late start of corona currents.

7. Therefore, in the quasi-uniform field, such as the sphere gap, where corona currents are of small amplitude or negligible at times to sparkover of one microsecond or more, the effect of wave shape on the sparkover characteristic is very small, the upturn of the volt-time curves is negligible, and the extent of the spark-over area is negligible. At times shorter than one microsecond the effect of corona current becomes considerable and the sphere gap should exhibit increasing extent of spark-over area and upturn of voltage.

8. Methods of co-ordinating system insulation on the basis of impulse spark-over areas rather than volt-time curves are pointed out.

9. The data presented here are only another step to a more complete understanding of spark-over phenomena. The classification of impulse wave shape by means of a simple ratio of effective front to time to sparkover, while not based on a precise scientific interpretation of the phenomenon, nevertheless gives excellent practical results.

References

1*a*. The Co-ordination of Transformer Insulation With Line Insulation, **V. M. Montsinger** and **W. M. Dann.** AIEE Transactions, volume 51, 1932, pages 923–4.

1*b*. Co-ordination of Insulation, **V. M. Montsinger, W. L. Lloyd, Jr.,** and **J. E. Clem.** AIEE Transactions, volume 52, 1933, pages 417–27.

1*c*. Insulation Co-ordination, **Philip Sporn** and **I. W. Gross.** AIEE Transactions, volume 56, 1937 (June section), pages 715–20.

2. Basic Impulse Insulation Levels, **Philip Sporn** and **C. A. Powel.** AIEE Transactions, volume 59, 1940 (October section), pages 596–8.

3. Flashover Characteristics of Rod Gaps and Insulators, AIEE Transactions, volume 56, 1937 (June section), pages 712–14.

4. Short-Time Sparkover of Gaps, **J. H. Hagenguth.** AIEE Transactions, volume 56, 1937 (January section), pages 67–76.

5. Impulse Voltages Chopped on Front, **P. L. Bellaschi.** AIEE Transactions, volume 55, 1936 (September section), pages 985–90.

6. Discussion on reference 4, **J. H. Hagenguth.** AIEE Transactions, volume 56, 1937 (July section), pages 885–7.

7. Recommendations for High-Voltage Testing, **EEI-NEMA Subcommittee Report.** AIEE Transactions, volume 59, 1940 (October section), pages 598–602.

8. Ionization Currents and the Breakdown of Insulation, **J. J. Torok** and **F. K. Fielder.** AIEE Transactions, volume 49, 1930, pages 352–7.

9. Impulse Voltage Strength of Insulators and Materials, **J. C. Dowell** and **C. M. Foust.** *General Electric Review*, March 1937.

10. Flashover Characteristics of Insulation, **P. H. McAuley.** *The Electric Journal*, July 1938.

11. Lightning Surges on Transmission Lines—Natural Lightning, **W. W. Lewis** and **C. M. Foust.** *General Electric Review*, November 1936, pages 543–55.

12. Resultate der Gewitter Messungen Inden Jahren, 1932–1933, **K. Berger.** *Bull. S.E.V*, April 27, 1934.

Transactions Section

Preprint of Corresponding Pages From the Current Annual Transactions Volume

Any discussion of these papers will appear in the December 1941 "Supplement to Electrical Engineering—Transactions Section"

Effect of Sapphire-Crystal Orientation on the Wear of Watt-Hour-Meter Bearings

J. H. GOSS
ASSOCIATE AIEE

Synopsis: This paper describes the most recent of a series of studies on the life of watt-hour meter bearing materials. It covers an investigation of the effect of jewel crystalline axis orientation upon jewel wear.

Lifetime stability of meter calibration is a function of bearing wear. A study of the wear (after several years' service) of the sapphire jewel cups of meters in relation to crystalline orientation confirms predictions of another investigator; and a corroborative theory, based upon the physics of crystals, is presented.

Introduction

THE importance of the induction type watt-hour meter in the complex structure of the modern distribution system is fully realized. Accurate metering is necessary because the electrical characteristics and the initial and sustained accuracy of the watt-hour meter are directly reflected in terms of revenue produced. Much work has been done over a long period of years to improve the electrical characteristics and to perfect the mechanical parts. The lower bearing which carries the load of the moving system has long been given close study because it plays a real part in sustained meter accuracy.

It is the purpose of this article to describe briefly the results of work that has shown a marked correlation between the wear of the sapphire jewel cups used in the lower bearings and the direction with which the cups are cut with respect to the sapphire crystal structure. The wear of the jewel cups affects the useful life of the lower bearing and the sustained accuracy of the watt-hour meter.

For many years, it has been generally known that certain crystalline substances exhibit different hardnesses on various crystal faces. In 1931, V. Stott[1] working in the National Physical Laboratory experimented with the wear of sapphire watt-hour meter jewel cups cut at various known angles with respect to the major axis of the sapphire crystal.

In 1936 V. Stott released a further account of work done in the National Physical Laboratory in a special report.[2] This report gave the results on 156-watt-hour meter jewel cups cut in definite crystal directions. The report indicated quite conclusively that there was a definite relation between wear and crystal direction. The apparatus used in making these tests was described in the first paper[1] and while it was designed especially for the work, represented a laboratory test which gave different operating conditions than a bearing experiences in a watt-hour meter.

It is desirable at this point, in order to understand properly the meaning of the term, "orientation" which is used to designate the direction with which the sapphire cup is cut with respect to the crystal axes, to consider briefly the subject of crystals and crystal structure.

Crystal Structure

Sapphire is crystalline alumina, Al_2O_3 and is a form of the mineral corundum. It is crystalline in structure and belongs to the hexagonal crystal system.[3] Sapphire is found in nature usually in rough rounded pebble-like masses, though frequently outer crystalline forms are evident. The material is also made synthetically by the Verneuil[3] process.

Figure 1*B* shows a wooden model of a sapphire crystal of hexagonal prism shape. This shape is frequently found in nature. The axis of the long direction of the crystal is defined for the purpose of identification as the *C* axis and is the reference axis of the crystal that will be used for this discussion. This axis will be called the vertical axis and is parallel to the optic axis of the crystal. Figure 1*A* shows a cross section of a watt-hour meter jewel cup cut with the axis of the cup at right angles to the *C* axis. This cup is said to be oriented to an angle of 90 degrees ($\theta = 90$ degrees). Figure 1*C* shows another cross section of a cup where the *C* axis of the crystal and the axis of the

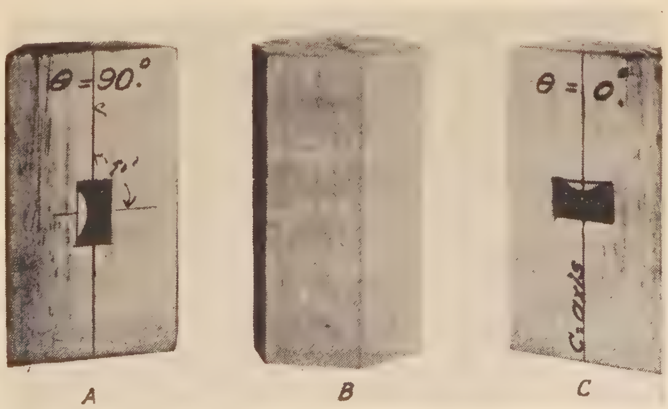

Figure 1. Models of sapphire crystal showing orientation angles of watt-hour-meter jewel cups

Paper 41-106, recommended by the AIEE committee on instruments and measurements, and presented at the AIEE summer convention, Toronto, Ontario, Can., June 16–20, 1941. Manuscript submitted November 13, 1939; made available for preprinting May 3, 1941.

J. H. Goss is with the General Electric Company, West Lynn, Mass.

1. For all numbered references, see list at end of paper.

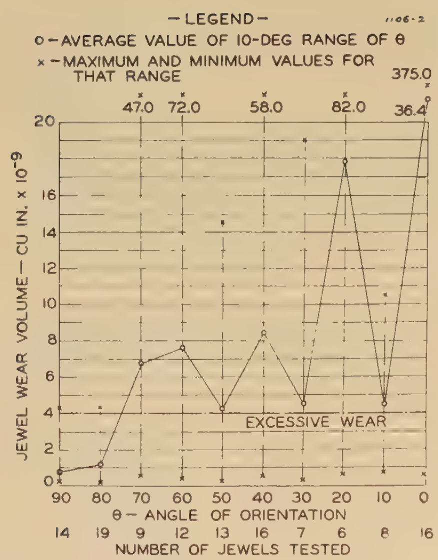

Figure 2. Jewel wear versus orientation

Composite curve of all jewels

jewel cup coincide. The orientation angle is 0 degrees ($\theta = 0$ degrees).

If a crystal is considered as being made up of small particles arranged in an orderly fashion, then a material that is noncrystalline, such as glass, may be thought of as being made up of particles with no systematic order of arrangement. A crystal that is allowed to form under ideal conditions will exhibit a definite geometric structure such as has been used in figure 1 to show one crystal form of sapphire.

If a sphere is formed from such a crystal as shown in figure 1, as might happen if it rolled in the bed of a stream for many years, it would be impossible to identify the substance as crystalline from its external shape. This is similar to what happens when synthetic sapphire boules are formed as they are more or less cylindrical in shape and exhibit few flat faces that make possible the identification of the boules as crystalline. Synthetic sapphire boules may give the appearance of globules of glass, yet actually they are identical in crystal structure to a piece of natural sapphire formed in nature which exhibits a perfect crystal shape as shown by figure 1. In the absence of the geometric form either optical methods[4] or X-ray[5] analyses can be used to orient and identify the crystal structure.

The most common method of identifying a sapphire crystal structure is to subject it to an analysis with polarized light and make use of the interference patterns which form definite optical figures.[4] The basal plane of the sapphire crystal may be determined by means of the optical figure. This is the plane in which all axes are equivalent. The axis at right angles to this basal plane is the vertical axis or *C* axis. This is the method of identification and orientation used in obtaining this experimental data.

Experimental Data

Following the publication of the material by V. Stott, it was desirable to check these results as the published data definitely indicated that an improvement in the life of watt-hour meter bearings could be obtained by controlling the orientation of the jewel cup to within the angle $\theta = 80$ degrees to 90 degrees. It was impractical to set up life tests with watt-hour meter jewels with known orientations and run them for a period of five to ten years to get this information. There were available in the laboratory several hundred watt-hour meters which had been operated for periods of five to six years under known conditions with jewel cups that had been cut at random with respect to the crystal direction. The logical procedure was to discontinue some of these life tests, examine the bearings for wear, and determine the orientation of each individual jewel cup. A system of measuring the orientation angle was devised and approximately 150 bearings were taken from life tests and examined. The wear was estimated from measurements made by means of a calibrated eyepiece in a 40 diameter magnification microscope. These data are plotted as a composite curve in figure 2. Here the jewels were grouped in accordance with their orientation angle, and the circles represent the average wear value for a

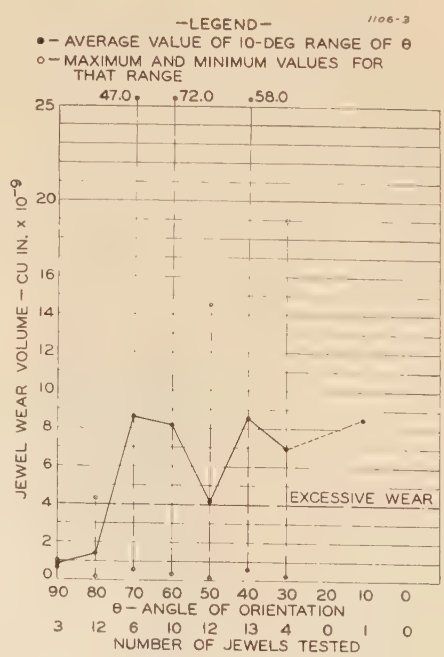

Figure 3. Jewel wear versus orientation

Composite curve of synthetic sapphire jewels

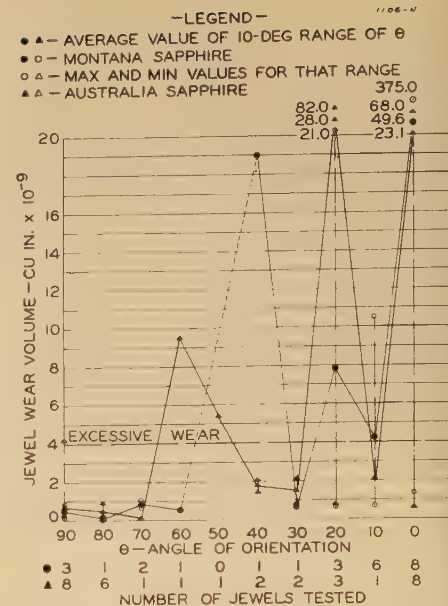

Figure 4. Jewel wear versus orientation

Composite curves of natural sapphire jewels

particular angular division. The minimum wear and the maximum wear for the angular division are shown by the crosses. It is interesting to note that there is a definite trend of increased wear as the jewels drop from an orientation of 90 degrees to an orientation of 0 degrees. In all cases the jewels oriented within 10 degrees ($\theta = 80$ degrees to 90 degrees) showed minimum wear and fortunately 33 jewels were found within this angular range. Figure 2 includes bearings from life test watt-hour meters with both natural and synthetic sapphire jewel cups. A further breakdown of these data is shown by figure 3 which shows the results for the synthetic sapphire cups and figure 4 which shows the results for natural sapphire cups. All of the watt-hour meters from which these bearings were removed were operating to simulate normal load conditions and were equipped with high carbon steel pivots in well-lubricated bearings.

Natural Versus Synthetic Sapphire

The experimental evidence shows the desirability of controlling the orientation angle as advocated by V. Stott.[2] It is impractical to orient natural sapphire jewel cups due to the fact that natural sapphire is frequently found in small pieces so that it is possible to make but two or three jewel cups from a single piece of raw material. The synthetic sapphire boules are quite large, and it is possible to make many jewel cups from one boule. As the optical procedure for determining the crystal direction of a boule is identi-

Figure 5. Atomic model of sodium chloride

Scale = two angstroms to one inch

Figure 6. Atomic model of sodium chloride

Scale = two angstroms to one inch

cal with that required for determining the crystal direction of a small fragment of natural sapphire, it is obvious that it is much more expensive to make the determination for natural sapphire on a commercial basis than on synthetic sapphire.

A careful review of extensive life test data on watt-hour meter jewel cups of random orientation, operating at both accelerated and normal speed, had already led to the conclusion that taken as a whole, natural sapphire and synthetic sapphire were giving equivalent performance.

Theory of Orientation

It was suggested that the difference in wear exhibited by the jewel cups cut in the different crystal directions was due to a phenomenon known as translation gliding in crystals. This is demonstrated in certain crystals, as for example rock salt. If the crystal is placed under tension or compression under controlled conditions, one portion of the crystal moves with respect to the other along a plane and rupture does not occur. No fractures are discernible even with polarized light or X-ray diffraction after the crystal has been stressed, even though one portion actually overhangs another portion. A theoretical explanation for this is shown most clearly by figure 5 and figure 6. Figure 5 is an atomic model of salt (sodium chloride, NaCl) actually built to a scale of one inch equals two angstroms (125 million to one). The large balls represent atoms of sodium. An examination of the photograph will show the nesting of the sodium balls between the chlorine balls. The model pictured consists of two parts. The bottom is a single layer, and the top is a triangular pyramid. The model represents but a small part of a crystal and must be thought of as repeating itself in all directions to form a crystal of salt. If the pyramid portion is moved with respect to the bottom layer in any direction except the direction represented by the top and bottom of the page, it will be noted that the chlorine balls tend to ride over and onto the chlorine balls in the bottom layer. As the chlorine particles are negatively charged, we have two negatives coming together with the result that a repelling force is present. If they are forced to move in that direction, the result will be that the negative charges will force the crystal apart. If, however, the pyramid is moved in the direction of the top and bottom of the page, it will be seen, as shown by figure 8, that a new position is assumed which is identical in the relation of the sodium and chlorine balls to that shown by figure 5, except that a portion of the bottom layer has been exposed. This portion of the bottom layer that has been exposed represents, therefore, the portion that is overhanging. This is the crystallographer's explanation of gliding and is substantiated by accepted scientific proof based on X-ray diffraction studies. This is, of course, a very simple example and is not intended to serve as an explanation for the orientation wear effect in sapphire.

Sapphire material has a much more complex crystal structure than salt, which is of the cubic form, the simplest crystalline form known. A model of sapphire was built at the Massachusetts Institute of Technology, under the direction of Professor M. J. Buerger.[10] Figure 7 shows the sapphire model which was made to the same scale as the sodium-chloride model. In figure 7, the reference *C* axis is represented by a vertical line joining the two hands. Figure 8 shows how the model was built to separate. The top half of the model is separate from the bottom half and may be moved with relation to it. While it cannot be seen from the photographs, the model demonstrates that gliding can occur. The gliding is in a plane at right angles to the *C* axis in sapphire.

If the assumption is made that the phenomenon of gliding is an indication of loose atomic bonding on that particular plane, a possible explanation of the results obtained experimentally can be given. That is, particles of the crystal may be more easily removed in this plane of the crystal than in other planes, because the atoms are held more loosely in place than in other directions. Crystals may have more than one plane of gliding, but in sapphire, we are primarily concerned with the plane at right angles to the *C* axis as borne out by the experimental evidence.

Consider a watt-hour meter jewel cup

Figure 7. Atomic model of sapphire

Scale = two angstroms to one inch

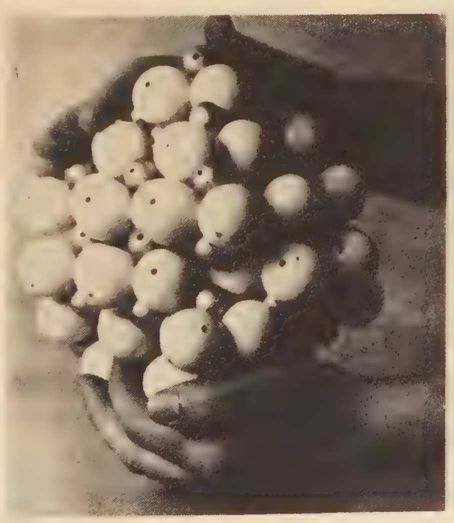

Figure 8. Atomic model of sapphire

View showing internal arrangement of atoms

Scale = two angstroms to one inch

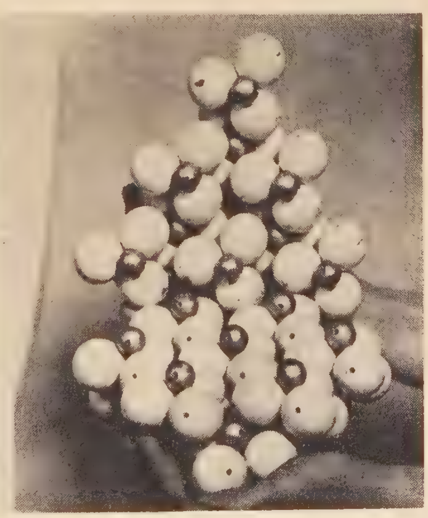

The Dielectric Strength of Glass—an Engineering Viewpoint

E. B. SHAND
MEMBER AIEE

Synopsis: The purpose of this paper is to provide the engineer with co-ordinated information and data regarding the dielectric breakdown of glass which will permit him to apply this insulating material more effectively for high dielectric strength. In the discussion of the subject, particular attention has been paid to "edge effects" and other factors which cause wide variations in breakdown voltages—variations which are responsible for many of the seeming inconsistencies found in published results on the dielectric failure of glass and other materials.

The author has concluded that it is possible to make a reasonable approximation of the breakdown voltage of glass, if the conditions of the test or of the application can be sufficiently well determined.

The characteristic breakdown curves of this paper do not represent the results of any one series of tests, but are rationalized from data selected from many sources, including unpublished tests.

The data curves included refer mainly to Pyrex* glass, but corresponding data have also been included on electrical porcelain because of the interesting comparisons shown.

I. Dielectric Failure of Glass

WITHIN the last few years the physicist has made pronounced progress in the study of dielectric failure, but in spite of this progress, our knowledge of the phenomena involved is still very incomplete. It is generally considered that the dielectric failure of insulating materials, such as glass and porcelain, may occur in one of two ways:

(*a*). In disruptive breakdown
(*b*). In thermal breakdown

Disruptive failure is one which results directly from an electrical overstress of the dielectric material without perceptible internal temperature rise. Recent research indicates that disruptive failure is caused by electronic ionization by collision within the molecular structure of the material.[1] In actual practice it is probable that pure disruptive failure occurs only under somewhat special conditions, and accurate test values of intrinsic dielectric strength are not easily obtained, even with the use of elaborate and careful procedure. The disruptive breakdown voltage is roughly proportional to the thickness, and may be expressed in volts per mil, or kilovolts per centimeter. Table I gives representative data for several materials which have been selected from various sources.

Paper 41-91, recommended by the AIEE committee on basic sciences, and presented at the AIEE North Eastern District meeting, Rochester, N. Y., April 30–May 2, 1941. Manuscript submitted October 19, 1940; made available for preprinting March 21, 1941.

E. B. Shand is with the product development department, Corning Glass Works, Corning, N. Y.

1. For all numbered references, see list at end of paper.

* Pyrex is a registered trade-mark of the Corning Glass Works and is applied to a group of products rather than to a glass composition. In this paper, glasses identified by Corning as 772, 774, and 776, etc., are referred to.

Table I. Disruptive Strength

Material	Disruptive Strength Kv/Cm. (Peak Value)
Lime glass	3,400– 4,500
Lead glass	3,100
Borosilicate glass (Pyrex)	3,900– 4,800
Fused quartz	5,000– 8,000
Electrical porcelain	320– 450
Mica	8,000–10,600

Thermal failure is one which results from the increased temperature of the insulation caused by the applied electrical stress. As the internal temperature rises the losses also increase, which, in turn, raise the temperature still more. Under certain circumstances a cumulative action of this kind may proceed until instability is reached, the current and losses rise suddenly, which represents the thermal failure of the insulation.[2]

Whether the limit of disruptive strength or that of thermal strength is reached first depends upon a number of conditions. In cases of thin glass sections, allowing the rapid dissipation of losses to the electrodes, of short periods of test, and of low ambient temperatures, the failure tends to be of the disruptive type; for the reverse conditions the failure tends to become thermal. When a series of tests is made with samples of successive steps of thickness, or at increasing temperatures, a transition from disruptive to thermal failure is found to

---

with a pivot bearing running in it.[6,7] Then assume a worn point on the pivot which is abrading the jewel surface. If the jewel cup is cut with an orientation $\theta = 0$ degrees (figure 1), the pivot is abrading the jewel cup in the most favorable direction for removing material, and it is reasonable to expect that the pivot will find it easier to remove particles of the jewel cup than if the angle $\theta = 90$ degrees. When $\theta = 90$ degrees the pivot is abrading the crystal right angles to the favorable direction in which material can be removed and the particles of sapphire may be thought of as in a locked position.

Conclusions

The experimental evidence demonstrates that orientation is a definite factor in the wear of watt-hour meter jewel cups, and its control represents another step in insuring longer bearing life.

The experimental data confirm V. Stott's findings that for optimum results, the angle θ should be controlled to within $\theta = 80$ degrees to $\theta = 90$ degrees.

A possible explanation based on elementary crystal theory confirms the experimental evidence.

References

1. Investigation of Problems Relating to Use of Pivots and Jewels in Intruments and Meters, V. Stott. National Physical Laboratory, volume 24, 1931.

2. Technical Report *T/T25*, British Electrical and Allied Industries Research Association.

3. Gems and Gem Materials, E. H. Kraus and E. F. Holden. McGraw-Hill Book Company, Inc., Copyright, 1925.

4. Elementary Treatise on Physics Experimental and Applied, E. Atkinson. Translated from Ganot's Elements de Physique, William Wood and Company, 1910.

5. Theories and Definitions of Hardness, S. R. Williams. *Instruments*, February 1937.

6. Lubrication Increases Life of Meter Bearings, T. A. Abbott and J. H. Goss. AIEE Transactions, volume 54, 1935 (April section), pages 428–31. Discussion, 1935 (September section), pages 992–3.

7. Watt-hour Meter Bearings, I. F. Kinnard and J. H. Goss. AIEE Transactions, 1937 (January section), pages 129–37.

8. Experiments Bearing on the Orientation of Quartz in Deformed Rocks, D. Griggs and J. F. Bell. November 1, 1938. *Bulletin* of the Geological Society of America, volume 49, pages 1723–46.

9. Kunstliche Schiebungen und Translationen in Mineralien, Von Kurt Veit in Kiel, Neuen Jahrbuch für Mineralogie, Geologie und Palaontologie, S. 121–148 und Taf. 1, Stuttgart, 1921, E. Schweizerbart'sche Verlagsbuchhandlung.

10. A Technique for the Construction of Models Illustrating the Arrangement and Packing of Atoms in Crystals, M. J. Buerger and Robert D. Butler. *American Mineralogist*, volume 21, number 3, March 1936.

occur. Certain tests of this sort made on very thin samples of glass have indicated that this transition occurs abruptly. For thicker samples, such as would apply to engineering practice, the indications are that the internal temperature effects within the sample modify the characteristics of disruptive failure very materially before the conditions of thermal failure are reached so that the transition becomes much less apparent.

Curve 1 of figure 1 represents the pure disruptive breakdown voltage of a material such as glass or porcelain as a direct function of thickness. Curve 2 represents the breakdown voltage as modified by thermal effects. For the lower part of the curve the failure is still considered to be substantially disruptive, but for thick sections it will be purely thermal. No definite point of transition is indicated by this curve.

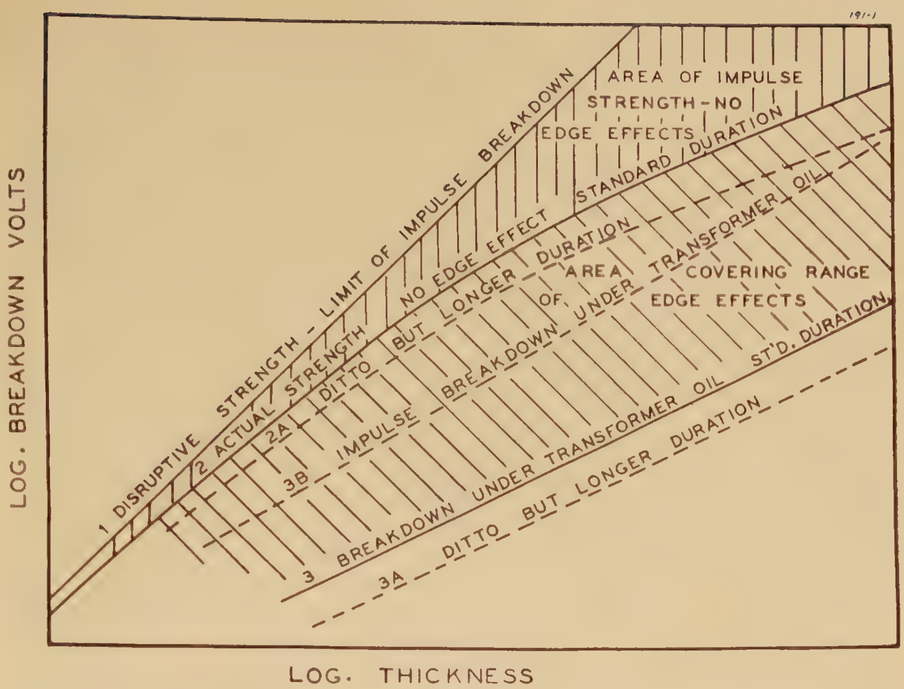

Figure 1. Graphic representation of breakdown characteristics

II. Factors Governing Breakdown

The principal factors governing breakdown may be listed as follows:

1. Characteristics of the dielectric material
2. Thickness of the section stressed
3. Temperature of the material
4. Duration of application of voltage
5. Characteristics of the applied voltage
6. Electrostatic field distribution in the dielectric and other "edge effects"

1. Wide differences in the characteristics of dielectric materials are indicated by the disruptive strengths listed in table I. Thermal failure is determined largely by the electrical and thermal conductivities of the material, and the variation of these properties with temperature. Glass and porcelain have widely different characteristics in disruptive failure, although in thermal failure these differences are much less pronounced.

2. The rate of change of breakdown voltage with thickness of section is dependent upon a number of conditions. As already stated, the breakdown voltage in pure disruptive failure may be considered to vary directly with the thickness. Mathematical analyses of thermal failure show that for thin sections the breakdown voltage will vary as $\sqrt{\text{thickness}}$, but that as the thickness is increased, this rate of increase is not maintained, and that a limiting condition is reached where a further increase in thickness will not result in any increase in the breakdown voltage. In other words there is a maximum voltage which a single thickness of insulation will withstand, regardless of its thickness. For Pyrex glass this limit has been calculated to be approximately 5×10^6 volts.

When materials such as glass and porcelain are immersed in insulating oil, this rate of change of breakdown voltage with thickness is determined mainly by the geometrical configuration of the insulator and the electrodes. For flat plates with thin electrodes, such as metal foil, the voltage will vary as $\sqrt{\text{thickness}}$ (see figure 1, curve 3). For power insulators of conventional design this ratio becomes approximately $(\text{thickness})^{0.7}$, as is indicated in figure 4.

3. Information regarding the quantitative effect of temperature on dielectric failure is not as complete as would be desired. However, various groups of data for both glass and porcelain indicate that in passing from room temperature (20 degrees centigrade) to 100 degrees centigrade, a reduction in breakdown voltage varying from 20 per cent to 40 per cent may be expected. At temperatures of 350 degrees centigrade or more these materials will have little remaining dielectric strength.

4. The period of time during which the voltage is applied to a dielectric is an important factor in determining the resulting breakdown voltage. Tests made under different procedures in this respect are not directly comparable. In general, it is found that for periods of stress extending from a few microseconds to an appreciable fraction of a second there is little change in the breakdown voltage, but from this point to a period of several minutes the reduction may be of the order of 50 per cent. Beyond this point to indefinite periods of time, further reductions are not great. This time characteristic of breakdown is probably connected with the stabilization of the internal temperature of the dielectric.

In figure 1, the disruptive strength (curve 1) represents the limit of breakdown voltage on impulse tests, curve 2 may be taken to represent the results of tests taken with the voltage raised continuously at the rate of 667 volts, rms per second, which is the standard procedure for insulator testing, while curve 2*A*, may be taken to represent the procedure of raising the voltage in one-minute steps, as is standard for apparatus testing. Curves 3*B*, 3, and 3*A*, are corresponding curves for other test conditions.

The breakdown voltage as measured by the one-minute hold test is usually of the order of 15 per cent to 25 per cent lower than when measured by the standard continuously rising voltage procedure.

5. The question of voltage, whether d-c or a-c, and if the latter, its frequency, must be considered. Evidence indicates that if the failure is purely disruptive, the breakdown is determined by the peak value of the voltage. However, the dielectric losses produced by alternating stresses, even at commercial frequencies, are much greater than the leakage losses caused by direct current, so that in the former case a lower breakdown voltage may be expected, except for very special conditions, such as where very thin sections are involved. For normal sections and commercial frequencies, this reduc-

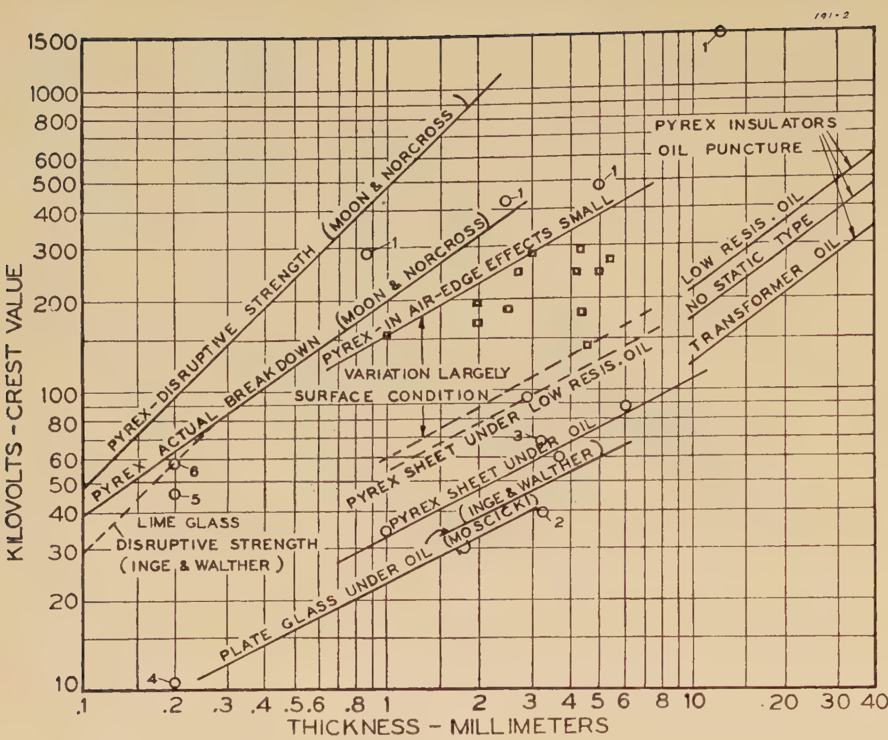

Figure 2. Selected dielectric breakdown data for glass

tion may be of the order of 20 per cent (peak value of the a-c voltage being considered).

As the frequency is increased the dielectric losses increase and the breakdown voltage drops. Some tests have indicated that at a frequency of 10,000 cycles the breakdown voltage may be about 40 per cent of that at 50 or 60 cycles, while for frequencies of the order of 1 megacycle this ratio may drop to less than 10 per cent.

6. In the actual application of insulation, it is not possible to avoid conditions which lead to local field concentrations and similar effects which reduce the breakdown voltage. These are generally referred to as "edge effects," because they were first observed at the edges of the electrodes, although they are not limited to these localities. Even in elaborate tests it is impossible to eliminate edge effects completely, and many discrepancies in the published data on the breakdown of glass result from this cause.

In addition to the edges of electrodes, these effects are found at points of imperfect contact between the electrode and the insulation, scratches in the electrode surface (when metal foil, or a silvered surface is used), voids or lack of homogeneity in the insulation itself, at changing sections of the insulation, and at imperfections of the surface of the dielectric, etc.

One of the principal reasons for the low disruptive strength of porcelain as compared with glass, is believed to be connected with the nonhomogeneous nature of the porcelain body which results in local field concentrations within the material. Glass, on the other hand, is homogeneous.† As a consequence of this, porcelain is much less sensitive than glass to certain edge effects of external origin. For instance in tests on glass it was found that with a rough ground surface under the electrodes, the breakdown voltage was only 16 per cent of the value obtained on a corresponding sample with polished surfaces. In the case of porcelain there was little difference in the two tests, and the breakdown voltages obtained on the porcelain samples were of the same order as those obtained on the rough ground glass samples of the same thickness.

Edge effects which result in local concentrations are ordinarily much less serious in the case of thermal failure than of disruptive failure. The temperature conditions resulting from the presence of local areas of high stress concentration will often produce a redistribution and partial equalization of stress, which does not occur when the failure is purely disruptive. Thus, within certain limits, thermal breakdown is in some degree analogous to the mechanical breaking of a ductile material such as soft steel, while the disruptive breakdown is more analogous to the tensile failure of a brittle material such as cast iron. Under certain conditions of test where edge effects are known to be present, a point of failure under the electrode, and away from the edges has been taken as indicative of a thermal failure, while a point of failure at the electrode edge or beyond the edge has been considered indicative of a disruptive failure. This distinction must be used with considerable care, as it is far from being a certain criterion to distinguish these conditions.

In order to avoid these edge effects it is important that the insulation used be without voids or surface imperfections, that the electrode should make a good contact with the insulation at all points, and that the stress at the electrode edges be equalized in some way. One effective method of reducing the edge stress is to thicken the insulation at the point where the electrodes terminate, without sudden changes in section.

Another type of edge effect not yet referred to specifically is one connected with certain phenomena in the ambient medium, such as insulating oil. Dielectric tests are frequently made under oil in order to eliminate flashover of the insulation sample. With the usual procedure for such tests, the electrostatic field at the electrode edges will fringe out into the oil. Insulating oils have a dielectric constant much lower than those of glass and porcelain so that the electrical stress in the oil will be materially higher than otherwise. Under these conditions corona discharges will form in the oil long before the true breakdown strength of glass is approached. As the voltage is raised beyond the corona point of the oil, streamers develop which will extend over the glass or porcelain. At the terminating point of these streamers on the surface of the insulation intense voltage gradients will exist, causing disintegration of the point attacked. If this action is allowed to continue for a sufficient time, it is probable that a hole will be drilled completely through thick sections of glass or porcelain causing dielectric failure.

This type of failure is determined almost entirely by the breakdown of the oil, and does not constitute a valid test of the insulating material, except for those cases where the insulation is to be oil-immersed in actual use.

Corresponding samples of various glasses and porcelain and of mica with wide differences of dielectric characteristics have been found to puncture at essentially the same voltage under this test, which demonstrates that breakdown is not a function of the properties of the insulating material.

† This, of course, is relative. Glass bodies may contain "stones, seeds, or blisters," which are not homogeneous with the remainder of the material. Any serious fault of this character, however, can be eliminated readily by visual inspection.

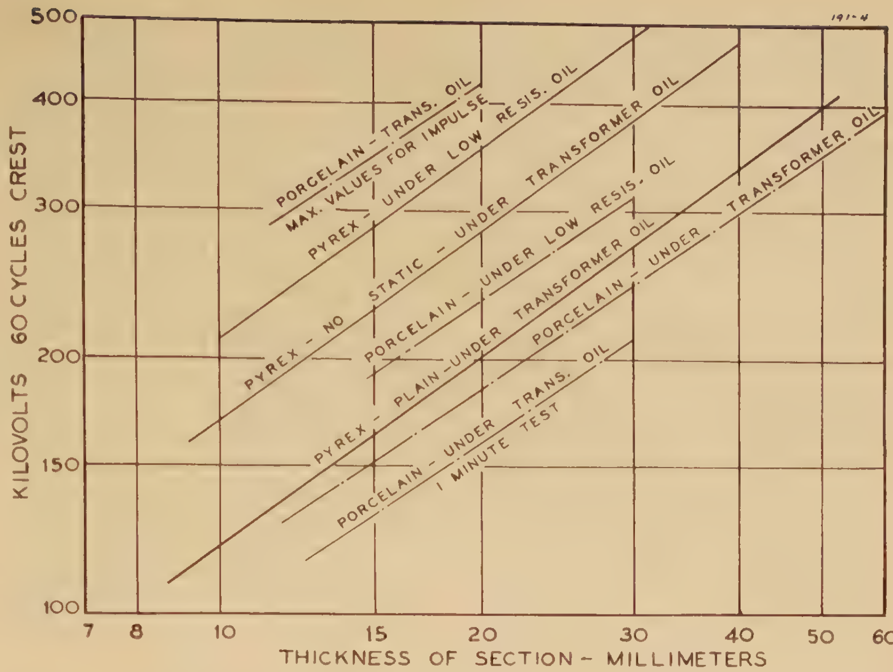

Figure 4. Oil puncture tests on power insulators

60-cycle voltage, raised continuously at 667 volts (rms) per second

Certain investigators state that when streamers occur in the oil the discharges have been found to be highly oscillatory, and that even if the puncture takes place under the area of the electrodes, the measured breakdown voltage may not be a true indication of dielectric strength because of the presence of the high frequency component of voltage.

One of the means used in overcoming this condition, at least to some extent, is by the use of semiconducting liquids in place of regular insulating oil. Oil with a high water content, mixtures of xylol and alcohol, etc., are effective in preventing the formation of corona to a very considerable extent. Semiconducting surfaces on the insulation adjacent the electrodes have also been used to produce the same general effect. In many practical applications the form of the insulation and the electrode can be selected so that the normal voltage stress in the oil is below its corona point. This procedure is commonly employed in the design of oil-immersed transformers. In this case, however, the insulation is usually composed of organic material.

There are still insulation test specifications which call for the oil immersion of the test piece, and many such tests of questionable validity are still made. For this reason an appreciation of the edge effects resulting from the ambient oil is of particular importance. As an instance of this, the oil puncture test is the standard procedure for testing power-line insulators, in spite of the fact that it is generally recognized that the results so obtained are not representative of their performance in service. Figure 4 gives average breakdown data as obtained from a large number of tests made on both Pyrex and porcelain insulators. The curves show that the puncture voltage may be raised either by reducing the resistivity of the oil or by using a semiconducting film on the insulator surface. Tests on Pyrex insulators indicate that, even when low-resistivity oil is used, the puncture results from edge effects, rather than from overstress of the glass.

III. Curve Data

Figure 1, representing the general dielectric charaeteristics of an insulating material such as glass or porcelain has already been discussed. It is to be noted, however, that a single group of such curves will not apply to all conditions. For instance, curve 1, the disruptive strength, may vary in some way with temperature. Curves 2 and 3 will shift to higher or lower voltages with variations of such factors as temperature, frequency, and duration of stress. These two curves represent certain limiting conditions of edge effect, so that for specific cases the relative severity of this factor must be estimated. This is necessarily very much of a guess, unless the engineer has a considerable background of experience to call upon. For actual design purposes there is the additional question of the proper factor of safety to be considered. This will, of course, depend upon the requirements of the type of application in view.

The data presented in the following figures refer to tests made at room temperature, and except when indicated otherwise, the values are for 60-cycle voltage raised continuously at the rate of 667 volts (rms) per second. In the case of some of the published data it was necessary to adjust the breakdown voltages to the condition. It will be noted, furthermore, that all voltages are expressed as peak values, rather than rms values.

Figure 2 includes a few representative

Figure 3. Selected dielectric breakdown data for porcelain

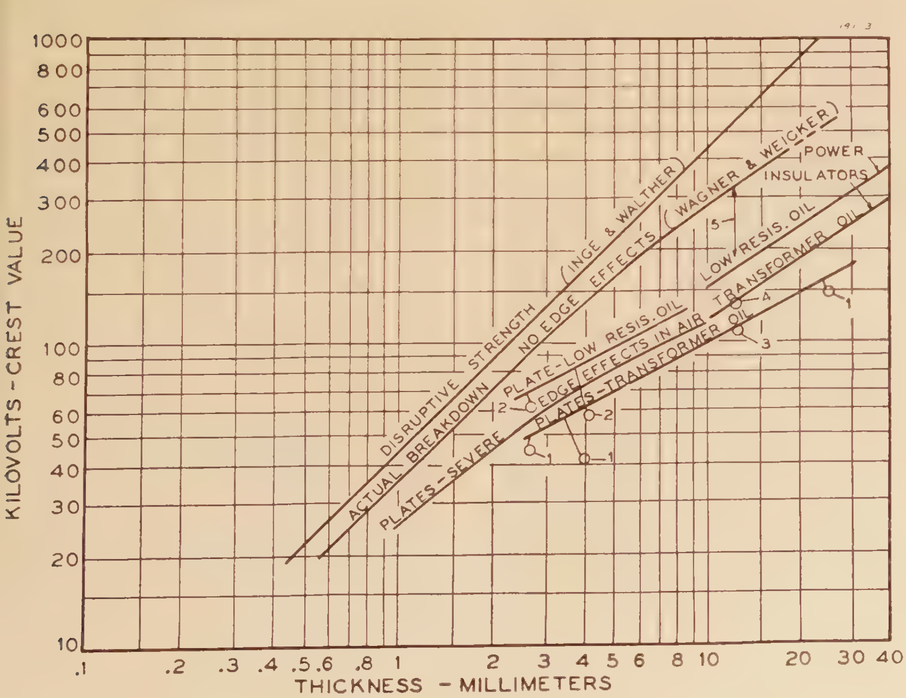

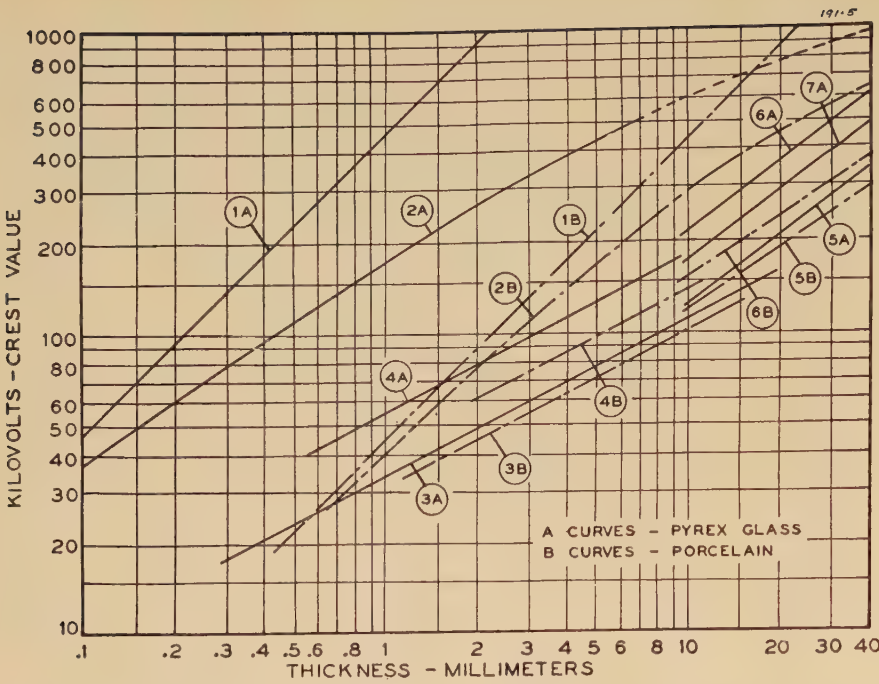

Figure 5. Dielectric breakdown characteristics of Pyrex glass and porcelain

Conditions—Room temperature and for 60-cycle voltage raised continuously at 667 volts (rms) per second

Curve 1—Disruptive strength
Curve 2—No edge effects
Curve 3—Under transformer oil
Curve 4—Under low-resistivity oil
Curve 5—Power insulators under transformer oil
Curve 6—Power insulators under low-resistivity oil
Curve 7A—Pyrex "no static" iridized insulators

data for glass. These are mainly for Pyrex glass, although some values for lime glass are included.

The disruptive strength of Pyrex glass, and also the breakdown values as actually modified by temperature effects are taken from the data of Moon and Norcross.[3] The results indicated by the square points were obtained from tests made by the Corning Research Laboratory on pin-type Pyrex insulators with the heads ground thin and polished to permit their puncture in air without flashover. Voids between the outer electrode and the insulator head, together with other surface irregularities, produced edge effects which were largely responsible for the wide difference in the breakdown values shown. Values indicated[1] represent impulse tests on Pyrex samples. Edge effects were experienced in these tests as well.

Other tests of the Corning Research Laboratory on plate glass under oil (point 2) check closely with the early data of Moscicki.[4] These tests were repeated with the use of semiconducting oil, with the result indicated by point 3. Corresponding tests made on Pyrex plate are seen to give materially higher breakdown voltages. The reasons for this difference are probably the lower dielectric constant of this glass (which will reduce the field strength in the oil), and the higher thermal resistance of Pyrex glass.

Data on lime glass, points 4, 5, and 6, are taken from the many tests of Inge and Walther.[5] They are for the following conditions:

4. Tests made under insulating oil

5. Tests with edge effects eliminated; duration ten seconds

6. Tests with edge effects eliminated; impulse tests

The curves for Pyrex insulators in figure 2 are replotted from figure 4.

Figure 3 corresponds to figure 2, except that the data apply to porcelain. The disruptive strength of porcelain is roughly ten per cent that of Pyrex glass, but when the breakdown is measured under insulating oil, there is very little difference between the two materials. For thick sections, which tend to result in thermal breakdown, the values of glass and porcelain tend to approach each other, even when edge effects have been eliminated from the test.

Points marked 1 and 2, for immersion in low and high conductivity oil respectively, refer to one-minute tests, and are consequently lower in value than the breakdown voltages taken with continuously rising voltages.

Points 3, 4, and 5 represent data published by Bellaschi and Manning[6] on porcelain insulator shells,

3. One-minute hold tests

4. Tests made with continuously rising voltage

5. Represents the limits of breakdown on impulse tests

The curves on power insulators have been replotted from figure 4 which has been discussed already.

Figure 5 combines the dielectric characteristics of Pyrex glass and electrical porcelain on one sheet. These characteristics are indicated in the same manner as figure 1, and the data are taken substantially from figures 2, 3, and 4, with minor modifications.

The information correlated in these curves, and in the data on other specific conditions mentioned above, is admittedly not developed to a point where an accurate prediction of the voltage at which Pyrex glass and porcelain will fail under certain conditions of test or of practical application, but it is believed that rough approximations can be made, and furthermore, that the methods proposed will allow the insulation engineer to obtain a better oriented view of the problems involved, and how the materials discussed might be used to better advantage. It is also hoped that with time, additional test results will allow the approximations to be made with improved accuracy.

References

1. Electric Breakdown of Solid and Liquid Insulators, A. von Hippel. *Journal of Applied Physics*, 1937, page 815.

2. The Theory of Thermal Breakdown of Solid Dielectrics, P. H. Moon. AIEE Transactions, volume 50, 1931, pages 1008–21.

3. Three Regions of Dielectric Breakdown, P. Moon and A. S. Norcross. AIEE Transactions, volume 49, 1930, pages 755–62.

4. Über Hochspannings—Kondensatoren, J. Moscicki. *Elektrotechnische Zeitschrift*, 1904, page 527.

5. Durchschlag von festen Isolatoren in homogenen und nicht homogenen elektrischen Feldern bei Beanspruchungen von langer und kurzer Dauer, L. Inge and A. Walther. *Archiv. f. Elekt.*, 1929, page 410.

6. Dielectric Strength of Porcelain, P. Bellaschi and M. Manning. AIEE Transactions, volume 58, 1939 (December section), pages 651–5.

Overvoltages in Polyphase Induction Motors During Single-Phase Operation

C. MACMILLAN
MEMBER AIEE

G. K. CARTER
ASSOCIATE AIEE

Introduction

IN the course of the starting, reversal, or normal operation of a polyphase wound-rotor induction motor, it occasionally happens that either the stator or the rotor or both may be allowed to operate single phase. In some cases it has been noted that the voltage of the open terminal or terminals under these conditions has a steady-state peak value well above its normal maximum. While scattered references to this effect may be found in the literature, and though the general subject of single-phase operation of polyphase induction motors has been discussed from time to time, apparently the magnitude of these voltages has not been the subject of a thorough and organized investigation. This paper is based on the results of a study, undertaken to determine analytically the maximum theoretical voltages of a three-phase induction motor under single-phase operating conditions, and, so far as possible, to check these calculated figures against actual test results.

Conclusions

The following conclusions were drawn from this study, for motor operation only; in general, high-voltage conditions would be worse for generator operation:

1. When a three-phase induction motor is operated from single-phase lines, the voltage from the open to either of the active terminals cannot exceed its normal three-phase value.

2. When a three-phase wound-rotor induction motor is operated with one rotor line open-circuited, the voltage from this open terminal to one of the active rotor terminals may reach a theoretical maximum of 2.3 times the rotor open-circuit voltage, assuming zero rotor resistance. This maximum would occur if the stator phase rotation were reversed and the secondary resistance were about 1.3 times the total leakage reactance referred to the rotor. The ratio of 2.3 for the terminal voltages is somewhat reduced in case part of the secondary resistance is internal.

3. When a three-phase wound-rotor induction motor is operated from a single-phase supply with one rotor line open, high voltages can occur on both the rotor and the stator open terminals. The theoretical maxima of these voltages, with resistance and saturation neglected, occur slightly below synchronous speed and recur twice in each slip cycle. The maximum theoretical line-to-line voltage on the rotor is $\sqrt{3}X_m \div 2X_0$ times the normal open-circuit rotor voltage (peak values); that on the stator is $\sqrt{3}(X_m - X_0)/2X_0$ times the normal line-to-line stator voltage (peak values).

4. The rotor voltage is somewhat analogous to the armature voltage of a synchronous machine with a single-phase short circuit.[1] In fact, the expression given here for the rotor voltage agrees with a previously derived expression for the transient voltage of the open terminal of a synchronous machine.[2] The stator open-terminal voltage in the induction motor has no counterpart in the normal synchronous machine. The presence of transient voltages in the induction motor of even higher magnitude than the steady-state voltage seems to correspond to the synchronous machine case when switching occurs at such time as to trap a d-c flux component in the short-circuited winding.

5. The magnitudes of voltages usually experienced are much lower than those calculated, because of various factors such as resistance, saturation, and supply system impedance, which were omitted to make the calculations feasible. In motors of small internal percentage resistance, the calculated values are most closely approached.

6. The conditions of operation and the abnormal voltages discussed in this paper can and do occur with existing systems of control of wound-rotor induction motors. They may be aggravated in cases in which one or the other of the open circuits is of a vibratory, or rapidly recurring, nature. An easy and effective safeguard is to avoid opening completely any one of the rotor lines, as tests show the voltages to be greatly reduced with even a relatively high resistance in the odd rotor phase.

Theoretical Investigations

A. Single-Phase Stator

The three-phase induction motor with single-phase excitation has long been studied from several standpoints: as a special case of an unbalanced polyphase machine,[3,4,5] as one type of single-phase motor,[6] and as a single-phase to three-phase phase converter.[7] Operation of this nature may readily be visualized by means of the revolving-field theory of Ferraris and its equivalent expression in terms of symmetrical components or by means of the two-axis method of resolution.[8] Both theoretical considerations and experience show that for this type of operation the open stator terminal will not reach a steady-state voltage greater than normal, so long as the rotor is symmetrical or nearly so.

B. Single-Phase Rotor

When a three-phase wound-rotor induction motor is operated with three-phase excitation and a single-phase secondary, the analysis becomes somewhat more difficult than for the case just considered. Nevertheless, adequate solutions have been obtained by the method of symmetrical components[4,5] and by the two-axis method;[9] this is also a special case of "internal cascade" operation,[10] in which tertiary nonsynchronous currents flow through the supply system, and are determined by its total impedance.

For purposes of visualization, with a sinusoidal terminal voltage the stator impressed field is of constant magnitude and rotates at synchronous speed with respect to the stator; thus, neglecting the resistance and leakage reactance drops, a maximum of twice normal voltage could be induced in the rotor if the stator phase rotation were reversed suddenly while the rotor was turning at full speed. A finite impedance connected between two of the rotor terminals allows a single-phase secondary current to flow with no direct mutual reaction on the open rotor phase, which thus keeps substantially twice normal induced voltage. Assuming zero machine resistance and a noninductive secondary resistor, the approximate secondary voltage vector diagram would be as indicated in figure 1, in which point 1 represents the open rotor terminal and points P and Q the rotor terminals shorted through the external resistor, point O being the center of the resistor. As the secondary resistance varies from infinity to zero, P and Q trace out the semicircles indicated. The maximum line-to-line voltage thus is seen to be about 2.3 times normal, for an external resistance of about 1.3 times the total leakage reactance. To account for the rotor resistance, points P and Q should be located on the same line, but a little closer together; they thus trace out

---

Paper 41-83, recommended by the AIEE committee on industrial power application, and presented at the AIEE North Eastern District meeting, Rochester, N. Y., April 30–May 2, 1941. Manuscript submitted November 16, 1940; made available for preprinting March 4, 1941.

C. MacMillan and G. K. Carter are both of General Electric Company, Schenectady, N. Y.

The authors wish to thank H. Maxwell for providing the opportunity of making this study and arranging for the tests, and J. A. VanLund for assistance in taking tests.

1. For all numbered references, see list at end of paper.

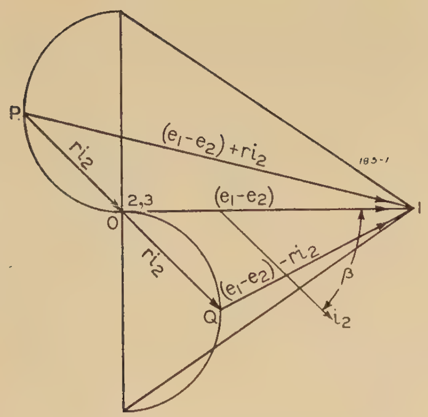

Figure 1. Vector diagram of rotor voltages, single-phase rotor, polyphase stator

curves slightly inside of the semicircles shown.

The conclusions drawn from this visualization are confirmed by an analysis by the two-axis method (appendix A).

C. Single-Phase Rotor and Single-Phase Stator

The operation of an induction motor with single-phase stator and rotor has been the subject of study for some time, both qualitatively and quantitatively. Steinmetz[7] discusses this connection under the heading of reaction machines, of which it is one type, and points out a number of interesting characteristics particularly associated with synchronous operation. Lyon[4] makes an analysis by symmetrical components, applying principles found useful in the case of the other types of single-phase operation. This analysis has been extended in a later paper,[11] which gives the equivalent circuit in the form of a ladder network.

Kron[9] has indicated symbolically the analytical solution in terms of a two-phase machine. A similar analysis may be based on the three-phase machine equations of Stanley,[12] also a two-axis resolution. Solutions by both of these methods were carried out for this study, resistance and saturation being neglected. The steady-state solution of Stanley's equations is outlined in appendix B. This solution indicates that the maximum voltages occur at a speed slightly below synchronism and are repeated twice in each slip cycle. The shapes of the calculated rotor and stator voltage waves at two points in the slip cycle are shown in figures 2 and 3. The maximum line-to-line voltage for the rotor is $\sqrt{3}X_m/2X_0$ times normal peak line-to-line voltage; for the stator, the ratio is $\sqrt{3}(X_m-X_0)/2X_0$.

In order to visualize the machine conditions corresponding to this state of operation, reference may be made to figures 4 and 5, which represent diagrammatically the physical arrangements of the machine parts and the approximate flux relations.

The voltages include components due to (a) transformer effects and (b) their modification due to speed of rotation. The first component is most easily recognized in the stationary condition. At any angle θ between the magnetic axes of the single-phase rotor winding and single-phase stator, the former may be assumed replaced by two quadrature coils in series, one of which is in maximum inductive relation to the stator winding, the other in noninductive relation with the excited stator phase, but in maximum inductive relation with the idle stator winding. There is thus a double transformation of stator impressed voltage into the idle stator and rotor windings involving a ratio of transformation dependent upon the angular position of the rotor axis, as illustrated in figure 6. With this variation of transformer ratio there is a corresponding variation of flux density, and of the additional voltage due to speed under running conditions.

When the motor is running, the machine voltages may be thought of as consisting of a speed voltage and also a transformer voltage. Since the curves of induced voltage of figure 6 might be thought of as proportional to the curves of "total flux of induction" for the open coils, the maximum speed voltage at any rotor angle, for constant rotor speed, may be thought of as proportional to the slope of these curves, or to the rate of change of "total flux of induction" with respect to angle (i.e., time). To this speed voltage must be added the transformer voltage itself; and for line-to-line quantities the effects of the excited phases must be considered.

Comparison may now be made with

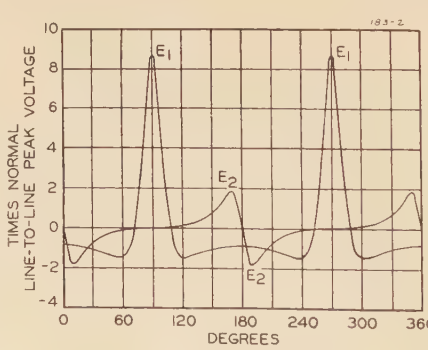

Figure 2. Calculated rotor voltage waves, single-phase rotor single-phase stator, $L_m/L_1 = 10$

E_1—At instant of maximum peak voltage
E_2—At one-quarter slip frequency cycle later

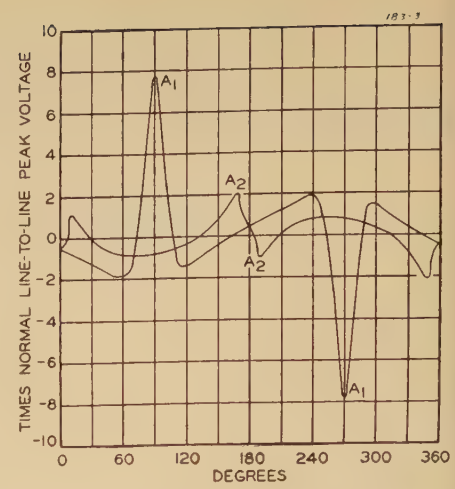

Figure 3. Calculated stator voltage waves, single-phase rotor single-phase stator, $L_m/L_1 = 10$

A_1—At instant of maximum peak voltage
A_2—At one-quarter slip frequency cycle later

the calculated voltage curves of figures 2 and 3. It is seen that the high-voltage curves fall off from their maxima to zero in about 17 degrees, as shown by the slopes in figure 6. They then acquire smaller negative values, which are appreciably shifted by the transformer and excited-phase voltages.

It is important to note from this analysis that, although very high voltages may exist, they are not the result of correspondingly high fluxes but of high rates of change of flux. Consequently, the effects of saturation will not be so great as might be supposed. The stator resistance should slightly reduce the magnitude of the currents and fluxes and introduce some phase shift; normal rotor resistance would also be expected to have a relatively small effect, but large values of external resistance would appreciably alter the impedance and result in lower voltages.

Of more importance in many practical cases is the impedance of the power source. This in effect adds to the motor impedances and reduces the current and voltage peaks accordingly. Including transformers as part of the source, the larger the system relative to the motor, the more closely are the theoretical voltage ratios approached.

Experimental Results

Tests were made on a standard three-phase wound-rotor induction motor rated 30 horsepower, 1,200 rpm, 60 cycles, 220/440 volts; the ratio X_m/X_0 for this machine, by test, was 12.8; the ratio of total resistance to total leakage reactance was 0.25. For some of the tests a

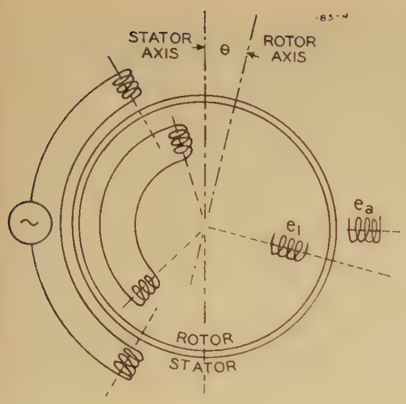

Figure 4. Diagrammatic sketch of three-phase induction motor operating single-phase on both stator and rotor

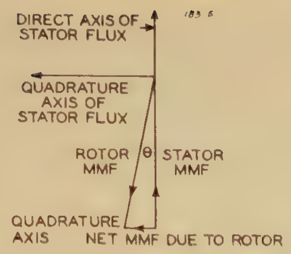

Figure 5 (above). Diagram illustrating vector flux and magnetomotive force relations of figure 4

standard cam-operated controller was used, to simulate operating conditions; in other cases knife switches were used, to give more positive control of the timing.

Prior to the running tests, curves of induced voltage versus rotor position were taken. For these, the stator was excited at a fixed voltage and all line-to-line voltages were measured by voltmeter as a function of rotor position, readings being taken with the rotor blocked. Since in some cases short-circuited rotor phases were involved, only one-fourth rated voltage was applied.

For the running tests, the motor was operated without load, giving a normal speed slightly below synchronism. Observation by means of a cathode-ray oscilloscope gave sufficient confirmation of the analysis for the two cases of three-phase single-phase operation to permit restriction of the further work to the more troublesome case of single-phase single-phase operation. For that case, the magnetic oscillograph was used to furnish permanent records.

Table I shows the comparison of the test and calculated voltage ratios, all on a line-to-line basis, for the single-phase single-phase case. All of these are steady-state voltages; in some of the oscillograms there was evidence of initial transient voltages, higher than the steady-state voltages, which appeared to build up under contactor vibration. Records of this sort of transient condition were obtained only for some of the lower voltage conditions in table I, the maximum observed transient peak being about 30 per cent greater than the corresponding steady-state peak.

Sample wave forms are shown in figure 7, which may be compared with the calculated wave forms of figures 2 and 3.

The tests indicate that resistance, in the normal range, slightly lowers the voltages. The effect of saturation is not indicated for the running condition, though this may be the explanation of the unusual standstill voltages (measured by voltmeter). System impedance, as shown by the effect of removal of the transformer, may modify the peaks to a large degree. Even without the transformer, however, the impedance of the system used was relatively high, resulting in the impressed voltage distortion evident in figure 7.

Table I. Test and Calculated Line-to-Line Voltages for Single-Phase Single-Phase Operation

	Rotor	Stator
Standstill: Ratios of rms voltages		
Calculated	1.61	1.93
Test	1.85	2.15
Running: Ratios of peak voltages		
Calculated (for an infinite bus)	11.1	10.2
Test: Motor connected direct to lines; rings shorted	5.0	4.45
Motor connected through transformer; rings shorted	3.35	3.05
Transformer in; external resistance in rotor circuit four times rotor resistance	3.0	2.55
Transformer in; rings shorted; odd rotor line tied to shorted rings with 300 times rotor phase resistance	1.1	1.0

Well-marked depressions in the supply voltage (wave B, figure 7), occurring simultaneously with maximum peak voltages in stator and rotor open phases, indicate the effect of limited supply system capacity in reducing the latter test voltage below calculated values. The wave shape is modified by this and other factors, so that the best comparison with calculated wave shape A (figure 3) is not obtained with the maximum induced voltages but at intervals of several impressed voltage cycles earlier or later, where the distortion at the peak has diminished. At these intermediate points in the quarter slip cycle between A_1 and A_2 states (figure 3), the similarity between the oscillogram and the calculated wave shape A_1 may be recognized more clearly despite the relative reduction of the oscillogram peak value.

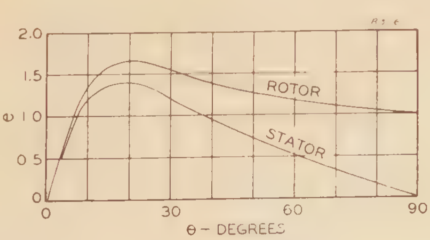

Figure 6. Ratio of induced voltage in open phase to normal phase voltage, as a function of rotor angular position for $L_m/L_l=10$

Appendix A. Maximum Voltage for Single-Phase Rotor in Three-Phase Stator

The two-axis resolution suggested by Stanley[12] will be applied. Stator resistance is neglected and the rotor resistance is combined with the external resistance, giving a total of r per phase; secondary terminal voltages are taken to the middle of the secondary resistor. With balanced stator terminal voltage (an infinite bus) and with rotor terminal 1 open, the conditions for equations 16 of reference 12 are

$$e_a = V \sin \omega t$$

$$e_b = V \sin (\omega t - 2\pi/3)$$

$$e_c = V \sin (\omega t + 2\pi/3)$$

$$i_a + i_b + i_c = e_2 - e_3 = i_1 = i_2 + i_3 = 0$$

The equations thus become

$$L_0 p i_a - \frac{2\sqrt{3}}{3} M_0 p(i_2 \sin \theta) = V \sin \omega t$$

$$-\frac{\sqrt{3}}{3} L_0 p(i_a + 2i_c) + \frac{2\sqrt{3}}{3} M_0 p(i_2 \cos \theta) = -V \cos \omega t$$

$$M_0 p i_a - \frac{\sqrt{3}}{3} M_0 [p\theta](i_a + 2i_c) - \frac{2\sqrt{3}}{3} l_0 (\sin \theta) p i_2 = \frac{2}{3} e \cos \theta + \frac{2\sqrt{3}}{3} r i_2 \sin \theta$$

$$-M_0 [p\theta] i_a - \frac{\sqrt{3}}{3} M_0 p(i_a + 2i_c) + \frac{2\sqrt{3}}{3} l_0 (\cos \theta) p i_2 = \frac{2}{3} e \sin \theta - \frac{2\sqrt{3}}{3} r i_2 \cos \theta$$

where

$$e = e_1 - e_2$$

These equations may be integrated, giving steady-state solutions for e and i_2. The actual terminal voltages are given by $e_R = (e_1 - e_2) \pm r i_2$. These voltages are shown in the vector diagram, figure 1. The maximum for motor operation is obtained for $[p\theta] = -\omega$, when

$$e_R = \frac{3M_0}{L_0} V \sin 2\omega t \pm \frac{\frac{\sqrt{3}M_0}{L_0} V r \sin (2\omega t - \beta)}{\sqrt{4\omega^2 \left(\frac{M_0^2}{L_0} - l_0 \right)^2 + r^2}}$$

$$\beta = \tan^{-1} \frac{-r}{2\omega \left(\frac{M_0^2}{L_0} - l_0 \right)}$$

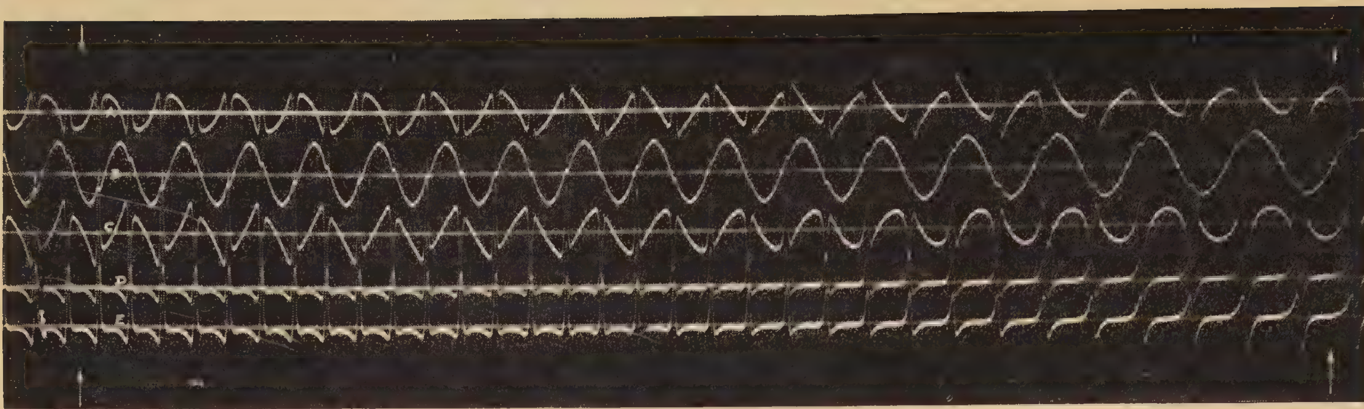

The peak value of normal rotor line-to-line voltage, obtained by setting $[p\theta]=0$ and $r=\infty$, is $|e_R|=\sqrt{3}M_0V/L_0$. Also the short-circuit inductance referred to the rotor is $l_l=l_0-M_0^2/L_0$. Thus,

$$\frac{e_R}{|e_R|}=\sqrt{3}\sin 2\omega t \pm \frac{r\sin(2\omega t-\beta)}{\sqrt{r^2+X_l^2}}$$

$$\beta=\tan^{-1} r/X_l$$

As r varies from 0 to ∞, the diagram of figure 1 is traced out.

Maximum voltage occurs for $r/X_l=1.33$; it is $e_R/|e_R|=2.30$. If part of r is internal to the machine, that fraction of the resistance drop is subtracted (vectorially) from the terminal voltage.

Appendix B. Maximum Voltage for Single-Phase Rotor in Single-Phase Stator

Stanley's equations will be applied to this case, as in appendix A, assuming sinusoidal applied voltage (an infinite bus) with all resistance neglected. The terminal conditions then are

$$i_1=i_a=i_2+i_3=i_b+i_c=e_2-e_3=0$$

$$e_b-e_c=V\cos\omega t$$

The equations to be solved are as follows:

$$\frac{-2\sqrt{3}}{3}M_0p(i_2\sin\theta)=e_a$$

$$2L_0pi_b+2M_0p(i_2\cos\theta)=V\cos\omega t$$

$$M_0[p\theta]i_b-l_0(\sin\theta)pi_2=(\sqrt{3}/2)e_1\cos\theta$$

$$M_0pi_b+l_0(\cos\theta)pi_2=(\sqrt{3}/2)e_1\sin\theta$$

Finally evaluated, the steady-state phase voltages are the following:

$$e_1=\frac{\dfrac{l_0V}{\sqrt{3}M_0}}{\dfrac{L_0l_0}{M_0^2}-\cos^2\theta}\left\{\sin\theta\cos\omega t+\left[\frac{p\theta}{\omega}\right]\cos\theta\sin\omega t-\frac{2\left[\dfrac{p\theta}{\omega}\right]\sin^2\theta\cos\theta\sin\omega t}{\dfrac{L_0l_0}{M_0^2}-\cos^2\theta}\right\}$$

$$e_a=\frac{\dfrac{V}{\sqrt{3}}}{\dfrac{L_0l_0}{M_0^2}-\cos^2\theta}\left\{(1/2)\sin 2\theta\cos\omega t+\left[\frac{p\theta}{\omega}\right]\cos 2\theta\sin\omega t-\frac{(1/2)\left[\dfrac{p\theta}{\omega}\right]\sin^2 2\theta\sin\omega t}{\dfrac{L_0l_0}{M_0^2}-\cos^2\theta}\right\}$$

The line-to-line voltages are

$$e_R=(3/2)e_1$$

$$e_S=-(3/2)e_a\pm(1/2)V\cos\omega t$$

Maximum values for e_R occur when $\cos\theta=\pm1$, $\sin\omega t=1$; then

$$e_{R\max}=\frac{\dfrac{\sqrt{3}l_0}{2M_0}V}{\dfrac{L_0l_0}{M_0^2}-1}$$

Maxima of e_S occur when $\cos 2\theta=\pm1$, $\sin\omega t=1$; then

$$e_{S\max}=\frac{\dfrac{\sqrt{3}V}{2}}{\dfrac{L_0l_0}{M_0^2}-1}$$

Calling the stator self-inductance L_0 the magnetizing inductance L_m, and the short-circuit inductance $L_0-M_0^2/l_0$ the total leakage inductance L_l, the ratios of the peak voltages as calculated to the normal peak voltages are

$$\frac{e_R}{|e_R|}=\frac{\sqrt{3}}{2}\frac{L_m}{L_l}$$

$$\frac{e_S}{|e_S|}=\frac{\sqrt{3}}{2}\left(\frac{L_m-L_l}{L_l}\right)$$

The former corresponds to equation $24f$ of reference 2.

In practice, the motor may not be connected to a system of low enough impedance to be taken as an infinite bus. In this case, if the generated internal voltage is substantially constant, it may be taken as the source, with the generator reactance transferred to fictitious motor circuits; the generator and line reactances would be expected to have approximately the effect of additions to L_m and L_l in the voltage expressions, giving

$$\frac{e_R}{|e_R|}=\frac{\sqrt{3}}{2}\frac{L_m+L_{ext}}{L_l+L_{ext}}$$

$$\frac{e_S}{|e_S|}=\frac{\sqrt{3}}{2}\frac{L_m-L_l}{L_l+L_{ext}}$$

These voltages would apply to fictitious points within the generator; the actual motor terminal values would differ slightly.

The standstill, or transformer, voltages can also be obtained from the foregoing expressions by setting $[p\theta]=0$. Then the line-to-line voltages to the open terminals are

$$\frac{e_R}{|e_R|}=\frac{\dfrac{\sqrt{3}}{2}\dfrac{L_0l_0}{M_0^2}\sin\theta}{\dfrac{L_0l_0}{M_0^2}-\cos^2\theta}$$

$$\frac{e_S}{|e_S|}=\frac{\dfrac{\sqrt{3}}{4}\sin 2\theta}{\dfrac{L_0l_0}{M_0^2}-\cos^2\theta}\pm\frac{1}{2}$$

The respective maxima are

$$e_R=\frac{\sqrt{3}L_m}{4\sqrt{L_l(L_m-L_l)}}$$

$$e_S=\frac{1}{2}+\frac{\sqrt{3}(L_m-L_l)}{4\sqrt{L_mL_l}}$$

Figure 7. Oscillogram of operating conditions with single-phase stator excitation and with single-phase short circuit on rotor, 30-horsepower, 12,00-rpm, 3-phase, 60-cycle, 220/440-volt induction motor

A—Stator line-to-line voltage
B—Stator line-to-line voltage (impressed)
C—Stator line-to-line voltage
D—Rotor line-to-line voltage
E—Rotor line-to-line voltage

For measured peak values, see table I

Appendix C. Nomenclature

i_a, i_b, i_c = stator phase currents
i_1, i_2, i_3 = rotor phase currents
e_a, e_b, e_c = stator phase terminal voltages
e_1, e_2, e_3 = rotor phase terminal voltages

Photographic Study of A-C Arcs in Flowing Liquids

J. SLEPIAN
FELLOW AIEE

T. E. BROWNE, JR.
ASSOCIATE AIEE

I. Introduction

THE importance of fluid flow in aiding arc extinction in circuit interrupters has long been known. Two general types of explanation of the large effect found have been offered. Slepian[1,2,3] who seems to have been the first to stress the importance of the motion of the gases liberated by the arc from the surrounding oil or solid insulation in oil breakers and expulsion fuses, sought the explanation in reduced arc section at current zero, and increased diffusion rate of ions and molecules arising from the turbulence. Other investigators have expressed similar views, at least in part.[4,5]

Another theory attributes the rapidly rising dielectric strength at current zero to the cutting of the arc path by a film of cool, un-ionized fluid, which grows in thickness at a rate comparable with the fluid velocity, so that a simple relation may be expected between fluid velocity, fluid dielectric strength, and limiting recovery rate of circuit voltage at which extinction takes place. Such a relation is said to have been established experimentally for an oil flow breaker,[6,7,8] but this has not been universally accepted.[9]

Paper 41-92, recommended by the AIEE committee on protective devices, and presented at the AIEE North Eastern District meeting, Rochester, N. Y., April 30–May 2, 1941. Manuscript submitted November 6, 1939; made available for preprinting March 14, 1941.

J. SLEPIAN and T. E. BROWNE, JR., are both with Westinghouse Electric and Manufacturing Company, Mr. Slepian in East Pittsburgh, Pa., and Mr. Browne in Trafford, Pa.

1. For all numbered references, see list at end of paper.

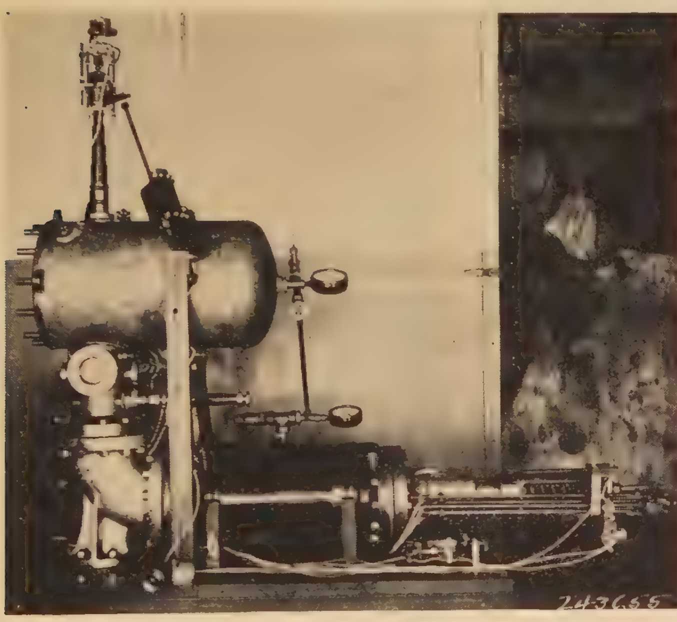

Figure 1. General view of the test structure

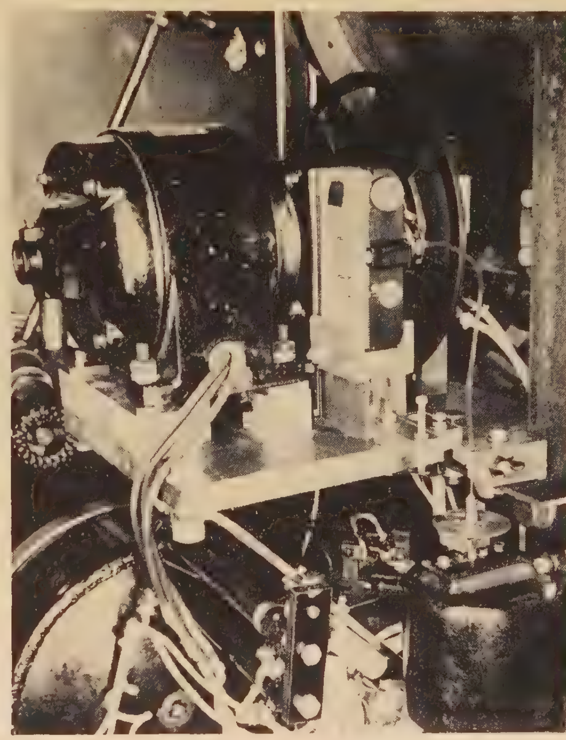

Figure 2. Camera with its synchronous shutter

---

e_S = stator line-to-line voltage
e_R = rotor line-to-line voltage
V = maximum value of impressed voltage
$\omega/2\pi$ = frequency of impressed voltage
θ = rotor position angle
$[p\theta]$ = rotor angular velocity
L_0 = stator inductance per phase
l_0 = rotor inductance per phase
M_0 = mutual inductance between rotor and stator per phase
L_l = leakage inductance referred to the stator
l_l = leakage inductance referred to the rotor
L_m = stator magnetizing inductance
L_{ext} = inductance of supply system
X_l = reactance corresponding to l_l
X_m = reactance corresponding to L_m
X_0 = reactance corresponding to L_l
r = secondary phase resistance

References

1. Discussion by J. H. Fortenbach of Edith Clarke, C. N. Weygandt, and C. Concordia's paper, OVERVOLTAGES CAUSED BY UNBALANCED SHORT CIRCUITS. AIEE TRANSACTIONS, volume 57, 1938 (August section), pages 453–66.

2. SYNCHRONOUS MACHINES—IV, R. E. Doherty and C. A. Nickle. AIEE TRANSACTIONS, volume 47, 1928, pages 482–92.

3. INDUCTION MOTORS UNDER UNBALANCED CONDITIONS, E. O. Lunn. AIEE TRANSACTIONS, volume 55, 1936 (April section), pages 387–93.

4. APPLICATIONS OF THE METHOD OF SYMMETRICAL COMPONENTS, W. V. Lyon. McGraw-Hill Book Company.

5. SYMMETRICAL COMPONENTS, Wagner and Evans. McGraw-Hill Book Company.

6. THEORETICAL ELEMENTS OF ELECTRICAL ENGINEERING, C. P. Steinmetz. McGraw-Hill Book Company.

7. THEORY AND CALCULATION OF ELECTRICAL APPARATUS, C. P. Steinmetz. McGraw-Hill Book Company.

8. THE CROSS-FIELD THEORY OF ALTERNATING CURRENT MACHINES, H. R. West. AIEE TRANSACTIONS, volume 45, 1926, pages 466–74.

9. APPLICATION OF TENSORS TO ROTATING ELECTRICAL MACHINERY, G. Kron. *General Electric Review.*

10. THEORY AND DESIGN OF ELECTRICAL MACHINES, F. Creedy. Pitman and Sons.

11. AN EXTENSION OF THE METHOD OF SYMMETRICAL COMPONENTS USING LADDER NETWORKS, W. V. Lyon. AIEE TRANSACTIONS, volume 59, 1940 (October section), pages 1025–30.

12. AN ANALYSIS OF THE INDUCTION MACHINE, H. C. Stanley. AIEE TRANSACTIONS, volume 57, 1938, pages 751–5.

13. ELECTRICAL ENGINEERING PAPERS, B. G Lamme. Westinghouse Electric and Manufacturing Company.

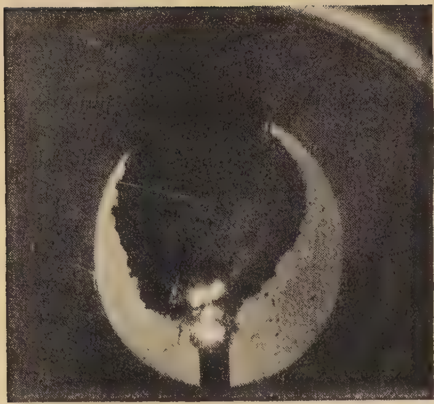

Photograph 272
Taken at current zero
Water velocity = 11 feet per second
Pressure at arc = 1 atmosphere
Circuit voltage = 2,300
Current = 530 amperes

Photograph 273
Taken 0.001 second after last current zero
Water velocity = 15 feet per second
Pressure at arc = 1 atmosphere
Circuit voltage = 2,300
Current = 509 amperes

Photograph 274
Taken one half-cycle after last current zero
Water velocity = 15 feet per second
Pressure at arc = 1 atmosphere
Circuit voltage = 2,300
Current = 515 amperes

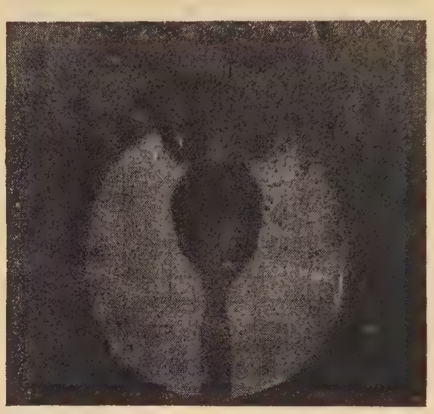

Photograph 237
Taken one-tenth half-cycle after last current zero
Water velocity = 40 feet per second
Pressure at arc = 1 atmosphere
Circuit voltage = 2,300
Current = 530 amperes

Figure 3. Arc photographs under water

With this uncertainty as to the nature of the arc extinction process in fluid flow, it is highly desirable that direct experimental investigation be made into the state of the arc near current zero. Short exposure photography near current zero would seem to be a powerful means of attack. High-speed motion pictures, at 5,000 frames per second, have been taken of arcs in a gas blast.[10,11] These show greatly reduced arc sections arising from the blast, but fail to show conclusively any sharp dividing line between a rapidly receding highly ionized luminous region and a growing dark region corresponding to freshly introduced gas in the arc path. Also, a criticism might be made that the location of the current zero is not determined with respect to the pictures. One cannot be certain that the continuous luminous column representing the arc space may not have existed for many microseconds after current zero, since it is quite possible that such a fine column, subjected to the local micro-turbulence inherent in the gas blast and high-temperature gradients, might have the capacity to withstand considerable voltage without breakdown.

Hoping to shed more light on these questions, particularly for the case where the flowing fluid was liquid, a series of investigations were carried on at the Westinghouse Research Laboratories, of which this is the first report.

The immediate objectives of this research were: (1) to determine the effect on the arc's interrupting ability of independent variations in fluid velocity, static pressure, type of fluid, arc length, electrode shape, baffle arrangements, and circuit natural frequency; and (2) to photograph the arc under these controlled conditions, hoping thus to learn something about the actual mechanism of the interaction between the flowing liquid and the arc in its gas bubble, especially near current zero. In this paper only the photographic results will be described.

II. Apparatus

An arc drawing structure with associated pump was so designed and built that the arc could be subjected momentarily to either longitudinal or transverse oil or water velocities up to 200 feet per second in a 3-inch channel and to independently controlled static pressures up to 15 atmospheres. Figure 1 shows the general arrangement of the structure. The fluid is directed upward from the horizontal pump cylinder through a Micarta and glass liner within the vertical tube and into the discharge tank above. Windows are provided on opposite sides of the arc tube at the point where the arc is drawn.

For photographing the arc, a miniature camera is mounted in front of one of the windows, as shown in figure 2.[12] It is provided with the synchronously driven rotating shutter shown for taking pictures of the arc and its associated gas bubble at any point on the current cycle. Contacts on a rotating drum attached to the shutter disk serve to synchronize the camera shutter with it and to record on an oscillogram exactly when the picture was taken. Because of the importance of that moment, pictures were taken generally at or near to current zero, the exposure time (with a much narrower slit than shown) being about $^1/_{3,000}$ second. The arc bubble was shown in silhouette against a very brightly illuminated background. In addition to the magnetic oscillograph, a cathode-ray oscillograph was available for observing the arc reignition or extinction voltage at current zero. A few high-speed moving pictures of the arc at about 2,000 frames per second were also taken.

III. Results

Such a large number of arc photographs have been taken that only a summary of the observations illustrated by a few samples can be presented here. Five hundred-ampere arcs, 1 and 2.5 centimeters long between one-fourth-inch (0.635 centimeter) electrodes subjected to parallel flowing oil and water were studied

first. The bubble shapes with oil and water were apparently identical, but because of greater transparency and the absence of carbon, the photographs with water were generally clearer than those with oil.

Parallel Water Flow

In figures 3 and 4, photographs 272, 273, 274, 237, and 284, are all of tests with parallel water flow. All were taken with the shutter adjusted to open near current zero. In 272, taken at current zero, the velocity (11 feet per second) is so low that droplets of incandescent copper can be seen falling against the flow and the gas bubble, or cloud, is large. In 273 the velocity was slightly greater and the photograph was taken nearly 0.001 second after the arc had been extinguished by opening the "back-up" circuit breaker. Here, streaks of light indicate that the arc terminals were still white hot, and it is evident that the fluid had not yet completely closed in between the electrodes, even though nearly 1,000 microseconds had elapsed since the disappearance of the arc. In 274, taken under similar conditions but one half-cycle after arc extinction, the interelectrode space had been swept clear except for a trail of bubbles still arising from the lower arc terminal. Remnants of the gas bubble were still visible around the upper electrode. The conditions of 237 were similar to those of 273, except that the velocity was considerably greater. Here no incandescence can be seen at the arc terminals, but some of the background light was transmitted through the "neck" of the bubble still existing between the electrodes. Comparison with 273 shows that the increase in velocity resulted in a still smaller tendency for the flow to close in above the lower electrode. This effect of fluid velocity is even more clearly illustrated by 284, in which, at a still higher velocity, the gas bubble at current zero just filled the space in the "wake" of the lower electrode and extended almost unchanged in section all the way to the upper electrode, which was 2.5 centimeters away instead of 1 centimeter, as in the foregoing pictures.

Of especial importance for the theory is the fact that the arc interrupted the 4,600-volt reactive circuit here, showing that this gas bubble of about one-fourth inch diameter was able to withstand $\sqrt{2}\times 4{,}600=6{,}500$ volts or a gradient of 2,600 volts per centimeter, shortly (less than 400 microseconds) after this current zero without the aid of any interposed layer of liquid dielectric. Actually, the oscillogram of the test showed that the arc

Photograph 284
Taken at last current zero
Water velocity = 87 feet per second
Pressure at arc = 1 atmosphere
Circuit voltage = 4,600
Current = 445 amperes

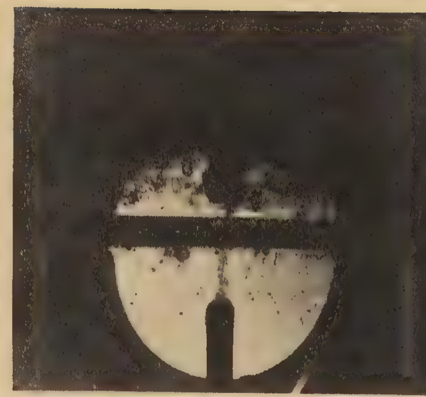

Photograph 299
Taken one half-cycle after last current zero
Maximum water velocity = 45 feet per second
Discharge pressure = 1 atmosphere
Circuit voltage = 2,300
Current = 442 amperes

Photograph 301
Taken just before current zero
Maximum water velocity = 38 feet per second
Discharge pressure = 1 atmosphere
Circuit voltage = 2,300
Current = 441 amperes

Photograph 302
Taken 1/40 half-cycle before last current zero
Maximum water velocity = 38 feet per second
Discharge pressure = 1 atmosphere
Circuit voltage = 4,600
Current = 474 amperes

Figure 4. Arc photographs under water

restruck one half-cycle later, presumably by thermal breakdown of the water[13] which must have by then entirely displaced the original gas bubble.

Nonparallel Water Flow

In addition to parallel flow, many other more complicated flow arrangements were studied. The first and simplest directing structure was merely a thin one-fourth inch thick) brass diaphragm placed across the flow channel and provided with a central round hole (usually one inch in diameter) through which the arc was drawn by the one-fourth-inch rod electrodes. Its location with respect to the electrodes in early tests is shown in photograph 299 of figure 4, taken one half-cycle after interruption of the circuit by the arc. The flow conditions roughly approximate those with many forms used in practice. Photo. 301, taken just before current zero, is the clearest obtained of a bubble form very often observed under these conditions, pear-shaped with the constricted neck only partially filling the outflow orifice. In contrast is 302, which was taken under apparently almost identical conditions, but which is entirely different. Such random variation in bubble size and shape was found to be characteristic of this type of flow at these moderate velocities. That bubble size was not, as one might expect, a function of instantaneous current is further shown in figure 5, by photograph 356, which was taken at peak current under otherwise similar conditions and shows a bubble of almost the same size and shape as that of 301 where the instantaneous current was near zero.

Associated with the variation in bubble

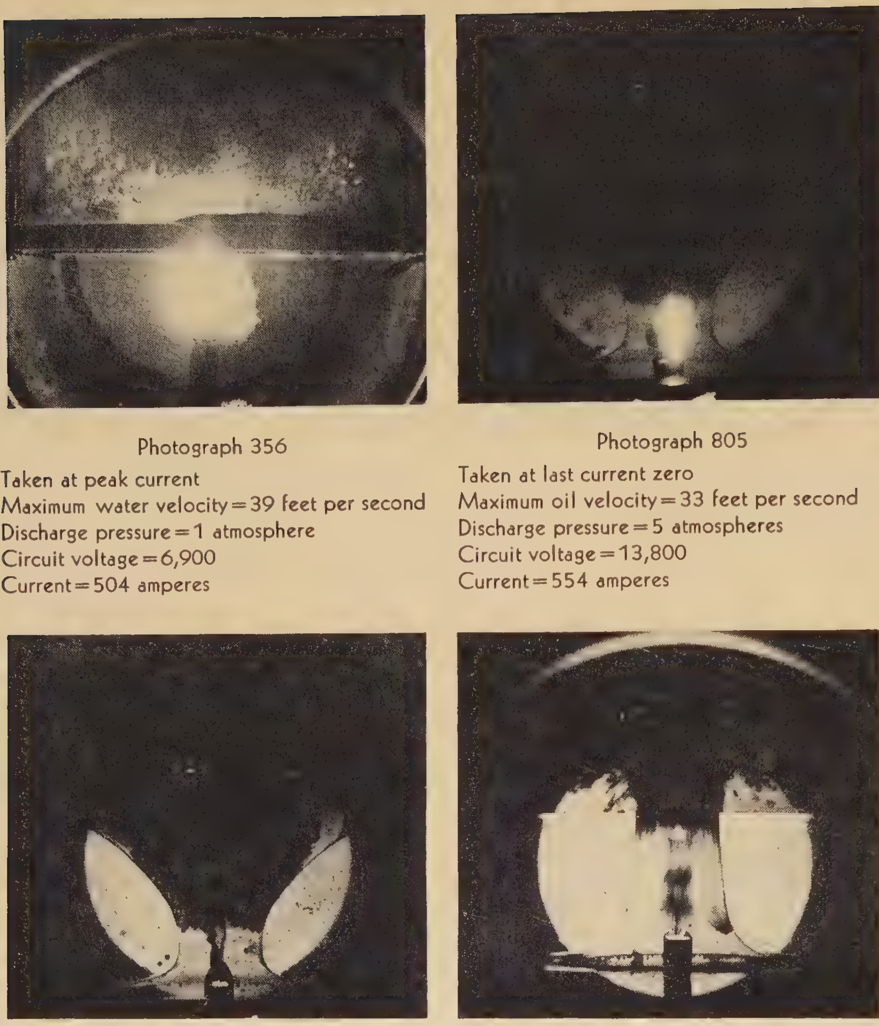

Photograph 356
Taken at peak current
Maximum water velocity = 39 feet per second
Discharge pressure = 1 atmosphere
Circuit voltage = 6,900
Current = 504 amperes

Photograph 805
Taken at last current zero
Maximum oil velocity = 33 feet per second
Discharge pressure = 5 atmospheres
Circuit voltage = 13,800
Current = 554 amperes

Photograph 806
Taken one half-cycle after last current zero
Maximum oil velocity = 23 feet per second
Discharge pressure = 5 atmospheres
Circuit voltage = 13,800
Current = 547 amperes

Photograph 890
Taken 1/20 half-cycle after last current zero
Maximum oil velocity = 22 feet per second
Discharge pressure = 1 atmosphere
Circuit voltage = 13,800
Current = 1,890 amperes

Figure 5. Arc photographs under water and oil

size was the variable interrupting performance of the arc under these conditions from one half-cycle to the next. The correlation between bubble size at current zero and tendency for the arc to reignite is illustrated well by photographs 301 and 302. Even though the circuit voltage in the case of 302 was 4,600 as compared with 2,300 for 301, the arc was extinguished after 302, but restruck with no appreciable pause after 301. Clearly, as one might expect, the small bubble was a very much better arc extinguisher than the large bubble.

Flow Oscillations

These wide and apparently random variations in bubble volume and interrupting ability at current zero are apparently due to the characteristically oscillatory nature of the flow of liquid and gas around the arc and through an orifice. These oscillations, which were first revealed by large-amplitude pressure variations in the vicinity of the arc and by corresponding periodic arc voltage peaks, always occurred when the conditions were such as to permit the formation of an appreciably large gas bubble on the high-pressure side of the orifice. The frequency, usually a few hundred cycles per second, depended linearly on the maximum fluid velocity through the orifice and was relatively independent of the orifice size and shape, and also of the arc current and arc length. The relation was $f=5V$ cycles per second, where V is the fluid velocity in feet per second. There was little, if any, tendency for the oscillation to synchronize itself with the 60-cycle current. Analysis of the oscillographic pressure records and of the mechanics of the flow indicated that periodic growth and collapse of the gas bubble surrounding the arc was an essential part of the oscillation.

Because of the lack of synchronization of the bubble oscillation with the current zero, the bubble diameter existing at current zero would be expected to vary in a random manner as it did in fact. Variability in interrupting performance was thus also explained. This oscillation could be prevented at moderate currents by so proportioning the flow channel and adjusting the driving pressure that bubble growth in front of the orifice was effectively prevented. Such arrangements gave somewhat better average interrupting performance with water but not with oil.

Photographs With Oil

Photographs 805, 806, 890, 975, 989, 990, 991, and 976 of figures 5, 6, and 7 are samples of a great number obtained while studying the interrupting ability of the arc with oil flow directed by variously shaped orifices. As these orifices were made of a transparent plastic material (Lucite), the effect of a cross-section view was obtained. Photographs 805 and 806 were taken under nearly similar conditions, except that 805 was at the last current zero and 806 followed the last current zero by one half-cycle. In 805, the arc bubble is comparatively small, but still large enough so that the flow was oscillatory. In spite of the design to accentuate radial flow, 806 shows that the flow had not completely closed in over the lower electrode even after one half-cycle, and that the arc terminal there was still luminous. Somewhat in contrast is 890, taken only $^1/_{20}$ half-cycle (400 microseconds) after extinction of a 2,000-ampere arc in an orifice of different shape. The arc terminals were still glowing brightly but the interelectrode space appears to have been swept almost clear of gas even at this comparatively low velocity of 22 feet per second (11 feet per second at the tip of the lower electrode).

A still different electrode and orifice arrangement is shown in photographs 975 and 976 referred to above. These apparently show successive stages near the beginning of the growth of an arc bubble. Strangely, extinction occurred after 975, but not after 976. All of these pictures illustrate the characteristically very large random variations in appearance of arc bubbles with orifice flow and these last also show the frequent impossibility of distinguishing between bubbles in which the arc will just reignite and those in which the arc will just fail to re-

ignite. This lack of distinction was characteristic of bubbles, whose volumes were always kept small by the flow, such as those in photographs 989, 990, and 991. These were all taken under identical conditions, except for the oil velocities, which were 209, 169, and 127 feet per second, respectively, measured at the constriction, which was here occupied by the arc. At the highest velocity some diminution in the bubble section may be noticed; but at 169 feet per second and 127 feet per second, which values were, respectively, above and below the critical value for ultimate arc extinction (143 feet per second), there was no detectable difference in the arc bubble appearance. However, it should be noted that photograph 990 was taken at a current zero prior to arc extinction.

More recently, sequence pictures have been obtained with a rotating-prism type high-speed motion picture camera[14] which reveal this bubble behavior clearly. The eight-frame sequence of figure 8 shows the gradual growth, collapse, and regrowth of an arc bubble under conditions similar to those of photographs 301 and 302 except that the fluid was oil flowing through the orifice at 68 feet per second, nearly twice as fast as in 301 and 302. The interval between successive pictures was about $^1/_{19}$ of a half-cycle, or 430 microseconds. Examination of the whole film leads to the conclusion that the current passed through a zero value in the vicinity of frames 4 and 5. Figure 9 is a similar sequence of an arc bubble like those of photographs 975 and 976 but also under oil flowing at considerably higher velocity. This sequence does not embrace a current zero. It is now revealed that photographs 975 and 976 represent near-minimum arc bubble sections which approximately coincided with current zeros only by coincidence.

Photograph 975
Taken 1/50 half-cycle before last current zero
Maximum oil velocity = 37 feet per second
Discharge pressure = 1 atmosphere
Circuit voltage = 13,800
Current = 490 amperes

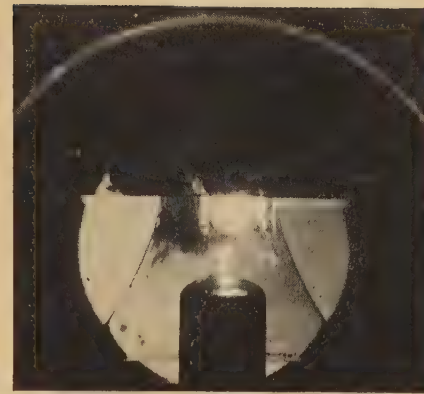

Photograph 976
Taken at current zero
Maximum oil velocity = 34 feet per second
Discharge pressure = 1 atmosphere
Circuit voltage = 13,800
Current = 486 amperes

Photograph 989
Taken 1/20 half-cycle before current zero
Maximum oil velocity = 209 feet per second
Discharge pressure = 1 atmosphere
Circuit voltage = 13,800
Current = 490 amperes

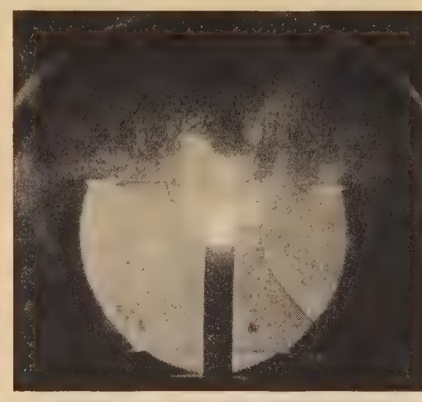

Photograph 990
Taken 1/20 half-cycle before current zero
Maximum oil velocity = 169 feet per second
Discharge pressure = 1 atmosphere
Circuit voltage = 13,800
Current = 490 amperes

Figure 6. Arc photographs under oil

IV. Conclusions

From a study of many hundreds of arc photographs represented here by only a few samples, the following conclusions have been drawn:

1. The gas bubble surrounding an arc under a flowing liquid is generally not displaced by a liquid barrier until some appreciable fraction of a half-cycle after the arc has been extinguished.

2. The existence of a large bubble section at current zero favors reignition of the arc while the existence of a small section favors its extinction.

3. Even under apparently identical conditions, the shape and size of the gas bubble may show very wide variations. These variations are the result of rapid bubble oscillations which are usually not synchronous with the arc current variation.

4. Where the arc bubble is uniformly small, there is no consistent difference between its appearance at a current zero at which the arc is extinguished and one at which it reignites, or between the characteristic bubble appearance at pressures or velocities just above the critical values for extinction and those just below these values.

With regard to the theory, it may be seen that conclusions 1 and 4 are wholly at variance with the idea that arc extinction *results from* the formation between the electrodes at current zero of a growing barrier of dielectric liquid. These and conclusion 2 suggest, rather, that extinction or reignition of the arc is usually determined by conditions existing within the remanent gas bubble at or just before current zero. These conditions probably relate to the character of the gas flow within the bubble, such as can be de-

Figure 7. Arc photograph under oil

Photograph 991
Taken 1/20 half-cycle before current zero
Maximum oil velocity = 127 feet per second
Discharge pressure = 1 atmosphere
Circuit voltage = 13,800
Current = 490 amperes

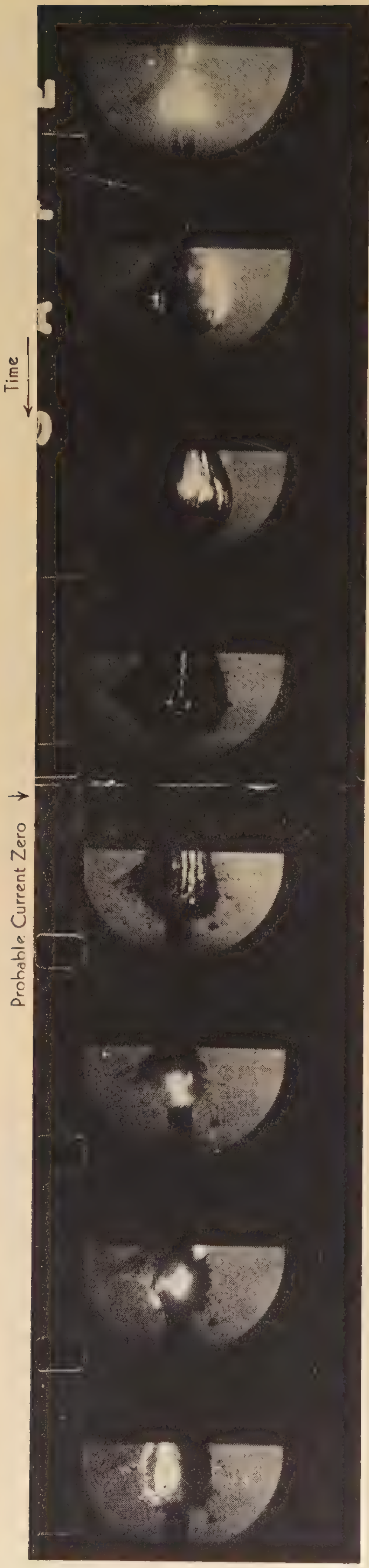

Figure 8 (left). Moving-picture sequence of arc under oil

Sequence taken at 2,300 frames per second

Oil velocity = 68 feet per second
Discharge pressure = 1 atmosphere
Circuit voltage = 13,800
Current = 500 amperes (rms)

scribed in terms of a mean velocity, and an intensity of turbulence. Once the arc has failed to reignite, of course, displacement of the bubble may follow very quickly.

Conclusion 3 seems to offer a plausible explanation for the well-known inconsistency of many types of fluid circuit breakers when tested near their interrupting limit.

References

1. Extinction of a Long A-C Arc, **J. Slepian.** Journal of the AIEE, volume 49, 1930, pages 310–14.

2. The Expulsion Fuse, **J. Slepian** and **C. L. Denault.** AIEE Transactions, volume 51, 1932, pages 157–65.

3. Displacement and Diffusion in Arc Extinction, **Joseph Slepian.** AIEE Transactions, volume 60, 1941 (April section), pages 162–7.

4. **O. Mayr,** *Elektrotechnische Zeitschrift,* volume 55, August 2, 1934, pages 757–60.

5. **F. Kesselring** and **F. Koppelman,** *Arch. f. Elektrot.,* volume 29, 1935, pages 1–33, and volume 30, 1936, pages 71–108.

6. The Oil-Blast Circuit Breaker, **D. C. Prince** and **W. F. Skeats.** AIEE Transactions, volume 50, 1931, pages 506–12.

7. **D. C. Prince** and **E. J. Poitras,** *Electric World,* Volume 97, February 28, 1931, pages 400–04.

8. The Theory of Oil-Blast Circuit Breakers, **D. C. Prince.** AIEE Transactions, volume 51, 1932, pages 166–70.

9. Discussion by **J. Slepian** of **T. E. Browne, Jr.'s** paper, Extinction of A-C Arcs in Turbulent Gases. AIEE Transactions, volume 51, 1932, pages 193–6.

10. **O. Mayr,** *Elektrotechnische Zeitschrift,* volume 53, January 28, pages 75–81; February, 11, 1932, pages 121–3.

11. **J. Biermanns,** *Allgemeine Elektrizitäts-Gesellschaft,* Revised Reprint from *Elektrotechnische Zeitschrift,* volume 59, February 17 and 24, 1938, pages 165–8 and 194–7.

12. **T. E. Browne, Jr.,** *Photo Technique,* February 1941, pages 52–4.

13. Dielectric Strength of Water in Relation to Circuit Interrupters, **J. Slepian, C. L. Denault,** and **A. P. Strom.** AIEE Transactions, volume 60, 1941, pages 389–95.

14. A Non-Intermittent High-Speed 16-Mm. Camera, **F. E. Tuttle.** *Journal of Society of Motion Picture Engineers,* volume 21, December 1933, pages 474–7.

Figure 9 (right). Moving-picture sequence of arc under oil

Sequence taken at 2,300 frames per second

Oil velocity = 56 feet per second
Discharge pressure = 1 atmosphere
Circuit voltage = 13,800
Current = 500 amperes (rms)

Theory of the Brush-Shifting A-C Motor—I

A. G. CONRAD
MEMBER AIEE

F. ZWEIG
ENROLLED STUDENT AIEE

J. G. CLARKE
ASSOCIATE AIEE

Synopsis: This is the first of a series of papers explaining the theory and principles of operation of the brush-shifting a-c motor. Operation of the machine, either as a motor or a generator, is explained on the basis of the superposition of currents. The theory of the primary current loci is developed for both high-speed and low-speed adjustments. A method of determining the primary current loci from no-load measurements is presented. Experimental data have shown the theory to be valid.

IN general, a-c polyphase motors are less adaptable to speed adjustment than are d-c motors. However, by use of a combination of regulating winding, a commutator, and brush-shifting facilities, a polyphase induction motor can be so constructed as to provide speed adjustment similar to that obtainable on a d-c shunt motor. These motors are essentially three winding motors. The primary winding placed on the rotor is supplied from the line through slip rings. The stator winding (see figure 1) is a phase wound secondary. The third winding is placed on the rotor and is provided with a commutator. Voltages collected from this commutator are inserted into the secondary circuit. Speed adjustment is obtained by changing the settings of the brushes. These a-c machines have speed-torque characteristics similar to those of the d-c shunt motor. Because of this similarity, they are sometimes called a-c shunt motors.

The authors have presented a simple explanation of the theory of this a-c adjustable speed, commutator type of motor based on ordinary induction motor theory which they have checked and found to be fundamentally sound. This explanation employs an extension of the application of the induction motor circle diagram theory. This new theory, meritorious because of its simplicity, is most helpful in explaining some of the motor characteristics such as power factor correction, design requisites for certain speed ranges, generator action, and its use for regenerative braking. The accuracies of the results obtained by this theory indicate that it may be found useful industrially as well as academically.

Paper 41-86, recommended by the AIEE committee on electrical machinery, and presented at the AIEE North Eastern District meeting, Rochester, N. Y., April 30–May 2, 1941. Manuscript submitted October 18, 1940; made available for preprinting March 7, 1941.

A. G. Conrad is a professor and F. Zweig and J. G. Clarke are members of the faculty of the School of Engineering, Yale University, New Haven, Conn.

The Motor

The speed of an ordinary induction motor can be changed by inserting into the secondary element a voltage of slip frequency, provided this voltage is in such a phase position that it forces a power component of current into the secondary (that is, this current produced in the secondary is not maximum when the flux surrounding the secondary conductors is zero). In the particular motor described here, this current (see figure 1) is obtained from an adjusting winding placed on the rotor. This adjusting winding is provided with a commutator and provision is made for collecting voltage from it by use of adjustable brushes which are connected to the secondary. The secondary is located on the stator and the primary on the rotor. The brushes are mechanically coupled so that they are spaced at the same distance for each secondary phase winding, thereby insuring equal voltages conducted to each secondary phase. When the brushes of each secondary phase are adjusted so that they are in contact with the same commutator segment, the secondary is short-circuited, and no voltage is supplied from the adjusting winding. Under these conditions, the motor behaves like an ordinary induction motor, and the adjusting winding is in no way operative. The speed can be reduced by separating the brushes in a given direction so the voltage collected from the brushes causes a component of secondary current which produces a negative torque. The machine can be operated above synchronism by shifting the brushes, that is, interchanging their positions (*a*) to (*b*), and (*b*) to (*a*)—figure 2, so that the voltage collected by these brushes is in such a direction as to force a current through the secondary which will produce positive torque. The motor can be reversed by reversing two of the leads supplying the primary.

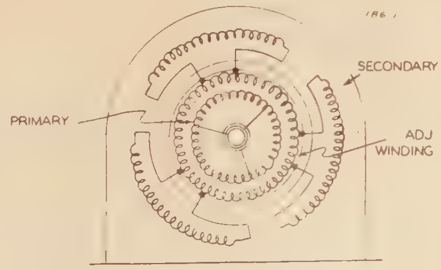

Figure 1. The motor circuit

The Theory of Speed Adjustment

Speed adjustment cannot be obtained merely by inserting a voltage into the secondary from the brushes unless this voltage is in such a direction as to cause a current that is torque producing. A voltage collected by the brushes even though large in magnitude may produce little or no change in speed if the current

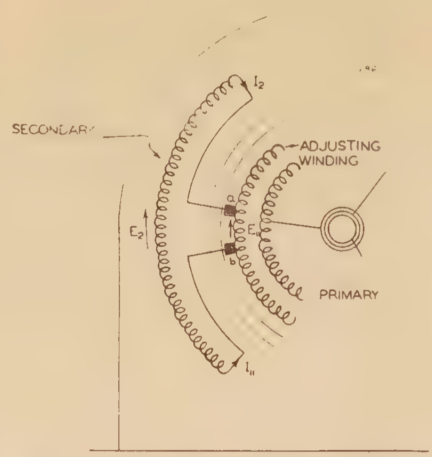

Figure 2. Currents and voltages in the secondaries

that it produces in the secondary conductors is in quadrature with the flux surrounding these secondary conductors. Such a condition will materially change the power factor of the motor without appreciable change of speed. Since it is possible to change both the magnitude and direction of this voltage collected from the adjusting winding, there is an infinite number of different brush settings that may give the same speed adjustment. However, there is but one setting of the brushes that will provide a given speed at a given power factor for a given load. Since all of these variables are interdependent, it is desirable that some form of explanation which shows their relation be presented. To show these relations, a specific brush setting will be chosen and the operation of the motor

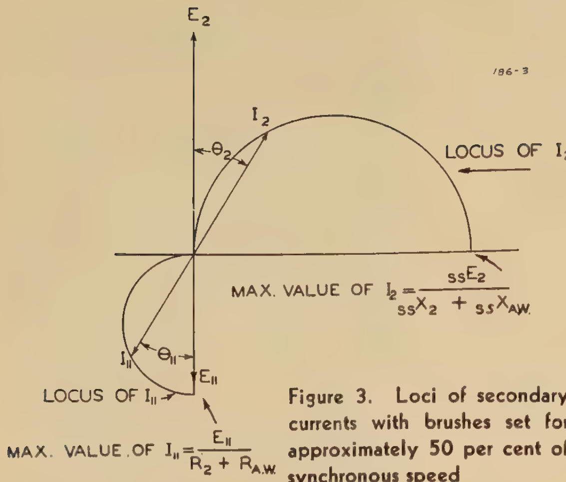

Figure 3. Loci of secondary currents with brushes set for approximately 50 per cent of synchronous speed

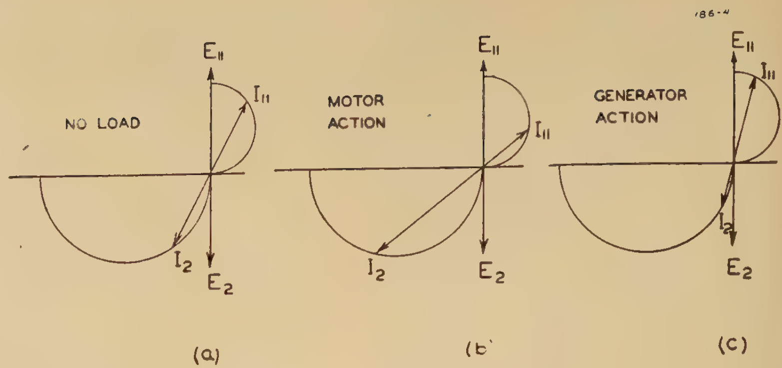

Figure 4. Relations of secondary voltages and currents when brushes are set to make E_2 opposite E_{11} and equal in magnitude at half speed

(a)—No load
(b)—Machine acting as a motor
(c)—Machine acting as a generator

explained for this setting. An understanding of the operation for this one brush setting will be most helpful in determining the conditions for other possible settings.

Operation Below Synchronous Speed

Let us assume that it is desired to operate this motor at half synchronous speed. This can be accomplished by spacing the brushes so that the voltage E_{11} induced in the adjusting winding between the brushes (*a*) and (*b*), figure 2, is exactly 180 degrees out of phase with the voltage E_2 induced in the secondary due to slippage of the secondary with respect to the flux. The separation of the brushes should be sufficient to make E_{11} equal to half the standstill value of E_2 in order to obtain a no-load speed equal to half synchronous speed. In figure 2 and in all following references this induced voltage due to slippage will be designated as E_2 and the current that it forces through the secondary and the adjusting winding included between the brushes will be designated as I_2. The voltage induced in the adjusting winding between the brushes will be referred to as E_{11}, and the current that it causes to flow is designated as I_{11}.

The total current flowing in the secondary for any condition of operation is the sum of the currents I_2 and I_{11}. The magnitude of this total current can be best understood by dealing with these two components separately to determine their nature, and then adding them to obtain the total current.

Assuming that the flux is constant for constant impressed primary voltage, the voltage per turn in the adjusting winding will be constant regardless of the speed. Therefore, for any given brush setting, E_{11} will be constant (independent of slip). The frequency of E_{11} changes with slip and at all times is the slip frequency of the motor. The voltage E_2 induced in the stator by this constant flux is directly proportional to the slip and is of slip frequency. Therefore E_2 and E_{11} are always voltages of the same frequency. The current I_2 which is caused by the voltage E_2 is impeded by the stator phase resistance R_2, the stator phase reactance X_2, the resistance of the adjusting winding R_{AW}, and the reactance of the adjusting winding X_{AW}. The current I_{11} is limited by the same impedance that limits I_2. Expressions for these currents are:

$$I_2 = \frac{E_2}{\sqrt{(R_2+R_{AW})^2+(X_2+X_{AW})^2}} \quad (1)$$

$$I_{11} = \frac{E_{11}}{\sqrt{(R_2+R_{AW})^2+(X_2+X_{AW})^2}} \quad (2)$$

Letting

E_2 at standstill be ${}_{ss}E_2$
X_2 at standstill be ${}_{ss}X_2$
X_{AW} at standstill be ${}_{ss}X_{AW}$
S = per cent slip

Then

$$I_2 = \frac{{}_{ss}E_2 S}{\sqrt{(R_2+R_{AW})^2+({}_{ss}X_2 S+{}_{ss}X_{AW}S)^2}} \quad (3)$$

or

$$I_2 = \frac{{}_{ss}E_2}{\sqrt{\dfrac{(R_2+R_{AW})^2}{S^2}+({}_{ss}X_2+{}_{ss}X_{AW})^2}} \quad (4)$$

$$I_{11} = \frac{E_{11}}{\sqrt{(R_2+R_{AW})^2+({}_{ss}X_2 S+{}_{ss}X_{AW}S)^2}} \quad (5)$$

It will be noted in the above equations that the secondary currents are limited by an impedance made up among other things of the reactance ${}_{ss}X_{AW}S$. This is the reactance offered to currents of slip frequency, and the voltages that are produced by this reactance and the secondary currents ($I_{2\,ss}X_{AW}S$ and $I_{11\,ss}X_{AW}S$) are independent of the primary supply frequency. At synchronous speed these voltages become zero and the secondary current is limited by the resistances only. This is on the basis of course that all the flux cuts all three windings.

On the basis of the equations 4 and 5, the vector diagram of the secondary circuit including its portion of the auxiliary winding can be constructed as in figure 3. From equation 4, it is evident that the extremity of the vector I_2 has a locus following the path of a semicircle as in an ordinary induction motor. Equation 5 shows that the vector I_{11} also has a circle locus. From equations 1 and 2, it is evident that the impedance offered to I_2 and I_{11} are the same, and therefore, these currents must lag their respective voltages by the same angle, therefore the angle $\theta_2 = \theta_{11}$. The maximum value of I_2 (diameter of circle) is equal to $\dfrac{{}_{ss}E_2}{{}_{ss}X_2+{}_{ss}X_{AW}}$ and the maximum value of I_{11} is obtained at 100 per cent power factor of the secondary or at synchronous speed and is equal to $\dfrac{E_{11}}{R_2+R_{AW}}$.

The current I_2 produces torque in the direction of rotation (positive) while the current I_{11} produces a negative torque.

The positive torque $= K\phi I_2 \cos\theta_2$
The negative torque $= K\phi I_{11} \cos\theta_{11}$

In these equations, ϕ = flux. It is assumed to be constant in magnitude, and that all of it cuts the primary winding,

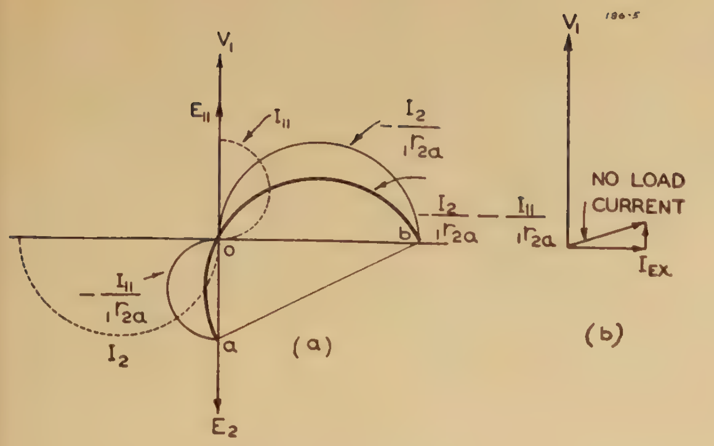

Figure 5. Currents

(a)—Of secondary reflected to the primary

(b)—Taken by primary at no load

the adjusting winding, and the stator winding. Since $\theta_2 = \theta_{11}$ for this brush setting, the total torque is—

$$T = K\phi(I_2 - I_{11}) \cos \theta_2 \qquad (6)$$

For a condition of no load (zero developed torque) I_2 and I_{11} are equal and opposite. Or in other words, the rotor must slip sufficiently to make I_2 increase to a value equal to and opposite to I_{11}. Since the brushes are so spaced that E_{11} is one-half E_2 at standstill, E_2 and E_{11} will be equal and opposite at 50 per cent slip, and the no-load speed will be one-half synchronous speed. If slippage is increased by further reduction of speed (loading), I_2 becomes larger, I_{11} smaller, and a positive torque will result. This is motor action and it occurs at a speed less than no-load speed. If now the machine is driven at some speed slightly above its no-load speed, I_2 will be reduced, and I_{11} increased. Under these conditions, the torque produced by I_{11} becomes higher than that produced by I_2 and the total torque is negative. This condition results in generator action. Thus with this machine generator action can be obtained at any speed within its speed range. These principles are illustrated further in figure 4.

Primary current for different conditions of load can be determined from the secondary currents and from the no-load exciting current in a manner similar to that used for the ordinary two-element induction motor. However, special consideration must be given to the turn ratios for the particular motor. Any turn ratio involving the adjusting winding is a function of speed adjustment (brush setting).

The effect of the secondary currents on the current taken by the primary can be explained from the diagram of figure 5a. This diagram shows the locus of the components of secondary current I_2 and I_{11} when E_2 and E_{11} are 180 degrees out of phase and the machine is adjusted at a no-load speed corresponding to approximately 50 per cent slip or one-half synchronous speed. The current I_2 flowing in the stator and through the adjusting winding will cause a current to flow in the primary of sufficient magnitude and direction so as to neutralize the flux produced by I_2. This component of the primary current is $\frac{-I_2}{{}_1r_{2a}}$ where ${}_1r_{2a}$ is equal to the ratio of the number of turns on the primary to the difference of the number of turns on the stator, and the number of turns in the adjusting winding that are placed in the secondary circuit by this particular brush setting, or ${}_1r_{2a} = \frac{N_1}{N_{2a}}$. The current I_2 passing through both the stator and the adjusting winding will produce fluxes in these two windings that are opposite in direction with respect to the primary circuit. The component of the primary current that neutralizes the magnetizing effect of I_2 is therefore a vector that has its extremity defined by the path of the circle $\frac{-I_2}{{}_1r_{2a}}$ shown in figure 5a.

Likewise, the current I_{11} will cause a component in the primary current which by the same reasoning as above must be 180 degrees out of phase with I_{11}. The magnitude of this primary component is $\frac{-I_{11}}{{}_1r_{2a}}$, and is defined by a current locus which is the path of another circle—figure 5a. If these two components of the primary current are now added vectorially, their sum would be $\frac{-I_2}{{}_1r_{2a}} - \frac{I_{11}}{{}_1r_{2a}}$ and the locus of this resulting current could be represented by another circle the diameter of which is $ab = \sqrt{\overline{oa}^2 + \overline{ob}^2}$. When the machine is running at no load the sum of these currents becomes zero. If the machine is operated at synchronous speed, the sum of these currents becomes oa. A resultant current below the line bo indicates generator action—a resultant current above this line, which has a component in the direction of the primary impressed voltage V_1, indicates motor action. The locus of motor currents and generator currents is defined by this circle boa. This circle however does not show the total primary current because of no-load losses and the requirements of an exciting current. Figure 5b shows the no-load loss and exciting components of primary current with respect to the impressed voltage V_1. The total primary current I_1 can now be obtained by adding the current defined by the circle locus aob of figure 5a to the no-load current shown in figure 5b. This construction results in a diagram, figure 6, which shows the relation of the primary current to the primary impressed voltage for different load conditions when brushes are set to reduce speed, to approximately 50 per cent of synchronous speed (${}_{ss}E_2 = 2E_{11}$).

Operation Above Synchronous Speed

The speed of this motor can be raised to a value above synchronous speed by

Figure 6. Circle diagram of primary current for brush setting corresponding to 50 per cent synchronous speed

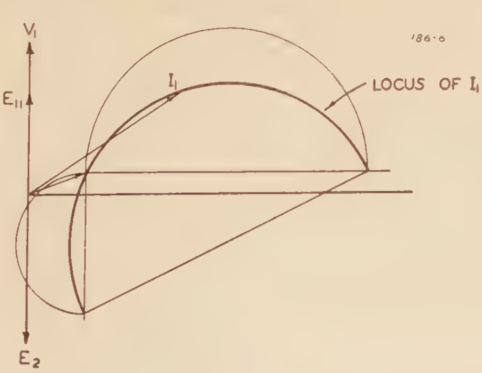

Figure 7. Current loci of secondary currents—brushes set for approximately 150 per cent synchronous speed

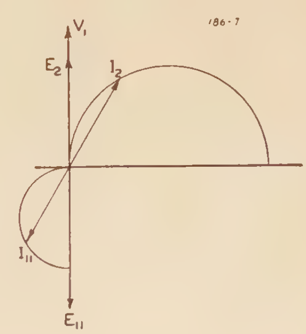

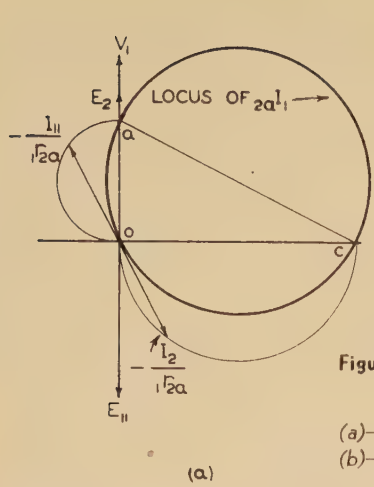

Figure 8. Currents for approximately 150 per cent synchronous speed

(a)—Secondary currents reflected to primary
(b)—Primary currents at no load

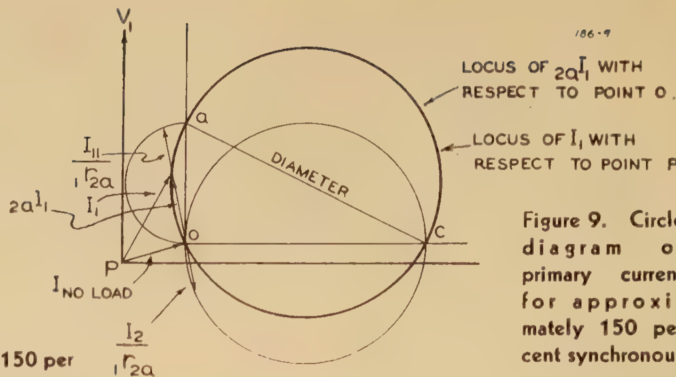

Figure 9. Circle diagram of primary current for approximately 150 per cent synchronous speed

reversing the potential E_{11} applied to the stator winding. This is done by transposing brush positions, i.e., in figure 2, brush *b* would be moved to the position of brush *a*, and brush *a* to the position of brush *b*. By reversing the direction of the voltage E_{11} applied to the stator, the current I_{11} will have a positive torque and tend to drive the motor at a high speed. For speeds above synchronous E_2 also reverses (since the flux reverses its direction of rotation relative to the stator), and I_2 now produces a negative torque tending to bring the motor back to synchronous speed. The vector diagram for this condition is shown in figure 7. It will be noted that both voltages are reversed with respect to the primary voltage V_1 from their position of figure 5*a*.

The current I_{11} flowing in the adjusting winding and stator will cause a primary current component $\frac{-I_{11}}{{}_1r_{2a}}$ where ${}_1r_{2a}$ is the ratio of the number of turns on the primary to the sum of the number on the stator and the adjusting winding between brushes. For this speed adjustment, the fluxes produced by the stator and adjusting winding are in the same direction with respect to the primary. Likewise, I_2 will cause a primary current component $-\frac{I_2}{{}_1r_{2a}}$.

When these currents of figure 7 are reflected to the primary circuit, with due regard to turn ratios, they provide a portion of the total primary current vector diagram shown in figure 8*a*. The total primary current resulting from the secondary currents in the adjusting winding, and the stator winding is the vector sum of the currents defined by the two current loci. Their vector sum is another current locus ${}_{2a}I_1$ which is defined by another circle *oac*. The complete vector diagram for the primary supply can now be obtained by superimposing the vectors of figure 8*a* on those of the no-load diagram of figure 8*b*. This complete diagram is shown in figure 9.

It will be noted that the resultant locus of the primary current of figure 9 is moved toward the vector V_1 from its position shown in figure 6. With this high-speed adjustment and with brushes set to make E_{11} opposite to E_2, the power factor of the motor can be made quite high at large loads, and the maximum power that the motor can develop is much higher than that of the low-speed adjustment described previously. This is indicated by the maximum power component of the primary current of figure 9 as compared with that of figure 6.

Experimental Check on Theory

In order to more fully verify the theory of the motor advanced thus far, an experimental check was made on one of these motors to see how closely the current taken under load followed the current predicted by the current loci circles. The machine, a General Electric B.T.A., 600–1800 rpm, 6 pole, 60 cycles, 4.1–12.5 horsepower, was first adjusted so that its no-load speed was 600 rpm (one-half synchronous speed). The brushes were set by opening the secondary connections at the brushes and adjusting the brushes so that the voltage across them, E_{11}, was one-half the voltage E_2 across the open-circuited stator coil at standstill. This gives only one of the necessary brush adjustments. The other adjustment for phase position of E_{11} is obtained by keeping the brushes fixed with respect to each other and moving them together on the surface of the commutator until the voltage E_{11} was 180 degrees out of phase with E_2. With this setting, the stator coils can now be reconnected to the brushes for operation at one-half synchronous speed for no load.

The current taken with this brush setting for different values of motor output is indicated by the encircled points in figure 10. The circle which should pass through these points can be located by measuring the no-load primary current (*po*), and the primary blocked rotor current (*pb*).

By erecting a perpendicular to the line *ob* one diameter of the current circle locus is established. If the line *ob* is extended to the point *f* so that $\frac{of}{bf} = \frac{{}_{ss}E_2}{E_{11}}$ the point *f* will fall on the locus of $\frac{-I_2}{{}_1r_{2a}}$. From points *o* and *f* the circle $\frac{I_2}{{}_1r_{2a}}$ can be constructed and consequently the point *e* is located. A perpendicular to *oe* will be another diameter to the primary current circle locus. The intersection of the two diameters establishes the center of the circle. The accuracy of this circle diagram is revealed by the proximity of the points obtained experimentally with the current circle locus *cob*.

To check the theory for higher speeds, the brush positions were interchanged so that the voltage E_{11} between them at standstill on open circuit was one-half the voltage E_2 induced in the open-circuited secondary and in phase with it. This adjustment provided a no-load speed of 1,800 rpm (150 per cent synchronous speed).

A current locus circle can be determined in the same manner as for the lower speed adjustment. This current locus along with the experimental points obtained by loading are shown for this speed adjustment (150 per cent synchronous speed) in figure 11. The circle locus predicted on the basis of no-load and short-circuit current provides a fair determination of the current characteristics of the machine. While there appears to be some divergence between this circle and the true current locus indicated by the curve through the encircled points, the actual differences as would be indicated on instruments as to power factor, magnitude of currents, etc., are small. The diagram

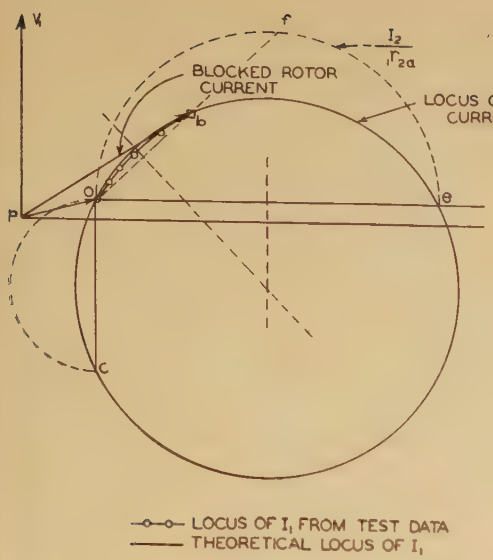

Figure 10. Theoretical primary current locus compared with test data—50 per cent synchronous speed

Figure 11. Theoretical primary current locus compared with test data—150 per cent synchronous speed

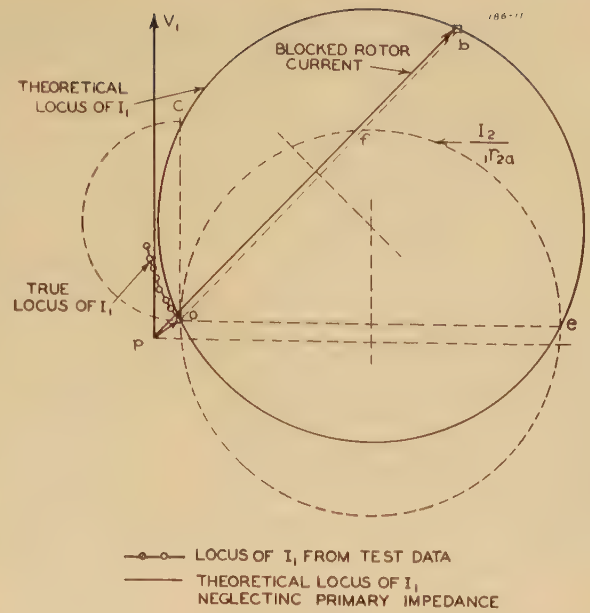

of figure 11 which displays this difference on a standard machine also, with proper interpretation reveals that the theory thus far developed is sound. However, the differences between the theoretical circle and the experimental current locus can be explained on the basis of the primary leakage reactance.

Effects of Primary Leakage Reactance

In a motor such as described here provision is made for two windings on the rotor and one on the stator. The necessary spacing of the primary winding with respect to the stator introduces primary leakage reactance. This reactance produces a voltage 90 electrical degrees ahead of the current in the primary which subtracts from the applied voltage in such a way that the voltage induced in the primary by the mutual flux (mutual to primary and to the stator) lags the applied voltage. Consequently at speeds above synchronism, this mutual flux must introduce a voltage in the stator winding which is ahead of the voltage that would be present if there were 100 per cent coupling between the two windings. The angle of lead of this voltage in the stator is exactly equal to the angle of lag between the total primary back electromotive force and the back electromotive force produced by the mutual flux. This lead in stator voltage will cause the circle with diameter *oe* of figure 11 to swing about the point *o* in the direction of the rotation of the vectors with increase in load on the motor. Since the leakage between the two rotor windings (primary and adjusting winding) is small, there is little shift of the circle *of* due to primary leakage fluxes.

It has been found experimentally that the true primary current locus represented by the points shown in figure 11 can be predicted from no-load data of three sets of measurements taken on the motor. These determinations are, as follows:

1. The no-load input current and watts.
2. The standstill input current and watts at reduced voltage.
3. The input current and watts on reduced voltage with the machine running.

The first and second determinations above are made in the customary manner. The third determination can be made by applying a reduced voltage to the primary sufficient to rotate the machine at no load at a speed somewhere intermediate between its no-load speed and standstill. A speed of approximately 50 per cent of no-load speed provides fair accuracy in construction of the circle.

From the data of the three above items, it is possible to calculate the current, power factor, etc., for normal voltage. From these three values of primary current and their respective power factors, it is possible to construct the circle locus of the primary current previously developed, and also to locate it in accordance with the shift created by the primary leakage reactance. This more accurate determination of the primary current locus is shown in figure 12. The current *PO* is the no-load current, the current *PS* is the standstill current for normal voltage determined from data taken at reduced voltage, and the current *PR* is a current that the motor would take when running on normal voltage under some load. This current *PR* is determined for a running condition at reduced voltage.

The center of the circle of figure 12 can be found by erecting perpendiculars to the chords *RS* and *OR*. Once this center *C* is located a circle can be drawn through the

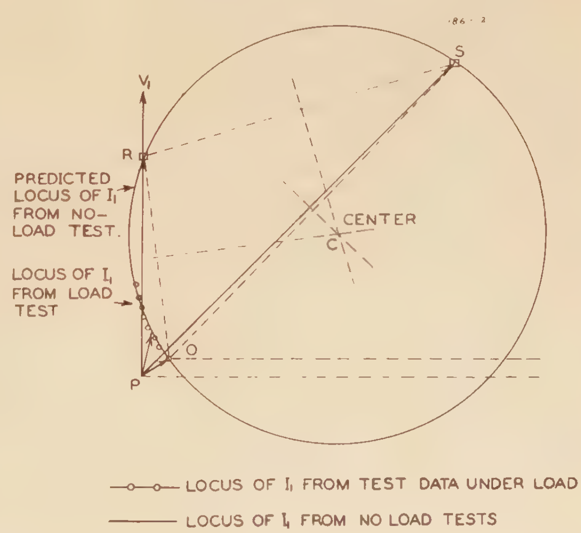

Figure 12. Comparison of primary current locus obtained from no-load tests with the true locus obtained by loading

Theory of the Brush-Shifting A-C Motor—II

A. G. CONRAD
MEMBER AIEE

F. ZWEIG
ENROLLED STUDENT AIEE

J. G. CLARKE
ASSOCIATE AIEE

Synopsis: In the preceding paper[1] of this series, a simple theory underlying the circle diagram of the brush-shifting a-c motor was presented. It is the purpose of this paper to advance this theory, and to show how it can be used to determine such quantities as efficiency, current, torque, and speed for different conditions of operation. The procedures outlined and explained have been checked experimentally, and found to be accurate for both high-speed and low-speed adjustments.

THERE is an infinite number of possible brush settings that can be made on the brush-shifting a-c motor. It is possible to move the brushes so as to change the magnitude or phase position, or both magnitude and phase position of the voltage collected from the commutator. Such movements can be used to change speed, or the power factor or both speed and power factor. Any change in brush setting will materially change the circle diagram proportions. Therefore, any circle diagram for this motor is useful only in determining the characteristics of the machine for one brush setting. However, an understanding of the use of the circle diagram for a particular setting of the brushes will be most helpful in obtaining a general understanding of the operation of the machine for other settings. Therefore, the diagrams used for a basis of explanation will be those corresponding to the settings described in Part I, i.e., when the machine is operated at 50 per cent of synchronous speed with the two secondary voltages in direct opposition, and when operated at 150 per cent of synchronous speed with the two secondary voltages in direct opposition. Characteristic circle diagrams for these brush settings are shown in the upper portion of figure 3.

Determination of the Circle Diagram

The circle diagram can be determined from three sets of readings taken at no load. These determinations are as follows:

(*a*). No-load input current and watts at normal voltage

(*b*). The standstill input current and watts at reduced voltage

(*c*). The no-load input current and watts at reduced voltage with the machine running at some speed between no-load speed and standstill

From the data of these three sets of readings, the circle diagram of figure 1 can be constructed. This diagram is characteristic of the machine for speed adjustments below synchronous speed. The line *po* shows the no-load current and its direction with respect to the impressed voltage V_1. It is obtained from determination (*a*) above. The standstill current I_{ss} for normal applied voltage is represented in magnitude and direction by the line *pb*. It is obtained from determination (*b*). A third point, *x*, on the circle is located from determination (*c*). This point is obtained from conversions made on data taken with reduced voltage. Having the points, *o*, *x*, and *b* on the circle, it is possible by erecting perpendiculars to two of its chords to locate the center *r*. Using *or* as a radius, the circle locus of the primary current *oxb* can be located.

Paper 41-87, recommended by the AIEE committee on electrical machinery, and presented at the AIEE North Eastern District meeting, Rochester, N. Y., April 30–May 2, 1941. Manuscript submitted November 16, 1940; made available for preprinting March 7, 1941.

A. G. CONRAD is a professor and F. ZWEIG and J. G. CLARKE are members of the faculty of the School of Engineering, Yale University, New Haven, Conn.

1. For numbered reference, see end of paper.

Determination of Characteristics From the Circle Diagram

Having established the currents *po* and *pb* in magnitude and direction with respect to the vector V_1, the lines *pe* and

points O, R, and S which very accurately predicts the primary current locus with respect to the impressed voltage. The accuracy of this method of determining this locus is evident from the proximity of the locus of the points determining the true locus obtained experimentally.

The theory presented here has been verified through experimental data. It is assumed to be fundamentally sound. An advancement of this theory for use in the analysis of the losses, slip, efficiencies, and power factor correction has been made, but falls without the scope of this paper. These advancements will be presented in a later publication.

List of Symbols

E_2—Voltage induced in one phase of stator

E_{11}—Voltage generated in adjusting winding between brushes supplying one phase of stator

I_2—Current flowing in stator and adjusting winding resulting from the voltage E_2

I_{11}—Current flowing in stator and adjusting winding resulting from the voltage E_{11}

I_{ss}—Standstill primary current

R_2—Resistance of stator per phase

R_{AW}—Resistance of adjusting winding per phase

X_2—Reactance of stator per phase

X_{AW}—Reactance of adjusting winding per phase

S—Per cent slip

${}_{ss}E_2$—Stator voltage at standstill (induced)

${}_{ss}X_2$—Stator reactance at standstill

${}_{ss}X_{AW}$—Adjusting winding reactance at standstill

θ_2—Angle of lag between E_2 and I_2 electrical degrees

θ_{11}—Angle of lag between E_{11} and I_{11} electrical degrees

θ—Angle of lag or lead between primary phase voltage and primary phase current

ϕ—Total flux produced by primary windings

K—Torque constant of the motor

T—Torque developed (synchronous watts)

${}_1r_{2a}$—Ratio of the number of turns on the primary to the effective number of turns on the secondary and adjusting winding

N_1—Number of primary turns

N_{2a}—Effective number of secondary turns per phase included in stator and adjusting winding circuit. This quantity is a function of speed adjustment as well as power factor adjustment

V_1—Primary impressed voltage per phase

I_1—Primary current per phase

I_{ex}—Exciting current in primary circuit per phase

${}_{2a}I_1$—Component of primary current flowing as a result of the currents in stator and adjusting winding

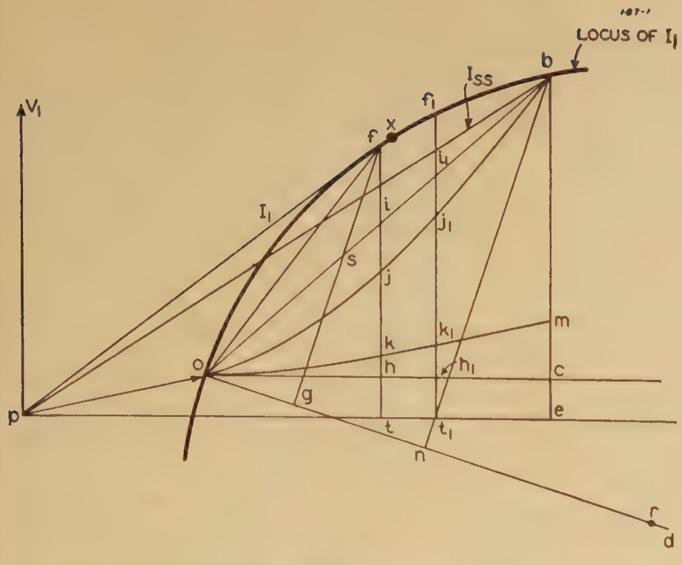

Figure 1. The circle diagram for the low-speed adjustment

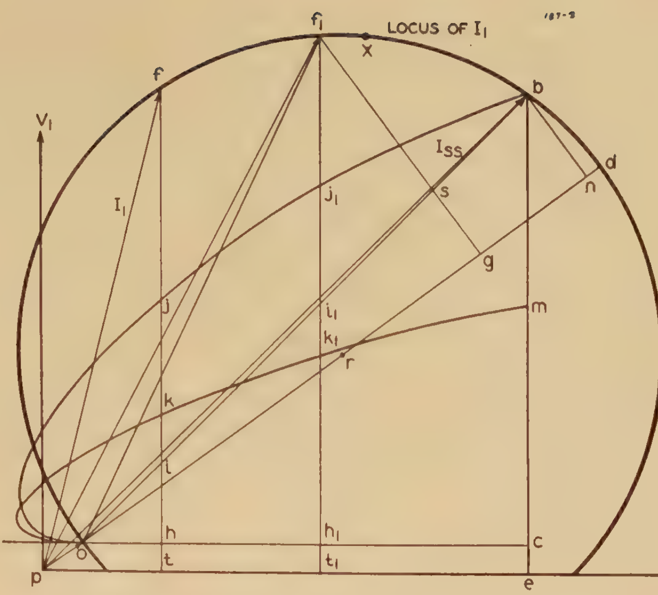

Figure 2. The circle diagram for the high-speed adjustment

oc can now be constructed perpendicular to V_1 and the line *be* perpendicular to *pe*. The power supplied to the motor at standstill per phase is the current *be* multiplied by the voltage V_1. The current *ce* multiplied by the voltage V_1 is the per phase iron loss of the rotor, the friction and windage losses, and a small amount of iron loss in the stator. By measurements of primary resistance, the primary copper losses per phase can be calculated for the normal short-circuit current. This loss is represented by the current *cm*. The loss in the adjusting winding and in the stator per phase for standstill conditions is $(bm)V_1$.

The copper losses can be estimated for any value of primary current in a manner somewhat similiar to that normally used with the ordinary induction motor. Thus for an input current of *pf*, it is assumed that the no-load current is one component and the loss associated with it, $(ce)V_1$, is constant regardless of the magnitude of the load. The other component of the primary current *pf* is *of*, and the losses associated with this component can be determined by the relations—

$$\text{Loss for current } of = \text{loss for } ob\left(\frac{\overline{of}}{\overline{ob}}\right)^2$$

Another method of determining the copper loss for the current *pf* is to erect a perpendicular *bn* from the point *b* to the diameter of the circle, and another perpendicular *fg* to the same diameter. The copper losses associated with the current *of* are expressed as—

$$\text{Loss for current } of = \frac{(bc)(sg)}{bn} V_1 \text{ watts per phase}$$

Having determined the total loss for this current *of* in terms of a current in phase with the voltage, this loss caused by the current *of* can now be laid off on a line *fh* drawn from *f* perpendicular to *oc*. In figure 1, it is labeled *hj*. Similarly, the total copper losses can be determined for other values of input current. Thus for an input current of pf_1, the total copper loss is h_1j_1. By successive determinations of losses, the curve *ojb* can be constructed to show the change in copper losses with different values of input current. If each of the distances *jh*, j_1h_1 are divided so that $\frac{jk}{kh} = \frac{j_1k_1}{k_1h_1} = \frac{bm}{mc}$ a new curve *okm* can be constructed so that the distance h_1k_1 shows the variation in primary copper loss, and k_1j_1 shows the variation in secondary (adjusting winding and stator) copper losses for different values of primary current.

The variables for the motor can now be determined for any value of input current I_1.

(1). Input $= (ft)V_1$ watts per phase
(2). Output $= (jf)V_1$ watts per phase
(3). Iron loss, friction, and windage $= (ht)V_1$ watts per phase
(4). Primary copper loss $= (hk)V_1$ watts per phase
(5). Copper losses of stator and adjusting winding $= (jk)V_1$ watts per phase
(6). Efficiency $= \left(\frac{jf}{ft}\right)$ 100 per cent
(7). Slip $= \left(\frac{jk}{kf}\right)$ 100 per cent of no-load speed
(8). Speed $= \left(1 - \frac{jk}{kf}\right)$ times the no-load speed
(9). Torque $= (kf)V_1$ synchronous watts per phase

For speeds above synchronism, a similar treatment can be applied. Figure 2 shows the circle diagram for the same motor as that of figure 1, except the speed is adjusted to approximately 150 per cent of synchronous speed. The standstill current I_{ss} for normal voltage is much larger, and maximum power output much greater. The circle is located from the three sets of no-load determinations described previously. The essential difference of this diagram as compared with that of figure 1 is the shape of the curves showing copper losses for different primary currents. The system of notations on figure 1 has been maintained in figure 2, so that the explanation of the use of figure 1 will suffice for the explanation of the use of figure 2.

Experimental Check on the Theories of the Circle Diagram

In order to check the validity of the theory thus far developed, tests were made on a General Electric B.T.A. 550–1,650-rpm, 4.17–12.5-horsepower, 6-pole, 60-cycle brush-shifting motor. The brushes were set by making the brush voltage E_{11} at standstill equal approximately one-half the voltage ${}_{ss}E_2$ in the stator coil to which they were connected. Care was taken to make these voltages opposite in direction. With this setting, the no-load tests described above under the headings (*a*), (*b*), and (*c*) were made to determine the circle locus of the primary current. The machine was then loaded and readings of speed, torque, current, watts, and volts were obtained for different values of output. The primary resistance was determined by measuring the resistance of the pri-

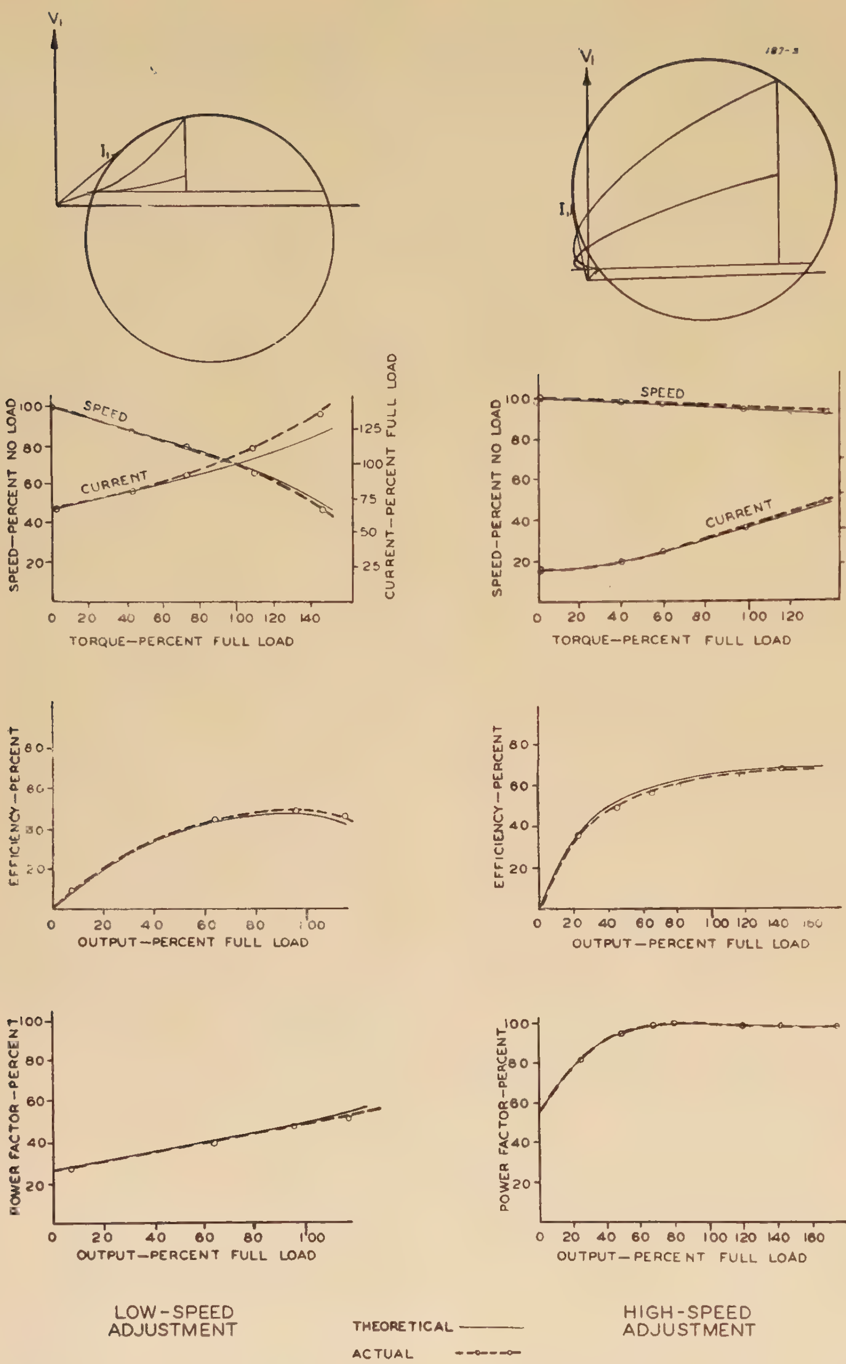

Figure 3. Comparison of the theoretical characteristics taken from the circle diagram with the actual characteristics obtained by tests for no-load speeds, approximately 50 per cent of synchronous speed, and 150 per cent synchronous speed

mary winding with direct current. From the no-load tests the circle diagram of the machine was constructed, and the characteristics determined from its proportions. The theoretical diagram for this machine with this low-speed setting is shown in figure 1.

A second experimental check was made with the brushes set to provide a speed of approximately 150 per cent of the synchronous speed. This can be done by making the voltage E_{11} across the brushes at standstill equal to one-half the stator voltage $_{ss}E_2$ of the stator coil to which they are normally connected. In addition to this, these two voltages should be in time phase with each other at standstill to provide proper running speed. No-load determinations similar to those described above were made and the circle locus of the primary current established for this speed adjustment. From this circle diagram, the characteristics of the motor were calculated. The machine was then loaded, and the characteristics again determined experimentally. The circle diagram for this higher speed adjustment is shown in figure 2.

A comparison of the theoretical characteristics with actual characteristics of the motor are shown in figure 3. The solid lines indicate the characteristics obtained by use of the circle diagram—the dotted lines indicate the characteristics obtained experimentally.

Conclusions

The proximity of the curves obtained from measurements made on the circle diagram to those obtained by the load test, indicates that the circle diagram developed and explained in this series of papers can be used to determine the operating characteristics of the brush-shifting motor accurately. While the circle diagrams of the motor have been shown and checked for only two speed adjustments, the explanation of the theory of the use of these diagrams can be applied to other diagrams constructed for different speed adjustment on the motor. A large portion of the theory thus far developed is directly applicable to the explanation of conditions within the motor when it is adjusted for power factor corrections; however, this is beyond the scope of this paper, and will be presented in another publication.

Symbols

V_1—Primary impressed voltage per phase
I_{ss}—Standstill primary current
I_1—Primary current per phase
$_{ss}E_2$—Voltage induced in stator at standstill
E_{11}—Voltage generated in adjusting winding

Reference

1. Theory of the Brush-Shifting A-C Motor—I, A. G. Conrad, F. Zweig, and J. G. Clarke. AIEE Transactions, volume 60, 1941 (August section), pages 829–34.

The Determination of Magnitude and Phase Angle of Electrical Quantities

ERIC A. WALKER
MEMBER AIEE

Synopsis: Although the three-voltmeter method for measuring the relative magnitude and phase angle of two voltages or currents is well known, the use of vacuum tube voltmeters, which draw negligible amounts of energy from the circuit, permits the use of the method for purposes which previously have not been considered. A further improvement of the scheme by balancing out one component of either voltage or current adds to the accuracy of the results. The method is considered for two purposes, namely: the measurement of the capacitance and power factor of imperfect condensers, and the measurement of the ratio and phase angle of current transformers.

Purpose

THERE are two well-known methods by which the constants of an unknown impedance may be determined. They are by balancing networks or bridges, of which there are many types,[1] or by the use of a wattmeter, voltmeter, and ammeter. Both methods are used successfully for a wide variety of impedances, even to the determination of the capacitance and power factor of cables and high-voltage bushings.[2,3,4]

There are also two principal methods by which the relative magnitudes of two voltages or two currents and the phase angle between them may be determined. They are by the use of an a-c potentiometer of the Tinsley-Drysdale type,[5] or by use of a modified bridge method.[6]

A third method for determining the magnitude and angle of an impedance, voltage, or current is known as the three-voltage, or three-voltmeter method.[7] The method has been known for a long time but it has been less widely used than the methods mentioned previously because of its supposed inaccuracy. For determining voltages, the method consists of measuring the two unknowns separately and then measuring their sum or difference. The scheme is inaccurate if the circuit on which the voltages are impressed is composed of high-impedance elements, and the instruments draw sufficient current to disturb the vector relations in the circuit However the development of vacuum tube voltmeters and amplifiers, which draw little or no power from the circuit and thus have negligible effect on circuit conditions, makes a re-examination of the method desirable.

This re-examination is made more important because there are cases when an unavoidable variation in the circuit parameters occurs during the test, making it very difficult to obtain a balance on a bridge. Furthermore there are cases, such as in the testing of current transformers, when it becomes necessary to design circuit elements to carry large currents. Then inductances become undesirable because of the magnetic fields which are produced and capacitors for large currents soon become unwieldy and expensive.

The Modified Three-Voltmeter Method

If one has two alternating voltages of the same frequency it is possible to determine their magnitudes and the phase angle between them by three-voltage measurements and a graphical or trigonometrical analysis. Figure 1*a* shows two voltages across two impedances on which three-voltage measurements can be made because of the common connection. In figure 1*b* E_1 is drawn along the real axis. Then arcs equal in length to E_2 and E_3 are drawn from the ends of E_1 and the phase angle θ is determined. If the measuring instruments do not disturb the distribution of voltage in the circuit the accuracy is limited only by the accuracy of the instruments and the personal error of the operator.

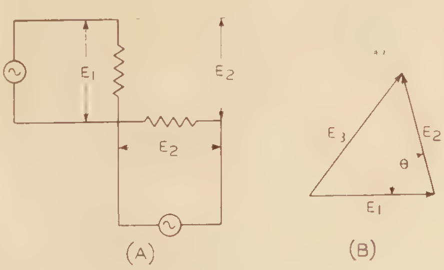

Figure 1. The three-voltage method for determining the magnitude and phase angle of two voltages

One difficulty is present if the two voltages E_1 and E_2 are nearly in phase and equal in magnitude for then a small error in the determination of either of them may result in recording three voltages which will not form a closed triangle. Such an error can be avoided by a procedure which balances out one component of a voltage in a manner which will now be explained. In figure 2*a* the circuit of figure 1*a* is shown with an added element. To the voltage E_2 a voltage E_2' is added which is variable in magnitude and 180 degrees out of phase with E_1. (This requires a transformer with exactly 180

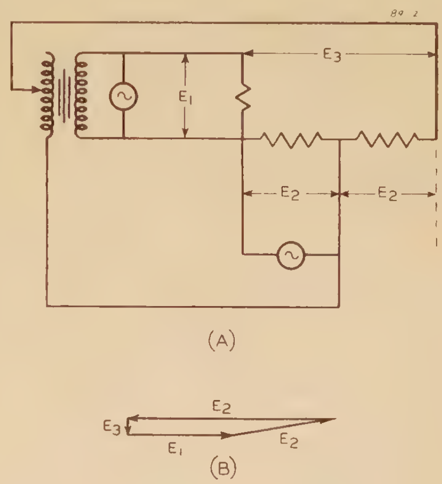

Figure 2. The method of balancing out one component of a voltage vector to determine the phase angle

degrees phase shift, a limitation which will be discussed later in this article.) Figure 2*b* shows the voltage relations in this circuit. It is evident that when the voltage E_3 is a minimum the phase angle between E_1 and E_2 is:

$$\theta = \sin^{-1}\frac{E_3}{E_2}$$

Therefore it is only necessary to determine these two voltages in order to find the phase angle. For very small angles a further approximation can be made:

$$\theta = \sin^{-1}\frac{E_3}{E_2} \approx \tan^{-1}\frac{E_3}{E_2}$$

$$\theta(\text{radians}) \approx \frac{E_3}{E_2}$$

These formulas are useful in studying the defect angle of condensers or of current transformers.

Paper 41-89, recommended by the AIEE committee on instruments and measurements, and presented at the AIEE North Eastern District meeting Rochester, N. Y., April 30–May 2, 1941. Manuscript submitted November 19, 1940; made available for preprinting March 11, 1941.

ERIC A. WALKER is a professor in the department of electrical engineering, University of Connecticut, Storrs, Conn.

1. For all numbered references, see list at end of paper.

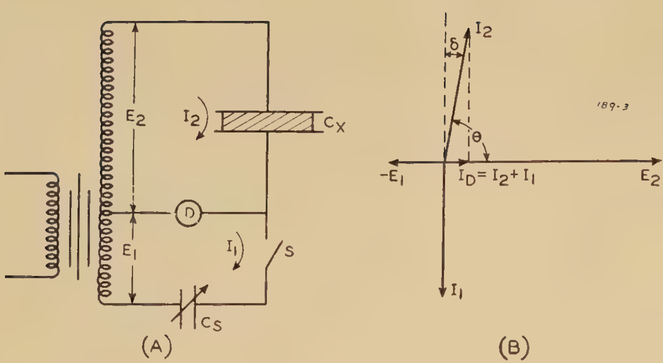

Figure 3. Circuit and vector relations for determining the defect angle of an imperfect condenser

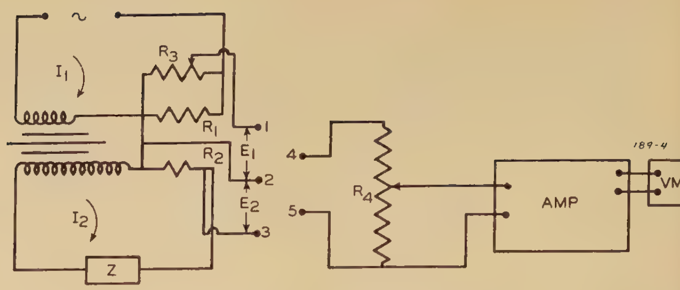

Figure 4. Circuit for determining the phase angle of a current transformer

Although this method has been discussed for voltages it is obvious that the vector relationship is applicable also to currents. Either the currents themselves can be measured or the voltage drop across resistors which are sufficiently small so that they do not appreciably affect the circuit.

Testing Condensers by the Measurement of Two Currents

In figure 3 a circuit is shown for measuring the power factor and capacitance of imperfect condensers. In this circuit the transformer has a 5,000-volt winding and a 100-volt winding, both shielded. The phase angle between the voltages of the two windings should be as small as possible. The imperfect condenser is connected to the high-voltage winding and a leading current flows through the detector D as is shown in figure 3*a*. This current leads the voltage by an angle θ and the condenser is said to have a defect angle δ, where $\delta = 90$ degrees $-\theta$. The defect angle is determined by closing switch S and varying the air condenser C until a minimum current is reached. This is

$$I_D = I_1 + I_2$$

Then

$$\delta = \sin^{-1}\frac{I_D}{I_2} \qquad \delta(\text{radians}) \approx \frac{I_D}{I_2}$$

Typical readings made on a high-voltage bushing are as follows:

$I_2 = 1{,}120$ microamperes at 5 kv and 60 cycles per second

$I_D = 60$ microamperes at 5 kv and 60 cycles per second

$$= \frac{60}{1{,}120} = 0.0535 \text{ radian}$$

$$C_x = \frac{1{,}120 \cdot 10^{-6}}{5{,}000 \cdot 377} = 594 \quad \text{micromicrofarads}$$

(approximately)

These measurements were checked on a Schering bridge. Although power factors which are too low to measure by this method can still be determined by a Schering bridge, this system showed one important advantage in the measurement of the power factor of wet oil. With the bridge the power factor of the oil changed too rapidly for a successful reading to be made, but with this circuit the variation could be followed without much difficulty because as I_d changes there is no appreciable variation in the out-of-phase component of I_2 and the power factor is approximately proportional to I_d.

This circuit is also useful in making tests where corona may be present at higher voltages. The circuit can be balanced at a low voltage and as the voltage is increased the current I_d should increase in direct proportion. Any sudden increase indicates a departure from linearity in the condenser being tested.

It is important to notice that the calibration of the air condenser C_S does not enter into the result. The only requirements are that the voltages E_1 and E_2 must be in phase and that the impedance of the detector be sufficiently low so that the phase angle is not affected. Both of these effects can be checked by placing an air condenser at C_x with a known resistance in series to give a known power factor. For a detector it is possible to use a rectifier type microammeter or, for lower impedance, a noninductive resistance with an amplifier and vacuum tube voltmeter can be used. A filter in the amplifier circuit to suppress all harmonics increases the accuracy of the results.

It must be noted that the capacitance of balancing condenser C_S must be larger than C_x by the ratio of E_1 to E_2. At times this makes it desirable to add fixed low-loss mica condensers in parallel with C_S to extend the range. The power factor of these condensers should be less than one per cent of the condenser being tested.

This circuit has been found very useful for measuring the defect angles of cables, bushings, and other impedances having defect angles from 0.005 to 0.1 radian. It is desirable to shield the device to keep stray currents out of the meter.

Application to Current-Transformer Testing

At present two methods are used for testing current transformers: the mutual inductance bridge method, and the "Silsbee" or comparative method. The first requires one or two calibrated mutual inductances, and the second requires a transformer similar to the one being tested but with a known ratio and phase angle. An arrangement requiring neither of these is shown in figure 4. In this circuit R_1 and R_2 are decade boxes, and Z is the burden with which it is desired to test the transformer. The resistance R_3 should be sufficiently large so that it diverts a negligible amount of current from R_1. A ratio of 10,000 to 1 or higher is usually used. The vacuum tube voltmeter consists of a three-stage, resistance-coupled, amplifier with 70 decibels gain and an input resistance of about one megohm. Readings are taken on a rectifier-type microammeter in the output circuit of the amplifier. With the method described here, a calibration of the amplifier-voltmeter combination is not necessary. Greater accuracy can be attained by inserting a 60-cycle band pass filter in the amplifier to eliminate any harmonic voltages from the voltmeter reading.

The method of making the test is as follows: the input terminals of the meter (terminals 4 and 5) are connected to points 2 and 3, and tap of R_4 is adjusted until full scale is indicated on the output meter. This value of R_4 is recorded as R_4'. Next the meter input is connected to points 1 and 2, and with R_4 unchanged the tap on R_3 is adjusted until full-scale deflection is obtained on the voltmeter. Call this setting on R_3, R_3'. Then:

$$E_{23} = E_{12} \qquad E_{12} = I_1 R_1 \frac{R_3'}{R_3} \qquad E_{23} = I_2 R$$

Transformer ratio $= \frac{I_1}{I_2} = \frac{R_2}{R_1} \cdot \frac{R_3}{R_3'}$

The next step is to connect the input terminals of the meter to points 1 and 3. This reading should be much less than the previous ones. If it is not the polarity of the secondary winding must be reversed. The tap on R_4 is now changed until full-scale deflection is obtained once more. This setting on R_4 is recorded as R_4''. One now has:

$$E_{12} \cdot \frac{R_4'}{R_4} = E_{13} \frac{R_4''}{R_4}$$

$$\theta = \sin^{-1} \frac{R_4'}{R_4''}$$

$$\theta(\text{radians}) = \frac{R_4'}{R_4''} \text{ (approximately)}$$

A typical set of readings are:

Rated primary current—50 amperes
Rated secondary current—5.0 amperes (nominal)

R_1 = 0.01 ohm R_2 = 0.10 ohm
R_3 = 10,000 ohms R_4 = 10,000 ohms
R_3' = 999.0 ohms R_4'' = 10,000 ohms
R_4' = 14.0 ohms

$$\text{Ratio} = \frac{0.1}{0.01} \times \frac{10{,}000}{999.0} = 1.0010$$

$$\theta(\text{radians}) = \frac{14.0}{10{,}000} = 0.0014 \text{ radian}$$

θ = 28.8 seconds

It is important to understand that the general method is not limited to the two cases cited. These are two illustrative examples where the method has proved of value and other examples can be found. The measurement of the voltage relations along an artificial transmission line or the measurement of the phase relations in resonant circuits might be mentioned.

References

1. ALTERNATING CURRENT BRIDGE METHODS, **B. Hauge.** Isaac Pitman and Sons, Ltd., London, 1930.

2. A HIGH SENSITIVITY POWER FACTOR BRIDGE, **Kouwenhoven and Banos.** AIEE TRANSACTIONS, volume 51, 1932, page 202.

3. THREE METHODS OF MEASURING DIELECTRIC LOSS, **Doyle and Salter.** AIEE TRANSACTIONS, volume 45, 1926, page 634.

4. THE USE OF A DYNAMOMETER WATTMETER, **E. S. Lee.** AIEE JOURNAL, volume 45, 1926, page 746.

5. A-C POTENTIOMETERS AND THEIR APPLICATIONS, **C. V. Drysdale.** *Journal* Institution of Electrical Engineers, volume 68, 1930, page 339.

6. EQUIPMENT FOR TESTING CURRENT TRANSFORMERS, **F. B. Silsbee, R. L. Smith, N. L. Forman, and J. H. Clark.** *Bureau of Standards Journal of Research*, volume 11, 1933, page 93.

7. ELECTRICAL MEASUREMENTS, **Frank Laws.** McGraw-Hill Book Company, N. Y., 1938, page 328.

Ampere-Squared-Second Recorder

T. A. RICH
ASSOCIATE AIEE

Synopsis: A device is described which records the ampere-squared seconds in an electrical impulse of less than 0.5-second duration. A number of these have been used in resistance-welding applications to monitor the electrical variables and have contributed greatly to the uniformity of welds. The problem of indicating $^1/_{60}$-second impulses at the rate of 100 a minute with the same device that will correctly integrate a half-second impulse has been solved by the use of a moving element with an infinitely long natural period, combined with a supplementary circuit which returns the element to the starting position in a fraction of a second.

Introduction

In resistance welding, it is necessary to control many variables to get optimum results. The control of the surface conditions of the material being welded, the size and shape of the electrodes, and the pressure between electrodes are mechanical and metallurgical problems. The control of the energy used in welding is a combined electrical, mechanical, and metallurgical problem. The electrical energy which produces the heat is a function of the square of the current, the time of application, and the resistance. The resistance at the weld will depend upon mechanical and metallurgical conditions which themselves must be subjected to careful control. It is logical then to measure as an electrical entity only those conditions which are responsive to electrical control, namely current and time or $\int i^2 dt$. The usual welding circuit is highly reactive and the resistance of the material being welded has but little effect on the current, and therefore the ampere-squared seconds are not greatly influenced by variables which should be controlled by nonelectrical means.

An ampere-squared-second recorder should:

1. Give a record for each weld.
2. Operate over the range of currents and time used in resistance-welding operations, and be adjustable to indicate 100 per cent for any specified value of $\int i^2 dt$.
3. Not limit the speed of welding.
4. Give an alarm when specified limits are exceeded.
5. Stand extreme overloads.

Paper 41-88, recommended by the AIEE committee on instruments and measurements, and presented at the AIEE North Eastern District meeting, Rochester, N. Y., April 30–May 2, 1941. Manuscript submitted February 28, 1941; made available for preprinting April 1, 1941.

T. A. RICH is an electrical engineer with the general engineering laboratory of General Electric Company, Schenectady, N. Y.

With such a device, the supervisor can adjust the sensitivity of the recorder to read 100 per cent for the correct electrical conditions for a given welding job. The operator then works in the usual way, and the device makes a record for each weld. If the electrical conditions change appreciably for any subsequent weld, an alarm is given, and, in some applications, the welding control is automatically locked.

The currents and times used in resistance-welding operations vary over a wide range, but by the use of transformers, any desired fraction of the current and therefore of the ampere-squared seconds in the circuit can be applied to the ampere-squared-second recorder. The most usual range of time is from $^1/_{60}$ to $^1/_2$ second, or from 1 to 30 cycles with a 60-cycle-per-second source. The rate of welding may be as high as 100 per minute on welds of a few cycles duration.

A conventional a-c ammeter can be used to indicate ampere-squared seconds if the duration of the impulse is short in comparison with the natural period of the instrument. If the moving element starts from rest, the maximum throw is directly proportional to ampere-squared seconds. Before the next impulse can be applied, the instrument must have come to rest again. For accurate work, the natural period should be ten or more times as long as the length of the longest impulse to be measured. When the longest impulse is 0.5 second, this would require a natural period of 5 seconds and the rate of welding on the shorter impulses would be less than 12 per minute.

Principles of a Suitable Mechanism

The arrangement finally developed is somewhat similar in operation to the Grassot fluxmeter. Instead of a mechanism for producing kinetic energy from the impulse and then converting to potential energy, as is done in ballistic measurements, a mechanism is used which produces an angular velocity proportional to the current squared which is maintained for the duration of the impulse.

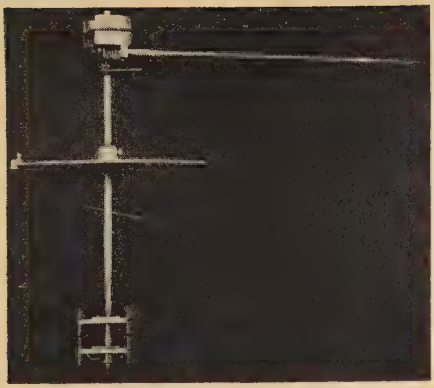

Figure 1. Moving element for ampere-squared-second recorder

The moving element consists of two separate iron-vane ammeter elements, an eddy-current damping vane, and a pointer, all on the same shaft, as in figure 1. One ammeter element produces clockwise rotation due to the impulse and the other counter-clockwise rotation from a separate source to return the element to the starting position. The deflecting element is at the bottom and the return element at the top in figure 1. The element can also be seen in position in figure 2.

If there were no physical limitations, the element would be made with no inertia, no spring torque, and no friction. Under these idealized conditions and with the element at rest, the torque applied when one ammeter element is energized is proportional to the current squared. The moving element instantly takes on a velocity such that the damping torque is equal to the applied torque. Since the damping torque is directly proportional to the angular velocity, it follows that angular velocity is proportional to the current squared. Under this condition of no inertia, the element will stop instantly when the impulse stops. The angular displacement then is proportional to the integral of i^2dt.

When inertia is present, the element will neither start nor stop instantly. In the appendix, it is shown that the angular displacement from a point of rest to a final rest position is independent of the inertia. In the derivation, friction is neglected because in a practical design the actuating torques will be large in comparison with friction torques.

The equations show that the deflection is proportional to $\int i^2dt$ when: (1) the electrical torque is proportional to the square of the current and independent of the angular position, and (2) the damping is proportional to velocity. In the recorder described, the damping is proportional to velocity, but neither of the other conditions are strictly met. The overall results, however, are such as to obtain substantially linear response with $\int i^2dt$.

Figure 3. Complete ampere-squared-second recorder

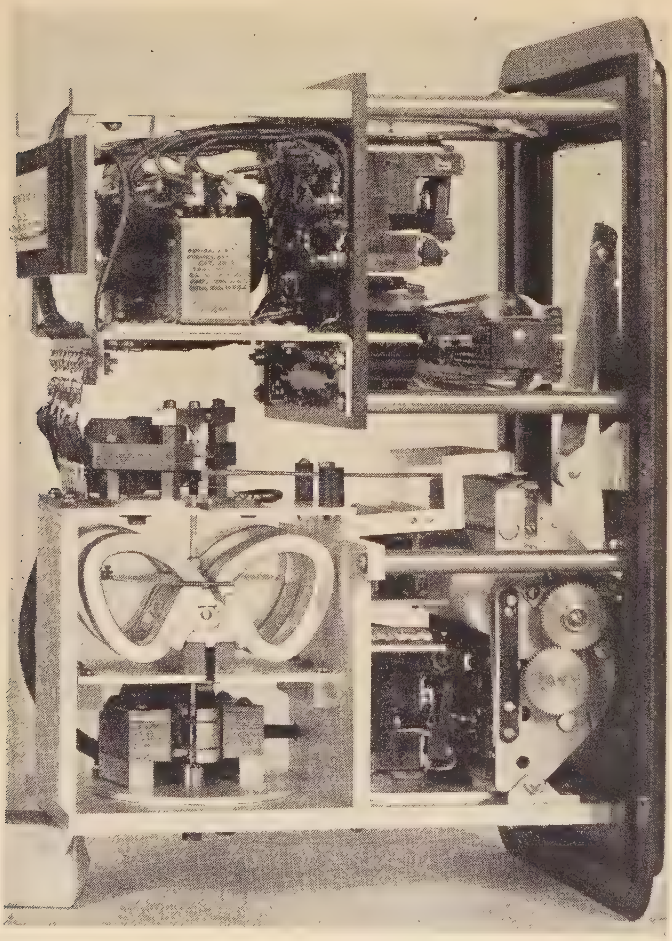

Figure 2. Side view of ampere-squared-second recorder with case off

Auxiliary Devices

The basic element described needs the addition of a recording and alarm mechanism and a device to control the sequence of events to make a complete instrument. (See figure 3.)

A. Method of Recording

A record of the maximum deflection of the pointer for each impulse is recorded on a strip chart. The chart drive is so arranged that the paper moves at a uniform speed as long as the welds are not spaced more than a few seconds apart.

A relay-operated print bar brings the pointer sharply against the strip chart (which is backed up by an inked roller ribbon) after the pointer comes to rest. This makes a short line on the back of the paper. The paper used is thin and the record shows through as a series of dots, one for each weld. The distance of the dot from the starting position is directly proportional to ampere-squared seconds. Once the record is printed, the other ammeter element is energized for a fixed time to return the element to the starting position.

The printing bar is carried by the Z-shaped member in figure 2. The printing bar is of metal except for an insulated

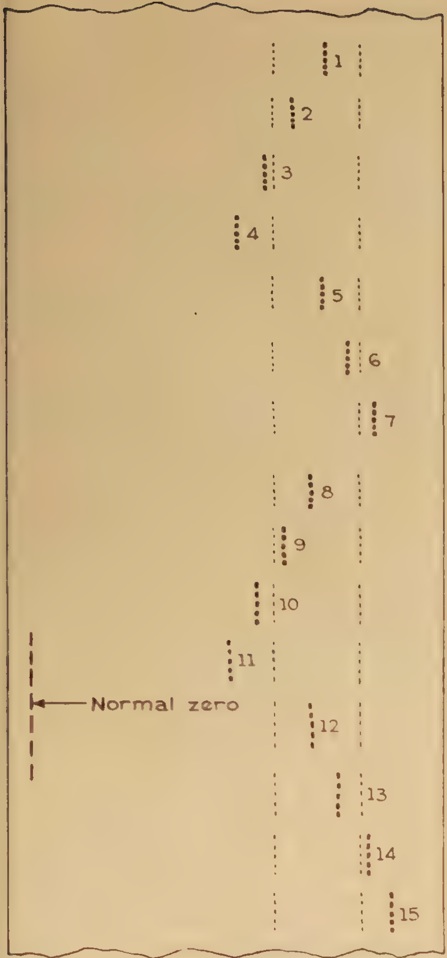

Figure 4. Tracing of an actual record from the weld recorder

Each of the darker dots represents one weld. The allowable limits are represented by the two parallel rows of light dots at the right. Groups 1 through 7 were made with 3 cycles current—the current changed as follows:

1—Current normal
2—Current reduced 5 per cent
3—Current reduced 10 per cent
4—Current reduced 15 per cent
5—Current normal
6—Current increased 5 per cent
7—Current increased 10 per cent

Groups 8 through 21 were made with current and voltage to the welder held constant and timing changed:

8—10 cycles
9— 9 cycles
10— 8 cycles
11— 7 cycles
12—10 cycles
13—11 cycles
14—12 cycles
15—13 cycles

insert at the point corresponding to 100 per cent deflection. An alarm is sounded if the pointer is not beneath the insulated insert when printing occurs. The length of the insert is determined by the tolerance allowed in $\int i^2dt$. Usual practice permits a variation of ±15 per cent in the ampere-squared seconds. An example of the type of record is shown in figure 4.

B. Sequencing Unit

The "brain" of the device is a unit which knows when to print the maximum deflection, when to energize the return element, and how long it must be energized to come to rest in the starting position.

The sequence of events is:

1. The impulse occurs and the pointer starts to move.
2. There is a waiting period while the pointer comes to rest.
3. The printer operates.
4. The moving element is returned to the starting position.
5. The device is made ready for the next impulse.

The waiting period must start when the impulse ends. The length of the waiting period depends upon the velocity at the end of the impulse, the moment of inertia of the system, the amount of damping, and the accuracy required.

The greatest velocity will be attained for the shortest weld and if the waiting period is sufficient for correct indication then, it will be more than adequate for any longer weld. The relationships used in determining the waiting time are shown in the appendix. On a one-cycle weld, with the recorder in figure 3, the pointer deflects approximately 25 per cent in the sixtieth of a second the impulse lasts and then coasts to nearly 100 per cent in the next tenth of a second. With the same recorder, it will deflect about 95 per cent of the final deflection during a 30-cycle weld, and in the next tenth of a second be substantially 100 per cent of final deflection. With the element used, a tenth-second wait was found adequate.

Since there is practically no control torque on the moving element, it will remain in any position it is placed. The zero position is determined by a stop, but a slight unbalance or shock might move the element in time. To provide a definite zero position, a small amount of magnetic material is attached to the damping vane. The damping magnets attract this material and hold the pointer against the stop. Only a small deflection is required to carry the magnetic material out of the field of the damping magnets.

Only a short time can be allowed for the return of the pointer, so it is necessary to accelerate it rapidly. On the other hand, if it hits the zero stop with high velocity, it will bounce and the return element will need to be energized until it comes to rest. The return element was designed to have high torque when the pointer was near full scale and to have the torque fall off rapidly as the element approached zero position. The return of the pointer from any scale position to rest at the zero position can be accomplished in 0.15 second.

A schematic diagram of the unit which controls the sequence of events is shown in figure 5. Under stand-by conditions, vacuum tube *T*-10 is conducting and relay *CR*-7 is energized. Tube *T*-9 is blocked by capacitor *C*-20 (which is charged to approximately 300 volts by current passed by *T*-9). The grids of both tubes are at filament potential. When an impulse is received, *CR*-6 is energized which connects the grid bias capacitors *C*-21 and *C*-22 in parallel with *C*-20. The grid bias capacitors then share the charge with the blocking capacitor and some current is passed by *T*-9 to again block itself, but this is not enough to operate *CR*-8. No visible change occurs except that *CR*-6 pulls in and stays in during the impulse. When the impulse ends, *CR*-6 drops out, connecting the charged bias capacitors across each grid. Both tubes are then well beyond cutoff and *CR*-7 drops out. This short-circuits the blocking capacitor *C*-20, but *T*-9 cannot yet pass current because of the high negative grid voltage. The charge on *C*-21 leaks off and 0.1 second

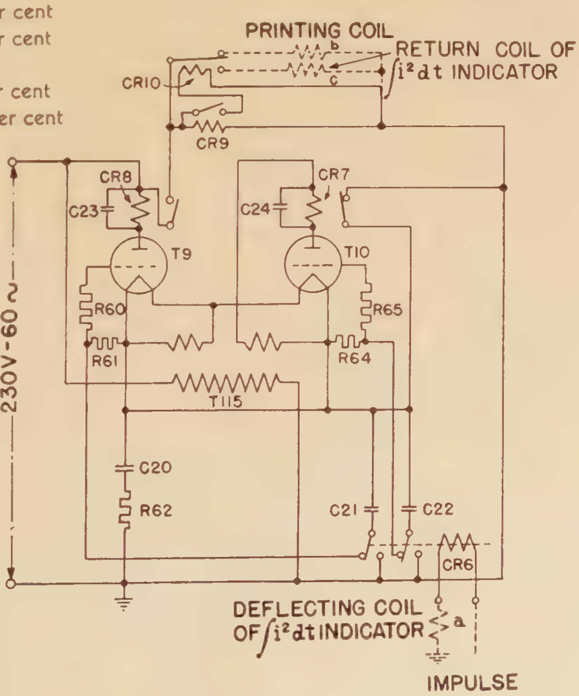

Figure 5 (right). Schematic diagram of sequence unit

after CR-6 opened, T-9 becomes conducting pulling in CR-8, which energizes the printing relay and CR-9. When CR-9 pulls in, it operates CR-10 which transfers power from the print coil to the return coil of the recorder. About 0.15 second after CR-8 operated (or 0.25 second after CR-6 dropped out) the bias of T-10 has leaked off enough to conduct and pull in CR-7. This removes the short circuit from the blocking capacitor C-20 and it charges up and stops the flow of current through T-9 and CR-8. Then CR-8, CR-9, and CR-10 drop out and the circuit is again ready for another sequence.

Conclusion

A considerable number of these recorders have been put in service in the last three years. In spite of the apparent complexity, the high-speed operation, and the rough usage they receive, their performance has been satisfactory. While the recorder is particularly designed for resistance-welding applications, the combination utilized represents a new measuring tool that may be valuable in other fields.

Appendix

Assume system starts at rest when $t=0$ (time) and $\theta=0$ (angular deflection). The impulse starts at $t=0$ and lasts for a second (producing a uniform torque) of D dyne-centimeter seconds. The torque is $\left(\frac{D}{a}\right)$ dyne-centimeter. When the system moves there will be a counter torque due to inertia $\left(J\frac{d^2\theta}{dt^2}\right)$ and one due to the damping magnets $\left(N\frac{d\theta}{dt}\right)$.

$$J\frac{d^2\theta}{dt^2}+N\frac{d\theta}{dt}=\frac{D}{a} \tag{1}$$

Let

$$N\frac{d\theta}{dt}-\frac{D}{a}=p$$

$$\frac{J}{N}\frac{dp}{dt}+p=0 \tag{2}$$

$$\frac{J}{N}\ln\frac{pa}{D}+t=0 \tag{3}$$

$$p=\frac{D}{a}e^{\frac{Nt}{J}}=\frac{D}{a}-N\frac{d\theta}{dt} \tag{4}$$

$$-\frac{J}{N}e^{\frac{-Nt}{J}}=t-\frac{Na\theta}{D}+c \tag{5}$$

When

$t=0 \quad \theta=0$

$$\theta=\frac{D}{Na}t-\frac{JD}{N^2a}\left(1-e^{-\frac{Nt}{J}}\right) \tag{6}$$

$$\frac{d\theta}{dt}=\frac{D}{Na}\left(1-e^{-\frac{Nt}{J}}\right) \tag{7}$$

At the end of the impulse $t=a$, $\theta=\theta_1$, $\frac{d\theta}{dt}=\left(\frac{d\theta}{dt}\right)_1$

$$\theta_1=\frac{D}{N}\left(1-\frac{J}{Na}\left(1-e^{-\frac{Na}{J}}\right)\right) \tag{8}$$

$$\left(\frac{d\theta}{dt}\right)_1=\frac{D}{Na}\left(1-e^{-\frac{Na}{J}}\right) \tag{9}$$

The torque due to current ceases at this point and letting

t' = time after impulse stops
θ' = angle traversed after impulse stops

$$J\frac{d^2\theta'}{dt'^2}+N\frac{d\theta'}{dt'}=0 \tag{10}$$

As before let

$$\frac{d\theta'}{dt'}=p'$$

$$\ln\frac{p'}{p_0'}+\frac{N}{J}t'=0 \tag{11}$$

$$\theta'=\frac{J}{N}\left(\frac{d\theta}{dt}\right)_1\left(1-e^{-\frac{Nt'}{J}}\right) \tag{12}$$

The deflection at any time (t) after the *start* of the impulse =

$$\Delta=\theta_1+\theta'$$

$$\Delta=\frac{D}{N}\left(1-\frac{J}{Na}e^{-\frac{N(t-a)}{J}}\left(1-e^{-\frac{Na}{J}}\right)\right) \tag{13}$$

at an infinite time

$$\Delta=\Delta_\infty=\frac{D}{N} \tag{14}$$

Special Case

In practice a certain deflection Δ will be required for a given $\int i^2dt$. The impulse D obtained from $\int i^2dt$, the moment of inertia J, and the damping constant N all depend upon the design of the moving element and are not independent. Of the many possible combinations, it will be assumed that $J=150$, $N=6{,}000$, and that $\Delta=0.4$ in the following illustration.

For an ultimate deflection of 0.4 radian

$D=0.4\times6{,}000=2{,}400$ dyne-centimeter seconds

If the impulse lasts 1 cycle, then $a=0.0167$ second and the deflection at the end of the impulse (from 8)

$$\theta_1=0.4\left(1-\frac{60}{40}\left(1-e^{-\frac{40}{60}}\right)\right)$$

$=0.107$ radian

From (9)

$$\left(\frac{d\theta}{dt}\right)_1=\frac{2{,}400\times60\times0.487}{6{,}000}=$$

11.7 radians per second

If we wait 0.1 second after end of impulse, the element will coast

$$\theta'=\frac{11.7}{40}(1-e^{-4})=0.287 \text{ radian}$$

$\Delta=\theta_1+\theta'=0.394$ radian

$\Delta_\infty=0.400$ radian

For the one-cycle case a change of 25 per cent decrease in the assumed wait of 0.1 second would make 3 per cent difference in overshoot or 2.2 per cent change in indicated value. An increase of 25 per cent will cause less change.

At 30 cycles, $a=0.5$ second

$$\theta_1=0.4\left(1-\frac{2}{40}\left(1-e^{-20}\right)\right)$$

$=0.380$ radian

$$\left(\frac{d\theta}{dt}\right)_1=0.8 \text{ radian}$$

Waiting 0.1 second, the element will coast

$$\theta'=\frac{0.8\times0.982}{40}=0.0196 \text{ radian}$$

$\Delta=0.399$ radian

Glass-Bulb Mercury-Arc Rectifiers for Traction Service

CHARLES E. WOOLGAR
MEMBER AIEE

Synopsis: The paper gives a general survey of the ability of glass bulb mercury-arc rectifiers to satisfactorily meet the stringent requirements of traction service. The subject matter is arranged on the assumption that engineers of the United States and Canada are not familiar with the use of this type of equipment for traction work, and the author has approached the subject from the point of view of an engineer considering the merits of different types of conversion equipment.

Major features pertaining directly to glass bulbs are discussed such as plant capacity, maintenance, efficiency, robustness, etc., but no attempt is made to include wider problems common to mercury-arc rectifiers as a class, namely frequency changing, inversion, harmonics, etc.

Introduction

THE first type of rectifier installed in England (1923) for traction service was a glass bulb mercury-arc rectifier, and installations of this type are widely used for traction service in Great Britain and countries served by British manufacturers. Glass bulb installations exceeding 5,000 kw in capacity are in service operating for the most part within the 500 to 1,600-volt range most commonly employed for D.C. traction. On the London Passenger Transport Board system alone approximately 80,000 kw of glass bulb rectifier plant (distributed among more than 50 substations) is installed for operating trams and trolley-busses. For railway electrification, glass bulb rectifiers are equally serviceable and widely used. Typical examples are London, Midland and Scottish Railway (recently, electrification of the Euston-Watford line required 17 substations each approximately 2,500 kw), Bombay, Baroda and Central India Railway, and the New Zealand Government Railways. In 1938, against world wide competition, one glass bulb rectifier manufacturer received 15,000 kw of a 19,800-kw contract for traction rectifiers in South America. Typical Canadian traction installations are: British Columbia Electric Railways (2–330 kw, 1–660 kw), City of Edmonton 1–700 kw), and Britannia Mining and Smelting Company (1–330 kw).

Approximate over-all dimensions of a 1,000-kw, 550-volt D.C. rectifier, excluding transformer, would be 23 ft long by 4 ft deep by 9 ft high.

The above information indicates that there is nothing new in using glass bulb rectifiers for traction service.

Plant Capacity

The current output of a single glass bulb being limited, engineers unfamiliar with the equipment question the advisability of operating a number of bulbs in parallel. They know that to obtain 2,000 kw at 800 volts D.C., i.e., 2,500 amp, it would neither be economical nor practicable to operate numerous rotary convertors in parallel, and naturally do not immediately appreciate that this arrangement can be utilized with glass bulbs to the greatest advantage. Eight or ten glass bulbs would be paralleled, depending on the size of bulb used.

Arc voltage drop being proportional to the arc current a number of parallel arc paths minimizes the voltage drop and thereby increases plant efficiency. For example, if a single tank rectifier has an arc drop of 20 volts at 500 amp and 25 volts at 3,000 amp, then a 3,000-amp equipment comprising 6–500 amp units would effect a saving of about 15 kw in arc drop. Allowing for extra fan and exciter losses, this may represent an efficiency gain of 1%.[1,4]

It is well known that an arc tends to concentrate within a small space on the anode and steel tank rectifier manufacturers have had to resort to baffles and shields to obtain more even distribution. Arc concentration overheats the anode and gives rise to conditions liable to cause backfire. It has been found that the best way to obtain effective increase in anode area, is not by increasing the size of anodes, but by increasing their number. For the 2,000-kw traction rectifier mentioned above, the steel tank rectifier would probably be equipped with 12 anodes, whereas 8 six-arm glass bulbs would have 48 anodes, thereby having an enormous effective anode area to ensure avoidance of hot spots.[1]

Should inspection or maintenance be necessary on a bulb cubicle, that cubicle can be readily cut out of service without disturbing operation of the remaining cubicles. Thus in the above case, the seven bulbs would share full load between them, slightly overloaded, until the other bulb was restored to service. With other conversion equipment such maintenance would probably entail shutting down the entire unit.

In Great Britain, general development of steel tank rectifiers is in the direction of air-cooled pumpless units whose present outputs are between 250 and 750 amp, and the chief engineer of one manufacturer of both steel tank and glass bulb rectifiers, states that the general trend of application is in the direction of operating convenient-sized units in parallel rather than employing large single units with numerous anodes.[1] The advantages of the multi-unit construction used by glass bulb manufacturers, are now becoming more generally recognized.

Characteristics of Conversion Equipment

The engineer must examine a number of important factors before reaching a decision on conversion equipment. The more important of these factors are discussed below and the degree to which glass bulb rectifiers meet desired characteristics is considered.

1. Initial Cost

(*a*) *Equipment.* The cost per kw varies considerably, but steel tank, steel bulb, and glass bulb rectifiers are all competitive and show to advantage over rotating equipment.

(*b*) *Buildings.* Glass bulb cubicles can, in general, be arranged in equal or less floor space than single tank rectifiers, and as they have no auxiliaries such as water cooling pipes, pumps, recoolers, blower motors, or special starting equipment, building costs are less than for other conversion equipment.

(*c*) *Installation.* The costly foundations required for rotating equipment are not necessary for rectifiers, and the uniform weight distribution of glass bulb

Paper 41-100, recommended by the AIEE committee on land transportation, and presented at the AIEE summer convention, Toronto, Ontario, Can., June 16–20, 1941. Manuscript submitted March 25, 1941; made available for preprinting May 9, 1941.

Charles E. Woolgar is in the power apparatus division of Northern Electric Company, Montreal, Quebec, Can. He is an associate member of the Institution of Electrical Engineers, London, England.

The author wishes to express his indebtedness to the Hewittic Electric Company, England, and the Northern Electric Company, Montreal, for permission to prepare and publish this paper, and to those authors whose papers were so freely consulted.

1. For all numbered references, see list at end of paper.

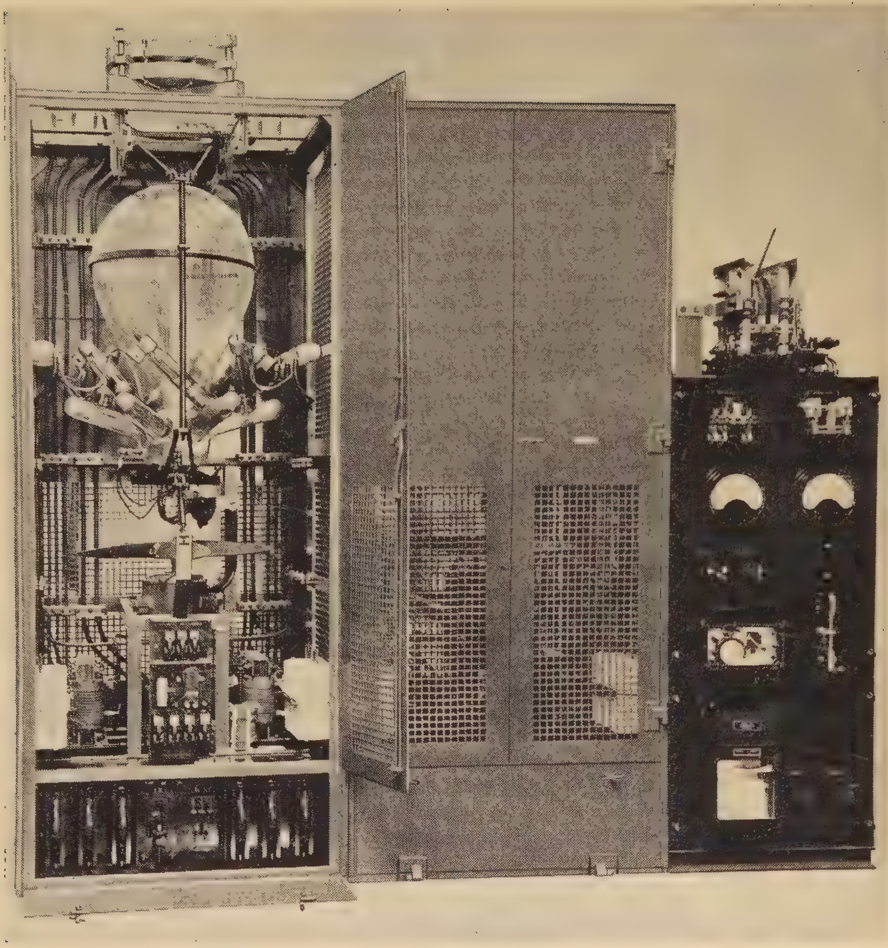

Figure 1. Street railway traction rectifier

330 kw, 550 volts d-c, double bulb unit complete with high speed circuit breaker panel, installed in British Columbia

cubicles can be sustained by a much lighter floor than that required by other types of rectifiers.

Since each cubicle is a self-contained rectifier unit with all auxiliaries (excluding main and auxiliary transformer) the installation, testing, and setting to work is much simpler than that required by more complicated types of conversion apparatus. This represents a considerable saving in initial cost.

2. Maintenance

(*a*) *Attention Required.* In common with other types of conversion equipment, glass bulb substations can be unattended, operating automatically or by remote control. No special attention is required.

(*b*) *Inspection.* Bulb transparency is of considerable practical value to operating engineers since by merely opening the cubicle doors it is immediately apparent whether the rectifier is firing properly. If required, individual bulbs can readily be removed from service and complete inspection carried out without interrupting supply to the remaining bulbs.

(*c*) *Sources of Trouble.* The sources of trouble of rotating equipment are well known and need not be discussed here, but it is advisable to draw some comparison between steel tank and glass bulb rectifiers in this respect.

In most steel tank rectifiers the great majority of breakdowns occur in auxiliary equipment, not in the rectifiers. On one large traction system, the records of 16 rectifiers over a period of 19 months showed maintenance carried out as follows: control gear—45.5%, vacuum pumps—31%, water system—21%, rectifiers—2.5%. Percentages refer to the number of failures. On those occasions when steel tanks must be opened and baked out, the expense involved due to outage of plant and cost of power for bake-out may be considerable.[2]

In glass bulb rectifiers connectors passing through the bulb wall have the same coefficient of expansion as the glass, thereby ensuring no leakage through the seals. The bulb itself is not porous and therefore perfect conditions for a permanent vacuum obtain. No pumping is required. Cooling is provided by a vertical-motor-driven fan, placed directly under the bulb. Ignition may be very simply accomplished with a dipping electrode attracted to a small, external electromagnet operated from the exciter transformer. The only moving parts are the fan and a small contactor which operates when starting. No other auxiliaries are required.

Glass bulb rectifiers, having a minimum of auxiliaries, require negligible maintenance.[6]

(*d*) *Bulb Life.* The life of a glass bulb is indefinite, as no wear occurs. Records show many bulbs in service 15 years without developing trouble. Possibly the best commentary is the fact that glass bulbs of reliable manufacture can be insured at $4^1/_2$% per annum to cover a period of 10 years. Experience has shown however, that maintenance and replacement costs are too small to justify even this small premium. For a 2,000-kw traction rectifier of 8 bulbs, insurance at the above rate costs approximately 20 cents per kw per annum.

3. Efficiency

The advantages of lower arc drop and resulting increased efficiency consequent upon multi-unit construction were briefly discussed under "Plant Capacity."

At the load factors encountered in traction service, the all-day efficiency of rectifiers shows to advantage over rotating equipment,[2] due largely to the relatively flat rectifier efficiency curve from $^1/_4$–$^5/_4$ load. Typical efficiencies (in per cent) for glass bulb traction rectifiers are:

D-C Voltage	Load $^1/_4$	$^2/_4$	$^3/_4$	$^4/_4$	$^5/_4$
600	93.75	94.2	94.1	94	93.8
1,200	95.6	96	95.9	95.6	95
1,500	96	96.5	96.5	96.2	95.6

4. Power Factor

The average power factor for glass bulb rectifiers is fairly flat over the normal operating range, varying from 0.90–0.94 approximately between one quarter load and full load.

5. Voltage Regulation

Glass bulbs, like steel tank rectifiers have a drooping voltage characteristic, the regulation being approximately 5%. Compounding can be effected by grid control, voltage regulator, or by means discussed in other papers.[5]

6. Overloads

(*a*) *Standard Ratings.* For glass bulbs standard overload ratings for traction service are:

25% overload..........2 hours
50% overload..........$^1/_2$ hour

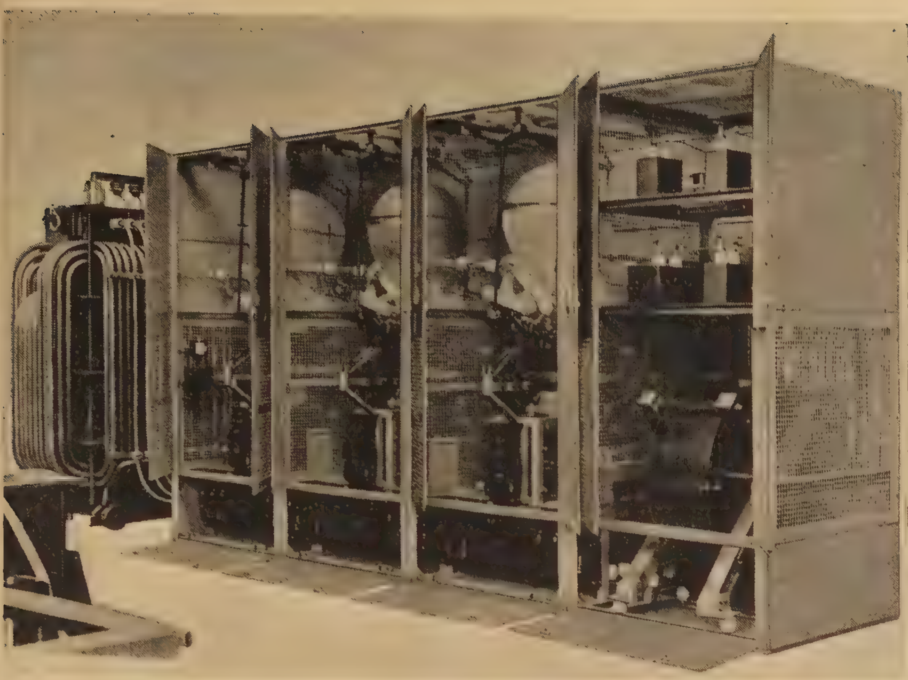

Figure 2. Railway traction rectifier

One of a set of six banks, each 600 kw, 650 volts d-c, with d-c smoothing equipment, England

100% overload..........5 minutes
200% overload..........momentary peaks

(*b*) *Non-Standard Ratings.* It is a simple matter to supply a glass bulb rectifier with any overload capacity required by simply installing the right number and type of bulb units with a suitable rectifier transformer. Actually each traction installation must be considered on its own merits and equipment supplied to meet particular load requirements.

(*c*) *Short Circuits.* Glass bulbs handle severe track short circuits without distress. Experience indicates that glass bulbs are less affected by short circuits than other types of conversion equipment. One engineer with wide operating experience of both rotating and static equipment confirmed that rectifiers are less sensitive than rotary converters and added that in his experience steel tanks were liable to backfire on track short circuits occurring within a half-mile of the substation but glass bulbs were not affected. The author does not intend this to represent a general condition but merely the experience of a particular engineer. It is of interest, however, that in 1938 another engineer stated "we employ a certain number of these (steel tank rectifiers) for traction purposes, but some of them have not approached the glass bulb type in respect of reliability."[1]

Multi-unit construction with its resultant low current density per anode, large effective anode area, and conditions of permanent vacuum contributes largely to stability under severe overload and short circuit conditions.

7. Stability and Robustness

(*a*) *A-C System Disturbances.* It is well known that rectifiers are insensitive to fluctuations of voltage or frequency in the A.C. network and in this respect ensure an absolute minimum interruption of traction supply not obtainable with rotary converters.[2,3]

(*b*) *Starting Time.* Ability to restart instantaneously after shut-down due to system disturbance, or to start up from cold in an emergency and to at once take on full load is of major importance. Glass bulb operation is largely independent of temperature and rectifiers of this type will start up and deliver full load current without delay. Pre-heating is not required except possibly in cold climates where the substation air temperature remains below freezing point for lengthy periods. Room temperatures from 4°C–40°C ensure immediate starting and stable operation.

(*c*) *Robustness.* Objections to glass bulbs are raised on the grounds of fragility and sensitivity to continued vibration or concussion. This has proved to be a fallacy. The bulbs are made of a special quartz type of glass and when handled with reasonable care breakages rarely occur. They are completely enclosed in individual sheet steel or expanded metal cubicles, and if anything, less liable to damage than the exposed commutators, brushes, relays, gauges, etc. of other types of conversion equipment.

The bulbs are secured firmly but flexibly in a suitable cradle and anode and cathode connections made through flexible copper conductors. Free from rigid connections of any type the bulbs are unaffected by continued vibration. Installations operating satisfactorily near gun testing locations at Woolwich Arsenal, underground in mines and subjected to blasting shocks, or in regions subject to earth tremors are ample evidence of their insensitivity to concussion.

Figure 3. Railway traction rectifier

3,600 kw, 1,200 volts d-c, installation comprising three 1,200-kw banks. One of two similar substations, England

A New Mercury Rheostatic Element for Regulation and Control

K. A. OPLINGER
MEMBER AIEE

Introduction

IN many regulating and control systems, the primary or actuating stimulus is available only at a low power level and must be amplified to obtain sufficient power output for the various control functions. This requirement, along with the increased use of automatic controls during the past few years has resulted in many industrial applications which require a simple, reliable power amplifier. Electronic tubes and special designs of rotating machines have been used for amplification where a continuous type of control is required, but in most applications it is difficult to justify the use of tubes or rotating amplifiers.

Contact Controls

Contact relays are often used for amplifying power in control circuits of the "on" and "off" type. For continuous control, a single pair of vibrating contacts makes a very simple amplifier. If the contacts are operated in a hovering position, their effective resistance varies with contact pressure and large changes in resistance, which will give large current changes, can be obtained with extremely small variations in pressure. The ratio between the change in resistance and the change in pressure is a measure of the contact amplification. It is possible to obtain very high values of amplification in this manner and to adjust this amplification by changing the amount of contact vibration. A practical application of the contact amplifier to speed regulators was described in a previous paper.[1] The power output of such an amplifier is, of course, limited by the current interrupting capacity of the contacts.

Rheostatic Control

Another simple device for controlling larger amounts of power is the rheostat. By using a large number of steps it is possible to secure practically continuous control. Novel rheostatic control members have been built which require very little force and movement to operate a large number of contacts.[2] In designing a rheostatic control, the following requirements are of importance in most regulating and control systems:

1. The power required to operate the rheostat should be small since the actuating stimulus is usually at a low power level.
2. Hysteresis resulting from frictional and magnetic forces should be small.
3. The inertia of moving parts and their displacement should be low to permit quick response.
4. The contacts should require no maintenance.

The above requirements become more difficult to meet as the output power of the rheostatic control is increased. By making use of the well-known advantages of the mercury switch, a new form of multicontact mercury rheostat has been developed to meet all of the above requirements and at the same time handle relatively large amounts of power. For convenience in describing this new device it has been called a "Mercurystat".

Design of Mercurystat

The contact element of the Mercurystat contains a large number of mercury switches so arranged that they can be operated by a small force and travel. The construction is shown by the schematic drawing, figure 1. A 40-step Mercurystat with its electromagnetic driver is shown in figure 2. Referring to these two figures, small flat terminals

Paper 41-98, recommended by the AIEE committee on industrial power applications, and presented at the AIEE summer convention, Toronto, Ontario, Can., June 16–20, 1941. Manuscript submitted March 26, 1941; made available for preprinting April 15, 1941.

K. A. OPLINGER is with the research laboratories of Westinghouse Electric and Manufacturing Company, East Pittsburgh, Pa.

The author wishes to acknowledge the assistance received from his associates in the laboratories and engineering departments and particularly the many helpful suggestions made by C. R. Hanna. The special speed control application described in this paper was made in co-operation with C. W. Drake and J. Z. Linsenmeyer. The speed matcher application was made in co-operation with C. E. Valentine and R. A. Geiselman.

1. For all numbered references, see list at end of paper.

---

8. Paralleling and Extensions

(*a*) *Paralleling Similar Units.* Each bulb unit of a multi-unit installation is adjusted at the factory for correct operation. In the two largest glass bulb substations in the world, 6,500 kw and 7,000 kw at 500 volts D.C. (industrial load) automatic, unattended, and remote-controlled, there are 44 and 40 bulbs respectively operating in parallel.

(*b*) *Paralleling Dissimilar Equipment.* Glass bulb units can and do operate in parallel with rotating equipment or steel tank rectifiers of equal or unequal capacities. Correct load sharing is arranged to suit plant conditions. To avoid considerable complication in grid control gear and high speed relays, it is desirable to arrange the rotating plant with a slight drooping voltage characteristic.

(*c*) *Extensions.* Glass bulb rectifier plant can be extended at any time and to any desired extent by adding the appropriate number of bulb units. This entails a considerable saving in capital cost as extensions to most conversion equipment necessitate installing units of large capacity.

Conclusions

Glass bulb rectifiers are suitable for traction service and in some respects show to advantage over other types of conversion equipment, particularly so in the multi-unit construction, lack of troublesome auxiliaries, high overall efficiency, reliability, negligible maintenance costs, and flexibility.

References

1. Recent Progress in Power Rectifiers and their Applications, **W. G. Thompson.** IEE *Journal*, volume 83, October 1938, and discussions.

2. Equipment and Performance of Steel-Tank Rectifier Traction Substations Operating on the Underground Railways of the London Passenger Transport Board, **A. L. Lunn.** IEE *Journal*, 1935.

3. Rectifier Equipments for Regenerative Working, **J. C. Read.** *B.T.H. Activities*, May–August 1940.

4. Ignitrons for the Transportation Industry, **J. H. Cox** and **G. F. Jones.** AIEE Transactions, volume 58, 1939 (December section), pages 618–22.

5. Voltage Control of Mercury-Arc Rectifiers, **G. R. McDonald.** AIEE Transactions, volume 58, 1939 (November section), pages 563–6.

6. Six Years of Glass-Bulb Mercury Arc Rectifiers, **J. H. Steede.** *Electrical News and Engineering*, June 1, 1938.

7. Frequency Changing With Mercury-Arc Mutators, **R. Feinberg.** IEE *Journal*, volume 85, October 1939.

each having a central hole, are assembled as shown with an insulating spacer between each pair of terminals. Stainless steel bellows with a plug to reduce the volume of mercury, are attached to the bottom of the terminal assembly. Displacement of the bellows raises and lowers a central mercury column which shorts out, or cuts in, sections of an external resistor connected to the ends of the terminals. A gas space is provided at the top of the terminal assembly to prevent an appreciable change in pressure from the slight changes in volume caused by the bellows displacement. The entire assembly, consisting of bellows, terminals, insulators, and gas space, is hermetically sealed by a special process so that the interior of the Mercurystat can be pumped out and charged with an arc-reducing gas such as hydrogen. It is then sealed off from the atmosphere to eliminate all contact maintenance.

Because of the large ratio between the area of the bellows and the area of the mercury column, only a small displacement of the bellows is required to short out all terminals. In the 40-step Mercurystat shown in figure 2, the terminal assembly is about two inches high but only a few thousandths of an inch displacement of the bellows is required to short out all steps.

Figure 1. Schematic diagram of Mercurystat

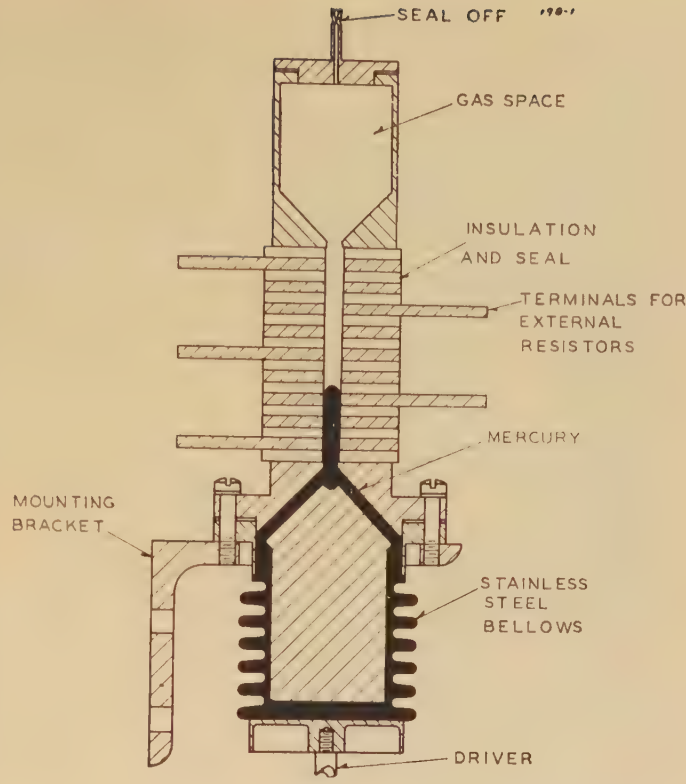

Power Capacity

The power capacity of the Mercurystat is fixed by the current interrupting capacity of the contacts and by the internal losses of a given design. The contact duty in a rheostat of this type is much less severe than in the ordinary mercury switch operated at line voltage. The large number of steps reduces the voltage across steps so that relatively high currents can be handled. For example, a small 40-step Mercurystat as shown in figure 2 can easily control six kilowatts. Life tests made with a unit this size operating in a 220-volt d-c circuit and varying the current from 12 amperes minimum to 30 amperes maximum showed practically no sign of contact wear after 5,000,000 cycles of operation.

At higher currents, the internal losses of the above design were greater than could be dissipated with a reasonable temperature rise. These losses result from the resistance of the terminals and the mercury column and from the contact drop between the mercury and the terminals. Greater power capacity can of course be obtained by increasing the cross section of the terminals and the mercury column. This will reduce the resistance of these parts and at the same time give a larger assembly capable of radiating more heat. The contact drop tends to remain constant as in the case of carbon brushes on slip rings and is in the order of about one-half volt for currents up to 100 amperes.

Design of Driver

In some applications the bellows of the Mercurystat can be operated directly by a lever or cam which is a part of the control system. In other cases it is desirable to have an electromagnetic driver so the Mercurystat can respond to electrical stimuli. A driver for this purpose should be free of friction and magnetic hysteresis and should have some reference standard such as a spring force for its calibration. Such a driving element is shown in figure 2. The driving arm is mounted on cross springs to provide a frictionless pivot. An insulating turnbuckle is used to connect the bellows to this arm. A calibrating spring is attached to one end of the driving arm while an iron armature is mounted on the other end. The armature travels in a magnetic circuit having a constant air gap and a laminated iron core. By proper armature shaping the negative magnetic stiffness of the driver can be made to match the positive stiffness of the Mercurystat and calibrating spring so that very small changes in coil current will cause the driver to move through a wide range. Typical response curves of a Mercurystat and driver are shown in figure 3. When working on the curve with a one per cent droop the entire resistance range is covered with only a 0.05 watt change in the driver coil. The change in power output of the Mercurystat may be say five kilowatts so that the power amplification, or ratio of output to input is 100,000. Lower values of amplification can be obtained by merely reducing the spring force. This will result in lower coil currents and a less perfect matching between the negative stiffness of the magnetic circuit and the positive stiffness of the spring. Different amounts of droop secured in this manner are shown by the curves in figure 3. The slight nonlinearity in response can be eliminated by grading the external resistance between steps to give a linear relation between input and output currents.

Changes in temperature and in atmospheric pressure may cause small variations in the calibration of the Mercurystat. The amount of these variations depends upon such factors as the type of drive, the dimensions of the Mercurystat, and its sensitivity when used in a regulating system. In any given application it is usually possible to proportion the design so that these variations are negligible. If the bellows position is positively fixed by the control, changes in atmospheric pressure will have no effect upon the calibration. Temperature changes will cause slight variations in the volume of the mercury which will change the height of the mercury column. These changes can be

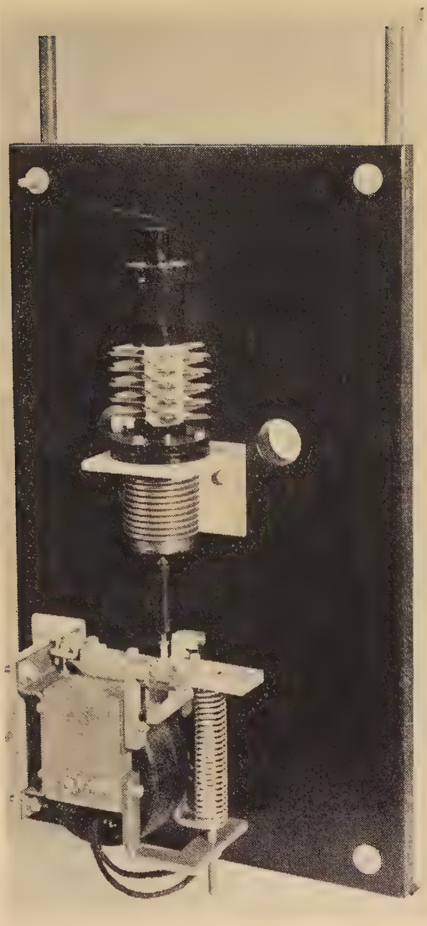

Figure 2. A 40-step Mercurystat and driver

kept small by decreasing the volume of mercury with a plug as shown in figure 1.

If the Mercurystat is used in a regulating system where the bellows are operated by an electromagnetic driver as shown in figure 2, the amount of error caused by variations in temperature and atmospheric pressure will depend upon the droop of the regulator. For example, if

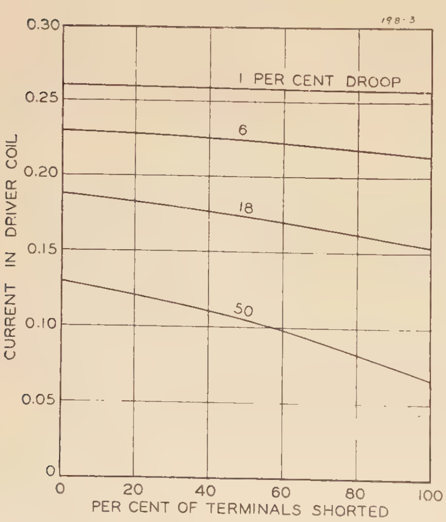

Figure 3. Mercurystat and driver response

Figure 4. Three-phase Mercurystat

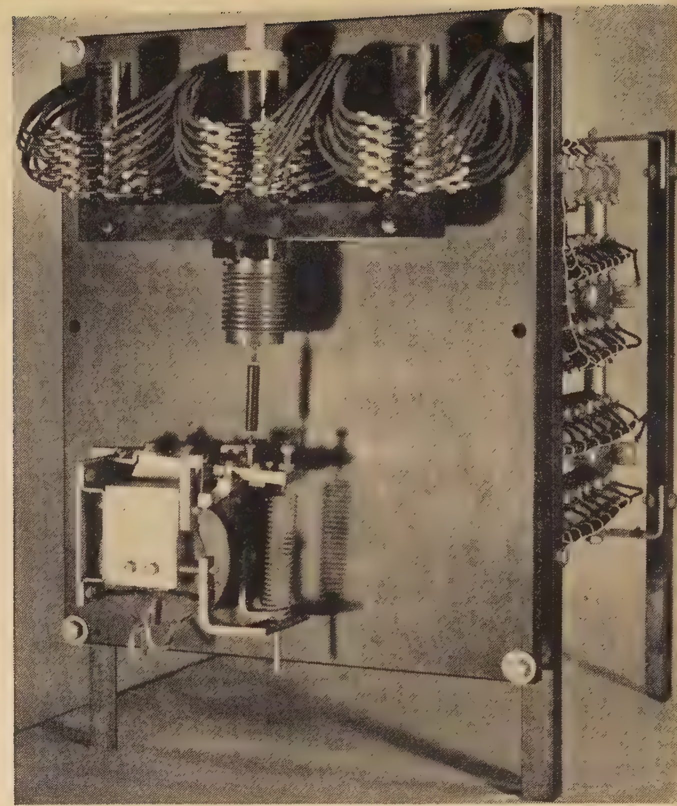

the regulator has no droop, any change in the height of the mercury column as a result of changes in temperature and atmospheric pressure will be corrected for with no error. If the regulator has a one per cent droop and changes in temperature and atmospheric pressure should cause the Mercurystat to swing through say 20 per cent of its range, the regulator will correct for this swing with a resulting error equal to one-fifth of one per cent. Errors due to variations in atmospheric pressure can be eliminated by attaching a duplicate sealed bellows to the driving arm in such a position that any change in atmospheric pressure will give equal and opposite moments to the driver arm. By making the volume of this second bellows equal to the gas space at the top of the mercury column, variations resulting from pressure changes of the internal gas with temperature can also be eliminated.

Applications

Numerous applications for the Mercurystat will be apparent to those who have worked with regulators and power amplifiers. A few applications will be briefly described to show how it can be adapted to typical control problems.

A Mercurystat designed for controlling the speed of three-phase, wound rotor motors is shown in figure 4. Three sets of terminal assemblies are mounted on a bar which has internal holes connecting the three mercury columns to a common bellows. Movement of the bellows will then give equal changes in external resistors which are connected in each phase of the rotor. If a voltage proportional to speed is applied to the electromagnetic driver of the Mercurystat, it will serve as a stimulus for regulating any speed within the range of the control resistance. When load changes occur which cause the motor speed and the voltage on the Mercurystat driver to change, the Mercurystat will automatically adjust the external resistors to maintain a constant motor speed. The control voltage, proportional to speed, can be obtained from a small electric tachometer driven by the motor. In place of an electric tachometer the voltage across slip rings can be rectified and used to control the Mercurystat. When the motor slip increases, this voltage will increase and the Mercurystat will short out resistance to bring the motor back to its regulated speed.

In another application of speed control, a special speed cycle was made possible by using a cam to drive two Mercurystats. One Mercurystat is used to change the resistance in the rotor of an a-c motor to adjust speed. The other Mercurystat is used to secure rapid changes in speed by controlling the dynamic braking of a d-c generator mounted on the same shaft as the a-c motor. This latter control is obtained by changing the resistance in series with the armature and series field of the d-c generator. The bellows of the two Mercurystats are so coupled that when

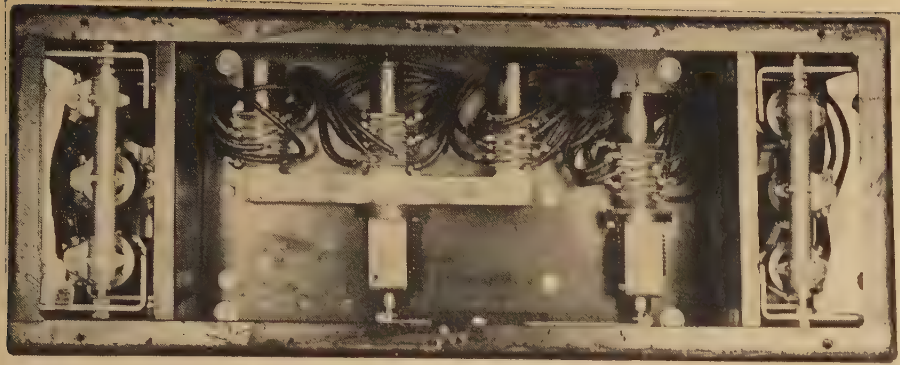

Figure 5. Special speed controller

one is inserting resistance in the rotor of the a-c motor to reduce speed, the other is shorting out resistance in the d-c generator to give increased dynamic braking. This arrangement gives a large number of speed settings which can be reached very quickly by adjusting the main control cam. Figure 5 shows this form of speed controller as built to meet special space limitations. The resistors required by the control are mounted on the sides and in the back of the Mercurystat panel.

In some applications where the operating stimulus is at a high power level, the amplification of the Mercurystat is not important. This was the case in applying the Mercurystat to a speed matching regulator. Here the Mercurystat was used because of its high-current capacity and its sealed-in contact structure. The Mercurystat is shown in figure 6 mounted on a panel which is supported by the synchronous motor and differential housing of an experimental speed matcher. It is a 100-step unit with the terminals connected to control resistors mounted in the rear of the panel. The synchronous motor drives one-half of the differential, and the cone pulley, located just below the Mercurystat resistors, is connected to the other half through the hollow shaft of the synchronous motor. If the speed of the cone pulley differs from the reference speed of the synchronous motor the movement of a traveling nut in the differential is transmitted to a lever on the side of the housing which operates the bellows of the Mercurystat in a direction to change the field excitation of the regulated motor and correct for the error in speed.

It will be apparent to those familiar with the design and application of voltage regulators that the new device can also be applied in this field. If used with an exciter, the Mercurystat has sufficient power capacity to regulate the voltage of medium and large size a-c generators. The circuits used in such regulating systems along with problems of stability and damping, have been described in a previous paper.[2]

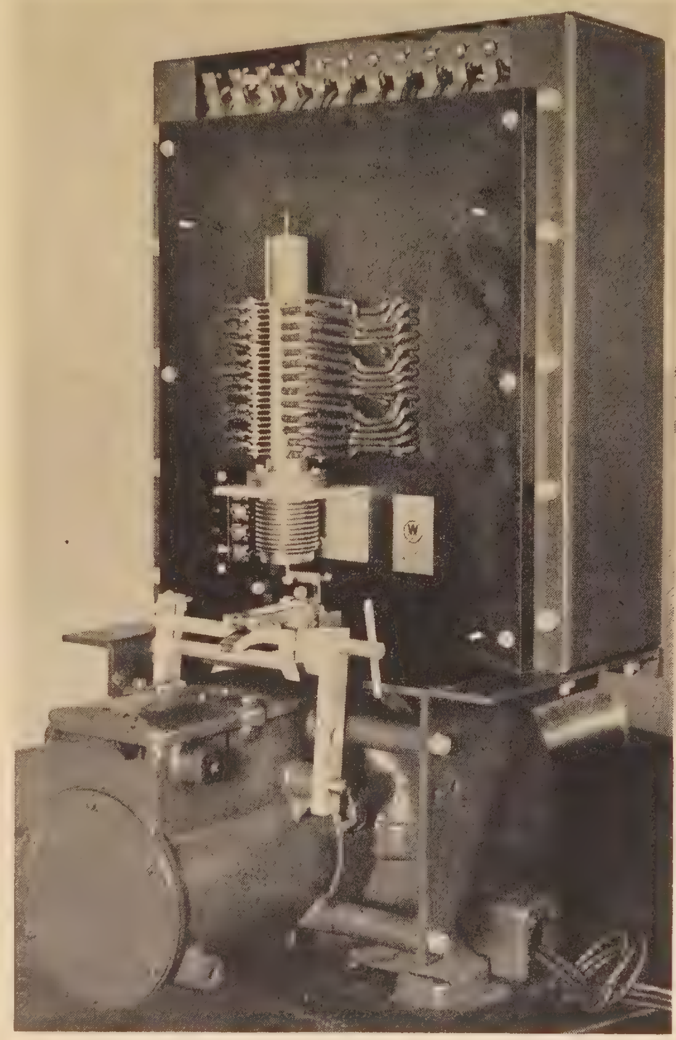

Figure 6. Speed-matcher regulator

Summary

The principal design features, along with several typical applications, were described for a new form of mercury rheostatic element which has been designated as the "Mercurystat". The unique features of the Mercurystat are its large number of hermetically sealed mercury contacts and the small force and travel required for their operation. It was shown that relatively large amounts of power can be controlled by the Mercurystat and because of the small input power required for its operation, power amplification in the order of 100,000 can be obtained. The performance of this new device along with its simplicity and absence of wearing moving parts should find many applications for it in automatic control systems.

References

1. Recent Developments in Speed Regulation, C. R. Hanna, K. A. Oplinger, and S. J. Mikina. AIEE Transactions, volume 59, 1940, pages 692–700

2. Recent Developments in Generator Voltage Regulation, C. R. Hanna, K. A. Oplinger, and C. E. Valentine. AIEE Transactions, volume 58, 1939, pages 838–44.

Modern Motors Serve City Transit Systems

W. J. CLARDY
MEMBER AIEE

C. A. ATWELL
ASSOCIATE AIEE

Synopsis: City transit motors operated today include many new mechanical and electrical features. Modern vehicles differ greatly from those of a decade ago and propulsion motors contributed substantially to the advances achieved. Meeting present-day needs has required designs for 300 and 600 volts involving extensive use of new materials, application to new types of drive, and suitability for dynamic braking. Mechanical design includes unusual developments in frame construction, method of mounting, lead arrangement, ventilation, housings, and bearings. Compactness has led to ingenuity in brushholder arrangement to secure accessibility. Armatures require judicious selection of materials for shafts, cores, and commutators as well as special seasoning and balancing procedure. Electrical design betterments have been introduced in armature slots, armature coils, field coils, and insulation. Provision for quietness and good commutation are also salient points. The new designs have resulted in high electrical and weight efficiency for series motors used on Diesel-electric busses, trolley coaches, and street cars in comparison with old type machines. Excellent commutation has produced outstanding stability at rapid accelerating and dynamic braking rates. Vehicle performance is exceptional with respect to safety, operating efficiency, available selection of accelerating and braking rates, and the broad speed range of the dynamic brake.

"PEOPLE must be served" has become the success axiom of city transit operators. Creative action has resulted to keep pace with present-day travel demands. The development of modern vehicles is closely associated with progress in propulsion motor construction. Machines in use today include many new mechanical and electrical features. Weight below ten pounds per horsepower, compared with almost three times this figure for old machines, is a measure of what has been achieved with modern designs. These advances have made possible the Diesel-electric bus, trolley coach, and the modern street car.

Performance Requirements

Motors used today differ greatly from older types and are the result of the solution of a number of interesting problems. Machines have been designed for 300 volts and applied two in series to reduce weight in comparison with 600-volt motors. In order to meet the limitations imposed by the space available, new materials have been used extensively. This has assisted in meeting the demand for motors much smaller than older types producing the same horsepower.

The change to different types of drive with spring-supported motors required fundamental departures from previous practices. Gear cases and axle bearings were no longer needed. The new method of mounting protected motors from road shocks and thus permitted lighter construction. An increase in gear ratio was practicable which gave a "step-up" in armature speed and a decrease in over-all weight. Modern vehicles use the motors for stopping as well as starting which introduced the added duty of dynamic braking.

Mechanical Design Features

An evolution has occurred in mechanical design features because of the experience gained during the transition from the axle-hung to spring-supported type machine. The rolled steel frame has replaced the cast type. This new construction has important manufacturing advantages and provides a more effective magnetic circuit. Hidden casting blowholes are eliminated, a condition which often reduced the area of the magnetic section and caused variation in speed between individual motors built in accord with identical designs. There is ample room for original assembly or servicing of the poles field coils, and field wiring between coils The method of motor support is dependent on the vehicles. For example, trolley coach motors are held at the two ends by feet cast on the housings which are suitable for bolting to horizontal cross members. Modern street car motors are supported by clamping them in circular grooves cut in the outside of the frames.

Flexible stranded cable with rubber insulation and heavy rubber jacketing is used for leads. Protection is provided for passage through frames by heavy rubber bushings. Four leads are needed by a series motor, two for the armature with the interpole field, and two for the main field. When field shunting is applied to increase speed, it is obtained by applying a shunt across the main field. The older method of field tapping required an additional lead. A novel terminal construction is used on the modern street car motor which employs four insulated stud type terminals. The construction is illustrated in figure 1. The terminals are made of brass and are tapered at the outer end. A stud bolt between each pair is used for clamping the internally tapered terminals of the car wiring tightly against the motor terminals. This scheme permits easy removal of the car wiring from motors in the restricted mounting space available on trucks.

Commutator and fan end housings are removable castings that fit accurately into the bore of the frame and are bolted to its extremities. Each housing includes its bearing assembly. The commutator end housing supports and provides access to the brush holders as well as being an inlet for the ventilating air. The fan end housing has space for the

Paper 41-104, recommended by the AIEE committee on land transportation, and presented at the AIEE summer convention, Toronto, Ontario, Can., June 16–20, 1941. Manuscript submitted April 17, 1941; made available for preprinting April 30, 1941.

W. J. Clardy and C. A. Atwell are both transportation engineers of Westinghouse Electric and Manufacturing Company, East Pittsburgh, Pa.

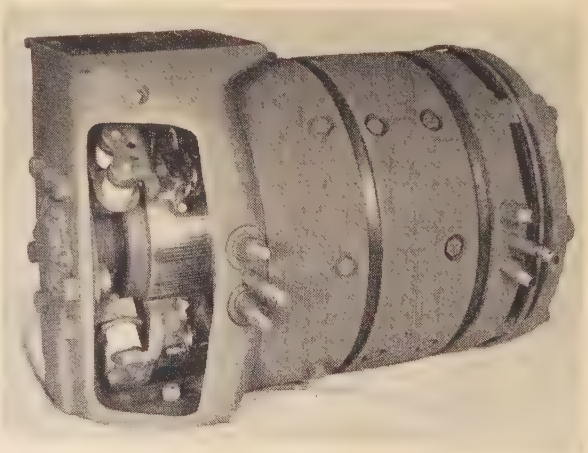

Figure 1. View showing novel lead arrangement of 300-volt, 55-horsepower street-car series motor

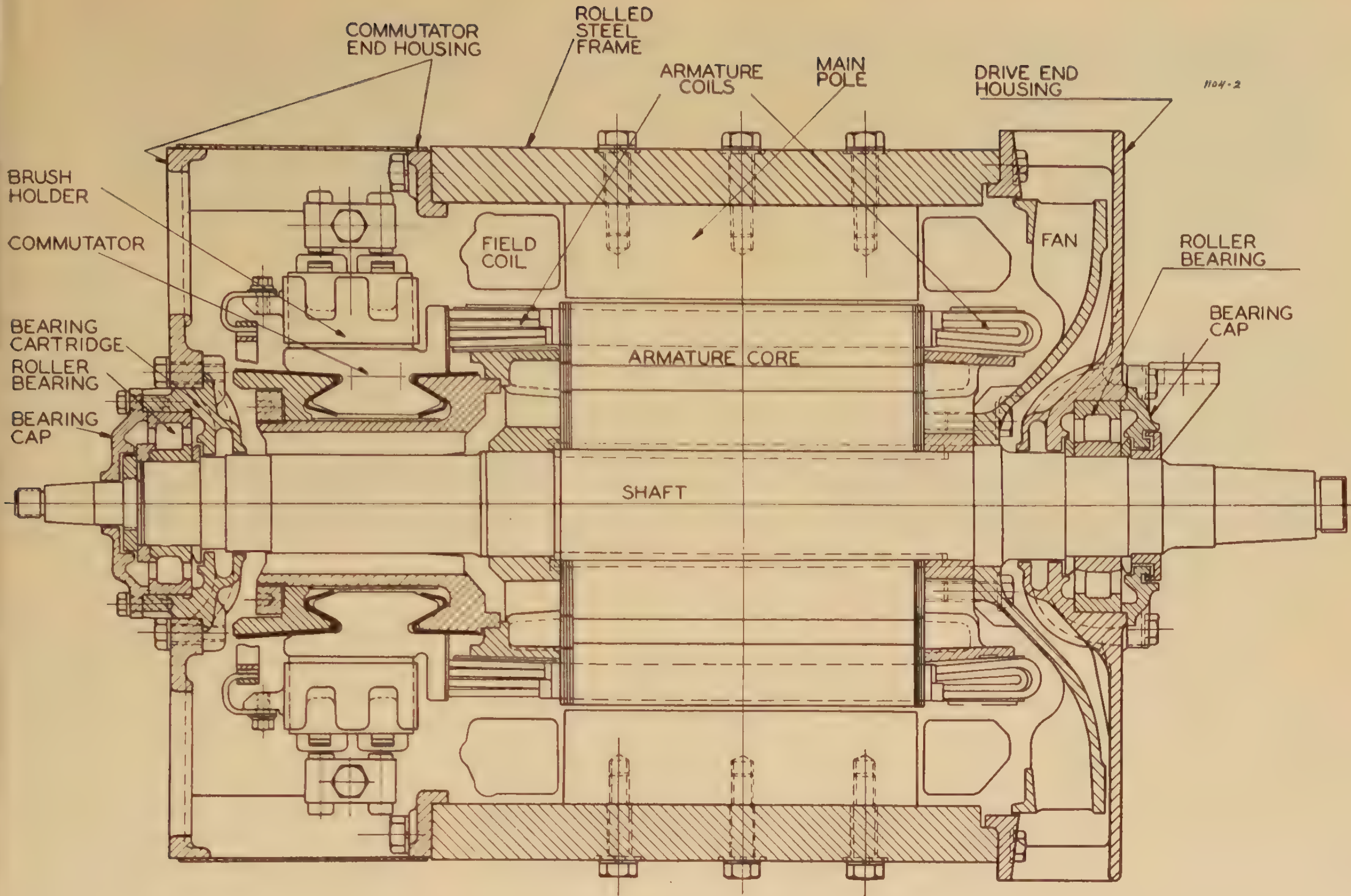

Figure 2. Construction of 600-volt, 140-horsepower trolley coach series motor

fan and is built with air outlets proportioned to give quiet and efficient discharge of the air leaving the fan blades. Adequate ventilation is obtained by the armature shaft fan. It draws air in at the commutator end, through spaces between the field coils and over the surface of the armature, as one path, and through longitudinal ducts in the armature core as a parallel path.

The support of bearings in housings and the method of enclosure have been carefully analyzed in conjunction with recent development work. Roller or ball bearings with grease lubrication are standard. Performance records[8] are exceptional for the designs of the past five or six years in comparison with those of 10 or 12 years ago. This is especially true in the case of roller bearings. It can be attributed to the proper initial internal clearances, the method of mounting and assembly in the housings, and the effective enclosure of the grease space by metal labyrinth seals.

The housing and bearing construction shown on figure 2 is typical. At the fan end, the bearing fits in a bore in the housing and has an outer bolted cap. At the commutator end, the bearing is carried in a separate cartridge having an outer enclosing cap. This cartridge fits in a bore in the commutator end housing and is also bolted to it. The commutator end roller bearing is of the thrust type and locates the armature longitudinally. A "free" type roller bearing is used at the fan end, allowing for expansion and contraction in the length of the shaft with respect to the stationary parts. An important advantage of this type of construction is that the complete armature with bearings may be removed without exposing either of the bearings to dirt. Such a removal is made by taking out the

Figure 3. Armature for 600-volt, 140-horsepower trolley coach series motor

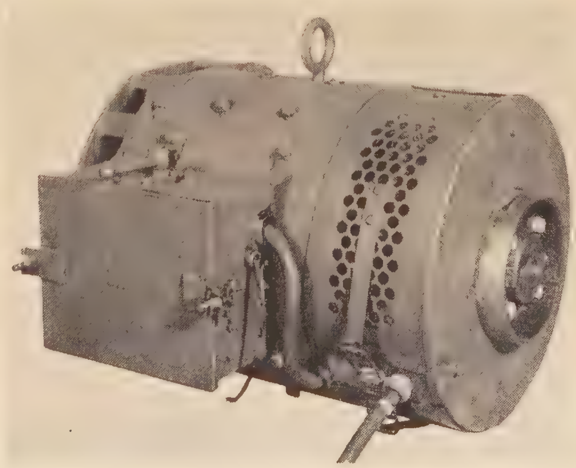

Figure 4 (right). Diesel-electric bus motor for use with 125-horsepower power plant

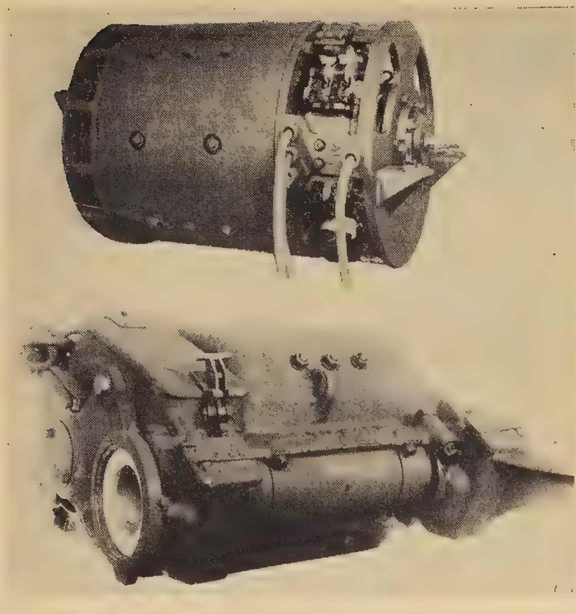

Figure 5 (left). Modern 600-volt, 140-horsepower trolley coach series motor compared with old type 600-volt, 125-horsepower machine

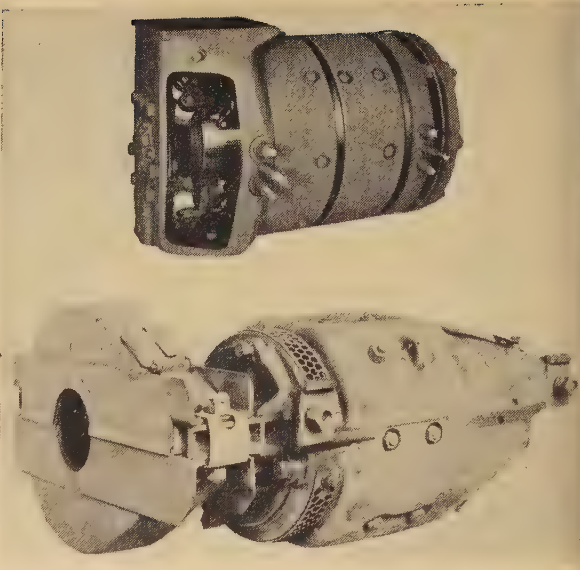

Figure 6 (right). Modern 300-volt, 55-horsepower street car series motor compared with old 600-volt, 50-horsepower machine

bolts holding the cartridge to the commutator end housing and the bolts holding the fan end housing to the frame. The complete armature with the fan end housing and the commutator end cartridge, as illustrated in figure 3, may then be drawn out of the motor at the fan end. This construction also permits a final grinding of the commutator surface while running in its own bearings. The procedure is to support the armature and housing assembly in a grinding fixture and rotate the armature by a small driving motor coupled to the shaft while grinding the commutator surface.

The commutator end housing construction is closely connected with the support and accessibility of the brush holders. Carbon brushes are subject to wear and the brush holders must be available for easy inspection and replacement of carbons. The brush holder used is the bronze box type with two insulated supporting pins. This provides a simple and accurately located mounting with means for radial adjustment as the commutator surface wears to a smaller diameter. Brush holders have adjustable steel clock springs to maintain the correct pressure of brushes against the commutator. The pressure finger and the carbons have flexible copper shunts. Spacing and position are set during manufacture by means of a jig which accurately locates the center line of the brushes relative to the center line of the commutating pole faces. After this setting is made, bolts holding the brush holder support block to the housing are welded in place. Individual brush holders are interchangeable.

Armatures are solidly constructed and capable of operating at high speeds without mechanical distortion. High-grade material in shafts and other parts contribute to this durability. The laminated core assembly with cast armature coil supports at each end of the punchings is arranged so that the shaft may be pressed out without disturbing the relation of punchings, armature windings, and commutator. Broken shafts rarely occur, but in case of injury to shaft ends, easy replacement is essential.

Commutators are seasoned at high temperature while being rotated near the maximum operating speed. This allows the mica between bars to become set to withstand movement at the maximum temperature and speed encountered in service. The seasoning process is a series of heatings and tightenings carried on under these conditions until the commutator runs smoothly either cold or hot at maximum speed. Armature balancing in a modern dynamic balancing machine is essential. The best construction provides for two dynamic balancings: one before the armature is wound, and one afterward. All of the unbalance of the armature except that due to the winding is permanently eliminated and if the armature is rewound, only the unbalance of the armature winding need be provided for. The coil support castings at each end of the punching assembly are provided with balancing pockets into which the required amount of melted lead is poured. This takes care of the unbalance before winding. The small unbalance of the armature winding is compensated for by adding solder to the wire banding on the armature coil ends.

Electrical Design Features

The electrical design of a d-c motor involves the selection of the number, size, and shape of the armature coils and slots and the arrangement and shape of the conductors in the slot. Commutation, flashing characteristics, and heating as well as complete motor size and weight are closely related to slot design. The newly developed insulating materials such as glass insulated conductors, glass fiber tape, and glass cloth backed mica wrappers for armature coils have done much to increase the efficiency of the slot design. The ratio of cross section of copper in the slot to the total cross section of the slot itself has been raised without sacrificing factors affecting commutation, flashing, and heating. Slot wedges for retaining the armature coils in the slots have replaced the use of wire bands on the core. The material used for wedges is usually micarta. The wedge construction is more reliable mechanically than core bands at high peripheral speeds. Their use eliminates eddy current losses produced in bands and the detrimental effect of core bands on commutation.

The small size of modern motors and the use of form wound, single turn, wave type armature coils, makes armature winding a simple procedure. Individual armature coils are varnish treated before winding and the wound armature is given a series of heatings, dippings, and oven bakings using a newly developed insulating varnish. The new varnish has improved characteristics of dielectric strength, more permanent set after baking, and provides a smoother surface that is more repellent to dirt and oil.

The field coil arrangement is made symmetrical around the armature by using the same number of commutating coils and poles as main coils and poles, usually four of each. The coils are either formed of strap copper wound on edge or flat

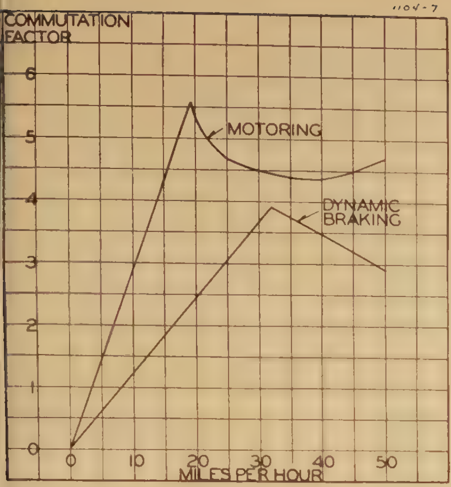

Figure 7. Commutation curve for 600-volt, 140-horsepower trolley coach motor

wound in sections depending on the particular design involved. The field coil construction has also benefited from the available new insulating materials. They occupy a minimum of space and are formed to fit accurately between the pole tips and the frame. The complete frame, pole, and coil assembly are given a dipping and baking treatment with insulating varnish similar to that used for armatures. A smooth hard coating over the insulated surfaces of coils and cable or strap lead connections is obtained. It has high dielectric quality and is resistant to water, dirt, or oil. Modern motors use insulation designated by the AIEE rules as class *B*. The materials consist principally of asbestos, mica, and glass fiber and are little affected by high overload temperatures often encountered in transit service.

Quiet operation is essential for use on vehicles with rubber tires or resilient wheels. Possible sources of motor noise are the brushes, bearings, fan, or armature teeth. All of these noises have been reduced in modern designs. Brush chatter or squeak is prevented by brush holder construction and smooth riding brushes. Bearing noise has been lowered to the point that a noisy bearing indicates that it is defective and must be replaced. Windage noise has been minimized by streamlining fan blades and air outlets. Magnetic noise from the armature is avoided either by skewing the slots or by using slots parallel to the shaft and giving careful attention to shaping of main pole tips and air gap taper. The latter method is more desirable because of greater ease of winding coils in straight slots and because slot skewing often widens the commutating zone under the commutating pole to an undesirable degree.

Commutation and flashing characteristics have been the subject of considerable study to secure long brush and commutator life and to permit the use of service dynamic braking. The higher rotational armature speeds tend to make this problem more difficult. This is largely offset by the use of single turn armature coils which compare with two or even three turn coils for older type machines. Also, the use of two 300-volt motors in series to utilize 600 volts from the trolley, has permitted designs with better commutation and flashing factors. In the case of the single motor for trolley coaches, a 600-volt commutator is required. However, the motor is of sufficient size to permit the use of a single turn armature coil, and other parts affecting commutation and flashing can also be well proportioned. While the commutation and flashing characteristics of a d-c motor are closely related, the design factors favorable to one are somewhat opposed to the other. A satisfactory balance must be obtained that will meet the requirements for both. For example, fewer armature conductors favor low "sparking volts" under the brush, but freedom from flashing calls for sufficient commutator bars, with the required armature conductors, to prevent the maximum volts per bar from becoming excessive at the maximum armature volts encountered in service. A flashover is started by the voltage between adjacent commutator bars becoming so high that arcs between bars are maintained after these bars pass under the brush. One precaution is to avoid main field strength distortion incident to the effect of the armature, thus preventing a peak in the field form. The series motor inherently averts an excessive armature distorting

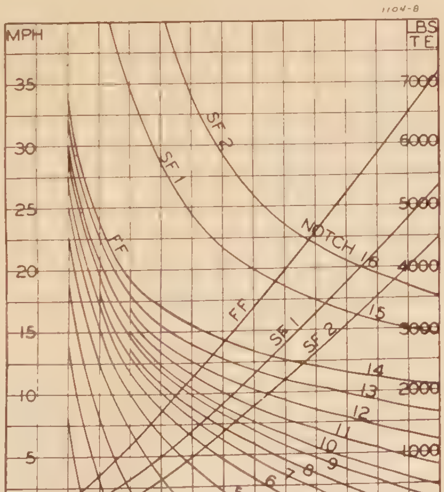

Figure 8. Acceleration curves for 600-volt, 140-horsepower trolley coach motor

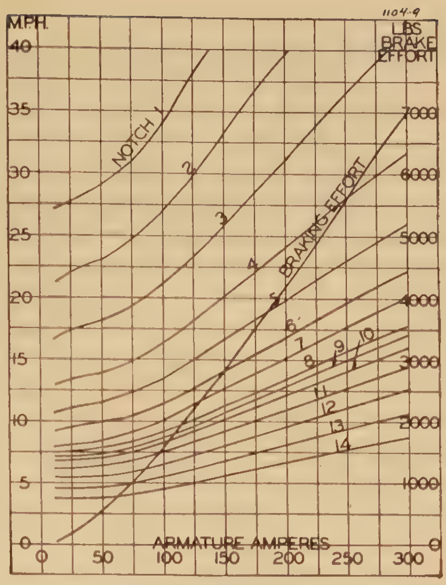

Figure 9. Dynamic braking curves for 600-volt, 140-horsepower trolley coach motor

effect because the ratio of armature to field ampere turns is constant and relatively strong in dynamic braking. Under the condition of acceleration with shunted field, some distortion can be allowed in the field form as the terminal voltage is never above the trolley voltage. The field shunt is made with the proper amount of inductance so that sudden changes of load will cause no transient weakening of the field. Good commutation under the condition of maximum accelerating amperes requires that the magnetic circuit of the commutating poles be unsaturated.

Typical Modern City Transit Motors

The Diesel-electric bus motor, designated as the 1435 type, is illustrated in figure 4. The machine is capable of handling the output of a 125-horsepower engine-generator power plant. The weight of the motor is 880 pounds which is exceptionally light for the available performance capacity.

The modern trolley coach would be impractical without the 1442-type motor which has been designed for this vehicle. The machine is illustrated in figure 5. It rates 140 horsepower at 600 volts and weighs 1,360 pounds—less than 10 pounds per horsepower. A picture of an old type 125-horsepower motor is shown in the same illustration to give a relative comparison. The latter unit weighs 3,430 pounds excluding gear and gear case—over 27 pounds per horsepower.

The development of the present-day street car is closely associated with the 1432-type, 300-volt motor shown in figure 6. This is a 55-horsepower machine

Measurements of Pre-Breakdown Currents in Dielectrics With a Cathode-Ray Tube

HUBERT H. RACE
FELLOW AIEE

A. Introduction

IN order to obtain more information regarding the mechanism of electrical breakdown in insulating liquids, a number of experimenters[1,2,3] have studied current flow as a function of applied voltage, using high-sensitivity d-c amplifiers with indicating instruments having relatively long-time constants. Such instruments will not follow rapid changes in current where the time intervals are of the order of milliseconds or less. Therefore we decided to investigate the possibility of using a cathode-ray tube as a current detector to follow current changes just preceding breakdown. This paper describes current measurements in liquids with 200-microsecond impulse voltage waves and current measurements in liquids and solids with gradually increasing unidirectional voltage applied to the specimens.

Paper 41-96, recommended by the AIEE committee on basic sciences, and presented at the AIEE summer convention, Toronto, Ontario, Can., June 16–20, 1941. Manuscript submitted January 29, 1941; made available for preprinting April 11, 1941.

Hubert H. Race is research engineer with General Electric Company, Schenectady, N. Y.

The author is indebted to R. A. Pfuntner for assistance in making these measurements and to N. Rohats for suggestions and circuit details connected with the cathode-ray equipment.

1. For all numbered references, see list at end of paper.

B. Measurements on Liquids Using Balanced Impulse Circuits

Breakdown in liquids gives no warning preceding its occurrence which can be used to trigger the sweep of a cathode-ray tube so as to make a breakdown self-indicating. Therefore we applied to the test cell a transient voltage increasing at nearly a constant rate of such a value that the test cell would break down on the rising portion of the voltage wave (figure 1). A sweep trip was built designed so that the sweep could be initiated at any predetermined time after the start of the voltage transient. Since the sweep time was also adjustable, the cathode-ray tube could be used to observe any portion of the voltage or current transient if the necessary single transient writing speed and deflection sensitivity could be obtained. A 15-kv cathode-ray oscilloscope[4] was used with photographic attachment to obtain the desired writing speed.

Because of the high rate of voltage rise necessary to obtain breakdown in one sweep of the cathode beam, the cell capacitance charging current would be much greater than the conductance current. Therefore two balanced, opposing impulse circuits were used, as shown in

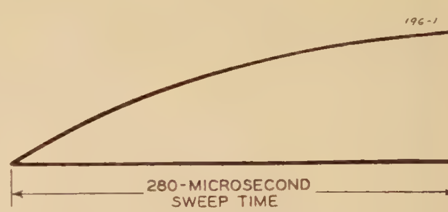

Figure 1. Impulse voltage-time curve

weighing 695 pounds—just over 12 pounds per horsepower. The same picture includes an old type 50-horsepower 600-volt motor and gives a visual indication of the progress made in the new design. The earlier type weighs 2,000 pounds or 40 pounds per horsepower.

Performance Characteristics

Satisfactory commutation requires minimum sparking at the brush faces under the most unfavorable combination of load and speed encountered in service. In figure 7, the "commutation factor" is a measure of the average voltage between bars under the brush. This figure shows how this factor varies throughout the speed range for motoring and dynamic braking for a 600-volt series trolley coach motor. The motor design is such that the maximum value of this "commutation factor" is below that which produces sparking at the brush faces. It is lower for dynamic braking than for motoring.

The series motor has the inherent advantage of a rapidly increasing dynamic braking effort as speed is stepped up. Thus, when a vehicle is gaining speed down grade and the dynamic brake is applied, any desired balanced condition may be quickly obtained. There is no possibility of the motor reaching an unstable condition and permitting the vehicle to run away if the mechanical brake fails. Dynamic braking with the series motor is effective when the trolleys leave the wire if battery operated control contactors are provided. When power for control operation is obtained from the trolley, the dynamic brake is unaffected as long as trolley voltage is sufficiently high to close the main circuit contactors. Thus, considerable voltage drop may occur without adversely influencing the dynamic brake.

Accelerating performance of the series motor is exceptionally smooth. Rates of acceleration, determined by the amount of pedal advance, permit an operator to start a vehicle at a rate selected to conform to traffic requirements. This gives the operating flexibility so necessary in city service. A set of acceleration curves, applicable to the modern trolley coach, is shown in figure 8.

The range of the dynamic brake obtained with the series motor is unusually broad. This is illustrated by the braking curves shown in figure 9. Braking current is effectively regulated to maintain any selected rate of braking up to the maximum capacity of the motor equipment. The uniform motor current which is obtained provides equal tractive effort values on all notches and thus maintains the desired braking rate. The series motor is capable of developing its full braking rate down to three or four miles per hour if these low speeds are desired.

New Motors Extensively Used

The new designs of motors for Diesel-electric busses, trolley coaches, and street cars have been generally applied on city transit systems. The machines available are the product of considerable engineering effort to reduce weight, increase efficiency, and improve output. Results are creditable as a contribution which has assisted in the development of modern transit vehicles.

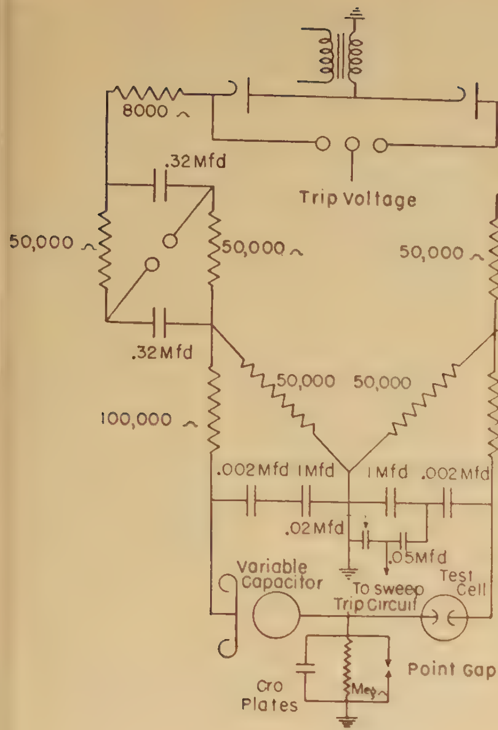

Figure 2. Balanced opposing impulse circuits to counterbalance capacitance charging currents

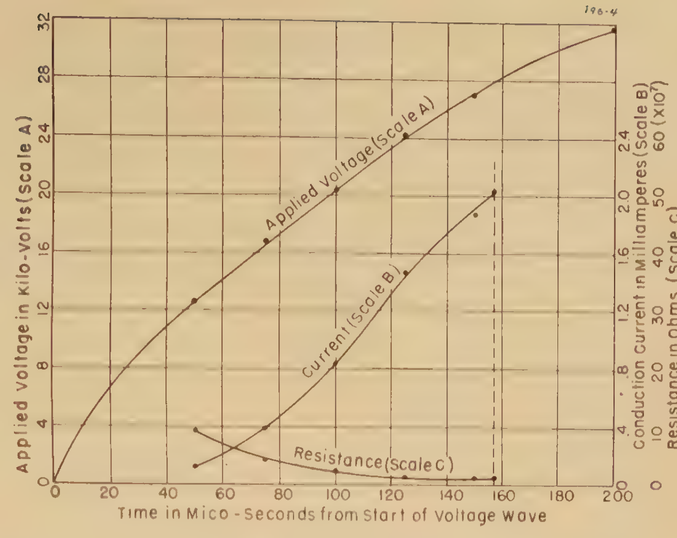

Figure 4. Current-voltage-time curves for a high-conductivity liquid

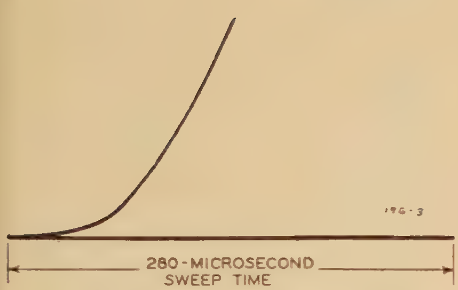

Figure 3. Breakdown current in a high-conductivity liquid

Diphenyl oxide + diphenyl

figure 2.[9] An adjustable air capacitor was used to balance out the capacitance current of the test cell. Under these conditions the voltage between point (*A*) and ground should be zero if the conductance current in the test cell were zero. Also if the cell conductance current were appreciable the voltage drop across the one-megohm resistor could be indicated by the cathode-ray deflection as a measure of this current.

Proper operation of this circuit depends upon equal voltage-time transients of opposite polarity being applied to the two sides of the circuit. The charging currents are then equal and opposite so that only the voltage drop due to the conductance current appears across the measuring resistor. If this resistor was larger than one megohm, the capacitance of the leads and cathode-ray oscillograph deflection plates provided a comparatively low-impedance shunt for the fast transients. Even with one megohm it became necessary to correct the resulting curves, both for the deflection plate capacitance and the circuit unbalance due to the drop in the resistor.

Good results were obtained on a mixture of commercial diphenyl and diphenyl oxide which was continuously circulated through a filtering and degasifying system.[5] Figure 3 is a good example of the type of curve obtained, and figure 4 shows the corrected curve plotted with time, current, voltage, and resistance scales. The pre-breakdown currents in this liquid were very high (one or two milliamperes). However, lower conductivity liquids could not be studied because of insufficient sensitivity. Figure 5 shows a typical shot taken on a low viscosity cable oil (GE number 5314) with a 22-microsecond sweep. After breakdown, the high-frequency damped oscillation is determined by the circuit constants, not the liquid. No pre-breakdown current can be seen, meaning *that the current was less than 10^{-4} amperes up to within a fraction of a microsecond of breakdown.*

C. Measurements on Liquids Using Gradually Increasing Voltage and Photographing Repeating Sweeps on a Cathode-Ray Tube

1. Apparatus

At a low rate of voltage application the capacitance charging current is negligible. Methods were worked out to trip the sweep circuit repeatedly at two-millisecond intervals and to use a continuous feed movie camera without shutter to record the resulting single traces. A 15-kv tungstate screen tube was used to get high photographic intensity. The film moved approximately parallel to the sweep direction at such a speed that successive sweeps uncovered or progressed about one-fifth of the length of a single trace on the film. A resulting hypothetical pre-breakdown current is shown schematically in figure 6. The slowly increasing unidirectional voltage-time curve was measured with a photoelectric recorder.[5] A manually operated selector switch (figure 7) was used so that the operator, while watching the cathode tube deflection, could vary the sensitivity and thus follow a slowly rising current as the voltage was gradually increased. The photographic setup was arranged so that the operator could view the tube screen from the side during the entire run. The 10^5 and 10^6 ~ resistors were wire wound, the others were electrolytic, using solutions of tetrabutyl ammonium picrate in a mixture of diphenyl and diphenyl oxide. Sealed off glass cells were used to prevent resistance changes with time and the concentration and cell dimensions were varied to give the desired resistances. Since the sweep time used is about 40 microseconds and the sweep interval is 2 milliseconds, we have a 2 per cent prob-

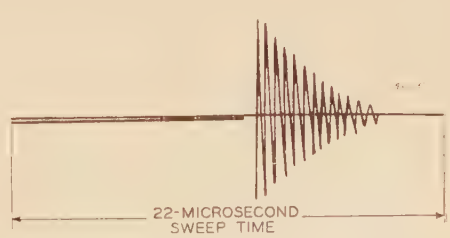

Figure 5. Breakdown in mineral oil

22×10^{-6} seconds sweep time

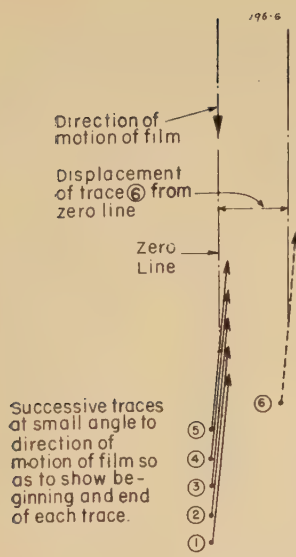

Figure 6 (left). Sketch of expected record on moving film

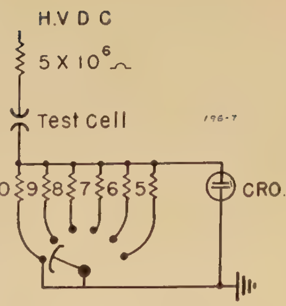

Figure 7 (right). Selector switch for varying the current sensitivity of a cathode-ray tube

Numbers correspond to the exponent to base 10 of the resistance in ohms

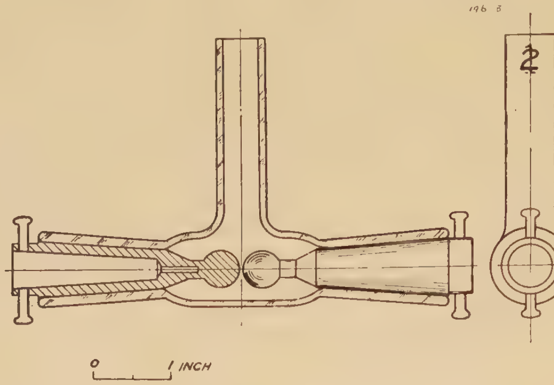

Figure 8 (right). Removable electrode gravity cell

ability of catching a breakdown transient if it is only of the order of microseconds duration.

2. Current-Time Data for a Low-Viscosity Mineral Oil (GE 5314)

For these experiments open cells (figure 8) having spherical electrodes of three different metals were used. The electrodes were polished on a dry clean buffing wheel. Then the electrodes and cells were chemically cleaned, steamed, and dried in a 100-degree centigrade oven as described by Dornte.[6]

Table I shows the last current readings and the breakdown gradients for this series of tests and figures 9 and 10 show the current-time data taken at intervals from the movie film record of the cathode-ray tube deflections. *These data give additional evidence for the conclusion that the conditions of the experiment particularly regarding the electrode surface are the important factors governing pre-breakdown current as well as the breakdown gradient.*[3,5]

3. Pre-Breakdown Current in Heptane

A hemispherical electrode, closed cell prepared and filled with *pure, dry* heptane by Dornte[3] was measured first with his FP54 amplifier below breakdown and then up to breakdown with the equipment described in this paper. The data taken from the records of the latter measurements are shown in figure 11.

It is interesting to examine these data in terms of two possible explanations of their cause. The Wien-Onsager[7] derivation* would predict that if $\log_{10}(I/E)$ is plotted against $\sqrt{\text{volts per centimeter}}$, the asymptotic slope equals

$$\frac{0.434}{T}\sqrt{\frac{8\times 9.64}{\epsilon'}} \tag{1}$$

for this experiment with heptane $\epsilon' = 1.91$, $T = 300$ degrees Kelvin so that the limiting slope $= 0.0092$. Figure 12 shows the data for heptane plotted in this form with the theoretical slope indicated.

Baker and Boltz[1] suggested that the limiting factor in conduction might be a potential barrier at the electrode-liquid interface so that a modified Schottky relation should apply.** Their derivation indicates that if $\log_{10} I$ is plotted against $\sqrt{\text{volts per centimeter}}$, the limiting slope should be given by the expression

$$1.91(\epsilon')^{1/2}/T \tag{2}$$

This relation gives a slope of 0.0089 for our data.

On the other hand, LePage and DuBridge[8] do not agree with the Baker-Boltz derivations and arrive at the relation.

$$1.91/(\epsilon')^{1/2}T \tag{3}$$

For heptane this gives a slope of 0.0045. The data for heptane are plotted in figure 13 with these two slopes indicated. The results for heptane fit the Onsager and Baker-Boltz derivations better than the LePage-DuBridge calculations.

* This theory is based upon increased dissociation of ion pairs at increased field strengths.

** This theory assumes that the controlling factor in current flow is the ability of electrons to escape into the liquid from the electrode surfaces and therefore is limited by a "work function" similar to that involved in electron emission into gases.

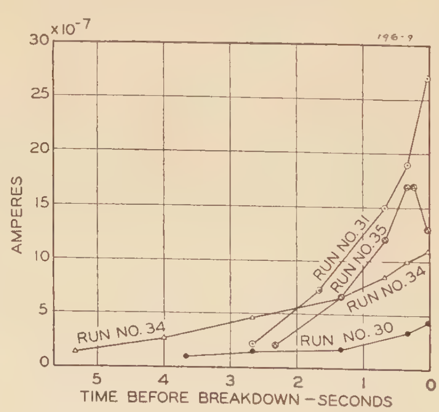

Figure 9. Pre-breakdown current in mineral oil

See table I

4. Pre-Breakdown Current in Conducting Liquids

To determine the effect of adding conducting ions, filtered, chemically pure toluene alone (run 66) and filtered toluene+0.025 per cent tetrabutyl ammonium picrate (run 72) were tested in the quartz cell with stainless steel spherical electrodes. The results are shown in figure 14. Before applying high voltage, the d-c resistance was measured at low voltage in each case as follows, run 66, $R = 1.8\times 10^{10}$ ohms, run 72, $R = 8.8\times 10^{8}$ ohms. The breaks in the current curves indicate definite changes in mechanism of conductance as the gradient is increased. Such breaks are commonly observed if the current-measuring equipment has a sufficiently wide range of sensitivity.

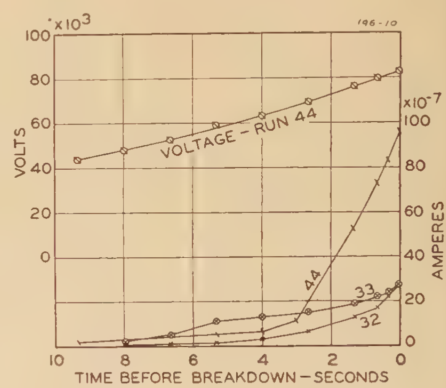

Figure 10. Pre-breakdown current in mineral oil

See table I

Since conducting ions have been added for run 72, the results should be checked against the Wien-Onsager theory. Therefore figure 15 is plotted but, contrary to expectations, the slopes of the conductances versus gradient lines were much

Table I. Pre-breakdown Conditions in 5314 Oil

Run No.	Symbol	Shot	B.D. Gradient (Kv/Cm)	Current before B.D. × 10^{-10} Amperes	Resistance Before B.D. × 10^{-10} Ohms	Electrode Material	Electrode Spacing (Cm)
30		1	600	4.3	8.5	Al	0.061
31	⊙	2	213	.27	0.5	Al	0.061
32	×	1	471	.27	2.6	Steel	0.15
33	⊗	2	208	.27	1.1	Steel	0.15
34	△	1	650	.11	4.0	Cu	0.069
35	△	2	265	.13	1.4	Cu	0.069
44	∮	1	550	.96	0.86	Steel	0.15

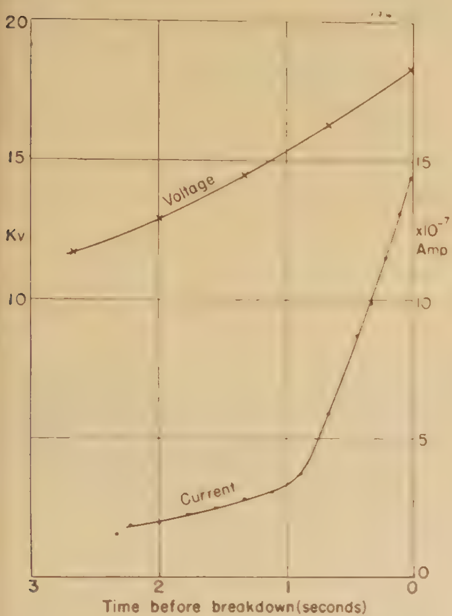

Figure 11. Pre-breakdown current and voltage in dry heptane

lower than would be required by the theory which predicts a slope of 0.008 for toluene. Likewise the same data are plotted in figure 16 to obtain a comparison with the potential barrier theory. The toluene containing conducting ions seems to check the LePage-DuBridge derivation but the toluene alone does not.

Unfortunately this investigation was discontinued before the above calculations were made so that the runs have not been repeated and checks are not possible at present. However, the results seemed worthy of reporting even though they are inconclusive as to the mechanism involved.

5. Discussion of Results on Liquids

In none of the breakdown records on liquids did we catch the breakdown transient. The last trace on each record was substantially like those immediately preceding it, showing the slowly increasing current with increased voltage as shown in figures 9, 10, 11, and 14. It seems reasonable to conclude that the observed current increases are ionic but that the final breakdown is electronic and occurs very fast (fractions of microseconds, see figure 5). Furthermore it seems that the pre-breakdown ionic current may be unrelated to the breakdown electronic current since the results of many investigations indicate that the breakdown gradient appears to be affected more by electrode surface conditions than by the ionic conductivity of the liquid.

D. Pre-Breakdown Currents in Solids

A number of experiments were tried to see whether the methods described in part *C* could be used to measure current just before breakdown in solids. The test pieces were prepared by drilling 3-millimeter coaxial holes from opposite ends of a 1.5×1.5×7-centimeter test piece. The ends of the holes were made hemispherical with a special reamer and the thickness of the test section between

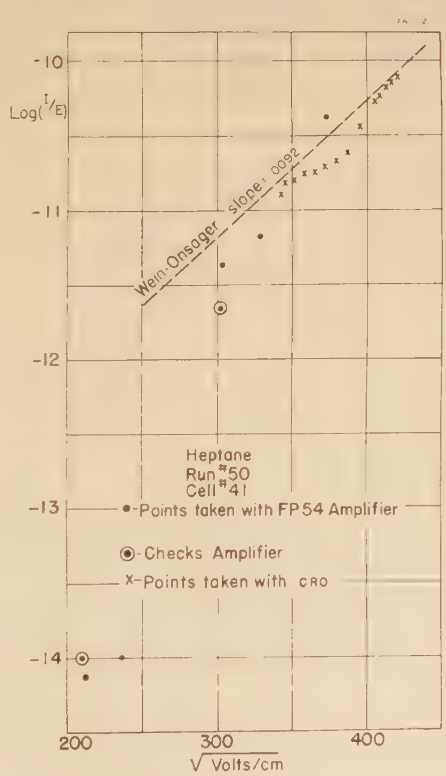

Figure 12. Plot of data for heptane to compare Wein-Onsager calculations

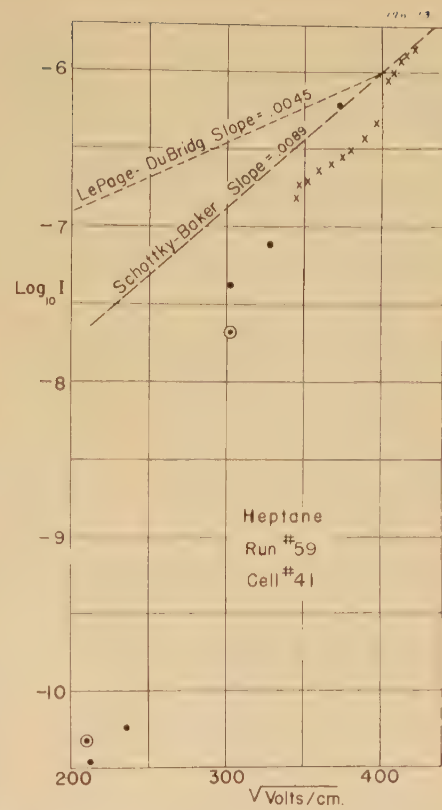

Figure 13. Plot of data for heptane to compare with Shottky-Baker hypothesis

the ends of the holes was accurately measured with a micrometer. Very finely divided graphite was then introduced into each hole and brass rod electrodes with rounded ends driven lightly into the graphite. In this manner the field distribution which exists between spheres in a homogeneous dielectric was obtained and corona between the electrode and the dielectric was eliminated.

Figure 18 shows a polystyrene specimen (run 53) after breakdown. This specimen had a test thickness of 0.053 centimeter and broke down at 77 kv, giving a breakdown gradient of 1.45×10^6 volts per centimeter. The current in this specimen was less than 1×10^{-8} amperes up to within four milliseconds of failure. The current record just before failure is interesting (figure 17), since the two sweeps before failure show currents of 40 and 106×10^{-8} amperes, respectively. Then failure occurred before the next sweep, which was back on the zero line. Another polystyrene specimen having a spacing of 0.033 centimeter did not fail at 83 kv, when tested at 100 degrees centigrade. This corresponds to a gradient $>2.5 \times 10^6$ volts per centimeter (6,350 volts per mil). A third specimen at 100 degrees centigrade having a test spacing of 0.013 centimeter failed at 34.2 kv corresponding to a gradient of 2.6×10^6 volts per centimeter (6,600 volts per

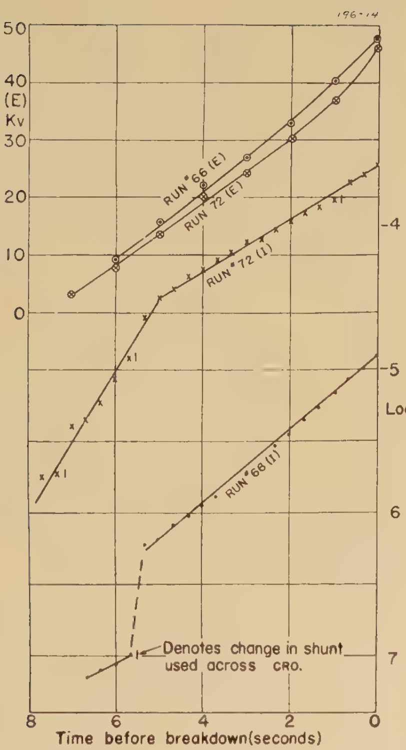

Figure 14. Pre-breakdown current and voltage data for chemically pure toluene (run 66) and toluene + tetrabutylammonium picrate (run 72)

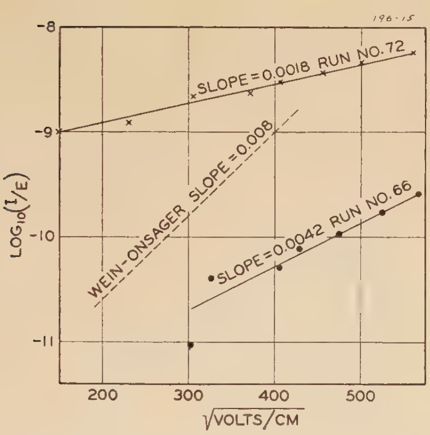

Figure 15. Plot of data for runs 66 and 72 to compare with Wein-Onsager calculations

mil). None of these specimens showed any measurable current before breakdown.

Several specimens of polyvinyl formal resin were tested in the same way. No pre-breakdown current was observed, the failure having occurred between successive sweeps in each case. One specimen

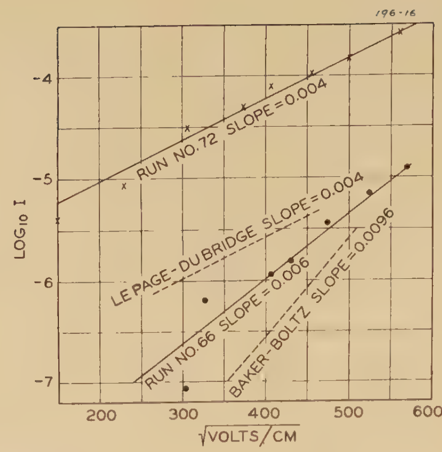

Figure 16. Plot of data for toluene alone (run 66) and toluene + 0.025 per cent tetrabutylammonium picrate (run 72)

having a spacing of 0.038 centimeter did not fail and had a current less than 10^{-8} amperes at 86 kv although the maximum potential was held for 30 seconds. This corresponds to a breakdown gradient $>2.3\times10^6$ volts per centimeter.

E. Summary

1. A method has been developed for photographing repeating traces on a cathode-ray tube which measure current in liquid and solid dielectrics with slowly increasing unidirectional voltage up to within two milliseconds of breakdown. The range of current sensitivity is from 10^{-8} amperes up. Current values at time intervals closer to the breakdown point could be measured by increasing the speed of motion of the film and decreasing the sweep interval. The probability of catching fast transient of the order of one microsecond duration is only 2 per cent (ratio of sweep time to sweep interval).

2. In liquids, the evidence so far obtained leads to the tentative conclusion that the final breakdown current increases from a substantially steady value to failure in fractions of a microsecond. This indicates that the final breakdown mechanism is electronic.

3. In liquids, it appears also that the pre-breakdown ionic current may be unrelated to the breakdown electronic current since the breakdown gradient appears to be affected more by the electrode surface conditions than by the ionic conductivity of the liquid.

4. In polystyrene and polyvinyl formal only one record was obtained showing any pre-breakdown current greater than 10^{-8} amperes up to within two milliseconds of failure at breakdown gradients of the order of 2.5×10^6 volts per centimeter.

Figure 17 (left). Photographic record of current rise immediately preceding failure in polystyrene (run 53)

Figure 18 (below). Section of polystyrene specimen after breakdown

References

1. **E. B. Baker and H. A. Boltz,** *Physical Review* volume 51, page 275, 1937.

2. **H. J. Plumley,** *Physical Review*, volume 52, page 140, 1937.

3. **R. W. Dornte,** *Industrial and Engineering Chemistry*, volume 32, page 1529, November 1940.

4. SOME RECENT DEVELOPMENTS IN IMPULSE-VOLTAGE TESTING, **C. M. Foust and N. Rohats.** AIEE TRANSACTIONS, volume 59, 1940 (May section), pages 257–62.

5. DIELECTRIC STRENGTH OF INSULATING LIQUIDS IN A CONTINUOUSLY CIRCULATING SYSTEM, **Hubert H. Race.** AIEE TRANSACTIONS, volume 59, 1940, pages 730–7.

6. **R. W. Dornte,** *Journal of Applied Physics*, volume 10, page 514, 1939.

7. **Lars Onsager,** *Journal of Chemical Physics*, volume 2, page 599, September 1934 (Equations 37 and 39).

8. **W. R. LePage and L. A. DuBridge,** *Physical Review*, volume 58, page 61, July 1940.

9. MEASUREMENTS OF SURGE VOLTAGES ON TRANSMISSION LINES, **E. S. Lee and C. M. Foust.** *General Electric Review*, March 1927, figure 4.

Any discussion of these papers will appear in the December 1941 "Supplement to Electrical Engineering—Transactions Section"

Bus Protection Independent of Current-Transformer Characteristics

G. STEEB
MEMBER AIEE

Synopsis: The paper describes the installation and operating results of a bus protective scheme, which uses a combination of high-speed directional ground relays on all sources of fault current and high-speed plunger type blocking relays on all outgoing circuits. The scheme described is independent of the ratios and characteristics of the current transformers.

Introduction

THE protection of station busses in the past has usually been accomplished by some form of differential relaying or by fault bus relaying.[1]

Differential relaying requires that the current transformers in each circuit on the bus have the same ratio and characteristic.[2] Sometimes auxiliary transformers are used to compensate for differences in the ratios of various current transformers.[3] It has often been necessary to give the differential relays a relatively high pickup and some time delay in order to prevent incorrect operations. The application of the harmonic current restraint relay has overcome some of the difficulties of differential relaying for bus protection.[4]

Fault bus relaying requires that all equipment be insulated from ground and connected to a common fault bus, which is grounded through a current transformer which operates some type of relay.[5]

Neither of the above schemes could be applied in a practical way to the bus layout shown in figure 1. Since each feeder has only one breaker, and each pair of feeders has selector disconnects to the busses, the application of current transformers for differential relay protection would not be feasible. This station is a 22-kv outdoor station which was built 20 years ago and does not lend itself readily to the application of the fault bus method.

Description of Bus Scheme

The difficulties in applying either of the two conventional methods of bus protection resulted in the development of a scheme which uses a combination of high-speed directional relays on all sources of fault current and high-speed plunger type current relays for blocking on all outgoing circuits. The method developed can be used for protection against any type of fault, but, after consideration of the speed of operation of the protective scheme and of the fact that the majority of faults in an outdoor station start as one wire to ground or two wires to ground faults, it was decided to install only ground fault protection. The total relay time of the protective scheme is from one to two cycles* and it was felt that this time was sufficiently short to insure relay operation before ground faults have sufficient time to develop into three-phase faults.

Figure 2 shows the simplified a-c connections for bus sections 1 and 2. Figure 3 shows the schematic d-c relay connections for bus sections 1 and 2. The connections for bus sections 3 and 4 are similar to those shown for bus sections 1 and 2.

Each of the high-speed ground directional relays used on circuits which are sources of ground current has one coil connected in the station neutral ground and its other coil in the respective residual current circuit. When de-energized, the contacts of these relays are open, and they close when ground current flows toward the protected bus section. A specially designed *b* switch on the oil circuit breaker in each circuit is connected across the

Figure 1. Circuit arrangement of 25-cycle, 22-kv outdoor station

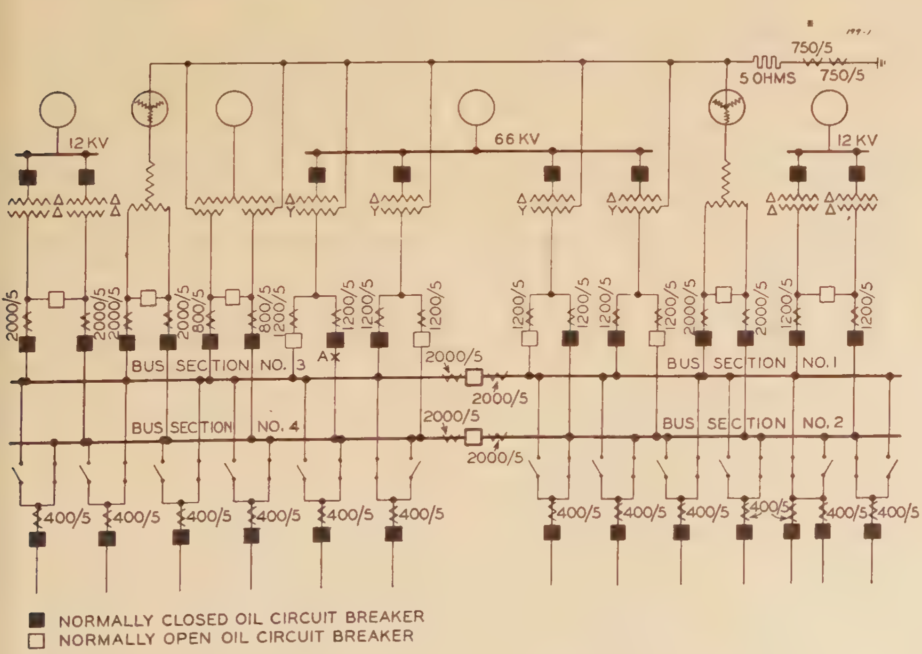

Paper 41-99, recommended by the AIEE committee on protective devices, and presented at the AIEE summer convention, Toronto, Ontario, Can., June 16–20, 1941. Manuscript submitted April 1, 1941; made available for preprinting May 5, 1941.

G. STEEB is with the Buffalo, Niagara and Eastern Power Corporation, Buffalo, N. Y.

1. For all numbered references, see list at end of paper.

* All times given are on a 25-cycle basis.

normally open contacts of these relays to prevent the relay scheme from being inoperative when a circuit is out of service.

All circuits which are not sources of ground current are provided with high-speed plunger type ground relays, each having two contacts both of which are closed when the relay is de-energized. Since the outgoing circuits can be connected to either one of two busses, it was necessary to use one contact of each of these relays in the protective scheme of each of these bus sections. Thus the are open. The tie breakers are normally open at least 90 per cent of the time.

To prevent an accidental operation of the bus scheme and also to prevent its operation on a high-resistance fault on a circuit off the bus, a high-speed plunger type overcurrent relay for each bus section is used in the station neutral ground. The contacts of this relay are connected in series with the operating coil of the gang trip relay, the normally open contacts of the ground directional relays, and the normally closed contacts of the plunger type ground relays for any bus section.

the station neutral and of the ground directional relays in the circuits which are ground sources close, energizing the gang trip relay which trips all the power sources on the bus. Since the outgoing feeder circuits carry no fault current, the contacts of the relays on these circuits remain in the normally closed position.

When a ground fault occurs on a circuit off the bus, the contacts of the plunger type ground relay on the faulted circuit open before the contacts of the overcurrent relay in the station neutral and the ground directional relays close and thus

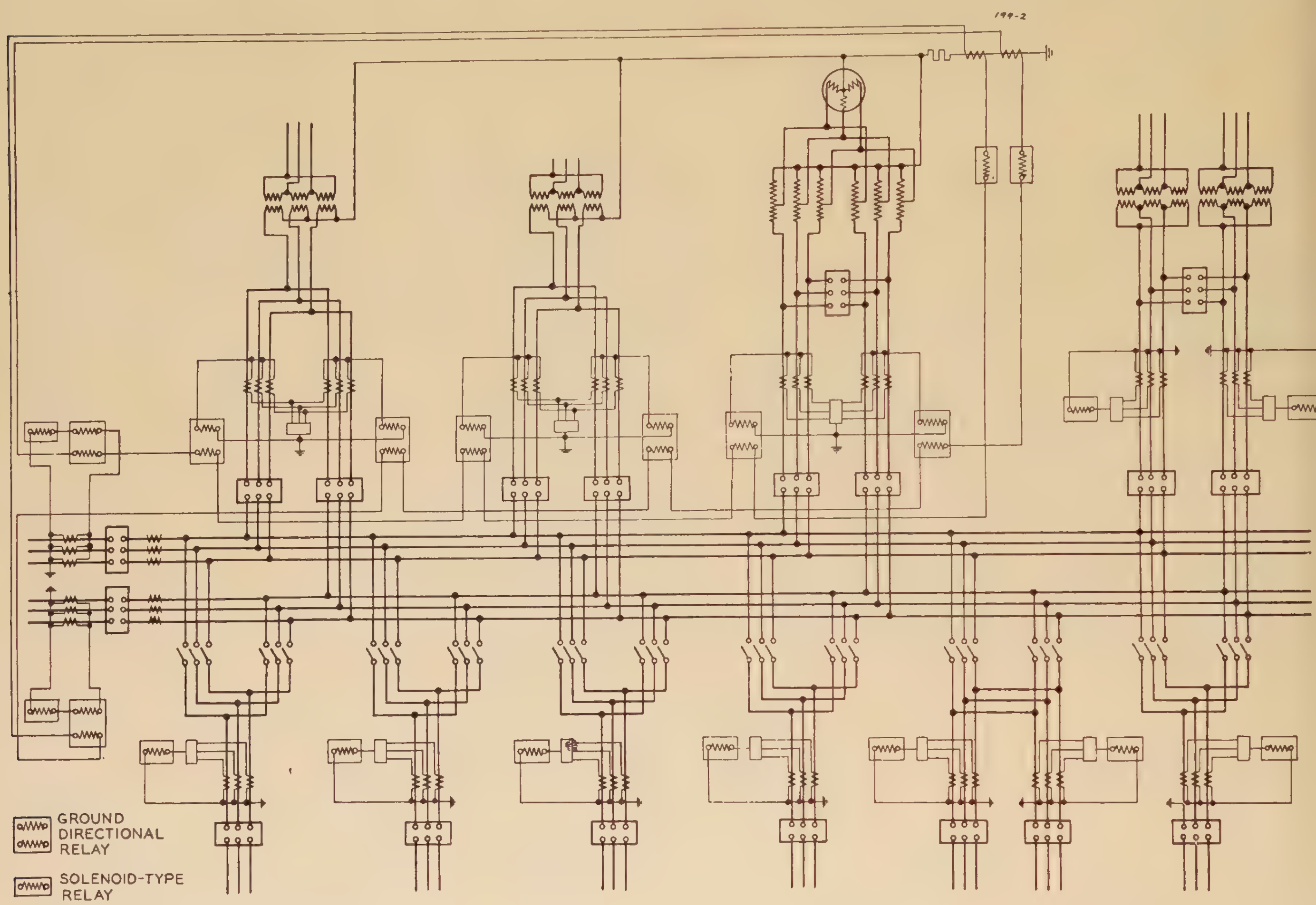

Figure 2. Simplified a-c connections for bus sections 1 and 2

operation of these relays, when a fault occurs on a circuit off the bus, blocks the bus scheme of both bus sections to which the circuit can be connected. The contacts of these relays are continuously supervised by indicating lights.

The tie breakers to adjoining bus sections are equipped with both high-speed ground directional relays and high-speed plunger type ground relays with their contacts connected in parallel. Since an adjoining bus section may or may not be a source of ground current, it was necessary to install both types of relays. The normally closed contacts of the plunger type ground relays of the tie breakers also serve as *b* switches when the breakers

Since the ground directional relays have a lower pickup than the plunger type ground relays on the outgoing circuits, the bus scheme would operate on a high-resistance ground fault were it not for the fact that the high-speed overcurrent relay in the station neutral has a higher pickup than the plunger type ground relays on the outgoing cables and prevents the operation of the bus relays on ground fault current below a predetermined value.

Sequence of Operation

When a ground fault occurs on the bus, the contacts of the overcurrent relay in

prevent the operation of the bus protective scheme. After the fault is cleared, the contacts of the station neutral relay, and of the ground directional relays, must reopen before the contacts of the feeder ground relay reclose.

Choice of Relays

The correct operation of this protective scheme requires that relay contacts open faster than they close.

To decide what types of relays would fulfill this requirement, a number of tests

were made in the laboratory, using an oscillograph, to check the relative opening and closing times of the various relays. It was found that satisfactory tolerance can be obtained between the opening of one contact and the closing of another, even on high-speed plunger type relays which are energized or de-energized simultaneously. The tests also showed that the contacts of five directional relays in series, operating simultaneously, give reliable results especially if the contacts are of the nonbounce type.

The relays that have been selected are all of simple design, and their operating times as recorded by the oscillograph, are described below.

The high-speed plunger type relays in the ungrounded circuits will open their contacts in a quarter of a cycle at all values of current greater than about 30 per cent above their setting, and after the current has been removed, the contacts will reset in one cycle. Of course the setting of these relays should be made as low as possible, because this determines the setting of the relays in the station neutral.

The high-speed plunger type overcurrent relays in the station neutral will close their contacts in a third of a cycle at the maximum obtainable current, which is 300 per cent of their setting. The closing time of the relay contacts increases, as the current decreases, i.e., at about 30 per cent above the setting the time will be one cycle and two cycles at 5 per cent above its setting. The contacts open in a quarter of a cycle after the relay becomes de-energized.

The high-speed ground directional relays have been adjusted to close their contacts in a time, varying from about two cycles at ten per cent above their setting to three-quarters of a cycle at the maximum obtainable current. These contacts will reopen in a quarter of a cycle after the relay becomes de-energized.

Additional tests showed that equally satisfactory results can be obtained with relays used on 60 cycles frequency.

Limitations of the Bus Scheme

1. If the unusual operating condition, should arise of a bus section being fed only through a tie breaker, it would be necessary to make the protective scheme nonautomatic on that section; since the *b* switches on every breaker that normally feed the bus section would be closed. The only contact that would then remain open in the d-c circuit of the bus scheme would be that of the overcurrent relay in the station neutral. Since these contacts close for a fault anywhere on the 22-kv system an incorrect operation of the bus protective scheme could result.

2. The bus protective scheme for a section would be inoperative if a breaker on a ground source circuit were in the closed position while its isolating disconnects were open. This is a situation that might arise while doing maintenance work on a breaker. If a bus ground fault should occur during this period, the ground directional relay on the circuit out of service could not close its contacts. This limitation of the bus scheme can be overcome by by-passing the *b* switch of the breaker on which maintenance work is being done.

3. The bus scheme of any section is inoperative while any of its relays is being tested. This, of course, applies to any bus scheme but with this one there are a greater number of relays to be tested than on a conventional scheme, and therefore more time is required.

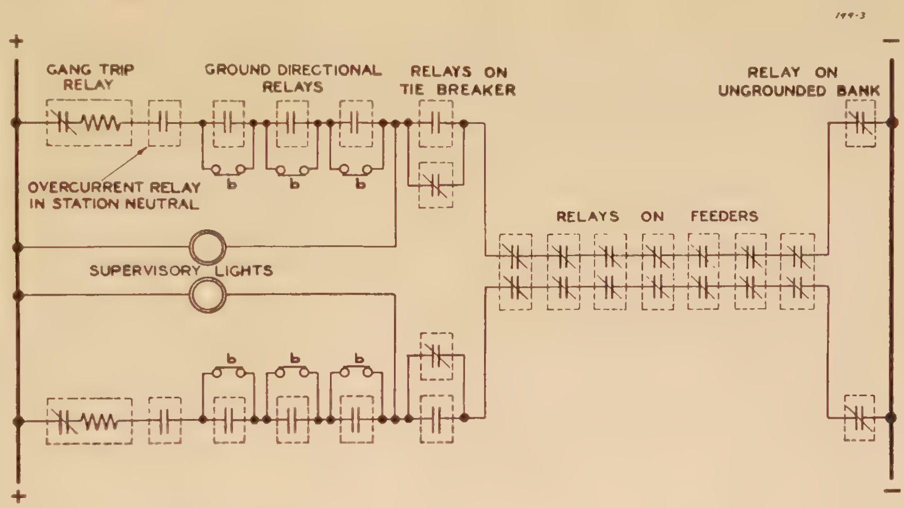

Figure 3. Schematic diagram of d-c relay connections for bus sections 1 and 2

4. This bus scheme does not operate if a bus fault starts as a phase-to-phase or three-phase fault or if a one wire-to-ground or two wire-to-ground bus fault changes to a three-phase fault in less than about one cycle after its start.

Staged Ground-Fault Tests

The various relays of the described bus scheme were installed and put in service in May 1939, but the trip circuits on the gang trip relays were left open temporarily. The purpose of this precaution was to determine, in actual operation, whether any of the relays would operate incorrectly on switching surges or external faults. During this period various disturbances occurred outside the four bus sections during which all the relays of the bus protective scheme performed correctly.

On May 12, 1940 a series of staged ground fault tests were made on each of the four bus sections and on circuits off the various bus sections. In each case the protective scheme operated correctly. Each of the bus faults was cleared in about seven cycles.

Operating Experience

Since May 12, 1940 when the bus scheme was put in service, there have been nine faults on circuits off the bus, and one fault on bus section 4.

The bus scheme was blocked correctly in all cases of faults off the bus.

The fault on the bus, which occurred on the bus side of the breaker bushings marked with the letter *A* in figure 1, was cleared in eight cycles through the operation of the bus protective scheme.

The record of the automatic oscillograph indicates that the disturbance started as a phase 3-to-ground fault. This condition remained for four cycles and after that the fault spread into a two wire-to-ground fault, involving phases 2 and 3.

Conclusion

The bus protective scheme has been applied to an important and rather complicated section of the system, where relatively large generators and power transformers are connected to the busses. Operating experience indicates that the reliability of this bus scheme is not adversely affected by either the magnetizing inrush currents of the power transformers or by the d-c component of the asymmetrical fault currents.

A Distribution System for War-Time Plant Expansion

J. L. McKEEVER
ASSOCIATE AIEE

Introduction

INDUSTRIAL distribution systems to meet the needs of expanding plant facilities for war and defense production are a very live issue today, both in Canada and in the United States. A great deal has already been written on the subject in a general way, as a guide to the proper tailoring of plant distribution to the type of plant and plant production. The purpose of this paper is not to generalize, but to offer a short description of the distribution system installed in the recently expanded facilities of the Peterborough plant of the Canadian General Electric Company, with reasons for the choice made. Many plants at the present time must be faced with distribution problems similar to ours and we feel that our solution has possibilities of wide adoption. It is obviously equally applicable to a new plant.

Description of Plant Extension

The plant extension now nearing completion consists of some 370,000 square feet of floor space in two single story buildings. One building of some 245,000 square feet was constructed to manufacture specialized mechanical equipment while the second building of 125,000 square feet area is to house our wire and cable manufacturing department. They will be designated in this paper as building *A* and building *B* respectively.

The types of load in the two buildings are quite different. In building *A* there will be a connected load of approximately 6,000 hp consisting very largely of small machine tools, plus 900 kva for heating and lighting, while in building *B* with a connected load of approximately 2,500 hp there are an appreciable number of motors in the order of 50 to 200 hp driving rubber mills, Banburys, strainers, etc.

Existing Distribution System

In laying out a distribution system for the new buildings the first thought naturally was to continue with the present system. Power is obtained from four sources, i.e.

Two small hydroelectric stations owned by the company

One steam turbine generator in the company's steam heating plant

Peterborough Utilities Commission

Paper 41-136, recommended by the AIEE committee on industrial power applications, and presented at the AIEE summer convention, Toronto, Ontario, Can., June 16–20, 1941. Manuscript submitted April 16, 1941; made available for preprinting May 15, 1941.

J. L. McKeever is general engineer with Canadian General Electric Company, Ltd., Peterborough, Ontario, Can.

Grateful acknowledgement is made of the help given in the preparation of this paper by G. R. Langley, chief engineer, and F. A. Athney, switchgear engineering department, Canadian General Electric Company, Peterborough Works.

1. For all numbered references, see list at end of paper.

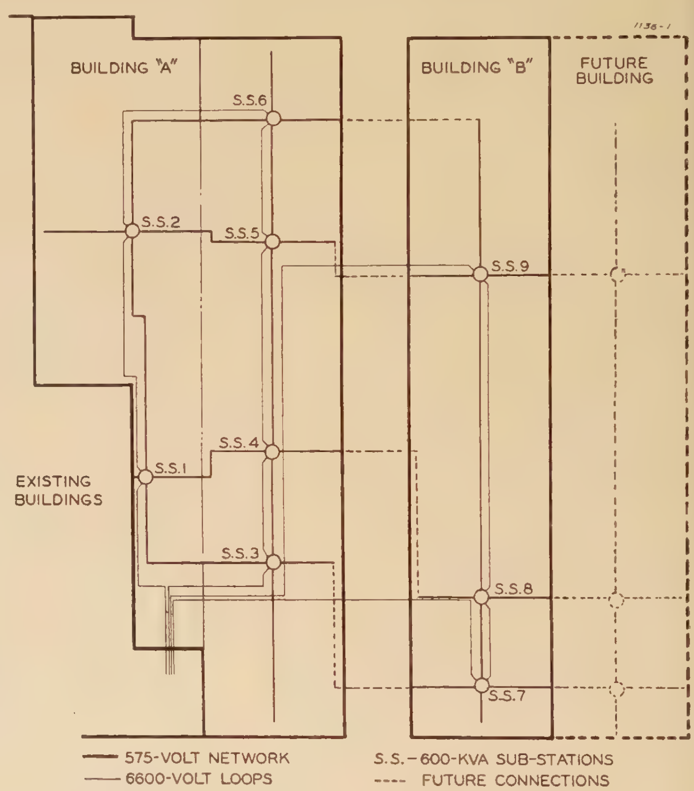

Figure 1. Approximate location of substations in buildings, showing 6,600-volt and 575-volt interconnections

---

While the installation requires a greater number of relays than conventional schemes, it avoids the use of additional current transformers and is independent of the current transformer ratios and characteristics, and can therefore be more readily applied to old stations. Economically it compares very favorably with other schemes.

The protective scheme as installed is practically foolproof. Mistakes made while working on the individual relays or on the various current circuits are not likely to operate the bus scheme. Troubles in the secondary wiring or the relays are more likely to prevent the scheme from operating than to cause an incorrect operation, a condition which is desirable from a system operating standpoint.

References

1. Bus Protection, AIEE-EEI committee report. AIEE Transactions, volume 58, 1939 (May section), pages 206–11.

2. Considerations in Applying Ratio Differential Relays for Bus Protection, R. M. Smith, W. K. Sonnemann, and G. B. Dodds. AIEE Transactions, volume 58, 1939 (June section), pages 243–52.

3. Relay Protection for Station Buses, W. A. Lewis and R. M. Smith. *The Electrical Journal*, volume 34, November 1937, pages 457–8.

4. Harmonic-Current-Restrained Relays for Differential Protection, L. F. Kennedy and C. D. Hayward. AIEE Transactions, volume 57, 1938 (May section), pages 262–71.

5. The Fault Ground Bus. Its Use and Design in Brunot Island Switch House of Duquesne Light Company, R. M. Stanley and F. C. Hornibrook. AIEE Transactions, volume 49, 1930, pages 201–12.

These sources are paralleled in the switch room of the steam plant and from there power is fed by 6,600-volt underground cables to four strategically located step-down substations. From these stations the existing plant of 790,000 square feet floor area is fed by conventional radial feeders at 575 volts for power and 115/230 volts for lighting.

Distribution Requirements

If the same radial type of distribution were to be used for the new buildings it was obvious that at least two new substations would be required and, considering the large area to be covered, it would be necessary to decentralize the 115/230-volt lighting transformer capacity by placing a number of small single phase units, either Pyranol or air cooled, throughout the buildings. This is of course in line with the best modern practice and the primaries could readily be connected to the 575-volt radial power distribution system, but there were other more serious problems to be solved.

While the load in building *B* both as regards amount and location was fairly well fixed before construction started, the situation with regard to building *A* was quite different. Here, for a variety of reasons, the final total of connected load could not be estimated at all closely and the layout was undergoing continual changes. Furthermore, due to the fact that the work for which this building was being erected was of a temporary nature, the distribution had to be laid out so that the building could be converted readily to a quite different type of manufacturing. In addition all concerned were interested in keeping costs to a minimum consistent with the conditions to be met.

Proposal

Mr. G. R. Langley, the chief engineer of the Peterborough Works, proposed the use of a number of unit substations with the primaries of the transformers connected into a 6,600-volt loop or ring main, and with the 575-volt secondaries interconnected to form a network. The lighting also was to be decentralized with the lighting transformer primaries supplied from the network. This scheme was adopted as a cost analysis showed that it would reduce the first cost and offer other advantages. While the idea of using a low voltage network for industrial distribution is not new, we believe that the scheme proposed has novelty in the use of the primary loop combined with a secondary network with simplified protection.

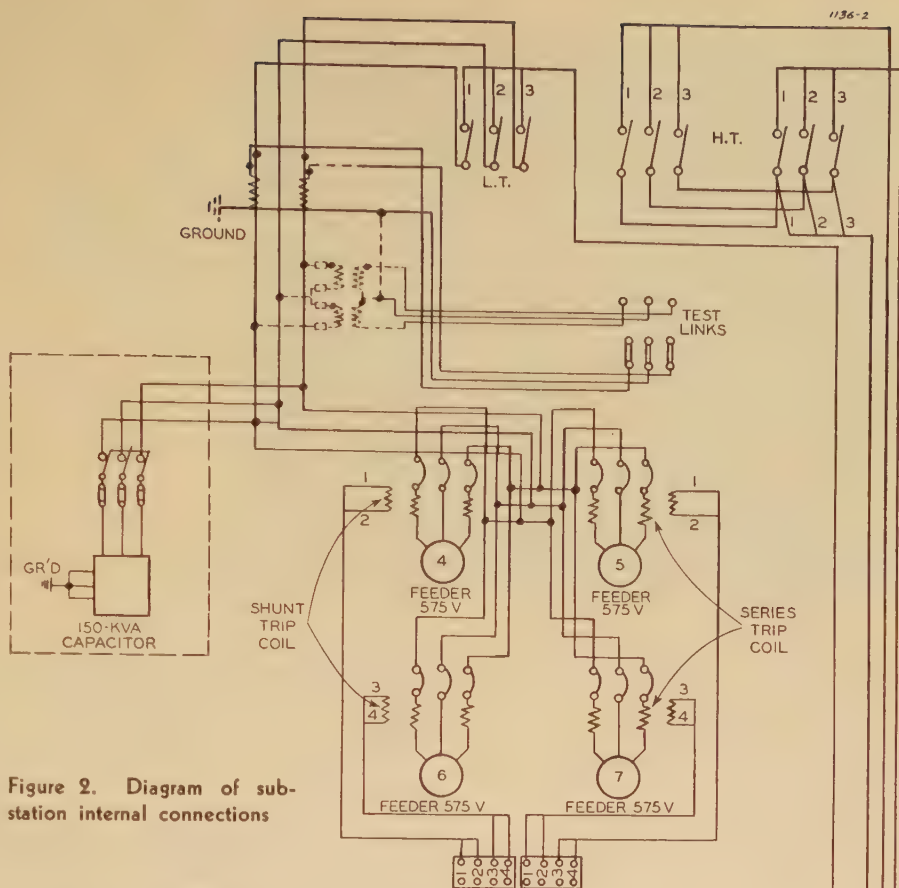

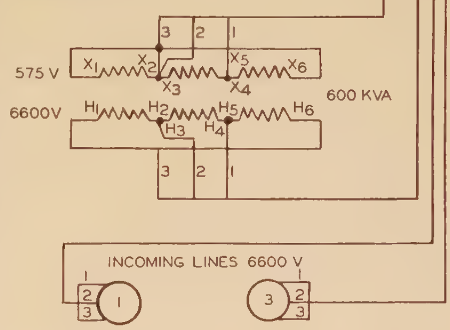

Figure 2. Diagram of substation internal connections

Actually it is an adaptation of the primary network idea as propounded some years ago by Mr. D. K. Blake and others of the General Electric Company.[1] A recent paper[2] pointed out that an industrial network must differ from the well-known 120/208-volt metropolitan type of network in that with the former, secondary cable faults cannot be allowed to burn themselves off. Thus protective means must be employed at each end of each secondary tie. The network diagram accompanying the above-mentioned paper[2] showed the network ties used simply as ties and protected by fuses or current limiters. The power feeders were taken off busses through air circuit breakers and network protectors were used between the busses and the transformers. Our system is admittedly not designed for uninterrupted service due to tie faults and simplifications were made in using the ties themselves as busses protected at each end by air circuit breakers and omitting the network protectors. So far as we are aware no similar system is at present in use in Canada or in the United States.

Evolution of Distribution System

Enquiries among other plants and at one plant in particular which had about the same type of load and approximately the same proportion of lighting, electric heating, and power load as we anticipated in building *A*, showed that we might expect a load factor of close to 50% and a power factor of between 70 and 75%. With a radial distribution system, allowance for growth and spare capacity would have necessitated the installation of about 4,500 kva in transformers for building *A* and between 2,000 and 2,500 kva for building *B*. With the network and loop system however, the ease with which a future additional substation can be connected into the system, together with its load dividing properties enables a considerable saving in transformer capacity. Incidentally this feature dispenses with one of the bug-bears of consulting engineers, namely the difficulty in drawing a mean between risk and over-conservatism in deciding upon transformer capacity. The capacity decided upon in our particular case was 3,600 kva for building *A* and 1,800 kva for building *B*. Investiga-

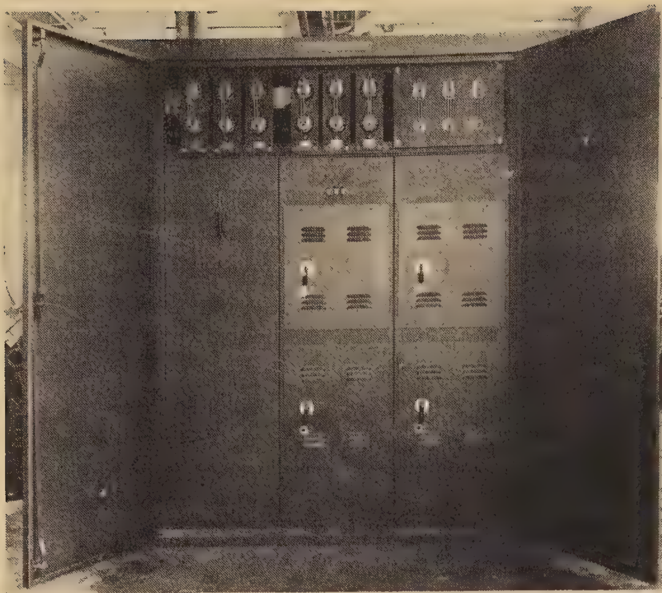

Figure 3. Front view of 600-kva unit substation

tion showed 600 kva to be the most suitable transformer size which meant a total of nine unit substations.

Consideration was given to using oil-cooled transformers in vaults below the floor level but it was found to be cheaper to use Pyranol filled transformers in the same enclosure with the switching. Floor space has minimum manufacturing value in the area along the line of the building columns where it cannot readily be serviced by cranes. Thus placing the substations on the floor backed against the columns represents no appreciable waste of space.

Figure 1 shows the approximate location of the substations in the buildings together with the 6,600-volt and 575-volt interconnections. Originally it was intended to have all the nine substations on one loop but a separate power contract for building *A* made it necessary to have two loops. This works out quite well however, as the wire building loop allows for the addition of three more substations in a future building alongside it so that actually the 6,600-volt cables for the two loops are identical.

The 575-volt switching in each station consists of four 400-ampere air circuit breakers of the dead-front type mounted two high as shown in figure 3. A low tension hook-operated disconnecting switch is provided for disconnecting the transformer from the air breakers, as shown on the top right of figure 3, while the two disconnecting switches appearing at the top left and centre permit the isolation of any section of the loop cable and also serve to disconnect the high voltage side of the transformer from the two ends of the loop.

It was mentioned earlier that the power factor to be expected in building *A* was between 70 and 75%. Each of the six substations in this building therefore is provided with a 150-kva capacitor controlled by the dead-front quick-break, fused knife switch showing at the left centre of figure 3. This is all the equipment provided in the substation except for one current transformer and some test links. Figure 2 shows the connections for the complete substation. The three substations in building *B* are identical with those in building *A* except for the omission of the capacitors.

Various designs of substation structure were considered and the final decision was to enclose transformer and switching in the same enclosure. This arrangement tends towards compactness as is evidenced by the dimensions which are 7 ft. 8 in. width, 8 ft. 6 in. depth, and 8 ft. 4 in. height. All wiring in the building for the 6,600-volt loop and the 575-volt network is overhead and the conduits are brought down the building column and through the roof of the substation.

Figure 1 shows the 575-volt interconnections between stations and the various stub feeders. From junction boxes, taps are taken to 50-kva single-phase Pyranol filled lighting transformers and to GE Trumbull Swing-Wa power panels. In one case in building *B* where a number of controls for large motors are placed in an enclosed force-ventilated control room, two runs of Trumbull Flex-a-power are used between the substations these runs passing through the control room, and connections for the controls are made to them.

Protection

Considerable study was given to the protection of this distribution system against faults in any part of it. Experience with our present system has shown that faults are extremely rare in the 6,600-volt cables and transformers, and this in conjunction with the fact that the rare short interruption of power is not particularly serious with the type of manufacturing involved, permitted simplified protection. The oil circuit breakers at either end of each loop are equipped with inverse-time induction type relays with instantaneous attachments. The loop cables are large enough to feed all stations on the loop from one end, and as already mentioned, disconnecting switches are

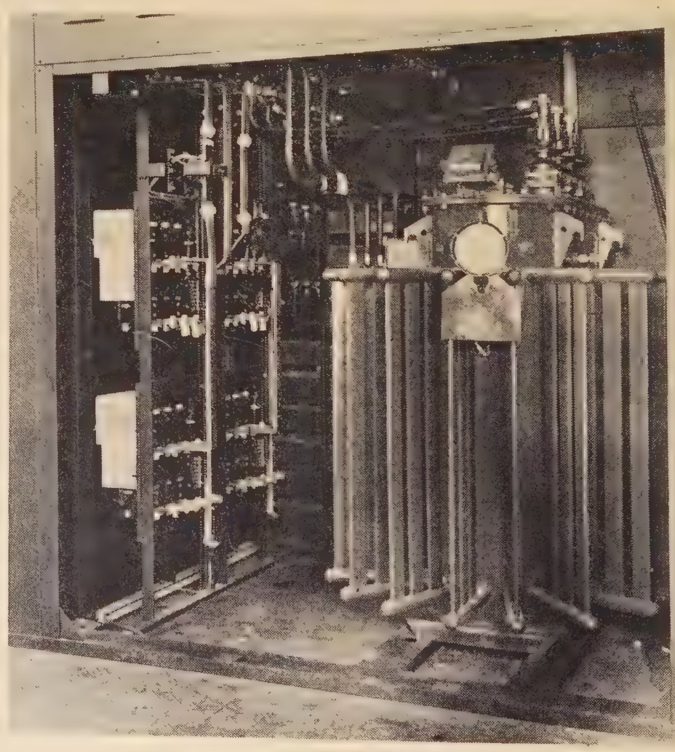

Figure 4. Internal view of 600-kva unit substation showing transformer, capacitor rack, and air circuit breakers

provided at each station so that any section of cable may be isolated. A temperature detector in the transformer winding will ring an alarm upon any serious temperature rise and should it become necessary to remove a transformer for examination or repair before a major fault develops, it can be removed from service without dropping load except on the stub feeders, by the following routine:

1. Trip the four 575-volt air circuit breakers to remove load from the transformer.

2. Open the loop disconnecting switches.

3. Open the 575-volt disconnecting switch and disconnect the transformer high tension leads.

4. Reclose the loop disconnecting switches and the four air circuit breakers.

An actual fault on either transformer or loop cable will open the loop oil circuit breakers and interrupt power for a short period but, as already mentioned, the inconvenience of such a shut-down does not, under our conditions, justify guarding against it.

The air circuit breakers in the network are provided with combination inverse-time and instantaneous overload trips which will give adequate selective protection. Calculations of fault currents have been made which indicate the maximum short-circuit current from all six stations at the terminals of any one of the air circuit breakers to be within safe limits. They also show the possible currents at the load side of the Swing-Wa power panels to be within the known tested rating of the standard cartridge fuses used. Actually the calculated fault currents are sufficiently low to allow considerable expansion beyond the six stations and indicate the feasibility of networks of larger capacity with the same standardized design of unit substation.

To provide peak load control, which may or may not be generally required, the network air circuit breakers are provided with shunt trips and a multi-conductor control cable is run from the operating room in the steam plant, allowing the operator to dump any section of the load if the contracted ten minute peak demand is liable to be exceeded. The stub feeders can obviously be disconnected without disturbing the network and in the case of the wire building where mention was made of two 575-volt network ties running through the large motor control room, one of these can be disconnected at each end dumping half the rubber mills but leaving the other half in operation on the other tie.

Direct-Current Supply

Direct current power is usually required for operation of cranes, boring mills, and certain other machines. In our case this power is supplied by motor-generator sets the induction driving motors of which are supplied from the network. With the load dividing feature of the network system such motor-generator sets can be connected into any convenient point close to the machines to be supplied without the prior thought necessary with radial feeders.

Figure 5. General view showing small space occupied by 600-kva unit substation

Comparison of Costs

In making a cost comparison between the network system described above and the radial system we would otherwise have installed we were fortunate in having access to the actual cost of a radial system recently installed in an Ontario plant of floor plan and area similar to building *A* in our plant. With the radial system the transformer capacity for building *A* alone would have been at least 4,500 kva and the costs from the other plant have been adjusted to this capacity. On this basis the network system showed a saving of $18^1/_2$%.

With the present radial system in our plant it has been the practice to use reduced voltage starters on all squirrel-cage induction motors of 50 hp and larger. The excellent voltage regulation characteristics of the network system, however, made reduced voltage starters unnecessary and the omission of these brought the saving with the network system to $22^1/_2$%, representing a figure in excess of $22,000 for building *A* alone.

Conclusion

The saving in capital expenditure realized by the use of the network system just described is sufficiently attractive in itself, but when this saving is coupled to the many other advantages the system offers, there seems to be good reason to expect its wide adoption.

Many plants in these days are faced with expansion problems similar to ours and it is hoped that our experience may be of value to others. The flexibility of the network system for increasing loads was impressed upon us recently by difficulties encountered with one of our existing radial substations in which the power transformer bank was seriously over-loaded. This substation had been built to take care of what at the time was thought to be ample future growth but it is now inadequate both in installed capacity and space for extension. In order to relieve the overloaded transformer bank it was necessary to split the 575-volt bus and feed part of it from a small transformer bank of incorrect characteristics for paralleling located in the test department substation several hundred feet away. Had we had a system similar to the one in our new buildings it would have been an easy matter to build another unit station and to connect it into the 6,600-volt loop and the 575-volt network.

The saving in transformer capacity, the saving in reduced voltage starters due to the good regulation, the high salvage value of equipment, and the simplicity of protection with the low-tension network and high-tension loop system of distribution have already been mentioned. These merits should assure its wide adoption in industrial plants.

References

1. Symposium on the Primary-Network System, D. K. Blake and others. *General Electric Review*, volume 35, number 6, June 1932.

2. Secondary Networks to Serve Industrial Plants, C. A. Powel and H. G. Barnett. AIEE Transactions, volume 60, 1941 (April section), pages 154–6.

An Improved Frequency Meter for Commercial Power Frequencies

K. J. KNUDSEN
MEMBER AIEE

Synopsis: While frequency meters of prior type admirably serve the purpose for which they are intended, their construction has been such as to necessitate the use of an external reactor. This external reactor is in most cases not objectionable, but for certain applications, where space is at a premium, a self-contained instrument is preferable.

This paper describes a frequency meter in which the external reactor has been eliminated by using an iron-core cross-coil instrument, the iron core serving the purpose of the normally external inductance, at the same time shortening the high reluctance air gap necessary for the moving coils.

Introduction

USING an iron core greatly reduces the ampere turns necessary to establish an adequate field intensity, which is proved by the fact, that while the power necessary to operate frequency meters

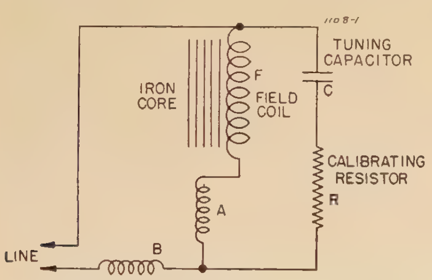

Figure 1. Schematic diagram of frequency meter

now being used range from 2.5 to 7.5 watts, depending on the design, this instrument consumes a maximum of 0.8 watt at 115 volts, or one-third the power of the prior instrument using the lowest power.

While the power consumption in most cases is insignificant with respect to the loss, it is important that a self-contained instrument use no more power than can be readily dissipated within the confinement of the case. Low power loss also simplifies compensation, as there is little change in temperature from the moment the instrument is energized till the temperature of the coils have reached constancy. In a self-contained instrument compensation is further simplified, because all components are mounted within the same container and therefore exposed to the same ambient temperatures, while if an external reactor is used, means must be provided to compensate for a possible difference of the temperature of the instrument proper and that of the reactor.

Theory

Referring to figure 1, the moving coil A is connected in series with the field coils F and therefore tends strongly to align itself with the magnetic flux in the air gap, the current through the coil being in phase with the flux. The capacitor C in series with the compensating resistor R, causes the resultant current in moving coil B to be 90 degrees out of phase with the air gap flux at the frequency corresponding to the center point of the scale. As the frequency varies from the center scale value, the power factor of the current in coil B will change, due to the altered impedance ratio between the field coils and the capacitor, resulting in a clockwise or counterclockwise deflection of the pointer, as the frequency increases or decreases.

As the power factor of the field coils, in series with coil A, is approximately 25 per cent, and the power factor of the current through coil B is about 97 per cent, four times as many turns, of correspondingly smaller size, may be used in coil B than in coil A for an equal heat loss in the two moving coils, resulting in a high order of deflection for a small change in power factor of the current in coil B.

The iron core is made from laminated "47-50" nickel iron due to its high resistance to corrosion and ease of stamping. Damping is provided by an aluminum vane moving through a strong unidirectional magnetic field established by an Alnico magnet.

Comments on Accuracy

The primary function of a frequency meter is, as the name implies, to indicate the frequency of an a-c circuit. Many causes tend to give an indication differing from the actual frequency, the most important of these are: Fluctuation of the line voltage, ambient temperature changes, and distortion of the voltage wave of the circuit.

Compensation for voltage influence has been accomplished by a high ratio of torque caused by the current flowing through the moving coils, to the torque of the ligaments connecting the moving coils to the stationary circuits. Figure 2 is a graph showing the voltage errors from 90 to 140 volts.

While conducting tests for voltage error on a number of instruments, some instruments would indicate erratically when high voltage was applied at certain frequencies. It was found that the two ligaments at one end of the moving coil assembly would short-circuit due to vibration of one of the ligaments, the vibration being set up by interaction between the magnetic flux in the air gap and the current through the ligament. The difficulty was overcome by cutting a turn of the ligament, thereby increasing its natural vibratory frequency above the measuring range of the instrument.

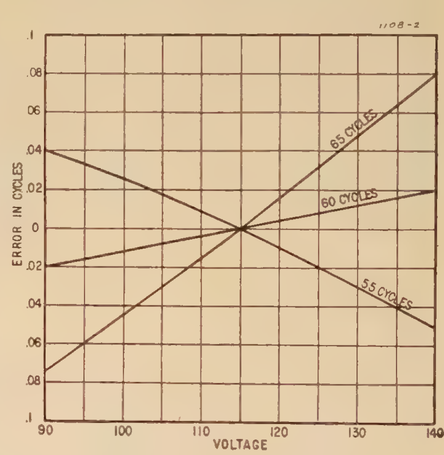

Figure 2. Voltage error curves

There are two main reasons for errors due to ambient temperature changes, they are: Resistance changes of coils and capacity changes of the capacitor used for tuning the field. In order to offset these errors, which have to be compensated simultaneously, a high temperature coefficient resistor is connected in series with the capacitor, thereby maintaining a constant phase relation between the current in the deflecting coil B (figure 1) and the magnetic flux in the air gap for a given frequency, at varying ambient temperatures.

It is important that a high-grade capacitor be used for an instrument, the purpose of which is to indicate small changes of reactance due to frequency changes.

Paper 41-108, recommended by the AIEE committee on instruments and measurements, and presented at the AIEE summer convention, Toronto, Ontario, Can., June 16–20, 1941. Manuscript submitted August 23, 1940; made available for preprinting May 5, 1941.

K. J. Knudsen is chief engineer of Hickok Electrical Instrument Company, Cleveland, Ohio.

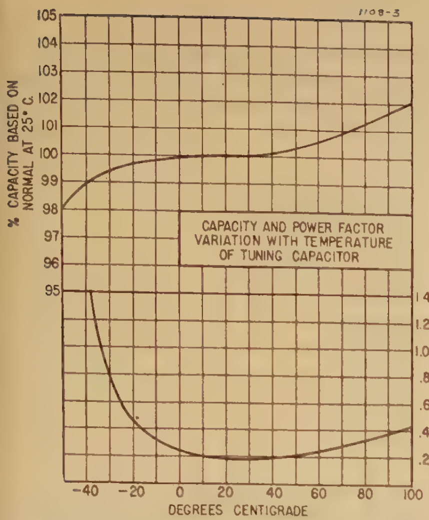

Figure 3. Capacitor-temperature capacity and temperature-power-factor curves

If considerable change of capacity would be caused by normal changes in ambient temperature, the instrument would be worthless as a frequency indicator; for this reason an oil-filled capacitor has been used, which has low and almost uniform temperature coefficient of capacitance within the normal range of temperatures. Figure 3 shows the capacity-temperature curve of the capacitor, and in addition the power factor-temperature curve. It will be noted that the power factor is almost constant within the measuring range, thus aiding the stability of the circuit.

As the temperature coefficient of capacitance is positive, it partly offsets the tendency of the instrument to read high at high temperatures, due to the increased resistance of the copper coils in the field circuit. Satisfactory compensation can be obtained between minus 20 and plus 45 degrees centigrade, by using a resistor in series with the capacitor, the temperature coefficient of the resistor having been adjusted to offset the combined causes tending to give an erroneous reading due to changes in temperature. Figure 4 shows the temperature error before and after compensation. While the capacitor has been under observation for a year, no change of capacity due to aging has been detected; it is however felt that insufficient time has passed to give exact data on aging characteristics.

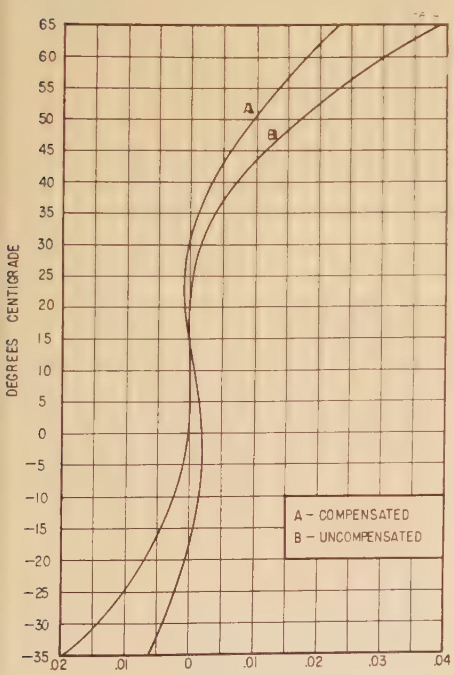

Figure 4. Temperature error of frequency meter

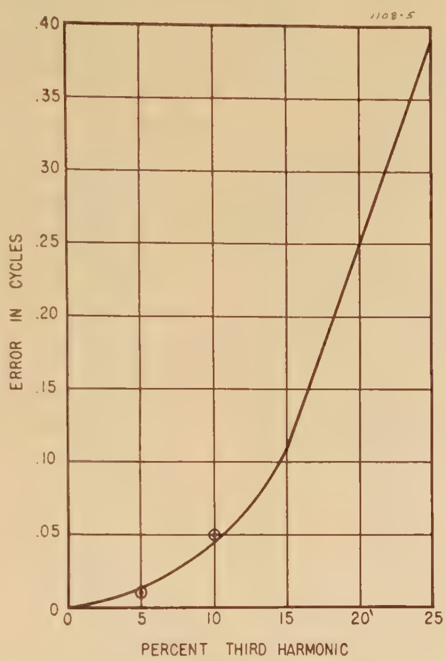

Figure 5. Third harmonic error

As the inductive reactance of the field circuit increases proportional to the frequency, and as the deflection of the pointer is caused by interaction between the moving coils and the magnetic flux of the field circuit, it will be seen, that the lower the harmonic present in the voltage wave, the greater is the tendency to indicate erroneously. Tests have been conducted to determine the effect of the third harmonic on the accuracy of the instrument, because this harmonic is the lowest commonly encountered in commercial supply lines. Figure 5 shows the error caused by varying magnitudes of third harmonic; changing the phase relation between the fundamental frequency and the third harmonic through 120 electrical degrees had no appreciable influence on the error indicated.

While the third harmonic influence seems rather high, it should be realized that the third harmonic, which is generally introduced into the voltage wave by the excitation of iron-core equipment due to the increased current at high saturation, seldom exceeds five per cent.

A four per cent seventeenth harmonic tooth ripple, present in the voltage of the generator used for calibration, had no influence on the accuracy, the indication being the same after eliminating the ripple by means of tuned by-pass filters.

Calibration

In order to obtain accurate calibration of the instrument without waste of time a multivibrator was used, having steps of 87,480, 29,160, 9,720, 1,620, 540, 180, and 60 cycles. The multivibrator is crystal controlled to one cycle in five million, its accuracy ascertained by comparing the time indicated by a synchronous electric clock, connected to the 60-cycles output stage, with radio time signals.

While the method of determining one frequency by its harmonic relation to another is not new, it is felt that it has been limited to a ratio, where it was possible to count the loops on the screen of the oscillograph. In the case where the harmonic ratio is more than 150 to one, counting the loops would be impossible without auxiliary means; a detailed description is therefore given of the method of calibration.

The instrument is calibrated by connecting the horizontal sweep circuit of an oscillograph to the 9,720-cycles stage of the multivibrator, and the vertical sweep to the variable speed generator used for calibration, the vertical sweep being amplified to extend beyond the limit of the screen, so as to show only two or three loops of the horizontal sweep, as indicated in figure 6.

Figure 6. Harmonic oscillograph sweeps

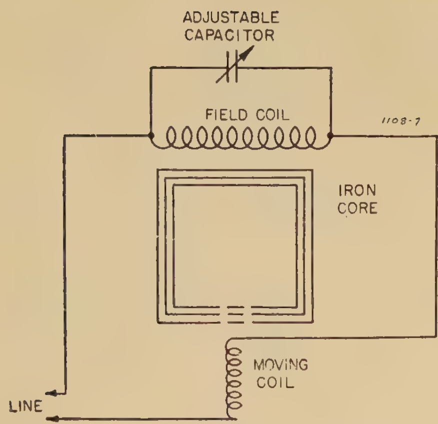

Figure 7. Schematic diagram of auxiliary frequency meter

As the frequency of the multivibrator is the 162nd harmonic of 60 cycles, some means must be employed to determine that the proper harmonic is used, there being only four-tenths cycle approximately between harmonics as compared to 60 cycles. A high-resistance voltmeter is connected in series with the 60-cycles stage of the multivibrator and the variable speed generator. The generator is adjusted until a steady reading equal to the sum of the voltages of the two supplies is obtained on the voltmeter. This reading is only obtainable when the voltages are synchronous and 180 degrees out of phase, the harmonic indicated on the screen must therefore be the 162nd.

In order to keep track of the harmonics used for calibrating the scale, an auxiliary frequency meter is used. The basic circuit of this instrument, shown in figure 7, is the same as that of the instrument under test, except that the restoring torque is provided by springs; the instrument is therefore accurate at only one point of the scale, the deflection at other points being dependent on the line voltage. An adjustable capacitor is used for adjusting the auxiliary instrument to center scale when the proper harmonic is found, by means of the voltmeter, at 60 cycles. As the sensitivity of the instrument is in the order of one-tenth cycle for full-scale deflection, it will be completely off scale if a wrong harmonic is used for calibration, and exact adjustment to center scale is therefore not necessary.

After the auxiliary instrument has been calibrated to 60 cycles, the setting of the adjustable capacitor is recorded and the speed of the generator is then slowly changed until the next harmonic appears on the screen. The auxiliary indicator again adjusted to center scale and the setting of the adjustable condenser recorded. Other points are determined in the same manner. By using harmonics from the 149th to the 177th, 29 points on the scale can be exactly calibrated and actual scale divisions determined by interpolation. Any harmonic can be readily redetermined by setting the adjustable capacitor to the proper value and adjusting the generator to the harmonic that permits the auxiliary indicator to read near the center of the scale.

Proper full-scale deflection of the frequency meter under test is obtained by connecting a calibrated resistor in parallel with either coil *B* or coil *A* (figure 1), thereby weakening either the deflecting or the restoring torque of the cross-coil moving element as the case may demand.

Table I

Generator Frequency	Subharmonic of 9,720 Cycles	RPM of Four-Pole Generator
54.915	177	1,647.5
55.227	176	1,658.8
55.543	175	1,666.3
55.862	174	1,675.9
56.185	173	1,685.5
56.512	172	1,695.3
56.847	171	1,705.3
57.176	170	1,715.3
57.515	169	1,725.4
57.857	168	1,735.7
58.207	167	1,746.1
58.552	166	1,756.6
58.909	165	1,767.3
59.268	164	1,778.0
59.632	163	1,788.9
60.000	162	1,800.0
60.373	161	1,811.2
60.750	160	1,822.5
61.132	159	1,834.0
61.519	158	1,845.6
61.911	157	1,857.3
62.308	156	1,869.2
62.710	155	1,881.3
63.117	154	1,893.5
63.530	153	1,905.9
63.947	152	1,918.4
64.371	151	1,931.1
64.800	150	1,944.0
65.235	149	1,957.0

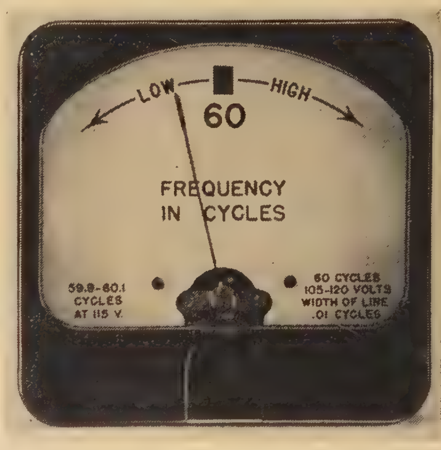

Figure 10. Auxiliary frequency meter in five-inch case

Table I shows the frequency and speed in revolutions per minute of a four-pole generator corresponding to the harmonics being used for calibration, it is included for the convenience of those, who may desire to use the same method of calibration.

Explanation of Pictures

Figure 8 is a photograph of the dynamometer; the damping magnet has been removed to give a better view of the cross-coil assembly and the parallel pole faces of the iron core.

Figure 9 shows the instrument mounted in a standard six-inch switchboard case, it has been calibrated in revolutions per minute of a four-pole generator.

Figure 10 shows the auxiliary frequency meter mounted in a five-inch case, the black center line has a width of approximately 0.01 cycle.

Conclusion

From the foregone description it is seen, that a self-contained frequency meter can be produced, the over-all accuracy of which is better than two-tenths cycle in 60 cycles, permitting a third harmonic

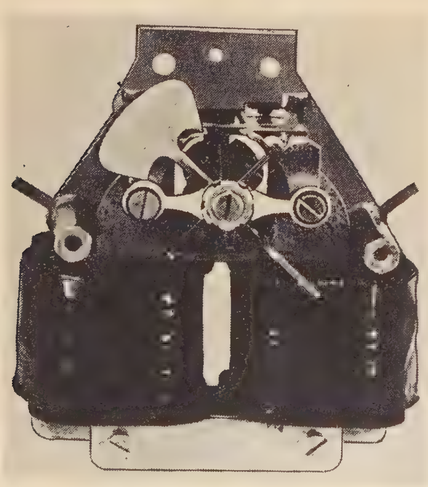
Figure 8. Frequency meter dynamometer

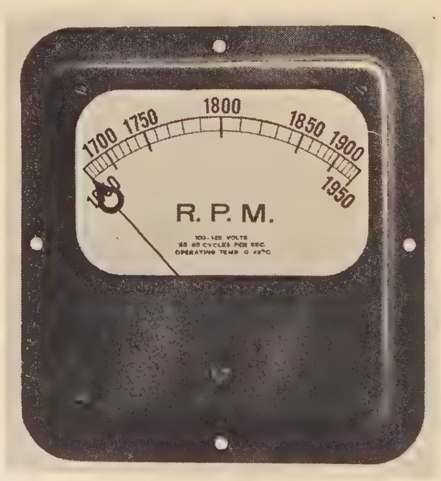

Figure 9. Frequency meter in six-inch case

Mechanical Simplicity of Air-Blast Circuit Breakers

H. W. HABERL
ASSOCIATE AIEE

OTTO JENSEN
ASSOCIATE AIEE

THE papers heretofore presented before the Institute on the subject of air blast circuit breakers have covered primarily their advantages in comparison with oil circuit breakers, the principles involved in current interruption by air blast, descriptions of interrupters developed by several manufacturing companies, the results of tests and related data. It is considered opportune to give an account of several other types of air blast circuit breakers ranging in voltage from 4 kv to 230 kv as developed and built by certain manufacturing companies in Canada and the United States in collaboration w th a large power company. The first machine of this general type was a 138-kv air blast breaker placed in service in 1934 at the Beauharnois generating station on lines to Montreal, this breaker having continued in service for six years successfully interrupting all faults; three additional breakers of the same general design with improved details have been placed in service at this station in later years.

Breakers of four types built by three manufacturing companies, all breakers having certain general features in common, will be illustrated by photographs and diagrams. In all of the breakers described, the general design of interrupting contacts is the same. This arrangement of contacts is suitable for the use of arc chutes utilizing any one of the elementary principles of pneumatic arc extinction or combinations of such principles.

Types marked "A" include breakers for 138 kv and 230 kv built by the English Electric Company of Canada.

Types marked "D" are 69-kv breakers built by the same company.

Types marked "B" are breakers of 15 kv to 37 kv built by the I-T-E Circuit Breaker Company, in Philadelphia.

Types marked "C" are breakers of 4 kv to 15 kv built by the Eastern Power Devices Limited, in Toronto.

The diagrams of each type are numbered 1 to 7 to show the sequence of operation.

Type "A"

Photograph *A* shows one of the 138-kv breakers in service. Figure 1*A* is a diagram of this breaker in the open position showing the main parts which are: the tank storing air at 100 lbs. per sq. in., the interrupter, and the isolating switch. In figure 2*A* the closing coil is being energized to close the breaker by admitting air from the tank to the cylinder and piston which closes the isolating switch. This coil is extremely small and becomes fully energized in a fraction of a cycle. The coil only has to move its plunger about one-eighth inch uncovering a port of one-eighth inch diameter, releasing about one-quarter cubic inch of compressed air from under a rubber diaphragm of about two inch diam. which is blown open by the opposing air pressure on the other side, thus opening the valve which admits air from the tank to the isolating switch cylinder and closes the switch. The cylinder of each pole is mounted under the bedplate of the interrupter, at line potential, as close as possible to the switch blade operated by a short link. Electrical, pneumatic, and mechanical inertia are reduced to the practical limit thus minimizing the closing time. A standard auxiliary switch to perform the usual functions, is operated from the isolating switch blade by a 90-degree rotation of the same porcelain tube (of one inch inside diameter) conveying closing air to the switch cylinder. Provision is also made for raising and lowering this porcelain tube one inch, to perform additional functions in connection with quick automatic reclosing.

The jaw contacts of the isolating switch are mounted on the cap of the pórcelain cone of the current transformer; this cap is purposely made extra heavy in weight and is supported on rubber bushings to minimize mechanical shock to the porcelain due to fast operation of the switch blade. The jaws are full-floating and swivel to facilitate cracking of ice film in opening; a large sleet hood also covers the contacts.

The interrupter has three identical interrupting elements in series in the 138-kv breaker and six in the 230-kv breaker. Each element has two stationary contacts bridged by one movable contact thus making two breaks in series per element. The movable contact is rigidly secured to a steel piston rod and piston working in a bronze cylinder insulated from adjacent cylinders. Figure 3*A* shows the breaker in the closed position.

As shown in the photograph *A*, the 138-kv breaker has one tank and three blast valves. The 230-kv breaker has three separate tanks to facilitate shipping and erecting the greater length. The 230-kv breaker is built up with the same parts as the 138 kv and almost all of the parts are interchangeable. Due to the greater height, the 230-kv interrupter is brazed with diagonal stacks of standard switch insulators.

The blast valve which is the same for 230 kv and 138 kv, is built into the side of the tank with an inlet of about three square feet section. The outlet of the valve is a funnel-shaped orifice of about 8″ diameter at the valve seat which is normally closed by a thick rubber diaphragm about 20″ diameter, reinforced by a light steel disk vulcanized to the rubber. The diaphragm moves down about one inch to fully open the valve. Air pressure at 100 lbs. is maintained underneath this diaphragm, to hold it closed. The volume of air under the diaphragm is less than one-twelfth of a cubic foot. To open the breaker this small volume of air is exhausted to atmosphere by two or three one-inch diameter orifices each normally held closed by a diaphragm and coil of the same size as

Paper 41-114, recommended by the AIEE committee on protective devices, and presented at the AIEE summer convention, Toronto, Ontario, Can., June 16–20, 1941. Manuscript submitted April 2, 1941; made available for preprinting May 9, 1941.

H. W. HABERL is with the electrical department of the Montreal Light, Heat and Power Consolidated, Montreal, Quebec, Can., and OTTO JENSEN is with the I-T-E Circuit Breaker Company, Philadelphia, Pa.

The authors gratefully acknowledge the assistance of H. Milliken, chief engineer and general superintendent of Montreal Light, Heat and Power Consolidated, in the preparation of this paper.

---

distortion of ten per cent, a voltage fluctuation of 90 to 140 volts, and an ambient temperature range of minus 10 to plus 40 degrees centigrade. The power consumed being eight-tenths volt-ampere at 97 per cent power factor.

As the complete instrument can be installed in a $3^1/_2$-inch case, it is well adapted for use where space is limited. The elimination of an external reactor reduces the work involved in wiring and installation.

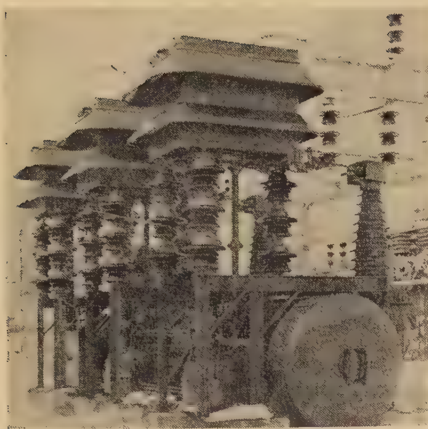

Figure A. General view of 138-kv air-blast breaker

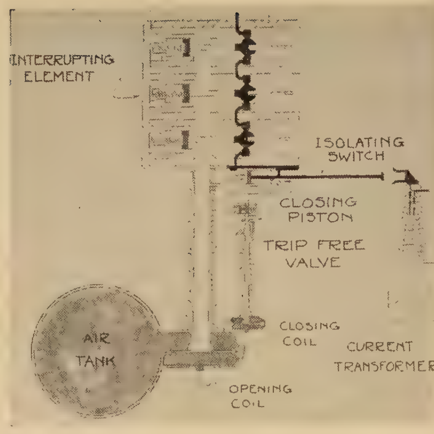

Figure 1A. Breaker in the normal open position

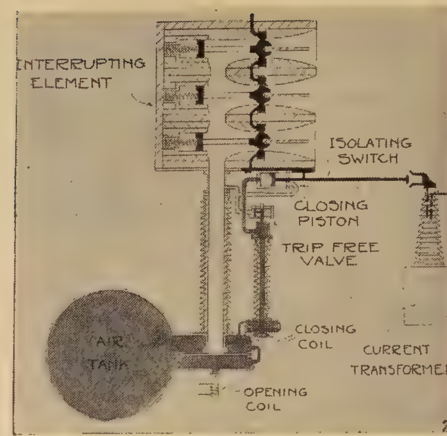

Figure 2A. Closing coil energized, isolator moving

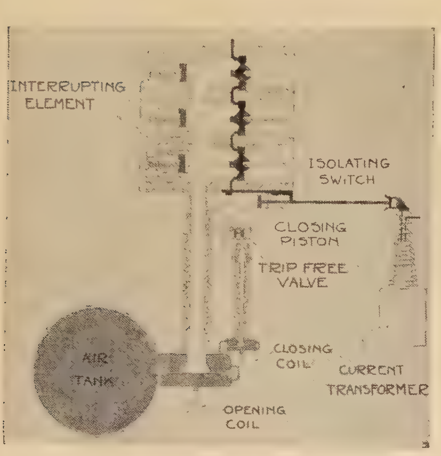

Figure 3A. Breaker in normal closed position

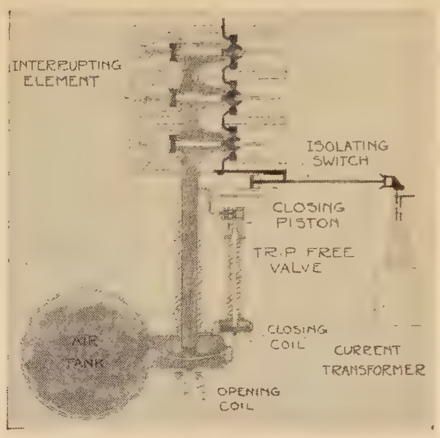

Figure 4A. Opening coil energized, air filling blast tube

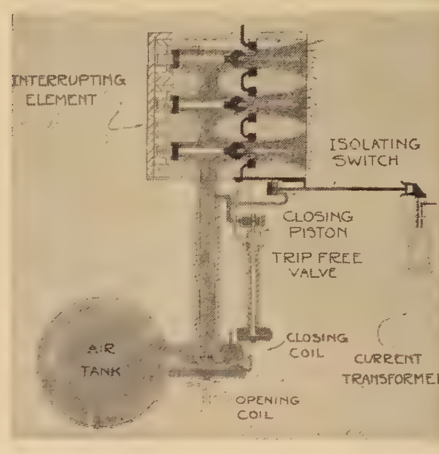

Figure 5A. Interrupter pistons open, arc drawn

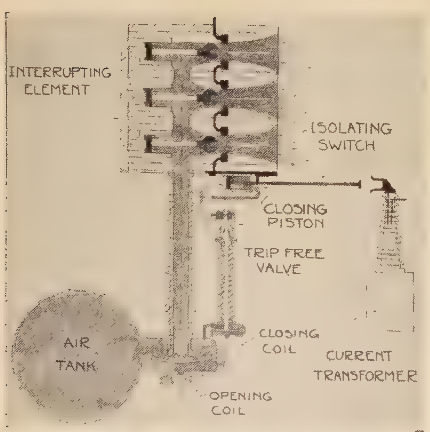

Figure 6A. Arc extinguished, isolator moving open

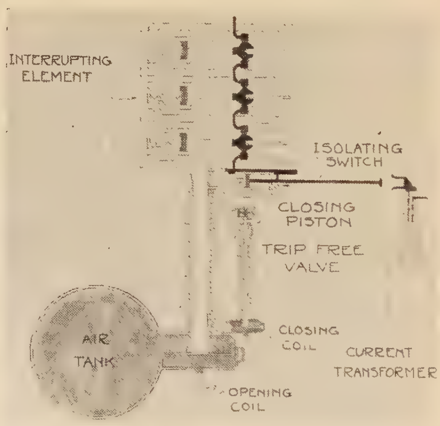

Figure 7A. Valves reset, breaker normal open

that described in connection with the valve used for closing the isolating switch. The weight of the moving parts of the blast valve is small, less than 5 pounds and the accelerating force is about 10,000 pounds, which gives an acceleration of about two thousand times that of gravity. This accounts for the very fast opening of these breakers, about one-sixtieth of a second from energizing the trip coil until parting of contacts, which of course is fast for a breaker of this large size. The interrupting element also contributes to this short opening time, the moving part having a weight of less than ten pounds and an accelerating force of about 2,000 lbs.

High-voltage air-blast breaker

For this type of breaker there are three interrupting elements in series, each individually air-operated

Figure 4*A* illustrates the conditions during the opening of the interrupter. The blast valve is open; a wave of air pressure is travelling up the porcelain blast tube, compressing the atmospheric air standing in the tube and header in the interrupter structure, similar to a sound wave, blasting the interrupter pistons to the left, opening the contacts and interrupting the arcs. A pressure wave is also travelling through a half inch pipe to the isolating switch cylinder but it cannot reach the cylinder in less than several cycles, leaving ample time for the interruption of the arcs before the isolating switch parts contact. This is shown in figures 5*A* and 6*A*.

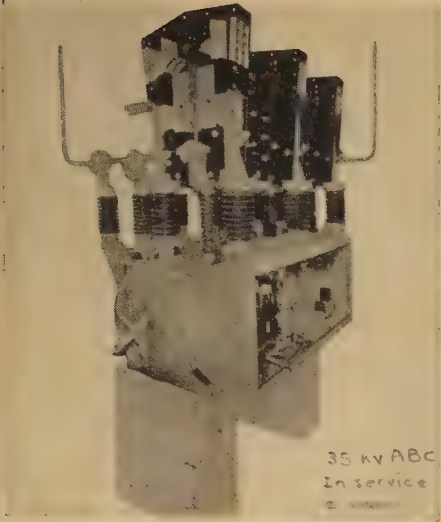

Figure B. General view of 35-kv air-blast breaker

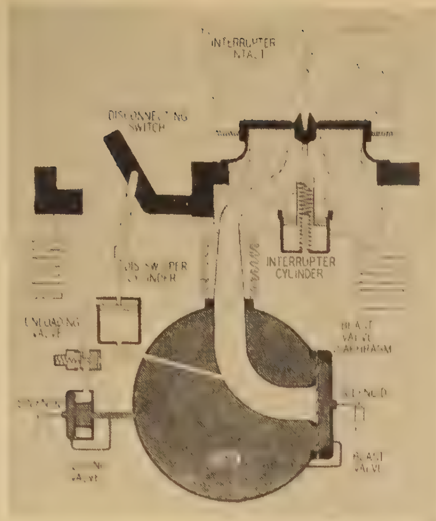

Figure 1B. Breaker in the normal open position

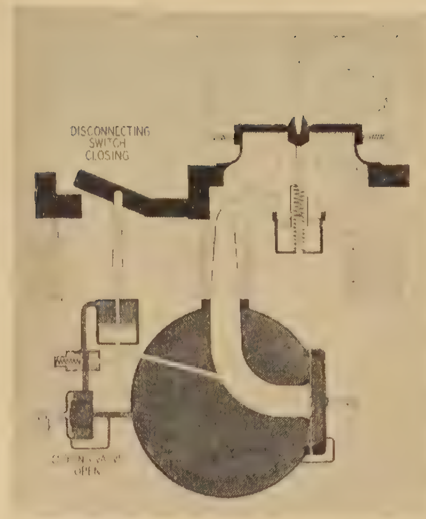

Figure 2B. Closing coil energized, isolator moving

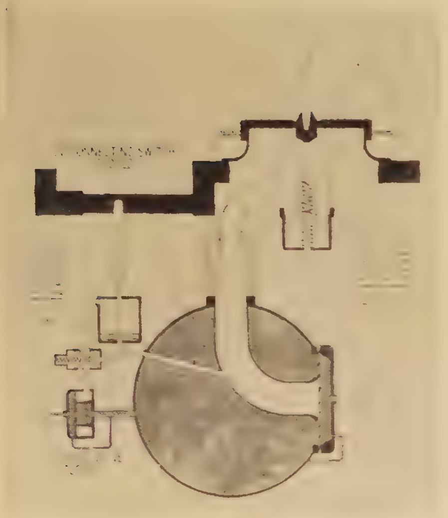

Figure 3B. Breaker in normal closed position

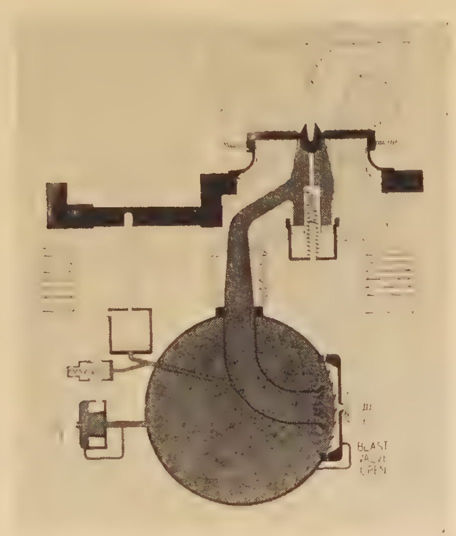

Figure 4B. Opening coil energized air filling blast tube

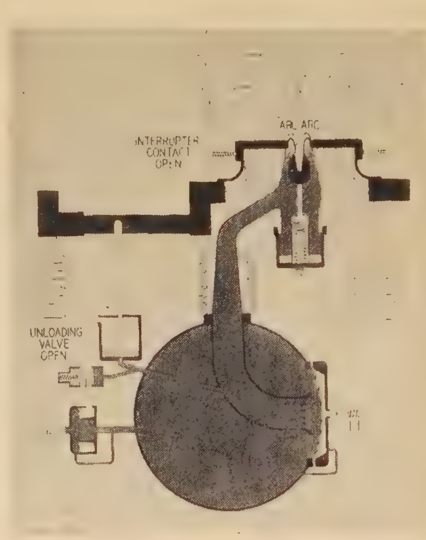

Figure 5B. Interrupter pistons open, arc drawn

Medium-voltage air-blast breaker

This type of breaker uses only a single blast valve for all three phases and only one interrupter element per phase

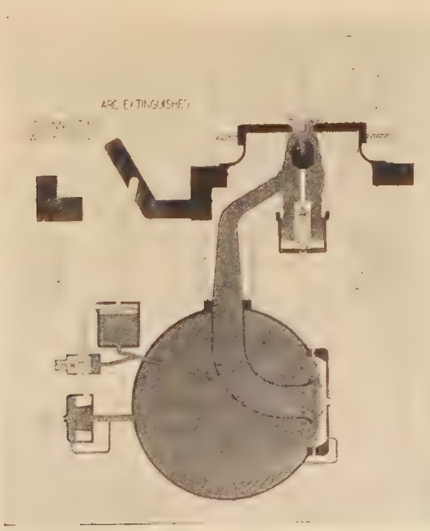

Figure 6B. Arc extinguished, isolator moving open

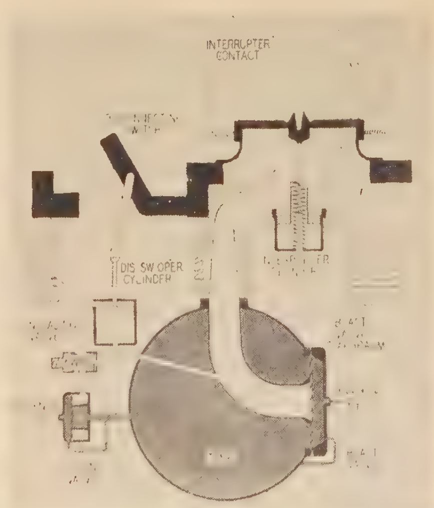

Figure 7B. Valves reset, breaker normal open

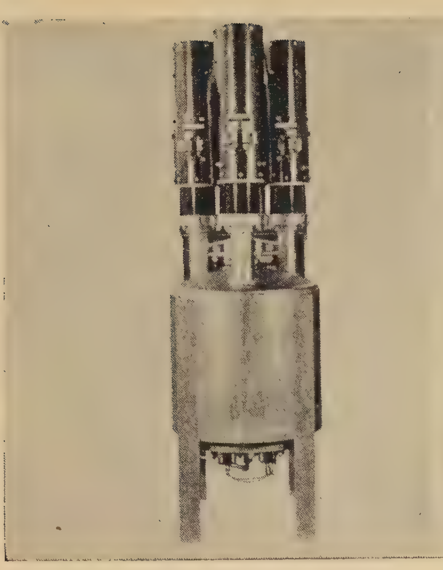

Figure C. General view of 12-kv air-blast breaker

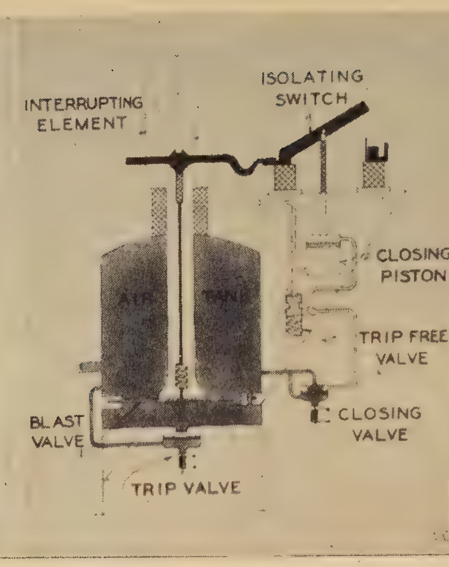

Figure 1C. Breaker in the normal open position

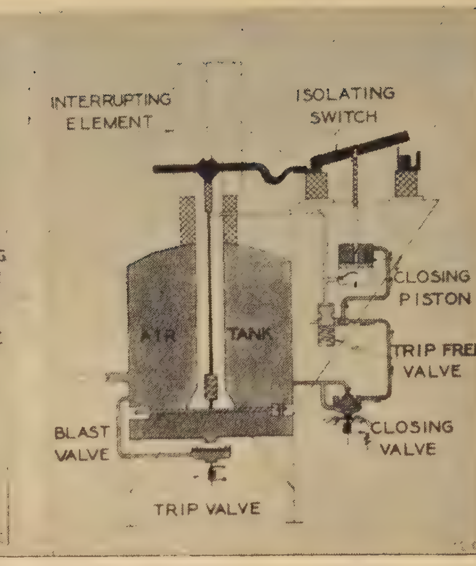

Figure 2C. Closing coil energized, isolator moving

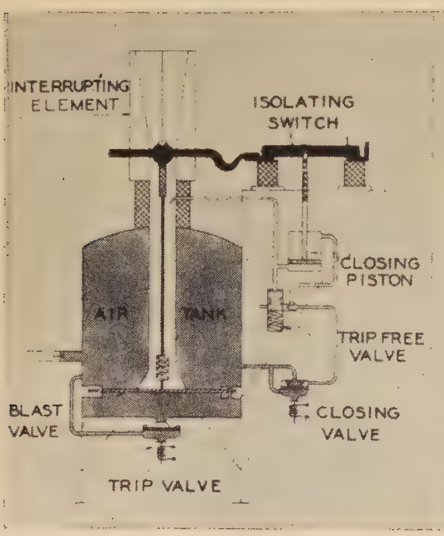

Figure 3C. Breaker in normal closed position

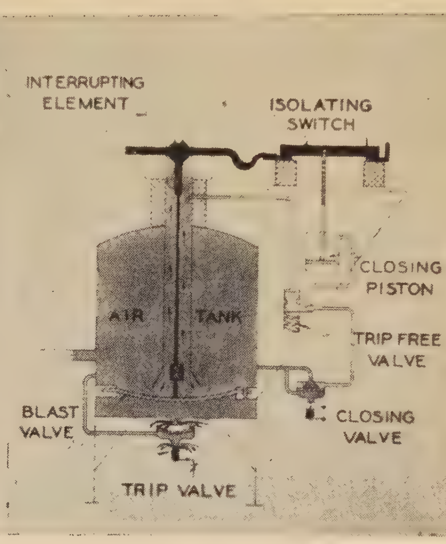

Figure 4C. Opening coil energized, air filling blast tube

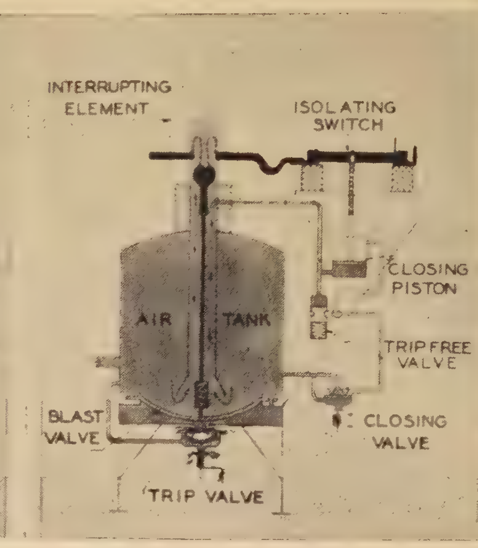

Figure 5C. Interrupter open, arc drawn

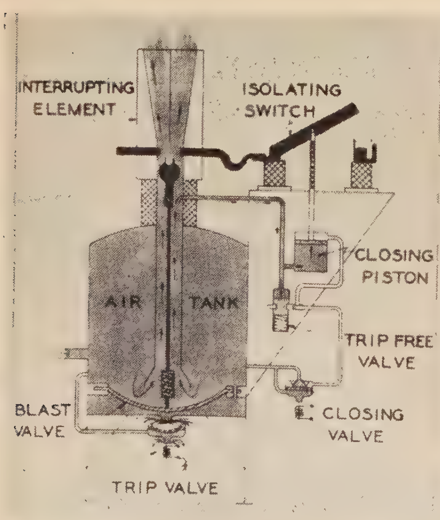

Figure 6C. Arc extinguished, isolator moving open

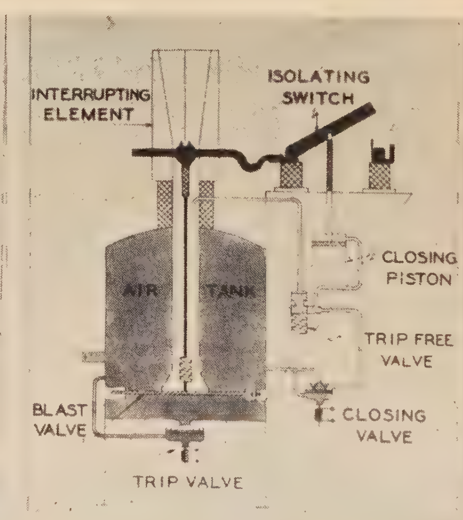

Figure 7C. Valves reset, breaker normal open

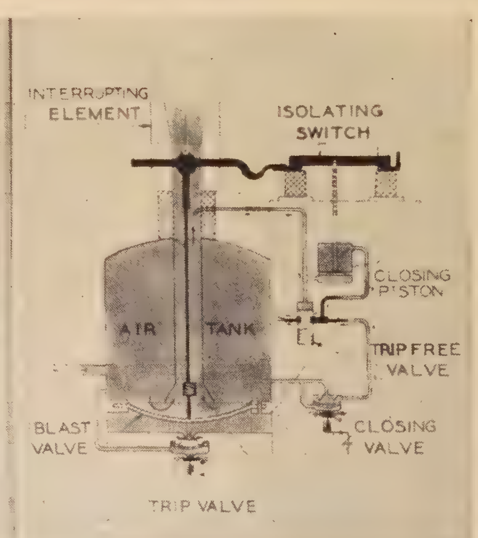

Figure 8C. OCO air trip-free valve draining closing air

Low-voltage air-blast breaker

In this type of breaker the main blast diaphragm operates the three phases of the interrupter elements

As the isolating switch is almost fully open, its auxiliary switch opens the trip circuit and the spring in the trip coil closes the trip valve permitting the re-establishing of pressure under the blast valve diaphragm by the flow from the tank. It has been found unnecessary to provide an area under the diaphragm greater than the area on top of it in order to make the diaphragm reseat, because there is an ejector effect which reduces the pressure near the center of the diaphragm due to the high velocity of the discharge and the diaphragm reseats promptly when the trip circuit is opened. Means have been developed for automatically shutting off the infeed of air from the tank to the lower side of the diaphragm while exhausting that space through the trip valve, but in service it has been found that satisfactory timing is obtained without such device. In general, the breaker can be blasted several times in quick succession before the tank pressure is reduced below the safe operating limit. When several breakers are installed in the same station, a common auxiliary storage tank is provided which quickly restores pressure in the breaker tank after which normal pressure is restored in the storage tank by the automatic starting of the compressor.

The 230-kv and 138-kv breakers are well adapted to single pole operation as there is no mechanical connection between poles. The switchboard operator can change the control from three-pole operation to single-pole operation by simply turning a control switch.

Type "B"

Photograph *B* illustrates a 35-kv breaker built by the I-T-E company which has been in successful service outdoors in New England for about two years at a location near the seashore where the salt spray constitutes a test of insulation even more severe than the St. Lawrence River mists on the higher voltage breakers. Figure 1*B* is a diagram of this 37-kv breaker in the open position. The interrupter has only one moving contact per pole; it is rigidly secured to a steel piston-rod and piston moving vertically in a cylinder which is at line potential. There is one blast valve and tank serving the three poles. The blast valve outlet divides three ways inside the tank and the three tubes pass through the tank to their respective poles. The blast valve is of the same general design as that of the higher voltage breakers, with certain modifications in detail, including springs to accelerate reseating of the diaphragm. The three poles of the isolating switch are operated by one cylinder at ground potential.

Figures 1*B* to 7*B* show the sequence of operation of this breaker. All breakers described in this paper are equipped with a pneumatic trip-free device operated by blast pressure to shut off compressed air supply to the closing end of the isolating switch cylinder and exhaust the air trapped in the closing end. The exhausting action is accelerated by the ejector effect of the nozzle in case the isolating switch closes on a short circuit.

Breakers of this same type also have been built by this company for 15 kv and 3,000 amperes. The current-carrying contacts are separate and part slightly before the interrupting contacts, all being rigidly fastened to the same operating piston-rod. In these breakers means are provided for surrounding the stationary contacts by air pressure to prevent premature parting of contacts before the moving contacts have moved away.

Type "C"

Photograph *C* illustrates a type of smaller breaker for 15 kv to 4 kv indoor service, 2,000 amperes, built by the Eastern Power Devices Limited. The main distinguishing feature of this type is the method of operating the interrupter contacts. The blast valve is of the same general design as in the other breakers except that the diaphragm has secured to its center, a steel operating tube which is rigidly connected to the interrupting contacts of the three poles through an insulating rod in each pole. When the valve diaphragm moves down it opens the blast and also mechanically opens the interrupting contacts. In order to insure that the contacts do not part before the blast arrives to interrupt the arc, a slight amount of slack is provided between the valve diaphragm and the operating rod so that the diaphragm moves down opening the valve part way before beginning to move the contacts. To minimize shock on the moving parts in opening, a spring is inserted between the diaphragm and operating tube.

Floor space is minimized by placing the tank vertically on end, the blast valve constituting the lower end of the tank. The blast valve outlet is shown in the diagrams as a single tube but actually it divides three ways passing up through the tank and out the top end of the tank in equilateral triangular formation; each of the three vertically projecting blast tubes is a 4″ standard pipe welded to the top of the tank and acts as the support for one pole of the interrupters. Each interrupter pole consists of a vertical cylinder of insulating material, 9″ inside diameter which provides sufficient space for interrupting elements of ample capacity.

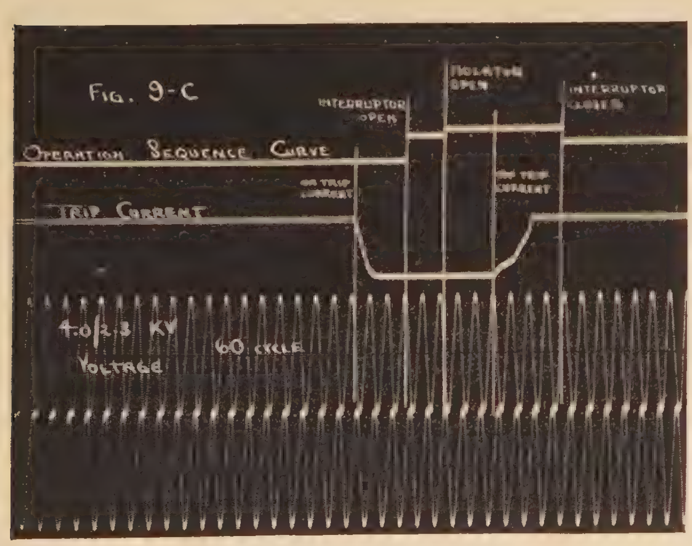

Figure 9C. Opening sequence

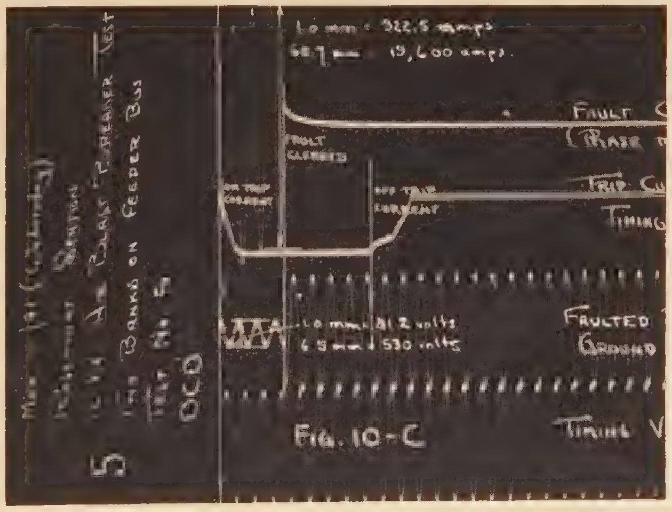

Figure 10 C. Oscillogram of interruption

A 2,000-amp. breaker of this type has a width of only 2′6″. This design is well adapted to various indoor layouts of stations and cell arrangements, including a draw-out arrangement of eliminating the usual disconnecting switches. This design can also be turned upside down and adapted to go into cells built for the old style oil breakers with live parts at the bottom.

Type "D"

Photograph *D* shows the general arrangement of 69-kv breakers built by the English Electric Company of Canada. It has one blast valve for the three poles, the valve being of the same design as the other breakers described. The blast tube passes horizontally through the tank to the external header tube parallel to the tank, serving the three poles through vertical stacks of porcelain blast tubes. Inside of each stack is an insulating operating rod opening and closing the interrupting contacts of the same design as in the other breakers. Each of these three operating rods is directly connected to a piston at the grounded end and in addition the three piston-rods are mechanically tied together through short links and a common shaft. The three poles of isolating switch blades are operated by a common cylinder at ground potential. The switch blade is a hollow bronze casting enclosing the hinge of a short toggle blade which makes a swiveling engagement with the stationary full-floating jaw contacts facilitating sleet cracking in opening. The blade is side opening facilitating sleet-hood protection and simplifying insulators, only two stacks per pole being required. A simple arrangement of arcing contacts has been found satisfactory in closing on short circuits with negligible burning; the operation of the isolating switch is very fast.

Figure D. General view of 69-kv air-blast breaker

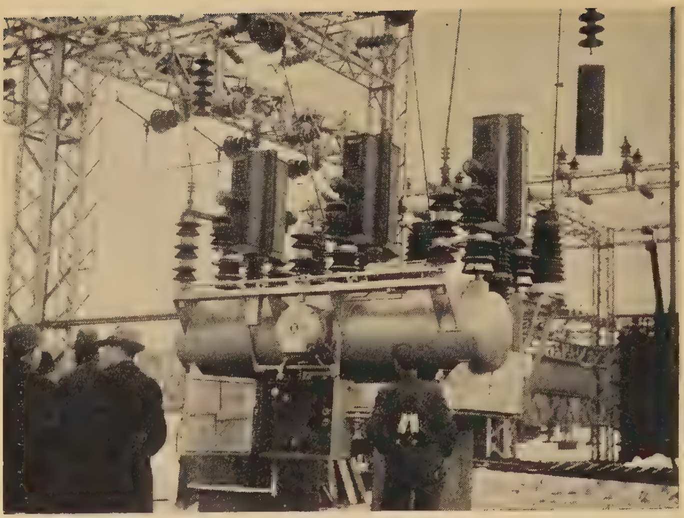

Operating Results

The service record of breakers of this general design dates from 1934 when the first 138-kv breaker was installed. Since that time breakers of the several other voltages have been placed in service and the record is now equivalent to 20 breaker-years of service. The number of breakers recently installed and on order is 30. There have been 15 breaker interruptions reported in service, with no failures.

Interrupting Ratings

The 230-kv breaker is rated 2,500,000 kva; single-pole interrupting tests on sections of this breaker have shown interrupting capacity equivalent to more than 3,000,000 kva on the complete 3-pole breaker. The 138-kv breaker is rated 1,500,000 kva; 69-kv breaker 1,000,000 kva.

Insulation

The standard specifications for breakers of the several voltages are complied with.

Operating Time

The opening time is three cycles or less, from energizing of trip coil to current interruption. Reclosing time is within 20 cycles from energizing trip coil.

Operating Current

Closing coil or opening coil takes ten amperes or less; can be reduced to one ampere.

The Shielding of Permanent Magnets From Transient Magnetic Fields

GEORGE J. WEY
ASSOCIATE AIEE

Introduction

CONSIDERABLE progress has been made toward the development of permanent magnets which are immune to disturbing conditions, such as temperature variation, mechanical vibration, natural aging, and extraneous flux fields. Contributions to this progress include new materials, improved processing techniques, and better manufacturing controls.

Constancy of flux is in most applications quite essential. This is particularly true of electromagnetic damping, in which the damping torque varies as the square of the air gap flux. The permanent magnet of a watthour meter is an example.

Despite the fact that the modern permanent magnet is remarkably stable, there have been cases in which the magnets showed changes in strength, generally becoming somewhat weaker. Isolated instances of such changes in watthour meter magnets have been found by the electric utility companies.

About four years ago, evidence gathered by various utilities pointed to lightning discharges as the probable cause of the demagnetization. After initial laboratory tests failed to demagnetize meter magnets by passing surge currents through the windings alone, it was realized that the demagnetizing field was primarily caused by surge currents in the service wiring itself. Figure 1, curve 1 shows the amount by which forged chrome steel magnets are weakened by a single surge of the value indicated by the abscissa using the test setup shown on the figure 2.

To date, there have been no extensive studies made of the magnitude and frequency of surge currents appearing on the secondaries of distribution systems. Figure 3 shows expectancy curves for lightning discharges in distribution system primary arrester ground leads from the investigations of McEachron and McMorris.[1] These curves show that in rural areas a discharge of 5,000 amperes may be expected at any one arrester location once in 14 years and a 10,000-ampere discharge once in 30 years. In attempting to apply these expectancy curves to the distribution secondaries, however, they should be considered as extremely pessimistic because of the reduced exposure of the secondary circuit.

It is evident from a consideration of the rarity with which high current discharges appear on distribution systems that any program designed to materially reduce the number of weakened magnets found on the system secondary must be applied to a large percentage of the total exposed installations. Thus, it would be desirable to protect not only new meters but also those in service.

Since there are millions of standard forged steel magnets in service, it would be desirable that surge protected magnets should not require new techniques or tools to service them.

High Coercive Alloys

The problem of making permanent magnets impervious to transient magnetic fields has been solved in two ways by the various meter manufacturers. One method has been to make the magnet from one of the new high coercive materials, such as Alnico. The coercive force, H_c, of these alloys ranges from 400 to 600 oersteds which means that when properly applied to a watthour meter such a magnet would withstand surges up to 25,000 amperes without appreciable weakening. Another advantage of these alloys over forged magnet steel is economy of space for a given air gap energy. However, before this advantage can be realized to any appreciable extent, the whole meter must be designed with this object in view. Also, a complete new magnet design must be made and manufacturing processes developed in order to utilize the new alloys.

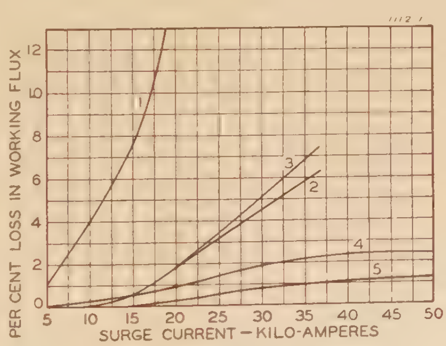

Figure 1. Demagnetization of chrome-steel magnets by transient currents

1. Unshielded
2. Plated with 0.002-inch thick copper
3. Schoop sprayed copper 0.02-inch thick
4. Copper clad (Roth process) 0.02-inch thick
5. High-speed copper plate 0.019 thick

Test waves
Curves 1, 2, 3—24x40 microseconds
Curves 4, 5—36x70 microseconds to 25,000 amperes; 30x50 microseconds 25,000 to 40,000 amperes; 20x35 microseconds over 40,000 amperes

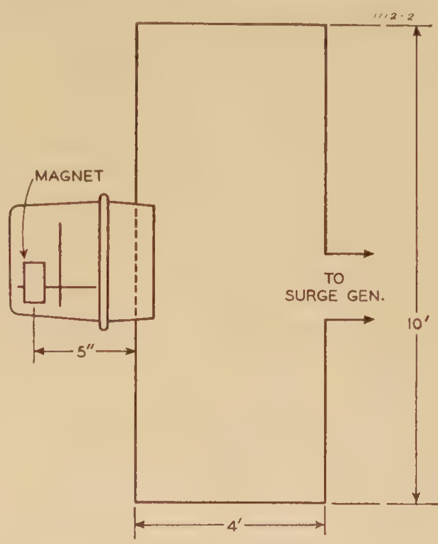

Figure 2. Setup for surge tests on permanent magnets

Electromagnetic Shielding

An alternate solution to the problem of transient fields and the one described in this paper is to use electromagnetic shielding around the existing forged steel magnets. While this principle of shielding is old,[2] it is felt that a description of its application to permanent magnets is new and may be of general interest.

The requirements of an efficient electromagnetic shield are: first, the shield must provide low resistance paths for the flow of eddy currents. Second, the shield must be continuous about the object to be shielded so the eddy currents can flow in any direction.

The above requirements immediately suggest plating the magnets with copper,

Paper 41-112, recommended by the AIEE committee on instruments and measurements, and presented at the AIEE summer convention, Toronto, Ontario, Can., June 16–20, 1941. Manuscript submitted April 23, 1941; made available for preprinting May 7, 1941.

George J. Wey is with Westinghouse Electric and Manufacturing Company, Newark, N. J.

1. For all numbered references, see list at end of paper.

since copper has low electrical resistance and a continuous sheath of the metal could be easily plated on steel. With the ordinary process of electroplating copper

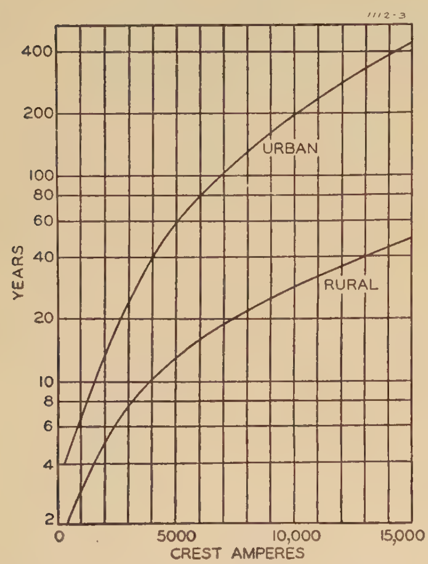

Figure 3. Discharge currents in distribution arresters

Number of years that may be expected to elapse for each discharge of at least the magnitude indicated through any one arrester

from a copper sulphate solution, however, it is impractical to build up a coat more than 0.002″ thick, and even this thickness requires upward of 24 hours plating time.

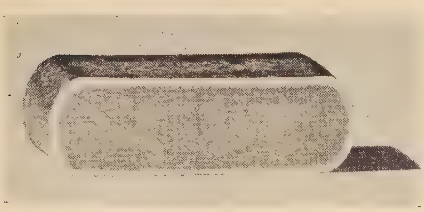

Figure 4. Cross section of plated magnet

Figure 1, curve 2 shows the shielding effect of a 0.002″ thick plated copper sheath using a 24x40 wave (24 microseconds to crest, 40 to half value). By comparing with curve 1 it will be seen that such a shield is quite effective against transients.

Another method of applying a metallic coating is by the Schoop spray process. By this means metallic coatings of any desired thickness can be applied to magnets. Figure 1, curve 3 shows the shielding effect obtained by this method. Due to the porosity and consequent high resistivity of the deposited metal and the difficulty of obtaining a uniform coating, this method was considered inadequate.

Good shielding can be obtained by the use of copper-clad steel made by any of the standard commercial processes. Figure 1, curve 4 shows the shielding obtained from a 0.020″ thick layer of copper formed by the Roth process. This process consists of placing a properly fluxed billet of steel in a vertical mold. After heating the mold and billet to a red heat, molten copper is poured around the billet. The mass is then rolled to the desired bar size. The principal disadvantage of copper-clad steel for magnets is that the conductivity of the copper is lowered during the heat treatment of the magnet steel. Also, the copper coat is not of uniform thickness, which reduces its effectiveness.

High-Speed Copperplating

Early experiments with a new high-speed copper-plating process invented by the E. I. du Pont de Nemours Company gave results worthy of further investigation.

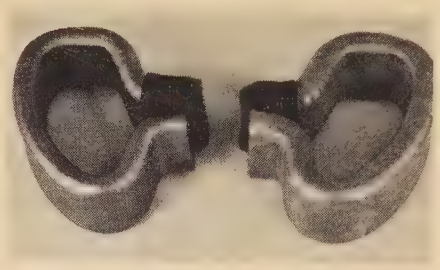

Figure 5. Left, magnet before plating; right, magnet after plating

The high-speed copper-plating process plates from a hot alkaline bath consisting of copper and sodium cyanides and sodium hydroxide. The work is placed in a rotating barrel, the speed of which is regulated to obtain the best burnishing action on the copper as the magnets tumble over each other.

With this process about 13.1 lb of copper can be deposited in 11 hours on 65 lb of magnets. This corresponds to an

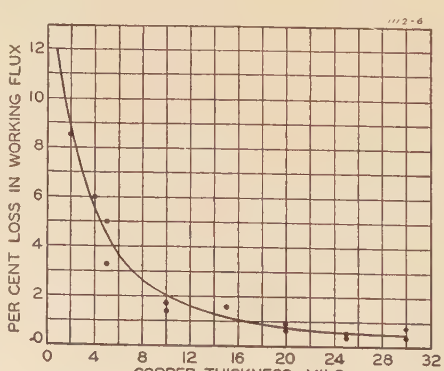

Figure 6. Effect of copper thickness on shielding of chrome-steel magnets

average deposition rate of 0.0017″ per hour.

It was found in developing this process for the plating of magnets that the conductivity of the copper plating decreased very rapidly after the solution was used a few times. This condition was traced to an excessive concentration of sodium carbonates in the electrolyte. Excessive amounts of this compound also cause the

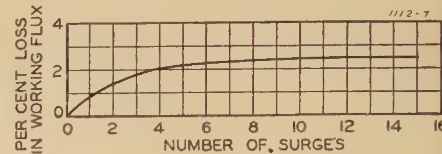

Figure 7. Effect of repeated 30x50 microsecond surges of 30,000 amperes on copper-plated chrome magnets

deposit to be rough and pebbly. It was found necessary to periodically chill the solution and allow the carbonates to crystallize out.

Figure 4 is an enlarged cross section of a plated magnet.

In order to obtain the maximum calibration adjustment on the assembled magnet, it is necessary to leave the upper pole tip unshielded. This is accomplished by placing a short length of rubber tubing over the upper pole tip before plating.

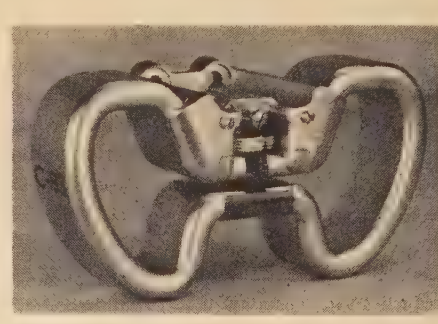

Figure 8. A complete assembly of copper-plated magnets

The tubing is thick enough to completely fill the air gap of the magnet, thus reducing the amount of material to be removed in the final grinding. Figure 5 shows a magnet before and after copper plating.

Since the effectiveness of the shielding depends on the resistance of the plating, this property is used to control the quality of the product. As absolute values are not necessary, the procedure is to measure the total ohmic resistance of the magnet between points just back of the poles using a Kelvin double bridge. The addition of the copper plating reduces the total resistance from 340 microhms for the

System Short-Circuit Currents

Proposed New Calculating Procedure for Application of Interrupting Devices and Relays

W. M. HANNA
ASSOCIATE AIEE

H. A. TRAVERS
ASSOCIATE AIEE

C. F. WAGNER
FELLOW AIEE

C. A. WOODROW
MEMBER AIEE

W. F. SKEATS
MEMBER AIEE

THE current flowing in a short circuit in a simple a-c system can be expressed as a function of time in the form of three exponentially decaying components and a term which is substantially constant. These components are termed the subtransient, the transient, the d-c components, and the steady-state component. In actual systems all these terms are affected to some extent by the number of machines and the phase angles between them and also by their excitations. The phase relations between machines may change during the period of short circuit and thus introduce further complications. Automatic voltage regulators also introduce another factor which tends to increase the short-circuit current, since their action causes increase in machine excitation. Consequently, the accurate determination of short circuit current at any instant may be and usually is quite difficult.

Fortunately such rigorous calculations are not generally required to determine the proper application of interrupting devices and relay settings, for many other factors having greater proportional effect than the variations cited above contribute to the determination of the limits for rational choice of circuit breakers, expulsion protective gaps, fuses, etc. It is, therefore, perfectly proper and logical to make certain approximations in the calculation of short-circuit current to permit simple solutions of electrical systems for the purpose of applications of equipment. Such assumptions have been in general use for a considerable time and recognized by the electrical engineering profession.[1] An early approximation took the form of decrement curves which could be utilized if the reactances of the component branches of the system were known. As the knowledge of machine performance with the resolution of currents into the transient and subtransient components increased and the use of symmetrical components for unbalanced conditions became more generally known and accepted, the original decrement curves were revised[2] and placed on a more substantial basis. These curves, the present decrement curves, included provision for the determination of three-phase, line-to-line and line-to-ground short-circuit currents. At the same time other and more elaborate approximations[3,4] were offered which, while giving more accurate results, involved more extensive and complicated calculations.

The growth and interconnection of systems has resulted in a condition such that if the curves are applied according to the rules, values of impedance outside the range of the curves are often obtained, thus making the curves useless. Recourse was often made to certain expedients, such as the division of the system into several groups, each of which fed short-circuit currents into the short circuit independent of the others. These were so chosen that all the generators in a certain group were approximately the same electrical distance from the fault. In addition, frequent errors have occurred, even among those accustomed to the use of the curves, in confusing the kva of the arbitrarily chosen base on which calculations are made, with the kva of the system. The need undoubtedly exists for

Paper 41-121, recommended by the AIEE committee on protective devices, and presented at the AIEE summer convention, Toronto, Ontario, Can., June 16–20, 1941. Manuscript submitted April 16, 1941; made available for preprinting May 14, 1941.

W. M. HANNA is with Consolidated Gas, Electric Light and Power Company, Baltimore, Md.; H. A. TRAVERS and C. F. WAGNER are with Westinghouse Electric and Manufacturing Company, East Pittsburgh, Pa., and C. A. WOODROW and W. F. SKEATS are with General Electric Company, Mr. Woodrow in Schenectady, N. Y. and Mr. Skeats in Philadelphia, Pa.

This paper is the report of a group assigned to investigate the problem under the auspices of the subcommittee on circuit breakers, switches, and fuses of the AIEE committee on protective devices.

1. For all numbered references, see list at end of paper.

---

steel alone to approximately 75 microhms for the combination.

Figure 6 shows the shielding effect of plated copper plotted against copper thickness. No appreciable increase in shielding is obtained after the coat is 0.020″ thick.

Figure 1, curve 5 shows the shielding effect of a 0.019″ thick plated copper shield using the surge values indicated on the figure.

Figure 7 shows the effect of repeated surges of the same magnitude on copper-plated magnets. Since the resistivity of the steel is fairly low (40.5 microhms/cm^3), an appreciable amount of self-shielding is obtained from the steel itself. This means that the demagnetizing effect of the first surge is limited to the outermost layer of magnet steel. After the surge has passed, the inner layers of steel remagnetize the outer layer, thereby weakening the whole magnet. Succeeding surges continue the process of demagnetizing fresh layers of steel until the demagnetized layer is so thick that the eddy currents induced in it are sufficient to prevent the further penetration of the transient flux. This is the same as saying that the demagnetization continues with succeeding surges until the intensity of the transient field minus the opposing intensity of the eddy current field equals the coercive intensity of the magnet material.

A complete copper-plated magnet assembly is shown on figure 8. This magnet is entirely interchangeable with unshielded magnets of similar design. Since the magnet material is the same as that used on unshielded magnets, the air gaps may be cleaned with magnetic cleaning tools without disturbing the calibration.

Summary

It has been shown that the problem of protecting permanent magnets from transient magnetic fields has been solved in a unique manner by the use of a new high-speed copper-plating process to apply a high conductivity copper shield over the conventional forged steel magnets.

Desirable features of this solution are complete interchangeability between unshielded and shielded magnets; forged steel material is used, which is fairly easy to obtain and on which unlimited operating experience is available.

References

1. DISCHARGE CURRENTS IN DISTRIBUTION ARRESTERS—II, K. B. McEachron and W. A. McMorris. AIEE TRANSACTIONS, volume 57, 1938 (June section), pages 307–12.

2. HIGH FREQUENCY MEASUREMENTS, August Hund. McGraw-Hill Book Co., 1933, page 47.

the simplification, if possible, of the present methods of the calculation of system short-circuit currents. Fortunately, due to the increased use of higher speed circuit breakers and faster relaying, this need can be satisfied for an extremely large proportion of the present applications. It is the purpose of this paper to discuss this general problem and recommend simplified methods of calculation for different types of apparatus.

The modern trend of practice is to speed up materially the clearing of short circuits in order to reduce damage and maintain continuity of service. But, in general, the more quickly a short circuit is cleared, the greater is the current to be interrupted. Thus it is quite easy, by speeding up the relay system, to jeopardize the breakers by requiring them to interrupt more current than that for which they were initially chosen. Also quite often there is a tendency to save investment in breakers by the use of slow speed relays to take advantage of the decrease in short-circuit current due to its decrement with time, but even with slow speed relays, there is no guarantee that a short circuit will not change its character and initiate a high current flow in a breaker while it is opening. And there is always the danger of shortening the time setting of slow speed relays, which will tend to increase the interrupting duty on the breaker. Provision of breakers with interrupting capacity adequate for fast relaying is thus at least as essential a part of planning for the future as the usual allowance for increase in generating capacity.

This being the case, the problem of interrupting device application resolves itself into a study of what happens in a system during the first few cycles of short circuit. Even with fast relaying, modern high speed breakers for 60-cycle systems may be expected to part their contacts in times no shorter than given below:

8-cycle breakers—4 cycles (0.0666 second)
5-cycle breakers—3 cycles (0.05 second)
3-cycle breakers—2 cycles (0.033 second)
2-cycle breakers—1 cycle (0.0166 second)

In the above intervals of time, the effects of change in relative phase position and change in excitation from voltage regulators are negligible and permit eliminating their influence in the calculation of short-circuit values. Values so calculated will also be on the conservative side where some types of breakers in the above classes part their contacts in slightly longer times.

Figure 1 gives, in the full-line curves, the magnitude of the three-phase short-circuit current expressed in terms of rated current for various reactances as obtained from the present decrement curves, for the four instants specified; namely, 4, 3, 2, and 1 cycles which are related to the 8, 5, 3, and 2-cycle breakers as discussed above. The rated current and reactances are based on the system kva. Curves are given for both the total rms current and the a-c component only, the difference between the two being due to the d-c component. The larger the d-c time constant,

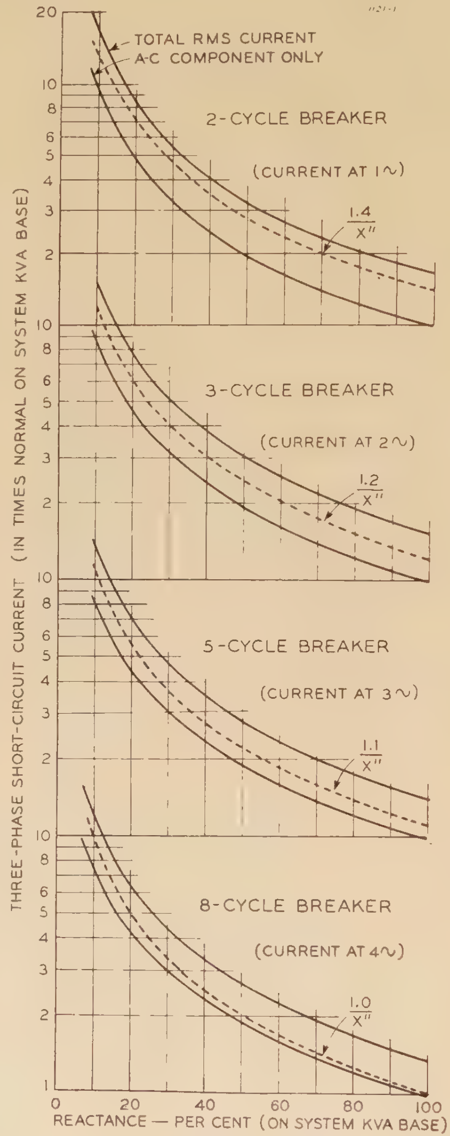

Figure 1. Comparison between decrement-curve calculations and calculations by the proposed method

the more closely is the total rms curve approached and the smaller the d-c time constant, the more closely is the a-c component curve approached. The time constant of the d-c component for which these curves were made is 0.15 second or 9 cycles. The d-c time constant may be expressed generally as equal to $\frac{1}{2\pi f}\cdot\frac{X}{R}$ in seconds, or $\frac{1}{2\pi}\cdot\frac{X}{R}$ in cycles, where X is the 60-cycle reactance and R the d-c resistance to the point of fault. Although ratios vary considerably, representative values of the ratio X/R for the major circuit elements for large equipment are given below.

		Corresponding Time Constant	
	X/R	In Seconds	In Cycles
Generators	80	0.21	13
Current-limiting reactors	50	0.13	8
Transformers	16	0.04	3
Transmission line	4	0.011	0.6
Cable	1.0	0.003	0.2

When any of these elements are connected in series relation the time constants of the combination become much smaller than that of a generator alone. Even a short length of transmission line has a marked effect upon the d-c component of current and a very appreciable effect upon the total short-circuit current. Table I shows the time constant of a particular combination for a fault at the generator, at the transformer terminals, and at two points out on an overhead line.

The Power Circuit Breaker Interrupting Problem

The reactances of figure 1 are based on the kva of the connected generator capacity. When the fault is near a generator the reactance is likely to be small and the d-c time constant large so that for small reactances the actual short-circuit current would approach the values given by the total current curves of figure 1. If, on the other hand, the fault is on the transmission line, the reactance is large and the time constant small. Thus, for large reactances the actual currents approach the values given by the a-c component only. The intermediate curves (dotted) of figure 1 for circuit breaker opening times of 4, 3, 2, and 1 cycles have been computed by the relation $1.0/X''$, $1.1/X''$, $1.2/X''$, and $1.4/X''$ respectively, in which X'' represents the system reactance to the points of fault, subtransient reactances being used for all generators. The factors in the numerators were arbitrarily chosen so that the curves lay between the curves for the total current and a-c component of current, and so the values were numbers that can be remembered easily.

In these curves the effect of the arc drop, which may be quite considerable in decreasing the d-c time constant, has been neglected. For a reactance of 30 per cent an arc drop of only 1.5 per cent in combination with one-half per cent resistance

in the system is all that is required to reduce the d-c time constant from the nine cycles used in the present decrement curves to three cycles. On a 440-volt basis this is equivalent to but 6.6 volts, a value that is easily attainable. A reasonably conservative value of arc drop is about 20 volts per inch so that on a 13,800-volt circuit, 1.5 per cent drop requires only about six inches of arc length.

Having shown through the medium of the decrement curves that the relations for 4, 3, 2, and 1-cycle opening times apply quite well for simple systems, the justification has been established for applying the same relations to more complex systems. The use of these simple relations circumvents practically all the disadvantages of the decrement curves enumerated previously. With this method of calculating it is necessary only to obtain the equivalent reactance, expressed in any manner, regardless of the system, and apply the appropriate factor to the reciprocal of the reactance.

The foregoing simplified rules cover practically all applications. For the few remaining, it is sometimes desirable to know the short-circuit current for times longer than four cycles. For these special cases, the present decrement curves[2] or more elaborate methods may be utilized.[3,4,5,7] However, these methods are discouraged in favor of the rules proposed in this paper.

In most cases, faults occur at a point in the system for which a certain amount of other apparatus intervenes between the generators and the point of fault, in which case, the d-c component decays rapidly and the actual current approaches the a-c component. Even if the fault occurs on a generator bus, it is likely that other generators contribute to the short-circuit current through transformers, transmission lines, or cables. Therefore, the calculated values of current will be conservative for most cases.

In extreme cases where all the fault current is produced by large generators located at the point of fault, an accurate calculation with all assumptions on the safe side might show values as much as 20 per cent higher than the values given by this procedure. For the most conservative practice, therefore, when this condition is approached the results may be increased or other methods of calculation used.

In the curves of figure 1 adequate allowance has been made for non-synchronous load. For most central station applications, the additional contribution from synchronous motors will be negligible but where there is an appreciable contribution from them, they should be taken into account. In industrial applications, synchronous motor contribution may be of the same order of magnitude as that from generators and hence must be taken into account.

Synchronous motors are usually operated at about unity power factor; hence the voltage behind their subtransient and transient reactances is but little above terminal voltage. They tend to increase the power factor of the load; hence indirectly they reduce the internal voltage of the system generators. In general, they are much smaller units than generators; hence all of their time constants are faster and the decay of their short-circuit current is more rapid. For all of these reasons, it is justifiable to make somewhat

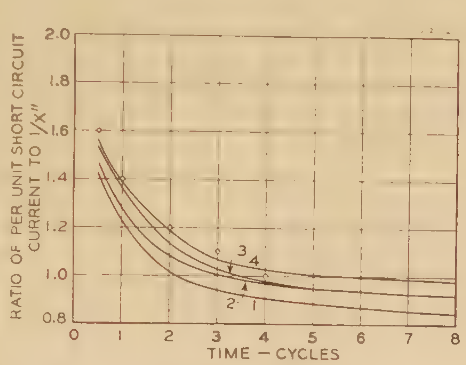

Figure 2. Three-phase short-circuit current from generators fully loaded at rated power factor

Arcing fault at one-fourth mile per kilovolt of transmission line

1. Steam-turbine generator, 0.8 power factor without transformer
2. Steam-turbine generator, 0.8 power factor with transformer
3. Hydroelectric generator, 0.9 power factor without transformer
4. Hydroelectric generator, 0.9 power factor with transformer

Circles show points proposed for calculating duty of equipment

less allowance for the short-circuit current of synchronous motors than for generators. Transient reactance may, therefore, be used in calculating their contribution.

The contribution of induction motors can always be safely neglected at times of two cycles or more.

The Momentary Problem

For many purposes, it is necessary to know the maximum possible rms current which can flow in the circuit. This is given by the current, including both a-c and d-c components, as calculated at one-half cycle. Allowing for overexcitation of generators on account of load, the rms value of current as calculated for zero time is about 1.8 times the value calculated by dividing leg voltage by subtransient reactance. As there will always be some decay even in the first half cycle, however, 1.6 times this value gives a safe figure.

In some instances, as when transmission line or cable reactance is an important factor in the limitation of current, the factor 1.6 may be higher than necessary.

In such applications, at 5,000 volts and below, the ratio of reactance to resistance is sufficiently low so that the d-c component decreases very greatly during the first half cycle. Thus within this voltage range, and except where the bulk of the power is supplied by generators at the point of fault, a standard factor of 1.4 may be used instead of 1.6. A standard factor is particularly desirable in consideration of the difficulties of obtaining actual resistance figures and the distribution of the d-c component among contributing short-circuit sources.[5]

Examples

All of the foregoing has been carefully checked by the calculation of specific examples. Figure 2 has been calculated for four representative simple cases as follows:

1. A representative turbine-generator with both transmission and fault at generator voltage.
2. A representative turbine-generator with a step-up transformer and both transmission and fault at 230 kv.
3. A representative hydro-electric generator with both transmission and fault at generator voltage.
4. A representative hydro-electric generator with a step-up transformer and both transmission and fault at 230 kv.

In each case the transmission line was assumed to have a length of one quarter mile per kilovolt and to have sufficient copper section to carry the entire generator output (either in one line or in several parallel lines) at a current density of 1 ampere per 1,000 circular mils. An arcing fault is assumed with an arc drop of 150 volts at generator voltage and of 2,000 volts at 230 kv.

The points corresponding to the coefficients 1, 1.1, 1.2, 1.4 and 1.6, at 4, 3, 2, 1, and 1/2 cycles respectively are shown on figure 2, and it will be observed that they represent with reasonable accuracy the currents obtained at their respective times.

Figure 2 may be considered representative of the general case in which although some power may be generated near the point of fault, the major part of the short-

circuit current comes from some distance away. Figure 3 has been calculated on a similar basis but without any transmission line between generator and fault point. Here it will be observed that the currents are somewhat higher, particularly for times from two to four cycles. It is for this reason that the recommendation is made that some additional allowance be made when the major part of the short-circuit current is obtained from large machines located at the point of fault.

Selection of Apparatus

It is suggested that the following procedure be followed in calculating short-circuit currents for use in applying various kinds of equipment.

Circuit-Breaker Interrupting Capacity

While there is a wide variation in system conditions, the following calculation will usually give a conservative value of required interrupting capacity.

(1). Calculate the highest value of initial rms symmetrical current on the basis of no load, normal voltage, whether for a three-phase, double-line-to-ground, line-to-line, or single-line-to-ground fault, using subtransient reactances for all synchronous generators. Use transient reactance of synchronous motors when their short-circuit contribution must be considered.

(2). Multiply by the appropriate factor for 60-cycle systems from those given below:

8-cycle breakers	1.0
5-cycle breakers	1.1
3-cycle breakers	1.2
2-cycle breakers	1.4

(3). When the condition is approached of a short-circuit fed solely by large machines at the point of fault, these results may be increased up to 20%.

(4). Low voltage (600 volts or less) air circuit breakers are often instantaneous in operation and part contacts during the first half cycle. These breakers, however, are rated on the basis of average current in the three phases, and circuits on which they are installed rarely have X/R ratios exceeding ten. This corresponds to an average rms current during the first cycle equal to 1.23 times the symmetrical current. Breakers may therefore be applied on the basis of $1\frac{1}{4}$ times the three-phase initial symmetrical current using subtransient reactance and including both synchronous and induction motors.[5]

In order to co-ordinate this method of application of low voltage breakers with the conventional method used for other types of breakers, it is interesting to note that an average current for the three phases equal to $1\frac{1}{4}$ times the symmetrical current corresponds to a total rms current in the phase carrying the maximum unsymmetrical current equal to 1.4 times the initial symmetrical component.

In making the calculation for the equivalent system impedances, it should be remembered that at low voltages small impedance values become of importance and all elements of the circuit including current transformers, disconnects, switches, circuit breakers, bus runs, lead wires, et cetera should be taken into consideration.

Mechanical Stresses and Momentary Rating of Circuit Breakers

The initial mechanical stresses due to the flow of electrical currents and the momentary rating of a circuit breaker are dependent on the maximum possible current which can flow at any time.

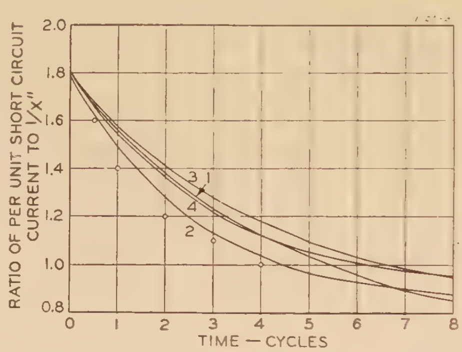

Figure 3. Three-phase short-circuit current from generators fully loaded at rated power factor

Arcing fault at generator or transformer terminal

1. Steam-turbine generator, 0.8 power factor without transformer
2. Steam-turbine generator, 0.8 power factor with transformer
3. Hydroelectric generator, 0.9 power factor without transformer
4. Hydroelectric generator, 0.9 power factor with transformer

Circles show points proposed for calculating duty of equipment

(1). Apart from cases covered by (2) below, the current to be used is 1.6 times the maximum value of rms symmetrical current using subtransient reactance values of both synchronous and induction machines.

(2). At 5,000 volts and below a factor of 1.4, instead of 1.6 should be used except on busses to which the major portion of total fault current is supplied either by directly connected synchronous machines or through reactors.

Directly connected synchronous machines are to be considered as those supplying fault current directly or through lines and transformers which reduce the contribution from those machines by less than 50%.

Protector Tubes

Inherent limitations of protector tubes require that a maximum and a minimum current rating be assigned to each tube for a given voltage. Because of the speed with which these devices become operative, it has been found possible to incorporate the variability of the d-c component into a rating which involves only the initial rms symmetrical a-c component of short-circuit current.[6]

Tubes should be applied so that the symmetrical short-circuit current at the point of installation of the tube, calculated on the basis of subtransient reactance for all combinations of connected synchronous machines and lines, should fall between the two limits assigned to the tube.

Fuses

Fuses are rated on total current and as the times involved are very short, their required interrupting capacity should be based on the total rms current at one-half cycle.

(1). In the general case, the current to be used is 1.6 times the maximum value of rms symmetrical current, using subtransient reactance for all machines, and including both synchronous and induction motor contributions.

(2). For fuses rated 15,000 V. or below with interrupting ratings not exceeding 3,000 amperes (except when applied on a generator bus) the resistance introduced by line and transformer is so great that the rms current of a maximum displaced wave in the first half cycle will not exceed 1.2 times the calculated symmetrical current, using subtransient reactance, and application on this basis may be considered safe.

Preliminary Relay Setting

High speed current actuated relays can be given settings based on, first, the highest initial symmetrical current, using subtransient reactance at maximum system conditions, and second, on the lowest initial symmetrical current using subtransient reactance for minimum system conditions. Time over-current relays are usually set by use of similar values of symmetrical current using transient reactance values.

The settings of distance and pilot wire relays are assumed independent of the magnitude of short-circuit current but their accuracy may be impaired if the currents are outside of the range for which they were designed. This range is determined by the maximum initial symmetrical current for maximum system conditions and the minimum initial symmetrical current for minimum system conditions using sub-transient reactance values if the relays are high speed, or similar values of current calculated with transient reactance values if slower relays are used.

For bus differential relays it may be necessary to make an accurate calculation of both a-c and d-c components for assurance that operation will be satisfactory.

Conclusions

The precise determination of short-circuit currents involves a calculation so laborious as to be wholly impractical. Thus some approximation is required and a degree of judgment is required in the application of any method proposed.

The following rules are proposed for the various applications:

A. Circuit-Breaker Interrupting Capacity

Determine highest value of rms symmetrical current for any type of fault using subtransient reactance for synchronous generators and transient reactance for synchronous motors.

1. *General Case.* Multiply by the appropriate factor for 60-cycle systems from those given below:

8-cycle breakers......................1.0
5-cycle breakers......................1.1
3-cycle breakers......................1.2
2-cycle breakers......................1.4

2. *Short-Circuits Fed Predominantly by Large Machines at the Point of Fault.* Increase results of the general case up to 20%.

3. *Air Circuit Breakers Rated 600 Volts or Less.* Apply on basis of average rms current in all three phases, which may be taken as 1.25 times the rms symmetrical current.

B. Mechanical Stresses and Momentary Rating of Circuit Breakers

Determine highest value of rms symmetrical current for any type of fault using subtransient reactance for both synchronous and induction machines.

1. *General Case.* Multiply by 1.6.

2. *At 5,000 Volts and Below Unless Fault Current Is Fed Predominantly by Directly Connected Synchronous Machines or Through Reactors.* Multiply by 1.4.

C. Protector Tubes

1. *Maximum Rating.* Use the highest value of rms symmetrical current determined as in *B* with no multiplying factor.

2. *Minimum Rating.* Use the lowest value of rms symmetrical current determined as in *B* for minimum system conditions, with no multiplying factor.

D. Fuses

Determine highest value of rms symmetrical current as in *B*.

1. *General Case.* Multiply by 1.6.

2. *At 15,000 Volts or Below With Interrupting Ratings Not Exceeding 3,000 Amperes.* Multiply by 1.2.

E. Basis for Preliminary Relay Settings

1. *High Speed Current Actuated*

(*a*). Highest rms symmetrical current based on subtransient reactance at maximum system conditions.

(*b*). Lowest rms symmetrical current based on subtransient reactance for minimum system conditions.

2. *Time Overcurrent.* Make the same calculations as for high speed relays, but use transient reactance.

As compared with the latest decrement curves,[2] this method of calculation of short-circuit currents is somewhat simpler and should reduce considerably the possibilities of misapplication.

This method is in accordance with the present trend toward high speed relaying and eliminates the possibility of exceeding breaker interrupting capacities by modernizing the relay system after installation of the breakers.

It recognizes the acceleration of the decay of the d-c component of short-circuit current caused by the relatively high resistance of circuit elements other than the generator.

Table I. Effect of Location of Fault Upon D-C Time Constant

Location of Fault	Impedance to Point of Fault X	Impedance to Point of Fault R	Total X / Total R	Time Constant In Cycles	Time Constant In Secs
Generator terminals	20	0.25	$\frac{20}{0.25}$	13	0.21
High-voltage side of transformer	28	0.75	$\frac{28}{0.75}$	5.9	0.10
Inclusion of line having 5 per cent reactance	33	2.0	$\frac{33}{2.0}$	2.6	0.044
Inclusion of line having 10 per cent reactance	38	3.2	$\frac{38}{3.2}$	1.9	0.031

All impedance on same base as generator.

In view of these advantages it is believed that this method will prove more satisfactory in practice than the present standard.

References

1. Rating and Selection of Oil Circuit Breakers, E. M. Hewlett, J. W. Mahoney, and C. A. Burnham. AIEE Transactions, volume 37, 1918, pages 123–38.

2. Standard Decrement Curves, W. C. Hahn and C. F. Wagner. AIEE Transactions, volume 51, 1932, pages 353–61.

3. Calculation of Short Circuits on Power Systems, C. F. Wagner and S. H. Wright. Published in pamphlet form as AIEE paper 32M4, and abstracted in Electrical Engineering, volume 51, 1932, number 2, page 131.

4. Decrement Curves for Specific Systems, W. C. Hahn. Published in pamphlet form as AIEE paper 32M5, and abstracted in Electrical Engineering, volume 51, 1932, number 2, page 131.

5. Short-Circuit Calculating Procedure for Low Voltage A-C Systems, A. G. Darling. AIEE Transactions, volume 60, 1941.

6. Protector Tubes for Power Systems, H. A. Peterson, W. J. Rudge, A. C. Monteith, and L. R. Ludwig. AIEE Transactions, volume 59, 1940 (May section), pages 282–91.

7. Symmetrical Components, Chapter V, by C. F. Wagner and R. D. Evans. McGraw-Hill Company, 1933.

Power-Circuit-Breaker Ratings

R. C. VAN SICKLE
MEMBER AIEE

CIRCUIT breaker application is being simplified. A subcommittee of the protective devices committee of the AIEE has studied methods of calculating short circuit currents and has prepared a report which presents a simplified procedure based on standardized contact parting times and typical current decrements.[1] To facilitate the use of this method, circuit breakers should have ratings which conform to the short circuit characteristics assumed in the calculations. At the present time, while the industry is preparing a revised list of short-time current ratings for circuit breakers, an opportunity exists to correlate the short circuit ratings so that a breaker selected for adequate interrupting current by the new method automatically has ratings adequate for the other short circuit currents.

The rating of a power circuit breaker as given by AIEE Standard 19-200 includes the following items:

(*a*). Rated voltage.
(*b*). Rated frequency.
(*c*). Rated continuous current.
(*d*). Rated short-time current.
(*e*). Rated making current.
(*f*). Rated interrupting current.

In addition definitions are given for the rated latching current and two short-time currents (the rated momentary current and the rated five second current).

The first three of these items are independent of each other. Breakers can be designed for any combination of rated voltage, rated frequency, and rated continuous current.

The rated making, momentary, five second, and interrupting currents are interdependent, being values of the maximum short circuit current permissible for the breaker.

The maximum short circuit current is determined by the impedance of the circuit and by the characteristics of the rotating machines supplying power to the short circuit. The initial current is composed of an a-c component determined by the subtransient reactance of the circuit, and a d-c component determined by the point on the wave at which the transient starts and by the circuit inductance and resistance. Both components are a maximum at the beginning and consequently the total rms current also is a maximum, figure 1.

This current during the first cycle is important as it is the maximum current to which the breaker will be subjected and corresponds to the rated momentary current and rated making current. In AIEE standards, "The rated momentary current is the maximum rms total current which the breaker shall be required to carry for any time however small up to one second.—" This current may be initiated either by a short circuiting of the system through some external means or by the breaker closing and completing a short circuit. Consequently, the first cycle current is also the current which the breaker must be capable of closing. By AIEE definition, "The rated making current of an oil circuit breaker is the maximum rms current including the d-c component against which the breaker must be capable of closing, without the welding of or undue damage to the breaker or contacts, with rated control voltage at the closing mechanism." Therefore, the rated momentary current and the rated making current should be at least equal to the maximum current which can be obtained during the first cycle.

Not all breakers are required to close completely and latch when making the rated current. For breakers having relatively low short circuit currents, the electromagnetic and other forces tending to oppose the closing of the circuit breaker may not impose much additional load on the closing mechanism and no difficulty may be encountered in the complete closing and latching of the breaker. Such breakers would have rated latching currents equal to rated making currents.

High interrupting capacity breakers for 15-kv service and below, have to make currents which may impose electromagnetic forces greatly in excess of the other forces opposing the closing, and may require a driving force considerably in excess of that needed for normal service. In this class of breakers, the closing and latching under short circuit conditions is a much more serious problem. The most advantageous position for carrying the current is with the contacts normally closed and the breaker latched, but with high speed tripping of the breaker it may be possible, without completely closing the breaker, to carry the current for the duration of the short circuit. However, the breaker contacts must be closed sufficiently to carry the short circuit current without undue burning or welding until such time as the short circuit is cleared elsewhere or the breaker tripped. In such cases the breaker will perform satisfactorily without latching and a rated latching current equal to the rated making current is not essential. Consequently, the rated latching current has no definite relation to the maximum short circuit current or to the rated interrupting current.

The sustained short circuit current must be carried by a breaker if it is not tripped. From its initial value, the current will decrease with the decreasing d-c and a-c components. The d-c component decreases approximately as a logarithmic function. The amount that the a-c component decreases will depend upon the effect of the short circuit on the generators. This effect is small if the generators do not form the principal limiting impedance and the a-c component may be sustained throughout the duration of the short circuit. Consequently, the maximum current which the breaker will be expected to carry for more than a few cycles while the d-c component is dying out, is the initial value of the a-c component. This value of the current corresponds to the 5 second rating of the breaker. By AIEE definition, "The rated 5 second current is the rms total current including the d-c component which the breaker shall be required to carry for 5 seconds." With increasing speed of breaker tripping this item is losing its significance.

Between the initial and the sustained currents is a current which the breaker must be able to interrupt. It is of great importance as it corresponds to the rated interrupting current which, by AIEE definition, "is the highest rms current at a specified operating voltage which the breaker shall be required to interrupt under the operating duty specified, and with a normal frequency recovery voltage equal to the specified operating voltage. The current shall be the rms value including the d-c component at the instant of contact separation as determined from the envelope of the current wave." The time at which the contacts separate and at which this current is measured depends upon the speed with which the breaker is tripped. It may be in the first cycle in the case of extremely high speed breakers, but is

Paper 41-116, recommended by the AIEE committee on protective devices, and presented at the AIEE summer convention, Toronto, Ontario, Can., June 16–20, 1941. Manuscript submitted April 15, 1941, made available for preprinting May 12, 1941.

R. C. Van Sickle is with Westinghouse Electric and Manufacturing Company, East Pittsburgh, Pa.

1. For all numbered references, see list at end of paper.

generally somewhat later in the short circuit. The interrupting current is between the initial and the sustained values of the current.

The basic rating of a circuit breaker is its interrupting capacity at rated voltage. The interrupting capacity determines the strength of the parts which must carry the short circuit and withstand the forces incident to the interruption of the current. The voltage determines the clearances required for insulation. The normal rated current is a less important factor in determining the size of the breaker, although it does determine to a large extent the cross section of the conducting path, the size of the conductors through the bushings, and the size of the contacts within the breaker. Therefore, the rated interrupting current at rated voltage is the basic rating, and establishes the principal dimensions of a group or class of breakers. Various modifications of this basic design are made to take care of variations in the normal current carrying capacity. For example—a breaker may be developed and tested for an interrupting ability of 500,000 kva at 15 kv and minor modifications will give the various rated normal currents.

Circuit breakers are frequently used at service voltages less than their rated voltage. At these lower voltages, the difficulty of interrupting a given current is less and higher rated interrupting currents can be assigned. Constant kva, or a rated interrupting current varying inversely with service voltage, is customarily assumed. The wider the range of service voltages at which constant kva is maintained, the greater the range of currents which must be interrupted by the breaker. For best designs which have as little compromise as possible, it is desirable to limit the interrupting current, and a limit is established which permits the use of the breaker at full kva down at least to the next lower standard voltage. This maximum permissible current is called the interrupting capacity current limitation and is about 1.5 times the rated interrupting current at rated voltage, but varies, specially for 15-kv breakers which cover a wider voltage range. This rating is one value of the highest short circuit current which the breaker can be required to pass.

The interdependent items of the circuit breaker rating, making current, momentary current, interrupting current, and five second current correspond to currents measured at various points on the short circuit transient current. If definite ratios exist among these values, the ratings of the circuit breaker should correspond to these ratios so that no one of the items becomes the limiting factor and so that if a breaker is selected for adequate interrupting capacity, it will automatically be able to make and to carry the currents associated with that interrupting capacity.

These requirements are related, but in the past variable times allowed for the tripping of the circuit breaker resulted in various durations of the length of the short circuit prior to the parting of the contacts and consequently a variation in the ratio between the initial current and the interrupting current. Consequently, it has not been possible to use definite ratios and any one of the ratings has been able to prevent the application of the breaker on a particular service.

Table 1. Favorable Relations of Interdependent Circuit-Breaker Ratings

Rating Item	Measured After Start of Short Circuit at Time Interval of (Cycles)	Current: Ratio of Rating Item to Interrupting Capacity Current Limitation	Current: Ratio of Rating Item to Rated Interrupting Current (Approximate)*
8 Cycle breakers			
Rated making current	0.5	1.6	2.4
Rated momentary current	0.5	1.6	2.4
Rated interrupting current	4	0.67	1
Interrupting capacity current limitation	4	1	1.5
Rated five second current	60	1	1.5
5 Cycle breakers			
Rated making current	0.5	1.45	2.2
Rated momentary current	0.5	1.45	2.2
Rated interrupting current	3	0.67	1
Interrupting capacity current limitation	3	1	1.5
Rated five second current	60	0.9	1.35
3 Cycle breakers			
Rated making current	0.5	1.33	2.0
Rated momentary current	0.5	1.33	2.0
Rated interrupting current	2	0.67	1
Interrupting capacity current limitation	2	1	1.5
Rated five second current	60	0.83	1.25
2 Cycle breakers			
Rated making current	0.5	1.14	1.7
Rated momentary current	0.5	1.14	1.7
Rated interrupting current	1	0.67	1
Interrupting capacity current limitation	1	1	1.5
Rated five second current	60	0.72	1.08

* The ratio beween the rated interrupting current and the interrupting capacity current imitation is a variable depending on the range of service voltages at which full interrupting kva is available. The table uses the ratio 1.5 which is the most common value, but it must not be assumed that this ratio applies to all breakers. Individual cases have conditions which justify using either arger or smaller ratios.

In the report referred to previously on the new method of calculating the current, the variable of the time of parting contacts has been eliminated by the assumption of definite contact parting times dependent only on breaker speed; after 1, 2, 3, and 4 cycles for 2, 3, 5, and 8-cycle breakers respectively. Likewise, the probable ratio between the initial a-c component and the total rms current during the first cycle and at the end of each of these cycles has been established. This new method assumes that the maximum asymmetry which can occur will make the total rms value of the current, at the time of the maximum peak, 1.6 times the a-c component, and that at the end of the first and succeeding cycles, this multiplying factor becomes 1.4, 1.2, 1.1, and 1.0. Consequently, the ratio of the current during the first cycle to the interrupting current for breakers parting contacts after 1, 2, 3, and 4 cycles are (1.6/1.4=)1.14, 1.33, 1.45, and 1.6, respectively. These factors are, therefore, the ratio of the initial current to the interrupted current of 2, 3, 5, and 8-cycle breakers respectively. They represent the minimum ratios between rated momentary current and rated interrupting current which permit utilization of the full rated interrupting current.

The values assigned to the interdependent items of a circuit breaker rating should be based on the interrupting capacity as this is the most important item. The interrupting capacity current limitation is determined from it by the range of voltages at which the breaker is to be used. This value is one measurement of the heaviest short circuit current which will be passed through the breaker. From it, the rated making, momentary, and five second currents can be obtained by use of the suitable factors. Table I shows the relations between these interdependent items as derived from the data in the report on the calculation of the interrupting current.

When low voltage breakers are used at service voltages, much below rated voltages, the making current may be high and require a very powerful closing mechanism. When used near rated voltage, the breakers may require much less energy for closing the corresponding making current. Such breakers could be adjusted to the requirements of the service by limiting the power input to the closing mechanism to that required for a making current corresponding to the rated interrupting current at service voltage. The saving in energy and wear on the breaker may justify this change which amounts of imposing a special rated making current and a special interrupting capacity current limitation which are determined by the reduced closing ability.

With ratings assigned in accordance with short circuit characteristics, circuit

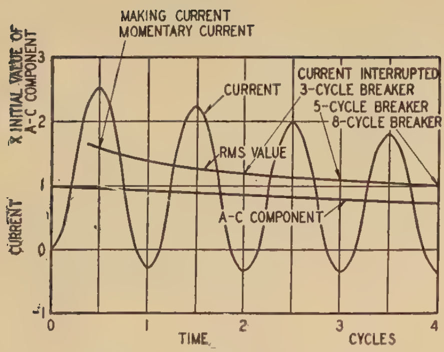

Figure 1. Short-circuit current

breaker application is simplified. Providing the current is calculated by the new method, the breaker can be selected on the basis of its rated interrupting capacity at the system voltage and the ratings of making current, momentary current, and five second current will automatically be adequate.

Since the rated making and momentary currents given in table I correspond to the interrupting capacity current limitations, they usually are higher than are required when a breaker is applied near rated voltage. When interrupting currents, calculated on the assumption of fast tripping, slightly exceed breaker ratings, a more detailed calculation using decrement curves might reveal that the making capacity is adequate and that the interrupting current is down to the breaker rating if a time delay of a few cycles is used.

If the advantages of the new method of short circuit calculation are demonstrated by experience and the method becomes used generally by the industry, another interesting possibility for the further simplification of breaker application should be considered. It gives exactly the same results as those obtained when breakers having ratings assigned in accordance with the assumed current transient are applied by the new method of calculation, but it eliminates from the calculation of the currents the factors dependent on breaker opening time and on special decrements for low voltage circuits.

Breakers could be applied on the basis of the initial a-c component of the short circuit current. The short circuit current calculations could be only the dividing of the voltage by the subtransient reactance to obtain the initial a-c component. The breaker ratings could consist of:

(*a*). Rated voltage.

(*b*). Rated frequency.

(*c*). Rated continuous current.

(*d*). Rated initial a-c component of short circuit current at rated voltage.

(*e*). Rated maximum initial a-c component of short circuit current at reduced voltage.

(*f*). Rated interrupting time.

(*g*). Rated latching current.

Breaker application could consist of selecting a breaker having these items at least as large as the system requirements. Circuit clearing time would depend on the speed of the breaker selected and the current calculation would be the same for 2-, 3-, 5-, and 8-cycle breakers.

Standardization rules could require of the manufacturer that his breakers be capable of closing carrying and interrupting currents having the rated a-c component at rated voltage and the a-c component current limitation at a corresponding lower voltage. Under these suggested rules, breakers would be capable of making a circuit having a total rms current equal to 1.6 times this maximum a-c component. They would be capable of carrying this momentary current. They would be capable of interrupting a total rms current equal to that specified for their contact parting time. They would be capable of carrying the a-c component for five seconds. Demonstrating or proving the performance of the circuit breakers would require these currents to have total rms values bearing the correct relations to the rated a-c component. On classes of breakers where special decrements are justified, for example 5 kv and below, the design of the breaker could be based on the special decrement characteristics and no change would be required in the current calculations. In other words, the requirements and results could be the same whether only the a-c component is specified and the testing requirements define the factors existing between the various currents, or whether as at present the various current values are calculated and checked for each application. Consequently, if the breakers were given rated initial a-c components of short circuit current at rated voltage and rated maximum a-c components at reduced voltage, the making, momentary, interrupting, and five second ratings could be eliminated.

In brief, the requirements would be determined by the initial a-c component of the short circuit current and a breaker selected which would have an adequate rated a-c component and which would be designed for making, carrying, and interrupting the corresponding total rms currents.

Conclusions

The ratings of a circuit breaker can be so correlated that full use can be made of the abilities of the breaker. With the new method of calculating the required interrupting capacity, and with breaker ratings assigned in accordance with the same current decrements, breaker application will be greatly simplified.

If, after trial, the new method of current calculation supplants the present method, a still further simplification in application can be obtained by rating a breaker on the initial value of the a-c component of the short circuit current which it can close, carry, and interrupt.

Reference

1. System Short-Circuit Currents, **W. M. Hanna, H. A. Travers, C. F. Wagner, C. A. Woodrow, and W. F. Skeats.** AIEE Transactions, volume 60, 1941 (September section) pages 877–81.

Lightning to the Empire State Building

K. B. McEACHRON
FELLOW AIEE

Synopsis: Lightning to the Empire State Building in New York City has been under investigation since 1935. Boys camera photographs of 62 strokes have been taken and 99 oscillograms. Twenty of these were taken simultaneously with photographs of the same stroke. Upward step leaders were discovered and continuing strokes were shown to be in the nature of a direct current arc. A brief résumé of the more important results up to the end of the 1937 season is given.

The paper is chiefly concerned with the oscillographic results of the 1938 and 1940 seasons. The low speed oscillograph in the Empire State Building recorded 17 of the 20 strokes to the building while the high speed oscillograph recorded 41 current peaks in 13 strokes.

1. Of 49 strokes recorded oscillographically during the years 1937–40, no stroke has been entirely positive although 41, or 84 per cent, were entirely negative. The first recorded current peak in stroke 13 was positive and had a crest current of 58,000 amperes.
2. Fifty per cent of the 49 strokes had charge of 25 coulombs or more, the maximum charge measured being 164 coulombs. These values are for the total stroke and not for current peaks.
3. Ninety-one per cent of all strokes recorded to the Empire State Building are classified as continuing, i.e. had a low current component.
4. Fifty per cent of the current peaks were found to have a crest current of 7,000 amp or more, while only 25 per cent of the 33 peaks measured in 11 strokes had a duration exceeding 40 microseconds.
5. The plotted data show that 50 per cent of the current peaks had a charge of 0.13 coulomb or more to half current value, although 5 per cent showed more than 1.5 coulombs.
6. A time of at least 1 microsecond is required to reach crest in 50 per cent of the current peaks, while 65 per cent reach the first crest in a time not greater than 1.5 microseconds—the time to crest of the present standard.
7. The results obtained show that rates of rise of the order of 10 to 20 kiloamperes per microsecond will be encountered quite frequently, and 30 to 40 kiloamperes per microsecond occasionally.
8. Errors as great as ±50 per cent may occur in connection with the highest rate of rise measurements; errors in connection with some of the other measurements may be as great as ±25 per cent, although most of the results will be more accurate than indicated by these figures.
9. It is pointed out that direct stroke data may be applied to transmission and distribution circuits if proper allowances are made for division of currents in the various paths including the effect of grounded neutral transformers. The current to be handled by lightning arresters will in general be much smaller than those measured in the direct stroke.

IN February 1939, the author published in the *Journal* of the Franklin Institute a paper[1] entitled "Lightning to the Empire State Building," and in May 1940 with K. G. Patrick, a book[2] titled "Playing With Lightning." These describe the Empire State investigation in some detail, while the instruments used have been described by Hagenguth,[3] Kettler,[4] and Flowers.[5] Therefore, only a brief mention will be made of the apparatus used, and a summary given of the important results obtained.

Equipment

At the Empire State Building are located two oscillographs—one arranged to record continuing currents up to one second duration, and the other to record the wave shape of individual current peaks. These have been called the low and high speed oscillographs respectively. At present both are of the hot cathode-ray type, although for several years the low speed oscillograph was of the electromagnetic type using a crater lamp for illumination. A schematic diagram of the operation of the high speed oscillograph is shown in figure 1. This equipment successfully[6] recorded in 1938 a multiple stroke consisting of (12) successive current peaks in 0.28 sec. Both of the oscillographs are connected to a non-linear shunt composed of thyrite and a linear shunt in parallel. With these shunts the low speed oscillograph records over a current range of 50 amps. to 24,000 amps., while the high speed range is 1,000 amps. to 200,000 amps.

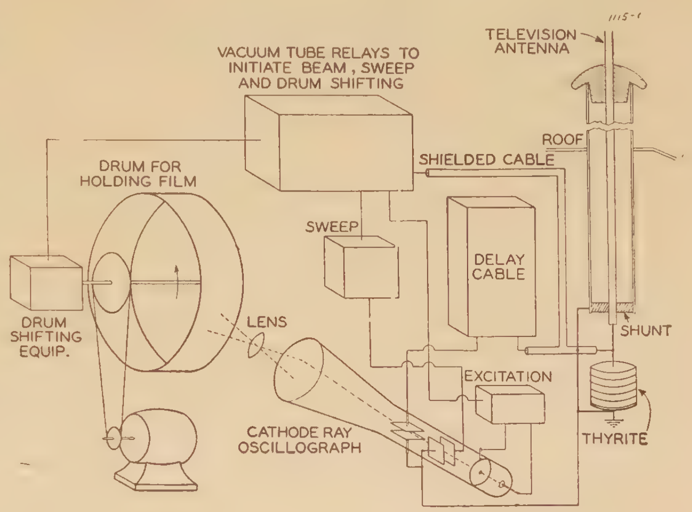

Figure 1. Schematic diagram of high-speed cathode-ray oscillograph equipment used for lightning investigation in the Empire State Building, New York City

Camera equipment is located at 500 Fifth Ave. a distance of 2,550 ft. to the top of the Empire State Building. Slow speed (1/2 rps) and (2 rps) Boys cameras are installed and also a high speed Boys camera normally having a film surface velocity of 124 ft. per sec. In addition, a moving film camera called a "multiple aperture camera" is used having four matched lenses so arranged that four images appear on the same moving photographic film along a horizontal axis. The lenses are provided with suitable filters and stop openings, so that a range of about one million to one may be obtained in exposure.

In addition to this equipment, another camera referred to as the "oblique camera" was installed on a building at the corner of 34th St. and 8th Ave. The purpose of this camera is to determine the shape of the stroke in a plane at right angles to that of the cameras at 500 Fifth Ave. so that a more accurate determination of the length of the stroke path might be made. This camera, controlled over a telephone circuit by the operator at 500 Fifth Ave., is not a Boys camera; its only purpose being to get the stroke shape, and no attempt is made to record detailed time effects.

A densitometer has been provided in the laboratory at Pittsfield for the study of changes in density found on the photographic records. All of the films used since the study began in 1935 have been provided with a sensitometer strip for calibration of the film against a known light source.

Means were set up in 1940 for the determination of visibility between 500 Fifth Ave. and the Empire State Building. This instrument was provided to make possible a fair determination of current from the Boys camera photographs, and studies are in progress to determine the change in current as one progresses up the

Paper 41-115, recommended by the AIEE committee on protective devices, and presented at the AIEE summer convention, Toronto, Ontario, Can., June 16–20, 1941. Manuscript submitted April 11, 1941; made available for preprinting May 9, 1941.

K. B. McEachron is research engineer, high voltage practice, General Electric Company, Pittsfield, Mass.

The author wishes to express his appreciation to the high voltage engineering laboratory staff at Pittsfield, particularly to J. H. Hagenguth, J. W. Flowers, John Russ, and Paul Edwards in connection with designing and operating the equipment, and to Harry Mason for assistance in the preparation of the material used.

1. For all numbered references, see list at end of paper.

stroke—thus obtaining some data on the space charge around the stroke channel.

Brief Résumé of Results Previously Reported[1,2,6]

Some of the more important results obtained in this study, particularly with the camera equipment, are listed briefly below. Only oscillographic data are discussed in the present paper.

1. Discovery of the initial upward step leader mechanism from the Empire State Building.

nism, explained by lack of mobility of charges in clouds compared to the earth, which does produce a return stroke with downward initial leaders.

6. Strokes to ground, whether started by upward or downward initial leader, seem to have same mechanism for successive current peaks without reference to how initiated.
7. The configuration of electrodes probably determines the direction of propagation of initial leader.
8. Thunderless lightning results from relatively slow rates of current rise of upward leader strokes, without successive current peaks.
9. Measurement of leader and stroke propagation velocities and approximate de-

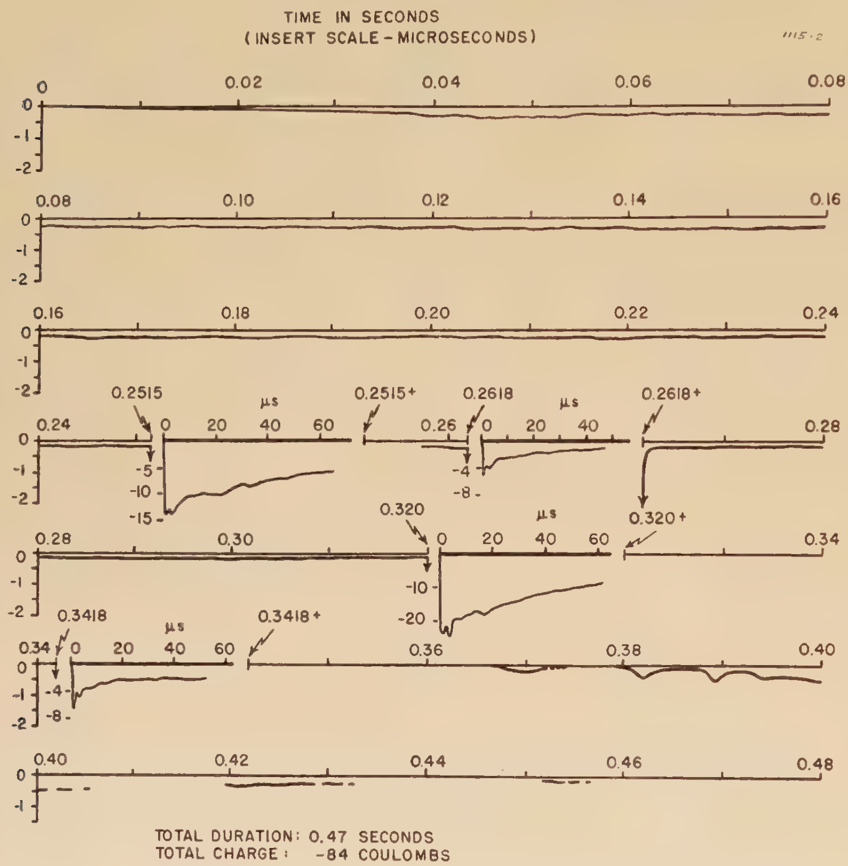

Figure 2. Composite replotted from low-speed and high-speed oscillograms showing our current peaks of stroke 3 to the Empire State Building

June 26, 1940 at 1:29.5 p.m.

2. Proof, both photographic and oscillographic of the existence of continuing current (substantially a direct current arc between line and ground).
3. Direct measure of charge in coulombs in lightning strokes, establishing a curve of frequency of occurrence for a given magnitude.
4. Oscillographic records show that out of 27 records all began with negative polarity, and 3 reversed polarity at end of the record, indicating that the base of the cloud is negative, and a positive region was reached in 3 cases only after a time interval.
5. Lack of so-called return stroke from clouds with upward initial leader mecha-

termination of current required by upward step leader.
10. Identification of the upward streamer from earth when the downward initial leader approaches the earth.
11. Determination of wave shape of direct strokes—front, crest, and duration of current peaks of strokes having single peaks and as many as 12 successive current peaks (total of 4 strokes recorded).
12. Strokes to the ordinary countryside, in those cases where the photography was such that good measurements could be made, show the same general photographic characteristics as do those to the Empire State Building, once the stroke is established.

Additional Results

Considerable additional data obtained in 1940 are now available with respect to the wave shape of current peaks. Although many correlating oscillograms and photographs were obtained in previous years, during 1940 most of the strokes were not recorded photographically because they did not occur at night. It is believed, however, based on past experience that most of the strokes recorded were initiated by upward step leaders.

During the 1940 season the low speed oscillograph recorded 17 of the 20 strokes to the building, while the high speed oscillograph recorded 41 current peaks in 13 strokes. The correlation between the low and high speed oscillograms was excellent, there being a detailed record of nearly every current peak of any importance appearing on the low speed record. Such a record for stroke 3 (1940) is shown in figure 2, where the high speed and low speed records have been reproduced together.

Polarity

Of the 49 strokes recorded oscillographically during the years 1937–40, no stroke has been entirely positive although 41, or 84 per cent, were entirely negative. Of the eight strokes having some positive, one is known to have begun with a small positive current (about 200 amps), while four strokes began with negative current. With two other strokes, the current recorded initially appeared to be negative, but had too small a magnitude to be certain. As for the remaining stroke, the first current recorded was positive, although the oscillograph had initiated more than 0.025 sec. before indicating the presence of a current, whose magnitude and polarity is, however, unknown. This stroke (No. 13, 1940) is of considerable interest, as the first recorded current was a positive peak having a crest of 58,000 amps., which is nearly double the highest heretofore recorded oscillographically[6] to the building. This was followed by three negative current peaks, as shown in figure 3. The current peaks appear to be connected together by continuing current, mostly negative.

Stroke Charge

The stroke charge in the entire stroke including current peaks for 49 strokes is given in figure 4, and indicates that at least 50 per cent of strokes have a charge of 25 coulombs or more, although the average charge is 37 coulombs. The maximum measured in New York is 164 coulombs obtained in 1937, while in 1940 the maximum was 150. Three per cent of the total charge measured to date was positive.

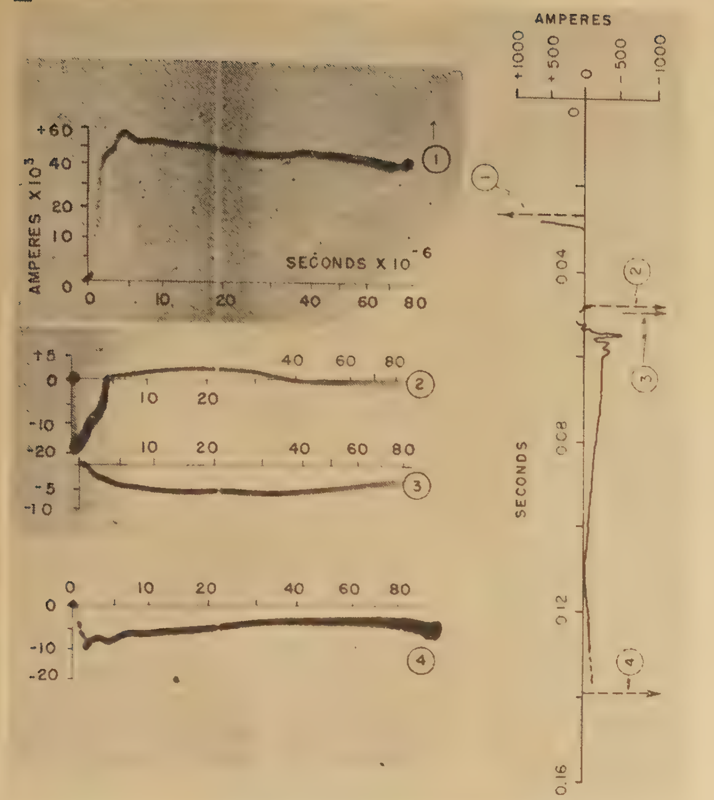

Figure 3. Low-speed and high-speed oscillograms showing four current peaks of stroke 13 to the Empire State Building

June 30, 1940 at 4:34 p.m. Time between peaks 0.021, 0.00092, and 0.087 second

Continuing Strokes

Of the 49 strokes recorded oscillographically, only seven did not show any signs of continuing current, and these due to lack of sensitivity might have recorded current under more favorable recording conditions. Of these oscillographic records 20 correlating Boys camera records were obtained—all but one showing the presence of continuing current. In addition to these photographic records 42 others were obtained—41 of which show the presence of continuing current. Thus 91 per cent of all strokes recorded in New York to the Empire State Building are classified as continuing.

It is of interest to record here that the results obtained thus far with the multiple aperture camera indicate that once a path is found between cloud and ground the current does not cease until the stroke is completed. The current merely increases and decreases in magnitude until the total stroke is completed.

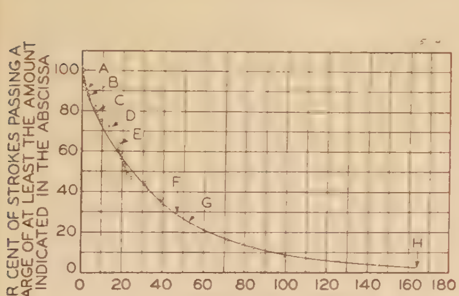

Figure 4. Frequency of occurrence of stroke charge based largely on low-speed oscillographic data

Total charge of lightning strokes recorded by low-speed oscillographs

Empire State Building, New York City 1937, 1938, 1939, 1940

Based on 49 strokes

Coulombs in two-polarity strokes

A	B	C	D	E	F	G	H
−1.4	2.0	5.4	12	8.2	30	36	160
+1.2	1.1	1.8	2.3	9.9	17	17	2.6

Other strokes negative charge only

Stroke Duration

The maximum stroke duration of 1.5 sec. reported in 1937 for a stroke to the building has not as yet been exceeded. Figure 5 shows that half of the 49 strokes recorded have a duration of at least 0.29 sec.

Current Peaks—Crest Current

The data given in figure 6 are plotted in terms of negative current peaks, since all the peaks recorded by the high speed oscillograph were negative but one, which is indicated. When comparing these data with those of other investigators, it is to be remembered that the magnetic link used in measuring currents through transmission towers[7] and distribution lightning arresters[8] indicate only the highest current peak occurring during the time the link is in service. In figure 6 each current peak in a stroke is plotted independently. It is not strange that Lewis and Foust give current values considerably higher than indicated in figure 6. The data given by McEachron and McMorris for distribution circuits are much lower in current magnitude, since the current was measured only at arrester locations, and in most cases is a measure of the traveling wave from some remote point. In many cases, too, the measured surge was the result of the release of a bound charge. The records do indicate arrester duty, but seldom the current magnitude in the stroke itself.

Duration

In terms of time to half value only 25 per cent of the 33 peaks measured in 11 strokes have a duration exceeding 40 microseconds, which is the present standard duration used in impulse testing in the United States. The maximum duration (figure 7) was 115 microseconds.

Charge

Since the tail of the current peak merges into the continuing current it is difficult to determine what is the current peak and

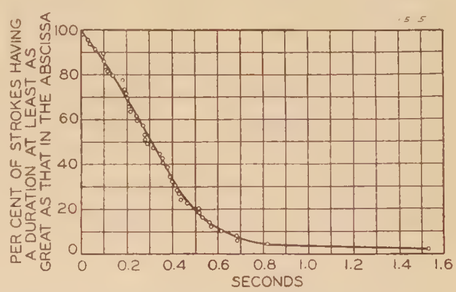

Figure 5. Stroke duration as a function of the frequency of occurrence

Values obtained from oscillographic records

Duration of multiple and continuing lightning strokes recorded by low-speed oscillographs

Empire State Building, New York City 1937, 1938, 1939, 1940

Based on 49 strokes

what is continuing current. Therefore, when determining the charge in each current peak the area under the current-time oscillogram has been limited to the point where the current has decayed to half value. Figure 8 shows that 50 per cent of the current peaks measured have a charge of 0.13 coulomb or more, although only 5 per cent showed more than 1.5 coulombs.

Since the cloud is not an infinite bus but has limited energy, one might expect that as the current increased the duration might decrease, but figure 9 indicates that

the charge is increasing more rapidly than the current, which means of course that the duration is also increasing with the current. If the rate of propagation of the so-called return stroke is independent of the current in the stroke, and if the duration of the tail of the current peak is the time taken to reach the cloud, it would appear then that in general the longer stroke path will contain the greater current. There is yet no real support for either of these assumptions, nor is there any direct measure of the length of the stroke path compared to its current. Furthermore, large and small current peaks are recorded in the same stroke, apparently indicating the presence of other factors beside the length of stroke which may influence the amount of current. While ground resistance may have considerable influence on the amount of current, yet it must be remembered that all of the current peaks recorded in figures 6 or 9, occurred to a structure whose ground

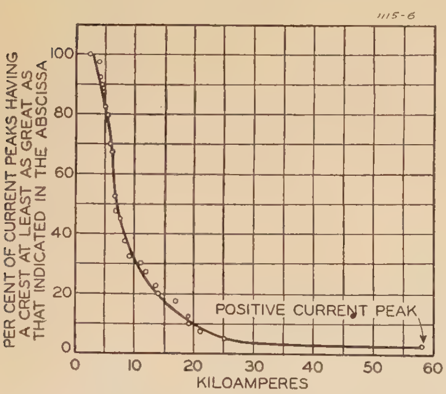

Figure 6. Frequency of occurrence of current peaks of various magnitudes determined oscillographically

Amplitude of current peaks recorded by high-speed cathode-ray oscillograph

Empire State Building, New York City

Based on 13 strokes

resistance was presumably quite constant —certainly it did not change during a stroke.

Wave Front

The time to the first crest is given in figure 10. These results show that a time of at least one microsecond is required to reach crest in 50 per cent of the peaks. Sixty-five per cent of the current peaks reach the first crest in a time of not more than 1.5 microseconds, the present standard time. It was of interest to plot the time to first crest against the crest value of current, but no trend could be found, except that higher currents usually required longer times to reach crest, but longer times did not necessarily mean a higher current peak.

Rate of Rise

The effective rate of rise in kiloamperes per microsecond, measured through the 10 and 90 per cent points is shown in figure 11. In considering these results it is well to bear in mind the difficulties encoun-

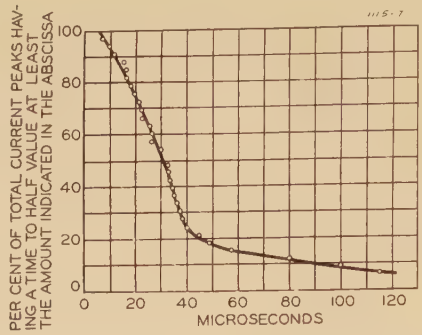

Figure 7. Duration of current peaks measured to half value as a function of frequency of occurrence

Based on 33 oscillographic records

Duration of current peaks recorded by high-speed cathode-ray oscillograph

Empire State Building, New York City 1938 and 1939

Based on 11 strokes

tered in recording and measuring accurately when the front becomes almost perpendicular to the time axis. It is clear that as the rate of rise increases the possibility of error increases, and therefore the highest values in figure 11 are to be taken with caution, since an error of the order of ±50 per cent may be present.

These results do indicate that rates of current rise of the order of 10 to 20 kiloamperes per microsecond will be encountered quite frequently in the stroke, and values as high as 30 to 40 kiloamperes occasionally. These values are to be compared with those of Norinder,[9] which are of the same general order of magnitude although obtained in Sweden by quite a different method.

Accuracy of Measurement

Measurement of the crest of the average current peak (9,000 amp.) is subject to an error of ±20 per cent. The major factors contributing to this error are difficulty in establishing a zero line, uncertainties in the measurement of deflections and in the value used for the oscillograph calibration including the lightning shunt. For smaller deflections, the error tends to be greater and may be less for the larger deflections.

Rate of rise measurements are subject

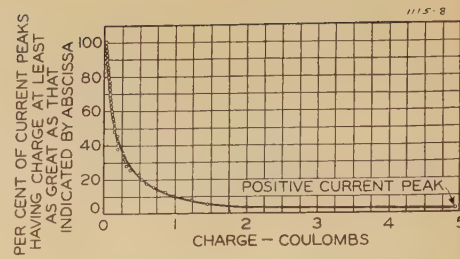

Figure 8. Charge of current peaks as a function of frequency of occurrence

Coulomb values based on time to half value of crest current

Charge in current peaks recorded by high-speed cathode-ray oscillograph

Charge passed until current decays to one-half of crest

Empire State Building, New York City 1938 and 1940

Based on 13 strokes

to error in measurement of both current and time. For a crest current of 9,000 amps. and a time of one microsecond, error in the rate of rise measurement may be of the order of ±25 per cent, while for steep fronts (0.1 ms) the error may be as great as ±50 per cent.

Measurements of charge are also subject to a possible error of ±25 per cent.

The low speed oscillograms are also subject to a possible ±20 per cent error in current magnitude; while currents smaller than 50 amps. are detectable, the accuracy is very poor, since the trace is often about 150 amps. in width.

It is believed, however, with the exception of the measurements depending upon fractional parts of microseconds, that the average accuracy is good for this type of measurement.

Discussion

Most of the oscillograms of current peaks show evidence of some oscillation near the crest (figures 2 and 3), having a magnitude of from 5 to 20 per cent and a period of about 2.5 microseconds. Since the building is 1,275 ft. high, perhaps this effect is the result of reflection phenomena at or near the base of the building. Of course the size of the building increases near the earth, which confuses the picture somewhat.

In applying these results to the case of lightning striking a transmission or distribution circuit, several assumptions must be made. It seems reasonable to assume that the sum of the currents flowing away from the point of contact with the lightning stroke will equal the current of the stroke, in view of what is now known of the mechanism of the stroke. Thus, if a line is struck at any point except close to

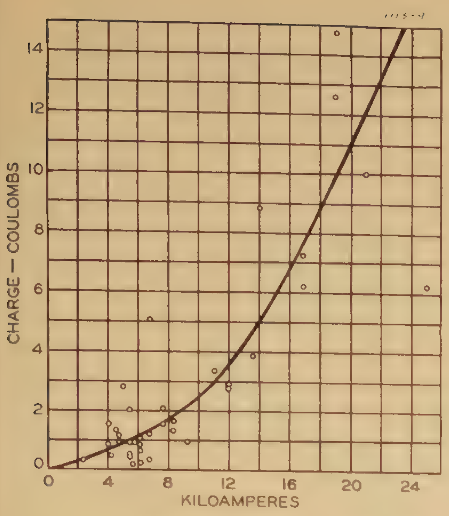

Figure 9. Effect of variation in crest current on the charge contained in each current peak

Relation between charge and crest current of negative current peaks

Charge passed until current decays to one-half of crest

Empire State Building, New York City 1938 and 1940

Based on 13 strokes

Charge of only positive peak recorded was 4.9 coulombs with crest of 58,000 amperes

its end, the current in the stroke will divide equally and will have half of the magnitude of the original measured stroke current. The time to crest and half value will be the same as measured in the stroke itself, thus the rate of rise in terms of amperes per microsecond would be reduced to half that found in this investigation of strokes to a well grounded steel structure.

Current waves traveling away from the point struck are associated with a traveling wave of potential equal to the surge impedance multiplied by the current. Thus stroke 13, figure 3, having a crest current of 58,000 amps., the highest yet measured oscillographically, would have a traveling wave current of 29,000 amps. This corresponds to a traveling wave potential of 14,500,000 volts (using a surge impedance of 500 Ω) which would flashover any insulation now in use, either wood or porcelain. If, however, the stroke made contact with an overhead ground wire at a tower having a ground resistance of 10 ohms, the potential at the tower top would be only 580,000 volts, neglecting the current flowing away from the stricken point which would be only a little over 2,000 amps. until reflections from adjacent towers returned to increase the current.

Thus the data obtained may be applied to transmission line conditions with reasonable accuracy. If the stroke is considered to have struck a considerable distance

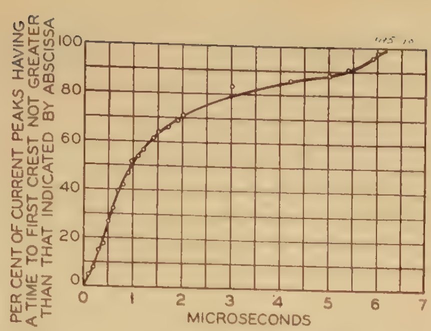

Figure 10. Time to first crest of current peaks as a function of frequency of occurrence

Recorded by high-speed cathode-ray oscillograph

Empire State Building, New York City 1938 and 1940

Based on 13 strokes

away from the ends of the line, then the traveling waves will contain a current half that shown in figure 6 and also a coulomb value of half that given in figure 8. If the stroke is at or very near the end of the line (within a few hundred feet) the traveling wave currents and corresponding voltages will be as originally given.

The wave shapes to reach apparatus will depend upon the point struck with reference to the apparatus, the insulation levels, surge impedance, coupling, and other factors. If overhead ground wires are used and the stroke does not initially make contact with the line conductors, the disturbance will be essentially local, if tower footing resistance is low enough and the line insulation high enough.

The total stroke consists not only of current peaks but also of long time low values of continuing current.

In the case of the transmission line, if the ground wire is struck these continuing currents find their way directly to ground. If the current peak was not of sufficient magnitude to cause flashover, the continuing current will not be of any importance, except for some burning of the ground wire which may result since this current is of the nature of a direct current arc.

If a continuing stroke causes an insulator flashover, the presence of the continuing current following arcover may interfere with the operation of the automatic reclosing equipment, if the latter is sufficiently rapid. Such continuing current in the conductors due to a stroke will be carried to ground through neutrals of transformers if grounded, while if the system neutral is isolated lightning arresters may be forced to carry such currents, which might possibly result in damage to the arrester, although in general the failures of arresters have been very small, indicating that currents of this character do not occur very frequently.

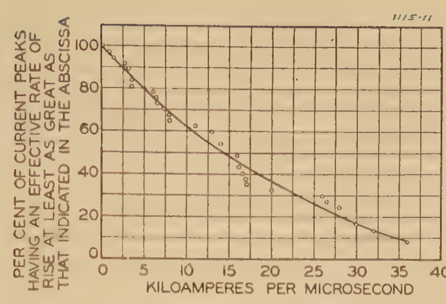

Figure 11. Effective rate of rise* of current peaks of lightning strokes as a function of frequency of occurrence

Recorded by high-speed cathode-ray oscillograph

* Slope of line through points on wave front at 10 per cent and 90 per cent of first crest

Empire State Building, New York City 1938 and 1940

Based on 11 strokes

In the case of distribution circuits, often several paths to ground exist over guy wires, through lightning arresters, and in the case of grounded neutrals continuing currents will find their way through many multiple paths to ground without undue duty on the lightning arresters. No doubt the continuing type of discharge is responsible for some of the fuses blown during lightning storms.

When using direct stroke data, such as given in this paper, to determine what may happen on either distribution or transmission circuits, proper consideration should be given to circuit conditions. Seldom, if ever, can direct stroke values be used directly.

It is also important to point out that there is good reason to believe that ground resistance will have an appreciable effect[1] on the current in a lightning stroke—the lower the resistance the higher the current, other factors being equal. The effect of ground resistance on wave fronts of direct strokes is not known, but one would expect that higher ground resistance would probably effect some increase in the duration of the stroke, although the effect of the cloud distribution of charge is probably controlling.[1]

Conclusion

For the first time, sufficient data relative to wave shapes of direct strokes are available to make possible the drawing of experience curves with respect to front, crest, and tail of current peaks. Similar data with reference to the total stroke are also available.

References

1. Lightning to the Empire State Building, K. B. McEachron. *Journal* of Franklin Institute, volume 227, 1939, pages 149–217.

The Basis for the Nondestructive Testing of Insulation

R. F. FIELD
MEMBER AIEE

Introduction

DIELECTRIC strength is the property of insulation that is most important to the operating power companies. The factor of safety determined by the ratio of breakdown voltage to operating voltage must be maintained. Yet this breakdown voltage cannot be measured on a finished piece of insulation. Actual breakdown, except in the case of liquids, destroys the insulation. Overvoltage less than that required for breakdown has been found to injure the insulation and leave it with a reduced factor of safety. Non-destructive testing at overvoltage is feasible only if some electrical quantity, such as current, is measured and used as a sensitive indicator of incipient damage. The use of d-c overvoltage from a tube rectifier for cable testing is an example.

Non-destructive testing of insulation, as currently practiced, is the measurement of certain electrical characteristics of the insulation, such as capacitance, dissipation factor,* and leakage resistance, at a voltage not greater than the operating voltage. Ordinarily a relatively low voltage at the operating frequency is used, 100 volts to 10 kilovolts. Of these three characteristics, dissipation factor has come to be considered the most reliable indicator of the condition of insulation. The standard practice is to measure the dissipation factor of insulation at the operating frequency at stated intervals of time after installation. A progressive increase of dissipation factor with time is believed to indicate deterioration of the insulation. Certain limiting values are set depending on the type of insulation. When these limits are exceeded, the insulation is removed from service. Frequently, greater weight is placed upon continual change in the value of dissipation factor than upon its absolute magnitude.

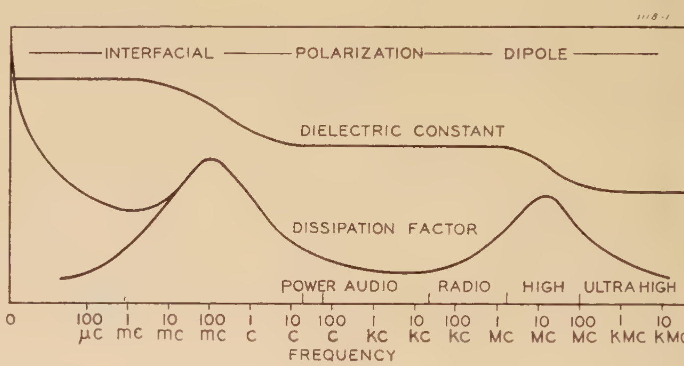

Figure 1. Schematic diagram showing changes in dielectric constant and dissipation factor with frequency (after Murphy and Morgan)

The upper branch of the dissipation factor curve shows the effect of d-c conductivity

Heretofore the assumption has been made that, when insulation deteriorates, a correlation exists between the decrease in dielectric strength and changes in dissipation factor, because the use of non-destructive testing has resulted in a decrease of insulation failures. It is, however, a fact that the greatest success has been attained with the simpler types of bushings and insulators, only fair success with transformers, and little success with generators and cables. This is probably true because the changes in dielectric strength on the one hand and in the three measurable electrical quantities on the other are all effects for which deterioration is the cause. It is also unreasonable to expect that sufficient information will be contained in measurments taken at a single frequency to allow the different kinds of deterioration to be recognized. It will be shown that only by taking measurements over a wide frequency range can all the information obtainable from the electrical characteristics be secured.

These considerations make it desirable to determine whether or not a satisfactory correlation should exist between dielectric strength and one or all of the electrical quantities which can be measured.

Deterioration

The many causes of deterioration occuring in insulation may be grouped under four heads, chemical, mechanical, and electrical changes and the introduction of foreign material. The processing of many commercial dielectrics is incomplete. Either polymerization is not complete or the solvents are not completely volatilized. During the subsequent changes, voids may form throughout the body of the material. Voids are also formed in laminated materials under the vibrational and mechanical forces to which insulation is subjected in rotating machines and in transformers.

Foreign materials, mainly dirt and moisture, may adhere to the surface of insulation or may penetrate throughout the volume, if the body is porous. This is not usually an irreversible change. Cleaning and heating will usually restore the original properties, but, as long as the foreign material is present, dielectric strength may be impaired.

The existence of voids and the presence of foreign material offer the possibility of ionization, even at operating voltage. The surface of the voids will eventually carbonize and add a semi-conducting path. On the outer surface of an insulator this produces tracking. Permanent damage is done in either case.

Paper 41-118, recommended by the AIEE committee on electrical machinery, and presented at the AIEE summer convention, Toronto, Ontario, Can., June 16–20, 1941. Manuscript submitted December 5, 1940; made available for preprinting May 12, 1941.

R. F. Field is an engineer with the General Radio Company, Cambridge, Mass.

1. For all numbered references, see list at end of paper.

* Dissipation factor is the cotangent of the phase angle, while power factor is the cosine.

2. Playing With Lightning, K. B. McEachron and K. G. Patrick, 1940.

3. Lightning Recording Instruments, J. H. Hagenguth. *General Electric Review*, volume 43, 1940, numbers 5 and 6, pages 195–201 and 248–55.

4. Cameras Designed for Lightning Studies, C. J. Kettler. *Phototechnique*, May 1940.

5. The Direct Measurement of Lightning Current, J. W. Flowers.

6. Wave Shapes of Successive Lightning Current Peaks, K. B. McEachron. *Electrical World*, volume 113, 1940, number 6, page 428.

7. Lightning Investigation on Transmission Lines—VII, W. W. Lewis and C. M. Foust. AIEE Transactions, volume 59, 1940 (April section), pages 227–32.

8. Discharge Currents in Distribution Arresters—II, K. B. McEachron and W. A. McMorris. AIEE Transactions, volume 57, 1938 (June section), pages 307–12.

9. Lightning Currents and Their Variations, H. Norinder. *Journal* of Franklin Institute, volume 220, 1935, number 1, pages 69–92.

Of these various kinds of deterioration the formation of voids and the absorption of moisture are most common.

Mechanism of Breakdown

Breakdown in solids has been studied extensively by von Hippel[1] and others. The application of a voltage produces a motion of free electrons and free ions toward the electrodes. If sufficiently long free paths exist, enough velocity is attained by these carriers of electricity to produce other ions by collision. As long as the motion of the carriers is limited, as by cleavage planes in crystals and by interfaces in mixtures, the insulation is stable. However, when the ionization becomes sufficiently intense, enough carriers are formed to blast an irregular path between the electrodes. This is breakdown.

Whatever increases the supply of free electrons and ions or lengthens their mean free paths lowers the breakdown voltage. This suggests that there may be a good correlation between dielectric strength and d-c conductivity.

Polarization

The values of dielectric constant and dissipation factor obtaining in insulation at any one frequency, or over a range of frequencies, are determined by the existing polarization. A value of dielectric constant greater than unity indicates polarization and an extra contribution to capacitance from polar groups. At optical frequencies a value of the refractive index greater than unity shows that some polarization exists. Any value of dielectric constant greater than the square of the refractive index indicates further polarization. A plot of dielectric constant against frequency has the general shape indicated in figure 1, which is after Murphy and Morgan.[2] The greatest value of dielectric constant occurs at zero frequency.

Two general types of polarization occur over the audio- and radio-frequency range, dipole and interfacial. The former was suggested by Debye and the latter by Maxwell, later amplified by Wagner. Dipole polarization is produced by polar molecules, in which the electrical centers of the positive and negative charges do not coincide. In an alternating electric field, such dipoles attempt to follow the direction of the field. At sufficiently low frequencies there is time enough during each half cycle for nearly all of the dipoles to place themselves in line with the field and that type of polarization is complete. The time required to carry the polarization to $1-1/e$ or 0.632 of completion is called the relaxation time. The corresponding frequency for which the polarization is complete usually appears in the megacycle range for the simpler polar molecules. For the more complex chain molecules, where dipoles occurring along the chain may produce a torsional vibration, this frequency may be found in the audio range.

The rotational motion of the dipoles is opposed by their own heat motion and the motion of the other molecules, with the result that a definite amount of energy is lost at each cycle. The power loss at any frequency is the product of the energy loss per cycle and the frequency. It decreases to zero at both zero and infinite frequencies and hence produces a maximum in dissipation factor at some intermediate frequency.

The d-c conductivity also contributes to the dissipation factor at very low frequencies and causes the numerical value of dissipation factor to become infinite rather than zero at zero frequency. This effect of d-c conductivity at very low frequencies is shown in figure 1, by the upper branch of the dissipation factor curve. For all ordinary dielectrics this contribution to dissipation factor is negligible at audio frequencies.

Interfacial polarization occurs at the interfaces of dissimilar dielectrics. These interfaces can occur as a few large surfaces between two materials or as innumerable small surfaces produced by finely divided particles. The free electrons and ions move throughout the volume of each dielectric and heap up at the interfaces. The charge accumulated at the interfaces during each half cycle contributes to the polarization in exactly the same way as does the lining up of the dipoles in dipole polarization. The resultant changes with frequency in dielectric constant and dissipation factor follow identical laws. In fact, it is not possible to distinguish the two types of polarization from the shapes of their frequency curves.

A condition necessary for the existence of interfacial polarization is an inequality in the product of dielectric constant and specific resistivity for the two dielectrics. This dependence of interfacial polarization on resistivity, and hence on free electrons and ions, suggests that there may be a good correlation between dielectric strength and the dissipation factor resulting from interfacial polarization.

Single Relaxation Time

For a polarization having a single relaxation time the changes of the various electrical characteristics with frequency follow definite laws. The polarization is completely defined[3] by the high-frequency dielectric constant K_∞, the low-frequency dielectric constant K_0 resulting from complete polarization and the relaxation time T. The maximum value of loss factor* is

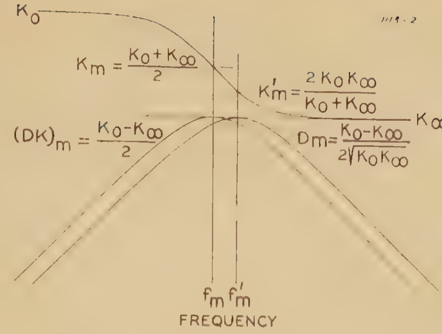

Figure 2. Change of dielectric constant, loss factor, and dissipation factor with frequency for a single-relaxation-time polarization

$$(DK)_m = \frac{K_0 - K_\infty}{2} \tag{1}$$

and occurs at a frequency

$$f_m = \frac{1}{2\pi T} \tag{2}$$

which may be called the relaxation frequency. The curve of loss factor is symmetrical about the relaxation frequency and is expressed by

$$\frac{(DK)}{(DK)_m} = 2\frac{f/f_m}{1+f^2/f_m^2} \tag{3}$$

where both loss factor and frequency have been normalized with respect to their values at the relaxation frequency.

The curve of dielectric constant also has a kind of symmetry about the relaxation frequency and is expressed by

$$K = K_\infty + \frac{K_0 - K_\infty}{1+f^2/f_m^2} \tag{4}$$

The value of dielectric constant at the relaxation frequency is the average value.

$$K_m = \frac{K_0 + K_\infty}{2} \tag{5}$$

The shapes of these curves are shown in figure 2, where frequency and loss factor are plotted logarithmically while dielectric constant is plotted arithmetically. The curve of dissipation factor is also plotted logarithmically in figure 2. In its normalized form the expression for dissipation factor is identical with equation 3 for loss factor, with a maximum value

$$D_m' = \frac{K_0 - K_\infty}{2\sqrt{K_0 K_\infty}} \tag{6}$$

*Loss factor is the product of dissipation factor and dielectric constant.

which occurs at a higher frequency

$$f_m' = f_m\sqrt{K_0/K_\infty} \tag{7}$$

Whenever it is inconvenient to obtain values of dielectric constant because of the irregular shape of the dielectric, the capacitance values may be used instead in these equations. Loss factor will have a different numerical value, while dissipation factor will remain unchanged.

Multiple Relaxation Times

The curves obtained for the various dielectrics and for commercial insulation have very much broader maxima than the curve for a single relaxation time shown in figure 2. In addition, the value of maximum loss factor is much less than that calculated from equation 1. The explanation given by Wagner and amplified by Yager[4] is that there exists a group of relaxation times distributed according to some probability law.

The curves shown in figure 3 are given by Yager[5] for a paper base phenolic, curves 15*D* for a dry specimen and curves 15*H* for the same specimen conditioned at 60% relative humidity. The maximum in loss factor at a frequency of ten megacycles is produced by dipole polarization of the cellulose filler and the curve is much broader than that shown in figure 2. The slight rise appearing at audio frequencies in curve 15*D* and caused by interfacial polarization is greatly increased by the moisture added under the conditions of curve 15*H*. The relaxation frequency of this polarization is well below the audio-frequency range. This curve is so broad that loss factor is increased even at ten megacycles.

Circle Diagrams

Cole and Cole[6] have recently offered a simpler and more fruitful explanation for the broad maxima. The properties of a polarization having a single relaxation time are such that a plot of loss factor and dielectric constant, as shown in figure 4*a*, is a semicircle with its center on the dielectric constant axis and with intercepts on this axis equal to the zero and infinite frequency dielectric constants. It becomes apparent immediately that the maximum loss factor must be one-half the change in dielectric constant as stated in equation 1.

The important discovery of the Coles is that when loss factor is plotted against dielectric constant for various insulating materials a circular arc results whose center is depressed below the dielectric constant axis by an angle ϕ as shown in figure 4*b*. The ratio α of this angle to a right angle is taken as the fourth parameter in defining the polarization. It can be considered as a storage coefficient, which determines the ratio of the stored energy to the dissipated energy for whatever mechanism is assumed for the polarization. The data of figure 3 for a paper base phenolic are thus plotted in figure 5. The circular arc is well defined for the dry material and the divergence of the points at the low frequency end shows the existence of a second polarization. For the wet material the effect of the interfacial polarization is very marked but the data were not carried to low enough frequencies to define its circle. Values of the four parameters for the high frequency polarization are given in table I.

Table I. Paper-Base Phenolic

	K_∞	K_0-K_∞	f_m Mc	α
15*D*	3.76	1.08	14	0.52
15*H*	4.01	2.72	20	0.63

The addition of moisture, while slightly increasing the storage coefficient δ, has its greatest effect on the change in dielectric constant K_0-K_∞.

Effect of Temperature on Polarization

The effect of increasing temperature on both types of polarization is to decrease the forces opposing the motion of the carriers and thereby to raise the relaxation frequencies. This moves upward on the frequency scale all the curves of dielectric constant and loss factor without greatly changing their numerical values. At a given frequency dielectric constant always increases with temperature at the lower temperatures and consequently its temperature coefficient is positive. The magnitude of this coefficient is by no means constant but depends both upon the amount of polarization and on the ratio of the measuring frequency to the relaxation frequency. After the polarization is complete at a high temperature, dielectric constant frequently decreases and the coefficient becomes negative.

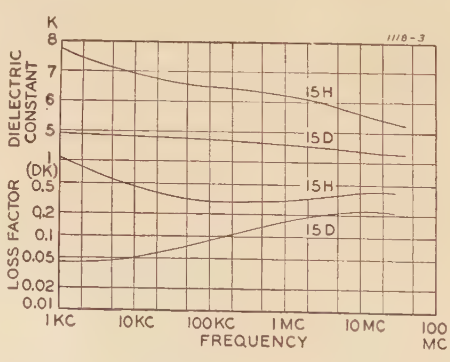

Figure 3. Change of dielectric constant and loss factor with frequency for a paper-base phenolic (after Yager)

15*D* dry, 15*H* conditioned at 60 per cent relative humidity

Loss factor and dissipation factor may increase or decrease with temperature depending on whether the measuring frequency is greater or less than the relaxation frequency. For most commercial insulation showing interfacial polarization the relaxation frequency is well below both audio and power frequencies, and the temperature coefficient is positive. It is always possible, however, for polarization from a single interface or from dipoles to occur at a higher frequency than the measuring frequency and make the temperature coefficient negative.

Effect of Voltage on Polarization

The effect on polarization of increasing voltage is to increase the amount of interfacial polarization because of the increase in the number of free electrons and ions. This will generally increase the value of maximum loss factor and decrease the d-c resistance.

Polarization in Commercial Insulation

Commercial insulation, as used in bushings and insulators, consists of a number of dielectrics in series and parallel. Interfacial polarization, with maximum dissipation factor occurring in the millicycle range,* is usual. Curves of capacitance and dissipation factor for a 25-kv compound-filled bushing are given in figure 6 for four different temperatures. These observations were taken on a Schering bridge operating at 100 volts. The shapes of the curves indicate the existence of both a high-frequency and a low-frequency polarization, but the frequency range is insufficient to allow the construction of circular arcs, even though the lowest frequency used was ten cycles.

The temperature coefficients are all positive and have the values given in table II.

The large variations in temperature coefficient indicate the difficulty of stating a single value applicable under all conditions.

*From 0.001 to 1 cycle per second. A frequency of one millicycle is 0.001 cycle per second.

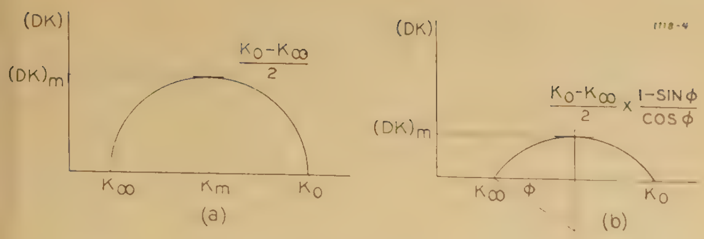

Figure 4. Circle diagrams (after Cole)
(*a*) Center of circle on dielectric constant axis
(*b*) Center of circular arc depressed by angle ϕ

Similar curves for a 66-kv multiple shell porcelain insulator are given in figure 7. Superposed on the low frequency polarization of the porcelain are the polarizations at the interfaces of the porcelain shells and the cement which holds the shells together. The changes in their relaxation frequencies with temperature amount to about 15% per degree centigrade. This is sufficient to cause the dissipation factor curves to cross each other

Table II. Temperature Coefficients for 25-Kv Bushing

f Cycles	C % Per Deg C	D % Per Deg C
10,000	0.24	0.7
1,000	0.25	1.1
120	0.27	3.1
60	0.29	3.8
10	0.45	3.5

and the capacitance curves to be anomalously spaced. The temperature coefficient of dissipation factor changes sign with both temperature and frequency and cannot be used for correcting to a standard temperature. The average temperature coefficient of capacitance at 60 cycles is 0.3% per degree centigrade.

The change in the interfacial polarization of porcelain and cement as the moisture content of the cement is changed is startling. In figure 8 is shown the effect of allowing water to stand in contact with the cement for $5^1/_2$ hours. The relaxation frequency is raised to 800 cycles. Further soaking for 4 days raises this frequency to 13 kilocycles. Characteristic changes also occur in the capacitance of the insulator. The existence of such polarizations complicates the determination of the main low- and high-frequency polarizations, but affords added information concerning the structure of composite insulation.

Figure 6. Effect of temperature on capacitance and dissipation factor of a 25-kv compound-filled bushing

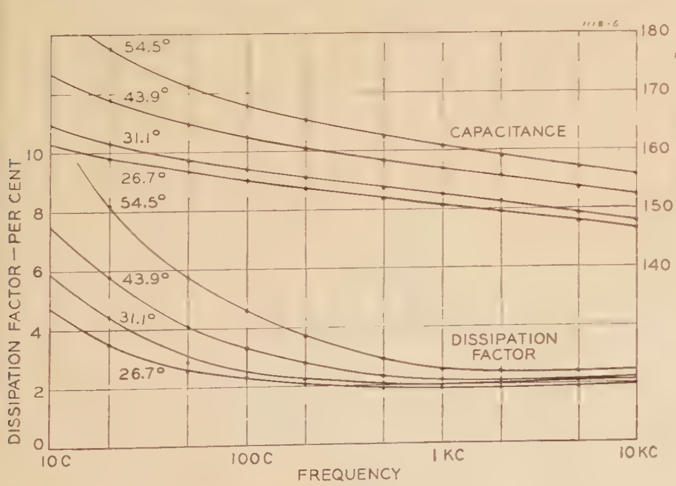

Current-Time Curves

The interfacial polarization occurring in commercial insulation has been shown to be of such a nature that its relaxation frequency is well below the range of bridge measurements and in many instances is not greater than a few millicycles. Curves of charging current against time when a voltage is applied, or of discharge current when the voltage is removed, offer a feasible means of measurement. The existence of this charging current has been a great annoyance in the measurement of d-c resistance, and has led to such arbitrary rules as the specification that d-c resistance shall be calculated from the current flowing one minute after the application of the voltage. It is now obvious that resistance calculated in this manner is only an apparent resistance, which actually is a partial measure of the existing polarization. The complete curve contains the information needed to determine all the parameters which define the polarization. Whitehead and Banos[7] in 1932 analyzed charging current curves for paper taken by means of a cathode-ray oscilloscope and obtained values of dissipation factor which agreed within 2% with measurements taken on a 60-cycle Schering bridge. Murphy and Morgan[8] in 1939 placed this method of analysis on a better theoretical basis. They showed that charge and discharge currents differ by the d-c leakage current only when the polarization during charge has been carried to completion. It is necessary either to subtract the leakage current from the charging current before beginning the analysis or to carry the charging to a time which is long compared with the relaxation time before beginning the discharge. It is very difficult to estimate the correct value of leakage current, and the latter method is preferable in spite of the extra time involved.

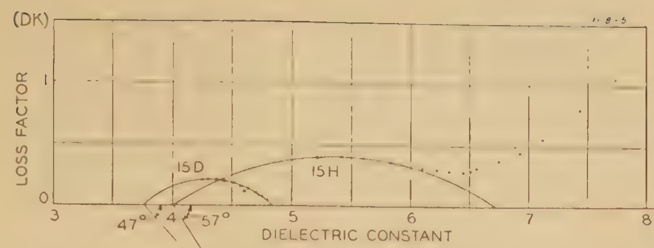

Figure 5. Circle diagrams for paper-base phenolic of figure 3

15*D* dry, 15*H* conditioned at 60 per cent relative humidity

The charging current at 500 volts for the 66-kv insulator is given in figure 9. After subtracting the leakage current of 0.62 $m\mu a$, the residual current was analyzed into the five exponentials shown, whose relaxation times vary from 0.4 to 63 seconds. The corresponding curves of dissipation factor are shown in figure 10. Their sum is the total dissipation factor

Figure 7. Effect of temperature on capacitance and dissipation factor of a 66-kv multiple-shell, pin-type, porcelain insulator

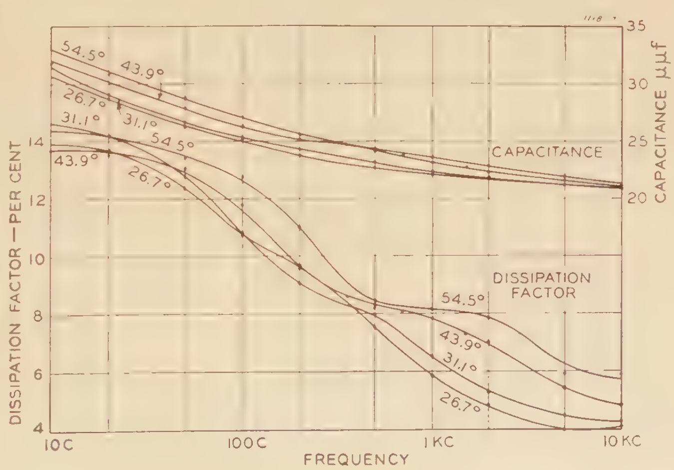

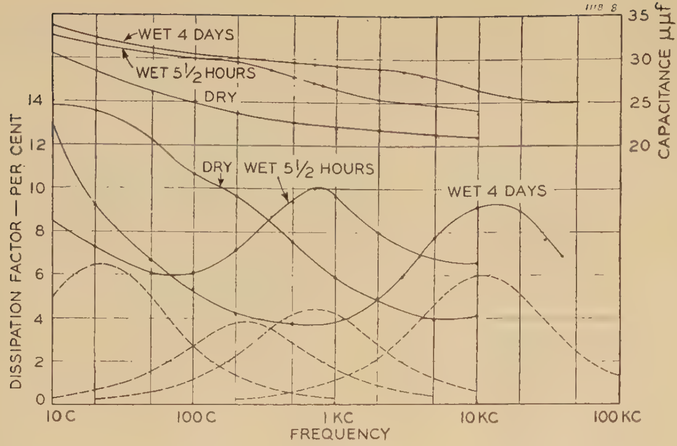

Figure 8. Effect of moisture absorption on capacitance and dissipation factor of a 66-kv multiple-shell porcelain insulator

The contributions to dissipation factor from the polarizations at the cement-porcelain interfaces are shown in dotted lines

produced by the interfacial polarization. The contribution from the leakage current is then added. The corresponding values of capacitance are also given. The resulting circular arc is shown in figure 11. The falling-off of the values of loss factor at the low-frequency end is caused both by the difficulty of estimating the leakage current correctly and by the lack of long time data. The charging current should have been observed for a considerably longer time than 15 minutes. At the high-frequency end the points diverge because of the extra polarizations from the porcelain-cement interfaces. The four parameters derivable from the circular arc are given in the first row of table III.

Table III. 66-Kv Porcelain Insulator

Method	C_∞ μμf	$C_0—C_\infty$ μμf	f_m Mc	α
Exponential	40.2	122.8	6	0.49
Graphical		115	5	0.4

The calculations required to obtain the four parameters in this manner are quite involved and take several hours to perform. Cole and Cole[9] in their most recent paper show that the current-time curves for any polarization have certain characteristic shapes, which are determined solely by the storage coefficient α, or depression angle ϕ of the center of the circular arc. The curve for $\alpha=0$ (center of circle on the dielectric constant axis) is a single exponential, which plots as a straight line on arith-log paper. It corresponds to the single relaxation-time polarization defined by equations 1 to 7. At the other extreme when $\alpha=1$ the curve is a 45° line when plotted on log-log paper. The family of curves are best plotted logarithmically on both axes. The observed current-time curve, plotted to the same scale, is matched to one of these curves and the values of storage coefficient α, relaxation time T, and current at that relaxation time noted. The residual current curve of figure 9 has been analyzed by this method with the results given in the second row of table III. The agreement between the two methods is reason-

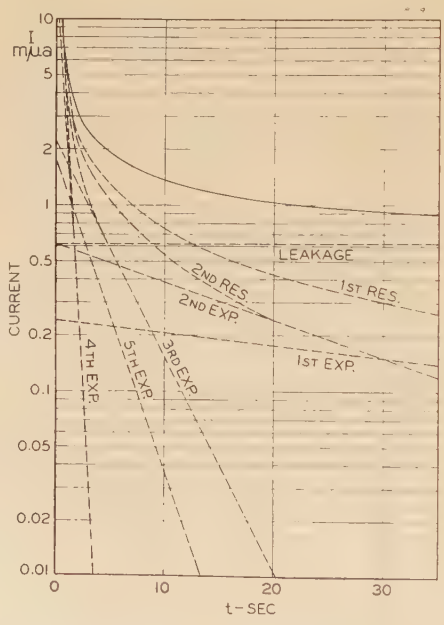

Figure 9. Analysis of the 500-volt charging current curve of a 66-kv multiple-shell porcelain insulator

$E=500$v
$A=806 k M\Omega$
$C_A=21.1$ μμf
$AC_A=17.0$ sec.

	B kMΩ	C μμf	BC_B sec.
1	2,084	30.1	62.6
2	805	25.9	20.84
3	227.2	16.50	3.74
4	33.0	11.62	.38
5	289.0	8.82	2.55

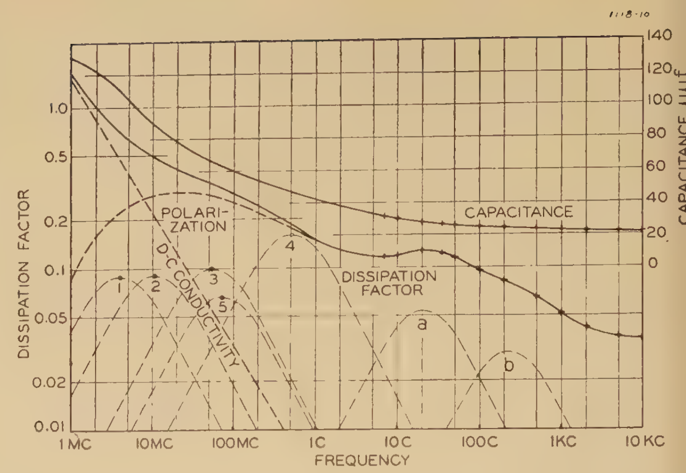

Figure 10. Capacitance and dissipation factor of a 66-kv multiple-shell porcelain insulator as calculated from the exponentials shown in figure 9

ably good. It is quite necessary in this graphical analysis to use a discharge-current curve which covers at least three time-decades symmetrically disposed around the relaxation time.

Effect of Deterioration on the Polarization Parameters

The most common types of deterioration in insulation have been shown to be the absorption of moisture and the formation of voids. In a way they go together, because the existence of voids furnishes an additional porosity which can increase the moisture absorption. This appears to be particularly true of the pasted mica insulation used in large generators. The added moisture increases the dielectric-constant change K_0-K_∞ both on account of the high dielectric constant of water and also because of the added interfaces and free ions. The relaxation frequency f_m is usually increased. The effect on the storage coefficient α is not known.

The voids formed by chemical or mechanical means provide additional interfaces at which ionization can occur. Under intense ionization these surfaces are damaged by carbonization and oxidation with a resultant increase in the dielectric-constant change K_0-K_∞: The effect of ionization on relaxation frequency and storage coefficient has not been determined.

Of the other chemical changes that may take place, polymerization appears to have little effect on the amount of polarization, and loss of volatile matter seems to decrease the polarization, as would be expected because of the loss of a foreign material.

It has already been shown that both dielectric strength and interfacial polariza-

tion depend on the abundance of free electrons and ions. The changes in the three parameters K_0-K_∞, f_m, and α will not only measure the amount of the deterioration, but will indicate the type of deterioration as well and hence will suggest the probable decrease in dielectric strength. The success of such interpretation will depend greatly on the thoroughness with which interfacial polarization in typical insulating materials is studied by means of current-time curves.

An important by-product of these studies will be numerical values for the temperature and voltage coefficients of the three parameters. At the present time only their signs are known.[10] The dielectric-constant change K_0-K_∞ decreases slowly with temperature, but increases considerably with voltage. Relaxation frequency f_m increases rapidly with temperature, frequently at the rate of a decade in frequency for a rise of ten degrees centigrade. Storage coefficient α often decreases with temperature. The effect of voltage changes on these two parameters is not yet known. The importance of knowing the temperature coefficients is that it will then be possible to reduce data taken at widely differing temperatures to a standard temperature. Difficulties from rapidly varying coefficients such as were illustrated in figure 6 no longer occur for these polarization parameters.

Single-Frequency Measurements

Only when the kind of deterioration and the type of insulation is known will measurements of capacitance and dissipation factor at a single frequency afford a reliable measure of the amount of deterioration. The relaxation frequency is so low that it makes little difference whether an audio frequency or the power frequency is used. There is no virtue in using the operating frequency and there is considerable advantage in choosing some neighboring frequency, because it will then be much easier to eliminate the effect of the intense electric field at the operating frequency in which many measurements must be made.

Measurements spread throughout the audio-frequency range will add little to the information obtained from single frequency data, except as they may disclose unusual polarizations of the type shown in figures 5 and 6, and as they provide values of the infinite frequency capacitance and dielectric constant. These frequencies will be too far removed from the relaxation frequency to be of any help in constructing a circular arc and thereby determining the polarization parameters. For this same reason even wide changes in the applied voltage will have little effect on capacitance and dissipation factor, even though the changes in zero frequency capacitance C_0 and maximum dissipation factor D_m' are appreciable. Measurements made at the power frequency of 60 cycles on both new and deteriorated bushings at voltages from 50 volts to 10 kv bear out this conclusion.

Conclusions

It has been shown that a satisfactory correlation can exist between dielectric strength and low-frequency interfacial polarization in insulation, because of their mutual dependence on the abundance and disposition of free electrons and ions throughout the material. Any decrease in dielectric strength caused by deterioration can therefore be measured by the corresponding changes occurring in this polarization. The polarization is defined by certain parameters and a new method for their measurement has been outlined, involving the graphical analysis of current-time curves.

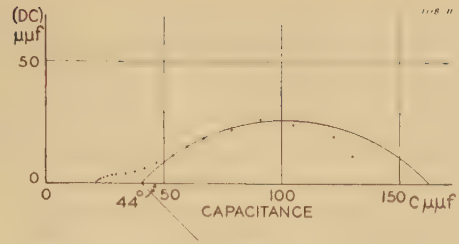

Figure 11. Circle diagram for a 66-kv insulator drawn from the data of figure 10

References

1. Electric Breakdown of Solid and Liquid Insulators, **A. von Hippel.** *Journal of Applied Physics*, volume 8, 1937, pages 815–32.

2. The Dielectric Properties of Insulating Materials, **E. J. Murphy** and **S. O. Morgan.** *Bell System Technical Journal*, volume 16, 1937 pages 493–512.

3. Capacitance and Loss Variations With Frequency and Temperature in Composite Insulation, **H. H. Race.** AIEE Transactions, volume 52, 1933, pages 682–92.

4. The Distribution of Relaxation Times in Typical Dielectrics, **W. A. Yager.** *Physics*, volume 7, 1936, pages 434–50.

5. Dielectric Constant and Loss of Plastics as Related to Their Composition, **W. A. Yager.** *Transactions*, Electrochemical Society, volume 74, 1938, pages 113–34.

6. Discharge and Absorption in Dielectrics, I, A-C Characteristics, **K. S. Cole** and **R. H. Cole.** *Journal of Chemical Physics*, volume 9, 1941, pages 341–51.

7. Predetermination of the A-C Characteristics of Dielectric, **J. B. Whitehead** and **A. Banos.** AIEE Transactions, volume 51, 1932, pages 392–409.

8. The Dielectric Properties of Insulating Materials, III. Alternating and Direct Current Conductivity, **E. J. Murphy** and **S. O. Morgan.** *Bell System Technical Journal*, volume 18, 1939, pages 502–37.

9. Transient Current in Dielectrics, **K. S. Cole** and **R. H. Cole.** Washington Meeting of American Physical Society, May 1–3, 1941.

10. Dielectric Properties of Organic Compounds, **S. O. Morgan** and **W. A. Yager.** *Industrial and Engineering Chemistry*, volume 32, 1941, pages 1519–44.

Radiobroadcasting in Canada

A. FRIGON
ASSOCIATE AIEE

Synopsis: The development of radio broadcasting in Canada has been very rapid and there are now 85 broadcast transmitters in daily operation. All broadcasting is under the control of the Canadian Broadcasting Corporation, an independent Government corporation, which in addition to its regulatory functions operates a coast to coast network connecting together, for a nation-wide service, its own ten modern stations with almost half of the privately owned transmitters. It cannot therefore be said that radio in Canada is owned and operated by the Government as the CBC is independent and free to apply its revenues derived from licenses and commercial operation, in the best interests of its radio audience. The Canadian system is one of co-operation between a semipublic service and private ownership. Parliamentary enquiries have always found it the best suited to Canada's needs considering its vast area and relatively sparse population.

RADIO broadcasting in Canada began at about the end of the last War when an experimental station originated programs for a few hours a day. Following this the first network broadcast in Canada took place on Christmas Day, 1923, when an experimental station in Ottawa was connected to a station in Montreal. In 1926–27 an Eastern Canada network was organized extending from Moncton, N. B. to Toronto; then in 1928–29 our first coast to coast network was inaugurated. Shortly before this time however, on the occasion of the Diamond Jubilee of Confederation, July 1, 1927, Canada's capital city Ottawa was linked for the first time in a nation-wide broadcast using the combined facilities of the Telephone and Telegraph Companies in Canada.

Thus, in 1932, when the Canadian Radio Broadcasting Commission was created by Parliament, the principal wire companies in Canada were already providing facilities for network broadcast. In 1936, the Commission was superseded by the Canadian Broadcasting Corporation which took over the facilities and personnel of its predecessor.

The present system of radio broadcasting in Canada has, since 1928, been considered the best available by all parliamentary committees of enquiry on this subject. Moreover, the present corporation is different from the Commission, which controlled radio from 1933–36, but the principle of accommodating privately owned stations and public service systems has been recognized as the best for Canada for a number of years. The voting in the House of Parliament and of its special committees treating on radio has always been unanimous.

Of the 85 broadcasting stations at present operating on the standard frequency band in Canada, ten are owned and operated by the CBC; the balance are privately owned. Twenty-five of the latter and the ten CBC stations constitute our national network.

The CBC itself is an independent Government corporation, quite free to run its business as it may please, not using public money in any manner but operating with revenues provided by the receiver license fees contributed to the corporation by every owner of a receiving set; this is supplemented by revenues obtained from the commercial operation of the stations. Outside of permitting the corporation to pay for part of the network cost, the national network, commercially run by the corporation, does not bring any appreciable profit.

The CBC is a non-profit enterprise, operating within its own revenues and serving the interests of the public. There are no shares, there are no bonds. The Board of Governors is entrusted with the administration of the revenues placed at its disposal and is responsible for the honest and efficient conduct of the business to a Minister of the Crown. Any surplus in operation is considered as such and invested in the business. It is not distributed as profits and not returned to the public treasury.

On the other hand, privately owned stations operate under conditions similar to those existing in the United States. They conduct their business as they please, and their operating profit is theirs but, as in the United States, they must, pertaining to program only, submit to certain regulations which in Canada are formulated by the CBC.

The restrictions as to program, self-imposed in the case of CBC stations, are such that restraint of private stations is, in my belief, not serious. For instance, the CBC will not carry commercial spot announcements. It will not carry certain types of commercial programs and generally does not accept a great number of the local commercial programs. These restrictions and many others do not apply to privately owned stations.

To emphasize on this freedom of the commercial side of the business, I may state that there are three privately owned stations in Canada which are outlets of the American networks and there are four CBC stations also having direct network connections with American networks. These facts will immediately prove to you that broadcasting in Canada is neither owned nor operated by the Government.

Our dependence on American networks for a good many of our best programs presents some difficulties at times, but generally speaking, it is considered as a very welcome asset and a great means of fostering closer understanding between our two countries.

From the network operating point of view we have problems in Canada which do not exist in the United States. The CBC network, which is the longest east to west network in the world extending over three thousand air miles, covers five time zones instead of the four south of the border. This great distance separating the two extremes of the network and more particularly the great difference in local time renders the problem of co-ordinating the program service very difficult. In addition we have a bilingual population, as almost one third of all Canadians speak French. In the province of Quebec we have besides our basic trans-Canada network a Regional French network. The French speaking minorities located throughout the other eight provinces are however constantly clamoring for more French programs. This presents a problem requiring a good deal of attention. Of course our greatest difficulty in Canada is the same as that faced by our transportation companies and is due to the wide scattering of a relatively small population across an extremely large area. This means low revenue and yet high cost of service. In the United States there is twelve times the population in five-sixths of the area, while in England the British Broadcasting Corporation serves four times the population concentrated in but one sixty-fifth of the area. In normal times this must, at least from the engineering standpoint, be a broadcaster's paradise, where the whole network is hardly longer than some of our local loops and where lines are only a few

Paper 41-113, recommended by the AIEE committee on communication, and presented at the AIEE summer convention, Toronto, Ontario, Can., June 16–20, 1941. Manuscript submitted April 10, 1941; made available for preprinting May 9, 1941.

A. Frigon is assistant general manager of the Canadian Broadcasting Corporation, Montreal, Quebec, Can.

hundred miles in length as compared to the five or six thousand miles some programs on this continent have to travel before reaching their destination.

The largest studios are located in Montreal and in Toronto where approximately 50% of our programs are produced. For exchange programs from or to American networks we have special switching facilities at Montreal and Toronto for the National Broadcasting Company Red and Blue networks, at Vancouver and Windsor exchanges with the Columbia Broadcasting System are handled, and again at Windsor for exchanges with the Mutual Broadcasting System and the Michigan Radio network. Broadcasts from the British Broadcasting Corporation in England are relayed to our network through our short-wave receiving station in Ottawa. At this station, we have directional aerials and diversity receivers constantly tuned to various points in Europe and South America. Before hostilities began important features or news gathered in this manner were broadcast over the network. From some of these sources activities are now necessarily curtailed. On the other hand, our relations with the British Broadcasting Corporation are even closer than ever. We have at the present time a number of our men in England working in conjunction with the British Broadcasting Corporation personnel.

One very interesting point is that the CBC is in the enviable position of being able to secure for its listeners, at any time, a greater variety of programs than are normally available to any other broadcasting system in the World. They are made up as follows: First it has access to the leading programs of all the principal networks in the United States. Second, broadcasts from Europe for the time being are limited to those from the British Broadcasting Corporation. Third, its own English network and fourth, its own French network.

Some special feature broadcasts have been of considerable credit to the CBC. An example of this was the Christmas Broadcast in 1935. During the two hour feature pick-ups were scheduled from some 35 different and in some cases almost inaccessible spots ranging from a point two miles under the Atlantic ocean to a golf course on an island in the Pacific. It was during this broadcast that eight choirs located at widely separated cities sang in perfect harmony with an orchestra at another point.

A more recent example involving still wider facilities was the Empire Day broadcast of May 24, 1939, during the visit of Their Majesties. The program which lasted an hour began with a rapid visit across Canada with Canadians speaking from Halifax, Montreal, Toronto, Winnipeg, Regina, Edmonton, and Vancouver then it carried the listener to Africa, Rhodesia, Australia, New Zealand, India, Jamaica, Newfoundland, Scotland, Northern Ireland, Wales, and England and then, to climax the broadcast, back to Winnipeg in Canada for the Empire Day message given by the King himself.

The Canadian contributions were brought together by land lines and those from other points of the Empire via short-wave radio relay lines. In Montreal all these elements were blended into a program which was relayed to 54 stations across Canada and 335 transmitters of the NBC, CBS, MBS, MRN in the United States and also to all parts of the British Empire by means of short-wave radio.

In all, we estimate that over 25,000 miles of telephone circuits and 100,000 miles of radio telephone links were used plus the services of some 2,000 technicians simultaneously engaged at the controls, constituting a program which was within the reach of millions of people.

Summing up, the CBC is mainly concerned with national and regional problems of broadcasting. This explains why it maintains a very elaborate network of broadcasting lines of a total length of over 7,000 miles reaching almost every broadcasting station in Canada. As a matter of fact, these lines are owned and operated for the CBC by our two main railway companies: the Canadian Pacific Railway and the Canadian National Railways. Under contract, the telegraph divisions of these two companies must maintain the wire line service between some 70 points across the country, the service being subject to certain specifications concerning the quality of transmission. This network permits the CBC to reach over 90% of the population of Canada within the primary coverage of some broadcasting station, that is within the 5 millivolts per meter contour of some station. If we consider that people living outside of these areas are for the most part isolated from industrial centers and can therefore obtain good reception from much lower field intensities, it may be said that the CBC network reaches practically all the population of Canada.

For commercial purposes, a group of stations has been organized as a network under the name of the National Network. This is composed of five regional networks which may be handled separately from a commercial point of view. Whenever some program of great national importance is handled by the CBC, for instance for all broadcasts of the Royal Visit or when our Prime Minister or your President has a message to send to the public, such broadcasts are offered to all stations in Canada. Those on the National Network carry the program, the others, while they are not obliged to, usually carry it of their own accord. This, I believe gives you a general outline of broadcasting in Canada.

It is difficult to give correct figures on privately owned stations as they are quite independent to run their show as they please and they are not required to submit a report on their financial operations except, of course, in so far as taxes or revenues are concerned, but files on these matters are not open to the public.

As I have said before, the CBC operates under a budget covering each fiscal year. Since its organization on the 1st of November 1936, the corporation has had a total operating surplus of $1,000,000—$600,000 of which has been re-invested in the corporation's plant. Our board is proud to have been able to operate a rather difficult business with a surplus each year. This is not always the case with organizations who may hope to obtain the help of the Government when they get into bad straights.

During less than five years since its inception, the CBC has built four 50-kw transmitters, one of 5 kw, a $7^1/_2$-kw short-wave transmitter, and new studios at two points. Besides this, a 5-kw transmitter was revamped as were two sets of studios. It also had the privilege of leasing from the Manitoba Telephone System the studios built by that organization in Winnipeg.

The Engineering Division is divided into five departments:

The Operation Department,
The Transmission & Development Department,
The Architectural Department,
The Design & Construction Department,
and the Purchasing & Stores Department.

Of a total staff of some 600 we have at present 185 employees in the main divisions of the technical service. Forty of these are graduate engineers and 100 are technicians and operators specialized in radio work.

Had it not been for the war we would probably have two important new buildings, one in Toronto and one in Montreal, to take care of our studio and office requirements at those points. The war has prevented heavy capital expenditures.

Although we ourselves fabricate a num-

Development in Lightning Protection of Stations

E. R. WHITEHEAD
MEMBER AIEE

Introduction

THE AIEE transformer sub-committee has recently sponsored a paper[1] on the protection of power transformers against lightning surges. The most effective method given combines overhead ground wires, line entrance gaps, and transformer mounted lightning arresters. Such a method does give a high degree of protection, but it is primarily applicable to high voltage, high capacity stations where the overhead ground wire system is justified for both line and station.

The conditions noted above are seldom fulfilled on subtransmission systems from 23 kv to 34.5 kv. Effective ground wires and low ground resistances are uneconomical, and the protection provided is usually a more or less modern arrester, not always located and grounded to the best advantage.

On the 23-kv subtransmission system of the Duquesne Light Company, the average transmission distance is approximately two miles. This means that most direct strokes will contact the line not more than one mile from some substation. Much of this transmission is now equipped with wood cross arm braces and guy insulators, and at some stations several spans adjacent thereto are carried on unguyed poles.

Under such conditions, it is possible for very high voltage waves to strike the station and result in arrester discharge currents having high rates of rise.

It is the purpose of this paper to outline briefly some of the field experience pointing to this factor as a cause of transformer and arrester failures, and to present a limited discussion of laboratory tests and calculations relating to a proposed method of achieving a high degree of protection for equipment so exposed.

Field Experience

After several years' experience with improved station insulation and modern types of carborundum block arresters,[2] it has become apparent that arrester failures are confined to a few exposed locations. Furthermore, most cases of insulation failure are associated with definite evidence of direct strokes to the line near the station.

In one station, no equipment failures have occurred, but arrester failures average one per year. In another station there have been no arrester failures, but transformer failures average one every two years. In still another case, the arrester suffered no damage but a transformer bushing flashed over. This particular bushing had an impulse strength over twice the arrester impedance voltage at 5,000 amperes on the standard AIEE test wave.

Paper 41-102, recommended by the AIEE committee on protective devices, and presented at the AIEE summer convention, Toronto, Ontario, Can., June 16–20, 1941. Manuscript submitted April 8, 1941; made available for preprinting May 6, 1941.

E. R. WHITEHEAD is with the Duquesne Light Company, Pittsburgh, Pa.

The author acknowledges the valuable assistance of C. M. Jackson in making the tests, and of E. L. Jarrett in the preparation of this paper.

1. For all numbered references, see list at end of paper.

Such instances have emphasized the necessity of providing some sort of back-up device which would come into play under extreme conditions only, yet not affect service under the great number of minor surges.

In one station, six-inch rod gaps were installed in parallel with the arresters two years ago, yet another transformer failure occurred in 1940.

As a result of this experience, it was decided to make a series of tests in the laboratory in order to determine if some method could be found to afford protection under such conditions.

Performance of Arresters

In analyzing the performance of lightning arresters subjected to high rates of current rise, it becomes apparent that the so-called *IR* voltage depends both on the rate of current rise as well as on the maximum value of the current. It has been found that a fair approximation to the actual characteristic can be obtained by using an equivalent circuit composed of a constant voltage, a constant resistance, and a constant inductance in series.

Such representation is, of course, entirely empirical, and serves merely to permit approximate calculations. The method of determining the constants is shown in figure 1. The value of the arrester voltage drop at the time of crest current is plotted for two well-separated values of crest current, and the line joining these points extrapolated to current zero to determine the value of E_a. The slope of this line determines the value of R_a. The difference between the crest of the arrester voltage and the value at the instant of crest current is a measure of the fictitious inductive drop at this time. These values are not strictly constant, but

---

ber of the minor parts of our equipment, we purchase the bulk of our plant from the usual equipment manufacturers. Our new 50-kw stations in Toronto and Montreal are Northern Electric transmitters. Those in Sackville and Watrous are RCA. We propose to co-operate with the Canadian Marconi in the operation of an F.M. transmitter on Mount-Royal, Montreal.

All our construction is designed and supervised by our own staff but actual building is assigned by tender to firms who are invited to bid.

Thus, it is seen that radio broadcasting in Canada is conducted under a dual system of individual privately owned stations and of a public service network operated by the CBC. This particular organization, besides having authority to regulate over program contents generally of private stations also owns and operates a number of its own stations and a network composed of both CBC and privately owned stations. Besides, the CBC acts as an agency in booking network programs on all network stations whether they are its own or privately owned. There is also a provision for the setting up of partial networks to meet special demands from sponsors or to take care of the overflow on the national or regional networks. This system has been in operation for more than five years and has proved to meet with the wishes of the very great majority of Canadians across the Country. The public service angle has proved extremely successful in certain instances of national importance and all indications are to the effect that present conditions will be maintained to the best satisfaction of the sponsors, artists, musicians, and the listening public.

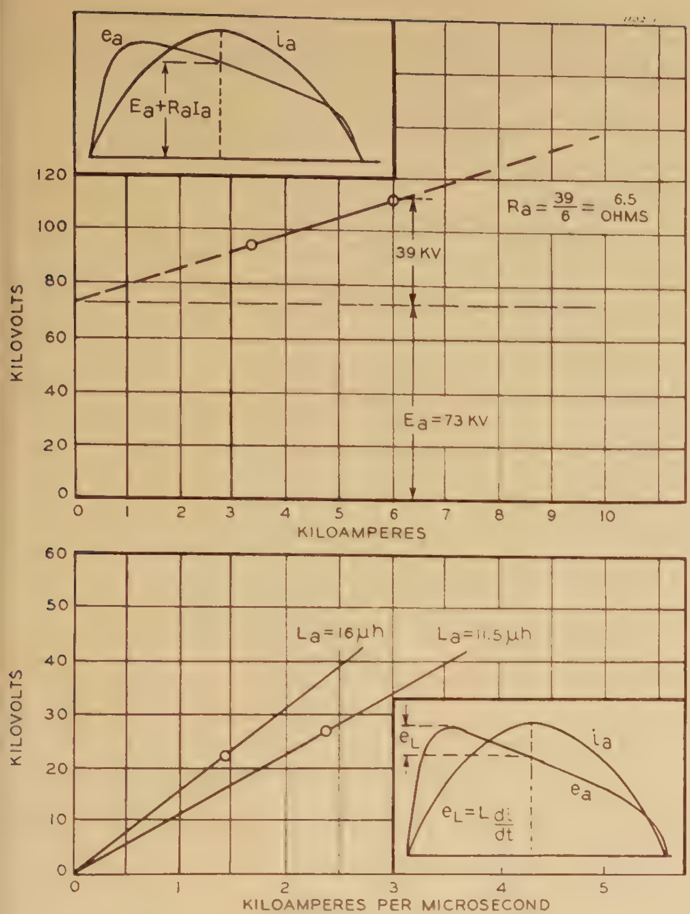

Figure 1. Method of determining constants for equivalent circuit of arrester

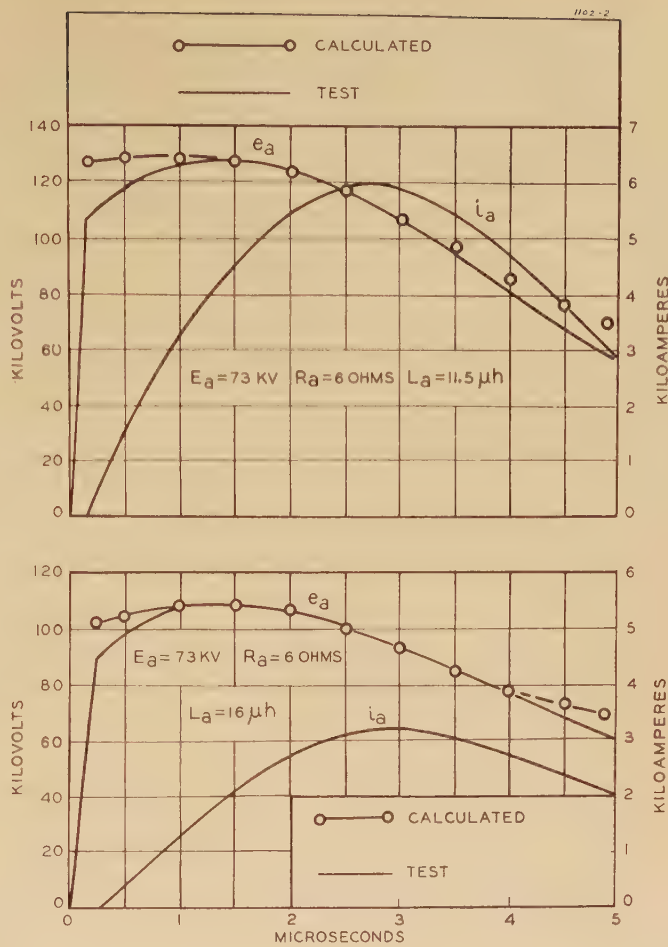

Figure 2. Comparison of test results and calculations from equivalent circuit

decrease with increasing discharge current. Values may be chosen for moderately high current and used with the knowledge that they will be conservative for extreme conditions. Figure 2 shows calculated and measured arrester voltages for the currents and arrester constants shown.

Transformer-Arrester Co-ordination

Because of the relative characteristics of gaps, transformers, and line type arresters, it is not possible to secure complete back-up protection for short times. This situation is illustrated in figure 3 where a modern transformer of the 23-kv class is compared with a modern arrester and a six-inch rod gap.

Gap-Reactor-Arrester Protection

Since the rate of rise characteristic of the arrester is simulated by an inductance, it seemed logical to add an external reactor which would increase the voltage at the gap location for high rates of current rise, and thereby at least partially offset the turn-up in the rod gap characteristic. This scheme is just the reverse of the old arrester-choke coil sequence in that the arrester is transformer-mounted and so limits the voltage at the vital point in the most effective way possible. In the old scheme, the arrester voltages for high rates of current rise were further aggravated by oscillations between arrester and transformer at the natural period of the choke inductance and effective transformer capacitance. In the new scheme, the basic protection is located at the transformer. The inductance and capacitance slope the wave front and lower the arrester breakdown, while the back-up gap is brought into action only when required to keep the arrester impedance voltage at a safe level.

Calculations for Theoretical Scheme

Figure 4 shows such a protection system. Through the substitution of the constant circuit elements to represent the arrester, it is possible to estimate the effect of any assumed terminal current. Although no "turn-up" is shown for the transformer strength, such an increase does exist and would actually provide a greater margin of safety than that indicated. The effect of this protection system at short times is roughly equivalent to the back-up protection of a 3.5-inch gap without the reactor.

Laboratory Tests

Impulse tests were made on the combination protective scheme in order to check the theory within the limitations of the laboratory equipment. Figure 5*a* shows the oscillogram of the voltage across the six-inch gap, while figure 5*b* shows the voltage across the arrester under the same conditions. Figure 5*c* shows the voltage across the arrester for a higher rate of rise of current, and without the reactor.

As a final test of the protection system, it was decided to make a complete set-up including a 100-kva, 3-phase, 22,000/460/230-volt transformer. The particular transformer chosen was an exact duplicate of those mentioned earlier as having flashed over or failed internally three times in six years. The surge generator was adjusted for maximum voltage and all series resistance was short-circuited. Under such conditions, the voltage, if unlimited by gap breakdown, would reach about 650 kv in something less than one-

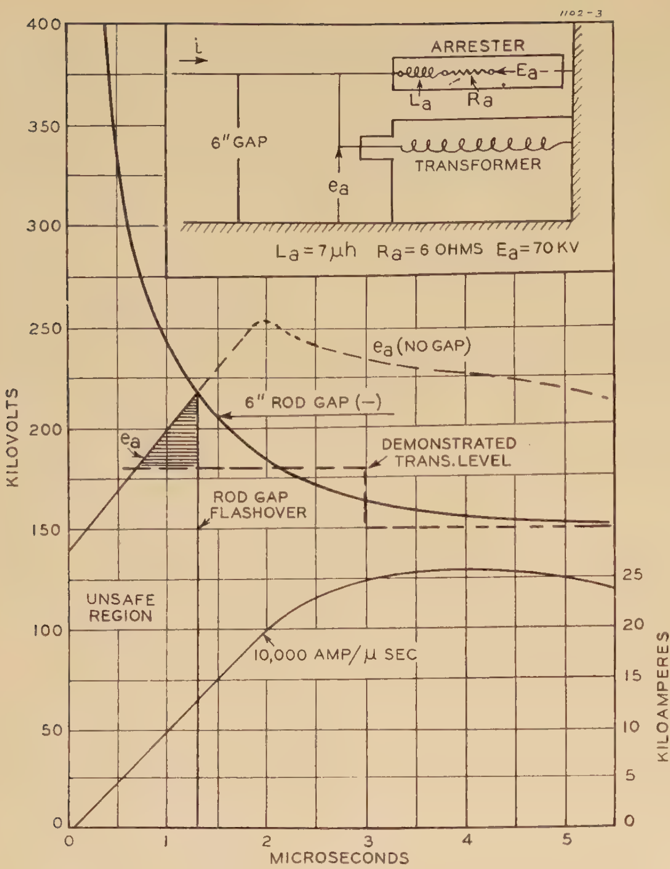

Figure 3. Co-ordination of gap-arrester-transformer combination

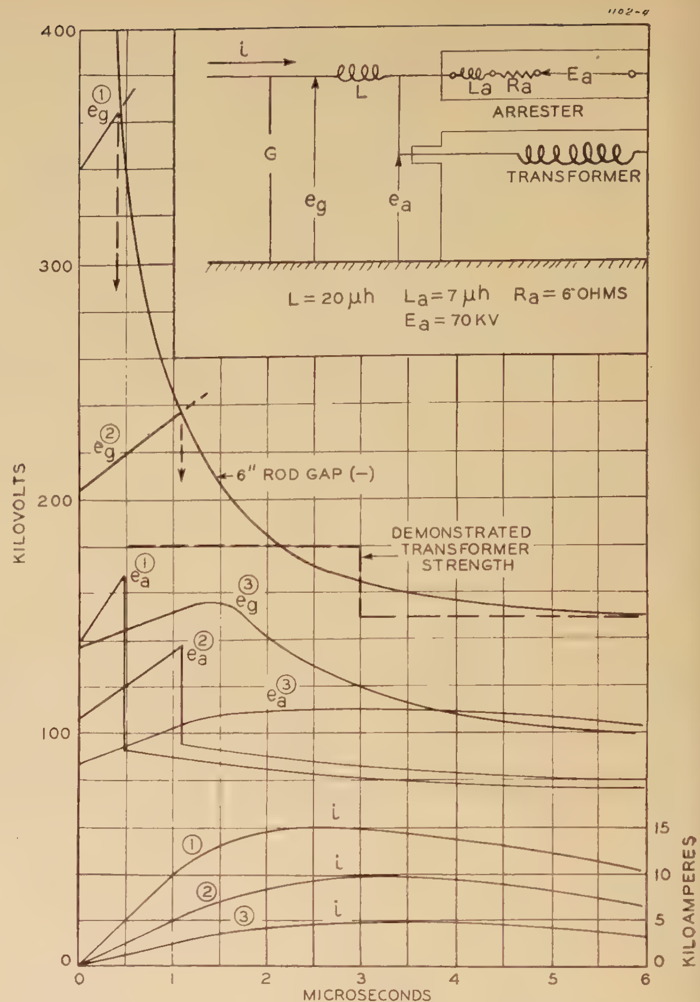

Figure 4. Calculated performance of gap-reactor-arrester protection scheme

half microsecond. Under these conditions, the generator was discharged into the system several times without damage to the transformer. A maximum voltage of 121 kv was recorded at the transformer bushing. Current measurements under such conditions were impossible, but it is estimated that the rate of current rise approximated 20 ka per microsecond.

Following this test, the transformer was subjected to both full wave and chopped wave tests slightly under the present AIEE standard values, and no evidence of insulation failure was detected.

Conclusion

It appears possible to employ a reactor or "choke coil" to compensate for the steep turn-up of rod gaps when the latter are used as back-up voltage limiting devices in conjunction with transformer-mounted lightning arresters. Moreover, such a combination gives promise of providing a high degree of protection to stations fed at subtransmission voltages over wood pole lines without overhead ground wires.

References

1. Protection of Power Transformers Against Lightning Surges, **AIEE Transformer Subcommittee.** AIEE Transactions, volume 60, 1941, pages 568–77.

2. Lightning Protection of 22-Kv Substations, **E. R. Whitehead.** AIEE Transactions, volume 57, 1938 (October section), pages 568–71.

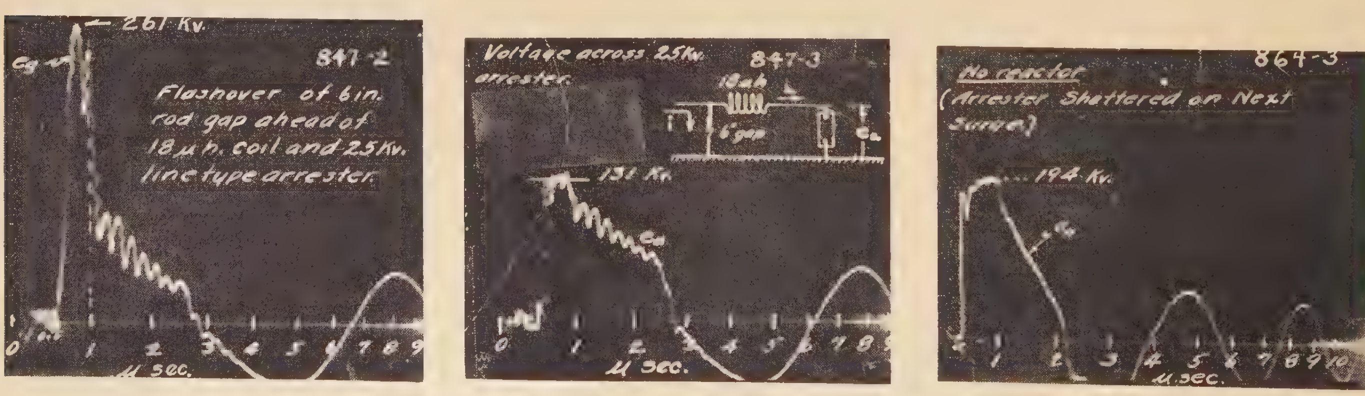

Figure 5. Laboratory tests on gap-reactor-arrester system

Current Rating and Life of Cold-Cathode Tubes

G. H. ROCKWOOD
MEMBER AIEE

Introduction

A COLD cathode tube is a gas discharge device capable of serving as a relay, a rectifier, or a voltage regulator.[1,2] It depends for its action upon the properties of gas discharges. The salient property employed is the fact that there is a difference between the breakdown voltage, or voltage necessary to initiate a discharge, and the sustaining voltage, or voltage drop across the tube when conducting. The principles involved are not new but a practical device capable of operating on voltages of 150 volts or less has awaited the relatively recent development of suitable cathode coating materials. The cathode surface employed at present consists of a coating of barium and strontium oxides applied to a nickel base. These oxides are partially broken down to barium and strontium metal during exhaust. During the operation of the tube the barium is continually removed from the cathode by sputtering and is replaced by further reduction of the oxide reservoir. The life of the tube is limited, therefore, by the amount of material present and by the rate of sputtering.

Because the cold cathode tube requires no cathode heating power it is well adapted to those applications in which the service is intermittent. The absence of a hot cathode implies no deterioration during idle periods and the ability of the tube to start instantly upon the application of an input signal. These properties have opened a wide field of use to the cold cathode tube and it is felt that this field may be widened if the tubes are so rated as to take cognizance of the fact that their life is determined by sputtering and the consequent exhaustion of the reservoir of cathode material. Other gas tubes, such as vapor rectifiers and thyratons, have been rated in terms of peak and average current. These ratings have been based on anode power dissipation and electron emission capability of the cathode surface. In the case of the cold cathode tubes it is desirable to have the rating bear a relationship to the rate of sputtering. For a tube of given manufacture, the rate of sputtering is determined solely by the current drawn. The general form of the life rating should be, therefore, a tabular relationship between the average life to be expected and the current. Several values of current and life are needed since the rate of sputtering is not proportional to the current.

If a cold cathode tube is operated until it fails in service certain changes may be observed visually. These are: first, a dark band on the tube walls in the vicinity of the cathode and, second, a change in color and surface appearance of the cathode. These observations may be accounted for by assuming that the cathode material is lost by either evaporation or sputtering. To test the idea of loss of material due to evaporation thermocouple measurements of the cathode were made. These measurements indicate that, in general, the cathode temperature is less than 250 C and invariably less than 375 C. These temperatures are so low as to make the theory of loss of material by evaporation untenable. For example, the cathode temperature at a current of 35 milliamperes was found to be 210 C and the average life 100 hours. Rudberg and Lumpert[6] have measured the vapor pressure of barium at low temperatures and give a formula by means of which their data may be extrapolated. From this knowledge of the vapor pressure of barium at 210 C and the total amount of barium present on the cathode the life may be calculated and it is found to be 45,000 hours compared to the 100 hours actually observed.

Microchemical examination of the tubes indicates that new tubes have considerable metallic barium on the surface of the cathode together with a much larger amount of barium in combination. Similar tests on tubes which have reached the end of their life indicate less metallic barium on the cathode and almost no barium in combination on the electrodes but the total barium which was present when the tube was made is to be found on other parts of the tube, notably the walls.

These facts lead to the conclusion that as the tube is operated barium is continually lost from the cathode surface by sputtering and is continually replaced from the reservoir of barium oxide provided in the cathode coating. When this reservoir is exhausted the tube reaches the end of its life.

Theory of Cathode Sputtering

Most of the literature on cathode sputtering relates to a discharge at relatively low pressures and with high voltage drops across the tube. The only comprehensive survey of sputtering in low voltage tubes is to be found in a paper by C. H. Townes.[3] A review of the conclusions reached by Townes is given below.

Townes divides the rate of sputtering into three factors: (1) the number of ions of a given energy striking the cathode, (2) the amount of material released by each ion, and (3) the fraction of material released from the cathode which diffuses away and ultimately reaches other surfaces in the tube.

There is good evidence that sputtering is due to ionic bombardment of the cathode and that the material sputtered leaves the cathode in all directions and in an uncharged atomic stage. In the low voltage cold cathode tube the cathode dark space, across which appears the cathode fall of potential has a thickness of several electron mean free paths. The mean free path for a positive ion being smaller than that for an electron, it is evident that very few, if any, positive ions reach the cathode with an energy corresponding to that of the cathode fall. The average energy of positive ions impinging on the cathode is found to be a little less than one electron volt. Not only the average energy is necessary but also the probability that an ion has any of the various possible energies. Appreciable variations in the total energy come principally from the variation in the energy acquired at the last free path of the ion. This follows from the fact that collisions between ions and gas atoms are collisions between particles of substantially equal mass so that on the average, an ion will lose half of its energy at each collision. On the average, therefore, the energy acquired by an ion in its last free path is double that which it had at the beginning of this last free path. The final expression for the distribution in energy of the positive ions striking the cathode is an exponential expression of the same form as that describing the distribution of molecular free paths in a gas. This is to

Paper 41-117, recommended by the AIEE joint subcommittee on electronics, and presented at the AIEE summer convention, Toronto, Ontario, Can., June 16–20, 1941. Manuscript submitted April 16, 1941; made available for preprinting May 12, 1941.

G. H. Rockwood is with the Bell Telephone Laboratories, Inc., New York, N. Y.

1. For all numbered references, see list at end of paper.

be expected since, as pointed out above, the principal variation in the energy comes from that acquired in the last free path, or in other words depends upon the length of the last free path.

Of the mechanisms suggested for the release of material from the cathode under positive ion bombardment the one most successful in explaining the experimental results is the theory of local heating and resultant evaporation of von Hippel.[4] According to this theory the positive ion delivers its kinetic energy to a small number of atoms on the surface which are temporarily given large random velocities and evaporate from the surface just as they would evaporate if the entire cathode were heated so that they had the same thermal energy. The local hot spot of course, cools very rapidly by sharing its energy with the surrounding atoms. Townes has developed an expression for the number of atoms removed from the cathode by each ion impinging with a given energy. For a cathode material such that an atom must have an energy of four electron volts to escape from the surface his expression leads to the following:

Atoms Removed Per Ion Striking Cathode	Energy of Impinging Ions
2×10^{-8}	4 e.v.
0.2	6 e.v.
2	8 e.v.

This demonstrates the rapid variation in the number of atoms removed per impinging ion as the energy of the impinging ions is increased. The expression for the total number of atoms released from the cathode considering the distribution in energy of the positive ions reaching it is complicated and will not be given here.

Since the mean free path of the sputtered particles is much smaller than the distance between the cathode and surrounding surfaces a large fraction of the atoms which leave the cathode will diffuse back to the cathode surface so that they do not represent a net loss of cathode material. Townes shows that for a fixed rate of evaporation of atoms at the cathode the actual rate of loss of material from the cathode is inversely proportional to the gas pressure and depends as well on the distance to the nearest surfaces where deposition may take place. A large number of the evaporated atoms return to the cathode surface. The exact number lost will, of course, depend upon the tube geometry.

The complete expression for the sputtering rate is given by Townes as:

$$I=AF\frac{J}{p}e^{-\left[\frac{V_0}{c}\left(\frac{p^2}{Vi}\right)^{2/5}\right]} \qquad (1)$$

where

- I is equal to the mass per second of sputtered material
- p is the gas pressure in millimeters of mercury
- V is the cathode fall in volts
- i is the current density in amperes per square centimeter
- V_0 is the energy in electron volts required to remove one atom from the cathode surface
- c is a constant characteristic of the gas. For argon $c=20$, for neon $c=33$
- J is equal to the total current
- F is a function determined by the geometry of cathode and collecting surface. For plain parallel surfaces $F=1/d$ where d is the distance between the surfaces
- A is another constant evaluated in terms of the properties of the cathode material in the gas

The constants in this equation may be approximately evaluated on theoretical grounds or they may be determined by experiment.

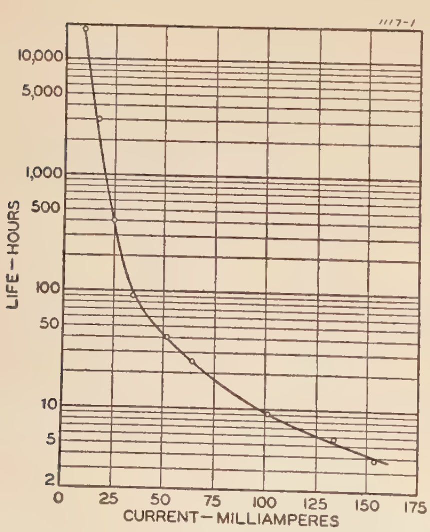

Figure 1. Life of the Western Electric 313C cold-cathode tube as a function of current

Experimental Results

A series of tubes have been operated at various currents to determine experimentally the relationship between current drawn and life. The cathodes of these tubes are coated to a nominal thickness of one-half milligram per square centimeter. This is an extremely thin coating and it is difficult to reproduce such coatings exactly from tube to tube. Considerable scattering in the test results must be expected therefore. The points on the curve of figure 1 each represent the average life of three tubes operated under the current conditions noted. The curve represents equation 1 with the constants so selected that it represents the best fit for the data. The agreement between the curve and the experimental data is seen to be quite satisfactory considering the scattering that must be expected in experiments of this type and suggests that the assumption at the outset that the life of the tubes was determined by the loss of cathode material due to sputtering is correct. This being so it seems reasonable to rate the tubes in such a manner as to reflect this fact.

The data presented in figure 1 relate to a Western Electric 313C vacuum tube and form the basis for the current ratings for this tube. The ratings employed are those currents which will give a life of 100, 1,000, and 10,000 hours. Because of the large scattering due to variations in coating thickness and gas pressure in individual tubes it is not expected that the life of a single tube can be predicted with an accuracy better than $\pm50\%$. In dealing with large numbers of tubes, however, the average life is predicted with a considerably better accuracy. It is practical, for instance, to use this curve in calculating the number of tube replacements required for a circuit which operates under given conditions.

Application of Current Ratings

Since the life of a cold cathode tube of given manufacture depends solely upon the current drawn a knowledge of the relationship between life and current drain is of vital importance to the circuit designer. In the use of cold cathode tubes it often happens that the duty cycle is so light that the life of the tube may be many times the life of the equipment in which it is used even though the tube, if operated continuously, might last but a few hours. If the circuit designer is furnished with the relationship between life and current drain and knows the duty cycle imposed on the tube he is in a position to determine the average life he may expect from the tube. With this knowledge it is often possible to apply small, inexpensive cold cathode tubes to circuits requiring considerable amounts of current for brief and infrequent intervals rather than to resort to larger tubes requiring hot cathodes and capable of supplying the current continuously. Likewise, it makes it possible for the designer to reach a reasonable compromise in decreasing the cost of associated equipment at the expense of increasing the current drain through the tube and therefore shortening the tube life.

If the current wave form through the tube is irregular the life may still be pre-

Dielectric Strength of Oil for High-Voltage Testing of Oil Circuit Breakers

H. J. LINGAL
MEMBER AIEE

W. F. SKEATS
MEMBER AIEE

H. D. BRALEY
ASSOCIATE AIEE

THE purpose of this paper is to report on work undertaken in response to a request, made to the Institute, to determine the minimum dielectric strength of oil for high potential testing of oil circuit breakers.

Many tests were made with 60-cycle and impulse voltages. The tests were made with a rod to plane gap, cone to disc gap, and on oil circuit breakers of commercial types and sizes. The results of these tests have been collected, analyzed, and are included in tabular form in the paper.

The impulse strength of oil circuit breakers was found to be practically unaffected by the 60-cycle breakdown strength of the oil within the range of 16 to 30 kv, as measured in a standard test cup.

The 60-cycle dielectric strength of oil circuit breakers is shown not to be changed in direct proportion to the differences in the dielectric strength of oil as measured in a test cup with 60-cycle voltage.

The effect of low dielectric strength oil on voltage breakdown is discussed and conclusions are drawn which show that it is desirable to test all oil circuit breakers with oil having dielectric strength of 22 kv or higher.

General

The general picture of oil breakdown for some years has involved the lining up of impurities over a period of time ranging from a small fraction of a second to several minutes, with breakdown taking place over the path so formed. From this standpoint it is to be anticipated that long gaps will be relatively less affected by the impurities in the oil than short gaps, and that breakdowns under impulse conditions, where time is not available for lining up of impurities would be less affected by impurities than breakdowns under a one minute test at operating frequency. This is supported by the fact that the impulse ratio of oil, as obtained by comparing Sorensen's[1] data on impulse tests with Miner's[2] data at 60 cycles is considerably greater than the impulse ratio for breakdowns over an air path. Hence, it would be expected that any equipment which will flash over in an air path in preference to an oil path at 60 cycles will have a good margin of safety for the oil under impulse conditions, and it is also to be expected that the dielectric strength of a completed assembly such as an oil circuit breaker would be much less affected by the presence of impurities, in the oil, particularly under impulse conditions, than would be

Table I. Rod-to-Plane Gap Impulse Tests
(See Figure 1)

Gap Spacing (Inches)	Oil	Highest Voltage Held Without Breakdown (Kv)	Lowest Voltage at Which Breakdown Occurred (Kv)
1	New	176	168
1	Old	165	166
2	New	200	186
2	Old	208	190

The tests were made with a $1^1/_2$–40 m.s. positive wave.

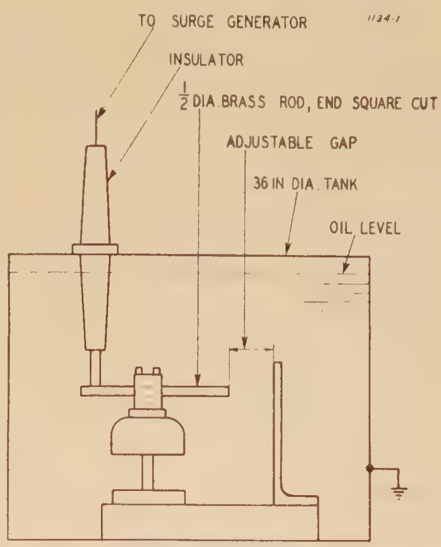

Figure 1. Rod-to-plane gap used in making tests shown in table I

Paper 41-134, recommended by the AIEE committee on protective devices, and presented at the AIEE summer convention, Toronto, Ontario, Can., June 16–20, 1941. Manuscript submitted April 15, 1941; made available for preprinting May 14, 1941.

H. J. LINGAL is with Westinghouse Electric and Manufacturing Company, East Pittsburgh, Pa., W. F. SKEATS with General Electric Company, Philadelphia, Pa., and H. D. BRALEY with Consolidated Edison Company, New York, N. Y.

The authors of this paper are the members of a working group of the circuit breaker switch and fuse subcommittee of the AIEE protective devices committee, who were appointed to investigate and recommend the proper dielectric strength of oil for high-potential testing of circuit breakers.

1. For all numbered references, see list at end of paper.

---

dicted by dividing the current wave into elements small enough so that the current in each element may be considered constant. Each of these currents may then be considered as lasting for a certain fraction of the cycle. For each of the current values obtained there is a life in hours which may be determined from figure 1. One then has a series of currents $i_1, i_2, \ldots i_n$ each lasting for a fraction $t_1, t_2, \ldots t_n$ of the entire cycle and a tube life corresponding to these currents of $l_1, l_2, \ldots l_n$. The fraction of life used up at each current per hour is, then t/l. The total fraction of life used up per hour is

$$\frac{t_1}{l_1}+\frac{t_2}{l_2}+\ldots\frac{t_n}{l_n}$$

and the socket life of the tube is

$$\text{socket life}=\frac{1}{\dfrac{t_1}{l_1}+\dfrac{t_2}{l_2}+\ldots\dfrac{t_n}{l_n}}$$

Conclusions

For tubes manufactured in any given manner the life will be determined solely by the current drawn. In view of the fact that the tubes do not deteriorate when they are not passing current it seems reasonable to operate them at very large currents if the duty cycle is sufficiently light. It is suggested, therefore, that the most useful type of rating for cold cathode tubes would be to state the current which will give a life of 100, 1,000, and 10,000 hours.

References

1. EIN NEUES RELAIS FUR EXTREM SCHWACHE STROM, H. Richter and H. Geffeken. *Zeitschrift für technische Physik*, volume 7, 1926, pages 601–06.

2. COLD-CATHODE GAS-FILLED TUBES AS CIRCUIT ELEMENTS, S. B. Ingram. AIEE TRANSACTIONS, volume 58, 1939 (July section), pages 342–6.

3. THEORY OF CATHODE SPUTTERING IN LOW VOLTAGE GLOW DISCHARGES, C. H. Townes, presented to the American Physical Society, Providence R. I., June 20, 1941.

4. KATHODENZERSTAUBUNGSPROBLEME, A. von Hipple. *Annalen der Physik*, volume 81, 1926, pages 1043–75.

5. THE VAPOR PRESSURE OF BARIUM, E. Rudberg and J. Lumpert. *Journal of Chemical Physics*, volume 3, 1935, pages 627–31.

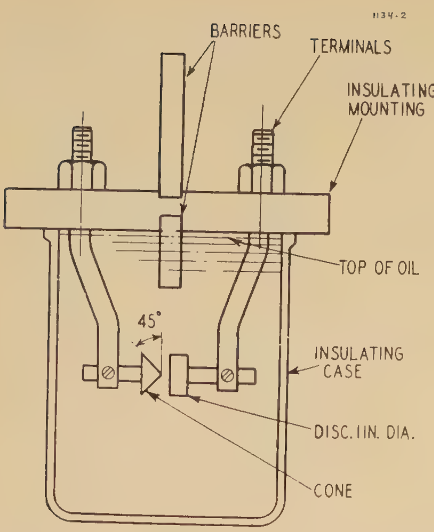

Figure 2. Cone-disc gap used in making tests shown in table II

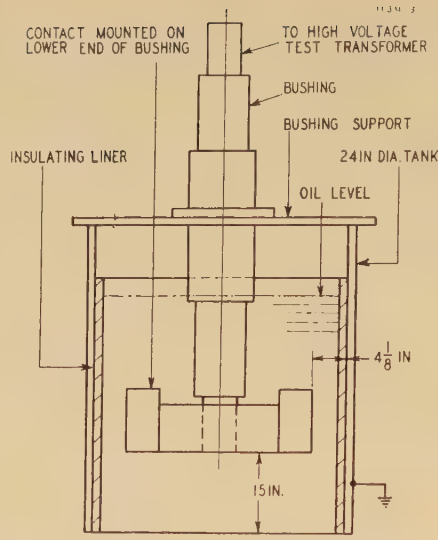

Figure 3. Large gap construction used in making tests in table III

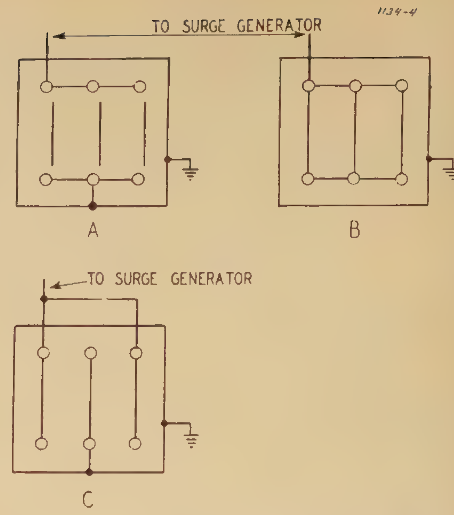

Figure 4. Connections for testing complete circuit breakers 1–10 inclusive, table IV

A. Test on oil across open breaker and to tank

B. Test on all bushings to ground

C. Test phase to phase and to ground

expected from values on oil dielectric strength obtained at 60 cycles in a standard test cup.

To verify this line of reasoning, impulse tests were made on sample gaps with good oil and oil deteriorated by the addition of carbon and moisture, 60-cycle tests were made under similar conditions on a gap much larger than that of the normal test cup, and finally tests were made on completed breakers of commercial design. As will be observed from the data set forth in the tables throughout the paper, these tests indicated in all cases less divergence of dielectric strength than shown in the standard test cup, and in the case of tests on the completed breakers negligible divergence.

Equipment Used

The data used by the authors in preparing this paper were obtained from tests made in the high voltage test laboratories of Westinghouse E.&M. Co. at East Pittsburgh, Pa., and General Electric Company at Schenectady, N. Y., and Philadelphia, Pa.

The oil circuit breakers on which the tests were made were complete commercial designs, sizes, and ratings.

The rod to plane gap was a special gap made by the laboratory and is shown in figure 1. When used for testing, the gap was immersed in a tank of oil.

The cone to disc gap on which tests were made is shown in figure 2.

The wet oil used in making the tests with the cone to disc gap was obtained by forming a saturated solution of water and oil at 80°C. and mixing in measured proportions with oil dried by bubbling dry air through it. The maximum water content was about 250 parts per million.

The used or carbonized oil was obtained from the dirty oil tanks in the laboratory and had previously been used for making oil circuit breaker tests until its dielectric strength had fallen to the point where it was considered necessary to recondition it before further use. In some cases the oil, having been taken from near the bottom of the tank, contained more than the usual amount of foreign material. When let stand without agitation for a short time, these materials tended to settle at the bottom of the tank. This accounts for the fact that in some cases the test value of the oil measured in a standard test cup with 60-cycle voltage varied from 4 to approximately 15 kv.

For the purpose of obtaining data on the dielectric strength of large gaps, using deteriorated oil, a 24-inch circuit breaker tank was filled with oil and a crosshead of corresponding size was supported in the tank in a position corresponding with that which it takes when the breaker is closed. An electrical connection was made to this crosshead through a high voltage bushing, and the tank itself was used as a ground terminal. See figure 3.

Impulse Tests on Rod-to-Plane Gap

Impulse tests were made on a rod to plane gap shown on figure 1. Tests were first made with new oil and then repeated with used oil. The new oil tested about 30 kv in a standard oil test cup. The

Table II. Cone-to-Disk Gap Impulse Tests (See Figure 2)

Ratio of Dielectric Strength Values

	60 Cycles		0.5 M.s.		1.5 M.s.		8 M.s.	
	Std. Gap	Cone Disk Gap	Cone Pos.	Cone Neg.	Cone Pos.	Cone Neg.	Cone Pos.	Cone Neg.
Good oil	1.00	1.00	1.00	1.00	1.00	1.00	1.00	1.00
Carbonized oil	0.43	0.48	0.83	0.89	0.72	0.76	0.60	0.62
Wet oil	0.26	0.40	0.89	0.78	0.89	0.80	0.86	0.70

Table III. Low-Frequency Tests on Large Gaps (See Figure 3)

	Oil Dielectric Standard Test Cup Strength		60-Cycle Test With a Large Gap			
	Kv	Ratio	Voltage Held Quietly (Kv)	Noisy (Kv)	Breakdown Voltage (Kv)	Ratio* Max. Quiet
Good oil	30		130	135	150	
Carbonized oil	9	0.30	115	**	118	0.89
Wet oil	14	0.47	112	115	146	0.86

*The values in this column are the ratios of the maximum voltage held quietly by the deteriorated oil, to the maximum voltage held quietly in good oil.

**No noisy region found between voltage held quietly and breakdown.

used oil was taken from a breaker which had undergone severe interrupting duty. The breakdown of the used oil was erratic, varying from 5 to 15 kv.

In these tests, the gap was immersed in the tank filled first with new oil and then with used oil. The tests indicated that the impulse breakdown of the low test oil was as high as that of the new oil. Tests were made with the gap set at one inch and at two inches with results as given in table I.

The small difference in test voltage shown for the two gaps is possibly due to corona forming on the gap electrode at the higher voltage and reducing the voltage required to break down the longer gap.

Impulse Tests Made With a Cone-to-Disk Gap

The tests were made with a 45° cone disc gap, figure 2, with a spacing of 0.025″ using:

(*a*). Good oil
(*b*). Carbonized oil
(*c*). Wet oil

The tests were made with the time to crest at 0.5 m.s. and 8 m.s.

From these values a figure for 1.5 m.s. has been interpolated for use in connection with the standard impulse wave. Table II shows the ratio of dielectric strength values between the good oil taken as 1.00 and the carbonized and wet oils respectively. Each of the impulse values in table II was determined by making approximately 100 tests.

It will be observed that the presence of carbon or water in the oil does not affect the ratio under impulse conditions to the same extent as under steady state voltage conditions.

Tests Made With 60-Cycle Voltage on Large Spacings

Tests were made to determine how the variation in the dielectric strength of oil as measured by the standard gap is reflected in the dielectric strength of a larger assembly such as an oil circuit breaker; the equipment used in making these tests was described previously, and is shown in figure 3. High potential tests were made to determine what 60-cycle voltage could be held for one minute without breakdown or audible internal disturbance. Results are given in table III.

It will be observed that there is a much lower spread in the dielectric strength of oil in a large gap than might be anticipated from the spread in dielectric strength values with the standard gap.

Impulse Tests on Complete Oil Circuit Breakers With New and Old Oil

Impulse tests were made with a $1^1/_2$–40 m.s. positive wave on 12 complete oil circuit breakers to determine if the impulse strength of breakers would be appreciably lowered by carbon or water or both in the oil. The breakers were tested with new oil and then retested with old oil.

The new oil used to test breakers 1–10 inclusive was taken from standard package containers and tested 30 kv in a standard test cup.[3] The used oil with which these breakers were tested was taken from the dirty oil tanks in the high power laboratory and tested from 4 to 16 kv.

Breakers 1–10 inclusive were small three pole breakers with all three poles in a common tank. The results of the tests on these breakers are given in table IV which follows immediately.

Table IV. Tests on Complete Common Tank Breakers

Tests on Completed Circuit Breakers 1 to 10 Inclusive

Breakers Tested	Lowest Flashover (Kv) New Oil Testing 30 Kv	Lowest Flashover (Kv) Old Oil Testing 4–16 Kv	Highest Full Wave Withstood (Kv) New Oil Testing 30 Kv	Highest Full Wave Withstood (Kv) Old Oil Testing 4–16 Kv
Breaker 1	44	44	46	44.5
" 2	40.5	42.5	41.5	40.5
" 3	51.5	51.5	52.1	52.7
" 4	49	52.1	53.5	54
" 5	63.4	65.5	76	78
" 6	80	83.5	81	84
" 7 Closed	97	97	106	108.5
" 7 Open	102	96	104	97.2
" 8 Closed	122	121	133	122
" 8 Open	115	120	115	127
" 9 Closed	119	118	130	121
" 9 Open	96	97	103	101
" 10	127	127	148	148

All flashovers were outside of breaker.

Each of the above values is the lowest flashover or highest full wave of 15 tests.

Tests on Complete Circuit Breaker 11

Breaker 11 was a single pole of a three pole breaker with each pole in a separate tank. The bushings in this breaker had a higher than usual flashover strength in relation to the breakdown strength of the oil between the contacts and the tank. This condition made it possible to obtain breakdowns through the oil in the tank. The tests were made with the breaker closed and both bushings connected to the surge generator. The results of the tests with oils of different dielectric strength are contained in table V. All tests were made with a $1^1/_2$–40 m.s. positive wave.

Test on Complete Circuit Breaker 12

The tests on breaker 12 were made on poles 1 and 2 of a three pole high voltage frame mounted breaker with each pole in a separate tank. Pole 1 was filled with good oil testing between 26 and 27 kv. Pole 2 was filled with oil taken from breakers in service on the shop lines. This oil tested slightly under 19 kv. For convenience in table VI these oils are considered to have test values of 26 kv and 19 kv respectively. The tests made on breaker 12 and shown in table VI show the 26-kv oil to have a slightly higher impulse breakdown value than the

Table V. Tests on Complete Separate Tank Breaker With Oversize Bushings to Secure Breakdown in Oil

	Oil at 30 Kv	Oil 34.5 Kv at Top and 16 Kv at Bottom	Oil at 23 Kv	Oil at 15–17 Kv
Breaker 11	250 kv *B*	226 kv	217 kv	294
	249 *B*	223	2-220	292
	246 *B*	229	223	297
	238 *B*	240 *B*	227	294
	237 *B*	240	228 *B*	302 *B*
	230 *B*	242	2-233	304 *B*
	235 *B*	245	228	2-293 *B*
	232 *B*	248	229	284
	223 *B*	2-256	231	278
	226 *B*	267	2-235	281
	2-226	272 *B*	244 *B*	287
	222	2-272	237	294
	224	278 *B*	2-236	295
	227	2-278	238	308
	226 *B*		239	2-297
	2-223 *B*		240	2-296 *F*
	225 *B*		242	294 *F*
	223		247 *B*	2-289
	226		2-246	294
	214 *B*		244	301
	212 *B*		2-250	303
	221 *B*		253 *B*	309 *F*
	227		2-260	
	228		2-265	
	226 *B*		265 *B*	
Average	228+	254−	241−	295+

B = Broke down through oil to tank.

F = Flashover bushing outside of breaker.

The numeral 2 appearing at the left of a test indicates that two tests were made.

Table VI. Tests on Complete Separate Tank Breaker With Various Striking Distances in Oil

	Full Striking Distance Through Oil		Striking Distance Through Oil Reduced to 35 Per Cent of Full Amount		Striking Distance Through Oil Reduced to 19 Per Cent of Full Amount	
	Oil at 26 Kv	Oil at 19 Kv	Oil at 26 Kv	Oil at 19 Kv	Oil at 26 Kv	Oil at 19 Kv
Breaker 12	3-351	3-351	3-258	2-258	258 *B*	3-192
	3-392	3-392	3-285	2-285	3-192	3-205
	3-432	3-432	3-312	2-312	3-205	2-218
	2-473*F*	2-473*F*	3-338	3-338	3-226	2-231 *B*
	5-432	452*F*	3-372	3-372	245	3-231
	2-459*F*	452	3-405	2-405	245 *B*	231 *B*
	459*F*	452*F*	446	405	245	231
	459	4-432	2-446*F*	446*F*	245 *B*	231 *B*
	459*F*	432*F*			245	5-244 *B*
	4-540*F*	432			2-258 *B*	
		3-452			2-258	
		452*F*			258 *B*	
		452			2-258	
		4-473*F*			2-258 *B*	
		4-554*F*			285 *B*	
					285	
					285 *B*	
					285	
					4-298 *B*	
					5-234	
					3-264 *B*	
					264	

The numerals 2, 4, 3, 5, appearing at the left of a number indicate the number of tests made at that particular voltage.

19-kv oil. This is contrary to the results obtained on breakers 1 to 11 inclusive and is probably due to the difference resulting from the two oils being tested in different tanks and on different poles of the breaker. All tests were made with the breaker open, one stud impulsed, frame and all other studs grounded. Approximately 15 seconds elapsed between tests. Both poles were tested and the results given in columns 1 and 2 of table VI. In these tests neither oil could be broken down. All flashovers—marked *F*—occurred in air over the outside end of the bushing. The poles under test were then changed by inserting 2″x1/4″ copper bar between the contacts and the tank cover to reduce the breakdown distance through the oil to the tank to 35% of the original distance. The tests in columns 3 and 4 were made and again the flashovers occurred through the air over the outer end of the bushing.

The breakdown distance through the oils was further reduced until it was only 19% of the original distance. Tests shown in columns 5 and 6 of table VI were then made. Breakdowns were obtained on pole 1 in good oil at a minimum of 245 kv. In pole 2 breakdowns were obtained through the 19-kv test oil at a minimum of 231 kv as indicated by the letter—*B*. All tests were made with a 1½–40 m.s. positive wave.

Discussion of Test Results and Conclusions

The test data indicate that the presence in the oil of moisture, carbon, and other materials, normally tending to lower the 60-cycle dielectric strength of oil, appears not to change appreciably the ability of oil circuit breakers to withstand impulse voltages.

Table I shows that the impulse strength of large gaps in oil is practically constant for oils of different dielectric strength, within the range regularly used.

Table II shows that the impulse strength of small gaps in oil varies, but not directly, with the 60-cycle strength of the oil.

Table III shows that the 60-cycle breakdown strength of the breaker is reduced when the dielectric strength of the oil is lowered, but much less than in proportion to the loss of strength in the oils as measured in a standard oil test cup.

Table IV shows that the impulse strength of ten small oil circuit breakers of different types and ratings was not lowered when they were tested with poor oil.

Data in table V, from tests made on a medium size outdoor breaker, show that the impulse strength of an oil circuit breaker might in some cases be better with poor oil than with good oil.

Data in table VI, from tests made on a large outdoor oil circuit breaker, show the impulse strength of large breakers to be practically unaffected by the 60-cycle strength of the oil within the range regularly used.

Oil for circuit breakers and transformers[4] is purchased with a minimum breakdown value of 22,000 volts. Since oil of this or higher strength is most easily obtained, the authors recommend that the oil used for high potential testing of oil circuit breaker, both 60 cycle and impulse, should have a dielectric breakdown strength of 22 kv or higher, the breakdown strength to be determined as prescribed by the American Society for Testing Materials.[3]

It is to be noted that apart from any reduction in dielectric strength resulting directly from the use of deteriorated oil as an insulating medium, there is a tendency for carbon particles to settle out from the oil upon insulating surfaces. This may in time decrease the creepage strength of these surfaces much more than the breakdown strength through the insulating medium is decreased, and constitutes the greatest danger from allowing poor oil to remain in the breaker. Consequently, the test results reported in this paper are not to be interpreted as suggesting any relaxation of maintenance activities in this respect.

References

1. Surge-Voltage Breakdown Characteristics for Electrical Gaps in Oil, Royal W. Sorensen. AIEE Transactions, volume 59, 1940 (February section), pages 78–81.

2. Oil Breakdown at Large Spacings, Douglas F. Miner. AIEE Transactions, volume 46, 1927, page 248.

3. Standard Methods of Testing Insulating Oils. ASTM *Standards* D117-36.

4. ASA Proposed American Standards for Transformers, Regulators, and Reactors. C57. 1-2.050.

Transactions Section

Preprint of Corresponding Pages From the Current Annual Transactions Volume

Any discussion of these papers will appear in the December 1941 "Supplement to Electrical Engineering—Transactions Section"

Conductor Vibration—Theory of Torsional Dampers

JAMES W. SPEIGHT
NONMEMBER AIEE

Synopsis: The paper is a theoretical treatment of the torsional damper which has been applied effectively to the protection of transmission line conductors from fatigue failures due to aeolian vibrations. The formulae of the energy dissipation are derived for three cases, viz., a single rigid damper, two rigid dampers at one end of a span, and a single damper with a resilient joint at the centre of gravity. The results are valuable in understanding the mode of operation of the torsional damper and point to certain optimum features of design. The formulae can be used for numerical calculations when the physical constants are known.

Introduction

FOR many years, electric power companies have been investigating the protection of transmission line conductors from fatigue failures that result from the vibrations excited by steady cross winds of low velocity. The methods of protection that have been proposed are very diversified in character, including the prevention of the vibration at its source with conductors of non-circular cross section, the reduction of concentrated stresses at the clamp by the use of reinforcing cables or rods, and the suppression of the vibrations by the application of damping devices. An energy-absorbing damper has proven to be the most practical solution up to the present time, and has been adopted for a number of lines in North America. An estimate of the efficiency of such devices has been determined, in a few instances, by experimental field studies and, more frequently, by operating experience.

The Hydro-Electric Power Commission of Ontario with power lines of all sizes throughout the province has, of course, been vitally interested in the problem of aeolian conductor vibrations. The need for an effective solution has been most important in recent years since, in modern construction using long spans and high tensions, the conductor is subject to more severe conditions of vibration than in the older construction with short spans and low tensions. To study the effectiveness of various protective schemes, a method was devised for recording the natural vibrations of damped and undamped lines and for analyzing the results statistically. Such experimental data on the frequency characteristics of a type of conductor are essential for the proper design of a protective device for that particular type.

In the year 1935, the theoretical and practical studies indicated that the conductor itself was available to absorb energy, if a suitable restraining force could be applied to the conductor to utilize the interstrand friction and the mechanical hysteresis loss. This force was accomplished with an offset weight attached to the conductor by a horizontal arm, so that a torsional motion was produced between the suspension clamp and point of attachment of the weight when the conductor vibrated. Additional damping was obtained by mounting the offset weights in pairs adjacent to and at different distances from the suspension clamp, when, for most frequencies of vibration, the section of conductor between the two offset weights was also in torsional motion. The torsional device which has become known as a torsional damper has been developed considerably in the last five years and is now practical.

Torsional dampers have been installed for the suppression of aeolian vibrations on the latest ACSR lines built by the Hydro-Electric Power Commission of Ontario. A torsional damper designed for 795,000 cir-mil ACSR is shown in figure 1 and is constructed with a resilient joint of rubber. In California, a rigid type of torsional damper has been adopted for the protection of H-H copper conductor on the exposed sections of the Boulder Dam transmission line.

Theory

The theoretical development of the torsional damper was studied along with the experimental work, and it is the purpose here to derive the theoretical formulae. The formulae were of great assistance in bringing the torsional damper to its present form and are valuable in designing dampers for specific conductors and predicting the approximate performance. The analysis of the torsional damper is limited here to the condition of steady state vibration, and does not include other possible beneficial effects which might exist under initial transient conditions. The reaction of the damper on the motion of the conductor is not taken into account either, since, for the suppression of vibration, the energy dissipative capacity of the damper is of prime importance and is affected only by the amplitude of the motion at the point of attachment, all the other factors being constant. The application of the formulae to actual numerical cases is direct, provided that the requisite physical constants are available.

The mode of vibration at a given point of a line conductor in service usually has a beat characteristic and not a constant maximum amplitude. However, the generality of the analysis is not affected, if it is considered that the conductor vibrates like a perfectly flexible string under tension[1] having the motion

$$\begin{aligned} y &= A_0 \sin (2\pi x/\lambda) \sin \omega t \\ &= A \sin \omega t \end{aligned} \tag{1}$$

Paper 41-94, recommended by the AIEE committee on power transmission and distribution, and presented at the AIEE summer convention, Toronto, Ontario, Can., June 16–20, 1941. Manuscript submitted January 29, 1941; made available for preprinting May 14, 1941.

JAMES W. SPEIGHT is assistant research engineer (physicist) in the laboratories of the Hydro-Electric Power Commission of Ontario, Toronto, Ontario, Can.

1. For all numbered references, see list at end of paper.

where

A_0 is the maximum amplitude
λ is the wave length
ω is the angular velocity $2\pi f$
f is the frequency

The differential equation for free torsional motion is

$$I\ddot{\theta}+q\dot{\theta}+\tau\theta=0 \quad (2)$$

where I is the moment of inertia and τ is the angular elastic constant.

With

$\alpha=q/2I$ and $\omega_c^2=\tau/I$

the solution is

$$\theta=B_e^{-\alpha t}\sin(\omega t+\phi)$$

in which B and ϕ are constants and $\omega^2=\omega_c^2-\alpha^2$. If $\alpha\ll\omega_c$,

$$\omega^2\approx\omega_c^2=\tau/I$$

Therefore, the quantity q which will be defined as the "torsional resistance" is given by

$$q=\delta\tau/\pi\omega \quad (3)$$

because $\alpha=\delta f$ where δ is the logarithmic decrement.[3]

For a rod of circular cross section, the angular elastic constant is inversely proportional to the length of the rod.[2,3] Hence, it is evident from relation 3 that the torsional resistance of a conductor is increased by decreasing the length of the effective part of the conductor.

Single Rigid Damper

The position of a single rigid damper at any moment can be represented as in figure 2. The notation is

M = mass of damper
$I=MK^2/g$ = moment of inertia about the axis of the conductor
$I_G=Mk^2/g$ = moment of inertia about the centre of gravity
l = distance from the centre of conductor to centre of gravity
θ = angular displacement from the horizontal
$y=A\sin\omega t$ = displacement of the point of support
h = distance of centre of gravity from position of equilibrium
$K^2=k^2+l^2$

The velocity of the centre of gravity for small oscillations is $(\dot{y}-l\dot{\theta})$. Considering the transverse energy of the conductor to be independent of θ, the kinetic energy of the damper is

$$S=M(\dot{y}-l\dot{\theta})^2/2g+I_G\dot{\theta}^2/2$$

The potential energy associated with the torsional motion is

$$\tau(\theta+\theta_0)^2/2-\tau\theta_0^2/2=\tau\theta^2/2+Ml\theta \quad (4)$$

since θ_0 is the static rotation and $Ml=\tau\theta_0$. The increase in the gravitational potential energy of the mass is

$$Mh\approx M(y-l\theta) \quad (5)$$

Therefore, the potential energy function is, adding 4 and 5,

$$V=\tau\theta^2/2+My$$

The Lagrangian function is $L=S-V$ and, from Lagrange's equation[4]

$$\frac{d}{dt}\left[\frac{\partial L}{\partial\dot{\theta}}\right]-\frac{\partial L}{\partial\theta}=0 \quad (6)$$

it follows that, adding the dissipative term,

$$\ddot{\theta}+2\alpha\dot{\theta}+\omega_c^2\theta=l\ddot{y}/K^2 \quad (7)$$

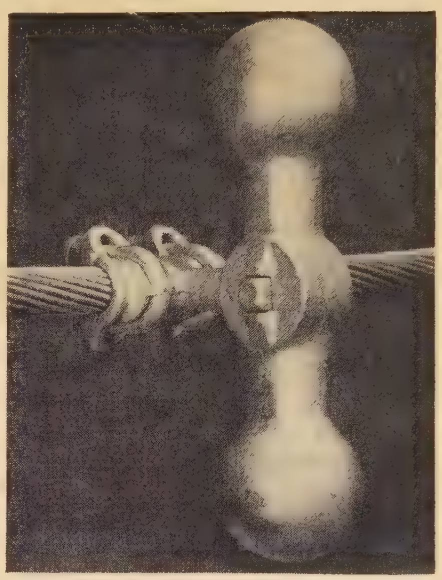

Figure 1. Torsional damper for 795,000-circular-mil steel-reinforced aluminum cable

The steady state solution of differential equation 7 is

$$\theta\doteq-\frac{lA\omega^2}{K^2Z}\sin(\omega t-\beta) \quad (8)$$

with

$$Z^2=(\omega_c^2-\omega^2)^2+4\alpha^2\omega^2$$

and

$$\beta=\tan^{-1}[2\alpha\omega/(\omega_c^2-\omega^2)]$$

The power dissipation is

$$P=\frac{1}{T}\int_0^T q\dot{\theta}^2dt$$
$$=ql^2A^2\omega^6/2K^4Z^2 \quad (9)$$

The graph of the frequency function $f^6/[\pi^2(f_c^2-f^2)^2+\alpha^2f^2]$ contained in equation 9 for constant amplitude is plotted in figure 3 with $f_c=5$ cps. and $\alpha=4$. Actually, most materials dissipate energy by solid damping[3] and then δ, not α, is constant with respect to frequency. From the curve, it is seen that to suppress a range of frequencies the damper has to operate on the region above f_c, i.e.,

$$\omega_c<\omega \quad (10)$$

In determining the damper spacing, the amplitude A which is a function of the frequency is considered in conjunction with the other factors. As a numerical example, let the velocity of propagation (λf) be 400 ft./sec. and the damper be 5 feet from the clamp. For a frequency range 5 to 20 cps.,

$$1\geq\sin(2\pi x/\lambda)>0.38$$

and the power loss at 20 cps. due to this

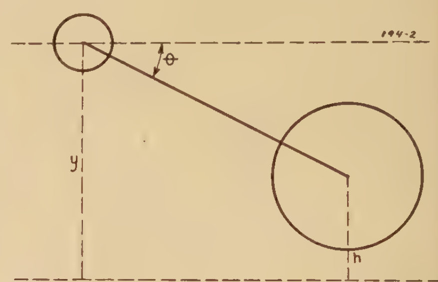

Figure 2. Schematic diagram of a single rigid damper in motion

factor is about seven times that at 5 cps. The magnitude of the divergence is reduced greatly, in practice, because the power loss associated with the transverse vibrations of a conductor excited by the wind increases rapidly with frequency and, consequently, the amplitude A_0 becomes smaller.[5] Thus, the spacing of 5 feet gives a satisfactory response to the frequency variations under these conditions.

If the condition $\omega_c\ll\omega$ is maintained, the optimum value of l is given by

$$\frac{d}{dl}(l^2/K^4)=0$$

or,

$$l=k \quad (11)$$

Then, the maximum power is

$$P_M=qA^2\omega^6/8l^2Z^2$$

from which it is deduced that the optimum optimum magnitude of l is the smallest value consistent with conditions 10 and 11.

For a damper with a heavy, concentrated mass and a long arm, $K\rightarrow l$; $\beta\rightarrow\pi$; $Z\rightarrow\omega^2$ and

$$\theta=(A/l)\sin\omega t$$

i.e., the centre of gravity remains stationary in space. This effect is observed in the field for the stated conditions. The power

dissipation for this case, substituting the value of q, becomes

$$P=\delta\tau f A^2/l^2$$

Two Rigid Dampers at One End of Span

In figure 4, the arrangement of two dampers having the same physical dimensions is shown schematically for the horizontal plane. The notation of the previous section is adopted with the subscripts 1 and 2 referring respectively to dampers 1 and 2. The quantities τ_1, τ_2 and τ_3 represent the angular elastic constants for the three sections of the conductor between the clamps and the two dampers. The displacements at the points of attachment are

$$y_1=A_1\sin\omega t$$

$$y_2=A_2\sin\omega t$$

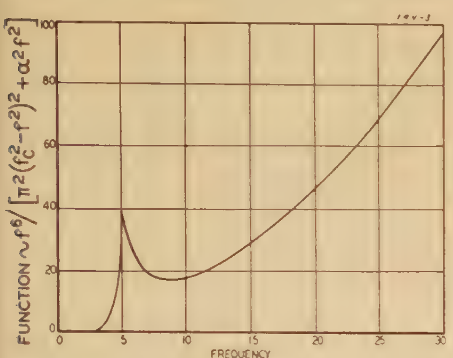

Figure 3. Graph of function for $f_c=5$ cycles per second and $\alpha=4$

The kinetic energy of the system is

$$S=(M/2g)[(\dot{y}_1-l\dot{\theta}_1)^2+(\dot{y}_2-l\dot{\theta}_2)]+I_G(\dot{\theta}_1^2+\dot{\theta}_2^2)/2 \quad (12)$$

Disregarding the gravitational potential energy function which does not contribute to the motion, the potential energy is

$$V=\tau_1\theta_1^2/2+\tau_2(\theta_1+\theta_2)^2/2+\tau_3\theta_2^2/2 \quad (13)$$

If the mutual torsional resistance is designated by q_3, the differential equations of motion with the dissipative terms are

$$\ddot{\theta}_1+2\alpha_1\dot{\theta}_1+\omega_1^2\theta_1+2\alpha_3\dot{\theta}_2+\Omega^2\theta_2=l\ddot{y}_1/K^2$$

$$\ddot{\theta}_2+2\alpha_2\dot{\theta}_2+\omega_2^2\theta_2+2\alpha_3\dot{\theta}_1+\Omega^2\theta_1=l\ddot{y}_2/K^2$$

with

$$\omega_1^2=(\tau_1+\tau_2)/I \quad \text{and} \quad \alpha_1=q_1/2I$$

$$\omega_2^2=(\tau_2+\tau_3)/I \qquad \alpha_2=q_2/2I$$

$$\Omega^2=\tau_2/I \qquad \alpha_3=q_3/2I$$

Making the substitutions

$$N_1e^{j\beta}=A_1(\omega_2^2-\omega^2)-A_2\Omega^2+2j\omega(\alpha_2A_1-\alpha_3A_2)$$

$$N_2e^{j\gamma}=A_2(\omega_1^2-\omega^2)-A_1\Omega^2+2j\omega(\alpha_1A_2-\alpha_3A_1)$$

$$De^{j\epsilon}=(\omega_1^2-\omega^2)(\omega_2^2-\omega^2)-\Omega^4+4\alpha_3^2\omega^{\prime\prime}-4\alpha_1\alpha_2\omega^2+2j\omega[\alpha_1(\omega_2^2-\omega^2)+\alpha_2(\omega_1^2-\omega^2)-2\alpha_3\Omega^2]$$

it follows that

$$\theta_1=-\frac{l\omega^2N_1}{K^2D}\sin(\omega t+\beta-\epsilon)$$

$$\theta_2=-\frac{l\omega^2N_2}{K^2D}\sin(\omega t+\gamma-\epsilon)$$

The power dissipated by the two dampers is

$$P=\frac{1}{T}\int_0^T[(q_1\dot{\theta}_1+q_3\dot{\theta}_2)\dot{\theta}_1+(q_2\dot{\theta}_2+q_3\dot{\theta}_1)\dot{\theta}_2]dt$$

$$=\frac{l^2\omega^6}{2K^4D^2}[q_1N_1^2+2q_3N_1N_2\cos(\beta-\gamma)+q_2N_2^2] \quad (14)$$

It is interesting to observe that the second term may increase or decrease the energy loss depending on whether N_1 and N_2 have the same phase or opposite.

If the moment of inertia is large and the arm is relatively long, the following approximations hold

$$\left.\begin{array}{l} N_1\rightarrow A_1\omega^2 \\ N_2\rightarrow A_2\omega^2 \\ D\rightarrow\omega^4 \\ K\rightarrow l \\ \beta\rightarrow\gamma\rightarrow\pi \\ \epsilon\rightarrow 0 \end{array}\right\} \quad (15)$$

Therefore, from equation 14,

$$P=\frac{\omega^2}{2l^2}(q_1A_1^2+2q_3A_1A_2+q_2A_2^2) \quad (16)$$

From relation 13 and the fact that the logarithmic decrement is equal to the energy loss per cycle divided by twice the maximum potential energy,[3] the power dissipation for conditions 15 may also be written

$$P=\frac{\delta f}{l^2}[(\tau_1+\tau_2)A_1^2+2\tau_2A_1A_2+(\tau_2+\tau_3)A_2^2] \quad (17)$$

The corresponding coefficients in expressions 16 and 17 are identical, so that the torsional resistances are

$$q_1=\delta(\tau_1+\tau_2)/\pi\omega$$

$$q_2=\delta(\tau_2+\tau_3)/\pi\omega$$

$$q_3=\delta\tau_2/\pi\omega$$

Single Damper With Resilient Joint at Center of Gravity

The inherent damping in some conductors is not sufficient in itself to suppress the vibrations adequately, even with two rigid dampers. Supplementary damping is introduced then by making a resilient joint near the centre of gravity with a material of high damping such as rubber. To facilitate the analysis, the damper is assumed to have the joint at the centre of gravity as in figure 5. In practice, the dampers are installed at both ends of the span and the power dissipation per span is twice the derived formula.

The notation will be the same as before with the subscript r designating the physical constants of the resilient material. The kinetic energy at any moment is

$$S=Mk^2\dot{\Phi}^2/2g+M(\dot{y}-l\dot{\theta})^2/2g$$

The potential energy is

$$V=\tau\theta^2/2+\tau_r(\Phi-\theta)^2/2$$

The damping force of the resilient joint is proportional to the relative angular velocity $(\dot{\Phi}-\dot{\theta})$. Hence, the differential equations of motion including the dissipative terms become

$$\ddot{\Phi}+2\alpha_r(\dot{\Phi}-\dot{\theta})+\omega_r^2(\Phi-\theta)=0 \quad (18)$$

$$\ddot{\theta}+2\alpha_N\dot{\theta}-2\alpha_r\frac{k^2}{l^2}(\dot{\Phi}-\dot{\theta})+\left(\omega_N^2\theta-\omega_r^2\frac{k^2}{l^2}(\Phi-\theta)=\ddot{y}/l\right)$$

where

$$\alpha_N=qg/2Ml^2$$

$$\alpha_r=q_rg/2Mk^2$$

$$\omega_N^2=\tau g/Ml^2$$

$$\omega_r^2=\tau_rg/Mk^2$$

But

$$y=A\sin\omega t$$

Therefore, making the substitutions

$$Q_1e^{j\mu}=\frac{A\omega^2}{l}(\omega_r^2-\omega^2+2j\alpha_r\omega)$$

$$Q_2e^{j\nu}=\frac{A\omega^2}{l}(\omega_r^2+2j\alpha_r\omega)$$

$$\Delta e^{j\zeta}=(\omega_r^2-\omega^2)(\omega_N^2-\omega^2)-\omega^2\omega_r^2k^2/l^2-4\alpha_N\alpha_r\omega^2+2j\omega[\alpha_N(\omega_r^2-\omega^2)+\alpha_r(\omega_N^2-\omega^2-\omega^2k^2/l^2)]$$

it follows that

$$\left.\begin{array}{l} \theta=-\dfrac{Q_1}{\Delta}\sin(\omega t+\mu-\zeta) \\ \Phi=-\dfrac{Q_2}{\Delta}\sin(\omega t+\nu-\zeta) \end{array}\right\} \quad (19)$$

The undamped natural frequencies of the damper are obtained by equating Δ, with the α-terms eliminated, to zero, i.e.,

$$f^4-f^2(f_N^2+f_r^2+f_r^2k^2/l^2)+f_r^2f_N^2=0 \quad (20)$$

The damper is designed so that the lower natural frequency is below the range of frequencies to be suppressed, as discussed in relation to figure 3. When

the torsional resistance of the resilient material is greater than that of the conductor, the range of frequencies below the higher natural frequency of equation 20 will not be suppressed adequately if the mode of vibration about the conductor has the lower frequency. In such a case, it is necessary to decrease the frequency f_r of the mode associated with the resilient material.

The rate of energy dissipation is

$$P=\frac{1}{T}\int_0^T [q\dot{\theta}^2+q_r(\dot{\theta}-\dot{\Phi})^2]dt$$

$$=\frac{\omega^2}{2\Delta^2}[qQ_1^2+q_r\{Q_1^2+Q_2^2-2Q_1Q_2\cos(\mu-\nu)\}] \quad (21)$$

The last term approaches a maximum contribution as $(\mu-\nu)\rightarrow\pi$, and its minimum as $(\mu-\nu)\rightarrow 0$. For an undamped condition, equation 18 can be written

$$(\omega_r^2-\omega^2)\Phi=\omega_r^2\theta$$

It is evident that $\theta=-\Phi$ is possible, in this case, only at one frequency, viz., $f=\sqrt{2}f_r$. The relation $\theta=\Phi$ can exist if $f=0$ or ω_r is very large. The first condition is not satisfied; the second is present for a large τ_r and the device would be a rigid damper. Consequently, the resilient joint has a dissipative effect at all operating frequencies, although it reaches a maximum displacement only at a unique frequency.

For a large mass, which is necessary to obtain the low undamped natural frequency, and a high conductor frequency, the following approximations hold:

$$Q_1\rightarrow A\omega^4/l$$
$$Q_2\propto\omega^3$$
$$\Delta\rightarrow\omega^4$$
$$\mu\rightarrow\pi$$
$$\nu\rightarrow\pi/2$$
$$\zeta\rightarrow 0$$

With these values, equations 19 and 21 become

$$\Phi\approx 0$$

$$\theta=(A/l)\sin\omega t$$

$$P=\frac{\omega^2A^2}{2l^2}(q+q_r)$$

Using the mathematical reasoning of the previous section and relation 3, it can be shown that

$$q=\delta\tau/\pi\omega$$

$$q_r=\delta_r\tau_r/\pi\omega$$

Physical Constants

The logarithmic decrement and angular elastic constant are required for numerical computations and can be found experimentally, in one way, from the decrement curves of free torsional motion.

To illustrate the magnitude of these quantities: For a 795,000 cir-mil ACSR, $\delta\approx 0.19$ and τ per foot varies from 230 lb.-ft./rad. at 3,000 pounds tension to 360 lb.-ft./rad. at 5,700 pounds tension. For a 336,000 cir-mil ACSR, $\delta\approx 0.20$ and τ per foot is 46 lb.-ft./rad. at 1,200 pounds tension increasing to a constant value of 78 lb.-ft./rad. at approximately 3,600 pounds tension.

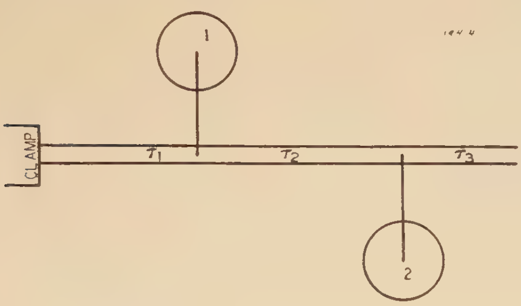

Figure 4. Schematic arrangement of two rigid dampers at one end of a span (horizontal plane)

Summary

In the theoretical treatment of the torsional damper, the following conclusions pertaining to the general design of dampers have been deduced:

1. The angular elastic constant and, thus, the torsional resistance are inversely proportional to the length of effective conductor.

2. The undamped natural frequency of the damping system has to be below the lowest prevalent conductor frequency to be suppressed.

3. The damper is placed at the point of highest amplitude, consistent with maintaining a low natural frequency and a high torsional resistance. The effect of amplitude variations over the frequency band on the determination of spacing is not very critical, because the damper has to be effective over such a large range of loop lengths (possibly 5 to 50 feet).

4. For a rigid damper, the distance from the centre of the conductor to the centre of gravity should be as short as possible and equal to the radius of gyration about the centre of gravity. The damper, applied singly, should be placed near the clamp and still satisfy conclusions 2 and 3.

5. With the arrangement of figure 4, the two rigid dampers are mounted in the same loop in order to take advantage of the mutual dissipation. The optimum spacings, which will be short for large torsional resistances, could be determined by calculation for specific cases.

6. The single damper with a resilient joint is required for conductors having a small damping capacity. This type of damper has an advantage over the rigid type in that the damping factor of the resilient material can be varied, whereas that of the conductor is fixed. The spacing for this device is found in the same manner as for the rigid damper. As an example, the torsional damper of figure 1 is installed 6 feet from the clamp on 795,000 cir-mil ACSR.

Appendix

The rigid analysis of the motion of a single rigid damper will be developed to show that the above solutions are approximations strictly valid for short spans.

The torsional wave equation

$$\frac{\partial^2\theta}{\partial t^2}=a^2\frac{\partial^2\theta}{\partial x^2}$$

in which

$a^2=Gg/\gamma$ = velocity of propagation squared
G = modulus of rigidity
γ = weight per unit volume

has a solution of the form

$$\theta=X\sin\omega t$$

Let one end of a span of length s be the origin and the damper be placed a distance b from the origin. For the end conditions

$$\theta=0 \text{ at } x=0 \text{ and } x=s,$$

the space function can be written

$$X_1=C\sin\frac{\omega x}{a}; \qquad 0\geq x\geq b$$

$$X_2=D\sin\frac{\omega(x-s)}{a}; \quad b\geq x\geq s$$

The conditions to be satisfied at $x=b$, with I_p representing the moment of inertia of the area of cross section of the conductor, are

$$\left.\begin{aligned}&\theta_1=\theta_2\\&I\frac{\partial^2\theta_1}{\partial t^2}=-GI_p\left[\frac{\partial\theta_1}{\partial x}-\frac{\partial\theta_2}{\partial x}\right]\end{aligned}\right\} \quad (22)$$

Eliminating C and D, the natural frequencies are given by

$$\tan\frac{\omega(b-s)}{a}\left[\tau'\cot\frac{\omega b}{a}-a\omega I\right]=\tau'$$

where

$$\tau'=GI_p$$

For a practical installation, $s\gg b$ and b is small. Then, with $\beta=\omega s/a$,

$$\tan\beta=\frac{\tau'b\beta}{\beta^2a^2bI/s-\tau's} \quad (23)$$

having consecutive roots $\beta_i(i=1, 2, 3\ldots.)$.

When β has a value such that $\tan\beta \rightarrow \beta$, the natural frequency becomes

$$\omega_c^2 \approx \tau'/bI \qquad (24)$$

which agrees with the approximate theory.

For forced oscillations, the solution in generalized co-ordinates is

$$\theta_1 = \sum_{i=1}^{i=\infty} x_i \sin\frac{\beta_i x}{s} : \qquad 0 \geq x \geq b$$

$$\theta_2 = \sum_{i=1}^{i=\infty} x_i \left(\frac{D}{C}\right)_{\substack{\beta=\beta_i \\ x=b}} \sin\frac{\beta_i(x-s)}{s} : b \geq x \geq s$$

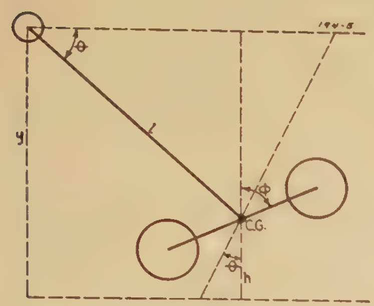

Figure 5. Schematic diagram of a damper with a resilient joint at the center of gravity

The potential energy function is

$$V = \frac{\tau'}{2}\left[\int_0^b \left(\frac{\partial\theta_1}{\partial x}\right)^2 dx + \int_b^s \left(\frac{\partial\theta_2}{\partial x}\right)^2 dx\right]$$

$$= \tau'\beta_i(A_i + B_i)x_i^2/8S^2$$

with

$$A_i = 2\beta_i\left[b - (b-s)\left(\frac{D}{C}\right)^2_{\substack{\beta=\beta_i \\ x=b}}\right]$$

$$B_i = s\left[\sin\frac{2\beta_i b}{s} - \left(\frac{D}{C}\right)^2_{\substack{\beta=\beta_i \\ x=b}} \sin\frac{2\beta_i(b-s)}{s}\right]$$

The kinetic energy function is

$$S = \frac{\gamma I_p}{2g}\left[\int_0^b \left(\frac{\partial\theta_1}{\partial t}\right)^2 dx + \int_b^s \left(\frac{\partial\theta_2}{\partial t}\right)^2 dx\right] + \frac{I_G}{2}\dot{\theta}_{x^2=b} + \frac{M}{2g}(\dot{y} - l\dot{\theta})_{x^2=b}$$

$$= \left[\frac{\gamma I_p(A_i - B_i)}{8g\beta_i} + \frac{I_G}{2}\sin^2\frac{\beta_i b}{s}\right]\dot{x}_i^2 + \frac{M}{2g}\left(\dot{y} - l\dot{x}_i \sin\frac{\beta_i b}{s}\right)^2$$

Applying Lagrange's equation, the differential equation for x_i is:

$$\left[\frac{\gamma I_p(A_i - B_i)}{4g\beta_i I} + \sin^2\frac{\beta_i b}{s}\right]\ddot{x}_i + \frac{\tau'\beta_i(A_i + B_i)}{4I_S^2} x_i = \frac{l\ddot{y}}{K^2}\sin\frac{\beta_i b}{s}$$

For the condition $\tan\beta \rightarrow \beta$

$$A_i \rightarrow B_i \rightarrow 2\beta_c b$$

and the differential equation simplifies to

$$\left(\sin\frac{\beta_c b}{s}\right)(\ddot{x}_c + \omega_c^2 x_c) = l\ddot{y}/K^2$$

Hence, for $K \rightarrow l$ and $\omega \gg \omega_c$

$$\theta_{x=b} = (A/l)\sin\omega t$$

The general solution of torsional dampers with the damping constants is obviously complex. The single natural frequency of the approximate solution is replaced by a series of frequencies in the general solution of a long span, since the distributed mechanical system of the conductor becomes a major part of the vibratory system. However, the lowest natural frequency of equation 23 is less than that of equation 24 for long spans and a damper designed for the approximate conditions will be effective when $\tan\beta \neq \beta$.

References

1. Principles of Mathematical Physics (a book), Houston, McGraw-Hill Publishing Company.

2. General Physics for Students (a book), Edser. Macmillan and Company.

3. Vibration Prevention in Engineering (a book), Kimball. John Wiley and Sons.

4. Vibration Problems in Engineering (a book), Timoshenko. D. Van Nostrand Company.

5. Laboratory Studies of Conductor Vibration, J. S. Carroll. AIEE Transactions, volume 55, 1936 (May section), page 543.

6. Dynamics of a Particle and of Rigid Bodies (a book), Loney. Cambridge University Press.

7. Vibration of Cables and Dampers, R. G. Sturm. AIEE Transactions, volume 55, 1936, part I, (May section), page 455; part II, (June section), page 673.

8. Vibration and Fatigue in Electrical Conductors, A. E. Davison, J. A. Ingles, and V. M. Martinoff. AIEE Transactions, volume 51, 1932, page 1047.

9. Conductor Vibration—Experience on Overhead Lines in North America, G. W. Preston. *The Electrician*, October 15, 1937.

10. Partial Differential Equations (a book) Bateman. Cambridge University Press.

The Protection of Solid Insulation by Lightning Arresters

D. D. MacCARTHY
ASSOCIATE AIEE

T. J. CARPENTER
ASSOCIATE AIEE

Introduction

THE protection of distribution transformers or other apparatus against lightning involves the basic problem of limiting the voltage applied to the insulation to a value adequately below the insulation strength. The effect on insulation of chopped waves and full waves of standard impulse wave shapes such as 1.5x40 microseconds has been thoroughly investigated in the past. However, there has been a lack of the information necessary to compare the effect of chopped waves with the effect of voltages of other than standard wave shape resulting from arrester breakdown followed by the impedance drop that occurs during the impulse current discharge. Also there have been little data available on the failure of low voltage insulation. For these reasons an investigation has been made using oil immersed solid insulation of a type used in distribution transformers. The puncture voltage and number of shots to failure were determined when the insulation was in parallel with lightning arresters or gaps which controlled the wave shape of the voltage applied to the insulation. These results have been correlated with the single shot puncture voltage determined from tests in which failure occurred on the wave front. It was found that repeated applications of voltages in excess of approximately 70 per cent of the single shot puncture voltage may damage the insulation.

Insulation Samples

The insulation tested consisted of pads of 10- by 10-inch sheets of kraft paper 5 mils in thickness. Thin sheets of paper were used so that the failure voltage could be varied in small steps by changing the number of sheets in series. The line electrodes were pancake coils 2 inches in outer diameter and 1 inch in inner diameter wound from 85- by 155-mil copper, see figure 1. The turns of the line electrodes were wrapped with paper insulation of a type used in transformers. This insulation raised the corona voltage and made the failure voltage of the insulation pads less erratic. The turns of the coils were tied with 15-mil thread since thread and tape are sometimes used on transformer coils. The maximum thickness of the coil insulation at points of contact with the paper was about 20 mils but was variable due to the thread and the paper wrapping. At the ends of the coil, the copper strips were bent perpendicular to the plane of the coil and brought up through a 15-lb cylindrical weight 2 inches in outside diameter used to assure good contact. These leads were connected in parallel to the impulse generator. The pads were immersed in transformer oil in a metal tray that served as the ground electrode. Both the coils and the paper were vacuum treated and oil impregnated before the tests to eliminate moisture and absorbed air. The samples were kept under oil at all times until failure. Although all of the materials in the pads are used for certain types of insulation in transformers, the pads as tested cannot be considered[1] as representing the actual insulation strength of transformers, since in transformers steep impulse waves may result in an unequal distribution of voltage along the turns and the major insulation does not consist of paper sheets alone. In designing the insulation test pieces, it was necessary to consider the requirement of simulating transformer insulation and the additional requirements of simplicity of construction to permit ready observation of the failure, and low cost so that a large number of samples could be tested.

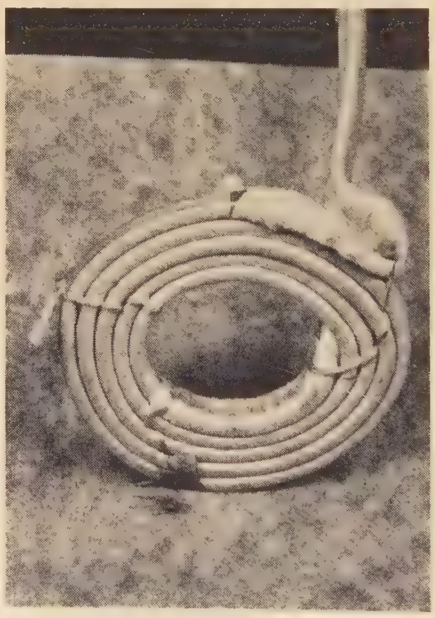

Figure 1. Insulation sample after puncture

A line electrode turned on edge to expose puncture and a small section of the sheet of 10- by 10-inch kraft paper used are shown. The bottom of an oil-filled metal tray formed the ground electrode

Single-Shot Puncture Tests

Tests in which puncture occurred on the wave front were made with impulse voltages of negative polarity that rose at a uniform rate until chopped by insulation puncture. A new line electrode and new sheets of paper were used for each test. The puncture voltage and time were determined, by means of cathode ray oscillograms, see figure 2, for line electrodes alone and line electrodes in series with pads of two, five, and eight sheets of paper. As the thickness of the insulation pads was changed the constants of the impulse generator circuit were adjusted so as to produce puncture at approximately the desired time. In those cases where the wave initially departed from a uniform rate of rise, the virtual zero was determined by a chord through the 30 and 90 per cent points on the voltage oscillogram. The results are plotted in figure 3. The failure in all cases was due to puncture through the paper and tended to occur near the outside of the line electrodes; corona was observed during tests of pads with five and eight sheets of paper.

Since it is desirable to base average curves on all of the available test data, the test results were correlated by means of figure 4 in which the average puncture voltage for failure times of 0.2, 1, and 8 microseconds was plotted against the paper thickness. The solid line curves of figure 3 give the puncture voltage from tests on line electrodes alone and pads with two, five, and eight sheets of paper; all of the original data points were plotted. The broken line curves for three, four, six, and seven sheets were obtained by interpolation from figure 4.

From figure 3 the puncture voltage at

Paper 41-133, recommended by the AIEE committee on protective devices, and presented at the AIEE summer convention, Toronto, Ontario, Can., June 16–20, 1941. Manuscript submitted April 15, 1941; made available for preprinting May 15, 1941.

D. D. MacCarthy and T. J. Carpenter are both with the lightning arrester engineering department, General Electric Company, Pittsfield, Mass.

1. For all numbered references, see list at end of paper.

0.25 microsecond is about 116 per cent of the value at 1 microsecond. Tests by Montsinger[1] gave a ratio of 160 per cent for the failure voltages at the same value of time. It is suggested that this difference is due to the considerable differences in the structure of the insulation samples tested in the two investigations and to differences in the applied voltage waves. Montsinger's tests were made on insulation barriers 0.64 and 2.5 inches in total thickness with relatively large oil ducts; the samples were designed to simulate the major insulation used in high voltage transformers.

From figure 4, it is evident that the average puncture voltage increased linearly with the total thickness of the paper sheets in the pad. This is evidence that the strength of the individual paper sheets and the distribution of voltage were uniform. Although the line electrode insulation measured 20 mils in thickness including the thread, it had a puncture voltage equivalent to 7.5 mils of the 5-mil paper. Failure tended to occur at the threads presumably due to a concentration of stress.

Puncture of Insulation in Parallel With Arresters or Gaps

A second series of tests was made with pads in parallel with 9-kv distribution arresters or gaps set for values of impulse breakdown within the range permitted by lightning protective devices used on 6,900-volt circuits. Several types of gaps were used among which were $^1/_2$-inch square rod gap set at $^{61}/_{64}$ inch and $2^1/_{16}$ inches; and sphere gaps 6.25 centimeters in diameter set at 16 millimeters. Cathode ray oscillograms were taken to show the failure voltage and time, see figure 5. A new line electrode and new sheets of paper were used for each test but not for each impulse. Although the applied impulse voltage wave was changed during the series of tests, each individual sample was punctured by repeated applications of the same voltage wave except that the tests were stopped in three cases after 100 or more shots. A total of 95 pads was tested and the results are summarized in the tabulation. In all tests the applied voltage rose at an approximate rate of 500 kv per microsecond until reduced by the arrester or gap or by puncture of the insulation. The rate of 500 kv per microsecond exceeds the rate of 100 kv per microsecond recommended in the appendix to "Standards for Testing Lightning Arresters," ASA C-62, and is perhaps representative of the steeper rates to which distribution arresters in service are

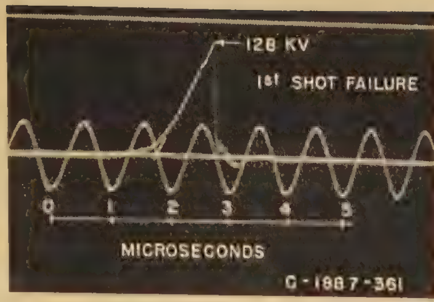

Figure 2. Volt-time oscillogram taken during single-shot puncture tests on eight sheets of 0.005- by 10- by 10-inch paper

subjected. The gap and arrester breakdown voltages in the tabulation exceed the values obtained from tests with voltages rising at 100 kv per microsecond. For example the 9-kv valve type arresters have a breakdown voltage of approximately 50 kv on the 100 kv per microsecond tests whereas a breakdown of 69 kv is given in the table for the 500 kv per microsecond wave. The time to breakdown of the arresters or gaps ranged from 0.13 to 0.30 microsecond on the 500 kv per microsecond wave. These values of time to breakdown of the arresters or gaps are small compared to the range of one to four microseconds required for the *IR* voltage to reach crest and are still smaller in comparison with the duration of the *IR* voltages produced by current discharges that decayed to half value in 40 microseconds.

When arresters were used, the impulse current had a crest of 5,000 amperes, an initial rate of 2,200 amperes per microsecond, and a time to half value of 40 microseconds. The value of 5,000 amperes crest was chosen for the current since 88 per cent of the discharge currents measured[2] through rural distribution arresters in service did not exceed this value. While comparatively little information is available[3] on rates of rise and duration of currents discharged by arresters in service, it is believed that the impulse discharge used in these tests was of more than average severity.

When gaps were tested, the impulse discharge current crest was 500 amperes or less and the time to half value was 40 microseconds. The value of approximately 500 amperes was selected for the magnitude of the discharge current as a matter of convenience and to give arc voltages and inductive drops that were small. For part of the tests, wire-wound resistors of 120 to 150 ohms were connected in series with the gaps to study the effect of *IR* voltage on insulation failure. Cathode ray oscillograms, see figure 5, showed whether the insulation failure occurred as the voltage was rising to gap breakdown or during the subsequent application of *IR* voltage to the insulation.

Comparison of Test With and Without IR Voltage

By means of the data in the tabulation, it is possible to compare the effect on insulation failure of breakdown voltage without subsequent *IR* voltage, with the effect of breakdown voltage followed by *IR* voltage. The per cent of single shot puncture voltage given in the tabulation is the ratio of the breakdown or *IR* voltage applied to the pad to the average single shot voltage determined from figure 3 for a pad with the same number of sheets. When valve arresters were tested the crest *IR* voltage occurred at one to two microseconds so the single shot puncture voltage curves were read at 1.5 microseconds; the wire-wound resistors gave crest *IR* voltages at two to four microseconds, and the curves were read at 3.0 microseconds. In tests 1 and 2 with valve type arresters puncture always occurred as the voltage was rising to gap breakdown; two-sheet pads failed in 1 to 5 shots and three-sheet pads in 3 to 14 shots. In test 3 with gaps set for

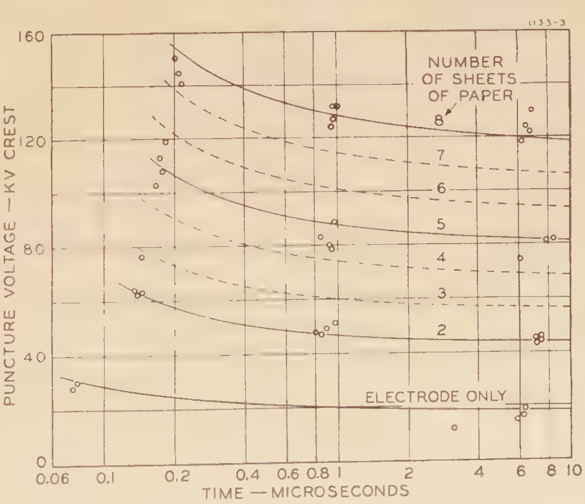

Figure 3. Volt-time curves for single-shot puncture from front-of-wave tests

The solid lines are the average volt-time curves from the original data as correlated by figure 4. All original data are plotted

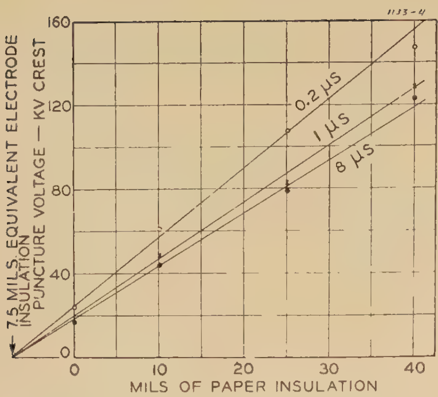

Figure 4. Average single-shot puncture voltage from front-of-wave tests

nearly the same impulse breakdown as in tests 1 and 2 but having no *IR* drop, two-sheet pads failed in one shot. In test 4, six of the three-sheet pads failed in one to nine shots (see footnote in tabulation) and the seventh pad withstood an abnormal number of shots. A comparison of tests 1 and 2 with tests 3 and 4 shows that valve arrester *IR* drops of 74 and 58 per cent of the average single shot puncture voltage did not reduce the number of shots required to fail the insulation.

However, it is evident that the *IR* voltage if sufficiently high will reduce the number of shots the insulation can withstand. This is seen from tests 4, 5, and 6 and tests 7, 8, and 9. The gap breakdown voltage was approximately equal for the three tests 4, 5, and 6. Test 4 was made with no *IR* voltage. In test 5 the *IR* voltage was 84 per cent of the single shot strength and puncture occurred on the *IR* voltage in two out of the seven tests. In test 6 with an *IR* voltage of 95 per cent of the single shot strength, puncture always occurred on the first shot during the *IR* voltage. These tests indicate that repeated shots with *IR* voltages in excess of 84 per cent of the single shot strength will deteriorate the insulation.

The three tests 7, 8, and 9 were all made with the same gap and give additional information on the effect of *IR* voltage. In test 7 there was no *IR* voltage and two pads each withstood 102 shots. In test 8 the *IR* voltage was 69 per cent of the single shot failure voltage and three of the pads tested punctured on shots 25, 34, and 86 while the fourth pad withstood 109 shots without failure. Although it might be inferred from a comparison of tests 7 and 8 that the *IR* voltage reduced the number of shots to fail the insulation, the number of pads are so few in test 7 and the range of shots so large in test 8 that such a deduction is questionable. On test 9 the *IR* voltage was 78 per cent of the single shot puncture voltage and failure occurred in fewer shots than in tests 7 and 8.

The remainder of the tabulation shows the number of shots required to puncture pads with various amounts of insulation when the voltage was chopped by gaps without series resistance. The protective ability of these gaps was approximately equivalent to a rod gap set two inches, since the breakdown voltages ranged from 112 to 125 kv and there was

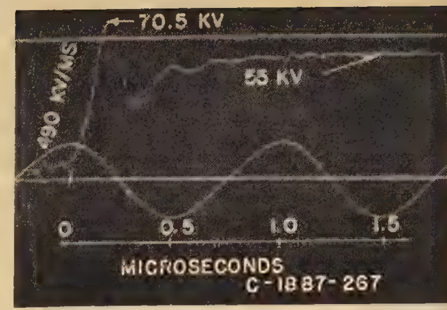

Figure 5. Volt-time oscillogram taken on pad with three sheets of paper

The pad was protected by 6.25-centimeter spheres set 16 millimeters with a resistance of 150 ohms connected in series. Puncture occurred during the *IR* voltage at about 1.7 microseconds. This oscillogram was retouched for reproduction

no *IR* voltage. With these gaps in parallel with the pads, it was necessary to have from five to eight sheets in the pads to withstand the same number of shots as were withstood by pads with two or three sheets when tested in parallel with valve arresters that had a breakdown voltage of 69 kv and an *IR* voltage of 34-kv crest.

Effect of Repeated Shots on Insulation Puncture

Thus far comparisons have been made between part of the individual tests listed in the tabulation. However, the effect of repeated shots can best be determined by putting the data from all tests on a common basis. This has been done in figure

Tests on Insulation Pads in Parallel With Gaps and Arresters

Test Number	No. of Sheets in Pads	Voltage Limited by	No. of Pads Tested	No. of Shots to Fail Pad	Pad Failed During	Average Voltage Applied—Kv Crest: Bkd. at 500 Kv/μs Bkd.	Average Voltage Applied—Kv Crest: 40 μs to Half-Current IR	Average Single Shot Strength, Figure 3—Kv Crest: Bkd.	Average Single Shot Strength, Figure 3—Kv Crest: IR	Ratio of Average Applied Voltage to Average Single Shot Strength—Per Cent: Bkd.	Ratio of Average Applied Voltage to Average Single Shot Strength—Per Cent: IR
1	2	Valve arr.	7	1–5	Breakdown	69	34	63	46	109	74
2	3	Valve arr.	8	3–14	Breakdown	69	34	80	59	86	58
3	2	Gap—no res.	4	1	Breakdown	69	0	64	0	108	
4	3	Gap—no res.	7	1–78[a]	Breakdown	72	0	78	0	92	
5	3	Gap and res.	7	1–2[b]	Bkd. or *IR*	79	49	77	58	103	84
6	3	Gap and res.	5	1	*IR*	70	55	80	58	88	95
7	4	Gap—no res.	2	102[c]		69	0	99	0	70	
8	4	Gap and res.	4	25–109[d]	Breakdown	69	48	99	70	70	69
9	4	Gap and res.	2	23, 27	Unknown	69	55	99	71	70	78
10	5	Gap—no res.	6	1–4	Breakdown	112	0	105	0	107	
11	6	Gap—no res.	2	3	Breakdown	112	0	120	0	93	
12	7	Gap—no res.	6	5–12	Breakdown	113	0	139	0	81	
13	5	Gap—no res.	6	1	Breakdown	112	0	105	0	107	
14	7	Gap—no res.	6	2–9	Breakdown	113	0	136	0	83	
15	8	Gap—no res.	1	25	Breakdown	115	0	133	0	86	
16	5	Gap—no res.	1	1	Breakdown	117	0	107	0	109	
17	6	Gap—no res.	5	1–2	Breakdown	119	0	119	0	100	
18	8	Gap—no res.	7	4–12	Breakdown	125	0	148	0	84	
19	6	Gap—no res.	4	1	Breakdown	118	0	119	0	99	
20	8	Gap—no res.	4	3–5	Breakdown	124	0	150	0	83	
21	9	Gap—no res.	1	12	Breakdown	120	0	165	0	73	

NOTES: [a]Number of shots to puncture pads: 1, 1, 1, 2, 4, 9, and 78.

[b]Five pads were punctured on the breakdown; two on the *IR* voltage.

[c]Two samples withstood 102 shots and tests were discontinued.

[d]Number of shots to puncture pads: 25, 34, 86, and one withstood 109 shots.

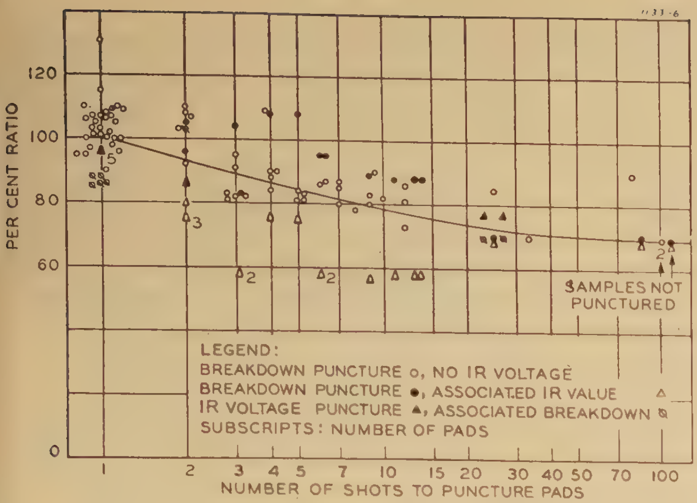

Figure 6. Tests with repeated shots

The applied voltage, in per cent of the single-shot puncture voltage, is plotted against the number of shots to puncture the pads. The insulation pads were in parallel with gaps or arresters

6 where the applied voltage expressed in per cent of the single shot puncture voltage was plotted against the number of shots to rupture the insulation. Data points were plotted from each of the 95 pads tested whereas the tabulation was condensed to include only averages or the ranges of data. A point was plotted for arrester or gap breakdown voltage and another for the *IR* voltage when it existed. The symbols indicate whether the puncture occurred as the voltage rose to gap breakdown or during the subsequent *IR* voltage. Since a large number of insulation punctures occurred on the first few shots, these points have been grouped about the ordinate through the actual shot number. Factors responsible for the scattering of the points include variations in the gap or arrester breakdown voltages, variations in the impulse generator discharge from shot to shot, and variations in the puncture voltage of individual pads.

The curve in figure 6 shows that the number of shots required to fail the insulation increases as the applied voltage expressed in per cent of the single shot puncture voltage is reduced. In all tests in which the insulation was ruptured, either the breakdown or the *IR* voltage was at least 70 per cent of the single shot puncture voltage. It is concluded from this plot that the insulation will withstand a large number of repeated shots provided the applied voltage does not exceed a value of approximately 70 per cent of the single shot puncture strength at any value of time. Within the limits of this investigation, this conclusion holds irrespective of whether the applied voltage is of short or long duration. On the basis that the curves of figure 3 are 100 per cent, it is concluded that curves drawn through 70 per cent of the voltage will approximate the shape of the highest voltage wave that can be repeatedly applied without reducing the number of shots the insulation will withstand. Montsinger[1] found that repeated shot injurious corona appears at voltages of 65 to 90 per cent of the single shot failure voltage and concluded that 80 per cent is a safe average value of voltage for repeated shots. The value of 70 per cent from the present tests is in good agreement with his results notwithstanding the differences in the structure of the insulation tested in the two investigations.

The Effect of Voltage Wave Shape on Insulation Puncture

One object of this investigation was to determine if arrester *IR* voltages of relatively low magnitude might possibly be more destructive to insulation because of long duration than voltages of relatively short duration preceding the breakdown of gaps. This was not found to be the case in these tests. The higher voltages necessary to puncture the insulation samples at short values of time are due to turn up of the insulation volt-time characteristic. Although figure 3 shows that higher voltages are required to cause puncture in short values of time, this might be offset in transformers by nonuniformity in distribution of voltage between the turns of the transformer coils which increases with the steepness of the voltage applied. Although these tests on insulation samples showed no evidence of deterioration of the insulation due to voltages less than 70 per cent of the single shot strength, the conclusion should not be drawn that chopped waves of this magnitude are necessarily harmless to turn insulation in actual transformers.

Conclusions

(1). The single shot puncture of the insulation increased linearly with the insulation thickness over the range tested in this investigation.

(2). The single shot volt-time puncture curves of the insulation tested in this investigation are relatively flat; the average puncture voltage for failure at 0.25 microsecond was found to be only 16 per cent more than the puncture voltage at 1 microsecond.

(3). This investigation shows that valve type arresters, of the type tested and the rating applied on 6,900-volt circuits, are superior to two-inch rod gaps for the protection of insulation when subjected to impulse discharges that are of more than average severity based upon field records.

(4). Tests with repeated applications of impulse voltages showed that as the ratio of the applied voltage to the single shot puncture voltage is reduced, the number of shots necessary to rupture the insulation increases.

(5). The insulation tested withstood a relatively large number of shots provided the applied voltage did not exceed a value of approximately 70 per cent of the single shot puncture voltage at any instant of time during the application.

(6). From life tests during which the insulation was subjected to voltage waves modified by the operation of protective devices, it is concluded that the insulation will withstand a relatively large number of shots provided the instantaneous voltage due to breakdown or *IR* voltages does not exceed approximately 70 per cent of the single shot puncture voltage.

(7). The results of this investigation suggest that in the application of protective devices, the upper limit of the stress that can be safely applied repeatedly to new insulation may be regarded as 70 per cent of the single shot puncture voltage; this is irrespective of whether the highest stress permitted by the protective devices is due to short or long time gap breakdown or short or long duration *IR* voltages.

References

1. Co-ordination of Power Transformers for Steep-Front Impulse Waves, V. M. Montsinger. AIEE Transactions, volume 57, 1938 (April section), pages 183–9.

2. Discharge Current in Distribution Arresters—II, K. B. McEachron and W. A. McMorris. AIEE Transactions, volume 57, 1938 (June section), pages 307–12.

3. The Lightning Stroke: Mechanism of Discharge, K. B. McEachron and W. A. McMorris. *General Electric Review*, October 1936, pages 487–96.

A New Transformer for Base-Load Stations

PHILIP SPORN
FELLOW AIEE

H. V. PUTMAN
MEMBER AIEE

Synopsis: This paper describes the application of Hipersil to three 40,000 Kv-a units for the Philo generating station of The Ohio Power Company. Because of Hipersil's ability to carry one-third more magnetic flux, appreciable savings in weight and dimensions are possible—in fact, the transformers will be shipped in oil completely assembled with bushings in place, ready to operate.

Forced-oil and forced-air cooling are provided, with proper relays for protection in the event of excessive copper temperature or failure of auxiliaries. Reliability, economy, ease of installation, and low maintenance have been the objectives sought in the design.

ALTHOUGH technical progress in the art of transmission of electrical energy has been considerable in the last two decades, it is a fact that no single significant contribution looking toward more economical transmission is readily called to mind. Most particularly is this true in the case of the transformer—the essential link in a-c transmission. Thus, major design and construction improvements have been made in impulse strength, in lightning protection, and in impulse testing of transformers. But these developments have only indirectly affected cost. Even more notable is the fact that a design trend of many years background in the direction of continually reducing losses has not been re-examined, nor most certainly altered in the face of decreasing costs of electrical capacity and energy. The development described here, it is believed, marks a definite step in altering that condition.

The essential element in this new design is a new steel, Hipersil.[1] Its outstanding characteristic is its ability to carry approximately one-third more magnetic flux in the transformer core. Figure 3 shows equipment used in a test made on two model cores identical in size—one of silicon steel and one of Hipersil. With the same exciting ampere-turns the flux measured in the Hipersil core was 38% greater than in the silicon steel core. It is hoped at a later date to present some more extensive information on the characteristics of Hipersil. This pushing forward of some of the design limitations which have heretofore held in check transformer designers, even though, for the present at least, the advantages of the new material must be limited to transformers where it can be used with the magnetic flux in line with the direction of rolling, is bound by itself to have a most material effect on transformer design economics and on transformer design art. In the development described, Hipersil has been coupled with forced-oil cooling, and with re-examined criteria for losses in the light of modern power and energy economics. But safety and reliability, as will be evident from the more detailed description to follow, have not been sacrificed.

Paper 41-124, recommended by the AIEE committee on electrical machinery, and presented at the AIEE summer convention, Toronto, Ontario, Can., June 16–20, 1941. Manuscript submitted April 25, 1941; made available for preprinting May 20, 1941.

PHILIP SPORN is vice-president and chief engineer of the American Gas and Electric Service Corporation, New York, N. Y. H. V. PUTMAN is manager of the transformer division of Westinghouse Electric and Manufacturing Company, Sharon, Pa.

1. A registered trade mark of Westinghouse Electric and Manufacturing Company.

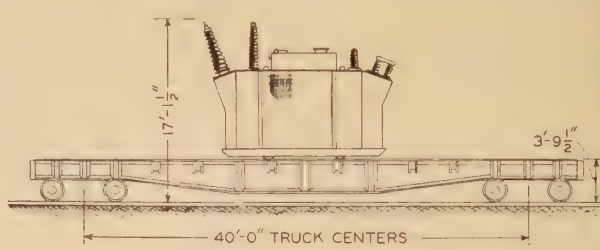

Figure 1. 40,000-kva 138-kv transformer mounted on standard flat car for shipment

In spite of the large size of this transformer, it will be shipped completely assembled with cooling equipment, oil bushings, and lightning arresters in place

Description of Transformer Units

This paper presents specifically the results of an analysis to see what the possibilities of this new material and new ideas would be in the design of large transformers for a base load station. The particular units under consideration are rated 40,000 Kv-a, 138 Kv, with non-solidly grounded neutral. The relatively lower cost of energy at the station bus was fully considered in evaluating the transformer losses and it made possible a closer use to the full of the inherent properties of Hipersil in reducing dimensions and the amount of active material required.

It was found that the smaller weights and dimensions resulting from the greater flux carrying capacity of Hipersil could be reduced still further through the use of forced-oil cooling, and in the light of the basic aim sought, this construction was adopted. Another factor bearing on the selection of forced-oil cooling for this application was the fact that little overload capacity is needed in a base load unit operating on the unit principle with generator and transformer in series switched as a unit.

As a result of these two basic ideas it was found possible to reduce weights and dimensions to a point where these large transformers could be completely assembled in the factory to be shipped in oil with bushings in place. Figure 1 shows an elevation of one of these units mounted on a standard flat car with significant dimensions. The cost of erection and starting in the field will obviously be reduced to a minimum.

Another interesting feature of these transformers is that due to the small size and the relatively small amount of oil involved it was possible to weld the cover on and seal the unit permanently against deterioration of the oil and insulation. There is no provision for breathing.

When operating at full load, these transformers have oil circulating pumps and fans in continuous operation, but much thought has been given to the question of reliability and protective devices. It is believed that with the arrangements described below, a degree of reliability comparable with that of other major apparatus in the generating station has been obtained.

It is interesting to examine the reduction in weights and increase in losses of this transformer compared with a standard self-cooled air-blast unit of the same rating:

Copper windings	reduction in weight	10%
Core	reduction in weight	25%
Losses	increase in weight	5%

Cooling System

The transformer itself is of shell-type construction and is mounted horizontally in the tank. Fin-type coolers employing round tubes of substantial cross-section are mounted on each side of the tank wall and provided with circulating pumps and cooling fans. The two radiator assem-

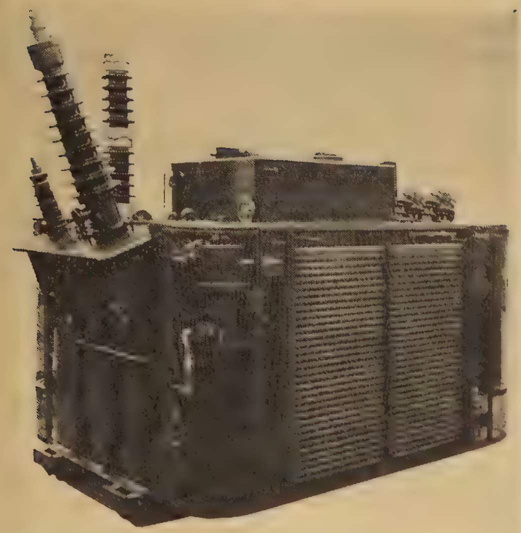

Figure 2. Side elevation of 40,000-kva 138-kv transformer showing principal over-all dimensions

The transformer is completely sealed with cover welded in place. No auxiliary gas equipment is required since adequate gas space is provided in the tank for maximum expansion and contraction due to temperature changes

Figure 3 (right). Test to demonstrate flux-carrying capacity of Hipersil

Two cores identical in size—one silicon steel, one Hipersil—were excited with 0.5 ampere through a coil of 154 turns. The voltage across the coil when assembled on the silicon steel core was 92—when on the Hipersil core, 127. Since the flux produced in the core is proportional to the voltage, the Hipersil core carried a flux greater than the silicon steel, in the ratio of 127 to 92, or approximately 38 per cent greater

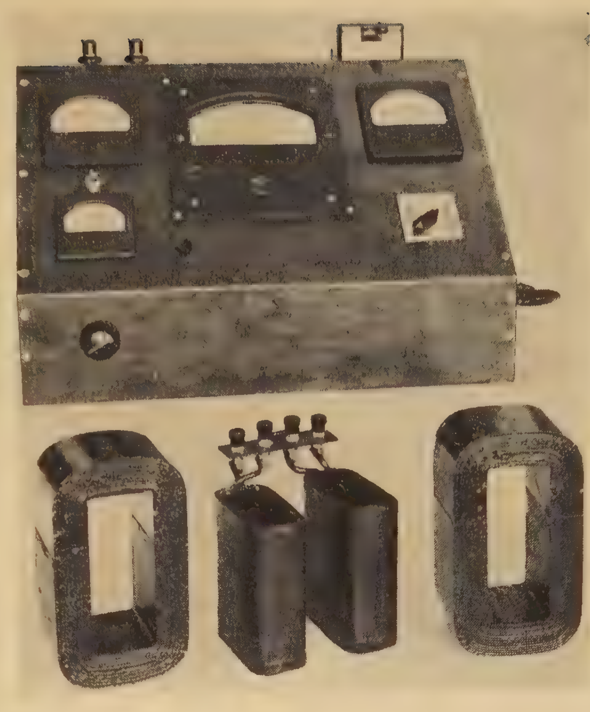

blies are operated as independent units. Power for the pumps and fans is supplied from two auxiliary transformers mounted inside the main unit—one auxiliary transformer taking care of one radiator bank. However, each of these auxiliary transformers is of sufficient capacity to supply power for the pumps and fans of both cooling units, and the control is so arranged that in the event one auxiliary transformer should fail, its fans and pump can be immediately connected to the other transformer. The control, too, is so arranged that both oil circulating pumps operate at no load but the fans come on as required; that is, when the oil temperature reaches 65°C, one set of fans comes into operation; at 75°C, the second set of fans comes into play.

Differential pressure relays are provided on each circulating pump. With only one pump in operation the capacity of the transformer would be reduced to 80%. Should the oil flow stop through one of the coolers due to failure of the pump or any other cause, the differential pressure relay would sound a warning to the station operator. Should both pumps stop, a signal to clear the unit from the line is given.

Operation by Copper Temperature

Since the thermal capacity of these transformers is small—comparatively little oil being required—excess copper temperatures could be reached in a relatively short time in the event difficulty should develop in the cooling system. For this reason relays are provided in each unit which operate on copper temperature. At 105 degrees centigrade copper temperature (measured by resistance), a warning signal is sounded to the station operator indicating that steps should be taken to reduce the load. It is not likely that the transformers would be actually overloaded due to the limitation of the generating equipment in the station, but it is conceivable that in the event of failure of fans or pumps on one side of the unit, even normal full load would exceed its reduced load carrying capacity. Should the copper temperature continue to increase and reach a dangerous point, the copper temperature relay signals the station operator for immediate shut-down.

Figure 4. Plan view showing oil circulation system

Pumps and fans are arranged in two independent assemblies each supplied from a separate auxiliary transformer mounted inside the main tank. Protection to the unit is provided in the event of failure of pumps by means of differential pressure relays and in the event of fan failure by copper temperature relays

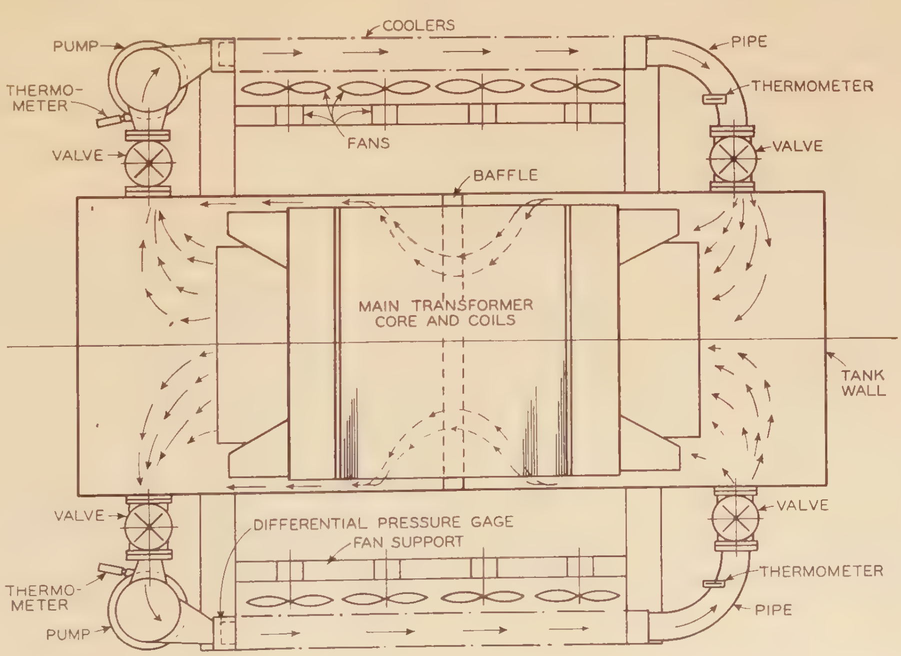

Fans and Pumps

A number of different blower arrangements were attempted during the course of the design but the use of simple air-

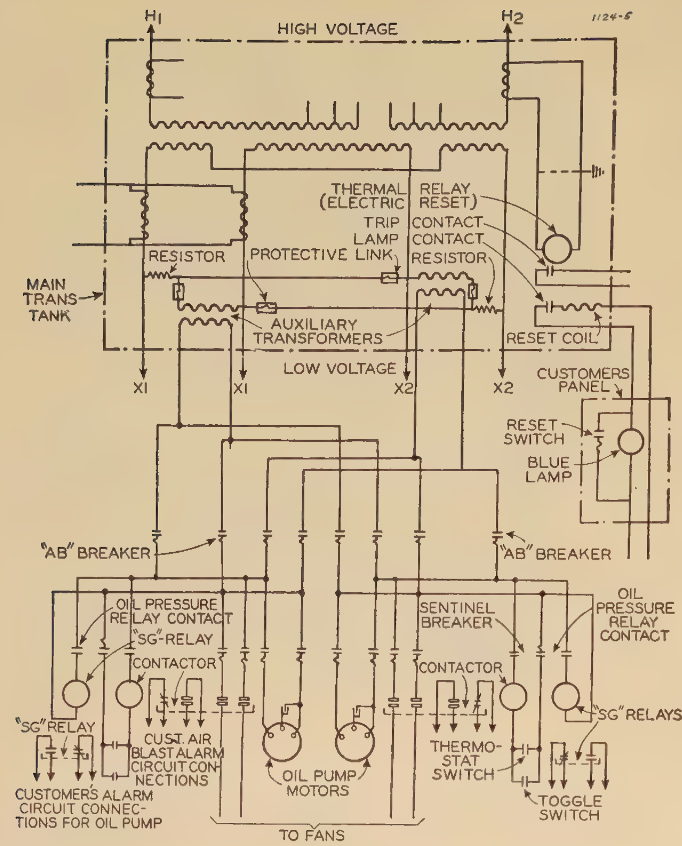

Figure 5. Schematic diagram showing arrangement of control apparatus mounted in control cabinets on transformer

Auxiliary transformers mounted inside main unit are provided with protective links to clear circuit in case of winding failures. Either auxiliary transformer will supply all pumps and fans by closing proper *AB* breakers. Fans are controlled from thermostatic relays operating on oil temperature. Pump motors run continuously. Copper-temperature relay protects against excessive copper temperature in the event of overload or failure of auxiliaries

Figure 7. Bird-wing fan mounted in removable assemblies of four units behind radiator coolers

Motors are outdoor capacitor-type equipped with "sealed-for-life" bearings. Capacitors are mounted in control cabinets on the transformer

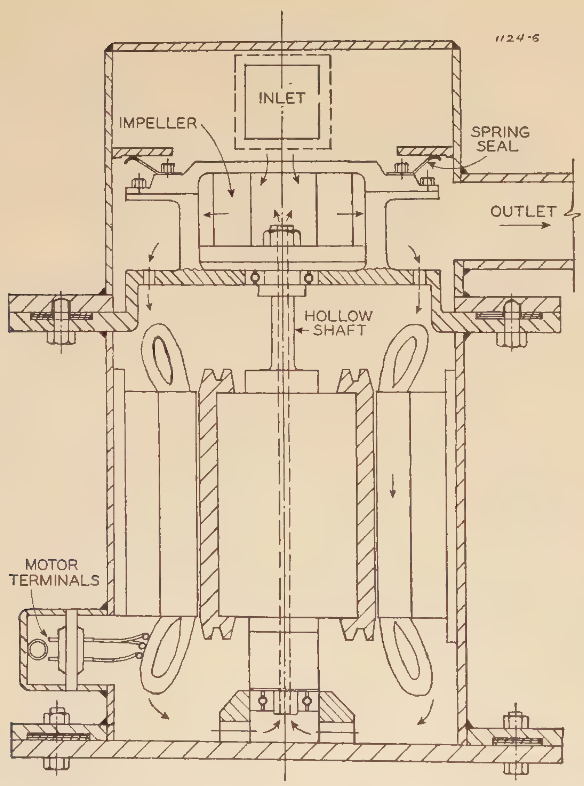

Figure 6. Section of oil circulating pump showing completely enclosed oil-immersed self-lubricating motor and pump rated 400 gallons per minute

blast fans equipped with motors having "sealed for life" bearings was finally adopted as the simplest and most economical arrangement. Sixteen fans are employed on each cooler, mounted in racks of four. Consideration has been given to easy replacement of these individual racks should that become necessary as a matter of routine maintenance.

The circulator pumps are of a type previously used for this application. They are equipped with a vertical shaft motor which is completely sealed and mounted in the oil circulation system so that both stator and rotor windings are submerged and bearings continually lubricated at all times by the transformer oil itself. Consideration has also been given to the problem of changing the pump motor and impeller assembly in the shortest possible time should that ever become necessary.

Conclusions

The development of Hipersil has opened up many new avenues for the design of transformers. As shown here, its use, coupled with other design ideas, has made possible production of large units more economically through reduction in size and amount of material required. Weights and dimensions become particularly important in very large units. Using standard magnetic steel these have had to be shipped in nitrogen gas in special containers to get by bridge and tunnel clearances. Upon arrival they required a considerable amount of erection work and expense prior to being placed in service. The use of Hipersil automatically extends the rating size before this becomes necessary. It is apparent, too, that the same development will make possible the extending of the practical size of the portable transformer whether on car or trailer. Finally, the authors believe that this development is but another proof of the vitality of the electric power art and of the ability of modern technology to move rapidly forward even in a well developed field.

The Measurement of Body Currents

ROBERT S. SCHWAB
NONMEMBER AIEE

IN these days of supersensitive amplifiers and recording apparatus, it is very tempting to define life and death in terms of electrical activity. Whether or not this concept is accurate, we can, on present knowledge liken living tissue to a B-battery and dead tissue to a burned out generator. The function of living tissue, however, is so closely allied with its electrical activity that knowledge of the latter has given us better understanding of the working of the human body.

Great names in electrical engineering contributed to our knowledge of the physiology of tissues. Galvani in 1780 made the really startling observation that the muscle of a frog's leg could be made to contract when stimulated with the voltage from the crude Voltaic pile. That the muscle itself, on contracting, gave off a charge of its own was shown in 1870 by D'Arsonval, who noted the deflection of the needle when the muscle contracted across the poles of his galvanometer.

With improvements and greater sensitivity in recording instruments, electrical waves were obtained from the human heart (Waller, 1885; Einthoven, 1903) and from the nerve and muscle (Lucus, 1906; and Piper). In 1929 Hans Berger, with string galvanometer and amplifiers, picked up the first electrical waves from the human brain with electrodes on the scalp.

The first type of body currents to be discussed here is the rather static, direct current potential difference. It is this ever-present E.M.F., found in all living matter, small (few millionths of a volt), but constant as to polarity and relatively unchanging in time or species, that brings up the easy analogy of life to the B-battery. The living cell shows a tiny potential difference between its surface and the centrally located nucleus (Freeman). In plants, we can find a few microvolts of D.C. potential and in one animal, the electric eel, we may find as much as 500 volts. There is strong evidence that these potentials are due to different metabolic rates or energy levels in different parts of the same structure. Thus the relatively inactive, transparent membrane covering the human eye-ball (cornea) is nearly a millivolt different from the highly active, photo-sensitive retina at the back of the eye.

Nearly anywhere in the body, such potential differences may be found and in some cases might be clinically useful. For example, if an electrode is placed in the vagina, and another on the surface of the skin of the abdomen, a sudden increase in the base-line voltage difference is said to indicate that ovulation is occurring in the underlying ovary. These D.C. potentials are always associated with the first and most important character of life, namely: absorbing energy, growth, and change in structure. We call these activities metabolism and catabolism. They are found, for example, in the rose from seed to death, although the flower never moves in the sense that animals swim, fly, walk, etc. The more active part metabolically speaking is negative to the less active part. Thus the former is essentially the $-$; zinc, or cathode of a battery and the less active tissue the $+$; carbon, or anode pole.

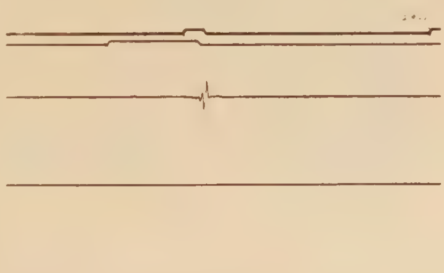

Figure 1. Electrical response of human biceps muscle to tap on tendon

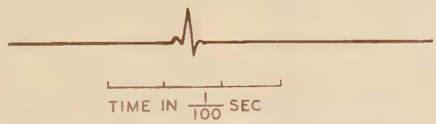

Figure 2. Action potential in a nerve fiber (from Gasser)

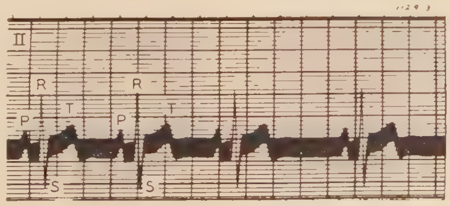

Figure 3. Action potentials of human heart (electrocardiogram—from P. D. White)

The second type of body currents is that associated only with the animal kingdom—the electrical activity of locomotion. It is nature's second and perhaps most interesting attribute of life, and is different from any of the D.C. potentials previously described. Contractile tissue is nature's first intrinsic movement in an environment of physical forces all in motion, such as wind, tides, rivers, etc. This tissue, when left alone "lives," i.e., has its D.C. potentials. But, when it is stimulated from without or from within, an astonishing change takes place. It moves actively, withdraws, strikes out. Associated with this defensive or aggressive movement there is an alternating current wave, a diphasic spike, which is lacking in the motionless tissues. An example of such tissue is a muscle fibre. When it is stimulated, it contracts, and a diphasic spike or group of such spikes occurs. This contractile tissue is primitive and found in all organisms that move, and is characterized by no electrical activity when quiet and by burst of such activity when stimulated to action (figure 1).

A similar structure, but more complicated, is nerve tissue. Primarily used to conduct stimuli to the contractile tissue, it acts like muscle in that it has no activity electrically when at rest, but when at work shows the same characteristic diphasic spike. Motion, as an inherent ability, however is not present in nerve tissue. (Figure 2.) In this tissue

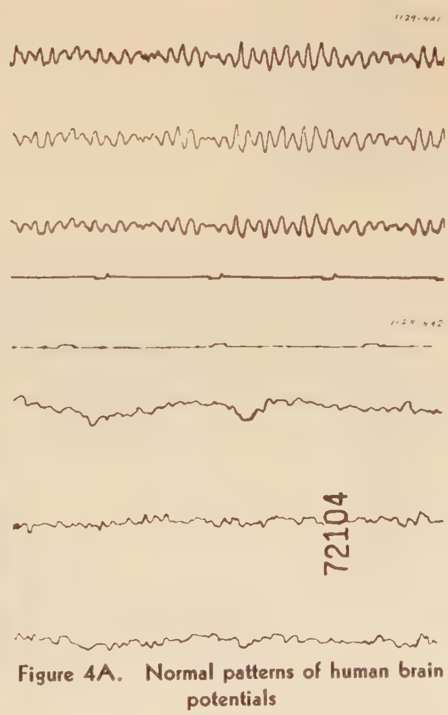

Figure 4A. Normal patterns of human brain potentials

Alpha rhythm above and beta rhythm below

Paper 41-129, recommended by the AIEE committee on communication, and presented at the AIEE summer convention, Toronto, Ontario, Can., June 16–20, 1941. Manuscript submitted April 25, 1941; made available for preprinting May 14, 1941.

ROBERT S. SCHWAB is associated with the brain wave laboratory of the Massachusetts General Hospital and the Harvard Medical School, Boston, Mass.

very rapid shifts of metabolic activity occur. For example, A, B, and C are points in line in such a piece of living matter. When at rest they are absorbing energy (being nourished, living) and are negative to their enveloping and supporting structures. Points A, B, and C are in, let us say, contractile tissue or nerve and have a much higher metabolic rate and complexity as far as molecular structure than the simple covering membrane. Hence they are all negative to it. If point A is stimulated its energy is released by a rapid chemical change and A loses its negative electrical charge. This in turn discharges or stimulates point B etc. These rapid changes produce the diphasic wave seen in muscle and nerve potentials. It is to be noted that in 3–4 thousandths of a second the whole process is completed. This nerve conduction proceeds not like electrons in a wire, but slowly as each adjacent point goes through a chemical breakdown and stimulates the next one. The rate of conduction of such an impulse is as far as 100 meters per second in man, but is much slower in lower animals (5 meters per second in reptiles).

A third type of electrical activity is associated with the more highly developed types of contractile tissue. Cilia, tubular digestive tracts, and heart muscle have a "beat" of their own and depend no longer on outside stimuli for their continuous, regular contractions and relaxations. Every "beat" has its accompanying bursts of diphasic waves. (Figure 3.) This shows a normal electrocardiogram. Metal (silver) discs covered with flannel soaked in salt are fastened with elastic bandage to the left wrist and left foot (lead II). Wires from the two discs lead to the poles of a sensitive string galvanometer. Bromide paper moved by clock works at 5 cm. per second receives the light beam from the mirror on the string. Thus electrical changes in the heart show up optically magnified on this recording paper when it is developed. Recording from each arm or right foot and left arm are some of the other leads (I and III). A vast and important field of clinical diagnosis has been developed in the interpretation of these EKG's as they are called. They indicate pathological changes in heart muscle, disturbances in rate, rhythm, and in circulation of blood in the heart muscle itself. No complete examination of the heart can be done without such a measurement. Every hospital now has one and many doctors have them at their disposal. In 1910 they were a curiosity in this continent.

The fourth type of body electrical currents is that associated with the complex tissue that makes up the central nervous system of animals. Here, as the function is continuous during life, the ganglia and brain cell tissues are ever-active electrically and show no periods of rest in the manner of muscle and nerve. (Figure 4.) Each brain cell does not actually beat alone, but by a system of interconnections keep each other stimulated to activity. These "chains" of neurones make up the bulk of the brain and spinal cord of man and animals. According to Herrick, in man, for example there are over $10^{2,783,000}$ possible neuronal combinations—a number far greater than the total sum of all atoms in the entire solar system 10^{76}.

It is this last form of living matter, the cells of the central nervous system that interests most physiologists today. In clinical medicine, the importance of the electrocardiogram in studying the function of the heart is completely established. The newer electroencephalogram or recording of the electrical activity of the

Figure 4B. Obtaining and recording human brain waves in the brain-wave laboratory of the Massachusetts General Hospital and the Harvard Medical School, Boston, Mass.

(Left). Electrodes used. Disc end fastened to scalp

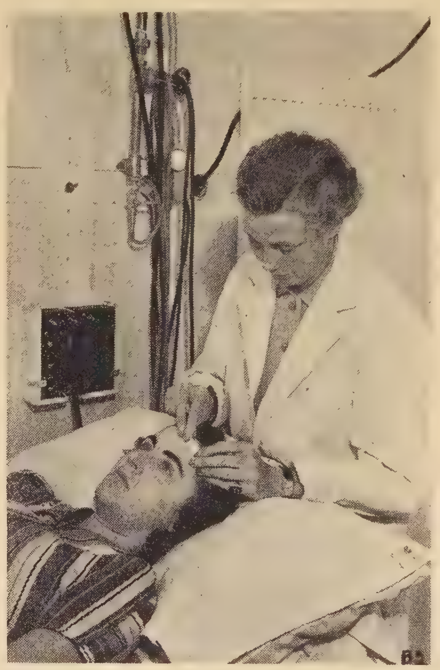

Placement of a frontal electrode. Note, at left, the box into which other end of electrode is plugged

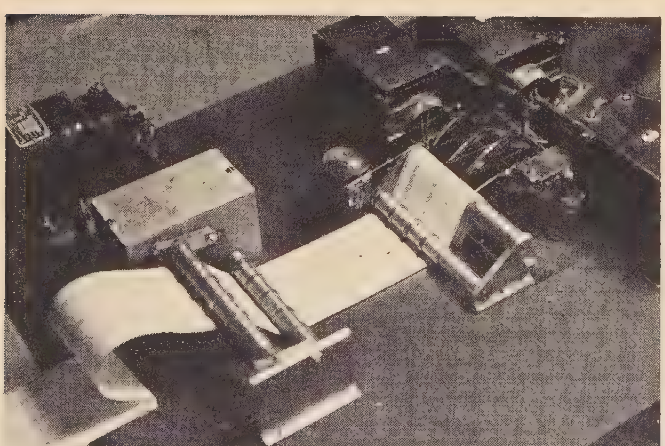

An ink-writing oscillograph recording a brain wave on moving paper

Apparatus room with two sets of amplifiers and two recorders

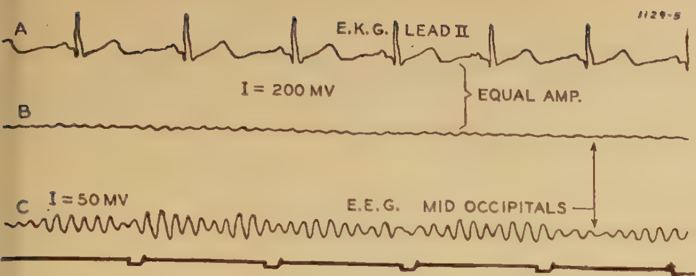

Figure 5. Comparison of human electrocardiogram and human electroencephalogram

In *B* the brain wave is at same amplification as the heart wave in *A*. In *C* the brain wave is at the standard amplification for recording

brain is rapidly becoming just as invaluable in the study of diseases and dysfunctions of the central nervous system. The recording of these brain waves, as the electroencephalograms are called, requires a much more sensitive type of apparatus. The heart currents obtained with surface electrodes on two of the extremities, as previously described, may reach nearly a millivolt and can be recorded directly by a string galvanometer. The brain currents picked up from small (5 mm.) lead discs attached to the scalp by electrode paste and collodion (needles or cutting the hair are not necessary) are only $^1/_{20\text{th}}$ of the heart's and require vacuum tube amplification before recording (see figure 4*A*, *B*). Albert Grass of Harvard and Dr. Alfred Loomis of Tuxedo Park both have developed rugged efficient battery and power-operated, push-pull amplifiers that operate ink-writing oscillographs. Offner of Chicago, Garceau of Holliston, Mass., and Rhem of New York, are other engineers who have apparatus in this field. By these brain wave machines the EEG, as the records are called, appear immediately as an ink line on the paper strip. The usual speed of the paper is 3 cm. per second and there are anywhere from 3 to 6 separate "channels" recording simultaneously. Normal human brain waves consist of two sorts. Alpha or 10 per second waves have voltages of 30 to 75 microvolts, are extremely regular, and when dominating the record are associated with easy-going stolid, reliable types (alpha type). The second type of normal activity is beta waves, 20–24 per second of voltages from 10 to 40 microvolts. They are often associated in general with tense, rather high strung people. There are so many exceptions and mixed types that the brain wave pattern is not a real index of personality, intelligence, or state of mind.

(Figure 5.) This shows a brain wave and a heart wave compared. Here is seen the regularity of the 10 per second alpha waves, their continual appearance and the smallness of the voltage as differing from the regularity, discreteness, and high voltage of the heart activity.

(Figure 6.) This shows the phenomenon of the disappearance of the alpha waves when light enters the eye. Professor Adrian of Cambridge University kindly lent me this slide. The lower tracing is from the brain of the famous Nobel Prize winner, the upper from his lowly compatriot, the English Water Beetle. Brain cells, wherever gathered together, act electrically much the same.

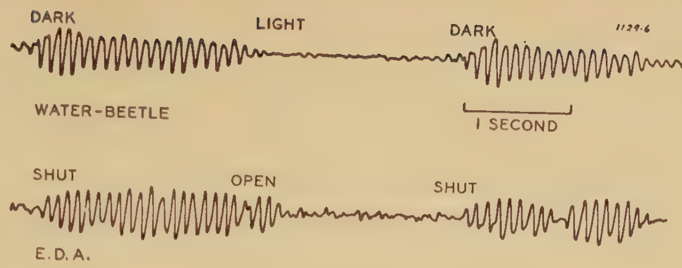

Figure 6. Comparison of the alpha rhythm in the beetle and human (from Adrian)

(Figure 7.) This shows what the human brain waves are like during sleep. Irregularity and increased voltage are characteristic. Response of the individual to outside stimulus is greatly prolonged. Here the reaction time was over five seconds. (Normal is $^1/_4$ of a second.) In very deep sleep, or when the individual is under anaesthesia, the rhythm becomes slower (3 per second) and the voltages increase. Such waves are called Delta waves. When the brain function is interfered with abnormal waves appear in the electroencephalogram. These seem to result from faster smaller waves being built up into some sort of synchrony. They appear as high-voltage spikes (100 to 200 microvolts) or high-voltage, slow waves (Delta waves). They are something like the sleep waves but usually of more voltage and slower. Periodic disturbances in the normal brain rhythm (cerebral dysrhythmia as it is called by Lennox) are found in patients who have epilepsy. The length and severity of the seizures (seconds to many minutes) are shown by the amount and voltage of these abnormal waves.

(Figure 8.) Record of brain waves of a person who has, clinically, a form of epilepsy. The seizures are short, lasting but a few seconds, and are often periods

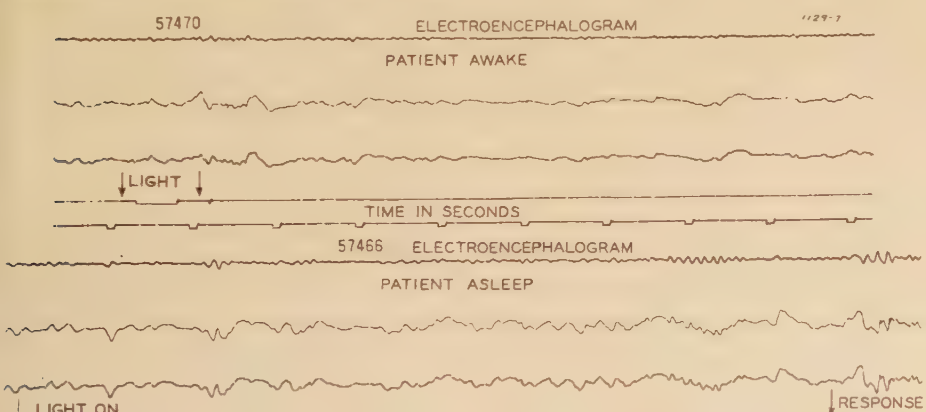

Figure 7 (above). Effect of sleep on brain waves and reaction

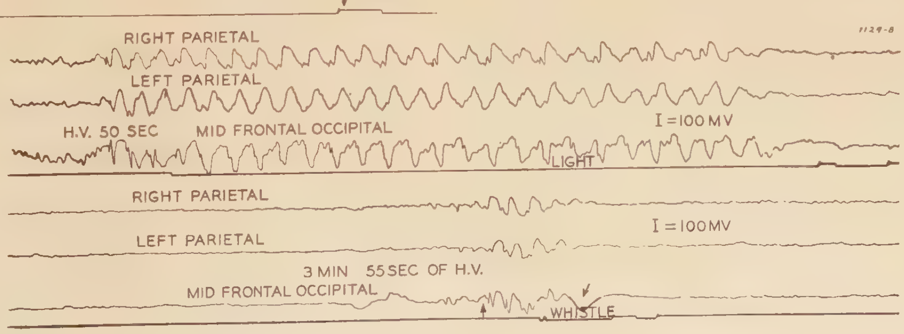

Figure 8 (right). Example of brain waves during a petit mal attack

Upper tracing shows long delay in responding to light. Lower tracing shows beginning of another attack probably stopped by whistle stimulus

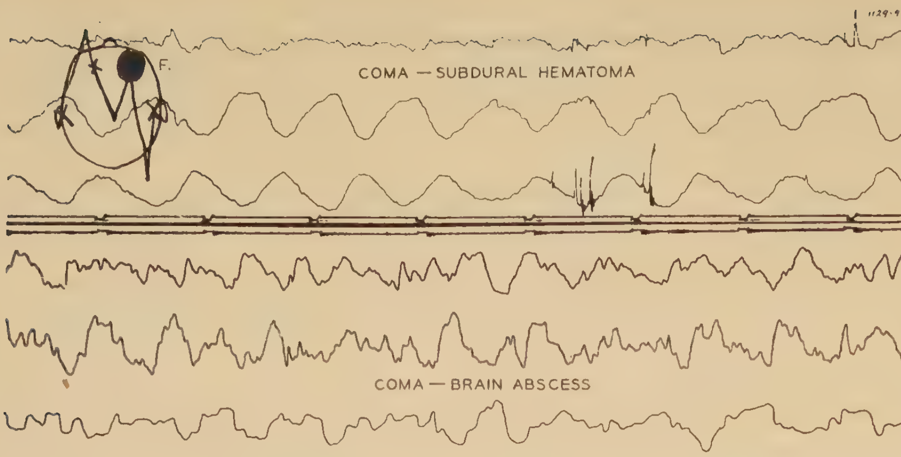

Figure 9. Brain waves from two patients in coma; upper waves from blood clot on brain and lower waves from brain abscess

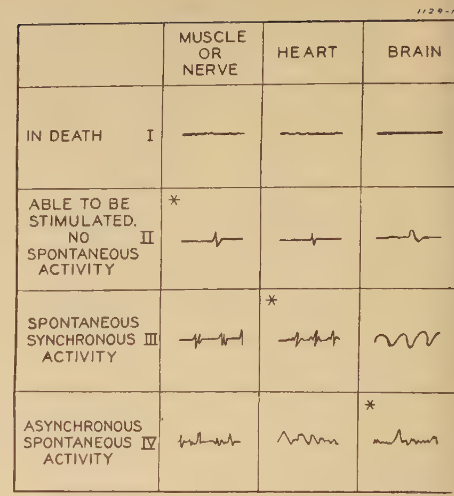

Figure 11. In death I all tissues show no electrical activity; in II only muscle and nerve are normal;* in III heart is normal;* muscle and brain abnormal; in IV only brain is normal*

of unconsciousness. Sometimes they show up as slight twitchings of various face muscles, but do not develop into a real convulsion. These lapses are accompanied by a characteristic wave pattern called *the wave-spike formation*, which is a slow delta followed by a short spike. In this case, the person did not respond to the neon light signal, but did to the extremely unusual stimulus of the sound of a tug-boat whistle. During severe attacks of this kind, many fail to respond even to such a noisy stimulus.

Blood clots and tumors of the brain also cause these high-voltage, abnormal waves. By means of triangulation and phase shifts with the multiple channel sets of apparatus accurate localization of these lesions is possible (84% accuracy in 400 verified cases at the Massachusetts General Hospital). An example of such an application of this technique is described. A 38-year old man was brought to the hospital in a coma with signs of pressure on the brain. A brain wave tracing showed a sharp, slow-wave dis turbance on the left side of his head. Operation revealed a tumor. Six weeks after this growth had been removed the

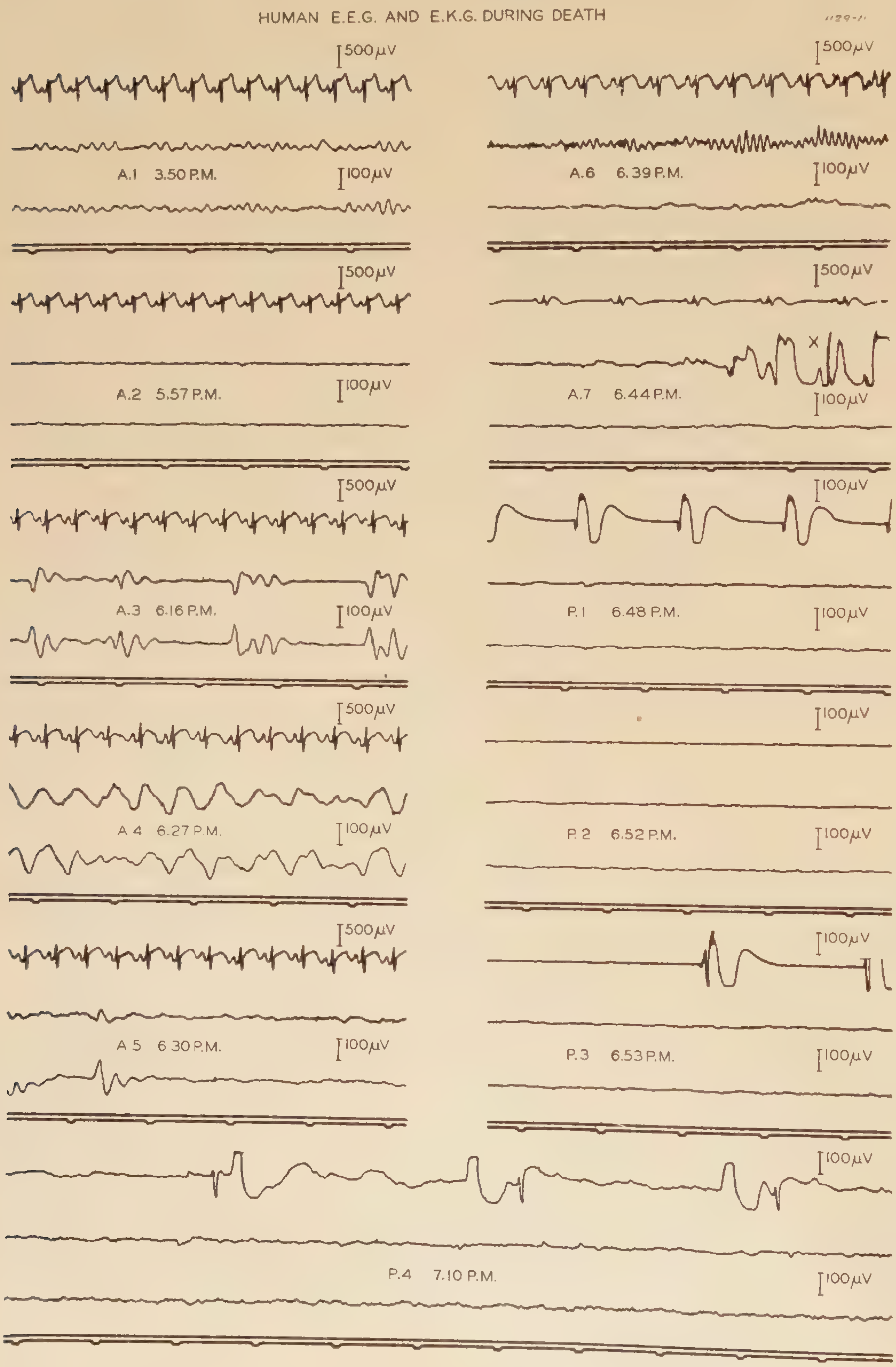

Figure 10. Brain waves and heart waves during death in a human

The electrocardiogram is top line and right and left brain waves are below. Brain waves disappear ten minutes before death. Legal death occurs at the spot marked (x) which indicates cessation of respiration and pulse. (x marks instant when intern placed stethoscope on chest to prove inaudible heart beat. The artifact produced by stethoscope touching electrode wire is shown in the tracing.) Electrocardiogram continues one minute after death, stops and then begins again. Thirty-two minutes after death heart still has three beats from pressure on chest

Damping and Synchronizing Torque of the Double-Fed Asynchronous Machine

M. M. LIWSCHITZ
MEMBER AIEE

I. Introduction

THE double-fed asynchronous machine has become important in recent times as fan drive with wide speed range. The system consists of five main machines and the fan (see figure 1). It has many springs, masses, and dampings and therefore many natural frequencies. In order to determine these frequencies, i.e. the dynamic stability of the system, the damping and synchronizing torques of all parts of the system have to be known. Some papers have been published concerning the torques of the synchronous machine. It is easy to determine torques for the D.C. machines of the system. The object of this paper is to derive formulas for the damping and synchronizing torque of the double-fed asynchronous machine. As in the case of the synchronous machine, a complicated derivation and complicated results cannot be avoided.

II. The Differential Equations of the Double-Fed Machine

In order to simplify the mathematical work a two phase machine will be considered, and the usual assumptions, i.e. no saturation and small oscillations, are made. The results will be generalized for the m_1-phase machine. The voltage equations of the two phase machine are (for the symbols see List of Symbols)

$$E_{L1} \sin \omega t = AB_{\mathrm{I}}' + L_1 i_{\mathrm{I}}' + r_1 i_{\mathrm{I}} \tag{1}$$

$$-E_{L1} \cos \omega t = AB_{\mathrm{II}}' + L_1 i_{\mathrm{II}}' + r_1 i_{\mathrm{II}} \tag{2}$$

$$E_{L2} \sin (s\omega t + \delta) = AB_d' + L_2 i_d' + r_2 i_d \tag{3}$$

$$-E_{L2} \cos (s\omega t + \delta) = AB_q' + L_2 i_q' + r_2 i_q \tag{4}$$

where

$$A = \frac{2}{\pi} \tau_p l_i \omega \times 10^{-8} \tag{5}$$

i_{I}, i_{II}, i_d, and i_q are the currents in the four windings. B_{I}, B_{II}, B_d, and B_q are the resultant inductions in the axes of the winding produced by all currents. Between the inductions consists the relation[1]

$$\begin{aligned} B_{\mathrm{I}} &= B_d \cos \gamma - B_q \sin \gamma \\ B_{\mathrm{II}} &= B_d \sin \gamma + B_q \cos \gamma \end{aligned} \tag{6}$$

where

$$\gamma = \frac{x}{\tau} \pi \tag{7}$$

is the angle between the axes of phase I of the stator and phase I of the rotor. For the inductions B_d and B_q the following equations hold

$$\begin{aligned} B_d &= \frac{x_m}{A\omega} (i_d + i_{\mathrm{I}} \cos \gamma + i_{\mathrm{II}} \sin \gamma) \\ B_q &= \frac{x_m}{A\omega} (i_q + i_{\mathrm{II}} \cos \gamma - i_{\mathrm{I}} \sin \gamma) \end{aligned} \tag{8}$$

With two new variables

$$\begin{aligned} I_d &= i_{\mathrm{I}} \cos \gamma + i_{\mathrm{II}} \sin \gamma \\ I_q &= -i_{\mathrm{I}} \sin \gamma + i_{\mathrm{II}} \cos \gamma \end{aligned} \tag{9}$$

the total torque of the machine will be[1,2]

$$T = A\omega (B_q I_d - B_d I_q) \tag{10}$$

With

$$\gamma = \frac{x}{\tau} \pi = \omega_{r\,\mathrm{av.}} t + \epsilon = \omega_{r\,\mathrm{av.}} t + \epsilon_0 \sin zt \tag{11}$$

and

$$\alpha = s\omega + z \quad \beta = s\omega - z \tag{12}$$

the following four simultaneous differential equations will be found after some conversions.

$$E_{L1}\left(\cos s\omega t + \frac{\epsilon_0}{2} \cos \beta t - \frac{\epsilon_0}{2} \cos \alpha t\right) = -A(B_d \beta' + B_q') - L_1 (I_d \beta' + I_q') - r_1 I_q \tag{1a}$$

$$E_{L1}\left(\sin s\omega t + \frac{\epsilon_0}{2} \sin \beta t - \frac{\epsilon_0}{2} \sin \alpha t\right) = A(B_d' - B_q \beta') + L_1 (I_d' - I_q \beta') + r_1 I_d \tag{2a}$$

$$E_{L2} \sin (s\omega t + \delta) = (1 + \tau_2) AB_d' + \frac{A\omega}{x_m} r_2 B_d - L_2 I_d' - r_2 I_d \tag{3a}$$

$$E_{L2} \cos (s\omega t + \delta) = (1 + \tau_2) AB_q' + \frac{A\omega}{x_m} r_2 B_q - L_2 I_q' - r_2 I_q \tag{4a}$$

III. The Torques

A straightforward solution of the four equations is possible. For the four variables has been found

$$B_d = -E_{L1} \frac{x_m}{A\omega}\left[(a_8 \cos s\omega t - b_8 \sin s\omega t) - \frac{\epsilon_0}{2}(a_{11} \cos \beta t - b_{11} \sin \beta t) - \frac{\epsilon_0}{2}(a_8 \cos \alpha t - b_8 \sin \alpha t)\right] \tag{13}$$

$$B_q = -E_{L1} \frac{x_m}{A\omega}\left[(a_8 \sin s\omega t + b_8 \cos s\omega t) - \frac{\epsilon_0}{2}(a_{11} \sin \beta t + b_{11} \cos \beta t) - \frac{\epsilon_0}{2}(a_8 \sin \alpha t + b_8 \cos \alpha t)\right] \tag{14}$$

Paper 41-110, recommended by the AIEE committee on electrical machinery, and presented at the AIEE summer convention, Toronto, Ontario, Can., June 16–20, 1941. Manuscript submitted April 14, 1941; made available for preprinting May 6, 1941.

M. M. Liwschitz is with Westinghouse Electric and Manufacturing Company, East Pittsburgh, Pa.

The author gratefully acknowledges the suggestions and assistance in solving the equations given by A. M. Wahl of the research laboratory, and the assistance in calculating of a specific problem given by J. C. Andreas of generator engineering department.

1. For all numbered references, see list at end of paper.

---

brain wave was normal again in this area.

(Figure 9.) Abnormal, slow-wave pattern obtained from a patient unconscious due to large blood clot on the brain. Abscesses and injuries to the brain can also be localized by this method.

(Figure 10.) Changes in the electrocardiogram and electroencephalogram occurring in a patient dying from cerebral hemorrhage. Electrical activity of the brain in this case ceased before that of the heart.

(Figure 11.) Table of comparison of normal electrical pattern of muscle, heart, and brain. A normal muscle lives at the second level of no electrical activity except on stimulus. When a muscle "beats" rhythmically and continuously, it is a diseased or dying tissue. The heart lives a normal life at this level of rhythmic discharge, and is abnormal when it depends on outside stimulus. The brain exists normally in the fourth level of continuous, arhythmic and asynchronous activity.

Summary

D.C. potentials are associated with static cellular life and are a product of metabolism.

A.C. potentials are associated with many tissues controlling or responding to movement.

Brain tissue is the most highly developed and exists normally in a state of constant, irregular electrical activity.

$$I_d=-E_{L1}\Big[(a_{14}\cos s\omega t-b_{14}\sin s\omega t)-\frac{\epsilon_0}{2}(a_{12}\cos\beta t-b_{12}\sin\beta t)-\frac{\epsilon_0}{2}(a_{13}\cos\alpha t-b_{13}\sin\alpha t)\Big] \quad (15)$$

$$I_q=-E_{L1}\Big[(a_{14}\sin s\omega t+b_{14}\cos s\omega t)-\frac{\epsilon_0}{2}(a_{12}\sin\beta t+b_{12}\cos\beta t)-\frac{\epsilon_0}{2}(a_{13}\sin\alpha t+b_{13}\cos\alpha t)\Big] \quad (16)$$

where

$$\lambda_1=\frac{r_2^2+\left(\frac{\alpha}{\omega}\right)^2(1+\tau_2)x_2x_m}{r_2^2+\left(\frac{\alpha}{\omega}\right)^2x_2^2}$$

$$\lambda_2=\frac{\frac{\alpha}{\omega}x_mr_2}{r_2^2+\left(\frac{\alpha}{\omega}\right)^2x_2^2}$$

$$\mu_1=\frac{r_2^2+\left(\frac{\beta}{\omega}\right)^2(1+\tau_2)x_2x_m}{r_2^2+\left(\frac{\beta}{\omega}\right)^2x_2^2}$$

$$\mu_2=\frac{\frac{\beta}{\omega}x_mr_2}{r_2^2+\left(\frac{\beta}{\omega}\right)^2x_2^2}$$

$$\nu_1=\frac{r_2^2+s^2(1+\tau_2)x_2x_m}{r_2^2+s^2x_2^2}$$

$$\nu_2=\frac{sx_mr_2}{r_2^2+s^2x_2^2}$$

$$a=r_2+K(r_1\cos\delta-x_1\sin\delta)$$

$$a_1=\frac{ar_2+bsx_2}{r_2^2+(sx_2)^2}$$

$$a_2=x_m+(r_1\nu_2+x_1\nu_1)$$

$$a_3=\frac{a_1a_2+b_1b_2}{a_2^2+b_2^2}$$

$$a_4=\frac{z}{\omega}(x_m+x_1\nu_1)$$

$$a_5=a_3a_4-b_3b_4$$

$$\alpha'=\omega+z$$

$$a_6=\frac{\alpha'}{\omega}x_m+\left(r_1\lambda_2+x_1\frac{\alpha'}{\omega}\lambda_1\right)$$

$$a_7=a_5+1+K\frac{z}{\omega}x_1\frac{r_2\sin\delta-sx_2\cos\delta}{r_2^2+(sx_2)^2}$$

$$a_8=\frac{a_6a_7+b_6b_7}{a_6^2+b_6^2}$$

$$a_9=\frac{\beta'}{\omega}x_m+\left(r_1\mu_2+x_1\frac{\beta'}{\omega}\mu_1\right)$$

$$a_{10}=a_5-1+K\frac{z}{\omega}x_1\frac{r_2\sin\delta-sx_2\cos\delta}{r_2^2+(sx_2)^2}$$

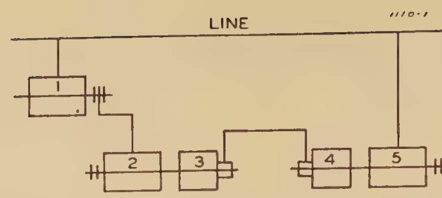

Figure 1. The double-fed asynchronous machine system

1. Double-fed asynchronous machine
2. Synchronous machine
3, 4. D-c machines
5. Synchronous machine

$$a_{11}=\frac{a_9a_{10}+b_9b_{10}}{a_9^2+b_9^2}$$

$$a_{12}=a_{11}\mu_1-b_{11}\mu_2$$

$$a_{13}=a_8\lambda_1-b_8\lambda_2$$

$$a_{14}=(a_3\nu_1-b_3\nu_2)+K\frac{r_2\sin\delta-sx_2\cos\delta}{r_2^2+(sx_2)^2}$$

$$b=sx_2+K(r_1\sin\delta+x_1\cos\delta)$$

$$b_1=\frac{br_2-asx_2}{r_2^2+(sx_2)^2}$$

$$b_2=-(r_1\nu_1-x_1\nu_2)$$

$$b_3=\frac{b_1a_2-a_1b_2}{a_2^2+b_2^2}$$

$$b_4=\frac{z}{\omega}x_1\nu_2$$

$$b_5=a_3b_4+b_3a_4$$

$$\beta'=\omega-z$$

$$b_6=-\left(r_1\lambda_1-x_1\frac{\alpha'}{\omega}\lambda_2\right)$$

$$b_7=b_5-K\frac{z}{\omega}x_1\frac{r_2\cos\delta+sx_2\sin\delta}{r_2^2+(sx_2)^2}$$

$$b_8=\frac{a_6b_7-b_6a_7}{a_6^2+b_6^2}$$

$$b_9=-\left(r_1\mu_1-x_1\frac{\beta'}{\omega}\mu_2\right)$$

$$b_{10}=b_5-K\frac{z}{\omega}x_1\frac{r_2\cos\delta+sx_2\sin\delta}{r_2^2+(sx_2)^2}$$

$$b_{11}=\frac{a_9b_{10}-b_9a_{10}}{a_9^2+b_9^2}$$

$$b_{12}=b_{11}\mu_1+a_{11}\mu_2$$

$$b_{13}=a_8\lambda_2+b_8\lambda_1$$

$$b_{14}=(a_3\nu_2+b_3\nu_1)-K\frac{r_2\cos\delta+sx_2\sin\delta}{r_2^2+(sx_2)^2}$$

From equations 10, and 13 to 16 the torques of a m_1-phase machine are

Constant torque

$$T_c=m_1E_{L1}^2x_m(a_3b_{14}-b_3a_{14})\text{ watts} \quad (17)$$

Damping torque

$$T_d=m_1E_{L1}^2x_m\frac{1}{2z}[a_8(b_{12}+b_{13})-b_8(a_{12}+a_{13})+b_{14}(a_8+a_{11})-a_{14}(b_8+b_{11})]\text{ watt-sec} \quad (18)$$

Synchronizing torque

$$T_s=m_1E_{L1}^2x_m\frac{1}{2}[a_8(a_{12}-a_{13})+b_8(b_{12}-b_{13})+a_{14}(a_8-a_{11})+b_{14}(b_8-b_{11})]\text{ watts} \quad (19)$$

A simple expression for the constant torque has been given in a previous paper.[3]

While the torques of the synchronous machine depend on the angle δ and the excitation, the torques of the double-fed asynchronous machine depend on the angle δ, the secondary voltage, and the slip.

The derivations made above are valid when the synchronous machine (machine 2, figure 1) is larger than the asynchronous machine, for example, when two or more asynchronous machines are connected in parallel to a single synchronous machine and the oscillation of one of the asynchronous machines is considered. In this case the secondary voltage can be assumed independent of the oscillation and proportional to the average slip (equations 3*a* and 4*a*). When the synchronous machine is of the same size as the asynchronous machine the change of the slip has to be taken into acount in the equations 3*a* and 4*a*. The results in this case become much more complicated than in the case considered.

List of Symbols

INDEX 1—STATOR—INDEX 2—ROTOR

E_L terminal voltage

$K=\frac{E_{L2}}{E_{L1}}$

l_i ideal core width

L leakage coefficient

m_1 number of phases of the stator

N number of turns per phase

r resistance

s slip

x leakage reactance

x_m reactance due to the main flux

z angular velocity of the oscillation

δ angle between primary and secondary voltage

$\tau_1=\frac{x_1}{x_m}$, $\tau_2=\frac{x_2}{x_m}$ leakage coefficients

τ_p pole pitch

References

1. DAMPING TORQUE AND DESIGN OF THE DAMPER WINDING OF SYNCHRONOUS MACHINES, **M. M. Liwschitz.** *Arch. f. Elektrot,* volume 10, 1921.

2. TWO REACTION THEORY OF SYNCHRONOUS MACHINES, I, **R. H. Park.** AIEE TRANSACTIONS, volume 48, 1929, pages 716–27.

3. POSITIVE AND NEGATIVE DAMPING IN SYNCHRONOUS MACHINES, **M. M. Liwschitz.** AIEE TRANSACTIONS, volume 60, 1941 (May section), pages 210–13.

Relative Accuracy of Three-Phase Metering Combinations

C. T. WELLER
MEMBER AIEE

Synopsis: This paper grades several three-phase combinations of instrument transformers and watthour meters under various conditions according to their approach to the best standard practice. The combinations are described and sources of uncertainty or of error are discussed. Diagrams are included to show the schematic connections of the component transformers and meters, both separately and in combination and of the power systems to be metered.

Introduction

FROM time to time questions arise in regard to the accuracy of three-phase metering combinations of instrument transformers and watthour meters. A definite estimate of the accuracy to be expected can usually be made for a given installation if sufficient details are available. However, in many cases all that is required is an idea of the relative accuracy obtainable. To meet such situations, relative accuracy under various conditions is here assigned to typical metering combinations now in use and to others sometimes proposed. These combinations are considered principally from the instrument-transformer standpoint. Operating and metering difficulties sometimes encountered with Y-connected potential transformers and the effects of various secondary interconnections on the metering accuracy are discussed. Much of this discussion applies to three-phase indicating wattmeters as well as to watthour meters.

A summary of the paper is given in table I, wherein the relative accuracy is graded from A to E. Grade A is assigned to cases where the metering combination and the conditions of application represent the best standard practice, which ordinarily embodies a close approach to the ideal. Three of the four power systems included are classified as three-phase, three-wire. There are five instrument transformer combinations and three types of watthour meters: 2-element, $2^1/_2$-element, and 3-element, respectively. In each case, sufficient comments are included to make table I reasonably self-explanatory. Table I is supplemented by figures 1 to 4, which show the schematic connections of the different parts and also of six complete metering applications.

It should be kept in mind that the ideal polyphase metering combination from the standpoint of accuracy is one that can be resolved into two or more component single-phase sections. Each section consists of one potential transformer, one current transformer, and one meter element. The instrument transformers can be checked for accuracy at any time and a portable single-phase indicating wattmeter or a watthour-meter standard can be added to the secondary meter circuits. Thus the accuracy of the polyphase combination can be verified to the satisfaction of any legal authority from the summation of two or more sets of single-phase results obtained simultaneously. For the highest accuracy, complete single-phase sections should be used as standards entirely separate from the polyphase combination. However, the accuracy obtainable with either method will not be uniform over wide ranges of power factor or load.

Power Systems

Three-Phase Three-Wire Systems

These systems may be classified according to the treatment of the system neutral. Systems with isolated neutral (figure 1*a*) or with a ground at one neutral point only (figure 1*b*) are common and require no special comments. Ordinarily it is immaterial from the metering standpoint whether the neutral is isolated or is grounded at one point either solidly or through low or high impedance; a ground-fault neutralizer (Petersen coil) constitutes an example of a high-impedance ground. Separate classifications for the two systems are justified, since single-phase loads could be connected between any line and ground with single-grounded neutral systems, particularly if the neutral is grounded through a low impedance, whereas such loading is not possible with isolated-neutral systems. For systems grounded at but one neutral point, it is assumed that there will be no line-to-ground loads.

Systems grounded at more than one neutral point (multiple grounds—figure 1*c*) in the manner shown probably should be considered as three-phase, four-wire systems, even if not so classified, not only because single-phase loads could be connected between any line and ground as just pointed out, but particularly because such loads can now be applied through the Y-Y-connected power transformers. These transformers often are provided with tertiary windings for closed-delta connection to take care of the triple harmonics in the exciting currents.

Three-Phase, Four-Wire Systems

This classification applies to systems having four metallic conductors (figure 1*d*). Such systems also are common and usually supply single-phase loads connected between any line and the neutral in addition to three-phase, three- or four-wire loads. The system neutral may or may not be grounded at one or more points.

Instrument Transformers

The principal functions of instrument transformers are to insulate low-voltage

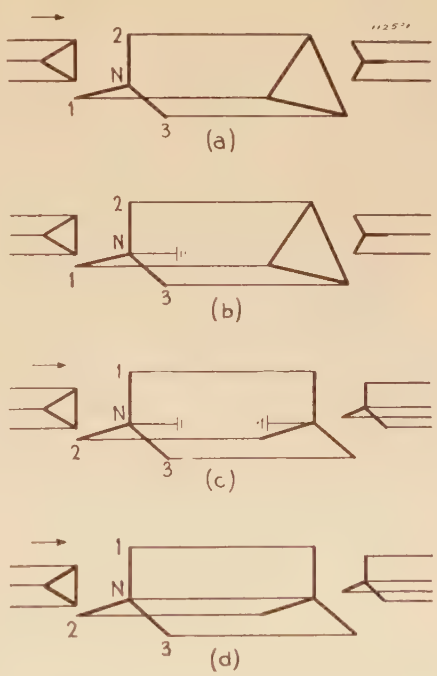

Figure 1. Three-phase power systems

Three-phase three-wire with
(*a*) Isolated neutral
(*b*) One neutral ground
(*c*) Multiple neutral grounds

Three-phase four-wire
(*d*) With or without neutral ground

Paper 41-125, recommended by the AIEE committee on instruments and measurements, and presented at the AIEE summer convention, Toronto, Ontario, Can., June 16–20, 1941. Manuscript submitted April 16, 1941; made available for preprinting May 14, 1941.

C. T. WELLER is an electrical engineer in the general engineering laboratory of the General Electric Company, Schenectady, N. Y.

1. For all numbered references, see list at end of paper.

measurement devices from dangerous-to-life line voltages and to act as multipliers for them. In the instrument transformer combinations under consideration (figure 2), the current-transformer primaries are connected in the proper lines and their individual secondaries supply individual meter-current circuits. On the other hand, the potential-transformer primaries are connected either line-to-line or line-to-neutral, so their individual secondaries either supply individual meter potential circuits or constitute part of a network.

The currents and voltages obtained from the secondaries of instrument transformers usually represent the corresponding primary quantities with acceptable accuracy without making corrections for the respective ratio and phase angle errors, but such corrections for either the actual or the "average" characteristics frequently can be applied when necessary. Several exceptions to these statements are discussed under "Metering Considerations" but some of a more general nature are mentioned here. Thus for the case of three potential transformers connected closed-delta-delta, the normal unit characteristics may be considerably altered because of a fairly large circulating current in the windings resulting from small differences between the units. However, line-to-line connected potential transformers are, in general, much freer from various disabilities than Y-connected potential transformers.

For the latter, the three line-to-neutral voltages with isolated primary neutral may contain appreciable triple harmonics due to the suppression of such harmonics in the respective exciting currents; this distortion actually may cause an erroneous voltage indication, to say nothing about rendering normal transformer corrections of doubtful value. If the primary neutral is grounded, but if the system neutral is ungrounded either permanently or temporarily, the potential transformer line-to-neutral voltages may become very badly distorted and the neutral point, in effect, may even get outside of the supply-voltage triangle due to switching surges.[1,2,3]

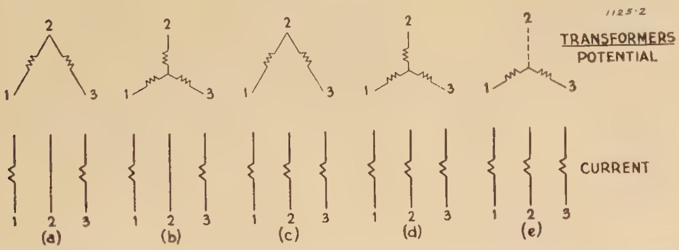

Figure 2. Instrument - transformer combinations for three-phase systems

Primaries of two current transformers and; *(a)* two potential transformers in open delta; *(b)* three potential transformers in wye. Primaries of three current transformers and; *(c)* two potential transformers in open delta; *(d)* three potential transformers in wye; *(e)* two potential transformers in part wye.

(a), (b), (c), (d) For three-phase, three-wire systems; *(d), (e)* for three-phase, four-wire systems

Watt-Hour Meters

Two-Element Meters (Figure 3*a*)

These meters have two separate driving elements, which may act either on separate disks mounted on a common shaft or on different segments of the same disk. Such meters are standard for three-phase, three-wire systems.

Two-and-One-Half-Element Meters (Figure 3*b*)

These meters also have two separate elements but each set of current coils is divided into two equal, separate sections. One section and the corresponding potential coil of one element are supplied from one system phase and the other similarly arranged element is supplied from a second system phase somewhat like a straight 2-element meter. Current from the third system phase flows in a reversed direction through the two extra meter current-coil sections in series and thus reacts with the voltages of the other two system phases applied to the two meter potential coils. The vector sum of these two phase voltages usually equals the voltage of the third phase, so it is evident that the "$^1/_2$-element" then operates correctly but with a synthetic instead of an actual third-phase voltage. However, this vector sum does not always correctly represent the third-phase voltage and under such conditions the "$^1/_2$-element" registration will be in error; of course, it contributes but one-third the torque and its error but one-third the effect in a balanced system.

These meters also are known as 2-element meters with split current coils. They are standard for three-phase, four-wire systems when the three voltages are approximately balanced and are used to avoid the extra potential transformer, wiring, and expense required for a 3-element meter.

Three-Element Meters (Figure 3*c*)

These meters have three separate elements which are supplied from the three phases of a three-phase, four-wire system for which they are standard under all conditions of load and of voltage balance. The meters are entirely satisfactory for three-phase, three-wire systems having one or more neutral grounds.

Metering Considerations

Single-Phase Metering

The metering of a single-phase system will serve as an introduction to the metering of polyphase systems. A single-phase system requires one potential transformer, one current transformer, and one watt-hour meter. Certificates for the two instrument transformers will give the respective ratio correction factors to within 0.1 per cent and the phase angles to within three minutes. The watthour meter can be adjusted to be correct within say 0.3 per cent over a medium load range. Thus an overall accuracy within 0.5 per cent over such a load range near unity power-factor could be expected, even if the errors were all in the same direction, which would be most unusual. Better accuracy can be obtained at a definite and fairly steady load point by taking the average of a large number of observations on a high-grade portable indicating wattmeter, which can be checked to within 0.15 per cent over the upper part of its scale. On a similar basis, an overall accuracy within 0.35 per cent could be expected under this condition.

The single-phase metering combination just described represents the simplest case, where the corrections determined for the individual parts can readily be combined algebraically and an estimate made of the best accuracy obtainable. Since a polyphase power system consists in effect, of two or more out-of-phase single-phase systems, it should be obvious that the highest accuracy can be obtained only if single-phase metering conditions are maintained. This accounts for long-standing cautions against some "secondary interconnections" in polyphase metering circuits.

Three-Phase Three-Wire Metering

Applying this idea to a three-phase, three-wire, ungrounded system, two current and two potential transformers and two single-phase watthour meters would

Table I. Relative Accuracy

Case	System	Neutral: Pot. Trans. Pri.	Neutral: Pot. Trans. Sec.	Neutral: Meter	Connections: Pot. Trans.	Connections: Meter	Comments	Figure	Accuracy Grade
3-Phase 3-Wire Systems									
2-element meter—2 current transformers—2 potential transformers									
1	*Isolated				Open Δ	Open Δ	Best standard practice	4*a*	A
2	**1 ground				Open Δ	Open Δ	Best standard practice	—	A
3	***Mult. gr.				Open Δ	Open Δ	L/N loads not metered correctly	—	D
2-element meter—2 current transformers—3 potential transformers									
4	Isolated	Iso./gr.	Gr.		Y-Y	Open Δ	Indeterminate	—	C
5	1 ground	Iso./gr.	Gr.		Y-Y	Open Δ	Indeterminate	4*b*	C
6	Mult. gr.	Iso./gr.	Gr.		Y-Y	Open Δ	Indeterminate; related to *case 3*	—	E
3-element meter—3 current transformers—2 potential transformers									
7	Isolated			Iso.	Open Δ	Y	Indeterminate	—	C
8	1 ground			Iso.	Open Δ	Y	Indeterminate	4*c*	C
9	Mult. gr.			Iso.	Open Δ	Y	Indeterminate	—	C
3-element meter—3 current transformers—3 potential transformers									
10	Isolated	Iso./gr.	Gr.	Iso.	Y-Y	Y	Indeterminate	—	C
11	1 ground	Iso./gr.	Gr.	Iso.	Y-Y	Y	Indeterminate	4*d*	C
12	Mult. gr.	Iso./gr.	Gr.	Iso.	Y-Y	Y	Indeterminate	—	C
13	Isolated	Gr.	Gr.	Gr.	Y-Y	Y	Neutral instability possible	—	C
14	1 ground	Gr.	Gr.	Gr.	Y-Y	Y	Best standard practice	—	A
15	Mult. gr.	Gr.	Gr.	Gr.	Y-Y	Y	Best standard practice	4*e*	A
3-Phase 4-Wire Systems									
3-element meter—3 current transformers—3 potential transformers									
16	Iso./gr. †	Iso./gr.	Gr.	Gr.	Y-Y	Y	Best standard practice	—	A
$2^1/_2$-element meter—3 current transformers—2 potential transformers									
17	Iso./gr. †	Iso./gr.	Gr.	Gr.	L/N	L/N	Standard practice	4*f*	B

NOTES: L/N = line-to-neutral; Iso./gr. = isolated or grounded.
*Figure 1*a*.
**Figure 1*b*—it is assumed that there will be no line-to-ground loads.
***Multiple grounds—figure 1*c*—these 3-phase, 3-wire systems probably should be considered as 3-phase, 4-wire systems and provision made for metering correctly single-phase loads connected between any line and neutral or ground.

†In *cases 16* and *17*, the potential-transformer and system neutrals are tied together; the system neutral may either be isolated from ground (figure 1*d*) or grounded at one or more points. See text for further comments on the $2^1/_2$-element metering combination.

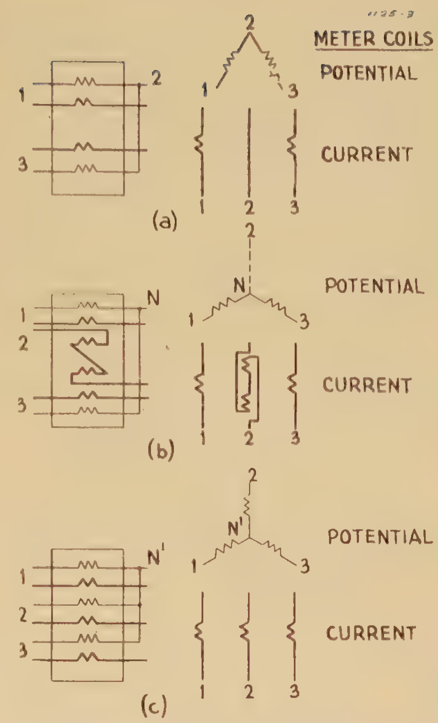

Figure 3. Polyphase watt-hour meters

(*a*) Two-element for three-phase three-wire systems

(*b*) Two-and-one-half-element for three-phase four-wire systems

(*c*) Three-element for three-phase three- or four-wire systems

be required and these would constitute two separate, single-phase metering circuits. Of course, such separate metering circuits are quite unusual, except for special tests. The meters are slightly handicapped by the fact that a phase displacement of 30 degrees exists between the line-to-line voltages and the line currents (at unity power factor).

Thus for *case 1* in table I (figure 4*a*), the first "secondary interconnection" occurs in the substitution of a 2-element polyphase watthour meter for the two single-phase meters, which necessitates an average correction for the instrument-transformer and meter-element errors. Other interconnections occur in the substitution of three secondary leads for four both for the current transformers and for the potential transformers. This tends to complicate the ratio and phase-angle tests, particularly if the secondary leads are long.

For balanced systems, the secondary current in the common lead will equal those in the other two leads, but will be 120 degrees out of phase with them and the resulting additional common burden for the two current transformers must be allowed for in making up the respective test burdens. If this common burden is large due to a long lead or to measurement or protective devices connected in series therewith, it will be necessary to know the phase sequence of the power system, as well as the actual phases in which the current transformers are connected in order to test them properly.

For two equal potential-transformer burdens, the current in the common potential lead will be $\sqrt{3}$ times those in the other two leads and 30 degrees out of phase with them; neglecting the voltage drop in the leads may cause appreciable errors in the ratio and phase-angle results. Further complications occur if a burden is connected across the open delta (third phase without potential transformer); even if its power factor is unity, it imposes its full voltamperes at 0.5 power factor on both potential transformers, leading in one case and lagging in the other, thus again making it necessary to know the phase-sequence of the power system and the connections of the individual transformers thereto: the importance of this proceeding increases with the magnitude of the burden. Somewhat similar considerations apply when double autotransformers are used to shift the phase of the potential transformer voltages to supply var- or voltampere-hour meters, since the net effect is to change the burden distribution. Interconnected, low-power-factor burdens sometimes have surprising effects: when two potential transformers supply such Y-connected burdens, not only does one transformer supply all the energy necessary, but it also tends to excite the other transformer secondary winding! This undesirable effect increases with the magnitude of the burdens and may be overcome by adding suitable non-inductive burdens.

In spite of the various uncertainties just outlined, some of which are inherent in the *case 1* metering combination, satisfactory accuracy is usually obtained. A similar statement applies when the power-system neutral is grounded at one point only as in *case 2*.* Thus the highest relative accuracy—grade A—is assigned to *cases 1* and *2*.

A much greater degree of uncertainty exists when three Y-connected potential

*Case 3 and others involving grounds at more than one power-system neutral point are discussed under "Three-Phase, Four-Wire Metering."

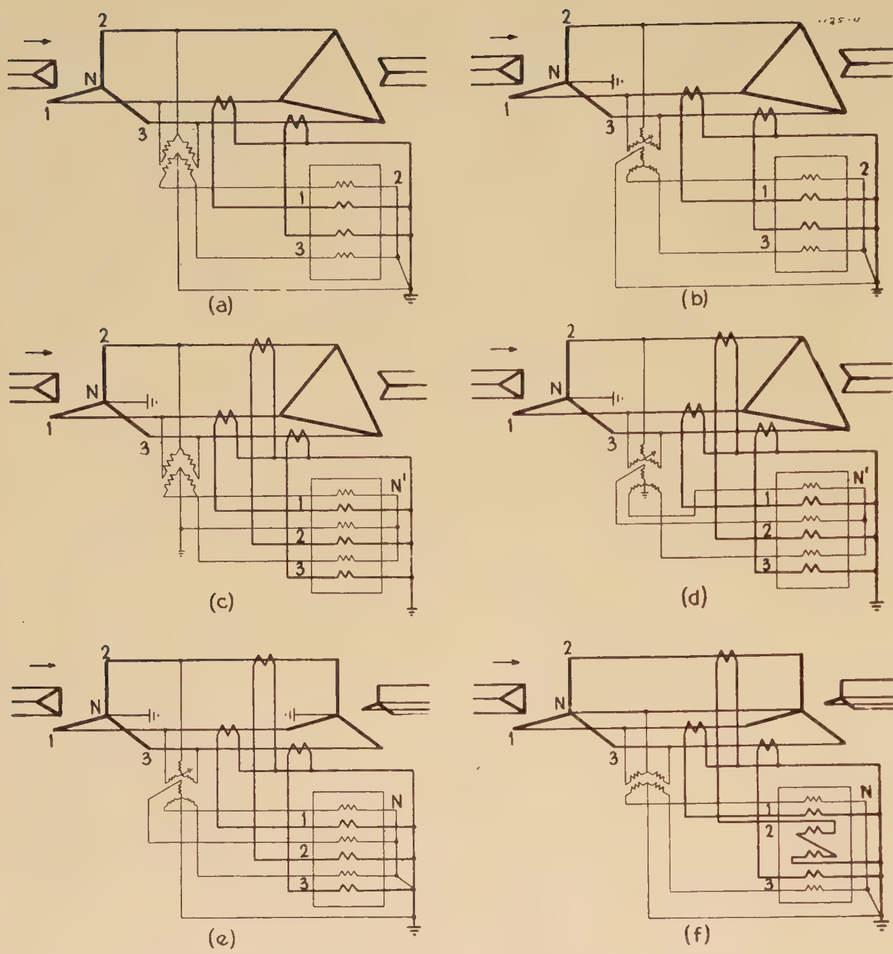

Figure 4. Schematic connections of three-phase metering combinations (cases outlined in table I)

(a) *Case 1* (figures 1*a*, 2*a*, 3*a*)
(b) *Case 5* (figures 1*b*, 2*b*, 3*a*)
(c) *Case 8* (figures 1*b*, 2*c*, 3*c*)
(d) *Case 11* (figures 1*b*, 2*d*, 3*c*)
(e) *Case 15* (figures 1*c*, 2*d*, 3*c*)
(f) *Case 17* (figures 1*d*, 2*e*, 3*b*)

transformers are substituted for two connected open delta to supply the two potential circuits of a 2-element meter as in *cases 4* and *5* (figure 4*b*). Here it is impossible not only to allocate properly the three individual potential transformer corrections, which may differ slightly, but also to resolve the combination into component single-phase metering circuits, which is much more important. The three line-to-neutral transformer voltages will be distorted (peaked) if the primary neutral is isolated and may be distorted if it is grounded with system neutral isolated, as was pointed out under "Instrument Transformers." However, the secondary line-to-line voltages applied to the two meter circuits will not be distorted, assuming sine-wave supply voltages. The uncertainty necessitates assigning a considerably lower relative accuracy—grade C—to *cases 4* and *5*.

A similar indeterminate situation exists when two open-delta connected potential transformers are used to supply the three Y-connected potential circuits of a 3-element meter as in *cases 7* and *8* (figure 4*c*), which is sometimes recommended for low-power-factor loads on three-phase, three-wire systems. Here the three line-to-neutral meter voltages are somewhat distorted due to the suppression of the triple harmonics in the exciting currents. Such distortion will not occur if the inductive meter circuits are replaced by noninductive wattmeters.

The foregoing situation is not improved by the substitution of three Y-connected potential transformers for the two in open delta, if the two secondary neutral points are not connected as in *cases 10* and *11* (figure 4*d*). Here again as in *cases 4* and *5*, the three line-to-neutral transformer voltages will be distorted if the primary neutral is isolated and may be distorted if it is grounded with system neutral isolated, but the secondary line-to-line voltages applied to the Y-connected meter circuits will not be distorted with a sine-wave supply.

The indeterminate features of *cases 10 and 11* are partly overcome by connecting the potential-transformer-secondary and meter-potential-circuit neutral points as in *case 13*. However, the three line-to-neutral voltages may be distorted and potential-transformer-neutral instability may result as with similar neutral conditions in *cases 4* and *10*, due to the attempt to ground the power system through the potential transformers. Because of this, *case 13* is assigned relative-accuracy grade C also.

Grounding the power-system neutral at one point as in *case 14* translates *case 13* into standard practice. *Case 14* closely approaches the ideal of component single-phase metering sections mentioned in the "Introduction." The eight secondary leads (as in figure 4*e*) are practically equivalent to twelve, since the currents in the two common leads normally are negligible. Three single-phase watt-hour meters may readily be added for verification purposes and each meter or meter element operates at the same power factor as that of the load in its respective phase, which is particularly advantageous at low power factors. This favorable condition does not exist with balanced three-phase loads in *cases 1* and *2;* however, these are entitled to share relative-accuracy grade A with *case 14* for most applications.

Three-Phase Four-Wire Metering

A 3-element meter with three current and three potential transformers as in *cases 14, 15* (figure 4*e*) and *16* is standard both for three-phase, three-wire systems with at least one neutral point grounded and for three-phase, four-wire systems. Relative-accuracy grade A is assigned to this metering combination. Three-phase, three-wire systems with multiple neutral grounds are equivalent in many respects to three-phase, four-wire systems, even if not so operated with single-phase loads connected between any line and the neutral ground.

A $2^1/_2$-element meter with three current and two potential transformers as in *case 17* (figure 4*f*) is standard for the usual condition where the three line-to-neutral voltages of the three-phase, four-wire system are fairly well balanced; relative-accuracy grade B is assigned to this metering combination.

Although designed primarily for three-phase, four-wire systems, it should be evident from a consideration of *cases 16* and *17* that the $2^1/_2$-element metering combination can be substituted for the 3-element metering combination in *cases 14* and *15*. Relative-accuracy grade B would then be assigned unless the system-neutral grounds are effected by means of ground-fault neutralizers; the line-to-neutral voltages may then be consider-

Impulse Strength as a Measure of Cable Quality

L. I. KOMIVES
ASSOCIATE AIEE

Synopsis: Testing cables by means of the impulse generator, originally developed for use in studying the effect of lightning on cables, is becoming recognized more and more as a useful method for determining cable quality. It is felt that the amount of data accumulated during the past ten years is sufficiently large to be used in formulating a theory concerning the factors governing the impulse strength of cables. It is indicated in this paper that maximum rather than average stress should be taken into account when impulse test results are evaluated, since the maximum stress at breakdown is a measure of the quality of the insulation alone. This view is contrary to that generally accepted in this country although some workers in this field abroad have accepted this theory for some time.

Introduction

THE Detroit Edison Company has in the past sponsored a number of tests to determine the impulse strength of various types of cable in relation to other electrical equipment. Results of some of these tests on "solid-type" impregnated paper (24 and 4.8 kv) and varnished cambric (4.8 kv) cables were published by McCabe[1,2] from time to time. About two years ago the scope of these tests was enlarged to include various types of impregnated paper insulated cables proposed for extra-high voltage service as no impulse test data were then available on such cables. Held and Leichsenring[3] and Foust and Scott[4] have since published results of impulse tests on oilfilled cables.

Oilfilled, oilostatic, compression, and gas-filled (Beaver) cables were in commercial use two years ago at voltages above those recommended for solid type cables. As gas-filled cable was not on hand, oilfilled, oilostatic, and compression cables having equal insulation thicknesses, were tested. The results of these tests indicated that maximum rather than average stress determines the impulse strength of the cable. In order to verify this statement, tests were made on solid type cables of various conductor diameters, conductor surfaces and insulation thicknesses, and on low gas pressure cables. In computing average stresses at breakdown on the solid type cables, no definite correlation could be established between these data and the quality of the insulation as observed by examination of the samples. On the other hand, when maximum stresses at breakdown were computed, values were obtained that showed pronounced increase with improving insulation, reaching a constant maximum value at the best obtainable impregnation. Further tests on oilfilled cables showed that uniformity of taping as determined by the Mildner diagram affects the maximum stress at breakdown in a similar manner as does the degree of impregnation. This correlation is a strong indication of the significance of the maximum stress as the criterion of quantitative breakdown.

Previous Work

No universally accepted theory has been proposed that would allow the computation of the impulse breakdown voltage of a cable of known construction details and known insulation qualities. A study of the published data on impulse tests of cables, however, permits the drawing of conclusions concerning certain factors that influence the impulse strength.

Paper 41-131, recommended by the AIEE committee on power transmission and distribution, and presented at the AIEE summer convention, Toronto, Ontario, Can., June 16–20, 1941. Manuscript submitted April 8, 1941; made available for preprinting May 14, 1941.

L. I. Komives is with The Detroit Edison Company Detroit, Mich.

The author wishes to extend his thanks to A. Gemant, F. M. Hull, and J. Sticher of The Detroit Edison Company for their collaboration and constructive criticism.

1. For all numbered references, see list at end of paper.

---

ably unbalanced due to unequal capacitances to ground of the three line conductors. Under this condition, the 3-element metering combination should be used. Of course, the straight 2-element metering combination (*case 2*) may be used for all such three-phase, three-wire systems if the single-phase loads to neutral are negligible or if these loads are balanced.

The limitations just placed on the application of 2-element metering combinations are important. In *cases 3* and *6*, for example, a load connected between the line without current transformer and ground would not be metered at all and the meter voltages would not have the proper magnitude or phase for loads connected between the other two lines and ground; this accounts for the low relative-accuracy grades D and E, respectively. The grade C accuracy assigned to the 3-element metering combination in *cases 9* and *12* is due to its being indeterminate and not to the possibility of incorrectly metering single-phase loads to ground.

In the foregoing discussion, the term "indeterminate" has been used to describe conditions where it is impossible to resolve the metering combination into component single-phase sections and thus to allocate instrument-transformer and meter corrections definitely. Although it need not be assumed that "indeterminate" is synonymous with "inaccurate," arguments advanced as to the correctness of such a metering combination may sound unconvincing. It should be emphasized that all important metering installations are at all times subject to verification or checking when questions arise in regard to their correctness.

Conclusions

A general idea of the performance to be expected from several three-phase metering combinations under various conditions is conveyed by the relative accuracy assigned thereto in table I. Among the many cases included, it should be possible to find examples approximating other cases sometimes used or proposed and thus permit grading them also. From the accompanying discussion, it should be evident that in cases where grade A is assigned to the metering combination, very satisfactory accuracy can be obtained if appropriate secondary connections are used and if the instrument-transformer corrections are properly applied.

References

1. Experiences With Grounded-Neutral, Wye-Connected Potential Transformers on Ungrounded Systems, C. T. Weller. AIEE Transactions, volume 50, 1931, pages 299–316.

2. Physical Nature of Neutral Instability, A. Boyajian and O. P. McCarty. AIEE Transactions, volume 50, 1931, pages 317–27.

3. Theory of Abnormal Line-to-Neutral Transformer Voltages, C. W. LaPierre. AIEE Transactions, volume 50, 1931, pages 328–42.

(a). Quality of Insulation

Held and Leichsenring[3] and Busse and Vogel[5] established that the use of denser papers results in higher impulse strength; and that temperature of the cable during the tests, provided the limits do not exceed those of commercial operation, does not measurably influence the impulse strength.[3] By inference, the latter signifies that the viscosity of the impregnating compound (which decreases as the temperature increases) has also a very limited effect on the impulse strength. Whether "straight" mineral oil is used to impregnate the cable or a mixture of mineral oil and rosin, appears to have no effect on the impulse strength of the cable. The degree of impregnation at a given temperature, however, seems to have a very decided effect.[1] That service aging of solid-type cables, which generally results in a decrease of the degree of impregnation, will also result in a proportional decrease of impulse strength is indicated[2] but this requires further study.

(b). Geometry of Cable and Surface of Conductor

The effect of conductor diameter (minimum radius) and conductor surface appears to have influenced the results of several workers. For instance when specially constructed copper conductors having the same diameter and smooth outer surface were used, the number of variables was reduced to such an extent that from the results obtained it was possible to disprove the theory still generally accepted in this country, that thinner insulation possesses a comparatively higher impulse strength.[3] Tests on cables with sector shaped conductors disclosed the fact that 80 per cent of the failures were on the "shoulder" (minimum radius of the conductor) of the sector.[1] The same author reports that strand-shielding improves the impulse strength considerably.[2] Davis and Eddy found that the impulse strength of rubber in sheet form is approximately 50 percent higher than that of rubber cable insulation of the same wall thickness.[6]

(c). Polarity of the Impulse Wave

Schneeberger,[7] in discussing the effect of polarity of the impulse wave on the impulse strength of a cable, indicated that when a positive wave was used, the breakdown value was 20 percent lower than with a negative wave. Later reports contradict this finding. One author has found no difference in oilfilled cables but in solid cables the impulse strength, using a negative wave, was from 5 to 13 percent lower than when a positive wave was used.[3] Another paper states that the authors found no difference in impulse strength due to variations in the shape and polarity of the impulse wave.[6]

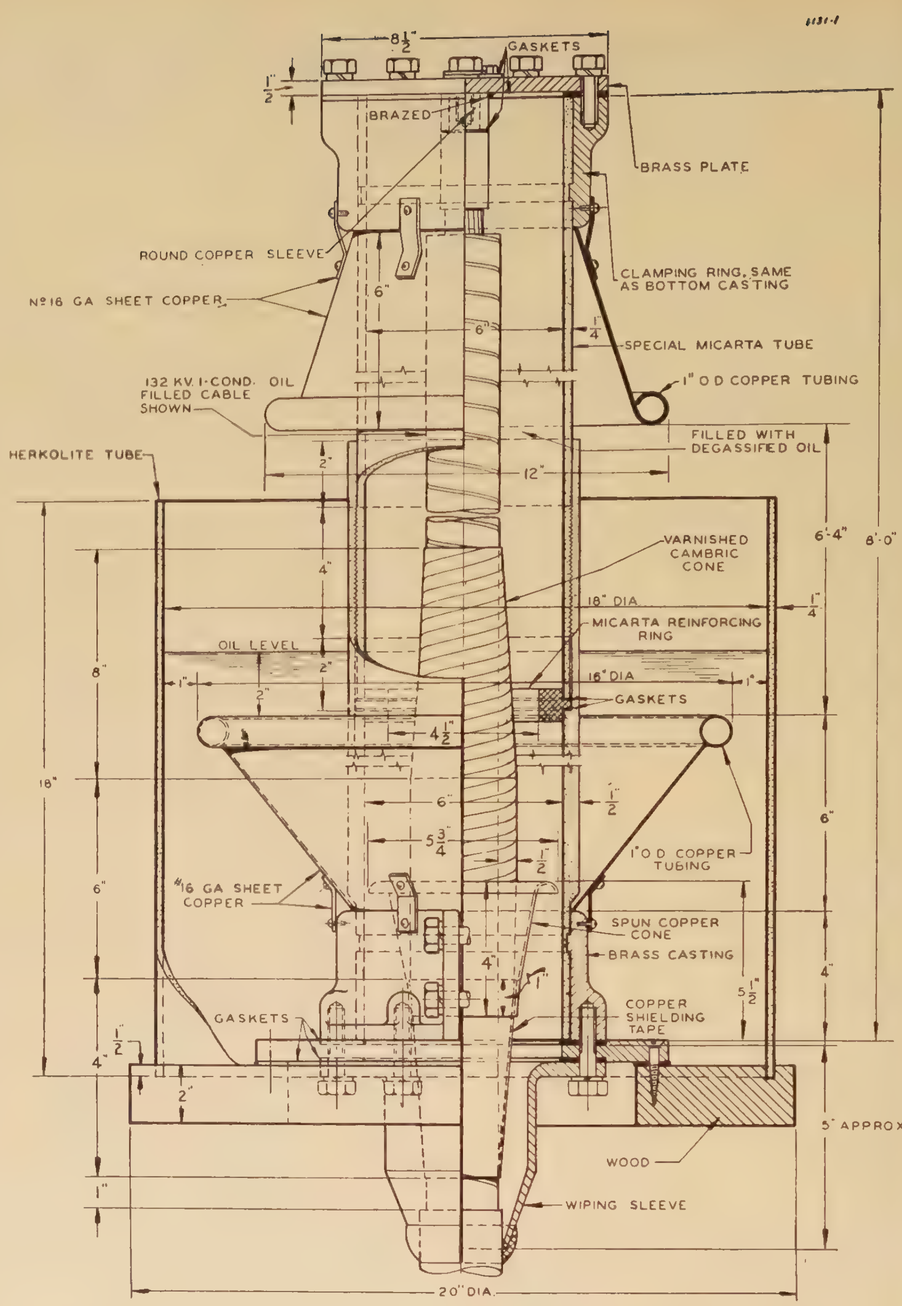

Figure 1. Impulse terminal assembly for high-voltage surge test

In view of the above data, no definite conclusion can be drawn in regard to the effect of the polarity of the impulse wave on the impulse strength of the cable. For this reason, small variations in absolute values reported by various authors may exist, but the relative rating of the individual samples will probably still remain the same.

Method of Test and Testing Equipment

Engineers of The Detroit Edison Company favor the impulse testing of electrical apparatus with a negative wave because field testing has shown the prevalence and greater importance of negative lightning strokes in connection with transmission line outages. A method of testing with sufficiently high potential surge to obtain breakdown with one surge is also favored for reasons of simulating conditions in the field. All tests described in this paper, therefore, were made with negative wave and attempts were made to obtain breakdown with one surge.

The impulse generator used has been previously described.[1] For these tests additional condensers were used in series and both ends of the cable were encased in terminals built to withstand 1,000 kv and

200 psi pressure. Figure 1 shows the terminal assembly. Figure 2 shows the method used in connecting the cable to the impulse generator. Figure 3 is an oscillogram of the incident wave (approximately 0.05×24 microsecond) with the cable disconnected, and figure 4 is a typical wave recorded during breakdown of sample $J1$. It should be noted that the steepness of the wave front is somewhat lessened when the cable is connected to the generator.

Presentation of Results and Description of Samples

The results of the impulse tests which form the basis of this paper, are graphically illustrated in figure 5, and complete data are supplied in tables I and II.

represents minimum values of groups of measurements.

Pertinent information regarding the Detroit samples is given in the following:

Samples $A1$, $A2$, $I1$, and $J1$ were solid type, single-conductor cables. The A samples had a small conductor and thin insulation. Sample $I1$ had a conductor diameter similar to that of samples $E1$ to $E4$ (compression and oilostatic) but an insulation thickness almost twice as great (170%). Sample $J1$ had a large conductor diameter similar to that of samples $F1$, $F2$, $G1$, $G2$, $H1$, and $H2$ (oilfilled) but greater insulation thickness (130 and 111% respectively).

Samples $B1$, $B2$, $B3$, $B4$, $B5$, and $B6$ were low gas pressure, three-conductor, sector, shielded, 27.6-kv cables. Samples $B1$, $B2$, and $B3$ represent three conductors of one section and samples $B4$, $B5$, and $B6$ the three conductors of another section of the same cable. Ten complete failures were observed in the six samples, seven of which were at the "shoulders" of the sector.

Samples $C1$, $C2$, $C3$, $D1$, $D2$, and $D3$ were solid type, three-conductor, sector, shielded, 24-kv cables. The C samples represent the three conductors of one cable, while the D samples are the three conductors of another cable. The two cables were identical except for the strand-shielding with semi-conducting tapes employed in the latter group. The manufacturer who made these cables used the same type of paper, same taping machine, impregnated the two cables in the same tank, and lead covered both on the same day. Therefore, except for the strand-shielding, there should be no other variables. Failures in all six samples occurred at or near the "shoulder" of the sector.

Samples $E1$, $E2$, $E3$, and $E4$ were taken from the same oval-shaped, single-conductor cable. Samples $E1$ and $E3$ were tested in a steel pipe containing nitrogen under 200 psi (compression cable). $E2$ was tested as an oilostatic cable, that is, the armoring and lead sheath were removed, and the pipe that contained the cable was filled with oil under 200 psi. $E4$ was tested without the application of pressure; in other words, as a solid type cable. All four samples failed near the major axis of the oval conductor. Figure 6 shows the Mildner-diagram of cable E.

Samples $F1$, $F2$, $G1$, $G2$, $H1$, and $H2$ were taken from three single-conductor oilfilled cables made by three manufactur-

Table I

Tested in Detroit

No.	Type of Cable	r.	w.	R.	n.	Breakdown Volt. Kv	G. Avg. V/Mil	G. Max. V/Mil	Qual. of Taping	Degree of Impr.
$A1$	Solid	145	156	301	7	230	1,475	2,715	Fair	Fair
$A2$						225	1,440	2,660	Fair	Fair
$B1$	Solid	167	240	407	"Compact" strand	280	1,170	1,880	Very good	Very ltd.
$B2$	Low gas press.	167	240	407	"Compack" strand	300	1,250	2,010	Very good	Very ltd.
$B3$						300	1,250	2,010		
$B4$						315	1,310	2,110		
$B5$						320	1,330	2,150		
$B6$						335	1,400	2,250		
$C1$	Solid	151	281	432	Compack strand	380	1,350	2,390	Very good	Very good
$C2$						390	1,390	2,450		
$C3$						400	1,425	2,520		
$D1$	Solid	166	261	427	Strand shield	480	1,840	3,060	Very good	Very good
$D2$						485	1,860	3,090		
$D3$						500	1,915	3,180		
$E1$	Compr.	290	386	676	18	570	1,475	3,010	Very good	Very good
$E2$	Oilost.					580	1,500	3,060		
$E3$	Compr.					585	1,515	3,080		
$E4$	Compr*					630	1,630	3,320		
$F1$	Oil-filled	542	386	928	37	730	1,890	3,250	Very good	Very good
$F2$						775	2,010	3,450		
$G1$	Oil-filled	514	450	964	25	590	1,310	2,360	Very irr.	Very good
$G2$						680	1,510	2,720		
$H1$						820	1,820	3,280	Very good	Very good
$H2$						825**	1,835	3,300		
$I1$	Solid	340	656	996	18	760	1,160	2,700	Fair	Fair
$J1$	Solid	576	500	1,076	24	830	1,660	2,980	Fair	Fair

*Without pressure.

**No failure.

r. Minimum radius of conductor, mils.

w. Thickness of insulation.

R. Minimum radius over insulation.

n. Number of strands in outer layer.

This chart was compiled to show breakdown voltage and maximum stress at breakdown, for all the samples tested in Detroit as well as those tested elsewhere, when sufficient data were available. It should be noted that the Detroit samples are designated by a letter and a number, each letter representing a cable and each number an individual measurement on a sample of the cable. The data published by Foust and Scott,[4] is represented by the same numbers the authors used in their paper. Number 34 refers to the paper cable sample used by Davis and Eddy[6] and numbers 35 to 40 represent the Held and Leichsenring samples.[3] It should be noted that this latter group

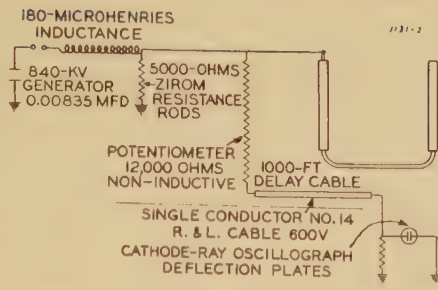

Figure 2. Impulse-generator wiring diagram

84 0.7-microfarad capacitors, 2 capacitors in series per bank. Capacitors charged to 20 kv per bank

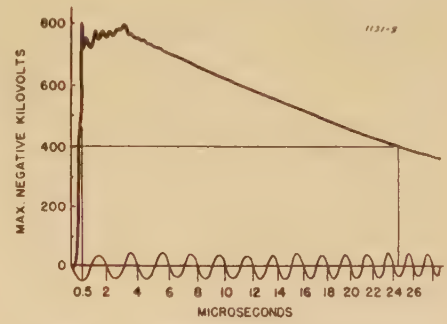

Figure 3. Oscillogram of incident wave

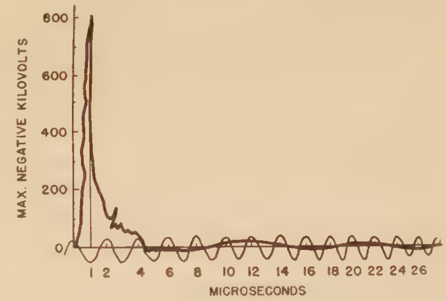

Figure 4. Typical breakdown wave

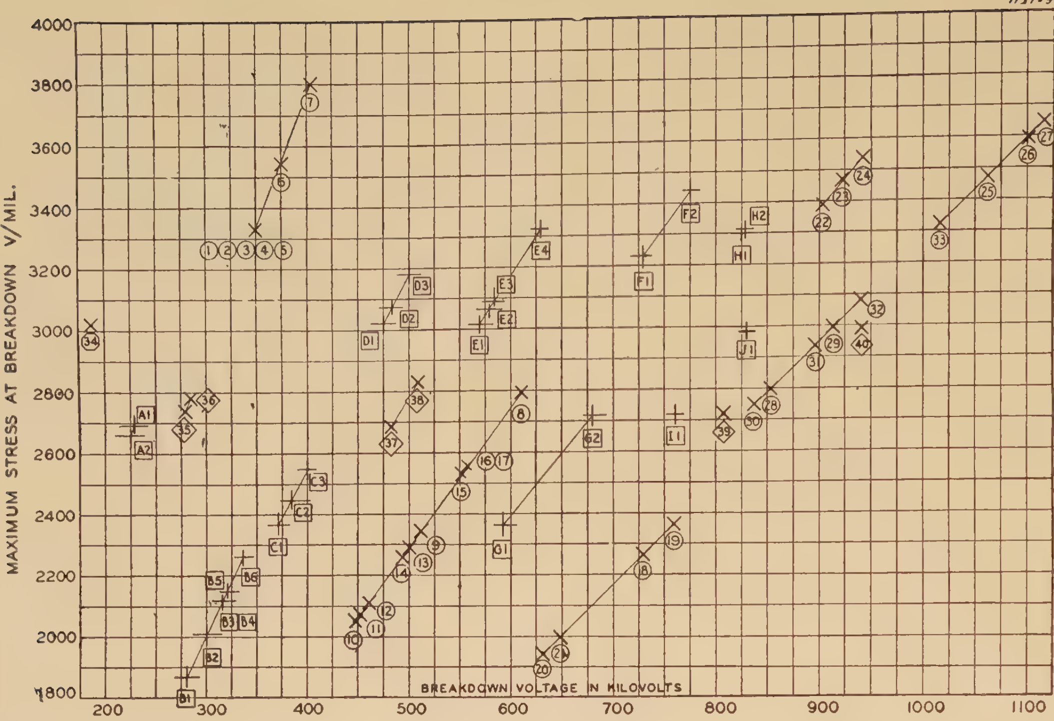

Figure 5. Graphical illustration of results

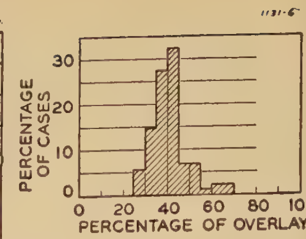

Figure 6. Mildner diagram of cable E

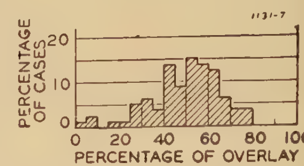

Figure 7. Mildner diagram of cable H

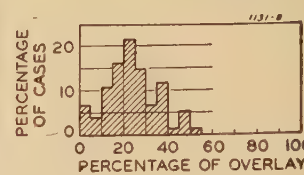

Figure 8. Mildner diagram of cable G

ers, respectively. All six samples were tested under an oil pressure of ten psi. The *F* samples were taken from a cable which was under accelerated aging test for eight years and which had the same insulation thickness as samples *E*1 to *E*4 (compression and oilostatic). Cable *G* which had never been in service, was identical in conductor size and shape, insulation thickness, etc. to cable *H*, made by a different manufacturer and which was under accelerated aging test for a short time. Figure 8 shows the Mildner-diagram of cable *G* and figure 7 of cable *H*.

Discussion of Results

Among the 26 samples tested in Detroit, *A*1, *A*2, *I*1, and *J*1 were single conductor, solid type cables, each having a standard stranded, round, copper conductor. Since the taping and impregnation were approximately the same for the four samples, they offer a basis for comparison of geometrically different constructions. Tabulating the average stresses at breakdown discloses a ratio of 1.43 between maximum and minimum values. Calculating on the basis of maximum stresses after correcting for stranding, yields a ratio of 1.11. This is clearly an indication that maximum rather than average stresses determine the breakdown voltage.

Further indication of the correctness of this theory is obtained in considering another group of three cables of equal insulation characteristics, namely samples *E*4, *F*1, and *F*2. Both cables from which these samples were taken had the same insulation thickness, uniform taping, and high degree of impregnation, but cable *F* had a conductor diameter very much larger than that of cable *E*. The ratio of average stresses of cables *E* and *F* was 1.2 in favor of cable *F*. The ratio of maximum stresses is, on the other hand, 1.01.

Having considered two different groups of cables separately, comparison of the two groups in relation to each other will now be made. The maximum stresses of the first group vary from 2,660 to 2,980 volts per mil, whereas the corresponding values for the second group are 3,250 to 3,450 volts per mil, the averages of the two groups being 1.21. Visual examination of the samples indicated that those in the first group exhibited a lesser uniformity of taping and a lower degree of impregnation than samples in the second group. Thus it can be concluded that the maximum stress, which has been shown to be independent of the geometry of the construction, depends solely upon the quality of the insulation, as measured by the uniformity of taping and the degree of impregnation.

Further and more specific proofs of this statement are supplied by results of tests on other groups of cables. The influence of taping and that of impregnation will be considered in separate paragraphs.

The best evidence in regard to the influence of the quality of taping on the impulse strength of cables was supplied when samples *G*1, *G*2, *H*1, and *H*2 were tested and examined. The cables from which these samples were taken, were identical in dimensions and, both being oil-filled, possessed the same high degree of impregnation. The samples differed from each other in only one respect, i.e. in the degree of uniformity of taping which again was manifested in much lower maximum stress at breakdown (23 percent) for the samples with inferior taping.

The importance of the degree of impregnation without the disturbing influence of variations in taping is demonstrated when the results of tests on the low gas-pressure cable, samples *B*1 to *B*6, are examined and compared with the results of tests on a well-impregnated solid-type cable, samples *C*1 to *C*3. Both types of cables contained sector shaped conductors having nearly equal minimum radii (167 and 151 mils, respectively) at the "shoulders," "compack" stranding was employed, producing approximately equally smooth surfaces; and the taping was equally uniform. The less complete impregnation in the low gas-pressure samples, therefore, appears to be responsible for the 15 percent decrease in maximum stresses.

The smoothness of the electrode surface has for some time been known to influence the impulse flash-over values in gases and liquids. How much practical importance should be attached to smoothing of the conductor surface in cables is indicated by comparing samples *C*1 to *C*3 ("compack" stranded) to samples *D*1 to

Table II

No.	Tested by	Type of Cable	r.	w.	R.	n.	Break-down Volt. Kv	G. Avg. V/Mil	G. Max. V/Mil
1–5	Foust and Scott	Solid	210	187	397	12	350	1,870	3,330
6							375	2,005	3,570
7							400	2,140	3,800
8	Foust and Scott	Oil-filled	945	315	1,260	48	610	1,935	2,895
9							512	1,625	2,430
10							448	1,420	2,120
11							453	1,440	2,150
12							461	1,465	2,180
13							500	1,590	2,370
14							490	1,555	2,320
15							555	1,760	2,630
16							559	1,775	2,650
17							559	1,775	2,650
18	Foust and Scott	Oil-filled	945	500	1,445	48	730	1,460	2,360
19							765	1,530	2,475
20							630	1,260	2,035
21							648	1,295	2,090
22	Foust and Scott	Oil-filled	515	500	1,015	25	902	1,805	3,345
23							928	1,855	3,440
24							940	1,880	3,485
25	Foust and Scott	Oil-filled	515	600	1,115	25	1,067	1,775	3,485
26							1,104	1,840	3,605
27							1,115	1,860	3,640
28							856	1,425	2,795
29							916	1,525	2,990
30							836	1,395	2,730
31							896	1,495	2,925
32							940	1,565	3,070
33							1,014	1,690	3,310
34	Davis and Eddy	Solid	81	94	175	Solid	188	2,000	3,030
35	Held and Leichsenring	Solid	349	118	467	Smooth surf.	280	2,370	2,745
36		Oil-filled	349	118	467		284	2,410	2,785
37		Solid	349	236	585		484	2,050	2,690
38		Oil-filled	349	236	585		510	2,160	2,830
39		Solid	349	472	821		809	1,710	2,715
40		Oil-filled	323	531	854		940	1,770	2,990

r. Minimum radius of conductor, mils.
w. Thickness of insulation.
R. Minimum radius over insulation.
n. Number of strands in outer layer.

*D*3 (strand shielded with semi-conducting tapes). The smoothness of the conductor surface in these samples increased the breakdown voltage by an average of 24 percent. In assessing the significance of this increase, the reduced effective insulation thickness in cable *D*, owing to the substitution of semi-conducting tapes for insulating tapes, near the electrodes, should be taken into account. With an equal thickness of effective insulation, this value would be nearer 30 percent.

The application of 200 psi pressure, gas or oil had a rather curious effect on the maximum stress at breakdown (samples *E*1 to *E*4). It was expected that pressure would increase the impulse strength. On the contrary the results indicated a ten percent decrease due to pressure. If the lower value had been found in only one specimen and the higher value in several specimens, the results might be ascribed to local conditions. However, the single specimen (sample *E*4) tested without pressure was found to have the highest value. Further investigation is recommended before final conclusions are drawn as to the effect of pressure on impulse strength.

Conclusions

The results of the impulse tests conducted by The Detroit Edison Company on various types of impregnated paper-insulated cables seem to indicate that with the type of impulse wave and method of application used in these tests, in a cable having the best obtainable insulation, breakdown occurs at a voltage for which the maximum stress is around 3,300 volts per mil. For a given insulation thickness, therefore, an increase in the minimum radius of the conductor and the use of smoother electrode surface should result in an increase in breakdown voltage. If the quality of the insulation is inferior, owing either to non-uniformity of taping or incomplete impregnation, or both, the maximum stress value can be expected to become less than 3,300 volts per mil. Therefore, the maximum stress obtained from impulse tests, compared with 3,300 volts per mil is a good measure of the uniformity of taping and the degree of impregnation of the insulation. The correlation obtained in these tests between the impulse strength value and the findings of visual examination, such as those shown in Mildner diagrams (also styrene wafers), shows that these visual tests in their turn can justifiably be used as a measure of the impulse strength of the cable insulation.

In view of the above mentioned results, solid, oilfilled, oilostatic, and compression cables should all have the same maximum stress at breakdown. For a given insulation thickness and conductor surface, the oilfilled cable, therefore, having the advantage of an intrinsically large diameter of the conductor will withstand the highest voltage before breakdown occurs.

The tests also indicated that this type of cable will retain this advantage even after aging. The solid, oilostatic, and compression cables, when new, belong to the same group as regards impulse strength. From the decrease of the degree of impregnation in service, it is logical to assume that service aged solid cables have a lower impulse strength than new ones and this assumption is borne out by test. By inference, it may be concluded that the care used in taping solid type cables is more important than the degree of impregnation since age decreases the beneficial effect of the latter, whereas the former will remain practically the same. Oilostatic and compression cables, on the other hand, can be expected to retain their original breakdown values even after aging, although there is as yet no direct experimental verification of this assumption. Low gas-pressure cables, although originally lower than solid-type cables as to impulse strength, are expected to retain this value after service aging and it is possible that they would then show even higher impulse strength than solid-type cables.

References

1. Impulse Tests on 24–27-Kv Paper and Lead Cable, G. B. McCabe. Transmission and distribution committee, Edison Electric Institute, Chicago, Illinois, May 1938.

2. Impulse Tests on Various Kinds of Cable, G. B. McCabe. Transmission and distribution committee, Edison Electric Institute, Atlanta, Georgia, October 1940.

3. The Impulse Strength of High-Tension Cable Installations, C. Held and H. W. Leichsenring. International Conference, Paris, June 1939.

4. Some Impulse Voltage Breakdown Tests on Oil-Treated Paper-Insulated Cables, C. M. Foust and J. A. Scott. AIEE Transactions, volume 59, 1940 (July section), pages 389–91.

5. Busse and Vogel, V.D.E. Fachbericht, 1935.

6. Impulse Strength of Cable Insulation, E. W. Davis and W. N. Eddy. AIEE Transactions, volume 59, 1940 (July section), pages 394–9.

7. Schneeberger, International Conference, Paris, 1937.

Appendix

1. In case of a cylindrical concentric cable with smooth surfaces of conductor and sheath, the field stress (S) at a point of the dielectric is given by the equation

$$S=\frac{E}{r_1 \log \frac{R}{r}} \quad \frac{\text{volts}}{\text{cm}} \qquad (1)$$

where

E = voltage applied between conductor and sheath

The A-C Dielectric-Loss and Power-Factor Method for Field Investigation of Electrical Insulation

FRANK C. DOBLE
ASSOCIATE AIEE

General

THE use of dielectric loss and power factor for testing the insulation of electrical equipment in service position in the field with one side grounded began with the advent of the apparatus and method described in this paper.

Through its use, tables of standard values have been set up indicating when insulation is "good" for continued operation with an adequate factor of safety or when it is "bad" to a degree that warrants investigation and possible replacement in order to insure continuity of service until the next scheduled test.

Types of insulation that were being discarded as inherently bad, judged by their high failure record, now are being re-established as good insulation after the tests have shown the defects to be largely of a secondary nature and removable or curable.

History

A series of high-voltage bushing failures occurring about 1925 emphasized the need for developing a practical field test for this type of insulation that would indicate the presence of certain types of fault or deterioration which inherently were not detectable by a non-destructive direct-current test.

A considerable amount of research and development work was done and several methods were tried and discarded before the ultimate discovery of the a-c dielectric-loss and power-factor method.

The voltage-distribution method for testing high-voltage live-line insulators which had been in successful use for several years was first tried but this method failed to reveal many types of defective insulation that were responsible for costly service interruptions.

Apparatus was then developed for measuring the charging current of a bushing at operating line voltage by isolating on an insulating support a current instrument arranged for connection in series between the terminal of the bushing and the live line normally leading to it. This test did not reveal certain types of defects in insulation and service interruptions continued to occur.

Finally the method described in this paper was devised in which voltamperes, watts, and the power factor of the insulation were measured in the field with portable instruments. The operation and application of the apparatus during the past ten years have been described in the papers listed in the bibliography. This paper is concerned with the technical electrical features and principles involved. There are different forms in which the apparatus may be constructed. For the purpose of discussion, the details of one form of the apparatus will be used to illustrate the general principles.

Paper 41-132, recommended by the AIEE committee on instruments and measurements, and presented at the AIEE summer convention, Toronto, Ontario, Can., June 16–20, 1941. Manuscript submitted November 22, 1940; made available for preprinting May 21, 1941.

FRANK C. DOBLE is president of the Doble Engineering Company, Medford Hillside, Mass.

1. For all numbered references, see list at end of paper.

Test Apparatus Elements

The elements of apparatus required in an a-c dielectric loss method for field investigation of electrical insulation are shown in figure 1.

A 110-volt supply feeds a step-up transformer, T.

From the high-voltage terminal of the high-voltage winding, a cable connection leads to one side of the specimen, C_xR_x, which is grounded.

The measuring means, M, is connected between one side of the high-voltage winding of the transformer, T, and the grounded specimen under test.

Technical Problems

There are special technical problems involved in apparatus designed to measure losses in insulation as installed in the field with one side permanently grounded and subject to electrostatic induction from adjacent or surrounding circuits and apparatus. Because the ground connection can-

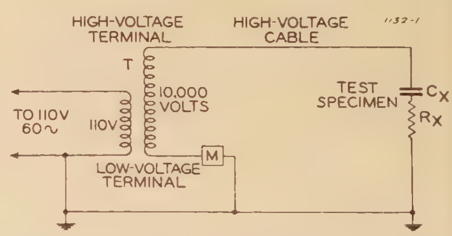

Figure 1. Apparatus to measure a-c dielectric loss in grounded insulation

---

r_1 = radial distance of the point from the center of the cable
r = inner radius of insulation
R = outer radius of insulation

Maximum stress for a given cable will be at the surface of the conductor when $r_1 = r$ and the equation will be

$$S = \frac{E}{r \log \frac{R}{r}} \tag{2}$$

2. For sector shaped conductors with paralleling ground (shielded cable), and smooth surface of conductor and shielding, the portion of the sector containing the points with the greatest stress, is what is known as the "shoulder" of the sector, having the minimum radius of curvature. In cables with sector-shaped conductors maximum stress was estimated by substituting these minimum radii in equation 2.

3. For elliptical (oval shaped) conductors same consideration as in 2, was applied.

4. To calculate the effect of stranding in cables other than those with compacted stranding, the following formula developed by Serguis Vesselowsky of The Detroit Edison Company was used:

$$S = \frac{0.572nE}{r\left(0.119 + n \log_{10} \frac{R}{r}\right)} \tag{3}$$

where

n = number of strands in outer layer
E = voltage applied between conductor and sheath
r = inner radius of insulation
R = outer radius of insulation

Above formula appears to be sufficiently accurate for high values for n (greater than 6).

5. In case of compacted stranding, the maximum value should be somewhat higher than that found in similar cable with smooth conductor surface. However this type of conductor does not lend itself to ready calculations because of differences of smoothness of conductor surface.

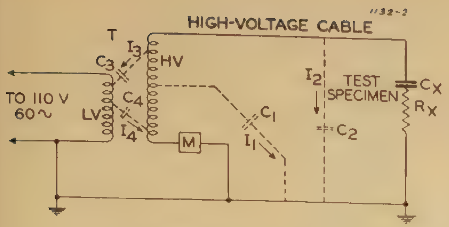

Figure 2. Simplified circuit diagram showing charging currents originating in the test apparatus itself

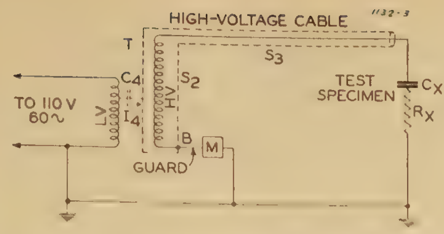

Figure 3. Test circuit diagram with shields to divert I_1, I_2, I_3

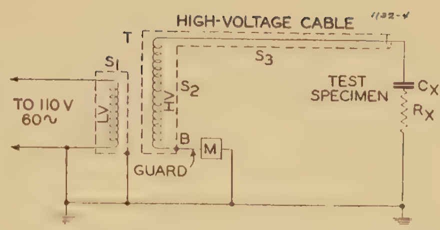

Figure 4. Test circuit diagram with shields to divert I_1, I_2, I_3, I_4

not be removed or even temporarily disconnected, the measuring means cannot be connected between the specimen and ground, and so cannot be connected directly in series with the insulation it is desired to measure. Consequently, the permanent ground limitation may cause the measuring apparatus to be subjected to electrical influences other than the losses in the insulation. For example, there may be:

Charging currents originating in the measuring apparatus itself.

Changes in phase angle and current caused by variations in capacitance.

Effects from extraneous electric fields.

Charging Currents Originating in the Apparatus Itself

In figure 2 the charging currents originating in the apparatus itself are indicated on a simplified diagram of the test equipment without any shielding. The distributed capacitance between the high-voltage winding of the transformer and ground is represented by a single capacitance, C_1, and the resulting charging currents are represented by I_1. The distributed capacitance which extends the entire length of the high-voltage cable is shown conventionally as a single capacitance, C_2, and the charging current as I_2. The distributed capacitance and current from the high-voltage end of the 10,000-volt coil of the transformer are shown as C_3 and I_3. Likewise the distributed capacitance and current between the 110-volt coil and the low-voltage end of the 10,000-volt winding are shown as C_4 and I_4. All of these charging currents, I_1, I_2, I_3, and I_4, flow through the measuring means, M, in addition to the current through the specimen which alone it is desired to measure. It is realized that these currents involve both capacitance and loss components but for brevity they are referred to as charging currents.

In figure 3 there have been added to the circuit of figure 2 guard shields S_2 and S_3 around the high-voltage winding of the transformer and the high-voltage lead. Charging currents I_1, I_2, and I_3 are diverted from the measuring means, M, by these shields, but I_4 continues to flow through M.

In figure 4 there has been added to the circuit of figure 3 a grounded shield S_1 around the low-voltage winding of the test transformer. This shield, S_1, diverts charging current, I_4, from the measuring means, M. This is important because the phase displacement of I_4 may be such that it will cause large errors in the watts measurement.

Changes in Phase Angle and Current Caused by Variations in Capacitance and Effects From Extraneous Electric Fields

From a study of figures 3 and 4, it is obvious that the capacitance between ground and the shields S_2 and S_3 is in parallel with the measuring means, M. This capacitance shunt diverts some of the test specimen current away from M. Correction for this shunting effect can be made by means of a compensating circuit or network. If this shunting capacitance is kept substantially constant, need for adjusting the network is practically eliminated. One method for maintaining constant capacitance is shown in figure 5 where, in addition to the shields S_1, S_2, and S_3 there are grounded shields S_4 and S_5 which surround the guard shields S_3 and S_2 on the high-voltage cable and the apparatus. Means for compensating the shunting effect are provided by the adjustable network R and C.

An additional function of the grounded shields S_4 and S_5 is to prevent currents induced from extraneous sources from flowing through the measuring means. By reference to figures 3 and 4, it will be seen that currents induced in the shields S_2 and S_3 from extraneous sources, such as adjacent high-voltage circuits, would flow to ground through the measuring means, M, thus vitiating the measurement. The shields S_4 and S_5 conduct such currents directly to ground.

This grounded shielding also contributes greatly to the safety of the operator by providing a direct path to ground for stray currents due to accidental breakdown of the insulation of the test circuit or contact with external high-voltage sources. In actual practice, lives of operators have been saved by this ground shielding when defective operating mechanism caused bushings under test to be accidentally alive at line voltages.

Even with the test apparatus and the test cable protected from external fields, the bushing or other test specimen may be so positioned as to have a considerable voltage induced at its high-voltage terminal due to extraneous sources. Voltage so induced in the specimen may in turn produce currents to ground which will flow through the measuring instruments, and it is essential to have means in the set itself for making corrections for these effects. A reversing switch, *SW* (figure 5), performs this function.

In practice, if the test voltage is less than 90 degrees out of phase with the current induced in the test specimen due to external fields, the resultant current and watts, as determined by the instruments, will be too great. If, however, the phase of the induced current is more than 90 degrees out of phase with the test potential, the watts and current indicated on the instruments will be too small. The actual value of watts loss in the insulation under test may be determined by taking two readings, first with the reversing switch in one position and then in the other. The algebraic average of these two readings is the actual watts loss in the specimen, and the algebraic average of the current is substantially the current flowing through the test specimen due to the test voltage. Thus, power factor can be calculated from watts-loss and current values determined under severe conditions of interference.

For example, let W_1 and W_2 be the observed values on the wattmeter, and I_1 and I_2 be the current readings, with the reversing switch first in one position and then in the other. The algebraic average of the watts loss will be $\frac{W_1+W_2}{2}$, and the algebraic average of the current will be $\frac{I_1+I_2}{2}$.* The resulting power factor will

* In practical application it is found that the current from induced voltages is small in comparison with the current through the specimen due to the test voltage, and hence its effect on the phase of the test current may be disregarded.

be $\frac{W_1+W_2}{E(I_1+I_2)}$. The accuracy of power-factor values thus derived from field readings of watts loss and voltamperes is well illustrated by a comparison with the true power factor of the same test specimen free from induction interference, as follows:

Observed values in the field:

$E = 10{,}000$ volts
$W_1 = 1.9$ watts
$W_2 = -1.6$ watts
$I_1 = 895$ microamperes
$I_2 = 685$ microamperes

The formula $\frac{W_1+W_2}{E(I_1+I_2)} =$

$$\frac{1.9+(-1.6)}{10{,}000(895+685)10^{-6}} = 1.9\% \text{ power factor}$$

True power factor, no induction $= 2.0\%$.

In passing it is interesting to note that it is not possible to compute the correct power factor by averaging power factors obtained under conditions of electrostatic interference by direct and reversed connections of the test voltage respectively. The algebraic expression for averaging power factor would be $\frac{\frac{W_1}{EI_1}+\frac{W_2}{EI_2}}{2}$, which equals $\frac{W_1I_2+W_2I_1}{2EI_1I_2}$. Applying this formula to the example cited above gives:

$$\frac{1.9(685)(10^{-6})+(-1.6)(895)(10^{-6})}{20{,}000(895\times10^{-6})(685\times10^{-6})} = -1.1\% \text{ power factor}$$

which negative result obviously is incorrect and in this case meaningless.

Test Frequency—60 Cycles

A test frequency of 60 cycles is most desirable because, other things being equal, a test at normal operating frequency reflects actual operating conditions. Moreover, the power factors due to defects in composite insulation are more pronounced at 60 cycles than at higher frequencies, consequently the differential between good and bad insulation is greater. Field trials have revealed that power-factor measurements at 1,000 cycles are limited in their scope as compared to 60 cycles.[5] The thousand-cycle power-factor test proved inadequate to indicate types of serious deterioration which were readily found by the 60-cycle power-factor test.

Test Voltage

A successful field testing apparatus requires a test potential adequate to detect deterioration in insulation of all voltage ratings up to and including the highest kv rating in practical use, which at the present time is 287 kv.

In practice, the operating company is interested principally when insulation has deteriorated to a point where it has become a failure hazard or represents a radio interference problem.

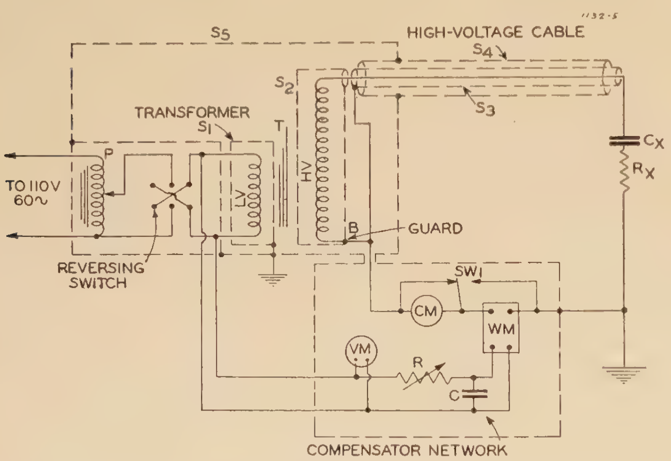

Figure 5. Simplified diagram of the watts-loss and power-factor tester

From a design standpoint the manufacturer is interested also to learn of inherent defects or incipient faults which may ultimately cause deterioration even though the resulting destruction of insulation value may not represent an electrical failure hazard until after many years of service operation.

Considering specifically the manufacturers' interest in new design, a test potential equal to or higher than operating voltage might furnish valuable data if it were possible in the field to separate the true loss from abnormal losses due to corona and extraneous interference conditions. However, except for studies of new design the advantages to be derived by the use of over-voltage in routine field testing are heavily outweighed by its obvious disadvantages. Extensive investigation of bushing insulation in the field showed that power-factor measurements at over-voltages introduced complications of analysis that are of no immediate practical value to the power company.

From a technical standpoint, the test voltage chosen should be as high as efficiently possible to meet the requirements of surface contact difficulties, ample unit stress on the insulation under test, and the minimizing of extraneous influences. On the other hand, the difficulties of segregating corona losses from insulation losses and the problems of portability, power supply, and regulation (all of which increase with voltage) compel a compromise in the interest of economy and efficiency. Tests at 10 kv appear to avoid a maximum of the difficulties. Data from ten years' experience with field tests on insulation rated from 10 kv to 287 kv indicate that a 10-kv test potential is adequate to solve the operating maintenance problem and also to make contributions useful to the manufacturer in his design problems.

Collar Tests

Need for localized high-voltage stress under special conditions, such as occur in voids in compound-filled bushings, is met by applying a metal band or "collar" to critical parts of the insulation so that the application of 10 kv produces higher unit stress at these local parts than would be produced by a test at full line voltage on the insulation as a whole. For example, tests at 10 kv impressed on metal collars placed under the first or second petticoat of a bushing will produce stresses that will indicate the presence of moisture, voids, and other abnormal and deleterious conditions in their incipient stages. In testing compound-filled bushings, the power-factor measurement is almost universally supplemented by the collar test. The trend of both measurements is carefully tabulated from consecutive tests and both are taken into consideration in the final analysis of the bushing condition.

Test Apparatus Details

In the particular circuit illustrated by figure 5, it will be noted that the measuring means consist of a voltmeter, wattmeter, and current instrument. In the following description (to differentiate this set from other types of measuring equipment which could be used), this equipment will be referred to as the "watts loss and power factor apparatus."

Figure 6 is a wiring diagram of a complete watts loss and power factor insulation test set, shown pictorially in figure 7.

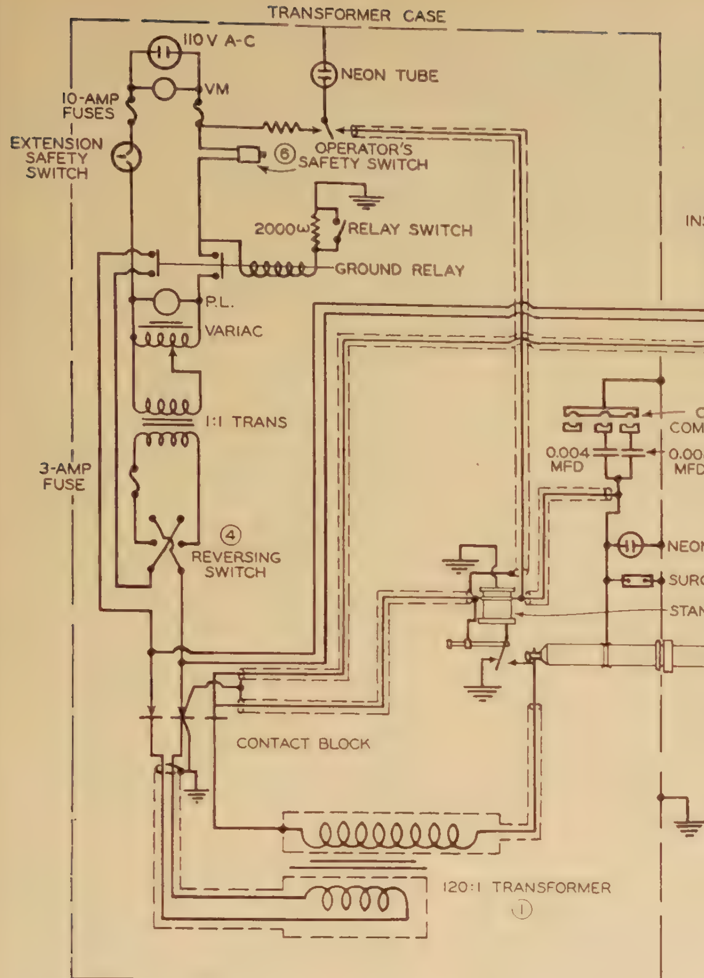

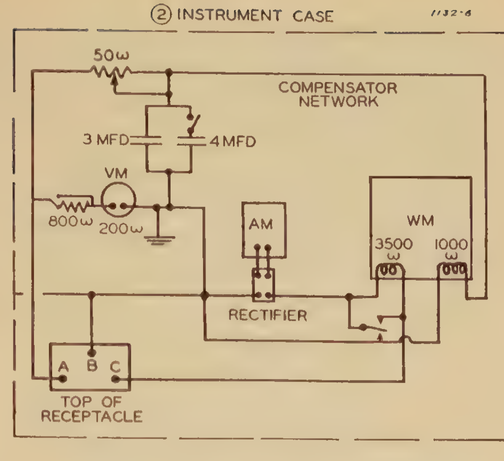

Figure 6. Watts-loss and power-factor tester

The set comprises:

1. Shielded step-up test transformer as a test voltage supply (120:1 trans.).
2. Shielded set of measuring instruments (voltmeter, ammeter, wattmeter in instrument case).
3. Multi-shielded cable for connection to the specimen under test.
4. Reversing switch.
5. Standard capacitor.
6. Safety relay and switches.

The test voltage supply is a 120:1 ratio, 13,200-volt, 60-cycle potential transformer capable of delivering 150 milliamperes at 10 kv.

The shielded set of measuring instruments includes:

A voltmeter calibrated for a range from 0 to 12.5 kv.

An ammeter having four scales, calibrated to cover a range from 0 to 10,000 microamperes.

A wattmeter of special dynamometer type having two scales with ranges of 0 to 2.4 and 0 to 12.0 watts. (Actual sensitivity of the wattmeter: 0.02 watt full scale.)

The multi-shielded cable has four concentric conductors separated by graded insulations of 500 volts, 10,000 volts, and 500 volts, respectively.

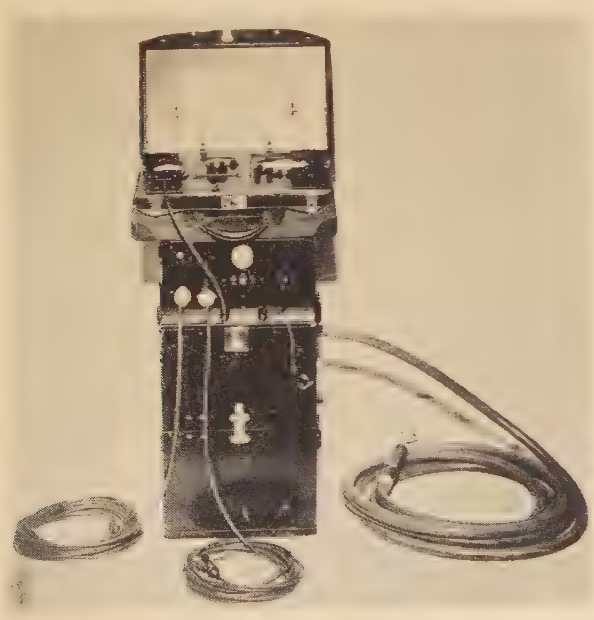

Figure 7. Watts-loss and power-factor tester assembled for use

Safety

Important safety features shown in the circuit diagram include a protective relay, series switches, and a safety grounded shielding system surrounding the entire test apparatus including the high-voltage test cable except a hook at the end for contact with the test specimen. Danger from contact with the test voltage is practically eliminated since the hook is the only exposed live part. The arrangement of the shielding is particularly effective in protecting the test operator against trouble arising outside the test apparatus itself, such as the remote but extremely dangerous possibility of accidental direct contact of the hook with the live line, or possible abnormal conditions due to serious voltages induced in the test circuit by short-circuit or ground occurring in neighboring equipment.

Range of Test Apparatus

The testing range of the apparatus described in this paper is from 0 to 2,000 milliamperes, or 2 amperes, at 10 kv.

To meet more special testing conditions, the apparatus has been adapted to convenient ranges of 10, 30, 150, and 2,000 milliamperes. The larger ratings are used for testing power transformers and cables. The design and physical dimensions of the apparatus are substan-

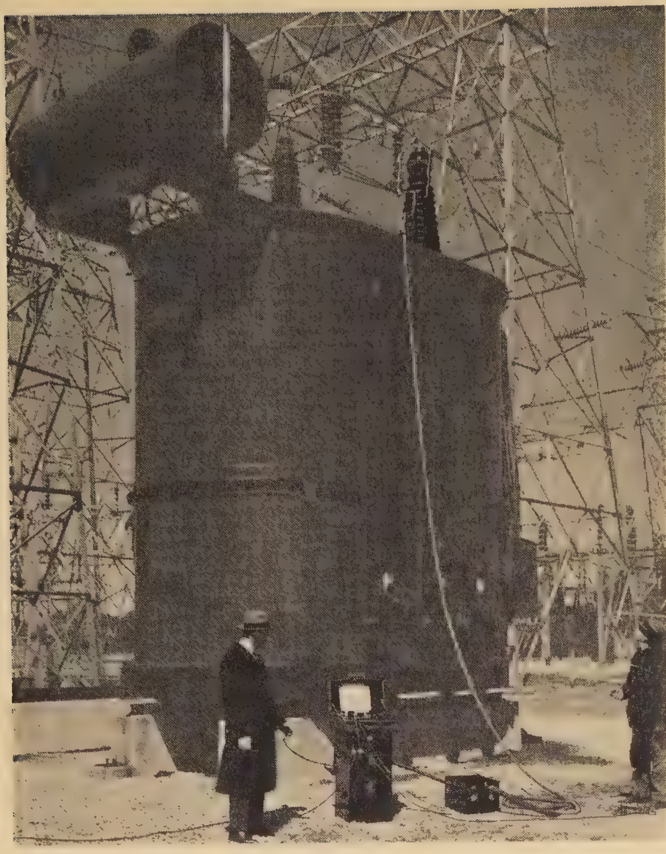

Figure 8. Testing a 220-kv bushing of the draw-lead type independent of the winding in a 220 / 110 / 13-kv transformer with the 30 tester and hot-guard attachment

tially the same up to and including 150 milliamperes, beyond which range additional equipment is required.

Auxiliary Test Equipment

For special tests a shielded current transformer, called "hot guard" transformer, is used in combination with regular testers. For example: in addition to making an overall test on a power transformer, it is advantageous to be able to test the transformer bushings individually without disconnecting the windings at the lower end of the bushing under oil. For this purpose, when the transformer winding terminates in a draw lead through the bushing, a "hot guard" attachment is used to supplement the regular test equipment. Figures 8 and 9 show a set with the "hot guard" attachment arranged for making tests on a transformer bushing in a 23,000-kva transformer. In this apparatus, a shielded current transformer, *CT*, is inserted in series with the high-voltage lead so that transformer bushings of the draw-lead type readily can be measured independently of the transformer winding. The test voltage is applied between the metal tube electrode *A* and ground and only current flowing from this electrode *A*, through the insulation of the bushing, to ground actuates the measuring instruments by flowing through the transformer primary, *W*.

By means of the guard circuit S_6S_7 which is connected to the lead of the transformer at *L*, the charging current flowing into the winding of the transformer through the capacitance *CW* to ground is by-passed from the measuring instruments. The wiring diagram of the "hot guard" test set as adapted to testing transformer bushings is shown in figure 9. It will be noted that the guard circuit, S_6S_7, which by-passes the current transformer winding is at nearly the same potential as that applied to the specimen. Thus, for test purposes, the insulation between the draw lead and the bushing tube need be only sufficient to withstand low voltage. In the test cable already described in connection with figure 6, the concentric (hot guard) shield nearest the center conductor is provided for this special test, and during a "hot-guard" test another shield, called the cold-guard shield, is connected to ground.

For testing generators and cables requiring charging currents up to 2 amperes at 10,000 volts, a shielded resonating choke is connected directly across the high-voltage winding of the test transformer and adjusted until the inductance of the choke and the capacitance of the test specimen are anti-resonant at 60 cycles. Under this condition the test transformer is required to supply only the losses in the choke-specimen resonant system, and 2 amperes at 10,000 volts may be obtained with a supply to the 110-volt side of the transformer of only 20 amperes which easily can be obtained from an ordinary lighting circuit. Without the choke the corresponding current on the 110-volt side of the transformer would be about 200 amperes which is very difficult to obtain in practice, and its complete regulation by portable equipment practically is an impossibility.

Application of Tester

The technique of applying the tester to the varied forms of insulation as found on the modern power system has been thoroughly covered in the literature of the AIEE,[1,2,3,4] and other publications,[5,7,9,10,11] listed in the bibliography.

Designed primarily for a bushing problem, the successful results in this investigation led to an extension of the application of the tester until it is now used for checking the condition of all types of insulation in service position, and also for acceptance tests on new and reconditioned insulating structures.[1,2,3,4]

Test Data and Their Interpretation

The criteria used for rating the serviceability of insulation from field dielectric-loss and power-factor tests are derived from the correlation of thousands of field tests, and many investigations. They are based on certain well known facts about insulation.

The correct interpretation of field dielectric-loss tests requires a knowledge of the detailed construction of the apparatus being tested and the characteristics of the particular types of insulation used. For example, each type of bushing has certain characteristics peculiar to its construction; defective internal insulation of an oil circuit breaker shows up in different ways depending upon the breaker construction.

The dry type porcelain bushing is subject to corona formation which must be considered in analyzing the test data. The condenser type bushing may show a normal power factor but have several condenser layers shorted out; this is revealed by an increase in charging current (capacitance) during the routine dielectric-loss test. A decrease in charging current for some types of compound-filled bushings indicates a break in the ground shield connection. The oil-filled type bushing may have a high power factor as a result of deteriorated oil; if the oil is replaced promptly, there may be no injurious after-effects. Collar tests will reveal defects in compound-

embedded bushings that otherwise would be masked.

The condition of the internal insulation of an oil circuit breaker is revealed by a comparison of the sum of the watts loss for the two bushings in a tank during the open-breaker test, with the combined loss of these same two bushings during the closed-breaker test. A study of these data will indicate defective lift rods or flash barriers, defective cross braces, wet or dirty de-ion grids, and many other forms of operating hazards.

No piece of insulation should be condemned until it has been completely isolated, cleaned, and compensated for temperature. Experience has shown that approximately two-thirds of the cases of high over-all dielectric loss initially found are due to bad operating condition such as carbon deposit, etc., that can be removed by ordinary servicing.

Standards for evaluation of test results appear in the literature,[2,3,4,7,9,11] as well as voluminous data concerning the results of their application to the insulation tests of typical operating companies.[1,2,3,4,5,7,9,10,11]

Typical test results[2] have indicated that defective equipment testing high enough to be removed from service is distributed among various types of apparatus in the following order:

	Percentage in "Remove" Class
Oil circuit breaker bushings..	2.1
Oil circuit breaker tank faults	1.6
Transformer bushings.........	3.2 to 3.9
Spare bushings....................	8.8
Instrument transformer windings....	7.7
Power transformer windings........	3.1

By the use of the technique and apparatus described, defective insulation can be detected in time for removal from service before it fails.[1,2,3,4,5,7,9,11] Such anticipation of failures not only prevents service interruptions but also makes possible the rehabilitation of defective insulation which otherwise might have been destroyed.

Figure 9. Schematic diagram of the essential portions of the tester circuit when the shielded current transformer "hot guard" is employed for testing transformer bushings of the draw-lead type

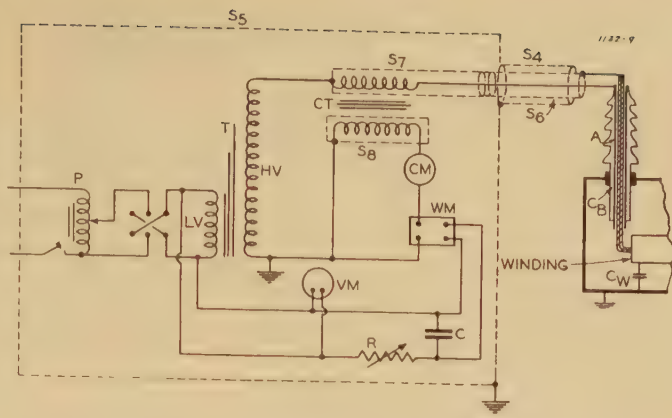

Of a large number of bushings tested and indicated defective to a point needing attention, about one-half of the faults were found to be external to the main insulation of the bushing and a considerable percentage of the faults that are in the main insulation can be cured or improved by servicing.[7]

"Insulation faults develop in all types of equipment such as bushings, transformers, wood insulation, and oil regardless of equipment design as it exists today. These faults may develop critically within test period intervals of 18 months to two years, as shown by the experience cited above, and appear, in a few cases, to develop to a lesser degree in a shorter period of time. Periodic testing, therefore, is necessary if a high standard of insulation is to be maintained."[2]

Conclusions

The use of the apparatus and method described in this paper makes it possible successfully to measure the a-c dielectric loss and power factor of all types of high-voltage insulation in service position. Such measurements provide an adequate non-destructive method for economical maintenance of insulation and for detecting deterioration in time to prevent failure.[4] The use of the equipment for tests at regular intervals and proper interpretation of the results will reduce to a minimum service interruptions due to faulty insulation.[2] Experience has proved that the period between tests of equipment in important locations should not exceed one year.[4]

References

1. Discussion of C. F. Hill, T. R. Watts, and G. A. Burr's paper, Portable Schering Bridge for Field Tests. AIEE Transactions, volume 53, 1934, pages 618–22, 478–81.

2. Field Testing of Bushings and Transformer Insulation by the Power-Factor Method, I. W. Gross. AIEE Transactions, volume 57, 1938 (October section), pages 589–99.

3. Field Power-Factor Testing of Transformer Insulation and Operating Experience, E. W. Whitmer. AIEE Transactions, volume 60, 1941, pages 605–11.

4. Bushing and Associated Insulation Testing by the Power-Factor Method, C. C. Baltzly and E. L. Schlottere. AIEE Transactions, volume 60, 1941 (June section), pages 308–12.

5. Doble Method of Testing Bushings, Frank C. Doble. Presented at meeting of Electrical Apparatus Committee, New England Division, NELA Harvard Faculty Club, April 28, 1931.

6. A Portable Power-Factor Apparatus for Studying the Deterioration of Insulation, Frank C. Doble. National Research Council, *Report* of Committee on electrical insulation of the division of engineering and industrial research for the year 1932, pages 43–4.

7. Testing Bushings and Insulation by Power-Factor Method, I. W. Gross and H. E. Turner. *Electrical World*, January 13, 1934, page 20.

8. Progressive Engineering Pays, Philip Sporn. *Electrical World*, June 9, 1934, pages 831–5.

9. Bushing Power-Factor Tests Show Failure Cause, E. L. Schlottere. *Electrical World*, March 28, 1936, pages 34–7 (894–7).

10. Analyze Transformer Insulation Faults, E. W. Whitmer. *Electrical World*, September 9, 1939, page 71 (747).

11. Power-Factor Testing of Transformer Insulation, Frank C. Doble and G. H. Browning. *Electrical World*, December 2, 1939, pages 49, 50, 128, 129 (1583–4, 1662–3).

Bushing Tests

A. L. BROWNLEE
ASSOCIATE AIEE

W. H. WICKHAM
ASSOCIATE AIEE

Introduction

MORE complete information on the dielectric characteristics of high-voltage bushings has been obtained from power-factor tests by extending the test voltage above the values generally used and by supplementing the ordinary power-factor tests with laboratory examinations of deteriorated bushings.

Most power-factor tests on high-voltage bushings have been made at a relatively low voltage, about 10 kv, regardless of the operating voltage of the bushing. These tests have been valuable in determining the general condition of the insulation. But by extending the test voltage to higher values, even above the operating voltage, it has been possible to detect defects in new bushings which would shorten their useful life and to detect certain types of deterioration in older bushings, both of such a nature that they are not shown by a low-voltage test.

Laboratory examinations of deteriorated bushings have been valuable in determining the nature, extent, and cause of bushing deterioration. Such information is needed to properly evaluate power-factor test results.

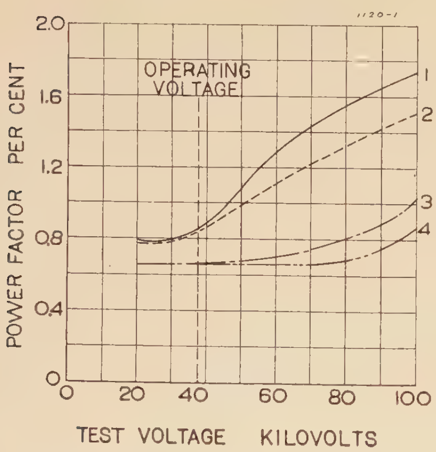

Figure 1. Power factor versus voltage curves, 66-kv condenser-type bushings

The purpose of this paper is to give the results of tests made at higher voltages and their significance and to describe the nature of deterioration in bushings as found by laboratory examinations of bushings with high power factor.

High-Voltage Power-Factor Tests

Power-factor tests on bushings at voltages equal to or above the operating voltage have shown defects in new bushings which would not have been found by a low-voltage test.

Ionization in two new 66-kv condenser-type bushings at a voltage below their operating voltage is shown by the sharply rising power-factor vs. voltage curves No. 1 and 2 in figure 1. Curves No. 3 and 4, taken on similar bushings, are given for comparison and show satisfactory power-factor-voltage characteristics. Curves 1 and 2 show an abnormal increase in power factor with voltage. Corona was present within these bushings at their normal operating voltage, 38 kv, as indicated by the breaks in the curves below that point. The ionization probably occurred in voids in the insulation which may be formed by wrinkles made in wrapping the paper which forms the condenser layers. The photograph of figure 2 shows a condenser-type bushing which was dissected and showed such wrinkles.

Corona has a deleterious effect on the insulation. Discoloration of the insulation around voids has been found in bushings which have been dissected. The action of corona will, in time, produce weak spots in the insulation and might lead to ultimate failure. New bushings in which corona is present at the operating voltage, as shown by high-voltage power-factor tests, are not acceptable.

Power-factor tests at these higher voltages have also shown up deterioration in older bushings which would not have been found by a low-voltage test.

The partial failure of a 44-kv condenser-type bushing is shown by the power-factor and capacitance vs. voltage curves of figure 3. The increasing power factor with increasing voltage, together with the abrupt change in capacitance above 60 kv, indicate that the insulation of one of the condenser layers was deteriorated so that it became partially conducting at the higher voltages. This was confirmed by measurements on the individual layers as given in table I. The outer layer had a very high power factor, 29.6%, compared with an average of 1.65% on the inner seven layers. The high power factor of the outer layer was found to be confined to the area under the ground flange as shown by the curve of figure 4 which gives the power-factor variation longitudinally over the outer layer. The insulation of this outer layer had become contaminated with glycerine from the litharge and glycerine cement used in cementing the ground flange to the condenser.

Partial failure of an oil-filled bushing is shown by the power-factor and capacitance vs. voltage curves of figure 5. While the fault had progressed so far that the power factor was high even at the initial voltage of 10 kv the increasing capacitance with increasing voltage and the changing power factor indicate the nature of the fault—a carbonized path within the bushing. The lower ends of the four inner insulating barriers between the conductor and the equalizing shield were badly burned and heavily carbonized. This conducting path gave rise to the high power factor and to the changing characteristics with increasing voltage.

Figure 2. Condenser-type bushing with outer layers of insulation removed

Wrinkled paper at the lower end of the section (left) shows how voids may be formed, in which ionization occurs

Laboratory Examinations

Laboratory examinations have been useful in determining the penetration of moisture in bushing insulation and the effectiveness of drying methods. Figure 6 shows a sketch of a 66-kv condenser-type bushing which had a high power factor due to moisture absorption and table II gives the results of the examinations made to determine the distribution of moisture in the insulation and the effectiveness of drying. The power factor of this bushing was not reduced by drying at atmospheric pressure; on the contrary,

Paper 41-120, recommended by the AIEE committee on instruments and measurements, and presented at the AIEE summer convention, Toronto, Ontario, Can., June 16–20, 1941. Manuscript submitted April 14, 1941; made available for preprinting May 15, 1941.

A. L. Brownlee is meter engineer and W. H. Wickham assistant engineer, electrical measurements, with Commonwealth Edison Company, Chicago, Ill.

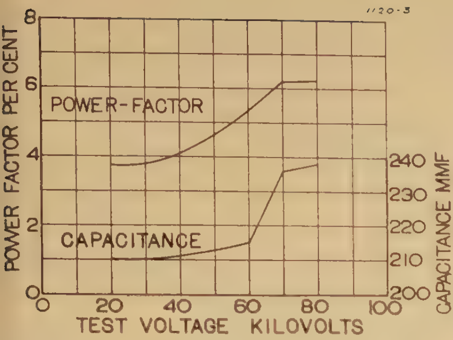

Figure 3. Power factor and capacitance versus voltage curves, 44-kv condenser-type bushing

it increased slightly. Moisture had entered the top of the bushing. This was confirmed by separating the ground wire into two sections, *A* and *B* of figure 6, and measuring the power factor to the upper and lower parts. The power factor was higher under the upper part, *A*. Further drying reduced the power factor somewhat because the separation of the outer layer between *A* and *B* afforded the moisture a means of escape. By measurements on the condenser layers it was established that moisture had penetrated to the second outer layer and that the inner eight layers had not been affected. Also, after prolonged drying at atmospheric pressure the second outer layer still contained a considerable amount of moisture.

Drying under vacuum has been much more effective in reducing high power factors caused by moisture. The curves of figure 7 show the results of drying four condenser-type bushings in vacuum The power factors of all four were reduced to satisfactory limits in reasonable time.

While moisture has generally been considered the chief cause of high power factor in bushings, laboratory examinations have also shown contamination from substances other than moisture.

In the 25-kv solid-type bushing sketched in figure 8*A*, the impregnated paper had been contaminated by acid compounds formed by deterioration of the varnished cloth. The variation of power factor longitudinally is shown in figure 8*B*, curve 1. The power factor was highest in the area under the ground shield. Curve 2 was taken after removing 0.2″ of the outer paper and curve 3 after removing 0.1″ more. A comparison of these curves shows that the power factor was highest n the outer part of the impregnated paper which was nearest the varnished cloth.

In a 37-kv solid-type bushing shown in the photograph of figure 9, the impregnated paper had been contaminated with a mixture of oil and filling compound. The power factor of this bushing was 9%.

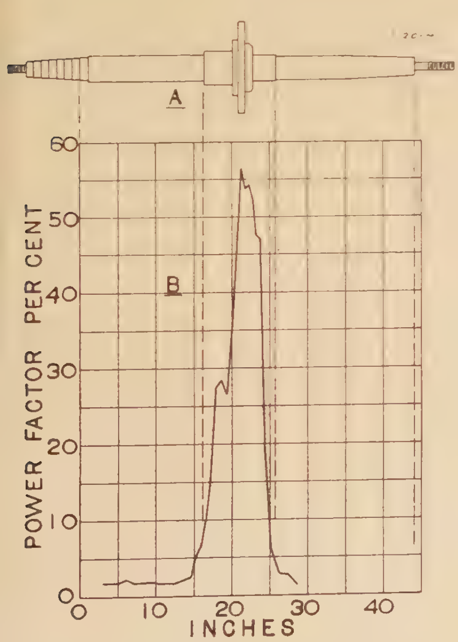

Figure 4. (A) Sketch of 44-kv condenser-type bushing; (B) power factor of outer layer

Table I. 44-Kv Condenser-Type Bushing, Power Factor of Condenser Layers

Layer No.	P.F. %
1	1.83
2	1.81
3	1.77
4	1.61
5	1.44
6	1.21
7	1.88
8	29.6

NOTE: The layers are numbered from the conductor outward.

Table II. Power-Factor Test Results on 66-Kv Condenser-Type Bushing of Figure 6

1. Bushing as received	Conductor to 10	3.8%
2. After drying in air for 8 days at 90 deg C	Conductor to 10	3.9%
3. After drying in air for 12 days at 110 deg C	Conductor to 10	4.1%
With section of ground wire and outer insulation removed at *C*, figure 6	Conductor to 10*A*	9.4%
	Conductor to 10*B*	3.0%
4. After drying in air for 11 more days at 110 deg C	Conductor to 10*A*	3.4%
	Conductor to 10*B*	2.3%
	Conductor to 1	1.3%
	1 to 2	1.2%
	2 to 3	1.0%
	3 to 4	1.0%
	4 to 5	1.0%
	5 to 6	1.5%
	6 to 7	1.1%
	7 to 8	1.9%
	8 to 9	24.0%
	9 to 10*A*	7.0%
	9 to 10*B*	4.1%
	Conductor to 9	2.2%
	Conductor to 8	0.7%

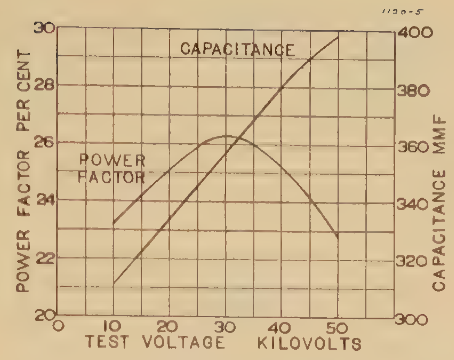

Figure 5. Power factor and capacitance versus voltage curves, oil-filled bushing

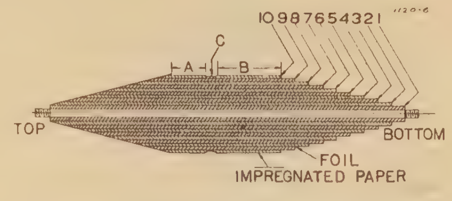

Figure 6. Sketch of 66-kv condenser-type bushing

Power-factor test results are given in table II

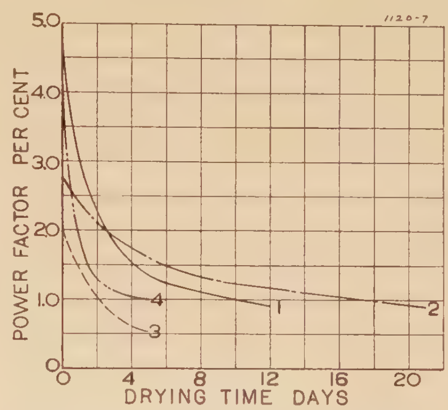

Figure 7. Vacuum drying of condenser-type bushings

Curves showing power factor versus drying time

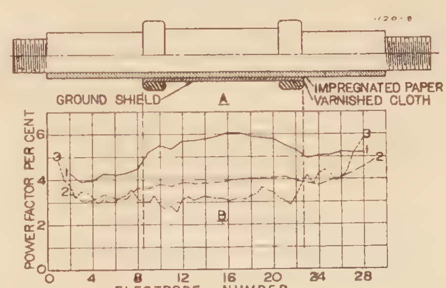

Figure 8. (A) Sketch of 25-kv solid-type bushing; (B) Power factor of impregnated paper

(1) Full thickness, 0.375 inch
(2) Turned down to 0.175 inch
(3) Turned down to 0.075 inch

Figure 9. Solid-type bushing with section of insulation removed to show contamination

The path of oil up through the bushing can be seen at the lower end (left). The dark portion in the center shows the penetration of dissolved filling compound from the top

Figure 10. Oil-filled bushing, porcelain-barrier type

View of internal parts showing deposits of disintegrated varnish compounds at the top and of litharge in the folds of the varnished cloth near the center

Power-factor tests on sections of the bushing showed that the power factor was 37.2% at the upper end above the ground shield and 1.78% at the lower end. Examination of a longitudinal section of the insulation showed that oil had migrated from the lower end, through separations in the impregnated paper, to the compound in the top. Compound dissolved in the oil had penetrated the insulation from the upper end. The paths of the oil and compound can be seen in the photograph.

Contamination of the oil has been found in oil-filled bushings of the porcelain-barrier construction. In one instance a 66-kv bushing of this type had a power factor of 26.1%. The power factor of a sample of oil was 84.9% and the dielectric strength of the oil was 14 kv. A photograph of the interior of this bushing is shown in figure 10. Examination showed deposits of disintegrated varnish compounds from the varnished cloth with which the conductor and the ends of the barriers were wrapped. Also, there were heavy deposits of litharge from the litharge and glycerine cement which was used to cement the barriers together.

Deterioration of oil and of impregnated paper under oil has been found by examination of oil-filled bushings of impregnated-paper barrier construction. Table III shows the results of examination and test of the component parts of two 66-kv bushings of this type. On No. 1 the power factors of the core and the barriers were satisfactory. Evidently deterioration of the oil gave rise to the power factor of 2.47% since the power factor was reduced to 0.49% using the same impregnated-paper parts with new oil. On No. 2 the impregnated paper of the core had a high power factor which was not reduced by drying. The insulation had become contaminated by the products of deterioration in the oil. The core was replaced.

Table III. Reconditioning of Oil-Filled Bushings

	Volume, Percentage	Surface, Percentage	
No. 1			
Power factor as received		2.47%	
Power factor of parts:			
Core	0.71	0.99	
Cylinder No. 1	1.09	1.06	
2	1.19	1.05	
3	1.23	1.31	
4	1.42	0.94	
Power factor of bushing assembled and filled with new oil		0.49%	
No. 2			
Power factor as received		6.60%	
Power factor of parts:			
Core	5.52	7.48	Volume power factor not improved by drying. Replaced.
New core	0.97	0.95	
Cylinder	2.02	1.82	
Power factor of bushing assembled and filled with new oil		0.71%	

Summary

The value of power-factor tests on bushings at higher voltages has been demonstrated. Tests at low voltages, while valuable, are inadequate. The power-factor and capacitance vs. voltage characteristics at voltages up to or above the operating voltage are important in judging the condition of the insulation.

The nature of bushing deterioration and the significance of high power factor have been shown by laboratory examinations. The findings help to establish a basis for power-factor limits, and for improvements in design and maintenance.

Excitation Circuits for Ignitron Rectifiers

H. C. MYERS
NONMEMBER AIEE

J. H. COX
ASSOCIATE AIEE

Introduction

THE development of the ignitron type of mercury arc rectifier, with its outstanding advantage in efficiency, introduced the need of a new type of excitation circuit. For the theory of how the arc is initiated, the reader is referred to the previous papers on ignitrons.[1,2]

Associated with each anode of an ignitron rectifier is an ignitor for initiating the arc. Each ignitor requires a positive impulse of current once each cycle to start the arc at the beginning of the conducting period of the main anode. In order to accomplish control of the output voltage of the rectifier, it must be possible to adjust the phase position of these impulses with respect to the supply voltage, either manually or by automatic provisions. Although the instantaneous current and power of the impulses are quite high, the impulse duration may be such that the average power is low and does not seriously affect the efficiency of rectifiers with the ratings usually encountered.

If an excitation system such as "main anode" is used with which only enough energy is applied to the ignitor each cycle to ignite the arc, the average power is very small. However, with separate excitation systems, every impulse must have the same energy and this must be adequate to ignite the arc under the most adverse conditions encountered.

The wave shape of the impulse is not critical, but the peak value of power required for reliable excitation varies considerably with the time rate of rise of current. With a high rate of rise, the voltage at which a cathode spot is formed is higher than if the voltage is applied more slowly. For a given rate of rise, this voltage varies somewhat from cycle to cycle, depending upon the exact condition of the contact of the mercury and the ignitor. This, of course, influences the time of pick-up of the main anode, so the impulses must be steep enough so that any such variations are negligible.

With the assumption that the impulses have the shape of the positive half of a sine wave, figure 1 has been plotted to show the average power of 60 impulses per second applied to a load with impulses of various peak powers and durations. The duration of the impulses is indicated by the base of the wave in terms of degrees of a 60 cycle wave. The values given by the curves must be increased by the losses in the circuit elements to obtain the total power requirements for excitation. The various systems have varying efficiencies. Circuits with which the authors have had experience have varied in their total power requirements from 75 to 300 watts per ignitor.

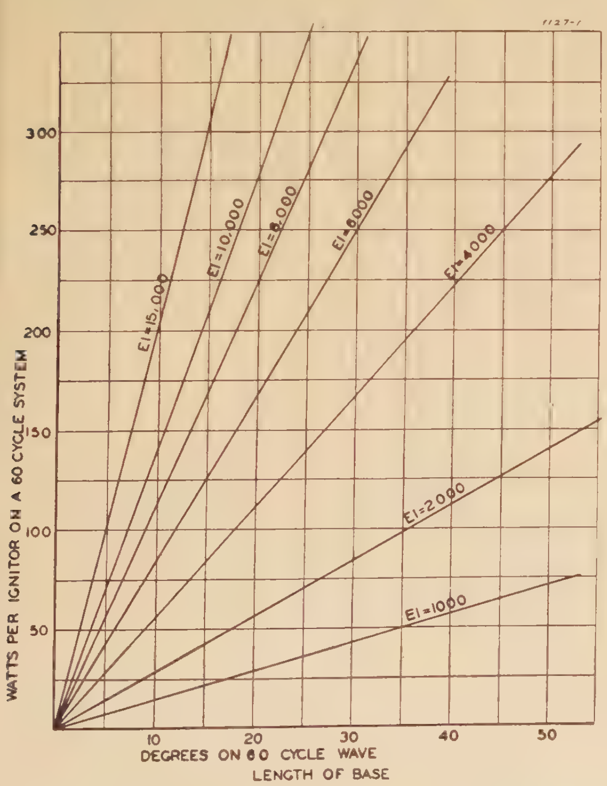

Figure 1. Average power output of a 60-cycle ignitron excitation circuit producing pulses of various durations and peak powers

There are four types of ignitron excitation circuits that have been used quite extensively in commercial applications which might be termed as follows:

(1). main anode
(2). capacitor-thyratron
(3). rotating impulse generator
(4). saturating reactor

All of the above have been applied with variations, as the art progressed, and depending upon the application. The following is a list of some of the circuits that have been worked on experimentally, but as yet have not proven sufficiently attractive to be applied commercially:

(1). peaked-wave transformers
(2). sine wave transformers phased back with thyratrons
(3). multi-anode control rectifier
(4). rotating commutator or other contact mechanism

A disadvantage of all circuits using thyratrons is that these tubes, having thermionic filaments, have limited life and constitute a replaceable item. An advantage, of course, is that voltage control is extremely flexible, simple, and efficient, since voltage control can be obtained by control of the thyratron grids. This control can consist of a bias voltage on the neutral of a sine wave grid transformer or a phase shifter in the primary of either a sine wave or a peaked wave grid transformer. A suitable phase shifter consists essentially of a wound rotor induction motor with the rotor locked in the desired phase position.

The conventional thermionic cathode of a thyratron is an average rated element; it is not suited to high over currents and thus not best suited to ignitron excitation. Ignitors require relatively high currents for short times. If only average currents were involved, ignitron excitation could be accomplished with very small and inexpensive thyratrons.

For purposes of reliable anode pick up, as well as certain control functions, it is desirable to provide a small excitation current to the main anode shield. Since this is only a nominal amount of power, it can be taken from any of the readily available sources. The figures used to

Paper 41-127, recommended by the AIEE committee on electrical machinery, subcommittee on electronics, and presented at the AIEE summer convention, Toronto, Ontario, Can., June 16–20, 1941. Manuscript submitted April 17, 1941; made available for preprinting May 16, 1941.

H. C. Myers is rectifier engineer and J. H. Cox rectifier section engineer with Westinghouse Electric and Manufacturing Company, East Pittsburgh, Pa.

1. For all numbered references, see list at end of paper.

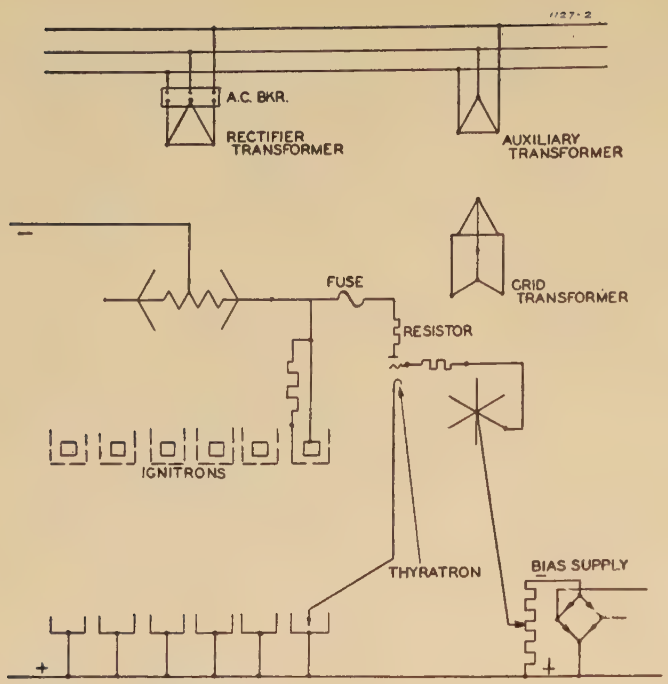

Figure 2. Diagram of a double three-phase ignitron rectifier with main anode excitation and bias control

illustrate the various excitation systems show the shield excitation accomplished in a variety of ways.

Main Anode Excitation

Figure 2 shows a schematic diagram of a simple anode fired ignitron rectifier using a grid bias method of control. A conventional double three-phase rectifier circuit is indicated for the power connections. The excitation circuit is completed for only one phase since the others are duplicates.

In this system, when an anode becomes positive with respect to its cathode, if the thyratron grid is positive, current is passed through the shunting thyratron and ignitor circuit. When this current reaches the value at which the cathode spot is formed by the ignitor, the main anode picks up and the thyratron path is short-circuited by the arc. The rate of application of voltage on the ignitor is a function of the voltage of the rectifier and the amount of grid delay used. The ignitor voltage collapses sharply when the main anode picks up. In this circuit only sufficient energy to ignite the arc is used each cycle and the average excitation power is very small. The major portion of the loss is the power required for heating the thyratron filament. Also, there is ample power available, since it comes from the rectifier transformer.

Although this system is highly efficient and most positive in action, it has certain limitations. Since the ignition voltage must come from the main transformer, arc pick-up does not take place until the anode voltage has reached ignitor voltage. This voltage is such that a 300 volt ignitron rectifier with anode firing operates at a minimum grid delay of approximately 8 degrees. Furthermore, because of the cycle to cycle variation in ignition voltage, this delay angle is not strictly uniform. This tends to cause some unbalance between main anodes, between phase groups, and between more than one rectifier on the same bus, all at low loads. At loads of one-quarter full load and higher, this effect vanishes.

In this circuit the ignition current must also pass through the load. Therefore, at loads below ignition value the entire load current passes through the thyratrons. Actually this is not very important since currents below ignition currents are well within the limits of the thyratrons used, even though maintained for the full load-conducting period.

With main anode excitation, the duty on the thyratron is probably more severe than in separate excitation circuits using thyratrons, since in the former, if an ignitor does not pick up, the current in the thyratron is limited only by the load demands, the resistance in the thyratron ignitor circuit, and the collapse of the interphase transformer voltage.

Capacitor-Thyratron Excitation

Figure 3*a* shows an excitation circuit in which a capacitor is charged through a resistor from a sine wave transformer. At a point near maximum positive charge the capacitor is discharged through the ignitor by triggering the thyratron. The principal voltage and current waves are shown in figure 3*b*. The front of the wave produced is very sharp and the tail is determined by the capacity and resistance of the circuit. The front can be sloped if desired by placing an air core reactor in the discharge circuit.

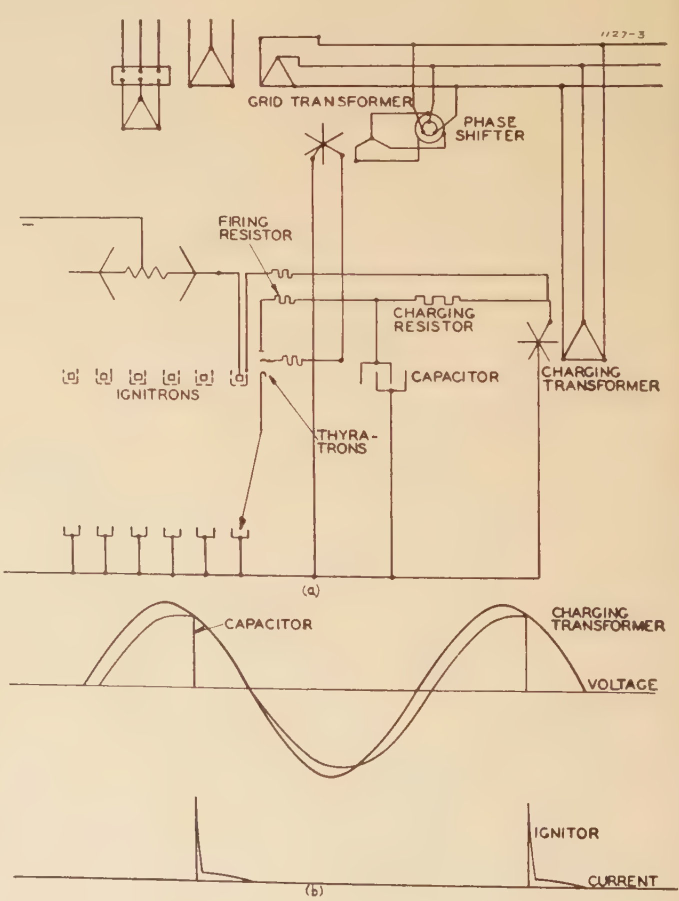

Figure 3. Ignitron rectifier circuit using capacitor - thyratron excitation with resistance charging

(*a*) Circuit diagram

(*b*) Voltage and current waves

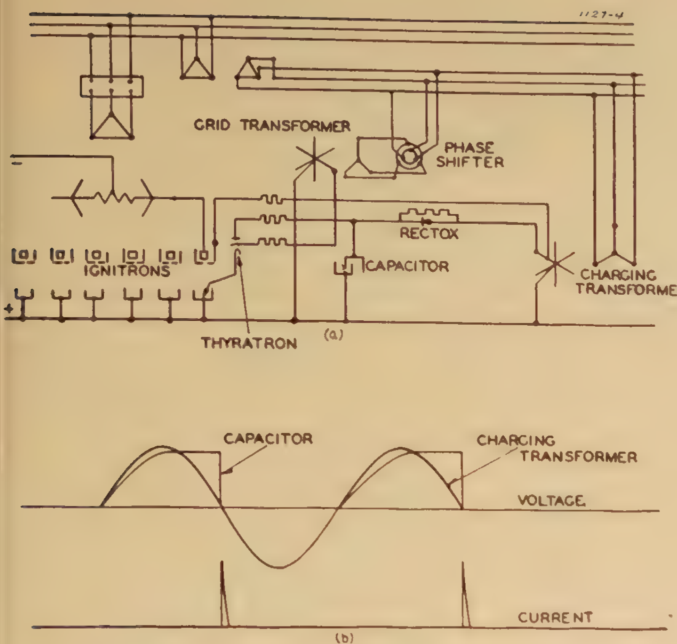

Figure 4. Ignitron rectifier circuit using capacitor - thyratron excitation with Rectox charging

(*a*) Circuit diagram
(*b*) Voltage and current waves

This circuit is simple and direct, and has the advantage of some follow-up current from the charging transformer after the pulse, which maintains an arc for 30 or more degrees and aids pick up of the main anodes at very low loads where the interphase transformer does not function. However, since the capacitor is charged through a resistor and this resistor must limit the follow current, the circuit is limited in the voltage that can be used without prohibitive loss.

The circuit permits a grid delay range of approximately 60 degrees. If a greater delay angle is desired, a transfer switch is necessary to shift connections between the charging transformer phases and the thyratrons. The power consumption can be reduced somewhat by using a reactor in place of the charging resistor. However, with a reactor the range of grid delay is considerably less and the power saved does not justify its use.

A modification of the capacitor-thyratron circuit, in which the capacitor is charged through a Rectox instead of a resistor, is shown in figure 4. This method of charging reduces the power requirements by about 50% and permits a wide range in choice of voltage with a corresponding range in impulse power. The power drawn from the line for either circuit has a power factor of nearly unity.

This circuit permits a wide range of grid delay, without switching terminals. However, if a wide range is used, it cannot be done with a grid bias, but it is necessary to use a phase shifter and a peaking transformer.

Impulse-Generator Excitation

By using concentrated fields and a suitable distribution of armature winding, a rotating synchronous generator can be built which produces impulse voltages. Such a winding arrangement, together with the waves produced and the connections to an ignitron rectifier are shown in figure 5. The impulses produced by units that have been built have a length of about 20 degrees on a 60 cycle base.

Grid delay with this type of excitation is obtained in either of two ways. In one, the generator is driven with a wound rotor induction motor, the necessary d.c. field being provided by d.c. in a pair of the windings. The phase position of the rotor is shifted by shifting the d.c. excitation from one to another of the pairs. Another method is to use a synchronous driving motor with frame shifting equipment.

The impulses provided by rotating impulse generators are highly satisfactory for ignitron excitation and the power requirements compare favorably with other types of efficient separate excitation systems. Furthermore, there are no replaceable parts except field brushes within the normal life of small synchronous M-G. sets.

The impulse generator has the disadvantage of being a rotating device somewhat bulky and noisy. For some applications a more serious objection is the synchronous motor's tendency to hunt and the reflected effect on the output voltage of the ignitron rectifier. By suitable choice of driving motor, this tendency to hunt can be kept to a value having negligible effect on the load where the rectifier capacity is small compared to the supply system. However, where

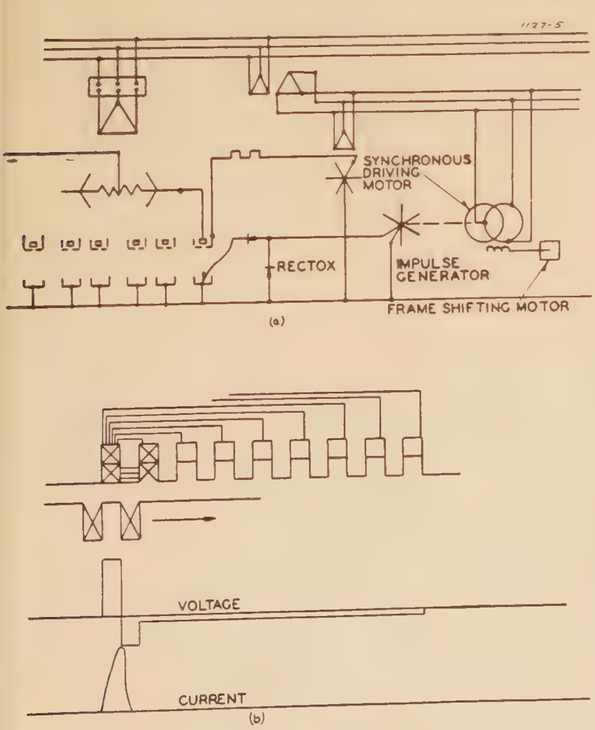

Figure 5. Ignitron rectifier circuit using a rotating impulse generator

(*a*) Circuit diagram

(*b*) Voltage and current waves

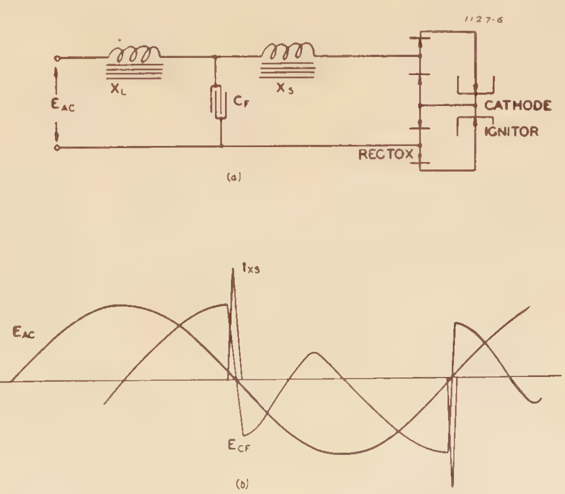

Figure 6 (right). Saturating reactor excitation circuit for gnitron rectifiers

(*a*) Circuit diagram

(*b*) Voltage and current waves

E_{AC} = supply voltage
X_L = linear reactor
C_F = firing capacitor
X_S = saturating reactor

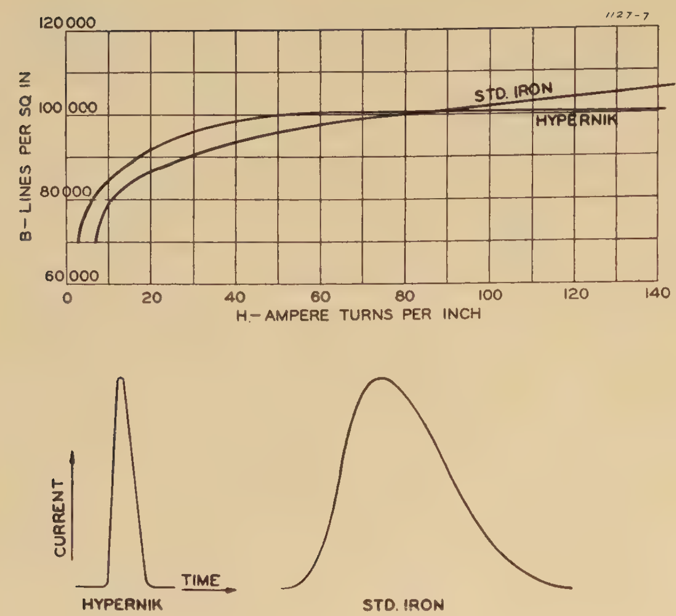

Figure 7. Current wave shapes of a saturating reactor excitation circuit with different types of reactors

the rectifier load is so large that fluctuations in the load affect the frequency of the supply system, it is possible for the natural periods of the impulse generators and the supply system to be such that violent fluctuations build up. Since the size and maintenance features of impulse generators limit their attractiveness to large installations, the danger of hunting practically precludes their use.

Saturating-Reactor Excitation

Figure 6*a* shows a circuit, utilizing reactors and capacitors, which will produce power impulses suitable for ignitron excitation. The linear reactor in this circuit has an iron core with an air gap and is designed to have a constant reactance for various voltages up to the rated voltage and frequency of the circuit. For a 60 cycle circuit, this reactance is approximately 30% of the reactance of the firing capacitor. The saturating reactor is built with a closed iron core and a winding such that at the rated voltage of the circuit, it will draw a large peak of magnetizing current. This peak of magnetizing current occurs when the capacitor, C_F, is charged to its peak value of voltage; hence the capacitor discharges through the saturating reactor and a large peak of current results. By using the Rectox units shown in figure 6*a*, it is possible for one circuit to supply excitation power to two ignitron tanks which are diametrically opposite in phase position in the rectifier circuit. Figure 6*b* shows a set of curves illustrating the voltage and current for a cycle of operation.

The shape of the current wave for the impulse developed by this circuit is affected considerably by the shape of the magnetization curve of the material used as a core for the saturating reactor. Saturating reactors with different core materials have been tried. Figure 7 illustrates the current wave shape developed for each case. One curve applies to a reactor with ordinary transformer iron having less than 1% silicon, and the second curve is for a reactor with Hypernik core. With a saturating reactor using a Hypernik core, it is possible to develop a peak power one hundred times the average power input. Some tests were made using this circuit with a resistor load to show the peak voltage and current it could develop for various values of constant resistance, and the results are plotted in figure 8.

In this circuit, the phase position of the impulses, which control the ignitron voltage, must be controlled by shifting the input voltage to the excitation circuit. This may be accomplished by means of a phase shifter which must shift the entire excitation power. The phase shift-

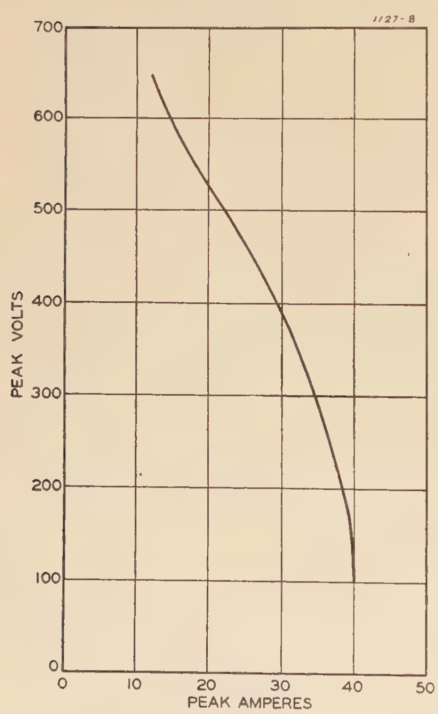

Figure 8 (left). Peak voltage and current developed by the saturating-reactor circuit using a Hypernik reactor

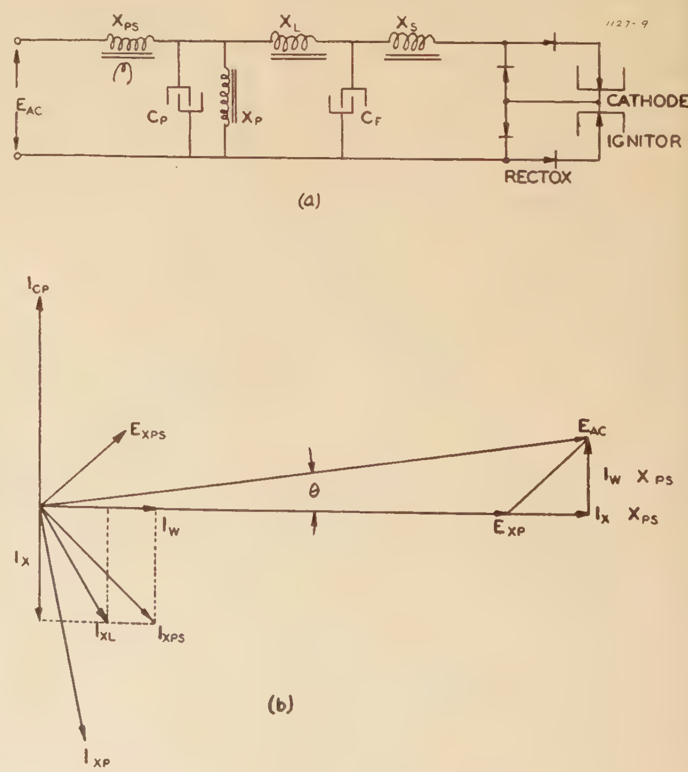

Figure 9. Phase-shifting network for a saturating-reactor excitation circuit

(*a*) Circuit diagram

(*b*) Vector diagram

E_{AC} = supply voltage

X_{PS} = phase-shifting reactor

C_P = parallel capacitor

X_P = parallel reactor

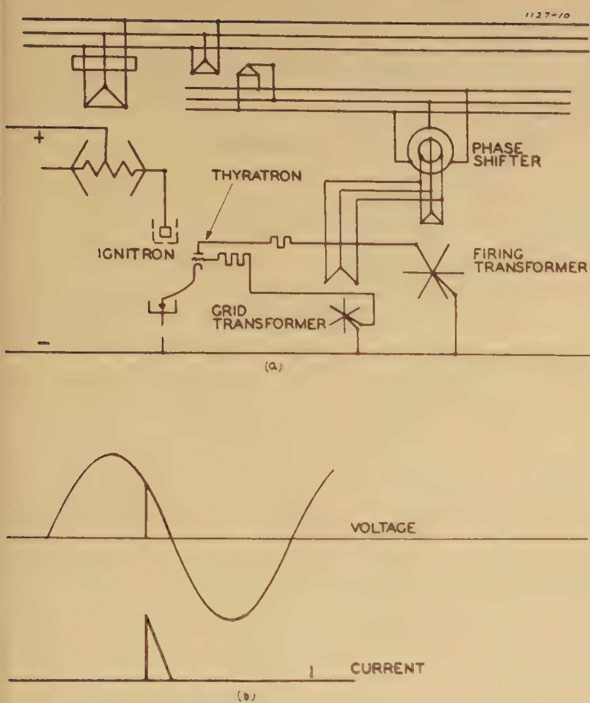

Figure 10. Ignitron rectifier circuit with sine-wave phased-back excitation

(*a*) Circuit diagram

(*b*) Voltage and current waves

ing may also be accomplished by means of a phase shifting network. Figure 9*a* shows a diagram of such a network.

The phase shifting circuit contains all the elements of the circuit shown in figure 6*a* with three additional components. The phase shifting reactor is capable of a gradual change in reactance over a 10 to 1 range by means of d.c. saturation. The parallel reactor and capacitor operate with a circulating current larger than that drawn by the excitation circuit and act as a power source for that circuit. The phase position of the voltage across the parallel combination can be adjusted by controlling the phase shifting reactor.

If the parallel reactor has a closed iron core, and is designed so that normally it operates with considerable saturation, then the voltage across X_P and C_P will remain almost constant with considerable fluctuation in line voltage or change in the reactance of the phase shifting reactor. Figure 9*b* is a vector diagram illustrating the voltage and current phase relations in this circuit.

As shown here, the loss component of current through X_{PS} determines the phase shift for a given value of reactance in X_{PS}. The reactive component of current in X_{PS} operates to maintain constant voltage across C_P and X_P. This reactive component is a balance between current taken by C_P and X_P which varies according to line voltage due to the fact that X_P is saturating. In practical operation this permits a 90° phase shift with no perceptible change in peak voltage output. The line voltage may likewise change 30% with only a 1% change in voltage across C_P and X_P.

Peaked-Wave-Transformer Excitation

The impulse produced by a conventional peaked wave transformer has the shape desired for ignitron excitation. Such a transformer, connected to block out or by-pass the negative peaks, is a satisfactory circuit. However, in a peaked wave transformer the impulse energy is stored periodically in the magnetic circuit and it is found that a transformer to produce impulses of the magnitudes required for ignitron excitation is prohibitively large.

Sine-Wave Phased-Back Excitation

Ignitors can be fired with 60 cycle sine waves. However, if the ignition is permitted to take place on the front of the wave from a circuit having capacity enough to supply the instantaneous power required by ignitors, the power loss is prohibitive. To avoid this high loss the voltage can be phased back or blocked by a thyratron, until a later point in the cycle where the follow current is much less. Such a circuit is shown in figure 10. In any event, the degree to which ignition can be phased back is limited and the minimum follow power attainable results in rather high excitation losses. Furthermore, the power consumption varies greatly with the angle of phase back so the range of grid control is very limited and the highest loss is at the minimum delay angle where rectifiers operate the majority of the time. Practically, control of rectifier voltage with this type of excitation requires that a phase shifter be placed in the power supply to the excitation circuit.

A modification of the circuit shown in figure 10 can be made by placing a single resistor in the neutral of the excitation transformer instead of the individual resistors in the ignitor leads. Such a resistor would cause the circuit to produce 60 degree pulses as in a six phase rectifier.

Multianode-Control Rectifier

The sine wave-phased back circuit can be modified as shown in figure 11, so so as to permit the use of a miniature multianode grid controlled rectifier. Since such a rectifier has a common cathode,

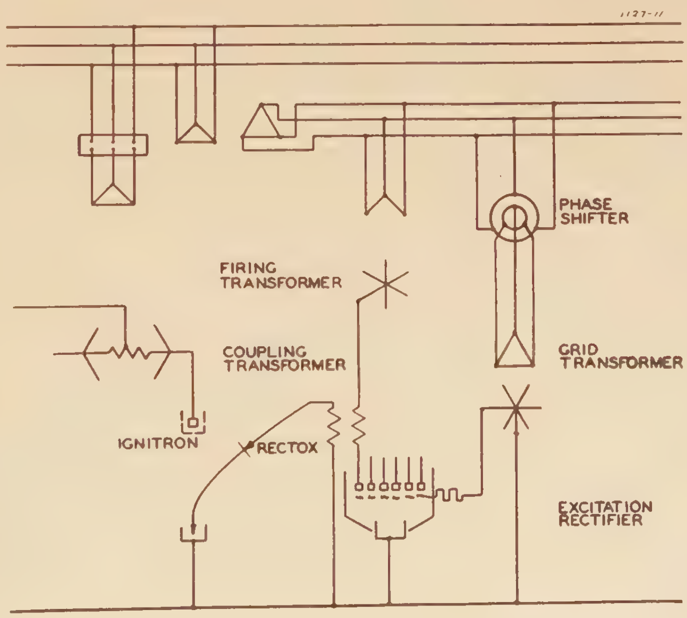

Figure 11. Ignitron rectifier circuit with miniature grid-controlled rectifier excitation

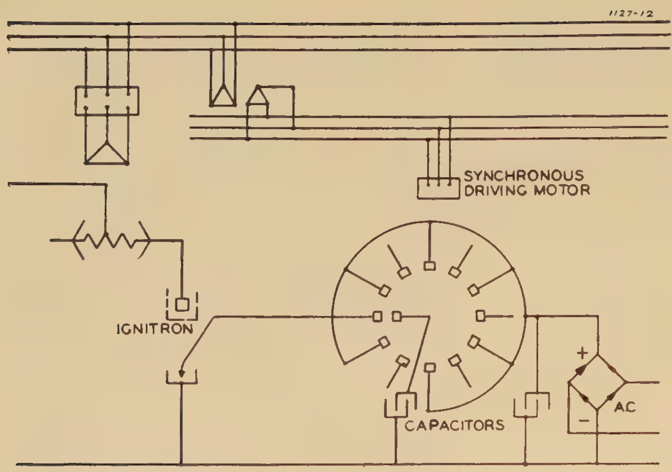

Figure 12. Rotating-commutator excitation system for ignitron rectifiers

coupling transformers are required in order to segregate the individual ignitor circuits.

The advantage of this circuit is that it retains low energy electronic control comparable to thyratron control, but eliminates the replaceable tubes. Its attractiveness is limited to pumped ignitrons where the addition of a small auxiliary pumped device involves little disadvantage. The range of grid control available with this circuit is limited, unless the entire excitation power is shifted, since, in common with the phased-back circuit, the excitation power varies widely with the phase back angle.

Rotating-Commutator Excitation

Figure 12 shows a system of excitation in which a rotating contact member is driven by a synchronous motor. As the moving contact passes under the brushes connected to the d.c. source, the capacitor is charged and when it passes under the brushes connected to the ignitors, the capacitor is discharged through the ignitor. Obviously, the capacitor could be connected to the stationary member and the ignitor contacts rotated if dictated by convenience. Control of voltage can be obtained either by means of rotating the stationary contact members or by any convenient means of shifting the phase position of the driving motor.

This system is most efficient and flexible as regards circuit constants, but it has the disadvantage of including a rotating member and sliding contacts with the resulting maintenance requirements.

Conclusions

In general, the development of the ignitron has progressed to a point where several circuits are available for excitation. These will provide positive and accurate ignition independent of load, and their attractiveness depends upon the application. Any of the circuits described in this paper which are in commercial use have a power consumption sufficiently small that the effect on overall efficiency is less than .1% for large units, and does not exceed .4% on units as small as 200 K.W.

The use of thyratrons in an excitation circuit provides a flexibility and speed of response that cannot be matched by any circuit using elements depending on mechanical movement or change of current in an inductive circuit, to provide control.

The saturating reactor excitation system, consisting entirely of static devices, by elimination of tube replacement appears to offer practical advantages for many applications.

When used with a phase shifting network, the saturating reactor system can be controlled with small power devices or compensating circuits, and has a speed of response adequate for most applications.

References

1. A New Method of Initiating the Cathode of an Arc, **J. Slepian** and **L. R. Ludwig.** AIEE Transactions, volume 52, 1933, page 693.

2. Ignitrons for the Transportation Industry, **J. H. Cox** and **G. F. Jones.** AIEE Transactions, volume 58, 1939 (December section), page 618.

3. Regulation of Grid-Controlled Mercury-Arc Rectifiers, **L. A. Kilgore** and **J. H. Cox.** AIEE Transactions, volume 56, 1937 (September section), page 1134.

4. A New Ignitron-Firing Circuit, **H. Klemperer.** *Electronics*, December 1939.

A Simple Method for Determination of Ratio Error and Phase Angle in Current Transformers

Correlation of Significant Constants of Current Transformers

E. C. WENTZ
ASSOCIATE AIEE

Synopsis: Up to the present time current transformer performance has been described by curves which show ratio error and phase angle over a range of current at various values of burden, (ohms) power factor, and frequency. The number of curves that are required to cover all possible conditions is so great as to render them, by their very bulk, practically useless. Another limitation is that they do not describe performance under transient conditions.

Performance of other types of transformers and certain other apparatus is invariably calculated from a few easily measured constants, according to simple standard formulas. Up to the present time, available methods for calculation of current transformer performance have had the disadvantage of either being difficult to use, or of depending on constants difficult to measure, or else they have not been sufficiently accurate for general use.

A method is described which depends on the following constants:

1. Open-circuit saturation curve measured in the usual way.
2. Secondary coil resistance.
3. Equivalent leakage reactance calculated from the voltage of an exploring coil enclosing the maximum value of leakage flux.

The method includes several important short cuts in the calculation which reduce the numerical work to a practical minimum. Curves are plotted which allow direct reading of the exact components of exciting current which cause ratio error and phase angle.

The objects of the paper are:

1. To present a practical method of calculation.
2. To establish constants (1), (2), and (3) as the fundamental quantities which determine real excellence of the transformer.

I. The Need for a Simple Method for Description of Current-Transformer Performance

THE conventional ratio and phase-angle curves for a current transformer are often inadequate for solution of a particular problem. Furthermore, the tests from which such curves are plotted are expensive, and the data are not available for many of the older transformers now in service.

A simple method for determining current transformer performance from a few easily measured constants (as power transformer performance is determined from copper and iron loss and impedance measurements) has been earnestly sought. This paper will present a method which the author believes to be the best so far proposed.

II. Theory of Current Transformation

The general principle of calculation of current transformer performance is very simple. The ampere turns in the secondary coil are less than those in the primary coil only because of the ampere turns lost in circulating flux in the core. Hence, we need only to calculate the ampere turns or magnetomotive force drop around the magnetic circuit.

However, on account of the leakage flux in the core, this is not as simple as it sounds. This leakage flux is principally the flux which passes between primary and secondary windings, and completes its path in the core outside the primary winding (figure 1). The current transformer is different from other transformers in that this leakage flux is relatively large, often larger than the working flux. This flux has been investigated experimentally[1] and theoretically,[2,3] but no method has been developed by which it can be exactly calculated. Furthermore, it is well known that it enters the core, not at one point, but all over the whole surface, so that it is not the same at any two points in the core

If any one of a number of approximate methods is used to calculate the leakage flux, the ampere turns to circulate it through the core can be calculated by dividing the core into a number of parts, assuming a constant equivalent flux in each part. This is the basis of the method described by Mr. Sinks,[3] and this method, although still not absolutely correct (its limitations are fully described by Mr. Sinks), is the most nearly correct method now available. Its real limitation is the great amount of numerical work involved.

III. Assumptions Which Simplify Calculation

Certain methods have been developed for simplifying this calculation. The most simple method, which does very well for ring type transformers, is to neglect the leakage flux altogether.[4] Another method assumes an experimentally determined flux, approximately related to an average value of leakage flux, to flow in the whole core.[5] These methods are not suitable for general use, because they do not use the real magnitude and distribution of the leakage flux.

IV. Combination of Best Features of All Methods

Giving first consideration to the fundamental soundness of the method, we can say that the method should—

1. Consider division of the core into several parts, as discussed in II with different leakage fluxes in the different parts.
2. Base the distribution of the leakage flux and the division of the core, on values of leakage flux actually existing in the core as measured by exploring coils (figure 2). The exploring coil can be simply ten turns of fine wire.

Giving second consideration to the aspects of economics and convenience, we can say that the method should not divide the core into more parts than is necessary for the required accuracy. Here a good deal of experience is required. Any particular division of the core into any finite number of parts is an empirical device, and can be justified only by general experience which shows that it works. The final result cannot be shown, in any rigorous way, to be the best possible result.

It will help to remember the primary objects of the investigation, and to make the division of the core accordingly. The first object is to calculate an error that is at least as large as the real error, to be on the safe side. The second is to get consistent results, to be able to compare transformers on a true basis. The first object can be obtained if the average flux values in each part of the core are taken to be sufficiently large, even if the

---

Paper 41-109, recommended by the AIEE committee on protective devices and instruments and measurements, and presented at the AIEE summer convention, Toronto, Ontario, Can., June 16–20, 1941. Manuscript submitted February 20, 1941; made available for preprinting May 6, 1941.

E. C. Wentz is with Westinghouse Electric and Manufacturing Company, Sharon, Pa.

The author wishes to thank J. B. Gibbs of the Westinghouse transformer engineering department for invaluable assistance in organizing and arranging the material.

1. For all numbered references, see list at end of paper.

core is not too well divided. The second object will be obtained if the flux measurements are made in the same way on all transformers of the same type.

Of course, we do not want to calculate an error too much larger than the true value. This is the disadvantage of not dividing the core at all, but considering the measured value of leakage flux to flow in the whole core; the calculated error will always be too large.

Division of the core into two parts, with the real leakage flux measured by exploring coils, is a compromise which the test results to be cited, and other tests, show to be suitable for general use with dry type transformers. This compromise is, however, definitely not fundamental; the general method to be described can be used with any desired division of core.

When the ratio error exceeds five per cent, the iron is usually working near saturation, and much of the leakage flux which is in the iron at normal flux densities leaves the core at the higher density and completes its path in the air leaving less flux in the core than would be expected. The result is that this method of calculation will give errors which are considerably too large when the error exceeds five per cent. As the method is conservative, it is still useful.

Actually less than the value of flux as measured by the exploring coil shown in figure 2 exists in practically all of the core. It is obviously conservative to assume that it exists in the half of the core which is outside the primary coil. Mr. Sinks has shown that the leakage flux at the center of the core inside the secondary is effectively reversed to the leakage flux in part of the core just outside the secondary. A reasonable assumption, confirmed by tests, is that the average effective value of leakage flux in the inside half of the core is zero, and that the only flux to be considered is the working flux.

V. Simplification of Numerical Work

The proposed method of determining the leakage flux and its distribution does not solve a real difficulty attending the problem—the amount of numerical work for a solution.

Several short cuts have been worked out which do not detract from the accuracy of the calculation. These are:

1. Substitution of equivalent reactance for the leakage flux. It can be shown (appendix I) that the transformer with magnetic circuit divided into two parts, one with, one without, leakage flux, can be represented by the equivalent circuit of figure 4, where the

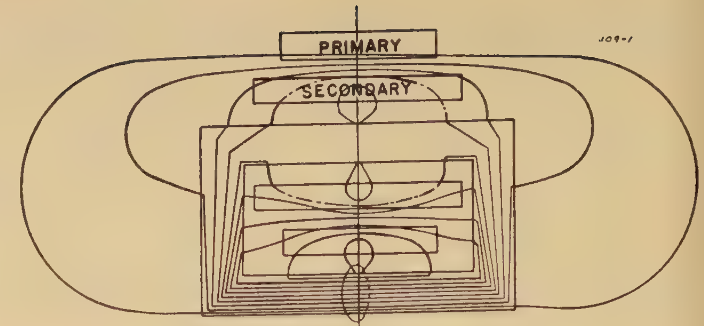

Figure 1. The leakage flux passing in the space through and between coils completes its path through the core

The leakage flux is relatively large in a current transformer

reactance X_L corresponds to the leakage flux and can be determined from the exploring coil voltage at normal current by—(see appendix II)

$$X_L=\sqrt{\left(\frac{N_s}{N_x}\frac{E_x}{I_s}\right)^2-R_s^2}$$

I_s = secondary current
R_s = secondary coil resistance
N_s, N_x = number of turns in the secondary and exploring coils, respectively
E_x = induced voltage in the exploring coil

(2). When the transformer is considered as the equivalent circuit in figure 4, the problem of calculating primary (input) current from the secondary (output) current is simply vector algebra. The fact that we have limited the method to five per cent ratio error (approximately five per cent total exciting current maximum) justifies the assumption that the voltage drop in X_L is not $(I_s-I_{e1})X_L$ (see figure 4) but I_sX_L, and the voltage on the number 2 exciting branch is $I_s(Z_b+R_s+X_L)$ (adding vectorially). The calculation of performance is then exactly as if the two exciting branches were two separate current transformers, one with burden Z_b+R_s, the other with burden $Z_b+R_s+X_L$, and the ratio and phase-angle errors will be the sum of the errors of the two.

3. It is well known[7] that the component of exciting current which produces ratio error is:

$F\cos\theta+M\sin\theta$
F, M = watt reactive components of exciting current, respectively
$\cos\theta$ = burden power factor

This value, added to the secondary current, gives the primary current reversed. The formula is:

$$\text{per cent ratio} = \text{per cent turns ratio} + \frac{100\,(F\cos\theta+M\sin\theta)}{I_s}$$

I_s = secondary current

Calculating the value of $F\cos\theta+M\sin\theta$ from the ordinary open-circuit secondary saturation and power factor curves is not difficult, but calculation of a number of points is tedious. Now the ordinary saturation curve is plotted between exciting current, which is $\sqrt{F^2+M^2}$, and secondary voltage. It is not much more difficult to plot $F\cos\theta+M\times\sin\theta$ for a number of values of $\cos\theta$, instead of $\sqrt{F^2+M^2}$, and the desired value can then be read directly.

$$\text{Phase angle}=\frac{3438}{I_s}(M\cos\theta-F\sin\theta)$$

The phase-angle component is $M\cos\theta-F\sin\theta$, and a similar set of curves can be plotted for this value.

Figure 5 is an example of such a set of curves for one transformer and figure 7 is a set of $F\cos\theta+M\sin\theta$ curves for a different transformer. The log-log co-ordinates of figure 5 are more useful if the lower range of the curves is important. This idea was originated by A. M. Wiggins.[6]

The data needed for calculating performance then are:

(1). Saturation curves of the form $F\times\cos\theta+M\sin\theta$ and $M\cos\theta-F\sin\theta$ plotted against secondary voltage, for a number of values of $\cos\theta$ (see figure 5).

(2). Secondary winding resistance.

(3). Leakage reactance X_L measured according to appendix II.

The procedure is:

(1). Given burden and power factor, determine the total burden on the right hand exciting branch of figure 4. (Burden + secondary resistance $=Z_1$.) Also determine the sum of this burden $+X_L$, which is the burden on the left hand exciting branch. $Z_1+X_L=Z_2$. (Vectorial addition.)

(2). From these two values of burden in ohms and the secondary current, calculate the voltages on the two exciting impedances.

$E_1=I_sZ_1$
$E_2=I_sZ_2$

(3). From the $F\cos\theta+M\sin\theta$ curves, read values for E_1 and E_2 and find per cent ratio by—

$$\text{per cent ratio}=\text{per cent turns ratio}+\frac{100}{2}\times\left[\frac{(F\cos\theta+M\sin\theta)_1}{I_s}+\frac{(F\cos\theta+M\sin\theta)_2}{I_s}\right]$$

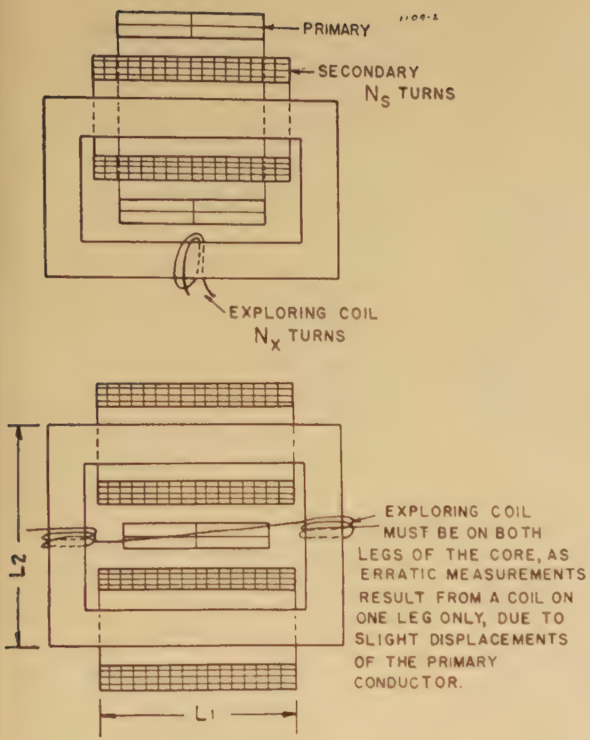

Figure 2. The most direct and simple as well as the most nearly correct method for determination of leakage flux is measurement by exploring coils

The lengths $L1$ and $L2$ represent relative (not absolute) lengths of the part of the magnetic circuit which can be considered to carry no leakage flux and all the leakage flux, respectively, in a through-type transformer

The subscripts 1, 2, refer to the two parts of the core; the division by 2 takes account of the fact that each component is for only half of the core, whereas the saturation curves are for the whole core. It will be noted that the exact turns ratio must be known. This ratio is often difficult to measure, but the manufacturer can always supply it. It may also be difficult to place the exploring coil on a transformer. This also is easy for the manufacturer, however. General use of this method will probably depend on the manufacturer's measurements of exact turn ratio and leakage flux.

$$\text{Phase-angle minutes} = \frac{3{,}438}{2} \times \left[\frac{(M \sin\theta - F\cos\theta)_1}{I_s} + \frac{(M\cos\theta - F\sin\theta)_2}{I_s}\right]$$

VI. Comparison of Tests and Calculations

The constants which determine the performance of the transformer at a given frequency are:

(1). The secondary coil resistance.

(2). The secondary leakage reactance X_L measured according to appendix II.

(3). The $F\cos\theta + M\sin\theta$ and $M\cos\theta - F\sin\theta$ curves for exciting current plotted against secondary voltage.

(4). The burden.

(5). The secondary current.

The fact that this method gives correct results for ring type transformers, in which there is no leakage flux, has been amply demonstrated.

The method has been demonstrated on several wound type transformers, and the constants for one wound type and one through type transformer will be given, together with calculated and measured results.

(a) Wound-Type Transformer

Secondary coil resistance:

0.3 ohm. (R_s)

Secondary leakage reactance:

Exploring coil voltage E_x 0.148 in 10 turns ($N_x = 10$)
At I_s = secondary current = 5 amperes
N_s = secondary coil turns = 239
From equation 7, appendix I

$$X = \sqrt{\left(\frac{0.148 \times 239^2}{5 \times 10}\right) - 0.31^2} = 0.638 \text{ ohm}$$

The $F\cos\theta + M\sin\theta$ and $M\cos\theta - F\times \sin\theta$ curves are given in figure 5.

The calculation of a given point is as follows:

Secondary current = 5 amperes	
Burden = 0.6 ohm, 90 per cent power factor =	$0.54 + j\,0.262$
Add R_s (secondary coil =	0.31
(Z_1 = 0.89 ohm, 96 per cent power factor) Z_1 =	$0.85 + j\,0.262$
Burden voltage $E_1 = 4.45$	
Add X_L =	$j\,0.638$
Z_2 = 1.24 ohms 69 per cent power factor	$0.85 \quad j\,0.9$
Burden voltage $E_2 = 6.2$	

From figure 5, at $E_1 = 4.45$, $(F\cos\theta + M\sin\theta)_1 = 0.0133$
at $E_2 = 6.2$, $(F\cos\theta + M\sin\theta)_2 = 0.0229$

$$\text{Per cent ratio} = \begin{cases} \text{per cent turns ratio} = 99.584 + \\ \dfrac{100}{2}\ \dfrac{(0.0133 + 0.0229)}{5} = \dfrac{0.362}{99.946} \end{cases}$$

Test value = 99.89

The curves of figure 6 were calculated in the same way, and one who desires to may check them very rapidly by the use of tabular calculations.

(b) Through-Type (Two-Coil) Transformer

Good results are generally obtained by dividing the core into two equal parts, in the case of a wound type current transformer, but the division should not be made quite this arbitrarily for a through type current transformer. If the length of magnetic circuit not enclosed by the coils is taken as the part carrying leakage flux, and the axial length of the coil is taken as the part not carrying leakage flux, better results are generally obtained. These two lengths are, more often than not, nearly equal, so that the final division is usually not far from division into two equal parts, but some designs are made with unusually long yokes which carry the leakage flux, and account should be taken of their length. The lengths of these parts of the circuit are usually easily measured, according to figure 2.

The particular design in question was such that the core could be considered to be divided into equal parts.

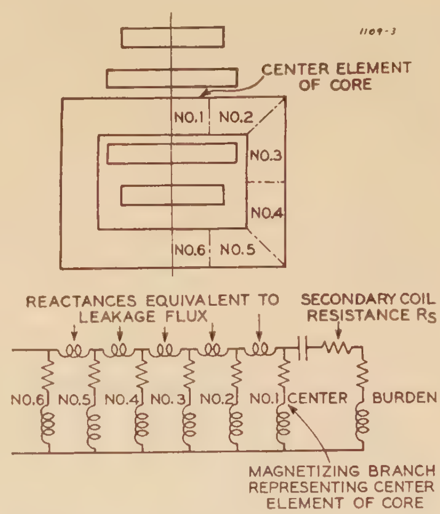

Figure 3. The flux at the center of the core inside the secondary coil is actually less than enough to generate the total burden voltage, because the "leakage" flux passing through the body of the secondary coil actually links some of the secondary turns and induces a part of the secondary voltage

This real reduction of flux in the center element of core can be represented exactly by a negative series reactance or a capacitor C

Each successive element of the core, starting from the center element, carries a greater part of the real leakage flux, represented by added series reactances, and the network is an accurate equivalent

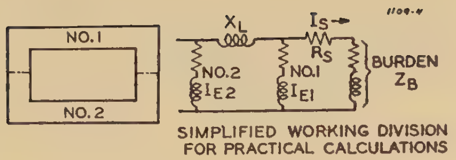

Figure 4. A practical working equivalent for figure 3 is the two-branched network

The curves for this transformer are given in figure 7.

The secondary resistance was 0.345 ohm. (R_s)

The secondary turns (N_s) were 280; ratio 1,400/5 amperes.

Two exploring coils were used, one on each yoke of the core, ten turns each, in series as in figure 2 ($N_x=20$). Erratic results would be obtained from measurements on only one exploring coil, as only slight displacement of the primary conductor causes considerable shifts in leakage flux, which has negligible effect on performance, but which causes considerable difference in individual coil voltages.

The total voltage of two exploring coils (E_x) was 2.15 volts at $I_s=15$ secondary amperes, and thus

$$X_L=\sqrt{\left(\frac{280}{20}\,\frac{2.15}{15}\right)^2-0.345^2}=1.98=2.0 \text{ ohms}$$

The details of calculation need not be given, but the test and calculated data are—

Burden Ohms	Secondary Current Amperes	Per Cent Ratio Error Test	Per Cent Ratio Error Calculated
1.0	50	0.5	0.59
	75	3.0	4.5
2.0	25	0.1	0.28
	50	3.3	3.1
	55	4.2	4.7
4.0	25	0.7	0.75
	35	5.5	5.4

At larger currents, where errors are much larger, the test values do not agree with calculation.

This design is typical of two-coil through type transformers, and the two-ohm equivalent internal reactance is also typical for this ratio. The burden may often be less than the equivalent internal impedance, so that the performance of the transformer may sometimes not be much affected by burden.

If the ratio is higher than 1,400/5 the internal impedance will be higher, increasing approximately as the square of the ratio, and if the core section is increased the internal impedance will increase almost in proportion. The result is that a two-coil through type current transformer of conventional design will not perform well at primary currents much above 25,000 primary amperes, regardless of the amount of iron in the core.

VII. Other Uses for Saturation Curves and Secondary-Coil Resistance Data

(1) Transient Performance

The use of the secondary coil resistance and saturation curve for determining per-

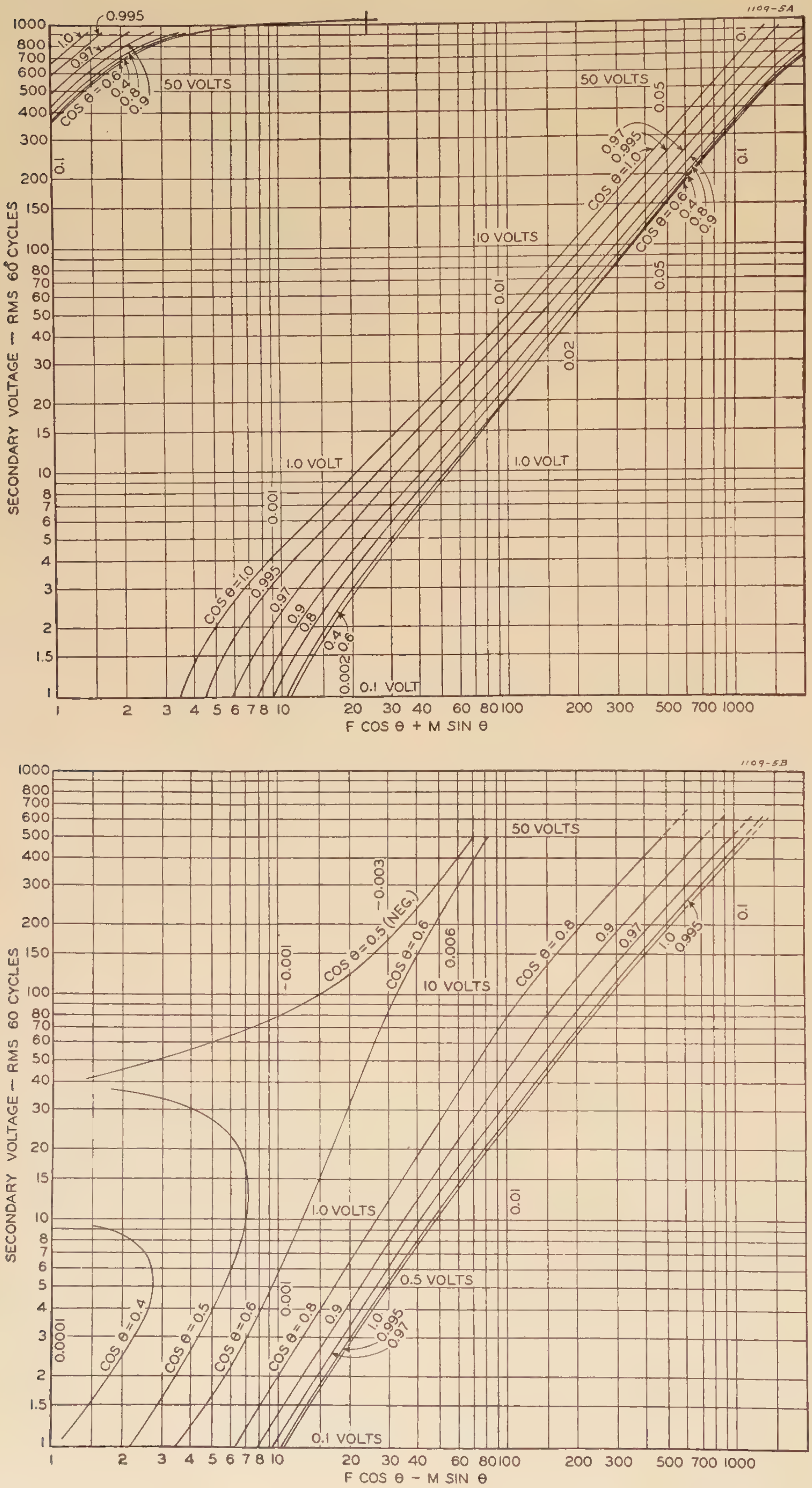

Figure 5. F cos θ+M sin θ and M cos θ − F sin θ curves for a typical transformer

These are calculated from the watt (F) and reactance (M) components of the open-circuit secondary saturation curve. Cos θ is the burden power factor

formance at transient currents has been fully described in previous papers.[8,9]

(2) Parallel Connection

When current transformers are connected in parallel, the primary current of one of the transformers may be very low, or even zero. If it is very low, while the burden voltage is relatively high because of current supplied by the other transformers in parallel, the effective burden impedance (:volts/current) is very high, higher than any usual burden, and the performance of the current transformer

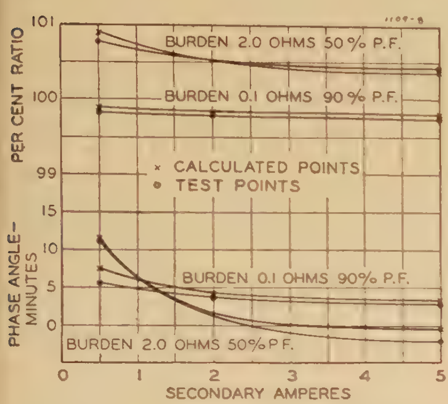

Figure 6. Calculation versus test

Wound-type current transformer calculated from figure 5, and secondary resistance = 0.31, leakage reactance 0.638

at such a burden will seldom be given by the standard performance curves. The performance can then easily be determined by the method given.

If the primary current is zero (primary circuit open) the exciting current drawn by the dead current transformer can be read from the same saturation curve, and its effect on the current supplied to the burden calculated in the same direct way.

VIII. Constants Determining the Excellence of a Current Transformer

The real excellence of a current transformer is determined by examination of ratio and phase-angle data. However, it is not economical, as has been pointed out, to measure ratio and phase angle at every possible condition, and comparison of overcurrent data on two current transformers is usually awkward, and often inconclusive.

When current transformers operate relays, ratio errors of less than five per cent are usually of no consequence. The power factor of the total burden with the usual relays will be in the neighborhood of 60 per cent. If the primary current is the common figure of 10 times normal, or 50 amperes secondary current, $F\cos\theta+M\sin\theta$ must be 2.5 to produce an error of 5 per cent. Then the magnitude of the voltage, according to the $F\cos\theta+M\sin\theta$ curves, at which $F\cos\theta+M\sin\theta$ will be 2.5 is one general measure of the excellence of the current transformer (see figure 5).

The resistance of the secondary winding and the equivalent value of X_L determine how much must be added to the connected burden to determine how much burden the transformer has to carry. Hence these figures also are measures of the excellence of the current transformer.

Thus two indices of excellence which can be readily compared are:

(1). Secondary voltage at which $F\cos\theta+M\sin\theta$ for 60 per cent power factor is 2.5.

(2). Internal resistance and reactance.

IX. Conclusions

A simple method for calculation of current transformer performance has been developed. It is not new in fundamental principles, but it is an improvement and simplification of the most accurate existing method.[3]

It is more direct in its use of leakage flux; it uses a real measured value in its calculations; furthermore, the measurement of flux is easily done with exploring coils without other special equipment. The exploring coil can be threaded through the space between core and coil in many transformers, especially older models.

The method is flexible. If further experience shows the necessity for further division of the core, two sets of exploring coils can be used with a division of the core into three parts. It can be made to be as accurate as desired.

It proposes a simple equivalent circuit for calculations which includes an internal reactance. This simplifies the calculation, and isolates and defines a constant of the transformer: the equivalent internal reactance of a current transformer is that reactance which as burden would require an additional flux equal to the maximum measurable value of leakage flux in the core. A formula for the reactance in turns of exploring coil measurements is included.

The errors in the method are on the conservative side. The real exciting current is less than the calculated value, and at the higher values, corresponding to saturation of the core, where the ratio error usually exceeds five per cent, the calculated ratio error is usually much too high. Thus, the method is useful even where it is not too accurate.

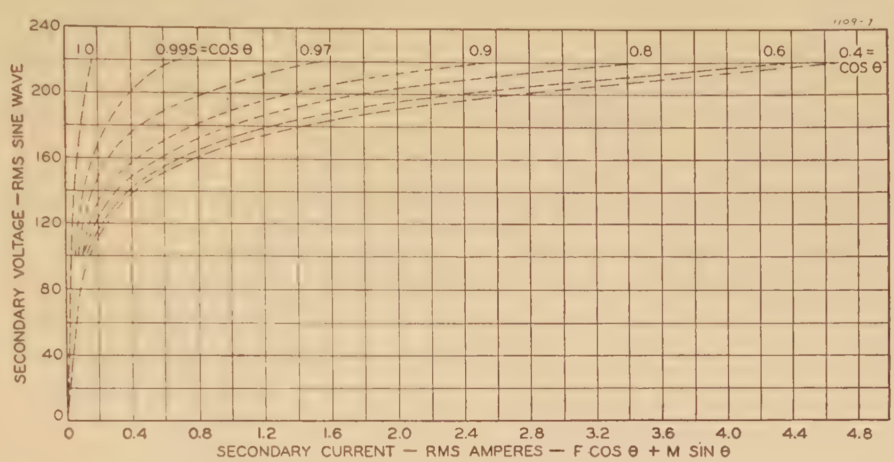

Figure 7. $F\cos\theta+M\sin\theta$ curve for a through-type current transformer

$F\cos\theta+M\sin\theta$ is the component of exciting current which must be added to the secondary output current to get primary input current reversed (1/1 ratio basis). Example: burden four ohms at 80 per cent power factor, secondary current 50 amperes, exciting current (from curve) at $4\times50=200$ volts = 1.8 amperes. Primary current reversed = 51.8, ratio = 100 (51.8/50) = 103.6 per cent

Curves are proposed for simplification of the vector algebra. This expedient is of great value when many calculations are to be made. However, this part of the method is not essential. Any correct method of vectorially adding exciting current to secondary current can be used.

The performance under transient conditions, at unusual burdens or currents (including performance of parallel transformers) can all be determined from the characteristics listed above, using available methods[8,9] for transient performance, and the method described above for performance at unusual burdens or currents.

The performance of a current transformer is shown to depend on a few simple constants of the transformer:

(1). Internal resistance

(2). Internal reactance as defined

(3). Open-circuit saturation curve

Comparison of (1), (2), and one point on curve (3) allows formation of judgment about the relative excellence of transformers.

Appendix I. Equivalent Circuit for Current Transformers

An inductance burden on a current transformer requires a voltage 90 degrees ahead of the current, and as the flux to induce the voltage is, in turn, 90 degrees from the voltage, the flux is in phase with the primary current. So we may say:

1. The flux required by an inductive burden is in phase with the primary current.

Furthermore, it is well known that—

2. The leakage flux is also in phase with the primary current.

We can combine statements (1) and (2) and say—the flux required by an inductive burden has the same phase position as the leakage flux.

As both fluxes are directly proportional to the current, they are equivalent fluxes, and the leakage flux can be represented, if desired, by an equivalent inductance in the burden.

As shown by Mr. Sinks,[3] the leakage flux at the center of the core inside the secondary coil has, in effect, a negative value, but has higher values in each succeeding element of the core. For purposes of analysis, we can separate the core elements and represent each one by an equivalent exciting branch. The fact that each element carries a certain leakage flux can be represented by an equivalent inductance in series with the current circuit, as in figure 3. The fact that the leakage flux at the center corresponds to a negative inductive reactance is represented by a capacitance in series with the first branch.

For practical work in which the core is divided into only two parts, one of which is assumed to carry no leakage flux, the circuit takes the simpler form shown in figure 4, in which the series equivalent inductance is determined according to appendix II.

Appendix II. Exploring Coil for Flux Determination

If the secondary winding of a current transformer is short-circuited, the total real linkages of flux with the secondary coil are just enough to circulate the current against the resistance of the winding. This flux can be calculated as an equivalent flux ϕ_s which links all the secondary turns.

$$\phi_s = \frac{I_s R_s 10^8}{4.44 f N_s} \tag{1}$$

I_s, R_s, N_s = secondary current, coil resistance, and turns, respectively.

This amount of flux may be considered as a working flux flowing all around the core.

If an exploring coil is placed on the outer part of the core at a point where leakage flux exists, it will develop a voltage corresponding to ϕ_s plus (vectorially) the leakage flux ϕ_L.

The exploring coil voltage will be—

$$E_x = 4.44(\phi_s + j\phi_L) f N_x 10^{-8} \tag{2}$$

j expresses the fact that the vector ϕ_L is at right angles to the vector ϕ_s. In absolute values,

$$\left(\frac{E_x 10^8}{4.44 f N_x}\right)^2 = \sqrt{\phi_s^2 + \phi_L^2} \tag{3}$$

$$\phi_L = \sqrt{\left(\frac{E_x 10^8}{4.44 f N_x}\right)^2 - \phi_s^2} \tag{4}$$

$$\phi_L = \sqrt{\left(\frac{E}{N_x}\right)^2 - \left(\frac{I_s R_s}{N_s}\right)^2}\ \frac{10^8}{4.44 f} \tag{5}$$

The leakage flux ϕ_L can be expressed as an equivalent reactance referred to the secondary winding of N_s turns and peak current $\sqrt{2}\, I_s$

$$X_L = \frac{2\pi f N_s \phi_L 10^{-8}}{\sqrt{2} I_s}$$

$$= \frac{2\pi f}{\sqrt{2}}\ \frac{10^8}{4.44 f} \sqrt{\left(\frac{N_s}{N_x}\ \frac{E_x}{I_s}\right)^2 - R_s^2}\ 10^{-8} \tag{6}$$

$$X_L = \sqrt{\left(\frac{N_s}{N_x}\ \frac{E_x}{I_s}\right)^2 - R_s^2} \tag{7}$$

Bibliography

1. Papers on Current Transformers, H. W. Price and C. Kent Duff. *Bulletin 2*, section 4, University of Toronto school of engineering research, 1921.

2. Calculation of Ratio Errors and Phase Angle in Current Transformers, With Particular Reference to Leakage Flux, E. C. Wentz. Thesis for the University of Pittsburgh, 1936.

3. Computation of Accuracy of Current Transformers, A. T. Sinks. AIEE Transactions, volume 59, 1940 (December section), pages 663–8.

4. Overcurrent Performance of Bushing-Type Current Transformers, C. A. Woods and S. A. Bottonari. AIEE Transactions, volume 59, 1940 (September section), pages 554–60.

5. A Proposed Method for Determination of Current-Transformer Errors, G. Camilli and R. L. TenBroek. AIEE Transactions, volume 59, 1940 (September section), pages 547–50.

6. Ring-Type Current Transformers—Limitations in Design, A. M. Wiggins. *Electric Journal*, December 1927, page 621.

7. A Study of the Current Transformer With Particular Reference to Iron Loss, P. G. Agnew. Reprint 164, *Bulletin* of the Bureau of Standards, volume 7, number 3.

8. Current Transformers and Relays for High-Speed Differential Protection, With Particular Reference to Offset Transient Currents, E. C. Wentz and W. K. Sonnemann. AIEE Transactions, volume 59, 1940 (August section), pages 481–8.

9. Current Transformer—Excitation Under Transient Conditions, D. E. Marshall and P. O. Langguth. AIEE Transactions, volume 48, 1929, pages 1464–74.

Transactions Section

Preprint of Corresponding Pages From the Current Annual Transactions Volume

Any discussion of these papers will appear in the December 1941 "Supplement to Electrical Engineering—Transactions Section"

Symmetrical Nomenclature of Three-Phase Circuits

BRYCE BRADY
MEMBER AIEE

Synopsis: Two methods of identifying three-phase conductors, voltages, and currents are in general use today. One method, used extensively on power systems and based on 30° voltage relations, is called "standard" nomenclature.[1,2,3] The other method, used frequently for analytical purposes and based on 90° voltage relations, is called "symmetrical" nomenclature.[4]

The following advantages of the symmetrical plan are discussed:

1. It is easier to use.
2. It identifies single-phase currents.
3. It requires fewer angles.
4. It is universal.
5. It is symmetrical.

Introduction

THE transformations most commonly used on three-phase power systems are the delta-Y and Y-delta connections which always introduce voltage phase shifts in the circuit, and the delta-delta and Y-Y connections which sometimes do. It is important to operating and design engineers that the voltage phase position of each terminal and conductor be identified by some arbitrarily adopted system of nomenclature. Such identification becomes more and more necessary as the number of successive transformations is increased.

The two nomenclature methods in general use are contrasted in figure 1 for a delta-Y transformation. Corresponding symbols are assigned to conductor-to-neutral voltages which differ by 90° in the symmetrical plan, and to voltages which differ by 30° in the standard plan. Both methods are expanded in figure 2 to provide a comparison with several variations of delta-Y and Y-delta connections. The two plans are identical with reference to delta-delta and Y-Y transformations, so these are omitted for the sake of brevity. Balanced voltage with counterclockwise (*ABC*) sequence is assumed throughout.

Ease of Application

A simple *ABC* rule facilitates the application of symmetrical nomenclature to all delta-Y and Y-delta transformer connections. For example in figure 2*a*, Y conductor *A* always corresponds with delta conductors *B* and *C* regardless of whether the connection is delta-Y or Y-delta, or whether the polarity is additive or subtractive, or whether the voltage displacement is lagging or leading. There is no exception to this easily remembered rule.

The rule for application of standard nomenclature is more complicated as illustrated in figure 2*b*, for sometimes Y conductor *B* and sometimes Y conductor *C*, corresponds with delta conductors *B* and *C*. This variability not only makes the rule more difficult to remember and use, but it renders standard nomenclature incapable of identifying single-phase fault currents

Fault-Current Identification

This same *ABC* rule positively identifies the flow of single-phase fault or load current through delta-Y and Y-delta transformations, if symmetrical nomenclature is used. For example in figure 3*a*, conductor *A* always supplies 100% current to a fault between conductors *B* and *C* on the load side of the transformation. Conversely, conductors *B* and *C* always supply 100% current if the fault occurs on conductor *A*. There is no exception to this simple rule.

Figure 3*b* illustrates the fact that such identification is impossible without supplementary data if standard nomenclature is used, for 100% current is sometimes supplied by conductor *B*, and sometimes by conductor *C*, through such transformations to single-phase faults between conductors *B* and *C*.

This failure of standard nomenclature to provide definite current identification is a major limitation of the method which cannot be evaded by standardization of connections, for both lagging and leading connections are necessary in a series of transformations to cancel voltage shifts and to obtain zero voltage displacement.

Fewer Angles

If either lagging or leading voltage displacement is allowed to accumulate in a series of transformations, only four kinds of three-phase voltages can result, such that parallel operation between circuits with different kinds is impossible. These four kinds are interpreted quite logically by the symmetrical plan to be the four multiples of 90°, as illustrated in figure 4*a*.

In such a series, the displacement be-

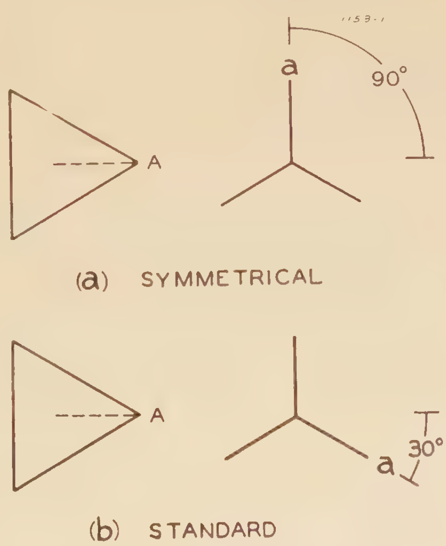

Figure 1. Symmetrical versus standard plan

Paper 41-153, recommended by the AIEE committee on power transmission and distribution, and presented at the AIEE South West District meeting, St. Louis, Mo., October 8–10, 1941. Manuscript submitted June 23, 1941; made available for preprinting August 11, 1941.

BRYCE BRADY is with the engineering department, Oklahoma Gas and Electric Company, Oklahoma City, Okla.

1. For all numbered references, see list at end of paper.

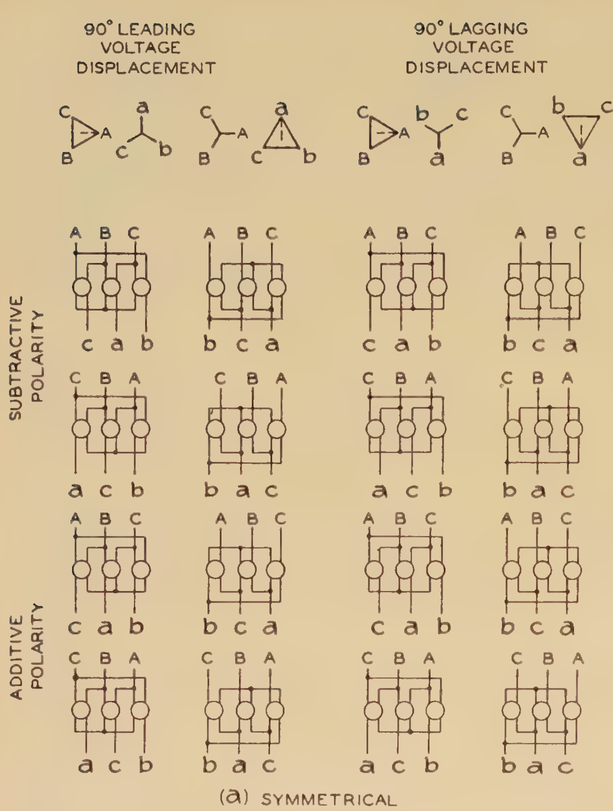

Figure 2. The symmetrical plan is easier to use

a. With the symmetrical plan, wye conductor *A* always corresponds with delta conductors *B* and *C*

b. With the standard plan, either wye conductor *B* or *C* may correspond with delta conductors *B* and *C*

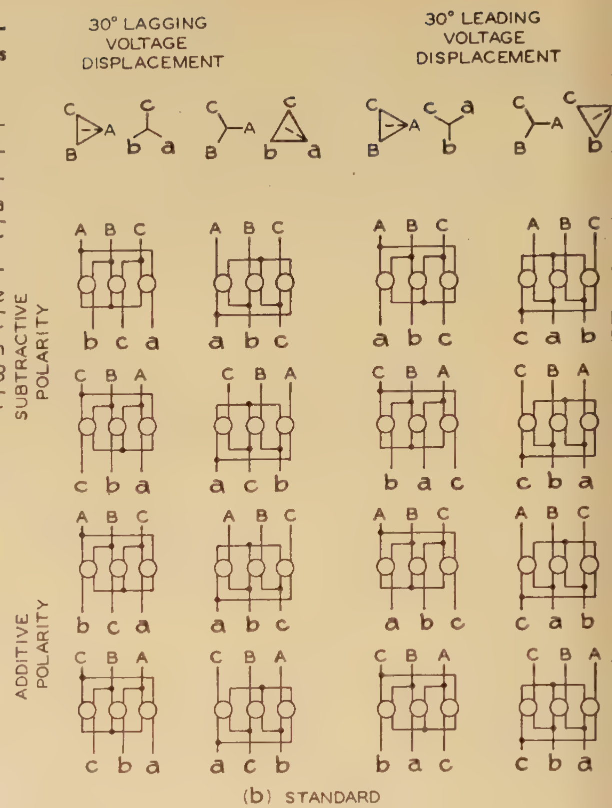

tween the same four voltage diagrams is interpreted at 30° intervals by the standard plan to present the illusion of twelve phase positions, as illustrated in figure 4*b*. The eight additional angles do not describe new phase positions, but merely represent rearrangements of symbols on the original four voltage diagrams. The use of such electrically duplicate angles, differing by 120° multiples, provides opportunity for confusion and error, and also destroys the ability of standard nomenclature to identify conductors with voltages that are in phase.

Universality

Situations frequently occur in practical applications where standard nomenclature fails to identify the conductors which must be interconnected for parallel operation. The connection diagram in figure 5*b* illustrates such a case where 4 kv conductor *A* originating in one substation must be connected to 4 kv conductor *B* originating in another substation, *B* to *C*, and *C* to *A*. Although all connections in the diagram are uniform and correct, the standard method of nomenclature causes confusion in the identification of 4 kv bus conductors. Circuit connections of this nature can occur in actual practice as a result of placing the 66 kv transformers back to back to reduce substation costs, or as a result of attempting to maintain uniform geographical phase sequence in all substations, such as phase sequence

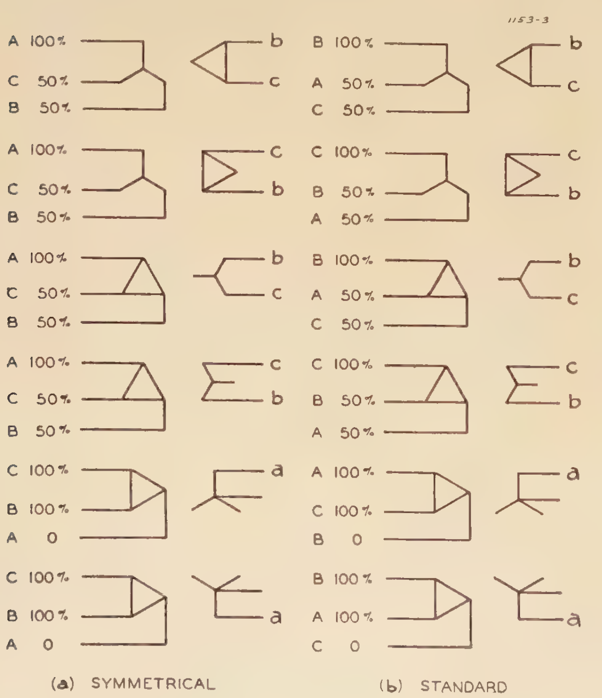

Figure 3. The symmetrical plan identifies single-phase currents flowing through delta-wye and wye-delta transformations

a. With the symmetrical plan, conductor *A* always supplies 100 per cent current to *BC* fault

b. With the standard plan, either conductor *B* or *C* may supply 100 per cent current to *BC* fault

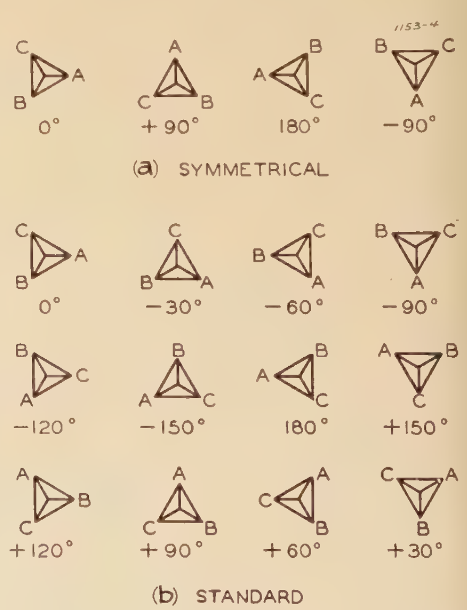

Figure 4. The symmetrical plan requires fewer angles, contains no duplicates

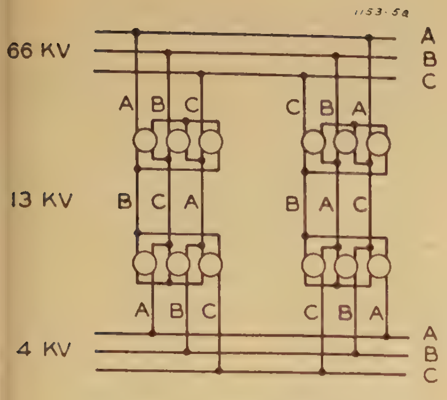

(a) SYMMETRICAL

a. With the symmetrical plan, circuits are always paralleled by connecting conductor *A* to *A*, *B* to *B*, *C* to *C*

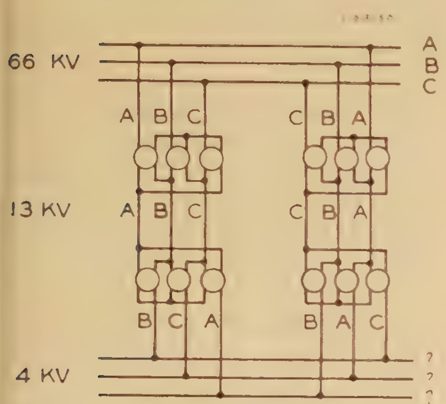

(b) STANDARD

b. With the standard plan, it is sometimes necessary to connect conductor *A* to *B*, *B* to *C*, *C* to *A*

Figure 5. The symmetrical plan is universal

ABC from north to south and from east to west. Such situations usually cannot be tolerated for safety, relaying, and other reasons and must be carefully avoided if standard nomenclature is used.

The symmetrical method does not have such limitations for conductors with in-phase voltages are always identified by corresponding symbols. For example in figure 5*a*, 4 kv conductor *A* originating in one substation is connected to 4 kv conductor *A* from the other substation, *B* to *B*, and *C* to *C*.

Symmetrical nomenclature is universal to the extent that it can always be applied without confusion to all conductors of a three-phase network, regardless of the sequences of delta and Y connections which may be used, and regardless of the number of interconnections and loops which may be added. It is the only nomenclature plan by which all in-phase delta and Y voltages on a three-phase network of unlimited complexity can be identified by the same symbol.

Symmetry

The symmetrical plan is based on the interpretation that all delta-Y and Y-delta transformations cause either +90° or −90° voltage displacement, and that all delta-delta and Y-Y transformations cause either 0° or 180° displacement. The symmetry of this classification is contrasted in figure 6 with the lack of symmetry of the standard classification.

The mathematical advantage of using such diametrically opposed groups is apparent in the treatment of polarity reversal or the equivalent connection reversal, for according to the symmetrical plan the effect of such reversal is always interpreted to be 180° displacement of voltage. If standard nomenclature is used, it is necessary to resort to the odd interpretation that such reversal causes 180° displacement in case the connection is delta-delta or Y-Y, but only 60° displacement if the connection is delta-Y or Y-delta. This anomaly results from the use of 30° angles to describe voltage phase shifts, and is the cause of many confusing situations in power transmission and distribution work.

The use of operator j is well developed in electrical engineering mathematics and fits perfectly with the symmetrical interpretation that the three-phase voltage displacement resulting from transformations is always a multiple of 90°. Change from standard to symmetrical nomenclature is accomplished by merely interchanging symbols on conductors and vector-diagrams after delta-Y and Y-delta transformations. It involves no change after delta-delta and Y-Y transformations; no change in physical connections; no change in vector diagram procedures; and no change in the use of arrows to identify instantaneous values.

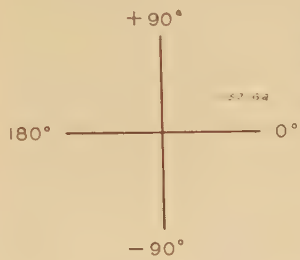

(a) SYMMETRICAL

Figure 6. Symmetrical nomenclature is based on the classification of all three-phase transformations in symmetrically related groups

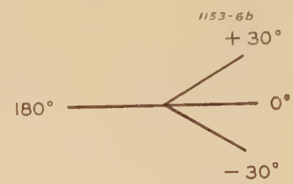

(b) STANDARD

Conclusions

The symmetrical plan of identifying three-phase conductors, voltages, and currents is worthy of more extensive use today and in the future because of the following advantages over the standard plan:

1. It is easier to use because symbols are applied by means of simpler rules.

2. It identifies the conductors which supply current through delta-Y and Y-delta transformations to single-phase faults—an impossibility by means of standard nomenclature.

3. It requires only four angles—the four multiples of 90°—to interpret all three-phase voltage displacement phenomena resulting from transformations. Standard nomenclature requires twelve angles—the twelve multiples of 30°—to accomplish the same purpose.

4. It is universal; it can be applied to transmission-distribution systems with unlimited delta and Y sequences and identify the conductors which must be interconnected for parallel operation. The standard plan sometimes fails to provide correct identification.

5. Mathematical advantages result from its perfect symmetry and the exclusive use of 90° multiples.

References

1. AIEE Standards, Transformers, Induction Regulators and Reactors (Revised), No. 13, May 1930, pages 17–21.

2. NEMA Transformer Standards, National Electrical Manufacturers Association. Publication number 32-12, seventh edition, 1932, pages 37–42.

3. ASA Rotation, Connections and Terminal Markings for Electric Power Apparatus, American Standards Association. C6, September 30, 1938, pages 29–30.

4. Symmetrical Components (a book), C. F. Wagner and R. D. Evans. McGraw-Hill Book Company, 1933. Pages 20–1, also 67–8.

The Recovery-Voltage Analyzer for Determination of Circuit Recovery Characteristics

G. W. DUNLAP
ASSOCIATE AIEE

Synopsis: Widespread interest in transient recovery voltage phenomena has led to the development of a device for determining the recovery characteristics of circuits and apparatus. The problem was solved by making use of the multiple surge testing technique which, in turn, involves the use of a low voltage repeating type surge generator. This paper describes the method and necessary equipment and indicates the range of conditions to which they may be applied. Demonstration tests on miniature and full scale circuits are also shown.

WHEN a current flowing in a circuit is interrupted, the voltage across the interrupting device rises or "recovers" rather rapidly in some characteristic wave shape from zero to the normal open circuit value. This phenomenon which has been defined as the "transient recovery voltage"[7] is illustrated in figure 1 where the voltage and current relations are shown for the application and clearing of a fault on a hypothetical circuit. The characteristic wave shape is dependent on the connected circuit and may consist of an oscillation at one or more frequencies corresponding to natural frequencies of various parts of the circuit.

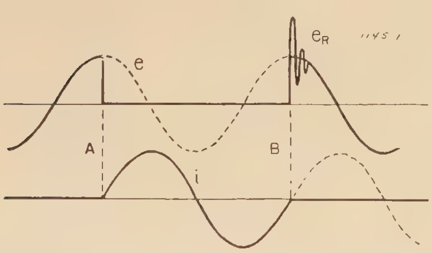

Figure 1. Diagram showing appearance of recovery voltage upon interruption of short-circuit current

e—System voltage
e_R—Recovery voltage
i—Short-circuit current
A—Point of fault application
B—Point of current interruption

The circuit interrupting device in performing its function of opening the circuit must contend with this voltage rise and must introduce insulation strength at a rate adequate to meet the stress of the rising voltage.

Since the comprehensive treatment of the subject in 1931 by Park and Skeats,[1] much has been written[2,3,4,5,6] concerning recovery voltages and their effect on the performance of circuit interrupting devices. The importance of the "transient recovery voltage" and "transient recovery voltage rate"[7] is now quite generally recognized and cathode-ray oscillograph measurements of these quantities are usually considered as part of standard test procedure for circuit breakers and other interrupting devices. Such measurements, though they involve expensive and time-consuming tests, are highly satisfactory and have proven of great value in the development work which has brought power circuit breakers to the present high level of performance.

Frequently, however, it is desirable to know the transient recovery voltage characteristics of a circuit where it is not practical to make interruption tests or cathode-ray oscillograph measurements, or where a breaker is not yet installed.

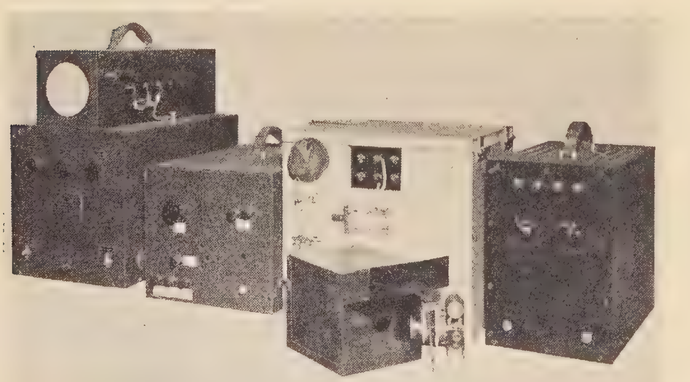

Figure 2. Recovery-voltage analyzer

Left to right, cathode-ray oscillograph, multiple-surge amplifier, multiple-surge transformer, and multiple-surge generator. Foreground, camera and mounting

Heretofore, the transient recovery voltage of the circuit was calculated by methods described elsewhere,[1,6,7] or it was sometimes possible to set up and analyze the circuit in miniature.[8,9,10] Such methods are dependent on a knowledge of the constants of the circuit in question. The accuracy of results is limited by the precision of this knowledge which involves many values of bushing and bus capacitance that in general can only be approximated.

By application of the multiple surge testing technique to the problem, a device known as the recovery voltage analyzer was developed. This analyzer permits the direct observation and measurement of the transient recovery voltage without full power interruption tests.

Technique

The multiple surge testing technique was developed as an adjunct to high-voltage impulse testing and the oscillograph electric transient analyzer[11,12] was built to utilize this method in the study of surge performance of a wide variety of apparatus. To briefly review this technique, it consists of the application to a test piece of a succession of low-voltage surges of controlled shape. In precise time coordination with these surges there is produced a series of sweep impulses for a cathode-ray oscillograph. When these voltages are put on the proper deflection plates of the cathode-ray tube, the successive surges superimpose on the tube screen and appear as a standing wave which may be viewed, traced, or photographed. In this way high-speed transient phenomena may be studied with the same facility had in reading steady state conditions with an ordinary voltmeter or ammeter.

Since the transient recovery voltage is also this type of phenomenon, the application of multiple surge testing to the problem was a logical step. This application was developed along two lines. The resulting methods will be distinguished by reference to them as the "substitution method" and the "current injection method" respectively.

Paper 41-145, recommended by the AIEE committee on protective devices, and presented at the AIEE Pacific Coast convention, Yellowstone National Park, August 27–29, 1941. Manuscript submitted April 12, 1941; made available for preprinting July 16, 1941.

G. W. Dunlap is with the general engineering laboratory of General Electric Company, Schenectady, N. Y.

The author expresses his thanks to C. M. Foust for his many suggestions and guidance and to G. F. Davis for his cooperation in the study of switchgear testing circuits.

1. For all numbered references, see list at end of paper.

a. Substitution Method

The substitution method was based on the idea of using the oscillograph electric transient analyzer to determine the constants of an unknown circuit or alternatively the constants of a simplified equivalent circuit. From these constants the transient recovery voltage could be calculated or read from curves of the type proposed by Boehne.[6] The justification of the method lies in the similarity of response to an applied voltage surge, of electrically equivalent circuits; and this was demonstrated by showing the transient responses of Boehne's circuits[6] to be identical for a wide range of applied voltage waves. Further demonstration was made by showing for the same wide range of waves that a full size power testing circuit with known constants behaved the same as a simplified equivalent circuit built up in the laboratory from lumped constants.

This method proved to be workable especially where the constants of a circuit are desired as in setting up a miniature representation of a system. However, it was less convenient than the current injection method for general usage.

b. Current-Injection Method

This method has the advantage that the transient recovery voltage is shown as an oscillogram of the same type as that obtained by high-speed cathode-ray oscillography in connection with interruption tests. The usual measurements of frequency, amplitude, and rate of rise may be made directly from this oscillogram in the accepted manner. In addition the validity of the method is immediately apparent and may be readily demonstrated by mathematical analysis.

The method utilizes the device ordinarily employed in calculations involving current interruption and demonstrated elsewhere[1,6,14]; i.e., a current wave of the same shape as that which is considered as being interrupted is injected into the circuit under study. The resultant voltage is identical with that which would appear on actual interruption, and is therefore the recovery voltage. If interruption of an alternating current at current zero is assumed, the injected current must be of sinusoidal form. However, for the time interval during which the transient recovery voltage is of interest, a sine wave is essentially a straight line so the injected current may be of the form i = constant × time. Off-zero interruption or interruption of d-c may also be simulated as will be described later; but the "ideal" interruption case is the most basic condition and the one on which most circuits will be comparable. This case will be considered in some detail.

A current of the desired linear form may be obtained by connecting a source of constant voltage to a linear inductance. Practically this is done by discharging the surge generator capacitance of an oscillograph electric transient analyzer through a suitable inductance. Of course when this arrangement is used to control the current applied to a test circuit the inductance must be sufficiently large in relation to the load so that there will be negligible distortion of the current wave.

Actually the problem was not as simple as it would appear. The inductance called for in the first design turned out to be too large and heavy for a portable equipment. It developed that a coil could not be built with low enough distributed capacitance to prevent the passage of an initial capacitance component of current which would appear as a "kick" at the beginning of the current wave. It was necessary to resort to a transformer in which the inductance could be utilized as before while the series capacitance path was virtually eliminated by electrostatically shielding the primary from the secondary. The same solution to the inductance problem was reached in England by Messrs. Trencham and Wilkinson[13,14] who applied their version of the oscillograph electric transient analyzer to the study of transient recovery voltages.

Further details of technique will become apparent as the various units of the recovery voltage analyzer are described.

Equipment

The present developmental model of the recovery voltage analyzer is shown in figure 2 and the several parts are described below.

a. Multiple-Surge Generator

This unit is a simplified oscillograph electric transient analyzer[11,12] The actual circuit used is shown inside the dashed lines in figure 3. Briefly its function is the generation of a succession of surges, the shape of which will depend on the elements connected to the terminal marked "surge." Synchronized with the appearance of these surges there are available at the terminals indicated, impulses for initiating the cathode-ray beam and for sweeping the beam across the screen at a predetermined speed.

To give this result the circuit operates as follows: Thyratron T_1 is fired once every cycle of supply voltage by a peaking transformer connected to its grid. This provides a series of positive impulses at the "trip" terminal to initiate the cathode-ray beam and at the grid of thyratron T_3 to trip the surge in synchronism with the sweep voltage produced by the current flowing through the variable resistance R and the capacitor C_2 during the conduction period of T_1. The series

Figure 3 (left). Multiple-surge generator circuit and connections for operation as a recovery-voltage analyzer

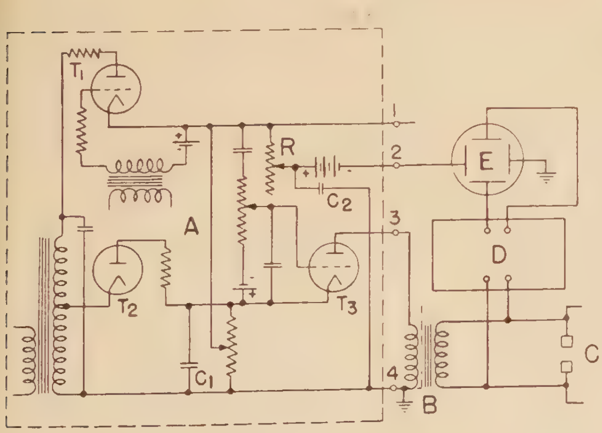

A. Multiple-surge generator
1. Trip-impulse terminal
2. Sweep-impulse terminal
3. Surge terminal
4. Ground terminal
B. Multiple-surge transformer
C. Test circuit
D. Multiple-surge amplifier
E. Cathode-ray oscillograph

Figure 4. Multiple-surge amplifier circuit

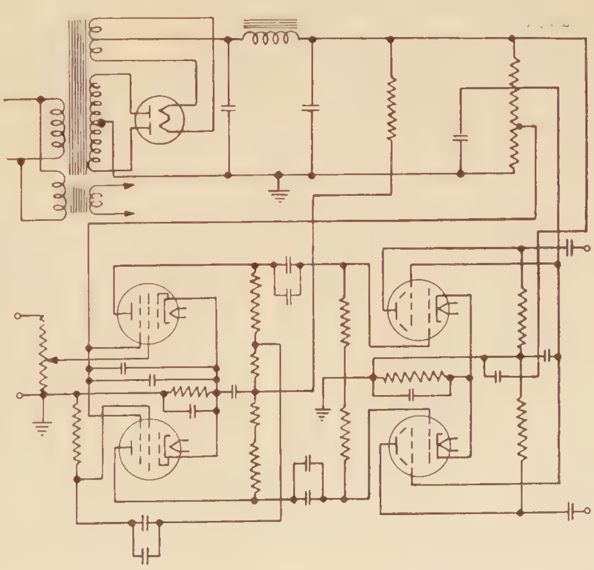

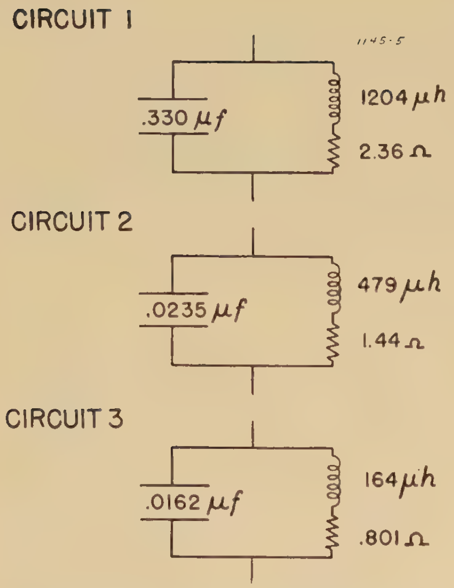

Figure 5. Lumped constant circuits for demonstration of recovery-voltage analyzer performance

Table I. Comparison of Calculated and Measured Recovery Characteristics, Figures 5 and 6

Quantity	Calculated	Measured
Frequencies		
f_1..........	8,000 cycles...	8,300– 8,400 cycles
f_2..........	47,500 cycles...	48,000–48,500 cycles
f_3..........	98,000 cycles...	97,000–98,000 cycles
Amplitude ratios (inductance ratios)		
$\frac{A_1}{A_2}$........	2.5 ...	2.1
$\frac{A_1}{A_3}$........	7.3 ...	5.8
$\frac{A_2}{A_3}$........	2.9 ...	2.8
Damping $\frac{E\phi_2}{E\phi_1}$		
Circuit 1...	0.94 ...	0.93
Circuit 2...	0.97 ...	0.87
Circuit 3...	0.97 ...	0.88

NOTE: Subscripts refer to the circuit with which the component indicated is associated.

$E\phi_2$ and $E\phi_1$ were measured between envelopes at times corresponding to ϕ_2 and ϕ_1 respectively.

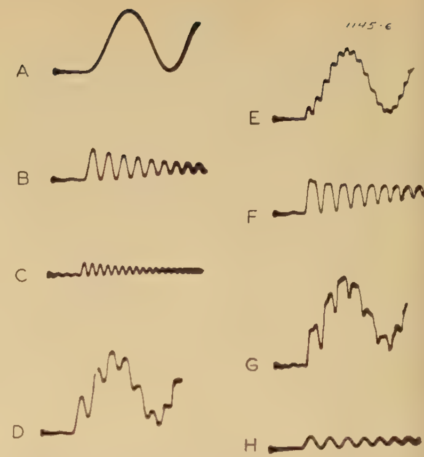

Figure 6. Recovery-voltage analyzer records obtained with the circuits of figure 5

A. Circuit 1
B. Circuit 2
C. Circuit 3
D. Circuits 1 and 2
E. Circuits 1 and 3
F. Circuits 2 and 3
G. Circuits 1, 2, and 3
H. 40-Kc timing wave

of surges is produced by the firing of thyratron T_3 which discharges the main capacitance C_1 through the circuit connected to the "surge" terminal. C_1 is charged through rectifier T_2 on each negative half cycle preceding the firing of T_3. Thus surges with synchronized beam control and sweep impulses are produced sixty times per second. This gives on the screen of the cathode-ray tube a stationary image of sufficient steadiness and brightness for viewing or photographing over the full range of sweep speeds giving sweep times of from 5 to 1,000 microseconds.

b. Multiple-Surge Transformer

The transformer is actually a set of interchangeable iron cored coils which viewed from the load side give a range of inductances from 60 millihenries to 4.5 henries. Each primary coil is electrostatically shielded by complete enclosure in a solid copper can with a gap between overlapping ends to avoid a short circuited turn. Experience showed that the shielding had to be very carefully designed to completely eliminate the objectionable "kick" mentioned before.

The function of this unit is the shaping of the wave to give the desired output of uniformly rising current surges. When the transformer is connected to the multiple surge generator as shown in figure 3, the repeated surges are discharged through the primary winding. Since for the time increments involved, the voltage applied to the primary is essentially constant, and since the transformer is operated well below saturation, the current flowing in the secondary is for the period of interest of the form $i=\text{constant}\times$ time. If the circuit to be measured is connected across the secondary, the current, controlled in form for all practical purposes by the transformer alone, will flow in the circuit and produce the desired response.

Since it is only necessary that the loading effect of the test circuit be negligible, the lower inductance transformer connections are used in conjunction with low impedance circuits in order to obtain a practical maximum of response. On the basis of inductance magnitudes available, circuits of up to 20 ohms impedance may be studied.

c. Multiple-Surge Amplifier

In order to keep the size and required power of the outfit within reasonable limits, it was found necessary to amplify the voltage waves appearing across the circuit to be measured. The amplifier was specially designed for this application and is shown diagrammatically in figure 4. It has an overall amplification of 180 times which falls off less than 10 per cent for frequencies down to 10 cycles per second and up as high as 500,000. Tests with the oscillograph electric transient analyzer showed that standard $1^1/_2$x 40 waves would be passed by the amplifier without measurable distortion. The output voltage is linear with respect to input up to 230 volts crest, while at 300 volts crest the output is only 8 per cent below the linear value. It might be noted that 230 volts gives full scale deflection on the cathode-ray oscillograph used. The input of the amplifier has a sufficiently high impedance so that the effect on the performance of the test circuit is negligible except in rare cases where 50,000 ohms shunt resistance will cause noticeable damping, or where 100 micromicrofarads additional capacitance will change the frequency appreciably. The amplifier contributes to the effective equipment capacitance which is about this value.

d. Cathode-Ray Oscillograph

The oscillograph used has a medium persistence screen 5-inch tube operated at 3,000 volts. All deflection plate leads are brought out directly to terminals and another terminal is provided which allows application of beam initiating impulses to the grid of the tube.

e. Camera

The camera used has an *F*2 lens with a 6.5 inch focus front lens and gives a record approximately $^1/_4$ the size of the actual image of the tube screen. Analysis of records is facilitated by projection of an enlarged image on a surface which may be provided with cross-section lines. With high-speed film good records may be obtained by exposures of $^1/_{50}$ to $^1/_5$ of a second, depending on sweep speed and beam intensity used. Of course, since the phenomenon appears on the tube screen as a standing wave, a slower camera could be used with correspondingly greater exposure.

Operation and Performance

a. Connection and Measurement

As may be seen from its picture in figure 2, the equipment is quite portable and may be set up at any point where a measurement is desired. The only re-

quirements are a source of 110–120 volt 60-cycle power and access to the circuit to be measured, which must be deenergized.

The units are connected together and to the circuits as indicated in figure 3. If the approximate impedance of the circuit is known as is generally the case, the proper combination of coils in the multiple surge transformer can be selected immediately; although if the impedance is not known, the operator is able with a little experience to make the selection by trial. With the equipment in place, measurements may be made directly and rapidly, since with the transient recovery voltage waves standing on the tube screen the effect of any change made in the circuit is immediately apparent.

b. Performance on Lumped-Constant Circuits

As a general demonstration of the analyzer performance, recovery voltage characteristics for the three lumped constant parallel L-C circuits of figure 5 singly and in various combinations are shown in the oscillograms of figure 6. It may be seen that the characteristic frequency, amplitude, and damping of each circuit as seen in curves A, B, and C are also present as component parts of the more complex waves of D, E, F, and G. Values measured from these records are compared in table I with values calculated from the known circuit values of capacitance, inductance, and resistance.

The comparison based on frequency, amplitude, and damping shows generally good agreement. The maximum deviation in frequency is 5 per cent and this is in the case where the measured value is based on a single cycle. Since the amplitudes should be proportional to circuit inductances, the comparison is made between inductance ratios and ratios based on y-axis intercepts of the voltage wave envelopes. Here again the measurement based on the single cycle is subject to some inaccuracy and the greatest deviation is about 20 per cent. For damping the greatest discrepancy of about 10 per cent is not unreasonable since no account was taken of the high frequency losses of the capacitor units.

The oscillograms of figure 7 show the increased damping provided by the connection of resistance in parallel with circuit No. 2. Calculation of damping for these conditions gives the same degree of agreement as found in table I.

Calibration of the time scale for these records is obtained by connecting the analyzer to a circuit with a known natural frequency. A 40 kc timing wave is included in both figure 6 and figure 7. Since it is only necessary that the current be of the desired linearity without restriction on the absolute rate of rise, the value provided by the most appropriate transformer connection is used and a convenient voltage amplitude is obtained by adjusting the amplifier gain. The amplitude of the wave appearing on the screen is therefore arbitrary. In cases where actual values of voltage are desired, a scale may be assigned by taking the axis of the lowest frequency oscillation as equal to the crest value of the rated normal frequency circuit voltage. The determination of this axis may sometimes be facilitated by introducing damping resistance as described in the preceding paragraph.

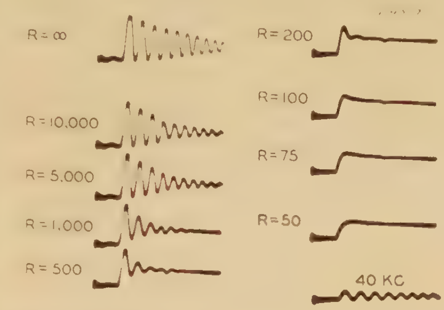

Figure 7. Recovery-voltage analyzer records showing damping effect on circuit 2 of parallel resistance of value indicated on each curve

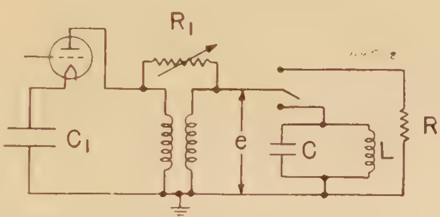

Figure 8. Connections for simulation of off-zero current interruption

C_1—Multiple-surge generator capacitance
R_1—Adjustable resistance 20,000 to ∞ ohms
e—Voltage measured with amplifier and oscillograph
C—0.0018 microfarad
L—1.35 millihenries
R—2 ohms noninductive resistor for current measurement

The range of load conditions under which satisfactory performance of the analyzer may be expected was established by measurements on circuits of the above type with natural frequencies ranging from 1 to 250 kc and with inductances up to 50 mh. While in special cases some lowering of frequency or increase in damping may be caused by the loading of the circuit by the equipment itself, particularly the amplifier as mentioned above, it may be said that the analyzer is adequate for the range of conditions which might be encountered in power circuits.

An interesting sidelight in the study of transient recovery voltage characteristics is the extension of the current injection method to simulate pre-zero interruption. This may be done by adding a d-c component to the normal injected current and is accomplished electrically by providing a resistance path directly between the multiple surge generator and the test circuit as shown in figure 8. Except that this resistance must be high compared to the load impedance, its magnitude may be varied to control the relative magnitude of the d-c component and hence the amount of pre-zero "chopping" simulated. Of course, if the "a-c" component is eliminated by disconnecting the secondary of the multiple surge transformer, interruption of d-c will be simulated.

A demonstration of the effect of pre-zero interruption on the transient recovery voltage is given by the oscillograms of figure 9 which were taken with the figure 8 circuit. The records of current were obtained by switching the analyzer output to a 2-ohm non-inductive resistor. Since the only variable was the resistance R, the relative amplitudes of the voltage waves represent over-voltage conditions caused by pre-zero "chopping."

c. Performance on Actual Power Circuits

A rather thorough check of field performance of the equipment was made on the test circuits of a high power switchgear testing station where some sixty different circuit arrangements were studied. Values measured from the analyzer oscillograms showed close agreement with those obtained from high-speed cathode-ray oscillograms taken during actual interruption tests, and in most cases with calculated values. Where there was disagreement between the calculated and analyzer results, the interruption test oscillograms checked with the analyzer records.

Typical transient recovery voltages are shown in the oscillograms of figure 10. Here analyzer records are superimposed on regular cathode-ray oscillograms and good agreement is shown. The small differences in the first part of the wave are due to modifications of the transient recovery by the circuit breaker used in obtaining the oscillograms. Also the method of determining the voltage calibration for the analyzer records is illustrated in this figure. As described above the axis of the lowest frequency oscillation is taken as a voltage equal to the crest

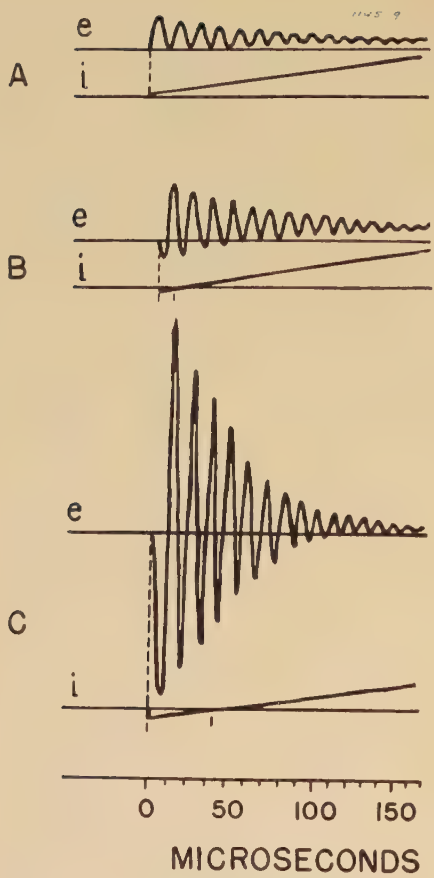

Figure 9. Recovery-voltage analyzer records obtained with figure 8 connections showing effect of off-zero current interruption

A. Voltage and current records, $R = \infty$ interruption at zero

B. Voltage and current records, $R = 200{,}000$ ohms, interruption 9 microseconds before zero

C. Voltage and current records, $R = 20{,}000$ ohms, interruption 34 microseconds before zero

value of the rated voltage of the circuit being measured. For *A* with a 4,200-volt circuit this value is 5.9 kv. For the 8,400-volt circuits of *B* and *C* it is 11.9 kv.

The analyzer has proven useful in determining the characteristics of test circuits, particularly special high recovery rate arrangements where this information was desired in advance of interruption tests. Analyzer records may also be used for comparison with conventional oscillograms to show modifications of the transient recovery voltage caused by the interrupting device itself. In addition, it is frequently desirable to know the characteristics of individual circuit elements and application has been made to transformers and reactors, illustrations of which have been published by Bewley.[15]

Conclusion

A portable device based on the multiple surge testing technique and utilizing the current injection method is now available for the determination of the transient recovery voltage characteristics of circuits and apparatus in the laboratory or field. These characteristics are obtained in the form of oscillograms which are analogous to the regular cathode-ray oscillograms ordinarily taken during interruption tests. They may be measured and interpreted according to standard practice[7] in the same way that the conventional records are. The range of conditions under which satisfactory performance may be expected includes natural frequencies from 1,000 to 250,000 cycles per second and load impedances up to 20 ohms.

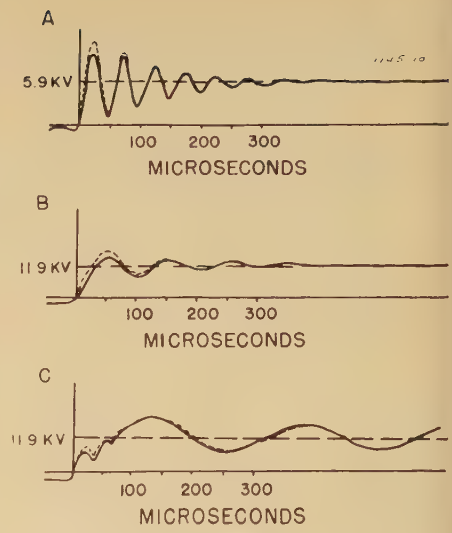

Figure 10. Typical transient-recovery voltages for switchgear testing circuits

Solid lines—cathode-ray oscillograms from interruption tests

Dotted lines—analyzer oscillograms

A. 4,200-volt circuit
B. 8,400-volt circuit
C. 8,400-volt circuit

References

1. Circuit-Breaker Recovery Voltages, **R. H. Park** and **W. F. Skeats.** AIEE Transactions, volume 50, 1931, pages 204–38.

2. Arc-Extinction Phenomena in High-Voltage Circuit Breakers, **R. C. Van Sickle** and **W. E. Berkey.** AIEE Transactions, volume 52, 1933, pages 850–7.

3. Oil Circuit Breaker and Voltage-Recovery Tests, **E. J. Poitras, H. P. Kuehni,** and **W. F. Skeats.** AIEE Transactions, volume 54, 1935 (February section), pages 170–8.

4. Breaker Performance Studied by Cathode-Ray Oscillograms, **R. C. Van Sickle.** AIEE Transactions, volume 54, 1935 (February section), pages 178–84.

5. Circuit Breakers for Boulder Dam Line, **D. C. Prince.** AIEE Transactions, volume 54, 1935 (April section), pages 366–72.

6. Determination of Circuit-Recovery Rates' **E. W. Boehne.** AIEE Transactions, volume 54, 1935 (May section), pages 530–9.

7. Alternating-Current Power Circuit Breakers, Proposed American Standard C37.4 through C37.9, January 1941.

8. System-Recovery Voltage Determination by Analytical and A-C Calculating-Board Methods, **R. D. Evans** and **A. C. Monteith.** AIEE Transactions, volume 56, 1937 (June section), pages 695–705.

9. Power-System Voltage-Recovery Characteristics, **H. A. Peterson.** AIEE Transactions, volume 58, 1939 (August section), pages 405–13.

10. An Electric Circuit Transient Analyzer, **H. A. Peterson.** *General Electric Review,* September 1939, page 394.

11. The Oscillograph Electric Transient Analyzer, **N. Rohats.** *General Electric Review,* March 1936, page 146.

12. Some Recent Developments in Impulse-Voltage Testing, **C. M. Foust** and **N. Rohats.** AIEE Transactions, volume 59, 1940 (May section), pages 257–65.

13. Restriking Voltage and Its Import in Circuit-Breaker Operation, **H. Trencham** and **K. J. R. Wilkinson.** *Journal* Institution of Electrical Engineers, volume 70, 1937.

14. Recurrent Surge Oscillographs and Their Application to Short-Time Transient Phenomena, **K. J. R. Wilkinson.** *Journal* Institution of Electrical Engineers, November 1938.

15. Equivalent Circuits of Transformers and Reactors to Switching Surges, **L. V. Bewley.** AIEE Transactions, volume 58, 1939, pages 797–802.

A Turbine-Governor Performance Analyzer

W. O. OSBON
MEMBER AIEE

Introduction

IN the modern interconnected power system the steam turbine governor plays a very important role. Its performance has an important bearing on system stability, effect of load swings, tie line load control, frequency regulation, and other related phenomena. Consequently, within the last few years there has been an increasing interest in the subject of steam turbine governor performance. Numerous papers[1] dealing with this subject presented at recent AIEE and ASME meetings provide ample evidence of this increased interest. These papers and the discussions which they have elicited reveal a need for improved means of obtaining complete and accurate measurements of turbine governor performance characteristics.

Operating engineers and turbine governor designers alike have felt the need for better measuring instruments. The principal concern of the central station engineer is the maintenance of a high quality of service for his consumers with the minimum operating cost. Accurate measurements of governor characteristics will often reveal imperfect operation and suggest means for improving performance or for increasing operating efficiency. The designer, on the other hand, is concerned with meeting the customer's requirements as to the operating characteristics of the governor. He must also contend with such design problems as the stability of the governor as a speed regulator, and the elimination of spurious effects such as may be caused by friction, mechanical imperfections in fly-ball governors, and by fluctuations in oil supply pressure in hydraulic governors. As a result of the designer's more recent efforts, the modern turbine governor has been developed to a point where existing measuring instruments are no longer adequate for determining its performance. The art of turbine control has, in fact, progressed to a stage where further major improvements are dependent to a considerable extent upon greatly improved instrumentation.

Previous instruments used for checking turbine governor performance have in general possessed limitations which leave their accuracy open to question, or which render them inconvenient to apply and use. Ordinary graphic frequency meters, pressure recorders, and recording tachometers, although entirely satisfactory for the purposes for which they were intended, do not respond rapidly enough to measure accurately the characteristics of the modern turbine governor. In many instances instruments for measuring certain essential quantities, particularly valve travel and hydraulic pressures, have been more or less makeshift, making their application to the turbine and the taking of simultaneous observations a difficult and irksome undertaking.

It is the purpose of this paper to describe a completely coordinated set of recording instruments which have been especially designed for analyzing the performance characteristics of steam turbine governors. These instruments are characterized by their wide range of measurements, their sensitivity, and by their ability to follow changes many times more rapid than can be followed by usual recording instruments capable of measuring similar quantities.[3,4]

General Requirements

The important governor characteristics; namely, sensitivity (or dead-band), speed regulation—both static and dynamic, speed of response, overspeed performance following a load dump, etc., can all be deduced from simultaneous measurements under appropriate conditions of instantaneous values of the following quantities:

1. Electrical output of the generator.
2. The mechanical travel of the turbine steam valve.
3. Various hydraulic pressures within the governor.
4. Angular velocity of the turbine shaft.

In order to overcome the limitations of previous instruments for measuring these quantities, certain features which were deemed essential to satisfactory measurement of the important governor characteristics were incorporated in the new governor performance analyzer. Some of these features which are common to the measurements of all the above quantities are:

First, unity of design permitting the recording of all quantities, or any combination of them, on a single chart thus allowing visual correlation of the various quantities to each other and to time.

Second, ability to record both direct and alternating components with frequency-response characteristics substantially flat from zero to 50 or 60 cycles per second if feasible.

Third, provision of indicating instruments so that the average value of each quantity can be determined at a glance.

Fourth, complete functional design so that makeshift and "haywire" set-ups can be avoided in the field.

Fifth, complete portability permitting the instruments to be set up and used with equal facility in the laboratory, in the shop, or in the field.

A sixth very desirable feature is the ability to record directly by pen or stylus on a paper chart, thus obviating the inconveniences of photographic recording. However, no multi-element recorder having a sufficiently high frequency response is now available, and due to the urgency of the governor analyzer development, it was considered inadvisable to undertake the development of such a direct-writing recorder for this application. It was decided, therefore, to use the standard oscillographic method of recording at least for the present. If a suitable direct recorder should eventually become available, the instruments to be described can be adapted to it with little difficulty.

Generator Output

For measuring electrical load delivered by the generator, it was thought desirable to provide various full scale ranges conveniently spaced between 1 and 200 megawatts with an accuracy of measurement of the order of ±2 per cent. The decision to use a standard oscillograph made the re-

Paper 41-158, recommended by the AIEE committees on power generation and instruments and measurements, and presented at the AIEE South West District meeting, St. Louis, Mo., October 8–10, 1941. Manuscript submitted April 16, 1941; made available for preprinting August 12, 1941.

W. O. Osbon is with the research laboratories of Westinghouse Electric and Manufacturing Company, East Pittsburgh, Pa.

The author acknowledges the work of F. T. Hague, manager of steam engineering, and of A. F. Schwendner, W. A. Wilson, and other turbine control engineers of the Westinghouse Electric and Manufacturing Company who proposed this project and who prepared the specifications for the instruments. He is grateful also for the helpful suggestions and encouragement of C. R. Hanna, under whose direction this work was done, and for the help of L. A. Bobula and M. D. Wilson, whose assistance in the design and construction of the instruments was invaluable.

1. For all numbered references, see list at end of paper.

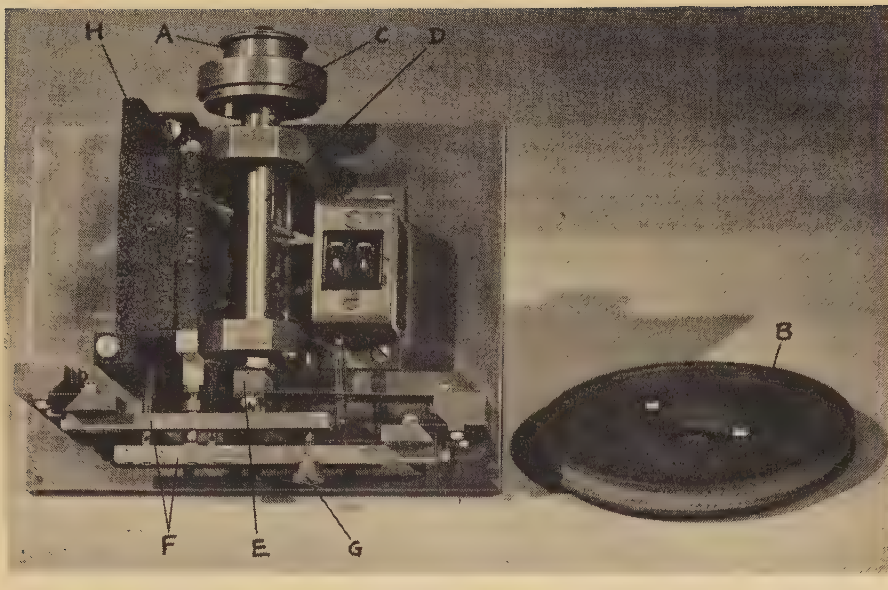

Figure 1. Valve travel recorder

A—Small pulley, *B*—large pulley, *C*—friction clutch, *D*—shaft, *E*—traveling nut, *F*—double-lever system, *G*—ratio-adjusting thumbscrew, *H*—magnetic strain gauge

cording of electrical load a simple matter, since there is already available a polyphase average watt oscillograph galvanometer which measures true watts in three phase circuits. The accuracy of this element is of the order desired, and the frequency response adequately meets the requirements, being flat to about 30 cycles per second, down approximately 10 per cent at 40 cycles per second, and down about 50 per cent at 60 cycles per second. The various full scale ranges can be obtained by using appropriate instrument transformers which are available in all central stations.

Steam-Valve Travel

The device for measuring turbine steam valve travel is illustrated in figure 1. A steel wire with one end attached to the valve operating lever is wrapped around one of the pulleys with the free end of the wire spring-loaded to insure accurate following. As the operating lever moves, the pulley and the shaft rotate proportionately. The traveling nut at the end of the shaft converts the rotary motion into linear motion, which is transmitted to a magnetic strain gauge[2] through the double lever system illustrated. The levers are mounted on crossed spring pivots to minimize friction and to eliminate lost motion.

Two pulleys are provided, one four inches in diameter and the other one inch in diameter. The smaller pulley can be exposed to use only by removing the large pulley, thus insuring the minimum moment of inertia when using either pulley. The ratio of the lever system can be adjusted to any one of four values by moving the thumb-nut to the appropriate tapped hole in the lower lever. The four lever ratios and the two pulley sizes provide a forty-to-one range of full scale motions. The instrument is proportioned so that valve motions of 0.2, 0.5, 1, 2, 4, and 8 inches give full scale deflection of the magnetic strain gauge. Motion of the strain gauge is converted into proportional variations of an electric current which are recorded by one element of the oscillograph. Thus the full travel of the largest steam turbine valve or operating piston, which may occur for example during a load dump test, may be recorded by the instrument as well as the minute motions of the order of $^1/_{16}$ inch or less which occur during normal operation of a highly sensitive governor.

A spring-loaded friction clutch is interposed between the pulleys and the shaft. This clutch, operating in conjunction with a pair of pins in the base and shaft clutch plate respectively, limits the rotation of the shaft to slightly less than one revolution. This feature serves to protect the instrument when the pulley is rotated through more than one revolution as may occur when the speed changer setting of the governor is shifted while the instrument is connected to the valve operating arm.

The frequency response of the valve travel recorder is limited to a value somewhat less than the natural frequency as determined by the inertia of the rotating parts of the recorder and by the stiffness of the wire connecting it to the valve operating lever. In order to obtain as high a natural frequency as possible with a particular wire, the force required to drive the recorder and its moment of inertia have been kept as small as practicable. The conversion of motion by the recorder into a proportional electric current permits mounting the unit very close to the valve lever so that a short and consequently stiff connecting wire may be used. With reasonable care in connecting the unit to the lever no difficulty is experienced in obtaining substantially flat frequency response to 60 cycles per second or higher.

Hydraulic Pressure

The oil pressures of interest in measuring governor performance are (1) the main pump pressure, (2) the speed-sensing impeller pressure (in the oil governor), (3) the transformed pressure, and (4) the pressures acting on the top and bottom of the valve operating piston. In order to cover the range of instantaneous values of these pressures three full-scale ranges were considered necessary, as follows: One pound per square inch variation in any average pressure up to 75 pounds per square inch; five pounds per square inch variation in up to 75 pounds per square inch average; and 50 pounds per square inch variation in up to 150 pounds per square inch average.

The device developed to measure these pressures is illustrated in figure 2. The pressure being measured is applied to the inside of a bellows, one end of which is fixed while the other end is attached to a lever. The motion of the lever is restrained by a stiff calibrating spring and

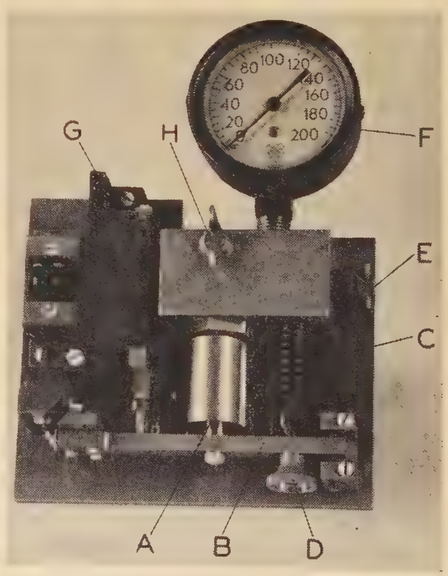

Figure 2. Oil-pressure recorder

A—Bellows, *B*—lever, *C*—calibrating spring, *D*—thumb nut for spring-force adjustments, *E*—needle valve for pressure gauge, *F*—pressure gauge, *G*—magnetic strain gauge, *H*—air drain

is measured by means of a magnetic strain gauge. The spring force can be adjusted by means of the thumb-screw to balance the force due to the average pressure within the bellows.

Two different units are provided. One is used for the one-pound and five-pound full scale ranges, the shift from one scale to the other being made in the electric circuit associated with the strain gauge. The other is used for the 50-pound full scale range. The two units are identical except for the size of the bellows and the stiffness of the calibrating spring. Both are provided with gauges to indicate the average pressure. The natural frequencies of the units as determined by the spring stiffnesses and effective inertias of the moving parts are of the order of 140 cycles per second for the low pressure recorder and 170 cycles per second for the high pressure unit. With natural frequencies of this order the frequency responses of the units will be flat to well above 60 cycles per second.

Angular Velocity

Although angular velocity of the turbine shaft is the quantity measured by the speed-sensing element of the governor, the ends of the shaft in many instances are not available for the attachment of a speed measuring device suitable for governor performance analysis. For this reason a small frequency-measuring synchronous motor driving two inductor generators is used. The motor is connected through a suitable transformer to the generator terminals so that its speed, within certain limitations to be discussed later, is an accurate measure of the generator frequency. Except for a small error due to variations in phase angle between the terminal and generated voltages, the generator frequency is in turn proportional to the speed of the turbine. Whenever it is necessary to avoid the error and limitations just mentioned, provision must be made for driving the inductor generators directly from the turbo-generator shaft. The synchronous motor drive has the advantage of simplicity and also permits the frequency meter described below to be used for the investigation of other problems not specifically related to governors, as for example, the relation between system frequency and tie line load variations.

Two full scale ranges are provided for the frequency meter: a wide range scale extending from 50 to 70 cycles per second to be used, for example during load dumping tests to measure overspeed characteristics; and a sensitive scale giving full scale deflection for ±0.25 cycle variation in a base frequency which may have any value between 59 and 61 cycles per second. In the instrument described below the sensitivity and accuracy are of the order of one per cent of the corresponding full scale ranges for the two scales.

The general scheme of operation of the frequency meter, which is by far the most complicated of the governor analyzer instruments, is illustrated by the block diagram, figure 3. One of the inductor generators produces a nominal frequency of 60 cycles per second for the wide scale range and the other generates a nominal frequency of 2,400 cycles per second for the sensitive range. As the turbo-generator frequency swings throughout the full range of the insensitive scale, the frequency of the 60-cycle generator varies between 50 and 70 cycles per second, and with constant excitation the generated voltage will vary proportionately. As it is desired to use only the frequency variations, an integrating circuit is interposed between the 60-cycle generator and the measuring circuits to eliminate the voltage variations. The output of this integrating circuit is then a true frequency-modulated wave whose amplitude is constant and whose frequency varies throughout the full scale range. This frequency-modulated signal is amplified and applied to a carefully designed discriminator circuit which, for a constant input voltage, gives an output proportional to the difference between the applied frequency and 50 cycles per second. The output of the discriminator is thus zero at 50 cycles per second, has a certain value at 60 cycles per second, and has twice this value at 70 cycles per second. The effect of the discriminator, then, is to convert the frequency-modulated signal applied to it into an amplitude-modulated signal. This signal is further amplified, rectified, filtered, and applied to an oscillograph galvanometer.

When using the sensitive scale the output of the 2,400-cycle generator is applied to a modulator circuit together with the output of a variable frequency oscillator. As the turbo-generator frequency swings throughout the full range of the sensitive scale the frequency of the 2,400-cycle generator will vary from 2,390 to 2,410 cycles per second for a base frequency of 60 cycles per second. If the oscillator is adjusted to produce a frequency of 2,340 cycles per second the modulator output then will be a frequency-modulated wave varying between 50 and 70 cycles per second or throughout

Figure 4. The inductor generators

The 2,400-cycle generator is nearer the motor. A brass collar at the end of the rotor corrects for the unbalance caused by truncating the 60-cycle rotor

Figure 3. Block diagram of frequency meter

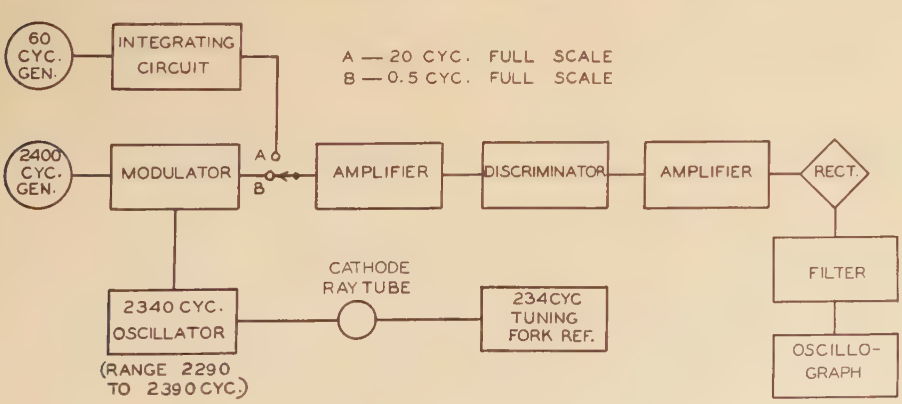

the same range as the output of the low-frequency generator during full scale swings on the insensitive range. By this process the turbo-generator frequency variations are increased forty times from ±0.25 cycle per second in 60 to ±10 cycles per second in 60. The output of the modulator is amplified, converted to an amplitude-modulated wave by the discriminator, and recorded similarly to the output of the integrator circuit when using the wide range scale. The voltage of the 2,400-cycle generator also varies with the driving motor speed, but these variations are not multiplied up as are the frequency variations. For this reason the error due to them is insignificant and consequently it is unnecessary to integrate the output of the 2,400-cycle generator.

In order that the base frequency for the sensitive scale be adjustable between 59 and 61 cycles per second, it is necessary that the oscillator frequency be adjustable from 2,300 to 2,380 cycles per second to give the same modulator output wave at all base frequencies. The oscillator control dial is calibrated directly in terms of base frequency.

It is evident from the foregoing discussion that accurate measurement of the average value of frequency when using the sensitive scale depends upon the constancy of the oscillator frequency. Consequently, great care has been taken to provide a highly stable oscillator circuit. In addition, a small cathode ray tube is provided for constantly checking the oscillator frequency, by means of a Lissajous figure, against the frequency of a very stable 234-cycle tuning fork which forms part of the equipment.

As implied above the oscillograph galvanometer will respond to voltage changes as well as to changes in inductor-generator frequency. It is necessary, therefore, to minimize voltage variations in the measuring circuits due to power supply fluctuations and temperature changes. Various expediencies are used to accomplish this end. The amplifier gains are stabilized by the use of large amounts of negative feedback. The discriminator circuit as well as certain other critical circuits are formed of stable elements with low temperature coefficients. The copper-oxide rectifier circuit is designed so that variations in resistance of the rectifier discs are insignificant. Finally, the voltage applied to the field windings of the inductor generators is stabilized by a gaseous voltage regulator tube. As a result of these precautions the oscillograph current varies less than 2 per cent of that corresponding to full scale range of frequency variation for ordinary room temperature changes and for power supply voltage fluctuations of 10 per cent.

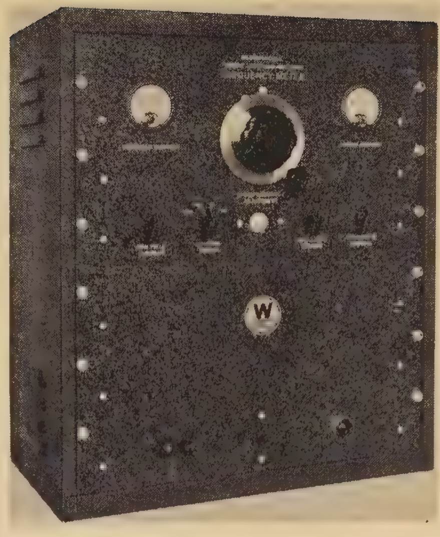

Figure 6. The frequency meter

Power-supply circuits are in the lower half and the measuring circuits are in the upper half

The inductor generators have several interesting and noteworthy features. To avoid erroneous readings it is essential that the wave shapes of the generated voltages be very nearly sinusoidal. Consequently, various arrangements have been used expressly to eliminate harmonics. As illustrated in figure 4, the two generators are combined in a single assembly. The rotor of the 60-cycle generator consists merely of a short cylindrical section truncated at one end by a plane at a slight angle to the axis. With this arrangement the length of rotor under any axial element in the pole face varies as the sine of the angle of rotation, and the voltage generated due to a uniform angular velocity is theoretically a sine wave. There is some distortion, however, mostly second harmonic, due to fringing of the flux at the edges of the rotor. This distortion is eliminated by using two diametrically opposed field structures with their windings connected so that the fundamental voltages add while the even harmonics cancel out.

In the 2,400-cycle generator even harmonics due to flux fringing are eliminated by a push-pull field arrangement similar to that used in the 60-cycle generator. The third harmonic and its multiples are eliminated by making the circumferential pole width equal to one third of the rotor tooth pitch. Finally, the fifth harmonic and its multiples are eliminated by a suitably proportioned trapezoidal rotor tooth shape suggested by Mr. C. R. Hanna. Thus the only harmonics not taken care of in the design of the generator are the 7th, 11th, 13th, 17th, etc. These are of such high order and have such small magnitude due to the smoothing effect of flux fringing that they are of no consequence.

The response of the frequency meter to sinusoidal variations in turbo-generator frequency is shown in figure 5. Curve *A* in this figure represents the frequency response of the synchronous motor which drives the inductor generators and illustrates the limitation mentioned earlier in connection with the relationship between motor speed and turbo-generator frequency. Mechanically, the motor consists of a rotating mass coupled to the revolving field produced by the voltage applied to the stator windings. The coupling is provided by the stiffness due to the synchronous torque of the motor and by the damping due to the squirrel cage winding on the rotor. Because it is not feasible to design synchronous motors with nearly perfect coupling, the response of the rotor to rapid variations in angular velocity of the revolving field is limited in the manner illustrated by curve *A*. This curve was computed, for the particular motor used, from calculated values of rotor inertia and damping and from a measured value of synchronizing stiffness. If better frequency response than this is required it will be necessary to couple the inductor generators directly to the turbine shaft. It is believed, however, that the response shown will be adequate in nearly every case.

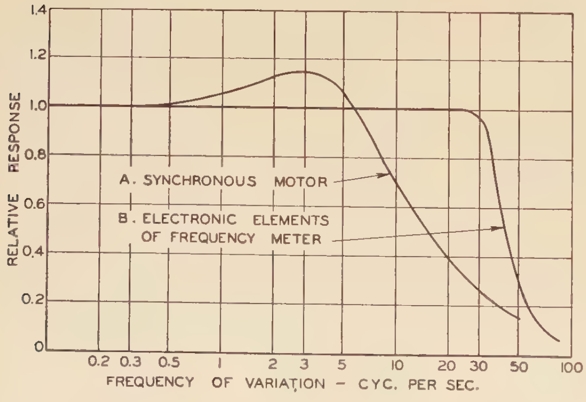

Figure 5. Response of the frequency meter to sinusoidal variations in turbogenerator frequency

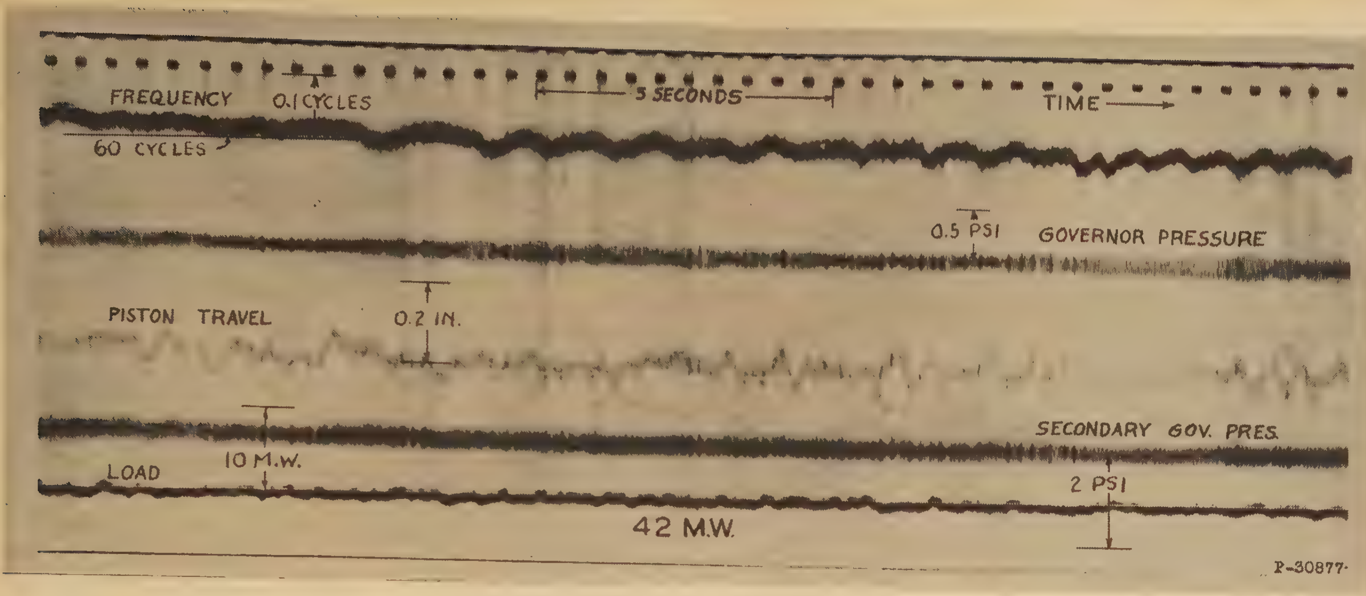

Figure 7. A typical record taken with the turbine-governor analyzer from a modern hydraulic governor controlling a 35,000-kw 3,600-rpm turbogenerator

Curve *B* in figure 5 shows the measured frequency response of the electronic parts of the frequency meter including the oscillograph. This response is very nearly the same as that of the smoothing filter connected between the rectifier and oscillograph, indicating that this filter is the limiting element. The response of the electronic elements of the frequency meter, therefore, can be improved if necessary by using a more elaborate filter.

The assembled frequency meter is shown in figure 6. The meters on the panel indicate generator field current and average turbo-generator frequency, respectively. For simplicity of operation the controls have been kept to a minimum. They include the following: base frequency adjustment, generator field current control, range selector switch, oscillator vernier, and sensitivity control. The cathode ray tube for checking the oscillator frequency is in the center below the base frequency dial. The tuning fork and the inductor generators with their driving motor form separate units.

Conclusion

It has been demonstrated in several applications of the new turbine governor performance analyzer to actual field tests that a minimum of time and effort is expended in both preparation for and during the tests. Furthermore, the information obtained is complete and easily interpreted by anyone familiar with governor characteristics. Figure 7 is a portion of atypical record. A complete test procedure for the use of the instruments was cutlined in a recent paper by A. F. Schwendner.[5]

The instruments themselves are rugged and foolproof and can withstand considerable abuse. When not in use and during transit they are contained in five rugged carrying cases which improve the portability of the equipment.

It is believed that extensive use of the new instruments will add greatly to the operating engineer's knowledge of the characteristics of his governors, and show the governor designer the way to noteworthy improvements in design.

References

1. The following papers are cited as examples:

CONSTANT SYSTEM SPEED AND THE STEAM-TURBINE GOVERNOR, **A. F. Schwendner.** American Society of Mechanical Engineers *Transactions*, volume 62, 1940, pages 199–206.

STEAM-TURBINE GOVERNORS, **Reed J. Caughey.** American Society of Mechanical Engineers *Transactions*, volume 62, 1940, pages 191–8.

THE FIELD OF SYSTEM GOVERNING, **Albion Davis.** American Society of Mechanical Engineers *Transactions*, volume 62, 1940, pages 207–19.

PRIME-MOVER SPEED GOVERNORS FOR INTERCONNECTED SYSTEMS, **R. J. Caughey and J. B. McClure.** AIEE TRANSACTIONS, volume 60, 1941 (April section), pages 147–50.

POWER-SYSTEM GOVERNING—THE PROBLEM, **J. J. Dougherty, A. P. Hayward, A. C. Monteith, and S. B. Griscom.** AIEE TRANSACTIONS, volume 60, 1941, pages 547–58.

EFFECT OF PRIME-MOVER SPEED-GOVERNOR CHARACTERISTICS ON POWER-SYSTEM FREQUENCY VARIATIONS AND TIE-LINE POWER SWINGS, **C. Concordia, S. B. Crary, Jr., and E. E. Parker.** AIEE TRANSACTIONS, volume 60, 1941, pages 559–67.

SYSTEM LOAD SWINGS, **H. A. Bauman, O. W. Manz, Jr., J. E. McCormack, and H. B. Seeley.** AIEE TRANSACTIONS, volume 60, 1941, pages 541–7.

2. AN INSTRUMENT FOR MEASURING SMALL DISPLACEMENTS, **B. F. Langer.** *Review of Scientific Instruments*, volume 2, 1941, pages 336–42.

3. OSCILLOGRAPH ANALYZES GOVERNOR PERFORMANCE, **J. E. Allen.** *Power*, volume 78, November 1934, pages 610–12.

4. APPLICATIONS OF THE PHOTO-ELECTRIC RECORDER, **W. L. Carson.** *General Electric Review*, volume 39, April 1936, pages 189–93.

5. ANALYZING GOVERNING-SYSTEM PERFORMANCE, **A. F. Schwendner.** Scheduled for publication in American Society of Mechanical Engineers *Transactions*, January 1942.

Sensitive Ground Protection for Transmission Lines and Distribution Feeders

ERIC T. B. GROSS
MEMBER AIEE

Synopsis: If ground fault coils are used in high tension overhead systems and underground cable networks, earth leakage relays may be employed to indicate the location of single ground faults. The influence of the contact resistance at the point of the ground is explained. Earth leakage relays in compensated networks, their operation in radial and meshed networks, and the means for determining their correct operation by tests, are described. The paper is based on the practical experiences gained from such installations in England and in Continental Europe.

1. Introduction

It has always been important to locate the line in a transmission or distribution network which is affected by a ground fault. A general satisfactory solution has not been found to this problem. Therefore, it seems advisable to report on the application of wattmeter-type relays for sensitive ground fault protection in compensated networks. Such relays have been used very successfully in overhead line and underground cable systems in European countries in the past.

The expression "compensated networks" means that earth fault coils (arc suppression coils, grounding arc suppressors, ground fault neutralizers, and resonant grounding reactors) are in use. This means that at the point of the fault the charging current to ground of the system is compensated by the inductive current of the earth fault coil. If the coil is exactly tuned, the fault current at the point of the ground is very small. It consists of the in-phase component of the fundamental wave of the charging current to ground and some higher harmonics. The harmonics shall not be considered in the following, as their influence on earth leakage relays is not of any importance.

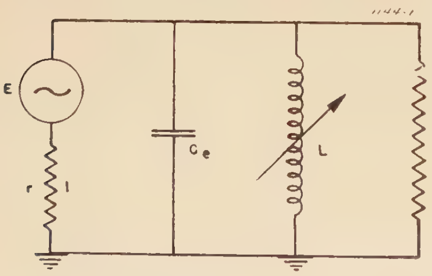

Figure 1. Simplified diagram of a compensated network, one phase of which is grounded through a resistance r

As far as ground faults in high tension systems are concerned there exist two protective schemes which are fundamentally different and which influence nearly every problem in connection with high tension power transmission and distribution. One scheme consists of the direct grounding of the power transformer star points, while the other uses earth fault coils. In the case of solidly grounded neutrals, which shall not be considered in this paper, ground faults are short circuits and the defective line has to be switched off; in the case of compensated networks

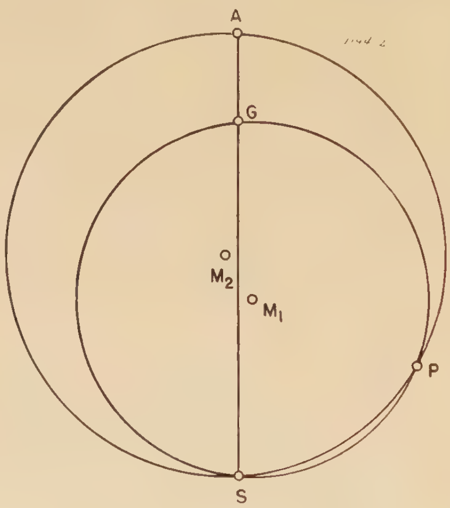

Figure 2. Circle diagrams

Circle M_1: displacement of the neutral corresponding to the simplified diagram, figure 1. Circle M_2: displacement of the neutral when no earth-fault coil is used, and when r varies

no dangerous short circuit currents occur in connection with single phase-to-ground faults. It is then possible and permissible to continue operation under steady ground fault conditions.

The earth leakage relays, which will be described more closely in the following, can be and have been used in radial systems both for signalizing the grounded feeder or switching it off. In interconnected systems, it is not equally easy to use these earth leakage relays for isolating the defective line, and the relays have been in use in the past mostly for signaling; however, for some systems a selective switching off system has been developed and has worked satisfactorily.

In this paper will be considered only how wattmeter-type earth leakage relays, influenced by the neutral-to-ground voltage and the residual current (mutual return of the three current transformers) operate in compensated networks. It is of special interest to investigate first how their sensitivity is influenced by the resistance to ground at the point of the fault. The theory and operation of earth fault coils has been covered in previous publications. We know from these investigations that the simplified diagram of a compensated network[1] is given by figure 1, where E is the negative phase voltage of the grounded conductor, impressed on the system at the point of the fault. The capacitance to ground of the lines is represented by C_e; L is the inductance of the earth fault coils; R is a resistance which represents the line losses and the losses in the coils; r is the contact resistance at the point of the fault.

The fault current I is greatly reduced when C_e and L are in resonance, as R is, on the average, from ten to twenty times greater than ωL. For this trap circuit I becomes $I=\dfrac{E}{R+r}$, and this is the in-phase component of the fault current. We can see from this immediately that the application of a "grounding transformer," for limiting the single phase short circuit current to about 20–40 amps. is[2] practically the same as a badly tuned earth fault coil, since the capacitances to ground will have an effect.

2. Influence of the Contact Resistance at the Point of the Ground

An exact analysis of the circuit leads to the conclusion that the fault current does not change very much when the tuning of the earth fault coil is not quite correct; as it is very easy to maintain nearly correct tuning, it may be considered in the following that the coil is in tune. The fault current becomes then exactly $I=\dfrac{E}{R+r}$. R will always be a rather high resistance in comparison with r. If

---

Paper 41-144, recommended by the AIEE committee on protective devices, and presented at the AIEE Pacific Coast convention, Yellowstone National Park, August 27–29, 1941. Manuscript submitted July 2, 1940; made available for preprinting July 18, 1941.

Eric T. B. Gross is with Cornell University, Ithaca, N. Y., and the College of the City of New York, New York, N. Y.

1. For all numbered references, see list at end of paper.

we assume, for example, that the ground fault I_c for an uncompensated 25 kv overhead line system is $I_c = \frac{E}{\omega L} = E\omega C_e = 20$ amps., then the in-phase component will be about 2 amps; hence we get $R = \frac{25{,}000}{2\sqrt{3}}$ $= 7{,}200$ ohms, and we see that I will vary only within narrow limits, if r varies between, say 0 and 1,000 ohms. One of the advantages of the earth fault coil in this connection is, therefore, that the earth leakage relays operate under a rather constant current.

As r is the contact resistance at the

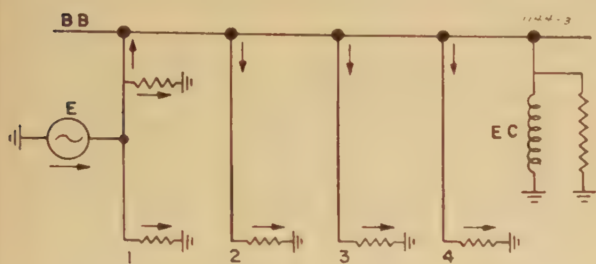

Figure 3. Radial network

Distribution of the in-phase component of the residual current. Ground fault on feeder 1

point of the fault, Ir is the voltage-to-ground of the conductor with the fault; the neutral-to-ground voltage then becomes IR. Since $IR + Ir = E$, we see in figure 2 that this vector SA is divided by the ground potential (point G) in the ratio $R:r = SG:AG$. Since r is much smaller than R, we may express the action of the earth fault coil as reducing the voltage-to-ground of the faulted conductor. Without the application of an earth fault coil the fault current I_u would be

$$I_u = \frac{E}{\sqrt{r^2 + 1/\omega^2 C_e^2}}$$

and for the voltage to ground we get $I_u r$. In this case we have neglected R, as its influence is rather small; however, figure 2 will give an accurate picture.

If we again assume $I_c = 20$ amps. as charging current to ground of a 25 kv network, we find $E = 14{,}400$ volts, $1/\omega C_e = 720$ ohms, and if $r = 720$ ohms, the voltage-to-ground of the faulted conductor becomes $I_u r = E \div \sqrt{2} = 10{,}200$ volts. On the other hand, if a correctly tuned earth fault coil is used, with the same $r = 720$ ohms, and the other data given as above ($R = 7{,}200$ ohms, $I = 2$ amps., $I_c = 20$ amps.), the voltage-to-ground of the faulted conductor becomes only

$$E\frac{r}{R+r} = 1{,}310 \text{ volts}$$

which is considerably smaller.

As already mentioned, the neutral-to-ground voltage is used for the polarizing of the earth leakage relays. Its value is the phase voltage of the system for a direct ground, and nearly as much for an earth fault through a contact resistance. As the voltage-to-ground of the grounded conductor is 1,310 volts in our example, the neutral-to-ground voltage becomes $SG = SA - AG$ or $SG = 14{,}400 - 1{,}310 = 13{,}090$ volts. In general we get $IR = \frac{ER}{R+r} \approx E(1 - r/R)$, as r/R is usually small compared with 1. This means that the earth leakage relays in a compensated network will operate also under a rather constant voltage.

Figure 2 shows the results of a precise analysis of the circuit.[3] The smaller circle, center M_1, is the diagram for the neutral-to-ground and the line-to-ground voltages when an earth fault coil is used and its tuning is changed steadily by varying L while C_e, r, and R are kept constant. The tuning is exact at G, and therefore $AG:SG = r:R$. The intersection of the two circles, point P, gives the voltages when the earth fault coil is switched off. The bigger circle, center M_2, is the diagram for the same voltages when no earth fault coil is applied; here, r is variable, and R and C_e are constant. The smaller circle is divided by S and G into two parts; at all points of the circle on the right side of SG there is undercompensation of the charging current to ground, i.e., the inductive coil current is smaller than the capacitive ground current. At all points on the left side of SG there is overcompensation. The coil is at resonance at G, at which point the fault current has no reactive component. Point P lies on the right part of the circle, since the coil is switched off at this point.

3. Earth-Leakage Relays

In a network with an insulated neutral and no earth fault coil in use, the point of the ground fault may be considered as that part of all the sections and lines of the whole system where the charging current to ground has its greatest value. We know that the neutral-to-ground voltage should be impressed on the network at this point to give the correct distribution of the charging-to-ground current over the system. This picture of the current distribution changes, as far as the reactive component of the charging current is concerned, when earth fault coils are introduced, since they are additional reactive connections to ground. However, the coils do not influence the dissipation of the in-phase component, since the in-phase component is due to losses, which are not compensated by the coils. This implies that, for getting selectivity, only relays can be used which act upon the in-phase component of the residual current i in each feeder. This means that the relays must react to the formula $ei \times \cos\phi$, where e is the neutral-to-ground voltage and $i \cos\phi$ the in-phase component of the residual current in the feeder. The operation of earth leakage relays in a compensated network will be shown in more detail in the following.

As first example, a radial network is drawn in figure 3, where each line represents a three phase feeder (lines 1, 2, 3, 4); BB are the busbars and EC is the earth fault coil. The resistances represent the losses which are, of course, uniformly distributed over the network. If a ground fault occurs on feeder 1, the distribution of the in-phase components $i \cos\phi$ of the fault current will be as indicated by the arrows. We see that its direction is the same in all the unaffected feeders, away from the busbars and opposite to

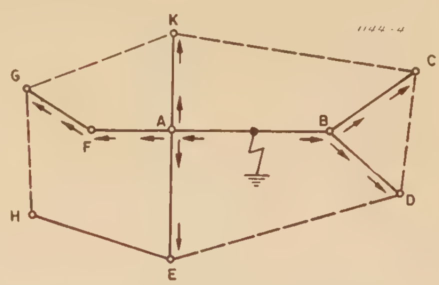

Figure 4. Interconnected network

Distribution of the in-phase component of the residual current. Ground fault on feeder AB

that in the faulted feeder 1. Hence a sensitive wattmeter-type earth leakage relay will detect the faulted feeder.

Similarly in a mesh or interconnected network, the in-phase component of the residual current is a maximum in the faulted line, and it is very easy to find this section of the transmission or distribution system from the operation of the signalizing earth leakage relays. Figure 4 shows a part of such an interconnected network, the dotted lines indicating that it is really a mesh network. If, for example, the fault occurs at the line AB, the distribution of the active component of the

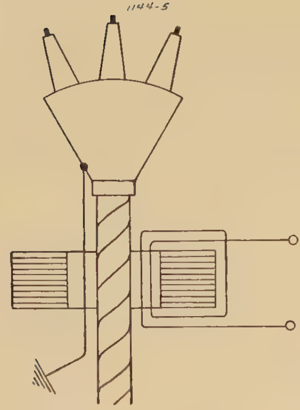

Figure 5. Ring-type current transformer

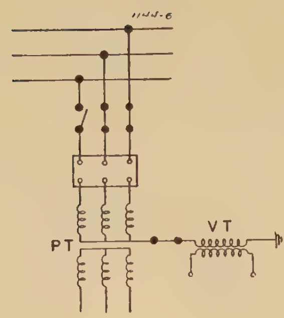

Figure 6. Testing connection when a single-phase voltage transformer is used for supplying the neutral-to-ground voltage

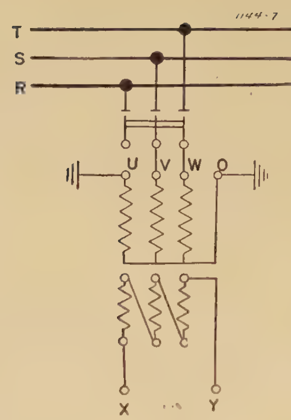

Figure 7. Testing connection when a three-phase voltage transformer is used for supplying the neutral-to-ground voltage

fault current will be as indicated by the arrows. The figure shows clearly that the earth leakage relays will operate on both ends of the faulted line, while on all other lines we find relays operating only on one end. On *BC*, for example, only the relay at *C* will operate thus indicating the direction in which the ground fault is located.

Relays acting on the in-phase component of the residual current could also be used in uncompensated (fully isolated) networks as the distribution of the inphase component of the residual current is independent of the presence of earth fault coils. However, earth leakage relays have been used mostly in compensated networks since the great reduction of the fault current permitted continuous operation under ground fault conditions. As the earth leakage relays are a means to find out rather quickly where the fault occurred, the faulted line can be isolated as soon as the necessary changes in interconnection have been made, thus preventing any substation from becoming deenergized. This method has been used in compensated networks in Continental Europe for many years and improved by past experience.[4] The method has proved to work very satisfactorily also in Great Britain, where earth fault coils and earth leakage relays have been used only for the last few years,[5] but are now being used in an ever increasing extent.

The earth leakage relays are wattmeter-type relays, polarized by the neutral-to-ground voltage and the residual current. The voltage coils in use are of the normal relay type, but the current coils are usually made from more turns of a smaller wire, in this way increasing the sensitivity of the relay. If accurate current transformers were at hand, they could be used successfully, even with an in-phase component of only 1 amp. or less, and with a current transformer ratio of 100/5 or 200/5 amps. For smaller primary residual currents special current transformers may be advantageous.[6] In Great Britain metal clad switchgear is used almost exclusively; therefore the overhead line sections are usually terminated through a short cable run, and ring-type transformers, figure 5, have been found as a cheap and good solution.

As the ground fault is no longer a single phase short circuit, no overcurrents now appear in connection with that kind of fault in a compensated network; hence it should not be necessary to protect the current winding of the earth leakage relays against damage by heavy excess currents. However, short circuit currents are possible through the earth leakage relay coil in the case of a double ground fault (i.e. two grounds on different line sections in different phases). In networks supplied by stations of very high generating capacity, additional excessive current protective relays in the asymmetry circuit have been used. These overcurrent relays shunt the sensitive earth relay coil and thus protect it against damage by the heavy short circuit currents in case of a double ground fault. Such overcurrent relays are useful too in another respect; they hinder the operation of earth leakage relays under double ground fault conditions. A detailed investigation shows that earth leakage relays might operate incorrectly in interconnected networks under double ground fault conditions.

4. Connections and Testing of Earth-Leakage Relays

The neutral-to-ground voltage can be taken from a secondary winding on the earth fault coil, which is the usual method in the case of a radial network, when the coil is located in the electrical center of the system. In other substations, it is possible to use a single-phase voltage transformer between a power-transformer star point and ground, or three single-phase voltage transformers with grounded neutral and the secondary winding in delta for supplying the neutral-to-ground voltage. As has been said, we consider only fundamental questions in this paper, hence we omit some results of theoretical investigations and practical experience by which correct operation of very highly sensitive earth leakage relays was attained.[4]

When earth leakage relays have been installed, it is advisable to check their correct operation by tests. There are two different ways of relay testing according to the various methods of getting the neutral-to-ground voltage.

(*a*). If the neutral-to-ground voltage is taken from the secondary winding of the earth fault coil, it is necessary to make actual ground faults, either on the busbars or on one or more feeders The use of a protective resistance as artificial contact resistance is advisable; its value in ohms should be[3] about $1/\omega C_e$. Then the earth leakage relays should be tested in correct wiring connections and also with reversed voltage. If the ground is made on the busbars, of course, the relays should operate only with reversed voltage, i.e., with the wiring connections reversed.

(*b*). If the potential transformers are used for supplying the voltage coils of the earth leakage relays, actual ground faults for testing the correct operation of the relays are not necessary. According to figure 6, one phase of the power transformer should be disconnected (if the power transformer can be de-energized), provided that only a single-phase potential transformer is used which is connected between the neutral of a power transformer and ground. The potential transformer is then under a voltage-to-ground which is of the same phase angle

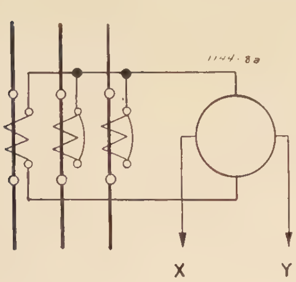

(a)

Figure 8. Testing connections of the three-current transformers of a line section

(*a*) Incoming power

(*b*) Outgoing power

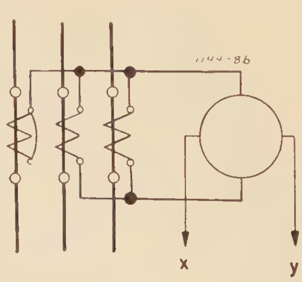

(b)

as if there were a ground in the disconnected phase; the amount of voltage being only half of its value under actual ground fault conditions. If, however, a bank of three potential transformers is used and a similar connection is made (figure 7), the secondary winding will give a voltage of correct phase-angle, but its amount will be only about $^1/_3$ of its maximum value under ground fault conditions; the phase angle will again be that of the opened phase of the potential transformer.

To get a corresponding current in the coil of the earth leakage relay, we now make an auxiliary connection on the secondary side of the current transformers on each outgoing feeder (as shown in figures 8*a* and 8*b*). We use figure 8*b* if power is outgoing and figure 8*a* if power is incoming.

With these auxiliary connections, in both voltage and current circuits, the earth leakage relays are supplied with voltage and current under exactly the same phase-angle as would exist between residual feeder current and ground-to-neutral voltage under ground fault conditions. The earth leakage relays should then operate. If they do not, we must change the connections by reversing either the voltage or the current wires. In similarity with a wattmeter or a watt-hour meter, we are able to find the correct connections only according to the polarized and marked terminals of the potential and current transformers; however, it is always advisable to make sure by actual tests that the relays are put into service with correct connections.

5. Conclusions

(*A*). The application of resonant neutral grounding makes possible the operation of radial and network systems with permanent ground faults. This has been proved by many installations abroad, both for overhead line and underground cable systems, and with line voltages from 3,000 volts up.

(*B*). The installation of wattmeter-type earth leakage relays would give an indication of the defective section of the line. The relays act upon the in-phase component of the residual current and the neutral-to-ground voltage of the system.

(*C*). The in-phase component of the residual current is in most cases large enough to secure correct operation of the relays.

(*D*). The operation of the relays can easily be checked by simple tests.

References

1. The Neutral Grounding Reactor, **W. W. Lewis.** AIEE Transactions, volume 42, 1923, pages 417–34.

Petersen Coil Tests on 140-Kv Systems, **J. R. North** and **J. R. Eaton.** AIEE Transactions, volume 53, 1934 (January section), pages 63–74.

Earth-Fault Coils in Transmission Lines and Distribution Networks, **Eric T. B. Gross.** *The Cornell Engineer*, volume 6, 1940, page 7.

2. Sensitive Ground Protection for Radial Distribution Feeders, **Lloyd F. Hunt** and **J. M. Vivian.** AIEE Transactions, volume 59, 1940 (February section), pages 84–90.

3. Adjustment of Earth-Fault Coils, **E. Gross.** *Bulletin Schweizerischer Electrotechnischer Verein*, volume 38, 1937, page 165.

4. Earth-Leakage Relays, **Eric T. B. Gross.** *The Electrician*, London, volume 123, number 3191, 1939, page 93.

Earth-Leakage Relay Sensitivity in Protection Systems, **E. Gross** and **W. Weller.** *Elektrotechnik und Maschinenbau*, volume 50, 1932, page 117.

5. Line Protection by Petersen Coils, With Special Reference to Conditions Prevailing in Great Britain, **H. W. Taylor** and **P. F. Stritzl.** *Journal* Institution Electrical Engineers (London), volume 82, 1938, page 387 and volume 83, 1938, page 708.

6. Zero-Sequence Current Transformers for Ground Protection, **J. W. Graff.** *Electrical World*, volume 102, 1933, page 822.

7. Testing of Earth-Leakage Relays, **E. Gross.** *Electrotechnik und Maschinenbau*, volume 46, 1928, page 1213 and volume 47, 1929, page 372.

8. Ground Faults in High-Voltage Systems (a book), **R. Willheim**, Berlin, 1936, Verlag von Julius Springer.

The Communication Facilities of the U. S. Forest Service

A. G. SIMSON
NONMEMBER AIEE

FOREST protection in the United States is a job of considerable magnitude. There are, roughly, 550,000,000 acres, which are equal to the area east of the Mississippi River, exclusive of Wisconsin and Illinois, under intensive protection against forest fires. Moreover, there are an additional 138,000,000 acres needing organized forest protection.

Of this vast area, state and private agencies are responsible for about 279,000,000 acres, the U. S. Forest Service for about 208,000,000, and other Federal Government agencies for about 60,000,000 acres.

According to U. S. Forest Service records the annual number of forest fires is increasing materially, though the average size of the fires is becoming progressively smaller each decade. The fact that the average fire is getting smaller, even though there are more of them, is one encouraging evidence of the gradually increasing effectiveness of fire suppression tools and fire control technique.

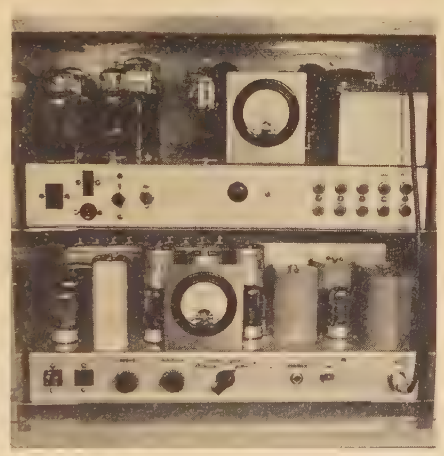

Dry-battery-operated ultrahigh-frequency automatic-relay station

Upper deck—transmitter; lower deck—receiver

Comparatively recent improvements in communication facilities have undoubtedly played an important part in reducing fire losses. It is generally true that the quicker one can attack a fire the fewer men are needed to put it out, which, of course, points the way toward faster communication and transportation.

One of many examples of the importance which fire fighters place on radio communication is contained in the following quotation from a news story on the recent forest fires in Maryland:*

"Two-way radio communication proved helpful on a large fire in northern Anne Arundel County which burned more than 3,000 acres. The department of forestry called three forestry radio cars into the area and directed them by radio from the Long Hill lookout tower in shifting fire-fighting crews from point to point.

"Had radio equipment been available on the fire trucks and other vehicles, forestry officials believe the fire could have been held to half its size and much of the forest saved."

Though it is probably true that few, if any, forest protection agencies have sufficient communication facilities, the extent of these systems is surprisingly great. For example, the U. S. Forest Service is

Paper **41-149**, recommended by the AIEE committee on communication, and presented at the AIEE Pacific Coast convention, Yellowstone National Park, August 27–29, 1941. Manuscript submitted June 11, 1941; made available for preprinting July 25, 1941.

A. G. Simson is radio engineer of the Forest Service, U. S. Department of Agriculture, Washington, D. C.

*"The Washington Post"—April 27, 1941.

Radio laboratory, Forest Service, U. S. Department of Agriculture, Portland, Oregon

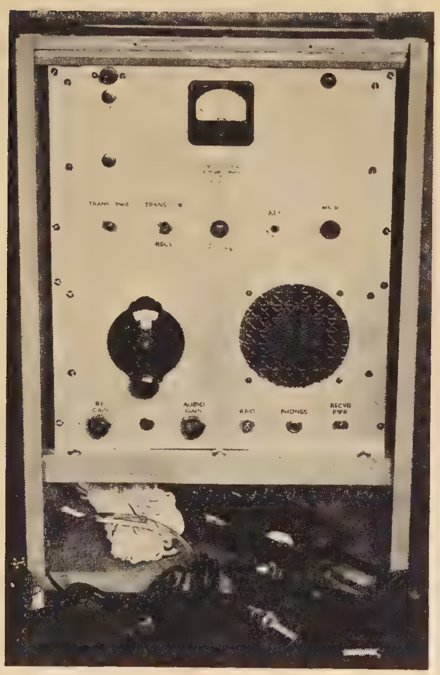

Forest Service type M semiportable radiophone

maintaining over 60,000 miles of telephone line and operates about 3,500 radio stations. State and private forest protection agencies are reported to have about 52,000 miles of telephone line and 1,500 radio stations.

Fundamentally, all forest protection agencies have pretty much the same job to do and go about it in a similar manner, though there are, of course, differences in organization and degrees of protection.

Since I am most familiar with the operations of the U. S. Forest Service, this discussion will deal mainly with that agency.

For administrative purposes, the Forest Service divides the continental United States, Alaska, and Puerto Rico into ten regions. Within each region there is a number of national forest units—a total of more than 150.

National Forest Communication Systems

Since the national forest is the administrative unit, the communication systems are set up on a national forest unit basis.

The backbone of the national forest communication is, of course, wire line—either Forest Service lines or commercial circuits if they are available.

Radio is used where no other satisfactory means of communication are available. Nearly all of the radio communication is of an emergency nature. Ordinarily, it is not considered desirable that both routine administrative and fire traffic flow over the same radio circuits, since in time of emergency the administrative traffic would have to give way to emergency needs which would disrupt the normal forest administration.

The communication system on a forest unit falls roughly into three general classes of use, namely: (1) administrative circuits, as between the forest supervisor and district ranger offices, and between district ranger and CCC camps, ranger stations, and logging camps; (2) fire detection circuits, as between fire lookouts and lookout to central fire dispatcher; (3) fire suppression circuits, as dispatcher to patrolmen, fire crews and fire trucks, communication between main base camp and sector camps on large fires, contact with foot and aerial scouts, freighting planes, communication along the fire line, base camp contact with regional equipment depots, and communication with the mobile fireweather forecast units.

Communication on Large Fires

Modern fire fighting, especially on large fires in heavily forested regions, assumes much of the aspect of a military operation with all its complexities of staff organization, service of supply, and front line attack.

Consider, for example, a fire of the "conflagration" class—say 50,000 or 75,000 acres. The perimeter of the fire will likely be 100 or 150 miles. Several thousand fire fighters will be employed. They will be split up in camps of about 200 men each appropriately spaced along the fire line. The fire line will be in the charge of a fire chief. Directly under him will be an assistant chief, chief of service of supply (SOS), transportation chief, equipment chief, head scout, communication chief, paymaster, and sector bosses. Each sector boss is directly responsible to the fire chief for his sector of the fire.

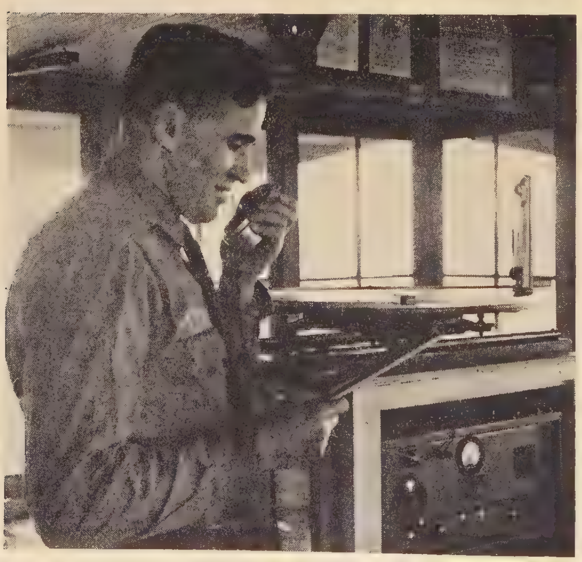

(Lower left) Typical radio installation in Forest Service lookout

Radiophone is designed to fit in standard firefinder pedestal

Interior of Forest Service radio trailer used on large fires

Radio communication on the fire line during "mopping up" phase of fire

Note two hose lines in use

(Right) Forest Service smokechaser "reporting in"

Fire pack includes tools, radio, emergency rations, and blanket

The main communication center will be at staff headquarters in the main base camp. From this point communication circuits will be established with the regional equipment depot, forest supervisor's headquarters, reconnaissance and transport planes, fireweather units, and the sector camps located along the fire line. The sector camps will set up local networks to communicate with the fire line, ground scouts, nearby lookouts, and various fire fighting units within the sector.

Before the advent of radio, communication along the fire line was largely by messenger, which at best is a slow and uncertain method. Consequently, there was too often a conspicuous lack of coordination among the various fire fighting units attacking a single fire. For example, one sector of the fire might be considerably overmanned or overequipped while other crews were losing ground through lack of reinforcements or apparatus. With the development of portable and mobile two-way radio, marked improvements in fire fighting tactics became possible. The entire forces can now be controlled from a single headquarters and men and machines shifted along the line as the vagaries of fire behavior dictate.

Radio Frequencies Used

Originally, forest protection radio communication was entirely in the 2–4 megacycle band. This part of the spectrum was selected because single channel transmitters were used and these frequencies exhibit the least variation in diurnal and seasonal sky wave propagation. The lower limit of the frequency band selected was also influenced by antenna length. In order to preserve portability and obtain reasonable efficiency, horizontal half-wave antennas are used. Experience has shown that the difficulty of finding a clear space in dense forests of sufficient size to stretch an antenna increases rapidly with

(Right) Automatic relay antenna, Mt. Hood, Oregon

Communication unit used on large fires

(Lower right) Portable radio installation in "sector" fire camp

length of the radiator and that 140 feet is a good compromise.

For the last seven or eight years the percentage of ultrahigh frequency stations—30 to 40 megacycle band—has increased rapidly. Frequencies in this portion of the spectrum were selected as representing the best compromise between the desirable characteristics of the ultrahigh frequencies such as minimum static, short antennas, circuit efficiencies, and the better coverage below line of sight obtainable with lower frequencies. Rapid growth in the use of the ultrahigh frequencies has been due both to improvements in apparatus and to increasing experience in the technique. Oddly enough, ultrahigh frequency systems have developed much more rapidly in the mountainous forest of the West than in the flat or rolling terrain of the East. One factor has been the discovery that, in general, the "blind" areas behind sharp mountain ridges are not nearly as sharply defined as they are in areas where the slopes are less precipitous.

Radio Equipment Requirements

Since fire behavior, suppression technique, and transportation facilities vary widely as between forest types, the types of radio apparatus employed also vary. Nevertheless, there are certain general requirements which all types must fulfill.

The equipment must have good reliability and must be consistently capable of withstanding hauling by truck over long distances on rough roads. It must withstand the vicissitudes of packhorse transportation and be workable after parachute delivery. The controls must be foolproof and the manipulation simple enough that untrained laborers may set up and operate the apparatus without difficulty. The component parts must be of standard design and commercially available to facilitate battery replacement and repairs without excessive delay, and because urgent equipment needs greatly exceed available funds costs must be kept to a minimum. In addition, the portable types must be truly portable. In regions where the standard smoke chaser's pack weighs about 35 pounds, 10 or 11 pounds are about the practical limit of additional weight he can carry for communication.

Since the portable radiophones must be low powered, it has been found desirable to restrict the power on even the semiportable units. An insufficient number of frequencies has made it necessary to repeat the same frequency well within interference range so that power must be held to a minimum if the signals from the lowest powered portables are to be protected against interference from the higher powered mobile and semiportable units.

High-Frequency Radiophones

The type *M* is the highest powered fire communication unit used by the Forest Service. It has a nominal output of 25 watts, although the full output is seldom used. The type *M* operates from an a-c power supply or portable generator. The complete unit weighs about 90 pounds, The tube line-up is: 6F6G oscillator, two 6L6G in parallel in radio-frequency amplifier, 6F6G speech amplifier, push-pull 6L6G modulators, and a pair of 83 rectifiers. A low-drift crystal maintains frequency stability. The output stage terminates in a pi matching network to accommodate a wide range of antenna or transmission line impedances.

The receiver section is a conventional superheterodyne having a minimum of operating controls.

The type *M* was designed for use at forest headquarters, central fire dispatchers, central equipment depots, and at communication centers on large fires. Since these radiophones may be expected to create interference over a radius of several hundred miles, lower powered units are substituted wherever possible.

A smaller unit of similar form designed to operate from an ordinary six volt automobile storage battery is also available. This unit has an output of $9^1/_2$ watts and is a substitute for the type *M* where commercial power is not available and where, because of "standby" requirements or for other reasons, it is not desirable to use a gas engine driven portable generator.

The most widely used three megacycle unit is the type *SPF*. For portable operation the complete unit weighs 21 pounds and has a rated working range of 20 miles. The transmitter section is crystal controlled and, as is the case in all Forest Service portable radiophones, receiving tubes are used throughout in both the transmitter and receiver sections. The nominal power output is 2.25 watts. The receiver section is a five tube superheterodyne having a sensitivity of about three microvolts absolute. Provision is made for continuous wave reception by either headphones or built-in loudspeaker.

For semiportable service a kitbox is supplied which contains heavy duty batteries and an additional half-wave antenna. This latter form was especially designed for secondary lookouts and road construction crews. The lookout installs the half-wave antenna at his station and operates his radiophone from the heavy duty kitbox batteries. When he goes to a fire he needs only to unplug the battery cable and drop the radiophone in its carrying bag to have a 21 pound portable radiophone complete with light batteries and antenna. Thus, he wastes no time in taking down the antenna and is assured

Forest Service type SX radiophone with loudspeaker unit as used at emergency lookouts and for semiportable operation

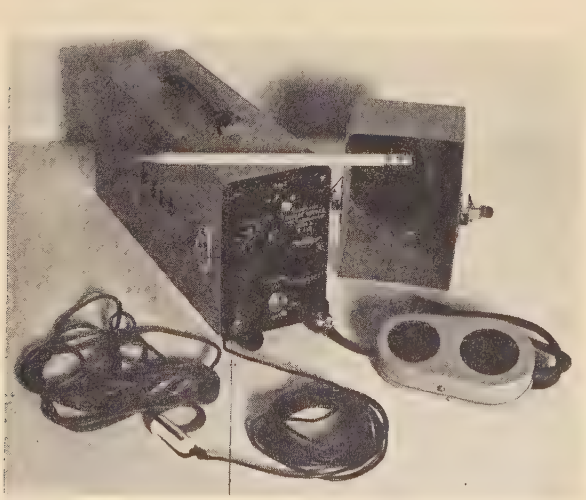

Portable radiophone used by Forest Service parachutist fire fighters

Forest Service portable type SX ultrahigh-frequency radiophone

of unused batteries for his emergency communication.

Similarly, some road crews use the half-wave antenna and heavy batteries while in camp and each morning take the portable outfit out on the job and set it up for contact with the fire dispatcher.

Though not designed for mobile operation, these units have been operated in planes, boats, and trucks where mobile equipment was not available.

Many of the fire trucks and patrol cars are equipped with two-way three megacycle radiophones. The consistent range of these installations is only about 20 miles, mainly because of antenna limitations.

Where fire trucks are employed intensively, two-way communication adds greatly to their usefulness, since it means the trucks are always "in service," even when making a run. It has enabled the dispatcher to recall trucks from false alarm runs and makes it possible to redispatch them without the necessity of returning to headquarters for orders.

The mobile transmitters are powered by dual vibrators rather than a motor generator in order to eliminate the more difficult servicing of rotating machines and to reduce the drain on the vehicle's battery. The input at the final radio-frequency stage is about 16 watts, but only a fraction is radiated because of antenna inefficiencies. Only a very short antenna can be installed because many of the trucks operate directly on the fire line and are driven through the forests where there are no roads, with a consequent high mortality in antennas, fenders, and running boards.

The shortcomings of the antenna are offset in part by a base loading and tuning unit, but withal the reliable range of this radiophone is only 20 miles, and when possible the ultrahigh frequencies are used, instead, for mobile communication.

Ultrahigh-Frequency Radiophones

In addition to the apparatus already described an increasing proportion of forest protection radio systems utilize the ultrahigh frequency 30–40 megacycle band. Where ultrahigh frequencies are usable they offer obvious advantages over the lower frequencies. Antennas are smaller, and there is substantially no fading or static. The last named feature is especially important since 44 per cent of all fires on the national forests are caused by lightning, and frequently these lightning storms destroy wire or telephones to the point of causing serious delays in the reporting of lightning fires, with consequent heavy fire losses.

Ultrahigh frequency radiophones are used for the same general purposes as the 3,000 kilocycle equipment and are especially effective for interlookout and mobile communication and where the utmost in light-weight compactness is required.

The unit designed especially for lookout installation (U. S. Forest Service type *T*) has a crystal controlled transmitter of two watts power.

The receiver contains a 1A7G converter, three stages of 4,050 kilocycle intermediate-frequency amplification using 1N5G tubes, a 1H5G detector and audio amplifier, and a call-buzzer circuit utilizing a 1N5G tube. The intermediate-frequency band width is approximately 50 kilocycles. This comparatively wide band permits reception of modulated oscillators. The buzzer-alarm circuit is useful for night calls and permits installation of extension bells in the towerman's residence.

The low-drain tubes employed in this radiophone give reasonable dry battery economy, even on continuous service.

A new all-purpose portable radiophone known as the type *SX* was developed last year. This complete unit weighs about ten pounds and is applicable to uses of scouts, smokechasers, and others requiring extreme portability. Provision for selecting any of three crystal-controlled transmitter frequencies adapts the unit for operation in fixed frequency networks or ready switching from one network to another. Another useful feature is a panel pushbutton which provides a marker signal and permits setting the receiver on any of the three transmitter frequencies.

For emergency lookout use a kitbox is supplied with the type *SX*, which contains heavy duty batteries and an additional unit containing an audio amplifier and loudspeaker.

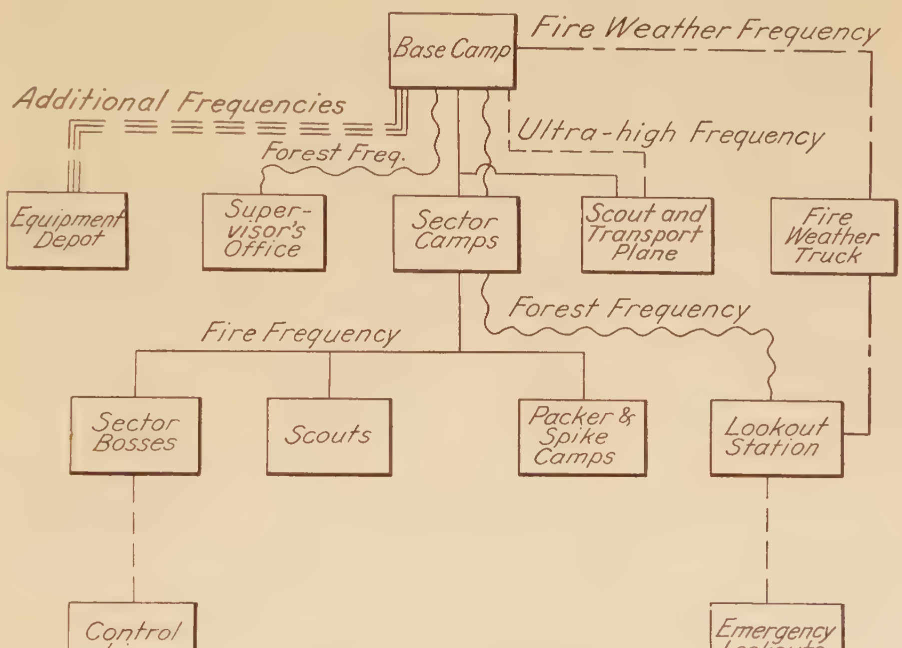

Radio net on "conflagration" fires

Forest Service parachute jumping fire fighters use a condensed version of this radiophone. The parachute jumper's model, which weighs a little less than six pounds, is designed to be carried in a pocket on the leg of the jumper's suit.

General use of ultrahigh frequency in mountainous regions has required the development of an automatic relay station. The transmitter section is conventional

design and where—as is usually the case—dry battery is the only source of power, has an output of two watts.

The receiver presents some interesting features. Twelve tubes are used distributed as follows:

Two signal radio-frequency stages
First detector
Crystal oscillator
Frequency multiplier
Three intermediate-frequency stages
Second detector (AVC)
Fifteen kilocycle noise amplifier and rectifier
Relay control tube
Audio amplifier

The system of relay control is based upon the inherent circuit noise and variations of this noise with signal input through operation of the AVC system by the signal. A filter which passes a narrow band centered at 15 kilocycles is branched off the audio input circuit and the resultant 15 kilocycle noise component is amplified and rectified to produce control bias for the relay tube. Fifteen kilocycles is chosen because it is well beyond the range of audio intelligence and, consequently, prevents the communication signal from energizing the relay tube The system operates with the relay, which controls the transmitter, *off* under maximum circuit noise, static crashes or other heavy noise, and relay *on* when an application of a signal causes a reduction in the 15 kilocycle noise component.

The circuit is so arranged and constants proportioned as to keep the noise at a relatively constant top level (in effect limited) so that operation is consistent with combined circuit noise and variable external noise. The circuit is reliable but is only relatively tolerant as to range of battery supply voltage. Some stabilization is effected because of the high gain throughout, which results in production of a small automatic volume control voltage from noise alone; this in turn tends to hold the noise delivered to the noise filter at a relatively constant value over a considerable range of battery voltage and temperature condition.

An inexpensive filter which is incorporated in the unit permits simultaneous transmission and reception on the same antenna.

Satisfactory antennas for high altitude relay stations where icing is especially bad, as well as for lookout house and tower installations, must be extremely rugged mechanically, must provide a heavy d-c path to ground for lightning protection, and must be easy to duplicate without special materials and insulators. An antenna with the best of electrical characteristics would be almost useless unless rugged and sufficiently simple in structure to permit duplication by mechanics in the average forest central garage or machine shop. The antenna structure consists of approximately quarter-wave radiator with an integral coaxial matching section and radial arms of quarter-wave length At one-tenth wave length the coaxial matching section has a resistance of about 65 ohms at the feed point. Line voltage is substantially constant and without standing waves on the transmission line. In field tests this antenna showed a voltage ratio of about 1.8 to that attained on the *J* type antenna.

An additional point of interest in the antenna is the absence of large exposed insulators. The only insulator involved in the antenna proper is the coaxial centering ring, which is placed well inside the coaxial tubing and is thereby not exposed to the weather.

Development

After trying commercially designed radio equipment the Forest Service was relunctantly forced to the conclusion that there was no equipment available that satisfied the peculiar and rigid requirement of forest protection communication. Primarily, the problem was not so much a matter of electrical circuits as of mechanical arrangement of the units.

Accordingly, the Forest Service established its own radio laboratory in Portland, Oregon, which is fairly central to the area of greatest fire and communication difficulty. The laboratory projects include development of new equipment as needed, revision of existing models to keep pace with the current state of the art, and developments in the application and technique of radio communication.

Procurement

The procurement and inspection of all radio equipment used by the entire U. S. Forest Service is centralized at Portland, Oregon. Centralized procurement permits consolidation of orders, helps insure purchase of uniform types of apparatus, and is the most practicable method we have found of filling emergency requisitions for apparatus to be used on going fires with a minimum of delay.

Manufacturing contracts are based on competitive bids Technical specifications are not used; instead, the contractor is required to build exact duplicates of a working model which is supplied him. The whole procurement program is designed to meet unpredictable emergency demands for radio units with a minimum of delay and without carrying large reserve stocks.

Maintenance

Usually Forest Service communication equipment, both telephone and radio, is serviced and maintained by regular personnel. Much of the work is done incidentally to other duties by employees having little or no electrical training other than on forestry radio. This situation requires special consideration in the design of the radio units and in the preparation of servicing instructions.

The variety of uses to which radio can be put in forest protection is increasing as we gain knowledge of its possibilities. At present we see a need for a simple, portable direction finder that can be operated by a lookout man in conjunction with his fire finder to guide smokechasers to "sleeper" fires in dense forests. These fires are often most difficult to find and have been known to smolder for weeks and to become a running fire during the next dry windy period.

A portable dry battery operated radio facsimile transmitter and receiver is needed for use by reconnaissance planes and for speeding up message traffic on large fires. Already the traffic load has reached a point where additional circuits must be established or unacceptable delay occurs.

The Modern A-C Network Calculator

W. W. PARKER
MEMBER AIEE

PRODUCTION requires power. The urgent necessity of meeting the immediate demands for electric power—due to national defense and natural growth—has created a challenge to the planning engineers. Local loads are increased and additional loads established, resulting in shifting of load centers. Such changes require increased generating and transmitting facilities. To provide for this expansion in power supply requires accurate planning to avoid waste of time, materials, or effort. The first step is the quick solution of all the electrical problems.

The A-C. network calculator provides accurate means for solving these problems. Therefore, it is appropriate to present the newly perfected features of the latest A.C. network calculators. These provide the means and methods for faster and more accurate analysis of existing or planned power systems and the solutions of electrical design and operating problems. The essential elements of a power system are reproduced in miniature replica, as illustrated pictorially in figure 1 for a simple radial feed from generator to load. The calculator reproduces systems with many generators or generating stations, transformers, lines, and loads. Readings of the miniature network on the calculator are readily converted into actual system quantities.

The electrical performance of the system can be obtained from the calculator studies. The principal studies involve:

1. Voltage regulation and load control studies for normal and emergency operation.
2. Short circuit studies for circuit breaker or protective relay application.
3. Steady state or transient stability studies for determining power limit of transmission systems.

For any of the above investigations, the various steps in the solution are:

1. Assemble and organize the data of the power system.
2. Convert these data to a base or scale suitable for use with the calculator voltages, currents, and impedances.
3. Set up the calculator network and adjust the loads and the generator outputs in accordance with the requirements of the specific problem.
4. Meter the network, obtaining the significant calculator readings such as voltage, current, phase angle, watts, and vars.
5. Reconvert these into system values.

For voltage regulation, load control, short circuit studies, and steady state stability studies, the calculator gives the desired quantities directly, requiring only conversion into system values. Transient stability studies require the same "step-by-step" method used in straight mathematical solutions. The calculator gives the electrical conditions for each step, thus not only saving tedious computations but also permitting the solution of multi-machine problems with more generators than can be solved by other methods.

The demand for calculator solutions has been so great that existing facilities have been taxed to full capacity and several new calculators are being constructed. A list of calculators is given in table I.

This paper describes the most recent A-C. network calculator which, although embracing fundamental designs proven over a period of eleven years, has incorporated improved features to facilitate the setting up and metering of the calculator miniature network. A typical calculator of modern design is shown in figure 2.

Fundamental Features of Design

The engineer who uses the calculator is interested primarily in quick, dependable, accurate results. In meeting these requirements, the designer of the calculator considers accuracy, convenience, speed, space, and cost. In these considerations the choice of frequency and power level are predominant factors.

Frequency

The choice of frequency is independent of the frequency of the system to be studied since impedances are used in terms of ohms. The cost and size of reactors and capacitors to cover the range of values needed indicated that a choice of frequency higher than normal would be desirable. The A-C calculator frequency has been established at 440 cycles.[2]

Power Level

The calculator has rated values for normal operation of 100 volts and 1 ampere, with maximum capacities of 400% for voltage and 300% for current. This power level was arrived at from considera-

Table I. Data on A-C Network Calculators in Use or Under Construction

Owner and Location	Date Installed	Frequency Cycles Per Second	Generators	Lines	Loads	Special Reactors	Capacitors	Auto Transformers	Mutual Transformers	Total
						Number of Units				
1. Massachusetts Institute of Technology, Cambridge, Mass.	1929	60	18	80	40	6	42	12	0	198
2. Westinghouse Elec. & Mfg. Co., East Pittsburgh, Pa.	1929	440	12	160	40*	20	70	24	30	356
3. Penn. R.R., Pennsylvania Station, New York City	1932	440	6	168	40	40	4	2	16	276
4. Commonwealth Edison Co., Chicago, Ill.	1932	440	6	72	48	12	24	6	6	174
5. General Electric Co., Schenectady, N. Y.	1937	480	12	150	50	0	30	12	15	269
6. Public Service Elec. & Gas Co., Newark, N. J.	1938	480	8	85	30	0	18	10	12	163
7. Tennessee Valley Authority, Chattanooga, Tenn. — Initial	1938	440	12	60	20	8**	16	12	10	138
Addnl.	1941	440	6	60	24*	0	18	12	12	132
Total			18	120	44	8	34	24	22	270
8. Bonneville Power Administration, Ampere, Wash.	1939	480	9	50	30	9	30	6	6	140
9. São Paulo Tram. Lt. & Pr. Co., São Paulo, Brazil	1940	440	6	26	14*	14	12	6	12	90
10. Potomac Electric Power Co., Washington, D. C.	1941	440	6	52	18*	18	12	6	8	110
11. Hydro Electric Power Comm. of Ontario, Toronto, Canada	1941	440	9	62	24*	24	18	12	8	157

*Equipped with load adjusters.

**Eight special high resistor-reactor circuits.

Paper 41-143, recommended by the AIEE committee on instruments and measurements, and presented at the AIEE Pacific Coast convention Yellowstone National Park August 27–29, 1941. Manuscript submitted April 14 1941. made available for preprinting July 10, 1941.

W. W. PARKER is with Westinghouse Electric and Manufacturing Company, East Pittsburgh, Pa.

1. For all numbered references see list at end of paper.

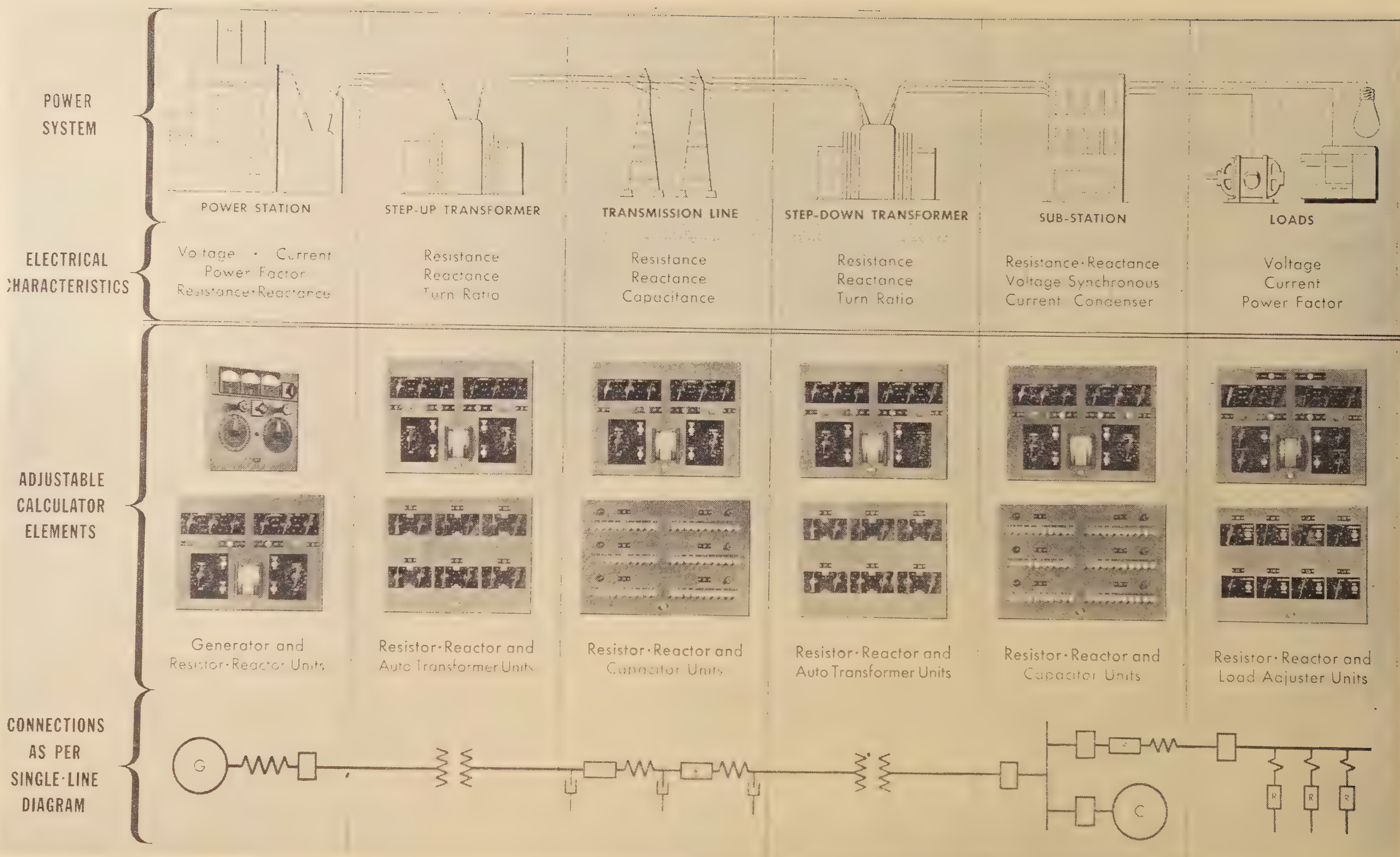

Figure 1. The a-c network calculator electrically reproduces actual power-system conditions

The a-c network calculator consists of a number of adjustable resistors, reactors, and capacitors, representing the corresponding constants of the actual system, wired to suitable cords so that an actual electrical network can be reproduced in miniature. Sources of voltage whose magnitude and phase position can be varied represent generators and other synchronous machines. Distribution of voltage and current throughout the system is determined by measuring the quantities in the calculator circuits and applying a multiplying factor fixed by the scale to which the network has been set up. The conditions in an existing or proposed system can thus be observed quickly, easily, and accurately

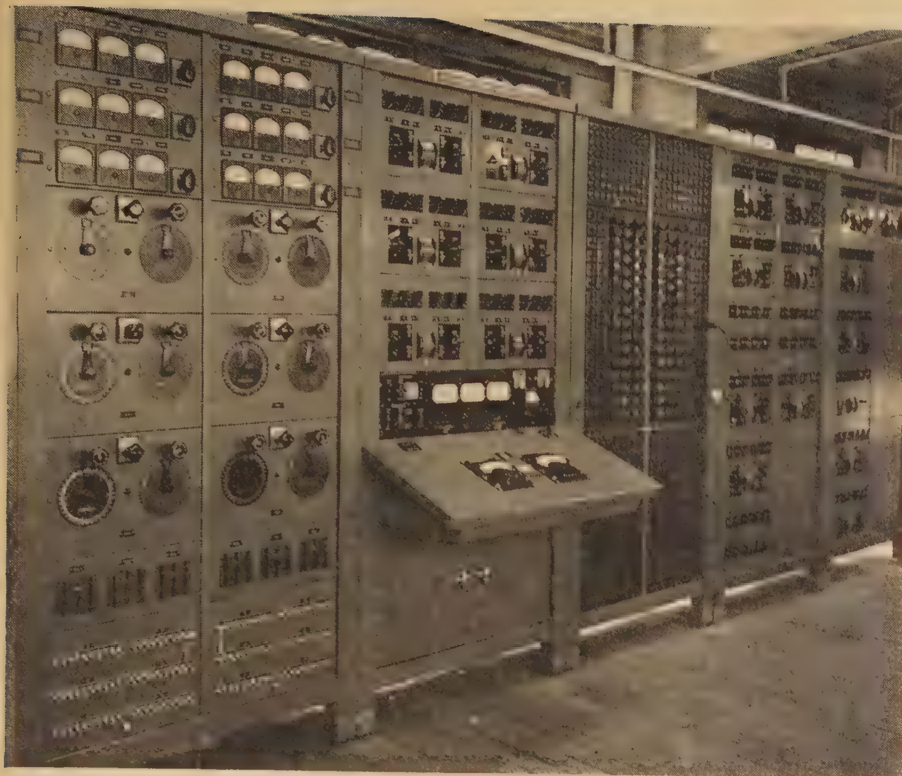

Figure 2. A typical a-c network calculator

The cabinet on the left contains six generator units with their associated instruments for measuring voltages, currents, and power. Below the instruments are the handles for independent adjustment of voltage and phase angle. The bottom drawers contain adjustable capacitor circuits. The next cabinet contains six impedance circuit drawer sections and the master instrument and control desk. (In the calculator described in this paper a separate control desk is used.) The third cabinet from the left is a connection cabiѳet in which all the circuit terminals are brought out for interconnection. The other cabinets contain load circuits with associated load adjusters, auto transformers, and other line circuits

tion of instrument characteristics and the desirability of avoiding errors due to capacitive or inductive coupling. If a lower voltage base were used, the current base would have to be lowered in proportion to avoid significant inductive coupling. This, in turn, would make the power level so low that, using standard torque instruments, errors would be introduced due to their burden, or high electronic amplification would be required. If the current level were reduced to any considerable extent without reducing the voltage, it would be difficult to avoid errors due to capacitive coupling.

Details of the New Calculator

In addition to these fundamental design features, the later calculators have improved methods of setting up the boundary conditions (i.e. desired loads and generator outputs) and inserting instruments into any element of the calculator network. As a result, accurate determinations of the system conditions are obtained with a minimum of time and effort devoted to manipulation of the calculator. Generally, the solutions are on a phase-to-neutral basis with the use of symmetrical components to solve unbalanced conditions. Complete three phase representation is possible but seldom used.

Generator Units

In order to represent generators or power stations, it is necessary to apply to the calculator impedance network, voltages which are adjustable in magnitude and phase angle. The voltage adjustment corresponds to changes in excitation, and the phase angle adjustment to changes in the governor position. In setting up a specific operating condition, the voltage regulator and phase shifter of the generator units are adjusted until their voltages and currents give the desired inputs. This adjustment requires a minimum of manipulation when there is negligible regulation in the calculator units and the controls of the voltage and phase angle are independent of each other.

Each generator unit has less than 2% regulation from 0 to rated load and has independent adjustment of phase angle and magnitude. This is achieved by means of a novel combination of induction voltage regulators and phase shifter, shown schematically in figure 3. The voltage regulator element consists of two independent, three phase induction regulators, electrically identical, with the rotors on a common shaft. The voltage outputs of the independent stators are equal in magnitude and are varied in phase angle by changing the position of the rotor, as is usual in a 3 phase induction regulator. The two regulator units are mounted mechanically opposite to each other so that turning the rotor shaft in one direction effects a clockwise rotation of the one

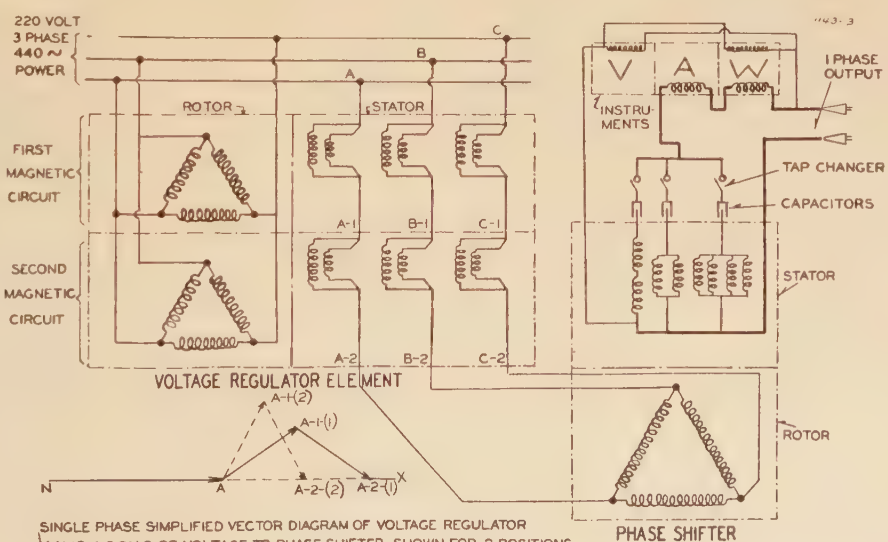

Figure 3. Calculator-generator unit

Actual system sources of synchronous emf are represented by a combination of voltage regulator and phase shifter. Independent control of voltage and phase angle is achieved by a combination of a double-unit three-phase regulator connected to a phase shifter. The voltage regulator has two electrically identical units physically arranged so that adjustment of the rotors does not shift the phase angle of the output to the phase shifter

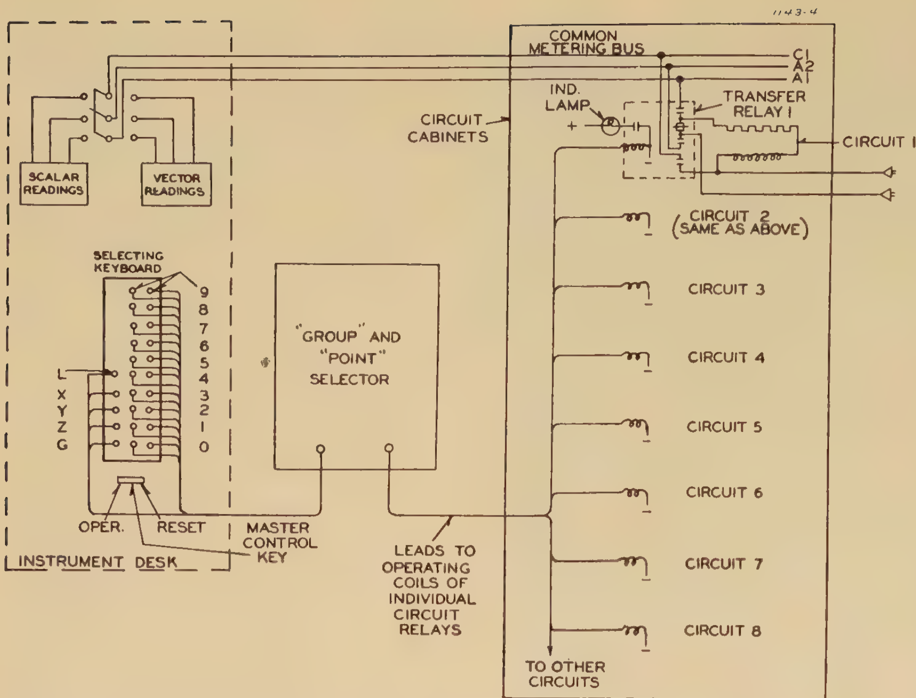

Figure 4. Schematic arrangement of circuit selector for a-c network calculator

The circuit selector consists of the keyboard, a "group" and "point" assembly of telephone-type supervisory relays, and one circuit transfer relay for each circuit. Only 25 keys are required for the selection of any of the present calculator circuits as well as for future additions up to a total of 599 circuits. To select a circuit three keys are pushed, one in each vertical row, and then the control key is thrown to the "operating" position. This closes the selected metering relay located directly behind the respective drawer section in the circuit cabinet. Closing the relay connects the circuit into the metering bus A guard relay is provided which prevents the selection of any other circuit until the control key is thrown to the "reset" position

stator voltage and a counterclockwise rotation of the other. The two stator windings are connected in series so that the changes in phase angle neutralize each other thus giving a voltage which is always in phase with the supply voltage. This induced voltage is added directly to the supply voltage, thus giving a scalar adjustment of voltage. As shown in the single phase vector diagram of figure 3 the voltage *NA* is the single phase line-to-neutral voltage of the power supply, voltages *A* to *A*-1 and *A*-1 to *A*-2 are the voltages induced in the stators. The output voltage *N* to *A*-2 is adjustable from 0 to twice *NA* in magnitude but always along the phase position as indicated by the dotted line *N*-*X*. The three phase output of the regulator is then put into the rotor of the phase shifter. A single phase output is taken from the stator for use in the network. Turning the rotor of the phase shifter changes the phase angle of the generator unit voltage as may be required.

In order to obtain negligible regulation, series capacitors are used to neutralize the reactive drop, while the units themselves are made large enough so that the resistive drop gives less than 2% regulation as previously mentioned. Because of the constant reactance of the three phase voltage regulator, the reactance is accurately and completely compensated for by fixed capacitance.

Instruments for Measuring Output of Generator Units

In a calculator network, as in the power system, the adjustment of one generator unit affects the current in the others. Therefore, it is very desirable to have simultaneous indications of the outputs of all the generator units. Since the output can be completely defined in terms of voltage, scalar current, and watts, a voltmeter, and ammeter, and a wattmeter are supplied. Each instrument is equipped with a red marker which can be set to indicate the desired output of the unit. Adjustments of the phase shifters and voltage regulators are made until the indicating pointers line up with the markers. The ammeter is used in short circuit studies and in obtaining equivalent networks. A wattmeter reversing switch is provided to obtain indication of reverse power. A voltage-selecting switch is also provided so that either terminal or internal values of the generator unit may be obtained if the associated impedance unit is set proportional to the internal reactance of the machine being represented.

Circuit Elements

As indicated in figure 1, actual system transformers, transmission and distribution lines, reactors, and capacitors are represented on the calculator by various combinations of resistor-reactor, capacitor, auto-transformer, and mutual reactor circuits. The circuit elements are so designed that for all normal problems there is no necessity for consulting calibration curves to compensate for reactance of resistors, or resistance of reactors.

The value of any resistor or reactor tap is within plus or minus $1^1/_2\%$ of the setting. The resistors are non-inductive and have negligible (−.00002) temperature coefficient. The iron cores of the reactors have large air gaps so that the permeability of the magnetic circuit is constant

Figure 5. Master instrument and control desk

The motor-generator set controls are mounted on the small vertical panel. Two independent sets of master instruments, the circuit selector, and metering controls are mounted on the sloping sections. Readings can be obtained of scalar or vector components of voltages and currents, watts, vars, and phase angle

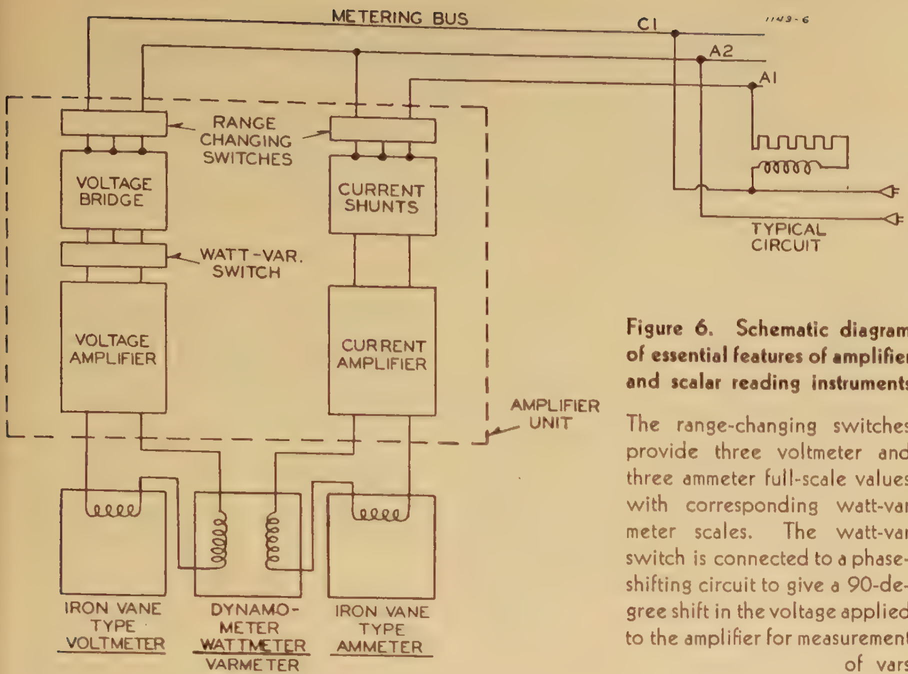

Figure 6. Schematic diagram of essential features of amplifier and scalar reading instruments

The range-changing switches provide three voltmeter and three ammeter full-scale values with corresponding watt-var meter scales. The watt-var switch is connected to a phase-shifting circuit to give a 90-degree shift in the voltage applied to the amplifier for measurement of vars

and hence the reactance is constant throughout the normal range of current. The reactors are designed to keep the resistance to such a low value that its effect can be neglected. This is achieved through the use of "U"-shaped Hypernik punchings (Hypernik having very low core loss at the density used) and by arranging the coils so that the ampere turns are divided equally across the two air gaps. Whenever it is deemed necessary to subtract the resistance of the reactor from the resistance component of the impedance representing an actual circuit element, an average value of 4% of the reactance value can be used.

Ratings

The range of values for the various classes of circuits is shown in the accompanying table.

All circuits are designed for operation at 220 volts, the normal base being 100. Reactors are capable of carrying 3 amperes (300% of normal).

Load and Load Adjuster Units

System loads are simulated on the calculator by means of series or parallel connection of the resistance and reactance elements of the load circuit. The value of this impedance is calculated from the desired kv-a. power factor and voltage at the load bus, using the following formulas:

Series connection

$$R=\frac{K(E')^2}{\text{Kv-a.}}\cos\phi$$

$$X=\frac{K(E')^2}{\text{Kv-a.}}\sin\phi$$

or *parallel connection*

$$R=\frac{K(E')^2}{\text{Kw.}}$$

$$X=\frac{K(E')^2}{R\text{-Kv-a.}}$$

Where K is the power multiplier, or the factor by which the volt-amperes in the calculator circuits are multiplied to give the kilovolt-amperes in the corresponding actual system circuit; E' is the calculator voltage at the load bus; Kv-a. is the 3 phase kilovolt-ampere load desired; and ϕ is the power factor angle.

Generally, the systems which are set up on the calculator contain several load points and more than one generator; and the voltages at the load busses are not known. For such cases, an assumed value of E' is used in the formula to determine the calculator values of resistance and reactance of the load circuits.

To adjust the values thus obtained to the desired values of load without changing impedances, a simple load adjuster is used. This consists of an auto-transformer with taps corresponding to 1% of the circuit voltage. This auto-transformer is connected ahead of and in series with the load impedance. By means of a reversing switch, the auto-transformer is inserted to increase or reduce the applied voltage. The load adjuster is set by selecting the proper tap and switch position so that the voltage applied to the impedance equals the assumed value. For example, if the assumed value was 100 volts and the voltage read at the load bus was 105, the auto-transformer tap would be set at 5%, and the reversing switch set to lower the voltage. The resistance and reactance do not have to be changed, yet the volt-ampere load taken at the load terminal is equal to the desired value because of the transformer action. The use of these load adjusters is a distinct advance in calculator manipulation.

Range of Circuit Elements

(Since Normal Base is 100 Volts—1 Ampere, 100 Ohms = 100%)

Element	Range	
Line impedance (series) $R+JX$	R 0–39 ohms	0 to 100 in 0.2 ohm steps; 100 to 399 in 1 ohm steps
	X 0–300 ohms	1 to 300 in smooth variation*
Load impedance (series or parallel) $R+JX$	R 0–3,990 ohms	0 to 1,000 in 2 ohms steps; 1,000 to 3,990 in 10 ohm steps
	X 0–2,400 ohms	1 to 2,400 in smooth variation*
Capacitance	C 0–4.10 mfd.	In 0.01 mfd. steps
Auto-transformer	%80 to 124.5	In 0.5% steps
Mutual reactors	Ratio 1 to 1†	

*Reactance values are obtained by a combination of fixed air-gap reactors in series with a variable air-gap reactor.

†Value of coupling is determined by impedance circuit connected across either primary or secondary.

Circuit Metering

A set of master instruments is provided for determining the electrical conditions of the network. There have been several stages in the development of means for connecting the circuits to the master instruments. The original design utilized manual plugging of an instrument switch associated with each circuit. Later, provision was made for metering a few selected circuits from pushbuttons on the master control desk. These operated transfer relays, one for each circuit. Such an arrangement for all the circuits on a large calculator would require excessive space on the operator's desk and thus would be inconvenient to handle. One of the outstanding features of the new calculator is the use of a 25 pushbutton selector, arranged in a compact assembly like a comptometer keyboard. By pushing the buttons corresponding to the digits of the desired circuit any one of the several hundred circuits is quickly connected to the master instruments. Only one circuit can be connected at a time because of me-

chanical and electrical interlocks. Figure 4 shows the schematic diagram for this equipment. This simple circuit selector saves valuable space and facilitates circuit connection.

The meter desk shown in figure 5 is the latest development in such equipment, being the result of experience with both horizontally and vertically mounted meters for this application. Having the circuit metering instruments and controls and the writing space on the same sloping plane has been found to eliminate fatigue and to facilitate the recording of readings.

Another distinct advantage of the new desk design is that sufficient space convenient to the operator is made available for using two independent sets of instruments. One set is designed for maximum convenience in obtaining scalar quantities by means of an ammeter, a voltmeter, and a watt-var meter. The second set of master instruments for vector readings, comprises a voltmeter and an ammeter. These, in conjunction with an instrument phase shifter, permit obtaining component values of current and voltage as well as associated phase angle relations. The significant factors in the given problem determine the selection of instruments. For example, the scalar instruments are generally chosen for the ordinary voltage regulation problem; while for stability problems, and certain relay studies where phase-angle and component quantities are desired, the vector instruments are better suited.

All of the master instruments are rugged high torque, instruments with knife edge pointers. The scales are approximately 5 inches long and very uniform so that with a minimum number of full scale values the entire range of electrical quantities can be accurately and quickly obtained. The instruments have a guaranteed accuracy of $1/2$ of 1% of full scale for any reading. In order to obtain better results on voltage regulation studies, the voltmeters are calibrated for 100% accuracy at the normal voltage values used in these studies.

Scalar-Type Instruments, Watt-Var Meter, and Thermionic Amplifier

The instruments provided for direct measurement of scalar current, scalar voltage, and watts or vars are connected into the network through a thermionic amplifier which is so designed that the energy taken from the calculator network is negligible. The schematic diagram is shown in figure 6. The amplifier is a negative feed-back type (current feed-back), so that the calibration is independent of temperature changes in the instrument, tube characteristics, and supply voltage variations.[6,8]

Vector Instruments

The vector instruments for measuring component values of current and voltage with respect to any reference or scalar values and relative phase angle are of the dynamometer type. Field coils in these instruments are energized from a phase shifter so that the instrument burden on the calculator network is negligible. The complete description of this scheme has been published previously.[3]

Conclusion

The modern A.-C. network calculator has so improved the technique of operation that little time or effort is required to set up, adjust, and take readings. Errors due to operator's fatigue are practically eliminated. More studies can be made in a given length of time. These benefits are of maximum significance during a period such as the present, when time is the most important factor in power system planning.

References

1. THE MIT NETWORK ANALYZER, H. L. Hazen, O. R. Schurig, and M. F. Gardner. AIEE TRANSACTIONS, volume 49, 1930, page 1102.

2. AN ALTERNATING-CURRENT NETWORK CALCULATOR, H. A. Travers and W. W. Parker. *The Electric Journal*, May 1930, pages 266–70.

3. MEASURING PHASE-ANGLE QUANTITIES, W. W. Parker. *The Electric Journal*, May 1933, page 187.

4. BOARD EARNS EIGHT TIMES ITS COST, T. G. LeClair. *Electrical World*, November 23, 1935, page 2776.

5. TVA INSTALLS A-C CALCULATOR FOR DETAILED SYSTEM STUDIES, V. J. Cissna. *Electrical South*, October 1938, page 30.

6. STABILIZED AMPLIFIER FOR MEASUREMENT PURPOSES, H. A. Thompson. AIEE TRANSACTIONS, 1938 (July section), page 379.

7. A NEW A-C NETWORK ANALYZER, H. P. Kuehni and R. C. Lorraine. AIEE TRANSACTIONS, volume 57, 1938 (February section), page 67.

8. AN AMPLIFIER-WATTMETER COMBINATION FOR THE ACCURATE MEASUREMENT OF WATTS AND VARS, G. S. Brown and E. F. Cahoon; discussion by W. O. Osbon and W. W. Parker. AIEE TRANSACTIONS, volume 59, 1939 (November section), page 598.

Line-Type Lightning-Arrester Performance Characteristics

AIEE LIGHTNING ARRESTER SUBCOMMITTEE

THIS report contains the performance data for the line type arresters rated 20 to 73 kv. The characteristics of line type arresters were submitted as a committee report in AIEE TRANSACTIONS, volume 57, 1938 (November section), pages 661–2. The lightning arrester subcommittee felt that it was desirable to bring the data up to date at this time; also, that the characteristics of the arresters should be made available for discharge currents up to 20,000 amperes, as well as a curve showing the volt-time gap breakdown characteristics.

The data in this report were obtained from the data submitted by the manufacturers for their respective products. The average values in the report are the average of the manufacturer's average values.

The tolerance from average curve was found to be ±25% for arrester breakdown and ±20% for arrester *IR* discharge voltage.

The arresters covered in this report have a sixty cycle spark potential which is at least 1.5 times the arrester maximum permissible line-to-ground rating.

Table I shows the arrester breakdown values taken on a wave rising to breakdown at the rate of 100 kv/ms per 12 kv of arrester rating. For this wave the breakdown occurs at about 0.4 microsecond. The table also includes the *IR* discharge voltage for currents of 1,500, 3,000, 5,000, 10,000, and 20,000 amperes on a 10×20 wave.

The relation between arrester breakdown voltage for the several voltage ratings is shown in figure 1. The tolerances are also shown.

Paper 41-138, recommended by the AIEE committee on protective devices, and presented at the AIEE Pacific Coast convention, Yellowstone National Park, August 27–29, 1941. Manuscript submitted April 20, 1941; made available for preprinting July 2, 1941.

Personnel of the AIEE lightning arrester subcommittee: H. W. Collins, chairman; H. N. Ekvall, F. R. Ford, I. W. Gross, Herman Halperin, H. G. Lloyd, L. R. Ludwig, W. J. Rudge, J. R. McFarlin, A. H. Schirmer, H. K. Sels, L. G. Smith, H. R. Stewart, E. R. Whitehead.

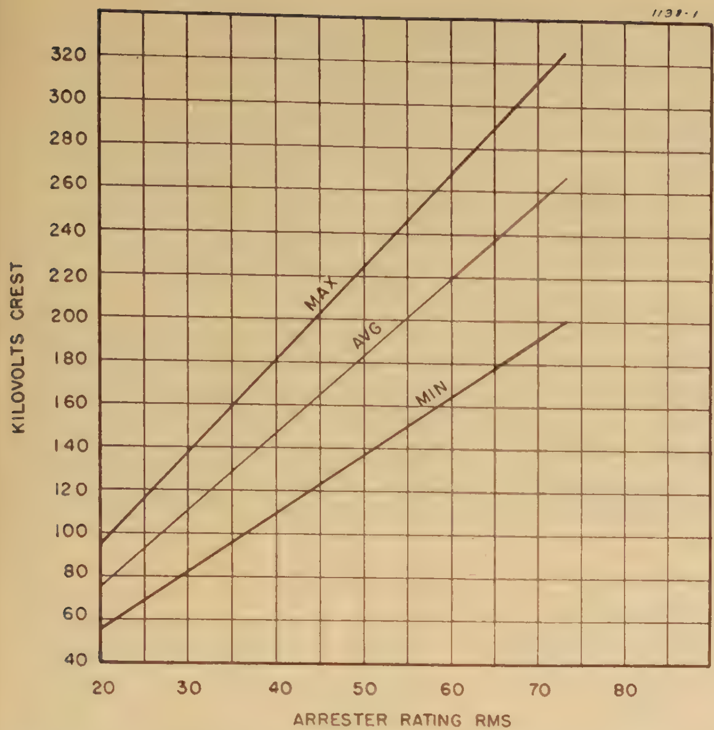

Figure 1. Arrester breakdown voltage at 100 kv per microsecond per 12 kv of rating

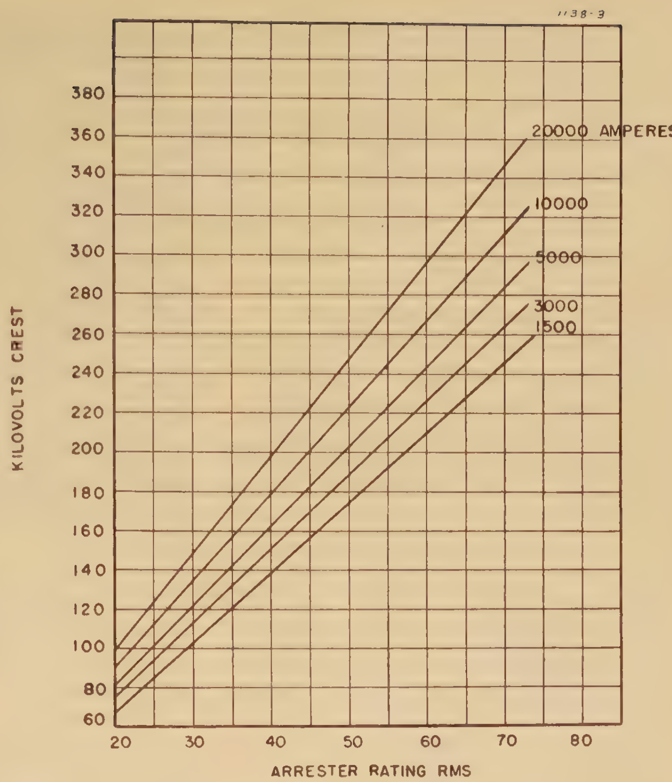

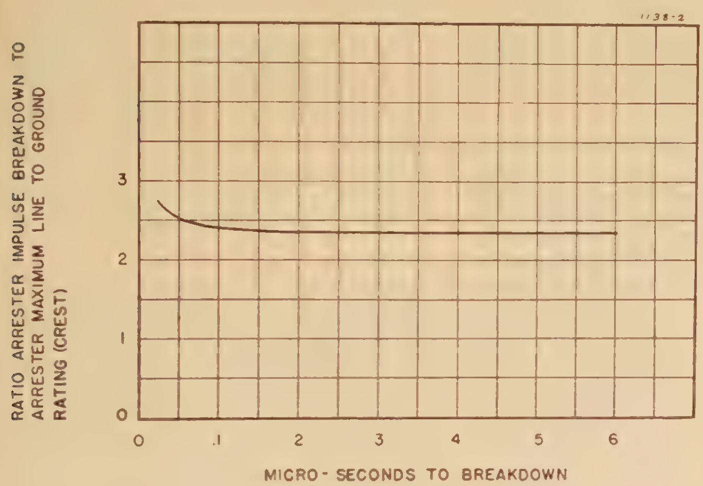

Figure 2. Volt-time impulse-gap breakdown

Figure 3 (upper right). Arrester IR discharge

Voltage 10×20
Average values
Tolerance ±20 per cent

The arrester volt-time breakdown characteristics are shown in figure 2. The breakdown values are given for times as small as 1/4 microsecond and as great as 6 microseconds.

Arrester average *IR* discharge voltages are shown for all ratings at currents of 1,500, 3,000, 5,000, 10,000, and 20,000 amperes, 10×20 wave.

The data in this report will assist in the evaluation on a volt-time basis of the margin between the arrester performance and the insulation to be protected. Consideration must also be given in such evaluations to other factors including rate of voltage rise, distance (circuit feet) between the arrester and the apparatus, ground resistance, selectivity required.

Performance Characteristics Line-Type Arresters (20–73 Kv)

Arrester Maximum Rating	Arrester Breakdown AIEE Rate			IR Discharge Voltage on 10×20 Current Wave														
				1,500 Amp			3,000 Amp			5,000 Amp			10,000 Amp			20,000 Amp		
	Min	Avg	Max	Min	Avg	Max	Min	Avg	Max	Min	Avg	Max	Min	Avg	Max	Min	Avg	Max
20	56	75	94	57	72	86	62	78	94	66	83	100	73	92	110	81	101	121
25	70	93	116	69	86	103	74	93	111	81	101	121	89	111	133	97	121	145
30	82	110	138	83	103	124	92	115	138	97	121	145	108	135	162	119	149	179
37	102	136	170	102	128	153	111	139	167	119	149	179	131	164	197	145	181	217
40	110	147	181	110	138	165	120	149	183	129	161	193	140	177	213	157	196	235
50	137	183	229	138	172	200	150	187	225	161	202	242	177	222	265	194	243	283
60	165	220	274	168	210	252	181	227	273	193	242	290	217	271	325	238	298	358
73	200	267	333	205	257	308	221	277	333	237	297	355	261	328	392	288	360	432

A Cathode-Ray Oscillograph With Rotating-Drum Camera

E. G. DOWNIE
ASSOCIATE AIEE

THE equipment and methods to be described have been developed to meet a need for a simple and effective means of photographing recurring or non-recurring waves viewed on the screen of the cathode ray oscillograph. The recording camera is simple and easy to operate and very economical of film. The recording method also provides for photographing any number of voltage or current waves, and later comparing the phase angles of all the waves. This oscillograph is designed primarily for slow speed work, particularly on waves of 60 cycle fundamental frequency, and in this feature is entirely different from the high speed cathode ray oscillograph described by Kuehni and Ramo.[1]

The cathode ray tube used is a high vacuum, seven inch screen tube. The screen is of the "fast" type with a highly actinic spot of short persistence. A suitable enclosing sheet steel case and a separately boxed 3,000 volt d-c power supply unit were constructed. When the equipment is used for visual work, sweep voltage is applied to one pair of deflecting plates from an independent sweep circuit.

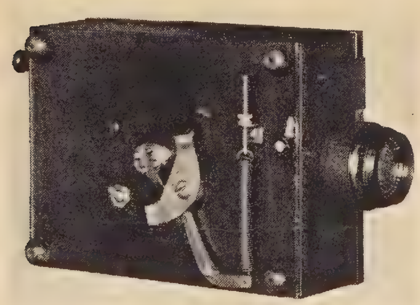

Figure 1. Camera arranged for spring operation of drum

Permanent records of the screen images are obtained with a revolving drum camera focused on the screen. No sweep voltage is used so that the wave to be photographed appears as a single straight line on the screen; with the moving film providing the time axis. The camera consists of an $8^1/_2$ in. by $6^1/_2$ in. by 3 in. sheet steel box with light tight cover, a $5^1/_2$ in. diameter drum (taking 35 mm. film) mounted on a single ball bearing with shaft and control arm extending out of box; and a Biotar lens of 50 mm. focal length, *F*1.4 aperture. In use, the camera is spaced approximately 15 in. from the tube screen by a light tight tapered sheet steel shield. This spacing is such that the image of the screen approximately fills the usable width of the perforated 35 mm. film.

Rotation of the film drum is accomplished by two methods. The first method, involving only a single revolution of the drum, is used for low film speed, and has been found especially useful for recording 60 cycle wave forms. As shown in figure 1, the drum control lever is locked at the beginning and end of a revolution by spring catches. At the start, the lever is given a short impulse by a spring tensioned lever, when released from the first spring catch. The ball bearing mounted drum has sufficient inertia to make the revolution at practically constant speed, and at the end is stopped by the rubber padded bolt and held by the second spring catch. Drum speed is controlled by changing the impulse lever spring tension and is fairly constant at a fixed setting during successive exposures. The film exposure is made by opening a simple shutter at the start of the revolution and closing it at the end. Transients may be initiated at about one third of the drum revolution by the small toggle switch operated by the drum control lever. The switch is double throw, so it may be used to open or close a circuit, as may be required.

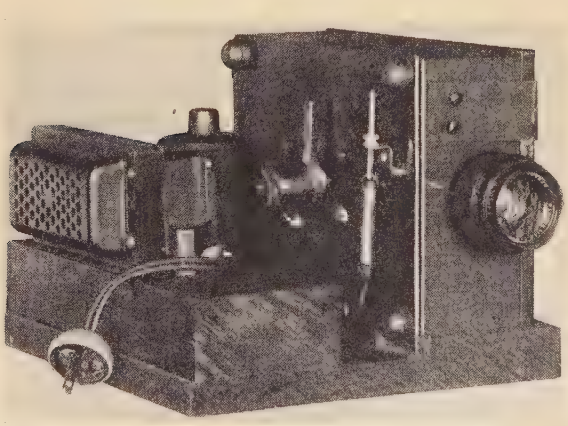

Figure 2. Camera with synchronous motor drive

The second method of drum operation is by synchronous motor drive. Continuous rotation is permitted by removing the stop and spring catch assembly. The motor most frequently used was made from a synchronous phonograph motor by special gearing, to give a speed of 550 rpm. The resulting film speed is 13.6 ft. per sec. and the span of one cycle of a 60 cycle wave is 2.72 in. This is a convenient speed for 60 cycle phase angle measurements to be later described. Exposure of the film in this case is made by opening of the shutter during a single revolution, or $^1/_{10}$ second. Synchronization of the shutter with the drum is desirable but not absolutely necessary. The motor and camera assembly are shown in figure 2 and the complete assembly with oscillograph in figure 3. In use, of course the tapered shield fits tightly in the end of the oscillograph case. Available materials made it more convenient to mount the $^1/_{10}$ second shutter in the shield, instead of on the camera proper, as would be more desirable.

The film drum is removed from the case for convenient loading of the film. The 35 mm. film (either unperforated or the standard perforated motion picture film) is cut to proper length, wrapped tightly around the drum, and fastened at the ends with a small piece of adhesive tape. Loading must of course be done in a dark room. Film used is the most sensitive obtainable, Eastman Super-XX, or Agfa Ultra-Speed Panchromatic; and is developed to high contrast in a "maximum energy" developer such as formula D-82. Such extreme sensitivity is not needed for low frequency waves, but is required when high frequency surges are to be recorded. In practice the intensity of the oscillograph beam is the only factor changed to provide proper exposure at different frequencies. Too high in-

Paper 41-155, recommended by the AIEE committee on instruments and measurements, and presented at the AIEE South West District meeting, St. Louis, Mo., October 8–10, 1941. Manuscript submitted March 23, 1938; made available for preprinting August 11, 1941.

E. G. DOWNIE is with the General Electric Company, Fort Wayne, Ind.

1. For all numbered references, see list at end of paper.

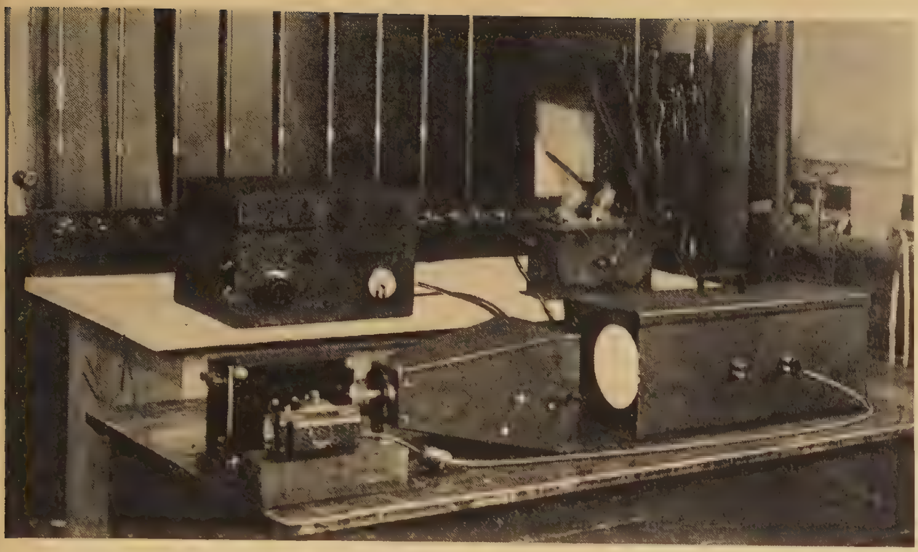

Figure 3. Camera and oscillograph assembly

tensity beam at low frequencies will cause screen retention and blurring on the recording film. The film may conveniently be developed, four lengths at a time, in a small tank such as used for 36 exposure miniature camera film.

The synchronous motor drive provides a uniform time axis, for comparison of successive films. A reference point of phase position on each film then, would also permit comparison of phase angle of waves on successive films. This reference point in each half cycle is obtained by superimposing a small peaked voltage on the wave being studied. This is provided by a coil mounted outside the tube carrying current from a special transformer[2] which produces a small peaked voltage of approximately 5 degrees duration in each half cycle. The magnetic field from the coil deflects the cathode beam in conjunction with the electrostatic field from the internal plates. This transformer must be excited from the same source as the waves being recorded. The voltage shows up on the film as a peak or ripple superimposed on the original wave. It can be easily identified on any except very irregular high frequency waves.

Adjustment of the phase position of the peaked voltage is often desirable to place the peak where it will least interfere and be easiest distinguished on the test wave. Some models of the peaked voltage transformer provide a limited phase shift by a variable resistance in one part of a divided primary winding. A three-phase original voltage source can also be utilized to provide a suitable phase position.

A series of films taken by the above method may be analyzed as shown in figure 4. The films are first arranged in careful register, with respect to the peaked voltage, on a printing frame and a negative film copy made from them. Enlarged prints are then made from this negative, giving black lines on a white background. The vertical line drawn through the peaks is the phase reference, from which measurements may be made on the various waves. Figure 4 shows oscillograms taken of luminous tube transformer secondary voltages, to show the phase relation between no load and various tubing load conditions. This is not conveniently done with a mechanical oscillograph, since only the cathode ray oscillograph, through a capacitance voltage divider, gives a true indication of luminous tube voltages.

In recording an unknown or mixed frequency wave, such as produced by

Figure 4. Phase-angle measurement of luminous tube transformer voltages

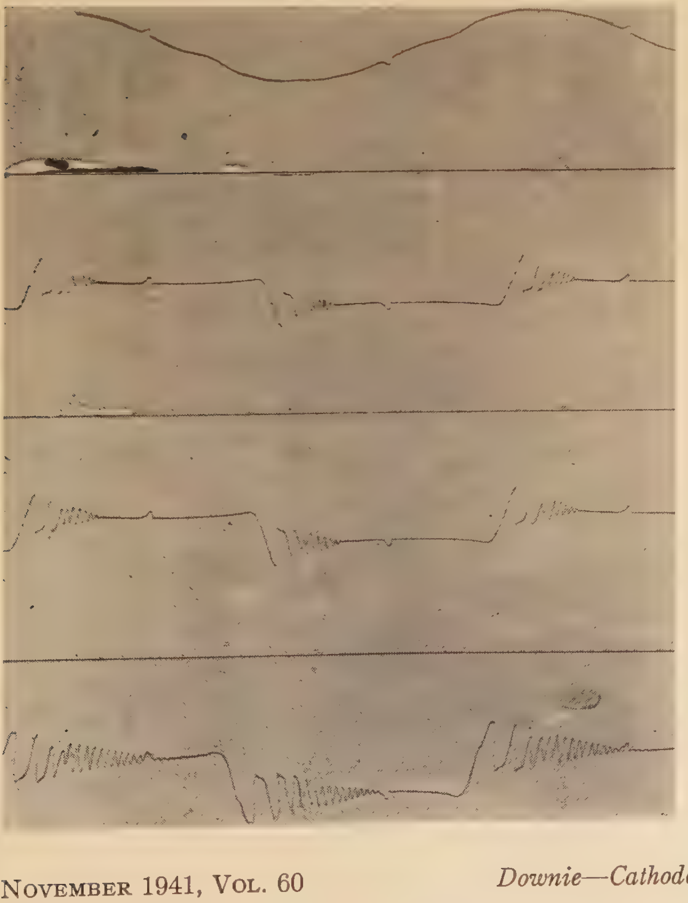

Figure 5. Oscillograms taken with spring operation of drum

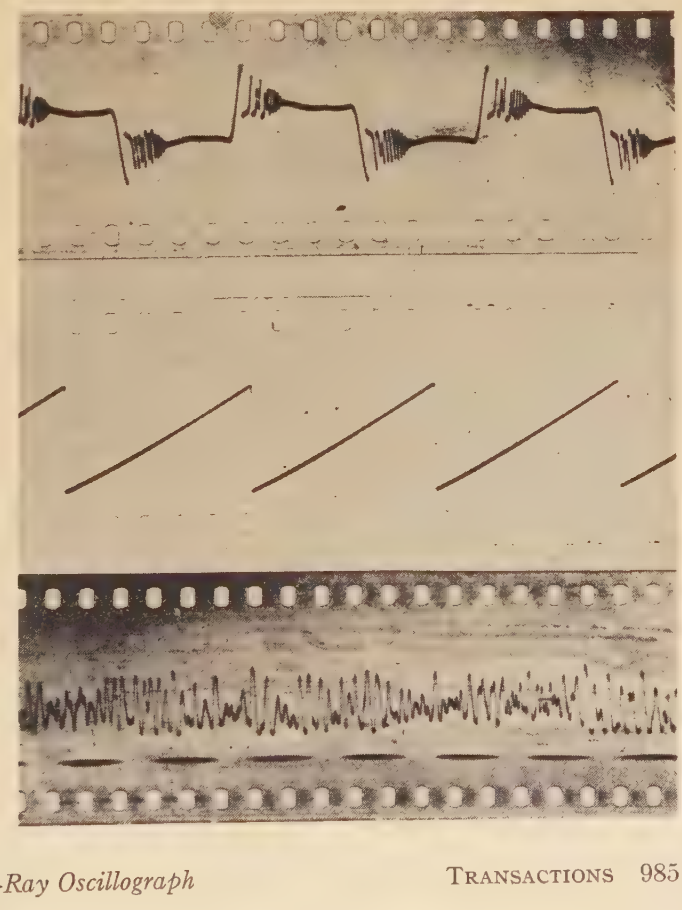

High-Voltage D-C Flashover of Solid Insulators in Compressed Nitrogen

JOHN G. TRUMP
ASSOCIATE AIEE

JAMES ANDRIAS
ASSOCIATE AIEE

HIGH-voltage apparatus insulated by compressed gas requires the use of solid insulating supports. It is generally recognized that even in a uniform field the flashover voltage of such solid insulation is considerably lower than for the gas-filled gap of equal length. An increase in the allowable gradient along such insulators would in general result in a reduction in the size, weight, and cost of gas-insulated apparatus, and must therefore be considered an important and fundamental objective of high-voltage engineering. It is probable that the flashover strength of solid insulators may be brought closer to that of the gases in which they are immersed, or to their inherent volume breakdown strength, through a better understanding of the influence on insulator flashover of such factors as material, surface condition, corrugations, and gas pressure.

Paper 41-146, recommended by the AIEE committee on basic sciences, and presented at the AIEE Pacific Coast convention, Yellowstone National Park, August 27–29, 1941. Manuscript submitted April 22, 1941; made available for preprinting July 30, 1941.

JOHN G. TRUMP is assistant professor at Massachusetts Institute of Technology, Cambridge, Mass. JAMES ANDRIAS is with the Naval Ordnance laboboratory, Navy Yard, Washington, D. C.

The Isolantite test pieces were obtained through the courtesy of Isolantite, Inc., of New York, N. Y.

1. For all numbered references, see list at end of paper.

Most of the scant literature on this subject is restricted to relatively low alternating voltages, small samples of solid dielectrics, or to special insulator shapes in non-uniform fields.[1] Reher studied the flashover of plain cylinders of ebonite, paraffin, and porcelain in dry air at pressures up to 15 atmospheres, using alternating voltages up to 140 kv maximum.[2] Goldman and Wul[3] have investigated the flashover of plain ebonite cylinders in nitrogen with alternating voltages up to 125 kv maximum and pressures up to 20 atmospheres. The present paper reports d-c flashover values up to 250 kv across short cylindrical insulators placed in the uniform field between metallic electrodes. These studies were made on both plain and corrugated cylinders of three dissimilar insulating materials immersed in dry nitrogen at gauge pressures up to 400 lbs. per square inch.

Apparatus

The test insulators were mounted between six-inch-diameter steel electrodes supported within a 13-inch-diameter steel pressure chamber. One of these electrodes was fastened to the end of a high-voltage bushing capable of bringing into the tank voltages up to 500 kv; the other, to a movable support which was insulated from ground so that the pre-flashover currents could be measured. The electrode gap was of such shape that a substantially uniform field existed in the central gap area for all spacings up to $1^1/_2$ inches. Windows were provided in the tank so that the appearance of corona and flashover could be observed.

The voltage source was a 500-kv electrostatic generator of the Van de Graaff type. The voltage was measured by a special spiral-line, high-voltage resistor with an estimated error of less than 3 per cent. Dry commercial nitrogen, which is similar in its electrical properties to air and other permanent gases, was used in this work.

Test Pieces

Three types of solid-insulator materials known by the trade names, Lucite, Textolite, and Isolantite, were studied. Lucite is a polymerized methylmethacrylate which has properties of high dielectric strength and resistivity, homogeneity, and machinability, with moderate mechanical strength. Textolite (No. 2029) is a laminated plastic with a paper base bonded with a phenolic compound. This material has a high dielectric strength across laminations and a moderately high resistivity. These two materials have basic differences which influence their performance as insulators, and each may be regarded as representative of a large group of plastics which are useful as solid insulation in high-voltage applications. Lucite is homogeneous in the volume, has the high volume resistivity of 10^{15} ohm cm, and may be given a smooth, nearly optically perfect surface finish; while Textolite is laminated, has moderate sur-

---

noise or vibration, a permanent timing record on the film is desirable. The superimposed peak is not distinguishable on such a wave. Another method of adding the timing record was devised and found to be quite satisfactory. A small hydrogen filled 110 volt incandescent light bulb is enclosed in a shield to emit a small spot of light, and placed at the edge of the tube screen. The filament of the hydrogen filled bulb, operated on 60 cycle alternating current, completely darkens every half cycle and makes a broken trace at the edge of the oscillographic film. A luminous gas bulb, of sufficient intensity to record on the film, could be used as well. A film recording vibration, with timing trace by this method, is shown in figure 5. The other items in figure 5 show a luminous tube voltage wave form and a "saw-tooth" sweep voltage. These were taken with the single revolution method of drum operation.

The oscillograph and camera equipment has been used in regular laboratory testing and developmental work during the past two years. In addition to the above mentioned application, they have been used in analysis of high frequency ripple in output of direct and alternating current generators; measurement of radio frequency surges in both windings of ignition, high potential testing, and luminous tube transformers during high and low side switching; and noise and vibration analysis of motors. Recently the equipment was transported 200 miles by automobile and returned with oscillograms of high potential testing voltages on an assembly line. It is clear that this type of oscillograph does not attempt to replace the mechanical oscillograph, the cathode ray oscillograph with single high speed condenser discharge sweep, or the newly developed multibeam cathode ray tube, but it has been found very useful in a class of work not well covered by any of these.

References

1. A NEW HIGH-SPEED CATHODE-RAY OSCILLOGRAPH, H. P. Kuehni and Simon Ramo. AIEE TRANSACTIONS, volume 56, 1937 (June section), pages 721–8.

2. TRANSFORMERS WITH PEAKED WAVES, O. Kiltie. ELECTRICAL ENGINEERING, volume 51, November 1932, pages 802–04.

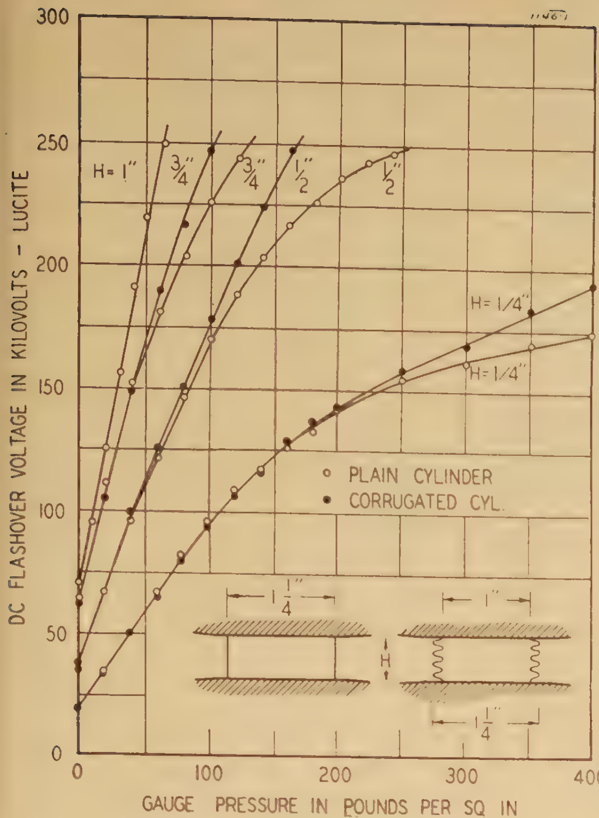

Figure 1 (left). D-c flashover strength of Lucite cylinders immersed in dry nitrogen at high pressures. Uniform field

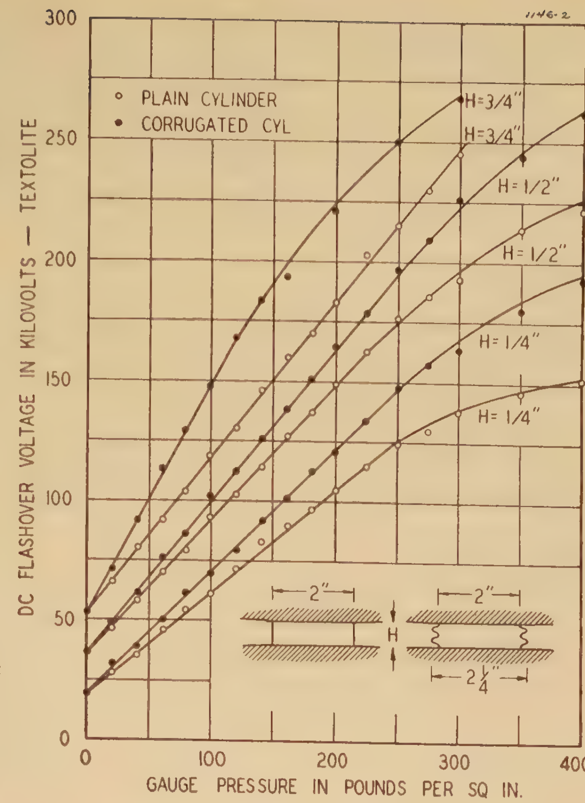

Figure 2(right). D-c flashover strength of Textolite cylinders immersed in dry nitrogen at high pressures. Uniform field

face resistivity and a volume resistivity of about 10^{11} ohm cm, and can readily be given only a moderately smooth surface finish. Isolantite is a porcelain ceramic which has magnesium silicate as its chief ingredient. This material, which may be considered as representative of most electrical porcelains in this application, has high surface resistivity and volume resistivity of about 10^{14} ohm cm, is uniform in the volume, and has the surface smoothness and mechanical properties characteristic of porcelains. The approximate dielectric constant of these materials in the order mentioned above is 4.2, 4.6, and 6.1.

The test insulators were circular in cross section so as to provide axial symmetry, and were $^1/_4$, $^1/_2$, $^3/_4$, and 1 inch in length. The plain cylinders of Textolite and Isolantite were 2 inches in diameter, while those of Lucite were $1^1/_4$ inches in diameter. All of the corrugated pieces had four corrugations per inch, with a 2-inch root diameter for the Textolite and Isolantite, and a 1-inch root diameter for the Lucite. The laminations of the Textolite test pieces were perpendicular to the axis of the cylinders. The cylindrical surfaces of the Isolantite test pieces were glazed.

To ensure good electrical contact between the test insulators and the electrodes, the end surfaces of the former were carefully coated to within $^1/_{32}$ inch of the edges with a conducting graphite mixture. This method was found to be the best of the several means of securing end contact which were tried. To ensure a dry and clean surface condition, the specimens were cleaned with carbon tetrachloride and stored for several days in an atmosphere in which the relative humidity was maintained at less than one percent.

Test Results

The d-c voltage which the insulators could withstand was in every case limited by surface flashover rather than volume breakdown through the material. Figure 1 gives the d-c flashover of plain and corrugated cylinders of Lucite placed in the uniform field between metal electrodes in compressed nitrogen. It is to be noted that with this homogeneous and high-resistivity material the advantage of corrugations becomes considerable only at the higher pressures. The flashover voltages increase linearly with pressure at first, and then more slowly. The flashover values increase nearly directly with the length. Figures 2 and 3 give similar data for Textolite and Isolantite. At the higher pressures Textolite shows a considerably lower flashover voltage than Lucite. For reasons that are discussed below, the influence of corrugations in raising the flashover voltage is pronounced. The flashover values obtained with plain cylinders of Isolantite were normal at atmospheric pressure but increased relatively slowly with pressure. This material was markedly benefited by corrugations.

In figure 4 the flashover strengths of $^1/_2$-inch corrugated cylinders of these three materials between flat electrodes in compressed nitrogen are compared, over the same pressure range, with the breakdown strength of the gap alone. At the lower pressures the flashover strength of corrugated Lucite is nearly the same as that of the gas gap, the departure increasing more rapidly the higher the pressure. At 100 lbs. per square inch the relative flashover strengths of the Lucite, Textolite, and Isolantite cylinders, on the basis of 100 percent strength for the nitrogen gap, were 80 percent, 48 percent, and 40 percent, respectively.

Influence of Surface Irregularities on Flashover

The fact that surface flashover limits the voltage which can be applied to a solid insulator placed between plane parallel electrodes in a compressed gas, may be explained by physical and electrical surface irregularities and by the field-distorting influence of surface-bound space charges. Since solid insulators usually possess dielectric constants in the range from 2 to 6, and are immersed in a compressed gas whose dielectric constant is substantially unity, the effect of physical irregularities—such as a depression—is to distort the otherwise uniform electric field and to increase the electric field intensity on the insulation of the lowest dielectric constant. Figure 5*a*

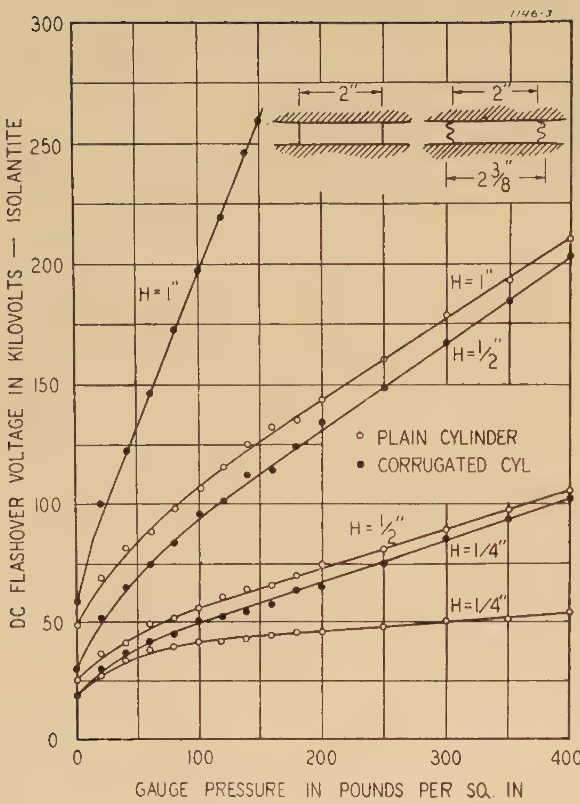

Figure 3 (left). D-c flashover strength of Isolantite cylinders immersed in dry nitrogen at high pressures. Uniform field

Figure 4(right). D-c flashover strength of nitrogen and of corrugated cylinders of Lucite, Textolite, and Isolantite immersed in nitrogen at high pressures. Uniform field, $^1/_2$-inch gap

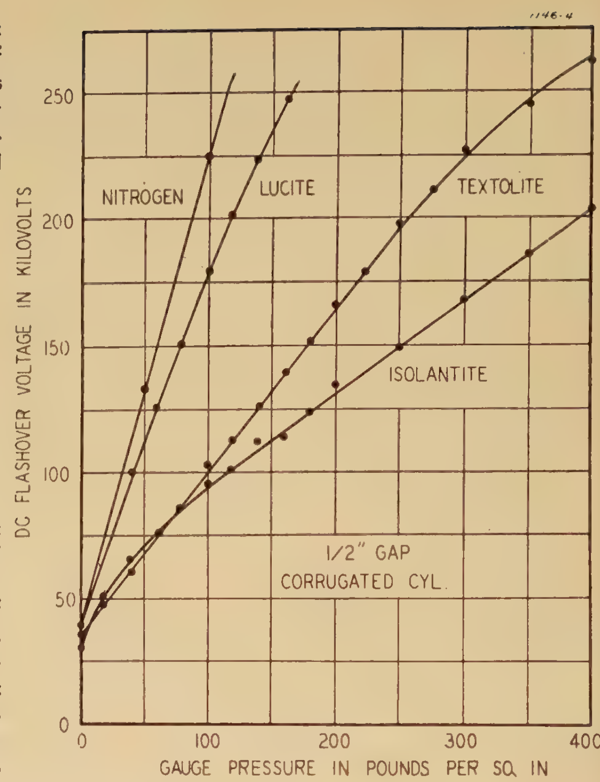

shows the equipotential lines and lines of electric flux in the region of an ideal insulator placed in the uniform electric field between parallel electrodes. Figure 5*b* shows the concentration and distortion of the field caused by a depression in such an insulator. The stress in the region of this depression is nearly *k* times the average stress of the gaseous medium where *k* is the dielectric constant of the solid. Thus, although the average gradient may be substantially less than that required for the breakdown of the gas, the gradient in the region of the irregularity may be sufficient for local ionization. Although the space charge which builds up on the surface of such a defect tends to correct the unfavorable field situation, this local ionized condition of the gas and surface will lead to flashover at a lower voltage than would otherwise be required. This self-healing by ionization in the vicinity of defects in solid insulation is much less effective when alternating potentials are applied, since in this case energy must be expended continuously in the overstressed region. The discussion below is based on applied constant potentials only and should not be assumed to hold in the case of alternating potentials.

Influence of Surface Leakage

Another factor entering into the d-c flashover strength of insulators is the modification of the potential distribution along the insulator surface by leakage. If the surface and volume of the insulator have a uniform leakage resistance, the gradient along the surface is constant and the potential distribution is ideal. Such uniformity of leakage is difficult to obtain, however, particularly when high resistivities such as that of solid insulators are involved. Factors of two in the resistivity of dry, carefully conditioned surfaces of the same insulating material are not uncommon, and the influence of moisture or surface contamination may cause local variations of the resistivity differing from the average by several orders of magnitude. While such nonuniform surface leakage may be modified in some cases by the more uniform leakage through the volume of the insulator, it has the effect of imposing a less favorable distribution of potential along the insulator surface. Local ionization and breakdown of the surrounding gas will originate in the regions of high field intensity, and complete flashover of the insulator will take place at a lower voltage than would be required under uniform leakage conditions.

Effect of Surface-Bound Charges

Again, distortion of the electric field in the vicinity of the surface of an insulator may result from charge accumulations on the surface. This effect should be most pronounced on insulators in which the surface and volume leakage is very small. Such surface-bound charges may be produced by sparking or by corona from an electrode projection. It was observed, in the case of the Isolantite insulators, that at the higher pressures the voltage diminished with repeated flashover to about 50 percent of the normal value, but that the normal voltage was recovered after a lapse of 15 to 30 minutes. This effect was apparently due to the accumulation of surface-bound space charges which distort the electric field. The charge could also be caused to leak off more rapidly by reducing the gas pressure to atmospheric pressure. This effect was not observed with Lucite, although Lucite has even higher resistivity than Isolantite. This is probably because considerable corona preceded flashover in the case of Isolantite, due to the relatively poor end conditions mentioned below. A corresponding space-charge effect has been observed in porcelain high-voltage x-ray tubes. When the inside porcelain wall of such a tube is insufficiently shielded, charge accumulations may occur on the porcelain because of secondary emission. Such an accumulation may displace the electron beam, and this displacement may persist for long periods of time. By introducing air, so as to change from vacuum insulation to a relatively conducting state, this bound charge is quickly removed.

End Effects

A cause of lower flashover voltage can often be found in the improper contact between the solid insulation and the metal

electrodes between which it is mounted. It was ascertained that the low flashover voltage of the Isolantite, for example, could be ascribed largely to this condition. As illustrated in figure 5*c*, the ends of these cylinders fitted imperfectly against the flat electrodes, leaving small wedge-shaped gas-filled gaps between electrode and insulator in which ionization readily occurred in the manner described above. This ionization, which may show as a continuous and visible discharge, both lowers the breakdown strength of the gas and distorts the electric field around the insulator by surface-bound charges. In order to confirm this cause of lower flashover, the ends of one of the Isolantite cylinders were reground to secure an improved contact with the electrodes. Though contact was still not ideal, this procedure increased the flashover values by about 20 percent. This difficulty was not observed with either Lucite or Textolite, since these materials could be machined quite accurately, and since their plastic nature insured excellent contact at the electrode-insulator boundaries. The influence of end contact must be regarded as of particular importance because ionization in this region can be supplied with unlimited amounts of power from the electrodes.

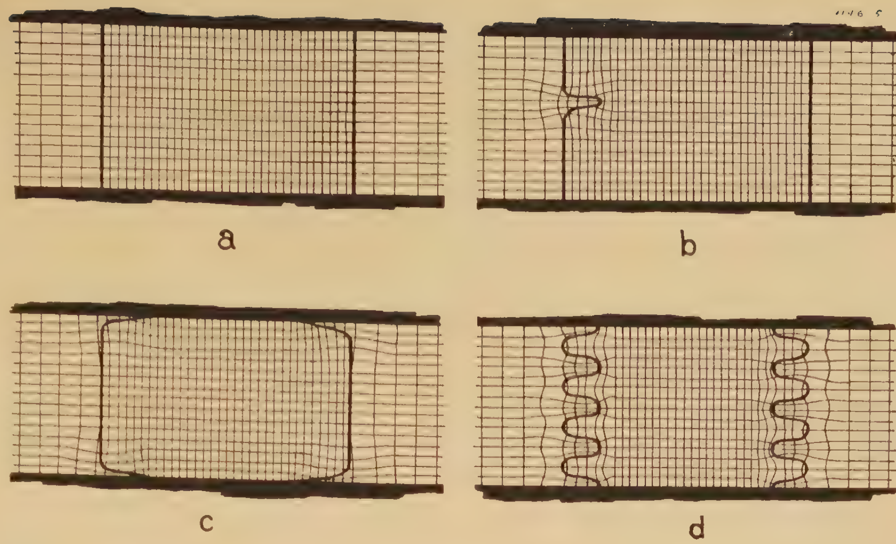

Figure 5. Field pictures of an ideal plain insulator in a uniform field (a), an insulator with a wall defect (b), an insulator with unfavorable end conditions (c), an ideal corrugated insulator (d)

Effect of Corrugations on Insulator Flashover

It can be seen from figure 5*d* that the electric field is distorted in the vicinity of corrugations and that the electric field intensity acting on the gas between corrugations is materially higher than average because of the interposition of material of relatively high dielectric constant. It is to be noted, however, that this field distortion is a not-altogether-unfavorable effect, and that the increase in field strength between corrugations is by a factor of about 2 rather than k, as in the case of the wall defect of figure 5*b*.*

In the case of plain insulators, the imminence of flashover is often revealed by a succession of faint gliding discharges originating on one electrode at the edge of the insulator and proceeding along the insulator surface toward the opposite electrode. On further increase in voltage, these surface gliding discharges increase in brilliance and length, and finally develop into complete and intense flashover. Corrugations, aside from increasing the surface length of the insulator, provide a shielding and localizing effect against such discharges which more than compensates for the field distortion and increased field intensity. The insulator surfaces on the side walls of the corrugations lie in a protected region of low intensity where the disturbing effect of discharges penetrates with difficulty. This is shown by the fact that the final flashover does not in general follow the contour of the corrugated insulator but glides over the tips of the corrugations and leaps across the gas gap between the corrugations.

The net effect of corrugations is to establish longitudinally along the insulator surface regions of alternately high and low field intensity which tend to localize the influence of surface defects, poor end contact, and space charge, and which interrupt the progress of gliding discharges. Corrugations, accordingly, should be expected to play the greatest role in those cases in which most of these conditions exist. The flashover strength of the Isolantite was markedly increased by corrugations, as can be seen from figure 3. In this case, local ionization at the ends caused a surface-bound charge to appear on the nearest corrugation, which reduced the tendency toward further ionization leading to flashover. In the case of Lucite these adverse factors were not present to any considerable extent, so that little advantage from corrugations was obtained until the higher pressures and gradients, at which all influences become more important and critical. It should, however, prove advantageous in general to employ corrugations in all practical applications of solid insulators in compressed gases, since —even with favorable initial conditions— it is probable that imperfections in the insulator surface, non-uniform leakage, or surface-bound charge arising from projections on the electrode may appear in time.

There is considerable tendency in the design of corrugated insulators for use in compressed gas or in high vacuum to have the maximum diameter at the insulator ends. This is intended to avoid the higher gradient which would be found immediately adjacent to the electrode, were the insulator to terminate in the root diameter. It is to be pointed out, however, that very small defects or crevices in the contact will result in local ionizing gradients, and that when this condition exists on the large-diameter ends, the ensuing gliding discharges may proceed from the fault toward the opposite electrode with little opposition. It appears preferable to terminate the insulator in the root diameter, as shown in figure 5*d*, in order that the nearest corrugation may act as a space-charge shield.

Conclusion

The d-c flashover strength of certain solid insulators in compressed gases is less than that of a corresponding gas-

*If a layer of gas of thickness d_1 and a layer of solid insulation of thickness d_2 and dielectric constant K_2 are arranged in series between parallel electrodes, the electric field intensity acting on the gaseous portion of the gap may be shown to be $G = K_2V \div (d_2 + K_2d_1)$ where V is the total applied voltage If d_1 is small in comparison with d_2, the field intensity acting on the gas approaches K_2 times that which would exist in the gap if it contained gas alone. This approximates the situation in the case of an insulator having a narrow fissure or cleft, as in figure 5*b*, or one which has poor end contact, as in figure 5*c*. When the thickness of the two dissimilar dielectrics are equal, the field intensity on the gaseous gap is $2K_2V/(1+K_2)d$ where $d = d_1 + d_2$ or $2K_2/(1+K_2)$ times that of a completely gas-filled gap. This approximates the situation in the corrugated portion of an insulator, as in figure 5*d*. The field intensity in the gas is in all cases K_2 times greater than in the solid dielectric in series with it. This explanation assumes that the electric field is due to charges on the electrodes alone.

The Equal-Volt-Ampere Method of Designing Capacitor Motors

P. H. TRICKEY
MEMBER AIEE

Introduction

IN September 1932, the writer presented a method of designing capacitor motors, known as the "balanced" method. Since that time an improvement on that method has been devised which has certain definite advantages.

The Equal-Volt-Ampere Method

The "equal-volt-ampere" method is fundamentally based on the "balanced" method, and consists in departing from the balanced winding in a certain prescribed manner so that the essential features are obtained with a smaller capacitor. The steps are as follows:

1. The motor is calculated as a two phase motor with both phases the same as the main winding of the proposed motor.

2. Using the formulas of the "balanced" method, a balanced winding and capacitor are designed by balancing at the full load point. The performance of this motor is calculated by the balanced method. If the performance is satisfactory, and if the capacitor is not operating up to its rated voltage, an "equal-volt-ampere" winding may be designed.

3. Choosing a value of capacity to be used in the proposed motor (usually the nearest size to give a capacitor voltage slightly less than the rated volts of the capacitor), calculate the new capacitor voltage as the square root of the the ratio of the balance point microfarads to the proposed microfarads.

4. Since the phase angle between the winding voltages is practically 90°, the capacitor winding voltage is obtained as the square root of the difference of the squares of the new capacitor voltage and the line voltage.

5. The winding ratio "K" (which is the ratio of the effective capacitor winding conductors to the effective main winding conductors) is the ratio of the new capacitor winding volts to the line or main winding volts.

6. Calculate the new "K_a" from the ratio $K/K_a = a$ constant, which should be kept the same as in the original balanced motor

$$K_a = \frac{r_{1a}}{Kr_{1m}}$$

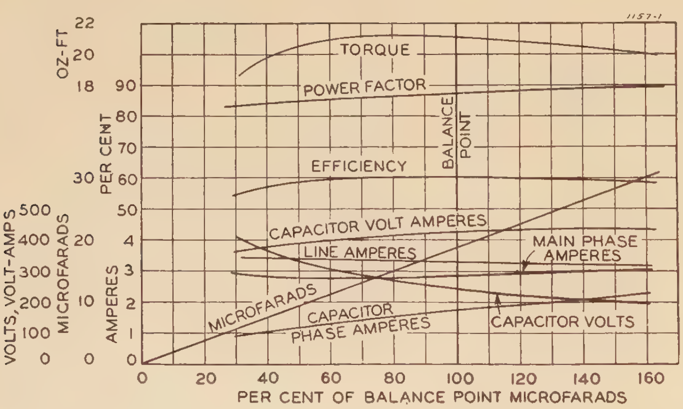

Figure 1. Effect of departure from the balance point while keeping approximately constant capacitor volt-amperes

filled gap or than the puncture strength of the material. It is strongly influenced by surface defects, non-uniform surface leakage, surface-bound space charges, and by end conditions. The flashover strength benefits substantially by increase in the dielectric strength of the gas, and may approach the value of the free-gas gap when favorable field configurations, insulator materials, and proper surface and end conditions are included in the design.[4]

References

1. Durchschlag und Uberschlag in Luft bei Drucken von 1 bis 30 at, C. Reher. *Archiv für Elektrotechnik*, volume 25, 1931, pages 277–98.

2. Die Durchbruchsfeldstärke komprimierter Gase und ihre Verwendung zur Hochspannung-Isolation, A. Palm. *Archiv für Elektrotechnik*, volume 28, 1934, pages 296–302.

3. The Breakdown and Flashover of Solid Dielectrics in Compressed Nitrogen, I. Goldmann and B. Wul. *Technical Physics of the USSR*, volume 3, 1936, pages 519–27.

4. A Compact Pressure-Insulated Electrostatic X-Ray Generator, J. G. Trump and R. J. Van de Graaff. *Physiological Review*, volume 55, 1939, pages 1160–5.

where

r_{1a} = capacitor winding resistance
r_{1m} = main winding resistance

In other words, the weight of wire in the capacitor phase is kept the same.

7. Choose the capacitor winding turns and wire size to give the new values of K and K_a. The nearest wire size is usually close enough.

Results of the Method

The determination of K and K_a completes the design of the "equal-volt-ampere" motor. Its performance will be almost identical to that of the "balanced" motor except for a slight decrease in power factor. This is best illustrated by the example below:

Example Motor

$^1/_4$ hp 1140 rpm 115 volt 60 cycles three speed capacitor motor (speed change obtained by voltage control through regulator)

Balance Point

$K = 1.746 \quad K_a = 2.50 \quad \text{mfd} = 18.85 \quad E_c = 231$

Desired Capacitor

Mfd = 12.6 (nominal value 12) rated at 330 volts

New Capacitor Volts

$$E_c' = 231\sqrt{\frac{18.85}{12.6}} = 283$$

New Capacitor Winding Volts

$$E_a' = \sqrt{283^2 - 115^2} = 259$$

New Winding Ratio

$K' = 259/115 = 2.25$

New Resistance Ratio

$K_a' = 2.50(2.25/1.746) = 3.22$

where

$$K = \frac{CKw_a}{CKw_m} = \frac{\text{effective series conductors in capacitor phase}}{\text{effective series conductors in main phase}}$$

$K_a = r_{1a}/Kr_{1m}$
r_{1a} = resistance of capacitor winding
r_{1m} = resistance of main winding
E_c = capacitor voltage
E_a = capacitor winding voltage

Paper 41-157, recommended by the AIEE committee on electrical machinery, and presented at the AIEE South West District meeting, St. Louis, Mo., October 8–10, 1941. Manuscript submitted December 10, 1941; made available for preprinting August 12, 1941.

P. H. Trickey is with the Diehl Manufacturing Company, Elizabethport, N. J.

1. For all numbered references, see list at end of paper.

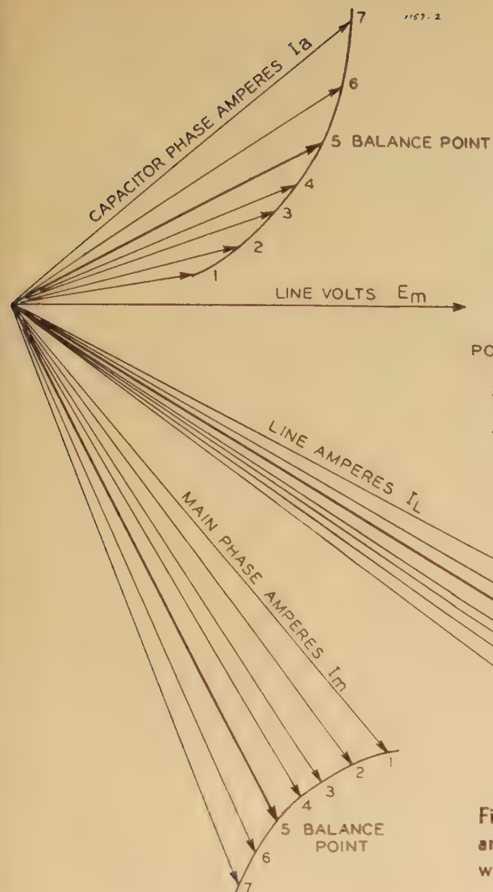

Figure 2 (left). Changes in vector diagram with departure from the balance point

POINT	PER CENT OF BALANCE POINT MFD
1	33.3
2	50.0
3	66.8
4	79.5
5	100.0
6	126.3
7	159.0

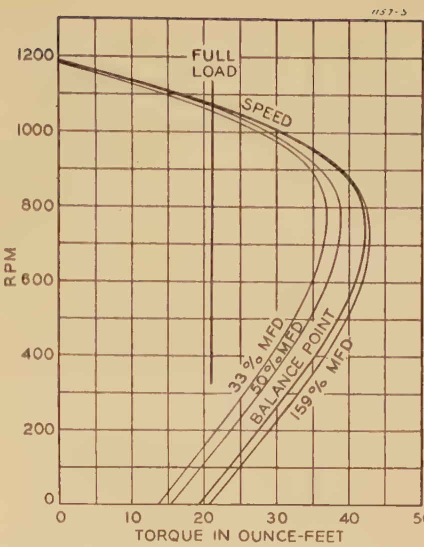

Figure 5 (right). Effect on the speed-torque curve of departure from the balance point while keeping approximately constant full-load capacitor volt-amperes

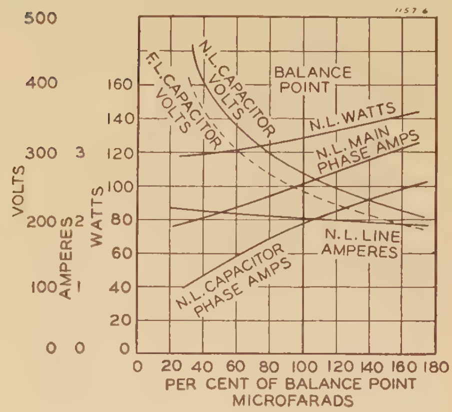

Figure 6 (right). Effect on no-load performance of departure from the balance point while keeping approximately constant full-load capacitor volt-amperes

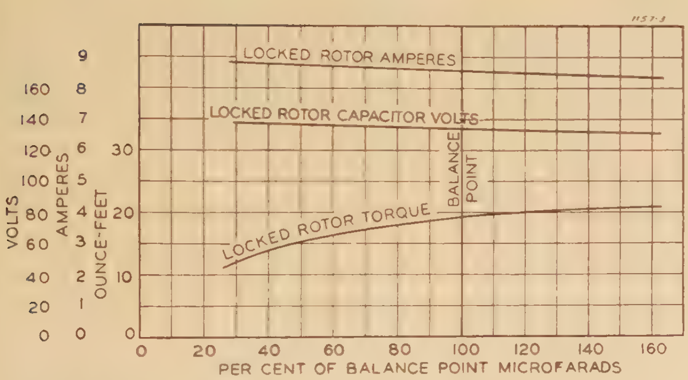

Figure 3 (left). Effect on starting performance of departure from the balance point while keeping approximately constant capacitor volt-amperes

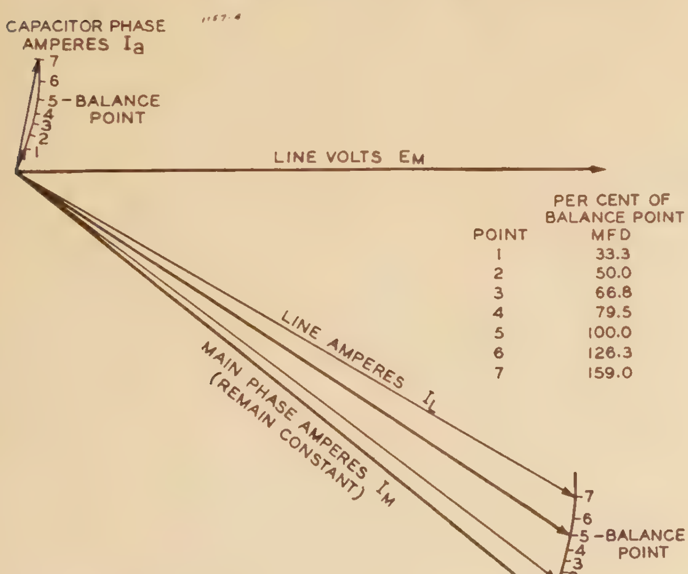

POINT	PER CENT OF BALANCE POINT MFD
1	33.3
2	50.0
3	66.8
4	79.5
5	100.0
6	126.3
7	159.0

Figure 4. Effect on standstill vector diagram

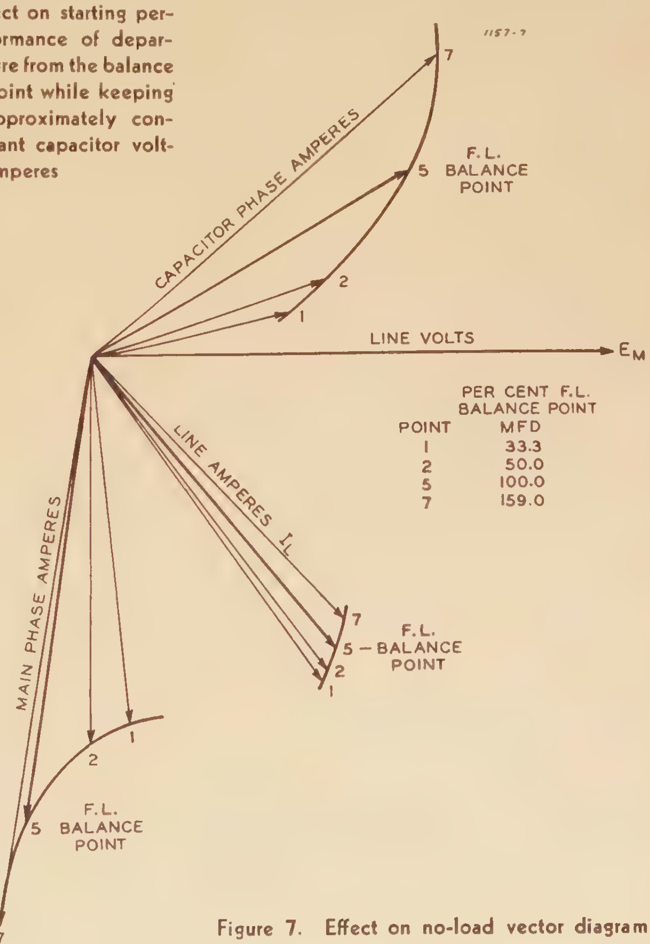

POINT	PER CENT F.L. BALANCE POINT MFD
1	33.3
2	50.0
5	100.0
7	159.0

Figure 7. Effect on no-load vector diagram

Performance	Balance Point	Equal-Volt-Ampere Point
Full-load amperes	3.32	3.40
Full-load watts	334	335.2
Full-load rpm	1,070	1,070
Full-load efficiency	60.0	59.7
Full-load power factor	87.5	85.8

Figure 1 illustrates the effect on full load performance as the equal-volt-ampere winding departs from the balance winding with either more or less microfarads. (It should be noted at this point that while the method is called "equal-volt-ampere" there is a slight variation from exactly constant volt-amperes.)

Figure 2 illustrates the effect on the current vectors. With less than balanced point microfarads, the currents are less than 90° apart, and with more than balance point microfarads they are more than 90° apart.

Figure 3 shows the effect on starting torque and current.

Figure 4 shows the effect on the standstill vector diagram.

Figure 5 illustrating the effect on the speed-torque curve, shows that reduction of the microfarads by this method, results in a slight reduction in the maximum torque.

Figure 6 shows the effect on the no load performance which is a slight improvement with reduced microfarads.

Figure 7 shows the effect on the no load vector diagram.

Figure 8. Effect on starting conditions using windings chosen by the equal-volt-ampere method, but using starting microfarads to give maximum starting torque

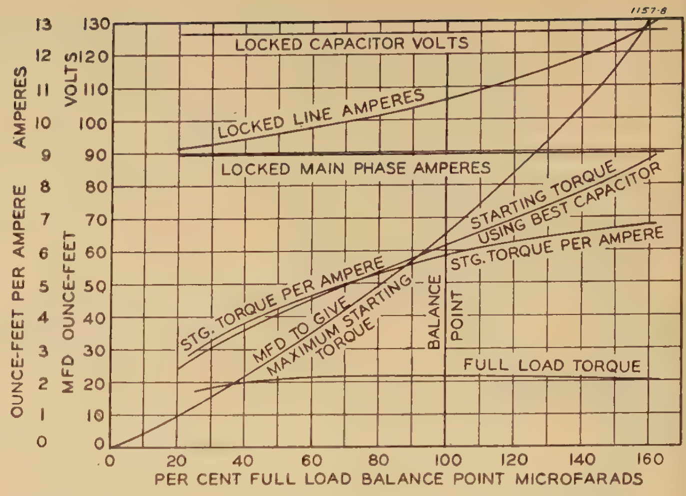

Figure 8 shows how this method affects the possible starting torque of a two value motor. It illustrates definitely that K can not be increased too far if it is necessary to obtain a high value of starting torque on the starting capacitor. In this case, the value of K and K_a would have to be determined by the necessary starting performance. Then the proper value of "equal-volt-ampere" running microfarads would have to be chosen to agree with these values of K and K_a.

Conclusions

The "equal-volt-ampere" method is a very simple and straightforward method of design. A motor is obtained which is well proportioned between performance and cost. All the necessary performance values of efficiency, speed, losses, and heating are obtained by relatively easy calculation formulas. That is, the performance is calculated by the "balanced" method, and used as the performance of the "equal-volt-ampere" motor.

References

1. The Design of Capacitor Motors for Balanced Operation, P. H. Trickey. AIEE Transactions, volume 51, 1932, pages 780–4.

2. The Revolving-Field Theory of the Capacitor Motor, W. J. Morrill. AIEE Transactions, volume 48, 1929, pages 614–29.

3. Performance Calculations on Capacitor Motors, P. H. Trickey. AIEE Transactions, volume 60, 1941 (February section), pages 73–6.

The Inherent Overheating Protection of Single-Phase Motors

C. P. POTTER
FELLOW AIEE

THE problem of controlling and restricting the temperatures of motor windings, is of vital importance to the motor manufacturer, the motor user, and the general public. The motor manufacturer is anxious to have winding temperatures restricted to a safe value, so that his products may have customer acceptance. The motor user is interested in winding temperatures because they affect motor life and maintenance cost. The general public is not conscious of any interest in the matter, but is certainly affected in all cases where excessive temperatures result in fire hazards.

In the early days of the industry, motors did not have adequate protection against overheating, because suitable protective equipment was not available. Motor circuits were fused, but the fuses had to be large enough to accommodate the motor starting current and were, therefore, too large to properly restrict the running current or protect the windings. However, the lack of proper protection was partially offset by the special attention which was given motors by their owners and attendants.

The shortcomings of fuses led to the development of magnetic type relays provided with dash-pots, which retard the operation of the relays to such a point that they can be set to operate close to the full load current of the motor and still have enough time delay to allow the motor to start. These relays were incorporated in motor starting switches and in most cases provide adequate motor protection, but they have one undesirable characteristic. Their operation depends entirely on motor current, while the temperature of motor windings depends upon the room temperature as well as the motor current. A magnetic type relay which will protect a motor located in a room of normal temperature may therefore not protect the same motor when it is operated in a high ambient temperature.

Thermal type relays were the next development and are widely used today in motor starting switches. As the name indicates, these devices are actuated by the heating of a resistor, the temperature of which depends upon both the ambient temperature and the motor current. If the thermal characteristics of the resistor are like those of the motor, and if the relays have the same ambient temperature as the motor, thermal relays installed in starting switches should be entirely adequate for the protection of motor windings. The first of the above conditions is only approximated and the second one cannot always be met, therefore, starting switches provided with thermal relays must also be used with discrimination.

Paper 41-154, recommended by the AIEE committee on electrical machinery, and presented at the AIEE South West District meeting St. Louis, Mo., October 8–10, 1941. Manuscript submitted July 30, 1941; made available for preprinting August 28, 1941.

C. P. Potter is with the Wagner Electric Corporation, St. Louis, Mo.

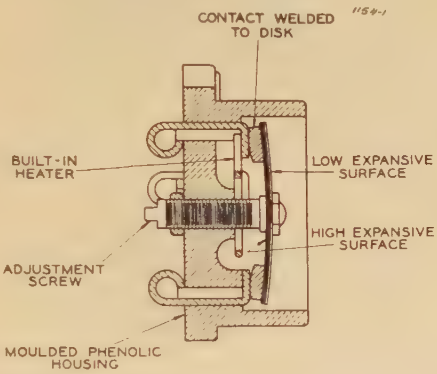

Figure 1. Cross-section of protector with heater coil

Inherent Overheating Protective Devices

Motor overheating is usually due to overloading, but may also be caused by too frequent starting, by foreign material becoming lodged in the motor openings, by installing the motor in a non-ventilated compartment, or in a number of similar ways, and such overheating cannot be prevented by any device which is mounted outside of the motor. Complete protection of motor windings can only be obtained by using thermal devices which are mounted inside the motor enclosure and which make use of resistors or "heater coils" through which the motor current passes. These devices are ordinarily known as "motor protectors" and are designated by the Underwriters' Laboratories as "Inherent Overheating Protective Devices."

Motor protectors have many modifications. When applied on certain types of service they are of the automatic reset type and as the name implies such a protector stops the motor when it reaches a dangerous temperature and automatically starts the motor when its temperature decreases to a safe value. For other types of service, protectors are of the manual reset type which must be reset by an attendant, who presumably inspects the installation to find out what caused the protector to open, before resetting it. Protectors which are used in motors 1 hp and smaller usually break the line current, thus eliminating the necessity of providing the ordinary overcurrent protection required by the Underwriters' Laboratories. Protectors which are used in motors larger than 1 hp do not ordinarily break the line current, but are connected in the pilot circuit of the magnetic switch which starts and stops the motor.

Motor protectors of the automatic reset type contain some sort of a thermostatic device such as a bimetallic disk or strip, which may be mounted adjacent to a heater coil through which the motor current flows. Figure 1 shows a cross-section of a device employing a heater coil, manufactured by the Spencer Thermostat Company. In other types the heater coil is omitted and the bimetallic strip acts as a resistor. A protector of the latter type manufactured by Cutler-Hammer, Inc., is shown in figure 2. In both cases the bimetallic elements carry contacts which are normally closed and which are connected in the motor line. These protectors are mounted inside the motor and when the temperature inside the motor reaches the maximum safe value, the bimetal snaps to its hot position, the contacts open, and the motor is disconnected from the line. When the temperature of the motor decreases sufficiently, the bimetal snaps back to its normal position and the motor is automatically started. Automatic reset protectors are used on motors which drive stokers, fans, blowers, pumps, small refrigerating outfits, etc. Automatic reset protectors are built in many styles, some of which are illustrated in figure 3.

Motor protectors of the manual reset type may employ a bimetallic element or they may have a thermal device of the

Figure 2. Protector without heater coil

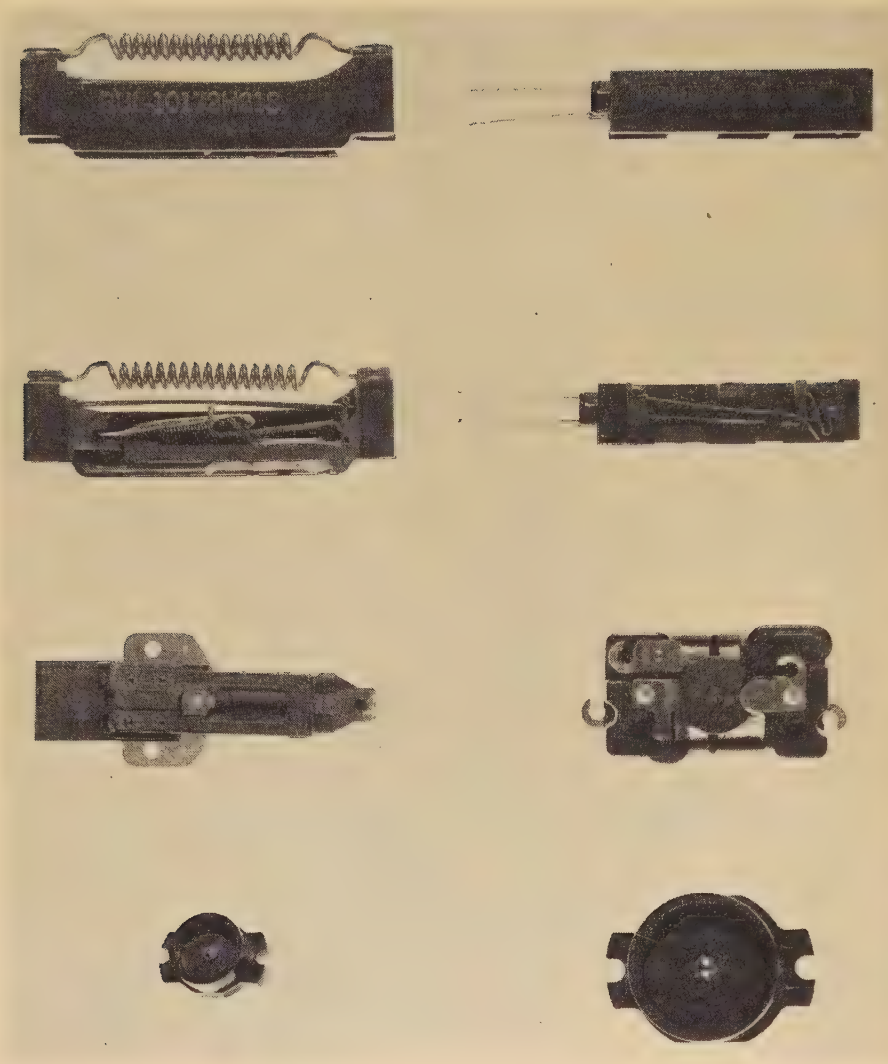

Figure 3. Assortment of automatic reset protectors

"solder pot" variety, mounted adjacent to a heater coil which carries the motor current. Figure 4 shows one of the former manufactured by the Micro Switch Corporation, while figure 5 illustrates a protector of the solder pot type manufactured by Cutler-Hammer, Inc. These protectors are actuated by the temperature inside the motor, but must be reset manually and cannot be permanently reset until the motor has cooled considerably. Manual reset protectors are used principally on motors which operate oil burners and other devices where it is desirable to investigate the cause of motor stoppage before restarting the motor.

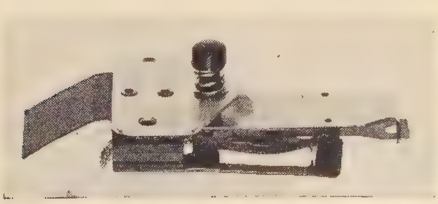

Figure 4. Manual reset protector with bimetallic element

Standard Tests on Motor Protectors

Several temperature tests are required by the Underwriters' Laboratories to determine the suitability of a protector for application on a motor. All temperatures are measured by means of thermocouples which are placed on the surface of the windings and enough thermocouples are used to be sure that the "hottest spot" is located. A series of temperature tests is made with the motor running at about 5% more than normal voltage and with gradually increasing loads, until the protector opens. A single test is made with the rotor stalled at about 5% more than normal voltage, and the protector is allowed to continually trip and reset until the temperature of the windings becomes constant. The object of these tests is to determine the maximum winding temperatures under these abnormal conditions, and restrict them to a safe value. If the temperatures thus taken are found to be reasonable, the application of the protector is considered satisfactory and it is assumed that the motor cannot be damaged no matter how it may be operated. It will be seen that tests have not been mentioned to determine the effect of high ambient temperatures, high or low voltage, high or low frequency, etc., and it would seem to be desirable to make such tests on a representative motor and determine whether motor protectors which have been applied in accordance with accepted rules, actually protect the motors on which they are installed, under all conditions of operation.

Special Tests on Motor Protectors

In order to obtain this information, special tests were made on a 1/3 hp, 1,725 rpm, 110/220 volt, 60 cycle, single phase, repulsion start induction motor equipped with an automatic reset protector, both running and with the rotor locked, at voltages above and below the rated voltage, at frequencies above and below the rated frequency, at various ambient temperatures and with the motor ventilation progressively restricted and finally eliminated. The results of these tests are plotted in figures 6 to 14 inclusive and in order to avoid repetition the term "protector limited temperature" is used to describe the maximum winding temperature which exists when the protector trips. The protector limited temperature

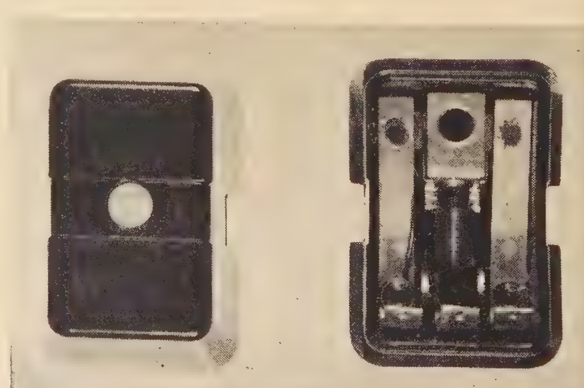

Figure 5. Manual reset protector with "solder-pot"

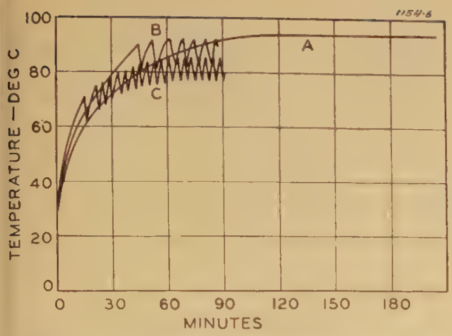

Figure 6. Winding temperature versus time

Normal voltage and frequency. $^1/_3$-horsepower repulsion-start induction motor with protector

Curve *A*: At maximum current permitted without interruption by protector

Curve *B*: At current 10 per cent greater than that of curve *A*

Curve *C*: At current 20 per cent greater than that of curve *A*

is usually much less than the ultimate temperature which would be reached without a protector.

Curve *A* in figure 6 shows the relation between time and winding temperature for the maximum current which the protector will allow the motor to carry continuously when it is operating at normal voltage and frequency. In this case the protector does not trip but any additional load would cause it to do so. The maximum winding temperature is 94°C, which is much lower than could be allowed. Curve *B* is plotted for a current 10% greater than the maximum current which the protector will carry continuously and curve *C* is plotted for a current 20% greater than the maximum current which the protector will carry continuously. In both these curves the protector trips and resets several times before the winding temperature reaches a constant value,

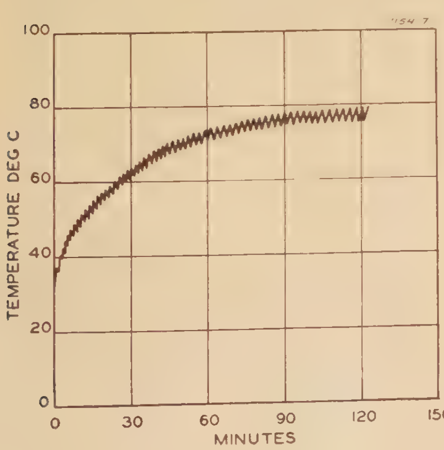

Figure 7. Winding temperature versus time

Rotor locked. Normal voltage and frequency. $^1/_3$-horsepower repulsion-start induction motor with protector

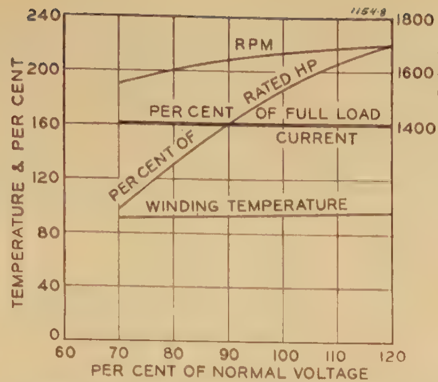

Figure 8. Motor characteristics versus voltage at maximum loads permitted by protector

Normal frequency. 28 degrees ambient. $^1/_3$-horsepower repulsion-start induction motor

and in both cases the protector limited temperature is less than the ultimate value for curve *A*.

Figure 7 shows the relation between time and protector limited temperature of the $^1/_3$ hp repulsion start induction motor at normal voltage and frequency with the rotor stalled. This is an abnormal condition, but is one which might exist in case of a mechanical defect in the motor or the machine which it drives. The protector trips and resets many times before the winding temperature reaches a constant value, which, however, is considerably less than for the running condition and is well within safe limits.

Tests were made with the motor operating at voltages above and below normal, to determine the effect of voltage on the winding temperatures permitted by the protector, and the results are shown in figure 8. It is interesting to note that under these conditions the protector is essentially a constant current device and allows the same current to flow at voltages from 70 to 120% of normal voltage. The protector limited temperatures at 70% voltage are slightly less, and at 120%

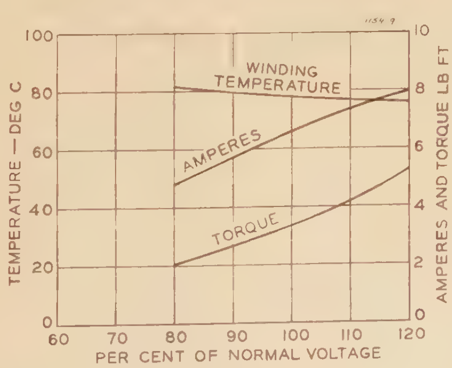

Figure 9. Locked characteristics versus voltage

Normal frequency. 31 degrees ambient. $^1/_3$-horsepower repulsion-start induction motor with protector

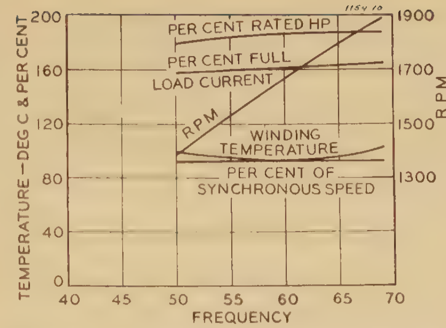

Figure 10. Motor characteristics versus frequency at maximum loads permitted by protector

Normal voltage. 28 degrees ambient. $^1/_3$-horsepower repulsion-start induction motor

voltage are slightly greater than the values shown in figure 6, but for all practical purposes the protector limited temperatures are not affected by the voltage. Motor loads and speeds are also plotted and as might be expected, they change quite rapidly with the voltage. It will be seen that if this motor is driving a compressor or pump and is considerably overloaded, it will be unable to carry the load at the lower voltages, because the protector will trip and disconnect the motor from the supply circuit.

Locked tests were also made at various voltages and the results are plotted in figure 9. In this case the locked current varies at about the same rate as the voltage, but the protector limited temperatures change very little as the voltage varies. This difference in protector operation between running and locked condition is due to the fact that when the motor is locked, the protector is essentially a constant temperature device and its operation depends almost entirely on the temperatuie of the heater coil which is adjacent to the bi-metal. Since the heater coil temperature and the winding temperature both depend on time and motor current, it logically follows that

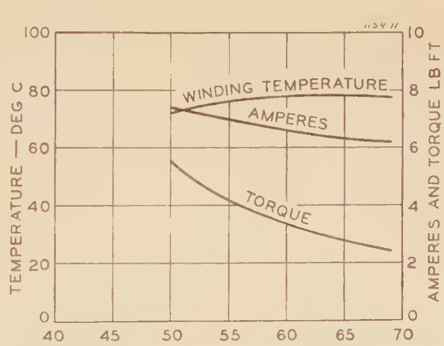

Figure 11. Locked characteristics versus frequency

Normal voltage. 31 degrees ambient. $^1/_3$-horsepower repulsion-start induction motor with protector

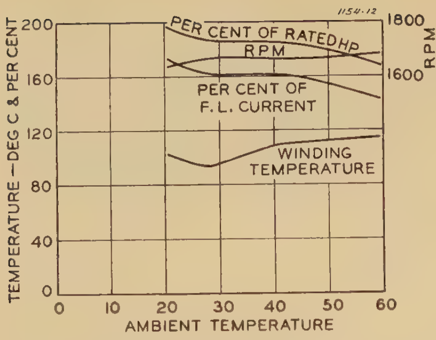

Figure 12. Motor characteristics versus ambient temperature at maximum loads permitted by protector

Normal voltage and frequency. $^1/_3$-horsepower repulsion-start induction motor

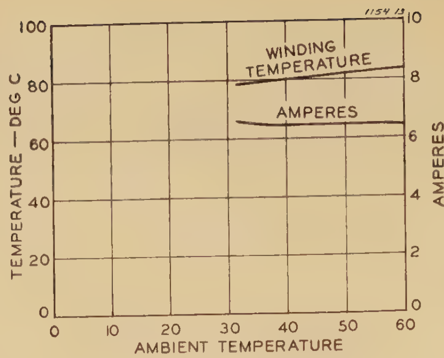

Figure 13. Locked characteristics versus ambient temperature

Normal voltage and frequency. $^1/_3$-horsepower repulsion-start induction motor with protector

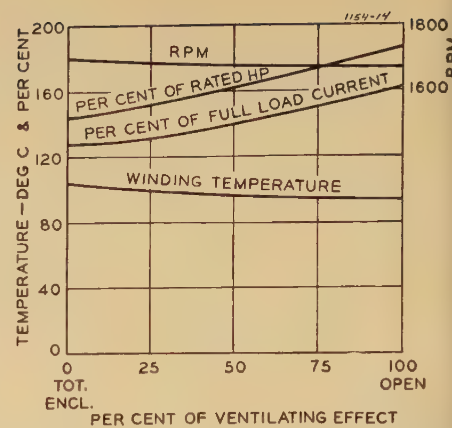

Figure 14. Motor characteristics versus ventilating effect at maximum loads permitted by protector

Normal voltage and frequency. 28 degrees ambient. $^1/_3$-horsepower induction motor

while the time required for the protector to trip a locked motor will vary with the current, the temperatures of the protector and the motor windings when the protector trips are not materially affected by the motor current, and, therefore, do not depend on the voltage applied to the motor terminals.

Figure 10 shows the effect of variations in frequency on the winding temperatures permitted by the protector, while the motor is running. The protector limited temperatures at high and low frequency are only slightly greater than they are at normal frequency and the motor protector takes care of frequency variations while the motor is running, quite satisfactorily. While this motor will carry the same horsepower load at a wide range in frequencies, it obviously cannot operate at frequencies much greater than the normal value because at the higher frequencies, the speed, horsepower, and motor current also increase and the protector will not be able to carry the increased current.

Figure 11 shows the effect of variations in frequency on the protector limited temperatures of the motor with the rotor locked. The operation of the protector with the rotor locked and the frequency varied is much the same as when the frequency is fixed and the voltage varies. The winding temperatures for comparatively wide variations in frequency are practically constant and no difficulty should be experienced with a locked motor at either high or low frequency.

The tests which are plotted in figure 12 were made with the motor running at normal voltage and frequency, but with various ambient temperatures. It was found that with ambient temperatures between 30 and 40°C the protector trips at a fixed value of current and the winding temperature increases at the same rate as the ambient. Above 40°C the protector trips at a smaller value of current and, therefore, the winding temperature does not increase as fast as the ambient. Below 30°C the protector trips at a higher value of current and the winding temperature increases in spite of the decreased ambient. It is evident that the protector limited temperature may increase considerably when the motor is running in a high ambient temperature.

Locked tests at various ambient temperatures were made and the results plotted in figure 13. In this case the winding temperatures do not change materially with the ambient, indicating that the protector trips when the temperature of the bi-metal reaches a definite value, and it makes little difference whether this temperature is produced by the heat of the motor or the surrounding air.

When open type motors are installed in locations where excessive amounts of foreign materials are present, the ventilating openings may become partially or even completely obstructed, and the motor may have an excessive temperature rise. Tests were made to determine whether a motor protector will take care of such a condition and the results are plotted in figure 14. With all the openings in the motor frame enclosed, the protector limited temperature increases 10° and the load which the motor can carry without tripping the protector is reduced 22%. It is unlikely that an open type motor will ever be completely enclosed either accidentally or deliberately; therefore, the probable increase in temperature resulting from foreign materials will be considerably less than 10°.

Variations in Winding Temperatures of a $^1/_3$-Horsepower Repulsion-Start Induction Motor Protected by an Inherent Overheating Protive Device

Abnormal Condition	Change in Temperature (Degrees Centigrade) Motor Running	Motor Locked
120% normal voltage	2 increase	2 decrease
80% normal voltage	2 decrease	4 increase
117% normal frequency	Inoperative	1 decrease
83% normal frequency	6 increase	6 decrease
60° ambient	6 increase	3 increase
All ventilation eliminated	10 increase	No change

Summary

Motor protectors are selected and applied so that they restrict the motor winding temperature to specified values at normal voltage and frequency and a room temperature of 40°C. The accompanying table shows the probable increase (or decrease) in winding temperatures which may occur on account of abnormal voltages, frequencies, or ambient temperatures, or with restricted ventilation.

Conclusions

The variations in temperature shown in the table are small and lead to the conclusion that inherent overheating protective devices mounted inside fractional horsepower single phase motors completely protect them against all abnormal operating conditions.

Criteria for Neutral Stability of Wye-Grounded-Primary Broken-Delta-Secondary Transformer Circuits

H. S. SHOTT
ASSOCIATE AIEE

H. A. PETERSON
MEMBER AIEE

Synopsis: This paper presents the results of an investigation made to determine and evaluate the effect of the factors affecting neutral instability of Y-grounded potential transformer circuits. The method used employs the medium of miniature system representation. The results therefore include the effect of saturation. The effects of the shape of the saturation curve, normal operating voltage, resistance of the winding, system capacitance, and impedance in the broken Δ secondary or across each phase are illustrated. Regions of instability are shown which should be avoided in applying Y-connected potential transformers as ground fault detectors. The analysis shows by means of oscillograms the conditions under which incorrect indications of faults may be obtained.

GROUNDED-NEUTRAL, Y-connected potential transformers with Y- or broken Δ-connected secondaries have been applied to three-phase circuits, the neutrals of which are temporarily or permanently ungrounded. The broken Δ secondary connection affords a means of ground fault detection, the voltage across the break in the Δ under such fault conditions being used to operate relays or otherwise indicate the presence of a ground fault.

In some cases, experience has shown that such a circuit is unstable. The phenomena involved have been described for limited ranges of circuit parameters.[1,2] One oscillographic investigation, however, describes the various conditions of instability in some detail.[3]

More recently other cases of difficulty with this type of circuit have been encountered. While correct indications of true faults were always obtained, indications of faults were sometimes obtained when no faults actually existed. These false indications sometimes resulted in higher than normal fault indicating voltages appearing across the break in the Δ secondary. This phenomenon was traced to the inherent instability of a circuit of this type when the amount of capacitive reactance to ground and the magnetizing reactance of the transformers involved are in certain relative proportions. As a consequence, a comprehensive analysis of the circuit was undertaken, using the miniature system transient analyzer,[4] which disclosed the regions of instability and methods of eliminating such instability. This paper presents the results of that investigation.

Basis of Study

The miniature system shown in figure 1 was selected as a basis for the study. The reactance of the sine wave generator was negligible compared with the external miniature system impedances. Thus balanced sinusoidal line-to-line voltages were applied at the transformer terminals. Consequently the phenomena were independent of positive sequence capacitance so that only zero sequence capacitive reactance, x_{co}, was involved.

Transformers used were single phase and their saturation characteristic is shown in figure 2. Curve #1 is representative of most transformers, and therefore was used throughout the study except for one case in which the #2 curve was used to indicate the effect of more abrupt saturation. The value of x_m is the ratio of normal line-to-neutral rms exciting volts to normal phase rms exciting amperes at normal frequency as defined by the saturation curves. The circuit can be completely defined by the ratio of x_{co}/x_m when the saturation curve used and the normal operating voltage are specified.

Provision was made to control the excitation of the miniature system sine wave set so that system voltage could be varied. It was not deemed practical to operate at voltages higher than normal, as indicated on the saturation curves, since in the system studied, a line-to-ground fault would result in extremely high magnetizing currents in the two unfaulted phases.

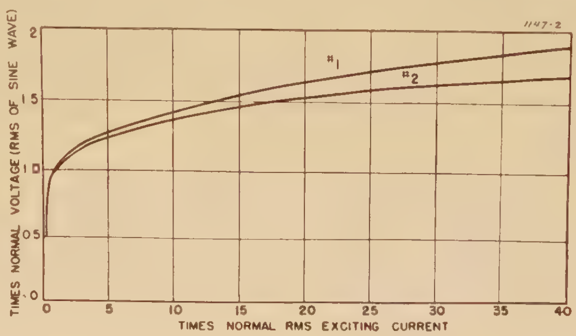

Figure 2. Transformer saturation curves used in the miniature system

1—Typical saturation curve

2—Curve having more saturation than curve 1

The study was made with and without load impedance in the break in the Δ. This is equivalent to putting load impedance across each phase in the case of Y-connected secondaries, the total ohmic resistance being the same in either case. Various impedances were used as burdens to determine the effect of impedance burden magnitude and power factor, both lagging and leading.

In practically all cases studied, the abnormal conditions were obtained by suddenly energizing the miniature system

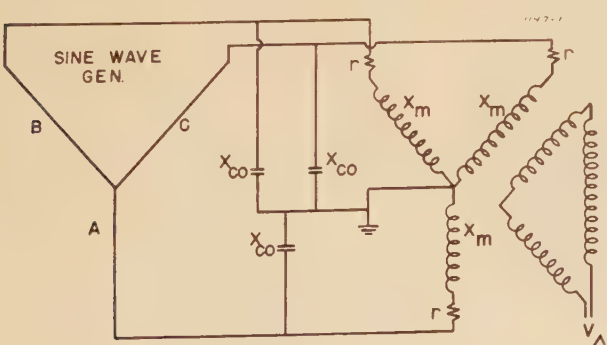

Figure 1. Miniature system studied

x_{co}—Zero sequence capacitive reactance

r—D-c resistance of transformer winding

x_m—Ratio of rms sinusoidal leg volts to rms phase current at a point on the saturation curve corresponding to $E=1.0$ in figure 2

Transformer turn ratio 1:1

Paper 41-147, recommended by the AIEE committees on protective devices and instruments and measurements, and presented at the AIEE Pacific Coast convention, Yellowstone National Park, August 27–29, 1941. Manuscript submitted May 15, 1941; made available for preprinting July 16, 1941.

H. S. Shott and H. A. Peterson are both with Central Station engineering department of the General Electric Company, Schenectady, N. Y.

1. For all numbered references, see list at end of paper.

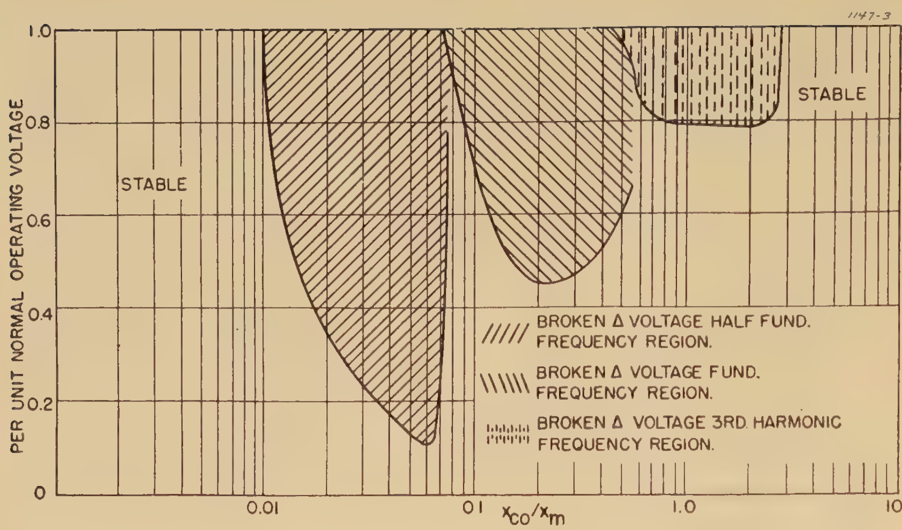

Figure 3. Regions of possible instability of the circuit of figure 1 with transformer saturation corresponding to curve 1 of figure 2

$r/x_m = 0.0003$ for the transformer

r—D-c resistance of the winding

x_m—Ratio of rms sinusoidal leg volts to rms phase current at a point on the saturation curve corresponding to $E = 1.0$ in figure 2

or by applying and removing a fault to ground on one phase, although in some cases, instability could be obtained by gradually raising the excitation of the sine wave generator. However, the manner of obtaining the abnormal circuit conditions, as long as it is reasonable, is of secondary importance relative to the question as to whether abnormal behavior of the circuit is possible or not for given constants. The study is primarily concerned with answering this question.

It is of interest to point out in this connection that regions of possible abnormality may overlap with regions of possible normal circuit behavior. In other words, in regions of abnormal circuit behavior it is sometimes possible for the circuit to behave normally also, but it is never possible in a region designated as stable to have an abnormal circuit condition of the type under discussion in this paper.

It should also be pointed out that the regions of instability are regions where the abnormal conditions persist in the steady-state condition. It is possible for relatively long-time transients to exist near the border line in the stable region. These will die out eventually, however, and normal conditions will always be restored ultimately.

Discussion of Results

For a particular set of transformer characteristics the regions of neutral instability of the system shown in figure 1 are defined in terms of the ratio of system parameters x_{co}/x_m and of the system voltage E where E is the per unit system operating voltage. $E=1$ corresponds to system operating voltage of $E=1$ on the saturation curves of figure 2. In the application of potential transformers as a means of ground fault detection, it is customary to select a transformer rated line-to-line system voltage and operate it at system leg voltage; that is $E=0.58$. In some instances, however, circuits for which $E=1.0$ may be encountered if in a normally grounded system the Y grounded transformer bank is temporarily connected to an otherwise ungrounded circuit, or if single-phase transformers are connected line-to-neutral in a three-phase system which has an open circuit in the neutral at the system grounding point.

The data of figure 3 were obtained using a low-loss transformer with typical saturation characteristics, curve 1, of figure 2. The regions outlined are those in which instability may occur as the result of a shock, such as a line-to-ground fault applied and removed. Stable operation may be obtained within portions of the unstable regions if system voltage is gradually applied or if the Δ secondary is closed until normal steady-state conditions exist.

At each test value of x_{co}/x_m the system voltage was raised to a value corresponding to $E=1.0$. If the application and removal of a line-to-ground fault created an unstable condition as indicated by the presence of an abnormal voltage across the break in the Δ, the system voltage was then reduced to the boundary value at which the unstable Δ voltage collapsed.

As indicated on figure 3 neutral instability for this case may occur in one of three distinct modes, depending on the values of x_{co}/x_m and E. For values of x_{co}/x_m less than 0.01, no instability can occur for values of E less than 1.0. For values of x_{co}/x_m between 0.01 and 0.07, corresponding to relatively large values of zero sequence capacitance, the unstable voltage appearing across the broken delta is approximately of one-half normal frequency. Intermediate values of x_{co}/x_m (between 0.07 and 0.55) give rise to a fundamental frequency Δ voltage, and large values of x_{co}/x_m (between 0.55 and 2.8) give rise to a third harmonic Δ voltage.

The first of these three abnormal conditions is illustrated by the oscillograms in figure 4*a*. For the case $x_{co}/x_m=0.026$ and $E=0.58$, oscillogram 76-10 shows the broken Δ voltage V_Δ with a single line-to-ground fault on phase *a*. This, of course, is of fundamental frequency and approximately three times normal leg voltage. Oscillogram 77-5 shows the transient V_Δ to the same time and amplitude scale following the removal of the fault on phase *a* at a normal current zero without any subsequent restriking in the fault. It will be observed that this transient voltage is approximately half fundamental frequency. Oscillogram #77-6 shows, with the same calibration, the ultimate steady-state voltage appearing across the break in the Δ. It can be seen that this also is approximately one-half fundamental frequency, of very good wave form, and essentially of the same amplitude as though a line-to-ground fault were on the system.

This phenomenon is referred to as being essentially of $^1/_2$ frequency. Actually it differs from one-half fundamental frequency by a small amount such that line-to-neutral voltages vary with time at a very low beat frequency. Oscillogram 77-7 shows the transient recovery voltage on phase *a*. 77-11, 12, and 13 show the steady-state line-to-neutral voltages on phases *a*, *b*, and *c*, respectively. Oscillograms 77-14, 15, and 16 show the same three respective voltages at a later time to illustrate how slowly the voltages to ground are shifting, due to the "slip" frequency involved giving rise to a beat frequency component of voltage. Phase voltages reach a maximum of two times normal line-to-neutral crest for this case. Transformer currents may be very high for this condition because of the presence of this low frequency component of voltage as will be shown later.

The fundamental frequency phenomenon is illustrated by the oscillograms in figure 4*b* for $x_{co}/x_m=0.123$ and $E=0.58$. Oscillograms 32-1, 2, and 3, show steady-state voltages to ground on phases *a*, *b*, and *c*, respectively, while 32-8 shows the sustained voltage appearing across the break in the Δ. This condition is very nearly the same as if a fault existed

on phase c to ground. The voltage on phase c is very low—in fact, the fundamental frequency component appears to be practically zero. Voltages to ground on phases a and b are essentially line-to-line voltages of fundamental frequency, and the broken Δ voltage gives every indication of a fault without there being any fault on the system. The presence of subharmonics of one-half and of one-ninth frequency are evident in the oscillograms.

The third harmonic phenomenon is illustrated in figure 4*c* for $x_{co}/x_m=0.594$ and $E=1.0$. Oscillograms 32-9, 10, and 11 show voltages to ground (one cycle of fundamental frequency) on phases a, b, and c, respectively, while 32-16 shows the voltage appearing across the break in the Δ. The broken Δ voltage is of third harmonic frequency with good wave form and of higher magnitude than that obtained for a fault on the system. Voltages to ground on all three phases are the same in magnitude (about four times normal line-to-neutral crest). There are no sub harmonics present in this case.

The normal condition for the same system ($x_{co}/x_m=0.594$) and operating voltage ($E=1.0$) is illustrated by the oscillograms in figure 4*d*. While the system constants are identical with those for the case discussed in the preceding paragraph

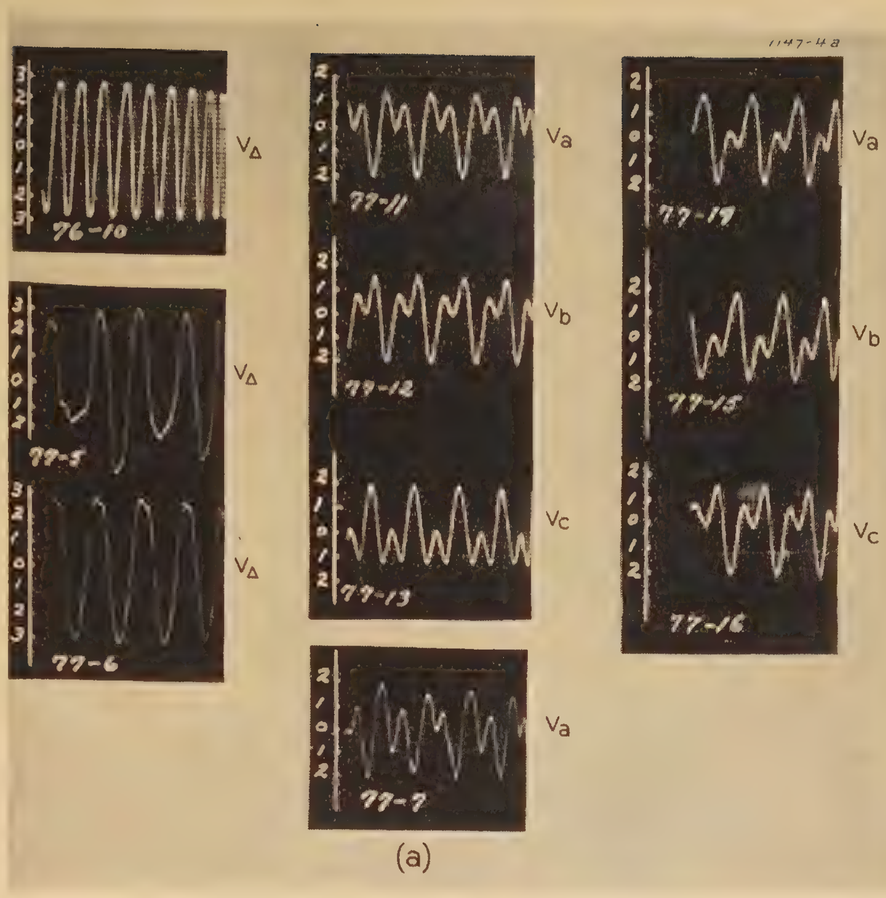

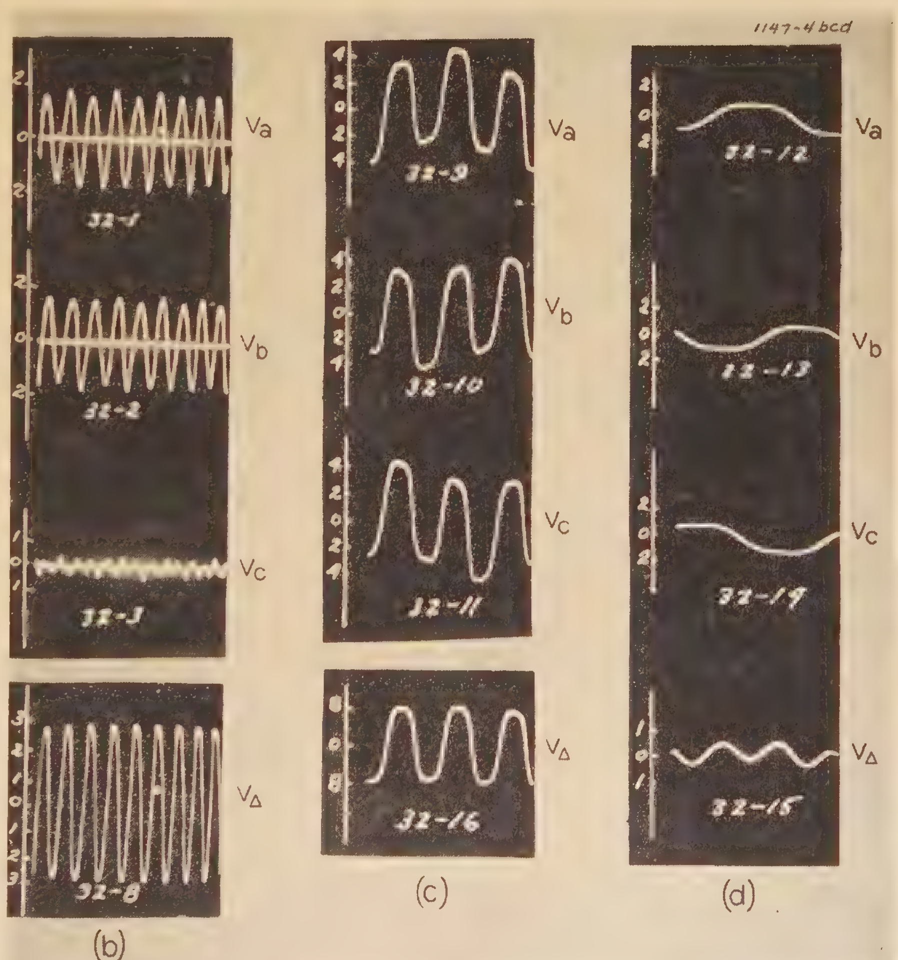

Figure 4a (upper right). Oscillograms illustrating the abnormal condition giving rise to one-half normal frequency broken Δ voltages and balanced phase voltages-to-ground

$x_{co}/x_m=0.026$, $E=0.58$

Note: All voltage calibrations are times normal line-to-neutral crest voltage on the system side of the transformer

Figure 4b. Oscillograms illustrating the abnormal condition giving rise to fundamental frequency broken Δ voltages and unbalanced phase voltages-to-ground

$x_{co}/x_m=0.123$, $E=0.58$

Note: All voltage calibrations are times normal line-to-neutral crest voltage on the system side of the transformer

Figure 4c. Oscillograms illustrating the abnormal condition giving rise to third harmonic broken Δ voltages and balanced phase voltages-to-ground

$x_{co}/x_m=0.594$, $E=1.0$

Note: All voltage calibrations are times normal line-to-neutral crest voltage on the system side of the transformer

Figure 4d. Oscillograms illustrating the normal condition of some third harmonic voltage across the Δ break with balanced voltages-to-ground

$x_{co}/x_m=0.594$, $E=1.0$

Note: All voltage calibrations are times normal line-to-neutral crest voltage on the system side of the transformer

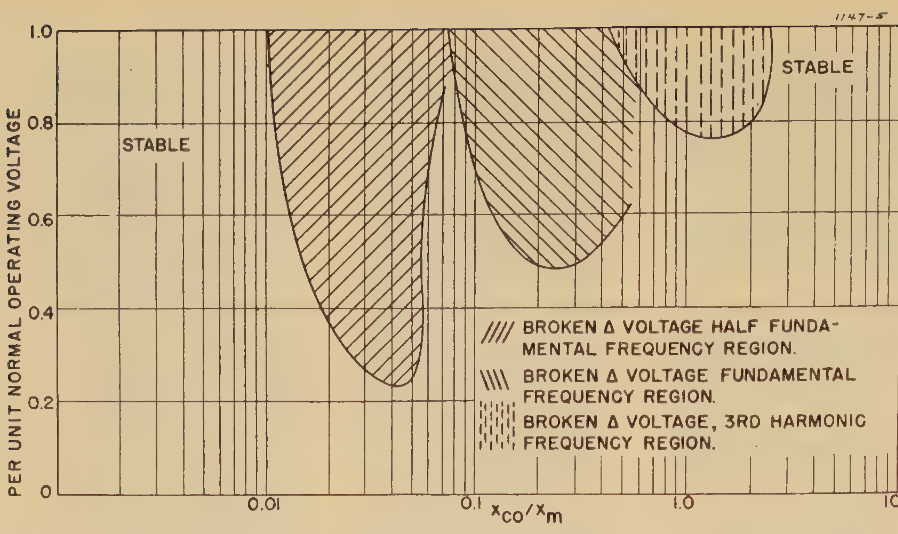

Figure 5. Regions of possible instability of the circuit of figure 1 with transformer saturation corresponding to curve 1 of figure 2

$r/x_m=0.0007$ for the transformer r—D-c resistance of the winding

x_m—Ratio of rms sinusoidal leg volts to rms phase current at a point on the saturation curve corresponding to $E=1.0$ in figure 2

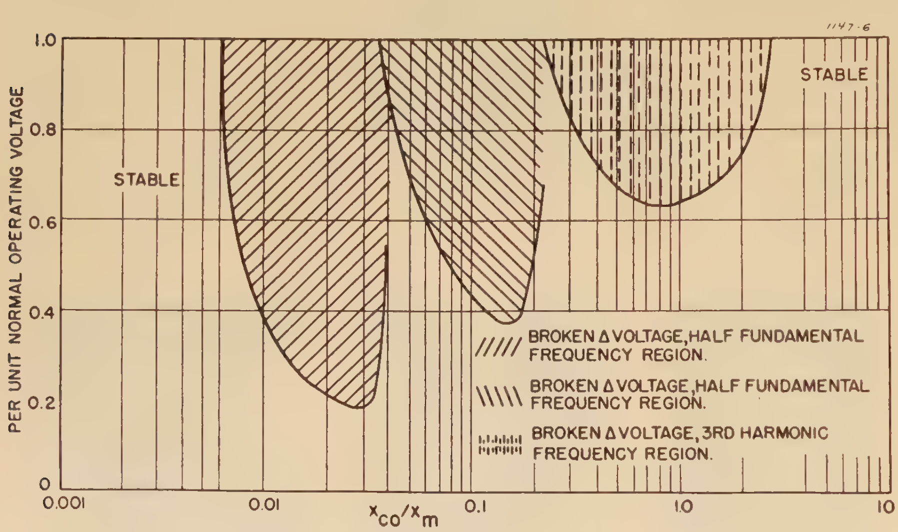

Figure 6. Regions of possible instability of the circuit of figure 1 with transformer saturation corresponding to curve 2 of figure 2

$r/x_m=0.0003$ for the transformer r—D-c resistance of the winding

x_m—Ratio of rms sinusoidal leg volts to rms phase current at a point on the saturation curve corresponding to $E=1.0$ in figure

the voltage conditions are quite different, corresponding to "normal" behavior of the circuit. As shown previously, circuits involving saturable impedance elements may give rise to voltage and current conditions which are not single valued functions of the circuit parameters.[5] For this case ($E=1.0$ and $x_{co}/x_m=0.594$), as in many others which could be used as illustrations, either of these conditions may be obtained, the one "abnormal" and the other "normal." Oscillograms 32-12 to -14, inclusive, show the balanced voltages-to-ground on phases a, b, and c, respectively, while 32-15 shows the broken Δ voltage. A third harmonic component is in evidence in this case also, but it is only a very small fraction of that present for the abnormal condition illustrated in oscillograms 32-9 to -11, inclusive, and 32-16. It is also much lower in magnitude than that obtained for the condition of a fault on the system.

Dividing lines between these three distinct modes of instability are not very clear-cut in all cases. For example, in the vicinity of $x_{co}/x_m=0.01$ but in the unstable region, $^1/_4$ frequency components of voltage were in evidence, although the $^1/_2$ frequency components predominated, other subharmonics were also present. sometimes of very low frequency, in this portion of the unstable region.

In the vicinity of $x_{co}/x_m=0.08$, the unstable phenomenon was mainly a combination of fundamental frequency and $^1/_2$ fundamental frequency. The dividing line might be considered as an indication of where for increasing values of x_{co}/x_m the phenomenon changes gradually from something predominantly of $^1/_2$ fre-

Figure 7 (below). Abnormal voltage and current conditions obtained for the circuit of figure 1

Transformer saturation corresponding to curve 1 of figure 2

$E=1/\sqrt{3}=0.58$ $r/x_m=0.0003$

——— Voltage - - - - - - - Transformer current

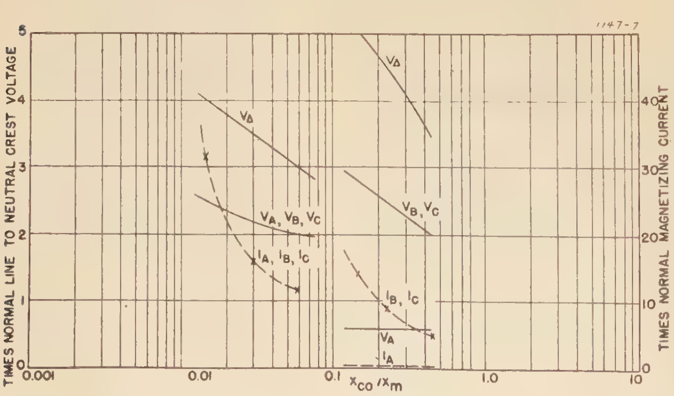

Figure 8. Effect of resistance burden R in the broken Δ on regions of instability

Saturation curve of figure 1 $r/x_m=0.0003$

Note: The total amount of resistance in the Δ is three times the amount of R indicated by the curves since R/x_m is on a per leg basis

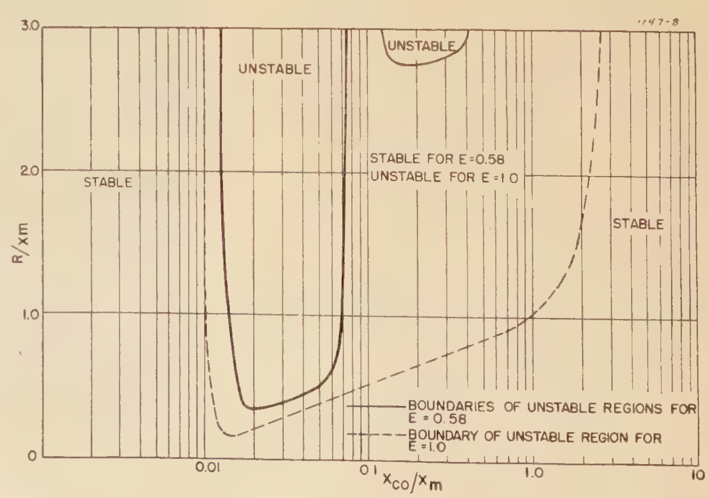

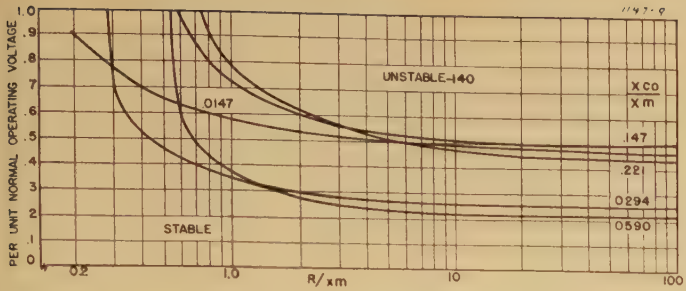

Figure 9. Illustration of the relationship between operating voltage and resistance burden to obtain stability for various values of capacitive reactance

quency to something of predominantly fundamental frequency.

In the vicinity of $x_{co}/x_m=0.5$, the phenomena included a component of approximately twice normal frequency. This was observed only for a very limited range of values of x_{co}/x_m, and the other abnormal conditions occurring over greater ranges of this ratio, were considered of far greater importance.

These facts are pointed out merely to indicate the physical consistency of the information plotted in figure 3. The ratio x_{co}/x_m is proportional to the square of the natural frequency of the circuit studied. For very small values of this ratio, the circuit is always stable. As the ratio is increased beyond a certain value instability is encountered and the unstable phenomena are characterized in succession by voltage components of $^1/_4$, $^1/_2$, 1, 2, and 3 times normal frequency. Thus the predominant frequency of the phenomena is seen to increase consistently with the natural frequency of the circuit.

The effect of increased transformer resistance is shown in figure 5, i.e., greater than that shown in figure 3. It is of importance to note that the regions of instability are only very slightly affected by resistance over a practical range. This fact makes the results of the investigation much more widely applicable.

The results shown in figure 6 were obtained for the saturation curve #2 of figure 2. This curve is somewhat steeper than that likely to be encountered in most actual cases, but the results are of interest in that they show how the unstable regions are broadened and shifted so as to extend the range of instability to lower values of the ratio x_{co}/x_m. This effect is consistent with other phenomena observed in connection with circuit analysis involving saturable impedance elements.[5] The effect of saturation is to broaden the range of abnormality, the broadening effect increasing with increasing abruptness of saturation.

For line-to-line voltage rated potential transformers connected line-to-neutral $E=0.58$ and the regions of instability given in figure 3 are $0.013<x_{co}/x_m<0.075$ and $0.125<x_{co}/x_m<0.45$. Crest values of broken delta voltage, line-to-ground voltage, and of transformer current that may be obtained within these regions are given in figure 7. In the region corresponding to the fundamental frequency broken Δ voltage the voltage-to-ground of one phase is of small magnitude. The voltages-to-ground on the other two phases are approximately equal. Thus line voltages-to-ground as well as the broken Δ voltage are essentially the same as if a fault were on the system.

In the region corresponding to the one-half frequency broken Δ voltage condition, the voltages-to-ground are the same in magnitude on all three phases. However, an interval of several seconds must be considered for this to be true because of the slow "slip" frequency involved as previously described.

The transformer current values shown in figure 7 are of interest also. In the region of one-half frequency phenomena these currents may reach values of 35 times normal magnetizing current in the vicinity of $x_{co}/x_m=0.015$. These currents are the same in magnitude in all three phases. In this range it might be possible to blow potential transformer fuses under such abnormal conditions. In the region of fundamental frequency phenomena the currents are smaller in general, and furthermore, the current in one phase is lower than normal. It is a significant fact that while the voltage conditions in this range of x_{co}/x_m approximate those obtained during a single line-to-ground fault, the currents flowing in the Y winding of the potential transformer may be 10 or 15 times as high as those obtained during a single line-to-ground fault condition, depending upon the ratio of x_{co}/x_m.

Figure 8 shows the results of inserting resistance, R, in the break in the Δ secondary. The curves show that the heaviest burden (lowest resistance) to insure stable operation is required when x_{co}/x_m is about 0.02 or slightly less depending upon the normal system operating voltage. At the lowest point, $R/x_m=0.15$ for operation at $E=1.0$ and $R/x_m=0.34$ for operation at $E=0.58$. These values are on a basis of resistance per leg in per unit of magnetizing impedance per leg for $E=1.0$ on the saturation curves of figure 2. Therefore the curve gives the resistance required per phase for Y-connected secondaries. The value of impedance required across the break in the case of broken Δ secondaries as in figure 1 is three times the quantity R/x_m of figure 8.

The effect of normal operating voltage E on the R/x_m ratio required for stabilization is shown in figure 9. It is of importance to note that as E decreases, the ratio of R/x_m required for stability increases. The values of x_{co}/x_m used in preparing these curves were purposely selected in the range requiring the lowest ratios of R/x_m as indicated in figure 8.

The effect of an inductive reactance burden x_L (power factor=0.2) is indicated in figure 10. A lower ratio of x_L/x_m is required for stabilization than of R/x_m as discussed in the preceding paragraph. The ratio of x_L/x_m at its lowest point is 0.04 for operation at $E=1.0$ and 0.28 for operation at $E=0.58$.

The effect of a leading power factor (capacitive) burden in the break in the Δ was investigated and the results indicated that pure capacitance was not satisfactory. The same conclusion holds for wave traps

Figure 10. Effect of inductive reactance burden x_L(0.2 power factor) in the broken delta on regions of instability

Saturation curve 1 of figure 2

Note: The total amount of reactance in the delta is three times the amount of x_L indicated by the curves since x_L/x_m is on a per leg basis

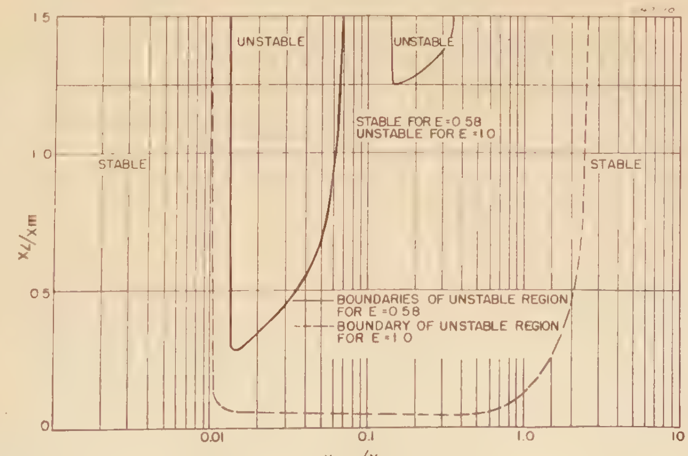

which were made up of a reactance and capacitance tuned to the third harmonic. These were not effective because other complicating phenomena were encountered which were difficult to account for. Consequently a resistance burden appears to be the simplest and most effective means of insuring stability by means of a secondary burden. Reactance was effective, although a reactance ohmic value would have to be smaller than that of a resistance to insure stability.

Conclusions

1. In using Y grounded primary broken Δ or Y-connected secondary potential transformers for metering or relaying, it is necessary to consider the amount of capacitance to ground that may be permanently or temporarily connected at the terminals of the transformer in order to avoid the possibility of abnormal voltage conditions brought about by circuit instability which might cause incorrect indications of faults. For line-to-line voltage rated potential transformers connected line-to-neutral, corresponding to general practice in the application of such devices ($E=0.58$ in the paper), the range of possible abnormality is defined approximately by $0.012<x_{co}/x_m<0.6$. If a given circuit is found to fall within this range, normal behavior can be insured by:

(*a*). Adding shunt capacitance to ground on the system side of the transformer until the resultant ratio of x_{co}/x_m becomes equal to or less than 0.012, or

(*b*). Connecting load across the break in the broken Δ secondary or in each phase in the case of Y-connected secondary. If resistance is used, it should have a value per phase of 33% of the magnetizing reactance x_m per phase or less; if reactance is used, its ohmic value per phase should not be greater than 28% of x_m per phase. In either case, x_m is referred to the secondary side in accordance with the transformer turn ratio. The impedances required for stabilization are high enough so as not to interfere with the normal functioning of the device.

For these criteria, x_{co} is the zero sequence capacitive reactance to ground on the Y grounded side of the transformer and x_m is the magnetizing reactance per leg corresponding to $E=1.0$ on the saturation curve 1 of figure 2.

2. The regions of abnormality as well as the abnormal phenomena observed are practically unaffected by resistance in the transformer windings or by losses in transformer iron over a practical range.

3. Increasing the steepness of the saturation curve tends to increase the range of possible abnormal circuit behavior. In particular, the region of abnormality is extended to lower values of x_{co}/x_m as the steepness of saturation is increased.

4. For conditions of operation above transformer flux densities corresponding to the normal practice of using *L-N* connected potential transformer with *L-L* voltage rating ($E=0.58$ in the paper), abnormal circuit behavior is extended to include a range of $0.01<x_{co}/x_m<3.0$ approximately for $E=1.0$. Furthermore, the impedance in the open Δ must be made smaller if stability is to be insured. For $E=1.0$, a resistance in the break in the Δ not greater than 45% of x_m (15% of x_m per phase) or a reactance not greater than 12% of x_m (4% of x_m per phase) would be required to avoid abnormal circuit behavior independent of x_{co}/x_m.

References

1. Theory of Abnormal Line-to-Neutral Transformer Voltages, **C. W. LaPierre.** AIEE Transactions, volume 50, 1931, pages 328–42.

2. Physical Nature of Neutral Instability, **A. Boyajian** and **O. P. McCarty.** AIEE Transactions, volume 50, 1931, pages 317–27.

3. Experiences With Grounded-Neutral Wye-Connected Potential Transformers on Ungrounded Systems, **C. T. Weller.** AIEE Transactions, volume 50, 1931, pages 299–316.

4. An Electric-Circuit Transient Analyzer, **H. A. Peterson.** *General Electric Review*, volume 42, September 1939, number 9, pages 394–400.

5. Abnormal Voltage Conditions in Three-Phase Systems Produced by Single-Phase Switching, **Edith Clarke, H. A. Peterson, P. H. Light.** AIEE Transactions, volume 60, 1941, pages 329–39.

Field Testing of Generator Insulation

EEI SUBJECT COMMITTEE ON GENERATOR INSULATION AND TESTING

I—Introduction

NEED for a practical as well as a reliable nondestructive test that will determine the condition of generator insulation has long been recognized by the industry. Simple methods now in general use, the high voltage proof test and the insulation resistance test, do not accurately or positively disclose the overall condition of windings, indicate the degree of deterioration, or necessarily locate weak spots. This lack of suitable insulation tests has been emphasized recently by the return to service of a number of machines either after long shutdown periods during the depression years or from standby service to low pressure elements used in connection with topping units; in these cases knowledge of insulation condition is vital.

As a result of this situation the Edison Electric Institute electrical equipment committee undertook active work on the problem in 1935.[1] In 1937 a special subject committee was appointed on "Generator Insulation and Testing," with the ultimate object of developing a reliable test procedure for determining the condition of generator insulation. The investigation has been carried out by various member companies of the EEI and others in the industry interested in the problem, under the guidance of the subject committee. Close contact has also been maintained with the manufacturers who have made many valuable suggestions, assisted in testing, and given aid in analyzing data.

The study is by no means complete and this paper should not be construed as a final report with definite conclusions, but rather as a progress report on an investigation still under way.

II—Present Status of Insulation Testing

Present testing practice in this country was surveyed in 1938, revealing a wide variation in testing methods and procedure. High voltage proof testing which consists merely of the stressing of the insulation by the application of an alternating potential according to the rules in the AIEE Standards is generally used for acceptance tests for new and repaired machines. There is no general agreement as to advisability of routine proof testing nor magnitude nor frequency when such tests are applied to machines in service. Insulation resistance testing is a common practice though generally a definite routine is not followed. In the past the procedure often has consisted of a "crank and read" type of measurement. Today, increasing recognition is being given the fact that insulation resistance values may be misleading unless careful account is taken of the many factors which may affect the results. No definite practice seems to be established regarding other methods of test, such as high voltage d-c resistance, dielectric loss or power factor tests.

Comparatively few operating companies maintain regular schedules of periodic insulation testing, from which records may be obtained to serve as a guide of the progressive condition of the insulation. Such special tests as are made are carried out usually after a machine winding has been repaired or an inspection indicates it to be in questionable condition.

Foreign practice in this respect also indicates a lack of uniformity. In some countries, notably Germany and Switzerland, experiments have been made with dielectric loss measurements, and it is felt there that this type of measurement has some promise of value as an index of changing insulation condition. A few experiments have made use of a recording instrument giving a curve of dielectric losses versus time during machine operation. It has been suggested that this method may give a definite index of changing conditions within the insulation. The method has not received broad use.

III—Scope of Work

Originally it was the objective of the subject committee to conduct destructive and nondestructive tests on insulation of machines about to be scrapped, rewound, or repaired and to develop from these a workable nondestructive method of determining insulation condition. Valuable information has been obtained from these tests but inasmuch as many of the data consist of "spot" readings taken under a variety of conditions, it has not been possible to correlate all of the data nor to draw definite conclusions. Real need for periodic and standardized measurements has become apparent. The scope of the investigation has been broadened to include and encourage the collection of periodic nondestructive test data on machines in service. By this means information is being accumulated on all classes of insulation, from the old to the new.

Insulation characteristics of both armature and field windings are undergoing investigation. Table I summarizes the machines tested or under test. The machine ratings vary from 1,500 kva, 2,700 volts to 200,000 kva, 16,500 volts

Table I

Type of Test	Number of Machines
Insulation resistance	106
Power factor of insulation	27
Ionization	8
Voltage strength a-c	21
Voltage strength a-c versus d-c	6*

* Includes 2–2.3 kv motors.

Paper 41-17, recommended by the AIEE standards committee, and presented at the AIEE winter convention, Philadelphia, Pa., January 27–31, 1941. Manuscript submitted November 6, 1940; made available for preprinting December 6, 1940.

Personnel of EEI subject committee on generator insulation and testing: C. M. Gilt and B. Van Ness, Jr., subject sponsors; R. L. Webb, chairman; J. E. Allen, E. F. Dissmeyer, O. E. Fawcett, A. P. Hayward, R. J. Woodrow.

The subject committee wishes to acknowledge the assistance and co-operation rendered in this work by EEI member companies and engineers, by other engineers and utility companies, and by the manufacturers.

1. For all numbered references, see list at end of paper.

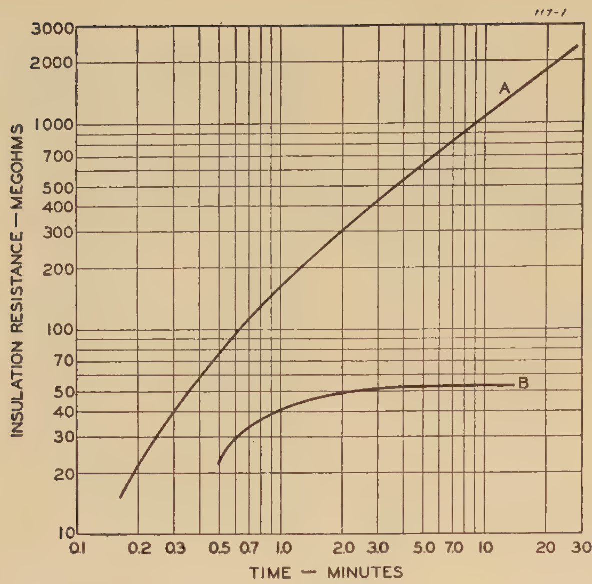

Figure 1. Armature-winding insulation resistance versus time

A—200,000-kva single-barrel generator, 16.5 kv, 60 cycles, 1,800 rpm (insulation dry)

B—18,750-kva single-barrel generator, 13.2 kv, 60 cycles, 1,800 rpm (insulation moist)

The subject committee, recognizing the need for uniform practice in insulation testing, has prepared a guide to be used in making such tests. Copies of this are available to the industry through EEI headquarters.

IV—D-C Insulation Resistance

Although d-c insulation resistance is among the most commonly used methods for testing the insulation of electrical apparatus, records obtained have been baffling of interpretation, and the factors which affect the results are to some extent unknown and often unappreciated. The fundamental that different types of insulating materials may have different volume resistances is obvious; but there are other variables which affect successive tests on a given piece of apparatus and cause widely varying results.

Tests have been directed to establish the manner in which the insulation resistance varies with

(*a*). Differences in insulation materials and structures
(*b*). Duration of voltage application
(*c*). Existing charge in windings
(*d*). Insulation temperature
(*e*). Test voltage magnitude
(*f*). Insulation moisture content
(*g*). Previous operating condition of the generator
(*h*). Various types of winding damage or deterioration

These investigations have confirmed findings obtained in similar experiments made by others and have gone somewhat further in extending the limits to which such tests have been conducted in the field.

Instruments

Experiments made so far have indicated that any one of several types of test instruments will give satisfactory insulation resistance results. Commercial forms of insulation resistance testers perform satisfactorily provided they are calibrated periodically and tested to assure their voltage output is proper. The maximum voltage at which measurements have been made with these instruments is 5,000 volts, d-c. Motor driven devices or other constant voltage generators are necessary for taking long time insulation resistance curves. Hand operated units may be used for short time readings.

The voltmeter method may be used with fair accuracy if the insulation resistance is less than 10 megohms. To insure accuracy of readings a high resistance voltmeter should be used.

Considerable success has been attained with electronic rectifier sets having d-c outputs from 100 to 5,000 volts and with dry cell battery sets up to 1,500 volts. These use a voltmeter and a microammeter for measurements which permit calculation of insulation resistance. They must be carefully shielded and guarded.

Higher voltages may be obtained from Kenotron test sets. Tests may be carried to any reasonable limit of voltage with this type of equipment, though 5,000 volts appears to be the present limit for sets portable by hand. In all rectifier sets it is essential that a steady supply of voltage be available to prevent fluctuation in charging current to the generator winding capacitance, an automatic voltage regulator being used if necessary.

Where protective resistors are used in test instruments their effect on the voltage magnitude applied to the insulation should be carefully taken into account.

Duration of Voltage Application

While many insulation resistance measurements have been taken by the "crank and read" method, Wieseman[2] and others have shown that the insulation resistance of a winding varies with duration of voltage application. Insulation resistance of a dry winding in good condition may continue to increase for as long as a day or more with the test voltage applied continuously at a steady value. Normally an approximately final value, which is termed "apparent insulation resistance" may be reached after 10 to 15 minutes. Insulation resistance after 30 seconds to 60 seconds may be as little as 10 per cent to 20 per cent of the 15-minute reading.

In figure 1 insulation resistance versus time curves, commonly referred to as dielectric absorption curves, are shown for different conditions of generator insulation. Curve *A* is a good example of the effects of "bone dry" and clean insulation on the final value of insulation resistance and on the shape of the dielectric absorption curve. This curve represents an unusually high insulation resistance for a machine whose rating is 200,000 kva, 16,500 volts, in one stator winding. Curve *B* was taken on an 18,750-kva, 13,200-

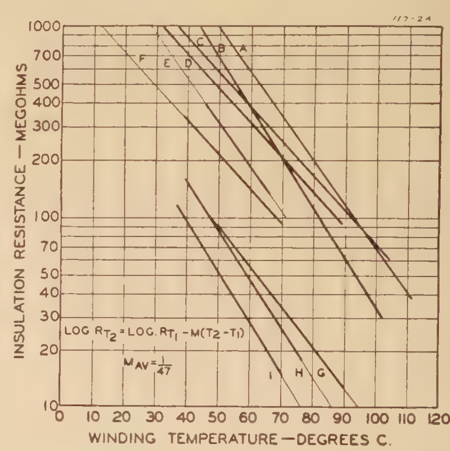

Family having more common slope. Data taken at 500 to 20,000 volts after ten minutes

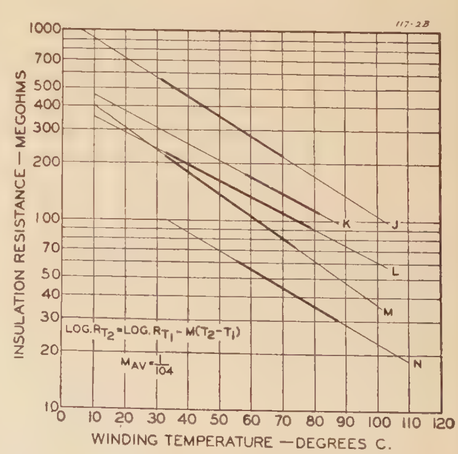

Family having lowest slopes. Data taken at 1,000 to 8,000 volts after one to ten minutes

Figure 2. Insulation resistance versus temperature

volt generator which had been exposed to varying degrees of atmospheric humidity for several years. Considering size alone this smaller unit would be expected to have a higher insulation resistance than the larger unit. However, the insulation conditions are such that the reverse is the case. Leakage resistance effects predominate and the curve flattens rapidly between the 30-second and the 3-minute readings.

Information contained in curves of this nature discloses the reason for at least one difficulty in past attempts to correlate insulation resistance readings, for it is obvious that "spot readings" made without regard to definite time of voltage application can give widely varying results.

Many dielectric absorption curves have been collected. While it is believed that these data give information as to dryness and cleanliness of winding, spot curves have not disclosed a positive relation between insulation resistance and insulation condition. Therefore, periodic curves are being taken and the behavior of the dielectric absorption factor over a long period is being observed and analyzed.

Effect of Existing Charge on Winding

Comparative values of winding insulation resistance are markedly affected by residual charges retained in a winding. For this reason windings should be grounded and discharged for at least ten minutes before applying insulation resistance tests.

Insulation Temperature

Tests have indicated that the insulation resistance of windings is affected greatly by temperature. The most marked effect occurs in class *A* windings but even in class *B* insulation structures, the insulation resistance may vary as much as 10 to 1 for a winding temperature change from approximately 25 degrees centigrade to 75 degrees centigrade, the insulation resistance being lower at the higher temperature.

It is desirable that insulation resistance readings be taken at temperatures as close to 75 degrees centigrade as possible, to secure an indication of resistance at operating temperatures, eliminating the effect of humidity and requiring minimum temperature correction.

Figure 2 gives the results of field tests undertaken with the objective of establishing factors which will permit readings taken at one temperature to be transferred to a lower or higher temperature. The results so far indicate two families of curves, with similar characteristics of in-

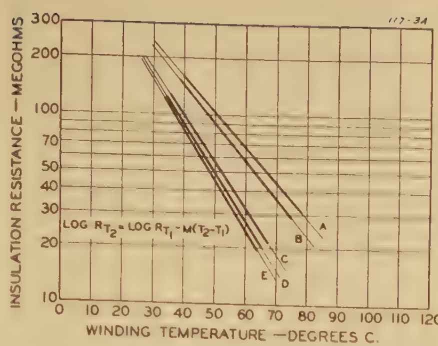

68,750-kva turbogenerator, 13.2 kv, 60 cycles, 1,800 rpm

Data taken following acceptance test run

A Insulation resistance at 10 min.—$M = 1/_{58}$
B Insulation resistance at 4 min.—$M = 1/_{50}$
C Insulation resistance at 1 min.—$M = 1/_{41}$
D Insulation resistance at 30 sec.—$M = 1/_{39}$
E Insulation resistance at 15 sec.—$M = 1/_{38}$
Avg.—$M = 1/_{44}$

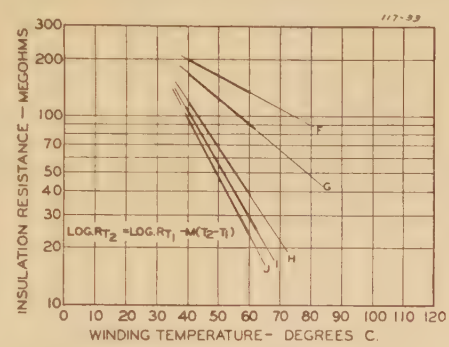

Data taken following about two years of base-load service

F Insulation resistance at 10 min.—$M = 1/_{115}$
G Insulation resistance at 4 min.—$M = 1/_{74}$
H Insulation resistance at 1 min.—$M = 1/_{41}$
I Insulation resistance at 30 sec.—$M = 1/_{36}$
J Insulation resistance at 15 sec.—$M = 1/_{34}$
Avg.—$M = 1/_{60}$

Figure 3. Insulation resistance versus temperature for different periods of voltage application

sulation resistance versus temperature in each group. The curves may be represented by the formula:

$\log R_{t_2} = \log R_{t_1} - M(t_2 - t_1)$

where R_{t_2} and t_2 are the unknown resistance and temperature at which the resistance is desired, R_{t_1} and t_1 are the measured resistance and the related winding temperature and M is a constant equal to the reciprocal of change in temperature for $\log R = 1$. Insulation resistance doubles for each 14 degree centigrade reduction in winding temperature for the curve whose $M = 1/_{47}$, and doubles for each 31 degree centigrade reduction for the curve whose $M = 1/_{104}$.

Although it might be assumed that the two families of curves bear definite relation to insulation class, this is not the case. Machines with both class *A* and class *B* windings appear in each group.

Operating conditions apparently have a large effect on these characteristics, for data indicate that even after years of operation changes in the value of M for a given machine may occur from year to year. This is evident from figure 3 in which the curves having an average value for $M = 1/_{44}$ were taken in 1938 shortly after a new generator was placed in service. The curves having an average value for $M = 1/_{60}$ were taken on this same machine approximately two years later. The machine had been operated about 72 per cent of the elapsed time at an average of 95 per cent of rated capacity and had been run for several days, well loaded, before the last test. It is apparent, therefore that the value of M may vary for a given machine but it is not known definitely whether this variation is due to differences in moisture or volatile matter content in the insulation, or whether it is due to some aging or curing action which has been under way during the many continuous hours of high load operation. It is believed that moisture is the most likely cause of the variation.

While extrapolation of the curves of figure 3 appears to meet in a point at low temperatures other data indicate parallelism or a meeting at high temperatures. The reason for and meaning of these variations are not known.

No definite formula applicable to all machines, or even to the same machine under various conditions, can be given at this time for the relation of insulation resistance to temperature. Two readings taken at the same date on a machine will establish a curve for that machine for a definite condition of the insulation. A change in slope of an insulation resistance-temperature curve indicates a change in the insulation condition.

Effect of Moisture Content

Accurate insulation resistance data are very useful in determining the progress of drying machine insulation. It is customary to dry a machine until the insulation resistance readings at constant temperature approach a constant value when plotted with regard to time. When drying out, the attainment of a constant insulation resistance at a constant temperature is a better indication of dryness than is the attainment of some previously selected value.

Figure 4 indicates the variation of insulation resistance of a new turbo-generator whose winding is being dried. Each point of insulation resistance was taken after ten minutes application of test voltage. The insulation resistance dropped rapidly as the winding temperature in-

creased and then recovered as the moisture was driven from the insulation. When the test was terminated, the insulation resistance rose rapidly as the winding temperature decreased.

Figure 5 gives another method of plotting similar data as taken on the initial dry-out run of a 37,500-kva water-wheel generator and illustrates the value of the one- and ten-minute readings in obtaining a clear picture of the conditions during machine dry-out. It will be noted that as the run progressed the separation between the curves increased, indicating an effective drying of the insulation and the resulting increase of absorption effect in the dielectric.

by the increased machine temperature.

An interesting case, illustrating the use of insulation resistance curves in determining the effects of moisture, concerns a machine which had been subjected to flood waters. After dry-out, the insulation resistance increased to a satisfactory though not a high value and the machine was placed in service. The unit was operated with cooling air supplied through a spray system equipped with baffles for removing water from the air before it reached the generator. Later, after fairly continuous service, the generator was found to have low insulation resistance. The cooling air was suspected of carrying moisture into the machine and preventing thorough

Effect of Test-Voltage Magnitude

Insulation resistance measurements at 75 degrees centigrade of dry insulation in good condition will be affected very little by wide variations in test voltage. The effect appears to increase somewhat at lower temperatures as will be noted on figure 7. Windings having high leakage due to moisture or dirt, or other types of deterioration, may show a more pronounced reduction in insulation resistance as the test voltage is increased.

Results of complete tests on two machines, have indicated there may be some merit in comparisons between insulation resistance measurements at two different d-c voltages, at the same winding tem-

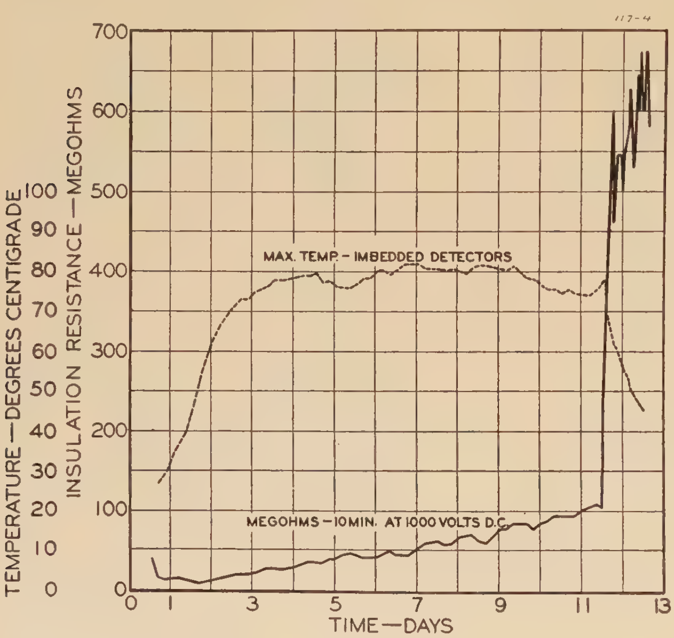

Figure 4. Change in ten-minute insulation resistance with time during generator dry-out

35,300-kva turbogenerator, 13.8 kv, 60 cycles, 1,800 rpm

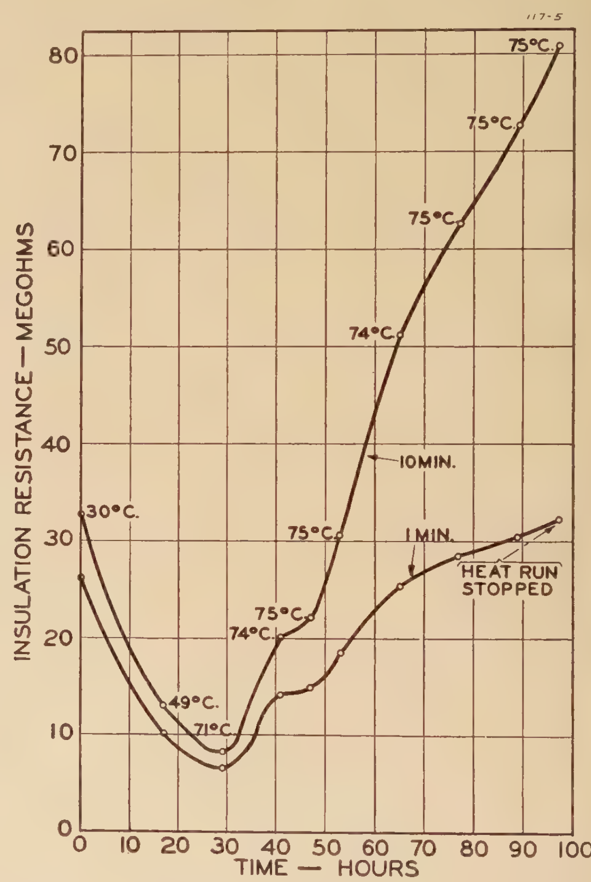

Figure 5 (right). Change in one-minute and ten-minute insulation resistance with time during generator dry-out

37,500-kva hydrogenerator, 13.3 kv, 25 cycles, 100 rpm

The degree of moisture content in the outer layers of generator winding insulation has a very marked effect on the insulation resistance. A machine which has been running regularly will generally have a much higher insulation resistance at room temperature than the same machine after being idle for several weeks in a humid atmosphere. A relatively low insulation resistance resulting from exposure to moist air does not necessarily mean that the insulation is inferior or that the machine is not safe for operation. If the insulation resistance is still reasonably high for the machine in question as shown by reference to periodic test data it may be returned to service and the moisture will be driven from its windings

drying. The unit was operated under test load for two hours using relatively dry turbine room air for generator cooling to learn of its effect on insulation resistance. Curves *A* and *B* of figure 6 show the insulation resistance results before and after this change in cooling air. As a result of these tests the unit, and several others in the same plant were equipped with surface coolers and a closed ventilating system, with improvement in insulation resistance as shown by curve *C* of figure 6.

Spray type air washers have not caused similar trouble at certain other locations where the same type of tests were made on generators whose windings had not been submerged.

perature. A 25,000-kw generator winding section was given a dielectric absorption test at 2.5 kv and at 15 kv d-c. The coils were then punctured on a 60-cycle high potential test and the insulation resistance values at the two voltages were again taken. The first test gave a ratio of approximately 2 to 1 with the 2,500-volt measurement being higher. The second test gave an insulation resistance ratio of approximately 6 to 1 after the insulation had been punctured. This test was repeated on another coil group and the ratio changed from approximately 2 to 1 to a ratio of approximately $4^1/_2$ to 1.

The stator winding of a 30,000-kva synchronous condenser was found in very

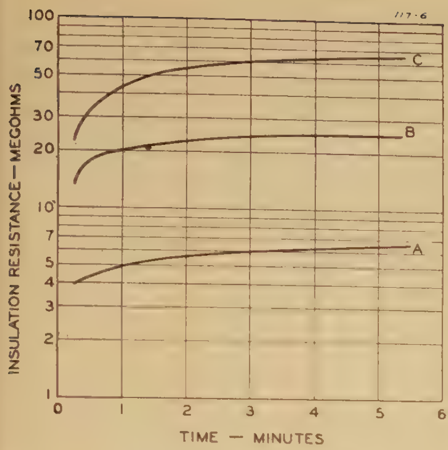

Figure 6. Armature-winding insulation resistance versus time

25,000-kva generator, 13.2 kv, 60 cycles, 1,800 rpm

Tests made at 500 and 1,000 volts d-c. Winding temperature—74 degrees centigrade

A—After using a water-spray air washer. Cooling air humidity—78 per cent

B—After using turbine-room air at approximately 38 per cent humidity during a two-hour load run made immediately after test *A*

C—After using a closed ventilation system and surface coolers for about one month

bad condition on visual inspection in a plant where two machines of the same rating and age were operating. The insulation resistance of the winding which had to be replaced was found to have a ratio of more than 7 to 1 between the 2,500-volt and 20,000-volt tests, respectively. The insulation resistance of the other machine was found to have a relation of approximately 1.25 to 1 for the 500-volt and 10,000-volt tests and 1.2 to 1 for the 2,500-volt and 10,000-volt tests, respectively. The winding of this machine appeared to be in excellent condition.

While sufficient data have not been accumulated to permit final conclusions, they do indicate that a wide difference in insulation values determined by low and high voltage tests should lead one to suspect irregularities in the insulation. Efforts at conducting voltage tests under staged conditions by mechanical damage have met with poor success because of the difficulty of keeping reductions in the dielectric strength of armature bar insulation under control.

V—Insulation Power Factor

Power factor testing of generator windings is not in common use. Experiments have been made, however, to determine whether some test of this type may be useful and practical. The 60-cycle power factor of generator insulation has been studied for different winding temperatures and impressed voltages.

Equipment

Any well constructed and properly shielded power factor measuring equipment is satisfactory. Circuits of the test instruments must be thoroughly shielded and guarded to prevent interference from other energized equipment. Use of the ordinary wattmeter, voltmeter, and ammeter is not likely to give satisfactory results. Suitable commercial measuring equipment is available from several sources. A testing supply of ample capacity to furnish the charging current at the measurement voltage should be used.

Park and Skeats[4] have shown that generator winding capacitance can be determined fairly accurately by use of the formula $C = K_c \dfrac{\text{MVA}}{\sqrt{kv}(1+0.08\ \text{kv})}$ microfarads per phase.

The constant K_c has the following values:

	K_c	Assumed Peripheral Speed Ft/Min
Solid round rotors	0.0187	22,000
Salient-pole generators without amortisseurs	0.0347	10,000
Salient-pole generators with amortisseurs	0.0317	11,000

C is approximately inversely proportional to peripheral speed.

Capacitance of connecting cables must be added if included in the test.

Charging current at high voltage may be 25 per cent to 100 per cent above that determined by the capacitance constant alone, depending upon the extent of the corona losses, which vary with the impressed voltage.

Results

Power factor measurements on machine insulation may be affected by many conditions, most of which are similar to those outlined for d-c insulation resistance. The time of voltage application appears to have little effect on winding power factor unless it causes heating within the insulation. Winding temperature and moisture content will have a pronounced effect, and winding capacitance is, of course, an important factor. Voltage magnitude has an effect on power factor causing it to increase as the voltage is increased over the normal test range.

Insulation power factor should be nearly constant at each voltage below the ionization value.

Figure 8 shows the typical variations of winding power factor with different values of applied alternating voltage at different temperatures.

Power factor measurements have thus far produced little data which may be used to indicate insulation condition, other than moisture content.

No experiments have been conducted on dielectric loss characteristics by the subject committee. European engineers have had some success with this method, particularly as applied to control of manufacturing processes. It has received little attention as a means for supervising the insulation characteristics of an operating machine.

VI—Ionization Measurements

Both qualitative and quantitative ionization measurements[5] have been investigated to determine whether such measurements can be used to detect insulation irregularities in generator insulation. The quantitative tests were designed to obtain a characteristic showing the relative magnitudes of ionization discharge from a generator winding as the applied a-c voltage was varied, and to determine whether this might have any relation to the physical condition of the insulation or to its dielectric strength. Qualitative tests were designed to locate ionization points in the winding on the supposition that ionization would be present at weak points in the insulation.

Apparatus used for the qualitative tests is shown in figure 9. Equipment for the quantitative measurements was connected as indicated in figure 10. Complete shielding of the apparatus is necessary, and even then external disturbances due to radiations from energized equipment nearby are bothersome. For the quantitative tests the radiations in the radio frequency range were amplified, rectified, and measured by a sensitive d-c instrument. The measurements were relative only and not of any definite figure in amperes of ionization current.

Results of Qualitative Measurements

The qualitative ionization tests determined not only the impressed voltage at which ionization began, but were reasonably successful in determining the locations at which more severe ionization was present. On 6.6-kv and 11.4-kv generators having old winding designs varying in insulation structure from 100 per cent class *B* to all class *A* construction in the slot section, the voltage at which ionization was noted varied from about 1,000 volts to approximately 7,000 volts. The

Table II. Summary of Generator-Winding Insulation Tests* 1935–1940

Rating (Kva)	Voltage	Speed (RPM)	Armature Insulation: Age (Yrs.)	Armature Insulation: Type	Armature-Insulation Resistance: Megohms	Time (Min.)	Voltage	Temp. (°C)	Armature-Insulation Power Factor: Per Cent P.F.	Temp. (°C)	Voltage (Kv)	High-Voltage Breakdown (Kv): Armature 60 Cy.
12,000	11,400	750	16	B	2,000	6	500	20				35
12,000	11,400	750	15	B	1,150	10	500	20	11	20	6.6	45
20,000	6,600	1,500	22	B	300	10	500	22	6.7	22	3.8	39
20,000	6,600	1,500	22	B	350	10	500	22	6.5	22	3.8	43
14,000	7,800	720	30	A	310/185	10	500/5,000	20	11	20	4.5	46
					54/35	10	500/5,000	47				
68,750	13,800	1,800	0	B	200	10	8,000	36				
			2	B	208	10	8,000	36				
33,000	11,000	360	15	B	38/28	10	1,000/5,000	56				
55,000	11,000	360	5	B	285	20	5,000	48				
00,000	16,500	1,800	7	B	2,200	25	1,000	22				
15,000	13,200	94.7	2		36	10	1,000	22				26 (Before rewinding)
18,750	6,600	112.5	16	A	33	10	8,000	32	10	35	2.5	
									13	35	8	8 (Min.) 21.4 (avg. of 18 coils)
30,000	12,000	1,800	10	B	32/26	10	5,000/15,000	28				
30,000	9,250	1,500	0	B	700/500	10	4,000/9,000	30	7.5/9.0	30	4/10	
3,500	12,000	1,200	27	A	16and17	1	1,000	6	22 to 29 (Arm & Fld.)	1	3.5	22.5 Min. (avg.—51.5 kv) (2 units—same rating)
28,600	13,800	1,800	11	B	74	10	470					8 to 14 (3 coils tested)
23,750	11,000	1,200	21	B	40,000/coil	3	500	11	6.7 (Avg.)	11	6	17 to 35 (1/3 of coils)
23,750	11,000	1,200	12	B	460	1	470	21	3.2	35	0.5	
3,500	2,300	1,800	9	B	1,000	1	470	21				
4,000	2,300	1,800	25	B	200	1	470	21				
8,000	11,000	1,800	23	B	340	1	470	21	8.9	31	0.5	
20,000	11,000	1,800	14	B	195	1	470	21	6.7	23	0.5	
23,750	11,000	1,200	14	B	955	1	470	21	3.5	50	0.5	
23,750	11,000	1,200	14	B	345	1	470	21	9.8	46	0.5	
43,750	11,000	1,800	10	B	140	1	470	21	5.4	24	0.5	
10,000	11,000	94	26	B	475/275	10	1,000	36/60				
10,000	11,000	94	25	B	670	10	1,000	63				
13,750	11,000	94	15	B	265	10	1,000	69				
10,000	11,000	94	15	B	235	10	1,000	60				
10,000	11,000	94	27	B	845/157	10	1,000	28/70				
12,000	11,000	116	26	B	311	10	1,000	69				
12,000	11,000	116	25	B	136	10	1,000	73				
12,000	11,000	94	24	B	540	10	1,000	29				
15,000	13,200	94.7	2	B	36	10	1,000	22				26 (Before rewinding two years earlier)
15,000	13,200	94.7	14	B	35	1	1,000	80				
12,500	13,200	1,800	11	B	1,270/200	10	1,000	41/79				
12,500	13,200	1,800	13	B	820/164	10	1,000	44/73				
30,000	12,000	1,200	6	B	10/7		4,000/12,000	(Room)	10	(Room)	10	14 (Old winding replaced in 1939)
			0	B	37/31		4,000/12,000	(Room)	8	(Room)	10	(New winding)
1,500	2,700	1,200	36	A	65	10	1,000	20	20	20	3	3.5
2,500	2,300	3,600	13	B	150/phase	2	1,000	20	18	20	3	6.5
27,777	13,200	1,800		B	1,500/phase	10	2,500	40	4.3	53	10	25 (38°C)
27,777	13,200	1,800		B					6.2	53	10	18 (53°C)
30,000	13,600	720	11	B	2,200/1,900	10	2,500/10,000	25				
30,000	13,600	720	11	B	6,500/2,500 (Ph-1)	10	2,500/10,000	30				26.3 (Avg.)
					5,800/2,700/800 (Ph-2)	10	2,500/10,000/20,000	30				
30,000	13,600	720	0	B	400 (1-Ph)	10	2,500	20				
					920 (All Ph)	10	2,500	20				
58,824	13,800	3,600		B	950	10	1,000	28				
30,000	13,270	300		B	1,000	10	2,500					
14,000	6,000	720	27	A	135/105	10	1,000/8,000	28	22/15	28	6	
1,500	11,000	375	0	B	1,200	5	25,000	30				
80,000	14,400	1,800	0	B	100	1	1,000	70				
					350/200	Final	1,000/10,000	33				
80,000	14,400	1,800	3	B	80	10	1,000	43				
80,000	14,400	1,800	2	B	19	10	1,000	45				
18,750	13,200	1,800	24	B	99/12	10	500	32/63				
18,750	13,200	1,800	24	B	125/25	10	500	28/74				
25,000	13,200	1,800	18	B	520/50	10	500	37/75				
31,250	13,800	1,800	3	B	900/190	10	500	34/72				
30,000	6,600	1,500	22	B	170/110	10	1,000/20,000	37	10	52	5	32.7 (Avg.)
24,000	13,800	1,800	21	B	100	10	1,000	47				
23,500	13,800	720	3	B	950	10	1,000	34				
58,800	13,800	3,600	0	B	1,500/2,100	10/35	1,000	27				
188,500	13,800	1,800/1,200	13	B	15/19	10	1,000	33				
188,400	13,800	1,800	13	B	40/21	10	1,000	25/43				
160,000	11,400	1,500	12	B	560 & 660	10	1,000	27	(Machine has two independent windings)			
24,000	13,200	1,800	21	B	330	10	1,000	21				
23,500	13,800	720	3	B	120	10	1,000	35				
35,000	11,400	1,500	17	B	1,000	10	1,000	42				
35,300	13,800	1,800	0	B	460	10	500	50				

* Insulation resistance data on 40 machines not listed because of lack of full rating information.

machine on which ionization was detected at 7,000 volts and 21 degrees centigrade, was a 7.8-kv class *A* insulated unit. When this winding temperature was raised to 47 degrees centigrade, ionization could be detected at about 5,000 volts.

Ionization was detected at 1,000 volts on a 6.6-kv machine with mica insulation at a point where the coil passed through an air duct at the center of the stator winding. Though signs of corona pitting were expected in the insulation and heavy paper protective covering actually no evidence of such damage was found.

Where an aerial was used for detection, the only radiations due to ionization which were picked up in the slot sections of the stators were at air ducts and at the outer edges of the stator iron, even though the voltage was raised to more than two times machine rated voltage. This may be explained partially by the shielding effect that the stator conductors receive in the slot sections. Ionization was detected at the end turns of all machines tested by this method, at voltages varying from 25 per cent to 50 per cent of machine rated voltage.

An attempt was made with the search aerial to locate points where intentional damage had been inflicted to the insulation of various generators, by bruising the insulation with hammer blows, by cracking the insulation in bending, and by cutting into the insulation structure with a knife. The qualitative measurements gave no clear indication that ionization had increased or that it developed at a lower voltage.

Results of Quantitative Measurements

Quantitative ionization tests were made to determine the relation of ionization discharge with change in impressed voltage and to determine whether the rate of change could be used to detect insulation damage or deterioration. Figure 11 shows the curves obtained on a class *A* insulated machine for all three phases, two phases separately, and for a section of another phase winding whose insulation had been intentionally damaged as previously described. It was thought that the curve would show a step type characteristic giving sudden increases of ionization units at increasingly rapid steps as the impressed voltage was increased. This characteristic does seem to be partially realized in the curves for the two separate phase tests, though not to the degree anticipated. The results on the winding section which had been damaged were somewhat surprising since the winding failed to ground as the voltage was approaching 16 kv. This is only 1,000 volts above the highest voltage at which a measurement of ionization units was made. The curve shape gives no indication of approaching failure.

VII—High-Voltage Tests—A-C and D-C

A survey of coil insulation strengths was made on a number of machines where the machine was being removed permanently from service or where the winding was to be replaced. The work consisted of a-c high potential tests, to breakdown, on different phases and different coil sections and, in some cases, was supplemented by tests using d-c voltage from Kenotron testing equipment. These tests were made in conjunction with other measurements on winding sections as found and on coil sections which had been subjected to various types of mechanical damage intentionally inflicted. Special attention was also given to determination of the relative a-c and d-c strength of winding insulation.

Effect of Age on Dielectric Strength

Generator armature winding insulation strengths were found remarkably high even after 20 to 30 years of service, as will be noted by reference to table II. There were occasional failures at voltages less than twice normal rated voltage attributable to mechanical injury which had developed in the insulation and which could not be seen until the winding was disassembled. Most of the breakdown voltages were far in excess of the voltage specified for new machines in the AIEE Standards. A 6.6-kv generator with 1915 class *B* insulation failed at the end-turns at approximately $6^1/_2$ times rated terminal voltage on several tests. This is the machine on which ionization was detected in the slot section at the air duct with an impressed potential of only 1,000 volts. It was impossible to obtain a failure on one of the armature bars after the end-turn brackets had been disassembled, though the voltage was raised momentarily to 72 kv and held at 68 kv (over 10 times normal) for a period of 5 minutes. This case is exceptional and is not intended to convey the thought that armature bar insulation has this safety factor as a general thing.

Rotor Dielectric Tests

Ten turbogenerator fields were tested to destruction, with breakdown voltages varying from 1 to 5.5 kv. Six of the fields punctured at values between 1 and 2 kv which indicates that, in order to prevent undue stress, routine field testing should preferably be done with a 500-volt source rather than with a 1,000-volt source.

Dielectric Strength—A-C Versus D-C

Numerous tests have been made to determine the relative strengths of generator insulation as determined by breakdown voltage using a-c and d-c test equipment. An established ratio between the two types of tests will permit use of low capacity d-c testing equipment on large armature windings.

Such tests were made by selecting a group of four to six coils, each at different locations, around the periphery of the stator for each type of test. Unusually low breakdown strengths were disregarded as being caused by abnormal weaknesses in the coil. Experiments made to date have given the following results:

Table III

Machine	Average Insulation Breakdown Strength: A-C Voltage (RMS) Kv	D-C Voltage Kv	Ratio D-C/A-C (RMS)
2.3-kv motor	13.2	20.8	1.6
2.3-kv motor	11.7	21.0	1.8
13.8-kv, 30-mva synchronous condenser	28.3	38.5	1.46
6.6-kv, 30-mva turbo-generator	34.0	46.7	1.38

Similar tests have been performed in the laboratory on a group of spare generator coils, no end-turn supports were used. The slot sections of the coil were grounded carefully by clamping them into metal troughs. The average 60-cycle breakdown was 65 kv. The d-c value varied from 150 to 175 kv. The ratio is approximately 2.5, which approximates values to be expected in cable insulations. It is thought the test set-up, by reducing ionization, may have more nearly represented a cable structure than it did a generator coil structure.

Relation Between Insulation Resistance and Dielectric Strength

Since the ultimate objective of this investigation has been to determine a test method or a group of tests which could be used to determine the true quality of generator insulation with regard to its ability to withstand high voltage, much time has been spent in attempting to find a relation between dielectric strength as determined by a-c and d-c breakdown and various d-c insulation resistance measure-

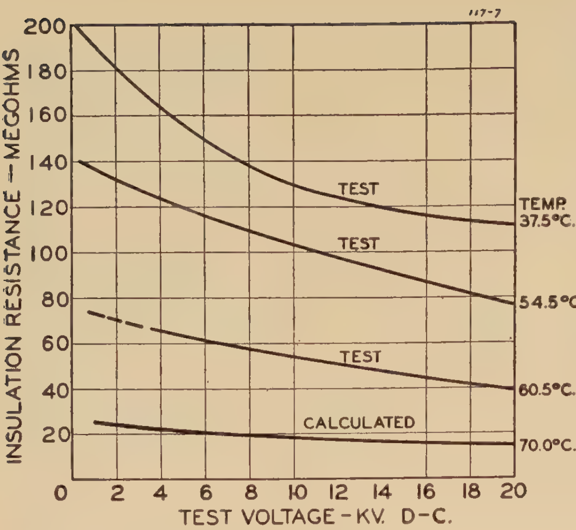

Figure 7. Insulation resistance versus test voltage at different winding temperatures

30,000-kw turbo-generator, 6.6 kv, 25 cycles, 1,500 rpm

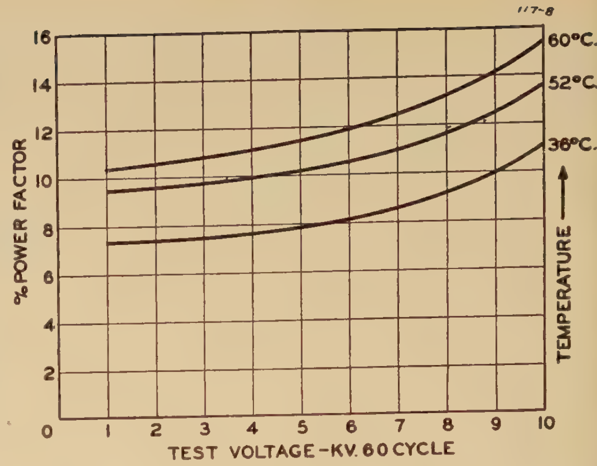

Figure 8 (right). Insulation power factor versus test voltage at different winding temperatures

30,000-kw turbo-generator, 6.6 kv, 25 cycles, 1,500 rpm

ments made at non-destructive voltages. In the early work, insulation resistance magnitudes were compared with 60-cycle breakdown strength on many coils. The investigation has been enlarged to include comparisons between insulation strength determined by a-c breakdown tests with dielectric absorption curve shapes and variations in insulation resistance characteristics at widely varying values of d-c voltage. Comparative insulation resistance and a-c breakdown tests have also been made under many conditions of deliberate mechanical damage to the insulation.

At present, no claim can be made that the ultimate objective has been attained. Comparisons between single insulation resistance measurements and dielectric strength seem to have little or no value and, under certain circumstances, the insulation resistance at moderate d-c voltages has been found to increase after the winding has been punctured on an a-c high potential test.

Location of Dielectric Failures

Stator winding insulation failures on breakdown tests occurred frequently at the end-turns. In some machines several coils were punctured, using both a-c and d-c, without a single failure occurring in the slot section. As indicated in table II the insulation strengths varied widely but invariably if a number of coils were tested, it was found that the weakest portion of the winding structure was at the end-turns.

Most end-turn failures occurred from the winding to the supporting brackets which always involved a flash through a short air gap. The insulation recovery after these failures was such that insulation resistance measurements did not detect any change in the winding characteristics. The failures which occurred in the slot sections appeared at the end of the slot or at the edge of an air duct in the stator iron. It is possible that ionization or swelling of the insulation at these points caused damages which reduced the dielectric strength but we have not been able to confirm the predominating cause. Very few machines have shown severe distress as a result of corona. In the few cases where effects of corona have been noted, the class *A* outer layer only has been affected. There has been no case where direct injury to mica insulation due to corona action has been discovered.

VIII—Conclusions

1. The industry will obtain increased value from its insulation testing if the known causes for variations in the results are carefully taken into account.

2. Insulation resistance varies widely with type and speed of machine, type and condition of winding, degree of cleanliness, temperature, moisture content, and extent of d-c charge on the winding. "Spot" readings, particularly, may be misleading unless carefully corrected for various factors affecting the reading. However, periodic

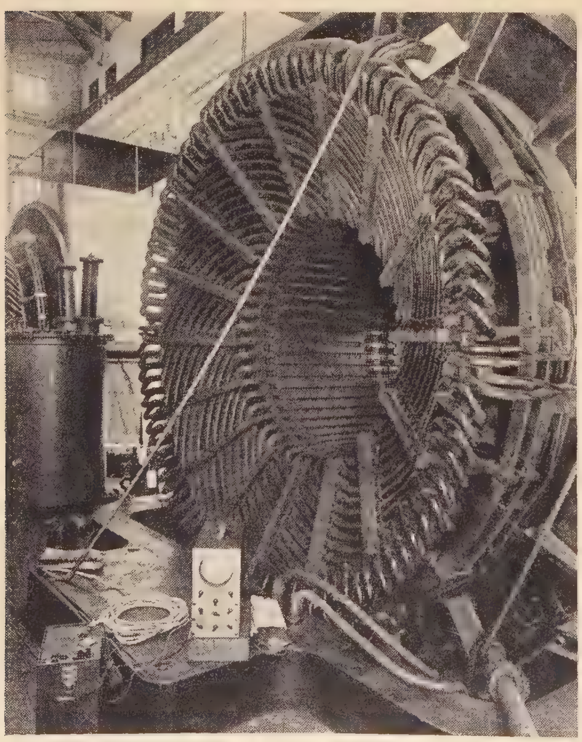

Figure 9 (left). Ionization detection apparatus ready for use

Figure 10. Connections of apparatus for measurement of ionization intensity in generator windings

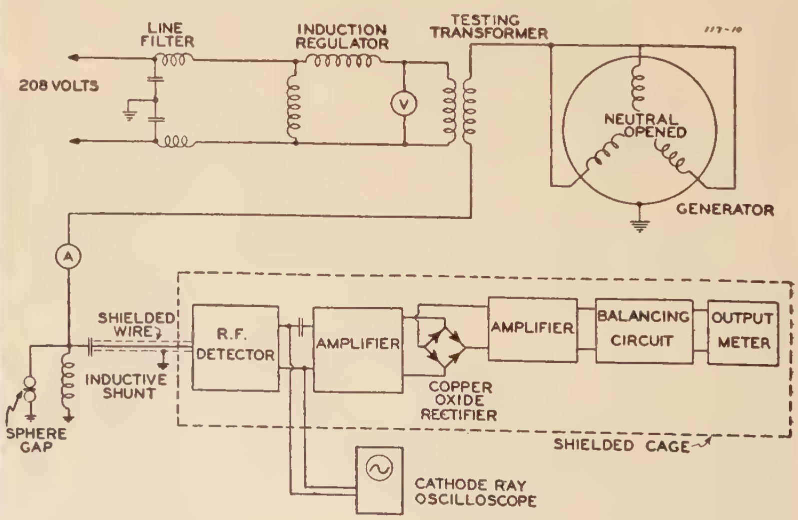

readings may indicate a trend of the general condition of the insulation.

3. There is at present insufficient data to permit accurate correction of insulation resistance readings for all factors affecting these readings.

4. Slopes of the resistance-time curves may be of value as an indicator of insulation condition. They are satisfactory indices of excessive moisture content in the insulation.

5. Insulation resistance-time curves are extremely useful to indicate the progress of winding dry-out.

6. Comparisons of insulation resistance-time curves taken at widely different d-c voltages may prove of value in determining insulation condition.

7. The voltage effect on winding insulation resistance appears to be greater as the winding temperature is reduced, or as the moisture content is increased.

8. Power factor tests have given little indication of value in locating faults or incipient faults in generator windings. However, power factor measurements may prove to be an indicator of the trend of the general condition of the insulation including moisture content in a given machine if records are kept of periodic readings.

9. Sixty-cycle ionization tests have given no indication of value in predicting generator insulation condition or locating weak spots in windings.

10. D-c/a-c (rms) relative dielectric strength of generator insulation appears to approach $\sqrt{2}$. Additional tests must be made to establish this more accurately.

11. Dielectric strengths of old armature windings have been found to be generally high.

12. The end-turns of old generator windings appear to be weaker dielectrically than the slot sections.

13. Preferably, field windings should not be stressed to more than 500 volts d-c in routine testing.

Figure 11. Ionization intensity measurements on each phase of a generator winding

14,000-kw vertical turbo-generator, 7.8 kv, 60 cycles, 720 rpm

A—Phase 3
B—Phase 2
C—Phases 2 and 3 and section of phase 1
D—Section of phase 1

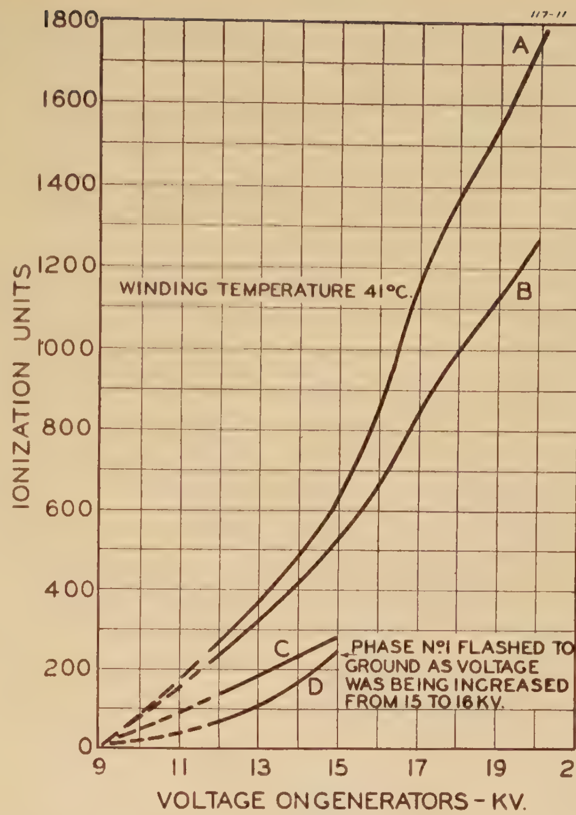

References

1. Progress Report—Investigation of Test Methods for Determining Operating Condition of Generator Insulation, H. R. Stewart. Electrical Equipment Committee, EEI, Eighth Meeting, Chicago, Illinois, October 7 and 8, 1935.

(Editors Note: EEI headquarters at 420 Lexington Avenue, New York, N. Y., advises that the foregoing item is out of print, but that a supplementary mimeographed pamphlet, "Guides for Initial, Periodic, and Experimental Testing of Generator Insulation" is available in a limited quantity.)

2. Insulation Resistance of Armature Windings, **R. W. Wieseman.** AIEE Transactions, volume 53, 1934 (June section), pages 1010–21.

3. The Characteristics of Insulation Resistance, **S. Evershed.** *Journal* of the Institution of Electrical Engineers, volume 52, number 224, December 15, 1913, pages 51–83.

4. Circuit-Breaker Recovery Voltage, **R. H. Park** and **W. F. Skeats.** AIEE Transactions, volume 50, 1931, pages 204–38.

5. University of Illinois engineering experimental station *Bulletins* 259 and 260.

6. Review by **T. Rich** of **G. J. T. Bakker** and **J. C. Van Staversen's** paper, The Insulation of Large High-Tension Synchronous Generators. *Electrician*, volume 102, number 25, June 21, 1939, pages 249–50.

7. Predetermination of the A-C Characteristics of Dielectrics, **A. Banos, Jr.,** and **J. B. Whitehead.** AIEE Transactions, volume 51, 1932, pages 392–403.

8. Insulation Tests of Electrical Machinery Before and After Being Placed in Service, **B. L. Barns** and **C. M. Gilt.** AIEE Transactions, volume 48, 1929, pages 656–65.

9. Insulation for High-Voltage Alternators, **J. F. Calvert** and **C. M. Laffoon.** AIEE Transactions, volume 54, 1935 (June section), pages 624–31.

10. Testing Breaker Insulation by Power-Factor Methods, **F. C. Doble.** *Electrical World*, volume 98, number 9, August 29, 1931, pages 374–5.

11. Testing Electrical Insulation, **E. L. Doty.** *Electric Journal*, volume 35, May 1938, pages 183–5.

12. Insulating Materials—Conditions Which Cause Deterioration, **A. R. Dunton.** *The Electrician*, volume 107, October 9, 1931, pages 483–5.

13. Dielectric Strength Ratio Between Alternating and Direct Voltages, **W. N. Eddy** and **J. L. R. Hayden.** AIEE Transactions, volume 42, 1923, pages 593–9; discussion, pages 612–20.

14. Reconditioning Flood-Damaged Electrical Equipment. Publication number *F13*, Edison Electric Institute, December 1938.

15. The Effect of Heat on the Electric Strength of Some Commercial Insulating Materials, **W. S. Flight.** *Journal* of the Institution of Electrical Engineers, volume 60, February 1922, pages 218–35.

16. Testing Bushings and Insulation by Power-Factor Method, **I. W. Gross** and **H. E. Turner.** *Electrical World*, volume 103, numbers 2 and 3, January 13 and 20, 1934, pages 68–73 and 111–16.

17. The Properties of Dielectrics in Electric Fields Comprising Unidirectional and Alternating Components, **L. Hartshorn** and **E. Rushton.** The British Electrical and Allied Industries Research Association, London, WC2; *Technical Report* L/T 79, July 28, 1936.

18. Improvements in Insulation for High-Voltage A-C Generators, **C. F. Hill.** AIEE Transactions, volume 47, 1928, pages 845–52.

19. High-Voltage Measurements on Cables and Insulators, **C. L. Kasson.** AIEE Transactions, volume 46, 1927, pages 635–47.

20. An Automatic A-C Potentiometer and Its Application to the Nondestruction Testing of Insulating Equipment, **G. Keinath.** AIEE Transactions, volume 58, 1939, pages 887–90.

21. The Influence of Moisture Upon the D-C Conductivity of Impregnated Paper, **G. T. Kohman** and **D. C. McLean.** *Journal* of the Franklin Institute, volume 226, August1938, pages 203–20.

22. The Predominating Influence of Moisture and Electrolytic Material Upon Textiles as Insulators, **E. J. Murphy** and **R. R. William.** AIEE Transactions, volume 48, 1929, pages, 568–75.

23. Testing of Insulation, **C. R. Reid.** *Electrical News and Engineering*, volume 46, July 1, 1937 page 212.

24. Temperature Limits and Characteristics of Mica as Used in Conjunction With Class "B" Insulation, **Robert H. Spry.** AIEE Transactions, volume 58, 1939 (June section), pages 287–9.

25. The Physics of Insulating Materials, parts I–V, **A. M. Thomas.** *World Power.*

I—Faraday, Kelvin, Maxwell, Mossotti, Debye, Hopkinson, J. J. Thomson, volume 14, December 1930, pages 485–91.

II—Dielectric Absorption and A-C Losses, volume 15, January 1931, pages 23–7.

III—Conductivity of Dielectrics, volume 15, February 1931, pages 113–15.

IV—Failure of Dielectrics Under Electric Stress—Gases and Liquids, volume 15, March 1931, pages 196–8.

V—Failure of Dielectrics Under Electric Stress—Solids, volume 15, April 1931, pages 307–10.

26. Generator-Insulation Tests, **B. Van Ness.** Edison Electric Institute *Bulletin*, volume 6, May 1938, pages 204–06, 231.

27. The Drying of Cellulose Insulation and Electrical Measurements as Measures of Dryness, **Emerson Venable.** Abstracted in Electrical Engineering, volume 58, January 1939, page 41.

28. Gaseous Ionization in Built-up Insulation, **J. B. Whitehead.** AIEE Transactions, volume 42, 1923, pages 921–39. Discussion, pages 953–8.

29. Gaseous Ionization in Built-up Insulation—II, **J. B. Whitehead.** AIEE Transactions, volume 43, 1924, pages 116–26.

Factors Contributing to Improving Electric Service by Means of High-Speed Switching and Utilization of Stored Energy

J. T. LOGAN
ASSOCIATE AIEE

JOHN H. MILES
NONMEMBER AIEE

Synopsis: The quality of electric service as reflected through variations in motor speeds resulting principally from voltage surges is about as important to many manufacturing processes as is the continuity of such service. This paper sets forth the effects of voltage surges on an extremely speed-sensitive manufacturing process and describes how the effect can be minimized to the extent of becoming harmless. Test data are given which show the effects of voltage surges, of varying duration and magnitude, on the process, and the voltage surge is shown engraved in the finished product as the purchaser sees it. The maximum tolerable driving motor speed variation, without impairment to the product, is established and means are described for preventing a greater variation irrespective of the voltage surge intensity. An alarm system is described which is capable of instantly responding when variations in speed exceed tolerable limits. Use of a synchronous condenser, to supply energy during the interim of severe voltage disturbances or brief power failures, is effective in preventing motor-speed variations from exceeding the tolerable limits. These and other recent improvements will provide highly reliable electric service for the requirements of those manufacturing processes which are very exacting as to speed variations.

ACCORDING to reliable statistics, approximately 85 per cent of automatic interruptions to overhead power circuits result from transient disturbances which are removed within a fraction of a second after the circuit is de-energized, leaving the circuit undamaged. Experience backed by tests conducted in various classes of industrial plants has established the fact that power failures of from one-half to one second duration do not constitute a failure of service, provided the energy stored in current consuming apparatus is utilized during the interim such apparatus is disconnected from the normal power supply. It follows, therefore, that when a power circuit is interrupted from transient causes, if reconnected to the normal power source quickly enough, an interruption to service is averted. Under this practice the circuit breaker employed for controlling the power circuit, in effect, becomes a device which removes disturbances from the power system without impairing service. This paper describes the use of circuit breakers in this manner, together with related factors in the order of their contribution to the improvement in reliability and quality of electric service.

I. High-Speed Circuit Reclosure

A series of tests was made on the Georgia Power Company's system in June 1931 for establishing the feasibility of high-speed circuit reclosure. An automatic circuit breaker reclosing relay, providing for reclosing the breaker without delay after its initial tripping, was applied to a circuit breaker through which some 6,000 kw of industrial load was supplied over a 38-kv overhead circuit. The breaker controlling this circuit was capable of making the complete operation, from closed position to open and closed position again, in about 40 cycles. (All references to frequency are on a 60-cycle basis.)

Time-delay undervoltage-type push-button stations were installed for controlling several motor contactors in one of the textile plants served from this circuit, replacing conventional instantaneous-type push-button stations. The 38-kv circuit was then short circuited several times by drawing pieces of fuse wire across phases. In every test the arc was extinguished by the circuit breaker opening and did not restrike when the circuit was reconnected to the power source, after having been disconnected for about 40 cycles. All motors in the plant equipped with instantaneous-type push-button stations were shut down from the voltage disturbances, but those controlled by the time-delay undervoltage devices continued in operation. The maximum speed drop of these particular motors which were driving twisting frames varied between 10 and 15 per cent during the interim. According to textile experts these speed variations did not appreciably lower the quality of the yarn, and the strain on the motors appeared to be less severe than restarting them from a standstill.

The tests attracted considerable interest and new reclosing relays, or modified conventional reclosing relays, were developed for this new reclosing practice, which was quickly adopted by several power companies in the Southeast.

High-speed circuit reclosing with a duty cycle of 0–15–120 seconds was applied on most of the circuit breakers controlling overhead circuits on Georgia Power Company's system. Certain motor operated breakers necessitated delaying the second reclosure for 45 seconds or more, in order to provide time for the operating mechanism to relatch after tripouts immediately following the first reclosure. After about 15,000 automatic operations of circuit breakers equipped for high-speed circuit reclosure, not one breaker failure has been traced to this reclosing practice.

An early obstacle to the application of high-speed circuit reclosing was the time required for certain types of protective relays to part contact after closing to trip the breaker. The geared-type relays, in particular, then required about three-fourths of a second to part contact and obviously would retrip the breaker upon the initial reclosure. New contact arrangements providing for contact separation in one-fourth second or less were employed.

More than 12,000 interruptions to circuits supplying loads varying from a few hundred kilowatts up to 25,000 kw have been prevented on the Georgia system through the medium of high-speed circuit reclosure during its ten years' use, the effects of circuit tripouts being no more harmful than ordinary voltage surges. Below is a table showing the ten years' performance of certain circuits equipped for high-speed reclosure:

Number of Circuit Tripouts	10,090	100%
Successful Reclosures:		
1st instantaneous	8,400	83.25%
2nd 15–45 seconds	1,084	10.05%
3rd 120 seconds	143	1.42%
Circuit Lockouts	533	5.28%

Actually, the proportion of successful first reclosures including all operations is

Paper 41-164, recommended by the AIEE committee on protective devices, and presented at the AIEE Southern District meeting, New Orleans, La., December 3–5, 1941. Manuscript submitted August 29, 1941; made available for preprinting September 24, 1941.

J. T. LOGAN and JOHN H. MILES are both with Georgia Power Company, Atlanta, Ga. 1. For all numbered references, see list at end of paper.

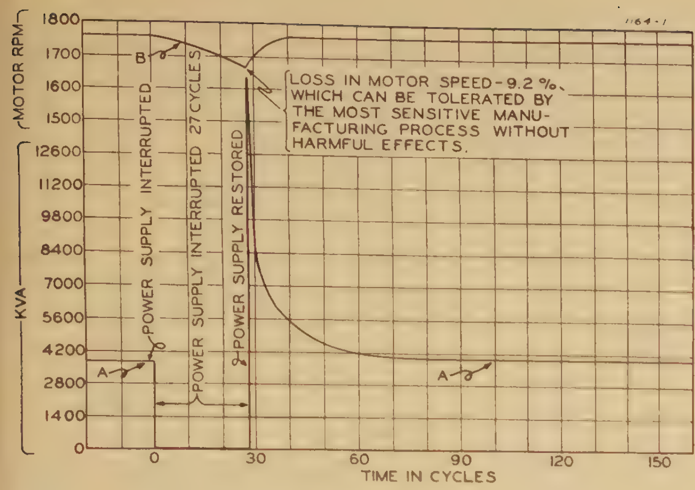

Figure 1. Results from oscillographic analysis of effectiveness of high-speed circuit reclosure in preventing interruptions

Note that load, curve *A*, after circuit tripout and reclosure is practically normal within one-half second after being reconnected to the power supply, and that the speed variation, curve *B*, of a 7.5-horsepower motor is negligible

above 85 per cent instead of the 83.25 per cent shown, because the tabulation includes 2.3-kv and 4-kv circuits, the performances of which are hampered by tree grounds; and omits some 5,000 operations of 38-kv and 44-kv circuits supplied from automatic or semiautomatic stations where the records might be questioned for lack of devices capable of accurately recording the sequence of breaker operations.

Power consumers, particularly the industrial class, receive the greatest benefits from high-speed circuit-reclosing practices. According to records and observations a power failure, if for only a few seconds, stops completely or seriously curtails the average industrial plant output for five to ten minutes and in many cases as much as one-half hour.[1]

The portion of the load that actually "coasts through" the time required for clearing faults from and reconnecting the circuit to the power source varies, but when motor controls are adapted for this practice, as described under section II following, the service interrupted is negligible, the effects being no more harmful than disturbances that cause moderate light flicker. Figure 1 shows oscillographic results of a test for determining the amount of load actually interrupted during the interim the circuit is disconnected from the power source. The load was disconnected from the normal power source for 27 cycles during which time stored energy supplied the requirements. The fact that the magnitude of the load was practically normal within one-half second after being reconnected to the normal power source is proof enough that for all practical purposes there was no service interruption.

II. Application of Time-Delay Undervoltage Devices

Control apparatus usually supplied with motors incorporates undervoltage protection for the larger or more important motors. Unless specified by the purchaser, this protection is generally of the instantaneous response type and will shut down the motors for voltage dips on the power supply.[2,3] This necessitates restarting the motors after each voltage dip, with resulting loss in production and, in many cases where continuity is essential, of upsetting the entire process for extended periods of time with consequent heavy loss in raw material. Application of suitable time-delay undervoltage protective apparatus will reduce such losses to the practical minimum.

This improved type of undervoltage protection is becoming standard practice, the older instantaneous types having proved entirely unsatisfactory for use on important motors supplied from large interconnected power systems, because of the large number of voltage surges resulting from atmospheric disturbances usually in the form of lightning or sleet. The great majority of these voltage disturbances are cleared from power systems within one second or less, or the fault is so far removed that the surge voltage at the particular location does not drop below 65 per cent of normal. Consequently, the disturbances should be of little concern when the motors are properly protected by time-delay undervoltage devices

Voltage surge tests conducted in many textile plants employing speed-sensitive manufacturing processes indicate that the drop in motor speed in event of a

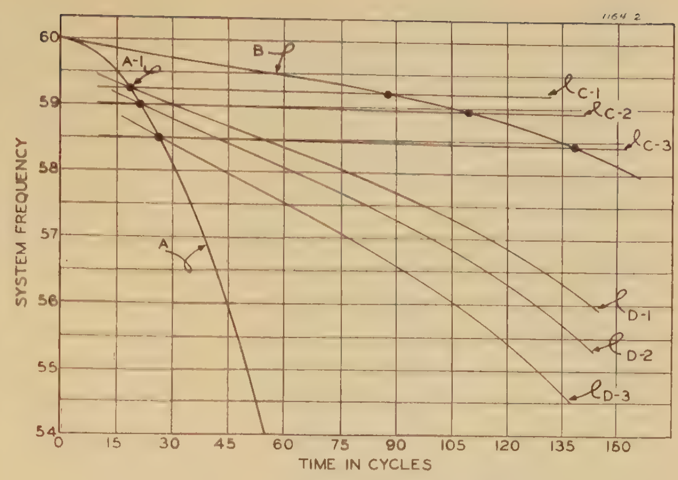

Figure 2. Inertia-relay operating characteristics

Curves *A* and *B* represent, respectively, speed changes for complete and partial loss of power source. Curves *C*-1, *C*-2, *C*-3, and *D*-1, *D*-2, *D*-3 represent, respectively, three of several possible relay-response slopes without and with the inertia element damped. The relay closes contact where slope, say *C*-1, crosses curve *A* or *B*

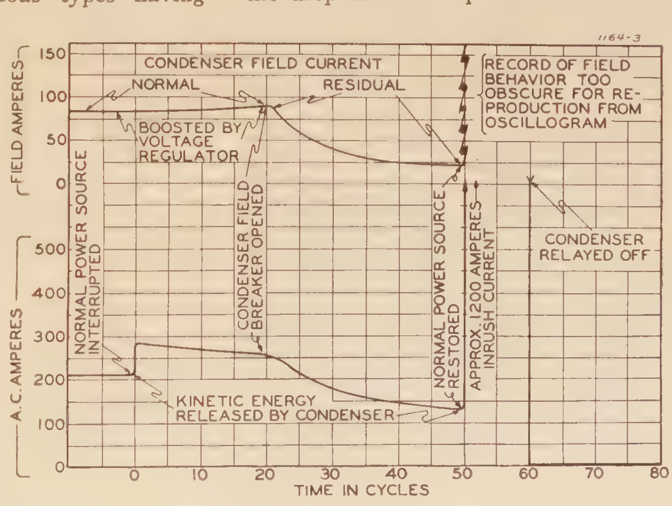

Figure 3. Graphic representation showing effects of high-speed circuit reclosure on synchronous condensers left connected to the circuit with the excitation source removed

Slow decay in field current makes this an unsafe practice. Condenser should be disconnected some 10 to 15 cycles in advance of restoring normal power source

complete power failure for one second is generally less than 20 per cent and that shutting down motors for such speed variations would do more harm than good, even ignoring the trouble of restarting. In fact, the practice of allowing essential motors to be shut down for voltage disturbances of any duration, so long as the motor continues to rotate, is questionable. There are links in many manufacturing processes that are adversely affected by rapid and prolonged speed changes, but usually stopping the process only aggravates matters. Such processes or links in processes should be given special consideration with the view of preventing objectionable voltage surges from being reflected on to the power source driving the particular motors. Means for accomplishing this are discussed under section V.

Continuity of operating through voltage disturbances is not essential, from the standpoint of production or quality of the product, for certain motors in most industrial plants. Whether these motors should be protected by time-delay undervoltage devices is a matter of individual consideration.

Synchronous motors, of course, require special consideration and generally should be disconnected from the line as quickly as possible following an out-of-step condition, unless the motor has excellent pull-in torque characteristics. Even then it would probably be better to provide field removal and restoring features and, possibly, automatic unloading devices.

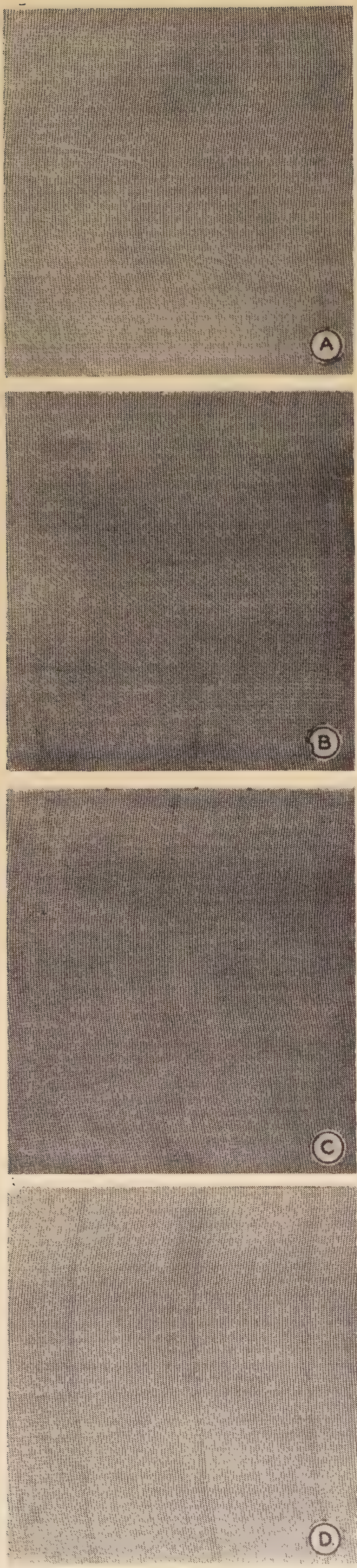

Figure 4. Swatches of hosiery tubing knit from yarn produced under conditions of repeated voltage surges imposed on the power supply

	Surge Voltage (Per Cent)	Surge Duration (Cycles)	Motor-Speed Variation (Per Cent)	Yarn Quality
A	60.0	61	2.2	Good
B	0.0	31	10.2	Good
C	14.7	61	13.7	Defective
D	13.5	122	27.9	Poor

III. Treatment of Synchronous Apparatus

A 3,000-kva synchronous condenser connected to one of the circuits originally equipped for high-speed circuit reclosure required that the initial reclosing time be delayed to allow the fault more time to clear. The condenser in some instances prolonged the arc. An analysis of this problem revealed that suitable relays were not available for the purpose of removing the condenser from the line quickly enough, in order to avoid purposely delaying the initial reclosing time as much as one second or more, thereby defeating the purpose of high-speed circuit reclosure.

Reverse power and frequency responsive relays were tried but when adjusted to operate in about one-fourth of a second, the maximum allowable without purposely delaying the circuit initial reclosure, the condenser would often be unnecessarily disconnected.

In order to solve this problem, the authors developed a relay operating on a new principle, that is, the rate of speed or frequency change. This device, called an inertia relay, combines high speed response with reliability and is ideally suited for not only this application but for other uses discussed later.[4]

The relay differentiates between the relatively gradual rate of speed or frequency change on large power systems where millions of pound-feet^2 of inertia are involved and the rapid and erratic changes that occur on small portions of the system suddenly cut loose from the main power source and left without, or greatly deficient in, power supply.

Referring to figure 2, which shows the inertia-relay operating characteristics,

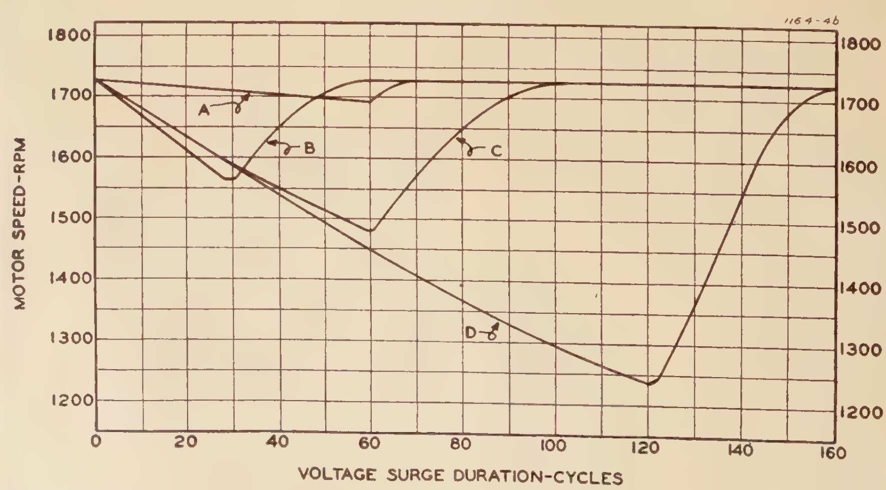

the relay can be adjusted to operate at any desired point along curve A, say at point A-1, for disconnecting synchronous condensers or an overloaded generating plant from circuits equipped for high-speed reclosing, this being accomplished in time to allow reconnecting the circuit to the system without delaying the reclosure. The maximum speed change expected on a power system under conditions of ordinary frequency disturbances follows some line usually well above curve B, to which the inertia relay will not respond if adjusted to operate on the slope represented by characteristic curves D-1, D-2, D-3 or some other of this family of curves. The relay can be adjusted to operate on the slope represented by curves C-1, C-2, C-3, and so on, if desired by simply lessening the damping effect on the inertia element. Also, the relay can be adjusted to respond within ten cycles or less for curve A. However, this would usually be undesirable because of waste in the kinetic energy stored in the rotors of spinning capacity so disconnected.

One of these relays is employed on the Georgia system for sectionalizing a 45,000-kw load in a manner for leaving load within capacity on a local 16,000-kw generating plant when the primary power source, a 110-kv transmission line, is involved by transient disturbances.[4] The relay detects the loss of the 110-kv source and accomplishes sectionalization in time to permit high-speed circuit reclosure to the transmission line without intentional delay, thus avoiding interrupting any portion of the load for transient faults involving the 110-kv source.

Five synchronous condensers and five small automatic hydroelectric plants connected to circuits equipped for high-speed circuit reclosure are also supervised by these relays. Four other installations for similar purposes are now under way.

Incidentally, the relay in addition to sectionalizing the 45,000-kw load area referred to above has proved to be faster and more positive than protective relays in disconnecting the faulted 110-kv line from the hydroelectric plant in time to prevent "swamping" the plant. This could not be done satisfactorily with conventional power directional relays, consequently, two other applications of the inertia relay for similar purposes are being studied.

Whether to disconnect synchronous condensers operating on circuits equipped for high-speed reclosure or to remove their sources of excitation only, during the interim the circuit is disconnected from the power source is a question frequently referred to the authors. Figure 3 shows the results of removing the excitation source only, and indicates that the magnetic energy stored in the machine is not dissipated in the field discharge resistor rapidly enough to make this a safe practice.

IV. Variation Tolerance in Motor Speeds

The foregoing sections of this paper deal primarily with improving the quality of electric service by reducing what otherwise would be momentary interruptions to electrical disturbances no more harmful than ordinary voltage surges.

Moderate voltage disturbances can be tolerated by the majority of users of electric service without harmful effects. However, some manufacturing processes are adversely affected from voltage surges to the extent that precautionary measures must be taken for minimizing the effects. In many instances the effects of voltage disturbances have been considered so damaging to the finished product that a local power supply is provided in preference to accepting the consequences of voltage surges that accompany electric service supplied from large transmission systems. A few of the processes which are unusually sensitive and adversely affected by voltage disturbances are employed in the manufacture of rayon and silk; high quality cloth; pulp and paper; broadcasting stations; printing presses.

The damaging effects of voltage disturbances are transmitted to the finished product generally through driving motor speed changes that result from the drop in voltage. Realizing the seriousness of this problem the authors have conducted extensive tests jointly with industries served by Georgia Power Company for the purpose of establishing what might be called a voltage "tolerance factor." The precision with which such a tolerance factor has been established for an unusually delicate or speed-sensitive process should be of interest, particularly to those who question the ability of a power system, subject to frequent lightning storms, to render satisfactory service to industries employing processes which require almost constant speed.

The test procedure provided for spinning yarn while the spinner driving motor power supply was being subjected to repeated artificial voltage disturbances of varying intensity and duration. Oscillographic records of the voltage disturbances and motor speeds were obtained for each series of tests and the yarn marked in a manner for identifying that made under each of four surge test conditions. The quality of the yarn with respect to variations in size and dyeing characteristics, was determined with uncanny accuracy by textile engineers. So accurate were the methods employed, that the yarn size could definitely be tied in with the motor speed, even to the extent of distinguishing that produced during the period of decreasing motor speeds from that produced during the period of accelerating speeds which followed immediately the restoration of normal voltage.

Sections of the four batches of yarn produced under power surge conditions were next knit into hosiery tubing and dyed in a sensitive shade for bringing out dyeing defects. Figure 4 is a reproduction of a photograph of the swatches of hosiery tubing which were knit from yarn spun during the four surge tests. Associated with each swatch is a motor speed curve, corresponding alphabetically with the swatch designation, showing the motor-speed variation for each artificial voltage surge which was repeated every 20 seconds during the test. The effects of the voltage surges as reflected through the driving motor can be seen as bars, faintly in swatch C and clearly in

Motor-speed variations in the area above curve A, do not damage material produced under extremely speed-sensitive processes. Curve B represents the frequency produced by a 2,000-kva synchronous condenser when supplying 2,700 kw of load. Curve C represents speed of motors so driven. Load was disconnected from condenser at B-1 and reconnected to the normal power source; otherwise, motor speed would have followed trend of B-2

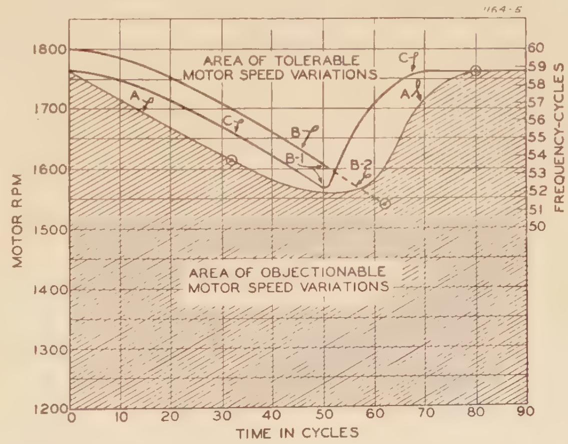

Figure 5. Tolerable and objectionable motor-speed variations

swatch *D*. The yarn produced under surge conditions represented by swatches *A* and *B* is classed as normal production by the textile engineers.

A summary of conclusions reached after analyzing the test results follows:

1. The principal interest of the textile company in regard to the effects of electrical disturbances may be measured by the degree to which the spinning machine driving motor speed is affected. Motor-speed variations of not more than 10 per c nt in one-half second can be accepted without great concern. Motor-speed variations of 15 per cent during a one-second period lead to variations in yarn size and dyeing disturbances which may be considered objectional. Speed variations on the order of 25 to 30 per cent during a two-second interval lead to pronounced loss of dye quality, due to marked variation in yarn size.

2. A signal system responding to motor-speed changes greater than that tolerable could be employed to advantage for advising the spinning production supervisor that yarn being spun was outside acceptable limits and should be segregated from regular production.

3. Voltage disturbances which do not reduce the driving motor torque below the pullout value are of little concern as the motor slip is increased less than ten per cent. Disturbances that reduce the torque below the pullout value, usually about 65 per cent normal voltage, must be limited to one-half second if the yarn spun is kept within acceptable limits.

4. The effects of voltage disturbances can be reduced to tolerable limits by means of high-speed clearing of faults, or the use of synchronous apparatus for maintaining voltage during system disturbances, to a value above the motor pullout point.

The signal system referred to in (2) above would require an initiating relay of unusual accuracy; otherwise yarn outside acceptable limits might get through unnoticed until too late, thereby causing a large shipment to be rejected as being outside acceptable limits. The inertia relay is ideally suited to initiate a signal for this purpose.

V. Prevention of Objectionable Motor-Speed Changes

Voltage-tolerance factors for various manufacturing processes can be established through suitable tests, similar to those described under section IV in connection with the manufacture of yarn. Having determined the voltage requirements for rendering satisfactory service to a particular speed-sensitive manufacturing process, means for restricting motor-speed variations to within tolerable limits can be considered.

High-speed clearing of faults offers an effective means for preventing damaging motor-speed changes. It was determined from tests described under section IV that zero voltage for one-half second was not objectionable in this particular extremely speed-sensitive process, in that the quality of the yarn was not appreciably lowered by subjecting the spinning motor power source to repeated power failures of one-half second duration. Refer to *B*, figure 4. For reasons more attractive than the prevention of damaging motor-speed variations, high-speed clearing of faults on transmission networks is very desirable and in many instances essential in order to promote system stability and reduce damages from power arcs. Unfortunately, however, this means for preventing motor-speed variations cannot be universally applied, principally because of fuse coordination problems which are encountered on most power circuits supplying industrial plants.

Objectionable motor-speed variations resulting from voltage disturbances reflected on to industrial plant power sources from the transmission system can be prevented where local generation is available and at a very reasonable cost. This may be accomplished by inserting a reactor between the plant bus and the transformer bank connecting the plant to the transmission system. The impedance of the reactor should be such that the local generating source can maintain voltage on the plant bus in excess of motor pullout values, usually about 65 per cent normal. Such an arrangement would limit motor-speed changes during the time of voltage disturbances on the transmission system to less than ten per cent or to within tolerable limits for even the most delicate or speed-sensitive manufacturing processes. Refer to *A*, figure 4. The reactor should preferably be normally short circuited by a high-speed circuit breaker controlled automatically by the transmission system voltage The circuit breaker should be opened only when the transmission system voltage, as measured on the transformer side of the reactor, is below motor pullout values.

Synchronous condensers offer a reliable means for preventing objectionable motor-speed variations. Kinetic energy stored in condenser rotors is generally sufficient for supplying a load equal to the kilovolt-ampere rating of the condenser for one second or more before the frequency drops to a value detrimental to speed-sensitive processes. This would involve high-speed switching, the load and synchronous condenser being disconnected from the main power source the instant the bus voltage dropped below motor pullout values. When voltage returned to normal on the main power source, the condenser would be disconnected from the load a few cycles in advance of transferring the load back to the main power source The condenser would then be returned to normal operation in the usual manner, preferably by automatic means

Figure 5 shows results when supplying 2,700 kw of load from a 2,000-kva synchronous condenser for 50 cycles, curve *B* representing the frequency supplied by the condenser. Motors driven from the synchronous condenser followed curve *C* which remained above curve *A*, the boundary of tolerable motor-speed variations for unusually speed-sensitive manufacturing processes. The condenser was disconnected from the load at *B*-1, a few cycles in advance of reconnecting the load to the main power source. Transfer of the load from the failing power source to the synchronous condenser and back again to the normal power source was accomplished smoothly by automatic control means. The voltage regulator controlling the condenser excitation prevented the bus voltage from dropping below 80 per cent normal which was well above the motor pullout value.

The use of synchronous apparatus connected to circuits equipped for high-speed reclosure for reducing voltage and frequency disturbances during the interim the circuit is disconnected from the normal power source is standard practice on the Georgia Power Company system. This practice is made possible through the inertia relay development which provides for positive isolation of the synchronous apparatus a few cycles in advance of reconnecting the circuit to its normal power source. The result gives the appearance of a short interval of reduced rather than apparent zero voltage. Best results are had by keeping the synchronous apparatus connected to the load until some 10 to 15 cycles prior to the restoration of the normal power source Reference to figure 3 shows that by this practice a great deal of kinetic energy can be fed into the load from synchronous machines thereby reducing the severity of voltage disturbances.

References

1. Faster Reclosing Breakers Needed, **J. T. Logan.** *Electrical World*, April 21, 1934, pages 571–2.

2. Notes on Motor and Circuit Control for Textile Mills, **Marshall E. Lake.** *Textile Bulletin*, July 1, 1940, pages 25–7.

3. Decreasing Lost Machine Time With the Undervoltage Time Delay, **Edwin M. Clapp.** *Cotton*, August 1933.

4. Inertia Relay "Anticipates" to Facilitate Reclosure, **J. T. Logan and J. H. Miles.** *Electrical World*, April 6, 1940, pages 69–72.

High-Pressure Gas as a Dielectric

GORDON C. NONKEN
ASSOCIATE AIEE

Synopsis: Impulse and 60-cycle breakdown strength of sphere gaps, rod gaps, and of samples built up of solid and fluid dielectrics are reported. The tests were made in nitrogen up to 200 pounds per square inch gauge pressure and in Freon up to 70 pounds per square inch gauge pressure. Dielectric strength values were compared with the breakdown of transformer oil between the same electrodes. Gap conditions were found for which the 60 cycle breakdown was twice its impulse breakdown.

RECENT interest in the dielectric strength of gases under pressure has been stimulated by the steadily increasing voltages used in power transmission as well as in X-ray and atomic physics work and by the shortcomings of atmospheric air and of oil insulation. Although scores of articles have been published on high pressure gas dielectrics during the last forty years, they contain practically no information on the impulse dielectric strength of gases at high pressure. This is a serious omission from the point of view of those interested in generating and distributing apparatus since the kind and amount of insulation in these apparatus are influenced greatly by impulse strength. The theoretical background related to the breakdown of gaps in gases is much too incomplete to permit the extrapolation of available data much beyond the exact conditions under which the data were obtained. Therefore, numerous general as well as specific breakdown data must be accumulated in order to make the proper utilization of high pressure gases as dielectrics.

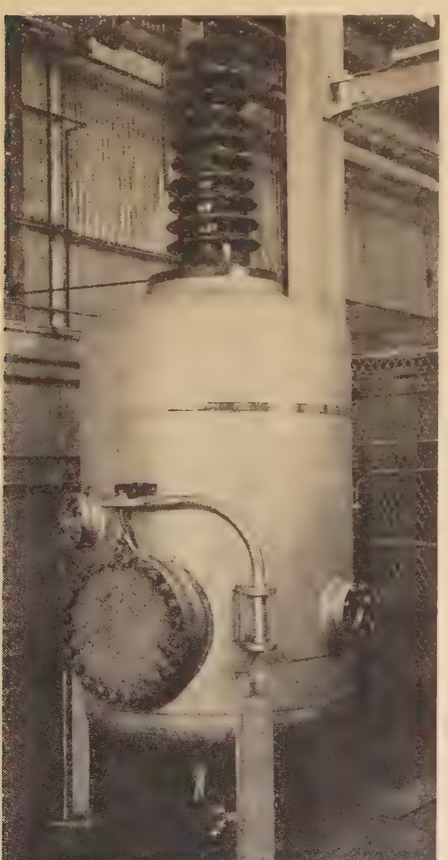

Figure 1. High-pressure electric test tank

This paper will present impulse and 60-cycle breakdown data between gaps in nitrogen up to 200 pounds pressure and in dichlorodifluoromethane (dichlorodifluoromethane, commercially known as "Freon" will be referred to in this paper as CCl_2F_2) up to 70 pounds gauge pressure. In each case, a comparison will be made with the breakdown of transformer oil at atmospheric pressure between the same gaps.

Recent Work

Several valuable contributions have been made to our fund of engineering knowledge of high pressure gas dielectrics during the last decade. Paschen's law, which was looked upon by many as a basic law of the dielectric strength of gaps at different spacing and pressure, has been shown to diverge far from the data at pressures above about six atmospheres. This law states that the sparkover voltage of a uniform field gap in a gas is directly proportional to the product of the gap spacing and the absolute pressure. The breakdown of a fixed gap is lower than the breakdown predicted by Paschen's law at pressures above 100 pounds per square inch. In fact the data[1,2] indicate that for air tested between spheres at a pressure of 600 pounds per square inch the actual sparkover is 55 percent of that predicted from atmospheric pressure data by Paschen's law.

Some gases have been found[3] which have as much as three times the 60 cycle dielectric strength of nitrogen when tested in a uniform field at atmospheric pressure. Notable among them are CCl_3F with a dielectric strength of three times that of nitrogen and CCl_2F_2 the gas commercially known as Freon and in common use in mechanical refrigerators, with a dielectric strength of 2.4 times that of nitrogen at atmospheric pressure.

Most of the earlier dielectric strength tests were made at low pressure or small spacings. Recently d-c breakdown tests[2] on spheres have been made at pressures up to 600 pounds per square inch and 450 kv breakdown. These data show also how slight roughnesses of the electrodes reduce the breakdown by as much as 50 per cent at 600 pounds pressure. Other investigators[4] made test in air and nitrogen up to 1,700 pounds per square inch. They indicate that the rate of increase of dielectric strength of air with increasing pressure continues to decrease at least up to 1,700 pounds per square inch pressure. This and other work[5] indicate that although the dielectric strength of air and nitrogen are practically the same at atmospheric pressure, the dielectric strength of nitrogen increases less rapidly than that of air with increased pressure, particularly above 100 pounds per square inch.

Apparatus

The experimental data presented in this paper were obtained by tests in the special pressure tank shown in figure 1. The pressure tank is four feet in diameter by seven feet high. Although it was tested hydrostatically up to 400 pounds per square inch pressure, it has not been used above 200 pounds gas pressure for safety reasons. It has three five-inch diameter sight windows made of discs of

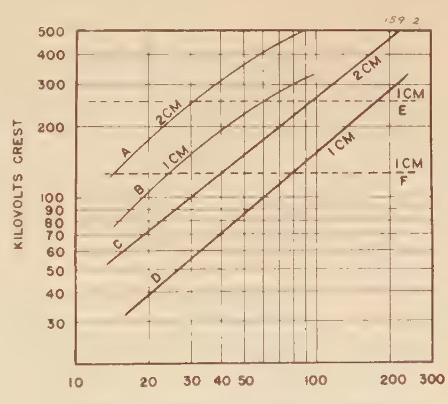

Figure 2. 60-cycle and impulse breakdown between 6.25 centimeter spheres

Curves *A* and $B = CCl_2F_2$, impulse and 60-cycle
Curves *C* and *D* = nitrogen, impulse and 60-cycle
Curve *E* = oil, impulse at atmospheric pressure
Curve *F* = oil, 60-cycle at atmospheric pressure

Paper 41-159, recommended by the AIEE committee on basic sciences, and presented at the AIEE South West District meeting, St. Louis, Mo., October 8–10, 1941. Manuscript submitted August 5, 1941; made available for preprinting September 8, 1941.

GORDON C. NONKEN is with the works laboratory of General Electric Company, Pittsfield, Mass.

1. For all numbered references, see list at end of paper.

methyl-methacrylate and an 18 inch steel door. A single high voltage bushing was used to carry the voltage into the pressure tank. This bushing was of the oil-filled type with a porcelain shell. The bushing was the same size both inside and outside the tank so that it could be used at maximum voltage with atmospheric pressure in the tank.

Two devices were used to adjust or change the electrodes inside the tank without opening the tank. One consisted of a screw which was operated by a shaft passing through the tank wall to a calibrated hand wheel. The gap electrode was mounted on the end of the screw and could be spaced accurately from the outside of the tank. The other consisted of a revolving platform installed in the bottom of the tank. The test samples which were made up of solid and gaseous dielectrics were good for only one breakdown determination. As many as twelve of these solid dielectric samples were placed on the revolving platform. These samples were connected, one at a time, to the voltage source by turning the turn table in the proper position with a driving mechanism which ran through a packing gland in the tank wall. These mechanisms saved a large amount of time by avoiding the necessity of opening the tank after each test.

Gases used were of a commercial grade obtained in high pressure tanks. The nitrogen was dried by passing it through a trap surrounded by liquid air. The CCl_2F_2 with high liquefying temperature was dried in columns of calcium chloride.

The CCl_2F_2 was drawn from the test tank through a compressor which recondensed the gas into its liquid phase and pumped it into a high pressure storage tank for future use.

The 60 cycle test voltage was supplied by a 350 kv, 1,000 kva testing transformer. The voltage was varied by controlling the field on the alternator connected to the testing transformer. The impulse voltage was supplied from a 500 kv impulse generator. The impulse voltage wave shape was checked and the breakdowns were observed with a cathode ray oscillograph connected across the test electrodes through a resistance divider. All impulse data presented herein were obtained with a $1^1/_2$–40 microsecond impulse wave.

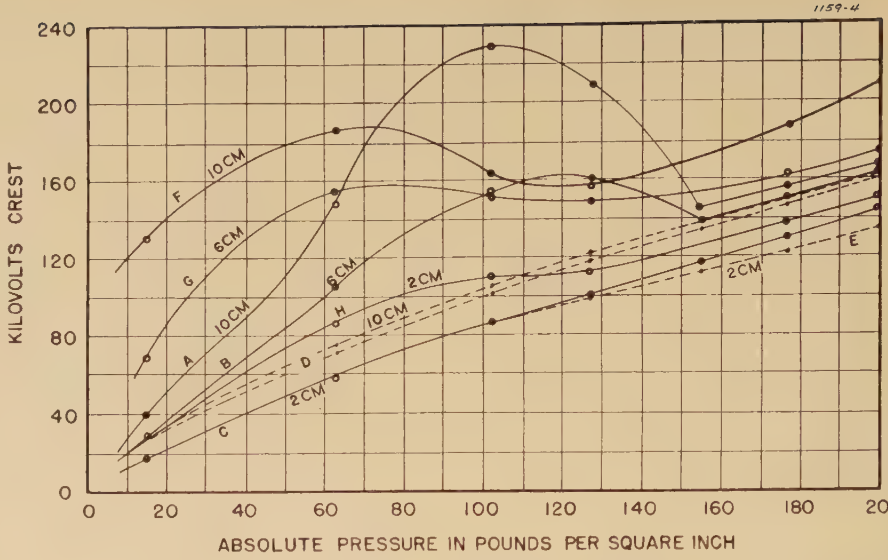

Figure 4. 60-cycle and impulse breakdown between one-half-inch square rod gaps in nitrogen

Curves *A*, *B*, and *C*=60-cycle breakdown
Curves *D* and *E*=60-cycle corona starting voltage
Curves *F*, *G*, and *H*=impulse breakdown

Test Results

Breakdown tests were made with the following three types of electrodes:

1. 6.25 centimeter diameter brass spheres.
2. Standard $^1/_2$ inch square brass rod gaps and
3. Electrode arrangements which included solid dielectrics.

The results of experiments made between the 6.25 centimeter spheres are summarized in figure 2. These data show the dielectric strength of nitrogen to increase as the 0.86 power of the pressure instead of increasing as the first power of the pressure in accordance with Paschen's law. The dielectric strength of CCl_2F_2 increases at a slightly smaller power of the absolute pressure than does the dielectric strength of nitrogen.

These gas breakdown curves represent both the crest value of the 60 cycle breakdown voltage and the crest value of the impulse voltage breakdown with a $1^1/_2$–40 microsecond voltage applied. The 60 cycle tests were made by increasing the voltage at a rate such that the voltage increased from approximately half of breakdown voltage to breakdown in one minute. An elapsed time of one minute was allowed between successive voltage applications. The average of ten breakdown determinations was used to establish a single datum point. The maximum spread of individual values was rarely over five per cent for the 60 cycle tests.

The impulse tests were made by applying five impulses of the same voltage at five or more steps two per cent apart in voltage, above and below the breakdown voltage. The voltage was lowered in two per cent steps until none of the five impulses broke down the gap. The voltage was also raised in two per cent steps until each of the five impulses at a particular voltage broke down the gap. The statistical voltage at which half of the impulses resulted in breakdown was taken as the breakdown value of the gaps. The maximum spread of individual values was with

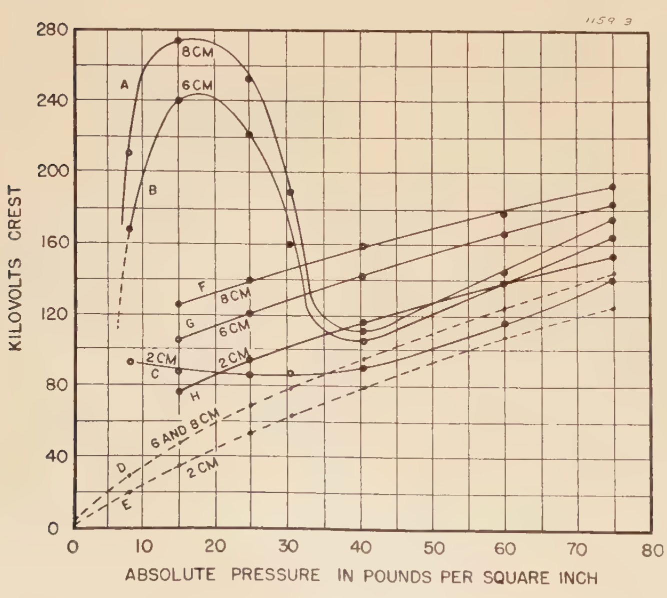

Figure 3. 60-cycle and impulse breakdown between one-half-inch square rod gaps in CCl_2F_2

Curves *A*, *B*, and *C*= 60-cycle breakdown

Curves *D* and *E*= 60-cycle corona starting voltage

Curves *F*, *G*, and *H*= impulse breakdown

few exceptions not greater than eight per cent of the breakdown value.

Observations showed that the breakdown of a gap was lower immediately after a breakdown. Therefore a procedure was followed such that a five minute interval elapsed between a flashover and the succeeding impulse application. Only one-minute interval was used after a voltage application that did not result in breakdown of the gap before another impulse was applied. This spread in the impulse data was probably increased by the fact that there was no effort to increase the free ion concentration within the tank by radioactive salts or an ultra-violet light source.

Breakdown of 6.25 centimeter spheres spaced one centimeter apart in 10-C transformer oil is plotted here for comparison. The oil breakdown tests were made at atmospheric pressure only. The transformer oil had a 60 cycle breakdown of 33 kv in a standard oil test cup with 0.1 inch gap spacing. The impulse strength of transformer oil with a $1^1/_2$–40 microsecond wave is slightly over two times its 60 cycle dielectric strength, while the impulse and 60 cycle breakdown strength of spheres in the high pressure gases are the same.

Rod-Gap Tests

Requirements of commercial high voltage apparatus other than the electrical insulation strength often dictate that the conductors adjacent to the insulation be made of some other shapes than spheres or curvatures of large radii. The standard $^1/_2$ inch square rod gap was therefore chosen for test electrodes to characterize the more severe conditions of non-uniform field encountered in high voltage apparatus.

60 cycle and impulse breakdown tests were made on this $^1/_2$ inch rod gap mounted in a vertical plane in the high pressure test tank, figure 1. Tests were made with both 60 cycle and $1^1/_2$–40 microsecond impulse voltages in nitrogen and CCl_2F_2 at various pressures and gap spacings. Figures 3 and 4 give the results of these tests. The corona starting voltage shown on figures 3 and 4 was taken by means of a cathode ray oscillograph which received its voltage from a high frequency amplifier placed across a shunt in series with the test gap

The 60 cycle breakdown of the rod gaps does not steadily increase with pressure. Figures 3 and 4 show how the breakdown voltage increases with pressure up to a critical pressure and then decreases with further increase in pressure until the breakdown of the gap is only slightly above the corona starting voltage of the gap. This critical pressure in the case of nitrogen is about 100 pounds per square inch gauge, while for CCl_2F_2 the critical pressure is only a few pounds above atmospheric pressure. The critical pressures are lower than those found by other investigators[1,4] on tests with point-plain electrodes. Goldman and Wul found the critical pressure for nitrogen to be about 150 pounds per square inch as compared with 100 pounds as shown in this report.

The impulse breakdown of rod gaps in nitrogen and CCl_2F_2 under pressure has only a remote resemblance to the 60 cycle breakdown curves. The impulse breakdown for rod gaps in nitrogen spaced at six and ten centimeters has a negative slope between 70 and 120 pounds per square inch, while the impulse breakdown of rod gaps in CCl_2F_2 increases steadily with increasing pressure. Figure 5 gives the impulse and 60 cycle breakdown of rod gaps spaced six centimeters apart in CCl_2F_2, nitrogen, and in transformer oil. The 60 cycle breakdown of CCl_2F_2 is about 2.2 times the impulse breakdown at

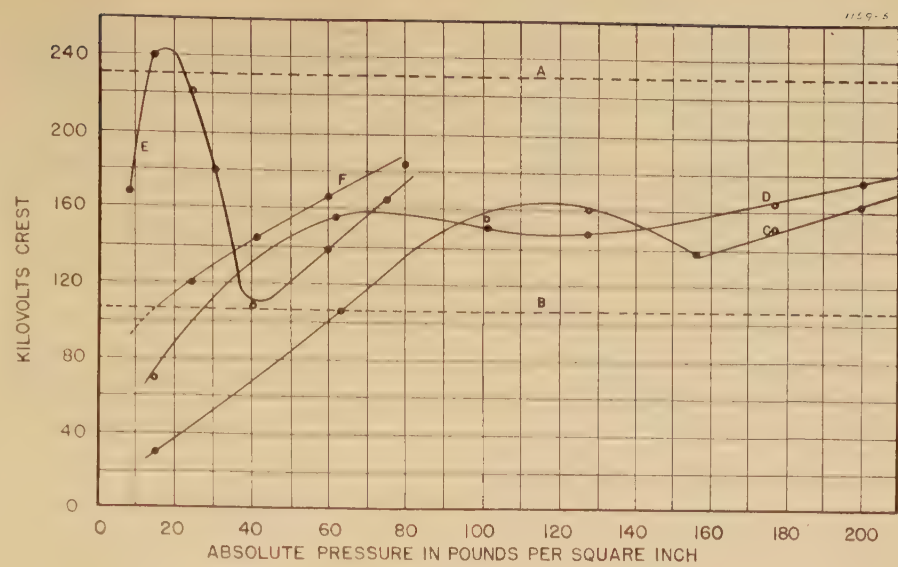

Figure 5. 60-cycle and impulse breakdown between one-half-inch square rod gaps spaced six centimeters in nitrogen, CCl_2F_2, and transformer oil

Curve A = impulse breakdown in oil
Curve B = 60-cycle breakdown in oil
Curve C = 60-cycle breakdown in nitrogen
Curve D = impulse breakdown in nitrogen
Curve E = 60-cycle breakdown in CCl_2F_2
Curve F = impulse breakdown in CCl_2F_2

Table I. Relative Dielectric Strength of Solid and Fluid Dielectric Arrangements in Transformer Oil and in Gases Under Pressure

1159-T

INSULATION SET-UP	TYPE OF VOLTAGE	CREST BREAKDOWN IN PERCENT OF No. 1 SAMPLE 10-C OIL BREAKDOWN		
		10-C. OIL	NITROGEN 200 LBS./SQ. IN. GAUGE PRESSURE	C Cl_2 F_2 70 LBS./SQ IN. GAUGE PRESSURE
① 1/8" PRESSBOARD 10" BY 10"; 1/2" DUCT; PRESSBOARD FILLER STRIPS; 5CM. TERMINALS	60 CYCLE PUNCTURE	100	88	132
② 1/8" PRESSBOARD 10" BY 10"; 5CM TERMINAL; 3 1/2"; 1/2" DUCT; METAL PLATE	60 CYCLE CREAPAGE	72	77	120
	1.5/40 µS. IMPULSE	142	115	143
③ 1/32" PRESSBOARD 10" BY 10"; 1/8" DUCT; 5 CM. TERMINALS	60 CYCLE PUNCTURE	56	37	
④ 1/8" PRESSBOARD SPACERS; .5" BY .06" COPPER WIRE .018" PAPER + .007" COTTON.	60 CYCLE	41	26	
	1.5/40 µS. IMPULSE	48	31	
⑤ 4"; LEAD FOIL ELECTRODE; PORCELAIN TUBE 1" DIA. BY 1/4" WALL	60 CYCLE	102	100	78

atmospheric pressure. It is very unusual to have a condition where the impulse breakdown of a gap is less than the 60 cycle breakdown. For example, the impulse breakdown with a $1^1/_2$–40 microsecond wave for a rod gap in air at atmospheric pressure is about 1.8 times the 60 cycle breakdown.

The fact that the impulse breakdown is greater than the 60 cycle breakdown for rod gaps in air has been explained on the basis of time lag before the gap is ionized in such a manner as to make it highly conducting. The condition in CCl_2F_2 gas where the 60 cycle breakdown greatly exceeds the impulse breakdown should be worthy of additional study. The reason for this unusual increase in the 60 cycle breakdown is not clear. There is evidence that the space charge in the gap is responsible for this unusually high breakdown.

Solid-Fluid Dielectric Combinations

Five different arrangements of solid and fluid dielectrics were tested for breakdown when immersed in 10-C oil, nitrogen, or CCl_2F_2. Schematic arrangements of the dielectrics and a comparison of voltage breakdowns are made in table I. Extreme care was taken in preparing the samples for these tests to see that the oil samples were completely impregnated and free from bubbles and that the gas-filled samples were thoroughly vacuum-dried and kept dry until they were tested. All of these dielectric arrangements have very non-homogeneous fields. The dielectric constants of the paper, pressboard, and porcelain used in these tests are all two or more times as large as the dielectric constant of transformer oil. Therefore, where the oil and solid insulation are in series, the oil must stand a disproportionately large part of the voltage stress. Since the dielectric constant of the compressed gases is substantially unity as compared with 2.2 for that of transformer oil, the voltage across the gas dielectric in series with solid insulation is considerably more than the voltage across the oil if it were made to replace the gas. This condition alone puts the gas dielectric to a considerable handicap when used in series with solid dielectrics.

It may be seen from table I that in general these combinations of solid and fluid dielectrics had higher dielectric strengths in transformer oil than they did in nitrogen at 200 pounds per square inch pressure or CCl_2F_2 at 70 pounds per square inch pressure.

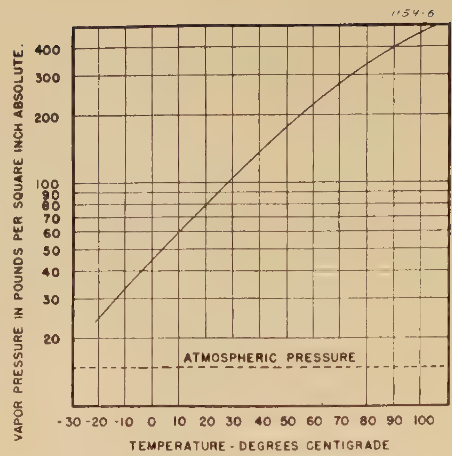

Figure 6. Vapor-pressure temperature curve of CCl_2F_2

Temperature Effects

High voltage apparatus filled with compressed gases may be subjected to a wide range of temperature either by virtue of their ambient conditions or by the heat liberated within them.

This change in temperature will change the dielectric strength of the gaseous dielectric in different ways according to the manner in which the gas is supplied to the vessel. The following are generalizations based upon theoretical considerations and checked experimentally for CCl_2F_2 between spheres.

(*a*). If gas were supplied in a manner such that a constant gas pressure was maintained, the dielectric strength of the gas would change inversely as the absolute temperature.

(*b*). If the total quantity of gas in the system is unchanged, the dielectric strength of the gas should remain unchanged with change in temperature. This follows from the fact that the dielectric strength of a gas is proportional to its density.

(*c*). If the gas is in a closed system similar to condition (*b*) but the gas is saturated and an excess of liquefied gas is present in the system, the gas pressure will change with temperature according to the vapor pressure of the gas at the particular temperature. The dielectric strength of the gas will change in such a system nearly the same as the vapor pressure of the gas. Vapor pressure of CCl_2F_2 is shown in figure 6. It is obvious that such a system has much greater change in dielectric strength of the gas with change in temperature than do the systems (*a*) and (*b*).

Summary

1. The impulse and the 60 cycle crest breakdown strength of nitrogen are substantially the same when tested between spheres at less than radius spacing; the impulse and 60 cycle crest breakdown strength of CCl_2F_2 are likewise the same. Nitrogen at 175 pounds per square inch absolute pressure, CCl_2F_2 at 62 pounds pressure and 10-C transformer oil at atmospheric pressure break down at the same impulse voltage when tested between 6.25 centimeter spheres spaced at one centimeter. Under the same conditions the 60 cycle breakdown voltages of the three fluids are the same with nitrogen at 80 pounds absolute pressure, CCl_2F_2 at 25 pounds absolute pressure, and 10-C oil at atmospheric pressure.

2. The fact that there is a condition where the 60 cycle breakdown of a rod gap in CCl_2F_2 is over two times the impulse breakdown of the same gap under the same condition is disturbing to the orthodox theory surrounding the electrical behavior of spark gaps in gases.

The 60 cycle breakdown between rod gaps is substantially higher in nitrogen above 60 pounds per square inch absolute or in CCl_2F_2 above atmospheric pressure than in transformer oil. On the contrary, the impulse breakdown between rod gaps is considerably lower in nitrogen under 215 pounds per square inch absolute pressure and CCl_2F_2 below 85 pounds per square inch absolute pressure than in transformer oil.

3. The breakdown strength of solid insulations tested in nitrogen at 215 pounds per square inch absolute pressure and in CCl_2F_2 at 85 pounds per square inch absolute pressure as compared to its breakdown in transformer oil indicates that with but one exception the tests made in transformer oil showed higher strength than when made in the gases at the above pressures.

References

1. Breakdown of Compressed Nitrogen in a Nonuniform Electric Field—II, **I. M. Goldman** and **B. M. Wul.** *Journal of Technical Physics*, USSR, volume 3, 1935, pages 16–27.

2. Breakdown Studies in Compressed Gases **A. H. Howell.** AIEE Transactions, volume 58 1939 (May section), pages 193–204.

3. Dielectric Strength of Insulating Fluids **E. E. Charlton** and **F. S. Cooper.** *General Electric Review*, volume 40, 1937, pages 438–42.

4. Durchschlaguntersuchungen in komprimierten Gasen und in flüssiger Kohlensaure, **O. Zeier.** *Annalen der Physik*, volume 14, 1932, pages 415–47.

5. Der Elektrische Durchschlag Verschiedener Gase Unter Hohem Druck, **E. Finkelmann.** *Archiv für Elektrotechnik*, volume 31, 1937, pages 282–6.

An Automatically Reclosing Breaker for Co-ordinating Distribution Systems

H. L. RAWLINS
ASSOCIATE AIEE

J. M. WALLACE
ASSOCIATE AIEE

Synopsis: The increasing spread of distribution systems in which fault protection is afforded by fuses has resulted in long outages and high maintenance costs. Excellent coordination is possible with modern fuses, but their inability to differentiate between a permanent and a temporary fault results in frequent outages and costly service trips.

A new automatically reclosing circuit breaker with pronounced inverse time current tripping characteristics makes possible an improved radial distribution system in which outage and maintenance are reduced to a minimum. The effectiveness of coordination is increased to a point where an outage is confined to the immediate neighborhood of a permanent fault. Service trips are no longer necessary unless there is a permanent fault condition to be removed from the system.

Extended Distribution Systems Require New Type of Protective Equipment

IN recent years there has been a large increase in the number of distribution systems having long lines and small loads scattered over considerable territory. Such systems represent an increase in the use and application of electricity as well as affording users the benefits and conveniences of a reliable source of power. The continued extension and successful operation of these systems depends upon a low initial cost and a low maintenance cost.

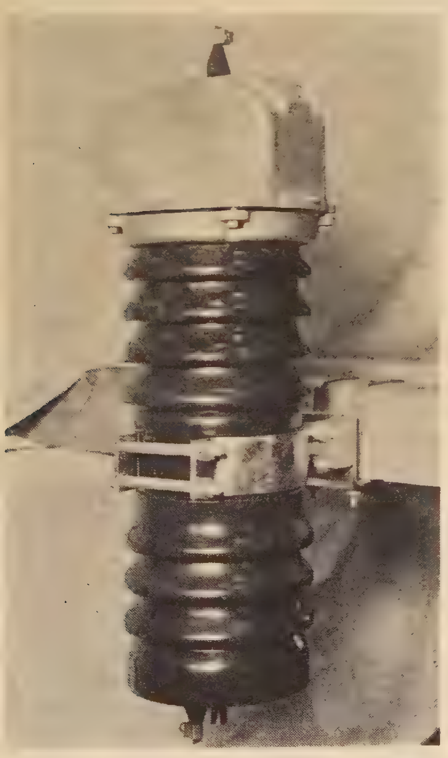

Figure 1. Single-pole automatically reclosing circuit breaker

The use of expensive lines and conventional apparatus for fault protection would result in low maintenance costs, but the installation cost could not be justified. Inexpensive lines with simple fuse protection for faults provide a low installation cost but result in high maintenance cost and unsatisfactory service. A high percentage of the maintenance cost of these extended systems is chargeable to the servicing required by faults. More than 80% of all faults are temporary and will not prevent the immediate restoration of service, so the elimination of service trips on such faults will materially reduce maintenance costs. The successful extension of such systems, therefore, depends upon the low installed cost of a device that will interrupt all faults and then restore service after all temporary faults.

The fault currents on these systems are relatively low and of such a value that distribution cutouts are used for sectionalizing, even to the use of five or more cutouts in series. The excellent coordination possible with modern fuses permits definite restriction of outages to the immediate neighborhood of a fault. On such systems, outages are of long duration and their restriction to limited areas greatly increases the quality of service. Therefore, a further requirement for a device to provide fault protection on such systems is its adaptability to an extensive coordination scheme. This will be accomplished if the device has a time current characteristic approximating that of modern fuses.

The necessarily inexpensive construction used on these systems, together with their length and exposure, has multiplied the number of faults to the point where simple fuses are inadequate for sectionalizing duty. Repeating fuses reduce the necessity for immediate service trips but require a periodic servicing and may not differentiate between a permanent and a temporary fault due to their short reclosing time. Close coordination is not dependable with repeating fuses, for a fuse is a thermal device and the heat stored in a protected fuse may result in its melting upon repeated operations of the fuse protecting it. It is seen, therefore, that an additional requirement is a time current characteristic which is not affected by repeated operations of the preceding protective device.

Since only a limited interrupting capacity is required, it is possible to make an inexpensive automatically reclosing oil circuit breaker to fulfill all of the requirements for operation on extended distribution systems. The requirements are:

1. Adequate interrupting ability.
2. Automatic reclosing to permit restoration of service after a temporary fault.
3. Pronounced inverse time current characteristic to permit close coordination on an extensive system.
4. Consistent time delay on tripping which is not affected by previous circuit conditions.
5. Reliable operation and low oil deterioration to reduce service trips to a minimum.
6. Low cost and a light weight to reduce the total installed cost to a minimum.

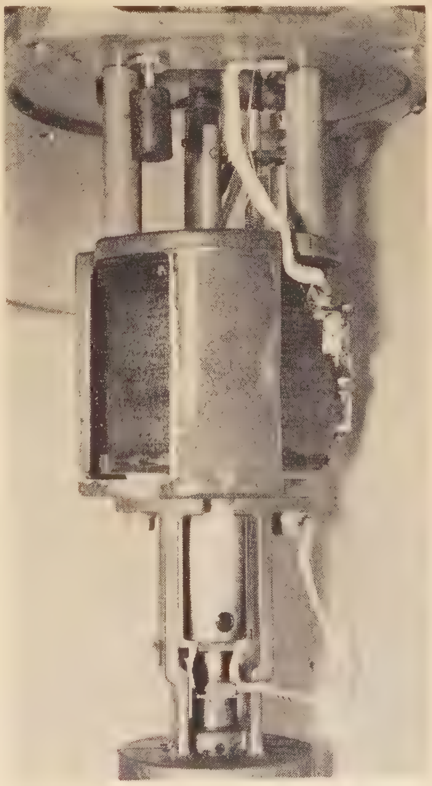

Figure 2. Interrupter and operating mechanism assembly withdrawn from porcelain tank

Paper 41-142, recommended by the AIEE committee on protective devices, and presented at the AIEE Pacific Coast convention, Yellowstone National Park, August 27–29, 1941. Manuscript submitted April 16, 1941; made available for preprinting July 10, 1941.

H. L. Rawlins and J. M. Wallace are both with Westinghouse Electric and Manufacturing Company, East Pittsburgh, Pa.

1. For all numbered references, see list at end of paper.

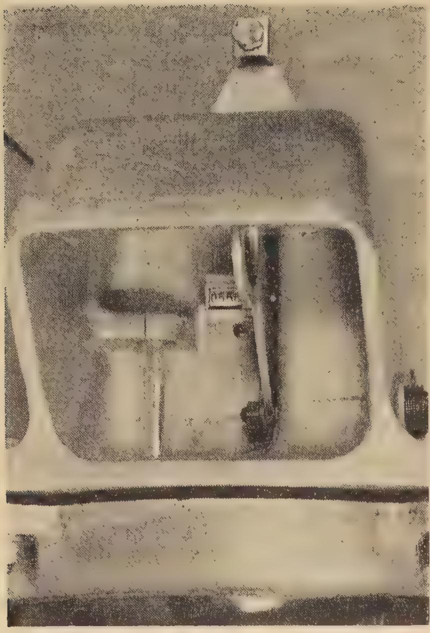

Figure 3. Indicating handle, oil gauge, and operation counter grouped under protecting hood

Figure 4. Sectional view of breaker with side view of lockout trip

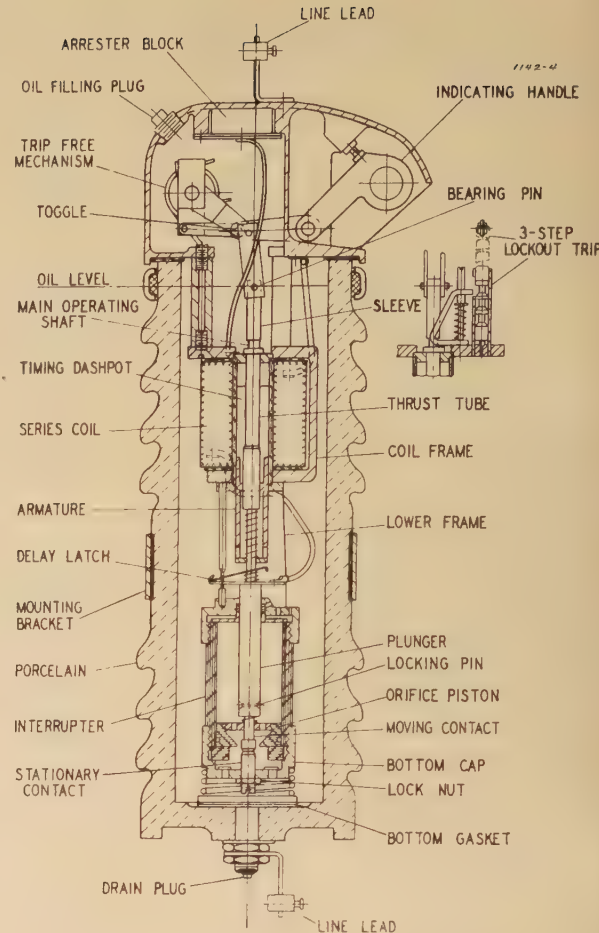

7. Complete self protection in that no overload current (within the interrupting rating) or surge voltage shall damage the device.

From the application viewpoint the most important of these requirements is the inverse time current characteristic. The coordination possible with a breaker having the proper time characteristic greatly increases the scope of its application and makes possible the economical extension of low capacity distribution lines.

Construction and Operation of New Breaker

All of the above application requirements are fulfilled by the single pole automatically reclosing circuit breaker shown in figure 1. In addition, it has many other inherent features such as trip free closing; immediate manual reclosing after lockout; lockout on first interruption when manually reclosed against a fault; and multitap coil to permit ready change in rating. The interrupting chamber and all operating parts are easily removed in one unit as shown in figure 2. The indicating handle, oil gauge, and operation counter are grouped under an integral protecting hood, as shown in figure 3.

Figure 4 is a cross sectional view showing all principal elements of the breaker. The breaker is normally biased closed by the contact pressure springs, except during lockout. This differs from more conventional breakers in that, on tripping, the contacts are forced apart against spring pressure instead of being opened by accelerating springs. The energy required to operate the breaker is obtained from a series coil. The small size of coil used to operate the breaker and continuously carry overload currents just below the minimum tripping current is made possible by using an efficient type of interrupter that requires only a short travel. Wide separation of the contacts on lockout is obtained by releasing a spring that opens the breaker in the conventional manner and is reset, on closing, by means of the handle. Additional energy to interrupt heavier currents is obtained from the interrupter itself after the initial separation of the contacts.

Referring to figure 4, the armature when actuated by an overcurrent through the series coil moves upward and forces the entrapped oil from the timing dashpot. This action provides the inverse time characteristic on tripping. The shape of the time current curve is a function of dashpot size and port area together with the magnetic circuit and other factors. After a predetermined travel, the dashpot is opened, permitting the free armature to drive the moving contact open against the contact pressure springs. The moving contact opens rapidly for a short distance and then picks up the orifice piston which forces oil into the arc path resulting in interruption at the end of the first half cycle after the orifice piston starts to travel. On high currents the pressure developed within the interrupter will produce an additional driving force on the plunger thereby forcing oil into the arc path under a pressure proportional to the value of current being interrupted. The moving contact is free to move upward through the armature thus permitting overtravel on high current interruptions. The moving contact is prevented from reclosing at once by the delay latch which is not released until the armature again reaches its starting position. This results in a reclosing time of approximately five seconds. The time interval before reclosing permits the escape of gas from the top of the interrupter and entrance of fresh oil into the bottom. This flushing takes place through washer type valves that close instantly upon the appearance of pressure during interruption.

There is provided a simple, three step lockout trip which is notched up by the travel of the armature during each interruption. On the third interruption it breaks the toggle that holds the trip free mechanism in the closed position, thereby permitting the contacts to be driven to the extreme open position. The manual

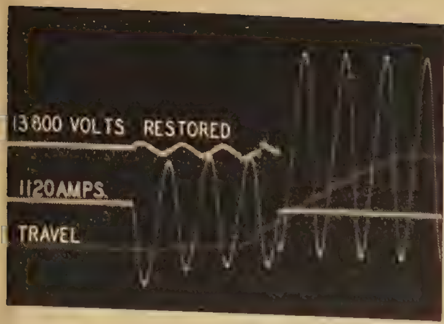

Figure 5. Interruption of 1,120 amperes at 13,800 volts

Note the increased overtravel at high currents

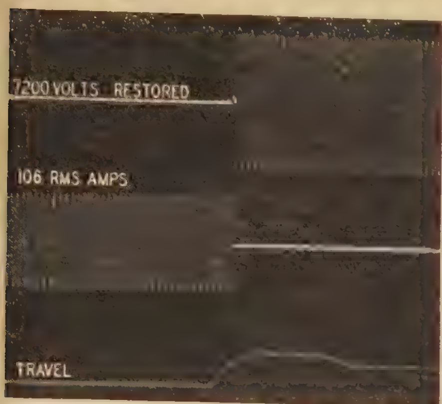

Figure 6. Interruption of 106 amperes at 7,200 volts

Figure 8 (right). Tripping-time current characteristics of new breaker

Note similarity to fuse link and relay curve

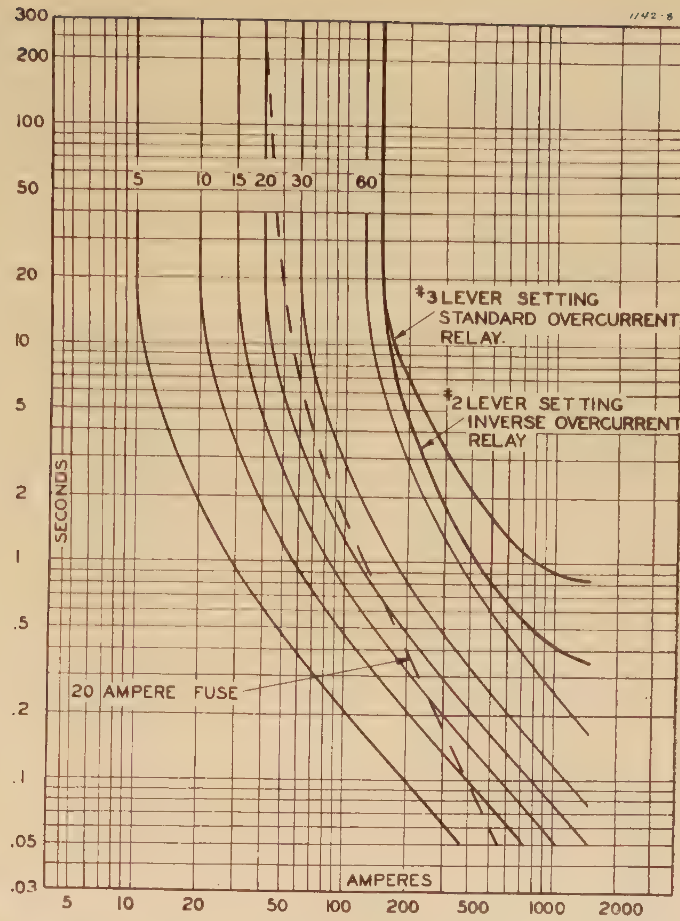

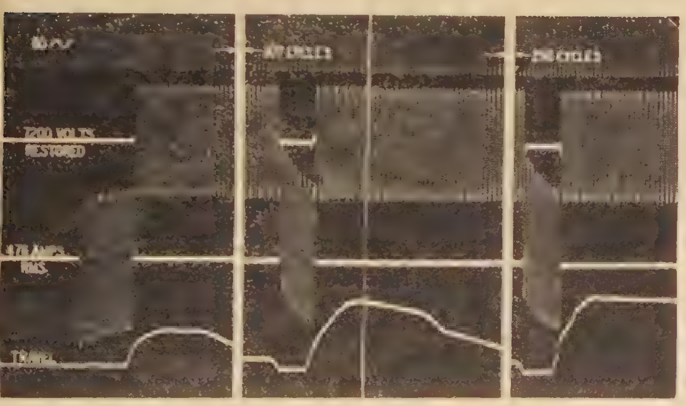

Figure 7. Three interruptions and lockout, 476 amperes at 7,200 volts

Note the travel of the contacts to the full open position after final interruption. (Portions of film showing breaker open between reclosures have been deleted from the original eight-foot film)

return of the indicating handle to the closed position will reset this toggle and the lockout trip and permit the breaker to close after the usual time delay. The lockout trip will be reset only to its second position from which it will lock out the breaker if there is a further interruption. If the fault has been removed from the line, the lockout trip will slowly reset to provide three step lockout on subsequent faults.

The series coil is made up of four separate windings. By connecting these windings in series, series-parallel, and parallel it is possible to obtain the six ratings from two coils, one coil furnishing the 5, 10, and 20 ampere ratings and the other coil furnishing the 15, 30, and 60 ampere ratings. To prevent damage to the coil from transient voltages, a suitable arrester is connected directly across its terminals.

Interruption and Lockout Tests

Repeated interrupting tests at both high and low currents on extremely fast circuits have demonstrated the high efficiency and low oil deterioration of the breaker. Indications are that the breaker can be in service many years before an oil change is required. The interrupting ability of the breaker is determined by the short-time current rating of the series coil rather than by any limitations in the interrupter. Figure 5 shows an oscillogram of a single interruption of 1,120 amperes at 13,800 volts. Figure 6 shows a single interruption of 106 amperes at 7,200 volts. Compare the travel record and note the additional travel of the contacts on the higher current interruption. Figure 7 shows three interruptions and lockout on 476 amperes at 7,200 volts. Note the tripping time, the reclosing time, and the travel of the contacts to the extreme open position after lockout.

Co-ordination Characteristics

The important attribute of this breaker is the time current characteristic. More time delay on tripping allows more time for coordination and therefore permits closer coordination between adjacent ratings. Consequently, as great a time delay as possible has been incorporated in this breaker particularly at the lower values of current just above the minimum tripping current. Since the different ratings are obtained by varying the number of turns on the series coil the curves will be parallel and identical in shape with only a shift in the current axis. Figure 8 shows the time current characteristics for the six ratings of 5, 10, 15, 20, 30, and 60 amperes. The time values have been obtained from oscillographic records of interrupting tests. Sufficient time delay has been provided so that all of these ratings can be coordinated in series. The possibility of coordination between these

breakers and fuses is further demonstrated by superimposing a 20 ampere fuse curve upon the breaker curves. The fuse curve is for a 20 ampere universal fuse link as used in distribution cutouts and is a representative curve for such links.

The coordination of these breakers with each other is relatively simple. There are, however, three possible applications in coordinating the breaker with fuses.

(1). A fuse can be selected such that it will be completely protected by the breaker, that is, the breaker will operate three times and lockout without melting the fuse. This would be a rather infrequent application.

(2). The fuse can be used to completely protect the breaker, that is, the fuse would clear the circuit without a single operation of the breaker. This arrangement might be used with transformer protective links.

(3). The fuse can be selected so that the breaker will clear the circuit once to permit the fault to clear, and then on the second operation, if the fault persists, the fuse will blow due to the stored heat remaining in it from the first operation. On the second reclosure the breaker will remain closed and the fault will be isolated by the fuse. In this arrangement the fuse would be the outermost protective device in the sectionalizing scheme.

The shape of the time current curve further suggests the coordination of the breaker with relays. The relay curve shown in figure 7 is for a standard overcurrent relay of the moving disk type. By adjusting it to the proper lever setting and proper current ratio, it is possible to have the relay curve very close to that of the breaker. With the setting shown, the breaker will consistently protect the relay and thus prevent tripping an entire substation. The time delay between operations of the reclosing breaker is sufficient to allow the relay disk to return to its starting point, so the coordination will be the same for each operation. With reclosing fuses, a much larger margin between the fuse curve and the relay curve would be necessary due to the short reclosing time. Here the relay disk would not return to its original position and there would be cumulative turning of the disk and consequent operation of the relay.

A further advantage of this breaker for fault protection on low capacity systems lies in the economies offered by the use of simple gaps for lightning protection. On this type of system a temporary outage is not serious and, with the coordination afforded by these breakers, such an outage due to lightning is confined to a small area and is removed upon the first reclosure.

Conclusions

An automatically reclosing circuit breaker meeting all of the requirements for use on extended distribution systems has been developed and proven by repeated tests. A particularly important aspect of this breaker is the pronounced time delay on tripping that permits coordination of several breakers in series and coordination of the breakers with standard fuses of comparable ratings. The coordination possible with this breaker greatly increases the scope of its application and permits the economical extension of low capacity distribution systems with improved quality of service.

References

1. A New Service Restorer, E. F. Sixtus and W. R. Nodder. AIEE Transactions, volume 56, 1937 (January section), pages 180–2, 152.

2. The Oil Circuit Recloser and Its Operation, L. S. Hobson. *General Electric Review*, November 1935.

Short Circuits in Synchronous-Machine Armatures

R. A. GALBRAITH
ASSOCIATE AIEE

Synopsis: An approximate solution is obtained for the current in a short-circuited coil or group of coils in the armature of a synchronous machine operating under load. The solution is expressed as the sum of a series of harmonics whose terms are in geometric ratio. The results obtained are similar in form to those previously obtained for the short circuit of a complete phase winding, and they reduce to that for the single-phase short circuit in the limiting case when the coil group comprises a complete phase. An experimental check of the theory is given for the case of a short circuit of a single armature coil, and it is shown that close agreement is obtained between theory and test with respect to the fundamental component of current, though not with respect to the small higher harmonics of current.

Solutions for single-phase and three-phase short circuits of synchronous machines have been obtained by several authors, those of Park[1] and of Doherty and Nickle[4] being notable. These analyses, however, have considered only complete phase windings, and it is the purpose of this paper to extend the theory to treat short circuits of a single armature coil or group of coils. The solution obtained is applicable to machines operating under load, the effect of the load currents being obtained by an approximation that is sufficiently accurate for practical purposes.

As one coil or a group of coils is essentially a single phase, the analysis is similar in form to that of Doherty and Nickle for the single-phase short circuit. Following their procedure, a general expression is obtained for the magnetic flux linkages of armature and field windings. The constant-linkage theorem, which states that the magnetic flux linkages in any closed electric circuit are constant if the resistance is neglected, is applied to determine the initial currents when the short circuit occurs. From physical considerations, these currents are then separated into their sustained and transient components, and the proper decrement factors are applied to the latter.

Assumptions

For simplification, this analysis is applied to an ideal synchronous machine.[2] In such a machine, linear relationships exist between magnetic flux and currents in any part of the machine, so that the principle of superposition applies. The phase windings are identical and symmetrically placed about the armature, and there are only two field circuits, the main field winding in the direct axis and a short-circuited winding in the quadrature axis, both of which are symmetrical about their respective axes. Only fundamental harmonics of magnetomotive force and voltage appear in the phase windings.

In addition to the assumption regarding the ideal machine, other simplifications are made. The resistances of the group of short-circuited armature coils and of the field circuits are neglected in deter-

Paper 41-163, recommended by the AIEE committee on electrical machinery, and presented at the AIEE South West District meeting, St. Louis, Mo., October 8–10, 1941. Manuscript submitted July 3, 1939; made available for preprinting September 4, 1941.

R. A. Galbraith is assistant professor of electrical engineering, University of Texas, Austin, Texas.

The material in this paper is part of a dissertation presented to the graduate school of Yale University in partial fulfillment of the requirements for the degree of Doctor of Philosophy.

1. For all numbered references, see list at end of paper.

mining initial currents in these windings but are taken into account in obtaining approximate values for the decrement factors. It is also assumed that the effect of the relatively large load resistance is to attenuate the unidirectional and even harmonics of induced current in the load circuit so quickly that these transient elements may be entirely neglected.

The solution is further simplified by making the assumption that, owing to the small mutual inductance between the phases and the coil group, the load currents are unaffected by the short circuit. The value of short-circuit current obtained under this assumption is regarded as the first approximation to the correct result. The effect of this current upon the load currents is then determined, and if the latter are changed an appreciable amount, the analysis is repeated, assuming that the load currents change by this amount. The second approximation is usually sufficiently accurate for all practical purposes, making further refinement unnecessary.

Analytical Development

Since the theorem of superposition is applicable to the ideal synchronous machine, the extension of Blondel's two-reaction method developed by Doherty and Nickle[3] is applied in appendix I to obtain expressions for the inductances of the field and armature circuits. Without loss of generality, the armature winding of which the short-circuited coils are a part is designated as phase A, and the angle between the axis of the coil group and that of phase A is β. Equations are then developed for the self and mutual inductances for the coil group, and it is found that these inductances may be conveniently expressed as functions of known design constants of the machine and the conventional inductances per phase.

Following the procedure that has been outlined, the inductance equations are used in appendix II to obtain the armature and field linkages of the machine. It is found that the results may be conveniently expressed in terms of the currents i_d and i_q defined by

$$i_d = i_a \cos\theta + i_b \cos(\theta-120°) + i_c \cos(\theta-240°) \quad (1)$$

$$i_q = i_a \sin\theta + i_b \sin(\theta-120°) + i_c \sin(\theta-240°) \quad (2)$$

The linkages in the short-circuited coil group are then

$$\psi_s = K_s\{(2/3)L_d i_d + M_d I_d\}\cos(\theta-\beta) + K_s\{(2/3)L_q i_q + M_q I_q\}\sin(\theta-\beta) + \{L_{SD}\cos^2(\theta-\beta) + L_{SQ}\sin^2(\theta-\beta)\}\times(i_s - i_a) \quad (3)$$

where i_s is the short-circuit current in the coil group. Expressions for the inductances and for the constant K_s are given in appendix I. The corresponding field linkages are

$$\psi_D = M_d i_d + K_s M_d (i_s - i_a)\cos(\theta-\beta) + L_d I_d \quad (4)$$

$$\psi_Q = M_q i_q + K_s M_q (i_s - i_a)\sin(\theta-\beta) + L_q I_q \quad (5)$$

These linkage equations will be used to obtain the solutions for the initial currents after the short circuit.

In conformity with the usual practice in the literature, the equations that follow are expressed in terms of reactances instead of inductances. The reactance corresponding to any inductance is the product of the latter and ω, where $\omega = 2\pi f$, f being the rated frequency of the machine. Thus $X_{SD}' = \omega L_{SD}'$.

Solution for Currents

When the short circuit occurs, spontaneous unidirectional components of current appear in the coil group and the field circuit tending to sustain the linkages at their initial value. The voltages that support these transient currents are generated through the collapse of the magnetic fields existing at the instant of short circuit.

As the machine rotates, the transient unidirectional current in the field induces a transient fundamental component of current in the coils, and this in turn causes a second harmonic in the field. This "reflection" from field to coils and back again gives rise to a series of even harmonics in the field and a series of odd harmonics in the coils, all of which are proportional to the average induced field current and all of which decay at the rate determined by the field decrement factor σ_f. Similarly the transient unidirectional current in the short-circuited coils causes a series of even harmonics in the coils and a series of odd harmonics in the field that decay to zero according to the decrement factor of the coil group, σ_s.

The rotating magnetic field due to the average field current supported by exciter voltage causes fundamental and higher harmonics of sustained current to appear in the short-circuited coils and also causes a series of even harmonics in the field.

Owing to the relatively large resistance of the load the transient unidirectional and even harmonics of current induced in the phases by the short circuit will be damped out very quickly and may be neglected. Because of the small mutual inductance between the coil group and the phases, only the fundamental of the induced odd harmonics that also appear is of appreciable magnitude. This component, being due to the fundamental of the short-circuit current in the faulty coils and the transient element of the average field current, will have a sustained and a transient value. The latter decays according to the field decrement factor. Neglecting the small harmonics, therefore, the induced load current can be represented by a sustained and a transient fundamental component. These must be added to the load current existing before the short circuit to get the total phase currents. The corresponding currents i_d and i_q, defined by equations 1 and 2, will then have the form

$$i_d = i_{d1} + (i_{d0} - i_{d1})e^{-\sigma_f t} \quad (6)$$

$$i_q = i_{q1} + (i_{q0} - i_{q1})e^{-\sigma_f t} \quad (7)$$

where i_{d0} and i_{q0} are the initial values before the short-circuit and i_{d1} and i_{q1} are the final sustained values. Approximate expressions for i_{d1} and i_{q1} are given in equations 19 and 20.

First Approximation to Short-Circuit Current. Following the procedure previously outlined, the first approximation to the short-circuit current is obtained by assuming that the load currents are unchanged. When the constant-linkage theorem is applied, it is shown in appendix III that if the short circuit occurs at $\theta = \theta_0$, the initial current in the coil group is

$$i_s = i_a + i' + i'' \quad (8)$$

The components i' and i'' are

$$i' = \frac{-2e_{SD}}{X_{SD}' + \sqrt{X_{SD}'X_{SQ}'}}\{\cos(\theta-\beta) + B\cos 3(\theta-\beta) + B^2\cos 5(\theta-\beta) + \ldots\ldots\} \frac{-2e_{SQ}}{X_{SQ}' + \sqrt{X_{SD}'X_{SQ}'}}\{\sin(\theta-\beta) + B\sin 3(\theta-\beta) + B^2\sin 5(\theta-\beta) + \ldots\ldots\} \quad (9)$$

$$i'' = \frac{e_{SD}\cos(\theta_0-\beta) + e_{SQ}\sin(\theta_0-\beta)}{\sqrt{X_{SD}'X_{SQ}'}}\times\{1 + 2B\cos 2(\theta-\beta) + 2B^2\times\cos 4(\theta-\beta) + \ldots\ldots\} \quad (10)$$

where

$$e_{SD} = K_s\{(2/3)X_d i_{d0} + X_{md} I_{d0}\} \quad (11)$$

and

$$e_{SQ} = K_s\{(2/3)X_q i_{q0}\} \quad (12)$$

are the direct and quadrature components of the voltage in the coil group prior to the short circuit, and

$$B = \frac{\sqrt{X_{SQ}'} - \sqrt{X_{SD}'}}{\sqrt{X_{SQ}'} + \sqrt{X_{SD}'}} \quad (13)$$

is a constant.

By the assumption made, i_a is unchanged, so that the additional current that is due to the short circuit is represented by the components i' and i''. The latter contains the d-c and even harmonics that arise to maintain the linkages at their initial value; therefore it is transient in character and decays to zero at the rate determined by σ_s. The other component, i', contains the odd harmonics and is proportional to the average field current.

As shown in appendix III, the average field current just after the short circuit occurs is

$$I_d(\text{average}) = G_0 I_{d0} \tag{14}$$

where G_0 is a constant defined by equation 60. Since the average sustained field current is I_{d0}, it is $1/G_0$ times as great as the initial value. The sustained value of i', therefore, is $1/G_0$ times as great as the initial value expressed in equation 9. The remaining portion $(1-1/G_0)i'$, is a transient and decays according to σ_f. The first approximation to the short-circuit current in the coil group is therefore

$$i_s = i_a + \frac{1}{G_0} i' + \left(1 - \frac{1}{G_0}\right) i' e^{-\sigma_f t} + i'' e^{-\sigma_s t} \tag{15}$$

The effect of the change in load currents being small, it will be found that this expression gives results that do not differ greatly from those obtained by the more accurate expression, equation 21.

The additional current introduced in the coil group by the short circuit is $(i_s - i_a)$, and for the reasons previously mentioned, its fundamental component is the only one that has appreciable effect upon the load currents. From equations 9 and 15, the sustained value of

$$(i_s - i_a)(\text{fundamental}) = I_1 \cos(\theta - \beta - \alpha_1) \tag{16}$$

where

$$I_1 = \frac{1}{G_0}\left[\left\{\frac{e_{SD}}{X_{SD}' + \sqrt{X_{SD}'X_{SQ}'}}\right\}^2 + \left\{\frac{e_{SQ}}{X_{SQ}' + \sqrt{X_{SD}'X_{SQ}'}}\right\}^2\right]^{1/2} \tag{17}$$

and

$$\alpha_1 = \tan^{-1}\left\{\left(\frac{e_{SQ}}{e_{SD}}\right)\frac{X_{SD}' + \sqrt{X_{SD}'X_{SQ}'}}{X_{SQ}' + \sqrt{X_{SD}'X_{SQ}'}}\right\} \tag{18}$$

Taking approximate account of the effect of this current, it is shown in appendix IV that the sustained values of i_d and i_q corresponding to equations 6 and 7 are

$$I_{d1} = -\frac{3}{2}\,\frac{x_q + X_L}{r^2 + (X_d + X_L)(X_q + X_L)}\left[X_{md} I_{d0} + K_S X_D \frac{I_1}{2}\cos\alpha_1 + \frac{r}{X_q + X_L} K_S X_Q \frac{I_1}{2}\sin\alpha_1\right] \tag{19}$$

$$i_{q1} = \frac{-r}{X_q + X_L} i_{d1} - \frac{3}{2(X_q + X_L)} K_S X_Q \frac{I_1}{2}\sin\alpha_1 \tag{20}$$

The corresponding expressions for i_{d0} and i_{q0} are obtained from those for i_{d1} and i_{q1} by putting $I_1 = 0$.

Second Approximation to Short-Circuit Current. The next step in the solution for the short-circuit currents is to assume that i_d and i_q have average values given by equations 6 and 7. Following the same procedure as before, the linkages of the coil group and the field circuits may be obtained and solved for the initial currents in the coil group and the field winding. Separated into its sustained and transient components and with the proper decrements applied, the second approximation to the short-circuit current in the coil group is

$$\begin{aligned} i = {} & \frac{2}{3}\{i_{d1}\cos\theta + i_{q1}\sin\theta\} - \\ & \frac{1}{G_1}\Bigg[\frac{2\{e_{SD} - K_S(^2/_3)X_d'(i_{d0} - i_{d1})\}}{X_{SD}' + \sqrt{X_{SD}'X_{SQ}'}} \times \\ & \{\cos(\theta-\beta) + B\cos 3(\theta-\beta) + \ldots\} + \\ & \frac{2\{e_{SQ} - K_S(^2/_3)X_q'(i_{q0} - i_{q1})\}}{X_{SQ}' + \sqrt{X_{SD}'X_{SQ}'}}\{\sin(\theta-\beta) + \\ & B\sin 3(\theta-\beta) + B^2\sin 5(\theta-\beta) + \ldots\}\Bigg] + \\ & e^{-\sigma_f t}(^2/_3)\{(i_{d0} - i_{d1})\cos\theta + (i_{q0} - i_{q1})\sin\theta\} - \\ & \frac{1e^{-\sigma_f t}}{G_1}\left[\frac{\{(G_1-1)e_{SD} - K_S(^2/_3)X_d'(i_{d0} - i_{d1})\}\cos(\theta-\beta) + \{(G_1-1)e_{SQ} - K_S(^2/_3)X_q'(i_{q0} - i_{q1})\}\sin(\theta-\beta)}{(^1/_2)(X_{SD}' + X_{SQ}') + (^1/_2)(X_{SD}' - X_{SQ}')\cos 2(\theta-\beta)}\right] + \\ & e^{-\sigma_s t}\frac{\{e_{SD}\cos(\theta_0-\beta) + e_{SQ}\sin(\theta_0-\beta)\}}{\sqrt{X_{SD}'X_{SQ}'}} \times \\ & \{1 + 2B\cos 2(\theta-\beta) + 2B^2\cos 4(\theta-\beta) + \ldots\} \end{aligned} \tag{21}$$

where

$$G_1 = \frac{X_{SD} + \sqrt{X_{SD}'X_{SQ}'}}{X_{SD}' + \sqrt{X_{SD}'X_{SQ}'}} \times \left[1 + \frac{2(X_d - X_d')(i_{d0} - i_{d1})}{3X_{md}I_{d0}} + \frac{X_{SD} - X_{SD}'}{X_{SD}' + \sqrt{X_{SD}'X_{SQ}'}}\cdot\frac{2X_d i_{d1}}{3X_{md}I_{d0}}\right] \tag{22}$$

The solution for the coil current for the case of short circuit at no load is obtained by letting $i_{d0} = i_{q0} = i_{d1} = i_{q1} = 0$ in equation 21. This is equivalent to making $e_{SQ} = 0$ and $e_{SD} = K_S X_{md} I_{d0}$.

Because of the relatively small mutual inductance between the coil group and the phase and field circuits $(i_{d0} - i_{d1})$, $(i_{q0} - i_{q1})$, and $(G_1 - 1)$ are ordinarily small. Therefore it is usually possible to neglect the terms involving $e^{-\sigma_f t}$ when making calculations using equation 21. For the sake of completeness, however, they have been included.

One component of the sustained short-circuit current is equal to the sustained load current $(^2/_3)\{i_{d1}\cos\theta + i_{q1}\sin\theta\}$. The other component is the sum of two odd harmonic series whose terms, in ascending order, are in geometric ratio. The ratio, B, is given in equation 13.

The expression for the short circuit current of the group of coils is similar in form to that given by Doherty and Nickle[4] for the single phase short circuit and their discussion of the effects of the machine constants upon the form of the solution applies equally well here. In the limiting case when the coil group comprises a complete phase, the solution for the condition of no load is exactly the same as theirs.

Decrement Factors

Expressions for the decrement factors may be obtained by the approximate method used by Doherty and Nickle,[4] which they have discussed fully. It is then found that the decrement factor for the coil group is

$$\sigma_s = \frac{\omega r_s}{\sqrt{X_{SD}'X_{SQ}'}} \tag{23}$$

where r_s is the resistance of the shorted coils, and that for the field is

$$\sigma_f = \frac{X_{SD} + \sqrt{X_{SD}'X_{SQ}'}}{X_{SD}' + \sqrt{X_{SD}'X_{SQ}'}}\cdot\frac{R_d}{L_d} \tag{24}$$

when R_d is the total resistance of the field circuit.

Experimental Confirmation of Theoretical Results

To verify the theory, experimental measurements were made of the short-circuit current in a single coil of a 125-horsepower, 440-volt, 60-cycle, 900-rpm, three-phase, synchronous motor. This machine had a full-pitch armature winding, no amortisseur on the rotor, and was a specially built laboratory machine with the leads to the armature coils brought out to a terminal board, making each coil accessible for measurements. The measured values of the reactances and resistances of the machine are given in table I.

Table I. Measured Reactances* and Resistances of Test Machine

$X_d =$	1.520 ohms	$X_D =$	1.050 ohms
$X_d' =$	0.445 ohm	$X_D' =$	0.266 ohm
$X_q = X_q' =$	1.205 ohms	$X_Q = X_Q' =$	0.970 ohm

$X_0 = 0.237$ ohm
$X_{md} = 37.3$ ohms
$r_a = 0.048$ ohm at 25 C (line to neutral)
$R_d = 23.5$ ohms at 25 C

* Measured by static test method.

Using the equations that have been developed, it is found that for a single armature coil of the machine,

$K_s = 0.0434$

$X_{SD} = X_{SQ} = X_{SQ}' = 0.0126$ ohm

$X_{SD}' = 0.01109$ ohm

The short-circuit current was measured by taking the voltage drop across a 0.000243-ohm, non-inductive shunt in series with the coil. The wave form of the current was obtained from an oscillogram of this voltage, and the magnitudes of the sustained harmonic components were measured with a vacuum-tube harmonic analyzer.

The coil used in the test was in the center of phase A, so that $\beta = 0$. The current was calculated analytically and checked experimentally for short circuits occurring under two different operating conditions, one when the machine was loaded, and one at no load. Both tests were made at reduced voltage to eliminate the effect of saturation as far as possible.

For the short circuit under load, the machine was operating with a pure resistive load of 2.45 ohms per phase and a field current of 0.992 ampere. The short circuit occurred at $\theta_0 = 215°$. The calculated current for the short-circuited coil was

$$i_s = -164.0\cos(\theta - 17.28°) - 5.13\times\cos(3\theta - 23.16°) - 0.161\times\cos(5\theta - 23.16°) - \ldots - e^{-0.0133\omega t}[4.80\times\cos(\theta + 19.85°) + 0.116\times\cos(3\theta + 13.38°) + \ldots] - e^{-0.1987\omega t}[163.3 + 10.27\cos 2\theta + 0.324\cos 4\theta + \ldots]$$

where $215° < \theta$ and $\omega t = (\theta - \theta_0)$ in radians. In table II the magnitudes of the harmonics of the calculated sustained current are compared with the actual values as measured with a harmonic analyzer.

The short-circuit at no load occurred at $\theta_0 = 180°$ and the field current was 0.988 ampere. The calculated current is

$$i_s = -185.5\cos\theta - 5.85\cos 3\theta - 0.184\times\cos 5\theta - \ldots - e^{-0.1987\omega t}[191.5 + 12.06\cos 2\theta + 0.38\times\cos 4\theta + \ldots]$$

where $180° < \theta$ and $\omega t = (\theta - \theta_0)$ in radians. The magnitude of the sustained harmonics of the calculated and measured currents are compared in table II.

Considering only the fundamental components of sustained current, the data in table II show that the calculated and measured values agree very closely. The analytical and experimental results for the higher harmonics, however, do not agree. This is probably due in large part to the fact that the higher harmonics of mutual linkages between the coil and the other

Table II. Comparisons of Peak Values* of Harmonics of Sustained Current in a Single Coil

	Fundamental	Third	Fifth
Machine loaded			
Calculated	164.0	5.13	0.161
Measured	165.5	29.1	6.69
No load			
Calculated	185.5	5.85	0.184
Measured	190.7	30.85	3.49

* All values are given in amperes.

machine circuits were neglected in the analysis. While the voltages due to higher harmonics of flux are ordinarily small in the complete phase due to the effects of fractional pitch and distributed windings, they may be much more important in one or two coils. To neglect these harmonics of flux, therefore, may introduce considerable error in the higher harmonics of current in the short-circuited coils. As they have little effect on the fundamental voltage, however, they may be disregarded in determining the fundamental component of current.

Oscillograms were made of the short-circuit current, and these were compared with a graphical plot of the calculated current. The agreement between the calculated and test results was fairly good, both during the transient period and after the transient components had died out. The effect of the larger values of the harmonics in the actual current was noticeable, however, the actual waves being slightly more peaked than those which were calculated.

Had the test machine been operated at higher flux densities, the effect of saturation would probably have been noticeable. As pointed out by Doherty and Nickle, this would not prevent the use of the results of the theoretical analysis, as the effect of saturation may be taken into account by proper shading of the machine constants.

Appendix I

Inductance Equations

Expressions for the inductances of the field and armature circuits may be obtained by application of the extension of Blondel's method previously mentioned. With the assumptions that have been made, only the fundamental component of magnetomotive force need be considered in obtaining the mutual linkages due to any machine circuit. The procedure is to resolve this space sinusoid into two components, one in the direct axis and one in the quadrature axis, determine the corresponding fundamental linkages due to each component acting separately, and combine these linkages to get the resultant. The fundamental linkages in any other circuit of the machine per unit current in the exciting circuit are equal to the mutual inductance between the two. That portion that is due to the space fundamental of air gap flux is the inductance of armature reaction, and the remainder, which is due to flux in the slots and end windings, is leakage inductance.

Self-Inductance of Armature Reaction of a Complete Phase Winding

Let the flux density per unit magnetomotive force at the armature surface be represented by the even harmonics series[3]

$$P = P_0 + P_2\cos 2\lambda + P_4\cos 4\lambda + \ldots \quad (25)$$

The fundamental component of the linkages with the complete phase A winding of the air-gap flux due to the fundamental component of magnetomotive force of phase A may be expressed as

$$\psi_{aa} = i_a\{L_{AD}\cos^2\theta + L_{AQ}\sin^2\theta\} \quad (26)$$

where

$$L_{AD} = 3.2Dl(yN_cK_dK_p)^2\{P_0 + (1/2)P_2\} \quad (27)$$

$$L_{AQ} = 3.2Dl(yN_cK_dK_p)^2\{P_0 - (1/2)P_2\} \quad (28)$$

are the static inductances of armature reaction for one phase.

Mutual Inductances Between Coil Group and Phase and Field Windings

If the space fundamental of magnetomotive force for the coil group is considered, it may easily be shown that the linkages of armature reaction in phase A due to the current in the coil group are

$$\psi_{as} = i_sK_s\{L_{AD}\cos(\theta - \beta)\cos\theta + L_{AQ}\times\sin(\theta - \beta)\sin\theta\} \quad (29)$$

where

$$K_s = \frac{sK_{ds}}{pyK_d} \quad (30)$$

and s is the number of coils in the group, y the slots per phase per pole, p the number of poles, K_d the phase belt distribution factor, and K_{ds} the distribution factor for the s coils; that is, sK_{ds} is the ratio of the fundamental of magnetomotive force for the coil group to that for a single coil. The corresponding linkages in phase B are obtained by replacing $\cos\theta$ and $\sin\theta$ by $\cos(\theta - 120°)$ and $\sin(\theta - 120°)$ respectively, and those for phase C may be obtained by using $(\theta - 240°)$ instead of $(\theta - 120°)$. The linkages per unit current in these expressions are equal to the mutual inductances of armature reaction between the phase windings and the coil group. The corresponding mutual leakage linkages will have the same form except that, being independent of rotor position, they will be the same for direct and quadrature axes. These mutual leakage inductances are $K_sL_l\cos\beta$, $K_s2L_{lm}\times\cos(\beta - 120°)$, and $K_s2L_{lm}\cos(\beta - 240°)$ for phases A, B, and C respectively. Adding these components to those due to armature reaction, it is found that the mutual inductance between the coil group and phase A is

$$L_{as} = K_s\{L_D\cos(\theta - \beta)\cos\theta + L_Q\times\sin(\theta - \beta)\sin\theta\} \quad (31)$$

The corresponding expression for the mutual

inductance between the coil group and phase B is

$$L_{bs}=K_s\{(L_D-L_0)\cos(\theta-\beta)\cos(\theta-120°)+(L_Q-L_0)\sin(\theta-\beta)\sin(\theta-120°)\} \quad (32)$$

and that for phase C is similar to equation 32 with $(\theta-240°)$ instead of $(\theta-120°)$.

The procedure followed in the preceding paragraph may be used to obtain the mutual inductances between the coil group and the field windings. These inductances are then found to be

$$M_{sd}=K_sM_d\cos(\theta-\beta) \quad (33)$$

$$M_{sq}=K_sM_q\sin(\theta-\beta) \quad (34)$$

It should be noted that all of the mutual inductances for the coil group are expressed as the product of the constant K_s and the inductances of the machine per phase.

Self Inductance of a Coil Group

Although space harmonics of magnetomotive force cannot appear in the complete phase winding of an ideal machine, they must be considered in obtaining an expression for the self inductance of a coil group. In the work that follows, therefore, the complete magnetomotive force of the coil group will be considered.

As the inductance of a coil group is a function of the self and mutual inductances for the individual coils in the group, the first step in this analysis will be to develop an expression for the self inductance of a single coil. The next step will be to obtain a general expression for the mutual inductance between two coils. These self and mutual inductances may then be combined to obtain the total self inductance of the coil group.

Assuming that the current i_s in a single coil of N_c turns is distributed in a line at the armature surface and that the iron has infinite permeability, the magnetomotive force distribution of the coil over the coil span ρ is a square-topped wave of magnitude

$$A_1=(1-\rho/p\pi)(0.4\pi N_ci_s) \quad (35)$$

If the relation between the flux density and magnetomotive force is expressed by equation 25, the linkages, with the coil, of the air-gap flux due to this magnetomotive force may be shown to be

$$\psi_{ss}=[(p-\rho/\pi)\{\pi^2/8(pyK_dK_p)^2\}]\times\{(\rho/2\pi)(L_{AD}+L_{AQ})+(1/\pi)\times(L_{AD}-L_{AQ})\sin\rho\cos 2(\theta-\beta)\} \quad (36)$$

when the small higher harmonics are neglected.

Since the path of the leakage flux in the slots and end windings is practically the same for a single coil and a complete phase and since there are $1/py$ as many turns for the single coil as for the phase winding, the ratio of the leakage linkages for the coil to those for the phase is approximately $1/(py)^2$. As indicated by equations 26 and 36 this is much smaller than the corresponding ratio for the linkages due to air-gap flux. The leakage component is, therefore, only a small percentage of the total linkages of the coil. Since $2L_{lm}$ is also very small in comparison to $(1/2)(L_{AD}+L_{AQ})$, the assumption will be made that the total linkages of the coil can be expressed in a form similar to equation 36 with

$$(1/2)(L_D+L_Q)-L_0=(1/2)(L_{AD}+L_{AQ})+2L_{lm}$$

substituted for $(1/2)(L_{AD}+L_{AQ})$. Although this assumption may introduce considerable error in the leakage linkages added, it will make only a small discrepancy in the total linkages, and the equation may be put in a much more convenient form for calculation. The total self inductance of a single coil is then

$$L_{ss}=L_{SD}\cos^2(\theta-\beta)+L_{SQ}\sin^2(\theta-\beta) \quad (37)$$

where

$$L_{SD}=[(p-\rho/\pi)\{\pi^2/8(pyK_dK_p)^2\}]\times[(\rho/\pi)\{(1/2)(L_D+L_Q)-L_0\}+(1/\pi)(L_D-L_Q)\sin\rho] \quad (38)$$

$$L_{SQ}=[(p-\rho/\pi)\{\pi^2/8(pyK_dK_p)^2\}]\times[(\rho/\pi)\{(1/2)(L_D+L_Q)-L_0\}-(1/\pi)(L_D-L_Q)\sin\rho] \quad (39)$$

The magnetomotive force distribution of the single coil over the armature outside the coil span will be a square-topped wave of magnitude

$$A_2=-(\rho/p\pi)(0.4\pi N_ci_s) \quad (40)$$

Using equations 27 and 28 and making the same assumptions regarding leakage linkages that were made in deriving equation 37, it may be shown that the mutual inductance between two coils separated a small angle Δ is approximately

$$L_{ms}=\{(p-\rho/\pi)(\pi^2/8)/(pyK_dK_p)^2\}\times[\{\rho/\pi-\rho\Delta/(p\pi-\rho)\}\{(1/2)(L_D+L_Q)-L_0\}+(1/\pi)\cos\Delta\sin(\rho-\Delta)\times\{(L_D-L_Q)\cos 2(\theta-\beta)\}] \quad (41)$$

The total self inductance of a group of coils may be obtained from the relationship

$$L_{ss}=L_{11}+L_{22}+L_{33}+\ldots+2(L_{12}+L_{13}+L_{23}+\ldots) \quad (42)$$

where L_{11}, L_{22}, ... are the self inductances of each coil given by equation 37 and L_{12}, L_{13}, ... are the mutual inductances between coils 1 and 2, 1 and 3, etc., as given by equation 41. It is apparent that the total self inductances of the coil group can be put in the form of equation 37 if L_{SD} and L_{SQ} are given the proper values. Equation 37, therefore, is a general expression for the total self inductance of a group of armature coils whether the group consists of one, two, or more coils.

Transient Inductances

The transient inductances L_{SD}' and L_{SQ}' are defined by

$$L_{SD}'=L_{SD}-K_s^2(M_d^2/L_d) \quad (43)$$

$$L_{SQ}'=L_{SQ}-K_s^2(M_q^2/L_q) \quad (44)$$

The inductances L_d', L_q', L_D', and L_Q' correspond to the transient reactances X_d', X_q', X_D', and X_Q' as ordinarily defined in the literature.

Appendix II

Linkage and Voltage Equations

The armature and field linkages for an ideal synchronous machine under normal conditions have been given by Park.[1,2] Following his analysis, it may be shown that if

$$\psi_d=(2/3)(L_d+L)i_d+M_dI_d \quad (45)$$

$$\psi_q=(2/3)(L_q+L)i_q+M_qi_q \quad (46)$$

then the following voltage equations may be obtained:

$$-\frac{d\psi_d}{dt}-\psi_q\frac{d\theta}{dt}=\frac{2}{3}ri_d \quad (47)$$

$$-\frac{d\psi_q}{dt}+\psi_d\frac{d\theta}{dt}=\frac{2}{3}ri_q \quad (48)$$

where r is the combined resistance of one phase of the machine and load.

When the machine contains another circuit of a group of short-circuited coils, the linkage equations must be modified to include the effect of the additional current in the faulty coils. This may be done by making use of the expressions for the mutual inductances between the coil group and the phase and field windings.

It is convenient to consider the magnetomotive force of the portion of the phase A winding that is outside the faulty coils as the difference between that due to a current i_a in the complete phase winding and that due to the coil group carrying the same current i_a. Similarly, the linkages in this portion of the phase A winding due to other currents may be obtained by subtracting the linkages in the faulty coils from those in the complete phase.

When the inductance equations developed in appendix I are used, the modified forms of equations 45 and 46 become

$$\psi_d=(2/3)(L_d+L)i_d+K_sL_D(i_s-i_a)\times\cos(\theta-\beta)+M_dI_d \quad (49)$$

$$\psi_q=(2/3)(L_q+L)i_q+K_sL_Q(i_s-i_a)\times\sin(\theta-\beta)+M_qI_q \quad (50)$$

It may then be shown that, to a close approximation, the voltage equations 47 and 48 are applicable to the short-circuited machine when ψ_d and ψ_q have the values given in equations 49 and 50.

Appendix III

Short-Circuit Currents Assuming Load Currents Constant

At the instant of short circuit, $\theta=\theta_0$, $i_d=i_{d0}$, $i_q=i_{q0}$, $I_d=I_{d0}$, and $I_q=0$. Applying the constant linkage theorem, the linkages in the coil group and the field windings are

$$K_s\{(2/3)L_di_d+M_dI_d\}\cos(\theta-\beta)+K_s\{(2/3)L_qi_q+M_qI_q\}\sin(\theta-\beta)+\{L_{SD}\cos^2(\theta-\beta)+L_{SQ}\sin^2(\theta-\beta)\}(i_s-i_a)=K_s\{(2/3)L_di_{d0}+M_dI_{d0}\}\cos(\theta_0-\beta)+K_s\{(2/3)L_qi_{q0}\}\sin(\theta_0-\beta) \quad (51)$$

$$M_di_d+K_sM_d(i_s-i_a)\cos(\theta-\beta)+L_dI_d=M_di_{d0}+L_dI_{d0} \quad (52)$$

$$M_qi_q+K_s(i_s-i_a)\sin(\theta-\beta)+L_qI_q=0 \quad (53)$$

In accordance with the method of analysis that has been outlined, the first approximation to the solution is obtained by assuming

that $i_d = i_{d0}$ and $i_q = i_{q0}$ remain constant. Then a simultaneous solution of equations 51, 52, and 53 gives

$$(i_s - i_a) = \frac{e_{SD}\{\cos(\theta_0-\beta) - \cos(\theta-\beta)\} + e_{SQ}\{\sin(\theta_0-\beta) - \sin(\theta-\beta)\}}{(1/2)(X_{SD}'+X_{SQ}') + (1/2)(X_{SD}'-X_{SQ}')\cos 2(\theta-\beta)} \tag{54}$$

$$I_d = I_{d0} - \frac{X_{SD}-X_{SD}'}{K_s X_{md}}(i_s - i_a)\cos(\theta-\beta) \tag{55}$$

where e_{SD} and e_{SQ} are defined by equations 11 and 12. These may also be expressed as

$$(i_s - i_a) = i' + i'' \tag{56}$$

$$I_d = I_d' + I_d'' \tag{57}$$

where i' and i'' are given by equations 9 and 10 and I_d' and I_d'' are

$$I_d' = I_{d0} + \frac{X_{SD}-X_{SD}'}{K_s X_{md}} \frac{e_{SD}}{X_{SD}' + \sqrt{X_{SD}'X_{SQ}'}} + \frac{X_{SD}-X_{SD}'}{K_s X_{md}}\left[\frac{e_{SD}(1-B)^2}{2\sqrt{X_{SD}'X_{SQ}'}}\{\cos 2(\theta-\beta) + B\cos 4(\theta-\beta) + \ldots\} + \frac{e_{SQ}(1-B^2)}{2\sqrt{X_{SD}'X_{SQ}'}} \times \{\sin 2(\theta-\beta) + B\sin 4(\theta-\beta) + \ldots\}\right] \tag{58}$$

$$I_d'' = \frac{(X_{SD}-X_{SD}')(1+B)}{2K_s X_{md}\sqrt{X_{SD}'X_{SQ}'}}\{e_{SD}\cos(\theta_0-\beta) + e_{SQ}\sin(\theta_0-\beta)\}[\cos(\theta-\beta) + B\cos 3(\theta_0-\beta) + \ldots] \tag{59}$$

The average field current is

$$I_d(\text{average}) = I_{d0} + \frac{X_{SD}-X_{SD}'}{K_s X_{md}} \frac{e_{SD}}{X_{SD}' + \sqrt{X_{SD}'X_{SQ}'}} = G_0 I_{d0} \tag{60}$$

where G_0 is the value of G_1 obtained from equation 22 by setting $i_{d1} = i_{d0}$.

The component of field current, I_d'', contains the odd harmonics and is due to the unidirectional component and even harmonics of the current $(i_s - i_a)$ to which it is directly proportional. It therefore decays to zero according to the decrement factor σ_s.

The current I_d', containing the unidirectional component and even harmonics, must have an average sustained value I_{d0} since it is supported entirely by the exciter voltage. Its sustained value is therefore $(1/G_0)i_d'$. The remainder $(1-1/G_0)I_d'$, is transient in character and, being proportional to the average field current, decays at a rate fixed by σ_f.

Separated into sustained and transient components and with the decrement factors applied, the field current at any instant after the short circuit is

$$I_d = (1/G_0)I_d' + (1-1/G_0)I_d'e^{-\sigma_f t} + I_d''e^{-\sigma_s t} \tag{61}$$

Appendix IV

Short-Circuit Currents Assuming Change in Load Currents

A second approximation to the solution for the short-circuit current is obtained by assuming that i_d and i_q have average values given by equations 6 and 7. It will first be necessary, however, to develop expressions for the currents i_{d1} and i_{q1}.

The currents i_{d1} and i_{q1} may be obtained by use of the voltage equations given in appendix II. Considering only average values, $d\psi_d/dt = d\psi_q/dt = 0$. The average value of $(i_s - i_a)\cos(\theta-\beta)$ is $(1/2)I_1\cos\alpha_1$ and that of $(i_s - i_a)\sin(\theta-\beta)$ is $(1/2)I_1\sin\alpha_1$, where I_1 and α_1 are defined by equations 17 and 18. Likewise, the average value of I_d is I_{d0} and the average of $I_q = 0$. Then from equations 47, 48, 49, and 50,

$$(2/3)(X_q + X_L)i_{q1} + (1/2)K_s X_Q I_1 \sin\alpha_1 + (2/3)r i_{d1} = 0 \tag{62}$$

$$(2/3)(X_q + X_L)i_{d1} + (1/2)K_s X_D I_1 \cos\alpha_1 - (2/3)r i_{q1} = -X_{md}I_{d0} \tag{63}$$

These may be solved simultaneously to obtain the currents i_{d1} and i_{q1}. The results are given in equations 19 and 20.

With currents i_d and i_q given by equations 6 and 7, the linkage equations for the short-circuited coils and field windings may be obtained. Following the same procedure as before, these may be solved for the initial currents. When the short-circuit current is separated into its sustained and transient components and the proper decrements are applied, the second approximation to the solution is that given by equation 21.

Nomenclature

i_a, i_b, i_c = currents in phases A, B, and C
i_s = current in short-circuited coil group
I_d = current in main field winding
I_q = current in field winding in quadrature axis
K_d, K_p = distribution and pitch factors for armature phase winding
K_{ds} = distribution factor for the group of s coils as discussed following equation 30
$K_s = (sK_{ds}/pyK_d)$ is a constant
L_D, L_Q = total static inductances, single phase, in the direct and quadrature axes, respectively. These correspond to the commonly used reactances, X_D and X_Q
L_d, L_q = total three phase, line to neutral inductances in the direct and quadrature axes corresponding to the synchronous reactances X_d and X_q
$L_0 = (L_l - 2L_{lm})$ = zero sequence inductance corresponding to X_0
L_l, L_{lm} = self and mutual leakage inductances per phase
L_{SD}, L_{SQ} = inductances of coil group in the direct and quadrature axes. See appendix I
L = load inductance per phase corresponding to X_L
M_q = maximum mutual inductance per phase between quadrature axis field winding and armature
M_d = maximum mutual inductance per phase between main field and armature
s = number of coils in short-circuited coils
X_d, X_q, X_d', X_q' = usual three phase, line to neutral, synchronous and transient reactances for the direct and quadrature axes
$X_{md} = \omega M_d$
X_D, X_Q, X_D', X_Q', = usual static single phase and transient reactances in the direct and quadrature axes
X_{SD}, X_{SQ} = reactances corresponding to L_{SD}, L_{SQ}
$X_L = \omega L$ = reactance of load per phase
β = angular displacement, in electrical radians, of the axis of the group of s short-circuited coils from that of phase A
ρ = coil pitch in electrical radians
θ = angular displacement of direct axis from that of phase A, measured in electrical radians
σ_f = decrement factor of main field, defined by equation 23
σ_s = decrement factor of short-circuited coils, defined by equation 24

References

1. Two-Reaction Theory of Synchronous Machines, Part I, R. H. Park. AIEE Transactions, volume 48, 1929, page 716; Part II, AIEE Transactions, volume 52, 1933, page 352.

2. Definition of Ideal Synchronous Machine and Formula for the Armature-Flux Linkages, R. H. Park. *General Electric Review*, volume 31, 1928, page 332.

3. Synchronous Machines—I, R. E. Doherty and C. A. Nickle. AIEE Transactions, volume 45, 1926, page 912.

4. Synchronous Machines—IV, R. E. Doherty and C. A. Nickle. AIEE Transactions, volume 47, 1928, page 457.

5. Synchronous Machines—V, R. E. Doherty and C. A. Nickle. AIEE Transactions, volume 49, 1930, page 700.

6. A Simplified Method of Analyzing Short-Circuit Problems, R. E. Doherty. AIEE Transactions, volume 42, 1923, page 841.

Transient Overspeeding of Induction Motors

RAYMOND W. AGER
ASSOCIATE AIEE

Synopsis: A transient swing above synchronous speed has been observed when a certain standard squirrel cage induction motor was started without load. This paper presents an explanation of the phenomenon based on the frequency modulation of the power supply caused by the rapid variation of the power taken from the line. Mathematical relations are developed and applied to the operating conditions of this motor. The agreement of the mathematical and test curves indicates that the explanation is basically correct although some secondary effects, not considered, may be present.

A TRUE induction motor cannot, of itself, operate at or above synchronous speed. The torque developed by this type of motor passes through zero at synchronous speed. It should, therefore, never be able to send the motor above that speed. Yet, in making some acceleration tests, a certain motor was consistently found to go above synchronous speed for a few cycles each time it was started.

This motor was from a standard line of squirrel cage induction motors. It had a cast aluminum rotor with deep, narrow slots. There were no salient-pole structures on the rotor, and, further, the rotor bars were skewed so that there was no tendency for the rotor to lock into synchronism. After the motor was up to speed and had settled down, the slip at no load became constant at less than 0.1 per cent.

The tests in which this behavior was observed were similar to those described in a previous paper.[1] A bakelite disc having 500 divisions accurately engraved around the periphery was mounted on the motor shaft. This disc was illuminated by light pulses from a stroboscopic lamp flashing 60 times per second, and the disc's position was photographically recorded at each flash. The motor was reversed on the line and readings were taken as the motor speed dropped from full speed in one direction to zero and then came back up to full speed in the opposite direction. Velocities were calculated by taking position differences, and accelerations were calculated by taking velocity differences. Since the friction forces were very small the entire torque of the motor was used in producing accelerations. The accelerations observed were converted to torques and plotted against speed in figure 1. Figure 2 shows a section of the velocity versus time curve for the same test. In this test the motor was operated at rated voltage. Due to the high torques developed and the low inertia of the rotor, the motor dropped from full speed in one direction to zero and returned to full speed in the opposite direction in a little over one-half second.

Paper 41-150, recommended by the AIEE committee on electrical machinery, and presented at the AIEE Pacific Coast convention, Yellowstone National Park, August 27–29, 1941. Manuscript submitted May 8, 1941; made available for preprinting July 16, 1941.

RAYMOND W. AGER is of the school of electrical engineering, Cornell University, Ithaca, N. Y.

The data used in this paper were obtained by C. N. Williamson, a former student of the University of California, now with the U. S. Navy engineering department.

The curve of figure 2 shows that the motor passed through synchronous speed about 35.5 cycles after the test was started, and that it rose almost two per cent above synchronous speed on the first over-swing. A second over-swing was recorded and a third one indicated. Reference to the torque curve of figure 1 shows that the torque developed was practically equal to full-load torque as the motor passed through synchronous speed the first time.

The reason for this peculiar behavior was fiist qualitatively described as follows. The input to the motor had both power and lagging components. The power input to the motor was approximately proportional to the torque developed. The curve of figure 1 would indicate that during the first part of the test the power input was relatively constant. After passing the maximum torque at about 85% of synchronous speed the power taken from the lines dropped very rapidly. The lagging component of the line current, however, certainly did not vary in the same way. A more gradual change of this component would be expected. The power component would reverse if the motor changed from motor to generator action. Such reversal would not occur in the magnetizing component. From full load to no load the lagging component should be nearly constant and therefore cause constant IR and IX drops. Since it is the rapid variation of these impedance drops which is important and not their magnitudes the effects of the lagging component may be neglected. The power was supplied from a transformer bank connected to a 4,000 volt system. The bank had an appreciable reactance. Neglecting the resistance of the bank and the lagging component of the motor current, the vector diagram would be as indicated in figure 3. In this diagram E_1 represents the transformer primary voltage vector which may be taken as constant in magnitude and rotating at a constant velocity ω_1. E_2 is the motor-voltage vector and IX is the reactance drop in the transformer due to the power component of the motor current. As long as the power component is constant the vector E_2 must rotate at the same speed as the vector E_1, although lagging behind it. If the power component decreases the impedance drop must decrease and the vector E_2 must catch up with vector E_1. Therefore during this transient period the vector must rotate at a velocity ω_2 greater than that corresponding to the normal line frequency. With a frequency greater than 60 cycles impressed on the motor terminals, even if only for a few cycles, the motor may attain a speed greater than the 60 cycle synchronous speed if very lightly loaded.

A more quantitative analysis following the above ideas has indicated that this reasoning is correct. The motor on which the tests were made is no longer available and accurate measurements of its constants had not been made. Approximate values of some of these constants had been determined and the others may be estimated accurately enough for present purposes. All values used are thought to be within 3% of the correct values except

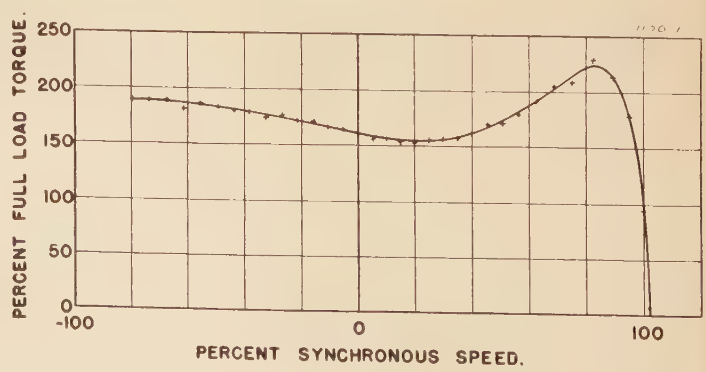

Figure 1. Speed-torque curve for a 15-horsepower four-pole squirrel-cage motor

Curve was determined under transient conditions for rapid acceleration under no load

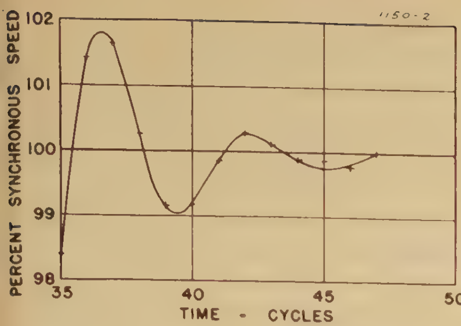

Figure 2. Section of velocity-versus-time curve for same test as figure 1

the full load slip. The full load slip was not determined but the motor manufacturer was consulted before assigning the value used.

Near synchronous speed the torque developed is proportional to the slip, and this torque will all be used in accelerating the rotor if the friction forces are negligible.

$$T = K_1 S = \frac{WR^2}{g} \times \frac{d\omega}{dt} \tag{1}$$

Where S is the slip and ω is the angular velocity of the rotor in radians per second. The full load torque of the motor was 45 pound-feet, and the full load slip was about 2.0 per cent. Therefore the constant K_1 was 45/0.020 or 2,250. The inertia of the rotor, coupling, and disc was 4.0 pound-feet-squared.

From figure 3

$$\omega_2 = \omega_1 - \frac{d\alpha}{dt} \tag{2}$$

The line frequency was 60 cycles per second so that $\omega_1 = 2\pi 60 = 377$. Equation 2 is on a 2-pole basis while equation 1 is for a general p-pole machine. Converting equation 1 to the 2-pole basis it becomes

$$T' = \frac{2K_1}{p} S = \frac{4WR^2}{p^2 g} \frac{d\omega'}{dt} \tag{3}$$

The slip which must be used in these relations depends upon the angular velocity of the rotor and the frequency applied to the motor terminals, and is not the apparent slip based on the nominal line frequency. Therefore

$$S = \frac{\omega_2 - \omega'}{\omega_2} \tag{4}$$

From this

$$\omega_2 = \frac{\omega'}{1-S} \tag{5}$$

Combining (2) and (5)

$$\frac{\omega'}{1-S} = \omega_1 - \frac{d\alpha}{dt} \tag{6}$$

But α is a function of the slip. In the

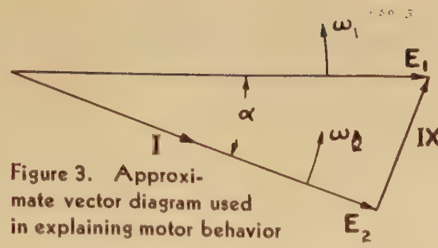

Figure 3. Approximate vector diagram used in explaining motor behavior

region of interest where the slip is small the lagging component of motor current is nearly constant while the power component is directly proportional to the slip. The angle α therefore varies directly with the slip in this region.

$$\alpha = K_2 S \tag{7}$$

The reactance which must be used in computing α is not just the transformer and lead reactance. The motor reactance must be included in this total and will usually be the largest item. For full load the reactance drop was estimated to be 20% of E_1. The angle α was therefore 11.5° or 0.20 radian for 2% slip, and the constant K_2 equal to 10.

Combining equations 6 and 7

$$\omega' = (1-S)\left(\omega_1 - K_2 \frac{dS}{dt}\right) \tag{8}$$

This value of ω' may be substituted in equation 3 giving

$$\frac{2K_1 S}{p} = \frac{4WR^2}{p^2 g} \frac{d}{dt} (1-S)\left(\omega_1 - K_2 \frac{dS}{dt}\right) \tag{9}$$

Differentiating after multiplying by $\dfrac{p^2 g}{4WR^2}$

$$\frac{K_1 pg}{2WR^2} S = (1-S)\left(-K_2 \frac{d^2S}{dt^2}\right) - \left(\omega_1 - K_2 \frac{dS}{dt}\right)\left(\frac{dS}{dt}\right) \tag{10}$$

Rearranging and dividing by K_2

$$(1-S)\frac{d^2S}{dt^2} + \left(\frac{\omega_1}{K_2} - \frac{dS}{dt}\right)\frac{dS}{dt} + \frac{K_1 pg}{2K_2 WR^2} S = 0 \tag{11}$$

Since the slip is very small in the region of interest the term $(1-S)$ is nearly equal to 1. Also the term $\left(\dfrac{\omega_1}{K_2} - \dfrac{dS}{dt}\right)$ is not very different from $\dfrac{\omega_1}{K_2}$. In figure 2, $\dfrac{dS}{dt}$ has a value of about 1.8 as the motor passes through synchronism the first time. The tests were made on a 60 cycle supply so that $\dfrac{\omega_1}{K_2} = 37.7$. Making these approximations, equation 11 becomes

$$\frac{d^2S}{dt^2} + \frac{\omega_1}{K_2}\frac{dS}{dt} + \frac{K_1 pg}{2K_2 WR^2} S = 0 \tag{12}$$

The roots of this equation are

$$D = -\frac{\omega_1}{2K_2} + \sqrt{\frac{\omega_1^2}{4K_2^2} - \frac{K_1 pg}{2K_2 WR^2}} \tag{13}$$

Substituting the numerical values corresponding to the tests in this equation

$$D = -18.8 + \sqrt{355 - 3{,}622}$$
$$= (-18.8 + j57.2)(-18.8 - j57.2) \tag{14}$$

By choosing zero time as the first time the motor passes through synchronous speed or zero slip, and further making the slopes of the two curves the same at this point, the slip equation becomes

$$S = -0.0315\epsilon^{-18.8t} \sin 57.2t \tag{15}$$

This is a damped oscillation having a frequency of 9.1 cycles per second. The frequency of the damped oscillation shown in figure 2 is about 10 cycles per second. The damping is nearly the same in the two cases. A plot of equation 15 is shown in figure 4. The test curve of figure 2 is replotted for comparison. Negative values of slip have been plotted above the axis and the ordinate scaled in terms of synchronous speed so that the curve will appear the same as figure 2. The discrepancies between the test results and equation 15 are due to several causes. First the determination of the constants of the motor were not as accurate as desired. Second the setting up and solution of the differential equation involved approximations. Third the motor was changing speed so rapidly that one might expect that the functions K_1 and K_2, called constants, might not be strictly constant, and their numerical values under these transient conditions might be different from values determined by steady state tests.

Equation 13 indicates that oscillations will be present when the quantity under the radical is negative. This condition exists when

$$\frac{K_1 K_2 p}{WR^2} > \frac{\omega_1^2}{2g} \tag{16}$$

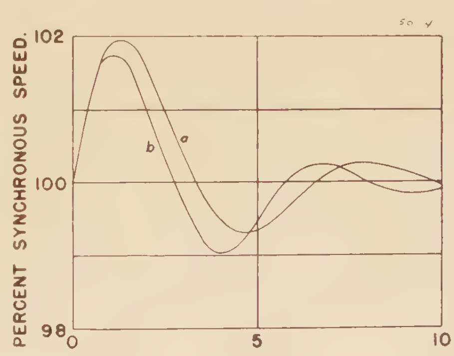

Figure 4

(a) $100(1-S) = 100 + 3.15\epsilon^{-18.8t} \sin 57.2t$

(b) Experimental curve shown in figure 2

A Cathode-Ray Method of Wave Analysis

VINCENT O. JOHNSON
ASSOCIATE AIEE

Synopsis: Complex periodic functions, when transformed into a corresponding voltage wave, may be analyzed with the use of a cathode ray oscillograph. The complex wave is represented upon the fluorescent screen of the cathode ray tube by a vertical displacement at the same time that a sinusoidal horizontal oscillation exists. If the frequency of the sinusoidal oscillation bears an integral relation to the fundamental frequency of the complex wave, a Lissajous figure is viewed on the screen. The areas of these Lissajous figures are directly related to the coefficients of the Fourier series of the complex wave. The area is determined by measuring a photograph of the figure using a polar planimeter. The method is based on the theory developed by Mr. L. W. Chubb in connection with the Chubb Polar Analyzer.[4] Advantages of the method are that it is quick and convenient, only standard laboratory equipment is necessary, and with special equipment, it promises to make possible the analysis of ultrahigh frequency waves.

PERIODIC waves, such as the vibration of mechanical bodies or the variation of current and voltage in electric circuits, are often complex. In electric circuits, sinusoidally varying functions usually give the most satisfactory operation. Calculations are much easier, values may be expressed graphically in vector diagrams, and vector equations may be used. The same is true of mechanical vibration. Hence, in order to handle complex waves conveniently, it is desirable that they be separated into their sinusoidal components. It is the purpose of this paper to describe and explain a new method of wave analysis using a cathode ray oscillograph. The underlying theory is not new, but the method is thought to be faster and the results more complete than other methods of wave analysis using ordinary laboratory equipment. It is hoped that this method will prove useful in other laboratories.

Application of Lissajous Figures to Wave Analysis

The electron beam in a cathode ray tube is deflected by electrostatic forces. If the beam be deflected in one direction by an alternating voltage, and at the same time by another voltage in a direction at right angles to the first, the resulting position of the beam at any instant of time is a function of both voltages. If one frequency is an even multiple of the other, the resulting pattern upon the screen is a Lissajous figure.

In order to begin a study of Lissajous figures, a simple Lissajous figure is shown in figure 1. The two functions to be compounded are $f(\theta)=A_1 \sin \theta$, and $g(\theta)=A_2 \sin (\theta+\alpha)$. The Lissajous figure is an ellipse with a maximum vertical dimension of $2A_2$ and a maximum horizontal dimension of $2A_1$. If $\alpha=0$, the ellipse becomes a single straight line; if $\alpha=90°$, one axis of the ellipse will be vertical and equal to $2A_2$, and the other axis will be horizontal and equal to $2A_1$; if $\alpha=90°$ and $A_1=A_2$, the Lissajous figure becomes a circle. More complex Lissajous figures are obtained if either or both functions are complex. In this case the fundamental frequencies of the functions must be the same or bear an integral ratio to each other.

The Fourier series for a complex function may be expressed as follows:

$$f(\theta)=A_0+C_1 \sin (\theta+\theta_1)+C_2 \sin 2(\theta+\theta_2)+ \ldots +C_n \sin n(\theta+\theta_n)+ \ldots \quad (1)$$

where θ is a function of time equal to $2\pi ft$. However, due to the difficulty of using the harmonics in their various phase positions, each harmonic is usually resolved into two quadrature components thus:

$$f(\theta)=A_0+A_1 \sin \theta+B_1 \cos \theta+A_2 \sin 2\theta+B_2\times \cos 2\theta+ \ldots +A_n \sin n\theta+B_n \cos n\theta+ \ldots \quad (2)$$

As a result, wherever complex periodic waves are encountered they are usually resolved into their harmonic components in order to permit a simpler mathematical treatment. The process of harmonic analysis, then, reduces merely to a problem of evaluating the coefficients A_0, A_1, B_1, etc., in the above series. This can be done in a great number of ways.

Experiments have been conducted in the laboratories of the A. & M. College of Texas using a low voltage cathode ray oscillograph for wave analysis. The complex wave is applied to the horizontal plates which give the cathode beam a vertical displacement. This pair of plates will be referred to hereafter as the horizontal plates, and the other pair of plates as the vertical plates. Ordinarily

Paper 41-156, recommended by the AIEE committee on instruments and measurements, and presented at the AIEE South West District meeting, St. Louis, Mo., October 8–10, 1941. Manuscript submitted June 19, 1941; made available for preprinting August 15, 1941.

VINCENT O. JOHNSON is with engineering laboratories and standards, Westinghouse Electric and Manufacturing Company, East Pittsburgh, Pa.

1. For all numbered references, see list at end of paper.

For K_1 and K_2 may be substituted their values in terms of full-load torque, slip, and angular phase shift.

$$\frac{T\alpha p}{WR^2S^2} > \frac{\omega_1^2}{2g} \quad (17)$$

This relation indicates that overspeeding may be reduced by increasing the WR^2 of a machine. Large machines have large values of WR^2 but also produce large torques. The inertia constant usually increases more rapidly than the torque, as the machine size is increased, so that these larger motors should show less tendency to over speed. The most important factor is the full-load slip since it occurs in the function as a squared term. Motors with low full-load slip should have much greater tendencies to overspeed than high-slip motors. Operation at reduced voltage would decrease this tendency by changing the relation between the torque, slip, and angle.

Various acceleration methods have been considered as a means of determining the speed-torque curves of induction motors. The above analysis indicates that precautions must be taken to avoid conditions similar to those found in these tests if accurate results are to be obtained. However the errors involved are appreciable only near synchronous speed where the frequency change represents a large percentage of the rotor frequency. Where acceleration methods are used to determine only the low-speed part of the curve, errors due to this frequency modulation should not be important.

Reference

1. SOME ACCELERATION TESTS ON LARGE SYNCHRONOUS PUMP MOTORS, R. W. Ager, AIEE TRANSACTIONS, volume 60, 1941, page 416.

the vertical plates receive a saw-tooth shaped voltage wave, which produces a linear horizontal sweep and allows visual observation of the shape of the complex wave. For wave analysis, the vertical plates are connected to a generator which will produce a nearly pure sine wave.

Since equation 2 is an expression representing a complex wave $f(\theta)$, let it represent the complex wave that is applied to the horizontal plates of the oscillograph. Also let $g(\theta) = -K \cos k(\theta + \alpha_k)$ be the sinusoidal wave applied to the vertical plates. The function $g(\theta)$ has a frequency k times the frequency of the fundamental of $f(\theta)$, so if k is an integer, a Lissajous figure will appear upon the oscillograph screen. The amplitude of $g(\theta)$ is K, and the angle α_k in the expression indicates the phase angle between $g(\theta)$ and the cosine term of the kth harmonic of $f(\theta)$.

Referring again to figure 1 and the discussion of plotting Lissajous figures, it is evident that the shape of the Lissajous figure depends upon the phase angle $k\alpha_k$. There is an infinite number of shapes that may be assumed as $k\alpha_k$ may assume an infinite number of values between 0 and 2π. If the frequency of $g(\theta)$ is not exactly a multiple of the frequency of $f(\theta)$, that is, if the two waves are not synchronized, the figure will gradually change through a complete cycle of shapes as the phase angle changes from 0 to 2π.

The area S_k of one of these figures may be calculated from the expressions of the two functions $f(\theta)$ and $g(\theta)$, and is as follows:

$$S_k = kK\pi(A_k \cos k\alpha_k + B_k \sin k\alpha_k) \qquad (3)$$

It will be noticed that this expression contains only two coefficients of the series

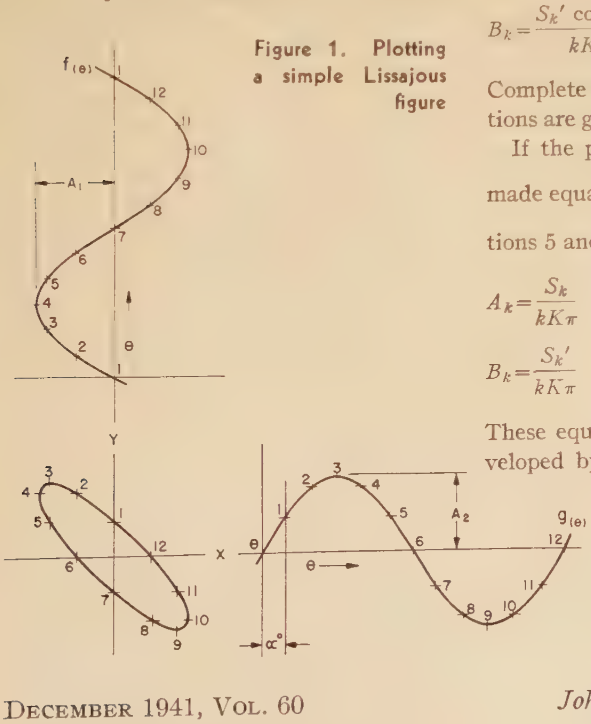

Figure 1. Plotting a simple Lissajous figure

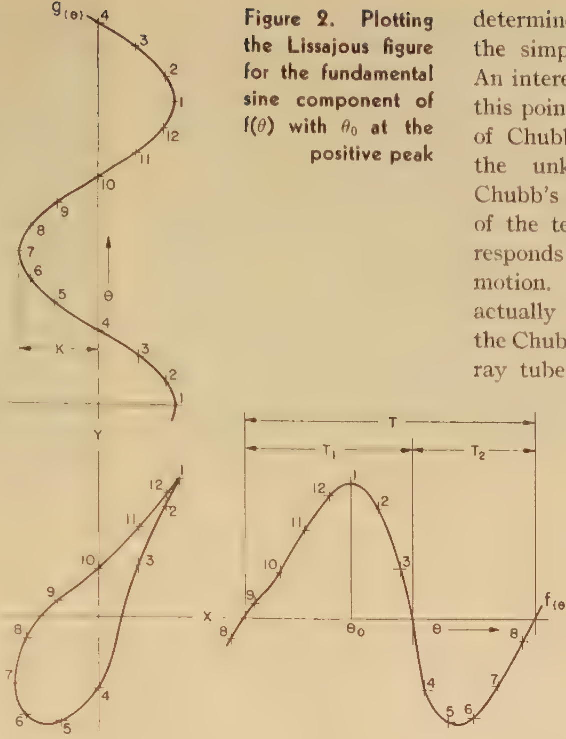

Figure 2. Plotting the Lissajous figure for the fundamental sine component of $f(\theta)$ with θ_0 at the positive peak

for $f(\theta)$. However, it is necessary to be able to solve for one of the coefficients independently. This may be done if another expression can be derived that will contain the same two coefficients. If the phase angle α_k were allowed to change to a new value, say β_k, the area of the figure would change to a new value S_k'. This area may be expressed similarly as

$$S_k' = kK\pi(A_k \cos k\beta_k + B_k \sin k\beta_k) \qquad (4)$$

If equations 3 and 4 are combined, the resulting expressions for A_k and B_k are as follows:

$$A_k = \frac{S_k \sin k\beta_k - S_k' \sin k\alpha_k}{kK\pi \sin k(\beta_k - \alpha_k)} \qquad (5)$$

$$B_k = \frac{S_k' \cos k\alpha_k - S_k \cos k\beta_k}{kK\pi \sin k(\beta_k - \alpha_k)} \qquad (6)$$

Complete derivations of the above equations are given in the appendices.

If the phase angles $k\alpha_k$ and $k\beta_k$ were made equal to 0 and $\frac{\pi}{2}$ respectively, equations 5 and 6 would reduce to

$$A_k = \frac{S_k}{kK\pi} \qquad (7)$$

$$B_k = \frac{S_k'}{kK\pi} \qquad (8)$$

These equations correspond to those developed by L. W. Chubb in connection with the Chubb polar analyzer.[4] However, the fact that it is difficult to accurately adjust the frequency and phase angle of the sine wave generator to a predetermined value precludes the use of the simple expressions in (7) and (8). An interesting analogy may be drawn at this point between this method and that of Chubb's. The vertical deflection of the unknown wave corresponds to Chubb's mechanical deflection by means of the template, and the oscillator corresponds to Chubb's simple harmonic motion. The cathode ray method is actually a simplification in apparatus of the Chubb method, making use of cathode ray tubes and oscillators to replace the Chubb mechanical apparatus. Like the Chubb method, this method will not apply to a determination of the constant term A_0 in a Fourier series. The constant term is relatively unimportant, and if it exists in a circuit, it may be determined by means of a direct current instrument.

It is interesting to note that the expressions 5 and 6 are both in terms of some area divided by π. The graphical method of analysis introduced by C. Runge[2] makes use of a theoretical area obtained by multiplying each ordinate by a function of the corresponding angle. The Lissajous figure automatically produces this same area as an actual figure that may be measured, with the exception that the area is multiplied by K the amplitude of $g(\theta)$, and k the order of the harmonic. Hence both K and k appear in the denominator of expressions 5 and 6.

Discussion of Experimental Procedures

In experimental analysis by means of the cathode ray method, several serious problems have been encountered; (1) the area of the Lissajous figure must be determined easily and accurately, (2) the sine wave source must be of a variable frequency and have very low harmonic content, (3) the frequency must be adjustable to synchronize with the fundamental of the complex wave, (4) the phase angle between the sine wave and the complex wave must be readily determined, and (5) results must be obtained in suitable units.

The Lissajous figure remains stationary on the screen only as long as the two waves are properly synchronized. With a little practice it may be possible to estimate the net area of a figure on the screen. A better practice, however, is to photograph the figure and later measure the area with an ordinary polar planimeter.

Figure 3 (left). Transformer exciting current wave

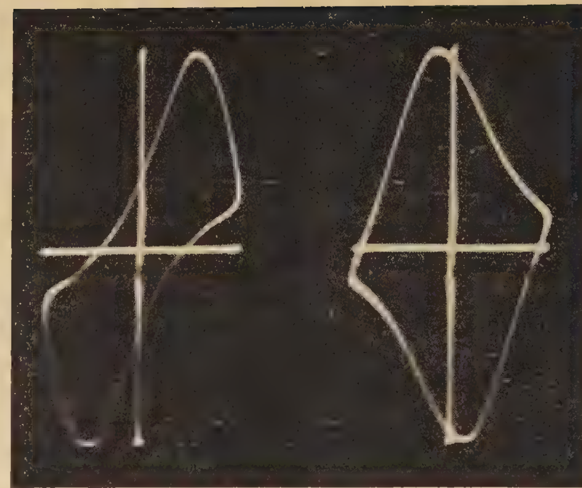

Figure 4 (right). A pair of Lissajous figures for determining the fundamental harmonic

The camera used is important, although an expensive one is not necessary. Better results will be obtained if the room is slightly darkened, but complete darkness is more of a handicap than a help. Since speed is more important than depth of focus, a fast lens is desirable. Also, the size of the image on the film demands that the camera be focused at distances in the vicinity of one or two feet. Once the camera is focused, however, it should not be changed during the process of analyzing a wave, as a change of focus would change the scale of units upon the film.

The sine wave source may be either a mechanical generator or an oscillator. The mechanical generator, of course, would be adaptable only at lower frequencies. In the 60 cycle range, the seventh harmonic is 420 cycles, and a generator producing from 60 to 420 cycles is a rare and expensive piece of equipment and may still develop a high percentage of harmonics. The most desirable characteristic of a mechanical generator would be the accuracy with which synchronism and phase relations could be worked out by mechanical gearing. In general a good quality variable frequency oscillator is more convenient to handle and more easily adjustable.

A number of different types of oscillators may be used. The only requirements are that the oscillator have a nearly constant amplitude over the proper frequency range and that the harmonic content be very small. The power required to maintain voltage across the plates of the tube is very small, so the power rating of the oscillator is relatively unimportant. However, if the output voltage is low, the oscillograph must have an amplifier to produce a figure of the desired size upon the screen.

The frequency of the oscillator must coincide exactly with that of the complex wave if a Lissajous figure is to remain stationary, and frequency drift of either the oscillator or the complex wave will cause the figure to change. There are a number of automatic synchronizing methods which might be used.[5] However, in all cases tried the method depends upon the interconnection of the oscillator with the complex wave, and the advantages are offset by a loss in the quality of the output wave of the oscillator. For this reason manual control of the frequency is desirable and a good frequency control is an important feature of the oscillator.

When the frequencies are synchronized so that the Lissajous figure remains stationary, there are a number of different shapes that the figure can assume. These depend upon the phase angle between the two waves. It is important to be able to determine this phase angle since it enters into the expression for the coefficients of the Fourier series, equations 5 and 6. In figure 2 a complex wave $f(\theta)$ has been plotted on the horizontal axis and a sine wave $g(\theta)$ has been plotted on the vertical axis. The Fourier series for $f(\theta)$ depends upon the location of a reference point where all the sine terms of the series are zero and all the cosine terms have a positive maximum value. Call this point θ_0. In many methods of analysis, the point where the complex wave crosses the axis is chosen for θ_0. For the cathode ray method of analysis, the maximum positive peak of $f(\theta)$ is thought to be a more suitable point for θ_0. The general expression for $g(\theta)$ in figure 2 is $g(\theta)=-K \cos k(\theta+\alpha_k)$. Since θ_0 is a value of θ such that $\sin(\theta_0)=0$ and $\cos(\theta_0)=+1$, θ_0 is some multiple of 2π. Hence, $g(\theta)$ for $\theta=\theta_0$ reduces to

$$g(\theta_0)=-K \cos k\alpha_k \tag{9}$$

In figure 2, the Lissajous figure has been plotted for the case when $\alpha_k=0$, and $g(\theta_0)=-K$. It will be noted that the Lissajous figure has a peak in the upper right corner a distance $-K$ from the Y axis. If α_k has a value other than zero, $g(\theta_0)$ will be reduced in magnitude and the peak will have moved a distance $(K-K \cos k\alpha_k)$ to the left. The peak can always be located on the oscillogram and $g(\theta_0)$ may be measured directly. Then the angle $k\alpha_k$ is, from equation 11,

$$k\alpha_k = \cos^{-1}(g(\theta_0)/K) \tag{10}$$

From equation 10, $k\alpha_k$ may be either positive or negative since the cosine is the same for either case, but in writing the sine of $k\alpha_k$, it is important to know whether $k\alpha_k$ is positive or negative. It is positive if $g(\theta)$ has already passed its negative maximum at the time $f(\theta)$ reaches its peak value. The best way to determine this when viewing the figure on the oscillograph screen is to adjust the frequency of the sine wave generator to a value slightly greater than that of the harmonic and stop the figure by synchronizing the two frequencies after the peak has left the upper right corner moving to the left. If the peak is stopped before it reaches the midpoint, the angle will be between 0° and 90°, while if it is stopped between the midpoint and the upper left corner, the angle will be between 90° and 180°. It is good practice to make $k\alpha_k$ about 45° and $k\beta_k$ about 135°.

It is important in planimetering the area of the Lissajous figures, to move always in the proper direction around the loops, for some areas may be positive and some negative. A simple way to do this is always to start from the peak point on the Lissajous figure and move downward to the left, thus tracing through one complete cycle. The reading on the planimeter is or can be corrected to square inches.

Now if the scales for all figures are the same, A_k and B_k can be calculated from equations 5 and 6 in inches. However, it is usually better to convert each area by means of its scale constant to a hypothetical unit, which may be called square volts if a voltage wave is being analyzed,

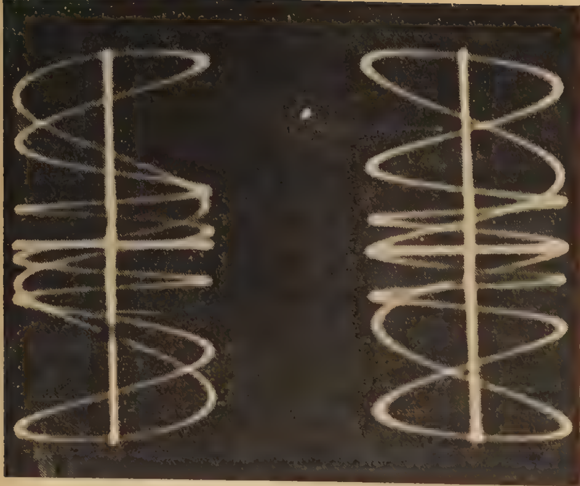

Figure 5. A pair of Lissajous figures for determining the seventh harmonic

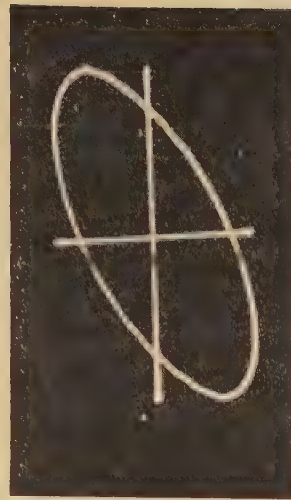

Figure 6. Calibration picture

or square amperes for a current wave. Then K (assumed constant) can be converted to the correct units, and the value of A_k is derived in those units. If K is not constant, equations 5 and 6 must be altered as follows:

$$A_k = \frac{S_k/K \sin k\beta_k - S_k'/K' \sin k\alpha_k}{k\pi \sin k(\beta_k - \alpha_k)} \qquad (11)$$

$$B_k = \frac{S_k'/K' \sin k\alpha_k - S_k/K \cos k\beta_k}{k\pi \sin k(\beta_k - \alpha_k)} \qquad (12)$$

The scale constant may be determined by taking a picture of a pure sine wave of known amplitude at the same time the other pictures are being taken. In fact, it is a good practice to take two or three calibration pictures during an experiment. Obviously, a change in amplification on the oscillograph or focus of the camera will alter the scale constant. If the scale constant varies slightly for unavoidable reasons, either an average constant must be used or individual constants must be assigned to each picture.

Experimental Results

In order to determine to some extent how practical the cathode ray method of wave analysis is, an exciting current wave for a potential transformer was analyzed. Figure 3 shows an oscillogram of the wave that was analyzed. The results of the cathode ray method were compared with results using another method of analysis. The other method was the graphical method of C. Runge using 72 points.[2] A comparison of results is shown in table I. The analysis was only carried as far as the seventh harmonic as the graphical method becomes very inaccurate for higher harmonics and correspondingly small magnitudes. It is thought that the two methods possess about the same degree of accuracy for low order harmonics up to the third, but for higher harmonics the cathode ray method is thought to be more accurate. The areas of the Lissajous figures for higher harmonics may be rather accurately determined because they are proportional to the order of the harmonic k times the magnitude of the corresponding coefficients.

Table I. Comparison of Results in an Experimental Analysis of a Transformer Exciting Current

	Cathode-Ray Method		Runge Method	
Harmonic	Magnitude Amperes	Phase Angle Degrees	Magnitude Amperes	Phase Angle Degrees
First	0.318	0	0.327	0
Third	0.1120	44.2	0.1135	50.0
Fifth	0.0267	54.5	0.0248	59.0
Seventh	0.00794	7.7	0.00725	12.6

Figures 4 and 5 show examples of some of the Lissajous figures that were used in the experimental analysis. The pictures were taken using a 35 mm. camera with an f-4.5 lens. Exposures were made at $^1/_{25}$ of a second. This was found to give a very good trace on the film when the intensity of the cathode ray was adjusted to a reasonable brightness. Since the light emitted from a cathode ray oscillograph screen is very small, a camera with a fast lens is a distinct advantage. Another desirable feature in this application is a short focus, since the size of the figures on the screen is hardly more than two inches high. The zero axes of the Lissajous figures were obtained by exposing the film once with the exciting current wave shorted out and once with the sine wave shorted out in addition to the exposure for the figure itself. Figure 6 is an example of one of the calibration pictures that were taken. It is a Lissajous figure similar to those in figure 4 except that both waves are sinusoidal.

Figure 7 shows the equipment as it was assembled for the experimental analysis. The cathode ray oscillograph had a 5 inch screen and the size of the figure could be adjusted through step up amplifiers on both the horizontal and vertical plates. The oscillator was a beat frequency type having a frequency range from 20 to 17,000 cycles and a practically constant amplitude over that range. Just in front of the oscillator and to the left is a small tuning condenser which was used in parallel with the main tuning condenser on the oscillator to give a finer adjustment of frequency.

Conclusion

It is important to note that only standard laboratory equipment is necessary for the cathode ray analysis. The method is much faster and less tedious than the graphical method, because most of the calculation is dispensed with. Harmonics that do not exist, or are negligible, are apparent at once from the areas of the Lissajous figures without further calcu-

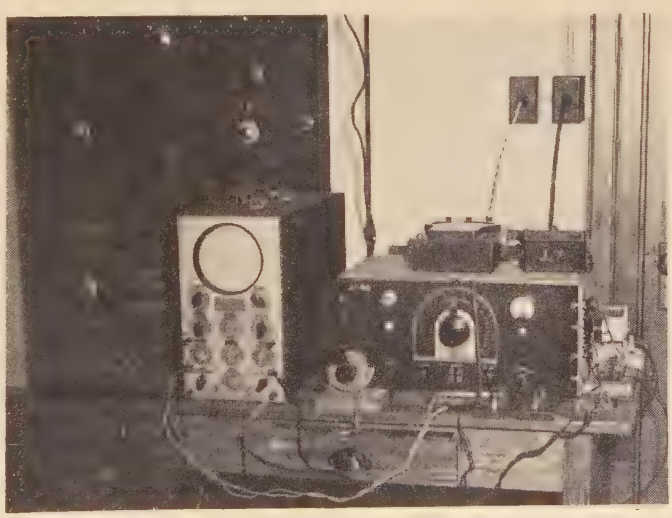

Figure 7. Apparatus used for the experimental analysis

lation. The other harmonics may be quickly calculated and converted to the correct units.

But much more important than any other advantage is the fact that the cathode ray oscillograph will respond effectively to much higher frequencies than any other type of oscillograph. The vibrator elements in most mechanical oscillographs have a natural frequency of 5,000 cycles per second undamped; so it is evident that any frequency in this range would be somewhat magnified and the results would be erratic. The cathode ray oscillograph may be used in the radio frequency range. Thus, high frequency waves may be analyzed with the same simplicity and completeness as are the power frequency waves.

With the possibility of completely analyzing higher frequency waves, the study of mechanical vibration may be accelerated and improved. A device that would couple the mechanical system to an electrical circuit and reproduce the mechanical oscillations as electrical functions would make possible the analysis of mechanical vibration with a cathode ray oscillograph.

The frequency range of cathode ray oscillographs has been still further increased with the invention of a new microwave oscillograph devised for the centimeter range of wave lengths, where ordinary oscillographs are not adaptable.[8] These high frequency waves are distorted in the ordinary cathode ray oscillograph because the finite time required for an electron to pass across a deflecting field is of the same order of magnitude as the time required for one cycle of the wave. Also, if the two deflection fields are spaced along the direction of the beam, the time lag between the two fields is an appreciable part of a cycle. In the microwave oscillograph, the deflection fields are made small and brought very close together. All dimensions of the tube are likewise reduced, and the image is thrown upon an especially fine grain fluorescent screen. The image itself is so small that it must be observed and photographed by means of a microscope. This new instrument should make ultra-high frequency wave analysis possible, with very little change from the method described in this paper.

Appendix I

Areas of Lissajous Figures

The general expression for the sinusoidal function is

$$g(\theta) = -K \cos k(\theta+\alpha_k) \tag{13}$$

and

$$\begin{aligned} dg(\theta) &= kK \sin k(\theta+\alpha_k)d\theta \\ &= kK(\cos k\alpha_k \sin k\theta + \sin k\alpha_k \cos k\theta)d\theta \end{aligned} \tag{14}$$

The area of the Lissajous figure is

$$S_k = \int_0^{2\pi} f(\theta)dg(\theta) \tag{15}$$

The complex function $f(\theta)$, given in equation 2, may be changed to the following form:

$$f(\theta) = A_0 + \sum_{n=1}^{\infty} A_n \sin n\theta + \sum_{n=1}^{\infty} B_n \cos n\theta \tag{16}$$

The integration may be carried out for each part of $f(\theta)$ independently as follows:

$$\int_0^{2\pi} A_0 kK \sin k(\theta+\alpha_k)d\theta = 0$$

$$\int_0^{2\pi} (A_n \sin n\theta)(kK \cos k\alpha_k \sin k\theta)d\theta = 0 \qquad \text{if } n \neq k$$

$$\int_0^{2\pi} (A_n \sin n\theta)(kK \sin k\alpha_k \cos k\theta)d\theta = 0 \qquad \text{for all } n$$

$$\int_0^{2\pi} (B_n \cos n\theta)(kK \cos k\alpha_k \sin k\theta)d\theta = 0 \qquad \text{for all } n$$

and

$$\int_0^{2\pi} (B_n \cos n\theta)(kK \sin k\alpha_k \cos k\theta)d\theta = 0 \qquad \text{if } n \neq k$$

If $n = k$

$$\int_0^{2\pi} (A_n \sin n\theta)(kK \cos k\alpha_k \sin k\theta)d\theta = A_k kK \cos k\alpha_k \int_0^{2\pi} \sin^2 k\theta d\theta = (A_k kK \cos k\alpha_k)\pi$$

and

$$\int_0^{2\pi} (B_n \cos n\theta)(kK \sin k\alpha_k \cos k\theta)d\theta = B_k kK \sin k\alpha_k \int_0^{2\pi} \cos^2 k\theta d\theta = (B_k kK \sin k\alpha_k)\pi$$

Only two terms remain in the expression for the area S_k,

$$\begin{aligned} S_k &= A_k kK\pi \cos k\alpha_k + B_k kK\pi \sin k\alpha_k \\ &= kK\pi(A_k \cos k\alpha_k + B_k \sin k\alpha_k) \end{aligned} \tag{17}$$

Since it is known that α_k may assume a new value β_k, the expression for S_k' may be written immediately,

$$S_k' = kK\pi(A_k \cos k\beta_k + B_k \sin k\beta_k) \tag{18}$$

Appendix II

Derivation of General Expression for the Coefficients

Equations 17 and 18 may be changed to the following form:

$$A_k \cos k\alpha_k + B_k \sin k\alpha_k = \frac{S_k}{kK\pi} \tag{19}$$

$$A_k \cos k\beta_k + B_k \sin k\beta_k = \frac{S_k'}{kK\pi} \tag{20}$$

These equations may be solved by determinants for the coefficients A_k and B_k.

$$A_k = \frac{\dfrac{1}{kK\pi}\begin{vmatrix} S_k, & \sin k\alpha_k \\ S_k', & \sin k\beta_k \end{vmatrix}}{\begin{vmatrix} \cos k\alpha_k, & \sin k\alpha_k \\ \cos k\beta_k, & \sin k\beta_k \end{vmatrix}} = \frac{\dfrac{1}{kK\pi}(S_k \sin k\beta_k - S_k' \sin k\alpha_k)}{\cos k\alpha_k \sin k\beta_k - \cos k\beta_k \sin k\alpha_k} = \frac{S_k \sin k\beta_k - S_k' \sin k\alpha_k}{kK\pi \sin k(\beta_k - \alpha_k)}$$

$$B_k = \frac{\dfrac{1}{kK\pi}\begin{vmatrix} \cos k\alpha_k, & S_k \\ \cos k\beta_k, & S_k' \end{vmatrix}}{\begin{vmatrix} \cos k\alpha_k, & \sin k\alpha_k \\ \cos k\beta_k, & \sin k\beta_k \end{vmatrix}} = \frac{\dfrac{1}{kK\pi}(S_k' \cos k\alpha_k - S_k \cos k\beta_k)}{\cos k\alpha_k \sin k\beta_k - \cos k\beta_k \sin k\alpha_k} = \frac{S_k' \cos k\alpha_k - S_k \cos k\beta_k}{kK\pi \sin k(\beta_k - \alpha_k)}$$

References

1. Wave Motion and Light (book), **E. P. Lewis.** Physics for Students of Science and Engineering, 1932.

2. Electric Circuit Analysis (book), **M. G. Malti,** 1930.

3. The Cathode-Ray Tube at Work (book), **John F. Rider,** 1935.

4. Analysis of Periodic Waves, **L. W. Chubb** *Electric Journal*, volume 11, 1914, pages 91–6.

5. Electrostatic Analyzer for Complex Waves of Small Amplitude, **J. C. Prescott.** *Journal* of the Institution of Electrical Engineers, volume 85, 1939, pages 302–08.

6. A New Frequency Transformer or Frequency Changer, **Isaac Koga.** *Proceedings* of the Institute of Radio Engineers, volume 15, 1927, page 669.

7. Automatic Synchronization of Triode Oscillators, **E. V. Appleton.** *Proceedings* of the Cambridge Philosophical Society, volume 21, 1922, page 231.

8. Ultrahigh-Frequency Oscillography, **H. E. Hollmann.** *Proceedings* of the Institute of Radio Engineers, volume 28, 1940, pages 213–19.

The Apparent-Impedance Method of Calculating Single-Phase-Motor Performance

WAYNE J. MORRILL
MEMBER AIEE

Synopsis: In the past several years there have been offered a number of calculation methods to be used in connection with predetermining the performance of single-phase induction motors. While such methods are usually based upon either the cross field or the revolving field theory, they differ from each other according to individual preferences.

In the present paper there is proposed a method which seems to be convenient and simple, and which, because of symmetry, involves a minimum of charts in carrying out the necessary calculations. The method is proposed because it has been used in one design department for a number of years and found to be very satisfactory as a practical method.

IN the calculation of performance of single-phase motors by the revolving-field theory, there appear repeatedly certain quantities which have been defined as apparent impedances. The actual determination of an apparent impedance when the characteristic impedances of the motor are known involves a considerable amount of labor and the use of complex quantities. This labor has caused some engineers to avoid a straightforward use of the revolving-field theory and to substitute artificial steps, or actually to use entirely different methods. In a case such as this it is often convenient to consider whether the labor of calculation could be avoided by the use of a suitable chart wherein the calculational work is done once and for all and, for a specific calculation, it is merely necessary to read the values from the chart. It is the principal purpose of this paper to indicate how such charts may be constructed for the determination of apparent impedance and to show how the use of such charts can be made to simplify induction-motor performance calculations.

Per-Unit Apparent-Impedance Charts

The values of the apparent impedances of a single-phase motor were given in equations 54 to 57, inclusive, of my 1929 paper[1] on the revolving-field theory. These values are indicated below in equations 1 to 4.

$$R_f=\frac{X_m^2\dfrac{R_2}{s}}{\left(\dfrac{R_2}{s}\right)^2+(X_2+X_m)^2} \tag{1}$$

$$X_f=\frac{X_m\left[\left(\dfrac{R_2}{s}\right)^2+X_2(X_2+X_m)\right]}{\left(\dfrac{R_2}{s}\right)^2+(X_2+X_m)^2} \tag{2}$$

$$R_b=\frac{X_m^2\left(\dfrac{R_2}{2-s}\right)}{\left(\dfrac{R_2}{2-s}\right)^2+(X_2+X_m)^2} \tag{3}$$

$$X_b=\frac{X_m\left[\left(\dfrac{R_2}{2-s}\right)^2+X_2(X_2+X_m)\right]}{\left(\dfrac{R_2}{2-s}\right)^2+(X_2+X_m)^2} \tag{4}$$

The right-hand members of each of the above four equations contain three independent variables, if R_2/s and $R_2/(2-s)$ be each considered as a single variable. Functions involving three independent variables are usually considered too complicated to chart since they involve families of curves. However, if the apparent impedances and each of the independent variables of the preceding equations be expressed as per unit of one of the independent variables, it is possible to reduce the number of independent variables by one. This can be done if both sides of the four above equations be divided by X_m and both the numerator and denominator of each of the right-hand members be divided by X_m^2. The resulting equations are given in 5 to 8 below:

$$\frac{R_f}{X_m}=\frac{\dfrac{R^2}{X_m s}}{\left(\dfrac{R_2}{X_m s}\right)^2+\left(\dfrac{X_2}{X_m}+1\right)^2}=\text{per unit forward field apparent resistance} \tag{5}$$

$$\frac{X_f}{X_m}=\frac{\left(\dfrac{R_2}{X_m s}\right)^2+\dfrac{X_2}{X_m}\left(\dfrac{X_2}{X_m}+1\right)}{\left(\dfrac{R_2}{X_m s}\right)^2+\left(\dfrac{X_2}{X_m}+1\right)^2}=\text{per unit forward field apparent reactance} \tag{6}$$

$$\frac{R_b}{X_m}=\frac{\dfrac{R_2}{X_m(2-s)}}{\left(\dfrac{R_2}{X_m(2-s)}\right)^2+\left(\dfrac{X_2}{X_m}+1\right)^2}=\text{per unit backward-field apparent resistance} \tag{7}$$

$$\frac{X_b}{X_m}=\frac{\left(\dfrac{R_2}{X_m(2-s)}\right)^2+\dfrac{X_2}{X_m}\left(\dfrac{X_2}{X_m}+1\right)}{\left(\dfrac{R_2}{X_m(2-s)}\right)^2+\left(\dfrac{X_2}{X_m}+1\right)^2}=\text{per unit backward-field apparent reactance} \tag{8}$$

In equations 5 to 8 the independent variables will have the following definitions:

$\dfrac{R_2}{X_m s}$ = per unit secondary resistance at slip s

$\dfrac{R_2}{X_m(2-s)}$ = per unit secondary resistance at slip $2-s$

$\dfrac{X_2}{X_m}$ = per unit secondary reactance

On the basis of the above definitions of the independent variables, there are only two independent variables in the right-hand members of equations 5 to 8. It therefore becomes possible to plot each of equations 5 to 8 in the form of a family of curves. Since the only difference between the expressions for per unit apparent forward field resistance and reactance and the similar expressions for the backward field is the use of R_2/s in place of $R_2/(2-s)$, the curves for the forward and backward field apparent impedances will be identical and only two families of curves need be drawn.

In figures 1 and 2 there are shown curves of per unit apparent resistance and per unit apparent reactance plotted for definite values of per unit secondary reactance and as a function of the reciprocal of the per unit secondary resistance for slips of s or $2-s$. The reciprocal of the per unit secondary resistance has been chosen as the independent variable because the resulting curves spread out in such a fashion as to make them more easily and more accurately read.

In order to make use of the charts and to obtain an actual value of apparent resistance or reactance, it is first necessary to obtain the per unit secondary reactance, X_2/X_m, to learn which of the curves

Paper 41-162, recommended by the AIEE committee on electrical machinery, and presented at the AIEE South West District meeting, St. Louis, Mo., October 8–10, 1941. Manuscript submitted August 14, 1941; made available for preprinting August 27, 1941.

WAYNE J. MORRILL is designing engineer of the fractional-horsepower motor engineering division of General Electric Company, Fort Wayne, Ind.

1. For all numbered references, see list at end of paper.

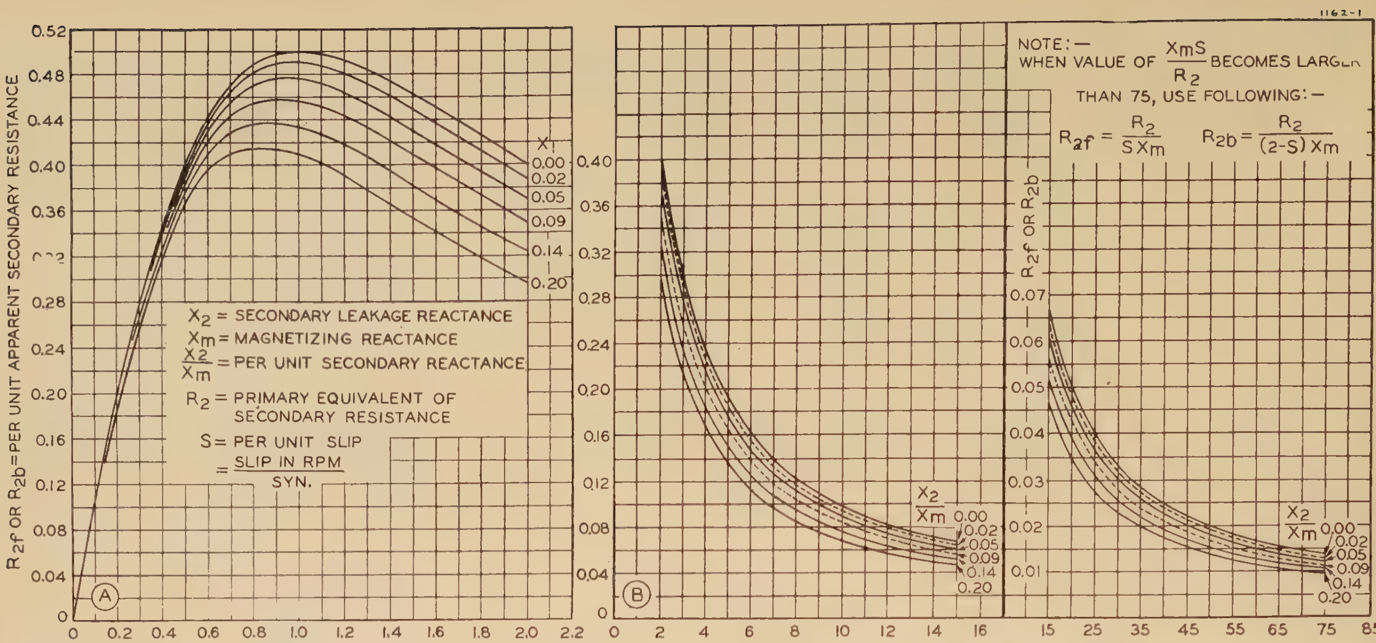

Figure 1 (above). Apparent-resistance chart

Figure 2 (below). Apparent-reactance chart

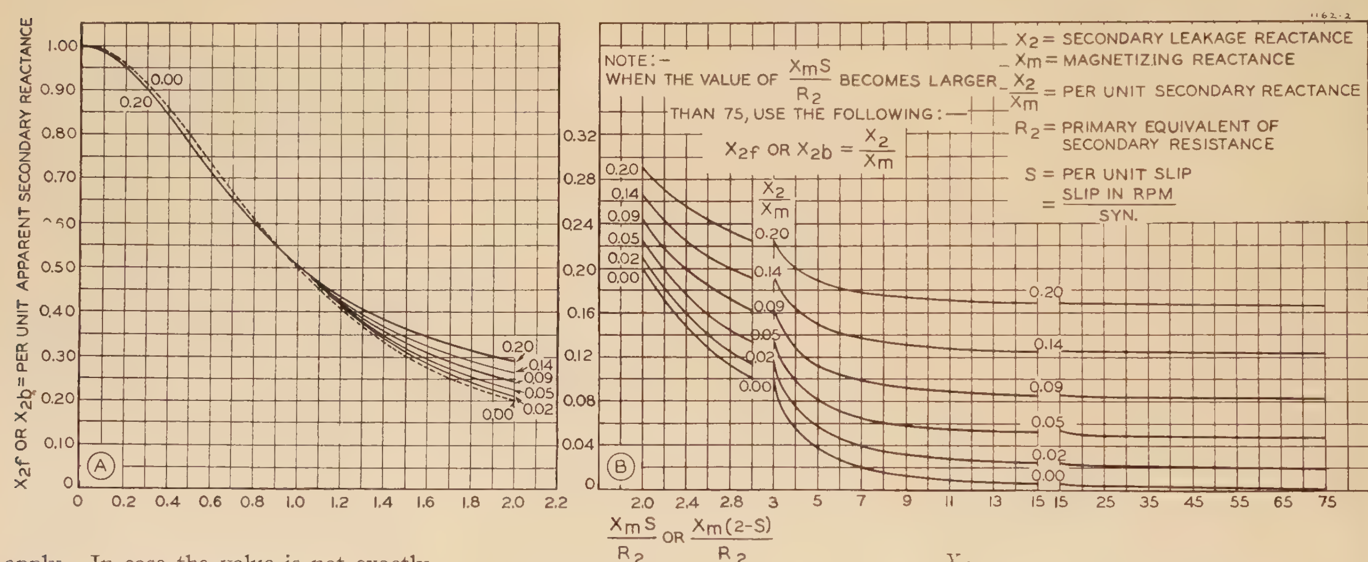

apply. In case the value is not exactly the same as that of a curve, it is, of course, necessary to interpolate between two adjacent curves.

Once the proper curve has been selected, the corresponding value of per unit apparent resistance or reactance may be read as the ordinate corresponding to the proper value of X_ms/R_2 or $X_m(2-s) \div R_2$. The actual apparent resistance or reactance is obtained as the product of the per unit apparent resistance or reactance by X_m, the magnetizing reactance.

As an example of actual use of these curves, consider the case of a single-phase motor having the following constants:

$$R_2 = 2 \tag{9}$$

$$X_2 = 1.7 \tag{10}$$

$$X_m = 34 \tag{11}$$

If this motor is operating at a slip of 0.05, the per unit forward and backward field secondary reactances will be

$$\frac{X_2}{X_m} = \frac{1.7}{34} = 0.05 \tag{12}$$

and the reciprocal of the per unit forward and backward field secondary resistances will be

$$\frac{X_ms}{R_2} = \frac{34(0.05)}{2} = 0.85 \tag{13}$$

$$\frac{X_m(2-s)}{R_2} = \frac{34(1.95)}{2} = 33.2 \tag{14}$$

Using these values and figures 1 and 2, the per unit apparent impedances and the corresponding actual impedance values are given below:

$$\frac{R_f}{X_m} = 0.475 \qquad R_f = 34(0.475) = 16.18 \tag{15}$$

$$\frac{X_f}{X_m} = 0.578 \qquad X_f = 34(0.578) = 19.65 \tag{16}$$

$$\frac{R_b}{X_m} = 0.0273 \qquad R_b = 34(0.0273) = 0.928 \tag{17}$$

$$\frac{X_b}{X_m} = 0.0482 \qquad X_b = 34(0.0482) = 1.638 \tag{18}$$

Calculation of Single-Phase-Motor Performance

In the calculation of motor performance it is usually desirable to proceed from a relatively simple idealized conception and to introduce phenomena of secondary importance by modifying the results obtained from the idealized concept. For example: The equivalent circuit for the single-phase motor which was given in figure 1 of my 1929 paper (figure 3 of the present paper), and which has appeared many times in publications by other authors, makes no provision for repre-

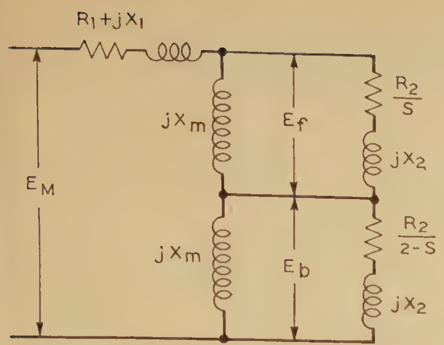

Figure 3. Single-phase-motor equivalent circuit

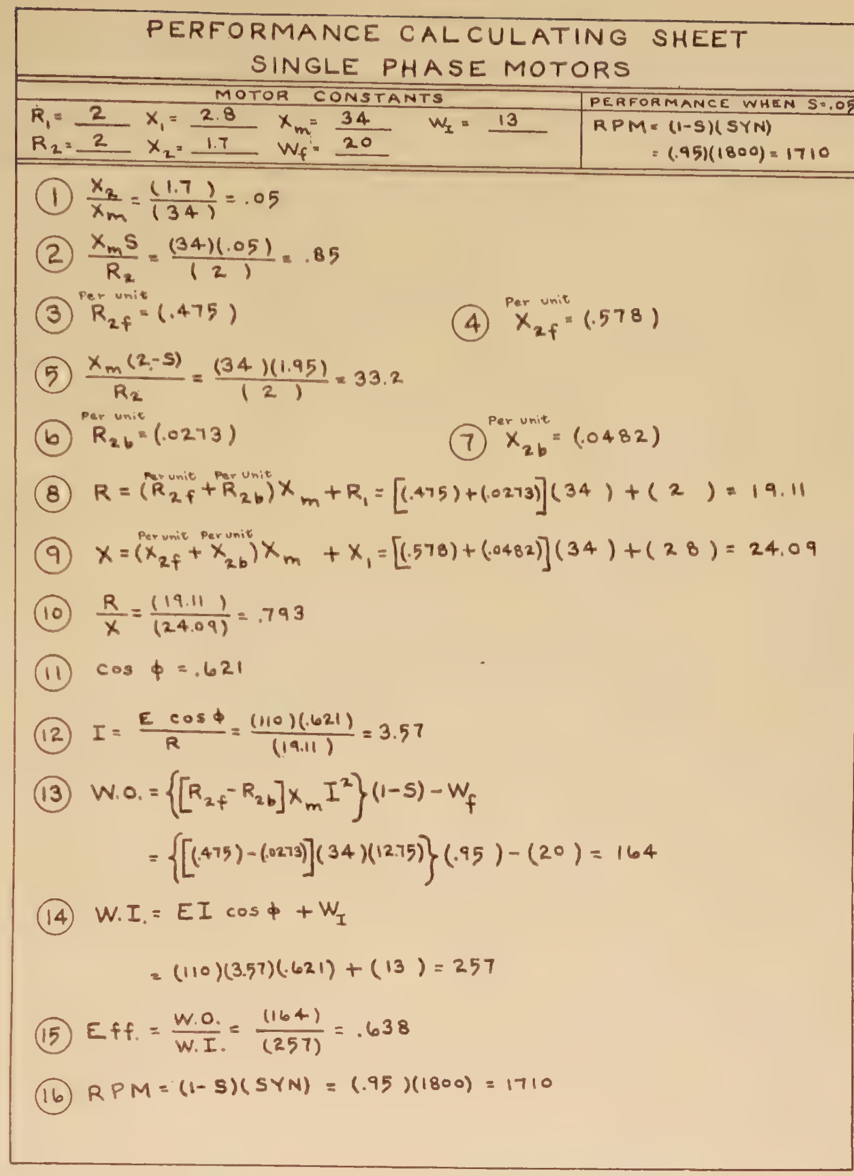

PERFORMANCE CALCULATING SHEET
SINGLE PHASE MOTORS

MOTOR CONSTANTS

$R_1 = 2$ $X_1 = 2.8$ $X_m = 34$ $W_I = 13$
$R_2 = 2$ $X_2 = 1.7$ $W_f = 20$

PERFORMANCE WHEN S=.05
RPM = (1-S)(SYN) = (.95)(1800) = 1710

(1) $\frac{X_2}{X_m} = \frac{(1.7)}{(34)} = .05$

(2) $\frac{X_m S}{R_2} = \frac{(34)(.05)}{(2)} = .85$

(3) Per unit $R_{2f} = (.475)$ (4) Per unit $X_{2f} = (.578)$

(5) $\frac{X_m(2-S)}{R_2} = \frac{(34)(1.95)}{(2)} = 33.2$

(6) Per unit $R_{2b} = (.0273)$ (7) Per unit $X_{2b} = (.0482)$

(8) $R = (\overset{\text{Per unit}}{R_{2f}} + \overset{\text{Per unit}}{R_{2b}})X_m + R_1 = [(.475)+(.0273)](34) + (2) = 19.11$

(9) $X = (\overset{\text{Per unit}}{X_{2f}} + \overset{\text{Per unit}}{X_{2b}})X_m + X_1 = [(.578)+(.0482)](34) + (2.8) = 24.09$

(10) $\frac{R}{X} = \frac{(19.11)}{(24.09)} = .793$

(11) $\cos\phi = .621$

(12) $I = \frac{E\cos\phi}{R} = \frac{(110)(.621)}{(19.11)} = 3.57$

(13) $W.O. = \{[R_{2f} - R_{2b}]X_m I^2\}(1-S) - W_f$

$= \{[(.475)-(.0273)](34)(12.75)\}(.95) - (20) = 164$

(14) $W.I. = EI\cos\phi + W_I$

$= (110)(3.57)(.621) + (13) = 257$

(15) $Eff. = \frac{W.O.}{W.I.} = \frac{(164)}{(257)} = .638$

(16) $RPM = (1-S)(SYN) = (.95)(1800) = 1710$

Figure 4. Single-phase-motor calculation sheet

senting the core-loss current. Such current could be shown as flowing through a high resistance which is connected in parallel with the magnetizing reactance of each forward and backward field. In actual practice it is usually found that the effect of the core-loss current on the motor performance is relatively small since the current itself is usually very small and since its time-phase relation is at 90 degrees with respect to the magnetizing current, which latter is usually relatively large. For this reason, it has usually been found desirable to consider the core loss as if it were the result of a high resistance in parallel with the entire motor and to neglect the effect of the flow of the core-loss current through the primary impedance of the motor. When this approach is employed, the core loss may be introduced as an input which is added to the input determined from the idealized equivalent circuit.

There are two other losses which must be accounted for in making an exact single-phase motor calculation and these are the rotational iron loss and the mechanical friction, sometimes called friction and windage. The rotational iron loss is indistinguishable from friction in its effect upon motor performance since the loss appears as a retarding torque tending mechanically to slow down the motor. The torque of rotational core loss differs from the torque of friction in that, in addition to being a function of speed, it is also a function of the currents in the stator and the rotor and, while an exact expression for the torque would be complicated, it and the corresponding power loss may be approximately represented as proportional to the second power of the stator current.

If it be presumed that the rotational iron loss and the mechanical friction are both known, and that the two rotational losses be classed as friction and represented by the symbol W_f, the effect of this combined rotational loss is properly accounted for if W_f be subtracted from the electrical output as determined from the idealized circuit.

On the basis of these remarks, the calculation sheet for a single-phase motor may be laid out as shown in figure 4 in which an actual calculation has been carried out using the constants which were employed in explaining the apparent-impedance charts, plus the values for the primary resistance and reactance, the iron loss, and the rotational losses as given below:

$$R_1 = 2 \quad (19)$$

$$X_1 = 2.8 \quad (20)$$

$$W_i = 13 \quad (21)$$

$$W_f = 20 \quad (22)$$

In carrying out the operation of determining the input current, it has been thought desirable to make use of figure 5

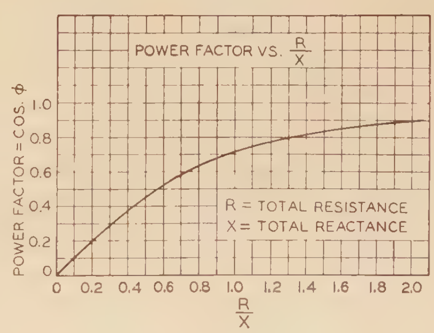

Figure 5. Power-factor versus R/X chart

and the total apparent secondary resistance, thus avoiding the necessity of squaring the impedances and extracting the square root or carrying certain quantities in mind during the calculation, as is necessary with other methods.

It will be seen from the calculation form that the number of steps required for the determination of the performance of a single-phase motor for any given

PERFORMANCE CALCULATING SHEET
CAPACITOR MOTORS

S =

R_{1m} = ____ X_{1m} = ____ $\frac{X_m S}{R_2}$ = ____ R_{2f} =
R_2 = ____ X_2 = ____ R_{2b} =
R_{1s} = ____ X_{1s} = ____ $\frac{X_m(2-S)}{R_2}$ = SUM ____ DIF. ____
R_c = ____ X_c = ____ X_{2f} =
W_f = ____ W_I = ____ $X_c - X_{1s}$ = ____ X_{2b} =
a = ____ X_m = ____ X_2/X_m = ____ SUM ____ DIF. ____

(1) $X_m(R_{2f}+R_{2b})$ = ( )( ) =

(2) $X_m(X_{2f}+X_{2b})$ = ( )( ) =

(3) $X_m(R_{2f}-R_{2b})$ = ( )( ) =

(4) $X_m(X_{2f}-X_{2b})$ = ( )( ) =

(5) $R_1 + (1)$ = ( ) + ( ) =

(6) $X_1 + (2)$ = ( ) + ( ) =

(7) $R_c + a^2(1)$ = ( ) + ( )( ) =

(8) $X_c + a^2(2)$ = ( ) + ( )( ) =

(9) $a\,(3)$ = ( )( ) =

(10) $a\,(4)$ = ( )( ) =

(11) $(9)^2 - (10)^2$ = ( ) − ( ) =

(12) $2(9)(10)$ = 2( )( ) =

(13) $(5)(7) - (6)(8)$ = ( )( ) − ( )( ) =

(14) $(5)(8) + (6)(7)$ = ( )( ) + ( )( ) =

(15) $(13) - (11)$ = ( ) − ( ) =

(16) $(14) - (12)$ = ( ) − ( ) =

(17) $(15)^2 + (16)^2$ = ( ) + ( ) =

(18) $\frac{E(15)}{(17)} = \frac{(\ \ )(\ \ )}{(\ \ )}$ =

(19) $\frac{E(16)}{(17)} = \frac{(\ \ )(\ \ )}{(\ \ )}$ =

(20) $(7) - (10)$ = ( ) − ( ) =

(21) $(8) + (9)$ = ( ) + ( ) =

(22) $(5) + (10)$ = ( ) + ( ) =

(23) $(6) - (9)$ = ( ) − ( ) =

(24) $(18)(20) + (19)(21)$ = ( )( ) + ( )( ) =

(25) $(18)(21) - (19)(20)$ = ( )( ) − ( )( ) =

(26) $(18)(22) + (19)(23)$ = ( )( ) + ( )( ) =

(27) $(18)(23) - (19)(22)$ = ( )( ) − ( )( ) =

(CONTINUED ON PAGE 2)

PG. 1

PERFORMANCE CALCULATING SHEET
CAPACITOR MOTORS

S =

(28) $(24) + (26)$ = ( ) + ( ) =

(29) $(25) + (27)$ = ( ) + ( ) =

(30) $\frac{R}{X} = \frac{(\ \ )}{(\ \ )}$ =

(31) $\cos\phi$ =

(32) $(24)^2 + (25)^2 + [(26)^2 + (27)^2](a^2)$ = ( ) + ( ) + [( ) + ( )]( ) =

(33) $(24)(27) - (25)(26)$ = ( )( ) − ( )( ) =

(34) $(32)(3)$ = ( )( ) =

(35) $2(a)(33)(1)$ = 2( )( )( ) =

(36) W.O. = $[(34)+(35)](1-S) - W_f$ = [( ) + ( )]( ) − ( ) =

(37) W.I. = $(28)(E) + W_I$ = ( )( ) + ( ) =

(38) Eff. = $\frac{(36)}{(37)} = \frac{(\ \ )}{(\ \ )}$ =

(39) $I = \frac{(28)}{(31)} = \frac{(\ \ )}{(\ \ )}$ =

(40) $T = \frac{(36)}{(1-S)}\left[\frac{112.7}{SYN}\right] = \frac{(\ \ )}{(\ \ )}(\ \ )$ =

(41) $(26)^2 + (27)^2$ = ( ) + ( )

(42) RPM = $(1-S)(SYN)$ = ( )( ) =

(43) KVA = $(41)(X_c - X_{1s})$ = ( )( ) =

(44) E_c = $\sqrt{(41)}\,(X_c - X_{1s})$ = ( )( ) =

PG. 2

Figure 6. Capacitor-motor calculation sheet

value of slip is very small. The time required for a single calculation should not exceed five to ten minutes and, where a number of calculations are done in parallel, even this time can usually be bettered.

Apparent impedance charts are not confined to the calculation of single-phase motors, but they may also be applied to polyphase motors, shaded pole motors, shading coils of relays, and other electrical devices. A calculation form for polyphase motors is too obvious and simple to present here, but in a similar way to that which has been used for the straight single-phase motor, it is possible to lay out a calculation form for an unbalanced two-phase motor such as the capacitor motor. An example of a calculation form of this type is shown in figure 6.

Advantages

The advantage of the apparent impedance method as herein outlined for the calculation of induction motor performance lies in the symmetry and naturalness of the approach. This symmetry is particularly indicated by the fact that the curves for the forward and backward field impedances are identical and the further fact that these impedances may not only be used in a simple fashion to obtain the input current, but the same quantities are also used in equally simple fashion in expressions for torque and output.

It is felt that the use of the apparent impedance charts not only eliminates considerable labor, but also a great deal of the possibility of error, for with the use of the charts, the calculational operations are reduced to arithmetic and complex quantities need not be considered.

A further advantage of the method lies in the assistance which it gives to a visualization of how the motor characteristics vary as the constants are changed. The separate points of a calculation are tied together mentally through the continuity of the curves.

In the determination of motor constants from test, the apparent impedance charts are used in reverse because apparent impedances at definite speeds are known and it is desired to find the true impedances.

Reference

Revolving-Field Theory of the Capacitor Motor, Wayne J. Morrill. AIEE Transactions, volume 48, 1929, pages 614–29.

A Novel Reclosing Relay

P. O. BOBO
MEMBER AIEE

Synopsis: This paper describes a reclosing relay for oil circuit-breaker control which is new in design, new in function, and new in operation. It was designed and built with additional features to meet certain reclosing requirements which cannot be obtained by use of standard reclosing relays. These reclosing requirements, brought about by complete automatization of high-voltage oil circuit-breakers in transmission networks and on lines containing automatic sectionalizing air-break switches, are herein described. Also several schemes of time-sequence-coordination are given for the operation of oil circuit-breakers with automatic line sectionalizing air-break switches. Of special interest is a scheme for materially reducing fuse outages, which utilizes the described reclosing relay for coordinating the operations of a breaker with fuse operations on the line served by the breaker.

BECAUSE of the greater exposure and higher potential stresses of the transmission system over those of the generation and distribution systems, most interruptions to electric service are caused by failures in the transmission process. Although transmission lines can be built almost interruption proof by utilizing modern design, the fact remains that the greater number of lines were built several years past when such quality lines, if at all possible, were so only at a prohibitive cost. Thus the major problem is simply an economical balance between what can be done to reduce the number of interruptions and what can be done to minimize or remove the adverse effects of those which do occur. It is a question whether to rebuild the older lines or accept the interruptions as inevitable and minimize their adverse effects upon service.

Paper 41-152, recommended by the AIEE committee on protective devices, and presented at the AIEE South West District meeting, St. Louis, Mo., October 8–10, 1941. Manuscript submitted July 8, 1941; made available for preprinting August 19, 1941.

P. O. Bobo is assistant protective engineer with Oklahoma Gas and Electric Company, Oklahoma City, Okla.

It is not the author's purpose to answer this question since each power company must work out its own problems. The author does wish, however, to discuss that side of the question regarding means for minimizing the adverse effects of service interruptions due to faults on the transmission system.

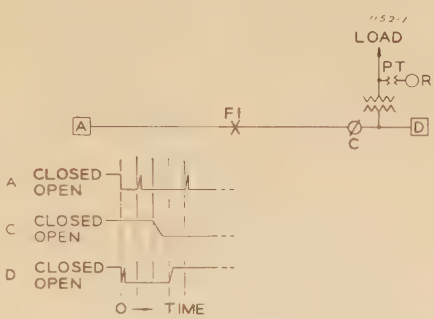

Figure 1. Operation-sequence diagram of line breakers and one automatic sectionalizing air-break switch with low side potential control for opening only

Service interruptions seldom result from failure of the conductor, but are caused by short circuits resulting from lightning. Accompanying voltage disturbances, however, can be practically nullified by the use of high speed relays, a fact which is repeatedly demonstrated on the Oklahoma Gas & Electric Company system. Large industrial motor loads now ride through all disturbances, whereas before installation of such relays these loads were occasionally lost. Moreover, since installing them permanent faults are a rarity and insulator replacements are few because the power is interrupted before burning action effects permanent damage.

Breaker-Reclosing Equipment, Transmission System

Although fast clearing of faults minimizes the voltage disturbance to remaining parts of system and greatly reduces the possibility of permanent line damage, it still interrupts service to consumers served from or through the faulted section. Through the modern practice of equipping breakers with automatic reclosing relays, the duration of such an interruption is greatly minimized. But when the breaker is located within a transmission network, its reclosing requirements necessitate the use of a reclosing relay having greater utility than the standard makes now available. The latter relays are generally designed for use on distribution feeders or radial transmission lines where the only requirements are to perform upon a breaker a certain number of closures at definite time intervals, and to lock out the breaker from further closures if the final closure is unsuccessful because of a permanent fault.

Such relays cannot be used in transmission networks because they are either unidirectional in operation, which requires extended resetting times, or they cannot be adapted to the conditions desired without use of extra equipment.

Need for a Reclosing Relay for Functioning Under Variable Line Conditions

A reclosing relay for transmission network use must be capable of distinguishing between energized and de-energized line conditions. Also, it must be adaptable for use in conjunction with synchronism-check relays for closing breakers on in-phase conditions. For example, it may be desirable to limit to one terminal the re-energization of a transmission line following tripouts, with closure of the remaining terminal breaker permitted only after successful re-energization of the line. The first requires closures on "de-energized line" only, and the second requires closures on "energized line" only which may also require synchronism-check.

For use in unattended and semi-attended substations a reclosing relay must be capable of one or more subsequent reclosures in addition to the immediate or delayed initial reclosure, since operating experience shows that out of the total tripouts about 85% are successfully re-energized by an immediate breaker reclosure, 10% by a second reclosure, 1% by a third reclosure, and 4% result in permanent faults. The percentage of successful immediate reclosures on circuits equipped with modern high speed fault clearing relays is above average and the percentage of permanent faults is far below average.

Need for a Fast Accurate-Timing Reclosing Relay

Transmission lines are customarily divided into several parts by airbreak switches so that any one section, on becoming faulty, can be removed and service restored to the remaining parts. Most airbreak switches are, as yet, manually operated but with service requirements becoming more exacting, automatization of certain airbreak switches affords an inexpensive means of speeding service restoration to loads tapped on transmission lines.

Airbreak switches are generally incapable of interrupting fault currents. They are designed to be opened under normal service conditions. Therefore, under fault conditions they must be opened after the line is de-energized and the time of opening must be coordinated with the time of re-energization of the circuit by the terminal breakers of the line. To accomplish this time coordination between the automatic sectionalizing switches and line breakers and yet restore service in minimum time, requires the use of a fast accurate breaker-control relay. Short time intervals between breaker reclosures are essential in order to minimize the time gaps between operations of the breakers and sectionalizing switches.

The extent to which an airbreak switch need be automatized depends upon service requirements of the load or loads protected and the quality of the transmission line serving the loads. Several schemes of time-sequence-coordination are given below as examples, in which the operations of airbreak switches are controlled from potential indications only.

Figure 1 shows a single airbreak switch C automatized for opening only. No high tension potential device is required for airbreak switch control, the potential indication to control relay $R1$ being received from low side of power transformer as indicated. This scheme is applicable for protecting a load tapped between a long and a short section of line where few

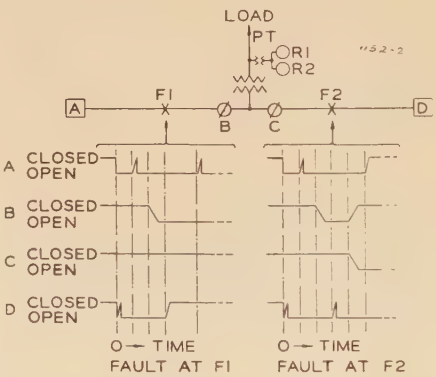

Figure 2. Operation-sequence diagram of line breakers and two automatic sectionalizing air-break switches with low side potential control

permanent faults are expected in the short section and practically all are expected in the long section. Since the airbreak switch is automatized only for opening, it is desirable that opening not take place until after some assurance of a permanent fault. For this reason at least two attempts are made to re-energize the line before the airbreak switch opens.

Figure 2 shows two airbreak switches controlled by relays $R1$ and $R2$, which also receive potential indications from the low side of power transformers. This scheme assures service to a load should a permanent fault occur on either side of the load.

Figure 3a shows two airbreak switches automatized for both opening and closing operations. This requires the use of potential devices connected to the line side of each airbreak switch for control. Since these switches will reclose automatically with line re-energized, less assurance is required that a fault be permanent before the switches automatically open. For this reason only one attempt at re-energizing the line is made before opening takes place. Switches B and C are identically equipped and controlled.

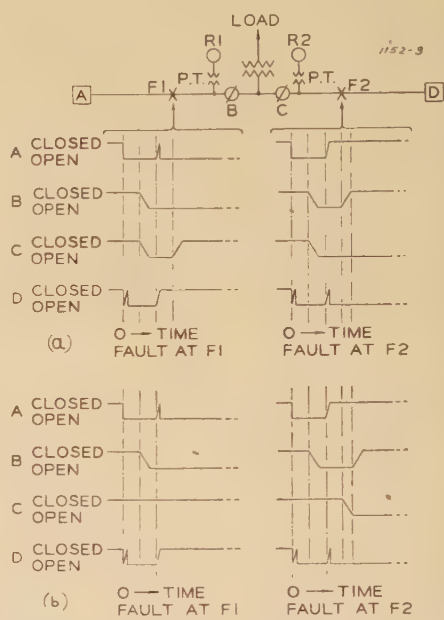

Figures 3a and 3b. Operation-sequence diagram of line breakers and two automatic sectionalizing air-break switches with high side potential control

They open simultaneously a definite time after initial attempt to re-energize line. After switches B and C open, breakers A and D close simultaneously; breaker A, closing on the fault, will reopen, and breaker D will remain closed. The line being re-energized to switch C will cause this switch to close and re-establish service.

Figure 3b shows two airbreak switches with equipment identical to that of the switches in figure 3a, but having different timing control. These switches are automatized so that only one switch is open at any given time. This scheme affords a faster means of service restoration than the scheme of figure 3a for faults in the $F1$ section, and slightly longer time for faults in the $F2$ section.

Need for a Quick-Resetting Reclosing Relay

To prevent possible hazards to service within a transmission system, a reclosing

relay is needed with quick resetting action following any successful reclosure. However, some time should elapse after a reclosure before permitting the device to reset quickly, as assurance that the reclosure was successful and that no permanent fault exists on the line. This time interval should be greater than the re-opening time of breaker under an existing fault condition, and its length is limited only by the permissible duty on the breaker. In no case, however, should the resetting time be extended until the device has traversed its complete reclosing cycle.

In the case of a breaker equipped with a unidirectional reclosing relay which trips on a transient fault, closes automatically and again trips on a second transient fault, the feeder customers would needlessly be without service until a subsequent reclosure point is reached. Even though this outage is momentary, important motor loads may be dropped, whereas with a quick resetting reclosing relay service would be immediately re-established upon the second tripout. In addition, if a transient tripout occurs during the timing interval between the final reclosure point and the lock-out position of a standard unidirectional reclosing relay, it will lock out without reclosing the breaker. Obviously such hazards can be serious, especially in a transmission system with isolated unattended or semi-attended substations, since it is possible for lines to be out of service or loop circuits to be open for lengthy periods when such unidirectional relays are so employed.

Likewise, on lines containing automatic sectionalizing airbreak switches and whose terminal breakers are controlled by unidirectional relays, subsequent tripouts as described above may cause these sectionalizing switches to open unnecessarily (due to loss of potential) and thereby seriously hazard service. Under these conditions the time coordination between the operations of the breakers and switches becomes disrupted.

Description of the Reclosing Relay

In view of the foregoing and the fact that automatic substations and motor operated sectionalizing switches have increased in number on the Oklahoma Gas and Electric Company system, the author designed an accurate timing, adjustable resetting, automatic reclosing relay for universal breaker application in the company's transmission system. It consists of an assembly of eleven standard telephone type relays mounted in a standard glass covered case as shown pictorially in figure 4 and schematically in figure 5. It contains no fabricated parts other than a terminal board and a mounting plate for the relays. Its principal features are:

Timer

The device contains no motor-driven gears, drum, or camshaft for interval timing. Timing is obtained by a vibrating reed relay acting in conjunction with slow-operate relays to pulse a stepping switch at intervals adjustable between 1 and 15 seconds. The vibrating reed relay *VR*, figures 4 and 5, on energization pulls-up and energizes slow-release relay *SR*, which seals in and de-energizes the *VR* relay; de-

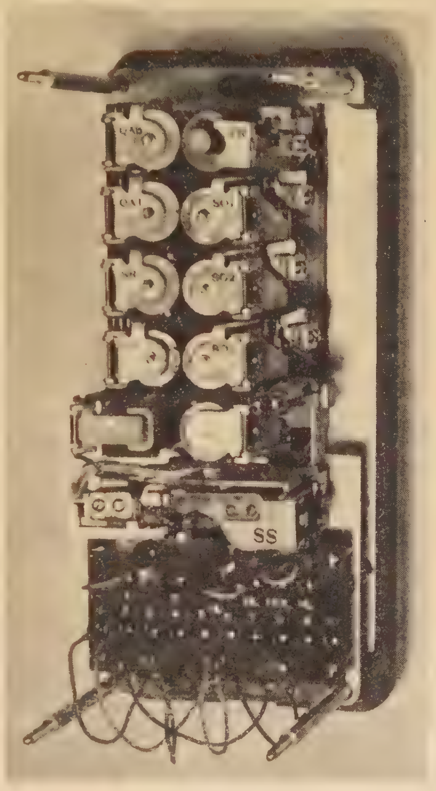

Figure 4. The reclosing relay, an assembly of 11 telephone-type relays

energization releases the reed which vibrates to rest, thus energizing (through break contacts) slow-operate relay *SO2*. Relay *SO2* in turn energizes slow-operate relay *SO3* to move the stepping switch one step by energizing the operating coil *SS*. Relay *SO3* de-energizes relay *SR* which causes repetition of the timing cycle for further movements of the stepping unit. The stepping switch has 10 steps which make possible a maximum time duration of $2^1/_2$ minutes for this reclosing relay. As many as 3 breaker reclosures can be made by it, and they can be accurately spaced from 3 seconds to $1^1/_4$ minutes apart.

Variable Conditions of Breaker Closure

The recloser contains a built-in "line potential checking relay" (*QAL*) which affords choice of breaker closures on "de-energized line only," "energized line only," or "energized and/or de-energized line." By means of an external terminal connection the device can be interlocked with a synchronism-check relay for closures on "energized line in-phase only" or "de-energized line and/or energized line in-phase."

Variable Conditions of Timer Movement

By this term is meant the conditions under which the stepping switch is advanced following the initial reclosure. For most applications the "conditions of timer movement" and the "conditions of breaker closure" should be the same in order that the timer not move the stepping switch past subsequent reclosure points to the "lockout position" while the conditions of breaker reclosure are incorrect. On the other hand, when the time coordination between operations of breakers and sectionalizing switches is close it is necessary that the reclosing relays serving both terminals of the line advance together regardless of breaker closing conditions.

Quick Reset

The most salient feature of the reclosing relay is its ability to reset following successful reclosures. Reset takes place immediately after the breaker has remained closed a definite time as assurance that the fault was not permanent. Retripping of the breaker before this time expires will cause the relay to progress toward subsequent reclosing points without resetting. This definite time limit is adjustable in impulse intervals of the stepping switch independently after each reclosure. The reset feature may be omitted from any reclosure, as is sometimes desired, to limit the possible rupturing duty that may be imposed upon a breaker with limited rating.

Antipump on All Reclosures

The relay is inherently anti-pump (electrically trip free) on all reclosures, that is, for each reclosure the closing circuit to the breaker is opened immediately upon closure and cannot be re-energized until a subsequent reclosing point is reached, and only then providing the breaker is open and closing conditions satisfy the settings made on the terminal board later described. This feature is obtained by energizing the closing relay *CL* through

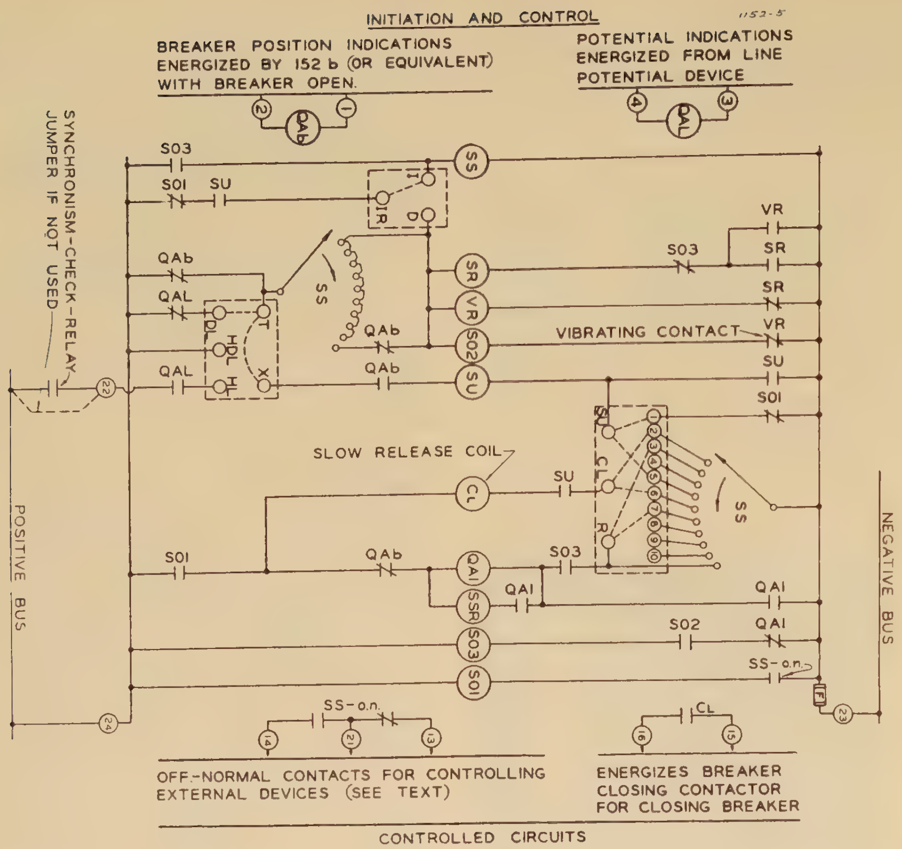

Figure 5. Schematic diagram of internal connections of reclosing relay

contacts of the set-up relay *SU* (figures 4 and 5), which is initiated from points of the stepping switch just preceding the points of closure, and is held energized by its own contacts until dropped by the control relay *QAb* on closure of the breaker.

Setting the Relay

The pulsing intervals of the stepping unit are adjustable between 1 and 15 seconds by screws which vary the reed amplitude of the vibrating reed relay (*VR*). All other settings are made electrically by inserting plug type jumpers in proper jacks on the terminal board, figures 4 and 5. The points of the stepping switch are terminated in a row of jacks numbered 2 to 10 on the board. The number 1 jack represents the zero point or normal position of the stepping switch—being controlled by slow-operate relay *SO*1, which is operated by an off-normal contact "*SS*-on" on the stepping unit.

Directly below this row of jacks is a row of 3 binding posts, *SU*, *CL*, and *R*, from which by use of jumper connections to the row of jacks time settings are made for: (1) initiation of the set-up relay *SU*, (2) energization of the closing relay *CL*, which closes the breaker, (3) resetting of the relay. Reset is accomplished instantaneously by energization of relay *QA*1 which seals in and maintains energized the reset coil *SSR* of the stepping switch until the unit has fully reset and relay *SO*1 is de-energized by the opening of "off-normal" contact "*SS*-on." Note that resetting cannot take place unless relay *QAb* is de-energized as indication that breaker is closed.

The conditions of breaker reclosure are set by placing jumpers from binding post "*X*" to jack "*DL*" for "dead-line" closing conditions, to jack "*HDL*" for "hot and/or dead-line" (non-restricted) conditions, and to jack "*HL*" for "hot-line" conditions. Jacks *DL* and *HL* are controlled by a break and a make contact respectively of line checking relay *QAL*. If synchronism-check is desired, the external terminal stud "22" is connected in series with the contacts of the synchronism-check relay to the positive bus; otherwise this terminal stud is connected directly to the positive bus. These connections to point "*X*" establish the conditions for which the set-up relay *SU* is energized.

The conditions of timer movement are set by placing jumpers from binding post "*T*" to the same jacks as those for the conditions of closure. Such connections to point "*T*" control the conditions for which the timer relays *SR*, *VR*, and *SO*2 are energized.

Immediate or delayed initial reclosure is chosen by inserting jumper from jack "*IR*" to jack "*I*" for "immediate" reclosure, or from jack "*IR*" to jack "*D*" for "delayed" reclosure. Connection to jack "*I*" permits immediate energization of operating coil *SS* of stepping switch, and connection to jack "*D*" interposes one impulse cycle of timing relays before energization of coil *SS*.

Other Features

As can be seen from schematic connection diagram figure 5, only one breaker auxiliary switch (152*b*) is required for operation, or in many cases the reclosing relay may be controlled directly from the breaker alarm or indicating light circuits instead, since the only requirement is energization of relay *QAb* when breaker is open.

The auxiliary relay *CL* which energizes the breaker closing circuit is equipped with a vacuum contact for the high-current capacity required in energizing breaker closing contactors. Its coil is slow releasing in order to permit ample time for the breaker to latch closed without any necessary critical adjustment of the breaker auxiliary switch.

The reclosing relay can be made for operating voltages from 24 to 250 volts d-c, or a-c with a rectifier unit.

A mechanical pointer fastened to the shaft of the stepping switch indicates when the relay is locked out by pointing to line marked "*LO*" on front of stepping unit.

The relay will automatically reset upon manual closing of breaker after lockout, provided breaker remains closed for one impulse interval of timer, otherwise it will remain in the lock-out position.

For remote supervisory indication and for other external functions of control associated with reclosing of breakers, two auxiliary "off-normal" contacts (*SS*-on) are brought out to terminal studs 13, 14, and 21. In attended stations where the relay is located away from control board, remote off-normal supervision indicates relay operations to the attendant. An important control function using an off-normal contact involving fuse operations is described below.

Method of Reducing Fuse Outages

To lessen the outages caused by transient faults on multibranch-fuse circuits served through a common breaker, the Oklahoma Gas and Electric Company is using a unique automatic scheme which permits instantaneous initial tripping of the breaker for a fault at any point on the circuit. Service is immediately restored by the breaker reclosing equipment. The instantaneous opening of the breaker

interrupts transient short-circuits before the branch fuses have time to blow. Service can then be restored to the fused branch immediately, instead of waiting until a fuse can be replaced. Of course, service to the entire circuit is momentarily interrupted, but it is doubtful whether such an interruption is more serious than the voltage disturbance caused by a longer clearing time of a fuse.

In order to protect customers on unfaulted branches when a permanent fault occurs, a reclosing relay fulfilling the following requirements is needed. It must remove the instantaneous tripping relays from service prior to the immediate reclosure of the breaker so as to permit coordination between breaker time-delay relays and sectionalizing fuses, and it should hold these instantaneous relays removed from service until it has reset and again is capable of an immediate reclosure, otherwise more than a transient outage may result needlessly to all customers.

The reclosing relay herein described with its auxiliary "off-normal" contact on the stepping switch fulfills all requirements. This "off-normal" contact (figure 5, terminal studs 13 and 21) is connected in series with the instantaneous tripping relay contacts and opens this circuit upon movement of the stepping switch off-normal just before closure of the breaker. The circuit remains open until the relay is fully reset.

The reset feature of the reclosing relay for this service is as useful in preventing fuse outages as the scheme itself.

Operating Experience

The accompanying table is an analysis of operations from January 1939 through June 1941 of the line breakers which are equipped with the reclosing relay.

Under (I) above, three of the successful sectionalizing operations were accomplished within 8 seconds by equipment utilizing the scheme of figure 3*b*. The four "line sectionalizing failures" were in no case due to improper functioning of the reclosing relays. One was caused by a blown fuse in an airbreak, switch mechanism; one was caused by the nature of the fault—open conductor, grounded on one end and in clear on the other; one was caused by the failure of a breaker to latch closed; the fourth was caused by manual interference with the automatic reclosing relay.

	Number	Per Cent
I. Breakers serving lines equipped with automatic sectionalizing air-break switches:		
Line terminals equipped	7	
Line faults	123	100
Normal service restored, initial reclosure	101	82
Normal service restored, second reclosure	7	6
Normal service restored, third reclosure	6	5
Relay lockouts	9	7
Reset feature, beneficial	12	10
Permanent faults	12	100
Line correctly sectionalized	8	67
Line sectionalizing failures	4	33
II. Breakers serving 66 kv-loop-circuit lines:		
Line terminals equipped	6	
Line faults	304	100
Normal service restored, initial reclosure	298	98
Normal service restored, second reclosure	3	1
Normal service restored, third reclosure	0	0
Relay lockouts	3	1
Reset feature, beneficial	40	13
III. Breakers serving multi-branch-fuse circuits:		
Line terminals equipped	1	
Line faults	46	100
Normal service restored, immediate reclosure	45	98
Normal service restored, second reclosure	1	2
Normal service restored, third reclosure	0	0
Relay lockouts	0	0
Reset feature, beneficial	3	6

The most important result shown by the analysis is the fact that the reset feature of the relay was beneficial in restoring service for 55 of the total 471 fault operations, that is, for approximately 12% of the faults, which faults occurred following a successful reclosure and within the total cycle of time for which the relays were set, the quick resetting action of the relay, in addition to speeding restoration of service, prevented the following possible service hazards. (Previously described under "Need for Quick Resetting Reclosing Relay.)

1. Disruption of time-sequence coordination between operations of automatic sectionalizing airbreak switches and line terminal breakers.

2. Longer than transient outages to important loads.

3. Loop circuits remaining open for lengthy periods.

4. Lockouts of reclosing relays without closing the breakers.

Conclusions

The relay meets the following requirements which are essential to successful operation of oil circuit breakers in an extensive transmission network:

1. Variable conditions of closure
2. Variable conditions of timing
3. Fast and accurate timing between closures
4. Anti-pump characteristics
5. Auxiliary off-normal contacts for external control and indications
6. Operation on either alternating or direct current
7. Quick resetting following successful reclosures

It is through the fulfillment of above requirements that the reclosing relay permits a transmission system to render maximum continuity of service. Interruptions caused by transient faults are minimized; hazards caused by untimely tripouts are eliminated; coordination between breakers and automatic sectionalizing switches is made faster and more effective; and fuse outages on certain circuits are greatly reduced. All of this has been definitely proved by 14 installations of the relay in the Oklahoma Gas & Electric Company's system over a period of $2^1/_2$ years beginning January 1939. Experience also has shown that the relay is dependable and virtually trouble free—a tribute to the versatile and highly developed relays originally created for automatic telephone systems.

Formulas for the Inductance of Rectangular Tubular Conductors

THOMAS JAMES HIGGINS
ASSOCIATE AIEE

THE formula for the inductance per unit length of two parallel conductors of rectangular cross section, obtained by using the formal expressions for the geometric mean distance of a rectangle to itself and the geometric mean distance between two rectangles with sides parallel, is exceedingly cumbersome. More than a score of logarithms and arc tangents must be evaluated when computing the inductance for a given conductor spacing and cross section. To circumvent such lengthy calculations when computing the reactance of like parallel rectangular strap conductors, Dwight[1, 2] has published curves, each plotted for a certain conductor spacing and cross section, from which the reactance can be obtained. Unless, however, the conductor spacing and the ratio of conductor thickness to breadth coincides with those values for which the curves are plotted, interpolation is necessary. Recently Roth[3] has expressed the inductance of such lines in the form of a rapidly converging series, the parameters of which are the spacing and dimensions of the conductors. Usually, a few terms of this series suffice to yield a value of inductance sufficiently accurate for all design purposes.

As regards rectangular tubular conductors, the only analytical literature is a paper by Dwight and Wang[4] giving formulas for *thin square* tubular conductors. These are derived on the assumption that the conductor walls are so thin that the sides can be considered as but line segments. The geometric mean distances for such segments are then used to calculate the inductance. Such a procedure is equivalent to asserting that the current flows solely on the surface of the conductors. It follows, then, that the values of inductance computed on this basis will be *less* than the actual values. Consequently, while these formulas suffice for many calculations on square tubular conductors, if accuracy is a desideratum of design this minimization of thickness restricts the range of application of these formulas to *very thin square* tubular conductors. Recognizing this restriction and noting, further, that commercial conductors have rounded corners, Dwight and Wang give formulas, empirically deduced, from which corrections for thickness and for rounded corners can be calculated.

The inductance of rectangular tubular conductors of appreciable thickness (and not necessarily square) can be obtained from equations given by the author[5] for the case of a line composed of two parallel conductors, the cross sections of which are geometrically similar but dimensionally different hollow rectangles. However, as these equations are implicit rather than explicit, they are ill suited to numerical computation. Yet, in light of the increasing use of rectangular tubular conductors for main bus bars, electric furnace installations, and other heavy current duties (especially feeders for batteries of welders), it is most desirable to have formulas with which one can calculate quickly the inductance for any conductor spacing or cross section. *Such formulas are derived in this paper*, it being assumed that the conductors are nonmagnetic, square cornered, of such length that end effects are negligible, and carry currents uniformly distributed over the cross sections of the individual conductors.

Although obtained through a procedure involving rather intricate analysis, the formulas themselves are simple in nature. With them a designer can calculate rapidly the inductance of a single-phase circuit composed of solid or tubular rectangular conductors; or of a three, six, or twelve-phase circuit composed of solid or tubular rectangular conductors, the axes of which lie in a plane.

I. The Formal Solution

With reference to figure 1, we seek A_1 which satisfies the differential equations

$$\nabla^2 A_1 = 4\pi w \text{ over } C_1 \tag{1}$$

$$\nabla^2 A_1 = -4\pi w \text{ over } C_4 \tag{2}$$

$$\nabla^2 A_1 = 0 \text{ over the remainder of the right half-plane} \tag{3}$$

and the boundary conditions

$$A_1 = 0 \text{ at infinity} \tag{4}$$

$$A_1 = 0 \text{ on the line } x = 0 \tag{5}$$

$$\frac{\partial A_1}{\partial y} = 0 \text{ on the line } y = 0 \tag{6}$$

The boundary conditions are obtained as follows: (4) from knowledge that the vector potential vanishes at infinity except for an arbitrary constant, taken here as zero; (5) from observation that the line $x = 0$ and the left-hand portion of the circle of infinite radius constitute, in the limit, a line of induction, whence, lines of induction being lines of constant vector potential, the vector potential is zero as on the circle at infinity; (6) from noting that the horizontal component of induction density vanishes on the line $y = 0$, or $B_x = \partial A_1/\partial y = 0$.

For the problem at hand, A_1 is an even function of y, an odd function of x. Accordingly, A_1 is expressed by the double Fourier integral

$$A_1 = (4/\pi^2) \times \int_0^\infty \int_0^\infty \int_0^\infty \int_0^\infty A_1(X, Y) \sin Mx \times \cos Ny \cos NY \sin MX dX dY dN dM \tag{7}$$

the same satisfying (5) and (6) unconditionally, and (1), (2), and (3) providing $A_1(X, Y)$ or an integral containing $A_1(X, Y)$ is appropriately determined. Thus, if the double Fourier integral expressing the current density at any point in the conductors,

$$\begin{aligned} w &= (4/\pi^2) \int_0^\infty \int_0^\infty \int_0^\infty \int_0^\infty w(x, y) \times \sin Mx \cos Ny \cos NY \times \sin MX\, dX dY dN dM \\ &= (4/\pi^2) \int_0^\infty \int_0^\infty \int_0^h \int_{d-e}^{d+e} w \sin Mx \times \cos Ny \cos NY \sin Mx\, dX dY dN dM \\ &= (8w/\pi^2) \int_0^\infty \int_0^\infty \frac{1}{MN} \sin Mx \cos Ny \times \sin Nh \sin Md \sin Me\, dN dM \end{aligned} \tag{8}$$

is substituted in the right-hand member of

$$4(M^2+N^2)/\pi^2 \times \int_0^\infty \int_0^\infty \int_0^\infty \int_0^\infty A_1(X, Y) \sin Mx \times \cos Ny \cos NY \sin Mx\, dX dY dN dM = 4\pi w \tag{9}$$

obtained by substituting (7) in (1), we

Paper 41-168, recommended by the AIEE committee on basic sciences, and presented at the AIEE Southern District meeting, New Orleans, La., December 3–5, 1941. Manuscript submitted July 23, 1941; made available for preprinting October 6, 1941.

THOMAS JAMES HIGGINS is assistant professor of electrical engineering, Tulane University of Louisiana, New Orleans, La.

This paper is based upon a thesis submitted by Professor Higgins to the faculty of Purdue University in June 1941 in partial fulfillment of the requirements for the degree of doctor of philosophy.

1. For all numbered references, see list at end of paper.

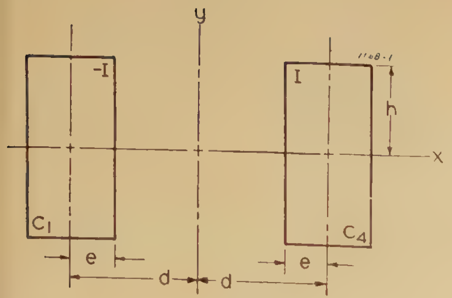

Figure 1

have, on comparing the two members of the resulting equation

$$\int_0^\infty \int_0^\infty A_1(X, Y) \cos NY \sin MX \times$$
$$dXdY = 8\pi w \frac{\sin Nh \sin Md \sin Me}{MN(M^2+N^2)} \quad (10)$$

Finally, substituting (10) in (7), we have for A_1

$$A_1 = (32w/\pi)\int_0^\infty \frac{\sin Md \sin Me \sin Mx}{M} \times$$
$$\int_0^\infty \frac{\sin Nh \cos Ny}{N(M^2+N^2)} dNdM \quad (11)$$

For the current distribution of figure 2 we have, analogously,

$$A_2 = (-32w/\pi)\int_0^\infty \frac{\sin Md \sin ME \sin Mx}{M} \times$$
$$\int_0^\infty \frac{\sin NH \cos Ny}{N(M^2+N^2)} dNdM \quad (12)$$

Superimposing the current distributions of figures 1 and 2 results in that of figure 3. The corresponding vector potential is

$$A = A_1 + A_2 \quad (13)$$

The total electromagnetic field energy W is, by symmetry, four times that associated with the current flowing through the shaded portions of figure 3. Thus, from the usual expression, $W = {}^1/_2 \int AwdS$, we have

$$W = 2\int_0^h \int_{d-e}^{d+e} Awdxdy -$$
$$2\int_0^H \int_{d-E}^{d+E} Awdxdy \quad (14)$$

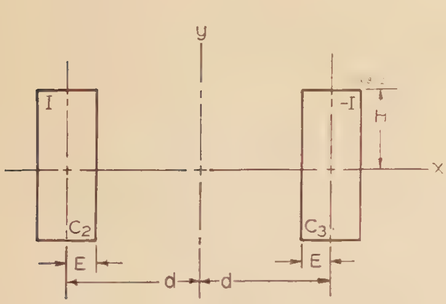

Figure 2

Substituting (11) and (12) in (13), and, in turn, (13) in (14), we have

$$W = (64w^2/\pi)\times$$
$$\int_0^h \int_{d-e}^{d+e} \int_0^\infty \frac{\sin Md \sin Me \sin Mx}{M} \times$$
$$\int_0^\infty \frac{\sin Nh \cos Ny}{N(M^2+N^2)} dNdMdxdy -$$
$$(64w^2/\pi)\times$$
$$\int_0^h \int_{d-e}^{d+e} \int_0^\infty \frac{\sin Md \sin ME \sin Mx}{M} \times$$
$$\int_0^\infty \frac{\sin NH \cos Ny}{N(M^2+N^2)} dNdMdxdy -$$
$$(64w^2/\pi)\times$$
$$\int_0^H \int_{d-E}^{d+E} \int_0^\infty \frac{\sin Md \sin Me \sin Mx}{M} \times$$
$$\int_0^\infty \frac{\sin Nh \cos Ny}{N(M^2+N^2)} dNdMdxdy +$$
$$(64w^2/\pi)\times$$
$$\int_0^H \int_{d-E}^{d+E} \int_0^\infty \frac{\sin Md \sin ME \sin Mx}{M} \times$$
$$\int_0^\infty \frac{\sin NH \cos Ny}{N(M^2+N^2)} dNdMdxdy \quad (15)$$

These integrals are such that the order of integration can be varied as desired. Accordingly, integrating first with respect to x and then with respect to y, we have after collecting terms

$$W = (128w^2/\pi)\int_0^\infty \frac{\sin^2 Md \sin^2 Me}{M^2} \times$$
$$\int_0^\infty \frac{\sin^2 Nh}{N^2(M^2+N^2)} dNdM +$$
$$(128w^2/\pi)\int_0^\infty \frac{\sin^2 Md \sin^2 ME}{M^2} \times$$
$$\int_0^\infty \frac{\sin^2 NH}{N^2(M^2+N^2)} dNdM -$$
$$(256w^2/\pi)\times$$
$$\int_0^\infty \frac{\sin^2 Md \sin ME \sin Me}{M^2} \times$$
$$\int_0^\infty \frac{\sin NH \sin Nh}{N^2(M^2+N^2)} dNdM \quad (16)$$

Now[6]

$$\int_0^\infty \frac{\sin NH \sin Nh}{N^2(M^2+N^2)} dN$$
$$= \frac{\pi}{2M^3}(MH - \epsilon^{-Mh} \sinh MH) \quad (17)$$

Substituting appropriately in (16), we have

$$W = 64w^2 \int_0^\infty \frac{\sin^2 Md \sin^2 Me}{M^5} \times$$
$$(Mh - \epsilon^{-Mh} \sinh Mh)dM +$$
$$64w^2 \int_0^\infty \frac{\sin^2 Md \sin^2 ME}{M^5} \times$$
$$(MH - \epsilon^{-MH} \sinh MH)dM -$$
$$128w^2 \int_0^\infty \frac{\sin^2 Md \sin ME \sin Me}{M^5} \times$$
$$(MH - \epsilon^{-Mh} \sinh MH)dM \quad (18)$$

The third integral in (18) can be written as the sum of two integrals, such that W is expressed as the sum of four like integrals. Doing so, we have

$$W = 64w^2 \int_0^\infty \frac{\sin^2 Md \sin^2 Me}{M^5} \times$$
$$(Mh - \epsilon^{-Mh} \sinh Mh)dM +$$
$$64w^2 \int_0^\infty \frac{\sin^2 Md \sin^2 ME}{M^5} \times$$
$$(MH - \epsilon^{-MH} \sinh MH)dM -$$
$$128w^2 \int_0^\infty \frac{\sin^2 Md \sin ME \sin Me}{M^5} \times$$
$$\left[\frac{M(h+H)}{2} - \epsilon^{-\frac{M(h+H)}{2}} \sinh \frac{M(h+H)}{2}\right] dM +$$
$$128w^2 \int_0^\infty \frac{\sin^2 Md \sin ME \sin Me}{M^5} \times$$
$$\left[\frac{M(h-H)}{2} - \epsilon^{-\frac{M(h-H)}{2}} \sinh \frac{M(h-H)}{2}\right] dM$$
$$(19)$$

Each integral of (19) is of the form

$$\frac{y}{2} f_1(x_1, x_2, x_3, x_4) - {}^1/_2 f_2(x_1, x_2, x_3, x_4, y) \quad (20)$$

As shown in the appendix

$$f_1 = \int_0^\infty \frac{1}{M^4} \sin Mx_1 \sin Mx_2 \sin Mx_3 \times$$
$$\sin Mx_4 \, dM$$
$$= \frac{\pi}{3!2^4} \sum_{i=1}^{8} (-1)^p |k_i^3| \quad (21)$$

k_i designating any one of the eight possible terms to be formed from

$$(x_1 \pm x_2 \pm x_3 \pm x_4)$$

by arbitrary selection of the plus and minus signs, while p is the number of minus signs in k_i.

For f_2 we have

$$f_2 = 2\int_0^\infty \frac{1}{M^5} \sin Mx_1 \sin Mx_2 \sin Mx_3 \times$$
$$\sin Mx_4 \epsilon^{-\frac{My}{2}} \sinh \frac{My}{2} dM$$
$$= \frac{1}{192} \sum_{i=1}^{8} (-1)^p F(k_i, y) \quad (22)$$

where k_i and p have the same significance as in (21), and

$$F(k_i, y) = (k_i^4 - 6y^2k_i^2 + y^4) \log (k_i^2 + y^2)^{1/2} + 4yk_i(k_i^2 - y^2) \tan^{-1}(k_i/y) - k^4 \log |k_i| \quad (23)$$

The fifth column of table I contains the values of k_i used in evaluating the first two integrals in (19), while those for the second two integrals of (19) are in the sixth column.

Defining new variables, $r=2e$, $R=2E$, $s=2h$, $S=2H$, $D=2d$, and $t=e-E=h-H$, evaluating each integral of (19) by means of (21) and (22), and collecting terms, we have for the terms of (19) taken in order

$$W = w^2\{W(r, s) + W(R, S) - 2[W(R+t, S+t) - W(t, S+t)] + 2[W(R+t, t) - W(t, t)]\} \quad (24)$$

where $W(r, s)$ is defined by

$$W(r, s) = \tfrac{1}{6}[2F(D, s) - F(D+r, s) - F(D-r, s) + 2F(r, s) - 2F(0, s) + 4\pi r^2 s(3D-r)] \quad (25)$$

Collecting the terms of (24), we have

$$W = w^2[W(r, s) + W(R, S) + 2W(t, S+t) + 2W(R+t, t) - 2W(R+t, S+t) - 2W(t, t)] \quad (26)$$

The energy W being known in terms of the dimensions and spacings of the conductors, the inductance can be obtained at once from the usual formula, $W = \tfrac{1}{2}LI^2$. Hence

$L = 2W/w^2(rs-RS)^2$ abhenries per centimeter of line length (27)

If $R=S=0$ we have solid conductors, and (27) becomes

$L = 2W(r, s)/(wrs)^2$ abhenries per centimeter of line length (28)

The 60-cycle reactance per thousand feet of conductor is obtained by multiplying L by 5.74×10^{-3}.

II. Series Expressions for L

We turn now to finding series expansions which enable one to calculate quickly each of the terms of (26). Expanding (25) in powers of r, we obtain

$$W(r, s) = \frac{1}{6}\Bigg[2F(r, s) - 2F(0, s) + 4\pi r^2 s(3D-r) - r^2 \frac{\partial^2 F(D, s)}{\partial D^2} - \frac{r^4}{2\cdot 3!}\frac{\partial^4 F(D, s)}{\partial D^4} - \frac{r^6}{3\cdot 5!}\frac{\partial^6 F(D, s)}{\partial D^6} - \ldots\Bigg] \quad (29)$$

The details of the expansion and expressions for the various derivatives, in terms of the dimensions and spacing of the conductors, are given in the appendix. Substituting appropriately in (29) and collecting terms, we have

$$W(r, s) = 2r^2\Bigg\{s^2\left[\frac{7}{12} + \frac{1}{2}\log\frac{D^2+s^2}{r^2+s^2}\right] - \left[\frac{D^2}{2} + \frac{r^2}{12}\right]\log\frac{D^2+s^2}{D^2} + \frac{s^4}{12r^2}\log\frac{s^2+r^2}{s^2} + \frac{r^2}{12}\log\frac{r^2+s^2}{r^2} + 2sD\tan^{-1}(s/D) - \frac{2}{3}rs\tan^{-1}(s/r) - \frac{2s^3}{3r}\tan^{-1}(r/s) - \frac{r^4}{180}\left[\frac{1}{D^2} - \frac{D^2-s^2}{(D^2+s^2)^2}\right] - \frac{r^6}{1{,}680}\times\left[\frac{1}{D^4} - \frac{(D^2-s^2)^2 - 4D^2s^2}{(D^2+s^2)^4}\right] - \frac{r^8}{7{,}560}\times\left[\frac{1}{D^6} - \frac{(D^2-s^2)^3 - 12s^2D^2(D^2-s^2)}{(D^2+s^2)^6}\right] - \ldots\Bigg\} \quad (30)$$

If r$<s$, (30) can be put in a more convenient form. Utilizing the power series for $\log(1+x)$ and $\tan^{-1}x$, we have after expanding appropriately in (30) and collecting terms

$$W(r, s) = 2r^2\Bigg\{\frac{s^2}{2}\log\frac{D^2+s^2}{s^2} - \frac{D^2}{2}\log\frac{D^2+s^2}{D^2} + 2sD\tan^{-1}(s/D) - \pi rs/3 + r^2\left[\frac{25}{75} - \frac{1}{12}\log\frac{r^2(D^2+s^2)}{s^2D^2}\right] - \frac{r^4}{180}\left[\frac{1}{D^2} - \frac{D^2-s^2}{(D^2+s^2)^2} - \frac{1}{s^2}\right] - \frac{r^6}{1{,}680}\times\left[\frac{1}{D^4} - \frac{(D^2-s^2)^2 - 4D^2s^2}{(D^2+s^2)^4} + \frac{1}{s^4}\right] - \ldots\Bigg\} \quad (31)$$

If $r<s$ and, in addition, $D>s$, we can expand (31) still further obtaining

$$W(r, s) = 2r^2s^2\Bigg\{\log\frac{D}{s} + \frac{r^2}{s^2}\times\left[\frac{25}{72} - \frac{1}{12}\log\frac{r^2(D^2+s^2)}{s^2D^2}\right] + \frac{3}{2} - \frac{\pi r}{3s} + \frac{1}{12}\frac{s^2}{D^2} - \frac{1}{60}\frac{s^4}{D^4} + \frac{1}{168}\frac{s^6}{D^6} - \ldots - \frac{1}{180}\frac{r^4}{s^4}\times\left[\frac{s^2}{D^2} - \frac{s^2D^2 - s^4}{(D^2+s^2)^2} - 1\right] - \ldots\Bigg\}$$

$$= 2r^2s^2\Bigg\{\log\frac{1}{m} + n^2\times\left[\frac{25}{72} - \frac{1}{12}\log n^2(1+m^2)\right] + \frac{3}{2} - \frac{\pi r}{3s} + \frac{m^2}{12} - \frac{m^4}{60} + \frac{m^6}{168} - \ldots - \frac{n^4}{180}\times\left[m^2 - \frac{m^2 - m^4}{(1+m^2)^2} - 1\right] - \ldots\Bigg\} \quad (32)$$

where $m=s/D$ and $n=r/s$.

If, however, $r<s$ and $s>D$, we have from (31)

$$W(r, s) = 2r^2s^2\Bigg\{\pi m + \left(\log m - \frac{3}{2}\right)m^2 - \frac{m^4}{12} + \frac{m^6}{60} - \frac{m^8}{168} + \ldots - \frac{\pi n}{3} + n^2\times\left[\frac{25}{72} - \frac{1}{12}\log n^2\left(1+\frac{1}{m^2}\right)\right] - \frac{n^4}{180}\times\left[\frac{1}{m^2} - \frac{m^2-1}{(m^2+1)^2} - 1\right] - \ldots\Bigg\} \quad (33)$$

where now $m=D/s$ and $n=r/s$.

If $r>s$, we have from (30)

$$W(r, s) = 2r^2s^2\Bigg\{\frac{1}{2}\log\frac{D^2+s^2}{r^2} - \frac{D^2}{2s^2}\log\frac{D^2+s^2}{D^2} + \frac{2D}{s}\tan^{-1}(s/D) - \frac{r^2}{12s^2}\log\frac{D^2+s^2}{D^2} - \frac{\pi s}{3r} - \frac{s^2}{6r^2}\left[\log\frac{s}{r} - \frac{25}{12}\right] + \frac{1}{180}\frac{s^4}{r^4} - \frac{1}{1{,}680}\frac{s^6}{r^6} + \ldots - \frac{1}{180}\frac{r^4}{s^2}\times\left[\frac{1}{D^2} - \frac{D^2-r^2}{(D^2+r^2)^2}\right] - \ldots\Bigg\} \quad (34)$$

If $r>s$ and, in addition, $D>r$, we have from (34)

$$W(r, s) = 2r^2s^2\Bigg\{\log\frac{D}{r} - \frac{1}{12n^2}\log(1+m^2) - \frac{n^2}{6}\log n + \frac{3}{2} - \frac{\pi n}{3} + \frac{25n^2}{72} + \frac{n^4}{180} - \frac{n^6}{1{,}680} + \ldots + \frac{m^2}{12} - \frac{m^4}{60} + \frac{m^6}{168} - \ldots - \frac{1}{180n^4}\left[m^2 - \frac{s^2(D^2-r^2)}{(D^2+r^2)^2}\right] - \ldots\Bigg\} \quad (35)$$

where $m=s/D$ and $n=s/r$.

If $r=s$, we obtain from (30)

$$W(r, s) = 2r^4\Bigg\{\frac{1}{2}\log\frac{D^2+r^2}{r^2} - \left[\frac{D^2}{2r^2} + \frac{1}{12}\right]\log\frac{D^2+r^2}{D^2} + \frac{2D}{r}\tan^{-1}(r/D) - 1.579393 - \frac{r^2}{180}\left[\frac{1}{D^2} - \frac{D^2-r^2}{(D^2+r^2)^2}\right] - \frac{r^4}{1{,}680}\left[\frac{1}{D^4} - \frac{(D^2-r^2)^2 - 4D^2r^2}{(D^2+r^2)^4}\right] - \ldots\Bigg\} \quad (36)$$

If $r=s$ and, in addition, $D>r$, we have from (36)

$$W(r, s) = 2r^4\Bigg\{0.805087 - \log m + \frac{m^4}{40} - \frac{11}{504}m^6 + \frac{13}{720}m^8 - \ldots - \frac{m^2}{180}\left[1 - \frac{1-m^2}{(1+m^2)^2}\right] - \frac{m^4}{1{,}680}\times\left[1 - \frac{(1-m^2)^2 - 4m^2}{(1+m^2)^4}\right] - \ldots\Bigg\} \quad (37)$$

where $m=r/D$.

III. Identification of the Terms of (24)

As (28) can be written in the form

$$L = 4\log(D_{14}/D_{11}) = 2W(r,s)/(wrs)^2 \quad (38)$$

where D_{14} is the geometric mean distance between C_1 and C_4, while D_{11} is the geometric mean distance of C_1 or C_4 to itself, these latter can be expressed as functions of the terms of (25). Our expressions are somewhat simplified if we introduce the new function

$$G(k_i, y) = F(k_i, y) - 2\pi y|k_i|(k_i^2 - y^2) \quad (39)$$

Comparison of $W(r, s)$ with expressions for log D_{14} and log D_{11} given elsewhere[6] reveals that

$$12r^2s^2\log D_{14} = 2G(D,s) - G(D+r,s) - G(D-r,s) - 25r^2s^2 \quad (40)$$

$$12r^2s^2\log D_{11} = -2G(r,s) + 2G(0,s) + 4\pi rs^3 - 25r^2s^2 \quad (41)$$

Similarly, from $W(R, S)$ we have

$$12R^2S^2\log D_{23} = 2G(D,S) - G(D+R,S) - G(D-R,S) - 25R^2S^2 \quad (42)$$

$$12R^2S^2\log D_{22} = -2G(R,S) + 2G(0,S) + 4\pi RS^3 - 25R^2S^2 \quad (43)$$

Like (28) written in the form of (38), we have[5] for (27)

$$L = \frac{4}{(rs-RS)^2}(r^2s^2\log D_{14} + R^2S^2\log D_{23} + 2rsRS\log D_{12} - r^2s^2\log D_{11} - R^2S^2 \times \log D_{22} - 2rsRS\log D_{13}) \quad (44)$$

Substituting (26) in (27) and comparing the resulting expression with (44), it follows that the as yet unidentified members of (26) must equal

$$-4rsRS\log D_{13} + 4rsRS\log D_{12} \quad (45)$$

Obviously, of the unidentified terms of (26), those containing D comprise the first component of (45), those not containing D comprise the second component of (45). We have, then,

$$12rsRS\log D_{13} = G(D+t, S+t) - 25rsRS\ G(D-t, S+t) - G(D+R+t, S+t) - G(D-R-t, S+t) - G(D+t, t) - G(D-t, t) + G(D+R+t, t) + G(D-R-t, t) \quad (46)$$

$$12rsRS\log D_{12} = 2G(t, S+t) - 2G(R+t, S+t) + 4\pi R(S+t)^3 - 2G(t,t) + 2G(R+t, t) - 4\pi Rt^3 - 25rsRS \quad (47)$$

where $(D-R-t) > 0$.

It is evident that (40) to (47) inclusive are of particular value: with them one can calculate the inductance or reactance of any arrangement of like solid or tubular busbars, the axes of which lie in a plane. For as detailed in most texts on transmission theory, if there are n conductors constituting a polyphase circuit, the reactance of an individual wire (for example, wire a) is given by

$$x_a = 0.2794\sum_{j=1}^{n}(I_j/I_a)\log(1/D_{ja}) \text{ ohms per mile at sixty cycles}$$

where

$$\sum_{j=1}^{n} I_j = 0$$

Or again, if n conductors constitute a single-phase circuit, the inductance is given by

$$L = \sum_{j=1}^{n}\sum_{k=1}^{n}(-2/I^2)I_jI_k\log D_{jk} \text{ abhenries per centimeter of line}$$

IV. An Illustrative Problem

As an illustration of the rapidity of convergence of the formulas developed in section III, we now calculate the reactance of a line composed of square tubular conductors. We use the dimensional data of a like problem to be found in the previously mentioned paper of Dwight and Wang,[4] and thus simultaneously determine the magnitude of the minimization in the basic formula presented therein, the same being due to neglecting the thickness of the conductors when deriving this formula, and the accuracy of the formula given for correcting for the effect of thickness. The data follow:

$r = s = 2.5$ inches; $t = 0.5$ inch; $D = 10$ inches;
$f = 60$ cycles per second;
$X = 0.0443$ ohm per thousand feet of conductor;
$L = 3.85$ abhenries per centimeter of conductor (calculated from X).

For the data given, we have from (26)

$$W/w^2 = W(2.5, 2.5) + W(1.5, 1.5) + 2W(0.5, 2) + 2W(2, 0.5) - 2W(2, 2) - 2W(0.5, 0.5) \quad (48)$$

Thus, to determine W/w^2 each of the terms of (48) must be calculated. From (37) we have for the terms taken in order:

$$W(2.5, 2.5) = 78.125(0.805087 + 1.386294 + 0.0000977 - 0.0000589) = 171.203$$

$$W(2, 2) = 32(0.805087 + 1.609438 + 0.000040 - \ldots - 0.000025) = 77.264$$

$$W(1.5, 1.5) = 10.125(0.805087 + 1.897120 + 0.000012 - \ldots - 0.000008) = 27.359$$

$$W(0.5, 0.5) = 0.125(0.805087 + 2.995732 + 0.000000 - \ldots - 0.000000) = 0.475$$

From (32) we have

$$W(0.5, 2) = 2(1.609438 + 0.035875 + 1.500000 - 0.261799 + 0.003333 - 0.000027 + \ldots + 0.000022 + \ldots) = 5.774$$

From (35) we have

$$W(2, 0.5) = 2(1.609438 - 0.003329 + 0.014441 + 1.500000 - 0.261800 + 0.021703 + 0.000022 - \ldots + 0.000283 - \ldots - 0.000026) = 5.761$$

The computation necessary to obtain each of these values of $W(x, y)$ was performed on an automatic calculating machine. As a check on both the computation and the series expansions, each value of $W(x, y)$ was then computed independently from (30). Agreement of the first five digits was interpreted as verification of the expansion and the first computations.

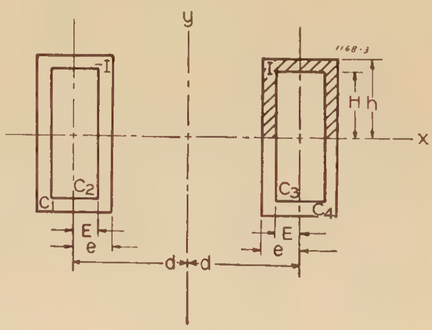

Figure 3

Substituting in (48) as indicated, we obtain

$$W/w^2 = 171.203 + 27.359 + 11.547 + 11.522 - 154.528 - 0.950 = 66.153$$

From (27) we have for the inductance

$$L = 66.153/(6.25 - 2.25)^2 = 4.135 \text{ abhenries per centimeter of conductor}$$

Multiplying L by $120\pi/10^9$ we obtain the reactance,

$$X = 496.1\pi/10^9 \text{ ohm per centimeter of conductor}$$

Converting to more suitable units, we have

$$X = 496.1\pi \times 2.54 \times 12 \times 10^3/10^9 = 0.0475 \text{ ohm per thousand feet of conductor}$$

Comparing this with the uncorrected value given by Dwight and Wang—namely, 0.0443 ohm per thousand feet of conductor, uncorrected—we find that

our value is 0.0032 ohm per thousand feet larger; or, the difference due to neglecting the thickness of the conductor is, in this case, 6.7 per cent. If the conductor were larger with correspondingly thicker walls, the per cent difference would probably be greater.

For this problem Dwight and Wang obtain from their correction formula 0.0026 ohm per thousand feet increase due to thickness. Accordingly, adding this value to the original value yields 0.0469 ohm per thousand feet of conductor. The difference is now but 0.0006 ohm per thousand feet of conductor. Accordingly, in view of this close agreement one might conjecture that in calculating the reactance of *identical, square* tubular conductors for purposes other than wherein extreme accuracy is required, that so far as time of computation is concerned the simpler formulas of Dwight and Wang can be used to the advantage of those given in this paper. If, however, the conductors are other than *both* square and identical the formulas of this paper must be used perforce.

A glance at the individual values of $W(x, y)$ will reveal the extreme rapidity with which they converge. As only three decimal places were used in calculating W/w^2 from (48), it would have been necessary to have computed only the first two terms in each of $W(2.5, 2.5)$, $W(1.5, 1.5)$, $W(2, 2)$, and $W(0.5, 0.5)$. Likewise, several terms could have been omitted in $W(2, 0.5)$ and $W(0.5, 2)$.

Appendix

I. Determination of the Integrals f_1 and f_2

We can transform f_2 as follows:

$$2 = \int_0^\infty \frac{\sin Mx_1 \sin Mx_2 \sin Mx_3 \sin Mx_4}{M^5} \times \epsilon^{\frac{-My}{2}} \sinh \frac{My}{2}\, dM$$

$$= \int_0^\infty \frac{\sin Mx_1 \sin Mx_2 \sin Mx_3 \sin Mx_4}{M^5} \times (1-\epsilon^{-My})\, dM$$

$$= \int_0^y \int_0^\infty \frac{\sin Mx_1 \sin Mx_2 \times \sin Mx_3 \sin Mx_4}{M^4} \epsilon^{-My}\, dM dy$$

Substituting the value of the infinite integral,[7] we have

$$f_2 = \int_0^y \frac{1}{3!2^3} \sum_{i=1}^{8} (-1)^p \left[(k_i^3 - 3y^2 k_i) \times \tan^{-1}\frac{k_i}{y} - (3yk_i^2 - y^3) \log (k_i^2 + y^2)^{1/2} \right] dy$$

Table I. Values of K_i for Evaluating Equation 19

x_1	x_2	x_3	x_4	k_i: $x_1 = x_2 = d$, $x_3 = x_4 = e$	k_i: $x_1 = x_2 = d$, $x_3 = e$; $x_4 = E$
+	+	+	+	$2d+2e$	$2d+e+E$
+	+	−	−	$2d-2e$	$2d-e-E$
+	+	+	−	$2d$	$2d+e-E$
+	+	−	+	$2d$	$2d-e+E$
+	−	+	+	$2e$	$e+E$
+	−	−	−	$-2e$	$-(e+E)$
+	−	+	−	0	$e-E$
+	−	−	+	0	$-(e-E)$

k_i designating any one of the eight possible terms formed from the member $(x_1 \pm x_2 \pm x_3 \pm x_4)$ by arbitrary selection of the plus and minus signs, while p is the number of minus signs in k_i. Integrating and collecting terms, we obtain

$$f_2 = \frac{1}{4!2^3} \sum_{i=1}^{8} (-1)^p \left[(k_i^4 - 6yk_i^2 + y^4) \times \log (k_i^2 + y^2)^{1/2} + 4yk_i(k_i^2 - y^2) \tan^{-1}\frac{k_i}{y} - k_i^4 \log |k_i| \right]$$

$$= \frac{1}{192} \sum_{i=1}^{8} (-1)^p F(k_i, y)$$

where $F(k_i, y)$ stands for the expression within the brackets.

Noting that

$$f_1 = \int_0^\infty \frac{\sin Mx_1 \sin Mx_2 \sin Mx_3 \sin Mx_4}{M^4} dM$$

$$= \lim_{y \to 0+} \int_0^\infty \epsilon^{-My} \times \frac{\sin Mx_1 \sin Mx_2 \sin Mx_3 \sin Mx_4}{M^4} dM$$

we obtain on substituting for the infinite integral

$$f_1 = \lim_{y \to 0+} \frac{1}{3!2^3} \sum_{i=1}^{8} (-1)^p \left[(k_i^3 - 3y^2 k_i) \times \tan^{-1}\frac{k_i}{y} - (3yk_i^2 - y^3) \log (k_i^2 + y^2)^{1/2} \right]$$

$$= \frac{1}{3!2^3} \sum_{i=1}^{8} (-1)^p \frac{\pi}{2} |k_i^3|$$

II. Expansion of W(r, s) in a Power Series

By definition

$$W(r, s) = {}^1/_6[2F(D, s) - F(D+r, s) - F(D-r, s) + 2F(r, s) - 2F(0, s) + 4\pi r^2 s(3D - r)]$$

Now

$$K(x, s) = 2F(D, s) - F(D+r, s) - F(D-r, s)$$

considered as a function of x alone, can be expanded in a power series about the point $x = D$. Accordingly, by Taylor's theorem we have

$$K(x, s) = -r^2 \frac{\partial^2 (FD, s)}{\partial D^2} - \frac{r^4}{2 \cdot 3!} \frac{\partial^4 F(D, s)}{\partial D^4} - \frac{r^6}{3 \cdot 5!} \frac{\partial^6 F(D, s)}{\partial D^6} - \ldots$$

where

$$F(D, s) = {}^1/_2(D^4 - 6D^2s^2 + s^4) \log (D^2+s^2) - D^4 \log D + 4(sD^3 - Ds^3) \tan^{-1}\frac{D}{s}$$

$$\frac{\partial F(D, s)}{\partial D} = (2D^3 - 6D^2s^2) \log (D^2+s^2) - 4D^3 \times \log D + 4(sD^2 - s^3) \tan^{-1}\frac{D}{s} - 3Ds^2$$

$$\frac{\partial^2 F(D, s)}{\partial D^2} = 6(D^2 - s^2) \log (D^2+s^2) - 12D^2 \times \log D + 24Ds \tan^{-1}\frac{D}{s} - 7s^2$$

$$\frac{\partial^3 F(D, s)}{\partial D^3} = 12D \log (D^2+s^2) - 24D \log D + 24s \tan^{-1}\frac{D}{s}$$

$$\frac{\partial^4 F(D, s)}{\partial D^4} = 12 \log (D^2+s^2) - 24 \log D$$

$$\frac{\partial^5 F(D, s)}{\partial D^5} = -\frac{24s^2}{D(D^2+s^2)}$$

$$\frac{\partial^6 F(D, s)}{\partial D^6} = 24\left[\frac{1}{D^2} - \frac{D^2 - s^2}{(D^2+s^2)^2}\right]$$

$$\frac{\partial^7 F(D, s)}{\partial D^7} = 48\left[-\frac{1}{D^3} - \frac{-D^3 + 3Ds^2}{(D^2+s^2)^3}\right]$$

$$\frac{\partial^8 F(D, s)}{\partial D^8} = 144\left[\frac{1}{D^4} - \frac{(D^2 - s^2)^2 - 4s^2D^2}{(D^2+s^2)^4}\right]$$

$$\frac{\partial^9 F(D, s)}{\partial D^9} = 576\left[-\frac{1}{D^5} - \frac{-D^5 + 10D^3s^2 - 5Ds^4}{(D^2+s^2)^5}\right]$$

$$\frac{\partial^{10} F(D, s)}{\partial D^{10}} = 2{,}880\left[\frac{1}{D^6} - \frac{(D^2 - s^2)^3 - 12s^2D^2(D^2 - s^2)}{(D^2+s^2)^6}\right]$$

References

1. Reactance of Strap Conductors, **H. B. Dwight.** *Electric Review,* volume 70, 1917, pages 1087–8.

2. Reactance Values for Rectangular Conductors, **H. B. Dwight.** *Electric Journal,* volume 16, 1919, pages 255–6.

3. Champ Magnétique et Inductance d'un Système des Barres Rectangulaires Parallèles, **E. Roth.** *Revue Générale de l'Electricité,* volume 41, 1938, pages 275–83.

4. Reactance of Square Tubular Busbars, **H. B. Dwight and T. K. Wang.** AIEE Transactions, volume 57, 1938, pages 762–5.

5. Inductance of Hollow Rectangular Conductors, **T. J. Higgins.** *Journal* of the Franklin Institute, volume 230, 1940, pages 375–80.

6. On the Geometrical Mean Distances of Rectangular Areas and the Calculation of Self-Inductance, **E. Rosa.** *Bulletin* of the Bureau of Standards, volume 3, 1907, pages 1–41.

7. Nouvelles Tables d'Intégrales Définies (a book), **D. Bierens de Haan.** Leyden, 1867. Table 173, number 20, and table 371, number 5.

1921

TIME *Marches On*

In 1921, NORMA-HOFFMANN introduced the Cup Mounting—the forerunner of all self-protected ball bearings. From this, through progressive stages (as shown above) has evolved the NORMA-HOFFMANN "CARTRIDGE" BALL BEARING—an ultra-modern type embodying 30 years of PRECISION BEARING manufacture and offering to industry the following distinctive advantages:

SIMPLER AND MORE ECONOMICAL MACHINE DESIGN, due to elimination of many costly mounting parts and machining operations, otherwise required; EASIER AND FASTER MACHINE ASSEMBLY AND DISASSEMBLY, since the "CARTRIDGE" BEARING is an integrally sealed unit needing no complementary mounting parts; 100% GREATER GREASE CAPACITY, due to double-row width creating a greatly enlarged grease reservoir; COMPLETE AND LASTING EXCLUSION OF DIRT AND FOREIGN MATTER by the use of tightly fitting, wearless, all-metal seals; SEALED FOR ANY POSITION, since the seals retain the lubricant regardless of shaft angle; EASY REGREASING AND INSPECTION WITHOUT DISMOUNTING, by means of refilling plug and removable seals.

Write for the Catalog. Submit your bearing problems for study and recommendation, without obligation. NORMA-HOFFMANN sales and service engineers, and distributors in principal cities stocking "CARTRIDGE" BEARINGS, are at your service.

"NORMA-HOFFMANN"

CARTRIDGE

BALL BEARING

PRECISION BALL, ROLLER and THRUST BEARINGS

NORMA-HOFFMANN BEARINGS CORP'N., STAMFORD, CONN., U.S.A. • FOUNDED 1911

ELECTRICAL ENGINEERING. Published monthly by the American Institute of Electrical Engineers; publication office 20th & Northampton Streets, Easton, Pa. Editorial and advertising offices, 33 West 39th Street, New York, N. Y. Subscription $12 per year to United States, Mexico, Cuba, Porto Rico, Hawaii, Philippine Islands, Central and South America, Haiti, Spain and Spanish colonies; $13 to Canada; $14 elsewhere; single copy $1.50. Entered as second-class matter at the Post Office, Easton, Pa., under the Act of Congress of March 3, 1879. Accepted for mailing at special postage rates provided for in Section 538, P.L. & R. Act of February 28, 1925. December 1941, Vol. No. 12 Number of copies this issue 25,000.

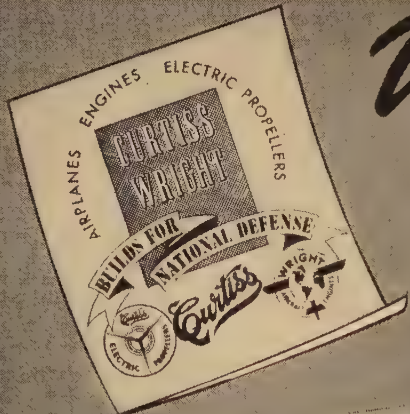

Wright Aeronautical USES IRVINGTON WIRE MARKERS

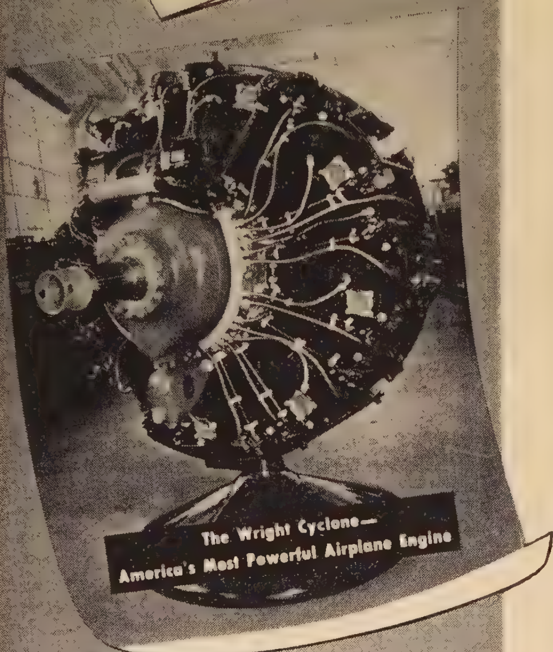
The Wright Cyclone—America's Most Powerful Airplane Engine

"more than 2000 horsepower"—18 cylinders. It's the world's most powerful air-cooled aircraft engine. Developed by Wright Aeronautical Corporation with the aid of the U. S. Army Air Corps. Among others provides power for the 52-passenger Consolidated Flying Boat, the 82-ton Douglas Bomber, the world's largest airplane; the Pan-American Clippers, TWA Stratoliners, and the U. S. A. "Flying Fortresses."

Irvington New Improved Wire Markers are used on these engines and other engines made by Wright Aeronautical for identifying the ignition wires.

Irvington Wire Markers for aircraft engine ignition systems, machine tools and many other applications where a number of terminal wires must be marked are made of lengths of insulation tubing, varnished impregnated inside-and-out for quick assembly. Suitable identification is printed with a special formulated ink.

Eliminates use of metal identification tags with the danger of short circuits in confined areas or die stamping the terminals.

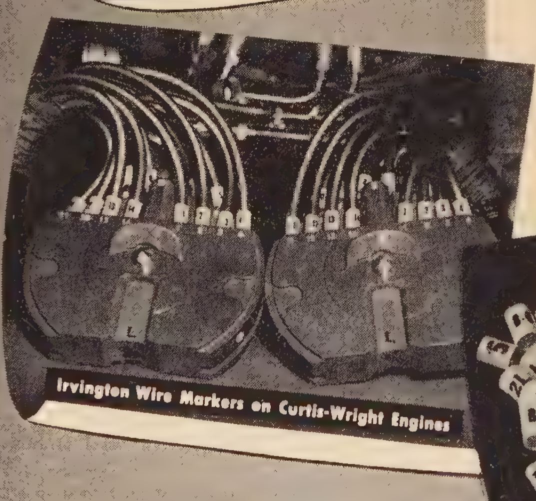
Irvington Wire Markers on Curtis-Wright Engines

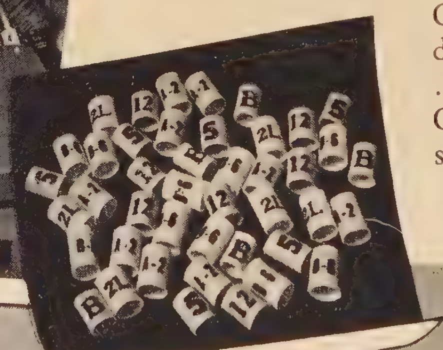

Comes in 2 standard lengths—2 diameters (nominal ID .263 or .294) and 2 lengths of symbols. Other sizes can be furnished on special order.

Write Dept. 36

IRVINGTON WIRE MARKERS MEET ALL AVIATION STANDARDS

Irvington VARNISH & INSULATOR CO.

IRVINGTON, NEW JERSEY, U. S. A.

STANDARD OF THE WORLD — IRVINGTON INSULATION — TRADE MARK REG. U. S. PAT. OFF.

PLANTS AT IRVINGTON, N. J. and HAMILTON, ONT., CAN.
Representatives in 20 Principal Cities

THE Standards of the American Institute of Electrical Engineers now comprise forty-five sections on electrical machinery and apparatus. They are chiefly devoted to defining terms, conditions, and limits which characterize behavior, with special reference to acceptance tests, and many of them are recognized officially as American Standards.

The Standards available are listed below, together with prices. A discount of 50%, on single copies only, is allowed to Institute members (except on Nos. C57.1, 2, 3, and C37.4). Such discount is not applicable on extra copies unless ordered for other members. Numbers of the Standards sections should be given when ordering. A binder (illustrated above) for standards is available with durable, stiff covers, resembling leather, lettered in gold. Price, $1.75 net.

AIEE STANDARDS

(Figures in Parentheses Give Dates of Latest Editions)

No.		
1	General Principles Upon Which Temperature Limits Are Based in the Rating of Electrical Machinery (6-40)	$ 0.40
1A	Principles for Rating for Short-Time, Intermittent or Varying Duty (9-41) (Proposed supplement to No. 1. No charge.)	
4	Measurement of Test Voltage in Dielectric Tests (6-40)	.40
*C50	Rotating Electrical Machinery, (Supersedes Nos. 5, 7, 8, 9, and 10) (4-36)	1.30
**11	Railway Motors (3-37)	.50
C57.1	Transformers, Regulators and Reactors (1940)	
C57.2	Test Code for Transformers, Regulators and Reactors (1940)	
C57.3	Guides for Operation of Transformers (1940) (C57.1, C57.2, C57.3, published as one booklet supersede A.I.E.E. Nos. 12, 13, 14, 100 and Test Code for Transformers. The member discount does not apply on price of this publication which is 75 cents net.)	.75
*15	Industrial Control Apparatus (5-28)	.40
*16	Electric Railway Control Apparatus (1-33)	.40
*17f	Mathematical Symbols (2-28)	.30
*17g1	Letter Symbols for Electrical Quantities (11-28)	.20
17g1A	Letter Symbols for Electric and Magnetic Quantities (3-40) (Proposed revision of No. 17g1. No charge.)	
**17g2	Graphical Symbols for Electric Power and Wiring (1-34)	.20
**17g3	Graphical Symbols for Radio (1-34)	.20
**17g5	Graphical Symbols for Electric Traction Including Railway Signaling (1-34)	.40
*18	Capacitors (6-34)	.20
19	Oil Circuit Breakers (4-38)	.40
C37.4	A-C Power Circuit Breakers (1-41) (A proposed revision of No. 19. The member discount does not apply on price of this publication which is 60 cents net.)	.60
20	Air Circuit Breakers (5-30)	.30
22	Air Switches and Bus Supports (6-40)	.40
*C37.1(23)	Relays Associated with Power Switchgear (1937)	.40
*C37.2(26)	Automatic Stations (1937)	.40
27	Switchboards and Switching Equipment for Power and Light (10-30)	.30
27A	Switchgear Assemblies (3-41) (A proposed revision of No. 27. No charge.)	
*28	Lightning Arresters (3-36)	.30
29	Wet Tests (11-41)	.40
*30	Wires and Cables (4-37)	.40
*C39.1(33)	Electrical Indicating Instruments (7-38)	.40
*36	Storage Batteries (2-28)	.20
*38	Electric Arc Welding Apparatus (1-34)	.40
*39	Resistance Welding Apparatus (1-34)	.30
*41	Insulator Tests (3-30)	.30
41A	Insulator Tests (3-41) (A proposed revision of No. 41. No charge.)	
45	Recommended Practice for Electrical Installations on Shipboard (7-40)	1.50
*46	Hard Drawn Aluminum Conductors (6-27)	.20
*C8.5	Specifications for Cotton-Covered Round Copper Magnet Wire. (See C8.7 for price.)	
*C8.6	Specifications for Silk-Covered Round Copper Magnet Wire. (See C8.7 for price.)	
*C8.7	Specifications for Enameled Round Copper Magnet Wire (1936) (C8.5, 8.6 and 8.7 published as one pamphlet.)	.30
**C8.11	Code Rubber Insulation for Wire and Cable for General Purposes (1936)	.20
**C8.12	Cotton Braid for Insulated Wire and Cable for General Purposes (1935)	.20
**C8.16	Tree Wire Coverings (1936)	.20
**C8.17	Class AO 30 Per Cent Rubber Insulation for Wire and Cable for General Purposes (1936)	.20
**C8.18	Weather-Resistant Wire and Cable URC Type (1936)	.20
*C8.19	Weather-Resistant Saturants and Finishes for Aerial Rubber-Insulated Wire and Cable (1939)	.20
*C8.20	Heavy-Walled Enameled Round Copper Magnet Wire (1939)	.20
500	Test Code for Polyphase Induction Machines (8-37)	.50
501	Test Code for D-C Machines (7-41)	.50
520	Test Code for Apparatus Noise Measurement (3-39)	.30
	Total Cost of Complete Set	$15.85

* *Approved as American Standard*

** *Approved as American Tentative Standard*

SECTIONS IN PREPARATION

Seven such sections are now available in report form for purpose of criticism, and copies will be sent without charge upon request. These sections are as follows:

- No. 6 Metal-Tank Mercury-Arc Rectifiers, Acceptance Test for (6–34)
- 21 Apparatus Bushings (3–41) (Including Test Code)
- 24 Protector Tubes (7–40)
- 25 Fuses Above 600 Volts. (7–41)
- 40 Electrical Recording Instruments. (6–33)
- 502 Test Code for Single-Phase Motors. (11–41)
- — Test Code for Synchronous Machines. (1–37)

American Institute of Electrical Engineers 33 West 39th Street New York

How "GF" (GAS FILLED)

New Self-supervising Cabl

MADE GOO

On First Test in Big City

AT the bottom of an excavation in downtown Manhattan*, Type GF cable met and passed its first test with ease. A workman with an air drill accidentally gouged into both the conduit and the sheath of a line of this new cable. Not being a cable engineer, the workman didn't report the accident at once. He didn't realize that such a puncture, sooner or later, means "lights out" not only for equipment on the circuit but also for the cable itself.

Because the cable was of the new G-E gas-filled type, this incident had a happy ending. In less than half an hour after the cable was punctured, up drove the power-company service men—without having been summoned by the workman. Repairs took little time because the break was *known in time*, and more serious damage was avoided.

The service truck had been called by the cable itself. When the sheath was punctured, reduction of pressure, caused by loss of gas, operated a pressure relay. This in turn sounded an alarm in the control room at the generating station.

A total of more than 140,000 feet of Type GF cable is in service. Do you have our booklet describing this cable? The number is GEA-3652. Ask the nearest G-E office for a copy. General Electric Company, Schenectady, N. Y.

**System of the Consolidated Edison Co. of New York, Inc.*

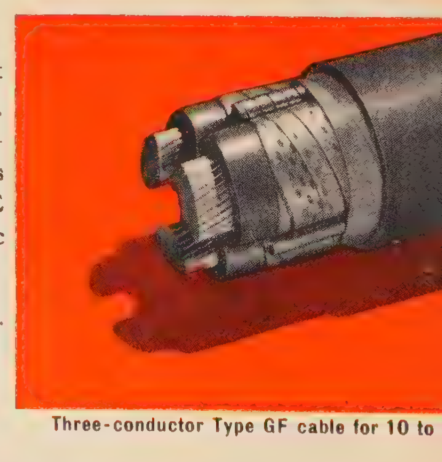

Three-conductor Type GF cable for 10 to

GENERAL ELECTRIC

501-7-1200

ANNOUNCING A NEW OUTDOOR POTENTIAL TRANSFORMER . . . .

The JE-3

TYPE JE-3

For outdoor metering applications
2300 volts and below

INSULATION

230, 460, and 575 volts—full-wave, 50 kv;
2300 volts—full-wave, 60 kv

ACCURACY

¼W, ¼X, ½Y

NOW, G. E. OFFERS... A complete line of outdoor current and potential transformers, 15 kv and below, which conform to ASA insulation standards

These new standards, which are met by this now complete line of transformers, provide a means whereby all apparatus on a line can be co-ordinated to have the same insulation strength. This facilitates the selection of adequate protective equipment.

All these transformers meet or exceed the highest accuracy standards and can be obtained in a wide variety of mechanical constructions to meet every installation need.

Ask your G-E office for a copy of our new bulletin, GEA-3650, which covers both outdoor current and potential transformers, 15 kv and below. Or write General Electric, Schenectady, N. Y.

GENERAL ELECTRIC

604-6-6400

Dies Is Preserved By Vapocarb-Hump Hardening

Manufacturers who have intricate cutting tools, dies, etc., to harden and temper, may be interested in the heat-treating practice of several makers of eyeglasses and spectacles.

Quenching an eyeglass-frame die, immediately after removing it from the Vapocarb-Hump Furnace which is standing open at right.

These plants use, in their heat-treating departments, the Vapocarb-Hump Method of hardening, the Homo Method of tempering and a pump-agitated quench tank. This equipment enables the heat-treater to make the best possible use of his skill, in the following ways: He can prevent the high heat of hardening from forming scale on the tools and thus spoiling the engraved lines; he can prevent soft areas from forming and thus shortening the life of the tool; he can be sure that each tool is heated to the exactly correct degree for longest life and greatest production. And, after giving the tool the exact degree of hardness he wishes, the heat-treater can "draw" as much or as little hardness out as his experience tells him is necessary to toughen the tool for its job.

In these ways the heat-treating department makes each tool do its best; reduces the total number required; may exert real influence on increasing the plant's production.

The Vapocarb-Hump and Homo Methods are described in Catalogs T-621 and T-625, sent on request.

Recorder For Furnace Current

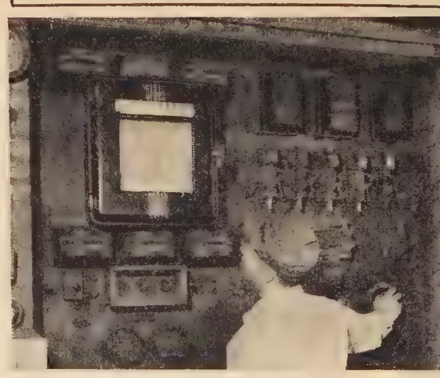

To help in operating big inductance-type and arc-type electric furnaces, several companies have added Micromax load recorders to the control panel. Note ease with which operator can see details of load record.

The recorder is almost identical with a thermocouple instrument, but requires even less maintenance. If interested, write for Catalog N-58-161.

"STRAIGHT-EDGE" CHARTS Are Hard To Get From MICROMAX Pyrometers

If you want pyrometer records to look as if they were drawn with a straight-edge, you may have trouble getting them from Micromax Controlling Pyrometers. For these instruments are "micro-responsive" in recording as well as in controlling—they not only *correct* the tiny temperature changes, but they *record* them. They put down the complete situation honestly and accurately, for the information of all concerned.

But, just as you'll find the tiny changes—the "wiggles"—shown in abundance, so you'll find practically no big changes in the record of any well-made, well-run furnace. And the reason, again, is the responsiveness of the Controller. The responsiveness which enables the instrument to correct the weaker upsets also makes it go after the stronger ones with correspondingly greater energy, and stop them before they become big enough to do more than jog the Controller. Temperature is thus held with the *steadiness* vital to uniform quality of product.

For further information about Micromax Control, write for literature.

Jrl Ad ENT-0600C(28)

LEEDS & NORTHRUP COMPANY, 4962 STENTON AVE., PHILA., PA.

LEEDS & NORTHRUP

MEASURING INSTRUMENTS · TELEMETERS · AUTOMATIC CONTROLS · HEAT-TREATING FURNACES


KERITE

Trade Literature

[Mailed to readers free—unless otherwise noted—upon request to companies named]

Insulator Tools.—Bulletin. Describes a live line tool set for safely changing to clamp top insulators without interrupting service. A. B. Chance Co., Centralia, Mo.

Motors.—Bulletin B6052-B, 8 pp. Describes the complete line of "Lo-Maintenance" motors in ratings from $^3/_4$ to 75 hp; open, enclosed and splashproof types; a-c and d-c. Allis-Chalmers Mfg. Co., Milwaukee, Wis.

Control Products Index.—Bulletin 585. A condensed-index covering air-operated and electrically-operated automatic control instruments, recording and indicating instruments; telemetering instruments for recording and remote automatic control, and engineering services. The Bristol Co., Waterbury, Conn.

Small Motors.—Folder F-8623, 8 pp. Describes small motors from $^1/_6$ to $^1/_2$ horsepower, 145 frame size, for general use. The standard parts making available more than 5,000 combinations of type, rating, and mounting are illustrated. Charts show motor characteristics plotting per cent synchronous speed against per cent full-load torque. Westinghouse Electric & Mfg. Co., East Pittsburgh, Pa.

Lamp Resistor.—Bulletin 26. Describes resistor, type K-40878, for use with six watt T-5 fluorescent lamps, on either alternating or direct current with a manual momentary contact starting switch. When operating the lamps on 120-volt circuits these resistors eliminate the need of an auxiliary. The resistor unit can be mounted in any standard fixture or wiring trough, and is insulated for 15,000 volts to ground. Ward Leonard Electric Co., Mount Vernon, N. Y.

Industrial Control Equipment.—Catalog 8301, 56 pp. Describes and illustrates 44 industrial controls and safeguards such as temperature controllers, pressure controllers, humidity controllers, float switches, combustion safeguards, etc. Complete specifications and informative details are given for all types. The first few pages contain a primer of automatic control. The three classes of such control,—electric, pneumatic and combined electric and pneumatic are fully covered. The Brown Instrument Co., Wayne & Roberts Aves., Philadelphia, Pa.

Fuse Links.—Bulletin 104, 8 pp. Describes series 100-E and 50-E universal fuse links, designed to comply with new NEMA standards. Other fuse links for cutouts are also covered. Contains considerable technical information and includes transformer fusing chart and fuse coordination table with directions for use. W. N. Matthews Corp., 3700 Forest Park Blvd., St. Louis.

Transformers.—Bulletin GEA-3650, 16 pp. Describes a complete line of outdoor type current and potential transformers of 15 kv and below. The bulletin is conveniently made up with accordion-fold pages, which allow insulation characteristics, accuracy classifications, ratings, and prices of the various units to be seen at a glance by spreading the contents out flat. General Electric Co., Schenectady, N. Y.

Analyzing Plate Solutions.—Booklet 48 pp. Gives simple and practical methods of analyzing many electroplating solutions, which may be followed by those without extensive chemical training. Contains reference tables and electrochemical data pertaining to the important metals. Methods of determining thickness of deposits at various times are described. Hanson-Van Winkle-Munning Co., Matawan, N. J.

Lubrication Manual.—Catalog 172 pp. This comprehensive publication is described as practically an engineering manual on the subject of lubrication for design engineers, and covers a complete line of devices for the application of fluid lubricants. Special sections are devoted to wick feed oiling, constant level oiling and multiple oiling; complete presentations are included on oil seals, oil cups, oil hole covers, gauges and sight gravity oilers. The catalog contains over a thousand illustrations. Requests for the publication should be addressed on business stationery to Gits Bros. Mfg. Co., 1846 S. Kilbourn Ave., Chicago, Ill.

CLASSIFIED ADVERTISEMENTS

RATES: Sixty cents per line; minimum charge based on use of five lines; maximum space not to exceed thirty-five lines. Copy is due the 15th of the month preceding publication date.

New Products

Rectifier Voltage Regulator.—The Benwood Linze Co., St. Louis, Mo., has developed a competitively priced voltage regulator, to be used in conjunction with its line of standard metallic rectifier electroplating units. The B-L voltage regulator, manually operated, is especially designed to provide a convenient and simple means for adjusting the voltage output of each individual or bank of rectifiers. The unit is available in a wall mounting cabinet so it may be installed adjacent to the plating tank within convenient reach of the operator and away from the rectifier units. The voltage regulator has 64 steps of adjustment, giving a voltage range from maximum down to one volt. The coarse control covers the full range in eight steps while the fine control provides eight steps for each step of the coarse control. In addition, the regulator provides a start-stop station permitting

remote control for starting and stopping the rectifier, thereby giving the operator complete control of each tank. One voltmeter and one ammeter record current and voltage of each individual rectifier. By this method of control, all the convenience of an individual tank rheostat is obtained, but the rheostat losses of bus bar control are eliminated. The elimination of no-load losses is possible because the operator can shut down the rectifier whenever a tank is not in use.

Decimal Equivalent Wall Chart.—A new large decimal equivalent chart, 26 by 39 inches, printed in black and red, brings all the equivalents from $^1/_{64}$ to $^{63}/_{64}$ inches within easy reading of the eye even at a distance of 50 feet. Copies will be mailed to interested readers upon request to The Frederick Post Co., 3650 N. Avondale Ave., Chicago, Ill.

Ohm's Law Calculator.—A unique, new, convenient Ohm's Law Calculator introduced by the Ohmite Manufacturing Company, gives the answer to any Ohm's Law problem quickly, with one setting of the slide. All values are direct reading. It

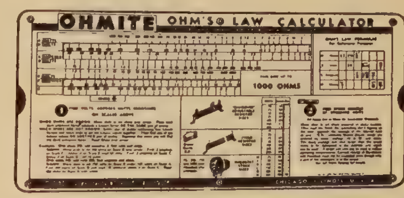

does not require any knowledge of a slide rule to operate. The Calculator has scales on both sides so as to cover the range of currents, resistances, wattages and voltages commonly used in the industrial, electronic, and radio fields. It covers the current and wattage range for motors, generators, lamps, other electrical apparatus and miscellaneous applications up to 100 amperes or 1,000 watts; also the low current high resistance radio, sound and electronic applications. The Calculator has a convenient Stock Unit Selector, listing hundreds of stock values, immediately available in Dividohms, fixed resistors (including Ohmite Brown Devils) and rheostats. A setting of the slide shows the stock number of the resistor or rheostat needed. Simple instructions appear on the Calculator. Multiplication, division, the finding of squares and square roots can also be performed on the Calculator. The Ohmite Ohm's Law Calculator is available to engineers, laboratory men, production managers, maintenance men, purchasing agents, etc. Request should be made on company letterhead, enclosing 10 cents to cover handling costs. Address the Ohmite Manufacturing Co., 4801 Flournoy St., Chicago, Ill.

"Nutshell" Soldering Kit.—A new, small, self-contained soldering unit that contains the correct amount of 50–50 solder and flux, sealed within a waterproof heat-generating outer shell, known as "Jiggers", has been introduced by Jiggers, Inc., of Chicago. To obtain a strong, perfectly soldered electrical connection, it is only necessary to push the wire splice into a Jigger and touch a lighted match to it as illustrated. The Jigger shell ignites and produces the proper temperature to flow the solder into the splice. The burnt shell is then dropped off and a smooth, perfectly soldered splice results. To demonstrate how practical, simple and easy "Jiggers" make the soldering job, free samples are offered. Address Jiggers, Inc., 215 W. Illinois St., Chicago, Ill.

(Continued on p. 18)

New Products

(Continued from p. 16

Decade Inductance.—A new type decade inductance, developed by the New York Transformer Co., 480 Lexington Ave., New York City, is available in decades from .001 henries per step to 10 henries. It has a Q of

approximately 25 with a useful range of 50 to 20,000 cycles per second. The accuracy is plus or minus 5 per cent, with an operating level up to 30db. These instruments may be had in either 2 or 3 decades in any of the inductance ranges desired. It is said to be in every respect a precision laboratory unit and a dependable aid in setting up experimental filters, equalizers, tuned amplifiers, phasing networks, etc.

Welding Terminal Panel.—Developed especially for use in shipyards and similar installations in connection with the constant potential system of welding feeders, by the O.Z. Electrical Mfg. Co., Brooklyn, N. Y., a new welding terminal panel provides opportunities to install at any desired points, panels that intercept the main welding feeders throughout the yard, with facilities for the welding leads. The panels (1) are a solid bronze casting mounted on an ebony asbestos block (2) which in turn is mounted in No. 10 gauge bent-up construction iron box (3), completely hot dipped galvanized after fabrication. The box top is slanted to shed water. Slots (4) in the bottom of the box provide entry for welding leads which are to be attached to terminal studs (5) on the panel. These stud bolts are force-fitted through the back of the casting. The removable plates (6) or clamps provide means for tapping the main feeder. Simple modification readily adapts the O.Z. Welding Terminal Panel to existing conditions on any given job, according to the manufacturer, who reports that an important installation has been made for defense work in one of the leading shipyards of the country and that other yards have shown active interest.

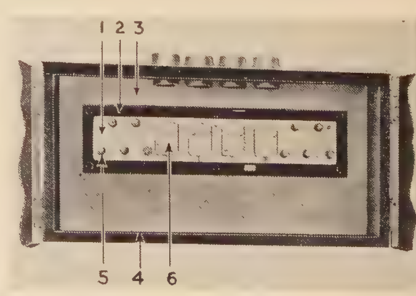

ELDORADO MAGIC!

Next to the man himself, the pencil plays the biggest part in creating drawings from which clear blueprints come. If there is magic in this, call it "Eldorado" magic.

The drawing forecasts the blueprint, as in some magic crystal!

Great drawing pencils come in 17 degrees of hardness of lead,—so does *Typhonite* "Eldorado." But no other drawing pencil has *Typhonite* leads. *Typhonite* is created in a literal whirlwind from natural graphite. There is no stopping the whirlwind and there is no stopping Dixon *Typhonite* "Eldorado" as it whirls along far in the lead.

TYPHONITE

ELDORADO PENCIL SALES DEPARTMENT 42-J12 • JOSEPH DIXON CRUCIBLE CO. • JERSEY CITY, N. J.

NEW DEVELOPMENTS IN AIEE STANDARDS

•

Proposed Test Code for Single-Phase Motors

A "Proposed Test Code for Single-Phase Motors," No. 502 has just been made available for a trial period for purposes of suggestion and criticism. This code has been prepared under the auspices of a subcommittee of the AIEE Committee on Electrical Machinery. The purpose of this code is to define acceptable methods of making tests to determine that the performance and other characteristics of single-phase machines comply with those guaranteed.

The following tests are covered: Resistance measurements, electrical input measurements, speed measurements, locked-rotor tests, torque measurements, efficiency tests, temperature tests, insulation tests, noise and vibration tests. There is no charge for copies of this pamphlet.

•

Standard for Wet Tests

A new AIEE "Standard for Wet Tests," No. 29 is now available in pamphlet form. This standard was developed by a special subcommittee under R. T. Henry, of AIEE Standards Coordinating Committee No. 3. The purpose of this standard is to establish a general standard method for use in making high-potential wet tests on insulators, bushings, switches and related apparatus. Only the requirements for spray and correction factors are covered. Requirements for mounting and method of voltage application for particular equipment are covered by particular apparatus standards. Cost 40 cents per pamphlet, with the usual 50 per cent discount to members on single copies.

Address: Order Dept.

AMERICAN INSTITUTE OF ELECTRICAL ENGINEERS
33 WEST 39TH STREET NEW YORK, N. Y.

TONG TEST A.C. D.C. AMMETERS

Help Keep Production Moving

Hundreds of plants, today, using TONG TEST Ammeters look upon them as one of their most important pieces of equipment. This is so because TONG TEST is the only clamp-type ammeter capable of measuring both A.C. and D.C. instantly, accurately, safely and without interrupting operations.

Guard against breakdowns, burned-out motors and transformers caused by current overloads, by measuring current with a TONG TEST. It is light in weight ($2^3/_4$ lbs.), precision built, measures 0–800 amperes and will pay for itself in the time it saves and the trouble it helps to avoid.

Send for a copy of the TONG TEST bulletin which tells the complete story.

COLUMBIA ELECTRIC MFG. CO.
4525 Hamilton Ave. Cleveland, Ohio

TONG TEST AMMETERS

THE COMPLETE TRANSFORMER LINE

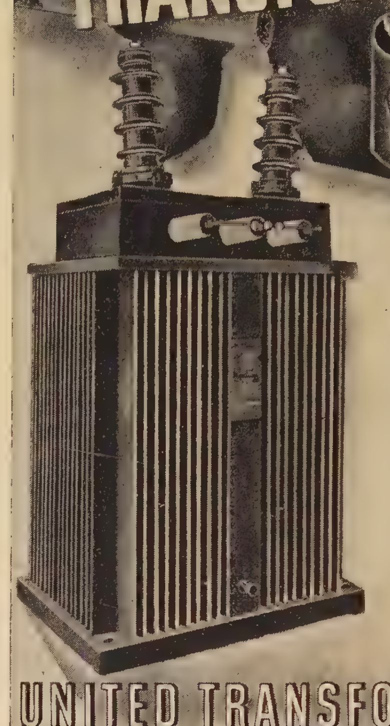

UNITS FROM 1/3 OUNCE TO 20 TONS

- Varitran voltage adjusters
- Automatic line voltage regulators
- Audio transformers
- Audio equalizers and filters
- Rectifiers and battery chargers
- Plate transformers
- Phase changers—booster transformers
- Instrument transformers

UNITED TRANSFORMER CORP.
150 VARICK STREET ★ NEW YORK, N. Y.
EXPORT DIVISION 100 VARICK STREET NEW YORK N Y CABLES ARLAB

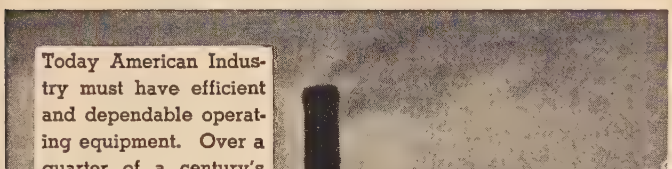

Today American Industry must have efficient and dependable operating equipment. Over a quarter of a century's experience in the manufacture of Oil Immersed Motor Control equipment is your assurance of dependability in Rowan products.

ROWAN CONTROL
THE ROWAN CONTROLLER CO., BALTIMORE, MD.

Science Abstracts

All electrical engineers actively engaged in the practice of their profession should subscribe to "Science Abstracts."

Published monthly by the Institution of Electrical Engineers, London, in association with the Physical Society of London, and with the cooperation of the American Institute of Electrical Engineers, the American Physical Society and the American Electrochemical Society, they constitute an invaluable reference library.

Through "Science Abstracts" engineers are enabled to keep in touch with engineering progress throughout the world, as one hundred and sixty publications, in various languages, are regularly searched and abstracted. "Science Abstracts" are published in two sections, as follows:

"A"—PHYSICS—deals with electricity, magnetism, light, heat, sound, astronomy, chemical physics.

"B"—ELECTRICAL ENGINEERING—deals with electrical plant, power transmission, traction, lighting, telegraphy, telephony, wireless telegraphy, prime movers, engineering materials, electrochemistry.

Through special arrangement, members of the A.I.E.E. may subscribe to "Science Abstracts" at the reduced rate of $5.00 for each section, and $10.00 for both. Rates to non-members are $9.00 for each section and $15.00 for both. Subscriptions should start with the January issue. The first volume was issued in 1898. Back numbers are available, and further information regarding these can be obtained upon application to P. F. Rowell, Secy., I.E.E., Savoy Place. Victoria Embankment, London, W. C. 2, England.

American Institute of Electrical Engineers
33 West 39th Street, New York

Employment Bulletin

Engineering Societies Personnel Service, Inc.

MAINTAINED for their members by the national societies of civil, mining, mechanical, and electrical engineers, in co-operation with other organizations. An inquiry to any of the four offices will bring full information.

A weekly bulletin of engineering positions open is available to members of the co-operating societies at a subscription of $3 per quarter or $10 per annum, payable in advance.

In the interest of effective service, it is essential that members using the employment service keep the bureau office serving them advised at reasonable intervals concerning their availability for employment, concerning any change in status, and immediately upon acceptance of any employment.

Employers interested in the following announcements should address replies to the key numbers indicated, and mail to the New York office.

Men Available

GRAD E.E., License; 29, family; 7 yrs experience in des, devpmt, testg, of motor generator sets, transfs, and accessories. Employed. Desires pos in elec des, devpmt, testg. E-925.

ELEC ENG; 42; wide exper constr, des, oprn, valuation, industrial plants, util, public works, now employed supervision elec work Federal project major magnitude, desires return private industry. Highest references, qualifications. E-926.

ELEC AND MECH ENGR, product devpmt type. 10 yrs Chief Engr elec mfg companies. Numerous patents. Broad exper des, devpmt, tooling and control of manufacture of elec and metal products. E-927.

TRANSM ENGR, university grad; 48, single; 16 yrs in transm des, elec and structural; 6 yrs valuation. Location, anywhere in U. S. E-928.

B.S.E.E., 1934; married; exper signal and substation instal. Chief Engr for high voltage pole line hardware mfr handle tests, specifications, des, maintenance. Desires permanent pos in maintenance or des. E-929.

LICENSED PROF ENGR, New York; 49, single; extensive and responsible exper in inventory, valuation, rate work on elec util; also des, draftg, of substations, pwr plants and light and pwr, all types of structures. South or West preferred. E-930.

ELECTRICIAN; 37, married. 21 yrs in steam-hydro plant oprn, maintenance. Exper in all types of eqpt used in generation, transm and distr. Employed. Available within 2 wks. E-931.

AIEE member; 45, married; 21 yrs with present pub util and its predecessors in supervisory and exec capacity, desires permanent pos with util or indus organization as oprn and/or maintenance engr. Now employed. E-932.

EXPER PATENT ATTORNEY seeks full or part time pos in South, Washington, D.C. or Ohio. Familiar with motors, instruments and transf; also accounting. HKN, Tau Beta Pi, Sigma Xi. E-933.

VALUATION ENGINEER; 7 yrs with pub util and 7 yrs with consulting firms, desires pos. E-934.

GRAD ELEC ENGR; 38; desires new connection as pwr engr. Extensive exper with elec machy and steam turbine instal with mfr, elec RR and insurance co. Location desired, Northeastern U. S. E-935.

ELEC DISTR ENGR; 40; exper includes supervision of des, constr, oprn, and appraisals; seeks responsible pos with util, industrial or consulting firm, with commensurate salary or prospects. E-936.

ELEC ENGR, elec and mech, for managerial or staff duties, exper in steel mill engg, oprn, maintenance, process or patent devpmt, employee relations, etc. E-937.

REGISTERED PROF E E; 39, married; 10 yrs exper maintenance engr of mech and elec eqpt in mfg plants and office bldgs. Desires pos as eqpt engr., supervision of sales. Metropolitan area preferred. E-938.

B.S.E.E., Lehigh Univ; 29, married; desires pos valuation or elec pwr sales and distr; 5 yrs engg exper; now employed. Desires pos with future. Location immaterial. E-939.

ENGINEERING SOCIETIES PERSONNEL SERVICE, INC.

NEW YORK 31 W. 39th St.
SAN FRANCISCO 57 Post St.
CHICAGO 211 W. Wacker Dr.
DETROIT 100 Farnsworth Ave.

Westinghouse Brings Safety to Seadromes with

LIGHT CONTROLLED BY RADIO

When ocean travel by air brought Rio closer to Miami, it also brought an entirely new problem to aviation—the problem of safe night landing on water for giant clipper planes.

But now a flashing red light, battery-powered and supported by a buoyant rubber float that will not damage a plane striking it, will warn surface craft away from the seaplane landing area. Lines of green, gold, or red fluorescent lights, visible from three to five miles, will mark the water landing lanes for pilots.

Portable units, designed for transportation by air to remote bases, are controlled by land radio. Boundary and contact lights can be operated separately. A single lane of contact lights or various lights within a lane can be controlled by the shore radio to meet the landing plane's requirements. Transoceanic flying will be revolutionized by this new light, developed by Westinghouse in collaboration with Firestone, that brings greater safety to seadromes.

Aviation, like other industries, is finding that electricity is the answer to many of today's rush production problems. A phone call to our local office will bring one of our representatives to help you with yours.

Westinghouse Electric & Mfg. Co., East Pittsburgh, Pennsylvania.

Westinghouse

Time-Saver For American Industry

ELECTRICAL POWER SPEEDS PRODUCTION

No American manufacturer can afford to overlook the modern methods and equipment offered by the electrical industry for speeding up production. A phone call will bring a Westinghouse representative to your office to discuss your problems.

Future advertisements on this page will describe how Westinghouse is helping in the aviation . . . mining . . . steel . . . metalworking . . . and other industries. Watch for these stories.

J-94446

Advertised Products Index

AMMETER COMPENSATING COILS
Minerallac Electric Co., Chicago

AMMETERS, VOLTMETERS
(See INSTRUMENTS, ELECTRICAL)

BRUSHES, COMMUTATOR
National Carbon Co., Inc., Cleveland, O.

BUS BAR SUPPORTS
Burndy Engg. Co., Inc., New York
General Electric Co., Schenectady, N. Y.

CABLE ACCESSORIES
General Electric Co., Schenectady, N. Y.
Minerallac Electric Co., Chicago

CAPACITORS
Aerovox Corp., New Bedford, Mass.
Behr, Leo, Philadelphia, Pa.
General Electric Co., Schenectady, N. Y.
Solar Mfg. Corp., Bayonne, N. J.
Westinghouse E. & M. Co., E. Pittsburgh

CIRCUIT BREAKERS
Air Enclosed
General Electric Co., Schenectady, N. Y.
I-T-E Circuit Breaker Co., Philadelphia
Roller-Smith Co., Bethlehem, Pa.
Westinghouse E. & M. Co., E. Pittsburgh
Oil
Allis-Chalmers Mfg. Co. Milwaukee, Wis.
General Electric Co., Schenectady, N. Y.
Roller-Smith Co., Bethlehem, Pa.
Westinghouse E. & M. Co., E. Pittsburgh

CONDENSERS, ELECTROSTATIC
Aerovox Corp., New Bedford, Mass.
General Electric Co., Schenectady, N. Y.
General Radio Co., Cambridge, Mass.
Solar Mfg. Corp., Bayonne, N. J.
Westinghouse E. & M. Co., E. Pittsburgh

CONDUIT PRODUCTS
General Electric Co., Bridgeport, Conn.
National Elec. Products Corp., Pittsburgh

CONNECTORS, SOLDERLESS
Burndy Engg. Co., Inc., New York
General Electric Co., Schenectady, N. Y.
Krueger & Hudepohl, Cincinnati, Ohio
National Elec. Products Corp., Pittsburgh

CONTROLLERS
Allis-Chalmers Mfg. Co., Milwaukee, Wis.
General Electric Co., Schenectady, N. Y.
Rowan Controller Co., Baltimore, Md.
Westinghouse E. & M. Co., E. Pittsburgh

CONVERTERS, SYNCHRONOUS
Allis-Chalmers Mfg. Co., Milwaukee, Wis.
General Electric Co., Schenectady, N. Y.
Westinghouse E. & M. Co., E. Pittsburgh

CORPRENE GASKETS & PACKINGS
Armstrong Cork Co., Lancaster, Pa.

DRAFTING PENCILS
Dixon Crucible Co., J., Jersey City, N. J.

ELECTRONIC TUBES
General Electric Co., Schenectady, N. Y.
Westinghouse E. & M. Co., E. Pittsburgh

FURNACES, ELECTRIC
American Bridge Co., Pittsburgh
General Electric Co., Schenectady, N. Y.

GASKETS, "CORPRENE"
Armstrong Cork Co., Lancaster, Pa.

GENERATORS AND MOTORS
Allis-Chalmers Mfg. Co., Milwaukee, Wis.
General Electric Co., Schenectady, N. Y.
Westinghouse E. & M. Co., E. Pittsburgh

GROUND RODS
Copperweld Steel Co., Glassport, Pa.

HEATING UNITS
General Electric Co., Schenectady, N. Y.

INSTRUMENTS, ELECTRICAL
Graphic
Ferranti Electric, Inc., New York
General Electric Co., Schenectady, N. Y.
Leeds & Northrup Co., Philadelphia
Roller-Smith Co., Bethlehem, Pa.
Westinghouse E. & M. Co., E. Pittsburgh
Weston Elec. Instrument Corp., Newark, N. J.

INSTRUMENTS, ELECTRICAL (Con't)
Indicating
Ferranti Electric, Inc., New York
General Electric Co., Schenectady, N. Y.
Leeds & Northrup Co., Philadelphia
Roller-Smith Co., Bethlehem, Pa.
Shallcross Mfg. Co., Collingdale, Pa.
Westinghouse E. & M. Co., E. Pittsburgh
Weston Elec. Instrument Corp., Newark, N. J.
Integrating
Ferranti Electric, Inc., New York
General Electric Co., Schenectady, N. Y.
Shallcross Mfg. Co., Collingdale, Pa.
Westinghouse E. & M. Co., E. Pittsburgh
Weston Elec. Instrument Corp., Newark, N.J.
Scientific Laboratory, Testing
Acme Elec. & Mfg. Co., Cuba, N. Y.
Du Mont Labs., Inc., Allen B., Passaic, N. J.
Ferranti Electric Inc., New York
General Electric Co., Schenectady, N. Y.
General Radio Co., Cambridge, Mass.
Leeds & Northrup Co., Philadelphia
Roller-Smith Co., Bethlehem, Pa.
Shallcross Mfg. Co., Collingdale, Pa.
Westinghouse E. & M. Co., E. Pittsburgh
Weston Elec. Instrument Corp., Newark, N. J.

INSULATING MATERIALS
Cloth
General Electric Co., Bridgeport, Conn.
Irvington Varnish & Ins. Co., Irvington, N. J.
Minerallac Electric Co., Chicago
Westinghouse E. & M. Co., E. Pittsburgh
Compounds
General Electric Co., Bridgeport, Conn.
Minerallac Electric Co., Chicago
Roebling's Sons Co., John A., Trenton, N. J.
Westinghouse E. & M. Co., E. Pittsburgh
Lava
American Lava Corp., Chattanooga, Tenn.
Moulded
General Electric Co., Bridgeport, Conn.
Westinghouse E. & M. Co., E. Pittsburgh
Paper
General Electric Co., Bridgeport, Conn.
Irvington Varnish & Ins. Co., Irvington, N. J.
Westinghouse E. & M. Co., E. Pittsburgh
Tape, Friction
Minerallac Electric Co., Chicago
Okonite Company, The, Passaic, N. J.
Roebling's Son Co., John A., Trenton, N. J.
Varnishes
General Electric Co., Bridgeport, Conn.
Irvington Varnish & Ins. Co., Irvington, N. J.
Minerallac Electric Co., Chicago

INSULATORS, GLASS
Corning Glass Works, Corning, N. Y.

INSULATORS, PORCELAIN
General Electric Co., Schenectady, N. Y.
Lapp Insulator Co., LeRoy, N. Y.
National Elec. Products Corp., Pittsburgh
Ohio Brass Co., Mansfield, O.
Universal Clay Products Co., Inc., Sandusky, O.
Westinghouse E. & M. Co., E. Pittsburgh

INSULATOR TESTING EQUIPMENT
Ferranti Electric, Inc., New York
General Radio Co., Cambridge, Mass.
Roller-Smith Co., Bethlehem, Pa.

LIGHTING EQUIPMENT, OUTDOOR
General Electric Co., Schenectady, N. Y.
Westinghouse E. & M. Co., E. Pittsburgh

LIGHTNING ARRESTERS
General Electric Co., Schenectady, N. Y.
Westinghouse E. & M. Co., E. Pittsburgh

LOAD RECORDERS—CONTROLLERS
Leeds & Northrup Co., Philadelphia

METERS, ELECTRICAL
(See INSTRUMENTS, ELECTRICAL)

MOTORS
(See GENERATORS AND MOTORS)

OSCILLOGRAPHS, CATHODE RAY
Du Mont Labs. Inc., Allen B., Passaic, N. J.
General Electric Co., Schenectady, N. Y.
General Radio Co., Cambridge, Mass.
Westinghouse E. & M. Co., E. Pittsburgh

PENCILS, DRAWING
Dixon Crucible Co., J., Jersey City, N. J.

POLE LINE HARDWARE
Ohio Brass Co., Mansfield, O.

PORCELAIN, ELECTRIC
Universal Clay Products Co., Inc., Sandusky, O.

RECTIFIERS
Allis-Chalmers Mfg. Co., Milwaukee, Wis.
Benwood Linze Co. The, St. Louis, Mo.
General Electric Co., Schenectady, N. Y.
Int'nt'l Tel. & Radio Mfg. Corp., New York
Westinghouse E. & M. Co., E. Pittsburgh

REGULATORS, VOLTAGE
Allis-Chalmers Mfg. Co., Milwaukee, Wis.
General Electric Co., Schenectady, N. Y.
General Radio Co., Cambridge, Mass.
Roller-Smith Co., Bethlehem, Pa.
Sola Electric Co. Chicago, Ill.
Westinghouse E. & M. Co., E. Pittsburgh

RELAYS
General Electric Co., Schenectady, N. Y.
I-T-E Circuit Breaker Co., Philadelphia
Roller-Smith Co., Bethlehem, Pa.
Weston Elec. Instrument Corp., Newark, N.J.
Westinghouse E. & M. Co., E. Pittsburgh

RESISTORS
General Electric Co., Schenectady, N. Y.
General Radio Co., Cambridge, Mass.
International Resistance Co., Philadelphia
Ohmite Mfg. Co., Chicago
Shallcross Mfg. Co., Collingdale, Pa.
Westinghouse E. & M. Co., E. Pittsburgh

RHEOSTATS, LABORATORY
General Electric Co., Schenectady, N. Y.
General Radio Co., Cambridge, Mass.
International Resistance Co., Philadelphia
Ohmite Mfg. Co., Chicago
Westinghouse E. & M. Co., E. Pittsburgh

STEEL, ELECTRICAL
Carnegie-Illinois Steel Corp., Pittsburgh

SWITCHBOARDS
Allis-Chalmers Mfg. Co., Milwaukee, Wis.
General Electric Co., Schenectady, N. Y.
I-T-E Circuit Breaker Co., Philadelphia
Roller-Smith Co., Bethlehem, Pa.
Westinghouse E. & M. Co., E. Pittsburgh

SWITCHES, AUTOMATIC TIME
General Electric Co., Schenectady, N. Y.
Minerallac Electric Co., Chicago

SWITCHES, DISCONNECT
General Electric Co., Schenectady, N. Y.
Roller-Smith Co., Bethlehem, Pa.
Westinghouse E. & M. Co., E. Pittsburgh

SWITCHES, GENERATOR FIELD
I-T-E Circuit Breaker Co., Philadelphia
Roller-Smith Co., Bethlehem, Pa.

TOWERS, TRANSMISSION
American Bridge Co., Pittsburgh

TRANSFORMERS
Acme Elec. & Mfg. Co., Cuba, N. Y.
Allis-Chalmers Mfg. Co., Milwaukee, Wis.
Chicago Transformer Corp., Chicago, Ill.
Ferranti Electric, Inc., New York
General Electric Co., Schenectady, N. Y.
General Radio Co., Cambridge, Mass.
Kuhlman Electric Co., Bay City, Mich.
Roller-Smith Co., Bethlehem, Pa.
Sola Electric Co., Chicago
United Transformer Corp., New York
Westinghouse E. & M. Co., E. Pittsburgh

TURBINES and TURBINE GENERATORS
Allis-Chalmers Mfg. Co., Milwaukee, Wis.
General Electric Co., Schenectady, N. Y.
Westinghouse E. & M. Co., E. Pittsburgh

VARNISHES, INSULATING
General Electric Co., Bridgeport, Conn.
Irvington Varnish & Ins. Co., Irvington, N. J.
Westinghouse E. & M. Co., E. Pittsburgh

WELDERS, ARC
General Electric Co., Schenectady, N. Y.
Westinghouse E. & M. Co., E. Pittsburgh

WELDING WIRE
American Steel & Wire Co., Cleveland, O.
General Electric Co., Schenectady, N. Y.
Roebling's Sons Co., John A., Trenton, N. J.

WIRES AND CABLES
Aluminum Co. of America, Pittsburgh
American Steel & Wire Co., Cleveland, O.
Belden Mfg. Co., Chicago
Copperweld Steel Co., Glassport, Pa.
Crescent Ins. Wire & Cable Co., Trenton, N. J.
General Cable Corp., New York
General Electric Co., Schenectady, N. Y.
Kerite Ins. Wire & Cable Co., New York
National Elec. Products Corp., Pittsburgh
Okonite Company, The, Passaic, N. J.
Okonite-Callender Cable Co., Passaic, N. J.
Roebling's Sons Co., John A., Trenton, N. J.

ADVERTISERS

** See previous issues.*

FACTS YOU CAN USE TO SELL MORE AND BETTER WIRING JOBS

FIRST... Measure All Three!

CODE WIRE TYPE R	PERFORMANCE TYPE RP	HAZARD PERFORMITE TYPE RH
Meets all "code" requirements but is limited to 50° C. operation.	This better grade insulation permits operation at 60° C. Carries heavier current loadings or allows use of smaller size conductors.	A superior insulation in every respect. Operating temperature 75° C. Permits still greater current loadings or even smaller conductors. Performite is super-aging... resistant to heat and moisture... lasts indefinitely... meets Federal Specs. J-C-106-a and J-C-121.

SECOND... Compare Typical Wiring Costs of All Three!

Conductor Size A W G	Carrying Capacity in Amperes 3 Cond. 30 Ambient			Relative Cost* per 100 Amp. — ft. (IAEI Bulletin, Jan. 1941)		
	Type R	Type RP	HAZARD Performite Type RH	Type R	Type RP	HAZARD Performite Type RH
2	80	96	115	$.867	.770	.670
4/0	160	193	230	$.970	.870	.740

**Naturally if the full carrying capacity of the conductors is not available because of excessive voltage drop, the comparison will have to be modified proportionately.*

WITH ALL ITS ADVANTAGES... HAZARD PERFORMITE COSTS LESS PER AMPERE CARRIED

There are the facts! Relative costs figured from actual installations show that even the first cost of HAZARD Performite is actually less than Type R wire in a great many cases. This is true because this superior insulation permits greater load carrying or makes it possible to use smaller conductors for the same load. Both ways bring important copper savings and add materially to the life of the circuit.

For full information on HAZARD Performite, Type RH or Type RHT (small diameter for new wiring and rewiring), WRITE TODAY.

HAZARD INSULATED WIRE WORKS
DIVISION OF THE OKONITE COMPANY
Works: Wilkes-Barre, Pennsylvania
Offices in Principal Cities

HAZARD
PERFORMITE TYPE RH